AGING AND DRYING OF GEL PRECURSORS PROMOTE NONTRONITE CRYSTALLIZATION DURING HYDROTHERMAL SYNTHESIS

Zhongyi Liu[1,6], Peixin Du[1,6*], Zhanshuo Dai[1,6], Zixuan Luo[1,6], Jing Liu[1,6], Jiacheng Liu[2], Dong Liu[3], Baifa Zhang[4], Shangying Li[5], Meiqing Chen[4], Peng Yuan[4]

1. State Key Laboratory of Lunar and Planetary Sciences, Macau University of Science and Technology, Macau, China
2. Department of Earth Sciences and Laboratory for Space Research, The University of Hong Kong, Hong Kong, China
3. Guangdong Provincial Key Laboratory of Mineral Physics and Materials, Guangzhou Institute of Geochemistry, Chinese Academy of Sciences, Guangzhou 510640, China
4. School of Environmental Science and Engineering, Guangdong University of Technology, Guangzhou 510006, China
5. School of Land Engineering, Chang'an University, Xi'an 710064, China
6. CNSA Macau Center for Space Exploration and Science, Macau, China

Abstract Nontronite exhibits heterogeneous composition, widespread occurrence but low abundance on Earth. Hydrothermal synthesis in laboratory is an effective method to obtain nontronite with controlled compositions and specific features. Numerous studies have investigated the parameters affecting nontronite synthesis, including temperature, pH, time, redox atmosphere, Fe/Si molar ratio, and types of raw materials. However, limited attention has been focused on the effects of precursor preparation prior to heating on nontronite synthesis. To this end, nontronite was synthesized with four different precursors: (1) a gel precursor without aging (the corresponding product was labeled Non), (2) a gel precursor aged for 24 h (Non-A), (3) a gel precursor aged for 24 h followed by drying at 60°C (Non-ADh), and (4) a gel precursor aged for 24 h followed by freeze-drying (Non-ADf). These products and two precursors (non-aged and aged for 24 h, respectively) were characterized via X-ray diffraction (XRD), Fourier transform infrared (FTIR) spectroscopy, visible and near-infrared (VNIR) spectroscopy, transmission electron microscopy (TEM), and X-ray photoelectron spectroscopy (XPS). The crystallinity of the four synthesized nontronite followed the order Non-ADh > Non-ADf > Non-A > Non, indicating that both aging and drying (including drying by heating and freeze-drying) played a positive role in formation of nontronite. These findings help to optimize the synthesis route of nontronite. Moreover, the synthetic nontronite samples exhibited an increase of Fe(III) contents with crystallinity, indicating oxidation of Fe(II) probably promotes the formation of nontronite.

Key words: nontronite, hydrothermal synthesis, drying, precursor, crystallinity

APPLICATION OF ARTIFICIAL INTELLIGENCE IN COLORED DIAMOND IMAGE COLOR GRADING

Wang Li-Nong[1], Huang Ching-Hsiang[1], Lui Wingtak[2,3],Huang Yu-Chen[2,3],Xing Rui-Rui[3], Chien Yu-Hsiang[1*]

1. Alishan Diamond Technology Co., Ltd., Taiwan, New Taipei, 241501
2. Taiwan Central Gem Laboratory, Taiwan, Taipei, 104035
3. MD minerals and Gem research (Nanjing) Co., Ltd., Nanjing, 210014

Abstract The value of colored diamonds in the jewelry market is closely linked to their color, making efficient and accurate color grading techniques crucial for the industry. In this study, we integrated the RGB, CIE, and HSV color models with artificial intelligence algorithms and employed machine learning on 514 certified colored diamond samples and images ranging in weight from 0.1 to 11.5 carats. After system optimization, our method can accurately identify the primary color and eight levels of intensity within 60 seconds and generate a detailed report. When compared with the color grading reports on the samples' GIA and IGI certificates, the accuracy reached 70%, effectively addressing the limitations of traditional visual assessment errors and significantly reducing the time required. In summary, this system is expected to facilitate the digital transformation of the jewelry industry, establish industry standards for broader cross-disciplinary applications, and promote the deep integration of artificial intelligence in the field of jewelry.

Key words: Colored Diamonds, Image Analysis, Color Identification, Artificial Intelligence

ATOMIC INSIGHTS INTO RARE EARTH ELEMENT ADSORPTION AT MINERAL-WATER INTERFACES

Gaofeng Wang[1,2,3,4], Lingyu Ran[1,2,3,4], Jianxi Zhu[1,2,3,4,*], Xiaoliang Liang[1,2,3,4], Jie Xu[5], Hongping He[1,2,3,4]

1. State Key Laboratory of Deep Earth Processes and Resources, Guangzhou Institute of Geochemistry, Chinese Academy of Sciences, Guangzhou, 510640, China
2. Guangdong research center for strategic metals and green utilization, Guangzhou 510640, China
3. Guangdong Provincial Key Laboratory of Mineral Physics and Material, Guangzhou Institute of Geochemistry, Chinese Academy of Sciences; Guangzhou 510640, China
4. University of Chinese Academy of Sciences; Beijing 100049, China
5. School of Environment, Hangzhou Institute for Advanced Study, University of Chinese Academy of Sciences, Hangzhou 310024, China

Abstract Regolith-hosted ion-adsorption deposits (IADs) are dominant global sources of strategically significant heavy rare-earth elements (HREEs). While clay minerals are primary rare earth element (REE) carriers, their role in the formation of such HREE deposits remains debated. Here, we report how clay minerals govern REE adsorption and fractionation at the atomic scale. Using in situ high-resolution atomic force microscopy, we directly visualized, at the atomic scale, light-REEs (LREEs) and HREEs adsorption on crystallographically distinct surfaces in aqueous solutions. Contrary to prevailing models emphasizing Al-basal planes, we find preferential REE adsorption on Si-basal planes, with strong affinity for HREEs over LREEs. These findings redefine atomic-scale mechanisms and pathways governing REE adsorption and fractionation at mineral–water interfaces, reshape surface reactivity paradigms for clay minerals, and offer new insights into the supergene weathering metallogeny of strategic metals beyond REEs.

Key words: Rare earth elements, atomic-scale imaging, in situ high-resolution atomic force microcopy, clay mineral-water interfaces, surface reactivity

ATOMIC-RESOLUTION OBF-STEM IMAGING OF STACKING FAULTS IN NACRITE

Hayato Miura[1], Toshihiro Kogure[2,3], Taiga Okumura[3] and Ichiro Ohnishi[1]

1. JEOL Ltd., Tokyo, Japan
2. Department of Earth and Planetary Science, School of Science, The University of Tokyo, Tokyo, Japan
3. Faculty of Education and Integrated Arts and Sciences, Waseda University, Tokyo, Japan

Abstract Stacking faults in kaolin-group minerals (KGMs), i.e., dioctahedral 1:1 phyllosilicates, are fundamental structural features strongly related to their crystallographic diversity, stability, and formation processes. Such faults have long been inferred mainly from diffraction-based techniques; however, the local atomic configurations responsible for the faults remain controversial because high-resolution electron microscopy observing them directly is severely hindered by the strong beam sensitivity of KGMs. In particular, discriminating stacking faults associated with intermixing of different polytypic groups requires atomic-resolution imaging along specific crystallographic directions under extremely low electron-dose conditions.

In this study, we investigated the atomic structure of stacking faults in nacrite, a KGM polytype classified into polytypic Group D as defined by Bailey (1988), using optimum bright-field scanning transmission electron microscopy (OBF-STEM) equipped with a segmented annular all-field (SAAF) detector. This technique enables the synthesis of phase-contrast images with sufficiently high signal-to-noise ratios even under low-dose conditions, making it especially suitable for beam-sensitive clay minerals. By carefully optimizing imaging conditions and specimen thickness, atomic columns, including oxygen, were resolved without inducing severe structural degradation.

Conventional bright-field TEM images acquired along the $\pm Y_i$ crystallographic directions of nacrite revealed distinct linear diffraction contrasts parallel to (001), suggesting stacking faults arising from stacking sequences different from those of Group D. Atomic-resolution OBF-STEM imaging along these directions showed that these faults correspond to stacking sequences characteristic of polytypic Group A inserted of the nacrite structure. The stacking geometry at the fault regions is unambiguously distinguished from that of pristine nacrite by the orientation of octahedral sheets and characteristic lateral displacements of silicon atomic columns between adjacent layers.

Complementary observations along the ±Xi directions further corroborate this interpretation. In these projections, the contrast patterns at the fault regions cannot be explained by any stacking arrangement intrinsic to nacrite; instead, they correspond to structural motifs typical of Group A polytypes, namely kaolinite and dickite. The consistency of these features across multiple fault occurrences indicates that stacking faults in nacrite are systematically formed by local intermixing

of Group A stacking sequences rather than by random disorder.

The coexistence of Group A and Group D stacking sequences within nacrite suggests that these polytypic groups are energetically close in stability despite substantial differences in the stacking sequences of the 1:1 layers. This finding provides insight into why, among the theoretically-derived numerous standard KGM polytypes, only a limited number (kaolinite, dickite, and nacrite) are observed in nature.

In addition to stacking-fault analysis, high-resolution OBF-STEM images revealed anomalously weak or absent contrast at specific oxygen columns corresponding to the inner hydroxyl (OH^-) and the nearest outer hydroxyl in nacrite, implying partial dehydroxylation of the crystal structure. Such dehydroxylation is likely induced either by electron irradiation during imaging or during specimen preparation by focused ion beam processing. This observation highlights an important caveat in atomic-resolution electron microscopy of hydroxyl-bearing minerals: even under low-dose conditions, subtle beam-induced structural modifications may occur and must be considered when interpreting local atomic arrangements. Simultaneously, these results provide implications for possible structures of partially dehydroxylated KGMs involving five-coordinated aluminum formed during heating.

Overall, this study demonstrates that low-dose OBF-STEM is a powerful approach for directly resolving local atomic arrangements, including stacking faults, in beam-sensitive minerals and provides new insights into their crystal chemistry, stability, and genesis.

Key words: OBF-STEM, low-dose imaging, nacrite, stacking faults, kaolin-group minerals

Acknowledgements We are grateful to Waka Tarora for the FIB operation to prepare thin film samples for TEM.

ATOMISTIC STUDY OF AQUEOUS SOLUTION IN THE IHOMOGENEOUS CLAY–QUARTZ SYSTEM

Artem A. Glushak, Evgeny V. Tararushkin, Grigory S. Smirnov

International Laboratory for Supercomputer Atomistic Modelling and Multi-scale Analysis, HSE University, Russia

Abstract The present work provides a heterogeneous model designed to study the structural and dynamical properties of aqueous solutions in the pores of a heterogeneous system of clay and quartz via molecular dynamics (MD). This model is created to study the aqueous solution between the basal surfaces of clay and quartz minerals to imitate “face-to-face” orientation of structures. Classical MD simulations are performed with the modified version of ClayFF-MOH interatomic potential. We discuss structural and dynamical properties of water in the pores of various sizes for heterogeneous clay-quartz system and compare results with homogeneous clay and homogeneous quartz systems. We have also studied the influence of the quartz-surface roughness on its interactions with water.

We have shown that the influence of surfaces is noticeable at distances of up to 15-20 Å. In this range, water near one surface is influenced by the other, as well as the influence on water between pores. Water near the surface of clay has a bidentate orientation, while water near quartz can be in both monodentate and bidentate orientation. Although water is more structured near the surface of clay, the total amount of water on the quartz side is higher.

The surface of rough quartz has been studied, showing reorientation of water on the surface of the mineral and its possibility to penetrate surface deeper into the crystal. Also, the introduction of defects increases the distance at which water begins to interact with the surface and form H-bonds with hydroxyls.

The dynamic properties of water in the pores of the studied systems are investigated. It is shown that the introduction of quartz reduces the mobility of water in the pore compare to the homogeneous clay system, which is associated with the formation of a dense complex H-bonds network on the surface.

Key words: Clay, Molecular Dynamics, Quartz, Surface Defects

Acknowledgements The work is supported by the HSE University Basic Research Program.

CARBONATE AND PHOSPHATE MATRIX REFERENCE MATERIALS DEVELOPED FOR LA-ICP-MS ANALYSIS

Chenzi Fan[1,2], Dongyang Sun[1], Linghao Zhao[1]

1. National Research Center for Geoanalysis, Beijing, China
2. State Key Laboratory of Deep Earth and Mineral Exploration, Beijing, China

Abstract This study presents CGSP carbonate and CGSP-P phosphate matrix reference materials for LA-ICP-MS analysis prepared by coprecipitation method. For carbonate references, the major and trace elements were dissolved from natural rare earth carbonate raw materials from Bayan Obo deposit in strong acid and precipitated with ammonium bicarbonate or ammonia to form carbonate matrix phases. For phosphate references, they were synthesised by co-precipitation with $CaCl_2$ and (NH4)3PO4 to form a hydroxylapatite matrix with adding in variable elements. The reference materials were ground and pressed into tablets for microanalysis. The element homogeneity and stability in CGSP reference materials were tested by LA-ICP-MS using a calibration strategy without an internal standard and evaluated mainly following ISO Guide 35: 2006, 2017 and JJF 1343-2012. The homogeneity of most of elements in the CGSP series were comparable with the repeatability obtained from homogeneous glasses, but some elements e.g. Mo, Se, Ga, Ge, Cd, Ni, Co, U were found to have some degree of heterogeneity. In the phosphate references, most of the elements (e.g. Mg, Ca, P, Mn, and REE) were homogenous within 10% RSD, and other elements (e.g. Si, Al, K, Rb, Cs, and Ni) were considered heterogeneous (with >20% RSD). All of elements passed the t-test evaluation in a 32 months stability examination except for Mo in CGSP-A, Na, Ge, Mo in CGSP-B, Ni, Cd, Sn in CGSP-C, and Al, P, Tb, Ho in CGSP-D. All of the elements passed the t-test except Ni in CGSP-P3, and V, Cr, Ni, Zr, Gd, Dy and Th in CGSP-P4 after a 29-months period stability examination by LA-ICP-MS. The certified element concentration values and uncertainties were determined with the characterization of a non-operationally defined measurand using various bulk analysis methods in multiple laboratories.

Key words: CGSP carbonate, CGSP-P phosphate, LA-ICP-MS, micro-analysis reference materials.

CATALYTIC PYROLYSIS OF POLYETHYLENE AND POLYPROPYLENE INTO LIQUID FUEL-LIKE PRODUCTS OVER CLAY MINERALS

Lyubov Furda, Dmitry Smalchenko, Sergei Golovin, Igor Tarasov, Ekaterina Migulina, Evgeniy Seliverstov, Evgeniya Tarasenko, Olga Kokoshkina, Olga Lebedeva

Department of General Chemistry, Belgorod State National Research University, Russian Federation

Abstract The accumulation of plastic waste has become a global environmental problem. The current goal is not simply to dispose polymer waste, but to make rational use of it by recycling into useful products. One of the simplest and most effective methods of recycling is considered to be the conversion of plastics into an oil-like set of hydrocarbons, which can be viewed as raw materials returning to the oil refining cycle or, with some further processing, as a means of producing motor fuel components.

An important requirement for polymer conversion catalysts is their availability and low cost. Such catalysts include natural materials as well as materials derived from industrial waste. In this regard, clay minerals are of considerable interest. The diversity of natural clays offers wide opportunities for the search for optimal catalysts among them.

In the present study, we conducted experiments on the degradation of plastic waste using a continuous flow fixed-bed reactor in inert atmosphere. Pristine clay samples from various natural deposits were used as catalysts. All samples were preliminarily characterized using XRD, FTIR spectroscopy, SEM and EDAX. The acid-base properties of the clay samples surfaces were investigated using the Hammett indicator method. TMB test was apply to estimate the oxidative properties of the samples. As a result, bentonite, kaolin and illite clays were demonstrated to give a sufficient yield of liquid hydrocarbons from polypropelene. The resulting liquid products were analyzed by gas-liquid chromatography and NMR spectroscopy.

Key words: clay minerals, pyrolysis, polyethylene, polypropylene, catalysts, liquid products

Acknowledgements The study was conducted under the state assignment, project № FZWG-2026-0007

COLOR AND SPECTRAL CHARACTERISTICS OF 24 COLOR-CHANGE NANOSITAL GLASS-CERAMICS USED AS GEM MATERIALS

Raksit Tantipisit, Pimlapat Kamkaew, and Parawee Sithisena

The Gem and Jewelry Institute of Thailand (Public Organization), Thailand

Abstract Artificial color-change glasses are commonly used to simulant for natural color-change gem- stones, such as alexandrite and color-change garnet. This study aimed at investigating the optical spectro- scopic and chemical composition of 24 artificial color-change glass samples in order to obtain their reliable separation criteria essential for gemological identification. Firstly, the basic gemological properties of those samples were measured including refractive index (RI) of 1.65 to 1.68 and specific gravity (SG) of 3.25 to 3.94. Their color-change behavior was documented under a D65 daylight-equivanent fluorescent lamp and incandescent illumination using a B-Light amber LED penlight and the observed colors were graded using the Munsell color system for standardized color description. Advanced analytical techniques including UV-Visible Spectrophotometry (UV-Vis), Fourier-transform infrared spectroscopy (FTIR), and Energy-dis- persive X-ray fluorescence spectroscopy (EDXRF) were also applied to examine spectral and elemental characteristics. Based on the visual color grading, the samples were classified into six color groups, namely blue, green, yellow, orange, pink, and purple. The UV-Vis absorption spectra varied among these groups, reflecting differences in the chromophores responsible for each hue and color-change effect. The FTIR spec- tra of the stones showed similar patterns, with a few samples displaying an additional hump at 5135 cm^{-1}. The Raman spectra showed different spectral patterns among the six color groups. The EDXRF analysis also revealed the variation of their major and trace element content among those six color groups. The stone hues and color-change effect are likely associated with the variation of Y_2O_3 in range of 27 to 32 wt% oxides, Nd_2O_3 from 10 to 14 wt% oxides, and the trace elements of La, Gd, Zr, Ba, Ce, Mg, and Ho. These varia- tions allowed us to systematically group the samples according to their color characteristics. This study has also provided the baseline gemological and spectroscopic features of these artificial color-change glasses, particularly their unique FTIR spectra and rare-earth trace element composition, to be distinguished from natural color-change gemstones.

Key words: Artificial, Glass, Color-change, Gemstone, Simulant identification

Acknowledgements The authors would like to thank The Gem and Jewelry Institute of Thailand (Public Organization) for providing samples, laboratory facilities, and analytical instrumentation, as well as the research advisors for their valuable guidance throughout this study.

COLOUR ZONING IN MELT-GROWN BLUE SAPPHIRE

Waratchanok Suwanmanee[1], Chutimun Chanmuang N.[1], Manfred Wildner[1], Bhuwadol Wanthanachaisaeng[2], Lutz Nasdala[1]

1. Institut für Mineralogie und Kristallographie, Universität Wien, 1090 Vienna, Austria
2. The Gem and Jewelry Institute of Thailand (Public Organization), 10500 Bangkok, Thailand

Abstract Synthetic gem-quality corundum can be created in a variety of colours, including the option to produce zoned or multiply coloured specimens. However, a remarkable observation is that the art of producing body-coloured blue sapphire using the (comparably low-cost) Verneuil technique seems to have been lost. Verneuil-synthesised blue sapphire typically exhibits non-uniform colouration: Boules have a several-mm-thick cornflower blue rim surrounding a colourless bulk. In the present study, we examined melt-grown blue synthetic sapphire with optical, spectroscopic and chemical analyses.

Boules were prepared as doubly polished wafers oriented perpendicular to the long axis of the boule. Single crystal X-ray diffraction revealed that the corundum's *c* axis is not parallel to, but nearly perpendicular to, the long axis of the boule (predetermined by the crystallographic orientation of seed crystals). Results of line scans of the chemical composition (EPMA) revealed that the outer blue zone contains approximately 0.11 wt% Ti and 0.07 wt% Fe. The concentrations of both elements gradually decrease with increasing depth from the boule's outer surface towards the colourless interior.

Raman spectra obtained from blue and colourless regions show vast differences. Spectra of the colourless interior are consistent with that of typical corundum, displaying characteristic bands at ~378, 417, 578, 643 and 750 cm^{-1}. In contrast, the blue rim exhibits additional spectral features, with major bands at ~180 and ~250 cm^{-1} and minor bands at 404, 475, 533, 667, and 704 cm^{-1}. These additional bands have already been observed quite often in previous studies. They have been controversially discussed in the literature; the additional spectral pattern is likely related to the trace-element incorporation causing colour formation. Optical absorption spectra of the blue rim show two strong absorption bands in the orange-to-red range at ~17,240 cm^{-1} (~580 nm, $E \perp c$) and ~14,280 cm^{-1} (~700 nm, $E \| c$). These bands are assigned to Fe^{2+}–Ti^{4+} charge transfer that accounts for the characteristic cornflower-blue colour in sapphire. An additional weak absorption band in the violet range may indicate minute amounts of O^- defects.

Achieving uniform blue colour in Verneuil synthesis remains to be challenging. Further studies are needed to better understand the factors contributing to the non-uniform distribution of minor elements and resulting colouration.

Key words: synthetic blue sapphire, colour zoning, Raman spectroscopy, optical absorption

spectroscopy, trace element composition

Acknowledgements The studied Verneuil boules were kindly provided by Thai Tech Sapphire Co., Ltd. We thank Andreas Wagner for sample preparation and Franz Kiraly (both Universität Wien) for performing the EPMA analyses.

DEFECT ENGINEERING IN GEM CRYSTALS: FROM COLOR CENTERS TO OPTICAL AND QUANTUM MATERIALS

LUI Wingtak[1,2],Huang Yu-Chen[1,2],Xing Rui-Rui[1]

1. MD minerals and Gem research (Nanjing) Co., Ltd., Nanjing, 210014
2. Taiwan Central Gem Laboratory, Taiwan, Taipei, 104035

Abstract The Gem crystals constitute a compelling family of wide-bandgap hosts in which point defects, impurities, and defect complexes govern both color and functional optical responses. Beyond gemology, these defect states can be engineered as addressable electronic and spin degrees of freedom for photonics and quantum technologies. We overview representative defect platforms across diamond (NV and group-IV vacancy centers), corundum (Cr^{3+}- and Ti^{3+}-related centers), and silicon carbide (divacancies, silicon vacancies, and vanadium-related centers). A process-to-property toolkit—growth doping, irradiation, ion implantation with post-anneal activation, isotopic purification, surface termination, and strain control—is summarized to tune defect yield, charge-state stability, spectral diffusion, and spin coherence. We highlight application frontiers including room-temperature quantum sensing and nanoscale magnetometry, deterministic single-photon sources with integrated nanophotonics, defect-enabled spectroscopy under extreme conditions (e.g., high pressure), and defect-mediated laser gain media. Finally, we discuss bottlenecks such as near-surface noise, implantation damage, and phonon-induced dephasing, and outline defect-by-design workflows that couple first-principles prediction with process–structure–property feedback for scalable device integration.

Key words: gem crystals, defect engineering, color centers, quantum sensing, single-photon emitters

DIFFERENTIAL HYDROXYL RADICAL PRODUCTION EFFICIENCIES OF FE-BEARING CLAY MINERALS UNDER VARYING PO_2 LEVEL

Qiang Zeng, Chang Xiong

Center for Geomicrobiology and Biogeochemistry Research, State Key Laboratory of Geomicrobiology and Environmental Changes, China University of Geosciences, Beijing 100083, China.

Abstract It has been documented that hydroxyl radicals (•OH) are generated during the oxygenation of soils and sediments in redox-dynamic subsurface environments. Fe(II)-bearing clay minerals, in particular, have been identified as primary contributors to •OH production during oxygenation, with these radicals playing a key role in contaminant degradation and elemental cycling. However, the mechanisms underlying •OH production via the oxygenation of Fe(II)-bearing clay minerals under varying partial oxygen pressure (pO2) levels remain unclear. The objectives of this study were to elucidate the mechanistic basis of •OH formation from Fe(II)-bearing nontronite under different oxygen concentrations and to decipher the electron transfer dynamics governing Fe(II) oxidation and subsequent •OH production. Chemically reduced nontronite was used as a model Fe-bearing clay mineral to explore how oxygen gradients modulate Fe(II) oxidation and •OH formation. •OH production and Fe(II) oxidation kinetics were systematically monitored under 5% or 20% O2. A broad range of spectroscopic and analytical techniques—including Fourier transform infrared spectroscopy (FTIR), X-ray photoelectron spectroscopy (XPS), X-ray diffraction (XRD), and Mössbauer spectroscopy—were employed to characterize the structural variations of Fe(II) sites and to trace electron transfer pathways within reduced nontronite (rNAu-2) and molecular oxygen. A strong linear correlation was observed between •OH yield and Fe(II) oxidation rate. Under low oxygen conditions, both Fe(II) oxidation and •OH generation proceeded at markedly slower rates. Notably, the efficiency of •OH production per unit of Fe(II) oxidized was substantially lower under 5% O2 than under 20% O2. Edge-bound Fe(II), previously identified as a key contributor to •OH generation, simultaneously acted as a dominant sink for •OH scavenging. Under 5% O2, greater accumulation of edge Fe(II) occurred due to limited oxidation, whereas under 20% O2, rapid Fe(II) consumption kept edge-bound Fe(II) levels low. This difference in Fe(II) availability at reactive edge domains critically governs •OH production efficiency under varying pO2 levels. These findings highlight that edge-bound Fe(II) controls oxygen-regulated •OH formation, offering broader implications for redox-driven contaminant attenuation and iron cycling in dynamic soil and sedimentary systems.

Key words: Clay minerals, Hydroxyl radical, Oxygen Concentration, Mechanism

DUAL PATHWAYS OF Fe^{2+} UPTAKE DRIVE INTRACELLULAR FENTON CHEMISTRY AND FERROPTOSIS-LIKE CELL DEATH OF *ESCHERICHIA COLI* UPON EXPOSURE TO REDUCED NONTRONITE

Zijing Rong[1], Qingyin Xia[1], Yizhi Sheng[1,2], Xiaoqin Tang[1], Hailiang Dong[1,2]

1. Center for Geomicrobiology and Biogeochemistry Research, State Key Laboratory of Geomicrobiology and Environmental Changes, China University of Geosciences, Beijing 100083, China
2. Frontiers Science Center for Deep-time Digital Earth, China University of Geosciences, Beijing 100083, China

Abstract Reduced iron-containing clay (RIC) minerals display strong antibacterial activity, yet the intracellular processes underlying bacterial cell death remain poorly understood. Herein, *Escherichia coli* knockout strains were exposed to a model RIC mineral, reduced nontronite (rNAu-2), to dissect iron influx pathways and the resulting oxidative damage. Two complementary mechanisms of Fe^{2+} influx were identified: (i) active transport through FeoB proteins and (ii) passive permeation across oxidatively compromised membranes. At low rNAu-2 loading, a *feoB* mutant accumulated less labile Fe and survived better than the *E. coli* wild-type, whereas at higher loading, passive permeation dominated and the genotypic differences diminished. Intracellular radical analysis revealed hydroxyl radicals (•OH) as the predominant cytotoxic species. Deleting superoxide dismutases (*sodA* or *sodC*) improved bacterial survival by limiting H_2O_2 availability, whereas loss of peroxidase (*ahpC*) or catalase (*katG*) activity elevated H_2O_2 and •OH production, and heightened cellular vulnerability. rNAu-2 exposure promoted lipid peroxidation and malondialdehyde accumulation, while increasing reliance on glutathione biosynthesis (*gshA*), indicative of ferroptosis-like cell death. Correspondingly, a recombination-deficient mutant (*recA*) was hypersensitive to rNAu-2, underscoring the role of oxidative DNA damage to bacterial cell death. These results elucidate the molecular mechanisms of RIC-mediated bacterial killing and significantly advance the current model of antibacterial clay activity.

Key words: Antibacterial clay, Reduced iron-bearing clay minerals, Fenton reaction, Ferroptosis, *Escherichia coli* mutants.

DUAL-CLAY COMPOSITE ELECTROLYTE WITH RIGID-FLEXIBLE INTERLOCKED ARCHITECTURE FOR SAFE LITHIUM METAL BATTERIES

Hao Liu[1], Zhangkuo Han[1], Shusen Zhou[1], Di Jiang[2], Guocheng Lv[2], Libing Liao[2]

1. School of Science, China University of Geosciences, Beijing 100083, China
2. School of Materials Science and Technology China University of Geosciences Beijing 100083, China

Abstract Developing solid electrolytes that combine high ionic conductivity, robust mechanical stability, and fast interfacial kinetics is critical for safe lithium metal batteries, yet these requirements are rarely met simultaneously in conventional polymer- or inorganic-dominant systems. Herein, we report a mineral-dominant dual-clay composite solid electrolyte (DCCSE, >50 wt% mineral content), in which montmorillonite serves as the continuous ion-transport phase, attapulgite acts as the rigid reinforcing framework, and their functional division enables a rigid-flexible integrated electrolyte architecture. Through a one-step organic-inorganic synergistic modification strategy, Na^+/Li^+ exchange in montmorillonite is coupled with the replacement of native interlayer water by dimethyl sulfoxide, thereby constructing a Lithium bis (trifluoromethanesulfonyl)-imide−dimethyl sulfoxide modified montmorillonite transport channel. Structural characterization and molecular dynamics simulations reveal that the negatively charged interlayer environment of Mnt, together with interlayer DMSO, enlarges the interlayer spacing, lowers the Li^+ migration barrier, and induces a weak-solvation-like transport state by suppressing $TFSI^-$ participation and reconstructing the local coordination of Li^+. As a result, DCCSE delivers an ionic conductivity of 2.1×10^{-4} S cm^{-1}, an activation energy of 0.48 eV, a Li^+ transference number of 0.64, and an electrochemical stability window of 4.5 V at 60 °C, together with significantly enhanced mechanical strength, thermal stability, and flame retardancy. Li|Li symmetric cells stably cycle for over 1700 h at 0.1 mA cm^{-2}, while LFP|DCCSE|Li full cells retain 94.1% of their capacity after 500 cycles at 0.5 C. This work proposes a new design concept for solid electrolytes based on the synergistic functional division of dual clays and confined-solvation regulation within minerals, providing a new design paradigm for constructing low-cost, highly safe, and mechanistically tunable solid-state lithium metal battery electrolytes from natural minerals.

Key words: Solid electrolyte, Clays, Confined solvation, Lithium metal batteries

EFFECT OF FLUORESCENCE ON THE COLOR PERCEPTION OF BANGKAJA YELLOW SAPPHIRE SAMPLES

Wiwat Wongkokua[1], Thanapong Lhuaamporn[2], Natthapong Monarumit[1], Phongsakorn Kajornboonsook[1], and Pornsawat Wathanakul[1]

1. Gem and Mineral Science Special Research Unit, Department of Physics and Department of Earth Sciences, Faculty of Science, Kasetsart University, Bangkok, Thailand
2. Gem and Jewelry Institute of Thailand (Public Organization)

Abstract Yellow sapphire is a variety of the mineral corundum (α-Al_2O_3) that is primarily composed of Al_2O_3 with iron (Fe^{3+}) and/or other impurities, depending, however, on their geological occurrences. The yellow color is caused by Fe^{3+} substituting for Al^{3+} in the corundum structure or by forming a yellow color center in combination with other elements such as Mg^{2+} or Be^{2+}. The absorption spectra of these two causes of yellow sapphires are clearly distinct. In addition, fluorescence from the impurities adds light to the transmittance spectrum, which can affect human eyes. However, the color measurement does not include fluorescence in the definition. In this work, we measure the color of yellow sapphire samples from Bangkaja, Thailand, which are hosted by basalt; hence, iron is responsible for their color. The transmittance measurements were made using monochromatic and polychromatic UV-Vis-NIR spectroscopy. The CIE 1931 standard observer matching function (2˚) and the spectral power distributions of illuminants D57, D65, and A were selected. The color indices with and without fluorescence are presented according to CIE $L^*a^*b^*$ and L^*C^*h. Trace elements and their concentrations are measured by X-ray fluorescence (XRF) to determine the cause of the color. The transmission spectra of the two UV-Vis-NIR spectrophotometers differ significantly, indicating that fluorescence is present in the polychromatic spectrum. The fluorescence can increase L^* and a^*, but reduce b^*, C^*, and h. However, the illuminance sources do not much influence the color indices, i.e., the color rendering is rather low among the different illuminants. Therefore, the fluorescence in Bangkaja yellow sapphire samples can influence the perceived yellow color.

Key words: UV-Vis-NIR, Polychromatic UV-Vis-NIR, CIE color indices, Yellow sapphire.

Acknowledgments The Gem and Jewelry Institute of Thailand (GIT), Department of Physics, and Department of Earth Sciences, Faculty of Science, Kasetsart University, and the Asian Institute of Gemological Sciences (AIGS) are thanked for the research facilities.

EFFECT OF KH550-FUNCTIONALIZED NANO-ACTIVE MAGNESIUM OXIDE ON THE PROPERTIES AND HYDRATION MECHANISM OF GYPSUM-BASED SELF-LEVELING MORTAR

Meirong Zong, Haozhe Ma

School of Urban Construction, Changzhou University, Changzhou 213164, Jiangsu, PR China

Abstract The surging demand for construction materials and the shortage of natural resources have created a sharp contradiction, urgently requiring sustainable pathways for waste resource utilization. Industrial by-product gypsum is generated in large quantities with few recycling routes, leading to massive accumulation. The development of gypsum-based self-leveling mortar (GSL) can rapidly promote the resource utilization of industrial by-product gypsum. This study investigates the effect of γ-aminopropyltriethoxysilane (KH550)-functionalized nano-activated MgO (KH-Mg) on the performance of GSL prepared from industrial by-product gypsum. First, the effects of adding 0.125%, 0.25%, 0.5%, 1%, and 2% nano-activated MgO on the fluidity, setting time, and mechanical properties of GSL were analyzed. Subsequently, the influence of the nanomaterial on mortar morphology, hydration characteristics, and hydration product crystal phases was thoroughly explored using XRD analysis, hydration heat analysis, thermogravimetric analysis, scanning electron microscopy, Fourier-transform infrared spectroscopy, and X-ray photoelectron spectroscopy. Finally, by comparison with ordinary GSL, the mechanism of action of KH550-functionalized nano-activated MgO on GSL was revealed.

The results show that KH550-modified nano-MgO exhibits good dispersion in the GSL slurry. With increasing KH-Mg content, both the fluidity and setting time of GSL show a decreasing trend. After the addition of KH-Mg, the mechanical properties of GSL first increase and then decrease, with the optimal performance observed at a KH-Mg content of 0.5%. At this content, the 28-day flexural and compressive strengths increase by 47.85% and 52.30%, respectively. When KH-Mg exceeds 1%, the strength of GSL decreases slightly, which may be attributed to microcracks induced by expansion stress due to excessive formation of $Mg(OH)_2$, as well as agglomeration of nanoparticles hindering hydration. The nucleation effect of KH-Mg promotes the formation of $C\hat{S}H_2$ and AFt, refines the crystals of hydration products, and enhances the phase transformation efficiency of the mortar. In addition, Mg^{2+} released from KH-Mg reacts with Al^{3+} and SO_4^{2-} in the GSL system to form layered double hydroxide (LDH) and a magnesium oxysulfate phase ($5Mg(OH)_2 \cdot MgSO_4 \cdot 7H_2O$, 5·1·7 phase), filling pores and strengthening the mortar skeleton. This study not only provides new insights for the strengthening of GSL but also offers theoretical data for the application of industrial by-product gypsum in construction materials, presenting a new pathway for the sustainable application of solid waste.

Key words: Industrial by-product gypsum, Self-leveling mortar, Nano-activated MgO, KH550 functionalization, Hydration mechanism.

FE^{3+} COMPETITIVE SUBSTITUTION OF TETRAHEDRAL SITES ON CRYSTAL GROWTH OF SAPONITE

Jie Yang [1,2], Bao Chen Guo [1,2], Chun Hui Zhou [1,2]

1. Research Group for Advanced Materials & Sustainable Catalysis (AMSC), State Key Laboratory of Green Chemical Synthesis and Conversion, College of Chemical Engineering, Zhejiang University of Technology, Hangzhou 310032, China.
2. Anhui International Exchange and Cooperation Base, Qing Yang Institute for Industrial Minerals, You Hua, Qing Yang, Chi Zhou 242804, China.

Abstract Saponite, a 2:1 trioctahedral clay mineral of the smectite group, exhibits isomorphous substitution in both tetrahedral and octahedral sites, which strongly influences its structural and geochemical properties. For example, status of different temperature of precursors will effect cation substitution mode in the octahedral and tetrahedral sites on saponite. However, the role of Fe^{3+} in competitive substitution within tetrahedral sites and its impact on crystal growth remains insufficiently understood. In this regard ,in this study, synthetic saponite was prepared using a semi-continuous flow reactor to investigate the substitution behavior of Fe^{3+} under controlled conditions. Nowadays, continues-flow chemistry has already used in the biocatalysis, photochemistry, pharmaceutical products synthesis and so on. Usual and advanced material like metal organic frameworks, layered double hydroxide, zeolites all can use continues-flow synthesis to get the production. In this study, synthetic saponite was prepared using a semi-continuous flow reactor to investigate the substitution behavior of Fe^{3+} under controlled conditions. A precursor system consisting of Si/Al gel (aged for 16 h) and Fe^{2+} and/or Mg^{2+} solutions was employed to simulate dynamic geochemical processes. The results reveal a competitive substitution relationship between Fe^{3+} and Al^{3+}, particularly in tetrahedral sites. This study affords mechanistic insights into Fe^{3+}-Al^{3+} competitive substitution and its critical role in controlling saponite crystal growth.

Key words: Synthetic saponite, Isomorphous substitution, Continuous flow synthesis

Acknowledgements The authors wish to acknowledge the financial support from the National Natural Science Foundation of China (42572045; W2433034; 22072136). This work was also supported by the Central Government Guided Local Science and Technology Development Fund Project (No. 2025ZY01113), and by the projects from Qing Yang Institute for Industrial Minerals (KYY-HX-20220336; KYY-HX-20170557).

GEM SCIENCE CHALLENGES: OXIDATION STATES OF COLOUR CAUSING ELEMENTS IN YELLOW, GREEN SAPPHIRES AND KYANITE

Natthapong Monarumit[1], Wiwat Wongkokua[1], Thanapong Lhuaamporn[2],Phongsakorn Kajornboonsook[1], and Pornsawat Wathanakul[1]

1. Gem and Mineral Science Special Research Unit, Department of Physics and Department of Earth Sciences, Faculty of Science, Kasetsart University, Bangkok, Thailand
2. Gem and Jewelry Institute of Thailand (Public Organization)

Abstract The research team at KU has carried out the in-dept research on oxidation states oftrace elements (Cr, Fe and Ti) in gem corundum varieties for over a decade using the XANES technique of Siam synchrotron facility at Synchrotron Light Research Institute (SLRI), Khorat, Thailand. The oxidation states of trace ele- ments in ruby and sapphires of yellow, blue as well as green varieties revealed as Cr (III), Fe (III) and Ti (IV) regardless their origins. We have used the band theory and the energy band model in explaining the causes of colours in gemstones including their fluorescence property. Most of the results are well fitted for both theoret- ical and experimental approaches, also confirmed by chemical analyses and other spectroscopic results such as UV-Vis-NIR and FTIR data. The XANES experiments on yellow and green sapphire samples from Bangkaja, Chanthaburi, Thailand also show Fe (III), and Fe (III) and Ti (IV) as their causes of colours, respec- tively. In the recent years the topics have been extended to other gemstone species and their varieties such as quartz (amethyst/citrine) and kyanite. Besides, kyanite samples with blue and white zones also show that Fe (III) and Ti (IV) are responsible for their blue component. The research would challenge gem scientists to explore more in depth in mineral science of gemstones and bring new results to discuss in our research com- munity as why this is different from the Fe^{2+}/Ti^{4+} IVCT concept.

Key words: Sapphires, Kyanite, Iron oxidation states, XANES

Acknowledgments SLRI, GIT, AIGS and Faculty of Science, Kasetsart University, Thailand are thankful for research facilities and funding.

HALLOYSITE-CONSTRAINED COPPER CATALYST UNDERGOES IN SITU RECONSTRUCTION FOR N_2O TO N_2 ELECTROREDUCTION

Meng Liu, Guocheng Lv, Libing Liao

School of Materials Science and Technology, China University of Geosciences (Beijing), 100083, China.

Abstract Nitrous oxide (N_2O) is a potent greenhouse gas with a high global warming potential. The electrocatalytic N_2O reduction reaction (N_2ORR) has emerged as a promising mitigation strategy, where copper (Cu)-based catalysts are considered a rational choice due to their biological relevance in natural N_2O reduction systems. However, the unavoidable and uncontrollable reconstruction of Cu-based catalysts during the electrocatalytic reduction process poses a significant challenge to maintaining their catalytic activity. Herein, we propose a strategy that synergistically integrates the confinement effect of halloysite nanotubes (HNTs) and the potential gradient between the inner Al-OH lumen and carbon-coated outer surface induced by the conductive carbon layer to regulate the reconstruction of Cu pre-catalysts. Our results demonstrate that under reductive potentials with alkali cation induction, well-dispersed Cu nanoparticles can be controllably generated on the HNT exterior surface without agglomeration, in contrast to non-confined commercial Cu nanoparticles. Furthermore, dynamic reconstruction evolution was observed across different electrochemical stages. Systematic electrochemical experiments revealed an optimal N_2 Faradaic efficiency (FE) of 96.3% and a yield rate of 9.8 mmol h^{-1} $mgmetal^{-1}$ at -0.6 V vs. RHE. Isotopic labeling experiments ($^{15}N_2O$) confirmed that the majority of N_2 products originated from the electrocatalytic reduction of N_2O, as evidenced by ^{15}N signal. Critically, the key Cu-N intermediate was experimentally and theoretically identified through in situ attenuated total reflection Fourier transform infrared spectroscopy (ATR-FTIR) and density functional theory (DFT) calculations, suggesting that the N-terminal adsorption configuration is energetically favored for N_2ORR. This work not only provides an effective approach to mitigate N_2O emissions but also establishes a novel strategy for achieving controllable reconstruction of Cu-based catalysts in electrocatalytic systems.

Key words: N_2ORR, Halloysite nanotubes, Reconstruction, Cu nanoparticles, Cu-N intermediate

HALLOYSITE-REINFORCED NANOCOMPOSITE HYDROGEL AS MULTIFUNCTIONAL INJECTABLE WOUND DRESSING

Li Wen Wong[1,2], Joash Ban Lee Tan[2], Pooria Pasbakhsh[3,4]

1. School of Environmental Science and Engineering, Guangdong University of Technology, China
2. School of Science, Monash University Malaysia, Malaysia
3. School of Engineering, Monash University Malaysia, Malaysia
4. Department of Infrastructure Engineering, The University of Melbourne, Australia

Abstract Nanocomposite hydrogels, formed by crosslinked polymer networks reinforced with clay minerals, offer versatile platforms for biomedical applications. This study reports the fabrication of an injectable nanocomposite hydrogel incorporating halloysite nanotubes (Hal), a naturally occurring aluminosilicate clay mineral, into a polymer matrix of oxidized bacterial cellulose and gelatin. Hal, an abundant and low-cost mineral resource, serves multiple complementary roles within the hydrogel system: (1) facilitating the sol-gel transition required for injectability, (2) acting as a sustained-release carrier for antimicrobial drugs, and (3) leveraging its inherent hemostatic properties to accelerate clot formation at wound sites. The resulting Hal-reinforced nanocomposite hydrogel enables targeted, sustained antibiotic delivery to infection sites while simultaneously promoting wound recovery through enhanced hemostasis. Its injectable nature allows for minimally invasive administration, conforming to irregular wound geometries while providing structural support, combating bacterial infection, and controlling bleeding, all in a single formulation. This work demonstrates the utilization of halloysite for biomedical applications, offering a multifunctional platform integrating infection management, bleeding control, and wound dressing tailored for diverse wound types.

Key words: Clay minerals, Drug carrier, Halloysite nanotubes, Hemostasis, Polymer-clay nanocomposites

HARNESSING THE DUAL-CHARGE CHARACTERISTICS OF HALLOYSITE NANOTUBES FOR HIGH-PERFORMANCE COMPOSITE POLYMER ELECTROLYTES IN LITHIUM-ION BATTERIES

Ke Wang, Guocheng Lv, and Libing Liao

School of Materials Science and Technology, China University of Geosciences (Beijing), China

Abstract Naturally occurring halloysite nanotubes (HNTs), a clay mineral characterized by a unique dual-charge architecture, offer a promising strategy for enhancing the performance of composite polymer electrolyte (CPE). In this work, HNTs are introduced as a low-cost, functional filler to simultaneously address two key limitations of poly(vinylidene fluoride-co-hexafluoropropylene) (PVDF-HFP)-based CPE: low ionic conductivity and inadequate lithium-ion transference number. The negatively charged outer surface of HNTs facilitates Li^+ transport, while the positively charged inner lumen confines anions such as $TFSI^-$. Controlled acid etching (6 M HCl, 12 h) further optimizes this structure by removing surface impurities and enlarging the lumen, thereby enhancing both charge-directed ion transport pathways. The resulting HNT-modified CPE achieves a high ionic conductivity of 6.1×10^{-4} $S \cdot cm^{-1}$ and a Li^+ transference number of 0.73. When assembled into Li||CPE||$LiFePO_4$ cells, the electrolyte enables stable cycling over 300 cycles at 0.2C, retains 119.2 $mAh \cdot g^{-1}$ at 2C, and delivers 85.7 $mAh \cdot g^{-1}$ even at 5C, demonstrating excellent cycling stability and rate capability. This study reveals the potential of mineral-derived nanomaterials, with their inherent structural and physicochemical properties, to serve as key functional components in high-performance batteries.

Key words: halloysite nanotubes, acid-etching, composite polymer electrolyte, ionic conductivity, lithium transference number

HOW HYDRATION AND SALINITY CONTROL ILLITE WETTABILITY: PERSPECTIVES FROM NANOMECHANICAL FORCE MEASUREMENTS

Lijuan Wang[1], Zhengdong Lei[1*], Yingfeng Peng[1], Yishan Liu[1], Xiaomei Zhou1, Nijun Qi[2, 3], Jiayao Zhang[2,3]

1. PetroChina Research Institute of Petroleum Exploration & Developent, Beijing, 100083, China;
2. School of Engineering Science, University of Chinese Academy of Sciences, Beijing 100049, China;
3. Institute of Porous Flow and Fluid Mechanics, Chinese Academy of Sciences, Langfang 065007, China;

Abstract Illite wettability is a critical factor controlling shale oil occurrence and migration in clay-rich reservoirs, particularly in the Gulong shale where illite constitutes over 60% of the clay fraction. Large-scale hydraulic fracturing, which is essential for shale oil development, inevitably introduces aqueous phases into the reservoir and induces illite hydration. Consequently, hydration-induced wettability alteration directly controls the occurrence and mobility of shale oil, and is therefore critical for the efficient development of such reservoirs. However, the mechanisms by which hydration and salinity regulate wettability evolution and water-wet/oil-wet transitions on illite surfaces remain poorly understood. Therefore, clarifying the effects of hydration and salinity on illite wettability is of great significance for improving shale oil recovery.

In this study, We employed with nanomechanical resolution (±5 pN) to quantify illite wettability under controlled hydration and salinity conditions. Water- and oil-functionalized AFM probes were used to measure adhesion forces between liquids and illite surfaces at the nanoscale, where adhesion force was used as a direct indicator of wettability strength. Six hydration conditions are designed, which can be categorized into three groups: (i) pre-hydration (pristine state); (ii) single-step hydration using deionized water, 5%, 14%, and 20% NaCl brine; and (iii) sequential hydration involving low-salinity hydration (5% NaCl) followed by high-salinity rehydration (20% NaCl). In addition, Surface morphology and charge distribution were characterized to elucidate underlying mechanisms.

The results show that pristine illite exhibits neutral to weakly oil-wet characteristics, with oil adhesion generally higher than water adhesion. Significant fluctuations in adhesion forces indicate strong local wettability heterogeneity caused by the exposure of different crystal faces. After hydration with deionized water, illite surfaces become predominantly water-wet due to enhanced hydrogen bonding interactions and the exposure of hydrophilic active sites. Salinity exerts a significant control on wettability evolution. Low-salinity brine (5% NaCl) greatly increases water adhesion and decreases oil adhesion, resulting in strongly water-wet behavior, whereas medium- to high-salinity brines (14% and 20% NaCl) promote oil-wet characteristics. Sequential hydration

experiments further demonstrate that high-salinity brine can reverse the water-wet state induced by low-salinity hydration, restoring illite surfaces to an oil-wet condition and highlighting the reversible nature of wettability evolution. The wettability transitions observed in this study are mainly controlled by salinity-dependent electrostatic mechanisms. Under low-salinity conditions, negative charge spillover from illite basal planes to edge surfaces enhances water–surface interactions and weakens oil adsorption. In contrast, under high-salinity conditions, charge screening and electrical double-layer compression promote oil adsorption on illite surfaces. These findings indicate that salinity is a key factor controlling illite wettability evolution. This study provides nanoscale experimental evidence for understanding fluid–clay mineral interactions in shale reservoirs and offers important implications for optimizing fracturing-fluid systems and enhancing shale oil recovery in continental shale reservoirs.

Key words: Illite Wettability, Nanomechanics, Salinity Effect, Shale Oil Recovery, Atomic Force Microscopy

IRRADIATION EXPERIMENTS ON COLORLESS AND PINK SAPPHIRES

Thanapong Lhuaamporn[1], Montira Seneewong Na Ayutthaya[1], Sirinapa Saengdech[1], Kannatee Fueangaksorn[1], Chanikarn Seangrit[1], Nongnuch Jangsawang[2] and Karnwalee Pangza[2]

1. The Gem and Jewelry Institute of Thailand (Public Organization), Thailand
2. Thailand Institute of Nuclear Technology (Public Organization), Thailand

Abstract Gamma irradiation has been used to improve the color of gem corundum for many years, but the effects of trace elements and the stability of irradiation-induced color are still not fully understood. In our first study, we have investigated natural colorless sapphires from Tanzania, Sri Lanka, and Madagascar in order to understand how gamma irradiation could produce color hue in colorless corundum containing different iron contents from various sources. Although all samples could develope yellow related color centers after irradiation, their visible yellow hue responses were different. Colorless sapphires from Sri Lanka and Madagascar, which contain relatively low to moderate Fe, showed stronger yellow coloration after irradiation, whereas many Tanzanian samples with higher Fe content exhibited only weak visible color changes. These results indicate that iron could suppress the occurrence of yellow color centers after irradiation, thus the presence of high iron concentration in the stone plays an important role in controlling the appearence of radiation-induced color. Our color stability test also revealed that those radiated yellow colors were unstable and faded after exposure using LED by Gemstone Color Stability Testing Carbinet, developed by GIT for 3 hours.

Based on the above results, our study was extended to natural unheated purplish-pink sapphires from Madagascar, which are widely traded in Thailand. Every year, large numbers of Madagascar sapphires are submitted to the Gem and Jewelry Institute of Thailand (GIT) for gem identification. However, fine natural unheated pink sapphires are relatively rare, whereas purplish-pink sapphires are much more common. In recent years, the prices of these purplish-pink stones have increased significantly, although they are still considerably less valuable than fine pink sapphires. GIT has also received information from the gem trade that some foreign traders may use the irradiation technique to improve the color of Madagascar sapphires. Therefore, this study is intended to investigate whether gamma irradiation could modify the color of natural unheated purplish pink Madagascar sapphires and whether the induced color remains stable under light exposure.

Six natural unheated purplish-pink Madagascar sapphires having low to moderate iron contents were irradiated with gamma rays at a dose of 500 kGy. Color changes were evaluated by visual observation, CIE L*a*b* color measurements, and UV-Vis absorption spectroscopy. Color stability testing was investigated using the Gemstone Color Stability Testing Carbinet, developed by GIT, after 60 and 180 minutes of light exposure.

Colors of all samples apparently changed from purplish pink before irradiation to orange-pink or yellowish orange after irradiation. The UV-Vis spectroscopy showed a marked increase in the absorption spectra due to the presence of the color center after irradiation, while the Cr^{3+} absorption bands still remained essentially the same. These spectral changes indicate that gamma irradiation could generate an additional radiation induced yellow color centers superimposed on the original pink Cr-related color, thus produce orange hue after irradiation.

The CIE L*a*b* results were consistent with the visual observations. Before irradiation, all samples showed negative b* values, while after irradiation the b* values shifted to positive values, confirming the formation of a strong yellow component. During the gemstone color stability testing, the b* values gradually decreased with increasing light exposure time, corresponding to the progressive reduction of the yellow component. Although the irradiation-induced yellow color faded during the stability test, the final color appearance did not completely return to their original purplish-pink hues. Instead, the remaining color was generally more pink indicating that irradiation could change the purple overtone of the stones to some degree.

The results from our earlier study on the colorless sapphires from Tanzania, Sri Lanka, and Madagascar, together with the natural purplish pink Madagascar sapphires have demonstrated that gamma irradiation could produce an unstable yellow related color center, and that the final color appearance strongly depends on both the iron content and the original body color of the stones. These findings improve the understanding of irradiation-induced color modification in gem corundum and provide additional evidence for evaluating gemstones currently circulating in the gem trade. The increasing availability of pink sapphires from Madagascar in the gemstone market, together with the significant increase in the value of natural unheated purplish-pink sapphires, highlights the importance of understanding possible color modification by irradiation. Nevertheless, further studies are still required to establish reliable identification criteria for irradiation treated corundum, because there is currently no validated laboratory method capable of conclusively identifying previously irradiated corundum after the radiation-induced color centers have faded.

Key words: Irradiation, Color center, Trace elements, Color stability

Acknowledgements The authors would like to thank the Gem and Jewelry Institute of Thailand (Public Organization) for providing laboratory facilities and would like to express their sincere gratitude to Dr. Visut Pisutha-Arnond and Mrs. Wilawan Atichat, GIT Advisors, for their valuable guidance and support throughout this research. We also thank to Amorngems for the unheated madagascar samples.

MINERAL CONTROL OF EXTRACELLULAR ENZYME ACTIVITY AT BIOGEOCHEMICAL INTERFACES

Yizhi Sheng, Zijing Rong, and Hailiang Dong

Center for Geomicrobiology and Biogeochemistry Research, State Key Laboratory of Geomicrobiology and Environmental Changes, China University of Geosciences, Beijing 100083

Abstract Extracellular enzymes catalyze the rate-limiting steps of organic carbon decomposition and therefore play a central role in regulating carbon persistence in soils and sediments. Although enzyme activities have been increasingly incorporated into predictive biogeochemical models, their catalytic efficiency, kinetic behavior, and functional lifespan vary widely across natural environments. Mineral surfaces are ubiquitous reactive interfaces that can adsorb extracellular enzymes, alter enzyme conformation, and modify substrate accessibility. However, the mechanisms by which minerals regulate enzyme activity remain insufficiently understood, particularly under redox-fluctuating conditions where Fe-bearing minerals can generate reactive oxygen species during oxygenation.

Here, we synthesize our recent studies on hydrolytic and oxidative enzymes to examine how mineral adsorption and redox-driven ROS production jointly regulate extracellular enzyme activity and longevity. For hydrolytic enzymes, enzyme activity was primarily associated with capacity-related mineral properties, including specific surface area and the surface-area-normalized amount of enzyme adsorption, rather than functional surface properties such as surface charge. Mineral adsorption generally reduced initial enzyme activity by inducing conformational changes and limiting substrate accessibility, but under anoxic conditions it prolonged enzyme functional lifespan. In contrast, under oxic conditions, oxygenation of reduced Fe-bearing minerals generated abundant hydroxyl radicals, with •OH production positively correlated with the extent of structural Fe(II) oxidation. These radicals induced enzyme conformational disruption and structural decomposition, thereby decreasing activity and shortening enzyme lifespan.

Our work on laccase, a model oxidase, further demonstrates that the effect of hydroxyl radicals on enzyme activity depends strongly on their spatial origin. Homogeneous •OH generated from soluble Fe(II) oxidation enhanced laccase activity, likely by promoting exposure of the copper-containing active site without causing substantial oxidative damage. In contrast, heterogeneous •OH produced on Fe-bearing clay mineral surfaces failed to stimulate laccase activity and instead caused pronounced inhibition by degrading histidine residues that coordinate active-site copper and oxidizing critical enzyme functional groups. These findings reveal that mineral surfaces do not act as passive enzyme carriers, but as dynamic biogeochemical interfaces where adsorption-induced protection and ROS-induced inactivation

compete to determine the active extracellular enzyme pool.

Together, these results disclose a previously underappreciated mechanism of mineral control over extracellular enzyme activity. They suggest that the fate of extracellular enzymes in soils and sediments depends on mineral surface area, adsorption configuration, Fe redox state, ROS production, and oxygen availability. Incorporating these mineral-mediated mechanisms into biogeochemical models will improve predictions of organic carbon decomposition and persistence in redox-oscillating environments.

Key words: Biological nitrogen fixation, Molybdenum paradox, Molybdenite, Pyrite, Great Oxidation event

MINERAL-SPECIFIC ELECTRON TRANSFER AND MICROBIAL COMMUNITY SHIFTS: HOW CLAY MINERALS MEDIATE AZO DYE BIODECOLORIZATION

Ying Zhang[1], Qi-Zhi Yao[2], Gen-Tao Zhou[1*]

1. State Key Laboratory of Lithospheric and Environmental Coevolution/School of Earth and Space Sciences, University of Science and Technology of China, Hefei 230026, China
2. School of Chemistry and Materials Science, University of Science and Technology of China, Hefei 230026, China

Abstract Azo dyes are widely used and frequently discharged into aquatic environments, creating serious ecological and health hazards. Anaerobic-aerobic biological treatment is considered one of the most cost-effective strategies for azo dye mineralization. However, its efficiency is often limited by the extracellular electron transfer (EET) step. To address this, various redox mediators (e.g., quinones) and functional materials (e.g., iron oxides) have been employed to facilitate EET. Even so, the application remains largely limited by high costs or potential environmental risks. In contrast, naturally abundant clay minerals offer an alternative class of reactive biogeochemical interfaces capable of supporting microbial colonization, buffering local pH, releasing essential nutrients, and in some cases, enhancing electron transfer through the redox cycling of structural Fe. Netherlands, whether and how different clay minerals exert mineral-specific control over electron transfer processes is still poorly understood. Against this backdrop, four common clay minerals montmorillonite, illite, kaolinite, and chlorite were selected to investigate their individual roles in the biodecolorization of Reactive Red X-3B (RRX-3B), a azo dye chosen for its extensive use in dyeing cellulose and blended fabrics, accounting for over 60% of global reactive dye consumption. Batch experiments revealed that supplementation with kaolinite, illite, or chlorite increased the azo dye decolorization rate by 1.6-, 1.9-, and 1.9-fold, respectively. In contrast, montmorillonite suppressed decolorization by 96%, an effect attributed to swelling-induced restrictions on microbial mobility and substrate accessibility. Among the clays that promoted decolorization, illite and chlorite significantly accelerated the porcess by strengthening electron transfer through multiple pathways. Illite promoted the formation of conductive microbial networks via pili production, thereby boosting EET. Chlorite enhanced the expression of ferredoxin-like electron carriers, facilitating redox-mediated electron transport. Both minerals stimulated cytochrome *c*- and flavins-mediated electron transfer, thereby modulating ATP generation and improving energy metabolism. Community profiling further revealed the enrichment of electroactive bacterial taxa, consistent with elevated EET at the community level. These findings demonstrated that clay minerals with specific structural and chemical properties can act as effective biogeochemical catalysts for azo dye biodecolorization, highlighting the broad application potential of mineral-microbe interactions in

anaerobic wastewater treatment.

Key words: Clay minerals, Azo dye, Electron transfer, Microbial metabolism, Microbial community

Acknowledgements This work was partially supported by the National Natural Science Foundation of China (Nos. 42430201 and 42472059).

MINERALOGICAL EVOLUTION AND SUSTAINABILITY OF LOW-CARBON 3D PRINTED MORTAR INCORPORATING HEMIHYDRATE PHOSPHOGYPSUM

Yuting Sun, Meirong Zong, Qifeng Lyu

School of Urban Construction, Changzhou University, Changzhou 213164, Jiangsu, PR China

Abstract The sustainable utilization of mineral based industrial by products is of great significance for reducing cement consumption and developing low carbon construction materials. This study investigates the use of thermally activated hemihydrate phosphogypsum (HPG) as a partial replacement for ordinary Portland cement in extrusion based 3D printed mortar. Seven mixtures with HPG replacement levels of 0%, 10%, 20%, 30%, 40%, 50%, and 60% were prepared to clarify the effects of HPG on printability, mechanical performance, water resistance, mineral phase evolution, pore structure, and carbon emission efficiency. The results show that HPG significantly affects the fresh properties of 3D printed mortar. As the HPG replacement level increased from 0% to 60%, the initial setting time decreased from 345 min to 163 min, while the final setting time shortened from 400 min to 188 min. The accelerated structural build up improved layer stacking stability at moderate HPG contents. The buildability index tanθ increased from 4.49 for the reference mixture to a maximum of 11.94 at 30% HPG, and then declined at higher dosages because of excessive flowability loss and a shortened printing window. The mechanical response of the printed mortar was strongly dependent on HPG content and loading direction. A low HPG dosage of 10% slightly improved early age strength, with the 3 d compressive strength in the Z direction increasing from 12.7 MPa to 14.1 MPa and the flexural strength in the Y direction increasing from 5.6 MPa to 5.8 MPa. However, excessive HPG incorporation led to a marked reduction in later age performance. Compared with the reference mixture, the 60% HPG mixture exhibited decreases of 59.1%, 58.7%, and 57.7% in 28 d compressive strength along the X, Y, and Z directions, respectively. The 28 d flexural strength decreased by 35.0% in the Y direction and 36.8% in the Z direction, while the interlayer splitting tensile strength declined from 2.65 MPa to 1.85 MPa, corresponding to a reduction of 30.2%. Water resistance also deteriorated progressively, with water absorption increasing from 7.9% to 11.6% and the softening coefficient decreasing from 0.86 to 0.48. XRD and TG DTG analyses indicate that HPG increased gypsum related crystalline phases and supplied sulfate for ettringite formation. SEM, EDS, and MIP results further show that high HPG contents weakened matrix continuity, enhanced the heterogeneous enrichment of sulfate bearing phases, and caused pronounced pore coarsening. As the HPG content increased from 0% to 60%, porosity rose from 21.27% to 27.64%, while the median pore diameter increased from 388.63 nm to 2141.66 nm. These changes explain the deterioration in long term strength, interlayer bonding, and water stability. Carbon emission assessment demonstrates

that HPG incorporation can improve the environmental performance of 3D printed mortar by reducing cement demand. The lowest carbon emission intensity index, 24.17 kg/(m^3·MPa), was achieved at 30% HPG. Overall, a 30% HPG replacement level provides the best balance among printability, microstructural stability, engineering performance, and low carbon benefit. This study highlights the potential of hemihydrate phosphogypsum as a sustainable mineral resource for advanced construction materials and provides a basis for the environmentally responsible design of low carbon 3D printed cementitious systems.

Key words: Hemihydrate phosphogypsum, 3D printed mortar, Mineralogical evolution, Low-carbon construction materials

MINERALOGICAL STUDY OF KENYAN RUBY BY FIB-KTD CHARACTERIZATION: IMPLICATIONS FOR GENESIS AND CRYSTAL ORIENTATION OF EXSOLUTED RUTILE INCLUSIONS

Jinglin Tian, Tao Chen*

Gemmological Institute, China University of Geosciences, Wuhan, China

Abstract Asterism effect (star effect) of gem-quality corundum often arises from light reflection of the oriented mineral inclusions within the crystal. Beyond its special gemmological appearance, the characteristic of the inclusions and trace element signatures of corundum can serve as indicators of the host rock's petrogenetic history. This study investigates the star rubies from John Saul Mine (Mangari area, Kenya), which occurs within the contacts of mafic-ultramafic intrusions and metasediments associated with the Pan-African Orogeny. These cabochon samples show rosy-violet, semi-trasparent appearances with significant fracturing. Distinct 6-ray stars can be observed in some samples, generated by three sets of oriented inclusions inside. All the three-directions oriented crystals distributed in $(0001)_{crd}$ basal plane of corundum host, intersecting at 120° angles. Determined by Raman Spectum and Scanning Electron Microscope (SEM), all the oriented inclusions are rutile (TiO_2), predominantly exhibiting an acicular (needle-like) morphology. The needle-like crystals measure 5~10 μm in length and 0.5~1 μm in width, with an interparticle spacing of 5~10 μm. Chemical analysis of the host rubies using X-Ray Flourescence (XRF) and LA-ICP-MS reveals a trace element profile defined by high Cr and low Fe content, consistent with previous regional literature. Areas exhibiting astrerism show obvious higher Ti concentration compared to non-asterism area in the host. Foil samples with both needle-like rutile and corundum host are prepared using Focused Ion Beam (FIB), and the Crystallographic Orientation Relationship (COR) of corundum and rutile is determined by Transmission Kikuchi Diffraction (TKD). The topotaxial relationship between corundum and rutile needdles established as $(0001)_{crd}$ // $\{100\}_{rt}$. This research applys FIB-TKD techniques to study microscale oriented rutile inclusions in natural corundum, thereby providing a new model for exsolution lamellae research and for understanding the thermal evolution of the Pan-African Orogeny.

Key words: ruby, corundum, exsolution, oriented inclusions, rutile

MINERALOGY OF WEATHERING FORMS OF A STONE COLUMN EXPOSED IN A POLLUTED URBAN ENVIRONMENT, AN EXAMPLE FROM BUDAPEST

Ákos Török*, Annamária Kis,

Department of Engineering Geology and Geotechnics, Budapest University of Technology and Economics, Hungary, *corresponding: torok.akos@emk.bme.hu

Abstract Urban air pollution often causes severe mineralogical changes in built structures. Limestone is one of the most sensitive lithotypes that shows various forms of weathering features in urban environments, including weathering crusts, dissolution features, and salt crystallization phenomena. In this paper, a 36 m high Corinthian-style stone column that forms part of the Millennium Monument of Budapest (Hungary) is studied. The stone column consists of half-ring-shaped limestone segments (drums) made of travertine. At the top of the column, a large rectangular stone block formed the base of a bronze statue. The stone column was erected in 1901, and it has been exposed to acid deposits and extreme weather conditions for more than 120 years. The current research provides an overview of the mineralogical changes of these freshwater limestone elements and provides some hints on the dissolution and precipitation processes of secondary minerals in the urban environment. Small samples were collected for laboratory analyses, and oriented samples were taken representing the north, east, south, and west directions, with different exposure to sun and precipitation, representing different microclimates. Textural analyses of samples were made by using optical microscopy, SEM-BSE, while mineralogical composition and elemental analyses were performed using XRF and thermogravimetric analyses. The travertine shows various weathering forms such as black crusts, dissolution features, and green staining of the stone surface from dissolved bronze. The composition of weathering crusts differs slightly, representing various orientations; wind and rain exposed parts or sheltered ones. The main secondary mineral is gypsum that prevails in black crusts. Gypsum crystals entrap soot particles and also small amounts of wind-blown fine silt-sized particles such as quartz or dolomite. The study helps in the preservation of the historic site, providing data for the restoration, describing mineralogical changes and decay mechanisms.

Keywords: travertine, mineralogical composition, air pollution, exposure, gypsum

MULTI-SCALE AMMONIUM SORPTION IN GLAUCONITE: EXPERIMENTAL AND COMPUTATIONAL INSIGHTS FROM GLOBULAR MORPHOLOGY TO INTERLAYER SITES

Maxim Rudmin[1], Ivan Khitrin[1], Evgeny Tararushkin[2]

1. Division for Geology, Tomsk Polytechnic University, Tomsk, Russia
2. International Laboratory for Supercomputer Atomistic Modelling and Multi-scale Analysis, HSE University, Moscow, Russia

Abstract Glauconite is a potassium- and iron-bearing dioctahedral 2:1 phyllosilicate that is widely distributed in marine sedimentary environments. The mineral commonly occurs as globular grains with a complex internal morphology. This morphology forms a heterogeneous system of sorption domains. Because of these properties, glauconite is increasingly considered a promising natural material for environmentally oriented mineral technologies. At the same time, the mechanisms underlying ammonium retention at different structural levels of the mineral remain poorly understood.

In this study, ammonium sorption in glauconite is considered as a multi-scale process. Experimental investigations include several morphological forms of the mineral. Natural glauconite globules possess a complex pore system that includes macro-, meso-, and micropores. Nanoporous domains are also present and are mainly represented by interlayer spaces within the crystal structure. These structural elements control both sorption and diffusion of solutions within the grains. Mechanochemical multistage treatment of the initial mineral progressively disrupts and transforms the globular structure into highly dispersed material. As a result, thin platy aggregates and individual glauconite nanosheets are produced. These structures represent the highest degree of mineral dispersion. They create an extended reactive surface and can be applied as mineral suspensions in emerging agricultural technologies. Morphological and structural-chemical features of different glauconite morphologies and glauconite nanocompositeswere studied using a set of analytical methods, including scanning electron microscopy with energy-dispersive analysis, transmission electron microscopy with selected area electron diffraction, X-ray diffraction, infrared spectroscopy, X-ray photoelectron spectroscopy, thermogravimetric and differential thermal analysis with mass detection, X-ray fluorescence analysis, inductively coupled plasma mass spectrometry, and BET surface area measurements.

Laboratory sorption experiments and molecular dynamics simulations were carried out on finely dispersed glauconite. The modelling results clarify the mechanisms of ammonium interaction with the mineral surface. Ammonium sorption occurs through a system of three coordination modes. Two of them correspond to inner-sphere coordination. One mechanism represents outer-sphere coordination. This three-level system of interactions is sensitive to solution concentration. A gradual

increase in ammonium nitrate concentration leads to a reorganization of coordination states and redistribution of ammonium between sorption sites. Nitrate ions show only outer-sphere interaction with the mineral surface. Molecular dynamics simulations also reveal the role of hydrogen bonding between ammonium ions, water molecules, and the glauconite surface. The modelling provides estimates of self-diffusion coefficients and orientational relaxation of ammonium in the interfacial water layer, which reflect changes in mobility and hydration structure near the mineral surface.

The results demonstrate that ammonium sorption in glauconite is controlled by processes operating at several structural levels. Globular morphology governs the distribution of pore space and diffusion of solutions. Finely dispersed particles and nnanosheetsprovide highly reactive surfaces. Interlayer domains act as stable sorption sites for ammonium. Together, these factors define the multi-scale interaction between aqueous solutions and the layered silicate structure of glauconite. These characteristics should be considered when designing mineral materials containing glauconite for various purposes, including as sorbents and controlled-release fertilizers.

Key words: Glauconite, Ammonium sorption, Phyllosilicates, Molecular dynamic simulation, Mineral morphology

Acknowledgements This research was financially supported by the Russian Science Foundation (grant 22-77-10002-P).

NATURAL HALLOYSITE NANOTUBES ON FUNCTIONAL SEPARATORS FOR LITHIUM-ION BATTERIES

Xiu Yun CHUAN, Qin Ting Deng

Key Laboratory of Orogenic Belts and Crustal Evolution (MOE), School of Earth and Space Sciences, Peking University, Beijing 100871; CHINA)

Abstract Nowadays, commercial polyolefin separators such as polyethylene (PE), polypropylene (PP) and their compounds are commonly used in LIBs owing to their excellent mechanical strength, good elec-trochemical stability and reasonable cost. However, their poor thermal stability causes separators to shrink easily at higher temperatures, which causes explosion accidents. HNTs was coated them on both sides of the PP separator, their physical and electrochemical properties of separators for LIBs was investigated. The cells assembled with a PP/HNTs composite separator deliver discharge capacities of 113.8 mA h g−1 (3 C) higher than PP of 92.3 mA h g−1.with good decreased thermal properties and high ionic conductivity. Natural mineral halloysite nanotubes can significantly improve the properties of PP/HNT composite separators for application in lithium-ion batteries.

Key words: Halloysite, nanotubes, separators, lithium-ion batteries.

NATURAL ROCK ASPHALT-DERIVED HIERARCHICAL POROUS CARBON FOR EFFICIENT REMOVAL OF TETRACYCLINE

Rui Cao[12], Shiyong Sun[13], Ke Wang[13], Jin Liu[1], Lin Gong[1], Xingyun Yang[1], Sen Lin[13]

1. Key Laboratory of Solid Waste Treatment and Resource Recycle of Ministry of Education, School of Environment and Resource, Southwest University of Science and Technology, China
2. School of Resources and Environment, Xichang University, China
3. Key Laboratory of Non-metallic Mineral Geology and Utilization in Sichuan Provincial Higher Education Institutions, Southwest University of Science and Technology, China

Abstract Natural rock asphalt (RA)—a globally scarce mineral resource with exceptional geological value (e.g, Longmenshan region from southwestern China)—serves as an ideal, eco-friendly carbon precursor due to its high carbon content (>80 wt%), chemical stability, and intrinsic N/S heteroatoms. Yet, prior studies underutilized its potential, reporting limited surface areas (SSA ≤ 1735 m^2/g) and overlooking self-doping advantages. Here, we address these gaps by developing a one-step carbonization-activation strategy to convert RA into N/S self-doped hierarchical porous carbon (RAPC) with breakthrough properties: (1) Ultrahigh SSA (3269 m^2/g) and microporosity (>68%), rivaling petroleum/coal-tar-derived carbons, (2) Exceptional adsorption capacity (1265 mg/g) of tetracycline (TC, a top-priority antibiotic worthy of immediate attention), outperforming most reported carbon adsorbents for this priority antibiotic via enhanced surface interactions, and (3) Inherent N/S self-doping (surface concentrations: N 3.63%, S 2.46%, O 6.71%), eliminating external dopants and leveraging RA's natural composition for tailored surface chemistry.

This work leverages RA's intrinsic heteroatom composition for synthesizing N/S self-doped hierarchical porous carbon via an established carbonization-activation approach - uniquely avoiding external dopants. We systematically correlate activation parameters (temperature/time/softening process) with pore structure evolution and surface functionality, enabling precise microstructure control. Critically, interfacial mechanisms (Freundlich isotherms, pseudo-second-order kinetics) and advanced surface characterization (XPS, FTIR, BET, TEM) reveal chemisorption-driven multilayered adsorption governed by pore filling, π-π interactions, hydrogen bonding, and electrostatic effects at the solid-liquid interface, where mesopores accelerate kinetics while SSA dictates equilibrium capacity.

This work presents an natural mineral derived porous carbon adsorbent combining ultrahigh SSA, abundant micro pores, and high adsorption capacity synthesized through a relatively simple process, and advances the high-value utilization of RA and presents.

Key words: Rock asphalt, Hierarchical porous carbon, N/S Self-Doped, Adsorption tetracycline

Acknowledgements This work was supported by the National Natural Science Foundation of China (NSFC, grant numbers 42061134018), Sichuan Provincial International Science and Technology Innovation Cooperation Project (2024YFHZ0262).

NEW DATA ON THE CRYSTAL STRUCTURES, STOICHIOMETRY, AND MODULARITY OF THE PALYGORSKITE-SEPIOLITE POLYSOMATIC SERIES

Sergey M. Aksenov[1], Hao Liu[2], Libing Liao[2]

1. FRC Kola Science Centre RAS, Russia
2. China University of Geosciences (Beijing), China

Abstract Compounds containing *TOT* modules exhibit a wide diversity of crystal structures. Among them, the palygorskite-sepiolite polysomatic series (or the palysepiole family) stands out, for which a large number of different structural representatives are known. The basis of their crystal structures is formed by tetrahedral layers with a 6^3 topology, similar to those in the structures of related phyllosilicates. Due to the different orientation of pyroxene chains that form these tetrahedral layers, all representatives of the polysomatic series, which includes structures of the palygorskite, sepiolite and kalifersite types, are formed. Adjacent tetrahedral layers are linked by ribbons of edge-sharing $M\varphi_6$ octahedra, which are cut-outs from an octahedral brucite layer, forming a heteropolyhedral framework with a system of wide channels running parallel to the *TOT* modules. The width of the channels directly depends on the width of the *TOT* modules. These structural features determine the diversity of physical and chemical properties of the representatives of the palygorskite-sepiolite polysomatic series.

According to the scheme for joining one-dimensionally extended *TOT* modules proposed by T. Zoltai, the crystal structures of known representatives can be written in the following idealized form:

- R–0–R–3/4 – for palygorskite;
- R–0–R–0–R–3/4 – for sepiolite;
- R–0–R–3/4–R–0–R–0–R–3/4 – for kalifersite.

By analogy with heterophyllosilicates, for representatives of the palygorskite-sepiolite polysomatic series one can derive a so-called “structure-generating function”, proposed by F.C. Hawthorne, which will describe the stoichiometry of all known representatives, as well as potentially possible structures and hybrid analogues. Since adjacent one-dimensionally extended *TOT* modules are linked only through the oxygens of tetrahedra, the octahedral chains or wide octahedral ribbons will be characterized by the presence of external unshared vertices. With this in mind, the joining of TOT modules to form a tetrahedral layer leads to the formation of structures that can be described by the following general formula derived

by S.M. Aksenov with colleagues:

$$S_n = X_i\{M_{(3n-3)}\Psi_{2(n-1)}(\widetilde{M}_{(2-k)}\emptyset_{2(2-k)})(\mathrm{Si}_{2n}\mathrm{O}_{5n})_2\}, \quad (1)$$

where *M* are the octahedral positions of the octahedral *O*-ribbon, and Ψ are the anionic ligands; $\widetilde{M}$ are the 'outer' octahedra of the *O*-ribbon, and $\emptyset$ are the 'dangling' anionic ligands coordinating the 'outer' octahedra; X_i are additional cations, anions, anionic groups, and water molecules that are located in the large channels. The value of the *k* coefficient controls the number of 'outer' $\widetilde{M}$ octahedra of the *O*-ribbon.

In the case where the crystal structure contains several types of *TOT* modules (as, for example, in the structure of kalifersite), then $n = a + b$, and formula (1) takes the form:

$$S_{a+b} = X_i\{M_{(3a-3)}\Psi_{2(a-1)}(\widetilde{M}_{(2-k)}\emptyset_{2(2-k)})(\mathrm{Si}_{2n}\mathrm{O}_{5n})_2\} \times \{M_{(3b-3)}\Psi_{2(b-1)}(\widetilde{M}_{(2-l)}\emptyset_{2(2-l)})(\mathrm{Si}_{2n}\mathrm{O}_{5n})_2\}. \quad (2)$$

The most representative group among the palygorskite-sepiolite polysomatic series is the group of compounds with the palygorskite structure type ($n = 2$), which includes the minerals palygorskite, yofortierite, tuperssuatsiaite, windhoekite, raite, and recently discovered in the Wind Mountain phonolite dyke (New Mexico, USA) windmountainite with the idealized formula $\{Fe^{3+}{}_2Mg_2(Si_4O_{10})_2(OH)_2(H_2O)_4\}\ 4H_2O$. Using (1), the general formula of minerals with the palygorskite-type structure can be written as:

$$|A_x(\mathrm{H_2O})_y|\{M_{3-z}\Psi_2(\widetilde{M}_{(2-k)}\emptyset_{2(2-k)})(\mathrm{Si_4O_{10}})_2\}. \quad (3)$$

where $0<z<1$.

The group of compounds with the sepiolite structure type ($n = 3$) is less representative and includes the minerals sepiolite, ferrosepiolite, loughlinite, and falcondoite; their general formula can be written as:

$$|A_x(\mathrm{H_2O})_y|\{M_{6-z}\Psi_4(\widetilde{M}_{(2-k)}\emptyset_{2(2-k)})(\mathrm{Si_6O_{15}})_2\}, \quad (4)$$

where $0<z<2$.

The only currently known representative of the palygorskite-sepiolite polysomatic series with a hybrid structure is the mineral kalifersite, in which *TOT* modules with $n = 2$ combine with modules with $n = 3$.

Key words: palygorskite, sepiolite, stoichiometry, modularity, crystal chemistry

OCCURRENCE MODES OF NICKEL IN CLAY MINERALS AND THEIR RESOURCE IMPLICATIONS

Chaoqun Zhang[1*], Fabien Baron[2], Jianxi Zhu[3], Sabine Petit[2], Hongping He[4]

1. Key Laboratory of PlanetaryScience and Frontier Technology, Institute of Geology and Geophyics, CAS, Beijing, China. *zhangchaoqun@mail.iggcas.ac.cn
2. Institut de Chimie des Milieux et Matériaux de Poitiers (IC2MP), UMR 7285 CNRS, Université de Poitiers, F-86073 Poitiers Cedex 9, France
3. State Key Laboratory of Deep Earth Processesand Resources, Guangzhou Institute of Geochemitry, CAS,Guangzhou, China
4. Chinese Academy of Sciences

Abstract: Mg–Ni clay minerals are important Ni-hosting phases in lateritic nickel deposits, yet the crystal-chemical mechanisms controlling Ni incorporation and redistribution in clay minerals remain insufficiently constrained. In this study, hydrothermal synthesis experiments were conducted to investigate Ni occurrence modes during the growth of trioctahedral Mg–Ni saponites. The Mg–Ni saponite system was selected as an analogue of Mg–Ni clay minerals in lateritic nickel ores. Moreover, the similar ionic radii of Ni^{2+} and Mg^{2+}, 0.70 and 0.72 Å, respectively, together with their contrasting atomic masses, make this system suitable for crystal-chemical characterization by FTIR spectroscopy and high-angle annular dark-field scanning transmission electron microscopy (HAADF-STEM). Mg–Ni saponites were synthesized from mixtures of Mg-saponite and Ni-saponite end-member precursors prepared under different crystallization conditions. FTIR and HAADF-STEM analyses show that the formation of Mg–Ni saponite solid solutions is strongly controlled by precursor particle size and crystallinity. Fine-grained precursors promote dissolution–reprecipitation and favor homogeneous Mg–Ni solid-solution formation, whereas coarse-grained precursors inhibit dissolution and preserve compositional heterogeneity. Mg–Ni solid solutions form more readily in systems containing quasi-amorphous Ni-saponite and well-crystallized Mg-saponite, suggesting that Ni^{2+} is more stable than Mg^{2+} in the saponite octahedral sheet and can substitute for Mg^{2+} during crystal growth. These results indicate that Ni in clay minerals can occur as structurally incorporated Ni within smectite solid solutions, rather than only as discrete Ni-rich phases. The combined FTIR–HAADF-STEM approach provides an effective means of identifying Ni occurrence modes at the crystal-chemical scale. This study provides new insights into Ni enrichment, mobility, and potential recoverability in Mg–Ni clay-bearing lateritic nickel deposits.

Key words: hydrothermal synthesis, Ni-clay, HAADF-STEM, FTIR

Acknowledgements This work was supported by the CSC program of the National Natural Science Foundation of China and the Student Research Grant of The Clay Minerals Society.

ORIENTED SPECTROSCOPIC CHARACTERISTICS OF CORDIERITE

Yimiao LIU[1], Liu LONG[1, 2], Ren LU[1]

1. Gemmological Institute, China university of Geosciences (Wuhan), China
2. Chongqing Natural History Museum, China

Abstract Cordierite is a common gemstone variety that has long been recognized for its distinct pleochroism, a property that arises from its anisotropic crystal structure. Despite being well known in gemmological practice, systematic studies on its spectroscopic properties with respect to crystallographic orientation remain relatively limited in the literature, particularly studies that integrate multiple spectroscopic methods under controlled polarization conditions. This paper presents an oriented spectroscopic investigation of natural blue cordierite along its three crystallographic axes, aiming to provide fundamental spectral data that may contribute to a better understanding of this gem material.

For this study, ten gem-quality cordierite samples were carefully selected and then precisely oriented and cut along the a, b, and c crystallographic axes. Polarized Raman, Fourier-transform infrared, and ultraviolet-visible-near infrared spectra were collected with the incident light polarized parallel to each axis, denoted as E // a, E // b, and E // c respectively. This experimental design allows for the direct comparison of spectral features across the three principal directions of the crystal.

The oriented spectra reveal several notable features that are closely related to the underlying crystal structure of cordierite. In the Raman spectra, the 1381 cm^{-1} band, which corresponds to the vibrational mode of CO_2 molecules, exhibits the highest intensity when measured in the E // a direction. This observation suggests that CO_2 molecules located within the structural channels are preferentially oriented along the a-axis of the crystal. Additionally, the intensity ratio between the 577 cm^{-1} and 555 cm^{-1} bands is found to vary regularly with changes in crystallographic orientation. In the FTIR spectra, absorption bands observed in the 3900 to 3300 cm^{-1} region and the 2600 to 2000 cm^{-1} region are attributed respectively to the presence of H_2O and CO_2 within the structural channels. The splitting patterns of the H_2O-related bands provide information that allows for the distinction between Type I and Type II water molecules occupying different channel sites. In the UV-Vis-NIR spectra, a broad absorption band centered near 570 nm is assigned to Fe^{2+}-Fe^{3+} intervalence charge transfer. This absorption band shows clear orientation dependence, being strongest in the E // b direction and weakest in the E // c direction. This variation correlates directly with the pleochroic colors observed in the samples, namely pale blue along the a-axis, violet-blue along the b-axis, and pale yellow along the c-axis.

Taken together, these results demonstrate that the spectroscopic features of cordierite are markedly orientation-dependent and that this dependence can be systematically traced back to features of its crystal structure. The oriented spectral data provided in this study may serve as a useful reference for the identification of cordierite and for future structural investigations of this and related gem materials.

Key words: Cordierite, Oriented spectroscopy, Pleochroism

Acknowledgements This research is supported by Deep Earth Probe and Mineral Resources Exploration - National Science and Technology Major Project 2025ZD1005100.

ORIGINS OF COLOR IN BROWN AND BLUE MAMMOTH IVORY

Tao Chen, Zhaoying Huang, Binyan Kang

Gemmological Institute, China University of Geosciences (Wuhan), China

Abstract Mammoth ivory, a precious organic gemstone, is predominantly found in blue and brown color variants, and the color genesis is closely related to mineral composition and diagenetic processes during burial. In this study, Fourier transform infrared spectroscopy (FTIR), X-ray powder diffraction (XRD), scanning electron microscopy (SEM) and energy dispersive spectroscopy (EDS) were employed to systematically analyze the mineral composition, surface morphology, chemical composition and functional group characteristics of blue and brown mammoth ivory samples. The results show that hydroxyapatite and collagen are the core basic components of both types of mammoth ivory, with organic matter gradually losing and the crystallinity of hydroxyapatite increasing from the dentine layer to the surface, and fissures and micropores on the surface and cementum layer providing space for the enrichment of chromogenic minerals. Vivianite is the exclusive chromogenic mineral of blue mammoth ivory, which is mainly enriched in surface fissures and microcracks near dentinal tubules, and its oxidation generates iron oxides forming brown stripes in blue areas. The brown color of mammoth ivory is jointly induced by iron and manganese minerals including hematite, pyrite, pyrolusite and manganite, which crystallize and accumulate in the fissures of the surface and cementum layer, with iron oxides and sulfides evenly distributed on the surface and manganese oxides and hydroxides mainly concentrated in fissures. Burial diagenesis is the key to the formation of chromogenic minerals: the loss of organic matter and the release of phosphate anions provide material basis, while microbial activities and changes in environmental physical and chemical conditions drive the valence transformation of iron and manganese ions and mineral phase conversion. In addition, the Schreger line angle of mammoth ivory is smaller than that of modern ivory, and surface color distribution can be an auxiliary identification method. This study clarifies the chromogenic mechanisms of blue and brown mammoth ivory, and provides mineralogical and geochemical basis for the identification and classification of mammoth ivory and paleoenvironment reconstruction.

Key words: Mammoth ivory, Color genesis, Vivianite, Iron-manganese oxides, Burial diagenesis

OXALIC ACID LEACHING OF PALYGORSKITE CLAY: STRUCTURAL ENGINEERING-DRIVEN SURFACE CHEMISTRY FOR MULTIFUNCTIONAL MATERIALS

Yushen Lu[1], Bin Mu[1,2]*, Xiaomei Wang[1], Aiqin Wang[1,2]*

1. Key Laboratory of Clay Minerals of Gansu Province, Research Center of Resource Chemistry and Energy Materials, Lanzhou Institute of Chemical Physics, Chinese Academy of Sciences, Lanzhou 730000, P.R. China
2. Center of Materials Science and Optoelectronics Engineering, University of Chinese Academy of Sciences, Beijing 100049, P.R. China

Abstract Palygorskite (Pal) is a one-dimensional clay mineral with a unique layered-chain structure, high surface area, and abundant active sites, making it attractive for nano-functional materials. Acid activation is commonly used to tailor its properties, yet the detailed structural evolution during acid leaching and its implications for material performance remain insufficiently understood. Therefore, we systematically investigated the gradient oxalic acid (OA) leaching of Pal from 1 h to 120 h using multi-technique approaches. OA leaching proceeded via surface-controlled dissolution, where OA molecules preferentially adsorbed onto active sites to selectively remove octahedral cations, creating widened grooves while preserving the 1D rod-like morphology. This structural dissolution progressively degraded long-range order, while modulating channel accessibility, specific surface area, surface acid-base properties, and electronegativity. Prolonged leaching beyond 96 h led to complete loss of long-range order, transforming Pal into amorphous silica nanorods rich in silanol groups. Structure-dependent active sites governed the adsorption selectivity for various adsorbates. Specifically, external surface area-driven adsorption dominated for bulky molecules such as toluene and water vapor, preserved channels and basic metal sites were essential for CO_2 capture, and optimized Brønsted acidity governed NH_3 uptake. The ability to independently tune surface chemistry provided a versatile platform for designing Pal-based materials. For Pal leached for 1 h showed superior procoagulant effects due to its intact nanorod morphology, increased negative surface charge, and release of Fe^{3+}/Mg^{2+} ions, which activated the intrinsic coagulation pathway and promoted fibrin formation. Meanwhile, Pal leached for 48 h served as an optimal nanocarrier for silver nanoparticles, achieving uniform dispersion and excellent broad-spectrum antibacterial activity via membrane disruption, ROS generation, and DNA damage. Moreover, the non-destructive nature of OA leaching preserved the relatively intact morphology while efficiently whitening brick-red mixed-dimensional Pal clay. This enabled the full utilization of both 1D palygorskite nanorods and 2D layered clay minerals, providing an ideal platform for constructing high-performance mixed-dimensional nanocomposites. Collectively, our findings demonstrated that controlled OA leaching transformed natural Pal clay into a family of

structure-tunable, surface-adaptable, and multifunctional materials, bridging the gap between fundamental mineralogy and practical applications.

Key words: Palygorskite, Oxalic acid leaching, Structural evolution, Surface properties, Multifunctional materials

REDOX-ACTIVE FE(II)-PILLARED SMECTITE

Joseph W. Stucki, * Martin P. Pentrak, and Linda A. Pentrak
University of Illinois at Urbana-Champaign, Urbana, IL 61801 USA

Abstract Redox-activated smectites have much potential as agents for various environmental and industrial purposes. Flow-through reactors are important devices for many such applications, but the utility of redox-activated smectites in such aqueous systems is generally not possible because of low permeability due to the very small particle size of the smectite. One possible way to overcome this problem is to increase the particle size of the clay mineral while preserving its reactivity. This may be done by placing pillars between the superimposed layers of the smectite (Sme), which stabilizes the smectite relative to swelling and shrinking and increases the particle size and porosity while preserving its high surface area, thus enabling them to be used in higher through-put membranes. A further interest is to construct the pillars with Fe, in order to enhance the possibility for redox activity. A previous study of Fe-pillared smectites found that the reduction reaction dissolves the Fe pillars and, thus, destroys the beneficial effect of Fe pillaring. The objectives of the present study were: (1) to find an alternative method of Fe pillaring that would prevent reductive dissolution of the pillars, (2) to measure the oxidation state of Fe in the pillars after chemical reduction, and (3) to compare wet chemical and spectroscopic methods for measuring the redox state in the Fe-pillared Sme. Samples were prepared at pillaring levels of 0, 5, 10, and 15 mmole Fe/g Sme. Pillaring was confirmed by XRD and XRF, and the Fe(III) state in the pillar was confirmed by Mössbauer spectroscopy. The greater the pillaring extent, the greater the particle size. Samples were reduced with citrate-bicarbonate-buffered Na-dithionite (CBD method), then washed free of excess salts using a controlled-atmosphere liquid exchanger (CALE). The total Fe content was measured by XRF, and the extent of reduction was measured by UV-Vis spectroscopy, Mössbauer spectroscopy, and wet chemical analysis using the 1,10-phenanthroline method. Results revealed that the Fe pillars in the Sme were not removed by the CBD treatment, contrary to earlier studies. In Fe-pillared Sme, not only did the pillars remain after reduction, but the intact Fe pillars contained >90% Fe(II). The relative areas of the Fe(II) and Fe(III) peaks in the Mössbauer spectra at 4K revealed a lower Fe(II)/Fe(III) ratio than the wet chemical method, suggesting that the recoil-free fraction for Fe(II) in the pillars differs significantly from that of the Fe(III). Upon reoxidation, the color of the Fe-pillared Sme returned to the Fe(III) state. The redox activity was then tested by reacting the samples with nitrate. Levels of nitrate removal from aqueous solution increased with increasing Fe pillar reduction

Key words: Fe-pillared smectites, Reductive dissolution, Fe(II)/Fe(III) ratio, Nitrate removal

RESEARCH ON WOUND HEMOSTATIC PROPERTIES OF MIXED-DIMENSIONAL ATTAPULGITE CLAY

Xiaomei Wang, BinMu*, Yushen Lu, Aiqin Wang*

Key Laboratory of Clay Minerals of Gansu Province, Research Center of Resource Chemistry

and

Energy Materials, Lanzhou Institute of Chemical Physics, Chinese Academy of Sciences,

Lanzhou 730000, PR China

Abstract: Rapid hemostasis is a critical step in clinical trauma care and surgical procedures. Clay minerals have attracted wide attention as hemostatic materials due to the unique crystal structure, abundant morphology and good biocompatibility. Attapulgite is a hydrated magnesium-rich aluminosilicate clay mineral with a unique chain-layer structure and nanorod morphology, which had been demostrated excelent hemostatic performances. Compared with the high-purity attapulgite, mixed dimensional attapulgite clay (MDAPT), composed of attapulgite, illite, chlorite, kaolinite, illite-smectite mixed-layer clay with unique advantages becomes a research hotspot in recent years. Here, an acid gradient etching strategy was employed to induce structural evolution of MDAPT. The structure-activity relationship between the structure and hemostatic performance was systematically studied, and the underlying hemostatic mechanism was clarified. Based on this, FeNPs/MDAPT nanocomposites were prepared using the extract of radix paeoniae rubra, which possesses hemostatic, anti-inflammatory, and antibacterial properties, as a reducing and stabilizing agent, and MDAPT as a carrier. Experimental results showed that the dispersion and hemostatic ability of FeNPs (ferric oxide nanoparticles) were effectively enhanced. The optimal *in vitro* coagulation activity was primarily attributed to the synergistic effect of MDAPT and FeNPs in enhancing the adhesion of red blood cells and platelets, as well as activating the coagulation pathway. The nanocomposite prepared by this green method possesses excellent biocompatibility, antibacterial and antioxidant properties, showing promise for wound management.

Key words: Mixed-dimensional attapulgite clay, structural evolution, Ferric oxide nanoparticles, Nanocomposites, Wound hemostasis

*Corresponding author: mubin@licp.cas.cn (B. Mu); aqwang@licp.cas.cn (A. Wang)

SEASONAL VARIABILITY OF SALT MINERAL ASSEMBLAGES IN POROUS LIMESTONE MASONRY

Annamária Kis*, Ákos Török

Department of Engineering Geology and Geotechnics, Budapest University of Technology and Economics, Hungary, *kis.annamaria@emk.bme.hu

Abstract Moisture-mediated salt transport and crystallization significantly influence the durability of porous construction materials. This study focuses on the mineralogical characterization and seasonal variation of salt assemblages in thick (3 to 4 m) masonry walls constructed from Miocene porous limestone at some places with volcanic tuff cores.

Sampling was performed during dry and wet seasonal conditions to assess temporal variability. Moisture distribution was determined in situ and through depth profiling using dry drilling. Salt phases were identified from drilled powder and surface samples by optical microscopy, X-ray fluorescence (XRF), X-ray diffraction (XRD), and thermogravimetric analysis (DTA-DTG).

The dominant salt minerals include gypsum, halite, and hygroscopic nitrate phases. Their vertical and depth distribution shows pronounced seasonal dependence, controlled by environmental moisture availability and transport mechanisms (capillary rise, infiltration). The results demonstrate that mineralogical transformations and salt redistribution are strongly governed by external climatic conditions, weathering forms, porosity and pore-size distribution. It is also controlled by the elevation from the ground level, since capillary water absorption has a crucial role in moisture transport and salt redistribution.

These findings underline the importance of mineralogical approaches in assessing the environmental performance and long-term stability of natural stone construction materials, and provide a basis for more sustainable conservation strategies through improved prediction of salt weathering processes.

Keywords: salt mineral assemblages, porous limestone, moisture transport, salt weathering, sustainable conservation

SELECTIVE ADSORPTION OF MAGNESIUM IONS AND STRUCTURAL RECONSTRUCTION IN ACIDIFIED PALYGORSKITE

Yi Zhou, Xin Liu, Meng Liu, Hao Liu, Guocheng Lv, Libing Liao

School of Materials Science and Technology, China University of Geosciences, Beijing 100083, China

Abstract Clay minerals play a crucial role in adsorption, crystallization, and elemental migration at interfaces, as reflected by such processes as the release of constituent elements and structural evolution in acidic aqueous solutions. In this study, acidification of palygorskite induces preferential Mg^{2+} dissolution from octahedral sites, creating distinct octahedral vacancy defects critical for selective cation adsorption. Acidified palygorskite exhibits exceptional Mg^{2+} selectivity in mixed ion solutions (Mg^{2+} >Ca^{2+} >Na^{+} >K^{+} >Li^{+}), surpassing affinities of competing ions by 1–2 orders of magnitude. The adsorption mechanism is predominantly governed by electrostatically induced chemisorption. Crucially, re-adsorbed Mg^{2+} drives structural reconstruction by occupying octahedral vacancies, as evidenced by SAED pattern restoration, Mg redistribution in TEM-EDS, FTIR recovery of Si-O-Mg vibrations (973 cm^{-1}), NMR resurgence of Q3(0Al) edge silicon sites (−92.2 ppm), and increased bound and structural water content in TG-DTG. DFT calculations confirm the mechanism that octahedral vacancies exhibit a lower formation energy (3.58 eV) than Si-leached defects (7.36 eV), and Mg^{2+} adsorption at vacancy sites (−1.95 eV) exceeds energies for other cations. This defect-mediated adsorption not only governs Mg^{2+} selectivity but also enables structural reconstruction via an adsorption-crystallization pathway, establishing a direct link between selective ion capture and mineral recrystallization processes. These findings advance predictive understanding of clay mineral reactivity in geochemical cycling and offer theoretical guidance for the development of novel adsorption materials.

Key words: Selective adsorption, structural reconstruction, acidified palygorskite, defect structure, clay minerals

SITE-SPECIFIC REACTIVITY OF TERMINAL AND BRIDGING HYDROXYLS ON γ-ALUMINA SURFACES REVEALED BY ^{19}F SOLID-STATE NMR

Jinhui Li, Wei Li*

State Key Laboratory of Critical Earth Material Cycling and Mineral Deposits, Key Laboratory of Surficial Geochemistry (Ministry of Education), Frontiers Science Center for Critical Earth Material Cycling (FSC-CEMaC), School of Earth Sciences and Engineering, Nanjing University, Nanjing 210023, China;

* Email of the corresponding author: liwei_isg@nju.edu.cn

Abstract The structure and reactivity of mineral surface hydroxyls at the mineral-water interface are of great significance for processes such as chemical weathering and ion adsorption. However, in classical studies, the mineral surface is often treated as a whole, as exemplified by the Electrical Double Layer theory. The Surface Complexation Model (SCM) can simulate surfaces with sites of differing reactivity, but conducting corresponding experimental controls is extremely difficult. Site-specific experimental characterization of mineral surfaces has become increasingly important, as it can help explain key issues such as the fractionation of rare earth elements during adsorption onto clay mineral surfaces and guide applications. Solid-state nuclear magnetic resonance (ss-NMR) is a powerful tool for investigating local structures and has been widely applied in fields such as catalysis, meanwhile its potential in mineralogy has yet to be broadly recognized. The application of ss-NMR techniques will help us establish a site-specific understanding of mineral surfaces.

In this study, γ-alumina, featuring six distinct surface hydroxyl sites which encompass all structural types of aluminum-bound hydroxyl sites found in clay minerals, was employed as a model mineral. Using ss-NMR techniques, including TRAnsfer of Populations in DOuble Resonance (TRAPDOR) and Heteronuclear Multiple Quantum Coherence (HMQC), we investigated the fluoride adsorption behavior of these sites. Single-pulse and HMQC experiments revealed that two types of surface hydroxyl groups bound to octahedral aluminum participate in fluoride adsorption. TRAPDOR experiments combined with DFT theoretical calculations further distinguished these as terminal hydroxyls (η-OH) and bridging hydroxyls (μ-OH) substituted by fluoride. By deconvoluting the fluoride spectra, we quantitatively differentiated the adsorption capacities of these hydroxyl groups under varying pH conditions. Additionally, surface reactions were fitted using the SCM, and the theoretical predictions aligned well with the quantitative results from ss-NMR, enabling accurate determination of the equilibrium constants for three reaction pathways in total at distinct hydroxyl sites. Combining ss-NMR experimental data with SCM theoretical calculations, we have achieved site-specific identification of surface hydroxyls on alumina minerals. Contrary to conventional assumptions, our results reveal the non-negligible reactivity of μ-OH relative to η-OH in surface adsorption process.

The observed fluoride displacement of multiple hydroxyl species at ambient conditions enables highly sensitive ss-NMR characterization of diverse hydroxyl site configurations. This

methodology can be readily extended to investigate various clay mineral surfaces. We employed fluoride as a probe to investigate the structure and reactivity of surface hydroxyls on boehmite. The results indicate the presence of η-OH and μ-OH on the boehmite surface that are structurally identical to those found on alumina. However, the η-OH includes two subspecies with distinctly different reactivity, which is well reflected in the reaction kinetics. We also observed that boehmite exhibits significant fractionation between light and heavy rare earth elements during surface adsorption, and η-OH, as the primary surface-active sites, may play a crucial role in this process. Further in-depth investigation into the origin of their property differences will help elucidate the fundamental cause of light and heavy rare earth element fractionation.

Key words: Surface hydroxyls, Site-specific reactivity, Solid-state NMR, TRAPDOR, Mineral-water interface

Acknowledgements We thank Professor Xiancai Lu, Professor Guangjin Hou, Associate Professor Chi Zhang, Dr. Lixin Liang, and Pengfei Shen for their support and assistance with this work. This research was funded by the National Natural Science Foundation of China (Grant No. 42421002).

SOILS AS RESERVOIRS OF HAZARDOUS FIBROUS ZEOLITES: EVIDENCE FOR ERIONITE IN SOILS AT GAWLER DOWNS, NEW ZEALAND

Satendra Kumar, Martin Brook, Melanie Kah, Ayrton Hamilton
School of Environment, The University of Auckland, New Zealand

Abstract Naturally occurring fibrous minerals represent a significant environmental hazard. Among these, the fibrous zeolite, erionite, has attracted considerable scientific attention due to its high carcinogenic potential and its strong association with malignant mesothelioma following inhalation exposure. While the occurrence of erionite in bedrock is well documented, significantly less research has been conducted on the presence of erionite in soil and on transfer pathways from bedrock to soil and, subsequently, into the air. Gawler Downs, New Zealand, provides a unique natural laboratory to investigate erionite in soils. The landscape preserves a complex geomorphic archive of relict glacial and periglacial landforms now buried beneath post-glacial soil horizons. This study investigates the occurrence and distribution of erionite in soils at Gawler Downs. Field investigations were integrated with high-resolution mineralogical analyses using scanning electron microscopy with energy-dispersive spectroscopy (SEM–EDS) and transmission electron microscopy (TEM). This dual-microscopy approach enabled the definitive characterisation of erionite fibre morphology and structural properties, particularly within heterogeneous soil matrices. The identified erionite fibers include elongate particles with high aspect ratios, physical traits that enhance their potential for atmospheric transport once liberated from the soil. The findings provide important evidence of the potential transfer pathway from rock to soil and into air, via natural weathering processes, as well as anthropogenic disturbance. By identifying these transfer pathways, this research underscores the role of soil as a critical, yet under-studied, reservoir for the release of hazardous mineral fibers into the environment.

Key words: Erionite, Naturally occurring asbestos (NOA), Transfer pathways, Geomorphology.

SONHARI MEMBER OF LAKI FORMATION, SINDH, PAKISTAN: A SOURCE OF IRON OXIDES AND ASSOCIATED CLAY MINERALS

M.H. Agheem*, G.M. Thebo, A.H. Markhand, A.A. Halepoto, Javed Ali

Centre for Pure and Applied Geology, University of Sindh, Jamshoro. Pakistan

Abstract The present study is carried out on iron ore deposits and associated clay beds in two sections of Sonhari member of Early Eocene age belonging to the Laki Formation in district Thatta, Sindh, Pakistan. The Sonhari member is exposed in different sections within the southern Khirther Fold and Thrust belt. The major objective of this study was to properly characterize and evaluate the iron-bearing and other associated clay minerals for their possible industrial use. During the field work, it was noted that the iron ores were alternative with a variety of clay minerals. The laminations and beds are variable both in size and shape and ranging from a few centimeters to as thick as 4-5 feet. The representative rock samples were collected and then were analyzed on the D8 Advance Diffractometer for XRD analyses for proper mineral characterization along with the EDS analyses exploring the chemistry in the Centre For Pure and Applied Geology, University of Sindh, Jamshoro. The XRD analyses indicate diverse iron oxides along with variety of clay minerals. The qualitative and semi-quantitative XRD analyses show that the hematite, goethite, and maghemite are the major iron phases present in various proportions in the analyzed samples while a significant proportion of diverse clay minerals including the quartz and clays are also present. Among the three identified iron-bearing minerals, the hematite is common with higher percentage while the maghemite is present in only four samples and goethite in eight samples. The XRD analyses of alternative clay beds show the presence of kaolinite, faujasite, calcite, illite, clinochlore, vermiculite, dickite, and boehmite. In addition, two titanium bearing minerals in the form of titanite and anatase are also identified. The evaporites are in the form gypsum and halite. The EDS analyses also confirm the presence of the minerals identified through the XRD. Both the iron oxides and clay minerals can be used for variety of industrial applications. Further, on the basis of such mineral assemblage, it can be concluded that the source of sediments was mixed and these were deposited in fluvial to deltaic environments; during the major phase of transgression and regression which occurred during the Late Paleocene and Early Eocene, the collision time of Indian and Eurasian plates.

Key words: Iron ore Deposits, Mineralogy, Sonhari member, Eocene, Laki Formation.

STRUCTURE–ACTIVITY RELATIONSHIP AND ACTIVITY REGULATION IN CLAY MINERAL-BASED ENZYME CATALYTIC SYSTEMS

Ke Wang, Shiyong Sun*

School of Environment and Resource, Key Laboratory of Solid Waste Treatment and Resource Recycle of Ministry of Education, Southwest University of Science and Technology, Mianyang, Sichuan, 621010, China.

Abstract Enzymes are efficient and specific biocatalysts that hold great potential for applications in various fields. However, their widespread use is limited by inherent drawbacks, including poor stability under non-physiological conditions, high cost, and difficulty in recovery. To address these challenges, our team has employed the unique properties and structures of clay minerals, such as high specific surface area, nanoconfinement microstructure, layered and porous characteristics, and good biocompatibility, as functional nanosupports to construct high-performance enzyme–clay mineral hybrid catalytic systems. These strategies integrate recent advances in mineralogy and applied research, providing an effective route to overcome the bottlenecks in enzyme applications.

In recent years, we have systematically explored various innovative strategies for constructing efficient enzyme–clay mineral hybrid catalytic systems, including covalent immobilization, allosteric regulation-assisted immobilization, cascade system construction, and oriented co-immobilization. Our works have elucidated the key mechanisms underlying these hybrid systems: (1) interfacial activation, where modifying the surface properties of clay minerals regulates enzyme catalytic activity; (2) support-induced allosteric effect, in which specific clay minerals induce synergistic conformational changes in enzymes to enhance catalysis; (3) nanoconfinement and substrate channeling, utilizing the interlayer nanostructure of clay minerals; and (4) rigid skeleton protection, wherein the stable mineral framework effectively protects enzymes from extreme catalysis environments. The synergistic action of these mechanisms significantly improves the performance of the hybrid catalysts, as evidenced by: (a) enhanced catalytic activity; (b) substantially improved stability in terms of thermostability, pH tolerance, and storage stability; and (c) excellent reusability, enabling multiple enzyme recycling and thus markedly reducing costs.

Our recent works not only provide innovative pathways for the green and high-value utilization of abundant, low-cost clay mineral resources, thereby promoting the practical application of novel high-performance, stable, and recyclable clay mineral-based biocatalysts in industrial biocatalysis, but also deepen the understanding of how clay minerals modulate biomolecular behaviors (e.g., conformation, activity, stability) at the micro/nanoscale. Furthermore, these work offers important experimental evidence and theoretical support for exploring the potential catalytic role of mineral surfaces in early Earth life processes and for understanding mineral–bio interfacial interactions.

Key words: Clay minerals, Enzymes, Nanostructured enzymes, Structure–activity relationship, Activity regulation

Acknowledgements This work was supported by the National Natural Science Foundation of China (grant number 42372056), Sichuan Provincial International Science and Technology Innovation Cooperation Project (grant number 2024YFHZ0262), and China Postdoctoral Science Foundation (grant number 2025M771277).

SYNERGISTIC THERMAL-MECHANICAL ACTIVATION OF POLYMINERALIC CLAYS FOR THE SUSTAINABLE STABILIZATION OF DREDGED SEDIMENTS

Gianluca Girardi[1], Francesco Genua[2], Rossella Petti[3], Isabella Lancellotti[2], Cristina Leonelli[2], Claudia Vitone[3], Daniela Pinto[1]

1. Department of Earth and Geoenvironmental Sciences, University of Bari, Italy
2. Engineering Department "Enzo Ferrari", University of Modena and Reggio Emilia
3. Department of Civil, Environmental, Territorial, Construction and Chemical Engineering, Politecnico di Bari, Italy

Abstract The construction industry urgently requires low-carbon solutions to mitigate its environmental footprint, with alkali-activated binders derived from pre-treated clays emerging as a viable and sustainable alternative to traditional Portland cement. Simultaneously, the valorization of waste streams, such as marine dredging sediments, into construction materials represents a key strategy for promoting circular economy and sustainable waste management. In this context, low-grade polymineralic clays represent a promising resource for producing high-performance binders. This study presents a systematic optimization of activation protocols (thermal, mechanical, and combined) applied to two clayey precursors, aiming to evaluate their potential in the mechanical stabilization of dredging sediments for building applications. Both raw materials and treated powders were characterized via XRD with Rietveld refinement, laser diffraction for particle size distribution, and thermal analysis, while chemical reactivity was quantified through dissolution tests (ICP-MS). Results demonstrate that a combined Thermal-Mechanical (T-M) route, involving 600 °C calcination followed by 10 minutes of high-energy ring-milling, achieves a peak reactive fraction (~73 wt.%) while significantly minimizing thermal input. The preliminary mechanical effectiveness of the optimized geopolymer binders was evaluated by stabilizing dredging sediments at different binder dosages. Geomechanical results suggest an encouraging improvement in consistency indices and a potential enhancement of the overall mechanical properties. Notably, the geopolymer-stabilized mixtures showed the capability to reach a mechanical performance approaching that obtained with traditional ordinary Portland cement (OPC) treatments. These findings highlight the feasibility of a synergistic upcycling route, suggesting that clays could be effectively transformed into sustainable binders for the reuse of dredging spoils in the construction sector.

Key words: Geopolymers, Polymineralic clays, Thermo-mechanical activation, Dredged sediments, Soil stabilization

THE BEHAVIOR OF THE 3161 CM^{-1} INFRARED BAND AT LOW TEMPERATURE HEAT TREATMENT IN CORUNDUM

Wasura Soonthorntantikul[1], Aaron C. Palke [2]

1. Gemological Institute of America, Bangkok, Thailand
2. Gemological Institute of America, Carlsbad, United States

Abstract The 3161 cm^{-1} infrared band can be found in untreated natural corundum of various colors, most commonly in yellow sapphire from metamorphic deposits. This band is often present with other less intense bands (3355, 3242, 3100, 2460, and 2420 cm^{-1} bands), known as the 3161 cm^{-1} series. The presence of the 3161 cm^{-1} feature is used frequently as supporting evidence of no artificial heat treatment. Previous works reported that the 3161 cm^{-1} feature in low iron yellow sapphire can be removed and sometimes transformed to the 3000 cm^{-1} band series (a prominent broad band at ~3000 cm^{-1} with the 2625 cm^{-1} band) after heating at 900°C and higher. The 3000 cm^{-1} band series can occur naturally, and it is previously seen in untreated yellow sapphires from basalt-related deposits. The presence of the 3161 cm^{-1} band with the 3000 cm^{-1} series was also reported in a few untreated Rock Creek sapphires. Two different infrared features, the 3161 cm^{-1} and the 3000 cm^{-1} band series, represent different specific forms of hydrogen incorporation in the corundum structure that may reflect thermal history of the stones caused by natural thermal annealing or artificial heat treatment.

In this study, several infrared spectra of untreated natural corundum from GIA's colored stone reference collection were surveyed. The samples have a wide range of colors and come from different deposits around the world. The results proved consistent with previous reports that three infrared patterns related with the 3161 cm^{-1} and the 3000 cm^{-1} features can be observed in untreated corundum: i) the 3161 cm^{-1}, ii) a combination of the 3161 cm^{-1} and the 3000 cm^{-1}, and iii) the 3000 cm^{-1}. After that, ten untreated samples containing strong intensity of the 3161 cm^{-1} band were heated in air to 650°, 700°, 750°, 800°, 850°, and 900°C for 5 hours at each temperature to study the thermal behavior of the 3161 cm^{-1} feature. It was found that three different infrared patterns can also be observed in the same sample at different temperatures. After heating between 800° and 850°C, the 3161 cm^{-1} band intensity significantly decreased in all samples, whereas the 3000 cm^{-1} band series was created in some samples. This suggests that natural corundum from different deposits possibly formed under different growth conditions such as temperature. Careful examination is required to identify heat treatment of unknown corundum when rely on the evidence of the 3161 cm^{-1} and/or the 3000 cm^{-1} features.

Key words: 3161 cm^{-1}, 3000 cm^{-1}, corundum, infrared spectroscopy, heat treatment

THE KIMBERLEY PROCESS AND THE GLOBAL GOVERNANCE OF NATURAL ROUGH DIAMOND TRADE: INSTITUTIONAL POWER, MARKET ACCESS, AND THE INTEREST STRUCTURE OF NON-RESOURCE NODE STATES

LIANG Weizhang[1], QIU Zhili[1*]

School of Earth Science and Engineering, Sun Yat-Sen University, Zhuhai 519082, China

Abstract The Kimberley Process Certification Scheme (KPCS) is more accurately understood as a certification-based arrangement for the governance of mineral trade than as a narrowly defined compliance mechanism directed only at "conflict diamonds." Existing scholarship has examined the internationalization of the conflict diamonds issue, the formation of the Kimberley Process, and the normative and implementation limits of the KPCS, yet the scheme is still often treated primarily as an instrument of conflict management. Such a reading is too limited to capture its wider institutional role in organizing the legal circulation of natural rough diamonds in the international market. Through the institutional combination of participation status, certificate accompaniment, and inter-member trade restrictions, legality is converted into a condition of market access, and state interests become embedded in a rule-based international trading order.

Qualitative institutional analysis, process tracing, and policy text analysis make it possible to identify how this governance arrangement operates and how it distributes interests. The relevant materials include United Nations resolutions, KPCS core documents, World Trade Organization waivers, the European Union implementing regulation, Chinese customs regulations, official Kimberley Process statistics, participant materials, and academic and policy literature. The central concern is not the net trade effect of the KPCS as such, but the way in which a certification-based trade-governance mechanism generates distributive consequences by organizing legality, access qualifications, and institutional participation. Four dimensions of institutional power emerge from this structure: rule-definition power, market-access power, interpretive power, and reform influence.

Several findings follow from this framework. First, the KPCS does not merely identify and exclude conflict-related goods. More fundamentally, it institutionalizes the legal trading status of natural rough diamonds and reconstructs the conditions under which rough diamonds can circulate internationally. Its significance therefore lies not only in conflict prevention, but also in the governance of legal market access for a high-value mineral commodity. Second, competition within the KPCS is not best understood as competition over resource possession alone. More important are struggles over who defines the boundary of "conflict diamonds," who remains inside the legal trading network, who interprets implementation standards, and who influences the future direction of institutional reform. The politics of the KPCS are therefore more usefully understood as struggles

over institutional power within a trade-governance framework than as simple disagreements over compliance.

The position of China helps clarify how such a system generates interests for participants that lack major upstream resource advantages but occupy important places within global trade networks. Dependence on external compliant supply, the mainland–Hong Kong composite trade-node structure, and sustained participation in Kimberley Process institutions together produce clear interests in market access, chain security, and rule participation. In this setting, the significance of the KPCS is not exhausted by formal compliance. Equally important are continued access to legal supply channels, maintenance of key trade and processing nodes, and participation in processes of institutional interpretation and adjustment. Interests in the governance of natural rough diamonds thus derive not only from resource possession, but also from access to compliant markets, nodal positioning, and institutional embeddedness.

The implications of diamond governance extend beyond the certification of natural rough diamond origins. The rise of synthetic diamonds points toward a broader governance space involving substitute materials, production capabilities, end-use boundaries, and fragmented compliance regimes. The KPCS accordingly belongs within a wider analytical framework concerned with the international governance of mineral resources, the ordering of global trade, and the distribution of institutional power.

Key words: Kimberley Process; natural rough diamonds; certification-based trade governance; institutional power; non-resource node states

THE STUDY OF PRODUCTS OF THERMOCATALYTIC DEGRADATION OF POLYOLEFINS OVER CLAYS BY NUCLEAR MAGNETIC RESONANCE SPECTROSCOPY

Sergei Golovin, Lyubov Furda, Olga Lebedeva, Dmitry Smalchenko, Igor Tarasov, Ekaterina Migulina, Evgeniy Seliverstov, Evgeniya Tarasenko, Olga Kokoshkina

Department of General Chemistry, Belgorod State National Research University, Russian Federation

Abstract Plastics have found a wide range of applications in many areas of modern life due to a number of their beneficial properties. However, the huge volume of production, low biodegradability and recycling difficulties have made plastic pollution a significant problem. Among the other methods of recycling plastic waste, thermocatalytic degradation remains an important and promising technique, and various clay-based materials can act as catalysts for this process.

One of the most informative methods for studying organic compounds and their mixtures is nuclear magnetic resonance (NMR) spectroscopy. For example, it is widely used for determination of composition of crude oils and its refined products, as well as pyrolysis oils obtained from various plant materials. Due to the similarity between products of thermocatalytic degradation of plastics and petroleum products, identical approaches are used for their analysis and characterization. ^{1}H NMR spectroscopy provides valuable information on the composition of plastics pyrolysis oils. For more simple interpretation of NMR spectra, it is convenient to split the chemical shift scale into several regions, in which the signals from the observed nuclei correspond to the specific structural elements. Integration of signals in these areas can be used to calculate some characteristic parameters, primarily the relative amount of paraffins, olefins and aromatic hydrocabons, as well as the degree of branching («isoparaffin index») and research octane number (RON). For more detailed studies ^{13}C and two-dimensional spectroscopy are used.

The scope of present work was to study products of thermocatalytic degradation of polyolefins over some clay catalysts using NMR spectroscopy, including both one-dimensional (^{1}H, ^{13}C) and two-dimensional (COSY, HSQC) techniques. Analysis of NMR spectra suggests that the decomposition of raw materials results in the formation of a complex mixture of hydrocarbonsm which predominantly consists of paraffins. The fraction of olefins and aromatic compounds is comparatively low. Several integral descriptors are also calculated. Overall, the resulting products are suitable for recycling as return oil.

Key words: clay minerals, thermocatalytic degradation, polyolefins, nuclear magnetic resonance

Acknowledgements The study was conducted under the state assignment, project № FZWG-2026-0007

THERMOELECTRIC PROPERTIES OF IRON-BEARING MINERALS IN TYPICAL SINTER AND PELLETS: FORMATION MECHANISM AND INDUSTRIAL APPLICATIONS

Bo-Wen Duan[1], Xiu-Li Han[1,2,3*], Jia-Hui Ren[4], Yu-Xin Xie[1], Feng-Jiu Li[1,3]

1. College of Mining Engineering, North China University of Science and Technology, Tangshan 063210, China
2. Yanzhao Iron and Steel Laboratory, Tangshan 063210, China
3. Collaborative Innovation Center of Green Development and Ecological Restoration of Mineral Resources, Tangshan 063210, China
4. College of Metallurgy and Energy, North China University of Science and Technology, Tangshan 063210, China

Abstract The thermoelectric properties of minerals are important physical properties that reflect their chemical composition, crystal structure, and formation conditions. Therefore, studying the thermoelectric properties of major iron-bearing minerals in sinters and pellets is crucial for understanding phase evolution during sintering and guiding industrial production. Using the ZY-RDY2000 thermoelectric coefficient testing instrument, the first systematic measurements of thermoelectric properties were conducted for major iron-bearing minerals in sinter and pellet samples under varied process conditions. The results showed significantly different thermoelectric properties among various iron-bearing minerals. Overall thermoelectric coefficients followed a descending order: skeletal hematite > eutectic of platy SFCA and magnetite > eutectic of needle SFCA and magnetite > recrystallized magnetite > primary magnetite > primary hematite/recrystallized hematite/secondary oxidized hematite. Both sinter and pellet exhibit significant thermoelectric effects, with the thermoelectric coefficients ranging from -60 $\mu V \cdot ℃^{-1}$ to -270 $\mu V \cdot ℃^{-1}$ and -40 $\mu V \cdot ℃^{-1}$ to -60 $\mu V \cdot ℃^{-1}$. Mechanistic analysis revealed that lattice defects induced by process constraints and isomorphous substitutions fundamentally govern these thermoelectric behaviors. The average thermoelectric coefficient of high-basicity sinter exhibits a negative correlation with the low-temperature reduction pulverization index ($RDI_{+3.15mm}$). Meanwhile, the distribution characteristics of the thermoelectric coefficient in pellet effectively reflect the uniformity of its mineralogical structure, thereby serving as a crucial basis for determining the appropriateness of its calcination temperature. Therefore, thermoelectric technology is expected to become a simple, green, and efficient method for quality assessment of both sinter and pellets.

Key words: Mineral thermoelectricity, Magnetite, Hematite, Silica-ferrite of calcium and aluminum (SFCA), Iron-bearing minerals thermoelectric mechanism

A SHARED CARBONATION PATHWAY: BRIDGING MINERAL, BIO-BASED, AND CIRCULAR MATERIAL SYSTEMS FOR CARBON NEUTRALITY

Pooria Pasbakhsh, Zipeng Zhang, Massoud Sofi

Department of Infrastructure Engineering, Faculty of Engineering and Information Technology, The University of Melbourne, Melbourne, VIC 3010, Australia

Abstract Mineral carbonation — the reaction of CO_2 with calcium- or magnesium-rich feedstocks to form stable carbonates — is well established in cement chemistry, but its role as a shared mechanism across otherwise disconnected material systems is rarely examined explicitly. This review proposes mineral carbonation as a unifying pathway linking three material classes central to low-carbon construction: reactive mineral resources (industrial byproducts and clay-based feedstocks), bio-based composites (lime-bound plant fibre systems, where carbonation of the binder compounds the biogenic carbon already stored in the substrate), and circular material systems (recovered polymers and CO_2-derived feedstocks). Using industrial case studies spanning slag mineralization, tailings valorization, in-situ concrete carbonation, and CO_2-derived polymer synthesis, we argue that these routes share a common driver — CO_2 availability and reactive mineral or chemical feedstock — despite differing substrates and processing conditions. We outline the mechanistic parallels and divergences across these systems and propose a research agenda for treating carbonation as an integrating design principle for carbon-neutral construction materials, rather than a cement-specific phenomenon. Finally, we highlight the potential of nanomaterial additions to reduce composite mass while imparting smart functionality to these carbonating systems, pointing to a further axis for future development.

Keywords: Mineral carbonation, calcined clay, carbon neutrality, clay-based feedstocks, lime-bound plant fibre systems

A STUDY OF THE MINERAL-ENHANCED BIOLOGICAL PUMP (MEBP) IN OCEAN SYSTEMS BASED ON MESOCOSM LAND-BASED SIMULATIONS

Yuguo Shen [1, 2], Dong Liu [1, 2*], Rongda Yu [1, 2], Xu Wang [1, 2], Peng Yuan [3], Nianzhi Jiao [4]

1. (State Key Laboratory of Advanced Environmental Technology/ Guangdong Provincial Key Laboratory of Mineral Physics and Materials, Guangzhou Institute of Geochemistry, Chinese Academy of Sciences, China)
2. (University of Chinese Academy of Sciences, China)
3. (Guangdong University of Technology, China)
4. (Carbon Neutral Innovation Research Center, Xiamen University, China)

Abstract Diatoms, as core components of the marine biological pump, play a crucial role in the global carbon cycle. However, due to the poor stability and high solubility of diatom opal (biogenic silica) in seawater, it is difficult for diatoms to transport a significant amount of photosynthetically fixed particulate organic carbon to the deep sea for sequestration, thereby limiting the efficiency of the biological pump. In previous small-scale laboratory simulations, we found that the addition of clay minerals such as montmorillonite could regulate the photosynthetic activity of diatoms and enhance biological pump efficiency, leading to the proposal of the "Mineral-enhanced Biological Pump (MeBP)" theory. However, it remained unclear whether this theory holds in larger-scale systems.

This study utilized the land-based mesocosm ocean environment and climate simulation system at Xiamen University to conduct in situ experiments on diatom bloom systems in 5-ton water columns with different concentrations of montmorillonite. The results indicate:(1) Carbonate particles were observed in the mesoscale simulated marine diatom biological pump system.(2) The addition of montmorillonite promotes carbonate formation by enhancing diatom activity, thereby improving the efficiency of the carbonate pump and mitigating ocean acidification.(3) The mineral-enhancing effect of montmorillonite stimulates diatom growth and strengthens the "ballast effect" of diatom shells, further boosting the efficiency of the diatom biological pump.

These findings preliminarily clarify the mechanisms behind the enhanced efficiency of the diatom biological pump and the formation of associated carbonates under the influence of typical clay minerals like montmorillonite. This study provides experimental support for research on the link between the mineral-enhanced marine biological pump and the marine carbonate pump, as well as theoretical and data-driven foundations for the practical implementation of the mineral-enhanced biological pump in actual marine environments.

Key words: Mineral-enhanced marine biological pump; Carbonate pump enhancement; Land-based mesocosm experiment

Acknowledgements This study was supported by the ONCE, the National Natural Science Foundation of China (42188102, 42272043 and 42172047), and Guang Dong Basic and Applied Basic Research Foundation (2024B1515040003 and 2023B1515120004).

AMINE-FUNCTIONALIZED ALLOPHANE FOR HIGHLY EFFICIENT CO_2 CAPTURE: CHARACTERIZATION AND PERFORMANCE EVALUATION

Yu Zimeng[1,2], Wei Haicheng[1,2], Min Xiuyun[3], Gao Chunliang[1,2], Yuan Peng[4], Wang Shun[1,*]

1. Key Laboratory of Green and High-end Utilization of Salt Lake Resources, Qinghai Institute of Salt Lakes, Chinese Academy of Sciences, Xining 810008, China.
2. University of the Chinese Academy of Sciences, Beijing 100049, China.
3. Salt Lake Chemistry Analysis Center, Qinghai Institute of Salt Lakes, Chinese Academy of Science, Xining 810008, China.
4. School of Environmental Science and Engineering, Guangdong University of Technology, Guangzhou, 510006, China.

Abstract CO_2 concentrations in the atmosphere have risen exponentially, leading to increasingly severe environmental problems such as global warming and ocean acidification. Solid adsorption offers advantages such as easy operation, low energy consumption, and high adsorption capacity. Many adsorbents have been designed, such as MOFs, mesoporous silica, graphene oxide frameworks (GOFs), and zeolites. Clay mineals possess unique structures and abundant active sites, making them exhibit huge potential for CO_2 adsorption. Allophane is a nano-sized clay mineral, showing hollow spherical nanoparticles with a diameter of 3.5–5 nm, which is commonly used as an excellent adsorbent. However, allophane has not yet been utilized for the preparation of CO_2 adsorption materials.

In this work, synthetic allophane was modified using two amino-organosilanes: γ-aminopropyltriethoxysilane (APTES) and N-(2-aminoethyl)-3-aminopropyltrimethoxysilane (AEAPTS) and then used for CO2 adsorption. The abtained materials were characterized by scanning electron microscopy (SEM), Fourier-transform infrared spectroscopy (FTIR), Diffuse Reflectance Infrared Fourier Transform Spectroscopy (DRIFT), nuclear magnetic resonance, and nitrogen adsorption-desorption. The CO_2 adsorption capacity of amino-modified allophanes was significantly enhanced, reaching a maximum of 1.73 mmol/g at 273 K, and gradually decreased with increasing temperature. After five cycles, their adsorption capacity remained above 92%. In addition, the amino-modified allophanes exhibited superior CO_2 adsorption kinetics. These findings indicate that allophane and its amino-modificaiton materials are excllent materials for CO_2 capture.

Key words: CO_2 adsorption, Allophane, Surface modification

Acknowledgements This work was supported by the Qinghai "Kunlun Talents" High-end Innovation and Entrepreneurship Talent Project (No. QHKLYC-GDCXCY-2024-461), the Western Young Scholars Talent Project (No. XBZGLZB2022027), and the generous funding of the International Cooperation Project of Qinghai Provincial Department of Science and Technology (2025-HZ-807).

BASALT MINERAL FOR CCUS: MINERAL CARBONATION PATHWAYS IN THE SUBSURFACE AND ON THE SURFACE

Michelle Tiong, Shizhang Cui, Qi Liu

1. Marginal Oil and Gas Development Technology Reseach Institute, Xi'an Shiyou University, China.
2. China University of Petroleum (Beijing), China.

Abstract Basalt formations have emerged as a promising medium for carbon capture, utilization, and storage (CCUS) due to their widespread availability, high content of divalent cations (Ca^{2+}, Mg^{2+}, Fe^{2+}), and strong potential for permanent CO_2 sequestration via mineral carbonation. This study presents a comprehensive evaluation of mineral carbonation pathways in basalt systems, encompassing both subsurface (in situ geological storage) and surface-based enhanced rock weathering (ERW) approaches. In the subsurface, CO_2 injected into basaltic reservoirs dissolves in formation water to form carbonic acid, which accelerates silicate dissolution and promotes the precipitation of stable carbonate minerals such as calcite, magnesite, and siderite. On the surface, finely ground basalt applied to soils, particularly reactive volcanic soils such as andosols—enhances natural weathering processes, enabling atmospheric CO_2 drawdown through similar geochemical mechanisms under ambient conditions. Recent advances highlight the role of temperature, fluid composition, and reactive surface area in governing carbonation kinetics, with geothermal conditions significantly enhancing dissolution rates and CO_2 mineralization efficiency. Furthermore, integrating basalt-based carbonation with renewable energy systems and industrial by-products offers opportunities to improve process efficiency and reduce lifecycle emissions. This paper reviews the current state of research on basalt carbonation, compares subsurface and surface pathways in terms of reaction mechanisms, kinetics, scalability, and permanence, and identifies key challenges, including reaction passivation, water demand, and monitoring, reporting, and verification (MRV) constraints. The findings underscore the potential of basalt as a versatile and scalable solution for long-term carbon storage, contributing to global decarbonization and net-zero targets.

Key words: basalt, CCUS, in-situ CO_2 mineralization, enhanced rock weathering, mineral carbonation

BIOGENIC MAGNETITE AS A KEY LINK IN IRON-FERTILIZATION-DRIVEN CARBON SEQUESTRATION DURING THE PETM

Xiaoodng Jiang[1], Weiqi Yao[2], Xiangyu Zhao[3], Andrew P. Roberts[4], Qingsong Liu[2]

1. The School of Marine Sciences, Hainan University, Haikou, 570228, China.
2. Department of Ocean Science and Engineering, Southern University of Science and Technology, Shenzhen 518055, China
3. School of Oceanography, Shanghai Jiao Tong University, Shanghai 200030, China
4. Research School of Earth Sciences, Australian National University, Canberra, ACT 0200, Australia

Abstract The Paleocene–Eocene Thermal Maximum (PETM), a period of rapid global warming, was accompanied by profound perturbations in the oceanic carbon cycle. However, the specific microbial feedbacks that mediated carbon cycling in the open ocean remain poorly understood. Through combined magnetic and geochemical analyses of sediments from the eastern equatorial Pacific Ocean, we find that iron fertilization by eolian dust and volcanic eruptions during the PETM significantly enhanced surface ocean productivity, thereby promoting enhanced organic matter export and burial. Notably, magnetotactic bacteria and their fossilized magnetofossils played a non-negligible role in this biogeochemical process. Thriving under elevated organic-matter fluxes, these bacteria biomineralize nano-sized magnetite crystals (magnetofossils), thereby converting bioavailable iron into a stable, mineral-bound form and directly influencing the iron biogeochemical cycle. Concurrently, the metabolic activity and subsequent degradation of magnetotactic bacterial cells provide an efficient pathway for transferring organic carbon into the sediment. Thus, variations in magnetofossil abundance and morphology not only record enhanced marine productivity and organic-matter flux during the PETM, but also reveal a tightly coupled relationship among iron fertilization, carbon burial, and microbial activity. Our findings highlight that, under global warming conditions, the iron-carbon feedback mediated by magnetofossils is a critical determinant of ocean carbon-sink efficiency. Although this process is loosely associated with changes in oxygen levels in intermediate waters, its more fundamental significance lies in demonstrating that magnetofossils – as a product of microbial activity – effectively link iron supply, organic matter production, and carbon sequestration. This provides a novel microbiological perspective for understanding the evolution of ocean carbon cycling under both past and future warm climates.

Keywords: Biogenic magnetite, PETM, Carbon cycling, Eastern equatorial Pacific

CARBON-NEUTRAL MINERALOGY: ROLES OF MINERALS AND MINERAL-BASED MATERIALS TOWARD CARBON NEUTRALITY

Peng YUAN

School of Environmental Science and Engineering, Guangdong University of Technology, China

Abstract Minerals play a fundamental role in the Earth's carbon cycle and are also indispensable components of industrial and agricultural systems, exerting broad influence over carbon generation, transformation, and storage. As a result, mineral-related processes are deeply embedded in both natural and anthropogenic carbon dynamics. Achieving carbon neutrality therefore requires a systematic understanding of greenhouse gas emissions, their cycling pathways, and mineral-associated sequestration mechanisms.

Although multiple pathways such as enhancing carbon sinks, optimizing energy structures, and advancing carbon capture, utilization, and storage (CCUS) have been widely explored, many of these approaches inherently involve mineral phases and mineral-mediated reactions. However, the underlying mechanisms governing these mineral-related processes remain insufficiently understood, highlighting the need for further research in this field.

In this context, this study proposes the concept of Carbon-neutral mineralogy (CNM), defined as a branch of mineralogy oriented toward achieving net-zero greenhouse gas emissions. CNM aims to elucidate the key mineralogical processes and controlling mechanisms of carbon cycling, and to develop theoretical approaches and material systems for carbon reduction, sequestration, and utilization.

Within this framework, CNM focuses on three main aspects: (i) The roles of minerals in the Earth's carbon cycle and climate change. (ii) The regulation of carbon migration and fate by carbon-bearing minerals and their phase transformations. (iii) The development of mineral-based technologies for carbon reduction and sequestration, as well as functional mineral materials for CCUS applications. These research directions are inherently interdisciplinary, with core scientific challenges centered not only on understanding mineral structures and interfacial reactivity, but also on elucidating their interactions with fluids, organic matter, and biological systems within relevant natural and engineered environments as well as industrial systems.

This presentation will briefly illustrate the roles and potential of minerals and mineral-based materials in achieving carbon neutrality through case studies of clay minerals in low-carbon construction materials and marine carbon sequestration. The results highlight emerging mineralogical pathways for carbon mitigation and contribute to advancing both the theoretical framework and practical applications of mineralogy in addressing global climate change.

Key words: Carbon neutrality, Carbon-neutral mineralogy, Mineral-enhanced biological pump, Low-carbon construction materials, Clay minerals.

CLIMATE-DRIVEN SHIFTS IN THE CARBON SEQUESTRATION EFFICIENCY OF REACTIVE IRON MINERALS IN THE ARCTIC SHELF

Jiazong Du, Limin Hu

College of Marine Geosciences, Ocean University of China, Qingdao, ChinaAffiliation

Abstract The organic carbon (OC) stored in the Arctic permafrost accounts for almost half of the global soil OC reservoir, with reactive iron oxides (Fe_R) playing a crucial role in sequestrating and stabilizing the labile permafrost OC. Under global warming and Arctic amplification in recent decades, the thawing of Arctic permafrost, increased river runoff, and enhanced coastal erosion have not only accelerated the release and transition of permafrost OC in the land-ocean continuum, but also likely altered the flux of Fe_R-associated OC (OC-Fe_R), thereby affecting the burial of permafrost OC in the marginal seas and its feedback to climate warming. Therefore, reconstructing the burial records of OC-Fe_R and the environmental response mechanisms in the Arctic is essential for accurately assessing the role of mineral protection in the carbon neutrality in a natural setting. This study investigated the burial of OC-Fe_R in sediments from the East Siberian Arctic Shelf over the last decades. It was found that an average of 19.82% of OC is bound to Fe_R, and this association occurs during terrestrial transport and marine deposition prior to burial. Comparing to the coastal erosion-affected region, the burial of OC-Fe_R in estuarine exhibits temporally-distinct responses to permafrost thawing dynamics in the watershed. By integrating permafrost environmental parameters in the Lena River watershed, such as permafrost temperature, moisture, active layer thickness, and precipitation, this study uncovered the response of OC-Fe_R burial to the terrestrial permafrost-climate dynamics. Specifically, during the pre-2000s, the progressive decline in OC-Fe_R coincided with watershed-scale soil moisture redistribution driven by gradual active-layer deepening, which preferentially retained OC-Fe_R in permafrost, attenuating its land-to-ocean fluxes. Since 2000s, although abrupt thaw has rapidly mobilized OC, ~19% of sedimentary OC remained stabilized as OC-Fe_R, thus partially decoupling abrupt thaw from immediate permafrost carbon-climate feedbacks. Therefore, this mineralogical buffering mechanism can attenuate the net climate impact of accelerating abrupt thaw across the Northern Hemisphere cryosphere.

Key words: organic carbon burial, iron-associated organic carbon, permafrost degradation, Arctic shelf

COUPLED MECHANISMS OF ARAGONITE PRECIPITATION AND CARBON FIXATION DRIVEN BY OLIVINE–BENTHIC DIATOM SYNERGY

Rongda Yu[1,2], Dong Liu[1,2*], Zhiming Liu[1,2], Yuguo Shen[1,2], Xu Wang[1,2],Guangcheng Huo[1,2], Peng Yuan[3]

6. State Key Laboratory of Advanced Environmental Technology, Guangzhou Institute of Geochemistry, Chinese Academy of Sciences, China
7. University of Chinese Academy of Sciences, China
8. School of Environmental Science and Engineering, Guangdong University of Technology, China

Abstract The weathering of silicate minerals such as olivine in seawater can consume CO_2 and release alkaline ions that increase seawater alkalinity, and is therefore considered a potentially effective pathway for marine negative emissions. However, how olivine input interacts with key marine organisms such as diatoms, and how it influences diatom carbon fixation and the efficiency of the biological pump, remain poorly understood. To address this issue, we investigated a benthic diatom–olivine system by integrating solution chemistry, mineralogical analyses, and microstructural observations to explore the effects of olivine addition on the marine carbon pump and its underlying mechanisms. Our results show that olivine input significantly enhanced organic carbon fixation in the benthic diatom system, as reflected by an increase in particulate organic carbon (POC), indicating greater accumulation of organic carbon within the system. Meanwhile, benthic diatoms were able to induce aragonite precipitation, and this process was further strengthened by the addition of olivine. Mineralogical and microstructural evidence showed that aragonite formed predominantly at diatom-associated extracellular interfaces, suggesting that this mineralization process was regulated by the bio–mineral interfacial microenvironment. Further analyses indicate that the promoting effect of olivine cannot be simply attributed to changes in bulk water chemistry, but is more likely associated with the induction of diatom metabolism by nutrients and dissolved components released during olivine dissolution, thereby stimulating extracellular polymeric substance (EPS) production and enhancing interfacial nucleation capacity. Considering that carbonate precipitation releases CO_2, while diatoms continuously assimilate CO_2 through photosynthesis, we propose that in this system olivine metabolically induces the simultaneous enhancement of particulate organic carbon (POC) and particulate inorganic carbon (PIC) formation, while allowing part of the CO_2 released during precipitation to be re-assimilated and fixed by diatoms. This results in a mineral–biological coupled process linking organic carbon fixation and inorganic carbon mineralization. Overall, this study reveals a coupled enhancement mechanism between diatom organic carbon fixation and aragonite mineralization under olivine input. Our findings indicate that the carbon sink effect of mineral

weathering is not determined solely by bulk water chemistry, but is regulated by key biological processes and further strengthened through mineral–biological interactions. These results provide new insights into the actual carbon sequestration potential of mineral weathering and its biological constraints.

Key words: Olivine, Benthic diatoms, Aragonite precipitation, Carbon fixation, Mineral–biological interactions.

Acknowledgements This study was supported by the ONCE, the National Natural Science Foundation of China (42188102, 42272043 and 42172047), and Guang Dong Basic and Applied Basic Research Foundation (2024B1515040003 and 2023B1515120004).

DEVELOPING PREDICTIVE POWER TO GUIDE THE USE OF ACTIVATED CLAYS IN LOW/ZERO CARBON CEMENTS

Alastair T.M. Marsh[1,2]

1. Laboratory of Construction Materials, Swiss Federal Institute of Technology Lausanne, Switzerland
2. School of Civil Engineering, University of Leeds, United Kingdom

Abstract Cement-based materials make up ~73% by mass of all human-made materials produced each year, and contribute ~7% of annual human-made CO_2 emissions. The cement industry's global target is to reach Net Zero by 2050. To minimise the reliance on costly Carbon Capture Utilisation and Storage (CCUS) technologies, a major decarbonisation strategy is to further reduce the proportion of carbon-intensive clinker in cements. This is achieved by replacing clinker with supplementary cementitious materials (SCMs). Activated clays have high potential to meet the increased global demand for SCMs in future years, due to the global abundance of clays. Activation methods for clays include both thermal routes (i.e. calcination), and mechanical routes involving intensive grinding. A challenge in the widespread adoption of activated clay SCMs is the inherent variability in the composition and mineralogy of clays. Adoption of activated clay SCMs has progressed fastest in tropical regions containing abundant quantities of kaolinitic clays, which are well-suited to thermal activation. In contrast, Europe has a prevalence of 'common clays' containing multiple clay minerals alongside various associated minerals. The European cement sector is familiar with using industrial by-products as SCMs (e.g. fly ash, blast furnace slag), which – unlike clays - have broadly consistent compositions. The mineralogical diversity of common clays thereby poses a challenge for selecting clays, and activation conditions, for manufacturing activated clay SCMs.

To overcome this challenge, I will present two complementary research approaches which can be used to develop greater degree of predictive power for the selection of clays and activation conditions. 1) Inductive reasoning: a generalized conclusion is drawn from a set of individual instances. I.e. Large numbers of naturally-occuring clays are investigated, and the influence of individual mineralogical parameters is inferred from semi-statistical trends. 2) Deductive reasoning: a generalized conclusion is established, and then applied to individual instances. I.e. Controlled experiments are carried out on 'synthetic clays' assembled from high-purity individual minerals, in which specific variables are isolated. Both research approaches have advantages and drawbacks. I will present examples from our recent research for how these two complementary approaches can be used to improve our fundamental understanding of processing-structure-properties relations for activated clays. And, how the greater predictive power from these findings can support guidelines for the industrial selection of clays and activation processes.

Key words: clays, clay minerals, cement, calcination, mechano-chemical activation

DIVERGENT STRATEGIES FOR ACCESSING PARTICULATE IRON IN DIATOMS UNDER PERVASIVE OCEANIC IRON LIMITATION

Jing Sun[1,*], Benjamin C. Bostick[2], Peng Yuan[3], Haohao Luo[1,4], Bo Jiao[1,4], Chao Li[1], Yue Cai[5], Fangyuan Meng[1,4], Chengshuai Liu[1,6]

1. Institute of Geochemistry, Chinese Academy of Sciences, Guiyang 550081, Guizhou, China
2. Lamont-Doherty Earth Observatory of Columbia University, Palisades, NY 10964, USA
3. Guangdong University of Technology, Guangzhou 510006, Guangdong, China
4. University of Chinese Academy of Sciences, Beijing 100049, China
5. Nanjing Institute of Geology and Palaeontology, Chinese Academy of Sciences, Nanjing 210008, Jiangsu, China
6. South China Agricultural University, Guangzhou 510642, Guangdong, China

Abstract Iron (Fe) supply to the surface ocean shapes the climate-relevant carbon cycle. Much of this Fe occurs as dust-derived mineral particulates and is widely assumed to become bioavailable only through slow dissolution. Here we show that phytoplankton with appropriate physiological machinery can exploit mineral-hosted Fe to sustain growth. We grew two globally distributed model diatoms, Phaeodactylum tricornutum and Thalassiosira pseudonana, on poorly soluble dust-relevant minerals in axenic cultures with identical bulk Fe concentrations. While T. pseudonana grew in proportion to each mineral's abiotic solubility, P. tricornutum overcame dissolution limitation through two additional strategies. It autonomously elevated the soluble unchelated Fe pool via proximal dissolution and accessed Fe from certain silicate minerals through a contact-dependent, solubility-independent pathway potentially involving iron starvation-induced protein 3 (ISIP3). These results indicate that particulate Fe bioavailability depends on Fe mineralogy and phytoplankton-mediated processes, challenging prevailing paradigms of dust-borne Fe utilization and redefining its ocean-climate impacts.

Key words: Dust-derived minerals, Iron mineralogy, Diatom iron acquisition, Ocean productivity

EFFECT OF CLAY MINERALS ON CARBON DIOXIDE HYDRATE FORMATION: INSIGHTS FROM MOLECULAR DYNAMICS SIMULATION STUDY

Yun Li

School of Petroleum Engineering, Xi'an Shiyou University, Xi'an 710065, China

Abstract Carbon capture and storage is an important clean energy technology that aims to capture the emission of carbon dioxide (CO_2) from industrial processes. CO_2 storage in the hydrate phase of natural gas hydrate deposits is considered a promising approach to greenhouse gas control. The mineral composition is an important factor affecting the formation of CO_2 hydrate. Clay minerals (i.e., montmorillonite, illite, kaolinite, mixed-layer mineral, etc.) are widespread in marine sediments. The layered structure and surface properties of clay minerals can potentially affect CO_2 hydrate nucleation. Therefore, exploring the nucleation mechanism of CO_2 hydrate in clay minerals would greatly improve our understanding of the role of minerals in the CO_2 hydrate formation.

Here we investigate the heterogeneous nucleation of CO_2 hydrate on the external surfaces of clay minerals (i.e., montmorillonite, illite, kaolinite, chlorite, and talc) by molecular dynamics simulations. The results showed that CO_2 hydrate nucleation occurred far away from the surfaces of montmorillonite and illite. No CO_2 hydrate nucleation occurs on the siloxane surface of kaolinite and talc due to the formation of CO_2 nanodroplets. Of particular interest is that the clathrate-like structures formed on the siloxane surface of chlorite due to its electric charge. Additionally, the clathrate-like structures were also formed between the interfacial water and hydroxyl surfaces of kaolinite and chlorite. The results of this study clearly indicate that the surface groups of clay minerals significantly affect CO_2 hydrate nucleation by changing the distribution of CO_2 and water molecules, which finally influences CO_2 storage in deposits and have profound impacts on related geochemical processes, such as interfacial interactions between water molecules and clay surfaces.

Key words: CO_2 hydrate, clay mineral, external surface, molecular dynamics simulation

FROM DISSOLUTION TO NETWORK INCORPORATION: MECHANISTIC INSIGHTS INTO THE ROLE OF IRON IN ACID-ACTIVATED GEOPOLYMERIZATION

Baifa Zhang, Peng Yuan, Ting Yu, Zhenhua Pan

School of Environmental Science and Engineering, Guangdong University of Technology, China

Abstract The transition toward carbon neutrality has driven increasing interest in developing low-carbon cementitious materials derived from mineral resources and solid wastes. Geopolymers, synthesized from aluminosilicate minerals, are promising alternatives to ordinary Portland cement due to their reduced carbon dioxide footprint and broad raw material availability. Among these resources, Fe-bearing minerals are widely distributed in natural systems and industrial wastes; however, their role in geopolymerization, particularly under acid-activation conditions, remains poorly understood from a mineralogical perspective.

In this study, the role of iron during acid-activated geopolymerization was systematically investigated using metakaolinite as a model mineral precursor. Two typical Fe-bearing minerals (hematite (HE) and magnetite (MA)) and two representative Fe sources (iron powder (IP) and ferric chloride (FC)) were selected to investigate the influence of mineral dissolution and Fe availability on reaction kinetics, structural evolution, and mechanical performance. The results demonstrate that Fe contribution was strongly governed by its dissolution behavior. Sparingly soluble phases (HE and MA) largely persisted as inert fillers, contributing limited to gel chemistry. Their addition slightly densified the matrix at low contents due to filler effects, whereas higher contents reduced strength due to dilution effect. Comparatively, acid-soluble Fe (IP and FC) actively participated in geopolymer network formation. Although low Fe contents initially impaired strength by inducing microstructural heterogeneity, increased Fe incorporation significantly enhanced compressive strength, with 28-d compressive strength increasing by 74.6% and 103.3% at 10% IP and FC, respectively. Spectroscopic analyses indicated that the release of Fe^{3+} can incorporate in amorphous geopolymer network as distorted octahedral units, forming Fe(III)-O-P-O-Al-O-Si network without new crystalline phases. Notably, the Fe^{2+} leached from IP can also participate geopolymerization prior to oxidation, forming Fe(II)-O-P-O-Al-O-Si network.

These findings highlight that controlling Fe dissolution and mineral transformation pathways is essential for optimizing geopolymer performance. This work provides new insights into the reactivity of Fe-bearing minerals and their transformation into functional binding phases, offering a viable pathway for the sustainable utilization of Fe-rich resources.

Key words: Carbon neutrality, Fe-bearing minerals, Geopolymerization, Acid activation, Kaolinite

MAGNESIUM EXTRACTION FROM OLIVINE VIA SULPHATION ROASTING FOR CO_2 SEQUESTRATION: REACTION MECHANISM, KINETICS, AND PROCESS OPTIMIZATION

Bojun Yin[1,2], Fang Xia[1], Hans C. Oskierski[1], Yuan Mei[1,2]

1. Sustainable Geochemistry and Mineral Sciences, School of Mathematics, Statistics, Chemistry and Physics, Murdoch University, Australia
2. CSIRO Mineral Resources, Australia

Abstract Olivine, a highly abundant Mg-rich silicate, is a promising feedstock for large-scale CO_2 sequestration through mineral carbonation. However, its practical application is severely limited by the extremely slow dissolution of olivine under ambient conditions, which restricts Mg extraction for reacting with CO_2 to form stable carbonates. Ammonium sulphate roasting has emerged as an effective approach to accelerate Mg extraction from olivine for subsequent mineral carbonation in industrial reactors. The process is promising for its reagent recyclability, environmental friendliness, and lower energy demands. Despite its potential, the reaction mechanisms, rate-controlling processes of sulphation roasting, and strategies to maximise Mg extraction remain poorly understood. To address these knowledge gaps, we conducted systematic sulphation roasting experiments in the temperature range of 300–500 °C and carried out a comprehensive investigation using powder X-ray diffraction (PXRD), scanning electron microscopy with energy dispersive spectroscopy (SEM-EDS), transmission electron microscopy with EDS (TEM-EDS), atomic absorption spectroscopy (AAS), *in situ* synchrotron PXRD, and kinetic analysis.

Results show that ammonium sulphate decomposes and melts rapidly at around 350 °C, forming molten sulphate phases within minutes. These molten sulphate phases rapidly react with olivine and extract Mg and Fe to form soluble metal sulphates and intermediate ammonium metal sulphates that form a porous outermost layer surrounding olivine particles. During roasting, the residual silicate framework of the reacted olivine simultaneously transforms to an amorphous silica layer that encapsulates the unreacted olivine core. This silica layer acts as a diffusion barrier, causing surface passivation and leading to a diffusion-controlled shrinking-core reaction mechanism. Kinetic analysis based on the *in situ* synchrotron PXRD experimental data confirm internal diffusion control with an apparent activation energy of ~33 kJ mol^{-1}.

Two effective approaches for overcome silica passivation were identified. Fine grinding significantly enhances Mg extraction from 42% for particles <75 μm to 60% by reducing the size to <20 μm and to 88% by reducing the size to <7 μm. Repetitive roasting–leaching cycles also provide an effective pathway to disrupt the passivating silica layer. For example, using particles <75 μm, Mg extraction increased from 42% in a single roasting–leaching step to 79% after five roasting–leaching

cycles.

These findings provide new mechanistic and kinetic insights into ammonium sulphate roasting of olivine and significantly advance the technical understanding of olivine-based mineral carbonation. The results also identify practical strategies to mitigate silica passivation, thereby improving the feasibility of using olivine for large-scale CO_2 sequestration.

Key words: Olivine, Ammonium sulphate roasting, Reaction mechanism, Kinetics, Silica passivation

MECHANISTIC INSIGHTS INTO MG CARBONATES FORMATION PATHWAYS

Yechan Chang, Kideok D. Kwon

Geology, Kangwon National University, Republic of South Korea

Abstract CO_2 mineralization using magnesium-bearing materials is a promising strategy for large-scale, permanent CO_2 sequestration. However, the mechanistic controls on Mg carbonate formation remain poorly constrained. Although magnesite ($MgCO_3$) is the most stable phase thermodynamically, laboratory precipitation at ambient conditions typically yields hydrated phases such as nesquehonite ($MgCO_3 \cdot 3H_2O$) and hydromagnesite ($Mg_5(CO_3)_4(OH)_2 \cdot 4H_2O$) instead of magnesite. This discrepancy suggests strong kinetic limitations, commonly attributed to its strong hydration energy of Mg^{2+} ions in aqueous solution, but the thermodynamic and kinetic barriers among these Mg carbonates are not clearly defined. In this study, we performed first-principles calculations based on density functional theory (DFT) to examine the relative energetics and nucleation barriers of anhydrous and hydrated Mg carbonates. Temperature-dependent reaction Gibbs free energies, $\Delta_r G$ (T), confirmed that magnesite is the most stable phase throughout all temperature range, while the relative stability of the hydrated phases varies with temperature. Nesquehonite is more stable than hydromagnesite below approximately 300 K but becomes less stable than hydromagnesite above this temperature. These results are consistent with experimental observation of the nesquehonite to hydromagnesite transition at elevated temperature and subsequent magnesite formation on further heating. To assess kinetic constraints, we calculated the nucleation energy barriers through surface energies of each phase; at 298 K, estimated barriers were 268 kJ/mol for magnesite, 43 kJ/mol for hydromagnesite, and 1 kJ/mol for nesquehonite. The substantially high barrier of magnesite arises from high surface energy relative to hydrous Mg carbonates, explaining its limited formation under ambient conditions. These results provide a quantitative thermodynamic and kinetic framework that reconciles observed precipitation pathways relevant for optimizing Mg-based CO_2 mineralization strategies.

Key words: DFT, thermodynamic stability, Mg carbonates, CO_2 mineralization

MINERAL-DEPENDENT CARBONATE AND GREENHOUSE-GAS FINGERPRINTS OF ENHANCED WEATHERING IN FLOODED RICE PADDIES

Zhaofeng Ouyang, Simon A.T. Redfern

Asian School of the Environment, NTU Singapore, Singapore

Abstract Enhanced rock weathering (ERW) in agricultural soils is commonly evaluated under upland cropland assumptions, yet flooded rice paddies impose a distinct hydrological and redox boundary on mineral dissolution, carbonate formation and greenhouse-gas exchange. Here we present a first-year field-scale MRV study from a replicated rice-paddy experiment in Chongqing, China, designed to compare basalt and wollastonite amendments under contrasting particle-size, dose, biochar and fertilization contexts. Across 36 main plots, we combined floodwater total alkalinity, TIC and TOC measurements with time- and depth-resolved soil chemistry, aggregate fractions, event-based CH_4, N_2O and CO_2 fluxes, crop traits, yield components, meteorological records and continuous pH sensing.

The dataset shows that paddy ERW generated mineral-dependent monitoring fingerprints rather than a uniform carbon-removal response. Wollastonite produced the clearest alkalinity-carbonate signal, expressed through stronger floodwater TA/TIC enrichment and soil pH/SIC responses, consistent with rapid Ca-silicate dissolution and carbonate-pathway activation. Basalt responses were detectable but more context-dependent, with relatively stronger expression in agronomic or structural co-benefits. Biochar modified these mineral pathways instead of acting as a universal weathering amplifier. Event-based gas analysis further showed that CH_4 and N_2O responses were not synchronized with carbonate indicators, emphasizing that non-CO_2 gases must be incorporated into paddy ERW-MRV. Strict quality control of continuous pH records revealed episodic and baseline-sensitive monitoring windows, indicating that pH can guide targeted TA/TIC calibration sampling but cannot replace alkalinity measurements. These results suggest that rice-paddy ERW should be evaluated as an integrated water-soil-gas-yield system, where mineralogy controls both carbon-removal fingerprints and deployment trade-offs.

Key words: Enhanced rock weathering, rice paddy, wollastonite, basalt, MRV

MINERALS CONTRIBUTE TO THE ENHANCEMENT OF THE OCEAN CARBON PUMP

Dong Liu[1,2*], Rongda Yu[1,2], Xu Wang[1,2], Yuguo Shen[1,2], Guangcheng Huo[1,2]

1. State Key Laboratory of Advanced Environmental Technology, Guangzhou Institute of Geochemistry, Chinese Academy of Sciences, China
2. University of Chinese Academy of Sciences, China

Abstract In response to the growing challenges of global climate change and rising atmospheric CO_2 levels, mineral-driven ocean negative emission technologies (such as mineral-enhanced biological pump, MeBP) have emerged as a promising solution for achieving carbon neutrality due to their cost-effectiveness, environmental compatibility and long-term carbon sequestration potential. This study presents, for the first time, a systematic investigation of minerals' multi-level enhancement mechanisms and proposes an innovative "mineral-mediated synergistic ocean carbon pump enhancement" strategy by coupling key ocean carbon pump processes, offering new theoretical and applied frameworks for marine negative emissions. Our findings reveal that minerals play key roles in strengthening the ocean carbon sink: 1) alkalify increase and carbonate precipitation through mineral weathering; 2) nutrient release optimization and diatom productivity improvement simultaneously; 3) accelerated refractory carbon formation and sinking via mineral-organic matter interactions. This enables synergistic effects between the carbonate pump, biological pump, and microbial carbon pump. Compared to conventional carbon sequestration approaches, our strategy overcomes the limitations of single-mechanism interventions through minerals' multifunctional coupling effects, providing both theoretical foundation and practical methodology for engineered marine carbon sink enhancement. These advances not only deepen our understanding of mineral-driven mechanisms in the global carbon cycle but also present innovative solutions for climate change mitigation and carbon neutrality achievement.

Key words: Mineral-mediated, Ocean carbon pump, Synergistic effects, Negative emissions, Carbon neutrality

Acknowledgements This study was supported by the ONCE, the National Natural Science Foundation of China (42188102, 42272043 and 42172047), and Guang Dong Basic and Applied Basic Research Foundation (2024B1515040003 and 2023B1515120004).

MONTMORILLONITE-OLIVINE COMBINATION FOR SYNERGISTIC ENHANCEMENT OF MARINE DIATOM-DRIVEN CARBON SEQUESTRATION

Fucheng Yao[1], Peng Yuan[1,*], Wei Yan[1], Rongda Yu[2], Dong Liu[2]

1. School of Environmental Science and Engineering, Guangdong University of Technology, Guangzhou 510006, China
2. State Key Laboratory of Advanced Environmental Technology, Guangzhou Institute of Geochemistry, Chinese Academy of Sciences, Guangzhou 510640, China

Abstract Building on the biological pump and the “iron hypothesis”, ocean iron fertilization (OIF) has been widely explored in high-nutrient, low-chlorophyll (HNLC) regions to stimulate phytoplankton blooms and enhance atmospheric CO_2 uptake. However, although OIF effectively induces phytoplankton blooms, it shows limited improvement in the efficiency of particulate organic carbon (POC) export to the deep ocean. To address this limitation in OIF, the “Mineral-enhanced Biological Pump” (MeBP) was proposed, aiming to enhance the transport of diatom-derived carbon to deep sea by adding clay minerals such as montmorillonite.Coastal enhanced weathering (CEW) represents another carbon dioxide removal strategy, involving the dispersion of silicate minerals in coastal environments to accelerate weathering, increase alkalinity, and facilitate CO_2 sequestration. Olivine, a magnesium iron silicate mineral, is characterized by high natural abundance (the most abundant mineral in the Earth's mantle) and relatively rapid weathering rate, and has been proposed as one of the primary candidate minerals for CEW applications.Montmorillonite and olivine are key candidate minerals for the MeBP and CEW strategies, respectively. However, the effects of their combined application in diatom-rich seawater on diatom-driven carbon sequestration remain unclear. In particular, whether the combination of clay minerals and olivine can synergistically enhance marine carbon sequestration under specific conditions has not yet been determined. These questions are important for developing effective diatom-driven carbon sequestration strategy but remain unexplored.In this study, microcosm experiments were conducted to investigate the effects of combined addition of montmorillonite and olivine on the growth and primary productivity of the diatom Thalassiosira weissflogii, as well as their interfacial interactions. The results showed that montmorillonite released more dissolved silicon than olivine in seawater over a short period, providing a richer silicon source for diatoms. This effectively promoted the diatom growth, total chlorophyll a concentration, and POC production. However, the addition of olivine alone had limited effects on promoting the diatom growth and the POC production. Notably, the combined application of both minerals exhibited a synergistic effect on diatom-derived POC accumulation and diatom growth. Meanwhile, aggregation between montmorillonite and diatom frustules and the incorporation of Al into frustule

structures can jointly enhance the protection of diatom-derived POC. In addition, the combined addition also increased seawater pH. These findings reveal the synergistic enhancement of the montmorillonite–olivine combination on the diatom biological pump, offering new insights and experimental evidence for the potentially comprehensive application of MeBP and CEW strategies to enhance marine carbon sequestration.

Key words: Clay minerals, Mineral-enhanced biological pump, Ehanced silicate weathering, Carbon dioxide removal, Carbon neutral mineralogy

Acknowledgements This study was supported by Science and Technology Planning Project of Guangdong Province (2023B1515120004), National Natural Science Foundation of China (42272043, 42188102, 42172047), Science and Technology Planning Project of Guangdong Province (2024B1515040003), Guizhou Province Technology Support Plan Project (2024031), and National Special Support for High-Level Personnel.

PROBING ORGANIC MATTER-MINERAL INTERACTIONS WITH AMINO ACIDS: A MOLECULAR PERSPECTIVE WITH A VIEW TOWARDS MEGASCALE CARBON SEQUESTRATION

Thomas Michael Blattmann

Asian School of the Environment, Nanyang Technological University, Singapore

Abstract Soils and sediments, the uppermost veneers of Earth's surface, play key biogeochemical roles as major pools storing and exchanging carbon with the atmosphere prior to geological sequestration. Today, Earth is facing unprecedented climate change due to human perturbation of the carbon cycle. To meet this global challenge, I advocate for research to understand biogeochemical processes from molecular to mega scale across the soil-sediment spectrum which essentially comprises complex mineral matrices embedded with carbon in the form of organic matter that are in tight association with one another. Among these organic constituents, amino acids represent one of the most ubiquitous classes of organic molecules essential for all life on Earth. The universal and abundant presence of amino acids allows us to compare their interactions with minerals across Earth's diverse environments. Investigations carried out on soil and sediment showcase direct evidence for the role of phyllosilicates in modulating the stabilization and preservation of amino acids. These patterns reflect molecular-level interactions consistent with laboratory-based experimental sorption studies yet also reveal processes operating beyond the observational range of laboratory experiment timescales. This study makes the case for using amino acids as molecular probes of organic matter-mineral interactions for understanding organic carbon sequestration in earthen matrices. These molecular perspectives will be placed in a megascale Earth system context for understanding the role of minerals in stabilizing organic matter and how this weighs against the impact of other mechanisms such as chemical weathering in natural and enhanced scenarios of carbon sequestration.

Key words: Amino acids, organic geochemistry, radiocarbon, organomineral, source-to-sink

THE ROLE OF MONTMORILLONITE IN IRON SUPPLY TO DIATOMS AND ITS POTENTIAL APPLICATION

Xu Wang[1, 2, 3], Dong Liu[1, 2, 3], Hao Liu[1, 2, 3], Rongda Yu[1, 2, 3], Mengyuan Li[1, 2, 3], Yuguo Shen[1, 2, 3], Guangcheng Huo[1, 2, 3]

1. (State Key Laboratory of Advanced Environmental Technology, Guangzhou Institute of Geochemistry, Chinese Academy of Sciences, China)
2. (Guangdong Provincial Key Laboratory Of Mineral Physics And Materials, Guangzhou Institute of Geochemistry, Chinese Academy of Sciences, China)
3. (University of Chinese Academy of Sciences, China)

Abstract Ocean Iron Fertilization (OIF) is the largest carbon-negative emission strategy to date, designed to mitigate atmospheric CO_2 by enhancing oceanic carbon pumps. However, the dissolution of diatom frustules (biogenic silica) during organic carbon sinking disrupts the ballasting effect, limiting the efficiency of the biological pump. The Mineral-enhanced Biological Pump (MeBP) strategy proposes that clay minerals such as montmorillonite can inhibit diatom silica dissolution, thereby improving the efficiency of the biological pump. Montmorillonite naturally contains iron, yet it remains uncertain whether this iron can be mobilized at the diatom-mineral interface, potentially stimulating diatom metabolism and enhancing carbon sequestration. To address this question, this study investigated the interactions between the marine diatom *Chaetoceros* sp and montmorillonite under iron-limited conditions, focusing on montmorillonite's role as an iron source. The results demonstrated that: (1) diatom-mineral interfacial interactions facilitated iron release from montmorillonite, with setae playing a key role in mineral-biological interactions; (2) montmorillonite effectively served as an iron source, promoting diatom proliferation: The chlorophyll a content increased by 46.15%during the 8-day logarithmic growth phase of the alga; and (3) montmorillonite as an iron source significantly enhanced carbon sequestration efficiency in the system. Its addition increased particulate organic carbon (POC) production by 24.63% compared to the control group. Furthermore, montmorillonite addition exhibited potential to amplify vertical carbon flux.

Key words: montmorillonite; diatoms; carbon negative emissions; iron fertilization; biological pump efficiency enhancement

Acknowledgements This study was supported by the ONCE, the National Natural Science Foundation of China (42188102, 42272043 and 42172047), and Guang Dong Basic and Applied Basic Research Foundation (2024B1515040003 and 2023B1515120004).

THERMAL–MECHANOCHEMICAL ACTIVATION MECHANISM OF MUSCOVITE CLAY

Weijie Chen, Mingshuai Zhang, Biqin Dong, Yanshuai Wang*

College of Civil and Transportation Engineering, Shenzhen Key Laboratory for Low carbon Construction Material and Technology, Guangdong Provincial Key Laboratory of Durability for Marine Civil Engineering, Shenzhen University, Shenzhen, 518060, China

Abstract Enhancing the reactivity of structurally stable T–O–T clay minerals such as muscovite remains a critical challenge for their use in alkali-activated materials. In this study, a sequential thermal–mechanochemical activation (T–MCA) strategy was proposed to improve the structural disruption and chemical reactivity of muscovite. The synergistic effects of thermal–mechanochemical treatment on muscovite's structural evolution and dissolution behavior were systematically investigated. Multi-scale structural analyses revealed that thermal treatment induced only partial dehydroxylation and minor atomic-level disorder, while mechanochemical activation introduced surface defects but failed to significantly alter the crystalline framework. In contrast, the T–MCA approach produced a higher degree of amorphization and disorder, leading to enhanced alkaline dissolution of Si and Al species and improved early-stage reactivity. Further results indicated that thermal pre-treatment weakened interlayer bonding, facilitating more extensive lattice disruption during subsequent mechanical processing. Such synergistic effect highlights the potential of the T–MCA strategy for activating highly crystalline aluminosilicates and offers a viable pathway for utilizing muscovite as an alternative precursor in alkali-activated materials, particularly in regions where conventional reactive materials are scarce.

Key words: Muscovite, Thermal–mechanochemical activation, Structural evolution, Dissolution behavior, Alkaline Reactivity

APATITE ARCHIVES REE BEHAVIOUR DURING FORMATION OF THE MOUNT WELD CARBONATITE, WESTERN AUSTRALIA

Anderson Santos[1], Artur Deditius[1], Arthur Vicentini[2], Hans Oskierski[1], Ganesh Bhat[3], Denis Fougerouse[2]

9. School of Mathematics, Statistics, Chemistry and Physics, Murdoch University, Australia
10. School of Earth and Planetary Sciences, Curtin University, Australia
11. Mt Weld Mining Pty Limited, Australia

Abstract Apatite is an excellent mineral archive that records the Earth's evolution through variation in its trace-element composition. In this study, 21 representative samples were collected from six diamond drill cores (maximum depth of 1020m) that probe the lithology of the circular (~4km in diameter) Mount Weld Carbonatite (MWC) intrusion. A combination of imaging and micro-analytical techniques helped identify five generations of hydroxyl- and/or fluorapatite (average Cl ~500 ppm) in calcite carbonatite and associated phoscorites, fluorocarbonatite-ferroan dolomite carbonatite (FDC), phosphate-ferroan dolomite carbonatite (PDC), and fluorite-apatite-ferroan dolomite carbonatite (FADC).

The first crystallising magmatic apatite (Ap1) in phoscorite and calcite carbonatite exhibits similar chemical composition but different textures. Pill-shaped Ap1a displays a blue-to-dark purple patchy cathodoluminescence (CL), contains calcite inclusions in the core, and has partially embayed rims. It occurs in phoscorite and is associated with magnetite, phlogopite, forsterite, calcite, and euhedral pyrochlore. Oscillatory-zoned Ap1b, characterized by alternating violet and green CL zones, formed cumulates of ovoidal grains in phoscorite and calcite carbonatite, and replaced Ap1a. Fine-grained, porous Ap2 of a consistent blue CL response contains microinclusions of Sr-Ba-REE carbonates. This metasomatic apatite is the most common apatite type in FDC, where it formed turbid overgrowths on or partially replaced Ap1b. Ap2 is associated with zoned Fe-dolomite, REE-fluorocarbonate, amphibole, and phlogopite. The late hydrothermal Ap3 is anhedral, fine-grained, and REE-depleted, displaying mottled yellow to green luminescence. The blue-violet in CL Ap4 is the dominant apatite type in the PDC, where it overgrew Ap3, formed massive aggregates, colloform bands, and pore linings. It is associated with monazite, sphalerite, phlogopite, and siderite. Ap5 occurs exclusively in FADC. It formed massive aggregates associated with fluorite and displays bright purple luminescence, recording a late-stage F-rich hydrothermal event.

The earliest apatite generations, Ap1 and Ap2, contain relatively low Sr concentrations (<1 wt.%). Strontium was enriched during the subsequent hydrothermal event associated with REE mineralization, as indicated by Ap3-Ap5 (2-4 wt.% Sr). Ap1 and Ap2 are relatively enriched in Si (1000-5000 ppm) compared with the later generations of Ap3-Ap5 (<500 ppm of Si). The relatively

high Mn concentrations in Ap1 (100-300 ppm) decreased during the formation of Ap2 (<<100 ppm), increased to 100-3000 ppm in Ap3 and Ap4, and then dropped to 10-20 ppm in Ap5. Sodium concentrations in all apatites are highly variable (500-5000 ppm). Uranium concentrations in all apatites range from below the detection limit to 40 ppm. In contrast, Ap2 and Ap3 are enriched in Th (30-1000 ppm).

Three main stages of REE mineralization were identified based on the variation in REE concentrations in apatite: (i) magmatic (Ap1) and metasomatic (Ap2) stages incorporating 800-20,000 ppm of REE_{total}; (ii) depletion of REEs during formation of Ap3 (300-1300 ppm of REE_{total}) conciding with crystallization of PDC; and (iii) final hydrothermal stages marked by renewed REE enrichment in Ap4 and Ap5, reaching up to ~2 wt.%, coeval with monazite precipitation. The steep chondrite-normalized REE patterns of Ap1 record LREE enrichment; $(La/Yb)_N$ from 33-170 and $(La/Sm)_N$ from 1-4. Similar slopes, but an order of magnitude depletion in REE occurs in Ap3. The HREE enrichment was recorded by Ap2, characterised by HREE/LREE ~1:1, $(La/Yb)_N$ from 0.5-20, $(La/Sm)_N$ from 0.1-2.5, and bell-shaped REE patterns (maxima from Nd-Tb). Ap4 and Ap5 show $(La/Yb)_N$ values of 20-120 but $(La/Sm)_N$ values of 0.6-3, documenting the increase in the MREE concentrations during the final stages of hydrothermal REE mineralization.

This study documents the complex behavior and distribution of REEs at Mt Weld. Early stages of the MWC emplacement witnessed LREE enrichment during formation of calcite carbonatite and phoscorite, followed by HREE metasomatic event during ferroan dolomite carbonatite formation, and final MREE enrichment driven by hydrothermal fluids.

Key words: apatite, carbonatite, phoscorite, rare earth elements, Mount Weld

Acknowledgements The authors acknowledge the funding from Mineral Research Institute of Western Australia (MRIWA; M10422), Lynas Rare Earth Limited, and the Exploration Incentive Scheme (Western Australian State Government). Additional support was provided by Curtin University and Murdoch University in Perth, WA. The authors extend their gratitude to the Microscopy and Microanalytical Facility at the John de Laeter Centre, Curtin University, and the Centre for Microscopy, Characterization, and Analysis at the University of Western Australia.

APATITE CA-SR SOLID SOLUTIONS FROM THE SAIMA PERALKALINE COMPLEX, CHINA: INSIGHTS INTO MAGMATIC-HYDROTHERMAL CONTROLS ON REE MINERALIZATION

Bin Wu[1], Wentao Li[1], Zhe Nan[2], Xingqing Xing[2], Fujun Zhong[1], Qingfei Wang[1]

1. National Key Laboratory of Uranium Resources Exploration-Mining and Nuclear Remote Sensing, East China University of Technology, China
2. No. 241 Group Co., Ltd., Liaoning Geological Exploration and Mining Group, China

Abstract Apatite, a significant host of rare earth elements (REE), is widespread in various rock types. Here we investigated a near-continuous Ca-Sr solid solution series in apatite (including a new mineral fluorsigaiite, $Ca_2Sr_3(PO_4)_3F$) from the Saima peralkaline complex, to trace REE behavior during magmatic and hydrothermal stages. Apatite grains from different paragenetic stages exhibit homogeneous initial $^{87}Sr/^{86}Sr$ (0.7083–0.7089) and εNd(t) values (-10.5 to -14.4), indicating a stable Sr-Nd isotopic system during crystallization and subsequent alteration. During the early magmatic sequence from primitive lamprophyre through syenite to nepheline syenite, the REE budget and LREE-HREE fractionation were dominantly controlled by apatite crystallization. Systematic decreases in apatite SO_3 content and volatile ratios (X_{Cl}/X_{OH}, X_{Cl}/X_F) record a decrease in melt oxygen fugacity and an increase in H_2O saturation, which efficiently promoted REE and volatile enrichment in the most evolved lujavrite, where intense REE mineralization produced relatively HREE-enriched silicates such as eudialyte. Subsequently, an autometasomatic fluid enriched in Na^+, Sr^{2+}, $LREE^{3+}$, CO_3^{2-}, PO_4^{3-}, and F^- exsolved from the lujavrite, decomposing earlier REE minerals and precipitating hydrothermal LREE-phosphates and carbonates at 220.0 ± 2.4 Ma. Hydrothermal apatite from this stage is characterized by coupled Sr and REE enrichment, facilitated by the fluid-mediated substitutions $Ca^{2+} \leftrightarrow Sr^{2+}$, $2Ca^{2+} \leftrightarrow REE^{3+} + Na^+$, and $Ca^{2+} + P^{5+} \leftrightarrow REE^{3+} + Si^{4+}$. The pronounced LREE-HREE fractionation observed in hydrothermal apatite is attributed to prior magmatic sequestration of HREE into early crystallized silicates and the higher compatibility and mobility of LREE in alkaline, carbonate-rich fluids. The Saima complex underwent three REE mineralization stages: an early magmatic stage dominated by disseminated apatite, a late magmatic stage concentrating HREE in eudialyte, and a hydrothermal stage precipitating LREE-enriched phosphates and carbonates.

Key words: Peralkaline rocks, rare earth elements, apatite Ca-Sr solid solutions, Saima complex

Acknowledgements This study was funded by the National Natural Science Foundation of China (Grant No. 42562011 and 42272087), and the Jiangxi Provincial Natural Science Foundation (Grant No. 20232BCJ23003 and 20242BAB27002).

CARBONATE AND SULFATE: KEY LIGANDS IN CARBONATITE-RELATED REE MINERALIZATION

Richen Zhong*, Hao Cui

Abstract Sulfate minerals are ubiquitous in carbonatite-related rare earth element (REE) deposits and are closely associated with REE minerals. In recent years, the role of sulfate-rich geofluids in REE transportation has been highlighted by natural sample analysis and geochemical experiments. However, recent studies argue that carbonate, rather than sulfate, plays dominant roles in REE mobilization, as evidenced by experimental results demonstrating that carbonate-rich geofluids can effectively dissolve REE minerals under alkaline conditions.

By integrating experimental results with observations from geological samples, this study evaluates the respective roles of both carbonate and sulfate in REE mobilization. Previous work has demonstrated that alkaline carbonate-rich fluids (e.g., Na_2CO_3 solutions) can dissolve significant amounts of bastnäsite, indicating that these fluids can co-transport REE and fluoride. This explains the REE enrichment observed in the Na_2CO_3-rich fluids (or brine-melts) during the early evolution of natrocarbonatite melts. However, as the carbonate-rich fluids (or brine-melts) interact with silicate country rocks (e.g., during anti-skarn metasomatism), the fluids become increasingly acidic, evidenced by the widespread presence of CO_2 bubbles in the fluid inclusions of carbonatite-related REE deposits (e.g., Maoniuping). Our experimental results show that $NaHCO_3$-rich fluids, which are more acidic than Na_2CO_3 fluids, have a very limited ability to dissolve bastnäsite. In contrast, experiments on bastnäsite dissolution in Na_2SO_4-rich solutions reveal that sulfate-rich fluids can also efficiently co-transport REE and fluoride, regardless of fluid acidity. This explains the geological observation that CO_2-rich fluid inclusions in carbonatite-related REE deposits contain large volumes of sulfate daughter minerals, but much less carbonate, along with bastnäsite daughter minerals.

Based on these results, we propose a genetic model highlighting the important roles of both carbonate and sulfate in REE transport. In the early-stage evolution of natrocarbonatite—the principal ore-forming melt for most REE deposits—Na_2CO_3 dominates the brine-melt composition and facilitates REE mobilization through carbonate ligand complexation. When fluid (or brine-melt)-rock interaction shifts the system from alkaline to acidic conditions, thereby destabilizing REE-carbonate complexes and diminishing the fluid's transport capacity. At this stage, sulfate ligands take over as the primary agents for REE mobilization.

CHALCOPHILE AND HIGHLY SIDEROPHILE ELEMENTS IN ORE-FORMING SYSTEMS - NEW INSIGHTS INTO GEODYNAMIC PROCESSES AND ACCUMULATION OF MINERAL DEPOSITS FROM THE UNESCO WORLD HERITAGE HARZ AND ITS ORE MINES

Sabine Dietrich

Alumna Technical University Berlin, Germany

Abstract Ore-forming systems in the Earth's crust commonly display rhythmic patterns such as banded formations, layered and folded structures, diapirs or cockade ores that can range in scale from just the micron, and even sub-micron-scale, up to several kilometres. This topic has been examined from a thermochemical-mechanical perspective for a long time, including chalcophile and highly siderophile elements bearing systems. Here, the concept of self-organisation is applied to ore-forming systems. Recognising ore-forming systems as ordered structures implies that they are considered as systems in which their components and properties are distributed in space and time, providing fundamental aspects to decipher their genesis. The complexity in describing connections and feedback between contributing key processes can thus be diminished, leading to an enhanced understanding and achievable numerical simulations.

The concept was proven by examination of a recent, early diagenetic banded iron-manganese mud in an abandoned underground mine that had accumulated over 40 years. Two years of in-situ testing revealed that the self-organising nature of the precipitated material was not only caused by fluctuations but also by interaction with redox, colloid, microbial, electrical, and Ostwald-ripening processes. A genetic model for the banded mineralisation was developed and successfully validated by numerical simulation. Moreover, gradients, such as concentration gradients, electric fields, and the like, as well as temperature and pressure, enabled a coupling of the ongoing processes that is spatially and temporally far-reaching. Such thinking could allow other information about geological and ore-forming processes to be revealed, which is otherwise hidden by time, environmental conditions or by location.

In the case provided here the concept is applied to the "richest ore" of Rammelsberg and the carbonate-rich iron ore of the Oberharzer diabase-lineament. An overview of the large-scale geological setting and ore types at the local scale will be given, along with the findings of the so-called Jacob-experiment, by which as an ore forming factor electric potentials are used, which commonly are going along with volcanic activities.

Key words: ore-forming systems, cross phenomena, electric field, self-organization, complexity

Acknowledgements The author would like to thank Professor Min Eng K.-H. Jacob, the colleagues at the former Department of Applied Geosciences and Mineral Deposits Research and the Department of Mathematics and Natural Sciences at the Technical University Berlin for the fruitful multi-year scientific cooperation.

CHALCOPYRITE DISEASE "IN-FECTION" IN SPHALERITE: NANOSCALE INSIGHTS INTO INCORPORATION AND ENRICHMENT OF INDIUM

Zhen Wang[1,2], Denis Fougerouse[1,2], Joachim Krause[3], Steven M. Reddy[1,2], David W. Saxey[1,2], William D. A. Richard[2], Zakaria Quadir[2], Laura Petrella[2], Jens Gutzmer[3,4]

1. School of Earth and Planetary Sciences, Curtin University, Perth, Australia
2. Geoscience Atom Probe Facility & Microscopy and Microanalysis Facility, John de Laeter Centre, Curtin University, Perth, Australia
3. Helmholtz-Zentrum Dresden-Rossendorf, Helmholtz Institute Freiberg for Resource Technology, Freiberg, Germany
4. Institute of Mineralogy, Technische Universität Bergakademie Freiberg, Freiberg, Germany

Abstract Chalcopyrite ($CuFeS_2$) disease was first coined to describe a naturally occurring ore texture in sphalerite from various sulfide deposits. It is characterized by the presence of a high density of (sub)micrometer-size inclusions of chalcopyrite within sphalerite. Such ore texture has been widely used to interpret the paragenesis of sulfide mineralization and understand the processes of ore formation. In addition, the occurrence and abundance of discrete sulfide inclusions are also often used to explain the enrichment and distribution of trace elements in sphalerite. Indium is a common trace element found in sphalerite and is globally recognized as a critical metal due to its vital role in modern technologies. Copper has been shown to play a fundamental role in the incorporation of In via coupled substitution Cu(I) + In(III) = 2Zn(II) and in many cases of In-rich sphalerite where chalcopyrite inclusions are common. However, much of our current knowledge on the correlation on In and Cu has been underpinned only at the microscale, and yet there is a lack of understanding of the processes responsible for both the formation of chalcopyrite inclusions and the incorporation of In in sphalerite at the nanoscale.

In this work, we present atom probe tomography (APT) and transmission electron microscopy (TEM) data to better understand the nanoscale relationships between the Cu and In in chalcopyrite-diseased, In-enriched sphalerite from the Hämmerlein skarn deposit in western Erzgebirge (Germany). Previous work by Bauer et al. (2019) (https://doi.org/10.1007/s00126-017-0773-1) has shown that the studied sphalerite crystals represent a second generation of sphalerite and are associated with chalcopyrite and pyrite that together form veins in a prominent unit of magnetite skarn. Our APT data reveal the heterogeneous nanoscale distributions of Cu, In, and Fe and the occurrence of discrete nanophases in the studied sphalerite. In specimen from the core of sphalerite crystals with moderate copper and indium content (around 2 at.%), nanoscale rhythmic bandings of Cu, In, and Fe are observed. These bands reflect the presence of crystallographically oriented nanoplatelets within the sphalerite matrix, possibly due to sub-solidus exsolution or epitaxial

intergrowth. This likely indicates a primary process for the incorporation of Cu and In (Cu/In atomic ratio ~1) during the formation of the sphalerite. In specimens from the crystal rims and healed cracks that are highly enriched in Cu and In (i.e., up to 20 at.% for Cu and 11 at.% for In), intricately intergrown chalcopyrite and roquesite ($CuInS_2$) with curviplanar boundaries are observed. The formation of these phases can be explained by diffusion-induced segregation during a secondary enrichment of Cu and In (Cu/In atomic ratio > 1) at oxidizing conditions. Overall, the results of our work reveal previously inaccessible nanoscale information about Cu, In, and Fe distribution in sphalerite and provide valuable mechanistic insights into chalcopyrite disease and In incorporation and enrichment. Such nanoscale information can be used to help identify and prospect new resources for critical metal In as well as improve its economic extraction from corresponding ore minerals and waste materials.

Key words: Critical minerals, Indium, Exsolution, Diffusion, Nanoscale investigation

Acknowledgements The authors acknowledge the access to the Geoscience Atom Probe Facility at the John de Laeter Centre, Curtin University, which is part of the Advanced Resource Characterization Facility (ARCF) supported by the Science and Industry Endowment Fund. This work was funded by a grant from the Helmholtz-Zentrum Dresden-Rossendorf, Germany to J.K. and the Australian Research Council Future Fellowship Project (FT240100041) awarded to D.F.

CHARACTERISTICS OF NB-TA ENRICHMENT IN DIFFERENT TYPES OF HIMALAYAN LEUCOGRANITIC SYSTEM

Kexin Xu, Lei Xie*, Rucheng Wang, Huan Hu

State Key Laboratory of Critical Earth Material Cycling and Mineral Deposits, School of Earth Sciences and Engineering, Nanjing University, Nanjing 210023, China

Abstract The Himalayan Orogen is characterized by the widespread occurrence of leucogranites related to variable rare-metal mineralization, particularly Be-Nb-Ta-Li-Cs enrichment. These rare-metal-bearing granites commonly contain accessory minerals, including beryl and Nb-Ta oxide minerals, while the associated granitic pegmatites exhibit additional minerals assemblages such as spodumene, lepidolite, and elbaite, characteristic of highly fractionated magmatic systems. These minerals crystallize throughout the entire magmatic-hydrothermal processes and display complex textures and compositions. To elucidate the interrelationship among rare-metal-bearing minerals during the magmatic evolution, this study investigates diverse types of rare metal-enriched leucogranites and granitic pegmatites in the Lhozhag district of eastern Himalaya, with particular emphasis on the Lalong dome and the eastern Kulakangri dome. The Lalong dome is dominated by Li-F-poor leucogranitic facies, exemplified by albite granites and beryl pegmatites. In contrast, the eastern Kulakangri dome hosts more abundant lithologies, including not only Li-F-poor albite granites and beryl pegmatites, but also contains Li-rich spodumene pegmatites and Li-F-rich lepidolite-elbaite pegmatites.

In Li-F-poor leucogranitic systems, Nb and Ta are mainly hosted in columbite group minerals (CGMs), samarskite group minerals (SGMs), and the Ta-rich phase tapiolite. Nb-Ta enrichment is mainly controlled by magmatic fractional crystallization, evidenced by compositional evolution toward Ta-rich endmembers. Moreover, tapiolite forms under non-equilibrium conditions during extreme magmatic fractionation. Contrastingly, in Li-(F-)rich leucogranitic system, Nb-Ta carriers expand to include CGMs, SGMs, and pyrochlore group minerals (PGMs), with Ta-rich phases dominated by microlite. Across lithologies, CGMs exhibit a systematic Mn-enrichment trend: from albite granites and beryl pegmatites (Mn-poor compositions) through spodumene pegmatite, to elbaite-lepidolite pegmatites (Mn-rich endmembers). This evolved trend likely reflects dual controls— magmatic fractional crystallization coupled intensive hydrothermal fluid activity. The presence of fluid-phase indicators such as lepidolite, hafnian zircon (with up to 37.31% HfO_2), and microlite further indicates the key role of volatile components (e.g., Li, F, B) in rare-metal enrichment within the Lhozhag district. Particularly, variable Cs-bearing minerals in Li-F-rich lepidolite-elbaite pegmatite, including pollucite (with up to 32.24% Cs_2O), lepidolite (up to 2.96% Cs_2O), and beryl (up to 2.19% Cs_2O). Pollucite occurs as individual crystals and aggregates, with Si/Al atomic ratios of 2.18-2.32 and 2.34-2.69, respectively, suggesting formation in two distinct stages—late fluid-rich magmatic stage and subsequent hydrothermal stage.

In summary, three distinct types of rare-metal leucogranitic systems have been identified within the Himalayan Orogen, Li-F-poor, Li-rich and Li-F-rich systems. The unique accessory minerals, especially the Nb-Ta oxide minerals, serves as critical indicators for deciphering the magmatic-hydrothermal evolutional pathways and degree of magmatic fractionation.

Key words: Nb-Ta oxide minerals, Magmatic-hydrothermal processes, extreme fractionation, fluxing components, Lhozhag

Acknowledgements This study was supported by the National Natural Science Foundation of China (Grant No. 42222202) and National Key Research and Development Program of China (2024YFC2909301).

CHARACTERISTICS OF ORGANIC AEROSOL AND MINERALS FROM COAL FIRE BASED ON HIGH-RESOLUTION MASS SPECTROMETRY

Ming Liang, Yuzhuo Liu

College of Geology and Environment, Xi'an University of Science and Technology, Xi'an 710054, China

Abstract A coal fire is a phenomenon in which a coal seam, following prolonged exposure to air, undergoes spontaneous oxidation leading to self-ignition; it subsequently develops into a substantial scale, posing a hazard to the surrounding environment. Such fires not only result in the loss of coal resources but also emit vast quantities of toxic and harmful gases, mercury, and particulate matter (aerosols), thereby posing a grave threat to both the ecological environment and human health. Given the complex composition and diverse origins of aerosols, their precise characterization remains a challenging task. Consequently, identifying molecular markers that are representative of coal fire sources is of paramount importance. Focusing on the typical coal fire zone in Wuda as our study area, we characterized and analyzed the organic components of collected particulate matter (PM2.5). Our findings revealed that the samples contained not only fly ash, aluminosilicates, and coal dust particles but also an abundance of polycyclic aromatic hydrocarbons (PAHs)—specifically, a complex molecular series comprising "16 PAHs + R-PAHs + HOOC-PAHs + HCO-PAHs." By integrating existing literature with statistical methodologies, we have preliminarily identified naphthalene and phenanthrene as a potential combination of molecular markers for organic aerosols originating from coal fires. This discovery holds promise for resolving the issue of unidentified sources of regional environmental organic aerosols, thereby providing a foundational basis for research into atmospheric environmental health.

Key words: Coal, Minerals, Particulate matter, Mass spectrometry

CHARACTERISTICS OF SEDIMENTARY LITHIUM RESOURCES AND THE APPLICATION OF LITHIUM ISOTOPES IN TRACING SURFACE WEATHERING

Na You, Hongfei Cheng*

School of Earth Science and Resources, Chang'an University, China

Abstract With the explosive growth in demand for lithium resources driven by the new energy industry, sedimentary lithium resources, an emerging strategic resource with abundant reserves and wide distribution, have made their metallogenic mechanism and efficient development a research hotspot. As abundant yet underutilized resources, the separation, extraction and efficient utilization of sedimentary lithium resources are restricted by their mineralization characteristics and lithium occurrence states. Simultaneously, the chemical weathering of continental silicate rocks — a key process driving atmospheric CO_2 sequestration and Cenozoic climate cooling —has been intensively studied using non-traditional lithium isotopes. As a critical component of global geochemical cycles, lithium (Li) is mainly hosted in silicate minerals and is little affected by carbonate weathering and biological uptake, making Li isotopes an ideal tracer for silicate weathering. During chemical weathering, primary minerals dissolve and release Li into aqueous solutions, while secondary clay minerals preferentially adsorb light ^{6}Li, leading to significant Li isotopic fractionation between dissolved and solid phases. This fractionation is modulated by hydrological conditions, mineralogy, and weathering intensity, enabling the reconstruction of weathering processes, paleoclimate shifts, and tectonic interactions across modern, glacial-interglacial, and deep-time scales. This leaching, transport, and clay-adsorption enrichment process is not only the core mechanism of continental chemical weathering but also the key metallogenic process of sedimentary lithium resources, especially clay-type lithium deposits. Current challenges include resolving controversies in isotope-weathering correlations, accurately interpreting sedimentary lithium isotope signals, and optimizing efficient lithium extraction technologies. Future research should integrate high-precision testing, multi-isotope systems, and mineralogical characterization to advance both fields, providing robust scientific support for China's lithium resource exploration, green extraction, and strategic energy security.

Key words: sedimentary lithium resources, Li isotopes, silicate weathering

CHARACTERIZATION OF HYDRATED REE-BEARING PHOSPHATES: INSIGHTS INTO REE MINERALIZATION IN A CRYPTIC SKARN REGOLITH SETTING FROM DORADILLA, NSW, AUSTRALIA

Rory Carter[1,2], Ian Graham[1], Indrani Mukherjee[1], David French[1], Mathias Kapo[1], Karen Privat[1,3], Oliver Davies[4]

1. Earth and Sustainability Science Research Centre, School of Biological, Earth and Environmental Sciences, University of New South Wales, Australia
2. Mineral Exploration Cooperative Research Centre, School of Biological, Earth and Environmental Sciences, University of New South Wales, Australia
3. Electron Microscopy Unit, Mark Wainwright Analytical Centre, University of New South Wales, Australia
4. Sky Metals Pty Ltd., Orange, Australia

Abstract The rare earth elements (REE) are a group of elements comprising the lanthanides (La-Lu) + yttrium (Y). Demand for the REE has been rapidly increasing in recent years due to critical applications in advanced technologies. As a result, many countries have classified the REE as critical elements, reflecting their importance to modern society.

Most current global production of REE comes from carbonatite-related systems (primary and weathered laterite profiles) and more recently discovered ionic adsorption clay-hosted deposits (IADs). REE enrichment is known in several additional settings such as alkaline igneous systems, heavy mineral sands, offshore placer deposits, and a growing number of clay-hosted settings over various protoliths that often show no appreciable REE concentration, with REE enrichment attributed entirely to weathering processes. In these clay-hosted environments, determining the mode of occurrence (detrital minerals, secondary mineralization or IADs) of the REE is critical to informing the enrichment mechanisms, particularly in cryptic, novel environments.

The Doradilla region, located in middle-northern NSW, Australia, is centered on a complex Sn-polymetallic skarn. Analysis of historic drill cuttings in the regolith revealed significant REE enrichment (up to 1.4 wt. % TREO) in weathered skarn horizons. Further analysis confirmed this enrichment throughout the entire 16 km+ strike length of the weathered skarn body at Doradilla. Preliminary metallurgical extraction using ammonium sulphate (AS) leaching at a solution pH of 4 and 3 was unsuccessful for economic extraction of REE. This suggests a negligible portion of ionically adsorbed REE within the regolith at Doradilla, and thus, the system is not an IAD. Therefore, REE enrichment at Doradilla must be hosted in minerals and this study was carried out to determine the REE-bearing mineralogy.

Results indicate that the REE mineralization in the regolith at Doradilla is dominated by REE-bearing phosphates. Textural evidence suggests thin horizons (commonly 1-3 m) of abundant, very fine-grained (200 nm – 2 μm) REE minerals. These frequently occur intergrown with secondary Fe and Ti oxides, in clusters infilling space within co-occurring gangue minerals. The dominant LREE-bearing phase has a La, Nd dominant EDS spectra, with minor Ca and trace S commonly noted. A marked Ce-depletion is commonly seen. This Ce-depletion is explained by the presence of cerianite. Cerianite is locally abundant, concentrated in zones with abundant Mn oxides, suggesting they served as effective oxidants during the oxidation of Ce^{3+} to Ce^{4+} and subsequent immobilization of Ce in cerianite (CeO_2) in the highly oxidizing sub-surface environment. The de-coupling of Ce through immobilization can explain the subsequent depletion in the LREE-rich phosphates. The only HREE phase identified displays an intimate association with detrital zircon, developing as a fine-grained rim. EDS of the HREE phase highlights a Y-dominance, with more subordinate HREE peaks (Dy – Lu), and, again, minor Ca is ubiquitous.

The common REE-bearing phosphates (monazite (LREE) and xenotime (HREE)) have hydrated analogues (rhabdophane (LREE) / churchite (HREE)). Identifying the presence of water in these minerals is critical to understanding how they formed (anhydrous phosphates = detrital system likely / hydrous phosphates = secondary mineralization). Laser Raman was utilized to analyze both the LREE and HREE-bearing phosphates. Peaks in the Raman shift were identified in the characteristic OH stretching region of ~3000 – 3500 cm^{-1}, thus confirming the presence of water, and that these minerals are hydrated.

As a result, the REE-bearing mineralogy at Doradilla is defined here as: rhabdophane-(La) ($La(LREE,Ca)PO_4 \cdot {}_nH_2O$) and churchite-(Y) ($Y(HREE,Ca)PO_4 \cdot 2H_2O$), formed in the secondary environment during weathering of the protolith skarn and regolith formation. The confirmation of the mineralogy in this novel, skarn regolith setting suggests that a wider range of currently known protoliths have the potential to produce significant clay-hosted REE enrichment through secondary mineralization.

Key words: Rhabdophane, churchite, regolith, skarn, rare earth element (REE)

CHARACTERIZING THE EVOLUTION OF BERYLLIUM MINERAL SEQUENCES IN GRANITE-RELATED MINERALIZING SYSTEM

Yutao Lin [1,2], Rucheng Wang[1,2*], Xudong Che[1,2], Jianjun Lu[1,2], Huan Hu[1,2]

1. State Key Laboratory of Critical Earth Material Cycling and Mineral Deposits, School of Earth Sciences and Engineering, Nanjing Universit, China
2. Frontiers Science Center for Critical Earth Material Cycling, Nanjing University, China

Abstract Beryllium (Be), a critical metal, is vital for its superior functional and structural material properties, and granite-related systems represent an important source of Be. The Shizhuyuan deposit in Hunan Province is a world-class giant polymetallic deposit located at the contact zone between the southeastern part of the Qianlishan granite complex and Devonian limestone. The orebody extends approximately 1200 m in length, 1000 m in width, and 50-500 m in vertical thickness, forming a lenticular geometry and is associated with W-Sn-Mo-Bi mineralization and accompanied by beryllium. It represents an ideal natural laboratory for studying the enrichment of rare metals in magmatic–hydrothermal systems. In this study, we focused on identifying Be-bearing minerals directly within the parent zinnwaldite granite and found abundant euhedral to subhedral beryl, revealing a series of spatially continuous Be mineralization from the proper magmatic granite type to greisen, skarn, and vein types in the Shizhuyuan deposit. We employed multiple in situ techniques (EMPA, LA-ICP-MS, FIB-TEM) to identify beryllium minerals across different types of mineralization. Fractional crystallization is consistent with the primary mechanism for magmatic stage enrichment, which leads to widespread beryllium mineralization in the system. The mineral sequence of beryllium provides an indicator of magmatic–hydrothermal geochemical evolution, where the spatial variation in mineral assemblages consistently reflects a dynamic regular variation of temperature and the relative chemical potentials (silica activity and alumina activity) from proximal to distal. Moreover, through comparisons with other granitic beryllium mineral systems worldwide, we provide a continuous beryllium mineral sequence model. This observed Be mineral sequence provides critical spatial vectors and geochemical indicators to effectively delineate mineralization loci in complexly metasomatized peripheral zones within the metasomatic halos of granite-related beryllium systems.

Key words: beryllium minerals, mineral sequence evolution, granite-related mineralizing system

COMPLEX SPODUMENE–PETALITE PEGMATITES FROM THE MOUNT QOMOLANGMA REGION, HIMALAYAN LEUCOGRANITE BELT: IMPLICATIONS FOR FLUID PROCESS AND LI MINERALIZATION

Zhi-Hao Xu [1], Ru-Cheng Wang [1*], Lei Xie [1], Xiao-Chi Liu [2,3], Fu-Yuan Wu [2,3]

1. State Key Laboratory of Critical Earth Material Cycling and Mineral Deposits, School of Earth Sciences and Engineering, Nanjing University, Nanjing 210023, China
2. State Key Laboratory of Lithospheric Evolution, Institute of Geology and Geophysics, Chinese Academy of Sciences, Beijing 100029, China
3. College of Earth and Planetary Sciences, University of Chinese Academy of Sciences, Beijing 100049, China

Abstract The Himalayan orogenic belt is characterized by widespread leucogranite magmatism, which is closely associated with lithium (Li) mineralization. This study focuses on complex spodumene–petalite pegmatites and their wall rocks from the Ra Chu section in the Mount Qomolangma region, aiming to constrain the key processes controlling Li enrichment within a coupled pegmatite–wall rock system. An integrated approach combining mineralogy, geochemistry, thermal modeling, and elemental diffusion modeling is applied to evaluate the contributions of magmatic differentiation, fluid processes, and tectonic activity to mineralization. The Ra Chu pegmatites belong to a highly evolved lithium–cesium–tantalum (LCT) pegmatite system, enriched in Li, Be, Nb, and Ta. Early magmatic crystallization led to progressive enrichment of Li in the residual melt, resulting in the formation of coarse-grained spodumene and petalite in the core under variable pressure conditions. The intermediate and wall zones record significant magmatic–hydrothermal overprinting, characterized by fine-grained petalite, vein-type petalite crosscutting earlier-formed minerals, and widespread alteration of spodumene, indicating exsolution and migration of volatile-rich fluids. In the surrounding marble wall rocks, Li-bearing minerals are also well developed, including spodumene and petalite—typically restricted to granitic pegmatites—as well as holmquistite. Late-stage volatile-rich, Li-bearing fluids released from the pegmatites migrated into the carbonate wall rocks along structurally controlled fractures. During fluid–rock interaction, decarbonation reactions, alkali consumption, and SiO_2 supply collectively regulated the local chemical environment, leading to the crystallization of spodumene, petalite, and holmquistite through metasomatism and mineral reactions. Thermal modeling indicates that the thermal effect induced by pegmatite emplacement was short-lived (on the order of tens of days) and spatially limited (~1–2 m), providing only the necessary temperature conditions for the formation of Li minerals in the wall rocks. Elemental diffusion modeling demonstrates that, within this timescale, solid-state diffusion is insufficient to account for Li transport over meter-scale distances and cannot explain the observed distal Li

enrichment in the wall rocks. Therefore, Li migration and enrichment were primarily controlled by advective transport of late-stage Li-rich fluids, with Li also incorporated into metamorphic minerals (e.g., biotite, scapolite, diopside, and tourmaline) as a result of fluid flow. At the regional scale, the South Tibetan Detachment System (STDS) facilitated magma emplacement, fluid exsolution, and fluid migration through extensional tectonics and decompression. Consequently, Li mineralization in the Ra Chu area reflects an integrated system in which pegmatites and wall rocks are not independent, but instead form a unified, tectonically controlled and fluid-driven Li metallogenic system. This study provides new insights into rare-metal mineralization processes and important implications for Li exploration in orogenic belts.

Key words: Himalayan leucogranite belt, Pegmatite–wall rock, Li mineralization, Fluid, South Tibetan Detachment System

CONTRASTING SPHALERITE GEOCHEMISTRY IN OROGENIC AND INTRACONTINENTAL HYDROTHERMAL SYSTEMS: INSIGHTS FROM THE HAOPINGGOU AND FANKOU DEPOSITS, CHINA

Dexian Zhang[1,2], Jinbo Liu[1,2], Ziqi Hu[1,2] and Dian Xiao[1,2]

1. School of Geosciences and In-physics, Central South University, China
2. Key Laboratory of Metallogenic Prediction of Nonferrous Metals and Geological Environment Mintoring (Central South University), Ministry of Education, China

Abstract As a ubiquitous sulfide in low-to-medium temperature hydrothermal systems, sphalerite serves as a robust geochemical archive of the physicochemical evolution of ore-forming fluids. Its crystal chemistry and trace element partitioning are sensitive indicators of temperature (T), sulfur fugacity (fS_2), and redox state (fO_2). This study conducts a systematic comparative analysis of sphalerite from two distinct metallogenic regimes: the Haopinggou orogenic gold-polymetallic deposit (Qinling Orogen) and the Fankou giant Pb-Zn deposit (South China Block). By integrating paragenetic constraints with in-situ LA-ICP-MS trace element analysis, EPMA, and sulfur isotope geochemistry, we delineate the typomorphic geochemical contrasts between orogenic and intracontinental mineralization and their implications for deep-seated fluid evolution.

Our results reveal fundamental disparities in the micro-textures and geochemical fingerprints of sphalerite between these settings. In the Haopinggou deposit, mineralization is intrinsically linked to Mesozoic collisional orogeny. Sphalerite primarily precipitated during the main polymetallic sulfide stage, coexisting with pyrite, chalcopyrite, and galena as disseminated or massive aggregates. Trace element signatures are characterized by significant enrichments in Fe, Mn, In, and Cu, consistent with high-temperature (mesothermal) and relatively reduced hydrothermal fluids. Elevated In/Ga and In/Ge ratios, coupled with high Fe concentrations, indicate a predominant contribution from metamorphic dehydration or magmatic-hydrothermal fluids. We propose a metallogenic model involving rapid fluid ascent along crustal-scale shear zones, followed by fluid mixing and boiling triggered by tectonic uplift and decompression during the late-orogenic phase.

Conversely, the Fankou deposit represents a quintessential intracontinental system governed by lithospheric extension and large-scale basinal brine migration. Fankou sphalerite manifests complex textural varieties, including colloform, rhythmic-banded, and brecciated structures with prominent oscillatory growth zoning. Geochemically, this sphalerite is Fe-Mn depleted but exceptionally enriched in critical metals and dispersed elements, specifically Ge, Ga, Cd, Tl, and Sb. The characteristically low In/Ga and In/Ge ratios, alongside a diagnostic "Ge-rich and In-poor" signature, identify the ore-forming medium as low-temperature, high-salinity basinal brines. Detailed substitution mechanism analysis suggests that Ge and Ga are incorporated into the lattice

via complex coupled substitutions: $Cu^{+} + Ga^{3+} \leftrightarrow 2Zn^{2+}$ and $2Cu^{+} + Ge^{4+} \leftrightarrow 3Zn^{2+}$. These signatures are fundamentally tied to intensive water-rock interaction and thermochemical sulfate reduction (TSR) within organic-rich carbonate sequences, which provided the reduced sulfur necessary for massive sulfide deposition.

In summary, the geochemical divergence between Haopinggou and Fankou sphalerite reflects the fundamental distinction between compressive-shear orogenic environments and extensional intracontinental settings. The former represents an Fe-In-rich system driven by deep crustal processes (metamorphism/magmatism), while the latter represents a Ge-Ga-rich system driven by geothermal gradients and basinal brine circulation. The contrasting Fe-Mn-In vs. Cd-Ga-Ge assemblages provide high-fidelity geochemical indicators for regional deposit classification. These findings underscore the utility of sphalerite trace element systematics as a discriminative tool for identifying tectonic settings and directing deep-seated mineral exploration in complex polycyclic orogenic belts.

Key words: Sphalerite geochemistry, LA-ICP-MS, Orogenic gold-polymetallic deposit, Intracontinental mineralization

CRYSTAL DEFECTS DRIVE GOLD REMOBILISATION IN SULPHIDES

Denis Fougerouse[1,2], Steven M. Reddy[1,2], David Saxey[2], Nicolas Thebaud[3], Laura Petrella[2], Zhen Wang[1,2], Joël Brugger[4]

1. School of Earth and Planetary Sciences, Curtin University, Perth, Australia
2. Geoscience Atom Probe Facility, John de Laeter Centre, Curtin University, Perth, Australia
3. Centre for Exploration Targeting, The University of Western Australia, Crawley, Australia
4. School of Earth, Atmosphere & Environment, Monash University, Clayton, Australia

Abstract Gold hosted in sulphides represents a large proportion of the gold resource globally. Sulphide-hosted gold is refractory, meaning that its liberation requires a full destruction of the crystals. Yet, gold can be remobilised naturally during geological processes through fluid-rock interaction and deformation. In pyrite, the general driving force of the re-equilibration reaction is the minimisation of free energy from a distorted pyrite lattice due to the incorporation of impurities, as well as tectonic strain, to a pyrite closer to stoichiometric composition and strain-free. In Arsenopyrite, fluid-mediated dissolution-reprecipitation has been proposed as the sole mechanism for gold remobilization. Yet, the mechanisms operating at the nanoscale for the remobilisation of gold in pyrite and arsenopryite remains poorly understood. Here, we apply a multiscale characterisation workflow using electron backscatter diffraction (EBSD), nanoscale and time-of-flight secondary ion mass spectrometry (NanoSIMS and ToF-SIMS), and atom probe tomography (APT) on selected gold-bearing pyrite and arsenopyrite to determine the factors controlling the remobilisation of gold. Pyrite from the Jundee (Yilgarn Craton, Australia) and Huangjindong (Jiangnan Orogen, China), and arsenopyrite from Fosterville (Lachlan Orogen, Australia) and Obuasi (West African Craton, Ghana) were investigated.

At the micrometre scale, a textural and microstructural analysis demonstrate that the crystals are oscillatory zoned and record minor to no evidence for crystal-plastic deformation. When deformed, the distribution of gold is noticeably affected, either depleted or enriched, in low-angle boundaries.

At the nanoscale, gold can either be depleted or enriched along dislocations. In pyrite, gold was enriched in dislocations forming a deformation-related low-angle boundary of the Huangjindong deposit and along a re-equilibration front at Jundee. In the arsenopyrite of Fosterville, gold was depleted in low-angle boundaries and at Obuasi, gold was weakly enriched in dislocations close to the re-equilibration front.

Taken together, our observations indicate that three main mechanisms are active in gold-bearing sulphides, including crystal-plastic deformation, fluid-mediated dissolution-reprecipitation and dislocation-mediated interfacial re-equilibration. In all cases, nanoscale data highlight the

importance of crystal defects, in particular dislocations, for the mobility of gold. Dislocations have been documented to collect gold through their migration during crystal-plastic deformation. Dislocations can also be utilised as fast diffusion and/or fluid pathways for localised dissolution-reprecipitation reactions to occur and the extraction of gold from the sulphides. Finally, dislocations located at the interface between arsenic-gold-rich pyrite and arsenic-gold-poor pyrite, control mass transfer and the progression of the re-equilibration reaction. These observations suggest that mineralogical processes such as fluid-mediated re-equilibration or chemical modification during recrystallisation are fundamentally controlled by dynamic crystal defects.

Key words: Fast diffusion, Element mobility, Invisible gold, Crystal-plastic deformation, Dissolution-reprecipitation.

Acknowledgements This study is supported by Australian Research Council (LP200200897 and FT240100041) and Mineral Research Institute of Western Australia funding.

DECIPHERING THE 'PURGE OF IMPURITIES' EFFECT: TIN SPECIATION EVOLUTION AND SELECTIVE DISSOLUTION DURING HYDROTHERMAL CASSITERITE RECRYSTALLIZATION

Yiqu Xiong, Hongfei Di

State Key Laboratory of Metallogenic Prediction of Nonferrous Metals and Geological Environment Monitor, Ministry of Education, School of Geosciences and Info-Physics, Central South University, Changsha 410083, China

Abstract Multi-stages superimposed tin (Sn) mineralizations in hydrothermal systems are commonly accompanied by the dissolution and reprecipitation process (DRP) of cassiterite. However, the role of cassiterite DRP in Sn enrichment remains ambiguous. To investigate this, a natural cassiterite (Yongde cassiterite) crystallized in a single metallogenic event with pure geochemical compositions, was used for crystallization experiments in $SnCl_2$–HCl–H_2O and $SnCl_4$–HCl–H_2O systems using both hydrothermal diamond anvil cell (HDAC) and cold seal pressure vessel (CSPV). HDAC experiments show that the Yongde cassiterite (Cst 1) was soluble in both the $SnCl_2$–HCl–H_2O and $SnCl_4$–HCl–H_2O systems during heating, while secondary cassiterite (Cst 2) crystallized in both systems during cooling. Notably, Cst 1 exhibited higher solubility in the $SnCl_2$–HCl–H_2O system, evidenced by its lower initial dissolution temperature (430 ℃) compared to the $SnCl_4$–HCl–H_2O system (500 ℃). Raman spectra collected on the Cl-bearing aqueous solution in the HDAC sample chamber suggests that Sn(II)–Cl is always significant in the hydrothermal transport of Sn, whereas Sn(IV)–Cl is significant only for relatively oxidized conditions. Major and trace element analysis of the Cst recovered after CSPV experiments demonstrates the enrichment and depletion of elements during cassiterite DRP. In the $SnCl_2$–HCl–H_2O system, SnO_2 is enriched, while Ti, Fe, and Zr are depleted in Cst 2. In the $SnCl_4$–HCl–H_2O system, Al, Sb, and W are enriched, while Ti, Fe, Zr, Hf, and Ta are depleted in Cst 2. The content variations of redox-sensitive elements (e.g., Al, Sb, W) and temperature-sensitive elements (e.g., Ti, Fe, Zr) reflect dynamic redox and temperature-driven purification during cassiterite DRP, wherein impurity elements (e.g., Ti, Fe, Zr) are expelled, enabling progressive Sn concentration. Our findings establish cassiterite DRP as a significant mechanism to generate Sn-rich fluids in multi-stages hydrothermal systems, driven by DRP that selectively removes impurity elements. This perspective enhances our understanding on Sn enrichment during superimposed Sn metallogenic events, with implications for analogous deposits involving oxides or sulfides.

Key words: Tin, Cassiterite, Dissolution and reprecipitation process, Hydrothermal diamond anvil cell, Cold seal pressure vessel.

DECIPHERING THE RELATIVE TIMING OF ALTERATION AND CU MINERALIZATION AT THE DEXING PORPHYRY CU–AU–MO DEPOSIT (SOUTH CHINA) USING THE TEMPORAL VARIATIONS OF CU ISOTOPE COMPOSITION OF CHALCOPYRITE

Jiafeng He, Guoguang Wang*, Weiqiang Li*

School of Earth Sciences and Engineering, Nanjing University, China

Abstract Porphyry Cu mineralization is generally considered to form early during the potassic alteration stage. Growing observations, however, suggest that the later phyllic alteration may play a critical role in the ore formation. Here, to address this contradictory timing of Cu mineralization, we integrate detailed vein characterization with systematic Cu isotope compositions of chalcopyrite at the Dexing porphyry Cu deposit in South China. At Dexing, there three well-characterized veining stages: stage 1 veins associated with potassic alteration, stage 2 veins with intense phyllic alteration halos, and stage 3 veins causing the late propylitic alteration event. One prominent feature of the Dexing deposit is that approximately two-thirds of the Cu ores are hosted in the phyllic alteration zones.

Forty-six chalcopyrite samples have a narrow variation in δ^{65}Cu values, spanning from -0.35‰ to 0.25‰, suggesting a hypogene origin devoid of supergene alterations. The Cu isotope compositions of chalcopyrite are largely invariable from stage 1 potassic alteration (-0.05‰ to 0.21‰) to stage 2 phyllic alteration (-0.03‰ to 0.24‰), implying limited sulfide precipitation. However, chalcopyrite in the barren veins related to stage 3 propylitic alteration (-0.35‰ to 0.02‰) have distinctly lighter δ^{65}Cu values. It suggests that during the acidic phyllic alteration, significant amounts of isotopically heavy chalcopyrite precipitated from the mineralizing fluids, decreasing the δ^{65}Cu values of residual fluids and accordingly stage 3 veins. This temporal variation in δ^{65}Cu values confirms the dominant Cu precipitation during the phyllic alteration stage, which is triggered by fluid cooling and acidic mineral alteration that buffers fluid pH. This study emphasizes that phyllic alteration can be significant to host ores. Combining our data with Cu isotope results from other porphyry deposits, we develop a comprehensive genetic model for porphyry Cu deposits that can host mineralization in either the phyllic or potassic alteration stages. Spatial mapping at Dexing suggests that sharp decreases in δ^{65}Cu values are likely indicative of the distal boundaries of Cu ore bodies. We highlight that Cu isotopes can be a powerful tool for characterizing the evolution of magmatic–hydrothermal systems.

Key words: porphyry copper deposit, chalcopyrite, copper isotopes, South China, Dexing

Acknowledgements This study was funded by the National Natural Science Foundation of China (42172072), the National Key Research and Development Program of China (2023YFF0804402), the "GeoX" Interdisciplinary Research Funds for the Frontiers Science Center for Critical Earth Material Cycling of Nanjing University (2024300247), and the Ministry of Education Basic Discipline Top Student Training Program 2.0 (20222068).

DEVELOPMENT OF HF ISOTOPE ANALYTICAL METHODS FOR COLUMBITE-GROUP MINEALS AND THEIR APPLICATION TO NB–TA MINERALIZATION

Zhi-Min Tang[1,2], Xu-Dong Che[2*], Ru-Cheng Wang[2], Yue-Heng Yang[3]

1. National Key Laboratory of Uranium Resources Exploration-Mining and Nuclear Remote Sensing, Jiangxi Provincial Key Laboratory of Genesis and Prospect for Strategic Minerals, East China Uni-versity of Technology, China
2. State Key Laboratory of Critical Earth Material Cycling and Mineral Deposits, School of Earth Sciences and Engineering, Nanjing University, China
3. State Key Laboratory of Lithospheric and Environmental coevolution, Institute of Geology and Geo- physics, Chinese Academy of Sciences, China

Abstract Columbite-group minerals (CGM; $(Fe,Mn)(Nb,Ta)_2O_6$) are among the most important ore minerals in Nb–Ta deposits. Their high Hf contents (up to 100–1000 ppm) and relative depletion in Yb and Lu make them excellent targets for Hf isotopic tracing. Moreover, as the primary economic minerals of Nb and Ta, CGM can provide direct information on the source of mineralization. Accurate determination of the $^{176}Hf/^{177}Hf$ ratio in CGM is therefore of great significance.

In this study, analyses of mixed standard solutions with varying Ta/Hf ratios revealed that high Ta contents severely interfere with $^{176}Hf/^{177}Hf$ measurements, causing the ratio to increase with increasing Ta concen- tration. To address this, we developed a two-stage ion-exchange column separation procedure (using Ln Spec and AG1-X8 resins) to effectively separate dominant Ta from trace Hf, thereby enabling solution- based Hf isotope analysis ofCGM. Furthermore, we established an in-situ Hf isotope determination method for CGM using LA-MC-ICP-MS. To circumvent the severe tailing of the ^{180}Ta peak that affects ^{180}Hf and ^{179}Hf signals, we propose a mass bias correction using $^{178}Hf/^{177}Hf = 1.4672$. This novel correction yields accurate $^{176}Hf/^{177}Hf$ ratios, as verified by solution analysis, demonstrating the robustness of the method.

We then applied this approach to trace the source characteristics of Nb–Ta mineralization in South China. A total of 24 Nb–Ta deposits were investigated, including 7 associated with metaluminous to weakly per- aluminous (MWP) granite systems and 17 associated with strongly peraluminous (SP) granite systems. Re- sults show that CGM from SP systems have $\varepsilon Hf(t)$ values ranging mainly from –16.45 to –0.60 and TDM2 model ages between 1.3 and 2.4 Ga, indicating that their mineralization materials were predominantly de- rived from reworking of ancient crust. In contrast, CGM from MWP systems exhibit more positive $\varepsilon Hf(t)$ values (–0.80 to 1.91) and TDM2 mode ages generally younger than 1.3 Ga, suggesting the contribution of juvenile crustal material. The Hf isotopic compositions thus reveal a marked

difference in the source regions between the two systems, a difference also mirrored in the contrasting geochemical compositions of the CGM themselves. Consequently, the Hf isotopic signature of columbite-group minerals holds great promise for directly tracing the sources of rare-metal (Nb–Ta) mineralization and provides a new scientific basis for the study and exploration of rare-metal deposits.

Key words: Columbite-group minerals, Hf isotopes, mineralization source, Nb–Ta, South China

Acknowledgements This study was financially supported by the Deep Earth probe and Mineral Resources Exploration-National Science and Technology Major Project (2025ZD1004706) and the National Science Foundation of China (42272067).

EFFECT OF CLAY MINERAL STRUCTURES ON LI^+ ADSORPTION

Wenbin Yu[1, 2], Zhiyi Deng[2], Zhen Wang[3], Quan Wan[2]

1. College of Earth Sciences, Guilin University of Technology, Guilin 541006, China
2. State Key Laboratory of Critical Mineral Research and Exploration, Institute of Geochemistry, Chinese Academy of Sciences, Guiyang 550081, China
3. School of Chemistry and Materials Science, Guizhou Normal University, Guiyang 550025, China

Abstract The rapid growth of lithium-ion batteries in electric vehicles and energy storage systems has led to an exponential increase in global lithium consumption. Clay-type lithium deposits, characterized by wide distribution, large reserves, and low mining costs, represent a promising Li resource. In these deposits, clay minerals serve as the primary hosts for lithium, and Li enrichment is largely controlled by the adsorption of Li^+ onto clay minerals. However, the influence of the structural characteristics of clay minerals on Li^+ adsorption remains poorly understood. To address this gap, this study systematically investigated Li^+ adsorption on four representative clay minerals—montmorillonite (Mnt), illite (Ilt), chlorite (Chl), and kaolinite (Kln). The effects of pH, temperature, and ionic strength on Li^+ uptake were examined. Additionally, desorption tests, ^7Li solid-state NMR, and FTIR spectroscopy were employed to elucidate the adsorption mechanisms associated with different mineral structures. The results showed that Li^+ adsorption on all four minerals reached equilibrium between 8 and 36 hours. Among them, Mnt exhibited the shortest equilibrium time, whereas Chl required the longest one. Mnt had the highest Li^+ adsorption amount, while Kln showed the lowest. Notably, Li^+ adsorption on Mnt and Ilt was less pH-dependent compared to the other minerals. Desorption experiments revealed that over 70% of pre-adsorbed Li^+ could be desorbed from Mnt. In contrast, only a small fraction was desorbed from the other three minerals, indicating that Mnt has the weakest affinity for Li^+. Mechanistically, Mnt adsorbs Li^+ primarily through outer-sphere complexation and cation exchange within its expandable interlayers, owing to the diffuse negative charge generated by octahedral substitution. In illite, Li^+ likely enters the pseudo-hexagonal sites due to the strong charge arising from tetrahedral substitution. For chlorite and kaolinite—characterized by fixed interlayers and limited isomorphous substitution, respectively—inner-sphere complexation between Li^+ and surface hydroxyl groups is likely the dominant adsorption mechanism. These findings reveal that the structural features of clay minerals play a key role in governing Li^+ adsorption, offering experimental insights into Li enrichment and guiding the exploration and processing of clay-type lithium resources.

Keywords: Clay minerals, Structure, Li^+, Adsorption, Mechanism

ELEVATED PH IN ORE-FORMING FLUIDS FACILITATED INDIUM ENRICHMENT IN SPHALERITE

Zhengbing Zhou[1], María Florencia Márquez-Zavalía[2,3], Hanjie Wen[4], Miguel Ángel Galliski[2]

1. National Key Laboratory of Uranium Resources Exploration-Mining and Nuclear Remote Sensing, East China University of Technology, Nanchang 330013, P.R. China
2. IANIGLA, CCT-Mendoza (CONICET), Mendoza 5500, Argentina
3. Mineralogía y Petrología, FAD, Universidad Nacional de Cuyo, Centro Universitario, Mendozab 5502, Argentina
4. School of Earth Sciences and Resources, Chang'An University, Xi'an 710054, P.R. China

Abstract Indium is an essential element in cutting-edge fields such as clean energy, electronics, and aerospace. This has led to a rapid increase in global demand, and it has been designated a "critical mineral" by multiple nations. As a highly dispersed chalcophile element, indium averages ~0.056 ppm in the upper continental crust, requiring $>10^3$ enrichment to achieve economic mineralization. Epithermal and skarn deposits are the principal In repositories, hosted predominantly in sphalerite. However, despite the observation of strongly heterogeneous indium enrichment across deposit, mineral, and elemental scales, the correspondence between indium enrichment and the evolution of physicochemical conditions in ore-forming fluids remains poorly constrained.

The Dulong skarn deposit (SW China) contains 88.61 Mt ore grading 4.00% Zn, 0.352% Sn, and 0.038% Cu. Indium is primarily hosted in sphalerite and with reported In resources exceeding 6,000 t. Skarn mineralization occurred at 88-81 Ma, genetically linked to the Laojunshan granitic magmatism. The Capillitas intermediate-sulfidation epithermal deposit (NW Argentina), hosted within the Farallón Negro Volcanic Complex (FNVC), has proven and possible reserves of 387,000 t grading 2.6 g/t Au, 108 g/t Ag, and 2.31% Cu. Indium is mainly associated with sphalerite and with contents up to 26.88 wt.%, being the In-richest variety of this mineral described in literature. Also, Indium independent mineral of roquesite and ishiharaite were reported in Capillitas.

Sphalerite from the Dulong deposit is characterized by the pervasive occurrence of micro-scale exsolution phases of chalcopyrite and pyrrhotite. Indium-rich sphalerite precipitated during the early paragenetic stage of sulfide mineralization and is distinguished by pronounced enrichment in Fe, Cu, In, and Mn, exhibiting mean concentrations of 11.25, 0.24, 0.36, and 0.13 wt.%, respectively. Micron-scale inclusions of extremely indium-enriched sphalerite have been identified locally, with indium concentrations attaining 17.35 wt.%. Fluorite is consistently observed in the immediate vicinity of these exceptionally indium-rich inclusions. In contrast, indium-rich sphalerite from the Capillitas lacks abundant exsolution of chalcopyrite or other sulfide phases, presenting a comparatively inclusion-free and texturally

pristine appearance. Furthermore, In-rich sphalerite formed during the final mineralization stages, coeval with the onset of rhodochrosite crystallization. Sphalerite from this deposit is characterized by low Fe contents (<0.2 wt.%) but exhibits elevated Cd, Ga and Sb concentrations (averaging 0.57, 0.54, and 0.11 wt.%, respectively). The spatial distribution of indium enrichment is further defined by rhythmic oscillatory zonation.

In both deposits, indium and copper display a well-defined positive covariance, and elemental mapping reveals a systematic spatial coupling of the distribution patterns of In and Cu. This observation indicates that indium enrichment is predominantly achieved through the coupled replacement of Zn^{2+} by In^{3+} and Cu^{+} within the sphalerite lattice. At Dulong, the intimate association of extremely indium-rich sphalerite with fluorite implies that indium may have been transported as fluoride complexes in the hydrothermal fluid. Subsequent fluid-rock interaction, specifically metasomatic reaction with carbonate-bearing lithologies, promoted the destabilization and decreased solubility of indium-fluoride complexes, thereby facilitating indium precipitation. Analogously, at Capillitas, the presence of svanbergite in the early, pre-indium-enrichment paragenesis indicates that the incipient ore-forming fluid was characterized by relatively low pH. Initial acidic fluids precipitated iron-arsenic sulfides (pyrrhotite, pyrite, arsenopyrite) and As-Zn-Cu minerals in quartz. As fluids cooled and pH rose, rhodochrosite became the main gangue and sphalerite became indium-rich. These low- to intermediate-salinity fluids likely originated from porphyry intrusions associated with the FNVC. Thermodynamic simulations of the complexation and transport behavior of In, Cu, and Fe in hydrothermal solutions corroborate this interpretation, demonstrating that elevated fluid pH reduces the solubility of indium complexes. Consequently, an increase in the pH of the ore-forming hydrothermal fluid is interpreted as a critical factor governing the enrichment of indium in sphalerite.

Key words: Sphalerite, Indium, Dulong deposit, Capillitas deposit, Magmatic hydrothermal

Acknowledgements This study was supported by the National Natural Science Foundation of China (Grant No. 42572108) and the National Scientific and Technical Research Council of Argentina (PIP 1489-CONICET).

ENRICHMENT AND MINERALIZATION OF REES IN CARBONATITES

Xueyin Yuan[1], Zhiming Yang[2], Xiaochun Li[3], Qi Li[3] and Zengqian Hou[2]

1. SKL-DeepMinE, Institute of Mineral Resources, Chinese Academy of Geological Sciences, China
2. SKL-DeepMinE, Institute of Geology, Chinese Academy of Geological Sciences, China
3. Institute of Geology and Geophysics, Chinese Academy of Sciences, China

Abstract The rapid development in high-tech and green energy industries has led to increased demand for rare earth elements (REEs). Globally, over half of the known REE resources are hosted by carbonatites, a unique igneous rock type that consists of carbonate minerals with subordinate phosphates, sulfates, fluorides and silicates. Extensive field and laboratory investigations, high pressure-temperature (P-T) experiments and thermodynamic simulations have investigated the REEs metallogenic processes in carbonatites, yet the factors governing the anomalous enrichment and the mineralization processes of REEs still remain enigmatic.

Here, we report our findings of the REE enrichment and mineralization processes in carbonatites, based on our high P-T experiments using a hydrothermal diamond anvil cell and melt-fluid inclusion studies of two large carbonatites REE deposits at the southeastern margin of the Tibetan plateau. Our high P-T experiment results show that REEs are highly soluble in aqueous Na_2CO_3 brine-melts, increasing from hundreds of ppm at 450 °C to >8 and 4 wt.% at 650 °C under silica-free and -saturated conditions, respectively. The REE concentrations are comparable to those in REE ore fluids (3 – 5 wt.%), demonstrating that alkaline carbonates are essential for the REE enrichment in the mineralizing liquids. Upon cooling REEs crystalize preferentially as burbankite or carbocernaite between 650 and 450 °C, even at the saturation of fluorite. However, while the systems contain substantial ferro- or alumino-silicates, the precipitation of alkaline silicate minerals (aegirine, cancrinite, etc.) suppressed the activity of Na, thus led REE crystalizing as bastnäsite at 720 – 550 °C.

Our findings are further verified by the results from melt-fluid inclusion studies. The inclusions studied contain abundant sulfate and carbonate daughter minerals (thénardite, celestine, baryte, calcite, nahcolite and burbankite) along with liquid water and small vapor bubbles under room condition. Upon heating, vapor homogenized between 100 and 228 °C, followed by dissolution of nahcolite (152 – 186 °C) and sulfates (thénardite, celestine and baryte, 320 – 465 °C). Burbankite remained stable before dissolving at 450 – 520 °C, leaving calcite as the last phase to dissolve at 470 – 600 °C. The sulfate and carbonate concentrations in these inclusions are estimated to exceed 50 and 20 wt.%, respectively, meanwhile the fluid pressure as determined by monitoring the Raman peak position shifts in sulfate daughter minerals increased linearly from 0 at vapor homogenization to 5.0 – 7.0 kbar at 500 – 600 °C. The homogenization P-T conditions and high carbonate-sulfate concentrations imply that the REE mineralization occurs during the melt-fluid transitional stage, with REE enrichment and crystallization processes being controlled by alkalis and carbonate ions.

Key words: Rare earth elements, carbonatites, Enrichment and mineralization process, brine-melts

EQUILIBRIUM FE-S ISOTOPE FRACTIONATION AMONG PYRITE PRECURSOR MINERALS: INSIGHTS FROM DENSITY FUNCTIONAL THEORY

Yin-Chuan Li [1, 2], Zhi-Jie Liu [1, 2], Hao-Long Li [1, 2]

1. School of Resources and Environment, Henan Polytechnic University, Jiaozuo 454003, PR China

2. Henan Key Laboratory of Coal Measure Unconventional Resources Accumulation and Exploitation, Jiaozuo 454003, PR China

Abstract Pyrite (FeS_2) isotopic compositions ($\delta^{56}Fe$ and $\delta^{34}S$) are widely used as paleoenvironmental tracers, but the interpretations are complicated by isotopic fractionation during transformation of metastable Fe–sulfide precursors (amorphous FeS/cubic FeS/mackinawite/greigite/marcasite → pyrite). While pyrite formation typically proceeds via metastable precursors, these transient phases are rarely preserved in geological records, which makes the determination of Fe–S isotopes during the phase transition process difficult. Herein, density functional theory (DFT) and DFT+U calculations were employed to determine the equilibrium Fe and S isotopic fractionation factors among these minerals across a temperature range of 0–700 °C. Our results establish distinct fractionation hierarchies: marcasite preferentially enriches heavy S (19.97‰) and heavy Fe (10.54‰) isotopes, while greigite hosts the lightest isotopes. Phase transitions induce significant isotopic fractionation, with the largest S isotope fractionation occurring between greigite and pyrite (–10.60‰ at 25 ℃) and the dominant Fe isotopic fractionation also observed between these two phases (–5.59‰ at 25 °C). Analyses of bond lengths and force constants confirm that 1000lnβ values are inversely proportional to Fe–S bond lengths and positively correlated with force constants. This study provides atomic-scale quantification of equilibrium Fe–S isotope fractionation during the transformation of pyrite precursors, yielding critical insights for interpreting isotopic records in sedimentary diagenesis, hydrothermal mineralization, and paleoredox reconstruction.

Key words: Fe–S isotopes, Equilibrium isotopic fractionation, Pyrite precursor minerals, Density functional theory, Phase transitions

Acknowledgements This research was financially supported by the National Natural Science Foundations of China (Grants Nos. 42203015) and the Opening Project of Joint Laboratory for Planetary Science and Supercomputing, funded by Chengdu University of Technology and the National Supercomputing Center in Chengdu (Grant No. CDCSZX-QT-2026-04).

EXPERIMENTAL DETERMINATION OF RARE EARTH ELEMENTS PARTITIONING BETWEEN TITANITE AND GRANITIC MELTS

Fangfang Huang[1], Jintuan Wang[1], Xiaolin Xiong[1,2], Mingdi Gao[1], Li Li[1], Chunxia Wei[1,2]

1. State Key Laboratory of Deep Earth Processes and Resources, Guangzhou Institute of Geochemistry, Chinese Academy of Sciences, Guangzhou 510640, China.
2. College of Earth Science, Jilin University, Changchun 130061, China.

Abstract Titanite is a favorable host for rare earth elements (REE) because the seven-coordinated Ca^{2+} site can be readily substituted by REE^{3+}. To investigate the factors controlling the partitioning of REE between titanite and melt, we conducted experiments under varying pressure (0.5–1 GPa), temperature (850–1000 °C), and oxygen fugacity conditions (~QFM+8 to ~QFM−4), using a piston cylinder apparatus. The obtained partition coefficients (D) of REE between titanite and melt are as follows: DLa = 3.65–18.14, DCe = 17.40–79.98, DPr = 18.46–150.81, DSm = 38.63–838.50, DEu = 7.46–603.03, DGd = 48.60–821.65, DDy = 34.84–587.48, and DYb = 15.82–110.64. All REE behave as compatible elements in titanite. The partitioning of the REE is mainly influenced by temperature and melt composition except for Eu, whose partitioning is also controlled by oxygen fugacity. Based on the Eu partitioning behavior, we developed an oxygen fugacity barometer using the (Eu/Eu*)D ratio of titanite. This barometer successfully estimates the oxygen fugacity conditions of the Fish Canyon Tuff magma.

Key words: rare earth elements, partition coefficients, titanite, granitic melts, oxygen fugacity

EXPERIMENTAL STUDY OF SYNTHETIC KOTULSKITE (PDTE): BISMUTH AND ANTIMONY SOLUBILITY

Jan Kamenský[1,2], Anna Vymazalová[1], František Laufek[1], Marek Tuhý[1,2]

1. Czech Geological Survey, Geologická 6, 152 00, Prague 5, Czech Republic
2. Institute of Geochemistry, Mineralogy and Mineral Resources, Faculty of Science, Charles University, Albertov 6, CZ 128 00, Prague 2, Czech Republic

Abstract The mineral kotulskite represents an important carrier of Pd mainly in Cu-Ni-PGE deposits related to mafic and ultramafic rocks. Kotulskite, in nature commonly dissolve a range of minor elements (eg. Bi, Pb, Pt, Ni, Sb). Among these, Bi and Sb show significant range of substition. In this study we experimentally investigated the Bi and Sb solubility in the synthetic analogue of kotulskite (PdTe). Experiment runs were performed using the evacuated silica-glass tube method at the temperatures of 400 °C and 500 °C. The products of synthesis were characterized by powder X-ray diffraction, reflected light microscopy and electron-microscopy techniques.

At 400 °C, Bi-rich experimental products in the Pd-Bi-Te system show a certain degree of inhomogeneity. To improve homogeneity, selected experiments were further heated at 500 °C. This additional heating resulted in more homogeneous run products, as reflected by diffraction patterns and electron microprobe data. At this temperature, our experimental data do not indicate the existence of a complete solid solution between PdTe and PdBi. The Bi content reaches $Pd_{0.99}(Te_{0.21}Bi_{0.80})_{\Sigma 1.01}$ (40.3 at.% Bi) and a compositional gap occurs between the Bi-rich kotulskite solid solution end member and the end-member PdBi (dissolves up to 1.6 at.% Te).

In the Pd-Sb-Te system, Sb-rich experimental products at 400 °C also exhibit degree of inhomogeneity. However, further heating at higher temperature (up to 500 °C) did not improve the homogeneity and instead led to the formation of a liquid. At 400 °C, the results suggest that a continuous solid solution between PdTe and PdSb does not occur. The solubility of Sb in kotulskite was confirmed up to the composition $Pd_{1.00}(Te_{0.18}Sb_{0.82})_{\Sigma 1.00}$ (41.1 at.% Sb). A compositional gap seems to occur between the Sb-rich kotulskite solid solution end member and the end-member PdSb. The phase PdSb, an analogue of sudburyite, does not dissolve Te.

The results indicate that, in contrast to interpretations based on natural occurrences, kotulskite (PdTe) does not form a complete solid solution with PdSb or PdBi under the investigated conditions. The incorporation of Bi and Sb in PdTe also affects structural parameters, reflecting changes in unit-cell volume, which increases with Bi substitution (from 84.7 to 87.3 Å^3) and decreases with Sb substitution (from 84.7 to 81.8 Å^3). In kotulskite structure (NiAs type), Bi and Sb substitute for Te.

These findings provide new experimental constraints on Pd-Bi-Te and Pd-Sb-Te systems and contribute to a better understanding of platinum-group assemblages.

Key words: kotulskite, Bi and Sb solubility, platinum-group mineral, solid solution, experimental study

Acknowledgements This is a contribution to the Strategic Research Plan of the Czech Geological Survey (DKRVO 2023-2027).

FLORENCITE PRECIPITATION UNDER HYDROTHERMAL CONDITIONS: MECHANISTIC INSIGHTS AND MINERALOGICAL IMPLICATIONS

Thiago Bezerra Lima[1,2], Fang Xia[1], Tobias G. Bamforth[3], Hans C. Oskierski[1], Joël Brugger[3], and Yuan Mei[1,2]

1. Sustainable Geochemistry and Mineral Sciences, Murdoch University, Australia.
2. CSIRO Mineral Resources, Australia.
3. School of Earth, Atmosphere and the Environment, Monash University, Australia.

Abstract The rare-earth elements (REEs, La-Lu, Y) are indispensable metals for the renewable energy transition. Florencite ($REEsAl_3(PO_4)_2.6H_2O$) is a ubiquitous mineral in many types of REE deposits that plays an important role in controlling REE concentrations and fractionation in REE sources and is emerging as a potential economic resource for these metals. Despite its significance, florencite has received limited scientific attention regarding the mechanisms, kinetics, and conditions under which it forms. This experimental study investigates hydrothermal florencite formation by reacting natural apatite with Al- and Ce-doped fluids at various temperatures and Al-Ce ratios. Through scanning electron microscopy (SEM), energy dispersive X-ray spectroscopy (EDS), powder X-ray diffraction (PXRD) and *in situ* synchrotron PXRD experiments, we show that at low temperatures (≤160 °C) florencite precipitated following apatite dissolution. Conversely, at higher temperatures (≥180 °C), it formed following the precipitation of metastable $AlPO_4$ phases. At low Al/Ce ratios, the formation of florencite was faster and smaller amounts of intermediate phases formed compared with high Al/Ce ratios. Monazite ($REEsPO_4$) formed almost exclusively at 140 °C as the stable secondary phase, and minimally as an intermediate metastable phase at higher temperatures. Mineral textures indicate that the metastable $AlPO_4$ phases that formed at higher temperatures did so by an interface-coupled dissolution reprecipitation mineral replacement reaction. Conversely, initial florencite precipitation occurred through the same mechanism. Mineral textures display nm-scale gaps separating florencite from $AlPO_4$ phases and apatite precursor minerals. However, precipitation later became decoupled from apatite and $AlPO_4$ dissolution, and at all temperatures florencite crystals formed throughout the supersaturated fluid. Compositional analysis by electron probe microanalysis (EPMA), laser ablation-inductively coupled plasma-mass spectrometry (LA-ICP-MS), and solution ICP-MS showed that florencite was consistently enriched in the light REEs (LREEs, La-Eu) compared to heavy REEs (HREEs, Gd-Lu), and also relatively more enriched in Th compared to U. Temperature and reaction time had no significant influence on florencite composition. Hydrothermal solution analysis revealed that florencite formation is associated with a decrease in pH and a relative enrichment in HREEs in solution. This experimental study indicates that natural florencite formation in the absence of Al-phosphate minerals may be

favored at relatively low Al/Ce ratios and temperatures, provided that the temperature is not so low that REE-phosphates (such as monazite) would stabilize instead. Such conclusions may apply to natural REE deposits, where florencite is rarely found associated with Al-phosphate phases and frequently observed alongside REE-phosphates and apatite. The results also indicate that higher temperatures may increase the stability and rate of florencite precipitation relative to REE phosphates, particularly in the presence of Al phosphates. Moreover, the ability of florencite to preferentially incorporate the LREEs (relative to the HREEs) indicates that the most valuable REEs (HREEs) are available to precipitate with other minerals or adsorb in clay-type minerals. Nevertheless, the uptake of economically important LREEs such as neodymium (Nd) by florencite highlights its importance as an emerging source of REEs in some deposits. The incorporation of Th represents a drawback for REE extraction from florencite, as it would require the management of radioactive elements during processing. However, in REE deposits where florencite is not the major REE resource, this characteristic may be beneficial, as florencite can act as an effective immobilizer of radioactive elements.

Key words: Rare earth elements, florencite, apatite, hydrothermal precipitation, *in situ* powder X-ray diffraction.

Acknowledgements We acknowledge the Australian Research Council for funding. TBL acknowledges a Murdoch University Strategic Partnership Scholarship, a Murdoch University International Tuition Fee Scholarship, and a CSIRO postgraduate top-up scholarship.

FLUID EVOLUTION AND ORE-FORMING PROCESSES IN THE SHAPINGGOU MO DEPOSIT, CENTRAL CHINA: INSIGHTS FROM LA ICP-MS MICROANALYSES OF FLUID INCLUSION AND SIMS OXYGEN ISOTOPES

Guoguang Wang, Zhiyuan Zeng, Pei Ni

School of Earth Sciences and Engineering, Nanjing University, China

Abstract The giant Shapinggou Mo deposit in Central China represent a porphyry system related to CO_2-rich ore fluid. However, the genesis of this type of Mo deposit remains unclear. This study aims to understand fluid evolution and metal enrichment mechanism of the Shapinggou Mo deposit, in which four stages of quartz veins have been identified. Early barren quartz (Q_1) contains intermediate-density inclusions with moderate Mo concentrations (~140 μg/g). Cathodoluminescence reveals two substages of main ore-stage quartz (Q_2): early bright-luminescing Q_{2a} and later dark-luminescing Q_{2b}. The brine inclusions in Q_{2a} exhibit strong Mo enrichment (up to 1100 μg/g), indicating that the partitioning of Mo into the brine phase during phase separation. Molybdenite is primarily spatially associated with Q_{2b}, demonstrating that retrograde quartz dissolution created porosity for ore deposition. The decrease in the Mo/(Na+K) ratio of brine inclusions during the main ore-stage shows a synergistic relationship with the decline in temperature, indicating that fluid cooling was the dominant mechanism for molybdenite precipitation. Moreover, elevated Sr/(Na+K) ratios in brine inclusions from Q_3 implies that minor Mo deposition is promoted via sericitic alteration. Q_4 exhibits the lowest $\delta^{18}O_{fluid}$, indicating a late-stage event of meteoric water incursion following molybdenite precipitation. This study reveals that the initial CO_2-rich fluids do not extremely enrich Mo but rather require a massive fluid supply for the formation of giant Mo deposits.

Key words: Fluid Evolution, LA ICP-MS Microanalyses, SIMS oxygen isotopes, Shapinggou, Central China

FLUID HALITE SATURATION DIRECTLY DRIVES CU-FE SULFIDE PRECIPITATION IN PORPHYRY DEPOSITS

Jiafeng He, Guoguang Wang*, Weiqiang Li*
School of Earth Sciences and Engineering, Nanjing University, China

Abstract Porphyry copper deposits supply approximately 75% of the world's Cu, yet the process that drives efficient Cu-Fe sulfide deposition within confined spaces remains unresolved. Fluid cooling is widely invoked, but it predicts a gradual decrease in Cu solubility and does not fully explain why ore formation commonly occurs at ~400°C. Halite saturation offers an alternative mechanism because precipitation of solid chlorides reduces the bulk Cu-transport capacity of ore-forming fluids; however, this process is difficult to recognize due to the high solubility of precipitated halite. Here we investigate the giant Dexing porphyry Cu deposit, South China, using fluid inclusion petrography and the first potassium isotope analyses of tiny fluid inclusions in quartz. From the main to late hydrothermal stages, the inclusion fluids show a sharp decrease in both $\delta^{41}K$ and Na/K. *Ab-initio* calculations indicate that halite (NaCl-KCl solid solution) is K isotopically heavier than the coexisting fluid, so K-bearing halite precipitation drives the residual fluid toward lower $\delta^{41}K$ while simultaneously lowering Na/K. This interpretation is consistent with fluid inclusion microthermometry indicating halite-saturated brines during the main mineralizing stage. Mass-balance modeling further shows that halite precipitation can trigger significant Cu deposition in the spatially restricted regions where saturated brines are concentrated, thus suggesting fluid halite saturation as an efficient driver for Cu deposition. Our results highlight that potassium isotopes in fluid inclusions provide an effective tracer of the transient salt precipitation in magmatic-hydrothermal systems.

Key words: porphyry copper deposit, fluid inclusion, potassium isotopes, halite saturation, Dexing

Acknowledgements We thank Junyi Pan for his help in fluid inclusion petrography. This study was funded by the National Natural Science Foundation of China (Grants 42425301 and 41772063), and the Fundamental Research Funds for the Central Universities of China (Grant No. 2025300349).

FORMATION MECHANISM OF KAOLINITE THROUGH THE MINERAL TRANSFORMATION PATHWAY

Shangying Li[1,2*], Hongping He[2], Qi Tao[2], Jianxi Zhu[2], Xiaoliang Liang[2]

1. School of Land Engineering, Chang'an University, China
2. Guangzhou Institute of Geochemistry, Chinese Academy of Sciences, China

[*] *E-mail: lsying2022@chd.edu.cn*

Abstract Kaolinite, a common 1:1 type clay mineral, is ubiquitous in the supergene environments of the Earth. It generally forms through the transformation of 2:1 type clay minerals and feldspars in weathering or hydrothermal environments. Understanding the transformation mechanism involved is of great importance to exploration of kaolin deposits and unraveling the evolution of palaeoenvironment in the areas where the transformations occur. We artificially realized the transformation of 2:1 type clay minerals (montmorillonite, illite, and rectorite) with different swelling and non-swelling properties as well as feldspars into kaolinite under hydrothermal conditions. The results revealed that 2:1 type clay minerals can be transformed into kaolinite via a local dissolution-crystallization mechanism, which starts mainly from the layer edges rather than the basal surfaces of the precursor 2:1 type clay minerals. The transformation of feldspars into kaolinite is dominated by a complete dissolution-recrystallization process that starts from the external surfaces of feldspars. In addition, the particle size and morphology of kaolinite that form through such dissolution-crystallization mechanisms are significantly affected by the precursor 2:1 type clay minerals and feldspars.

Key words: kaolinite, 2:1 type clay minerals, feldspars, transformation, morphology

GAS COMPETITIVE ADSORPTION IN TYPICAL CLAY MINERALS WITH DIFFERENT STRUCTURES: IMPLICATIONS FOR GEOLOGICAL CO_2 SEQUESTRATION WITH ENHANCED GAS RECOVERY

Yang Wang, Yichen Wang, Hongfei Cheng

School of Earth Science and Resources, Chang'an University, China

Abstract The escalating challenges of climate change and global warming have intensified the pursuit of sustainable technologies to reduce greenhouse gas emissions, particularly carbon dioxide (CO_2). Among the various mitigation strategies, geological sequestration has emerged as a promising solution. The CO_2 sequestration combined with enhanced natural gas recovery (CO_2-EGR) is a promising technology. Injecting CO_2 into hydrocarbon reservoirs induces a competitive adsorption process between CO_2 and CH_4, which not only facilitates significant CO_2 storage underground but also enhances hydrocarbon recovery. Clay minerals, which are abundant in oil- and gas-rich strata, provide numerous gas adsorption sites. This study employs a combined Grand Canonical Monte Carlo (GCMC) and Molecular Dynamics (MD) approach to investigate the competitive adsorption behavior of CO_2/CH_4 binary mixtures on clay minerals with different structures, specifically kaolinite and montmorillonite. Van der Waals forces predominantly govern the interaction of CO_2 and CH_4 with clay surfaces. The cations located between the isomorphously substituted montmorillonite layers exert stronger electrostatic interactions with CO_2, leading to an increased adsorption selectivity of montmorillonite for CO_2/CH_4. As pore size, pressure, and temperature increase, the selectivity of the binary mixture decreases. The presence of H_2O molecules counteracts some of the van der Waals forces between clay minerals and CO_2 and CH_4, almost entirely eliminating the electrostatic interactions between them. Kaolinite exhibits a more prominent competitive adsorption mechanism due to its rich surface hydroxyl groups; montmorillonite, owing to the ion-dipole interactions between surface, Na^+ and H_2O, shows stronger water-mediated synergistic adsorption, and the increase in water content further enhances the CO_2/CH_4 adsorption selectivity.

Key words: CO_2-EGR, Competitive adsorption, Kaolinite, Montmorillonite, Molecular simulation

Acknowledgements National Natural Science Foundation of China (42202148)

GENESIS OF THE BLACK-SHALE HOSTING LONGHUA HYDROTHERMAL NI–CO DEPOSIT, SOUTH CHINA: WHOLE-ROCK GEOCHEMISTRY, C-O ISOTOPE, FLUID INCLUSION, PB ISOTOPE AND ZIRCON (U–TH)/HE DATING CONSTRAINTS

Qiwenxiang, Guoguang Wang, Li weiqiang, Pei Ni
School of Earth Sciences and Engineering, Nanjing University, China

Abstract Hydrothermal Ni–Co deposits hosted in sedimentary rocks represent an increasingly recognized but poorly understood class of critical metal resources. In particular, the metals sources, mechanisms of transport and precipitation, and timing of mineralization remain debated for black shale-hosted systems. Here we investigate the Longhua Ni–Co deposit in the Qin–Hang metallogenic belt, South China, using integrated whole-rock geochemistry, C–O isotopes, fluid inclusion analyses, Pb isotopes, and zircon (U–Th)/He thermochronology. The host black shales in the deposit exhibit significant enrichment in nickel (average 823 ppm) and cobalt (average 199 ppm), with moderate Ir contents (~100 to 200 ppt) and radiogenic Pb isotopic signatures, indicating a crustal sedimentary origin rather than derivation from ultramafic rocks. Ni-Co ores and the black shale define a coherent Pb isotopic trend toward elevated $^{206}Pb/^{204}Pb$ and $^{207}Pb/^{204}Pb$ ratios, consistent with metal remobilization from U-enriched, organic-rich sediments. Mineralogical studies reveal that nickel and cobalt occur mainly as fine-grained sulfoarsenides within the shales or as isomorphic substitutions in calcite. Fluid inclusion studies reveal that the ore-forming fluids were low-temperature (150–210°C), low-to-moderate salinity (1.4–14.8 wt.% NaCl equiv.) H_2O-NaCl-$CaCl_2$ basinal brines. Carbon–oxygen isotopes further indicate extensive fluid–rock interaction with the organic-rich black shales. We propose that Ni and Co were transported predominantly as chloride complexes in weakly acidic fluids and precipitated via a pH increase during interaction with carbonate wall rocks, rather than by redox reactions. Zircon (U–Th)/He dating yields a mineralization age of 335.9 ± 25.2 Ma, providing direct constraints on the timing of low-temperature hydrothermal mineralization. These results demonstrate that metal pre-enrichment in black shales, coupled with basinal brine circulation and pH-driven precipitation, can generate high-grade Ni–Co mineralization. This model refines the genetic framework of "five-element" deposits by highlighting origin-rich sedimentary sequences as a primary metal source.

Key words: Hydrothermal nickel-cobalt deposit, Black shale, Fluid inclusions, isotopes, Sediment-hosted mineralization

GEODYNAMIC LIMITS ON FUTURE PORPHYRY COPPER FORMATION

Jakub Ciazela, Taras Gerya, Christian Verard, Robert Stern, Matthew Leybourne, Wenyong Duan

1. Institute of Geological Sciences, Polish Academy of Sciences

2. Institute of Geophysics, ETH Zürich, Switzerland

3. Earth Surface Dynamics Research Group, University of Geneva, Switzerland

4. School of Natural Sciences and Mathematics, University of Texas at Dallas, United States

5. Department of Geological Sciences and Geological Engineering, Canada

Long-term sustainability of human civilization depends on secure supplies of metals and critical minerals that underpin energy systems, infrastructure, and technology. By 2040, total mineral demand from clean energy technologies is expected to double to quadruple (iea, 2021), raising concerns about long-term supply sustainability because anthropogenic extraction operates on timescales and magnitudes unconstrained by geological ore-forming rates. Although recycling and substitution can mitigate pressure, widely adopted outlooks still require substantial expansion of primary supply and are commonly framed around reserves, production, and announced project pipelines.

We present a plate-kinematic framework to forecast ore deposit formation over the next 10 Myr by coupling tectonic setting-specific deposit-generation functions to a forward plate-motion model. Unlike reserve- or discovery-trend extrapolations, this approach explicitly links plate tectonics to mineralization rates, providing a first-order estimate of Earth's natural geological rate at which new mineralization may form. Before moving on to other tectonic settings and elements, we apply the method to Cu in porphyry-epithermal systems in continental arcs, parameterized by plate convergence rates and lithospheric factors (crustal thickness, slab composition, and proxies for slab oxidation state), reflecting how rapid convergence and thick crust favor porphyry formation, while explicitly accounting for melt-fluid-driven mass transfer of copper and oxidized species within subduction zones. Given that additional time is needed for the exhumation of deeper porphyry copper deposits, the erosion rate and the ratio of epithermal to porphyry deposits are included in the calculations. These parameterizations are integrated into a global 2°-resolution plate model based on the inventory of deposits (including those no longer preserved) over the last 50 Myr to test whether regional long-term trends are increasing, decreasing, or approximately constant. These trends are then extrapolated 10 Myr into the future to produce spatially explicit, time-dependent maps of ore-forming potential.

The first obtained distributions for the Americas are relatively uniform overall, with most intervals falling broadly between ca. 19 and 29 Mt Cu/Myr. Simple linear regressions indicate only weak first-order positive tendencies, with R^2 values of approximately 0.15. At this stage, the result is better interpreted as an approximately stationary first-order mean over the last 50 Myr than as evidence for a robust temporal trend. First-order projections for the next 5 (25.0 Mt Cu/Myr) and 10 Myr (25.6 Mt Cu/Myr) remain within the same broad range as the youngest observed bins. One numerically striking outcome is that the projected geological formation rates are approximately six orders of magnitude lower than present annual human consumption, based on current global refined copper use of ca. 28 Mt in 2025, according to preliminary ICSG data.

The resulting formation- and accessibility-weighted metrics provide benchmarks for Earth's geological ore-forming rate, against which scenario-based demand projections can be compared, thereby strengthening sustainability discussions with geodynamically grounded constraints. In addition, lithospheric copper budgets may be better constrained because the ratio of copper trapped in deposits to lithospheric copper can be more precisely determined.

GOLD CONTENT ANALYSIS IN GOLD ORES: 20 YEARS OF PROGRESS, CHALLENGES AND FUTURE DIRECTIONS

Ruifeng Gao*

Nanjing Institute of Product Quality Inspection, China

*Corresponding author's e-mail: ruifengg@hotmail.com

Abstract Gold content analysis of gold ores serves as the cornerstone for gold geological exploration, mineral resource assessment, mineral processing optimization, and product trade settlement. Over the past two decades, the global mining industry has confronted multiple challenges, including declining ore grades, increasing mining difficulties, stricter environmental regulations, and growing efficiency pressures, which have significantly driven innovations in gold analysis technologies. This article aims to systematically review the major advances in gold content analysis technologies since 2006, compare the performance of traditional and emerging techniques, identify the core issues and bottlenecks in current practices, and forecast future development trends based on technological evolution. This comprehensive review covers fire assay, atomic absorption spectrometry (AAS), inductively coupled plasma optical emission spectrometer (ICP-OES), inductively coupled plasma mass spectrometry (ICP-MS), X-ray fluorescence spectrometry (XRF), and the revolutionary PhotonAssay technology. It also discusses the integrated applications of automation, artificial intelligence (AI), and the Internet of Things (IoT), and deeply analyzes critical challenges such as sampling representativeness, the coarse gold particle effect, and the cost-efficiency balance. This article will provide a comprehensive reference for mining companies, analytical laboratories, technology developers, and researchers on the selection, optimization, and development of next-generation gold analysis technologies.

Key words: gold content, gold ore, review, fire assay, PhotonAssay

GOLD ENRICHMENT IN PYRITE: THE ROLE OF IMPURITY COUPLING

Zi-Yue Gao, Razvan Caracas

Université Paris Cité, Institut de Physique du Globe de Paris, CNRS, Paris 75005, France

Abstract Pyrite (FeS_2) is a key mineral phase in hydrothermal systems and commonly hosts a variety of trace metals, including gold and other economically important elements. Previous observations consistently show that gold is closely associated with arsenic-rich pyrite, implying that interactions among impurities play a fundamental role in metal enrichment. However, the processes governing such associations at the atomic scale remain insufficiently resolved. In this study, we apply *ab initio* simulations to examine how different impurities are incorporated into the pyrite structure, with particular emphasis on the relationship between gold and arsenic. A range of substitution scenarios is explored, and their energetic, structural, and electronic characteristics are systematically evaluated. The results indicate that the incorporation of single impurity atoms is generally unfavorable, whereas combined substitutions provide a more stable configuration. Arsenic, when substituting for sulfur, modifies the local structural environment and creates coordination geometries that are more accommodating for gold, allowing it to be retained within the crystal lattice.[1] Eletronic analysis shows that this stabilization is linked to adjustments in the electronic structure during co-incorporation. The presence of arsenic helps redistribute electrons in a way that avoids energetically unfavorable states, thereby enhancing the stability of impurity complexes. This behavior offers a coherent explanation for the frequent co-occurrence of gold and arsenic in natural pyrite. Overall, the results emphasize that coupled incorporation processes exert a primary control on trace-metal enrichment in pyrite and provide a framework for understanding element associations during ore-forming processes.

Key words: Ore depostis, pyrite, trace elements, electronic structure, *ab initio* simulations

GOLD SOLUBILITY IN CHALCOPYRITE PREDICTED BY ATOMIC SIMULATIONS

Jie Yao[1], Cristiana L. Ciobanu[1], Nigel J. Cook[1], Kathy Ehrig[2,1]

1. School of Chemical Engineering, Adelaide University, Adelaide, South Australia 5005, Australia
2. BHP Olympic Copper SA, 10 Franklin Street, Adelaide, South Australia 5000, Australia

Abstract Copper-iron-sulfide minerals are the dominant economic component of magmatic-hydrothermal ore deposits of porphyry, epithermal, volcanogenic massive sulfide and iron oxide copper-gold (IOCG) type. Although chalcopyrite ($CuFeS_2$) is the most widespread among the Cu-Fe-sulphides, bornite (Cu_5FeS_4) and members of the chalcocite group ($Cu_{2-x}S$) can be of major importance, notably but not exclusively in gold-rich intermediate- and high-sulfidation epithermal systems, IOCG deposits and some high-temperature Cu-Au skarns. Like most other sulfide-hosted trace and minor elements, gold (Au) may occur both dissolved within the sulfide crystal lattice and as nanoparticles (NPs) of discrete Au-(Ag)-minerals (native gold, electrum, Au-Ag-tellurides). Measured concentrations of Au in Cu-Fe-sulfides vary between 0.1 to 100 ppm. Establishing the solubility of gold (Au) in Cu-Fe-sulfide minerals assists interpretation of ore genesis and can also be important for grade model estimation and optimized processing. Previous experimental studies determined the maximum amount of Au able to dissolve within high-temperature bornite, chalcopyrite and pyrrhotite in porphyry environments. Experiments agree that bornite accommodates more Au than chalcopyrite and that Au solubility is greater with increasing temperature. However, individual studies show that measured concentrations of Au in bornite or intermediate solid solutions from 500 to 700 °C differ by an order of magnitude. This could result from differences in sulfur activity or the utilization of powder instead of capsule as a Au source for the experiments. The question of how much Au can be stored within high-temperature sulfide crystal structures thus remains controversial. During cooling, Cu-Fe-sulfides (especially bornite) undergo multiple phase transition into superstructures, which can reorganize cation/vacancy ordering, and therefore redistribute previously dissolved gold. This structural complexity, as well as sluggish kinetics to attain equilibrium, also make low-temperature solubility measurements almost impossible. Here, we calculate the equilibrium concentration of Au atoms within the chalcopyrite crystal structure from its Gibbs energy of formation, which is obtained from quasi-harmonic approximation (QHA). At 500 °C, the predicted solubility (1078 μg/g) was ~2 to 3 times greater than experimental values. The anharmonic part of Gibbs free energy in related phases can be included using machine learning-assisted thermodynamic integration, with the possibility of increasing the accuracy of prediction.

Key words: gold solubility, chalcopyrite, quasi-harmonic approximation, Cu-Fe-sulfides

Acknowledgements This research was funded by Australian Research Council grant DP250100308.

GRAPHITE AND ASSOCIATED CRITICAL ELEMENTS FROM BLACK PHYLLITES FROM HUNGARY

Lívia Leskóné Majoros, Boglárka Anna Topa, Máté Zsigmond Leskó, Ferenc Móricz, Délia H. Bulátkó-Debus, Sándor Szakáll, Ferenc Kristály

Institute of Exploration Geosciences, University of Miskolc, Hungary

Abstract The European Commission published an updated Study on the EU's list of Critical Raw Materials in 2023, which includes 34 critical raw materials. In the present study, we focus on selected critical elements and minerals, especially on natural graphite and geochemically related elements of graphitization: vanadium (V), niobium (Nb), titanium (Ti) and rare earth elements (REE).

Rock samples were collected from various geological settings in Hungary: from NE-Hungary (Uppony Mts. and Szendrő Mts.) and from NW-Hungary (Kőszeg Mts. and Sopron Mts.). All investigated areas underwent greenschist facies metamorphism, except Dédestapolcsány (Uppony Mts.), where anchimetamorphic conditions prevailed. The exposed formations are predominantly Paleozoic in age, with the exception of Velem (Kőszeg Mts.), where Mesozoic rocks occur. The collected samples are black colored, intensely deformed and schistose fine-grained phyllites; in contrast, siliceous black schists were sampled at Dédestapolcsány.

The samples were investigated with polarizing petrographic and ore microscopy (OM), scanning electron microscopy (SEM-EDX), X-ray powder diffraction (XRD), X-ray fluorescence spectrometry (XRF) and inductively coupled plasma mass spectrometry (ICP-MS).

Based on OM and SEM observations, the samples have metamorphic texture. The matrix consists of microcrystalline quartz grains (Dédestapolcsány), calcite and muscovite (Szendrőlád, Szendrő Mts.), and quartz and phyllosilicates (Szendrő, Meszes, Rakacaszend – Szendrő Mts., Velem – Kőszeg Mts., Fertőrákos – Sopron Mts.). In any cases, the mica plates (muscovite, muscovite with Na and phengite) found in the matrix often have vanadium content.

Many accessory minerals can be detected in the samples. As main Ti mineral, anatase and rutile are often found in the deformed zones with low Nb and V content. As REE-containing minerals, xenotime, allanite and monazite-(Ce) grains occur in all samples. Goyazite-gorceixite mixed crystals with low Ce and Nd content can be found in Dédestapolcsány samples, while REE-carbonate minerals (bastnäsite-(Ce)-parisite-(Ce), bastnäsite-(Ce)-parisite-(La), and bastnäsite-(Ce)-bastnäsite-(La) mixed crystals) can be detected in Szendrőlád, Szendrő, Rakacaszend and Velem samples. These minerals have low La, Nd, Gd, Th and U content based on EDX measurements. As Zr-bearing mineral, zircon is also frequent in all samples, mainly

linked to the deformed zones.

Graphite can also be observed in all samples, with different morphology and grain size (sometimes even within a single sample). Mainly two types of morphology can be distinguished: flaky appearance and aggregate appearance. The grain size of graphite moves in a wide range scale, from 1-20 μm to 100-300 μm. Sometimes low S content can be detected with EDX. By XRD, graphite cannot be detected directly on the diffractograms due to its low quantity and heavy peak overlapping with quartz peaks. However, its direct quantification is possible by Rietveld refinement.

Key words: critical elements, graphite, vanadium, REE, black phyllite

GRAPHITE FROM THE KROPFMÜHL DEPOSIT, GERMANY: REVIEWING ADVANTAGES AND DISADVANTAGES FOR LITHIUM INTERCALATION APPLICATIONS

Christoforos Zamparas[1,2], Elisabeth Eiche[1,2], Jochen Kolb[1,2]

1. Chair of Geochemistry and Economic Geology, Institute of Applied Geosciences (AGW), Karlsruhe Institute of Technology (KIT), Adenauerring 20b, 76131 Karlsruhe, Germany
2. Laboratory of Environmental and Raw Material Analysis (LERA), Karlsruhe Institute of Technology (KIT), Adenauerring 20b, 76131 Karlsruhe, Germany

Abstract The Kropfmühl graphite deposit is located near Passau, Bavaria, Germany. It is hosted in garnet-biotite-plagioclase gneiss of the Bavarian Forest. The gneiss and the graphite deposit formed during high-grade metamorphism during the Variscan orogeny, and are spatially related to quartzitic gneiss, quartzite, amphibolite, and calc-silicate rock. The present contribution focuses on discussing potential advantages and disadvantages of the Kropfmühl graphite in relation to Li-intercalation applications, and more specifically, Li-ion battery anode utilization. In this case study, the aim is to investigate the graphite crystallography spherically and to evaluate the quality for application in the Li-ion battery market as an EU-based mine. Our review does not consider the average particle size of the end product graphite as a factor for reliable Li-ion battery applications, because it is chosen by design and relative to industrial demand. Graphite in Kropfmühl exhibits an oriented mm-scale flake texture and is (a) either intergrown with sulfide minerals, mainly pyrrhotite, chalcopyrite, sphalerite and molybdenite, parallel to foliation, or (b) is oblique to foliation and associated with silicate minerals. Rhombohedral graphite-3R is the dominant identified graphite allotrope, while hexagonal graphite-2H is a minor or trace mineral. The relative amount of the two graphite allotropes was determined by comparing the 101_{3R} and 002_{2H} diffraction peaks in the XRD patterns. The fact that graphite-3R is the dominant graphite allotrope in the Kropfmühl deposit makes it a superior raw material for Li-ion battery anode utilization. This stems from the resistance of the graphene layers in this structure to exfoliate during the irreversible process of initial Li-ion doping. Additionally, graphite-3R superior behavior is a consequence of the lower capacity losses during subsequent electrochemical cycles. Furthermore, the lower vulnerability of rhombohedral graphite to co-intercalation of both lithium and solvents is also a significant reason. Despite these reasons for rhombohedral graphite superior material behavior, the hexagonal graphite is more thermodynamically stable in surface and battery usage conditions. In addition, the higher capacity of graphite-3R is not unequivocally attributed to lithium intercalation between graphene interlayers, but to lithium ion deposition at edged planes, making it a function of particle size and surface area to volume ratio. Moreover, space group – subgroup compatibility relationships between graphite-3R and lithiated graphite attest to this non-intercalation argument. Finally, our findings have a dual role. Firstly, they

pose the significance of a detailed mineralogical and crystallographic study for the optimization of a natural product's utilization and subsequently develop refined production chains for natural graphite. Secondly, they provide a transferable set of knowledge and practice on different raw materials, e.g., molybdenite-2H and -3R for lubrication, transition metal dichalcogenides for superconductivity applications, or pyrrhotite modifications for Li-ion or Li-S batteries.

Key words: graphite, allotropes, rhombohedral, Kropfmühl, Li-ion batteries

HIGH-LIGATION COMPLEXES UNLOCK EFFICIENT RARE EARTH ELEMENT TRANSPORT IN HYPERSALINE FLUIDS: EVIDENCE FROM FLUORIDE-BEARING SYSTEMS

Ye Wan[1], I-Ming Chou[2], Linbo Shang[1], Wei Zhang[3], Hao Zou[4], Wei Terry Chen[1], Haiyan Zhang[2], Xiaolin Wang[5]

1. State Key Laboratory of Critical Mineral Research and Exploration, Institute of Geochemistry (CAS), China
2. CAS Key Laboratory of Experimental Study under Deep-sea Extreme Conditions, Institute of Deep-sea Science and Engineering (CAS), China
3. School of Geography and Environmental Science (School of Karst Science), Guizhou Normal University, China
4. State Key Laboratory of Oil and Gas Reservoir Geology and Exploitation, Chengdu University of Technology, China
5. State Key Laboratory of Critical Earth Material Cycling and Mineral Deposits, School of Earth Sciences and Engineering, Nanjing University, China

Abstract Rare earth element (REE) mineralization is closely associated with hypersaline geofluids enriched in hard-base ligands (F^-, SO_4^{2-}, CO_3^{2-}), yet the mechanism enabling efficient REE transport in these fluids remains a subject of intense debate. Fluoride, in particular, presents a longstanding paradox: while it is abundant in REE-rich natural fluids, traditional experimental studies often characterize it as a precipitant due to the low solubility of REE-fluorides and the strong hydrolysis of fluoride. This study resolves the discrepancy by demonstrating that REE mobility is critically controlled by fluoride availability.Using in situ hydrothermal diamond anvil cell (HDAC) observations, synthetic fluid inclusion analyses, and ab initio molecular dynamics (AIMD) simulations, we investigated REE solubility and speciation in fluoride-bearing fluids up to 600 °C and ~150 MPa. Our results reveal that while low fluoride concentrations (1 mol/kg KF) indeed inhibit REE transport, hypersaline fluoride fluids (7 *m* KF) significantly enhance REE solubility at elevated temperatures. For example, HoF_3 solubility increases from ~100 ppm to over 25,000 ppm at 500 °C as KF concentration increases. Molecular simulations reveal that this solubility "surge" is driven by a fundamental shift in REE specition. In low-fluoride fluids, the dissolution of REE fluorides is dominated by low-ligation complexes (e.g., REE^{3+}, $REEF^{2+}$ and $REEF_2^+$), where F^- is released as a product. Under such circumstances, an increase in fluoride availability suppresses REE dissolution via the common-ion effect. However, in hypersaline fluids, previously neglected high-ligation complexes (e.g., HoF_4^- and HoF_5^{2-}) is preferentially stabilized and become the dominant species. Since the formation of these complexes requires external fluoride from the fluid, an increase in fluoride availability promotes their stability, thereby enhancing REE fluoride dissolution. This speciation transition allows REE transport to circumvent the solubility limits predicted by traditional low-

coordination thermodynamic models. By integrating these findings with analogous dissolution trends in sulfate- and carbonate-bearing systems, we propose that the enhanced stabilization of high-ligation REE complexes represents a universal mechanism for exceptional REE transport in evolved magmatic-hydrothermal fluids. This framework provides a thermodynamic "lever" that explains both the efficient scavenging of REEs in ligand-rich brines and their rapid precipitation during fluid cooling or dilution.

Key words: Rare earth elements, High-ligation complexes, Hypersaline fluids, Fluoride speciation

HIGH-SULFIDATION EPITHERMAL CU-AU DEPOSITS FORM BY LOW-SALINITY FLUIDS DERIVED FROM MAGMATIC VAPOR

Jun-Yi Pan[1,2*], Zhe Chi[2,1], Pei Ni[2], Christoph A. Heinrich[1]

pjynju2010@126.com

1. Department of Earth Sciences, ETH Zürich, Clausiusstrasse 25, 8092 Zurich, Switzerland
2. State Key Laboratory of Critical Earth Material Cycling and Mineral Deposits, Institute of Geo-Fluids, Nanjing University, 210023 Nanjing, China

Abstract High-sulfidation Cu-Au ore deposits are very rare, compared with their silicious host rocks leached by volcanic gases near the top of subduction-related magma systems. Yet, the richest examples include deposits of nation-building significance. Processes leading to this exceptional metal enrichment are debated, with proposals ranging from magmatic vapor, salty brines or even sulfide melts. Zijinshan, for decades one of China's most significant own copper and gold resources, allows sampling of vertically extensive geological exposures and contains fluid inclusions in clear textural context with pre-ore veins and rich Cu-Au mineralized breccias. Here, we applied modern methods of simultaneous analysis of S, B and ore metals in vapor-like fluids, aqueous liquid water and hypersaline brines, trapped as micro-inclusions in quartz and enargite. We show that ore formation occurred by aqueous liquid of low salinity (< 5 wt % total salts), formed by cooling and contraction of magmatic vapor-like fluids. Highly saline brines, even though richer in ore metals, did not significantly contribute to high-sulfidation mineralization, but were present at deep porphyry domain and locally entrained by preferentially ascending low-salinity fluids. These fluids with contrasting salinity can then remix at shallower level and result in isothermal dilution trend observed from fluid inclusions in pre-ore subvertical quartz-sericite-pyrite veins. Precipitation of Cu-rich sulfides including covellite (CuS) occurred below 300°C, by boiling and forceful mixing of the S-rich but relatively Fe-deficient ore fluid with much cooler (<200°C) and salt-free groundwater.

Key words: High-sulfidation epithermal Cu-Au deposit, fluid inclusion, element partition, vapor contraction

Acknowledgements We are grateful to Markus Wälle and Marcel Guillong for their invaluable assistence with fluid inclusion analysis at ETH Zurich.

HUANGSHANITE: A NEW Fe^{3+}-TA-DOMINATED WOLFRAMITE-GROUP MINERAL

Xinhao Duan[1], Lei Xie[1]*, Rucheng Wang[1], Xiangping Gu[2]

1. State Key Laboratory of Critical Earth Material Cycling and Mineral Deposits, School of Earth Sciences and Engineering, Nanjing University, Nanjing 210023, China
2. School of Gemology and Mineral Resources, Jiangxi Institute of Applied Science and Technology, Nanchang, 330100, China

Abstract Huangshanite (IMA 2025-067, symbol "Hus"), ideally $Fe^{3+}TaO_4$, is a new Ta-dominant member of wolframite group discovered within the Huangshan pluton in Anhui Province, China. The Huangshan pluton is composed of three lithofacies, coarse-grained porphyritic biotite granite, medium-grained porphyritic biotite granite and fine-grained porphyritic biotite granite from early to late stage. Huangshanite occurs as euhedral to subhedral tabular crystals with widths of ~10–20 μm and lengths of ~20–100 μm across all lithofacies. It mostly forms at the rims of rossovskyite ($Fe^{3+}NbO_4$) and intergrows with cassiterite in mineral assemblage. Average electron microprobe analysis (EMPA) yields the following composition (wt%): WO_3 8.31, Nb_2O_5 9.71, Ta_2O_5 51.24, TiO_2 5.18, SnO_2 4.82, Sc_2O_3 0.51, MnO 1.23, FeO 6.72, Fe_2O_3 12.83 summing to100.25%. Valence balance calculation indicate an Fe^{3+}: Fe^{2+} ratio of 64.3:35.7. This result is consistent with the X-ray photoelectron spectroscopy (XPS) analysis results, which show an Fe^{3+}:Fe^{2+} ratio of 60.3:39.7, confirming the EMPA-derived valence distribution. The empirical formula calculated on total cations= 2 and O=4 atoms per formula unit (apfu) is $^{M1}[Fe^{3+}_{0.33}Fe^{2+}_{0.16}Ta_{0.17}Nb_{0.11}Ti_{0.09}W_{0.05}Sn_{0.05}Mn^{2+}_{0.03}Sc^{3+}_{0.01}]_{\Sigma 1.00}{}^{M2}[Ta_{0.48}Fe^{3+}_{0.12}Fe^{2+}_{0.09}Nb_{0.10}Ti_{0.09}W_{0.05}Sn_{0.04}Mn^{2+}_{0.02}Sc^{3+}_{0.01}]_{\Sigma 1.00}O_4$.

The Raman spectrum of huangshanite is characterized by prominent peaks at 293, 366, 659, and 837 cm^{-1}. The first two peaks (293 and 366 cm^{-1}) are attributed to rotational vibrations within Ta(Fe, Nb)O_6 octahedra, while the latter two peaks (659 and 837 cm^{-1}) correspond to stretching vibrations of the same octahedra units. The crystal structure was determined by single-crystal X-ray diffraction. Huangshanite belongs to monoclinic system, space group *P2/c* (#13) with unit-cell parameters: a = 4.6956(4) Å, b = 5.6949(5) Å, c = 5.0921(4) Å, β = 90.270(8)º, and unit-cell volume V = 136.17(2) $Å^3$, Z = 2. The powder X-ray diffraction pattern exhibits the strongest reflections as follows [d, Å (I, %) (hkl)]: 3.617 (39) (110), 2.943 (100) (111), 2.543 (27) (002), 2.481 (21) (021), 2.340 (12) (200), 1.757 (15) (130), 1.705 (23) (221).

The Huangshan granitic pluton, formed at ~130 Ma within the Jiangnan Orogen, represents a typical example of metaluminous-peraluminous granite systems. Along with the Lingshan and Suzhou plutons, it distinguishes from the strongly peraluminous granites such as Yichun pluton through distinct petrogenetic characteristics. Spatially and temporally, the granitic lithofacies exhibit systematic evolution. From early to late stage, Fe-rich micas evolve from siderophyllite

toward zinnwaldite, reflecting the progressive enrichment of Li and F contents in the granitic system. The occurrence and composition of huangshanite, rossovskyite and cassiterite indicate they crystallized during the late magmatic-hydrothermal transition stage, a period marked by elevated concentrations of Ta, W and Sn in fluid-enriched environments. The increased Fe^{3+}/Fe^{2+} ratio preserved in these oxide minerals provide robust evidence for higher oxygen fugacity during the magmatic evolution. Crucially, the discovery of huangshanite serves as a vital indicator for the variable oxygen fugacity within the mineralizing system and the potential for W mineralization related to the granite-related hydrothermal processes.

Key words: Huangshanite, $Fe^{3+}TaO_4$, wolframite-group, metaluminous rare-metal granite, oxygen fugacity

Acknowledgements This study was supported by the National Natural Science Foundation of China (Grant No. 42222202) and National Key Research and Development Program of China (2024YFC2909301).

HYDROTHERMAL BERYLLIUM MINERALIZATION IN THE BAMIANSHAN ORE FIELD, NORTHWESTERN ZHEJIANG

Mianmian Ding[1], Can Rao[1], Xudong Che[2]

1. School of Earth Sciences, Zhejiang University, China
2. School of Earth Sciences and Engineering, Nanjing University, China

Abstract Beryllium (Be) is one of the nationally strategic critical metals, and research into its mineralization mechanisms, regularities, and resource potential holds significant value. Through investigations and explorations of beryllium deposits in the Bamianshan ore field of northwest Zhejiang, Gaowushan and Jiaokengwu Be deposits have been identified. By field investigation, petrography, whole-rock geochemistry, EPMA, LA-ICP-MS trace-element analysis, and U-Pb dating, we reveal occurrence, and timing of Be enrichment and the source. The whole-rock trace-element results show that altered rocks are strongly enriched in Be (305–4400 ppm). The granite and granite porphyry are peraluminous, F-rich, with anomalously high Be (7.81–12.1 and 15.8–28.6 ppm, respectively), whereas skarnized marble contains elevated Be (65.3–171 ppm). Beryllium minerals are dominated by phenakite and bertrandite, they occur mainly as veins and veinlets in altered rocks along the contact between fluorite orebodies and wall rocks. Normally, they are closely associated with fluorite- and K-feldspar-bearing assemblages. Hydrothermal K-feldspar from altered rocks show enrichment in Be, Li, Cs, Ba, and Sr, but depletion in Rb relative to granite-hosted K-feldspar. Late grossular-rich garnet contains higher Be (84.57–1093.95 ppm) than early andradite-rich garnet. Zircon U-Pb ages of the granite porphyry and granite are 126.3±0.92 Ma and 126.5±0.58 Ma, respectively, whereas garnet and calcite yield ages of 127.2±1.2 Ma and 122±22 Ma, suggesting Be mineralization from 126 to122 Ma. These mineralogical and geochemical results indicate that Be was derived from both magma and country rocks. It was initially concentrated in evolved F-rich magmas and subsequently mobilized and precipitated by hydrothermal fluids during K-feldspathization and fluoritization under low-temperature, high-Si, and low-Al conditions favorable. This study extends the range of hydrothermal Be mineralization in South China, and highlights granite-related fluorite systems as favorable exploration targets for the critical Be metal resource.

Key words: beryllium mineralization, hydrothermal alteration, ore-forming process, South China

HYDROTHERMAL ORIGIN AND SEDIMENTARY ACCUMULATION: EARLY-STAGE ORE FORMING PROCESS OF THE ÚRKÚT AND EPLÉNY MANGANESE ORE DEPOSITS (HUNGARY)

Máté Zs. Leskó[1], Boglárka A. Topa[1], Ferenc Móricz[1], Ferenc Kristály[1], Délia H. Bulátkó-Debus[1], Richárd Z. Papp[2], Tamás G. Weiszburg[3], József Pálfy[4,5], Tamás Vigh[6], Lívia Leskóné Majoros[1], Norbert Zajzon[1]

1. Institute of Exploration Geosciences, University of Miskolc, Hungary
2. UNEXMIN Georobotics Ltd., Hungary
3. Department of Mineralogy, Eötvös Loránd University, Hungary
4. Department of Geology, Eötvös Loránd University, Hungary
5. HUN-REN–MTM–ELTE Research Group for Paleontology, Hungary
6. BÁNYATERV Mérnökiroda Plc., Hungary

Abstract The global Toarcian Oceanic Anoxic Event (T-OAE) is one of the most extensively studied anoxic event in Earth's history. Its investigation is important not only because of the profound changes in flora, fauna, environment, and climate—which provide essential knowledge for understanding present-day processes—but also because significant raw material potential is associated with it.

Two industrial-scale manganese ore deposits accumulated during the Jenkyns Event in the Transdanubian Range (Hungary). The Eplény deposit was mined until the mid-1980s, whereas mining at the Úrkút manganese ore deposit ceased in 2016. Although the Úrkút deposit has been the focus of numerous geological and industrial studies over the past 70 years, yielding a wealth of information, several questions remain unresolved.

Our research focuses on the manganese mineralization at Úrkút. The main objective was to investigate the Upper Pliensbachian and Lower Toarcian strata—including footwall limestones, marly limestones, limestones, marls, black and grey shales, clays, and Mn-bearing layers—in order to better understand the initial phase of the Jenkyns Event. Through this approach, we aimed to address two key questions: (1) what was the source of the manganese responsible for ore formation, and (2) what geological processes led to the accumulation of industrial-scale ore exclusively in the Úrkút and Eplény basins.

Samples from four locations in the Transdanubian Range were studied: the Gerecse Mountains (Tölgyhát Quarry), the Bakony Mountains (Lókút, Hosszú Trench), and the manganese ore deposits of Úrkút and Eplény.

The applied analytical methods included X-ray powder diffraction (XRD), X-ray fluorescence spectrometry (XRF), scanning electron microscopy with energy-dispersive

spectroscopy (SEM–EDS), and inductively coupled plasma mass spectrometry (ICP-MS).

Based on new clay mineralogical results (identification of montmorillonite and beidellite interpreted as minerals formed in distinct environments—hydrothermal and sedimentary, respectively), geochemical data (Fe and Mn behaviour showing a general trend of increasing iron content at the start of the Toarcian followed by an increase in manganese; Co–Ni–Zn and Fe–Mn–(Co–Ni–Cu) ternary diagrams indicating hydrothermal source; and Cd/Mo ratios suggesting an upwelling system), and sedimentological observations (evidence for radiolarian blooms), we propose a new model for the early stage of ore formation.

During the Late Pliensbachian, associated with the opening of the Neotethys Ocean, seafloor currents transported part of the beidellite formed in the rifting zone. In the Úrkút and Eplény basins, an active upwelling system promoted the deposition of this beidellite. At the same time, the upwelling supported radiolarian blooms, providing the necessary silica for the formation of montmorillonite. Variations in the intensity of the upwelling system resulted in significant fluctuations in the ratio of authigenic montmorillonite to transported beidellite.

During the Jenkyns Event, anoxic conditions spread across the seafloor. Iron and manganese released from hydrothermal vents near the rifting zones remained dissolved in bottom waters under reducing conditions and were transported over long distances by deep currents. During upwelling, these reducing bottom waters mixed with oxygen-rich upper water layers. As redox potential (Eh) increased, iron precipitated first as goethite and hematite, followed by manganese as manganite. In Toarcian samples from all investigated sections and drill cores, we consistently observed an initial increase in iron content followed by a subsequent rise in manganese concentration, which eventually exceeded that of iron. These processes were subsequently followed by well-documented diagenetic processes such as bacterial carbonate reduction.

Key words: Manganese ore, Úrkút, Toarcian Oceanic Anoxic Event, Upwelling

HYPERSPECTRAL CHARACTERIZATION OF WHITE MICA IN OROGENIC GOLD SYSTEMS: IMPLICATIONS FOR ORE GENESIS AND EXPLORATION TARGETING

Hongjie Tan[1,2], Jakub Ciazela[2] Saeid Asadzadeh[3] Kun-Feng Qiu[1],

1. State Key Laboratory of Geological Processes and Mineral Resources, Frontiers Science Center for Deep-time Digital Earth, China University of Geosciences (Beijing), Beijing 100083, China
2. Institute of Geological Sciences, Polish Academy of Sciences, Poland
3. GFZ Helmholtz Centre for Geosciences, Telegrafenberg, 14473 Potsdam, Germany

Abstract Orogenic gold deposits account for about one third of global gold production and are commonly associated with hydrothermal alteration assemblages dominated by white mica, chlorite, carbonate, and quartz. These minerals form extensive alteration halos around orebodies and can be detected by hyperspectral remote sensing. Among them, white mica is particularly useful because its Al–OH absorption feature near 2200 nm records compositional variations related to temperature, fluid chemistry, and fluid–rock interaction.

In this study, we investigate lateral and vertical variations in white mica composition in two orogenic gold deposits in China using multi-scale hyperspectral data. By comparing two contrasting orogenic gold deposits, this study aims to assess how white-mica spectral variations reflect different fluid–rock interaction processes and their potential use as exploration vectors. At the Liba open-pit orogenic gold deposit in the West Qinling, we integrate GF-5B AHSI data, drill-core hyperspectral scanning, ASD TerraSpec point spectra, petrographic observations, and EPMA data. At the Qianchen orogenic gold deposit, nine representative drill cores from granitoid-dominated host rocks were analyzed using dense point spectroscopy, petrography, and EPMA.

The two deposits show contrasting white mica spectral patterns. At Liba, the Al–OH minimum wavelength ranges from approximately 2195 to 2212 nm. Longer wavelengths and higher white mica abundance are spatially associated with the orebody, whereas shorter wavelengths occur farther from mineralization. This pattern is interpreted to reflect compositional variation in white mica controlled by Tschermak substitution and evolving fluid chemistry. In contrast, the Qianchen deposit shows a narrower Pos2200 range, commonly around 2198–2205 nm, together with smooth and deep Al–OH absorption features near the ore-bearing zones. This pattern suggests strong fluid supply, high water–rock ratios, and efficient chemical re-equilibration under relatively closed or semi-closed conditions. More scattered and unstable Pos2200 values in host domains are interpreted to reflect limited fluid access, heterogeneous deformation, incomplete reaction progress, and multi-stage overprinting. These results show that hyperspectral mapping of white mica can be used to characterize fluid evolution and alteration architecture in orogenic gold systems. The two case studies define two contrasting exploration vectors: wavelength gradients that track evolving fluid chemistry toward mineralization,

and wavelength stability or clustered Pos2200 fields that indicate structurally focused ore-stage alteration under relatively stable fluid conditions.

Key words: Orogenic gold deposits, White mica composition, Imaging spectroscopy, Mineral chemistry, exploration targeting

Acknowledgements This research was financially supported by the National Natural Science Foundation of China (42521005, 92562302, 42203072).

IN SITU OBSERVATIONS OF AMORPHOUS PGE OXIDE IN PLATINUM MINERALISATION FROM THE KONDYOR URAL-ALASKAN ULTRAMAFIC INTRUSION, RUSSIA: EVIDENCE FOR EXTREMELY RAPID OXIDATION

Irina A Zhukova[1], Hugh O'Neill[2], Aleksandr A Stepanov[1]

1. State Key Laboratory of Geological Processes and Mineral Resources, School of Earth Resources, China University of Geosciences, Wuhan, China
2. School of Earth, Atmosphere and Environment, Monash University, Clayton, VIC 3800, Australia

Abstract Platinum-group elements are highly recognised for their resistance to oxidation, which governs their high-demand applications. Despite the chemical inertness of the PGEs, oxygen-bearing and hydrous PGE phases from the natural environment have been reported in supergene-oxidised rocks and alluvial deposits, but never from depth, such as drill-core samples. We investigated in detail PGM mineralisation within chromitite from the Kondyor Ural-Alaskan type complex in Russia. Chromitite is found within serpentinised dunite that, apart from olivine, also contains minor amounts of disseminated chromite and clinopyroxene. The chromitite consists mainly of euhedral chromium spinel with serpentinised contacts. Macroscopically visible platinum mineralisation of Pt-Fe alloy is largely confined to the spaces between chromite grains, concentrating near the contact of chromitite and dunite. An Ir-Ru-oxide phase was identified within the Pt-Fe alloy, typically in contact with native Os and sometimes in contact with Os-Ru sulfide (laurite-erlichmanite). The Ir-Ru-O phase appears as elongated aggregates reaching up to 70 μm in length. It has low hardness, as shown by a rough surface in polished sections, numerous cracks, and evidence of shrinkage. Both shrinkage and crack formation progress significantly once affected by the electron beam during EPMA and Raman analysis. The Ir-Ru-oxide composition is dominated by Ir, ranging from 42.5 to 49.8 wt.%, and also contains Ru (12.1-14.5 wt.%), minor amounts of Os (0.3–3.0 wt.%), Pt (1.3–4.7 wt.%), and Rh (0.8–1.5 wt.%). Oxygen contents measured by EDS and WDS EPMA vary between 16.8 and 30.4 wt.%, yielding an $(Ir,Ru)O_x$ stoichiometry where x falls between 1.6 and 3. TEM diffraction patterns of this phase show no distinct atomic plane reflections but rather diffuse rings, suggesting an amorphous structure. This contrasts with the perfect crystal structure of the adjacent native Os crystal. The presence of the Ir-Ru-oxide implies strongly oxidising conditions several orders of magnitude above the stability field of Ir-Ru alloys in temperature, pressure, and oxygen fugacity space. Furthermore, such oxidising conditions are inconsistent with the coexistence of native Os in direct contact with the oxide. We therefore interpret the Ir-Ru-oxide phase as a product of thermodynamic disequilibrium and discuss possible mechanisms for its formation. Stable under magmatic or hydrothermal conditions, primary PGE alloys turn reactive in near-surface supergene

settings when exposed to oxygen, acidic fluids, and chloride-rich solutions. Low-temperature, high-fO_2 chemical weathering oxidizes Pt-Fe and Os-Ir-Ru alloys. The former yields an oxygen-bearing Pt-Fe phase, while the latter partially dissolves to form Os-Ir-Ru oxides. This is evidenced by the Ru/Ir atomic ratio of the Ir-Ru-O phase, which matches that of native Os. Volatile Os oxide escapes the system, leaving behind an Ir-Ru-O phase alongside metallic Os low in Ir and Ru.

Key words: Chromitite, Ural-Alaskan Intrusions, PGE oxide, TEM.

INTENSIVE CARBONATE FRACTIONATION DRIVES GIANT REE ACCUMULATION: INSIGHTS FROM THE BAYAN OBO DEPOSIT

Xiaochun Li, Kuifeng Yang, Hongrui Fan

Institute of Geology and Geophysics, Chinese Academy of Sciences, China

Abstract The giant Bayan Obo deposit, China, represents the world's largest rare earth element (REE) resource, yet the mechanism responsible for its extraordinary REE enrichment remains highly debated. The central controversy concerns the origin of the ore-hosting dolomite. Because these dolomite rocks have experienced extensive hydrothermal overprinting, we conducted a texturally constrained in situ Sr isotopic study to determine their primary origin. The results show that unaltered dolomite domains exhibit $^{87}Sr/^{86}Sr$ ratios < 0.704, distinctly lower than those of Mesoproterozoic marine carbonates worldwide (> 0.705). These data demonstrate that the primary dolomite is mantle-derived and represents a carbonatitic protolith.

To further elucidate the petrogenetic evolution of the carbonatite, we investigated its two principal components: early-stage coarse-grained dolomite (CD; ~10 vol.%) and late-stage fine-grained dolomite (FD; ~90 vol.%). Compared with the CD, unaltered dolomite domains within the FD are enriched in FeO and MnO and display higher $\delta^{13}C$ (–4.9 to 0.3‰) and $\delta^{18}O$ (9.4 to 17.1‰) values. The FD also contains abundant REE- and volatile-rich hydrothermal minerals and Fe–Mg carbonates, which are rare in the CD. These geochemical and mineralogical characteristics collectively indicate that the melts forming the FD were significantly more evolved than those forming the CD. Based on melt Na contents estimated from apatite compositions, the parental melt underwent ~60–75% fractional crystallization of carbonates. Modeling demonstrates that such advanced differentiation can generate substantial REE enrichment in residual melts and exsolved fluids.

Compared with other carbonatite complexes worldwide, the Bayan Obo carbonatite suite is distinguished by its unusually large exposure (~48 km in outcrop) and the exceptional abundance of highly evolved carbonatitic components. The voluminous evolved carbonatite system provided a fundamental petrogenetic basis for the formation of this giant REE deposit.

Key words: Carbonatite, REE mineralization, Fractional crystallization, Bayan Obo

INVESTIGATION OF PRIMARY VOLATILE CONTENT AND EVOLUTION OF CHALCOPHILE ELEMENT OF BONINITIC MELT INCLUSIONS IN HIGH CRYSTALLINITY PICRITE, TROODOS OPHIOLITE

Ri Cao [1,2,5], Kun-Feng Qiu[2], Lee Saper[3], Wim van Westrenen[4], Igor Nikogosian[4], Geoff Bromiley[5]

3. School of Civil Engineering, University of Leeds, LS2 9LG

1. State Key Laboratory of Geological Processes and Mineral Resources, Frontiers Science Center for Deep-time Digital Earth, School of Earth Sciences and Resources, China University of Geosciences, Beijing 100083, China
2. Division of Geological and Planetary Sciences, California Institute of Technology, Pasadena, CA, USA
3. Department of Earth Sciences, Faculty of Science, Vrije Universiteit Amsterdam, Amsterdam, The Netherlands
4. School of Geosciences, University of Edinburgh, EH9 3FE

Abstract The Troodos ophiolite is an exceptionally preserved supra-subduction zone (SSZ) ophiolite, having chemical features typical for spreading centres near subduction zones. Over the past 70 years, extensive study of the structure, stratigraphy, and geochemistry of Troodos has been pivotal in the development of the theory of plate tectonics, seafloor spreading and subduction initiation, as well as our understanding of magmatic-hydrothermal processes associated with the formation of oceanic crust. Ascending from the base, the Troodos massif comprises tectonised harzburgite, layered intrusive rocks such as dunite, wehrlite, pyroxenite, and gabbro, followed by sheeted dykes and capped with extrusive rocks. Within the extrusive sequence, on the N. flank of the Troodos near Margi, exceptionally crystal-rich picritic lavas occur. Well-preserved olivines within these picrites record early fractionating processes which affected magmas across the ophiolite, but are typically poorly preserved in other units.

The metallogenic systematics of the Troodos Ophiolite are less clear, however, with uncertainties regarding precious metal enrichment in volcanogenic massive sulfide (VMS) deposits and the potential for magmatic-hydrothermal mineralisation in nascent arcs. The Troodos ophiolite is increasingly accepted to represent a ‘proto-arc’ formed during subduction initiation. Due to its volcanic glass record of magmatism and resource estimates for its VMS deposits, this ophiolite is well suited for elucidating this metallogeny.

To investigate the metallogeny and primitive volatile content of the Troodos Ophiolite, we selected 40 olivine crystals with three-phase MIs and performed 11 pioneer piston-cylinder experiments at 1.4 GPa and 1300 °C, in which we achieved complete homogenisation of 30 melt inclusions in high-forsterite olivines from different picrite bodies in Margi, followed by SIMS and EPMA analysis to more accurately capture the primitive volatile content and

chalcophile elements of those picrite. Our results show more enhanced primitive H2O content of boninitic parental magma than previously estimated by the 1-atm homogenised melt inclusion study, providing insight into the nature and extent of subduction-flux of fluids into mantle source regions for the Troodos.

Key words: Troodos Ophiolite, Chalcophile element, melt inclusion, volatile content

INVESTIGATION OF THE INDIUM BEARING SPHALERITE FROM NAGYBÖRZSÖNY, HUNGARY

Máté Zs. Leskó[1], Boglárka A. Topa[1], Róbert Arató[2], Viktor Bertrandsson Erlandsson[2], Phillip Gopon[2],
Délia H. Bulátkó-Debus[1], Norbert Zajzon[1]

1. Institute of Exploration Geosciences, University of Miskolc, Hungary
2. Department of Applied Geosciences and Geophysics, Technical University of Leoben, Austria

Abstract The Nagybörzsöny mining area is located approximately 50 km NNW of Budapest (capital of Hungary), in the central part of the Börzsöny Mountains. Nagybörzsöny is one of the oldest ore mining areas in Hungary, with documented extraction of gold, silver, lead, and sulfur dating back to the 14th century. The known mineralization is spatially associated with one Miocene (~14.6 Ma) caldera structure. The mineralization developed in dacitic lava rocks and pyroclasts. The following mineralization types can be distinguished:

- Epithermal breccia and vein mineralization with Bi-Pb-As-(Au-Ag-Te-Se), Zn-Pb-Ag-(Cu-Sb) and Au-Ag
- Mesothermal polymetallic mineralization with Zn-Pb-Cu-(W)
- Porphyry copper mineralization with Cu-Fe-(Au-Mo)

Sphalerite is the primary source of zinc and, due to its relatively simple crystal structure, can incorporate a wide range of trace elements, including e.g. Fe, As, Cd, Mn, Ag and Pb. In addition to being an important source of zinc, sphalerite is also known to host elevated concentrations of critical metals such as gallium, germanium, and indium. Consequently, sphalerite represents a significant ore mineral for these elements. Indium, which rarely forms sufficiently concentrated primary minerals, is produced almost exclusively as a by-product of zinc from sphalerite concentrates.

This study investigated sphalerite samples from several parts of the mining district, including the Lower Adit, Istenáldás Adit, Lower Rózsa Adit, Ludmilla Adit, and Kammerhof. During our research FIB-SEM-EDS (focused ion beam scanning electron microscopy) and LA-ICP-MS (Laser Ablation Inductively Coupled Plasma Mass Spectrometry) were used.

Indium was detected in all sphalerite samples, spanning a wide concentration range from a few tens of ppm up to 1245 ppm. No systematic spatial variation in indium enrichment was observed across the mining district; however, significant variability occurs even within individual sampling locations. We did not find clear evidence of a consistent correlation between indium and other trace elements. In some samples, indium shows a relatively strong

correlation with copper (up to 0.75), whereas in others this relationship is weak (around 0.25). A similar pattern is observed for silver: in some cases, the correlation is strong (up to 0.89), while in others there is no correlation (−0.02).

Key words: Indium, Sphalerite, Nagybörzsöny, Hungary,

Acknowledgements Project no. 2023-1.2.4-TÉT-2023-00045 has been implemented with the support provided by the Ministry of Culture and Innovation of Hungary from the National Research, Development and Innovation Fund, financed under the 2023-1.2.4-TÉT funding scheme.

LITHIUM ENRICHMENT IN CLAYSTONES OF THE JIUCAITANG DEPOSIT, SHIRENBEI BASIN, SOUTH CHINA

Shuai Huang[1], Xudong Che[1*], Rucheng Wang[1], Xiancai Lu[1], Fei Deng[2]

1. State Key Laboratory of Critical Earth Material Cycling and Mineral Deposits, School of Earth Sciences and Engineering, Nanjing Universit, China
2. Guangdong Province Geological Bureau Foshan Geological Survey Center,Foshan,Guangdong,China

Abstract Volcano-sedimentary (VS) Li deposits have recently been recognized as an emerging type of Li deposit. Although characterized by low grades, their large resource potential makes them highly promising Li reservoirs. However, this deposit type has so far been rarely documented in China. This study investigates the Jiucaitang lithium deposit in the Shirenbei Basin, northeastern Guangdong Province, South China, where Li mineralization is hosted mainly by fine-grained lacustrine claystones of the Late Cretaceous Yetang Formation overlying felsic volcanic rocks of the Yousheng Formation. We integrate whole-rock geochemistry, X-ray diffraction, SEM observation, mineral geochemistry, and zircon U-Pb geochronology to constrain the provenance, host phases, and enrichment mechanism of Li.

In ore-hosting claystones, Li content shows positive correlations with B and Rb, indicating that Li enrichment was coupled with fluid-related geochemical signatures. XRD and microtextural observations show that the claystone matrix is dominated by illite and illite-smectite (I-S) mixed-layer minerals, with minor chlorite and kaolinite. In-situ analyses demonstrate that illite and I-S mixed-layer minerals are the principal Li hosts. The highest-grade claystone is characterized by a homogeneous, clay-rich matrix, whereas lower-grade samples contain more quartz- and feldspar-rich silt, indicating that hydrodynamic sorting played an important role in controlling ore grade.

Detrital zircon U-Pb ages from the Li-rich claystone indicate a substantial contribution from coeval felsic volcanic materials to the Yetang claystones. Altered volcanic and volcaniclastic rocks record pervasive fluid-rock interaction, including mica zonation, volcanic-glass pseudomorphs, feldspar dissolution, kaolinization, and secondary quartz growth. Mineral chemistry further indicates substantial Li redistribution during alteration, with Li depletion in altered mica and enrichment in authigenic kaolinite replacing K-feldspar.

We propose that the Jiucaitang deposit formed through three processes: hydrothermal preconditioning of felsic volcanic source rocks, sedimentary concentration of Li-bearing clay-rich detritus in low-energy lacustrine settings, and diagenetic fixation of Li mainly in illite. The deposit is therefore best interpreted as a stratabound VS Li deposit. This model suggests that Late Cretaceous volcanic fault basins along the Southeast Coast Magmatic Belt of China are prospective where hydrothermally altered felsic source rocks, fine-grained lacustrine claystones, and coupled Li-B-Rb enrichment occur together.

Keywords: lcano-sedimentary Li deposit, Shirenbei Basin, Li claystone mineralizaton, illite

Acknowledgements Deep Earth probe and Mineral Resources Exploration-National Science and Technology Major Project (2025ZD1004706); the National Science Foundation of China (42272067).

MAGMATIC–HYDROTHERMAL EVOLUTION AT THE BARREN WUSHAN PLUTON, SOUTHEAST CHINA: INSIGHT INTO CONTROLS ON MINERALIZATION POTENTIAL

Zhe Chi, Jun-Yi Pan, Pei Ni

State Key Laboratory of Critical Earth Material Cycling and Mineral Deposits, Institute of Geo-Fluids, Frontiers Science Center for Critical Earth Material Cycling, School of Earth Sciences and Engineering, Nanjing University, Nanjing 210023, China

Abstract A-type granites are commonly associated with rare-metal enrichment and mineralization, including Mo and Sn deposits. Although Late Cretaceous A-type granites are widespread along the southeastern coast of China, significant mineralization has not yet been documented in this region. To evaluate the controls on the Mo and Sn metallogenic potential of this A-type granite belt, we conducted a detailed melt and fluid inclusion study of the Wushan pluton, located at its southernmost part, to constrain the metal and volatile contents of the melts and exsolved fluids and to reconstruct its magmatic–hydrothermal evolution.

The Wushan pluton displays distinct lithological zoning and consists mainly of medium-grained to porphyritic alkali-feldspar granite and fine-grained porphyritic granite, both of which contain abundant miarolitic cavities. Silicate melt inclusions in the two facies have rhyolitic compositions, with 76.7–85.3 wt% SiO_2, moderate F contents of 0.06–0.53 wt%, and relatively low H_2O contents of 2.0–3.5 wt%. Zr saturation thermometry and Ti-in-quartz thermobarometry indicate crystallization at 750–820°C and 1.4–2.5 kbar. Large variations in incompatible elements, such as Cs contents of 9–1977 ppm and Rb contents of 268–2601 ppm, indicate extensive magmatic differentiation.

The least evolved melt inclusions contain 2–5 ppm Mo and 3–10 ppm Sn. During magmatic evolution, Mo behaved as a highly incompatible element and became progressively enriched with fractional crystallization, although Mo concentrations remained nearly constant in highly evolved melts with Cs > 50 ppm. Rayleigh fractionation modeling suggests that exsolution of ore-forming fluids extracted substantial Mo from the residual melt, thereby limiting further Mo enrichment during late-stage evolution. In contrast, Sn showed only moderately incompatible behavior, increasing more slowly and reaching a maximum of approximately 30 ppm in highly evolved melts. Fractional crystallization of Sn-bearing minerals, including biotite, magnetite, and titanite, likely suppressed Sn enrichment in the residual melt.

Miarolitic quartz formed during the magmatic–hydrothermal transition and records fluid exsolution. Quartz cores preserve coexisting melt inclusions and intermediate-density fluid inclusions, the latter representing the initial fluid exsolved from the magma. Inclusion thermobarometry indicates trapping at approximately 700°C and 1.3–1.5 kbar. Quartz rims contain pseudosecondary assemblages of vapor-rich inclusions and high-salinity daughter-mineral-bearing inclusions, indicating fluid boiling caused by decompression and cooling. The intermediate-density fluid inclusions contain 120–

220 ppm Mo, whereas Sn contents are generally below 10 ppm. Based on coexisting melt and intermediate-density fluid inclusions, the fluid/melt partition coefficient of Mo ($D_{Mo,\ fluid/melt}$), is estimated at 16–19, whereas that of Sn ($D_{Sn,fluid/melt}$), is only approximately 1.

Global comparisons between mineralized and barren systems indicate that Mo mineralization is not simply controlled by metal contents in melts or fluids. Instead, lower melt viscosity and the development of apical cupolas may promote efficient extraction and focusing of metal-bearing fluids into small rock volumes. Thus, physical and structural conditions appear critical for Mo mineralization. For Sn systems, melt enrichment is necessary but not sufficient; the Sn content of the initial exsolved fluid is the key control. Our results suggest that the southeastern coastal A-type granite belt has some potential for Mo exploration but limited potential for Sn mineralization.

Key words: melt inclusion, fluid inclusion, LA-ICP-MS, mineralization potential

METHANE HYDRATE FORMATION IN THE KAOLINITE PARTICLES WITH DIFFERENT SURFACE CONTACTS: INSIGHTS FROM MOLECULAR DYNAMICS SIMULATION

Yun Li

School of Petroleum Engineering, Xi'an Shiyou University, Xi'an 710065, China

Abstract The nucleation behavior of methane hydrate in the presence of kaolinite was strongly affected by the surface contacts of kaolinite particles. Molecular dynamics simulations were performed to investigate methane hydrate formation in contact with different surfaces of kaolinite particles (*i.e., siloxane and hydroxyl surfaces*). The results show that methane hydrate can nucleate at the siloxane surface heterogeneously. Methane could be adsorbed onto the vacancy of the Si-O rings of the siloxane surface to form semi-cage structures. These structures not only help to minimize the structural mismatch between the siloxane surface and hydrate crystal but also facilitate the growth of methane hydrate. However, methane molecules cannot break through the hydration layer of the hydroxyl surface to nucleate. These results indicate that kaolinite particles with exposed siloxane surfaces facilitate methane hydrate nucleation but not those with hydroxyl surface in contact with solution. Thus, the surface properties of kaolinite particles are found to be crucial for nucleation, growth, and distribution of methane hydrate in natural sediments.

Key words: Methane hydrate, Kaolinite, Surface contacts, Molecular simulations

MICRO- TO NANO-SCALE INSIGHTS INTO GOLD ENRICHMENT IN HIGH-GRADE QUARTZ VEINS OF THE LONGTOUGOU GOLD DEPOSIT, SOUTH QINLING OROGEN

Ya-Fei Wu*, Ya-Ge Wu, Feng-Xia Huang

State Key Laboratory of Geological Processes and Mineral Resources, China University of Geosciences, Wuhan, Hubei Province 430074, China

Abstract Orogenic gold deposits represent one of the world's most important gold resources. However, the genesis of high-grade quartz veins in these systems remains unclear. This study combines laser ablation–multicollector–inductively coupled plasma–mass spectrometry (LA-MC-ICP-MS) and transmission electron microscopy (TEM) to characterize the micro- to nano-scale textures and geochemical features of auriferous pyrite in quartz veins (up to 48 g/t Au) from the Longtougou orogenic gold deposit in the South Qinling orogen, China, aiming to elucidate the processes and mechanisms responsible for gold enrichment in high-grade quartz veins.

Four generations of pyrite were identified: (1) early-stage euhedral Py1; (2) main-stage Py2 characterized by oscillatory zoning and abundant inclusions of native gold, galena, and tetrahedrite; (3) main-stage fine-grained porous Py3 that overgrows Py1 but lacks visible gold; and (4) late-stage Py4 intergrown with specularite. LA-ICP-MS trace element analyses reveal that Py1 contains low gold concentrations (mean = 1.72 ppm), occurring predominantly as lattice-bound solid solution. In contrast, Py2 shows higher Au contents (mean = 34.3 ppm), with Au spikes in ablation depth profiles indicative of gold inclusions. Py3 represents the most gold-rich generation (mean = 1031 ppm), with Au, As, and associated elements extensively incorporated into the pyrite lattice. Py4 has the lowest gold content (mean = 0.26 ppm). In situ sulfur isotope analyses reveal that Py1 has $\delta^{34}S$ values ranging from +1.75‰ to +5.70‰, consistent with a magmatic sulfur source. Compared with Py1, Py2 (+1.72‰ to +4.30‰) and Py3 (−3.64‰ to +3.44‰) display a progressively decreasing $\delta^{34}S$ trend, possibly suggesting that fluid oxidation played a key role in promoting gold deposition.

TEM analyses reveal the absence of gold nanoparticles in Py3, confirming that gold occurs predominantly as solid solution. Acicular to fibrous iron oxides are developed in Py3, indicating that the ore fluids were strongly oxidizing. The porous texture of Py3 is consistent with dissolution-reprecipitation processes of pyrite. These observations demonstrate that fluid oxidation and dissolution-reprecipitation reactions could have played important roles in gold enrichment in orogenic gold systems.

Key words: Auriferous pyrite, Gold enrichment, Longtougou gold deposit, South Qinling orogen

MINERAL CHEMISTRY AND PETROGENETIC IMPLICATIONS OF MONAZITE-(CE) AND ALLANITE-(CE) IN THE UYAYNAH CARBONATITES, UNITED ARAB EMIRATES

Mabrouk Sami[1*], Hamed Gamaleldien[2*], Xiao Han[2], Bahaa M. Amin[1], Xun ZhaO[1], Douaa Fathy[3]

1. Geosciences Department, College of Science, United Arab Emirates University, Al Ain, United Arab Emirates
2. Department of Earth Sciences, College of Engineering and Physical Sciences, Khalifa University, Abu Dhabi, United Arab Emirates
3. Geology Department, Faculty of Science, Minia University, El-Minia 61519, Egypt

*Corresponding authors (mabrouksami@uaeu.ac.ae; hamed.gamaleldien@ku.ac.ae)

Abstract The Uyaynah carbonatites of the United Arab Emirates represent an unusual extrusive carbonatite system distinguished by strong REEs enrichment and abundant phosphate mineralization. Within this assemblage, monazite-(Ce) and allanite-(Ce) are the principal REEs-bearing minerals and provide an important record of REEs sequestration during the late evolution of the carbonatite. Monazite is compositionally consistent with monazite-(Ce), showing clear dominance of the LREEs, particularly Ce and La, with subordinate Nd and Pr, low HREEs contents, and minor incorporation of Th, U, Ca, and Sr. Allanite is likewise Ce-rich and strongly enriched in the LREEs, indicating that both minerals acted as major sinks for REEs during crystallization and subsequent fluid-assisted modification. Texturally, monazite occurs as fine anhedral grains intergrown with allanite, whereas allanite is more abundant and occurs as disseminated grains and locally in late calcite veinlets. Their intimate association with apatite, calcite, and iron oxides suggests progressive redistribution of REEs from an initially apatite-rich carbonatite assemblage into secondary phosphate- and silicate-hosted reservoirs during late magmatic to magmatic-hydrothermal evolution, followed by metamorphic overprint. These data highlight a distinctive monazite-allanite mineral association in the Uyaynah carbonatites and emphasize the role of phosphate–silicate coupling in controlling LREEs enrichment in evolved carbonatite systems.

Key words: UAE carbonatites, Monazite, Allanite, REE enrichment, LREE sequestration

Acknowledgements This study was financially supported by the grants (No G00004879-12S155 and G00004980-12S218) from the United Arab Emirates University. This research was also funded by Khalifa University of Science and Technology through the RIG-2025 under Project ID: KU-INT-RIG-2025-8471000063.

MINERAL FORMATION MECHANISMS AND PALEOENVIRONMENTAL IMPLICATIONS OF IRON FORMATIONS DURING THE SNOWBALL EARTH

Jun Hu[1,2], Sanzhong Li[1,2], Shui-Jiong Wang[3,4]

1. Frontiers Science Center for Deep Ocean Multispheres and Earth System, Key Lab of Submarine Geosciences and Prospecting Techniques, MOE and College of Marine Geosciences, Ocean University of China, China.
2. Laoshan Laboratory, Laboratory for Marine Mineral Resources, Qingdao Marine Science and Technology Center, Qingdao, China.
3. State Key Laboratory of Geological Processes and Mineral Resources, China University of Geosciences (Beijing), China.
4. Frontiers Science Center for Deep-time Digital Earth, China University of Geosciences (Beijing), China.

Abstract The "Snowball Earth" hypothesis suggests that Earth experienced two global glaciations during the Neoproterozoic: the Sturtian (~ 717 – 660 Ma) and Marinoan (~ 650 – 635 Ma) ice ages. These events were among the most extreme climate events in Earth's history, significantly influencing the evolution of both the environment and life. The Sturtian glaciation is particularly unique, as iron formations (IFs) re-emerged after nearly a billion years of dormancy, providing a crucial window for studying the marine geochemical evolution and ice age dynamics of this period. In this study, we examine five representative Sturtian deglaciation IFs from the Nanhua Basin, integrating paleogeographic context, mineralogical features, and multiple geochemical indicators, including Ni-Fe-C isotopes. The results reveal a novel formation mechanism for magnetite and Mn-rich carbonate minerals within these IFs, controlled primarily by microbial-mediated metal-driven anaerobic oxidation of methane (AOM). The study further identifies that phosphorus (P) input predominantly comes from continental weathering, with the formation of authigenic apatite also constrained by AOM-driven Fe-Mn-P cycling. These findings highlight the complex "microbe-methane-metal-mineral" coupling interactions during the Sturtian glaciation, offering new insights into the genesis of IFs. Moreover, our results emphasizes the potential significance of CH_4-related biogeochemical processes and Fe-Mn-P cycling in extreme climate transitions, paleoenvironmental evolution, and early life evolution.

Key words: Magnetite, Apatite, Fe–Ni–C Isotopes, Iron Formations (IFs), Snowball Earth

MINERALOGIC AND GEOCHEMISTRIC STUDY OF SPHALERITE FROM THE DALINGKOU PB-ZN-AG DEPOSIT, ZHEJIANG, CHINA

Ying Xu[1], Haizhen Wei[1,2,*]

1. State Key Laboratory for Mineral Deposits Research, Department of Earth Sciences and Engineering, Nanjing University, Nanjing 210023, PR China
2. CAS Center for Excellence in Comparative Planetology, China, Anhui 230026, PR China

Abstract The Dalingkou Pb-Zn-Ag deposit is a typical representative of continental volcanic-hosted mineralization in southeastern Zhejiang Province. An in-depth study of this deposit is of great scientific significance for deciphering the intrinsic mechanisms of the Mesozoic volcano-magmatic-hydrothermal ore-forming system in the coastal area of Southeast China. In this paper, we present systematic investigations from four aspects: deposit geology, sphalerite mineralogy, major and trace element geochemistry, and silver isotope composition. The main conclusions are as follows:(1) Two generations of sphalerite have been identified: Sphalerite in the Dalingkou deposit formed mainly in the second mineralization stage (including Sp2a and Sp2b) and the third mineralization stage (Sp3). Sp2a and Sp2b, which formed in the early part of the main mineralization stage, are characterized by dark colors, good euhedral shapes, and common complex oscillatory zoning. Sp3, which formed in the late part of the main mineralization stage, is less abundant, has lighter colors, lacks well-developed internal zoning, and locally exhibits colloform textures. (2) The occurrence states and substitution mechanisms of trace elements have been clarified: Binary plots of trace elements and elemental mapping results indicate different occurrence states and substitution mechanisms for different trace elements. Fe, Mn, Cd, Ga, Ge, and In are dominantly incorporated into the sphalerite lattice via isomorphic substitution, whereas Cu, Ag, Sb, and Pb mainly occur as micro-inclusions or daughter minerals. (3) The temperature-sulfur fugacity evolutionary path of the ore-forming fluid has been quantitatively reconstructed: Calculations using multiple sphalerite geothermometers indicate that the average crystallization temperatures of sphalerite in the second and third metallogenic stages were approximately 298 °C and 227 °C, respectively. The sulfur fugacity (fS_2) during sphalerite precipitation ranges from $10^{-8.7}$ to $10^{-14.8}$, revealing a significant cooling process from the early to the late stage accompanied by a progressive decrease in sulfur fugacity. (4) The enrichment mechanism of silver in this deposit has been elucidated: During mineralization, Ag^+ was transported mainly as chloride complexes (e.g., $AgCl_2$) in the early stage. As temperature and sulfur fugacity decreased, silver was predominantly carried as hydrosulfide complexes ($Ag(HS)_2^-$) during the second mineralization stage, and eventually precipitated as fine-grained silver minerals in the third stage due to the dissociation of these complexes. This process is accompanied by a corresponding variation in Ag isotope distribution. The $\delta^{109}Ag$ values of the second stage are concentrated and stable (-0.002‰ to +0.318‰), reflecting

homogeneous fluid conditions. In contrast, the third stage shows wider fluctuations (-0.426‰ to +0.474‰), indicating environmental perturbation or a change in fluid source. Based on a comprehensive analysis of mineralization characteristics, fluid evolution, and geochemical indicators, this study proposes that the Dalingkou deposit belongs to the intermediate to low-sulfidation epithermal type. These findings are expected to deepen the understanding of metallogenic processes in continental volcanic rock regions of South China and provide new scientific evidence for further refining the regional metallogenic theory.

Key words: Dalingkou deposit, Sphalerite, LA-ICP-MS, Ore-forming physico-chemical conditions, Ag isotopes

MINERALOGICAL AND GEOCHEMICAL INVESTIGATION OF UV-FLUORESCENT SPHALERITES FROM MEŽICA, SLOVENIA

Norbert Zajzon[1], Máté Zs. Leskó[1], Róbert Arató[2], Viktor Bertrandsson Erlandsson[2], Máté Bíró[3], László Himics[4], Délia H. Bulátkó-Debus[1], Boglárka A. Topa[1]

1. Institute of Exploration Geosciences, University of Miskolc, Hungary
2. Chair of Geology and Economic Geology, Technical University of Leoben, Austria
3. Department of Mineralogy, Eötvös Loránd University, Hungary
4. Applied and Nonlinear Optics Department, HUN-REN Wigner Research Centre for Physics, Hungary

Abstract The Mississippi-Valley-Type (MVT) Pb–Zn ore deposits of Mežica in the Eastern Karawanken Mountains (Slovenia) have been exploited since Roman times, with intensive mining during the last ~500 years until depletion of known resources in 1994. The deposits, which are genetically related to the nearby Bleiberg and Raibl localities, consist of more than 350 orebodies formed by hydrothermal fluids migrating along subvertical Alpine fault systems hosted by Triassic karstic limestones. The youngest part of the system (Topla) is considered syngenetic. Primary ore mineralization is dominated by galena and sphalerite, which were subsequently oxidized by meteoric waters to depths of down to 2 km, forming a complex and world-famous secondary mineral association dominated by wulfenite, accompanied by anglesite, cerussite, hemimorphite, smithsonite, and descloisite.

During field tests of the Horizon 2020 Robominers project, in-situ UV observations and sampling were performed in two distinct orebodies: the Level 5 section of the Graben mine in Žerjav (sphalerite-rich) and the Mežica mine (Podzemlje Pece) in Glančnik (galena-rich). While massive galena-rich ores are easily identifiable visually, sphalerite-rich ores are inconspicuous in visible light and were effectively detected using UV illumination due to their strong and variable fluorescence. This pronounced UV fluorescence of sphalerite was therefore investigated in detail.

Galena, sphalerite, dolomite, and calcite were identified by X-ray powder diffraction in the samples. Optical microscopy revealed several generations of sphalerite, distinguishable under visible light and even more clearly under UV illumination by distinct fluorescent colours. Fluorescence spectra were recorded using a photo-spectrometer under monochromatic excitation. The textural relationships and trace element contents of the different sphalerite generations were also investigated with LIBS- and LA-ICP-MS-mapping.

The coarse-crystalline brown sphalerite displays blue luminescence with fine-scale zoning, ranging from deep dark to light blue, with darker outer zones adjacent to carbonates and brighter inner zones. Under 270 nm excitation, emission peaks occur between ~310–335 nm, while excitation at 365 nm produces an emission around ~460 nm. Subsequent zones consist of dark

brown to black sphalerite that exhibits intense deep red fluorescence under UV light, with pronounced fine and sector zoning visible in UV images, back-scattered electron images, and elemental maps. The red fluorescence intensity correlates with cadmium contents of a few tenths of wt%, whereas sector-zoned copper distribution results in fluorescence quenching. This sphalerite generation shows emission peaks at ~360 and ~440–450–460 nm with 270 nm excitation, and at ~560 and ~600–610 nm with 365 nm excitation.

The innermost zone is composed of a fine-crystalline mixed sphalerite mass exhibiting diverse luminescent colours, with spectra containing features characteristic of both brown and black sphalerite as well as dolomite, though black sphalerite peaks dominate. The zonation patterns are also prominent in monochrome SEM-cathodoluminescence images, where luminescence intensity may correlate with or oppose UV fluorescence intensity.

Associated dolomite exhibits strong violet-purple luminescence under UV light, with peaks at approximately 350 and 390 nm under 270 nm excitation, and dominant bands near 410, 440, and 490 nm under 365 nm excitation. Previous work reported minor Fe, Cu, As, Cd, Ag, Ga, Ge, Hg, Bi, Mn, Mo, Ni, Pb, Sb, and Tl in Mežica sphalerite, but without qualitative data or distribution patterns. Although several recent studies have linked fluorescent colours in sphalerite to trace elements, the exact effects of individual and simultaneous trace-element incorporation remain unresolved.

Key words: sphalerite, UV-fluorescence, trace elements, LA-ICP-MS-mapping, Mežica,

Acknowledgements This research was partly financed by the Robominers project, which has received funding from the European Union's Horizon 2020 research and innovation programme under grant agreement No. 820971.

MINERALOGICAL AND ISOTOPE-GEOCHEMICAL FEATURES OF SULFIDES IN NATIVE GOLD FROM THE GULI MASSIF (POLAR SIBERIA) AND THEIR GENETIC SIGNIFICANCE

Kreshimir N. Malich[1], Inna Yu. Badanina, Alexandr V. Ignatiev[2], Tat'yana A. Velivetskaya[2]

1. Department of Geochemistry and Ore-Forming Processes, Zavaritsky Institute of Geology and Geochemistry, Ural Branch of the Russian Academy of Sciences, Russia
2. Department of Stable Isotopes, Far East Geological Institute, Far East Branch of the Russian Academy of Sciences, Russia

Abstract The Guli massif of ultramafic, alkaline rocks and carbonatites is the primary source of large osmium placers, as well as small gold placers. This study presents the first results on the chemical and S-isotope composition of sulfides within polymineralic inclusions in native gold from the Quaternary deposits of the Gule and Dunitovaya rivers, located in close proximity to the Southern carbonatite stock of the Guli massif.

The composition of native gold and sulfide inclusions was determined using a CAMECA SX 100 electron probe microanalyzer equipped with five wavelength-dispersive spectrometers (Geoanalitik Shared Knowledge Center, IGG UB RAS). Sulfur isotope data for the sulfides were obtained using a femtosecond laser ablation system (NWR Femtosecond UC with Pharos 2mJ-200-PPam laser and HE-4Hi-A harmonics module) and a MAT-253 mass spectrometer (Thermo Fisher Scientific, Germany) at the Primorye Center for Local Elemental and Isotopic Analysis (FEGI FEB RAS, Vladivostok).

Sulfides within polyphase inclusions (70 to 150 microns in size) for which the sulfur isotope composition was determined consist of: (1) pentlandite (Pn), pyrrhotite (Po), chalcopyrite (Ccp), and galena (Gn); (2) Pn and Ccp; and (3) Ccp, Po, and Pn. These inclusions were identified in Au-Ag alloy grains of varying fineness with compositions ($Au_{77}Ag_{23}$) and ($Au_{52}Ag_{47}Cu_1$), as well as in a natural Au–Cu–Ag alloy where the concentrations of Au, Cu, and Ag are 87.53±0.85, 7.00±0.21, and 5.71±0.23 wt. %, respectively.. The $\delta^{34}S$ values for the sulfides vary within a narrow range from –0.1 to 2.5‰ (mean value of 1.70‰ with a standard deviation of 1.23‰, n = 4).

The difference between sulfides from placer gold ($\delta^{34}S$ = 1.70±1.23‰) and those from the phoscorite-carbonatite rock series ($\delta^{34}S$ from –3.0 to –6.9‰) can be considered within the framework of two alternative hypotheses:

1. The placer gold of the Guli massif originates from different primary sources. In this context, a portion of the gold (with a mantle signature of $\delta^{34}S \approx 1.7$‰), much like the Ru-Os sulfides, may be associated not with carbonatites, but with the earliest ultramafic rocks (dunites). This explains why the sulfur isotope composition of sulfides in gold is identical to that of detrital Ru-Os sulfides ($\delta^{34}S$=1.4±0.8‰, n = 10) but differs from that of carbonatites.

2. If the hypothesis of a genetic link between placer gold and carbonatites is accepted (based,

in part, on the similarity of mineral assemblages), the difference in sulfur isotope composition suggests that the gold crystallized from an early, undifferentiated portion of the carbonatite fluid. In this case, the "isotopically heavy" sulfur of the sulfides in gold corresponds to the "primary" mantle signature, whereas the "isotopically light" sulfur of sulfides from phoscorites and carbonatites results from the prolonged evolution of the magmatic fluid (even in the absence of sulfates, for instance, due to temperature fractionation or changes in the pH of the mineral-forming environment).

The fact that the sulfur isotope composition of placer gold matches that of platinum-group minerals within the margin of error, yet differs from carbonatite sulfides, serves as additional evidence for a deep-seated magmatic origin of the gold, unrelated to the final stages of carbonatite formation. It is concluded therefore that the gold is a product of an early high-temperature stage of the magmatic system. It acted as an inert "micro-container" that preserved the primary mantle sulfur and isolated it from subsequent processes of isotopic fractionation and fluid depletion in heavy isotopes, which are characteristic of the final stages of the phoscorite-carbonatite series formation.

Keywords: Guli massif, native gold, sulfide inclusions, sulfur isotopes, genetic significance.

Acknowledgements This study was supported by the Russian Science Foundation, project No. 25-17-00116.

MINERALOGICAL CONSTRAINS FOR THE PROCESS OF CS ENRICHMENT IN THE LCT PEGMATITE SYSTEM FROM THE GYIRONG PLUTON, HIMALAYA

Ennong Tian[1,2], Lei Xie[2], Rucheng Wang[2]

1. School of Gemology and Materials Science, Hebei GEO University, China
2. School of Earth Sciences and Engineering, Nanjing University, China

Abstract Lithium-Cesium-Tantalum (LCT) pegmatites are primary hosts for rare metal mineralization. Recent studies indicate that numerous LCT pegmatites within the Himalayan leucogranite belt are associated with Be, Li, Nb, Ta, Sn, and Cs mineralization. Notably, Cs mineralization has been identified in the Gyirong pluton, located in the central Himalaya. This study presents a detailed mineralogical investigation to constrain the magmatic-hydrothermal processes governing Cs mineralization.

The Gyirong pluton hosts various granitic and pegmatitic lithologies. Based on mica and tourmaline assemblages, these rocks are classified into two-mica granite, schorl-bearing muscovite granite, elbaite-bearing lepidolite pegmatite, and elbaite-rich lepidolite pegmatite. These units are predominantly composed of quartz, albite, K-feldspar, mica (muscovite/lepidolite), and tourmaline.

Due to its low abundance and large ionic radius, Cs typically occurs as a trace element in potassium-bearing minerals (e.g., micas and K-feldspar), except when forming discrete Cs-rich minerals such as pollucite, sokolovaite, and pezzottaite. In the two-mica granite and schorl-bearing muscovite granite, Cs is hosted primarily in mica and K-feldspar, exhibiting an elevated fractionation trend. For instance, Cs concentrations increase from trace amounts in the two-mica granite (~37 ppm in muscovite, ~990 ppm in biotite) to significantly higher levels in the schorl-bearing muscovite granite (~1680 ppm in muscovite and ~363 ppm in K-feldspar).

Furthermore, progressive fractional crystallization from elbaite-bearing to elbaite-rich lepidolite pegmatite resulted in enrichment of Li, Rb, and Cs. Micas in these pegmatites typically display a core-rim structure with muscovite cores and lepidolite rims. The cores show increasing Li and Cs concentrations from the elbaite-bearing to the elbaite-rich varieties (up to 13000 ppm and 4,000 ppm, respectively), consistent with magmatic fractionation trends. In contrast, the activity of F-rich fluids during the late magmatic stage caused a sharp increase in F, Li, and Cs contents from the muscovite cores to the lepidolite rims. Consequently, lepidolite rims in the elbaite-rich pegmatite contain higher concentrations of F, Li, and Cs (up to 8.53 wt%, 31200 ppm, and 8800 ppm, respectively) compared to those in the elbaite-bearing pegmatite (up to 6.80 wt%, 27400 ppm, and 5600 ppm, respectively). The Cs fluids released by the hydrothermal alteration of lepidolite eventually enhance the Cs concentration in the residual melts, and ultimately leding to the crystallization of Cs-rich minerals, including pollucite, sokolovaite, and Cs-rich beryl.

Key words: LCT pegmatites, Himalaya, cesium, micas

MINERALOGICAL EVIDENCE FOR CO–SE REDISTRIBUTION IN COBALT MINERALIZATION SITES OF THE LANPING–SIMAO BASIN: CONSTRAINTS FROM PYRITE OXIDATION AND TROGTALITE FORMATION

Yuxiang An[1], Fei Huang[1]*, Wenyuan Gao[1], Lichen Feng[1], Yang'ai Lei[2]

1. School of Resources and Civil Engineering, Northeastern University, China
2. Team 310 of Yunan Nonferrous Metals Geological Bureau, China

Abstract Newly discovered cobalt mineralization occurrences in the Lanping–Simao Basin, Southwest China, exhibit significant Co enrichment characteristics. In systematically collected samples, Co contents reach up to 4200 ppm, averaging approximately 2000 ppm, with local outcrop samples exceeding 1 wt.% Co. This Co enrichment indicates the possible presence of intensive Co activation, migration, and re-enrichment processes in this area; however, the mineral occurrence state of Co and its coupling relationship with Se remain unclear. To determine the carrier minerals of Co, the occurrence state of Se, and the formation mechanism of trogtalite, this study comprehensively employs X-ray diffraction, scanning electron microscopy, electron probe microanalysis, and transmission electron microscopy to conduct multi-scale mineralogical investigations of sulfides, iron oxides/hydroxides, and selenides in cobalt mineralization samples.

Combined X-ray diffraction, microscopic observation, and electron probe microanalysis data indicate that pyrite in this cobalt mineralization occurrence is generally enriched in Co, with contents typically ranging from 200–2500 ppm; some pyrites also contain minor Se, usually below 100 ppm. No microscopic evidence of independent Co mineral inclusions was observed in pyrite. Goethite is the dominant secondary iron mineral in the mineralized samples, accompanied by minor hematite; goethite commonly retains pyrite pseudomorphs and contains trace amounts of Co, typically around 0.1 wt.%. Comprehensive analysis of the above phenomena suggests that early Co was likely incorporated primarily into pyrite in an isomorphous form. Following intensive supergene oxidation, pyrite underwent oxidative alteration to form hematite-goethite mineral assemblages with pyrite pseudomorphs.

Trogtalite ($CoSe_2$) is mainly distributed in pores, fractures, and grain edges of residual pyrite and goethite, commonly occurring as 2–15 μm anhedral microcrystals or microcrystalline aggregates. Electron probe microanalysis shows that these microcrystals are composed primarily of Co and Se, with Co contents of approximately 16.66–19.66 wt.% and Se contents of approximately 60.42–74.38 wt.%. Transmission electron microscopy observations reveal that trogtalite grains exhibit distinct polycrystalline characteristics. Selected area electron diffraction patterns show diffuse concentric diffraction rings, among which the (110), (111), (200), and (220) crystal planes corresponding to $CoSe_2$ can be identified. High-resolution transmission electron microscopy images

and their fourier transform results indicate that both lattice fringes and diffraction spots are relatively blurred, demonstrating that Co and Se in this mineralization occurrence have been re-enriched into the important mineral phase trogtalite, with fine grain sizes and generally low crystallinity.

This study proposes that early pyrite was an important initial carrier of Co and minor Se. During subsequent supergene oxidation, pyrite decomposed, transforming into goethite and hematite; part of the S was removed from the local system as sulfate, while Co and Se were activated, migrated, and reprecipitated in micropores or at mineral boundaries. Under local low sulfur activity and relatively Se-rich microenvironments, Co and Se formed $CoSe_2$ with a pyrite-type structure, namely trogtalite, occurring as low-crystallinity polycrystalline aggregates between residual pyrite and goethite. This study demonstrates that trogtalite is not only one of the important Co-bearing minerals in the cobalt mineralization occurrences of the Lanping–Simao Basin, but also records the local retention, migration, and reprecipitation of the chalcophile element Se during pyrite oxidation. These results provide new mineralogical evidence for understanding the Co–Se coupled enrichment mechanism in sedimentary basin-type cobalt mineralization and the control of supergene oxidation modification on critical metal redistribution.

Key words: Trogtalite, Pyrite oxidation, Co–Se redistribution, Supergene enrichment, Lanping–Simao Basin

MINERALOGICAL INVESTIGATION OF THE NI – CO BEARING MINERALS OF THE FELSŐCSATÁR TALC SHIST (HUNGARY)

Máté Zs. Leskó[1], Boglárka A. Topa[1], Délia H. Bulátkó-Debus[1], Lívia Leskóné Majoros[1], László E. Aradi[2], Sándor Szakál[1]

1. Institute of Exploration Geosciences, University of Miskolc, Hungary
2. Hungarian National Museum, Archaeometry Laboratory, Budapest, Hungary

Abstract The Ni and Co enrichment of the Felsőcsatár talc deposit is known from the middle of the 20th century, but detailed mineralogical investigation was not carried out. Our aim is to identify Ni- and Co bearing phases, and explain their formation.

Felsőcsatár is located within the Rechnitz Window, a Penninic tectonic unit exposed along the eastern margin of the Alps. This window represents a deeply exhumed segment of an accretionary complex, consisting predominantly of oceanic and sedimentary sequences that were subducted and metamorphosed during Alpine convergence.

The lithological framework is dominated by two main complexes. The ophiolitic complex comprises serpentinized ultrabasic rocks and metabasic lithologies derived from MORB-type oceanic crust, typically represented by greenschist- to locally blueschist-facies assemblages. These rocks frequently underwent talc and serpentine alteration, forming the basis of the talc mineralization. The second major unit is a metasedimentary complex composed of phyllites, quartz-phyllites, and calcareous schists.

The metamorphic evolution of the Rechnitz Unit is polyphase. An early ocean-floor metamorphism under low-pressure, high-temperature conditions ($P \approx 1$ kbar, $T \approx 400 - 700$ °C) affected the ophiolites. This was followed by Alpine metamorphism under low-temperature, higher-pressure conditions (6–8 kbar, ~390–430 °C) during the Late Cretaceous (~65 Ma), corresponding to subduction-related burial. A later, lower-pressure overprint (~3 kbar, similar temperatures) occurred during Miocene exhumation.

The talc mine is closed, and availability of the drillhole samples is limited, so our samples were collected from the waste dump of the former talc mine. During our research SEM-EDS and Raman-spectroscopy were used.

We identified at least ten distinct mineral phases containing Ni and/or Co. The most abundant phases (~80 wt% of the total Ni- and Co-bearing phases) are Ni-rich pentlandite, with an approximately 55–45 wt% Ni–Fe ratio, and Ni-bearing pyrrhotite with ca. 3.5 wt% of Ni. These minerals are interpreted to originate from the original MORB-type oceanic crust; however, it remains unclear to which metamorphic stage their formation can be attributed.

The violarite–siegenite group represents the second most abundant assemblage, comprising

approximately 15 wt% of the Ni- and Co-bearing phases, and is interpreted to have formed via supergene alteration of the pentlandite.

In addition, we identified gersdorffite, cobaltite, Ni-bearing pyrite, ullmannite, millerite, and greigite; however, these minerals collectively account for less than 5 wt% of the total Ni- and Co-bearing phases.

Key words: Ni-Co mineralization, Felsőcsatár, Hungary

Acknowledgements Supported by the University Research Scholarship Program of the Ministry for Culture and Innovation from the source of the National Research, Development and Innovation Fund.

MINERALOGY AND GENESIS OF PYRITE WITH VARYING CRYSTAL MORPHOLOGIES IN COAL GANGUE OF NORTH CHINA

Lihui Liu[1], Yiyuan Huang[1], Qinfu Liu[2]

1. School of Environmental and Municipal Engineering, Lanzhou Jiaotong University, Gansu 730070, China
2. School of Geosciences and Surveying Engineering, China University of Mining and Technology (Beijing), Beijing 100083, China

Abstract Coal gangue is a blackish-gray rock with a lower carbon content and greater hardness than coal, formed in association with coal seams during the coal formation process. This study investigated the mineralogical and geochemical characteristics of coal gangue from the Taiyuan Formation of the Carboniferous within the Late Paleozoic coal-bearing basins of the North China Platform. The coal gangues are mudstones, silty mudstones and pelitic siltstones. They are mainly composed of kaolinite, quartz, feldspar, pyrite, illite, siderite and magnesite. Pyrite is ubiquitous in coal gangue for its reduced formation environment, which has great influence on the recircling utilization of coal gangue.

Pyrite with different crystal morphologies and geochemical characteristics that are typically employed to infer the bottom seawater microenvironment and diagenetic stages. In this study, five kinds of pyrite with different structures and morphologies were identified, framboidal pyrite, pentagonal dodecahedral pyrite, euhedral octahedral crystalline pyrite, semi-euhedral granular pyrite and irregular granular pyrite. Through the effective integration of polarizing microscopy, X-ray diffraction, scanning electron microscope, and nanoscale secondary ion mass spectrometry, the crystal structure, microscopic morphology, *in-situ* sulfur isotope content, and distribution of pyrite crystals were comprehensively analyzed. Pyrite with good crystallinity has a high S/Fe ratio, approximately 2.15; pyrite with poor crystallinity has a low S/Fe ratio, approximately 1.88. The NanoSIMS show that the varying morphologies and $\delta^{34}S$ values of pyrite closely correlate to the crystal growth pattern, sulfur source, and precipitation mechanism. Extremely negative $\delta^{34}S_{CDT}$ values ranging from -38.09‰ to -0.62‰ occur for framboidal pyrite and euhedral granular pyrite. The low $\delta^{34}S$ values suggest genesis from syn-depositional to early diagenetic periods in an open environment with unlimited diffusion of seawater sulfate. In the zones dominated by organiclastic sulfate reduction, morphological characteristics of pyrite are controlled by the redox condition of bottom seawater, which generally have relatively small particle sizes. In contrast, the irregular pyrite and cell-filling pyrite exhibit slightly larger particle size, with positive $\delta^{34}S_{CDT}$ values ranging from +8.93 to +10.15‰ and +5.55 to +16.16‰, respectively, indicating that they formed during the diagenetic stage under the influence of sulfate-reducing bacteria. The geochemical characteristics recorded in the microscale pyrites reflect substrate depletion effects in an increasingly closed system. This research highlights the vital relationship between grain shape and the mechanism of sedimentary pyrite formation in the

coal-forming environment, providing important theoretical support for the comprehensive utilization of pyrite-rich coal gangue.

Key words: Coal gangue, Pyrite, Crystal morphology, *In-situ* sulfur isotope

MINERALOGY AND ORIGIN OF AMMONIUM ILLITE IN COAL SEAM PARTINGS

Zhanjie Xu

Institute of Surface-Earth System Science, School of Earth System Science, Tianjin University, Tianjin 300072, China

Abstract This study investigates mineralogy and origin of ammonium illite within the No. 15 coal seam of the Taiyuan Formation in the Qinshui Basin, utilizing polarized light microscopy, XRD, FTIR, and TGA to systematically analyze its mineralogical features and genetic mechanisms. The results show that ammonium illite is predominantly concentrated in the fine-grained fractions of claystone interbeds within coal gangue. It forms via two primary pathways: diagenetic transformation of kaolinite and authigenic crystallization within fractures, both of which are closely associated with the occurrence and enrichment of critical metals. While nitrogen in the diagenetic ammonium illite is largely derived from the pyrolysis and biodegradation of organic matter, nitrogen in the fracture-hosted authigenic illite may be linked to magmatic hydrothermal activity. Therefore, diagenetic transformation, authigenic crystallization, and hydrothermal processes may control the enrichment of critical metals (e.g., Li, Rb, Cs) in the ammonium illite, primarily through isomorphous substitution or adsorption. These findings provide fundamental data and theoretical insights into the formation of ammonium illite in coal-bearing systems, critical metal enrichment, and future mineral exploration.

Key words: illite, nitrogen, origin, coal seam, Qinshui Basin

MINERALOGY, GEOCHEMISTRY, AND ISOTOPIC CONSTRAINTS ON THE GENESIS OF BORON DEPOSITS IN THE LIAO-JI BELT, EASTERN LIAONING PROVINCE

Chenyang Liu[1], Can Rao[1], Nan Ju[2], Yanfei Zhang[2]

1. School of Earth Sciences, Zhejiang University, China
2. Shenyang Center of Geological Survey, China Geological Survey, China

Abstract Boron deposits are strategic critical mineral resources essential to traditional industries and high-technology sectors. The boron deposits in eastern Liaoning Province, representing China's most significant boron resources, occur as stratiform or lenticular ore bodies hosted within Paleoproterozoic volcano-sedimentary sequences of the Liao-Ji Belt. However, the occurrence modes and metallogenic mechanisms of boron remain insufficiently understood. This study focuses on the Zhuanmiao deposit, with comparative analysis of the Wengquangou and Houxianyu districts, integrating regional geological context to examine boron occurrence and its relationship with regional Liaoji granites, thereby providing theoretical guidance for future mineral exploration.

As the Liao-Ji Belt represents the most typical Paleoproterozoic orogenic belt within the North China Craton, the Liaodong boron deposits are hosted by Paleoproterozoic Liaohe Group metamorphic rocks. Structurally, the region features near EW-trending linear, tight compound anticlines and synclines, with NNE-, EW-, and NW-trending fault systems. Ore bodies of the Zhuanmiao boron deposit primarily occur within boron-bearing serpentinized dolomitic marble. Formation of these deposits was influenced by volcanic and sedimentary processes, followed by multiphase metamorphism and deformation. Country rocks exhibit varying degrees of migmatization, with intense hydrothermal alteration proximal to ore bodies, including serpentinization, diopsidization, phlogopitization, chloritization, and marblization.

Petrographic and mineralogical analyses show szaibelyite and tourmaline are the principal boron-bearing minerals within six distinct paragenetic assemblages. Whole-rock geochemistry reveals that Zhuanmiao ores contain 20.74–30.46% B_2O_3 and 38.40–40.20% MgO, whereas boron-bearing serpentinized marbles have 8.53–12.43% B_2O_3, 28.10–34.50% MgO, and 22.48–24.19% SiO_2; serpentinite ores contain 44.61–45.65% SiO_2 with variable MgO (6.35–33.00%). Trace element patterns indicate LREE-enriched patterns with pronounced negative Eu anomalies, featuring Sr/Ba ratios (0.39–68.14) distinct from surrounding amphibolites (~0.9) and migmatitic granites (~0.5). Isotopic analyses yield a Sm-Nd age of 1935.6 ± 27.5 Ma and Pb compositions indicating derivation from U-Th-enriched orogenic upper crust. δ^7Li values range 5.45–14.11, while carbonate C-O isotopes ($\delta^{13}C$ = −5.56 to −1.21‰; $\delta^{18}O$ = −25.94 to −14.69‰) and Z-values (122.02–131.08) support a marine sedimentary protolith. These results

will provide theoretical foundations for exploration targeting and sustainable resource development in the Liaodong region.

Key words: Boron deposit, Szaibelyite, Liao-Ji Belt, Paleoproterozoic metallogenesis, Isotopic geochemistry

MULTI-SCALE MINERALOGICAL CONSTRAINTS ON ARC-RELATED FE-TI-(P) MINERALIZATION: A CASE STUDY OF THE DEVONIAN DAWUSUNANGOU LAYERED MAFIC-ULTRAMAFIC INTRUSION, NORTH CHINA CRATON

Sijia Yao [1], Shanshan Li [1], Kristoffer Szilas [2], Kunfeng Qiu [1]

1. State Key Laboratory of Geological Processes and Mineral Resources, Frontiers Science Center for Deep-time Digital Earth, China University of Geosciences, China
2. Natural History Museum of Denmark, Nordic Center for Earth Evolution, University of Copenhagen, Denmark

Abstract The northern margin of the North China Craton hosts numerous mafic-ultramafic intrusions associated with Fe-Ti-(P) mineralization along the Hongshila-Damiao fault zone, constituting one of the most important Fe-Ti-(P) metallogenic belts in northern China. Although these deposits have been extensively studied, the processes controlling Fe-Ti-(P) mineralization in hydrous arc-related mafic magmatic systems remain poorly constrained. The Dawusunangou deposit preserves Devonian Fe-Ti-(P) mineralization superimposed on Paleoproterozoic AMCG-related magmatism, providing an excellent opportunity to investigate the origin and evolution of Fe-Ti-(P) mineralization in a hydrous arc-related layered mafic-ultramafic intrusion. This study integrates petrography, whole-rock geochemistry, in-situ major and trace element analyses of rock-forming and ore minerals, biotite Rb-Sr geochronology, and apatite U-Pb geochronology to constrain the timing, magma source, magmatic evolution, and mineralization processes of the lower ore-bearing intrusion.

Geochronological data indicate that the lower layered mafic-ultramafic intrusion and associated Fe-Ti-(P) mineralization formed between 404 and 389 Ma, demonstrating a regional Devonian mafic-ultramafic magmatic event along the northern margin of the NCC. The intrusion is dominated by pyroxene amphibolite and pyroxenite and hosts both Fe-Ti and Fe-P mineralization. Pyroxene and amphibole thermobarometry reveals two crystallization stages at approximately 0.65–0.85 GPa and 900–940 °C, and 0.40–0.52 GPa and 850–875 °C, corresponding to middle-lower crustal and middle crustal magma reservoirs, respectively. These results indicate polybaric crystallization and evolution of a hydrous arc-related magma system. Amphibole from the Fe-P ores records relatively higher crystallization temperatures, suggesting that P enrichment was related to the evolution of a deep-seated, mantle-derived, P-rich, hydrous, and moderately oxidized mafic-ultramafic magma.

Trace element compositions of magnetite indicate that magnetite from both Fe-Ti and Fe-P ores crystallized within the same hydrous arc-magmatic system through Fe-Ti oxide crystallization and accumulation. The mineralization is distinct from both the high-Ti-V Fe-Ti oxide systems associated with the Emeishan mantle plume and the liquid-immiscibility-related Fe-Ti-P

mineralization recognized in the Damiao complex. Apatite and magnetite accumulated together within the layered intrusion. Apatite is characterized by LREE enrichment, HREE depletion, positive Ce anomalies, and weak positive Eu anomalies, indicating crystallization from a P-rich, REE-enriched, and relatively oxidized magma. Following ore formation, Ti-rich magnetite domains underwent subsolidus re-equilibration during cooling and increasing oxygen fugacity, producing ilmenite lamellae, trellis textures, and patchy Ti-rich oxide domains. Subsequently, hydrous and moderately oxidized magmatic-hydrothermal fluids infiltrated the Fe-Ti oxide assemblages along fractures, grain boundaries, and exsolution interfaces, resulting in localized dissolution-reprecipitation and element redistribution, and forming rutile, titanite, and aggregates of high-Ti magnetite.

The lower layered mafic-ultramafic intrusion is characterized by enrichment in LREEs (La, Ce, Pr, and Nd) and LILEs (Rb, Ba, and Pb), depletion in HFSEs (Nb and Ta), high Ba/Th ratios, low Th/La ratios, and relative enrichment of Pb and U. These geochemical characteristics indicate derivation from an enriched mantle source metasomatized by subduction-related fluids. The intrusion formed in a subduction-related continental arc setting following arc-continent collision between the northern margin of the NCC and the Bainaimiao arc. This study provides new insights into mantle source modification, the evolution of hydrous mafic magmas within a multi-level magma plumbing system, and the genesis of Fe-Ti-(P) mineralization in subduction-related continental arc environments.

Key words: North China Craton, layered mafic-ultramafic intrusion, Fe-Ti-(P) mineralization, Multi-level magma reservoir system, arc magmatism

NANOSCALE DISTRIBUTION OF ELEMENTS IN GOLD USING ATOM PROBE TOMOGRAPHY

Kimberly T. Tait[1,2] and Evan Hastie[2,3]

1. Royal Ontario Museum (Department of Natural History, Canada)
2. Ontario Geological Survey (Ministry of Energy and Mines, Canada)
3. University of Toronto (Department of Earth Sciences, Canada)

Abstract Critical minerals are essential components of modern technologies and play a central role in the global transition toward low-carbon energy systems. Many countries around the globe are investing time, effort and money in various strategies to respond to the global demand for critical mineral elements and materials to support the transition to a low-carbon economy. The growing demand for critical minerals, combined with increasingly complex geopolitical pressures, has highlighted the vulnerability of relying on foreign sources for these essential resources.

A collaborative project between the Ontario Geological Survey (OGS), the Royal Ontario Museum (ROM) and the Metal Earth project (MERC, Laurentian University) and dozens of industry partners called the Gold Fingerprinting Project was started in 2020. The primary objective of this project is to develop a robust methodology for gold characterization and to establish the chemical composition of gold samples from deposits around the world. To support this objective, the project team has analyzed more than 650 samples from over 330 gold deposits across the globe, with a focus on North America and Ontario, Canada. The resulting geochemical dataset provides a baseline for elemental concentrations in gold ores and associated tailings. Complementary petrographic and geochemical analyses have also been conducted to better understand the mineralogical deportment of key elements and critical minerals within these deposits. Fundamentally studying gold itself, not proxies for gold, such as quartz, is an important step forward in gold exploration, not only in Ontario, but globally.

Although gold may not be on many critical mineral lists, gold deposits offer the best opportunity to produce several elements as co-products or by-products. Many of the elements that are associated with gold and used as exploration vectors can also be highly enriched in gold deposits (e.g., antimony, arsenic, bismuth, copper, molybdenum, platinum group elements, selenium, silver, tellurium, titanium, tungsten and zinc). Of particular interest are semi-metals, such as bismuth, antimony and tellurium given that these are geochemically coupled throughout the natural gold refinement process in deposits. This presentation will explore our approach at studying gold samples with a correlative workflow including analytical techniques such as Laser Ablation Inductively Coupled Plasma Mass Spectrometry (LA-ICP-MS), electron microprobe analysis (EMPA), and Scanning Electron Microscopy (SEM) and Atom Probe Tomography (APT).

With this large dataset, we can selectively interrogate a variety of elements from different deposit types and how they substitute within gold using APT. Gold forms 12-coordinated cubic

closest-packed structures with metallic bonds. Most elements appear to have a homogenous 3D atomic distribution visually, but this can be investigated more closely by examining nearest-neighbor distributions of each element. These first nearest-neighbor (1NN) distributions can indicate the homogeneity (or randomness) of elemental distribution in the gold samples by being compared to distributions expected for a randomized dataset. Although several elements such as Ag, Cu, As, Pd, Pt are homogeneously distributed in several gold samples, Sb is notably different from that of the randomized data, with a clear shift in the distribution peak toward smaller 1NN distances. This deviation from the random distribution suggests the presence of Sb clusters. Many other elements also share similar metallic radii with Au, but it is likely that many of these are less commonly found within gold due to their preference for other minerals.

Key words: critical minerals, semi-metals, gold, atom probe tomography, atomic distribution

Acknowledgements This project is made possible by the collaborative effort of the OGS, ROM, and MERC at Laurentian University. The authors would like to thank Katherine Dunnell (ROM) for her support in sampling gold for the project. KTT is supported by a NSERC Discovery Grant. Atom probe tomography sample preparation and analysis was performed at the Canadian Centre for Electron Microscopy (also supported by NSERC and other government agencies) with special appreciation given to Brian Langelier, Gabe Arcuri, Nabil Bassim and Travis Casagrande.

NANOSTRUCTURAL CHARACTERISTICS OF ASBOLANE IN A CO-POLYMETALLIC MINERALIZATION SITE, LANPING–SIMAO BASIN, CHINA

Lichen Feng[1], Yuxiang An[1], Fei Huang[1]*, Wenyuan Gao[1], Yuanzhao Liang[2]

1. School of Resources and Civil Engineering, Northeastern University, China
2. Team 310 of Yunan Nonferrous Metals Geological Bureau, China

Abstract Cobalt is an important strategic critical metal. However, in supergene environments, its mineral carriers commonly exhibit low crystallinity, highly variable compositions, and ambiguous phase boundaries, rendering accurate identification challenging. Asbolane is a significant carrier mineral in weathering-type cobalt mineralization, chemically corresponding to Co- and Ni-bearing hydrous manganese oxide/oxyhydroxide. Nevertheless, owing to its layered structure, interstratification characteristics, and overlapping diffraction features and chemical compositions with phases such as lithiophorite, manganite, and heterogenite, asbolane remains difficult to identify conclusively.

This study systematically investigates the micrometer- to nanometer-scale mineralogical characteristics of asbolane in a Co-polymetallic mineralization site in the Lanping–Simao Basin, southwestern China. A comprehensive analytical approach, incorporating optical microscopy, scanning electron microscopy (SEM), electron probe microanalysis (EPMA), and transmission electron microscopy (TEM), was employed to systematically characterize nodular Co–Mn oxyhydroxide aggregates hosted within quartz interstices and pyrite-bearing veinlets. The nodules in the studied sample are predominantly 50–150 μm in diameter and exhibit distinct concentric zoning. EPMA spot analyses reveal that the outer zone is Co-enriched, with local Co contents reaching 55–68 wt.%, corresponding to a heterogenite-like (CoOOH) phase; the intermediate zone is Mn-enriched, showing decreased Co and elevated Mn contents; and the inner zone exhibits renewed enrichment of Co and Ni, forming a Co–Mn oxyhydroxide assemblage dominated by asbolane. Goethite inclusions are observed in the cores of some nodules.

TEM observations indicate that asbolane-dominated inner zones are porous and poorly crystallized, exhibiting lattice defects including discontinuous lamellae, dislocations, and localized structural vacancies. Selected area electron diffraction (SAED) patterns demonstrate that the inner Co–Mn-enriched zone has an interplanar spacing of approximately 0.928 nm, consistent with the basal spacing of asbolane, whereas the outer Co-enriched phase exhibits an interplanar spacing of ~0.475 nm, indicative of a layered structure analogous to that of heterogenite. Localized Al enrichment in the outer zone further indicates late-stage fluid modification and complex crystal-chemical adjustment.

Integrated mineralogical evidence demonstrates that asbolane formation in the study area was

controlled by multistage supergene alteration. Early-stage weathering of Co-rich pyrite released Co, which was subsequently oxidized, adsorbed, and structurally incorporated by Mn oxyhydroxides under oxidizing conditions. The nodular texture and concentric compositional zoning reflect periodic fluctuations in redox conditions and fluid chemistry within an open weathering system. This study suggests that asbolane should not be regarded as a simple mineral with fixed stoichiometry, but rather as a highly complex Co–Ni–Mn oxyhydroxide mineral assemblage that plays a critical controlling role in the enrichment, fixation, and preservation of Co in supergene cobalt deposits.

Key words: asbolane, cobalt mineralization, supergene enrichment, nanostructure, Lanping–Simao Basin

NEW PERSPECTIVE ON CRITICAL RAW MATERIALS POTENTIAL IN CENTRAL EUROPE: INSIGHTS FROM THE CZECH GEOLOGICAL SURVEY

Michal Poňavič, Martin Kubeš, Anna Vymazalová, Martin Štrba,
Czech Geological Survey, Klárov 131/3, 118 00 Praha 1, Czech Republic

Abstract The raw materials strategies are currently being reassessed worldwide. There is a new emphasis on the security of raw materials and energy supplies, promoting recycling, and increasing the use of secondary raw materials. Like other countries, the Czech Republic supports intensive research into Critical Raw Materials (CRM) through national and international research projects. One example is the Ministry of the Environment's national program "Environment for Life". As part of this program, the Czech Geological Survey is working on an extensive research project RENS (=Rock Environment and Natural Resources), which is subdivided into several basic research themes mainly focused on studying CRMs that have economic significance for the Czech Republic. The CRM currently being studied in the Czech Republic include graphite, lithium, manganese, tungsten, rare earth elements (REE), germanium, and feldspars. The research includes not only conventional exploration methods, such as geochemical heavy minerals prospecting and soil metallometry, but also modern methods of applied geophysics (satellite geophysical analysis, use of combined geoelectric techniques, etc.). Besides, an important part of the research is also the creation of 3D deposit and geological models with visualization of the newly acquired data. Furthermore, the current research activities include the verification of basic parameters of CRM processing technology with a focus on modern technologies producing minimum waste and the development of new ecological and low-energy processing methods. The attention is mainly focused on the processing of graphite, lithium, tungsten, REE and gold.

Another example is the international ERA-MIN project SuMREE (=Sustainable mining of REE in Europe), which provides important constraints on the distribution and major enrichment mechanisms of REE and other CRM (e.g. Ni, Co, Sc, platinum group elements = PGE) in Ni-rich lateritic soils associated with (ultra)basic complexes from the South Bohemian Region in the Czech Republic. Based on integration of in-situ chemical analyses (EMPA-SEM), X-ray diffraction (XRD), whole-rock elemental (ICP-MS) and Sr–Nd isotopic composition (TIMS), major carriers and sources of CRM in lateritic soils were identified. These include mainly Mn-oxides, which along with Ni-rich chlorite, serpentine (antigorite-lizardite), Fe-oxides (goethite) and clay minerals (smectite) may incorporate a significant amount of Ni, whereas Co is exclusively hosted by Mn-oxides. By contrast, distribution of REE lateritic soils appears to be more complex. The positive whole-rock correlation of ΣREE and Al_2O_3 suggests sorption of REE on clay minerals (mainly smectite). Furthermore, REE are occasionally present as detrital (monazite) and authigenic phases

(rhabdophane), reflecting diversity of REE mineral hosts in lateritic sediments. The variable Sr–Nd isotopic signatures of lateritic soils most likely reflect different REE sources, including (ultra)basic rocks with more radiogenic isotopic compositions (e.g. pyroxenites, eclogites) and/or granulites that typically enclose mantle-derived rocks tectonically emplaced to the crustal lithologies. Based on the whole-rock distribution of REE and other CRM in lateritic soils, in combination with the above-mentioned findings, geochemical maps illustrating a large-scale distribution of CRM were compiled to provide a reliable tool for targeting new potential occurrences of CRM associated with lateritic deposits in Central Europe.

Key words: Environment for Life, Critical Raw Materials (CRM), Czech Geological Survey (CGS), RENS, SuMREE

Acknowledgements The research is supported by the projects "SS02030023 Rock Environment and Natural Resources RENS" and "TH88020001 Sustainable Mining of Rare Earth Elements in Europe SuMREE" of the Technology Agency of the Czech Republic.

ORIGIN AND DIAGENETIC EVOLUTION OF CLAYSTONES IN THE CP_2 COAL SEAM, ADAOHAI MINE, DAQINGSHAN COALFIELD: EVIDENCE FROM MINERALOGY AND GEOCHEMISTRY

Ni He[1], Shangying Li[2], Hongfei Cheng*[,1], Zhenxiao Wu[3], Yichen Wang[1], Shaoxian Liang[4]

1. *School of Earth Science and Resources, Chang'an University, No. 126 Yanta Road, Xi'an 710054,*
2. *School of Land Engineering, Chang'an University, No. 126 Yanta Road, Xi'an 710054,*
3. *School of Resources Environment and Tourism, Anyang Normal University, No. 436 Qiangge Road, Anyang 455000, ChinaChina,*
4. *Geoscience and Surveying Engineering, Xi'an University of Science and Technology School, No. 58 Yanta Road, Xi'an 710054, China*

Abstract As the demand for non-metallic and strategic associated resources continues to grow, the comprehensive development and utilization of coal-associated resources have become a focal point in the mining industry's green transition. Among these, coal-bearing claystones, as vital clay resources, have attracted significant attention owing to their potential for development and economic value. The high-quality claystone layers within the coal-bearing strata of the Daqingshan Coalfield represent a vital reserve for enhancing the comprehensive utilization of regional resources. Although the basic geology and coal section characteristics of this mining area have been extensively studied, systematic mineralogical and geochemical evidence regarding the provenance, diagenetic evolution, and genesis mechanisms of coal-bearing claystones remains lacking.

The Daqingshan Coalfield in Inner Mongolia takes the CP_2 coal section (Shuanmazhuang Formation) as its primary mineable layer, with the CP_4 coal section (Zahuaigou Formation) as a local mineable layer. These coal sections contain abundant claystone resources. This study presents a systematic analysis of claystone samples from the CP_2 seam in the Adaohai Mine, integrating mineralogical and geochemical data to elucidate sediment provenance and diagenetic evolution. The dominant clay minerals include kaolinite, illite (with K^+ primarily occupying the interlayer sites), and NH_4^+-bearing illite (with NH_4^+ primarily occupying the interlayer sites), with minor non-clay phases such as quartz, pyrite, diaspore, anatase, and calcite. The provenance of the claystones in the study area mainly derives from the intermediate-felsic volcanic ash associated with the Late Paleozoic continental arc volcanic activities in the Inner Mongolia Uplift, which is located on the northern margin of the North China Block. During the Late Paleozoic, the Paleo-Asian Ocean Plate subducted beneath the North China Block triggered extensive volcanic activity in the Inner Mongolia Uplift along the northern margin of the North China Block. The erupted volcanic ash was deposited in the coeval peat swamp basins of the North China region. Kaolinite primarily formed through the alteration of volcanic ash in basins, with minor kaolinite originating from the

recrystallization of aluminosilicate colloidal solutions. Numerous fine-grained illite and NH_4^+-bearing illite exhibit textural characteristics of replacing kaolinite grains, indicating that illite and NH_4^+-bearing illite were formed by the transformation of the precursor mineral kaolinite under hydrothermal fluids associated with thermal anomaly activity in the Late Jurassic-Early Cretaceous of North China. These fluids, enriched in Ca, Mg, Al, Si, and N, can form fracture fillings predominantly composed of silexite, dickite, calcite, diaspore, and NH_4^+-bearing illite with fractures. Beyond providing thermal impetus for mineral alteration, the hydrothermal fluids also have provided the necessary elements supply for the compositional changes of the claystone, promoting mineral transformation.

This work highlights the complex interplay between volcaniclastic provenance and post-depositional hydrothermal processes in shaping clay mineral assemblages in coal-bearing sequences.

Key words: Altered volcanic ash, Kaolinite, NH_4^+-bearing illite, Hydrothermal fluids, Clay mineral evolution

Acknowledgements. The authors gratefully acknowledge the financial support provided by the National Natural Science Foundation of China (52474283; 42302039; 42172043) and the Fundamental Research Funds for the Central Universities, CHD (300102263301).

PETROLOGICAL, GEOCHEMICAL AND MINERALOGICAL CHARACTERISTICS OF KHOTGOR REE-RICH CARBONATITE, SOUTH MONGOLIA

Meng Feng[1,2], Cheng Xu[3*], Wenlei Song[4]

1. Collaborative Innovation Center for Exploration of Nonferrous Metal Deposits and Efficient Utilization of Resources by the Province and Ministry, Guilin University of Technology, Guilin 541004, Guangxi, China
2. Guangxi Key Laboratory of Hidden Metallic Ore Deposit Exploration, Guilin University of Technology, Guilin 541004, Guangxi, China
3. State Key Laboratory of Deep Earth and Mineral Exploration, Key Laboratory of Orogenic Belts and Crustal Evolution, School of Earth and Space Sciences, Peking University, Beijing 100871, China
4. State Key Laboratory of Continental Dynamics, Department of Geology, Northwest University, Xi'an 710069, China

Abstract The Khotgor carbonatite complex, hosting 40 Mt REO reserves, is located in the southern part of Mongolia in the Gobi Desert. Carbonatites are predominantly composed of calcite, associated with orthoclase, apatite, biotite, fluorite, barite, synchysite-(Ce) and parisite-(Ce). Zircon LA-ICP-MS U-Pb dating yielded crystallization ages ranging from 135.3 ± 4.2 Ma to 134.2 ± 1.7 Ma, indicating emplacement of the carbonatite dykes during the late Mesozoic. Geochemical data show that most of the carbonatite are rich in REEs with total REEs range from 347 ppm to 12458 ppm. Based on geochemical and textural characteristics, three types of calcite were identified. Elemental discrimination diagrams indicate a magmatic origin for Cc-1 and Cc-2, whereas Cc-3 formed during the hydrothermal stage. Three types of calcite share similar in-situ carbon isotopic compositions (-5.77‰~-2.72‰), suggesting they derived from the same mantle source. Based on the magmatic characteristics of Cc-1, it is inferred that the primary carbonatite melt was alkali-rich and lost alkalis through fenitization during magma intrusion, co-precipitating with abundant orthoclase. The presence of alkalis (e g., K and Na) might play an important role in REE exsolution and transportation. The common paragenesis of fluorite and barite with REE minerals indicates that REE precipitation occurred mainly during the hydrothermal stage, and that REE were transported primarily as sulfate complexes in F-rich fluids. The precipitation of REE minerals was mainly controlled by fluid-carbonate interaction and the increase in fluid pH. Barite precipitation removed sulfur from the fluid, destabilizing REE-sulfate complexes. This promoted REE precipitation and resulted in the low REE contents of Cc-3. The carbonatite has undergone varying degrees of hydrothermal fluid metasomatism and supergene weathering, which have altered primary calcite and formed Fe-Mn oxides, facilitating the mobilization and secondary enrichment of rare earth elements. The in-site Sr for the calcite (0.70376 ~ 0.70425) and Nd isotopic data for the parisite

(+0.4 ~ + 4.1) from the Khotgor carbonatite plot between the HIMU and EMI mantle end-members, near the East African Carbonatite Line (EACL). This suggests that the carbonatite magma were not directly from mantle plume, might be contaminated by crust materials.

Key words： Carbonatite; South Mongolia; Khotgor; calcite; REE enrichment

Acknowledgements This study was supported by the National Natural Science Foundation of China (Grant No 42272076).

PLATINUM-GROUP MINERALS AND THEIR PROPERTIES - EXPERIMENTAL STUDY

Anna Vymazalová[1], František Laufek[1], Jan Kamenský[1,2]

1. Czech Geological Survey, Prague, Czech Republic
2. Charles University, Faculty of Science, Prague, Czech Republic

Abstract There is a desired need for further investigation of critical metals chalcogenides, intermetallic phases, those occurring in nature likewise their synthetic counterparts. Platinum-group elements (PGE), belonging to critical metals, are also widely used in various industrial applications.

There are currently 170 platinum-group minerals (PGM), recognized by the Commission on New Minerals, Nomenclature and Classification (CNMNC) of the International Mineralogical Association (IMA). Amongst up to date 170 known PGM, there are 83 – palladium, 38 – platinum, 22 – rhodium, 16 – iridium, 7 – ruthenium and 4 – osmium dominant PGM. The largest class of minerals are sulphides – 41, followed by tellurides – 24, and arsenides – 23, reflecting the chalcophile character of PGE. There is also a significant class of alloys - 20 reflecting the siderophile character of PGE. Regarding the type locality, most PGM were described from the localities in Russia – 64, followed by South Africa – 18, Canada – 15 and China – 15. In terms of crystal structure, most PGM are cubic – 55, followed by orthorhombic – 30, hexagonal – 23 and tetragonal – 22. However, there is still a number of PGM with unknown or undetermined crystal structure that requires further detail investigations.

We have tried to synthetize the majority of PGM at the Laboratory of Experimental Mineralogy at the Czech Geological Survey. For the purpose of this study the silica-glass tube method was applied. The aim is to study in a detail the mineral properties and to advance the understanding of natural process that led to the PGM formation. A number of PGM have also shown specific unique properties.

Several PGM also display unique crystal structures (e.g.: sluzhenikinite, $Pd_{15}(Sb_{7-x}Sn_x)$ $3 \leq x \leq 4$; viteite, Pd_5InAs; or thalhammerite, $Pd_9Ag_2Bi_2S_4$). Mineral monchetundraite, Pd_2NiTe_2 was recently predicted as a new superconductor via machine learning. Mineral jacutingaite, Pt_2HgSe_3, has been receiving a vast attention due to its quantum spin Hall insulator (QSHI) behaviour, opening possibilities for low-power nanoscale electronic and spintronic applications. Mineral mitrofanovite (Pt_3Te_4), was proved to be a topological metal with termination-dependent surface band structure and spin polarization. One of the most common palladium mineral kotulskite (PdTe) was recently regarded as a candidate for Dirac semimetal and showing unconventional superconductivity. Palladium-based chalcogenides are being an innovative class of materials extensively studied as electrocatalysts.

A detailed knowledge of synthetic counterparts of PGM and their experimental study may help further characterize PGM not only from mineralogical point of view (defying thermal stabilities, solid solutions, structural mechanisms of various substitutions, predicting stable assemblages) but

also in terms of application in materials science and potentially in geometallurgy. Thoroughfull investigation of critical metal chalcogenides is still of a great interest from mineralogical point of view, socio-economical demand and applicational potential.

Key words: Platinum-group minerals, PGE, experimental study

Acknowledgements This is a contribution to the Strategic Research Plan of the Czech Geological Survey (DKRVO 2023-2027).

REACTION-DRIVEN MAGMATIC CRYSTALLISATION AT THE MAONIUPING CARBONATITE

Yan Liu[1], Michael Anenburg[2]

1. State Key Laboratory of Deep Earth and Mineral Exploration, Institute of Geology, Chinese Academy of Geological Sciences, Beijing, PR China
2. Research School of Earth Sciences, Australian National University, Canberra, Australia

Abstract Igneous rocks form by solidification of magmas through cooling or volatile degassing following decompression. Expelled H_2O is thought to trigger alteration around intrusions, leading to formation of metasomatic halos. This mechanism is often invoked to explain many magmatic–hydrothermal rock associations, some of them economically mineralised. Maoniuping in China is one of the four largest operating rare earth element (REE) mines globally, whose origin has been attributed to such hydrothermal exsolution. However, no direct evidence links hydrothermal fluids to the formation of Maoniuping and its associated REE mineralisation. Here we show that the REE deposit at Maoniuping formed magmatically from a carbonatitic brine-melt. Textural and chemical evidence reveals extensive interaction with its quartz syenite host, producing albitised fenites. Coupled metasomatism with these fenites led to silica contamination of the carbonatite melt, triggering crystallisation of refractory alkali–ferromagnesian silicates—an antiskarn. This solidified the melt due to removal of the fluxing elements Na and K. Thus, carbonatite melts can crystallise by element assimilation from their environments, precipitating alkali liquid fluxes into solid minerals. Temperature decrease and volatile degassing merely play a secondary role in this igneous rock-forming process. Solidification driven by coupled antiskarnisation and fenitisation affects both the mineral assemblage and ore fabric, and likely operated in most carbonatite-hosted REE deposits elsewhere.

Key words: Maoniuping, antiskarn, carbonatite-syenite complex

REDOX-CONTROLLED MAGNETITE ORE GENESIS AT BAYAN OBO

Shubham Choudhary[1], Michael Anenburg[2], Ross Chandler[2], Wenbo Xu[1], Runchao Liu[3,4], Zhijun Jin[3,4,] Renbiao Tao[1,4,*]

1. Center for High Pressure Science and Technology Advanced Research, Beijing, China
2. Research School of Earth Sciences, Australian National University, Canberra, Australia
3. Institute of Energy, Peking University, Beijing 100871, China
4. Peking University Ordos Institute of Energy, Ordos 017010, Inner Mongolia, China

*Corr. author: renbiao.tao@hpstar.ac.cn

Abstract The Bayan Obo carbonatite, the largest known rare earth element (REE) deposit, was originally exploited for iron due to its abundant magnetite. In other carbonatites, magnetite is typically an accessory, and not a major rock-forming mineral, with its abundance at Bayan Obo remaining unexplained. Here, we report dolomite-hosted graphite and methane inclusions from the northern part of the ore body, surrounded by silica-poor dolostone. In contrast, the southern silicate-bearing part is surrounded by silica-rich slate and lacks reduced carbon inclusions in the dolomite. Coexistence of magnetite and reduced carbon is prohibited in Si-bearing systems, imposed by oxygen fugacity buffers such as fayalite-magnetite-quartz. However, Si-absent systems are free from this constraint, and the coexistence of magnetite and reduced carbon is inexorable once CO_2 and FeO reach sufficient activities. We propose that in-situ redox reaction of an evolving iron-rich carbonatite melt, with its associated CO_2 and H_2O, led to abundant magnetite formation in a Si-poor environment, with byproduct graphite and methane. This process fractionated iron from the carbonatite melt and prevented it from forming magmatic ankerite and siderite, which are otherwise common rock-forming minerals in carbonatites globally.

Key words: Bayan Obo, Magnetite ore, Reodx, Inclusions, Thermodynamic modelling 5

RESOLVING "SCANDIAN IXIOLITE": IXIOLITE-(SC), A NEW COLUMBITE-SUPERGROUP MEMBER FROM THE HEFTETJERN PEGMATITE (NORWAY)

Dan Holtstam[1], Alice Taddei[2,3], Roy Kristiansen[4], Luca Bindi[2,3]

1. Department of Geosciences, Swedish Museum of Natural History, Box 50007, SE-10405 Stockholm, Sweden
2. Dipartimento di Scienze della Terra, Università degli Studi di Firenze, via La Pira 4, I-50121 Firenze, Italy
3. Museo di Scienze Planetarie-Fondazione Parsec, Via Galcianese 20H, I-59100 Prato, Italy
4. PO Box 32, N-1650 Sellebakk, Norway

Abstract Scandium (Sc) is a strategically important metal, essential for advanced technologies such as lightweight alloys used in the space and aeronautics industry and as a dopant in solid electrolytes of fuel cells. Close to 30 minerals known have Sc as an essential chemical component, although major resources exploited today are low-grade laterite deposits and REE ores where it is extracted as a by-product. The study of Sc minerals can increase knowledge about the enrichment processes of the element in geological environments. This work resolves the ambiguity surrounding scandium-rich members of the ixiolite group, which have been reported for decades from the Heftetjern pegmatite (Tørdal, Telemark, Norway), through the characterization of a new mineral species, ixiolite-(Sc), having the ideal formula $(Ta_{0.5}Sc_{0.5})O_2$ (IMA 2025-054). The mineral occurs as dull black, submetallic, opaque aggregates up to 2–3 mm in the type specimen, partially altered to a Sc-rich microlite-group phase. Ixiolite-(Sc) is associated with typical pegmatitic minerals including albite, quartz, fluorite, spessartine and microlite-group minerals, and is interpreted as a primary accessory phase that crystallized from late-stage, Sc-enriched fluids under relatively high fluoride activity.

Electron-microprobe data indicate a cation population dominated by Ta and Sc, yielding the empirical formula (calculated based on two oxygen atoms): $(Ta_{0.33}Sc_{0.27}Nb_{0.14}Sn_{0.08}Mn^{2+}_{0.07}Fe^{2+}_{0.06}Zr_{0.02}Ti_{0.02}W_{0.01})_{\Sigma 1.00}O_2$. Single-crystal X-ray diffraction indicates a structure with orthorhombic symmetry (space group *Pbcn*; a = 4.7673(4) Å, b = 5.7113(5) Å, c = 5.1564(5) Å, Z = 4) characterized by a single, disordered octahedrally coordinated site hosting all cations. This structural arrangement is consistent with the ixiolite-type structure and distinguishes the mineral from related, ordered columbite-supergroup members. Additionally, Raman spectra confirm the absence of water and highlight significant structural disorder through broadened bands linked to mixed cation occupancy.

Ixiolite-(Sc) is related to other members of the ixiolite group via heterovalent substitution mechanisms, and represents the Sc-dominant species within the group. It is dimorphous with

heftetjernite (monoclinic $ScTaO_4$), sharing the same locality but differing in cation ordering and, thus in symmetry and physical properties.

The identification of ixiolite-(Sc) clarifies the nature of the long-known "scandian ixiolite" from Hefte-tjern, expanding the compositional and structural diversity of the ixiolite group, and also provides new information on scandium behavior in pegmatitic environments. In particular, it highlights the role of fluoride-rich fluids and late-stage processes in concentrating Sc and promoting its incorporation into oxide phases, leading to a better understanding of rare-element mineralization in granitic pegmatites.

Key words: ixiolite-(Sc), scandium, Heftetjern pegmatite, columbite supergroup, ixiolite group

SPECTROSCOPIC INSIGHTS INTO OXIDE-SILICATE COUPLING IN POLYMETALLIC NODULES: SILICATE-INDUCED RESTRUCTURING OF VERNADITE AND PHILLIPSITE NUCLEATION

Weishi Zhang[1, 2, 3], Wei Li[1, 2, 3]

1. School of Earth Sciences and Engineering, Nanjing University, China
2. State Key Laboratory of Critical Earth Material Cycling and Mineral Deposits, Nanjing University, China
3. Key Laboratory of Surficial Geochemistry (Ministry of Education), Nanjing University, China

Abstract Marine polymetallic nodules are large-tonnage, critical-metal including Co, Ni, Cu, platinum elements and rare earth elements, where poorly crystalline Mn oxides, particularly vernadite-like phyllomanganates, provide reactive surfaces for the capture, redistribution, and stabilization of dissolved metals in abyssal environments. Among their mineral constituents, phillipsite represents the dominant aluminosilicate fraction which has been proposed to form on growing nodule surfaces coupled with Mn(II) oxidation, yet the role of this oxide-silicate association in the mineralogical evolution of critical-metal-bearing nodules remains poorly constrained. Here, we combine nanoscale observations of Si-rich ferromanganese nodules from the South China Sea with vernadite-silicate coprecipitation experiments to constrain the mineralogical pathway from Mn oxide growth to zeolite nucleation.

Aberration-corrected transmission electron microscopy and energy-dispersive X-ray spectroscopy show that the nodules are consist of authigenic Fe-Mn nanoparticles with coupled Si-Mn distributions. The Si-rich domains are dominated by poorly crystalline vernadite-like and more ordered birnessite-like Mn oxides, with Si/Mn mole ratios comparable to those reproduced in the coprecipitation products. These observations indicate that silica was fixed within growing Fe-Mn oxide assemblages at the nanoscale.

In the coprecipitation experiments, initial Si/Mn ratios from 0 to 200 produced a systematic mineralogical evolution. Low-Si conditions suppressed vernadite layer ordering and generated highly disordered Mn oxide nanoparticles. With increasing dissolved silicate, fourier-transform infrared spectra indicate a transition from monomeric silicate adsorption to silicate polymerization. Pair distribution function analysis further resolves Si-O dimers, ring-like Si-O oligomers, and structural features consistent with zeolite framework. At high Si/Mn ratios, X-ray diffraction identifies a phillipsite-bearing assemblage, while Mn K-edge EXAFS indicates reorganization of vernadite into disordered Mn-oxide nanoclusters, together with a second-shell Mn-Si contribution. These structural changes suggest that Mn oxide surfaces first provide reactive adsorption sites for dissolved silicate, then promote phillipsite formation through local Mn-Si bonding and Si-O

polymerization.

The combined natural and experimental evidence supports a mechanism in which vernadite acts both as a sink for silica and as a reactive template for authigenic zeolite formation in polymetallic nodules. This pathway provides a mineralogical basis for evaluating how oxide-silicate associations regulate metal partitioning and preservation in marine sedimentary systems.

Key words: polymetallic nodules, vernadite, dissolved silicate, zeolite, critical metals

Acknowledgements Polymetallic nodules from South China Sea were kindly provided by Prof. Huaiyang Zhou, Department of Ocean Science and Engineering, Southern University of Science and Technology (SUSTech), Shenzhen, China.

SUPERGENE SN MINERALIZATION: POTENTIAL FOR SECONDARY SN ENRICHMENT IN A CRYPTIC SKARN REGOLITH SETTING FROM DORADILLA, NSW, AUSTRALIA

Rory Carter[1,2], Ian Graham[1], Indrani Mukherjee[1], David French[1], Mathias Kapo[1], Karen Privat[1,3], Oliver Davies[4]

1. Earth and Sustainability Science Research Centre, School of Biological, Earth and Environmental Sciences, University of New South Wales, Australia
2. Mineral Exploration Cooperative Research Centre, School of Biological, Earth and Environmental Sciences, University of New South Wales, Australia
3. Electron Microscopy Unit, Mark Wainwright Analytical Centre, University of New South Wales, Australia
4. Sky Metals Pty Ltd, Australia

Abstract Tin has been classified as a critical element by many countries. This is due to its wide range of applications in solder, alloys, coatings and various other industrial applications. Mineralogically, economic production of tin is dominated by cassiterite (SnO_2). Tin is also found in a range of other minerals, including sulfides such as stannite (Cu_2FeSnS_4) and herzenbergite (SnS), silicates such as malayaite ($SnCa(SiO_4)O$ and Sn-bearing garnets (e.g. Sn-bearing andradite ($Ca_3(Fe^{3+},Sn)_2(SiO_4)_3$), and in the supergene environment, Sn is also found in a range of secondary species such as stokesite ($SnCa(Si_3O_9)\cdot 2H_2O$) and varlamoffite ($Sn_{1-x}Fe_xO_{2-x}(OH)$).

Sn-bearing skarns are a well-known source of Sn. In these systems, the Sn is generally only economic if it is hosted in cassiterite. The Doradilla skarn, located in middle-northern NSW, Australia, is a complex Sn-polymetallic skarn that hosts tin in cassiterite, but also a considerable proportion in malayaite and Sn-bearing andradite (commonly 1-3 wt. % SnO). The malayaite is observed in an almost complete solid solution with titanite, with SnO values ranging from <5 wt. % up to 50 wt. %. The overlying regolith displays significant Sn enrichment associated with particular horizons of the weathered profile. This study was undertaken to determine if there had been secondary enrichment of the Sn.

The deeper, saprock skarn horizons contain partially weathered laminated skarn. Garnet is largely retained, however, clinopyroxene (hedenbergite ($CaFe^{2+}Si_2O_6$) more common relative to diopside ($CaMgSi_2O_6$)) is observed to alter rapidly to an Fe-rich nontronite smectite ($Fe((Si,Al)_4O_{10})(OH)_2\cdot_nH_2O$ in the oxidizing regolith environment. Within these saprock skarn layers, Sn is noted to be enriched up to > 3 wt. % concentrations. Micro-X-ray fluorescence mapping and petrography of Sn-rich samples from this saprock skarn revealed that Sn is concentrated within garnet-rich bands, hosted primarily in malayaite clusters, commonly

500µm to 2mm in size. Further electron microscopy revealed at least three secondary Sn-bearing phases present as replacements and secondary rims of this malayaite. Electron microprobe analysis (EPMA) revealed the first of these to be a rim of stokesite ($SnCa(Si_3O_9)\cdot 2H_2O$) between the malayaite blades, suggesting the development of a reaction rim in the presence of a H_2O-rich environment. The second phase identified as a direct replacement of the malayaite is most likely a metastable phase which comprised approximately 78 wt.% SnO, 10 wt. % SiO_2, 1.5 wt. % CaO, and low totals (~ 95 wt. %) suggesting the presence of water. This is believed to be a metastable alteration product of malayaite during leaching and alteration in the oxide zone. Finally, the brightest BSE phase, particularly noted to overgrow/replace the metastable phase was cassiterite (SnO_2). The presence of cassiterite, appearing as anhedral, 2 – 10 µm grains, suggests that it was the final product of the low temperature oxidation, leaching, hydration, and eventual dehydration from original malayaite -> stokesite -> metastable phase -> cassiterite.

In the overlying, more saprolitic horizons of the weathered profile, Sn is noted to be hosted almost entirely in varlamoffite ($Sn_{1-x}Fe_xO_{2-x}(OH)$). The varlamoffite is observed as a paragenetically late rim and partial replacement of smectite sheets, as well as common space-fill in smectite, kaolinite, and partially weathered primary phases.

It is proposed that differential weathering of different primary lithologies, in different horizons of the regolith profile has produced these two different Sn occurrences in the regolith. In both cases, the primary Sn concentration has either been retained or more commonly enriched with the precipitation of these secondary Sn minerals. This study has implications for the mobility and retention of Sn in the regolith environment, with breakdown of complex, often uneconomic primary Sn-bearing calc-silicates and formation of new secondary species, including the primary ore mineral of Sn, cassiterite.

Key words: Cassiterite, stokesite, malayaite, regolith, supergene Sn

THE CRYSTAL CHEMISTRY OF RARE-EARTH OXIDES

Nancy L. Ross[1], Alix Ehlers[1], Jing Zhao[1], Carla Slebodnick[2], Robert J. Bodnar[1]

1. Department of Geosciences, Virginia Tech,USA
2. Department of Chemistry, Virginia tech, USA

Abstract The rare-earth elements, comprising the lanthanides (La-Lu) plus scandium and yttrium, exhibit unique structural chemistry characterized by large ionic radii, high coordination numbers, and distinctive electronic configurations. The systematic decrease in ionic radius across the lanthanide series, known as lanthanide contraction, provides an opportunity to study structure-property relationships in crystal chemistry. In this study, the structural parameters across major rare-earth compound families are examined, including rare-earth sesquioxides, phosphates, garnets and perovskites focusing on how geometric constraints and ionic size effects dictate crystal structure preferences. The profound impact of lanthanide contraction on structural chemistry is demonstrated. Key findings include predictable trends in bond lengths, coordination numbers, and polymorphic transitions that correlate directly with ionic radius changes from La^{3+} to Lu^{3+}. Distortion parameters increase systematically with lanthanide contraction, affecting optical and magnetic properties. These systematic trends demonstrate the power of comparative structural analysis in understanding and predicting rare-earth compound behavior. Furthermore, quantitative structure-property relationships provide valuable tools for materials design and property optimization.

Key words: Rare-earth oxides, crystal chemistry, structure-property relations

THE GEOCHEMISTRY OF THE DIABASE FROM THE WULIPING PB-ZN DEPOSIT, NORTHWESTERN GUIZHOU

WANG Ziyong

College of Urban Construction, Heze University, Shandong, China

Abstract The Wuliping Pb-Zn deposit is located in the northwestern part of Guizhou province. The exposed strata is mainly carboniferous. The orebodys occur in dolomite, biolimestone and bioclastic limestone. Igneous rocks are undeveloped, with only a few diabase beds invading the carboniferous strata, and have not been studied yet. Based on field geological observations of outcrops and borehole cores, and combined with geochemical data of concealed diabase, this paper devoted to discuss the petrochemical characteristics, rock-forming tectonic settings and genesis of diabase.

Samples are taken from different positions of CWzk46 drilling hole. The diabase is grayish green, dark green, has commonly diabasic texture and mainly composed of pyroxene and basic feldspar, with a small amount of olivine, magnetite, ilmenite. Samples element contents were analysed at the State Key Laboratory of Continental Dynamics (Northwest University). Major were determined by RIX2100XRF, . Trace and REE were determined by inductively coupled plasma mass spectrometry (ICP-MS).

The diabase rocks are characterized by low SiO_2 and high K_2O. The average content of total alkali is higher than that of N-MORB, and closes to OIB. The average contents of TiO_2 and P_2O_5 are apparently higher than N-MORB. The average contents of Al_2O_3 closes to OIB. The average content of CaO is lower than N-MORB. The average content of MgO is lower than N-MORB, and it is well below the reference values of primary basaltic magma. On TiO_2-Nb/Y diagram, the diabase rocks plot in the area of the tholeiite series. The K_2O /TiO_2 ratios of the diabase rocks are lower than 1. This suggest that samples fall into the range of continental tholeiite. The diabase has higher REE contents with enrichmen in light REE and without significant Eu, suggesting that frctionation crystallization of plagioclase was not evident during the magmatic evolution. The average values of Ta and Nb in the diabase are 2.3×10^{-6} and 27×10^{-6}, and the Hf/Th ratios are lower than 8, which are consistent with those of intra-plate basalt. And the Zr/Nb ratios are also similar to OIB (10). In the diagrams of Zr/Y-Zr and TiO_2-Zr, the diabase samples plot in the area of intra-plate basalt. Taken together, the geochemical characteristics suggest that the diabase belongs to continental intra-plate basalt.

The average Zr/Ba ratio is 0.57, indicating that the primary magma originated from the asthenospheric mantle (Zr/Ba > 0.2 suggests an asthenospheric source). The Cr and Ni concentrations are well below the reference values for primary basaltic magma, which may be related to both mantle metasomatism and magma fractional crystallization.

Key words: diabase, geochemistry, Pb-Zn deposit, northwestern Guizhou

THE DISCOVERY OF GRIMMITE ($NiCo_2S_4$) IN CHINA AND ITS GEOLOGICAL SIGNIFICANCE

Jinlu YANG, Jiaxi Zhou*

Key Laboratory of Critical Minerals Metallogeny in Universities of Yunnan Province, School of Earth Sciences, Yunnan University, Kunming 650500, Yunnan, China

* Corresponding author, Email: zhoujiaxi@ynu.edu.cn

Abstract Grimmite ($NiCo_2S_4$) was first discovered in the Příbram mining district, Czech Republic, with the ideal chemical formula $NiCo_2S_4$. This mineral is a rare nickel-cobalt thiospinel (cubic crystal system), exhibiting a creamy grey colour in reflected light, with no pleochroism or internal reflections. Its unit-cell parameters are (a=9.3933(9)Å, V=828.81(14)Å^3, Z=8), with Co atoms dominating the octahedral site (16c) and Ni atoms occupying the tetrahedral site (8b). The fundamental distinction between grimmite ($NiCo_2S_4$) and the Ni-Co thiospinel series ($Co_{3-x}Ni_xS_4$)lies in its Ni content, which ranges from 0.5 to 1.5 apfu. Based on systematic mineralogical investigations, this paper reports the first discovery of grimmite in China, at a mining area in Yanjin County, Zhaotong City, Yunnan Province. The mineral occurs predominantly as euhedral to subhedral microcrystals, associated with calcite, pyrite, and quartz. Electron microprobe analyses reveal a chemical composition with an atomic formula range of $Ni_{1.00}(Co_{1.59–1.71}Ni_{0.216–0.31}Fe_{0.078–0.1302})_{\sum 2.00}S_4$, where the Ni content remains stable between 1.216 and 1.31 apfu, conforming to the compositional criteria for grimmite defined by the International Mineralogical Association. The unit-cell parameters of grimmite from the Yanjin mining area are (a=9.3999(7)Å, V=830.56(19)Å^3, Z=8), with Co atoms dominating the octahedral site (16c) and Ni atoms occupying the tetrahedral site (8b). On a Ni-Co-Fe ternary diagram, the chemical composition of the Yanjin grimmite falls within the compositional field of previously documented grimmite occurrences, confirming that they are the same mineral species. The discovery of grimmite not only suggests its global distribution but also indicates a previously unrecognized hydrothermal cobalt mineralization event in the study area, where Ni-Co sulfides occur as independent minerals, providing an important clue for the exploration of independent cobalt deposits.

Key words: Grimmite, Cobalt-nickel sulphides, Independent cobalt minerals, Hydrothermal mineralisation system, Independent cobalt deposits

Acknowledgements This study is supported by the National Natural Science Foundation of China (U2444206), the Fundamental Research Major Project of Yunnan Province (202501BC070002), the Major Science and Technology Special Plan Project of Yunnan Province (202402AB080006), the Scientific and Technological Innovation Team (2025-01) and Master's Supervisor Team (2023-15) Projects of Critical Metal Metallogeny and Prospecting Prediction of Yunnan Provincial Education Department to J.-X. Zhou.

THE GREAT OXIDATION EVENT: AN INFORMATICS APPROACH TO THE OXYGEN-INDUCED MINERALOGY OF CRITICAL MINERALS

Yanzhang Li and Robert M. Hazen

Earth and Planets Laboratory, Carnegie Institution for Science, Washington DC, USA

Abstract The Great Oxidation Event (GOE), which saw the rapid rise of atmospheric oxygen starting ~2.5 billion years ago, triggered the greatest increase in mineral diversity in Earth's history. The formation of more than 2000 new mineral species was facilitated by the oxidation state transformations of over 20 redox-sensitive elements in newly oxidizing near-surface environments. Many of these new minerals incorporate the highest oxidation states of common elements. Of special importance were S^{6+}-bearing sulfates, arsenates with As^{5+}, and/or antimonates with Sb^{5+}. These anionic groups often occur in association with Fe^{3+}, Cu^{2+}, U^{5+}/U^{6}, V^{4+}/V^{5+}, Mn^{3+}/Mn^{4+}, and/or Mo^{5+}/Mo^{6+}.

Here we compile age and association records from large, open-access data resources of mineral compositions, structures, localities, and associations (mindat.org; rruff.net) and employ network analysis coupled with community detection and heat map analysis coupled with agglomerative clustering to focus on the patterns of diversity and distribution of representative critical minerals formed in the near-surface oxidative environments following the GOE—conditions that transformed Earth's near-surface mineralogy. As one of the results, we find that after the GOE hundreds of new copper and uranium minerals formed, with discrete communities based primarily on the source and anionic composition of metal-rich fluids. Considering that both Cu^{2+} and U^{6+} are orders of magnitude more soluble than their reduced counterparts, Cu^{1+} and U^{4+}, we proposed that the Earth's oxygenation increased their mobility and drove extensive mineral diversification. These results reveal fundamental controls on critical-metal mineralization in oxidizing environments and suggest informatics-based strategies in the search for new critical resources.

Key words: Mineral Evolution, Great Oxidation Event, Critical Minerals, Network Analysis, Heat Map Analysis

THE MINERALOGY OF THE CRITICAL MINERALS

Robert J. Bodnar, Nancy L. Ross
Department of Geosciences, Virginia Tech, Blacksburg, VA 24061 USA

Abstract The critical minerals, hereafter referred to as "critical elements" to distinguish between metals or elements of interest and the host phase(s) for those elements, often occur as minor or trace components in the ore minerals being mined. As an example, an ore mineral for the elements cadmium (Cd), gallium (Ga) and indium (In) is sphalerite (ZnS), and Cd, Ga, and In occur as trace to minor components by substituting for Zn in the crystal structure. Many other critical elements do not occur in an ore mineral in which that element is a primary constituent of the phase. Examples include (element/ore mineral): Ga/sphalerite, bauxite minerals; Ge/sphalerite, chalcopyrite; Hf/zircon; In/sphalerite, cassiterite, chalcopyrite; Ir/PGM; Sc/wolframite, Ni-ore minerals, ilmenite, rutile, davidite; Te/chalcopyrite, galena, pyrite; V/titaniferous magnetite; Co/pentlandite, chalcopyrite, pyrite, limonite in Ni laterites; Bi/galena, chalcopyrite, cassiterite, molybdenite, wolframite; Rb/lepidolite, carnallite, pollucite.

In order to develop efficient and cost-effective processes to extract the critical element of interest from the host phase, it is necessary to know the manner in which the elements are hosted within the ore mineral, including the crystallographic setting and the distribution within the host phase. For example, when Ga substitutes for Zn^{2+} in the sphalerite structure, each Ga atom is tetrahedrally coordinated by 4 sulfur atoms and mimics the normal Zn-S coordination in sphalerite. However, the Ga-S bond length is slightly shorter than that of Zn-S owing to the smaller ionic radius of Ga compared to Zn, and the Ga-S bond strength is slightly stronger (220-240 kJ/mol) than that of Zn-S (200-220 kJ/mol). The greater bond strength of Ga-S vs Zn-S means that slightly more grinding energy might be required to break Ga-S bonds during physical beneficiation (minor concern), and has a much greater effect on chemical extraction because stronger bonds generally lead to slower dissolution rates and require a higher activation energy to break the bond.

In this presentation, the ore minerals for the critical elements (minerals) will be described, representing a first step in developing efficient and cost-effective processes to produce critical elements.

Key words: critical mineral, critical element, trace element, minor element, crystal structure

TOMINGLEY GOLD PROJECT PYRITES: PATHFINDER TEXTURES AND TRACE ELEMENTS

Muhammad Fariz Bin Md Nasir[1], Indrani Mukherjee[2], Alexander Cherry[3], Ian Graham[2], Karen Privat[4], and Ivan Belousov[5]

1. Yarra Enviro Solutions Sdn Bhd (YESSB), Shah Alam 40160, Selangor, Malaysia
2. School of Biological, Earth and Environment Sciences (BEES), University of New South Wales (UNSW), Sydney, NSW 2052, Australia
3. Alkane Resources Ltd., 22 Cameron Place, Orange, NSW 2800, Australia
4. Electron Microscope Unit, Mark Wainright Facility, University of New South Wales (UNSW), Sydney, NSW 2052, Australia
5. CODES Analytical Laboratories, School of Natural Sciences, University of Tasmania, Hobart, TAS 7001, Australia

Abstract The Tomingley Gold Project (TGP) is a group of exploration and mining leases centred along an Ordovician volcanic belt (Mingelo Volcanics) near Tomingley, in the Central West region of NSW. Previous work on the TGP focused on regolith studies, the distribution of pathfinder elements, the biogeochemical potential of native vegetation etc., using conventional techniques. However, application of in-situ techniques has not been conducted in the TGP despite known excellent utility of such datasets. Therefore, this study focused on the application of sulphide chemistry and texture as a tool for Alkane Resources to explore for potential gold within the TGP area using in-situ techniques. A total of forty-one drill core samples from a variety of lithologies (volcaniclastic, monzodiorite, graphitic siltstone, dacite, andesite) were analysed using reflected light and scanning electron microscopy (SEM), elemental mapping (EPMA), and targeted trace element analysis of sulphide grains (LA-ICP-MS). The main objectives were to determine pathfinder textures and trace elements in TGP sulphides.

Findings show that pyrite and arsenopyrite are the major sulphides that host fracture-fill/inclusion of native gold and invisible gold. Pyrite rich in groundmass inclusions should be evaluated due to their characteristic high concentrations of both As and Au. Pyrite trace element chemistry (Sn, Bi, W, Sb, Au, and Se) was able to delineate mineralised and unmineralised samples for volcaniclastic, graphitic siltstone and andesite lithologies but were more challenging for lithologies like dacite and monzodiorite. The study also found that Au may have been introduced into the system earlier than previously thought and existed as invisible gold in pyrite. This study highlights the utility of in-situ techniques to differentiate mineralised vs unmineralised samples (from pyrite and arsenopyrite), and effectiveness compared to whole-rock techniques and the benefits of such datasets in mineral exploration.

Key words: Orogenic Au, Pyrite, LAICPMS, trace elements

Acknowledgements We would like to thank Alkane Resources for sponsoring the project.

TRACE ELEMENT GEOCHEMISTRY OF MULTI-STAGE QUARTZ VEINS: IMPLICATIONS FOR THE PORPHYRY GOLD MINERALIZATION AT BILIHE, NORTH CHINA CRATON

Hang-Fei Ge, Ya-Fei Wu*

State Key Laboratory of Geological Processes and Mineral Resources, China University of Geosciences, Wuhan, Hubei Province 430074, China

Abstract The mineralization of porphyry deposits is typically hosted in stockwork quartz veins at the apices of the porphyry stocks and in adjacent country rocks. These veins comprise multiple generations of quartz ± sulfide infilling, recording the complex evolutionary history of fracturing, vein filling, wall-rock alteration, and metal precipitation. The Bilihe deposit is the first large-scale, high-grade porphyry gold deposit (~50 t Au) discovered along the northern margin of the North China Craton and is characterized by multi-stage quartz veining. However, the formation mechanisms of different veins remain poorly understood, limiting a comprehensive understanding of the ore-forming processes. Based on detailed petrographic observations, we systematically characterized the textures and elemental compositions of different generations of quartz (-sulfide) veins using cathodoluminescence imaging and laser ablation-inductively coupled plasma-mass spectrometry (LA-ICP-MS). Seven vein types were identified: magmatic quartz phenocrysts, dendritic quartz, unidirectional solidification texture (UST) quartz, quartz-K-feldspar veins (A-type), banded quartz veins (B-type), sulfide veinlets (C-type), and quartz-calcite-pyrite veins (D-type).

LA-ICP-MS trace element analyses reveal a positive correlation between Al and monovalent cations in quartz, indicating that these elements are incorporated into the quartz lattice primarily through coupled substitution $Si^{4+} \leftrightarrow Al^{3+} + (Li^{+}, Na^{+}, K^{+}, Rb^{+})$. The Al contents increase progressively from the early magmatic stage (mean = 140 ppm) through the magmatic-hydrothermal transition (mean = 354 ppm) to the hydrothermal stage (mean = 1605 ppm), indicating a continuous decrease in pH during ore fluid evolution. The TitaniQ geothermometer results indicate that the UST quartz crystallized at temperatures up to 757℃, significantly higher than the subsequent two stages (676℃ and 678℃), reflecting rapid cooling during gold mineralization. B-type veins exhibit multi-stage fluctuations in Al and Ti contents, probably indicating pulsed injections of magmatic–hydrothermal fluids. Quartz intergrown with sulfide veinlets formed at ~443°C, within the retrograde quartz solubility field (350–450°C). Native gold in early gold-bearing quartz veins is significantly depleted where late sulfide veinlets overprint them, possibly indicating remobilization of early-precipitated gold and its reprecipitation in sulfides. Consequently, we suggest that gold enrichment at Bilihe resulted from multiple coupled processes, including rapid cooling, pulsed magmatic-hydrothermal fluid injections, and

remobilization of early-stage gold.

Key words: Quartz trace element, Multiple gold mineralization, Bilihe porphyry gold deposit, North China Craton

TRACE METAL MINERALIZATION IN MARINE OOIDAL IRONSTONES: MINERALOGICAL EVIDENCES FOR CRYPTIC HYDROTHERMAL FLUID ACTIVITY

Maxim Rudmin

Division for Geology, Tomsk Polytechnic University, Tomsk, Russia

Abstract Chalcophile elements play an important role in the formation of ore minerals in a wide range of geological environments. Their concentration is commonly associated with sulfide phases and hydrothermal fluids capable of transporting metals and producing characteristic mineral assemblages. Marine ooidal ironstones of the Phanerozoic are widely regarded as important archives of the chemical evolution of ancient marine basins and early diagenetic processes in sedimentary systems. However, the sources of metals and the mechanisms responsible for their incorporation into ferruginous sediments remain debated. In some models, continental input is considered the dominant source of metals, whereas other interpretations suggest that hydrothermal fluids penetrate the sediment column. Mineralogical indicators of metal input and ore-forming fluids in sedimentary iron-rich systems remain poorly documented. Identifying mineralogical and geochemical indicators of such processes is therefore essential for reconstructing the formation conditions of ferruginous sediments and potentially related ore accumulations.

This study examines the mineralogy and geochemistry of trace metals in Late Cretaceous and Paleogene marine ooidal ironstones of the West Siberian Basin. Particular attention is given to the distribution of Zn and associated chalcophile elements within different mineral domains of the ironstones. The analytical approach included scanning electron microscopy with energy-dispersive analysis, X-ray fluorescence analysis, and inductively coupled plasma mass spectrometry. Special attention was paid to the textures of ore minerals and their spatial relationships with carbonate cement, iron ooids, and the clay matrix.

Zinc mineralization is mainly represented by authigenic sulfide phases dominated by wurtzite (Zn, Fe)S. This mineral commonly occurs with galena and, locally, with pyrrhotite and greigite. Zn- and Pb-bearing minerals are mainly concentrated within massive or vein-like carbonate cement that binds iron ooids and detrital particles. Such carbonate often fills epigenetic fractures enriched in sulfides. More rarely, Hg- and As-bearing mineral phases occur within the same mineral assemblages. Wurtzite forms micro-inclusions in carbonate cement, framboidal aggregates within the clay matrix, and accumulations along contacts between siderite and phyllosilicates.

Fluid inclusions hosted by the carbonate cement and associated with wurtzite and/or pyrrhotite show homogenization temperatures up to ~300 °C. The gaseous composition of these inclusions includes hydrogen sulfide, carbon dioxide, and methane. These characteristics indicate the involvement of relatively high-temperature, metal-bearing, reducing hydrothermal fluids.

Geochemical data reveal consistent associations of Zn with elements typical of hydrothermal systems, including Co, Ni, Pb, Mo, and U. Their distribution suggests redistribution of metals between carbonate cement, clay matrix, and sulfide phases.

Mineralogical textures and geochemical signatures indicate a multistage history of ironstone formation. Primary iron ooids formed in a shallow marine environment. Later, reduced fluid input into the system, likely controlled by tectonic structures and deep fluid circulation within the basin. The results demonstrate that marine ooidal ironstones may preserve mineralogical evidence of cryptic hydrothermal activity and record the migration of metal-bearing fluids. Such systems are important natural archives of ore-forming processes in sedimentary basins. They may provide useful criteria for recognizing sedimentary-hosted polymetallic mineralization in ironstone-bearing basins.

Key words: Marine ooidal ironstones, Zinc mineralization, Chalcophile elements, Hydrothermal fluids, Fluid inclusions

Acknowledgements This research was financially supported by FSWW-2026-0076.

TYPOMORPHISM OF EUDIALYTE-GROUP MINERALS: FROM STRUCTURAL CHEMISTY TO MINERAL PROCESSING OF RARE-EARTH ELEMENTS

Sergey M. Aksenov[1], Julia A. Mikhailova[1], Alfia M. Safiulina[2,3], Nikita V. Chukanov[4], Ramiza K. Rastsvetaeva[5], Alexey A. Lizunov[2], Galina O. Kalashnikova[1], Igor P. Luybach[3], Evgeniy A. Rodionov[3], Ivan G. Tananaev[6]

1. FRC Kola Science Centre RAS, Russia
2. JCK A.A.Bochvar High-Technology Research Institute of Inorganic Materials, Russia
3. D. Mendeleev University of Chemical Technology, Russia NRC Kurchatov Institute, Russia
4. FRC of Problems of Chemical Physics and Medicinal Chemistry RAS, Russia
5. FRC Kurchatov Institute, Russia
6. I.V. Tananaev Institute of Chemistry and Technology of Rare Elements and Mineral Raw Materials, FRC Kola Science Center RAS, Russia

Abstract Eudialyte-group minerals (EGM) are widespread in agpaitic complexes, where they occur as typomorphic accessory minerals and sometimes as rock-forming minerals. Unlike most other rock-forming minerals, EGMs have the ability to concentrate a range of rare and strategic elements, making them of practical interest as a potential source of these elements.

The most interesting distinctive feature of EGMs is the unique complexity and variability of their crystal structure, which has led to the establishment of a large number of distinct mineral species. The crystal-chemical formula of EGMs is: $[N(1)_3N(2)_3N(3)_3N(4)_3N(5)_3]\{M(1)_6M(2)_3M(3)M(4)Z_3(Si_9O_{27-3x}(OH)_{3x})_2(Si_3O_9)_2Ø_{0-6}\}X(1)X(2)$, where $M(1)$ = Ca, Mn^{2+}, *REE*, Na, Fe^{2+}; $M(2)$ = $^{IV,V}Fe^{2+}$, $^{V,VI}Fe^{3+}$, $^{V,VI}Mn^{2+}$, ^{V,VI}Na, ^{IV,V}Zr; $M(3)$ and $M(4)$ = ^{IV}Si, ^{VI}Nb, ^{VI}Ti, $^{VI}W^{6+}$; Z = Zr, Ti, Nb; Ø = O, OH; $N(1)$–$N(5)$ are extraframework cations (Na, H_3O^+, K, Sr, *REE*, Y, Ba, Mn^{2+}, Ca) or H_2O molecules; $X(1)$ and $X(2)$ are extraframework anions (Cl^-, F^-, S^{2-}), anionic groups (CO_3^{2-}, SO_4^{2-}), and water molecules; x = 0–1.

Currently, 31 distinct mineral species are known in the eudialyte group. The distinction of mineral species within the eudialyte group is highly relevant, as these minerals are indicators of formation conditions and record the evolution of the mineral-forming environment, which may change its physicochemical parameters such as alkalinity, redox conditions, basicity, temperature, and others. Most species-defining elements (Fe, Ca, Mn, Zr, and others) can occupy several sites in the structures of eudialyte and its analogues. The distribution of these elements is the result of a combination of two factors: the competition of their activities in the mineral-forming environment and their affinity for different sites in the structures of minerals of this group. Thus, both geochemical and crystal-chemical factors are involved in the formation of each mineral species.

Different subgroups and families of EGMs are confined to different types and stages of evolution of agpaitic complexes. In the early stage of rock and pegmatite formation, eudialyte sensu

stricto crystallizes. With a sharp increase in alkalinity (high- and ultra-agpaitic stages), minerals of the oneillite structural family are formed, often enriched in Zr (the calcium-deficient genetic branch) or, under sufficiently high calcium contents, 24-layer high-sodium and titanium-bearing members of the group. In the late stages of mineral formation, characterized by decreasing alkalinity (including during metasomatic and autometasomatic processes with introduction of Nb, K, Ca and/or Sr, as well as CO_2, under decreasing temperature), minerals of the kentbrooksite crystal-chemical type crystallize. In the late hydrothermal stage, hydration of eudialyte and leaching of Na and Fe occur, leading to the formation of aqualite and other "hydroeudialytes" or (under high oxygen activity) "oxyeudialytes" or ikranite. The formation of "hydroeudialytes" is related to natural ion-exchange processes when sodium is replaced by hydrated proton complexes (predominantly, H_3O^+) and water molecules. These features are in good agreement with experimental data on synthesis and dissolution of EGMs, as well as theoretical data on element diffusion in the crystal structure.

Using eudialyte concentrate as an example, the effectiveness of a stoichiometric binary mixture of a phosphoryl podand and quaternary ammonium salts for the extraction of uranium, thorium, zirconium, hafnium, scandium, and titanium from leach solutions was demonstrated. Given the large balance reserves of eudialyte (with a significant gross concentration of *REE*s and other strategic metals in this mineral), such results could form the basis for a new industrial technology for recovering valuable ore components from eudialyte, as well as for waste conditioning in the production of rare and rare-earth metals from natural and technogenic raw materials.

Key words: eudialyte, crystal chemistry, rare-earth elements, typomorphism, alkaline massif

Acknowledgements This work was performed in accordance with the state task Nos. 122011300125-2 and 124013100858-3.

UNCOMMON BI-SE-TE MINERALS FROM THE TENNANT CREEK AU-BI-CU DEPOSITS, AUSTRALIA: MINERALOGICAL ADVANCES AND IMPLICATIONS FOR ORE GENESIS AND EXPLORATION

Damian Braize[1,2], Jeffrey Steadman[1], Sebastien Meffre[1]

1. Centre for Ore Deposit and Earth Sciences, University of Tasmania, Hobart, Australia
2. Guangzhou Institute of Geochemistry, Chinese Academy of Sciences, Guangzhou, China

Abstract Bismuth is increasingly recognised as a critical metal and a key tracer of hydrothermal processes, particularly where it occurs in complex mineral assemblages with selenium and tellurium. Its strong affinity with gold in reduced, low-sulfur systems makes Bi mineralogy a powerful tool for constraining ore-forming conditions and metal transport mechanisms.

This study investigates the mineralogical controls on bismuth and copper-gold mineralisation in the Tennant Creek Mineral Field (Northern Territory, Australia), a world-class Au-Bi-Cu province and a type locality for several Bi- and Se-bearing minerals. Comprehensive mineralogical characterisation using reflected light microscopy, SEM-EDS, EPMA, EBSD and TEM reveals a remarkably diverse assemblage of Bi-bearing phases. This includes native bismuth, members of the bismuthinite-aikinite and cuprobismutite series, and structurally complex selenides and tellurides.

The identified assemblages record multiple stages of fluid evolution and demonstrate strong partitioning of Bi, Se and Te during copper-gold deposition. Phase associations and textural relationships indicate a close link between bismuth mineralisation and key stages of Au precipitation, consistent with thermodynamic constraints with Bi acting as a collector and transport agent for Au under specific redox and sulfidation conditions.

The study documents and characterises previously unrecognised Bi-Ag-Se-bearing sulfosalts and unusually complex solid solutions among Se- and Te-rich minerals, significantly expanding the known diversity of bismuth mineralogy in the Tennant Creek district and globally.

These results contribute new mineralogical knowledge to the sulfosalt family, refine genetic models for Bi-bearing Cu-Au systems, and highlight the value of detailed mineralogical studies for understanding metal partitioning, critical-metal enrichment, and the use of Bi minerals as indicators for Cu-Au mineralisation.

Key words: Bismuth, Tennant Creek Au-Bi-Cu deposits, Sulfosalts, Economic Geology, Systematics

UNLOCKING INDIAS CRITICAL MINERALS: PXRD-EDXRF REVOLUTION FROM CRATON DEPTHS TO INDIGENIOUS CRMS

P V Sunder Raju

CSIR-NATIONAL GEOPHYSICAL RESEARCH INSTITUTE, INDIA Abstract

Abstract **Powder X-ray Diffraction (PXRD)** is a premier non-destructive analytical technique for the identification and quantification of mineral phases in crystalline and non-crystalline materials. Recent technological leaps in optics and detectors have dramatically lowered detection limits, while advanced software suites—utilizing similarity indices, whole-pattern fitting, and multivariate analysis—have revolutionized the search and identification process. In the wake of India defining a strategic list of **30 critical minerals**, PXRD has emerged as an indispensable mineralogical tool. Its reliance on Bragg's Law to reveal unique atomic arrangements provides unbiased structural data, making it a cornerstone for both terrestrial exploration and next-generation planetary missions, such as NASA's Mars 2020 Perseverance rover.

This study presents a comprehensive mineralogical and geochemical investigation of Rare Earth Elements (REEs) and critical minerals sourced from the **Dharwar and Central Indian cratons**. The examined specimens include scheelite, vanadiferous titanomagnetite, carbonatites, and nepheline syenites. A primary objective of this research is to evaluate the efficacy of **Energy Dispersive X-ray Fluorescence (EDXRF)** as a high-throughput, non-destructive alternative to traditional destructive chemical analysis. By eliminating the need for complex sample dissolution, EDXRF reduces the potential for erratic results and environmental waste. The **CSIR-NGRI** EDXRF laboratory participated in international round-robin testing to benchmark analytical procedures, focusing on the development and validation of Indian **Certified Reference Materials (CRMs)**, specifically **REE-2** and **NAS-1**.

The **PXRD methodology** employed a Bruker D-8 Advance diffractometer equipped with a Cu Kα radiation source and a high-precision LYNXEYE detector. Samples were micronized using a McCrone XRD mill to ensure optimal particle size and back-loaded to minimize preferred orientation. Data processing involved background correction and instrumental shift alignment against a corundum standard. Mineralogical identification was facilitated by the **ICDD PDF-5+** database, and quantitative results were refined using **Rietveld refinement (WPF)** via TOPAS software.

The **EDXRF analysis** utilized a PANalytical Epsilon 5 spectrometer featuring a 100 kV Sc/W anode tube and a 3-D polarized optical path. This configuration is particularly significant for REE exploration, as the high-voltage excitation allows for the analysis of heavy rare earth elements (Eu to Lu) using their more sensitive **K-lines**. This effectively bypasses the spectral interference and L-line overlaps common in traditional 2-D EDXRF systems.

Results indicate that while EDXRF data largely corroborates certified values, certain elements (e.g., Al, Er, Ho, K, and La) showed deviations of 0.5x to 2x the certified concentrations. These

discrepancies are attributed to inter-element interferences, peak overlaps, and Rayleigh or Compton scattering from the X-ray target. However, through the use of batch blanks and Compton normalization to correct for self-absorption and varying sample density, the EDXRF method demonstrated a high correlation with destructive analytical techniques.

The study highlights a critical gap in the industry: the shortage of matrix-matched CRMs specifically tailored to Indian lithological units. During early-stage exploration, where detecting subtle anomalies above background levels is paramount, the precision and cost-effectiveness of EDXRF are invaluable. We conclude that the integration of PXRD phase identification with EDXRF elemental analysis provides a robust, rapid framework for critical mineral prospecting. Furthermore, the successful characterization of REE-2 and NAS-1 underscores the necessity of developing indigenous CRMs to support the burgeoning Indian mineral sector and ensure analytical self-reliance.

Key words: Critical Minerals, Craton, India, PXRD, EDXRF

UNRAVELING MAGMATIC TO HYDROTHERMAL SCANDIUM ENRICHMENT IN THE BAYAN OBO CARBONATITE-HOSTED DEPOSIT, NORTH CHINA

Ya-Ting Xu, Ru-Cheng Wang*, Xu-Dong Che

State Key Laboratory for Mineral Deposits Research, FSC for Critical Earth Material Cycling, School of Earth Sciences and Engineering, Nanjing University, 163 Xianlin Avenue, Nanjing 210023, P.R. China

Abstract Scandium (Sc) is a critical strategic metal essential for aerospace and clean energy technologies, yet its enrichment mechanisms in carbonatite-hosted systems remain debated. The Bayan Obo deposit in North China, renowned as the world's largest rare earth element (REE) resource, hosts significant Sc concentrations across diverse ore types, though previous models predominantly favored hydrothermal enrichment due to a lack of direct magmatic evidence. This study integrates whole-rock geochemistry, detailed mineralogical characterization, and Th-Pb isotopic dating to constrain Sc speciation and evolution from magmatic to hydrothermal stages. Results identify magmatic Sc-rich columbite-(Fe)/ixiolite (up to 22.59 wt% Sc_2O_3) and aegirine (up to 2.46 wt% Sc_2O_3) as primary hosts, establishing a foundational magmatic enrichment stage. Subsequent hydrothermal processes, dated at ca. 421 Ma, facilitated Sc remobilization into high-grade thortveitite (up to 50.76 wt% Sc_2O_3) within fluorite-banded ores and secondary aegirine-jervisite assemblages via F-bearing fluid metasomatism, while late-stage veins contain only minor Sc. We propose a two-stage genetic model involving initial magmatic fractionation into Nb-Fe oxides and pyroxenes, followed by hydrothermal remobilization into discrete silicate phases. This work underscores the critical role of magmatism in Sc pre-enrichment within carbonatite systems and refines the genetic framework for Sc mineralization, offering new insights for exploration targeting in similar deposits globally.

Key words: Scandium mineralogy, Bayan Obo deposit, Carbonatite-hosted, Magmatic-hydrothermal enrichment, Metallogenic model

URANIUM ENRICHMENT IN GRANITIC PEGMATITES OF THE HUSAB DEPOSIT, NAMIBIA: CONSTRAINTS FROM THERMODYNAMIC MODELING AND LI-BA-SR ISOTOPES

Shan-Shan Li[1], Kun-Feng Qiu[1], Fang-Huang[2], Jun Deng[1]

1. State Key Laboratory of Geological Processes and Mineral Resources, Frontiers Science Center for Deep-time Digital Earth, China University of Geosciences (Beijing), Beijing 100083, China
2. CAS Key Laboratory of Crust-Mantle Materials and Environments, School of Earth and Space Sciences, University of Science and Technology of China, Hefei 230026, China

Abstract Granitic pegmatite-hosted ore systems, exemplified by the Husab uranium deposit in Namibia, are important sources of critical metals. Mineralogical studies reveal that uranium is primarily hosted in uraninite, accompanied by zircon, apatite, and monazite as accessory phases. Widespread alteration features, including albitization, silicification, fluoritization, sericitization, pyritization, and chloritization, indicate significant fluid-rock interaction. These mineral assemblages and alteration styles point to a magmatic-hydrothermal origin, prompting us to quantitatively evaluate uranium enrichment during partial melting, fractional crystallization, and fluid-rock interaction. To achieve this, we integrated thermodynamic phase equilibrium modeling with Li-Ba-Sr isotope. Our modeling results show that partial melting and fractional crystallization concentrate uranium by only tens of times relative to the source, whereas fluid-rock interaction leads to enrichment by hundreds of times. Li-Ba-Sr isotopic signatures indicate that magmatic fluids played a dominant role in mobilizing and precipitating uranium. We therefore propose that water-rock interaction is the primary driver for efficient uranium hyper-enrichment in pegmatite systems. These findings provide new insights into the ore-forming processes of the Husab deposit and highlight the critical role of fluid-rock interaction in the formation of giant pegmatite-type uranium deposits.

Key words: Granitic pegmatite, Uranium enrichment, Fluid-rock interaction, Thermodynamic modeling, Li-Ba-Sr isotopes

Acknowledgements This research was financially supported by the National Natural Science Foundation of China (42521005, 92562302, 42203072).

WATER-INDUCED ARCHEAN MANTLE OVERTURN AS A MECHANISM FOR EARTH'S FIRST LEAD PARADOX

Yudong Chen[1], Zhongqing Wu[1, 2*]

1. State Key Laboratory of Precision Geodesy, School of Earth and Space Sciences, University of Science and Technology of China, Hefei 230026, China
2. Mengcheng National Geophysical Observatory, University of Science and Technology of China, Mengcheng, 233500, China

Abstract The first lead paradox remains one of the most persistent unresolved problems in isotope geochemistry. Nearly all accessible terrestrial reservoirs exhibit excess radiogenic Pb relative to the bulk silicate Earth (BSE), yet the origin of this discrepancy has remained unclear for more than five decades. Previous explanations generally invoke hidden reservoirs or incomplete sampling of the deep Earth, but they do not explain how materials responsible for radiogenic Pb excess became incorporated into accessible Earth reservoirs. Resolving the paradox requires accounting for two fundamental constraints: (1) preferential Pb loss relative to U during early Earth differentiation, and (2) independent geological and isotopic evidence indicating that the μ ($^{238}U/^{204}Pb$) of accessible Earth increased during the Archean.

Here we present a quantitative evolutionary model showing that coupled sulfide segregation during basal magma ocean crystallization and water-induced Archean mantle overturn can reconcile these constraints within a mass-balanced framework. Sulfide segregation preferentially removes Pb relative to U, producing Pb-depleted residual silicate melts with elevated μ. Subsequent Archean mantle overturn transports these high-μ materials into the shallow mantle, where they contribute to the long-term evolution of accessible terrestrial reservoirs. Meanwhile, the sulfides segregated during BMO crystallization remain unsampled by accessible Earth materials, preserving the early U–Pb decoupling signature.

The modeled evolution reproduces both the Archean increase in μ inferred from geological records and the radiogenic Pb isotopic compositions characteristic of accessible Earth reservoirs. These results suggest that the first lead paradox may represent a natural outcome of early Earth differentiation and mantle dynamics rather than requiring hidden reservoirs or incomplete sampling of the deep Earth.

Key words: First lead paradox, Basal magma ocean (BMO), Water-induced mantle overturn, Pb isotope

Acknowledgements This study is supported by Deep Earth Probe and Mineral Resources Exploration-National Science and Technology Major Project (No. 2025ZD1005200) and by the National Natural Science Foundation of China (42350004, 41925017). The calculations were performed in Supercomputing Center of University of Science and Technology of China.

AB INITIO STRUCTURAL MODELS AND VIBRATIONAL PROPERTIES OF HYDROUS BRIDGMANITE UNDER HIGH PRESSURE

Kikuyo Inagaki[1], Jun Tsuchiya[2], Haruhiko Dekura[1], Yanyao Zhang[3], Fu Lin Jung[4], Shun-ichiro Karato[5], Jennifer Kung[6], ChingChien Li[6]

3. Geodynamics Research Center, Ehime University
4. High Pressure Material Physics Group, Osaka University
5. Department of Earth and Planetary Sciences, Stanford University
6. Department of Earth and Planetary Sciences, Texas University
7. Department of Geology and Geophysics, Yale University
8. Department of Earth Sciences, National Cheng Kung University

Abstract Water is abundant in the Earth's interior, and a portion of it is incorporated into minerals as hydro gen-related point defects. Bridgmanite (Brg ; $(Mg,Fe)(Si,Al,Fe)O_3$), the most abundant mineral in the lower man tle, is a nominally anhydrous mineral (NAMs), and can incorporate hydrogen through charge compen sation mechanisms associated with atomic vacancies (e.g., Mg and Si sites) and cation substitutions (e.g., Fe^{3+}, Al^{3+}) in its crystal structure (Zhang et al., 2025). This hydrogen could significantly affect various physical properties, including melting relations, phase stability, viscosity, and electrical conductivity, and thus plays a crucial role in the structure and evolution of the Earth's interior (Inoue, 1994 ; Karato and Jung, 1998 ; Karato and Wang, 2013). To evaluate hydrogen solubility , it is essential to under stand how hydrogen is incorporated in the crystal structure. However, reported water contents in Brg show large discrepancies among experiments, which have been attributed in part to differences in hy drogen configurations and defect structures (Fu et al., 2019 ; Bolfan-Casanova et al., 2003). In addi tion, theoretical studies have explored only limited structural models, and a systematic understanding of stable hydrogen configurations remains insufficient (Peng and Deng.,2024 ; Mohn et al., 2025).

In this study, we employed first-principles calculations to construct multiple hydrogen-bearing models incorporating cation substitutions and atomic vacancies, including $Mg^{2+} \leftrightarrow 2H^+$, $Si^{4+} \leftrightarrow 4H^+$, and $Si^{4+} \leftrightarrow Al^{3+} + H^+$ substitutions. We have also evaluated their structural stabilities. Furthermore, infrared ab sorption spectra were calculated for each model to investigate the relationship between hydrogen con figurations and vibrational properties. Our results show that the OH stretching frequencies systemati cally vary depending on hydrogen configurations. In addition, under high-pressure conditions, changes in vibrational properties associated with hydrogen bond strengthening and symmetrization were identified. The calculations are compared with experimental FTIR spectra of single-crystal bridgmanite crystals, suggesting the possible presence of multiple substitution models. This study provides a quantitative relationship between hydrogen configurations and spectroscopic features in bridgmanite.

Key words: Lower mantle, NAMs, Bridgmanite, Infrared spectra, Hydrogen bond symmetrization

ACCESSORY MINERALS OF ECLOGITES AND GROSPYDITES FROM THE ZAGADOCHNAYA KIMBERLITE PIPE

Nikolay V. Gubanov[1], Denis S. Mikhailenko[1], Sergey Yu. Skuzovatov[2], Anastasia M. Logvinova[3], Yi-Gang Xu[4], Andrey V. Korsakov[3]

1. Zavaritsky Institute of Geology and Geochemistry, UB RAS, Yekaterinburg, Russia
2. Institute of Geochemistry, SB RAS, Irkutsk, Russia
3. V.S. Sobolev Institute of Geology and Mineralogy, SB RAS, Novosibirsk, Russia
4. Institute of Geochemistry, Chinese Academy of Sciences, Guangzhou, China

Abstract Subduction of oceanic lithosphere to mantle depths is a key geological process facilitating interactions between Earth's reservoirs and the crust–mantle material cycle. According to current concepts of lithospheric mantle composition and evolution, eclogite xenoliths from kimberlites are considered the deepest representatives of subducted oceanic rocks.

Following the classic petrological definition, eclogite is a bimineralic rock composed of omphacite and garnet of the pyrope–almandine–grossular series. In recent decades, the interpretation of the term "eclogite" has significantly broadened, leading to the inclusion of a greater number of rock-forming and accessory minerals. The list of primary accessory minerals in eclogite xenoliths from kimberlites is very limited and includes rutile, coesite, sanidine, diamond, graphite, kyanite, corundum, and allanite. Secondary mineral assemblages are more diverse and their formation is typically attributed to mantle metasomatism, as well as to processes occurring during the transport of xenoliths to the surface by kimberlite melt. Thus, the appearance of LREE-enriched phases in eclogites serves as an important indicator of deep-seated metasomatic processes involving fluids or melts.

The Zagadochnaya pipe differs markedly from all diamond-bearing pipes in the world by its unique suite of deep-seated xenoliths, represented exclusively by eclogites and their high-calcium variety – grospydites (grossular, pyroxene, and kyanite), with a complete absence of typical mantle ultramafic rocks (peridotites, dunites, lherzolites). The mineral composition of these xenoliths is unique: they contain kyanite with exceptionally high Cr_2O_3 contents (up to 12.86 wt%), high-calcium garnets (Ca# > 80 %), rock-forming zoisite and sanidine, a peculiar variety of clinopyroxene (kosmochlor), rutile with elevated Nb_2O_3 contents (up to 10 wt%), as well as accessory allanite, apatite, zircon, and titanite. This indicates a strikingly different composition of the upper mantle beneath the pipe compared to the neighboring highly diamondiferous Udachnaya pipe.

Our preliminary results on the mineralogical and geochemical features of eclogites and grospydites indicate the absence of significant metasomatic overprints. The studied xenoliths show no evidence of material input or redistribution characteristic of intense metasomatic

alteration: the mineral assemblages preserve their original equilibrium relationships, and the rock-forming minerals (garnet, zoisite, sanidine, pyroxenes, kyanite) display no zoning related to external influences. At the same time, the unique mineral composition of the rocks, together with the geochemical characteristics of the rock-forming and accessory minerals, reflects a complex history of formation and subsequent evolution of the mantle block beneath the Zagadochnaya pipe.

Key words: Eclogites, grospydites, mantle metasomatism, kimberlites

Acknowledgements This work was financially supported by the Russian Science Foundation (project no. 25-77-10027).

COMBINED EFFECTS OF LIGHT ELEMENTS ON THE MELTING TEMPERATURE OF EARTH'S INNER CORE

Kai Wang*, Anatoly Belonoshko, Xiancai Lu

School of Earth Sciences and Engineering, Nanjing University, China

Abstract The temperature at the inner core boundary (ICB) is a fundamental parameter in deep Earth science as it controls the thermal state of the core, the growth history of the inner core, and the energy available to sustain the geodynamo. This temperature is set by the melting behavior of the inner core alloy at approximately 330 GPa. In addition to Fe and Ni, Earth's core is widely known to contain several light elements, including Si, S, O, C, and H, all of which may depress the melting temperature relative to pure iron. While the melting properties of pure Fe and binary Fe-X systems have been extensively investigated, the combined effect of multiple light elements, which represents a realistic core composition, remains largely unconstrained. Here, we employ molecular simulation based on machine-learning force-field (MLFF) to investigate the melting temperatures of multicomponent Fe alloys in the Fe-Ni-Si-S-O-C-H system, as well as the solid-liquid partitioning behavior of light elements under the ICB condition. These results are expected to provide improved constraints on inner-core temperature and composition, with important implications for the thermal structure, compositional evolution, and dynamics of Earth's core.

Key words: Earth's inner core, melting temperature, light elements, machine-learning force field

CONSTRAINTS ON THE LIGHT-ELEMENT BUDGET IN THE EARTH'S INNER CORE INFERRED FROM THE EQUATIONS OF STATE OF FE-SI-C-H ALLOYS

Ilya Kupenko[1], Efim Kolesnikov[2], Xiang Li[1], Susanne C. Müller[1,2], Arno Rohrbach[2], Stephan Klemme[2], Jasper Berndt[2], Aaron Rigoni[3], Mohamed Mezouar[1], Michael Hanfland[1], Carmen SanchezValle[2]

1. ESRF – The European Synchrotron, 71 Avenue des Martyrs, Grenoble, France
2. Institute for Mineralogy, University of Münster, Germany
3. Institute of Materials Physics, University of Münster, Germany

Abstract The Earth's inner core is thought to be composed primarily of iron with the addition of approximately 5–10 wt% nickel. However, the density of pure iron and iron-nickel alloys at inner-core conditions exceeds the observed inner-core density by 3–8 %, depending on the assumed temperature. This density deficit requires the presence of lighter elements in the core composition. The most likely candidate light elements are hydrogen, oxygen, silicon, carbon, and sulfur, given their high abundance in the solar system and their preferential partitioning into liquid iron during core formation. Understanding the effect of light elements on inner-core properties is crucial for constraining its composition.

We investigated the equations of state of six Fe-Si-C-H alloys by performing high-pressure diamond-anvil-cell experiments above 1 Mbar and extrapolated the results to inner-core conditions. In this contribution, we present our results and discuss the details of the extrapolation to inner-core conditions. These data provide constraints on the Earth's inner core composition consistent with seismological models.

Key words: Earth's inner core, Iron alloys, Light elements, Equations of state, High-pressure experiments

DEEP PHOSPHORUS RECYCLING REQUIRES EXCEPTIONALLY COLD SUBDUCTION

Qiwei Zhang[1,2], Frank E. Brenker[3],Suzette Timmerman[4], Steven B. Shirey[1], Thomas Stachel[2], Robert W. Luth[2], Andrew Locock[2], Richard A. Stern[2], Ingrid L. Chinn[5], Fabrizio Nestola[6], Xin Deng[1], D. Graham Pearson[2]

1. Earth & Planets Laboratory; Carnegie Institution for Science, U.S.A
2. Department of Earth and Atmospheric Sciences, University of Alberta, Canada
3. Schwiete Cosmochemistry Laboratory, Goethe University, Germany
4. Institute of Geological Sciences, University of Bern, Switzerland
5. De Beers MRM; South Africa
6. Department of Geosciences, University of Padova, Italy

Abstract Phosphorus is a key bio-essential element, yet the efficiency of its recycling into Earth's deep mantle remains poorly constrained. High-pressure phosphate inclusions in sublithospheric diamonds provide a rare opportunity to track deep phosphorus transport. Here we report tuite (γ-$Ca_3(PO_4)_2$) inclusions from two lower mantle-derived diamonds. A diamond from Juína, Brazil hosts a tuite inclusion co-occurring with low-Mg# (~65) ferropericlase and calcite. Trace-element and Sr–O isotope compositions of the tuite support its derivation from subducted altered oceanic crust. In contrast, a diamond from the DO-27 kimberlite, Canada, contains three tuite inclusions coexisting within a meta-peridotitic assemblage comprising high-Mg# ferropericlase (~90), retrogressed bridgmanite, CaSi-perovskite, and stishovite. These observations provide mineralogical confirmation that phosphorus is transported into Earth's lower mantle as tuite. However, thermodynamic calculations reveal that the formation of these diamonds and their inclusions requires the subducting slab to follow the coldest endmembers of slab geotherms observed in modern subduction systems. Such stringent conditions would have been rarely met and consequently minimized deep phosphorus recycling over geological time. Thus, phosphorus is dominantly retained in the crust through shallow mantle recycling, maintaining an accessible surface phosphorus reservoir critical for nutrient availability and the origin of life. The exceptionally cold subduction conditions not only enable deep phosphorus transport but also generate distinctive mineral assemblages of the slab mantle. Thermodynamic modeling of cold (<1080℃) harzburgitic slab mantle shows that it comprises ~44 wt.% stishovite + 55 wt.% ferropericlase + 1wt.% CaSi-perovskite. This newly recognized mineral assemblage drastically increases previous estimates of cold slab density and seismic velocity. Thus, temperature is a first-order control on slab mineralogy and rheology, determining slab stagnation or penetration at the transition zone–lower mantle boundary.

Key words: Superdeep diamonds, phospherous cycle, deep subduction

DEFORMATION OF BRIDGMANITE UNDER THE LOWER MANTLE CONDITIONS

Longli Guan[1,2], Daisuke Yamazaki[2,*], Noriyoshi Tsujino[3], Yuji Higo[3], Sho Kakizawa[3], Xiang Wu[1,*] & Junfeng Zhang[1]

1. State Key Laboratory of Geological Processes and Mineral Resources, School of Earth Sciences, China
2. University of Geosciences, Wuhan, China Institute for Planetary Materials, Okayama University, Japan.
3. Japan Synchrotron Radiation Research Institute, Japan

Abstract Seismic anisotropy in the Earth's lower mantle, particularly beneath subduction zones, points to dislocation creep as a dominant deformation mechanism. Globally, however, the lower mantle appears nearly isotropic for most of its depth, suggesting limited prevalence of this mechanism. Despite its key role, the rheological properties of bridgmanite, the most abundant lower mantle mineral, remain poorly constrained due to experimental challenges. Here, we report the temperature dependence of lattice preferred orientation (LPO) development in Fe-free and Fe-bearing bridgmanite from deformation experiments under conditions of the uppermost lower mantle (25 GPa, 1700-2100 K) using the D111-type apparatus. LPOs were observed across the temperature range, with the dominant slip system of [010](100) below 1800 K and [100](010) above 1800 K, negligibly affected by Fe content. High-temperature LPO exhibits weaker anisotropy under horizontal shearing, approaching isotropic behavior, while low-temperature LPO produces stronger anisotropy. These findings reconcile the strong seismic anisotropy observed beneath subduction zones and the global near-isotropic behavior, attributing to the temperature-dependent LPO of bridgmanite. Our results suggest that dislocation creep may be the dominant deformation mechanism in the lower mantle, providing new insights into the viscosity structure and mantle dynamics.

Key words: Lower mantle, bridgmanite, lattice preferred orientation, seismic anisotropy, deformation mechanism

DOMINANCE OF HIGH-SPIN FE^{2+} IN BRIDGMANITE AND POST-PEROVSKITE UNDER HYDROUS LOWERMOST MANTLE CONDITIONS

Ziqiang Yang[1], Xiang Li[2], Georgios Aprilis[2], Ilya Kupenko[2], Yuzhu Wang[3], Ho-kwang Mao[1,4], Li Zhang[1]

1. Center for High Pressure Science and Technology Advanced Research, China
2. European Synchrotron Radiation Facility, France
3. Shanghai Synchrotron Radiation Facility, Shanghai Advanced Research Institute, Chinese Academy of Sciences, China
4. Shanghai Key Laboratory of Material Frontiers Research in Extreme Environments, Institute for Shanghai Advanced Research in Physical Sciences, China

Abstract Water can be transported to the Earth's lowermost mantle through subducted slabs, but its effects on the physical and chemical properties of ferromagnesian silicate phases remain elusive. Here, we synthesized $(Mg,Fe)SiO_3$ bridgmanite and post-perovskite under hydrous deep lower mantle conditions at 102–135 GPa and 2100–2400 K using laser-heated diamond anvil cells. The valence and spin states of iron were determined by combining *in situ* X-ray diffraction (XRD) and synchrotron Mössbauer spectroscopy (SMS). The high-pressure SMS spectra of both bridgmanite and post-perovskite are dominated by one quadrupole doublet with a center shift of ~1 mm/s relative to α-Fe and an extremely high quadrupole splitting (QS) of ~3.9–4.1 mm/s. The high-QS doublet was previously attributed to Fe^{2+} in the intermediate spin state, and subsequently interpreted as high-spin Fe^{2+} in distorted sites on the basis of theoretical calculations. The SMS measurements on $(Mg_{0.6}Fe_{0.4})SiO_3$ bridgmanite decompressed to 5 GPa yield an $Fe^{3+}/\Sigma Fe$ ratio of 7.6(1.8)%, confirming the dominance of Fe^{2+}. Our results indicate that Fe^{2+} adopts high-spin state in both bridgmanite and post-perovskite under high pressure-temperature conditions corresponding to the deep lower mantle. The valence and spin states of iron in $(Mg,Fe)SiO_3$ bridgmanite and post-perovskite under hydrous conditions provide constraints on the chemical heterogeneity and complex seismic structures of the lowermost mantle.

Key words: bridgmanite, post-perovskite, ferrous iron, ferric iron, spin state, Mössbauer spectroscopy

Acknowledgements This work was supported by the National Natural Science Foundation of China (NSFC) (grant nos. 42525204 and 42150103). The synchrotron XRD experiments were performed at BL15U1 and BL17UM of Shanghai Synchrotron Radiation Facility (SSRF). The synchrotron Mössbauer spectroscopy experiments were performed at ID14 of European Synchrotron Radiation Facility (ESRF).

ELASTIC PRESSURE CONSTRAINT ON AN ECLOGITIC DIAMOND FROM MENGYIN KIMBERLITE: EVIDENCE FOR DEEP SLAB SUBDUCTION IN THE EASTERN NCC

Yongkang Ding, Hongfu Zhang

School of Earth Sciences, Zhejiang University, China

Abstract Given that the Paleozoic kimberlites of the North China Craton (NCC) lack eclogite xenoliths, eclogitic diamonds have become the only direct window into ancient subducted materials preserved in the lithospheric mantle of the eastern block. Defining the formation depth of these materials is critical to reconstructing the subduction dynamic. However, these diamonds rarely retain the mineral pairs required for traditional geochemical thermobarometers. Based on this, we use a coesite-in-diamond elastic barometry. This method is independent of mineral pairs and nearly independent of temperature assumptions. By measuring the residual elastic pressure of the coesite inclusions using Raman spectroscopy, we have constrained the formation depth of the primary eclogitic diamond in the NCC for the first time. Elastic barometric analysis of the coesite-bearing diamond SD-234 yields an estimated entrapment depth of ~200 km, suggesting that the subduction slab materials preserved in the eastern NCC reached at least the base of the craton root. This result provides significant new understanding of the subduction processes beneath the eastern NCC. Nevertheless, no reliable formation ages are available for these eclogitic diamonds, and the timing of the associated ancient subduction event remains poorly constrained. The geodynamic setting in which they formed, as well as their broader role in the formation and long-term stability of the NCC lithosphere, remain unresolved. Addressing these issues will require ongoing cooperative efforts of China's diamond research community.

Key words: North China Craton, Mengyin Kimberlite, Eclogitic diamond, Elastic barometry

ELASTIC PROPERTIES OF IRON-SULFUR ALLOY AT EXTREME CONDITIONS

Dennis Kosobokov[1], Xiang Li[1], Carolina Longa[2], Cheng Qian[3,4], Xiang Wu[4] Lianjie Man[5], Georgios Aprilis[1], Katarzyna Skrzynska[1], Mohamed Mezouar[1], Ilya Kupenko[1]

1. ESRF – The European Synchrotron, 71 Avenue des Martyrs, Grenoble, France.
2. Department of Earth and Environmental Sciences, University of Milano Bicocca, Milan, Italy.
3. Bayerisches Geoinstitut, Univerity of Bayreuth, Bayreuth, Germany.
4. State Key Laboratory of Geological Processes and Mineral Ressources, China University of Geosciences, Wuhan, China.
5. Department of Earth and Planetary Sciences, ETH Zürich, Zürich, Switzerland.

Abstract Iron-nickel alloys are the primary components of the cores of terrestrial planets, such as Earth. However, seismic models reveal a density deficit and reduced seismic velocities in Earth's core compared to pure Fe-Ni alloys, suggesting the presence of 4–7 wt% of light elements such as S, C, O, H, and Si. The concentration and combination of these light element candidates remain unknown.

Despite extensive discussion of sulfur as a plausible alloying element, experimental data remain scarce, and our knowledge of the Fe-S systems mainly arises from theoretical models that are highly constrained and include numerous assumptions. Most available experimental studies focus on the high-pressure/high-temperature behaviour of classical iron sulfide and iron-rich sulfide phases (FeS, Fe_2S, Fe_3S). Investigations of iron-sulfur alloys on the iron-rich side of the phase diagram are hindered by the insolubility of sulfur in iron at ambient pressure. However, the maximum solubility of sulfur in solid iron increases with pressure, rising from 0.8 wt% sulfur at 25 GPa to about 4 wt% at 250 GPa.

To better constrain the sulfur content in terrestrial planetary cores, we investigated the elastic properties of an iron alloy containing 1 wt% sulfur, pre-synthesized in a multi-anvil press, at high pressures using synchrotron X-ray diffraction and Nuclear Inelastic Scattering in diamond anvil cells. In this contribution, we will present the elastic behavior of iron-sulfur alloys under extreme conditions and compare our findings to available seismic models. Based on our results, we will discuss new constraints on the sulfur budget in the interior of terrestrial planets.

Key words: Sound velocities, Earth's core, Iron alloy, Extreme conditions

EMERGENCE OF NOVEL COMPOUNDS FORGED IN ATOMIC FIREBALLS

Luca Bindi

Department of Earth Sciences, University of Florence, Florence, Italy

Abstract High-energy impact and compression processes – ranging from planetary-scale collisions to laboratory shock experiments – are known to generate extreme, transient physicochemical environments that drive the formation of novel mineral phases inaccessible under equilibrium conditions. Nuclear detonations represent a unique anthropogenic analogue of such processes, producing ultrahigh temperature–pressure regimes, rapid decompression, and quenching rates comparable to those inferred for hypervelocity impacts and deep planetary interiors. Here, mineralogical and crystallographic data from new materials recovered in the debris generated by the Trinity (1945) and Hiroshima (1945) atomic explosions are presented.

In beach sands from Hiroshima Bay, a previously unknown high-entropy alloy (HEA) has been identified preserved within a glassy spherule (hiroshimaite) formed during the 6 August 1945 airburst. The μm-scale metallic grain is embedded in a quenched silicate matrix and exhibits a chemically homogeneous, multi-component composition dominated by Fe, Cr, Ni, Mn, Mo, Si, and Al. Single-crystal X-ray diffraction reveals that this phase crystallizes in space group $P2_13$ and adopts the ordered $AlAu_4$-type structure, an ordered derivative of the β-Mn topology. The compositional complexity and structural ordering of this alloy indicate formation via condensation from a high-temperature, mixed metallic vapor, followed by ultrafast quenching during fireball expansion. Such conditions mirror those expected in vapor plumes generated by large impacts, where rapid cooling can stabilize entropy-dominated metallic phases. The discovery of this HEA demonstrates that nuclear blast environments can act as natural laboratories for the synthesis of complex alloys, providing insight into nonequilibrium metal formation under extreme compression and decompression pathways.

Complementary evidence from the Trinity test further underscores the diversity of materials generated under these transient conditions. Within red trinitite, a new Ca–Cu–Si type-I clathrate has been found, with composition $(Ca_{3.3}Cu_{0.4}Fe_{0.3})_{\Sigma=4}Si_{23}$, hosted in a Cu-rich metallic droplet. Single-crystal X-ray diffraction confirms a cubic clathrate-I framework, marking the first crystallographically validated clathrate structure identified among nuclear detonation products. This phase occurs in close association with a previously reported Si-rich icosahedral quasicrystal formed in the same event, sharing similar chemical characteristics and textural context. The coexistence of these phases suggests that rapid fluctuations in temperature, pressure, and composition within the detonation plume can stabilize both periodic and aperiodic structures from a common precursor system.

To explore potential structural relationships between these phases, density functional theory

calculations on clathrate-based icosahedral models across a range of Cu contents have been performed. The results indicate that clathrate-derived icosahedral configurations are mechanically plausible and metastable at relatively low Cu concentrations (~10–11%), but become unstable as Cu content increases toward that observed in the Trinity quasicrystal. These findings constrain viable structural models for the quasicrystal and suggest that, although clathrate frameworks may represent a structural motif accessible under dynamic compression, the quasicrystal likely forms via a distinct pathway under more extreme or rapidly changing conditions.

Taken together, these results demonstrate that atomic explosions generate a spectrum of previously unknown materials – including high-entropy alloys, clathrates, and quasicrystals – through processes governed by extreme compression, rapid thermal gradients, and nonequilibrium kinetics. These environments provide a scaled analogue for mineral formation during hypervelocity impacts and potentially within the shock-compressed regions of planetary interiors, including super-Earths where high pressures and complex chemistries prevail. The study of nuclear-blast-derived materials thus opens a new avenue for exploring phase stability, structural complexity, and emergent order in matter subjected to dynamic compression, bridging mineral physics, materials science, and planetary science.

Key words: atomic explosions, Trinity, Hiroshima, clathrate, high-entropy-alloy

EXPERIMENTAL CONSTRAINTS ON THE THERMAL STRUCTURES IN EARTH'S DEEP MANTLE: GLOBAL AND REGIONAL

Wen-Pin Hsieh

Institute of Earth Sciences, Academia Sinica, Nankang, Taipei 11529, Taiwan

Abstract Earth's deep mantle is featured by several thermochemical heterogeneities with variable sizes, e.g., the large low shear-wave velocity provinces, ultralow-velocity zones, and subducted slabs. They co-exist and interact with each other over Earth history, impacting the thermochemical evolution of our planet. Thermal conductivities of these heterogeneous structures are pivotal to regulate Earth's available energy, dynamics, and thermochemical and geodynamo evolution. However, such important property remains poorly constrained. With our novel combination of an ultrafast optical spectroscopy and laser-heated diamond anvil cells, we have precisely measured the thermal conductivity of important lower mantle minerals with representative compositions. This allowed us to model the thermal conductivity profiles for pyrolytic lower mantle and iron-rich oxides or melts for the seismic ultralow velocity zones above the core-mantle boundary. I will discuss their effects on the thermochemical evolution at the lowermost mantle and core along with the geodynamo evolution.

Key words Thermal conductivity, diamond anvil cell, core-mantle boundary

FELDSPARS AND RELATIVES: CONNECTING CHEMISTRY, TOPOLOGY AND STABILITY

Liudmila Gorelova

Institute of Earth Sciences, Saint Petersburg State University, Russia

Abstract Feldspars are one of the most common minerals in the Earth's crust. Usually, feldspars are used to refer to potassium feldspars and plagioclases, i.e., minerals of the $KAlSi_3O_8$–$NaAlSi_3O_8$–$CaAl_2Si_2O_8$ series that are aluminosilicates with three-dimensional (3D) crystal structures. However, a whole series of minerals with a general formula MT_4O_8 (*M* – alkaline / alkaline-earth metals, *T* – semimetals/ post-transition metals), whose composition and structure are strikingly different from classic feldspars, exist in nature. These compounds can be considered members of the feldspar family and offer a new perspective on how the composition, structure, and stability of minerals are interrelated. Seven basic topologies (which can exist under ambient conditions) can be distinguished among MT_4O_8 minerals. Three types of framework topologies based on TO_4 tetrahedra ("feldspar" (e.g., albite), "paracelsian" (e.g. paracelsian) and "svyatoslavite" (e.g. svyatoslavite)), layered topology based on TO_4+TO_4 tetrahedra ("layered feldspars"; e.g., dmisteinbergite); and framework topology, based on TO_6 octahedra ("high-pressure feldspar"; e.g., hollandite) are known. Besides, layered topologies based on TO_4+ TO_5 and TO_4+ TO_6 polyhedra are known for synthetic compounds.

Over the past decade, we have investigated feldspars and other MT_4O_8 compounds (natural and synthetic) using a wide range of methods. Solid-state synthesis and melt crystallization methods were used to synthesize MT_4O_8 compounds. The minerals and synthetic compounds were studied at high pressures (up to 100 GPa) and high temperatures (up to 1200 °C). Diamond anvil cells, synchrotron and in-house powder and single-crystal X-ray diffraction, Raman spectroscopy, and DFT calculations were used to study their crystal structures. We have studied more than 30 compounds in which 18 cations act as species-forming ions.

We studied crystal structures for the first time of three compounds isostructural to feldspars ($SrZn_2P_2O_8$, $RbAlGe_3O_8$, $CdAl_2Si_2O_8$). These findings demonstrate that more feldspars could be discovered in nature. High-temperature studies of compounds with MT_4O_8 have revealed such pattern as: (1) compounds with feldspar topology are usually the most stable modifications; (2) compounds with paracelsian topology usually transform into feldspar topology above 900 °C; (3) layered compounds with dmisteinbergite topology are metastable (i.e. they are difficult to obtain) and usually undergo two polymorphic transformations upon heating with the preserving of layered topology. These studies allowed us to describe rare polymorphs of different feldspar-related compounds, including anorthite ($CaAl_2Si_2O_8$) and celsian ($BaAl_2Si_2O_8$), which can provide precise information about the temperatures and rates of crystallization of the host rocks.

High-pressure studies demonstrated that the most interesting polymorphic transformations are found for framework compounds with feldspar and paracelsian topologies. These compounds could contain unusual polyhedra like SiO_5, BeO_5, and PO_5 and edge-sharing BO_4 tetrahedra. The transformation pathway depends largely on the initial topology but can also differ significantly depending on the chemical composition of both framework-forming and extraframework cations. The obtained crystal structures with unusual structural units indicate the possibility of non-traditional pathways for the phase transformation of minerals in the deep layers of the Earth. An increase in the coordination number with increasing pressure affects the density of the substance, its plastic and elastic deformation, and, as a consequence, the density of the lithospheric plate and its behavior in the mantle.

In total, more than 30 new high-temperature or high-pressure polymorphic modifications of feldspar-related compounds were discovered. All of the above confirms the importance of the obtained results not only for experimental mineralogy and modeling of mineral formation processes but also for fundamental crystal chemistry.

Key words: feldspar, topology, polymorphism, high temperature , high pressure

Acknowledgements This research was funded by the Russian Science Foundation, grant number 22-77-10033-П.

FEO AS THE DOMINANT COMPONENT OF THE MARTIAN INNER CORE

Zhongxu Pan, Wenzhong Wang*, Zhongqing Wu*

Laboratory of Seismology and Physics of Earth's Interior, School of Earth and Space Sciences, University of Science and Technology of China, Hefei, Anhui 230026, China.

Abstract Seismic data from the InSight mission reveal that Mars possesses a structure comprising a crust, mantle, and core, with recent studies indicating the existence of a solid inner core. While the composition of the inner core of Mars remains unclear, but some scholars argue that it might be FeO and/or Fe3C. Here, the thermoelastic properties of high-spin antiferromagnetic B1-phase FeO was derived from first-principles calculations, and the composition of the core was inverted by combining with the previous experimental data. Additionally, the possible light element components in the Martian outer core have also been restricted. These results provide a new starting point for the composition of the Martian core and might have implications for understanding the chemical composition and magnetic evolution of the Mars.

Key words: First-principles, FeO, High-spin, Antiferromagnetic, Martian Core

FLUID INCLUSIONS IN COATED DIAMONDS: INSIGHTS INTO EPISODIC DIAMOND GROWTH

Fernando Cámara[1*], Maxwell C. Day[2], Fabrizio Nestola[2] & D. Graham Pearson[3]

1. Dipartimento di Scienze della Terra, Università degli Studi di Milano, Via Luigi Mangiagalli 34, 20133, Milan, Italy

2. Dipartimento di Geoscienze, Università degli Studi di Padova, Via Gradenigo 6, I-35131 Padova, Italy.

3. Department of Earth and Atmospheric Sciences, University of Alberta, 116 St & 85 Ave, Edmonton, AB, T6G 2R3, Canada.

***Presenting Author:** fernando.camara@unimi.it

Abstract Coated diamonds consist of a gem-quality core overgrown by a fibrous (fluid-rich) rim and are particularly informative as they record multiple diamond forming events associated with different fluids from potentially distinct sources. In this study, two coated diamonds (CTPS-1 and CTP-12) from the DRC were studied using FTIR and Raman spectroscopy. For CTPS-1, FTIR mapping revealed significantly higher nitrogen-aggregation states ($\%N_B$) in the gem core compared to the fibrous rim. This, in addition to a sharp core-rim contact, suggests a prolonged mantle residence period for the core prior to formation of the rim. Interestingly, the gem core of CTPS-1 also shows concentric growth zonation with $\%N_B$ ranging from 20-70% suggesting the core itself also formed during several discrete diamond-forming events.

For CTPS-12, the core and rim have similar $\%N_B$ (0-20%) and both show fine concentric growth zoning. Moreover, the core-rim boundary is relatively diffuse where fibres (observed as linear arrays of mineral inclusions) appear to extend from the fluid-rich rim into the gem-quality core. Raman spectroscopy revealed numerous silicate inclusions (~2-5 μm) in the core close to the core-rim contact and FTIR spectra show a silicic composition for high-density fluid (HDF) inclusions in rim.

Keywords: diamond, fibrous diamond, fluid inclusion, coesite, growth zoning

Acknowledgements the authors acknowledge funding from the ERC Advanced Grant MADAM (grant agreement n. 101199315)

FLUORINE-BEARING MELT INCLUSIONS IN DIAMONDS OF THE SIBERIAN CRATON

Vladislav S. Shatsky[1,2], Alexey L. Ragozin[1], Viktoria V. Kalinina[1]

1. V.S. Sobolev Institute of Geology and Mineralogy SB RAS, Russia)
2. Novosibirsk State University, Russia)

Abstract Here we report the first discovery of fluorine-bearing polyphase inclusions in diamonds from the Siberian Craton, based on a study of diamonds from alluvial placer deposits in the northeastern craton and the Internatsionalnaya kimberlite pipe. Six diamonds containing F-rich polyphase inclusions were examined using SEM-EDS and Raman spectroscopy. The samples include diamonds of ultramafic paragenesis (ISTD-124, INTS-10, INTS-32), uncertain origin (ISTD-119), and variety V diamonds (ISTD-193, XLS-147) following Orlov's classification. Variety V diamonds have been previously linked to subduction-related processes based on mineral inclusion assemblages and carbon isotope compositions.

In placer diamonds, fluorine in polyphase inclusions occurs predominantly in association with calcium. Polyphase inclusions in ISTD-124, ISTD-119, and ISTD-193 contain domains with Ca/F ratios of 0.38–0.58, closely approaching fluorite (CaF_2) stoichiometry. The polyphase inclusions contain regions composed of calcium fluorides and regions composed of iron oxides with carbonate admixtures, the presence of carbonatesconfirmed by Raman spectroscopy. Diamond ISTD-124 additionally contains olivine inclusions (Mg# = 91), indicating ultramafic paragenesis. In diamond ISTD-193, inclusions show complex internal structure with carbonate-fluoride mixtures in central region (Ca/F = 0.38–3.0) and nearly pure Ca-F regions. Diamond XLS-147 (V variety) contains several types of inclusions. Some are compositionally similar to aluminum fluoride, while others consist of both aluminosilicate and fluoride parts. Additionally, pure aluminosilicate inclusions without fluorine were also found.

Diamonds of ultramafic paragenesis from the Internatsionalnaya kimberlite pipe provide additional evidence for F-rich mantle. In INTS-10 and INTS-32, fluorine-bearing melt inclusions coexist with primary olivine (Mg# = 90.5–92.6), phlogopite (Mg# = 90.5–91.4), sulfides, and magnetite. Notably, the phlogopite inclusions contain no detectable fluorine but exhibit minor chlorine (0.1–0.2 at%). Sulfide inclusions in INTS-32 show Me/S ratios of 1.12–1.3, Ni# (Ni/Ni+Fe) of 0.5–0.7, and consistently contain 10–14 at% oxygen.

The fluoride melt inclusions display remarkable compositional heterogeneity. In INTS-10, fluorine varies from 43 to 58 at%, accompanied by Mg (1–18.7 at%), Ca (2.3–24.5 at%), Fe (0.9–3.6 at%), and O (11.4–27 at%), with minor Al, Si, K, and S. In INTS-32, inclusions are enriched in Mg (17.5–27.3 at%) and Fe (3.1–15.2 at%) but contain negligible Ca (<0.6 at%), defining a distinct Mg-Fe fluoride melt composition. A positive correlation between Fe and O suggests the presence of oxide components within the fluoride melt.

In a diamond of octahedral habit, INTS-13, inclusions consisting of anhydrite and calcium fluoride have been identified. In addition to fluoride and anhydrite inclusions, inclusions of olivine (Mg# 92.4), sulfides, and magnetite are present. The sulfides have a Me/S ratio of 0.98-1.0 and a Ni# of 0.94-0.96.

In diamonds ISTD-119, ISTD-124, and ISTD-193, along with fluorides, the inclusions also contain carbonates and magnetite. Therefore, a carbonatite melt can be considered as the primary melt for these inclusions. The absence of fluorine impurity in phlogopite inclusions in diamonds, together with the simultaneous presence of sulfide and anhydrite inclusions in diamond INTS-13, indicates the interaction of oxidized fluids from the subducting slab with the reduced lithospheric mantle.

The research was funded by the Russian Science Foundation (project No. 25-27-00492).

Key words: Siberian Craton, inclusions in diamonds, fluoride melts, diamond formation, mantle

HIGH-PRESSURE SYNTHESIS AND CRYSTAL STRUCTURES OF NOVEL IRON-BASED OXIDES-HYDROXIDES IN THE DEEP LOWER MANTLE

Hongsheng Yuan[1], Lianjie Man[2,3], Qingyang Hu[1], Daniel J. Frost[2], Leonid Dubrovinsky[2]

1. Center for High Pressure Science and Technology Advanced Research, China.
2. Bayerisches Geoinstitut, University of Bayreuth, Germany.
3. Institute of Geochemistry and Petrology, ETH Zürich, Switzerland.

Abstract Water-rock interactions at the lowermost mantle can be pivotal in generating chemical heterogeneities that may manifest as seismic anomalies, such as ultralow-velocity zones (ULVZs). Here, we present the discovery and structural characterization of several novel iron-based oxides-hydroxides, including $Fe_{\sim 2.5}O_6H_x$ and $Fe_{\sim 7}O_{12}H_x$ and $(Fe,Mg)_8SiO_{14}H_x$ phase, synthesized from hydrous, iron-bearing assemblages at pressures above 70 GPa and temperatures exceeding 2500 K. Using in situ single-crystal X-ray diffraction in laser-heated diamond anvil cells, supplemented by ex situ electron microscopy, we resolved the crystal structures of these materials. Our results demonstrate that these dense phases coexist with a comprehensive suite of lower mantle minerals, including bridgmanite, post-perovskite, davemaoite, silica polymorphs, and iron carbides. The exceptional thermal stability and high density of these newly identified phases provide a robust mineralogical framework for the origin of ULVZs, suggesting that iron-rich "pockets" formed via volatile-driven reactions are sustainable features of the deep Earth's thermochemical evolution.

Key words: single-crystal X-ray diffraction, water-rock interaction, iron-based oxides-hydroxides, lower mantle, laser-heated diamond anvil cell

HYDROUS ALUMINOSILICATES REGULATE WATER RECYCLING IN THE UPWELLING MANTLE

Fabin Pan, Xiang Wu, Junfeng Zhang

State Key Laboratory of Geological Processes and Mineral Resources, and School of Earth and Planetary Science, China University of Geosciences, Wuhan 430074, P.R. China

* Corresponding authors. e-mail: panfabin@cug.edu.cn

Abstract Aluminosilicates hold the ability to transport and store considerable amounts of water in the transition zone and lower mantle. The aluminum-rich basaltic fragments of subducted oceanic slab serve as the dominant reservoir for water in the deep mantle, whereas the water capacity of pyrolitic mantle remains inherently limited. Two aluminosilicates are found in hydrogen-rich olivine (formerly wadsleyite/ringwoodite) derived from the mantle transition zone. Type I is amorphous silica in association with Fe-Ni alloy nanoparticles, and represent breakdown of Al-bearing stishovite with an aluminum content up to 7 wt.%; Type II is a stoichiometric aluminosilicate (Al/Si = 1:1) in direct coexistence with spinel, formed via retrogression from a high-pressure silicate phase Egg. Notably, both Al-bearing stishovite and phase egg possess water retention capabilities reaching the weight percent magnitude, indicating their potential for substantial water storage. The coexistence of stishovite and phase Egg inclusions in olivine indicate that the olivine hosts formed in a water-saturated mantle transition zone (MTZ). The olivine grains exhibit $\delta^{18}O$ values of 5.4–5.8‰, consistent with pristine mantle signatures, rather than interaction with meteoric or hydrothermal fluids delivered by the deep subducted oceanic slab. These features confirm that hydrogen in the MTZ dominantly comprises primordial hydrogen with invisible subducted surficial water. Our findings provide compelling evidence for the occurrence, abundance, origin, and evolution of hydrogen in the deep mantle, shedding new light on Earth's internal water cycle.

IMPACT OF ALLOYING AND TEMPERATURE ON SHEAR MODULUS OF IRON IN THE EARTH INNER CORE

Anatoly B. Belonoshko[1], Grigory Smirnov[2], Sergei Simak[3]

1. Department of Earth Science, Nanjing University, Nanjing, China
2. Laboratory of Computer Simulation, HSE University, Moscow, Russia
3. Depatment of Physics, Linköping Universitty, Linköping, Sweden

Abstract The material in the Earth Inner Core (IC) is soft with extremely low shear modulus. We know that the body-centered cubic (bcc) phase of iron at the IC P-T conditions has the shear modulus almost identical to the material in the IC. The hexagonal close packed (hcp) phase of iron, according to numerous publications, has the shear modulus much larger than that in the IC. We can not exclude that the alloying by Ni increases the shear modulus of bcc phase while extreme proximity of hcp temperature to the melting temperature drastically decreases the hcp shear modulus. We have checked both factors and discovered that the bcc iron alloyed by 10 percent of Ni remains extremely low and close to that of the Preliminary Earth Model (PREM). Since the low shear modulus in bcc is related to the anomalously high diffusion, we checked whether the hcp atoms become highly diffusive on approach to melting. They are not. According to our results, hcp remains very rigid and bcc very soft. Therefore, bcc is very fitting candidate for the major phase of the material in the IC while hcp can not be there unless something else drastically changes elastic properties of the hcp phase.

Key words: Inner Core, bcc,hcp, shear modulus, diffusion

INTERNALLY CONSISTENT *P-V-T* EQUATIONS OF STATE AMONG PT, AU, AND MGO

Xi Zhu[1,2], Yu Ye[1], Wei Sun[1], Tomoo Katsura[3] and Razvan Caracas[2]

1. State Key Laboratory of Geological Process and Mineral Resources, China University of Geosciences, Wuhan 430074, China.
2. Institut de Physique du Globe de Paris, CNRS, Université Paris Cité, Paris 75005, France
3. Bayerisches Geoinstitut, University of Bayreuth, Bayreuth 95440, Germany

Abstract Accurate pressure scales are fundamental to high-pressure-temperature (high *P-T*) experiments, enabling direct comparison between laboratory experiments and geophysical observations of the Earth's interior. Platinum (Pt), gold (Au), and periclase (MgO) are the most widely used pressure scales. However, significant discrepancies still exist among their reported P-V-T equations of state (EOSs), particularly at high temperatures.

We present a set of internally consistent *P–V–T* EOSs for Pt, Au, and MgO. The EOS optimizations incorporate various datasets, including static compression and shockwave measurements, as well as high-*T* X-ray diffraction (XRD), elasticities, and heat capacities. The fitting residuals are generally within experimental uncertainties. The electronic and anharmonic phonon contributions to thermal pressure are highlighted; the effects of yield strength in shock experiments are also taken into account for the metals Pt and Au.

These EOSs are also utilized to reevaluate the *P-T* boundaries of the post-spinel and post-perovskite phase transitions, which are the main factors leading to the formation of the 660-km discontinuity and the D″ layer, respectively. The Clapeyron slopes (-2.1 ± 0.4 MPa/K for the post-spinel and +5.9 ± 1.1 MPa/K for the post-perovskite transition) are thus better constrained and agree with seismic observations. Additionally, the compositional effect is quite small on the slope of the post-perovskite boundary.

Key words: DAC, pressure scales, high pressure, mineral physics

INVESTIGATING THE REDOX STATE OF THE LITHOSPHERIC MANTLE: INSIGHTS FROM FE ISOTOPES AND FE^{3+}/FE_{TOT} OF MAGNESIOCHROMITE INCLUSIONS IN DIAMONDS

Davide Novella[1], Hugo Abe[2], Peng Ni[2], Valerio Cerantola[3], Nadia Malaspina[3], Maxwell C. Day[1], Martha G. Pamato[1], Fabrizio Nestola[1], Jeff W. Harris[4]

1. Department of Geosciences, University of Padova, Italy
2. Department of Earth, Planetary and Space Science, University of California, Los Angeles, USA
3. Department of Earth and Environmental Sciences, University of Milano - Bicocca, Italy
4. School of Geographical and Earth Sciences, University of Glasgow, UK

Abstract Mantle oxygen fugacity (fO_2) can be constrained through the investigation of different geochemical proxies such as Fe isotopes and the ration Fe^{3+}/Fe_{tot} in minerals from the deep mantle. Whilst in this regard the minerals in mantle xenoliths have been extensively studied, and provided crucial information regarding the redox state of the deep mantle, mineral inclusions in diamonds provide an alternative study of the pristine deep mantle. This is because of these minerals being incorporated in the strong and inert diamond, thereby isolating them from secondary events.

In this study, we investigated magnesiochromite – $(Mg,Fe^{2+})(Cr,Al,Fe^{3+})_2O_4$ – inclusions found in lithospheric diamonds from different cratonic areas. Magnesiochromite normally measure hundreds of μm in size and contain considerable amounts of FeO_t (e.g., 15 wt.%), which allows precise determinations of their Fe isotopic composition and Fe^{3+}/Fe_{tot}. The combination of these two different and important proxies determined on the same specimens allows to differentiate the effects of mantle redox state, mantle melting and mantle sources on fO_2 proxies. These results will provide new constraints on the redox state of parts of the lithospheric mantle.

Key words: diamond, inclusions, Fe isotopes, Fe^{3+}/Fe_{tot}, redox

IRON MONOSULFIDE DOES NOT INCORPORATE HYDROGEN INTO ITS STRUCTURE UNDER HIGH-PRESSURE AND HIGH-TEMPERATURE CONDITIONS

Hiroyuki Kagi[1], Masahiro Takano[1], Yuichiro Mori[1], Hiroki Kobayashi[1], Katsutoshi Aoki[1], Yoshio Takahashi[1], Yuta Ijichi[1], Sho Kakizawa[2], Noriyoshi Tsujino[2], Yuji Higo[2], Asami Sano-Furukawa[3], Taku Tsuchiya[4]

1. Graduate School of Science, The University of Tokyo, Japan
2. Japan Synchrotron Radiation Research Institute, Japan
3. J-PARC Center, Japan Atomic Energy Agency, Japan
4. Geodynamic Research Center, Ehime University, Japan

Abstract Iron monosulfide (FeS) is a major sulfide phase in planetary materials and has been proposed as a potential reservoir of hydrogen in planetary interiors. A previous study reported significant volume expansion and a decrease in the melting temperature of the high-pressure NiAs-type polymorph, FeS V, under high pressure and high temperature hydrogen-saturated conditions (Shibazaki et al., 2014). They attributed these changes to hydrogen incorporation into the interstitial sites, analogous to the behavior of iron and other metal hydrides. More recently, neutron diffraction experiments suggested hydrogen incorporation up to $FeSD(H)_{1.20}$ (Abeykoon et al., 2024). In contrast, some studies found little evidence for either substantial volume expansion or hydrogen incorporation in FeS V (Iizuka et al., 2021; Takano et al., 2024).

In this study, we propose that the discrepancy arises primally from differences in FeS stoichiometry and iron valence state. FeS synthesized under reducing conditions shows no measurable volume expansion upon exposure to hydrogen at high pressure and temperature. Our X-ray absorption spectroscopy and in situ X-ray diffraction results demonstrate that the volume expansion previously observed under hydrogen-saturated conditions is better explained by the reduction of Fe^{3+} to Fe^{2+} and the accompanying decrease in the δ value of Fe-deficient $Fe_{1-\delta}S$ rather than by hydrogen incorporation into the FeS lattice. Rietveld refinements of neutron diffraction data further show that a hydrogen-free structural model provides the best fit to the observed patterns, whereas a hydride model requires unrealistically large atomic displacement parameters. Consistently, first-principles calculations indicate that plausible FeS hydride configurations are energetically unstable. Based on these results, we estimate an upper limit of hydrogen in the FeS lattice as ~200 ppm up to 30 GPa. These results demonstrate that FeS is effectively hydrogen-incompatible under deep planetary interior conditions, implying that hydrogen preferentially partitions into metallic Fe during the early stages of core formation.

Key words: Iron sulfide, hydrogen, high pressure, high temperature, planetary cores

KINETIC HINDRANCE OF PHASE TRANSFORMATIONS IN DENSE $MgSiO_3$ POLYMORPHS UNDER SHOCK COMPRESSION

Sota Takagi[1,2], Donghoon Kim[1,2], Yingwei Fei[1], Sally June Tracy[1]

1. Earth and Planets Laboratory, Carnegie Institution for Science
2. Department of Earth and Environmental Sciences, Korea University

Abstract Equilibrium phase diagrams define the pressure–temperature stability fields of $MgSiO_3$ polymorphs, yet whether the corresponding phase transformations can proceed under shock compression remains poorly constrained. Here, we present in situ synchrotron X-ray diffraction measurements of pre-synthesized dense $MgSiO_3$ polymorphs—bridgmanite and akimotoite—subjected to laser-driven shock compression. The experiments were conducted at the Dynamic Compression Sector of the Advanced Photon Source, Argonne National Laboratory. Bridgmanite preserves its perovskite structure up to at least ~270 GPa, far beyond the equilibrium perovskite–post-perovskite boundary. Akimotoite retains its ilmenite structure up to ~100 GPa, well beyond the akimotoite–bridgmanite boundary. These observations provide direct evidence that neither the perovskite–post-perovskite transition from bridgmanite nor ilmenite–perovskite transition from akimotoite occurs under the shock conditions investigated. Our results indicate that kinetic limitations dominate $MgSiO_3$ transformations on nanosecond timescales, such that equilibrium phase relations cannot be directly applied at extreme short-timescale shock. Placed in the context of recent *in situ* XRD studies across a range of silicate minerals, these results indicate that the structural response to shock is governed not by thermodynamic stability alone, but by kinetic accessibility relating to crystal topology.

Key words: Shock compression, in situ XRD, $MgSiO_3$, bridgmantie, akimotoite

MAJORITIC GARNETS FROM THE MAPING KIMBERLITE, SOUTH CHINA: IMPLICATIONS FOR DEEP MANTLE PROCESSES AND DIAMOND EXPLORATION

Yuhua Zhu[1,2,3], William L. Griffin[4], Ruidong Yang[1,2], Junbo Gao[1,2*], Lei Wang[5], Yuren Zeng[1,2,3], Jianshu Chen[3], Miaoling He[3], Hongjuan Rao[6], Yonggang Li[6], Jiawei Zhang[1,3*]

1. College of Resources and Environmental Engineering, Guizhou University, Guiyang 550025, China
2. Key Laboratory of Karst Georesources and Environment, Ministry of Education, Guizhou University, Guiyang 550025, China
3. Guizhou Geological Survey, Bureau of Geology and Mineral Exploration and Development of Guizhou Province, Guiyang 550081, China
4. CCFS/GEMOC ARC Centre of Excellence, Department of Earth and Environmental Sciences, Macquarie University, Sydney, New South Wales 2109, Australia
5. Wuhan Center, China Geological Survey (Central South China Innovation Center for Geosciences), Wuhan 430205, China
6. 101 Geological Team, Bureau of Geology and Mineral Exploration and Development of Guizhou Province, Kaili 556000, China

Abstract Deep mantle-derived rocks provide unique insights into the Earth's interior. In this study, we identified characteristic ultrahigh-pressure minerals—majoritic garnets—in the kimberlites of the Maping diamond deposit within the Yangtze Craton, South China. These garnets are predominantly of the G9 and G1 types, with a notable absence of the G10 type, which is typically associated with diamonds. Their equilibrium temperatures range from 939 to 1274 °C under geopressures of 6.5–9.2 GPa, corresponding to depths of approximately 215–304 km. These conditions suggest a deep lithospheric mantle origin, confirming that the Maping kimberlite magma traversed the main diamond-forming region (often referred to as the 'diamond window') during its ascent. Additionally, these majoritic garnets exhibit complex europium anomalies (δEu), with values ranging from 0.51 to 1.92, where negative Eu anomalies may reflect metasomatic modification related to ancient subduction events and/or recycled crustal components in the mantle source. Overall, This discovery significantly advances our understanding of the Yangtze Craton's evolution, its deep structural composition, and its prospects for diamond exploration.

Key words: majoritic garnet, pyrope, kimberlite, diamond, Yangtze Craton

Acknowledgements This research was supported by the Guizhou Provincial Basic Research Program (Natural Science; Grant No. MS[2025]012), the Geological Research Project of the

Bureau of Geology and Mineral Exploration and Development of Guizhou Province (Nos. QDKKH[2020]26, QDKKH[2024]6, and QDKKH[2023]1), and the National Natural Science Foundation of China (Nos. 41963006 and 42363006). This abstract is based on a previously published article in the ***Journal of Earth Science*** (https://doi.org/10.1007/s12583-024-2021-9).

MARTIAN MANTLE COMPOSITION AND STRUCTURE CONSTRAINED BY INSIGHT AND FIRST-PRINCIPLES MINERAL PHYSICS

Bicheng Zhang, Zhongqing Wu, Wenzhong Wang

School of Earth and Space Sciences, University of Science and Technology of China, Hefei, Anhui 230026, P.R. China.

Abstract The internal structure of Mars offers a window into the differentiation of terrestrial planets, but current models face a fundamental impasse. Seismic observations from InSight suggest a large liquid core, yet the resulting light-element budget contradicts traditional cosmochemical models. To bridge this gap, recent hypotheses have relied on a basal molten silicate layer, though this interpretation is now challenged by emerging evidence of a solid inner core. In this study, we provide an alternative solution, showing that the "large core" architecture can be reconciled with Insight seismic datas and the Martian moment of inertia without a basal melt layer. This is achieved by utilizing thermodynamic phase-equilibrium modeling alongside a robust synthesis of mineral elasticity data. Crucially, by synthesizing our inversion with experimental Fe-S-O-C phase relations at high pressures and temperatures, we identify an outer core composition comprising 11–16 wt% S, 7–9 wt% O, and 0–4 wt% C. Furthermore, our results favor the formation of a solid FeO inner core. This framework resolves long-standing geochemical-geophysical contradictions and suggests that the Martian core's chemistry aligns more closely with standard planetary building blocks, offering new insights into its long-term cooling and dynamo history.

Key words: Martian interior, large core model, InSight seismic data, Mineral physics, Light element abundance

MELTING DURING GIANT IMPACT ON MERCURY: FROM PROTO-MERCURY'S MINERALOGY TO SHOCK CONDITIONS: OVERVIEW OF THE KEY VARIABLES

Laëtitia Allibert, Soetkin Willemyns, Eva Vets, Sietse Van Overstraeten and Olivier Namur
Department of Earth and Environmental Sciences, KU Leuven, Belgium

Abstract The joint JAXA–ESA **BepiColombo mission** is en route to Mercury, with orbit insertion planned for November 2026. This makes it a timely opportunity to develop predictive models and interpretative frameworks for the forthcoming data. BepiColombo will probe Mercury's present-day state, which reflects its complex evolutionary history. Establishing a robust framework is essential to translate current observations into insights on the planet's formation and past evolution.

In particular, surface composition measurements will help constraining the mantle's mineralogical structure. Estimating solidus and liquidus curves of Mercury's mantle is critical to connect surface mineralogy with magma ocean crystallization rates, which in turn inform the depth, shape, and composition of Mercury's last magma ocean.

Data suggest that current-day Mercury possesses a large metallic core in comparison to all other terrestrial planets in the solar system. Multiple scenarios for explaining this feature exist. We focus on the giant impact scenario that would be responsible for transforming proto-Mercury, the growing planet yet unaffected by a catastrophic event, into Mercury, the post catastrophe planet, which mass is the one of Mercury as observed today. This hypothesis suggests that a single giant-impact, where proto-Mercury was either the impactor or the target, stripped a large mass fraction of its mantle, without affecting the mass or size of its core. Such a catastrophic event, generating a large energetic shock wave, must in turn leave measurable prints/tracks. If this event occurred, that means that the thermochemical outcomes of such an event must be consistent with BepiColombo's observations. Among these, we focus on magma ocean formation upon impact. Outcomes in terms of melt production during a giant collision naturally depend on impact parameters, but it may also critically depend on proto-Mercury's initial structure, composition and mineralogy, which we aim to investigate. Thermodynamic modeling is therefore essential to define realistic internal structures and sizes of proto-Mercury prior to impact, providing initial conditions for collision simulations.

Here, we present thermodynamic modeling of a proto-Mercury with an enstatite-like composition, estimating pressure and temperature at its core–mantle boundary. We choose an enstatite composition because of the similar oxidation state compared to Mercury, that seems to be a first order good proxy of material that has accreted near the Sun. This constrains the planet's size and informs magma ocean crystallization modeling based on assumed initial composition. The results yield critical insights into proto-Mercury's interior, which serve as

input for **giant impact simulations** using **iSALE-3D**, a shock physics code tailored for planetary collisions. We incorporate realistic thermal profiles, interior structures, and solidus–liquidus curves from **MAGEMin**, accounting for Mercury's unique oxidation state. Using the peak shock pressure method to calculate melt production, we predict the shape and depth of the post-impact magma ocean. These predictions are aimed to be compared with experimental constraints on solidus and liquidus behavior, providing estimates of cooling rates for Mercury's last magma ocean and estimates of the chemical/mineralogical composition of Mercury's mantle and crust, which will be measured by BepiColombo.

Key words: Mercury, Giant impact, fusion curves, magma ocean, Interior

MICRODIAMONDS IN THOLEIITIC DOLERITES FROM THE NORTH CHINA CRATON

Yun Wang[1,2], Jingsui Yang[1,2], Zhiyun Lu[3]

1. State Key Laboratory of Critical Earth Material Cycling and Mineral Deposits, Nanjing University, China
2. IMMR, State Key Laboratory of Critical Earth Material Cycling and Mineral Deposits, Nanjing University, China
3. School of Earth Science, Zhejiang University, Hangzhou, China

Abstract Diamonds occur predominantly in deeply sourced magmas (e.g., kimberlites, lamproites, or ultramafic lamprophyres), and their occurrence in ultrahigh-pressure metamorphic rocks and impact-related rocks is also well established. However, the origin of microdiamonds recently recovered from the Lao'zhai'shan (LZS) tholeiitic dolerite intrusion in the southeast North China Craton (NCC) remains controversial. We integrate petrological, mineralogical, spectroscopic, geochronological, and geochemical data on diamond-bearing dolerites and microdiamonds to clarify their characteristics and origin.

These microdiamonds are Ib-IaA type with cubic-octahedral morphology, and they exhibit diverse resorption features: partial resorption (pseudohemimorphic diamond), laminar growth, triangular/tetragonal pits, deformation lines, and corrosion textures on their surface. These diamonds also have complex inclusion assemblages, including graphite, magnetite, ilmenite, clinopyroxene, coesite, Fe-Ni alloy, humite-group phase, fluorine-bearing phase, and newly discovered orthorhombic ZrO_2 (Ortho-I; likely retrograded from Ortho-II, i.e., >12.5 GPa), TiO_2-II, perovskite, and zirconolite. These inclusions display subduction-related geochemical fingerprints, and light C-isotope data of these microdiamonds point to deeply subducted slabs as the initial source.

Zircon geochronology dates the diamond-bearing intrusion to 906.4 ± 6.3 Ma, intruded under low oxygen fugacity ($\Delta\log fO_2$ = -1.0 to -3.7) at shallow crustal levels (0.56–3.44 kbar, 1138–1175 °C). The geochronology, geochemical, and isotopic data suggest that the LZS intrusion is part of the Neoproterozoic Dashigou Large Igneous Province (LIP). The host dolerites originate from interactions between an upwelling asthenosphere/plume and the juvenile lithospheric mantle in a rift system at shallow mantle depths. Notably, we have identified a suite of eclogitic garnets and Na-rich clinopyroxenes (components ranging from aegirine to omphacite with Na_2O contents of up to 2.86 wt. %, corresponding to 11.8 mol% Jd) in this intrusion. We explain that some diamond-bearing mantle fragments (e.g., garnet xenocrysts) were transported by early plume-associated magmatism to the shallow crustal level and later captured by tholeiitic magmatism. Low oxygen fugacity may have helped preserve the microdiamonds within this intrusion during magma emplacement. Plume-related slab-dehydration fluids/melts may have driven rapid diamond growth and transported them to the shallow crust shortly after diamond formation.

These findings challenge the traditional understanding of diamond host rocks, demonstrate that

unaggregated nitrogen diamonds are not exclusively lithospheric, and link diamond formation/preservation to plume-slab interactions during tectonic-thermal events in the NCC.

Key words: Microdiamonds, Plume-Slab Interaction, Mineral Inclusions, Dashigou LIP, Tholeiitic Dolerites

MINERAL PHYSICS OF A NEW PEROVSKITOID STRUCTURE FOR PHOTOVOLTAIC APPLICATIONS

Paola Comodi[1], Emanuele Priola[2], Azzurra Zucchini[1], Marco Milanesio[3], Mattia Lopresti[3], Luca Palin[4], Elisa Boccalon[5], Eliano Diana[2]

1. Department of Physics and Geology, University of Perugia
2. Department of Chemistry, University of Turin
3. Department of Science and Technological Innovation, "Amedeo Avogadro" University of Eastern Piedmont
4. Nova Res s.r.l., Via Baluardo Partigiani 5, Novara

Abstract Organometal halide perovskites (OMHPs) have emerged as highly promising materials for the ecological transition, owing to their low production costs, outstanding optoelectronic properties, and the possibility of finely tuning their characteristics through targeted design and synthetic strategies. Recently, a class of OMHPs in which triphenylsulfonium [$(Ph)_3S^+$] or trimethylsulfonium [$(CH_3)_3S^+$] are chosen as the organic cations, combined with lead- or bismuth-halide frameworks, has attracted growing attention. Their bulky (sterically large), hydrophobic, and positively charged nature allows them to optimize perovskite morphology, passivate bulk defects, and exhibit good moisture stability. These large cations generally form low-dimensional (0D, 1D or 2D) perovskite-like structures.

In this context, the present work investigates the structural and functional role of the triphenylsulfonium cation in lead-halide (I, Br, Cl) perovskite systems, with particular emphasis on the interplay between crystal chemistry, weak interactions, and optoelectronic behavior.

A series of novel OMHPs was synthesized via different solution-based approaches, including low-temperature aqueous precipitation, crystallization from volatile polar solvents, and slow evaporation from dimethylformamide (DMF). These methods yielded multiple new perovskite-like phases, with distinct structural arrangements. In most cases, the cystallized compounds were effimerous under room conditions, and just in a few cases we were able to isolate good crystals to refine their crystal structures. One of the most promising run products is a new bulky triphenylsulfonium lead iodide–DMF complex $(Ph)_3S[Pb_2I_5(DMF)]$ that was well stabilized by the fine tuning of the synthesis procedure, and structurally characterized by single-crystal X-ray diffraction. It crystallizes in the monoclinic space group $P2_1/n$ (No. 14), with unit cell parameters a = 9.3128(3) Å, b = 23.5999(9) Å, c = 14.1518(5) Å, β = 96.9090(10)°, and Z = 4.

The crystal structure reveals a one-dimensional perovskite-like framework based on lead–iodide units, where Pb^{2+} centers are coordinated by iodide anions and a DMF molecule, forming distorted octahedral environments. These octahedra connect into chains, generating a

1D inorganic backbone. The role of the coordinated DMF is interesting as it might play a key role in reducing the dimensionality and stabilizing the structure.

Vibrational spectroscopic data are presented to supports the crystallographic model, together with theoretically calculated band gap of the newly crystallized $(Ph)_3S[Pb_2I_5(DMF)]$ that results to be 2.30 eV at room conditions. High-pressure experiments and theoretical calculations are presented to investigate phase stability, potential memory effects upon decompression, and the evolution of electronic and transport properties. Preliminary results indicate the likely presence of phase transition and decrease in band gap during compression, resulting in a complete metalklic transition at extreme conditions.

These studies aim to deepen the understanding of structure–property relationships in sulfonium-based OMHPs and to assess their potential for advanced optoelectronic and energy applications.

Key words: High Pressure, Band Gap, Phase Transitions, Solar Cell, Organometal Halide Perovskites.

Acknowledgements The work was carried out with funding from the Ministry of Universities and Research (Italy) within the framework of the PRIN 2022 call (sliding list), project "EnVironmentally friEndly pSeudohalides mixed compounds for tunable Photoactive pErovskite mateRials (VESPER)" no. 20222MA3FE P.I. Prof. Emanuele Priola (CUP n. J53C24002460006).

MINERAL PHYSICS OF SUPER-EARTH INTERIORS

Jie Deng

Department of Geosciences, Princeton University, USA

Abstract With thousands of confirmed exoplanets—many of which likely possess differentiated core–mantle structures similar to Earth—the search for potentially habitable rocky worlds beyond our Solar System has entered an exciting new era. Yet the internal structure and mineralogy of super-Earths remain among the largest uncertainties in exoplanet science. Because interior structure exerts first-order control on thermal evolution, magnetic field generation, and long-term surface conditions, constraining deep planetary properties is essential for understanding habitability. Mineral physics provides a critical link between atomic-scale processes and planetary-scale structure. At pressures approaching the terapascal regime, novel silicate phases and unconventional thermodynamic behaviors emerge, fundamentally altering density, elasticity, and transport properties relative to Earth's mantle minerals. In this talk, I will present recent advances from state-of-the-art computational modeling that explore the composition, phase stability, and thermophysical properties of deep mantle materials under extreme conditions relevant to super-Earths. These results offer new perspectives on how the interiors of massive rocky planets may differ from Earth's, and what those differences imply for their thermal evolution, dynamics, and potential habitability.

Key words: Mineral physics, exoplanet, super-Earth, interior

MORPHOLOGY, SPECTROSCOPY AND INCLUSION CHARACTERISTICS OF DIAMONDS FROM SOUTHERN LIAONING KIMBERLITE DEPOSIT: IMPLICATIONS FOR THEIR FORMATION ENVIRONMENT

Dongsheng Li[1], Zhongwei Wu[2], Gungrong Ning[1], Weilai Zeng[1], Xiyue Xia[1]

1. College of Materials Science and Engineering, Guilin University of Technology, China
2. School of Jewelry and Art Design, Wuzhou University, China

Abstract Diamonds from kimberlite-hosted deposits are unique probes for deep mantle processes and lithospheric evolution. This study focuses on diamonds from the No.50 kimberlite pipe in Wafangdian, southern Liaoning, aiming to reveal their formation conditions and genetic history using morphological, spectroscopic, and inclusion analyses. More than 1200 diamond grains were observed, and 15 representa -tive samples were examined by Infrared spectroscopy, Ultraviolet-visible spectroscopy, Laser Raman spectroscopy, and 3D confocal Raman imaging. Macro-morphological results show that curved rhombic dodecahedra are dominant, followed by stepped octahedra and composite crystals, with rare regular octahedra and cubes. Surface microtextures, including triangular growth mounds, inverted triangular etch pits, and step growth striations, indicate intensive mantle resorption and multistage recrystallization. Infrared spectra demonstrate that most diamonds belong to type IaA, IaB and IaAB with aggregated nitrogen defects, suggesting long-term residence in high-temperature cratonic mantle. Ultraviolet-visible spectra display strong N3 center at 415.5 nm, consistent with the colorless to pale yellow appearance of the samples. Laser Raman spectra show a sharp characteristic peak at approximately 1332 cm^{-1}, confirming the typical cubic diamond structure, and weak peaks related to S–H impurities. 3D Raman imaging identifies multistage inclusions: forsterite enclosed in diamond inclusions in sample LN50-01, and coexisting perovskite and graphite in sample LN50-08. These inclusion assemblages indicate an upper-mantle peridotitic origin and record complex growth and resorption events. Integrated evidence from morphology, spectroscopy and inclusions confirms that the Liaoning diamonds are typical mantle-derived crystals formed in the high-pressure and high-temperature environment of the ancient North China Craton lithospheric mantle, modified during kimberlite magma ascent and emplacement. This study provides new mineralogical constraints for understanding diamond genesis and mantle evolution in eastern China.

Key words: diamond, kimberlite, morphology, spectroscopy, inclusion

NANOMETRIC MINERAL INCLUSIONS IN FLUID-RICH DIAMONDS

Fabrizio Nestola[1], Maxwell C. Day[1*], Yanjuan Wang[1,2], Francesca Innocenzi[1], Fernando Cámara[3], Matteo Ardit[1], Robert W. Luth[4], D. Graham Pearson[4], Yaakov Weiss[5], Suzette Timmerman[6], Martha G. Pamato[1], Davide Novella[1], Nicola Rotiroti[3], Jürgen Grässlin[7], Christian J. Schürmann[7], Anna Barbaro[1], Kai Qu[8], Zengqian Hou[2]

1. Dipartimento di Geoscienze, Università degli Studi di Padova, Italy.
2. State Key Laboratory of Deep Earth and Mineral Exploration, Chinese Academy of Geological Sciences, China
3. Dipartimento di Scienze della Terra, Università degli Studi di Milano, Italy
4. Department of Earth and Atmospheric Sciences, University of Alberta, Canada.
5. Institute of Earth Sciences, The Hebrew University of Jerusalem, Israel
6. Institute of Geological Sciences, University of Bern, Switzerland.
7. Rigaku Europe SE, Germany
8. Tianjin Centre, China Geological Survey, China

Abstract A particularly interesting type of diamond, known as fluid-rich or fibrous diamond, can provide crucial information about diamond-forming fluids and the recycling of volatiles in the deep Earth through the study of the fluid inclusions they contain. However, the minerals found within fluid-rich diamonds are often nanometric in size and thus not amenable to study using standard instrumentation, preventing application of chemical or elastic thermobarometry. Consequently, determination of the depths at which they form is extremely challenging and researchers have been unable to link information from fluid-inclusions to specific mantle environments associated with diamond formation. The MADAM research group (Discovering Mineral nAnoinclusions in DiAMond - ERC Advanced Grant - 2024) is working to solve this problem.

Using new single-crystal micro-electron diffraction (MED) instrumentation and a prototype device for crushing and extracting nanometric mineral inclusions, we can now structurally characterize, and thus rigorously identify, nanometric inclusions from different types of fluid-rich diamonds. A preliminary study of a fluid-rich diamond from the Kaapvaal craton (Kimberley region, South Africa) revealed nanometric inclusions of Sr-rich åkermanite ($Ca_2MgSi_2O_7$), unusual carbonates [norsethite – $BaMg(CO_3)_2$, monoclinic Ca-rich strontianite - $SrCO_3$ and nyerereite - $Na_2Ca(CO_3)_2$], sellaite (CaF_2) and anatase (TiO_2). We completed a crystal structure refinement with full anisotropic displacement parameters of one åkermanite crystal (100 × 40 × 10 nm) marking a milestone, the first complete structural characterization of a nanometric mineral inclusion in diamond. Åkermanite and monoclinic Ca-rich strontianite have not been previously observed as inclusions in diamonds and no natural analogue of

monoclinic Ca-rich strontianite is known. FTIR data from fluid inclusions, along with MED data, suggest this diamond formed from an alkali-silico-carbonatitic parental melt, related to recycling of crustal material into the lithospheric mantle beneath the Kaapvaal Craton. Using the experimental formation temperatures of synthetic åkermanite, combined with N-aggregation thermochronometry, the minimum diamond formation temperature was constrained to 1000 °C, at ~140 km depth (~4.6 GPa) along a typical 40 mWm^{-2} geotherm.

Key words: Diamond, mantle, diffraction, inclusions, minerals

Acknowledgements Chinese Academy of Geological Sciences Basal Research Fund (JKYDM2025205); Nest_Contratti_Ric_BIRD24_01; ERC Advanced Grant MADAM (grant agreement n. 101199315); ERC Starting Grant INHERIT (grant agreement n. 101041620).

NATIVE IRON ASSEMBLAGES IN EARTH'S CRUSTAL ROCKS-MINERALOGICAL ANALOGUES OF IRON-RICH ASTEROIDS

Oleg S. Vereshchagin and Sergey N. Britvin
Saint Petersburg State University, Russia

Abstract Iron (Fe) is one of the most abundant elements on Earth. Its mineral form depends largely on oxidation conditions. The Earth's core contains native iron, while in the Earth's crust, almost all iron is oxidized. Processes in the Earth's core (and that of other planets) are inaccessible to direct observation. However, it is assumed that iron meteorites and iron-rich asteroids are fragments of planetary cores and provide direct information about their composition and mineralogy. Unfortunately, very little data is currently available on the origin of iron meteorites, and the only mission to the iron-rich asteroid Psyche will not reach it until 2029.

It is interesting to note that in some cases, native iron forms in the Earth's upper crust. Based on their locality, these processes can be divided into three groups: very local (< 1 m³; e.g., fulgurites), local (1-50 m³; e.g., high-temperature combustion metamorphic rocks), and large-scale (> 50 m³; e.g., magmatic rocks). In all three cases, under the influence of high temperatures (~1000 to 2500 °C), native iron is reduced from primary Fe-bearing minerals through interaction with organic matter. It is important to note that native iron in Earth's upper crust rocks has been very well studied geologically, allowing one not only to obtain its mineral / material composition but also to identify the genetic features of its formation.

We studied anoxic mineral assemblages with native iron from fulgurites (Leningrad oblast and Kolyma region, Russia), high-temperature combustion metamorphic (pyrometamorphic) rocks (Hatrurim Comple, Israil and Jordan), and magmatic rocks (Disco island, Greenland; Krasnoyarsk region, Yakutia, Russia and Bühl, Germany). We also summarize data on the diversity of oxygen-free minerals in terrestrial native Fe-bearing crustal rocks and iron meteorites to further assess the formation conditions of metal-rich asteroids.

We listed 25 oxygen-free minerals as main constituents and accessory phases of iron. To the best of our knowledge, 10 minerals were unknown in terrestrial crustal rocks at the beginning of this study. Suprisingly, only 8 minerals (lonsdaleite, diamond, edscottite, carlsbergite, roaldite, perryite, joegoldsteinite, zolenskyite) of the 25 iron meteorite minerals have not yet been identified in native Fe terrestrial crustal rocks. However, the number of anoxic minerals specific for iron meteorites should be reduced to 4, given that (1) lonsdaleite, diamond and zolenskyite are formed from graphite and daubréelite, respectively by shock metamorphism atypical for iron meteorites, and (2) perryite is an aubrite rather than iron meteorite mineral.

Based on mineralogical and geological evidences we assume that the formation of metal-rich asteroids could have occurred at heating temperatures achievable in space (≈1000-1100 °C),

which easily lead to the formation of native iron melt from primary Fe-bearing silicate-rich matter. The chondrite substance contains a sufficient amount of organic molecules and carbon, which could act as a reducing agent. At the same time, the process does not require high pressures, which is consistent with data on iron meteorites. Depending on the primary composition of the bodies and their geological history, the resulting iron melts will have different geochemical and isotopic markers. At the same time, since the cooling of such melts occurs in space, it can be much slower than in terrestrial objects.

Key words : native iron, Fe, metal rich asteroid

Acknowledgements: The authors thank the Resource Center of X-ray diffraction studies, Geomodel Resource Centre, Center of Microscopy and Microanalysis and Nanophotonics Resource Centers of Saint-Petersburg State University for providing instrumental and computational resources.

PATH-DEPENDENT SALT INCORPORATION IN HIGH-PRESSURE ICE VII

Xi Zhu, Razvan Caracas

Université Paris Cité, Institut de Physique du Globe de Paris, CNRS, Paris 75005, France

Abstract High-pressure ices are believed to be the major constituents of the deep interiors of icy satellites and water-rich exoplanets. Incorporation of the impurities is a crucial problem as it controls the physical and chemical properties of high-P ices and thus the interiors of planets. However, the solubility of salt in ice VII remains poorly constrained. Different experiments have reported different estimates. Here, we address this discrepancy from a thermodynamic perspective.

We first developed a machine-learning interatomic potential based on the r²SCAN functional, covering a P-T range of 5–30 GPa and up to 1600 K. The predicted ice VII melting curve matches two recent experimental determinations across the investigated pressure range. Free-energy calculations indicate that the equilibrium solubility of NaCl in ice VII is limited to 0.23 mol.%, substantially lower than several previously reported experimental estimates.

Undercooling simulations of homogeneous saline liquids reveal rapid 3D nucleation and growth of ice VII. During this process, the crystallization front advances much faster than solute transport in the liquid, leading to efficient solute trapping and incorporation of salt at concentrations 6 times the equilibrium limit. We further performed interfacial simulations near solid–liquid coexistence conditions, which show that solute diffusion in the solid remains strongly limited unless the temperature is close to the liquidus.

These results reconcile previous experimental results and imply that salt incorporation in high-P ice is highly sensitive to the thermodynamic path. The extremely low diffusivity of salt in the solid also suggests that kinetically produced, supersaturated "salty" high-pressure ice can persist over long timescales at low temperatures. Increasing the temperature would enhance the salt diffusion inside the ice VII lattice and thus the secondary nucleation of halite.

Key words: high-pressure ice VII, salt solubility, ocean exoplanets

PHENGITE-MEDIATED F AND CL FLUXES FROM SUBDUCTION ZONES TO THE DEEP MANTLE

Yingzhuo Liu[1], Yu Wang[1,2*], Chunfei Chen[3], Mingdi Gao[1,2], Yi-Gang Xu[1,2]

1. State Key Laboratory of Deep Earth Processes and Resources, Guangzhou Institute of Geochemistry, Chinese Academy of Sciences, Guangzhou, 510640, China
2. Guangdong Research Center for Strategic Metals and Green Utilization, Guangzhou 510640, China
3. State Key Laboratory of Geological Processes and Mineral Resources, School of Earth Sciences, China University of Geosciences, Wuhan, China

Abstract The cycling of volatiles through subduction zones fundamentally shapes Earth's chemical evolution, yet how fluorine (F) and chlorine (Cl) are processed in the deep mantle remains enigmatic. Here, we use high-pressure experiments (5–11 GPa, 850–1200°C) on altered oceanic crust analogues to track deep halogen behavior. We show that phengite remains stable to 11 GPa and 1050°C, efficiently transporting F and Cl to ~330 km depth. Upon breakdown or melting, phengite strongly fractionates these halogens: Cl is released into fluids or melts, while F is sequestered in residual phases such as $KMgF_3$. The Cl-rich fluids produced (9.6–19.9 wt.% Cl) closely match high-density fluid inclusions in diamonds, implicating them as key agents of cratonic metasomatism. Our findings establish phengite as a critical carrier mediating post-arc fluxes of F (1.7-2.6 × 1012 g/yr) and Cl (0.52-1.1 × 1012 g/yr), providing a major pathway for replenishing deep mantle halogen reservoirs.

Key words: phengite, AOC, fluorine, chlorine, subduction

PLAGIOCLASE MEGACRYSTS AS RECORDERS OF RECHARGE-DRIVEN MAGMA CHAMBER DYNAMICS IN THE 1.83 GA WULONG GABBRO DYKES

Jianfeng Ma[1,2], Hamed Gamaleldien[1]*, Wen-Hong Qiu[3], Ross N. Mitchell[4,5], and Tai-Ping Zhao[2]*

1. Department of Earth Sciences, College of Engineering and Physical Sciences, Khalifa University, Abu Dhabi 127788, UAE
2. Key Laboratory of Mineralogy and Metallogeny, Guangzhou Institute of Geochemistry, Chinese Academy of Sciences, Guangzhou 510460, China
3. State Key Laboratory of Ore Deposit Geochemistry, Institute of Geochemistry, Chinese Academy of Sciences, Guiyang 550081, China
4. State Key Laboratory of Lithospheric and Environmental Coevolution, Institute of Geology and Geophysics, Chinese Academy of Sciences, Beijing 100029, China
5. University of Chinese Academy of Sciences, Beijing 100049, China

*Corresponding authors: hamed.gamaleldien@ku.ac.ae

Abstract Giant plagioclase aggregates preserve valuable yet poorly understood records of magma-chamber processes. The ca. 1.83 Ga Wulong porphyritic gabbro dykes of the North China Craton contain 1–6 cm plagioclase megacrysts characterized by flower-like petaloid clusters, flow-aligned fabrics, oscillatory zoning, and epidote-garnet inclusion bands. In-situ elemental profiles, especially Sr and Ba, display sawtooth-like patterns that record repeated thermal perturbations linked to multistage magma recharge. These patterns are interpreted to reflect partial dissolution of metastable plagioclase during heating, followed by reprecipitation during cooling, which redistributed Sr and Ba within the crystals. Recharge-driven convection also promoted aggregation of megacrysts into the observed macrotextures. Phase-equilibrium modelling indicates crystallization at ~1000 MPa and ~880 °C, whereas diffusion chronometry of garnet inclusions suggests a short magma chamber residence time of ~2 kyr. Thermal-kinetic simulations further show that near-liquidus storage was inherently unstable, and that mafic underplating ($\Delta T > 140$ °C) could rapidly trigger eruption or shallow emplacement. These results identify plagioclase megacrysts as sensitive recorders of pulsed open-system magma transport and reconcile their textural maturity with brief crustal residence.

Key words: plagioclase megacrysts, thermal cycles, magma convection, magma residence time

Acknowledgements This work was financially supported by the National Key Research and Development Project of China (grant 2020YFA0714803 to T.-P. Zhao) and Khalifa University of Science and Technology through the SFU-2024 under Project ID: KU-INT-SFU-2024-8474000697).

PRESSURE-DEPENDENT POTASSIUM INCORPORATION IN DAVEMAOITE

Jingjing Niu[1], Renbiao Tao[1], Qingyang Hu[1], Guoliang Niu[1], and Jintao Zhu[2,3]

1. Center for High Pressure Science & Technology Advanced Research, Beijing 100193, China
2. Institut des Sciences de la Terre d'Orléans, CNRS, France
3. Laboratoire Magmas et Volcans, Universit´e Clermont Auvergne, France

Abstract Potassium (K), a major radiogenic heat-producing element, plays an important role in Earth's thermal evolution, and its geochemical behavior in the lower mantle is controlled by both its storage capacity and incorporation mechanisms in mantle minerals. Davemaoite ($CaSiO_3$ perovskite) has been proposed as a potential host for K due to its relatively large A site, and K-bearing davemaoite has been reported in natural diamond inclusions. Still, its storage capacity and substitution mechanism remain poorly constrained. Here, we investigated K incorporation in Fe-bearing davemaoite using multi-anvil press and laser-heated diamond anvil cell experiments. K incorporation increases systematically with pressure, reaching up to ~0.08 apfu at 85 GPa, corresponding to deep lower-mantle conditions. At lower pressures, K incorporation is dominated by vacancy-related or mixed mechanisms, whereas the stronger near 1:1 K–Fe relationship observed at 85 GPa suggests a greater contribution from Fe-coupled substitution. These results indicate that both the solubility and substitution behavior of K in davemaoite are pressure dependent.

Key words: Davemaoite, Potassium, High pressure, Lower mantle, Substitution mechanism

Acknowledgements This work is supported by the Deep Earth Probe and Mineral Resources Exploration - National Science and Technology Major Project (2025ZD1005505). The authors express thanks to the staff at beamline ID31, High Energy Photon Source.

QUARTZ MICROSTRUCTURES AND DEFORMATION CONDITIONS IN THE JINZHOU–WANFU METAMORPHIC CORE COMPLEX

Dongling Jiang, Junfeng Zhang*, Zhenhua Xue

School of Earth and Planetary Sciences, China University of Geosciences (Wuhan), China

Abstract: Metamorphic core complexes are widely developed in continental extensional settings, and their detachment faults commonly record intense deformation and metamorphism under high-temperature conditions. Quartz, as one of the major constituents of the middle and upper crust, participates in a wide range of geological processes and is therefore a key mineral for investigating crustal deformation and tectonic evolution. Studies of quartz deformation provide an important link between microstructural geology and regional tectonics. Analysis of quartz deformation characteristics and mechanisms can be used to constrain deformation conditions and improve understanding of deformation processes in the middle–upper crust. In this study, the Jinzhou–Wanfu metamorphic core complex was selected as the study area. Gneiss samples were systematically collected from the core to the margin of the detachment fault zone. Quartz microfabrics were investigated by electron backscatter diffraction (EBSD), and deformation temperatures were estimated using the Ti-in-quartz thermometer. The aim was to explore the evolution of quartz crystallographic preferred orientation (CPO) and its relationship with metamorphic conditions. Quartz c-axis fabrics from four representative profiles across the Jinzhou–Wanfu metamorphic core complex reveal a pronounced temperature gradient and significant differences in recrystallization mechanisms from the core of the detachment fault toward its margins. Quartz CPO patterns show a transition from prism <a> slip to rhomb <a> slip, indicating that the deformation fabric evolved spatially under different metamorphic conditions. Trace element analyses of quartz were carried out to determine Ti concentrations in recrystallized grains, and deformation temperatures were calculated using the Ti-in-quartz thermometer. The results show that quartz Ti concentrations increase progressively away from the detachment fault core, indicating an overall increase in deformation temperature from the core toward the margin. These data provide an additional constraint on the relationship between quartz c-axis fabrics and deformation conditions. This study provides new microstructural evidence for the evolution of deformation mechanisms within metamorphic core complexes and offers further insight into intracrustal detachment processes.

Key words: Crystallographic preferred orientation (CPO), Dynamic recrystallization, Detachment fault, Metamorphic core complex, Ti-in-quartz thermometer

SEIFERTITE FORMATION CONDITIONS IN SHOCK-COMPRESSED CRISTOBALITE

Sota Takagi[1,2], Donghoon Kim[2], Sally June Tracy[1]

1. Earth and Planets Laboratory, Carnegie Institution for Science
2. Department of Earth and Environmental Sciences, Korea University

Abstract Seifertite (α-PbO_2-type SiO_2) is an ultrahigh-pressure polymorph found in shocked Martian and lunar meteorites. It is widely invoked as a mineralogical record of hypervelocity impacts, yet the shock pressure at which seifertite nucleates dynamically has never been directly constrained. Pressure estimates inferred from meteorite samples span nearly an order of magnitude (~11 to >85 GPa), reflecting a fundamental ambiguity in applying equilibrium phase boundaries to the dynamic, transient conditions of impact events. We performed laser-driven shock compression experiments on cristobalite (SiO_2) with simultaneous *in situ* X-ray diffraction (XRD) at the Linac Coherent Light Source MEC end-station, probing a pressure range of ~34–81 GPa. Shock pressures were determined by velocity interferometry via impedance matching. We directly observe seifertite formation from cristobalite at shock pressures of 34(4)–44(5) GPa — far below the equilibrium seifertite stability field (>100 GPa). With increasing pressure, seifertite gives way to a d-NiAs-type structure in a transitional pressure range, and stishovite becomes dominant above ~64 GPa. These results provide the first direct experimental calibration of seifertite as a dynamic shock barometer. The quantified 34–44 GPa formation window places firm constraints on the impact pressures and temperatures recorded in silica-bearing planetary materials. Placing these conditions in a geological context, our results support interpretations that seifertite in Martian shergottites (e.g., Shergotty, Zagami) records shock pressures in the range of tens of GPa, and demonstrate that nanosecond-duration shock events are sufficient to drive the cristobalite to seifertite transformation.

Key words: Shock compression, in situ XRD, SiO_2, cristobalite, seifertite

SEISMOLOGICAL IMAGING OF EARTH'S INNER CORE: FROM SURFACE FLOW TO ITS ENIGMATIC CENTRE

Hrvoje Tkalčić

Research School of Earth Sciences, The Australian National University

Abstract Earth's inner core (IC) remains one of the most difficult-to-observe and physically contentious regions of our planet. Despite being sampled by seismic waves for nearly a century, fundamental questions about the stable phase of iron, the nature and origin of its anisotropy, and whether it convects, remain unresolved. I present three interlocking lines of seismological investigation that together span the IC from its outermost shell to its very centre.

First, state-of-the-art Hamiltonian Monte Carlo tomography of the outermost ~100 km of the IC, combined with an independent attenuation quality-factor tomogram, reveals a pattern of velocity and attenuation anomalies more complex than the classical hemispherical dichotomy. The positive correlation between compressional-wave speed and attenuation across the IC surface is interpreted as the seismic expression of thermally driven convection, with the tomograms serving as proxies for the near-surface temperature field that drives present-day flow.

Second, the global coda-correlation wavefield, constructed from the late coda of large earthquakes and exploiting I2* as a counterpart to PKIKPPKIKP and higher order seismic reverberations, provides volumetric sampling of the innermost inner core (IMIC) that is largely insensitive to mantle heterogeneity and source-parameter uncertainties. This methodology reveals that the IMIC hosts the strongest anisotropy in the inner core, with the slow direction of P-wave propagation oriented at ~50–55° from Earth's rotation axis, fundamentally distinct from the outer IC, which has the slowest direction in the equatorial plane, and consistent across independent body-wave and normal-mode studies.

Third, ongoing joint inversion of PKIKP differential travel times within a Bayesian framework that accounts for the systematic underestimation of mantle heterogeneity that biases conventional PKP analyses provides new constraints on the depth-dependence of this anisotropic transition. Critically, the change in anisotropic character between the outer IC and the IMIC emerges as gradational rather than sharp, suggesting a continuous evolution in iron phase, crystal alignment, or composition with depth rather than an abrupt structural boundary.

Together, these observations demand a physically distinct innermost region with a unique fabric. I discuss what these observations require of mineral physics models, and where the seismological and experimental communities most urgently need to converge.

Key words: Earth’s inner core, seismology, body wave, PKIKP, coda-correlation wavefield

SHOCK EFFECTS IN PLAGIOCLASE FROM TWO-STAGE LIGHT GAS GUN EXPERIMENTS

Meng-Hua Zhu[1], Min Ding[2], Yangyu Lu[1], Jie Wang[1], Yingjie Gao[1], Zhicheng Jing[2], Tao Liu[1], Kenan Han[1]

1. State Key Laboratory of Lunar and Planetary Sciences, Macau University of Science and Technology, Macau, China
2. Department of Earth and Space Sciences, Southern University of Science and Technology, Shenzhen, China

Abstract: Impacts are the most fundamental geological processes affecting the surfaces and interiors of terrestrial planets in the inner Solar System. During an impact event, rocks and minerals are subjected to extreme and transient pressures and temperatures, which can produce shock metamorphism, melting, plastic deformation, and partial or complete vaporization. These processes modify mineral structures, textures, and phase relations, generating diagnostic features such as planar deformation structures, high-pressure polymorphs, diaplectic glass, melt products, and vapor-condensed phases. Because minerals can preserve a robust record of the pressure-temperature conditions and energy distribution associated with impact events, even after surface morphologies have been modified or erased, the investigation of shock-induced mineralogical effects provides critical constraints on planetary impact histories.

The two-stage light gas gun (TSLGG) is an effective tool for investigating shock effects in minerals under controlled conditions. We established a TSLGG system capable of launching projectiles 5-30 mm in diameter at velocities of 3-7 km/s hitting target in a cylindrical vacuum chamber (Φ3.0 m × L4.5 m). Although these velocities are lower than the typical impact velocities onto the terrestrial planets (e.g., 15 km/s for Moon's impact), the system can reproduce key characteristics of hypervelocity impacts, like high peak pressures, short loading durations, and rapid pressure release. This enables detailed examination of mineral responses, such as deformation, microfracturing, solid-state phase transformation, melting, and vaporization. Experimental results obtained from the TSLGG system therefore provide valuable calibration for interpreting shocked minerals in meteorites, returned samples, and remote sensing observations, which can also bridge the gap between natural impact observations, numerical simulations.

In this study, we will present new shock experiments on plagioclase, a mineral that is widespread on the lunar surface, and discuss how impact-induced modifications in plagioclase can be used to better understand the formation and evolution of the lunar crust.

Key words: Impact shock effects, Shock metamorphism, Two-stage light gas gun, Plagioclase

Acknowledgements : M. Z. is supported by National Natural Science Foundation of China (42525803) and the Science and Technology Development Fund of Macau (0132/2025/AFJ).

SHOCK-CONSTRAINED EQUATION OF STATE OF MOLTEN IRON INDICATES COMPOSITIONAL GRADIENTS IN THE LOWER OUTER CORE

Youjun Zhang

Institute of Atomic and Molecular Physics, Sichuan University, Chengdu 610065, China

Abstract Earth's outer core is composed of liquid iron with a small fraction of light elements, yet its detailed composition and dynamics remain limited constrained. A key limitation is the lack of an accurate equation of state for molten iron under core conditions. In this work, we remeasured the shock temperature of iron in the liquid state under shock compression. By combining these new measurements with existing data on pressure, density, and sound velocity along comparable shock conditions, we establish a self-consistent thermal equation of state for molten iron at the outer core conditions.

Our results reveal a clear depth dependence in the lower outer core, characterized by an increasing density deficit and a decreasing sound velocity excess with depth. These observations point to a compositionally heterogeneous basal outer core, with a gradient in light-element concentration. This compositional stratification provides strong support for ongoing compositional convection in the liquid outer core, with important implications for its thermal evolution and the geodynamo.

Key words: Earth's core, molten iron, shock compression, light element, geodynamo

SINGLE-CRYSTAL ELASTICITY OF LAWSONITE AT HIGH PRESSURE: IMPLICATIONS FOR HIGH POISSON'S RATIO AND V_P/V_S ZONES IN SUBDUCTION ZONES

Shuo Gao

Synergetic Extreme Condition High-Pressure Science Center, State Key Laboratory of High Pressure and Superhard Materialss, College of Physics, Jilin University, China

Abstract Conventional models attribute anomalously high Poisson's ratios in Earth's interior to the presence of fluids or melts. Here, we propose a fundamentally different mechanism, which is rooted in the unique crystal chemistry of lawsonite ($CaAl_2Si_2O_7(OH)_2 \cdot H_2O$). Our high-pressure experiments reveal anomalous changes in the elastic tensor of lawsonite at ~4 GPa and ~9 GPa, which are linked to phase transitions involving hydrogen-bond reorganization. Compared to typical mantle minerals, lawsonite exhibits moderately low P-wave velocity (V_P) and very low S-wave velocity (V_S). More notably, it is characterized by exceptionally high isotropic aggregate Poisson's ratio (0.32 – 0.38) and V_P/V_S ratio (1.92 – 2.27), which serve as diagnostic identifiers in the interpretation of seismic models. In hot subduction zones, such as Cascadia and Southwest Japan, lawsonite provides a key mineralogical mechanism for the high-Poisson's-ratio anomalies observed at 20 – 50 km depth, presenting a viable explanation distinct from conventional models that invoke overpressured fluid-saturated oceanic crust. In colder subduction systems such as NE Japan, the presence of 20 – 40 vol.% lawsonite can account for the regional-scale seismic anomalies observed at 50 – 90 km depth. Furthermore, we find that the localized ultra-low shear-wave velocity zone at 50 – 60 km depth in oceanic crust is most likely caused by lawsonite enrichment. The seismologically unique signature of lawsonite and its compatibility with seismic models underscore how this mineral could have a critical role in facilitating water transport into the deep mantle.

Key words: lawsonite, hydrogen bonding, elastic properties, hydrous minerals

SOLIDIFICATION OF A PROTO MAGMA OCEAN MODEL AND ITS IMPLICATIONS FOR THE ORIGIN OF LARGE LOW VELOCITY PROVINCES

Wenjie Wu, Kun Yin

State Key Laboratory of Geohazard Prevention and Geoenvironment Protection, College of Earth and Planetary Sciences, Chengdu University of Technology, China

Abstract The thermochemical differentiation of the early magma ocean shaped the composition and structure of Earth's interior. However, how this differentiation led to the large-scale seismic velocity anomalies observed in the present-day deep mantle remains unclear. By modeling the phase relations in a pyrolitic lithology composed of three prototypical lower-mantle mineral components (MgO–$MgSiO_3$–$CaSiO_3$), combined with seismic shear-wave velocity anomaly inversion, this study reveals that the origin of the large low velocity provinces (LLVP) is closely linked to the solidification process of the magma ocean. The systematic compositional difference between the solidus and liquidus in the model results in a final residual basal melt layer that is relatively enriched in $CaSiO_3$ and depleted in $MgSiO_3$. Critically, using the maximum likelihood estimation (MLE) method to invert the velocity and density anomalies of LLVP, and incorporating the effects of iron, the proportions of the three main lower-mantle minerals are quantitatively constrained. The resulting mineral proportions are highly consistent with the aforementioned solidus composition predicted by the ternary system composed solely of the three pure end-members. This consistency indicates that upon fractional crystallization, the seismic and volumetric properties of the basal melt layer are in excellent agreement with the observed characteristics of present-day LLVP. Consequently, the basal melt layer most likely served as the key material source or precursor of the LLVP. The primordial origin of such large-scale heterogeneities implies that certain portions of the mantle may have remained remarkably inactive with respect to solid-state convection induced by slab subduction and mantle plume upwelling, and have survived to the present day due to their unique compositional and rheological properties. This study establishes a unified petrogenetic model connecting the evolution of the early magma ocean with the most prominent seismic heterogeneous structures in the deep mantle, and provides new physical constraints on the thermochemical evolution of Earth's interior and the long-term stability of mantle heterogeneities.

Key words: magma ocean, fractional crystallization, LLVP, lower mantle, thermochemical differentiation

SOUND VELOCITY AND MELTING OF DAVEMAOITE UNDER SHOCK COMPRESSION

Ye Wu [1], Xun Liu [1], Haijun Huang [1], and Yingwei Fei [2]

1 School of Physics and Mechanics, Wuhan University of Technology, Wuhan, Hubei 430070, China

2 Earth and Planets Laboratory, Carnegie Institution for Science, Washington, DC 20015, USA

Abstract Davemaoite, as the third most abundant mineral in the lower mantle, constitutes significant amounts in pyrolite and mid-ocean ridge basalts mantle compositions. Its physical properties are essential to constrain the compositions and mineralogical models of the lower mantle. Because of its unquenchable nature, measurements by static compression techniques on its physical properties under lower mantle conditions are technically challenging. Here, we report Hugoniot equation of state, sound velocity and shock temperature of $CaSiO_3$ glass obtained by shock-wave experiments. $CaSiO_3$ glass transforms into davemaoite above ~80 GPa under shock compression. Davemaoite has lower longitudinal sound velocity than other major minerals in the lower mantle, providing the critical experimental data to model the sound velocity at the base of the lower mantle. Davemaoite melts above 4500 K at 110 GPa, which is lower than melting curves predicted by theoretical calculations. The measured sound velocity and melting temperature of davemaoite are significant for understanding the origin of large low-shear-velocity provinces above the core-mantle boundary and the evolution of early magma ocean in the deep Earth's interior.

Key words: davemaoite, Hugoniot equation of state, sound velocity, melting, shock compression

SOUND VELOCITY MEASUREMENT OF IRON ALLOYS AT HIGH PRESSURE AND TEMPERATURE AND ITS APPLICATION TO THE EARTH'S INNER CORE

Eiji Ohtani[1], Daijo Ikuta[2], Tatsuya Sakamaki[1], Hiroshi Fukui[3], Daisuke Ishikawa[4], Alfred Q.R. Baron[4]

1. Department of Earth Science, Tohoku University, Sendai, Miyagi 980-8578, Japan.
2. Institute for Planetary Materials, Okayama University, Misasa, Tottori 682-0193, Japan.
3. Japan Synchrotron Radiation Research Institute, Sayo, Hyogo 679-5198, Japan.
4. Materials Dynamics Laboratory, RIKEN SPring-8 Center, Sayo, Hyogo 679-5148, Japan.

Abstract The earth's core is one of frontier of the Earth Science. Previous experimental and theoretical studies indicated that the Earth's core is less dense compared to pure iron which is called the core density deficit, suggesting the core contains light elements. Several light elements such as silicon, sulfur, hydrogen, oxygen, and carbon have been suggested as the candidates of the light elements in the core.

The seismic velocity is the most accurate property determined by seismology, whereas density is less reliable compared to seismic velocity. Therefore, measurement of the sound velocity of iron compounds is essential for better understanding the earth's core. In spite of the importance, measurements of the sound velocity under the core conditions are limited to date due to technical difficulties. We have conducted Inelastic X-ray scattering experiments at high pressure and temperature to determine the compressional velocity of the earth's core materials. We extended our sound velocity measurements to the core pressures and high temperature by using the diamond anvil cell combined with synchrotron X-ray at the beamline BL43LXU of Spring-8. We developed a newly designed optical system, Soller screen, to improve S/N ratio of the IXS signal of the experiments. These improvements allowed us to successfully measure the compressional velocity of hcp-Fe pressures exceeding 300 GPa and at ambient temperatures. Additionally, we developed a portable laser heating system (COMPAT) for high-temperature generation at high pressure, and measured the compressional velocity of hcp-$Fe_{0.94}Ni_{0.06}$ alloy at temperatures exceeding 2500 K and high pressures to 205 GPa.

We measured the compressional velocity of pure Fe, $Fe_{0.94}Ni_{0.06}$, and $Fe_{0.84}Ni_{0.08}Si_{0.08}$ alloys with a hcp structure, and B2-$Fe_{0.68}Ni_{0.06}Si_{0.26}$ with a B2 (ordered bcc) structure to the core conditions by using the procedures described above. We found a linear relationship between compressional velocity and density, i.e., the Birch's law, at high pressure and temperature for these iron alloys. The density dependency of the compressional velocity, i.e., the slope of the Birch's law, is similar in all of these alloys and greater than that of the PREM inner core. We found the temperature dependency of the Birch's law for B2-$Fe_{0.68}Ni_{0.06}Si_{0.26}$ alloy is negligibly small, similar to bcc-Fe, fcc-$Fe_{0.8}Ni_{0.2}$, and B20-

FeSi alloys. Based on the measurements of the compressional velocity and density, we extrapolated the properties to the inner core conditions, and derived compositional models of the inner core which can explain the compressional velocity and density of the PREM inner core. Our analysis suggests that the compressional velocity and density of the PREM inner core can be explained by the iron-nickel-silicon alloy and a small amount of sulfur or hydrogen compounds which reduces both the sound velocity (v_p and v_s) and density under the inner core conditions.

Key words: Sound velocity, Inelastic x-ray scattering, inner core, high pressure, high temperature

Acknowledgements This study was supported by the JSPS KAKENHI Grant Number JP15H05748, JP20H00187, JP24K00722 (E.O.), Number JP24K00734 (D.Ik.), J-PEAKS Grant Number JPJS00420230010 (D.Ik.), and RIKEN SPring-8 Center (A.Q.R.B.). The synchrotron x-ray experiments were performed at the RIKEN SPring-8 Center at BL43LXU (proposal No. 2023011, 2023012, 2023013, 2024022, 2024023, 20250030, 20250035, 20250036).

SPIN TRANSITION AND MELT CURVE IN MG-FE-O SYSTEM STUDIED WITH LASER-DRIVEN SHOCK COMPRESSION

Carolina Camarda[1,2], Karen Appel[1], Khachiwan Buakor[1,3], Celine Crepisson[4], Marion Harmand[5], Alexis Amoureti[6], Lea Pennacchioni[7], Melanie J. Sieber[8], Christian Sternemann[2] on behalf of the DiPOLE Community (proposal 6656)

1. European X-ray Free Electron Laser (Eu.XFEL), Germany
2. Technische Universität Dortmund, Germany
3. Rostock University, Germany
4. University of Oxford, United Kingdom
5. Processes and Engineering in Mechanics and Materials (PIMM), France
6. SACLA-Japanese XFEL, Japan
7. Potsdam University, Germany
8. Technische Universität Berlin, Germany

Abstract Ferropericlase ((Mg,Fe)O) is the second most abundant mineral in Earth's lower mantle and is expected to be a crucial component in the mantles of Super-Earth rocky exoplanets, playing a central role in controlling their physical and chemical properties. The electronic spin state under extreme pressure–temperature (P-T) conditions of ferropericlase directly influences density, structure, and elasticity of the mantle creating some anomalies in the chemical and seismic properties.

In this study, we investigate the behavior Mg-Fe-O system under conditions of Earth's core-mantle boundary and outer core using laser-driven shock compression experiments. These conditions correspond to depths of ~2,800 km and 4,500 km within pressures about 135 GPa and 300 GPa, respectively. Experiments were conducted at the High Energy Density instrument at the European XFEL within the scope of DiPOLE community proposals. Time-resolved, in situ diagnostics were achieved using synchronized femtosecond X-ray pulses before and after laser drive, enabling direct comparison between ambient and shocked states. We combined X-ray diffraction (XRD), X-ray emission spectroscopy (XES), and Velocity Interferometer System for Any Reflector (VISAR) measurements to simultaneously constrain structural, electronic, and thermodynamic properties. Shock temperature was calculated using the Durvall-Graham approximation from the energy conservation equation of Rankine-Hugoniot.

XES measurements, performed using a von Hámos spectrometer, reveal a clear spin transition through characteristic spectral changes: a shift of the $K\beta_{1,3}$ peak toward lower energy and broadening of the $K\beta'$ satellite. To extract quantitative information from the spectral variation, we applied common analysis such as integrated absolute difference and $K\beta_{1,3}$ first momentum which confirm the pressure-induced spin crossover. XRD data show a shift of Bragg peaks to higher scattering vector under compression along the Hugoniot, allowing the determination of density and unit cell evolution.

Our results show that the spin crossover begins above ~45±09 GPa, consistent with a progressive high-spin to low-spin transition and is accompanied by changes in electronic structure and compressibility. Melting initiates at ~249±24 GPa/ ~7150K and coexists with solids. Sample was fully molten above ~348±30 GPa/ 9500K.

The combined results highlight key implications for deep Earth processes. The reduction in ionic radius associated with the spin transition promotes Fe partitioning into melts, as Fe becomes incompatible in ferropericlase, leading to Fe-rich liquids and Mg-rich residual solids. This behavior affects mantle mixing, seismic velocities, and rheology, challenging simplified geophysical models that overlooked spin transitions and compositional variability.

Overall, this work provides new experimental constraints on the coupled electronic, structural, and melting behavior of Mg-Fe-O system under extreme conditions along the Hugoniot, helping us understand the electronic changes in the Earth environment, as well as the melt curve in rocky exoplanets, which can also be useful to understand the early Earth evolution.

Key words: Mg-Fe-O system, shock compression, Hugoniot

Acknowledgment We acknowledge the European XFEL in Schenefeld, Germany, for provision of X-ray free electron laser beamtime at the Scientific Instrument HED (High Energy Density Science) and would like to thank the staff of European XFEL and DESY for their assistance. The authors are indebted to the HIBEF user consortium for the provision of Instrumentation and staff that enabled this experiment as well as Dominik Krauss (PI) and Thomas R. Preston (MP) for community proposal 6656. We thank the Deutsche Forschungsgemeinschaft (DFG, German Research Foundation) – PN: 521549147 / Grant: AP262/3-1, STE 1079/10-1 under Germany's Priority Programme "Reconstructing the deep dynamics of planet Earth over geologic time (DeepDyn)" SPP2404 – 500707704.

STABILITY OF AL-BEARING HYDROUS MAGNESIUM PHASES AND SOLUBILITY OF H_2O IN NOMINALLY ANHYDROUS MINERALS AND HYDROUS MAGMAS UNDER CONDITIONS OF THE MANTLE TRANSITION ZONE AND THE UPPERMOST LOWER MANTLE

Toru Inoue

Department of Earth and Planetary Systems Science, Hiroshima University, Japan

Abstract Water (H_2O) is one of the most abundant volatile components on Earth. Its presence in the deep interior of the Earth significantly influences the properties of minerals and mantle dynamics. The discovery of hydrous ringwoodite (Mg_2SiO_4) and phase egg ($AlSiO_3(OH)$) in diamonds originating from the mantle transition zone (MTZ) strongly supports the presence of water in the Earth's deep interior (Pearson et al., 2014; Wirth et al., 2007). Since phase egg is a high-pressure, hydrous mineral formed by the hydration of aluminum-rich crustal material under MTZ conditions, its presence suggests that crustal material is subduction into the MTZ.

High-pressure hydrous minerals form under low-temperature and/or high H_2O content conditions. Extensive research has been conducted on the stability of these minerals in hydrous peridotite, hydrous basalt, and hydrous sedimentary rock compositions. Our group is currently conducting experimental research focusing on the importance of mantle-crust interactions. In hydrous peridotite, various dense hydrous magnesium silicates (DHMS) form; however, their temperature stability is lower than that of the mantle geotherm. Conversely, hydrous aluminosilicates appear in hydrous sedimentary rocks, and their temperature stability exceeds that of the mantle geotherm. Therefore, elucidating the influence of these interactions on temperature stability is of the utmost importance.

When the water content within the system is low, the water is incorporated into nominally anhydrous minerals (NAMs). The high-pressure polymorphs of olivine, wadsleyite, and ringwoodite are classified as NAMs; however, it is known that these minerals can retain up to 3 wt% of water in their crystal structures (e.g., Inoue et al., 1995). Under high-temperature conditions where a liquid phase coexists, a clear temperature dependence is observed in the water content of these minerals. However, researchers disagree about the conditions under which hydrous minerals coexist at low temperatures. Our group is working to elucidate the cause of this disagreement.

Furthermore, when H_2O is not retained in NAMs or hydrous minerals, it is released as a fluid through dehydration reactions, which lead to the formation of hydrous magma. Although the water content of magma formed under high pressure is thought to depend strongly on temperature, systematic data are scarce. Our group has been conducting studies to determine the water content of magma generated under high-temperature, high-pressure conditions.

In this presentation, I will introduce our group's recent findings on the above topics. Through these findings, I aim to understand the storage patterns and transport processes of H_2O in the Earth's deep interior to elucidate mantle evolution and deep material cycling.

Key words: deep Earth water, hydrous phase, hydrous magma, mantle transition zone, water transportation

Acknowledgements The author gratefully acknowledges the contributions of students at Hiroshima University to high-pressure experiments, data analysis, and other aspects of this study. This work was supported by the Joint Usage/Research Center PRIUS, Ehime University, Japan.

STRONG TIDAL DISSIPATION IN SUPER-EARTH TRIGGERED BY THE WEAK EXTRATERRESTRIAL MANTLE

Bowen Chen, Wenzhong Wang and Zhongqing Wu

School of Earth and Space Sciences, University of Science and Technology of China, China

Abstract Tidal dissipation is a fundamental process that distinguishes many close-in rocky exoplanets from our Earth. As a dominant internal heat source, it profoundly reorganizes the planetary thermal evolution and thereby shapes long-term habitability. The efficiency of tidal dissipation depends not only on the planetary orbital parameters, but also on the viscosity and shear modulus of planetary materials, which remain poorly constrained under super-Earth mantle conditions. Here, we use first-principles calculations to determine the viscoelastic properties of three major mantle minerals relevant to super-Earth interiors: post-perovskite $MgSiO_3$, I-42d-type Mg_2SiO_4, and $P2_1/c$-type $MgSi_2O_5$. We find that, rather than monotonically increasing stiffness with depth, super-Earth mantles may instead experience multiple reductions on viscosity associated with mineral phase transitions, leading to the formation of several rheologically weak layers. The presence of these weak layers can substantially enhance tidal dissipation. For a modest orbital eccentricity of 0.01, tidal heating becomes comparable to radiogenic heating at an orbital period of ~10 days, and can reach Io surface heat fluxes at ~5 days. Such intense tidal heating can strongly enhance the volatile degassing from the deep interior and reshape the planetary surface tectonics, especially for planets orbiting M-dwarfs, whose close-in habitable zones amplify tidal forcing.

Key words: super-Earth, tidal dissipation, viscosity, elasticity, habitability

STRUCTURAL BEHAVIOR OF NATURAL LUDWIGITE UNDER HIGH PRESSURE: AN ANALOG OF BO_3 COORDINATION AT DEPTH

Xinxin Gao[1,2], Zhi Zheng[1], Jing Gao[1], Hao Yan[1]

1. Institute of Deep-sea Science and Engineering, Chinese Academy of Sciences, China
2. University of Chinese Academy of Sciences, Beijing, China

Abstract The migration of volatile elements and their isotopes is fundamental to understanding crust-mantle interactions, fluid evolution, and magma genesis. Boron is an effective tracer of fluid-rock interactions in subduction zones and of deep-mantle recycling. Its compatibility with minerals, and hence its isotopic fractionation, are both controlled by crystal-chemical defects. However, in situ characterization of boron in deep Earth minerals remains challenging due to its low abundance, low atomic mass, and volatility, limiting our understanding of boron deep cycling and isotopic behavior. To address this, ludwigite (Mg_2FeBO_5), a major natural boron reservoir commonly associated with peridotite, serves as an ideal analog for high-pressure investigations. Its high boron concentration and typical trigonal-planar BO_3 coordination environment make it particularly suitable for probing boron behavior under extreme conditions. In this study, the structural behavior of natural ludwigite was investigated using in situ high-pressure synchrotron powder X-ray diffraction in diamond anvil cells, using a 4:1 methanol-ethanol mixture as the hydrostatic pressure medium up to 10 GPa. Major element compositions were determined by electron probe microanalysis (EPMA). Chemical analyses showed MgO = 36.1–37.9 wt.%, FeO (total) = 40.1–41.8 wt.%, Al_2O_3 = 1.3–1.9 wt.%, B_2O_3 = 16.7–22.1 wt.%, and MnO = 0.4–0.5 wt.%. No structural phase transition was observed in the investigated pressure range. Pressure-volume data were fitted with a third-order Birch-Murnaghan equation of state, giving a bulk modulus B_0 = 183 GPa and a pressure derivative B'_0 = 4.1. The compressional behavior of ludwigite is anisotropic, with the *c* axis more compressible than the *a* and *b* axes. The rigid BO_3 trigonal planar units lie parallel to the ab plane, resisting compression along the *a* and *b* axes. Consequently, structural strain is primarily accommodated by distortion of the octahedral sites along the *c* axis. These results provide experimental constraints on the compressibility of natural ludwigite and support its potential role as a boron host phase in cold subducting slabs. Furthermore, they indicate that the BO_3 trigonal planar configuration, which favors the heavy ^{11}B, could remain highly stable under high pressure.

Key words: ludwigite, borate, boron reservoir, diamond anvil cell, deep mantle

Acknowledgements The authors would like to thank the financial support from Deep Earth Probe and Mineral Resources Exploration – National Science and Technology Major Project 2025ZD1005100. We thank the Shanghai Synchrotron Radiation Facility of BL15U1 for assistance

on synchrotron radiation X-ray diffraction measurements. We are grateful to Professor I-Ming Chou, Nanfei Cheng, Haiyan Zhang, and Junwei Li at IDSSE for their help in the ongoing follow-up work. We also thank Qijing Chen at IDSSE for her technical assistance with EPMA measurements.

SUPERIONIC H-SI-N-O COMPOUNDS AND TRANSITION ZONES IN ICE GIANT INTERIORS

Shidong Yu[1,2], Shichuan Sun[1], Simon A. T. Redfern[1,2*]

1. Asian School of the Environment, Nanyang Technological University, 50 Nanyang Avenue, Singapore 639798
2. School of Materials Science and Engineering, Nanyang Technological University, 50 Nanyang Avenue, Singapore 639798

Abstract About one third of known exoplanets resemble Uranus and Neptune, with icy mantles overlying rocky cores. Whether such planets possess sharp core-mantle boundaries or gradual 'fuzzy' transition zones depends on the miscibility of mantle ices and core silicates, yet the H-Si-N-O system had not been explored at the relevant conditions. Using ab initio random structure searching combined with density functional theory, we map the H-Si-N-O chemical space from 100 to 700 GPa and identify three thermodynamically stable compounds: HSiNO, H_4SiN_2O and H_2SiN_2. All three are built from corner-, edge- and face-sharing $Si(N,O)_6$ octahedra with hydrogen bonded to nitrogen, and their compositions lie on a balanced-redox plane connecting NH_3, H_2O, SiO_2 and Si_3N_4, demonstrating that they form by redox-conserving reactions between simple planetary ices and silicates. Ab initio molecular dynamics show that all three become superionic across much of the transition-zone window (4000 to 6000 K, 270 to 550 GPa), with protonic conductivities reaching about 54 S/cm. Their intermediate densities bridge the gap between icy-mantle and rocky-core materials, generating a natural compositional and density gradient running from NH_3 and H_2O through H_4SiN_2O, H_2SiN_2 and HSiNO toward SiO_2. Such a stratified, conductive transition zone can suppress convection, helping to explain the anomalously low luminosity of Uranus, and can host the conductive layer required to generate the eccentric, non-dipolar magnetic fields of both planets.

Key words: Superionic, High-pressure , Ice giant interiors, Crystal structure ,H-Si-N-O system

SUPERIONIC TRANSITON AND ITS EFFECTS IN EARTH'S DEEP LOWER MANTLE

Yu He[1,2,3]

1. State Key Laboratory of Critical Mineral Research and Exploration, Institute of Geochemistry, Chinese Academy of Sciences, Guiyang 550081, China
2. Key Laboratory of High-Temperature and High-Pressure Study of the Earth's Interior, Institute of Geochemistry, Chinese Academy of Sciences, Guiyang 550081, Guizhou, China
3. Center for High Pressure Science and Technology Advanced Research, Shanghai 201203, China.

Abstract The superionic state lies between the liquid and solid states. Under thermal excitation, superionic materials contain a large number of vacancy and interstitial defects, which facilitate ion transport and endow such materials with high ionic conductivity. The presence of defects and vacancies also leads to properties such as elastic softening and superior structural stability. Owing to these unique characteristics, superionic materials have become a research frontier in the exploration of Earth's interior. Recently, researchers have predicted the precence of hydrous phases, iron-hydrogen alloy, and oxygen-vacancy Davemaonite in the deep lower mantle through theoretical calculations. The special properties of superionic materials in the lower mantle offer new insights into deep water cycling, deep lower mantle heterogeneity and core-mantle interactions.

Key words: Superionic transition, ionic conductivity, lower mantle, deep water cycling

SUPERIONICITY IN THE DEEP INTERIOR OF ROCKY PLANETS

Zifan Wang[1], Yu He[2], Ho-kwang Mao[1,3], Duck Young Kim[1]

1. Center for High Pressure Science & Technology Advanced Research, Shanghai, China
2. Institute of Geochemistry, Chinese of Academy of Sciences, Guizhou, China
3. Institute for Shanghai Advanced Research in Physical Sciences (SHARPS), Shanghai, China

Abstract First-principles calculations and large-scale computational modeling have become essential tools for investigating novel phases of matter under extreme conditions of pressure and temperature. In regions that are difficult to probe experimentally, predictive calculations of material structures and properties, combined with subsequent experimental verification, provide a powerful framework for understanding Earth's deep interior. In this talk, I will present our recent studies on the possible emergence of superionic states in the deep interiors of Earth and other terrestrial planets. I will show how superionic phases predicted computationally have been validated experimentally, and highlight electride formation at ultrahigh pressure as a key mechanism promoting light-element diffusion. I will further discuss superionic behavior in light-element-bearing and oxygen-deficient minerals relevant to Earth's interior, and its geophysical implications for planetary interior structure and evolution.

Key words: Superionicity, Structure prediction, Computational, High Presure, planetary sciences

THE EFFECT OF GRAIN SIZE AND DISTRIBUTION ON THE ACOUSTIC VELOCITIES OF POLYCRYSTALLINE $MgSiO_3$ BRIDGMANITE

Cheng Qian[1], Alexander Kurnosov[2], Lianjie Man[3], Johannes Buchen[2], Tiziana Boffa Ballaran[2], Xiang Wu[1], and Daniel J. Frost[2]

1. State Key Laboratory of Geological Processes and Mineral Resources, China University of Geosiences (Wuhan), China
2. Bayerisches Geoinstitut, University of Bayreuth, Germany
3. Department of Earth and Planetary Sciences, ETH Zurich, Switzerland

Abstract It is widely accepted that bridgmanite is a primary mineral constituent of the Earth's lower mantle. Consequently, a thorough understanding of its elastic properties under relevant pressure–temperature conditions is essential for interpreting seismic observations and constraining the structure of the deep Earth. Criniti et al. (2021) measured the acoustic velocities of single–crystal $MgSiO_3$ bridgmanite up to 80 GPa at room temperature, providing constraints on the pressure dependence of seismic signature of bridgmanite at lower–mantle pressures, the results diverge significantly from those obtained on polycrystalline samples. While this study provided a reliable high-pressure reference for the seismic signature of this important mineral at lower–mantle pressures, the results differ significantly from those obtained from measurements on polycrystalline samples. The origins of these discrepancies remain debated.

In this study, we report Brillouin spectroscopy and X–ray diffraction measurements conducted on polycrystalline $MgSiO_3$ bridgmanite samples with varying average grain sizes. The samples were synthesized using a 1200–ton multi–anvil press at 24 GPa and at different temperatures to control the grain growth of bridgmanite. The recovered samples were polished into thin platelets (~15 μm thick) and subsequently shaped into circular disks using focused ion beam. High–pressure X–ray diffraction (XRD) and Brillouin spectroscopy measurements were conducted so far up to 35 GPa at room temperature using a diamond anvil cell with helium as pressure–transmitting medium. Our results demonstrate that the measured acoustic wave velocities depend strongly both on the grain size of the polycrystalline sample and on the orientational distribution. By comparing our data with the range of velocities expected for up to 10,000 randomly oriented grains, we infer that the acoustic velocities of polycrystalline bridgmanite are likely influenced by grain–boundary effects and preferred orientation, which may affect the Brillouin scattering signal.

Key words: Bridgmanite, Elasticity, Brillouin spectroscopy, Polycrystalline, High pressure

THE ELASTICITY OF NEW HYDROUS $MgSiO_4H_2$ PHASES AT DEEP EARTH CONDITIONS

Jiajun Jiang[1] and Taku Tsuchiya[1]

4. Geodynamics Research Center, PIAS, Ehime University, 2–5 Bunkyo-cho, Matsuyama, Ehime 790-8577, Japan

Abstract: Deep water circulation within the Earth not only controls the distribution of water in the deep mantle but also plays a fundamental role in the long-term evolution of planetary habitability. Dense hydrous magnesium silicates (DHMSs) are considered as the key carriers in this deep water cycle, transporting water into the deep mantle via subducting slabs. Of the DHMS, phase H ($MgSiO_4H_2$) has been demonstrated to be stable up to mid-lower mantle conditions (up to ~60 GPa and ~1600 K) as a dissociation product of phase D (Nishi et al., 2014; Ohtani et al., 2014; Tsuchiya, 2013; Walter et al., 2015). Consequently, the existence of phase H in cold slabs is pivotal for water cycling in the deeper part of the lower mantle. Despite extensive efforts have been devoted to investigating the properties of phase H, two new hydrous $MgSiO_4H_2$ polymorphs with $P2_1/c$ symmetry, denoted as α-and β-$MgSiO_4H_2$, were recently predicted using advanced structure search methods (Shao et al., 2024), which has significantly lower energies than the originally proposed P2/m structure (Tsuchiya, 2013; Nishi et al., 2014; Bindi et al., 2014;). Although phase H was suggested to exhibit strong elastic anisotropy (Song et al., 2022), the elasticity of these newly predicted phases remains poorly constrained. Here we first report elastic properties of α-and β-$MgSiO_4H_2$ under low mantle pressure using first-principles calculations. Our results show that whereas the sound velocities (V_P and V_S) of α-$MgSiO_4H_2$ are nearly indistinguishable from those of the $P2/m$ phase, both α- and β-$MgSiO_4H_2$ show significantly weaker elastic anisotropy under lower mantle pressure. This unexpected behavior can be reconciled by differences in the hydrogen bond configurations, in particular no hydrogen bond symmetrization in the α and β phases, and connectivity of MO_6 (M=Mg, Si) octahedron networks in these two structures. Several studies have discussed the seismologically observed anisotropy associated with the elastic anisotropy of Phase H (Nowacki et al., 2015; Song et al., 2022). However, the interpretations should be revised based on the elasticity of new $MgSiO_4H_2$ phases.

Key words: Hydrous phase, Elasticity, Anisotropy, Earth's mantle, First-principle

THE ELECTRONIC, MAGNETIC, AND STRUCTURAL PROPERTIES OF FEO UP TO CORE CONDITIONS

Xiang Li

European Synchrotron Radiation Facility - 71, avenue des Martyrs, 38043 Grenoble Cedex 9, France.

Abstract Iron oxides are important materials for geoscience but also for basic science and applied technologies. Iron monoxide (Fe_xO) is a fundamental component of the Earth's interior as the iron endmember of ferropericlase (Mg,Fe)O–the second most abundant mineral in the lower mantle. Moreover, oxygen is considered as an important light element in Earth's outer core. The stability and high-pressure properties of Fe_xO could, thus, determine its potential role in processes in Earth and planetary interiors.

Fe_xO has the NaCl (B1) structure at ambient pressure and temperature and transforms into the rhombohedral distorted-B1 phase (rB1) at about 16 GPa, which correlates with a transition from the paramagnetic state to the state with the antiferromagnetic order. A further transition from a rhombohedral rB1 phase to a hexagonal B8 phase has been proposed at 74 GPa and 900 K. Although numerous studies were focused on the investigation of the electronic and magnetic properties and phase diagram of Fe_xO, information on the magnetic and structural coupling of Fe_xO at high pressures and high temperatures is very limited.

I will present our investigation on the pressure dependence of the electronic, magnetic and structural properties of Fe_xO by means of Synchrotron Mössbauer Source spectroscopy and Single-Crystal X-ray diffraction in laser-heated diamond anvil cells up to 220 GPa and 3000 K. I will particularly discuss the electronic, magnetic and structural properties of Fe_xO and their potential role in the mineralogy, chemistry, and physics of the Earth's core.

Key words: FeO, oxygen in Earth's core

THE INCORPORATION AND EFFECTS OF CHROMIUM IN THE GARNET LATTICE: INSIGHTS INTO OXYGEN ISOTOPE EQUILIBRIUM FRACTIONATION

Jiling Zhou, Yu Ye, Erqiao Liu

State Key Laboratory of Geological Processes and Mineral Resources,

China University of Geosciences, China

Abstract Chroumium, as a critical strategic resource, mainly exits in nature as chromite, and tis application in alloys highlights its economic and national defense value. As an important host for chromium in the Earth's deep interior, garnet-group minerals are among the dominant silicate minerals in the upper mantle, mantle transition zone, and uppermost lower mantle (above 700 km depth). In particular, Cr-bearing pyrope is one of the most common mineral inclusions in peridotitic diamonds, providing key constraints for revealing the physiochemical conditions of diamond formation. The chemical composition of mantle garnet varies with pressure, making garnet a vital indicator mineral for estimation diamond formation depths. Previous geochemical studies of kimberlites have shown that some Cr-rich garnets are associated with diamonds and typically exhibit high Cr, Mg, low Ca, and low ^{18}O signatures. Therefore, investigating the enrichment mechanism of chromium in the Earth's interior uding garnet as a carrier is of great significance for understanding deep geochemical characteristics, diamond formation mechanisms, and choromite genesis.

In this study, three Cr-bearing garnet were synthesized using a multi-anvil press: uvarovite (Uvr_{100}), uvarovite-knoringite solid solution ($Uvr_{59}Knr_{41}$), and knorringite (Knr_{100}). Based on Raman spectroscopic measurements data, the isobaric (γ_{iP}) and isothermal (γ_{iT}) Grüneisen parameters, anharmonic parameters, and oxygen isotope ($^{18}O/^{16}O$) fractionation factors (β factors) of the three garnets at high temperatures were calculated. The main results are as follows: (1) Garnet composition and temperature exert significant effects on oxygen isotope fractionation. Among the three synthesized garnet solid solutions, the $10^3 \cdot \ln\beta$ value increases gradually with the rise of Mg^{2+} content. Compared with grossular (Grs_{100}), Uvr_{100} significantly reduces oxygen isotope fractionation in garnet, suggesting that the presence of Cr lowers the ^{18}O composition of garnet. Under isothermal conditions, garnet exhibits a geochemical signature of high Mg and low ^{18}O, consistent with previous work. (2) After anharmonic correction, the Cr effect on oxygen isotope fractionation in the garnet due to Cr^{3+} substitution for Al^{3+} was quantified. Each 1 mol.% increase in $X_{Uvarovite}$ reduces the $10^3 \cdot \ln\beta_{garnet}$ of the uvarovite-knoringite solid solution by 0.16 ‰ at 300 K and by 0.009 ‰ at 1500 K.

This study investigates the behavior of oxygen isotope equilibrium fractionation in the garnet and constrains the chromium effect on oxygen isotope equilibrium fractionation in garnet. It provides a valuable model for understanding chromium enrichment in the deep mantle and its influence on mineral properities, and also offers high temperature and high pressure experimental constraints for

interpreting the geochemical characteristics of garnets in diamond paragenesis. Combined with previous studies, we find that Cr substitution leads to the most significant reduction in the garnet oxygen isotope fractionation $\beta(T)$ factor. This provides a reasonable explanation for the low ^{18}O signature of Cr-rich garnets in damond paragenesis, which is mainly caused by their high chromium content.

Key words: Chromium, Garnet, Oxygen Isotope Equilibrium Fractionation

Acknowledgements This study was supported by the National Natural Science Foundation of China (Grant No. 42472061)

THE ORIGIN AND FORMATION ENVIRONMENT OF DIAMOND SPHERULITES INFERRED FROM PRIMARY INCLUSIONS

Hiroaki Ohfuji[1], Kouga Kanai[2]

1. Department of Earth and Planetary Science, Graduate School of Science, The University of Tokyo, Japan
2. Department of Earth Scinece, Graduate School of Science, Tohoku University, Japan

Abstract Some mantle-derived diamonds exhibit a spherulitic polycrystalline texture, consisting of needle-like crystals extending radially from the center, commonly referred to as “ballas”. Recent studies suggest that ballas represents an end-member variety of “coated diamonds” and that its crystallization occurs under extremely high driving forces. However, its origin and formation environment in the mantle remain unclear. In this study, we investigated primary inclusions in ballas diamonds through detailed SEM-TEM observations to gain insights into their formation environments.

We used ballas diamonds of 5-6 mm in diameter from Africa, which were laser-cut prior to polishing. Polished cross-sections were prepared by conventional mechanical polishing and also by Ar ion milling. Orientation contrast and CL imaging showed two-layered structure consisting of a relatively fine-grained, radiating fibrous crystals (bight in CL) in the interior, and coarser columnar crystals (dark in CL) in the rim, suggesting that they grew under different environments during early and late growth stages. SEM-EDS analysis revealed that spherulites often contain micro-inclusions that exhibit clearly different physicochemical features between the interior and the rim. In the interior, the inclusions exclusively occur as negative crystals raging from a few to several micrometers, and are commonly accompanied by daughter crystals of silicates (mostly phlogopite) and small voids, interpreted as traces of volatile components, in which fluid-mobile elements such as Ba and Cl were detected by EDS. On the other hand, the rim part contains elongated voids of tens to a hundred of micrometers in length, developed along the elongated growth of columnar diamond crystals. These inclusions are, in most cases, voids containing only a very small amount of precipitates composed mainly of Al and Si, and the void spaces are likely filled with CH4 and/or H2O as indicated by micro-Raman spectroscopy.

These results suggest that diamond spherulites were formed in a silicate melt containing a small amount of volatile components, and subsequently experienced significant overgrowth in a C–H–O fluid during the late stage. The ubiquitous occurrence of phlogopite in the inner inclusions implies that the formation depth was not extremely deep, but rather near the base of a thick lithospheric mantle where most single-crystalline diamonds are thought to form. The formation of diamond spherulites likely occurred in a carbon-supersaturated silicate melt generated through fluid-mediated metasomatic reaction between crustal and the mantle materials.

Key words: Diamond, C-H-O fluid, Inclusion

THE STABILITY OF A NEWLY DISCOVERED $CASIC_2O_7$ SILICATE-CARBONATE REACTING WITH EARTH'S LOWER MANTLE MINERALS

T. Tsuchiya, M. Isobe

Geodynamics Research Center, PIAS, Ehime University, Japan

Abstract The deep carbon cycle and carbon reservoir in the Earth's lower mantle are of great interest in high-pressure mineral physics since they are thought to have important contributions to the dynamical and chemical evolution of the solid Earth. A high-pressure silicate-carbonate, $CaSiC_2O_7$, has recently been discovered, but its stability in reactions with surrounding mantle materials remains unclear. To investigate this, we perform ab initio density functional calculations assuming several reactions with deep mantle mineral components. The calculated results show that this new class of carbon-bearing silicate compound is stabilized by the reactions of $CaCO_3$ and $MgCO_3$ with SiO_2, $CaSiO_3$ perovskite, and $MgSiO_3$ bridgmanite at different pressures and inversely inhibits the stabilization of $CaCO_3$, $MgCO_3$, and CaC_2O_5 above 60 GPa. These results suggest that $CaSiC_2O_7$ represents an important host for carbon in the Earth's deep mantle and influences the form in which carbon is stored and transported under lower mantle conditions.

Key wordsz: Carbonate, Subducted basalt, Lower mantle, Density functional theory

THERMAL CONDUCTIVITY CONTRAST BETWEEN RINGWOODITE AND BRIDGMANITE: IMPLICATIONS FOR THE LONG-TERM STABILITY OF CONVECTIVE REGIMES

* Youyue Zhang [1], Takashi Yoshino [2], Masahiro Osako [3] and Steeve Gréaux [1]

1. Geodynamics Research Center, Ehime University, Japan
2. Institute for Planetary Materials, Okayama University, Japan
3. National Museum of Nature and Science, Japan

Abstract The thermal evolution and internal dynamics of the Earth are fundamentally governed by heat transport across major internal boundaries. A central question in geodynamics is whether the physical properties of the Mantle Transition Zone (MTZ) and the lower mantle promote a single-system convective flow or a layered regime. As the primary constituent of the lower MTZ, ringwoodite occupies approximately 60% of its volume, effectively characterizing the bulk physical properties of this region. Correspondingly, beneath the 660 km discontinuity, bridgmanite, the most abundant mineral in the Earth's interior, defines the thermal and rheological state of the vast lower mantle. While density and viscosity have been extensively discussed in modelling work, the thermal transport properties of these dominant phases remain among the least constrained parameters. This knowledge gap is largely due to the technical challenges involved in synthesizing high-quality, large-volume samples of these high-pressure phases, which are essential for accurate measurements under well-defined boundary conditions.

To address this gap, we synthesized a dry $(Mg_{0.9}Fe_{0.1})_2SiO_4$ ringwoodite sample and Al,Fe-bearing bridgmanite with various compositions using a Kawai-type multi-anvil press. The synthesis was conducted under mantle conditions with oxygen fugacity controlled at the IW buffer to simulate the deep interior. The thermal conductivity and thermal diffusivity of these samples were measured simultaneously at high pressures and temperatures up to 1300 K using the pulse heating method. Our experimental results reveal that dry ringwoodite exhibits much higher thermal conductivity than previously reported values, which suggests a suppressive effect of water on thermal transport. At the 660 km discontinuity, the thermal conductivity of dry ringwoodite is 15% higher than that of decomposed post-spinel assemblages and 45% higher than Al,Fe-bearing bridgmanite. This represents a distinct, step-like change in conductivity across the boundary, followed by a consistent and stable gradient within the bridgmanite-dominant lower mantle. These findings provide a possible physical basis for Earth's long-term thermal evolution. Our data imply that the efficiency of heat exchange between deep and shallow reservoirs could be influenced by such mineralogical variations, offering a potential explanation for the maintenance of global thermal stability alongside episodic convective breakthroughs.

Key words: high pressure, thermal conductivity, ringwoodite, bridgmanite, geodynamics

THERMAL EQUATION OF STATE OF THE SPINELLOID PHASE AND ITS IMPLICATIONS FOR DEEP-FOCUS EARTHQUAKES

Fei Qin, Lixin Liu

School of Earth Sciences and Resources,China University of Geosciences (Beijing), China

Abstract Wadsleyite and ringwoodite, as the dominant mineral phases in the mantle transition zone, are crucial for understanding deep hydrous minerals and geophysical anomalies. As a potential transitional phase between them, the Spinelloid series minerals were first discovered in the nickel-aluminosilicate system. Subsequently, in the forsterite-fayalite-magnetite ternary system at 1100 °C and pressures up to 10.5 GPa, Spinelloid III to V phases coexisting with olivine were also identified. Among these, Spinelloid V is the most stable phase in the series; however, its compression behavior and thermoelastic properties under high pressure remain unstudied. In this work, a magnesium-rich Spinelloid V sample coexisting with wadsleyite was successfully synthesized using high-pressure and high-temperature synthesis in a multi-anvil press. Subsequently, the high-pressure-high-temperature behavior and thermoelastic properties of Spinelloid V were systematically investigated up to 27.5 GPa and between 300 K and 750 K by combining diamond-anvil cell techniques with high-pressure-high-temperature single-crystal X-ray diffraction.

In this work, a magnesium-rich Spinelloid V coexisting with wadsleyite was synthesized using high-pressure and high-temperature synthesis in a multi-anvil press. Subsequently, the high-pressure-high-temperature behavior and thermoelastic properties of Spinelloid V were systematically investigated up to 27.5 GPa and between 300 K and 750 K by combining diamond-anvil cell techniques with high-pressure-high-temperature single-crystal X-ray diffraction. The results show that within the experimental pressure-temperature range studied, the structure of Spinelloid V remains stable without phase transformation or decomposition. A BM3 equation-of-state fit yields the parameters: V_{T0} = 405.24(2) Å³, K_{T0} = 140.8 GPa, K'_{T0} = 5.59, and α_T = 4.15×10⁻⁵ K⁻¹. Its thermal expansion is notably higher than that of wadsleyite, which is attributed to the incorporation of a significant amount of Fe^{3+} into the Spinelloid V structure. Since Fe^{3+} tends not to enter olivine or wadsleyite, Spinelloid V may represent a potential Fe^{3+}-enriched phase at the 410 km depth, besides garnet. Its thermoelastic parameters could therefore help to explain the seismic velocity anomalies observed near this discontinuity, providing new mineral-physics constraints for interpreting wave-speed variations around the 410 km discontinuity.

Key words: Spinelloid phase, wadsleyite, Thermal EoS, single crystal, elasticity

THERMAL EVOLUTION OF MARS CONSTRAINED BY THE LATTICE THERMAL CONDUCTIVITY OF RINGWOODITE: IMPLICATIONS FOR INNER-CORE FORMATION AND DYNAMO HISTORY

Xiaowei Zhao, Zhongqing Wu, Dong Wang, Yu Zhang, ZhongXu Pan
University of Science and Technology of China, Hefei 230026, China

Abstract Recent studies suggest that Mars, like Earth, possesses a solid inner core and once hosted a strong global magnetic field. However, the evolutionary history of the martian inner core remains poorly constrained, and the duration of its dynamo activity is still under debate. Addressing these questions requires a better understanding of the thermal evolution of the martian core. Because heat transport from the core to the mantle is primarily governed by thermal conduction, the thermal conductivity of minerals near the core–mantle boundary plays a key role in constraining the cooling history of Mars. Under the pressure–temperature conditions of the martian core–mantle boundary, ringwoodite is expected to be one of the dominant mineral phases. Here we combine first-principles calculations with machine-learning interatomic potentials to determine the lattice thermal conductivity of ringwoodite, and incorporate the results into coupled core–mantle thermal evolution models. Our thermal evolution calculations provide new insights into the formation and evolution of the martian inner core, as well as the lifetime of the early martian dynamo.

Key words: Machine learning, Thermal conductivity of ringwoodite, Martian thermal evolution

THERMAL TRANSPORT PROPERTIES IN FERROPERICLASE ACROSS THE LOWER MANTLE

Zena Younes [1,2], Bernhard Massani [2] , Orianna Ball [2] , Hanns-Peter Liermann [3], Zuzana Konôpková [4], Karen Appel [4], Rachel Husband [3], Silvia Boccatto [5], Nicolas Jaisle [2], Guillaume Morard [5], Maxim Bykov [7], Eric Edmund [6], Carmen Sanchez-Valle [6], Stewart McWilliams [2] on behalf of EuXFEL beamtimes 3160, 8025,8032 & 8056

1. European Synchrotron Radiation Facility (ESRF), France
2. Centre for Science at Extreme Conditions, University of Edinburgh, United Kingdom
3. Deutsches Elektronen Synchrotron (DESY), 22607 Hamburg, Germany
4. European XFEL (EuXFEL), Schenefeld, Germany
5. Inst. Minéralogie, de Physique des Matériaux et de Cosmochimie (IMPMC), Sorbonne Universite, France
6. Institut für Mineralogie, University of Münster, Germany
7. Goethe University Frankfurt, Germany

Abstract Large scale dynamics within the Earth are the result of its secular cooling, heat is transported towards the surface by large scale convection and conduction processes that occur in the mantle, core and across the thermal boundary layers at the core–mantle boundary (CMB) and the lithosphere at different rates. Determination of thermophysical properties of lower mantle minerals, such as Ferropericlase is important to understand the thermal history of the Earth. There is a range of estimates for these thermal transport properties such as thermal conductivity (k) in the lower mantle which ranges between 4 and 16 W/(m K). This results from a lack of consensus on how to formulate the pressure & temperature dependency of k where different models often yield different extrapolations. Here a novel approach to study thermal conductivity of deep earth minerals at CMB conditions using XFEL-based time resolved MHz X-ray diffraction and heating in a diamond anvil cell (DAC) is used to examine the thermal conductivity of Ferropericlase solid solutions from MgO to FeO end-members. The hard X-ray beam (≈18 keV) at the European X-ray Free Electron Laser (Eu-XFEL) generates MHz pulse trains to perform time resolved measurements of heating dynamics in high pressure samples. Finite element modelling (FEM) is carried out utilizing volume change with temperature in a sample, extracted from the diffraction data, with temperature dependent thermal conductivity fitted to the data. We report thermal conductivity values of polycrystalline Ferropericlase with Fe content increasing from the MgO through to the FeO end member at relevant CMB pressures and temperatures.

Key words: Thermal Conducivity, Heatflow, CMB, DAC, FEM

THERMODYNAMICS OF SUPERIONIC PHASES IN EARTH'S INNER CORE

Zepeng Wu[1], Chen Gao[1], Liangrui Wei[1], Shunqing Wu[1], Renata M. Wentzcovitch[2-4], Yang Sun[1]

1. Department of Physics, Xiamen University, Xiamen 361005, China
2. Department of Applied Physics and Applied Mathematics, Columbia University, New York, NY 10027, USA
3. Department of Earth and Environmental Sciences, Columbia University, New York, NY 10027, USA
4. Lamont–Doherty Earth Observatory, Columbia University, Palisades, NY 10964, USA

Abstract Light elements profoundly influence the structure and properties of Earth's core. Recent studies have shown that, under inner-core conditions, iron–light-element systems can exhibit superionic states, in which light elements shows liquid-like mobility within a crystalline iron lattice. This state of matter can fundamentally reshape current views of inner-core structure and the distribution of light elements between the inner and outer core. Investigating the thermodynamic equilibrium between superionic and liquid phases is therefore essential for understanding the chemical composition and distribution in the Earth's core. Here, we introduce a first-principles framework to calculate the Gibbs free energy of superionic phases and apply it to the Fe–O and Fe–H systems under Earth's inner core conditions. Our results show that superionic oxygen influences the phase competition between bcc and hcp iron in the inner core and doubles the oxygen content in the inner core relative to previous estimates. Superionic hydrogen develops a radial concentration gradient in the inner core under chemical potential equilibrium, leading to a drier inner core center than the boundary. Our work provide new insights into how superionicity may reshape the composition and structure of Earth's core.

Key words: Earth's core, Superionic state, Phase diagram, Thermodynamics

ZOISITE-BEARING ECLOGITES FROM KIMBERLITE PIPE ZAGADOCHNAYA (SIBERIAN CRATON).

Denis S. Mikhailenko[1,2], Sergei Yu. Skuzovatov[3], Nikolay V. Gubanov[1], Andrey V. Korsakov[4], Alla M. Logvinova[4], Yi-Gang Xu[2]

1. Zavaritsky Institute of Geology and Geochemistry UB RAS, Ekaterinburg 620002, Russia
2. State Key Laboratory of Deep Earth Processes and Resources, Guangzhou Institute of Geochemistry, Chinese Academy of Science, Guangzhou, 510640, China.
3. Vinogradov Institute of Geochemistry SB RAS, 1A Favorskogo str., Irkutsk 664033, Russia.
4. Sobolev Institute of Geology and Mineralogy SB RAS, Novosibirsk 630090, Russia.

Abstract Subduction recycling of volatile components is a fundamental factor controlling the rheology, magmatism, and seismicity of the lithosphere in convergence zones. According to existing estimates (Peslier et al., 2017), the water content in the chemically depleted lithospheric mantle of cratons is extremely limited, and its heterogeneous distribution is controlled by nominally anhydrous silicates. Subduction of oceanic crust is proposed as the primary mechanism for water enrichment of the subcontinental lithosphere, with mantle eclogite xenoliths serving as an indicator of this process. In eclogites at depths of the subcontinental lithospheric mantle, water content is mainly controlled by hydrous phases, including lawsonite and zoisite (Poli and Schmidt, 1998), whereas major mineral phases have water contents comparable to those of mantle peridotite minerals.

Among xenoliths from the Zagadochnaya kimberlite pipe (Yakutia), a new, zoisite-bearing variety of high-Ca mantle eclogites was studied. The studied xenoliths are rocks with massive textures and medium-grained granoblastic structures composed of garnet (15–40 vol.%), omphacite (26–58 vol.%), kyanite (7–41 vol.%), and zoisite (8–18 vol.%). According to the classification (Sobolev et al., 1968), the rocks belong to grospydites — a high-calcium variety of eclogites. Garnet has a composition of $Grs_{50–70}$, $Prp_{16–25}$, $Alm_{12–28}$, that corresponds to garnets from group C eclogites (Coleman et al., 1965). Zoisite is homogeneous in composition, and its H_2O content, estimated based on mass deficit, ranges from 1 to 2.8 wt.%. Zoisite forms euhedral short-prismatic crystals 50–200 μm in size, which locate primarily around kyanite grains, often forming intergrowths with garnet and kyanite itself. The calculated equilibrium P-T conditions for the rock-forming assemblage (Nakamura, 2009) correspond to the range of 800–1000°C at pressures of 3–4 GPa, which corresponds to depths of 100–150 km. The calculated bulk water content in the studied grospydites ranges from 1600 to 4250 ppm, which is an order of magnitude higher than that in the surrounding peridotite mantle (Peslier et al., 2017). The obtained estimates significantly exceed the

values previously calculated for zoisite eclogites from other kimberlite pipes (Radu et al., 2022).

The presence of regular intergrowths of euhedral zoisite crystals with garnet and kyanite suggests that zoisite could be a product of prograde lawsonite breakdown in the temperature range of 800–900°C (Poli and Schmidt, 1998). The exceptional rarity of zoisite eclogites and grospydites in kimberlites is apparently related to the scarcity of lawsonite varieties, which is due to the specific composition of the protolith (Ziberna et al., 2013). The discovered zoisite-bearing varieties represent a new type of mantle lithologies, critically important for understanding the geochemical cycle of water at great depths. The high water concentrations in the studied grospydites allow considering these rocks as significant local water reservoirs in the cratonic lithosphere.

Key words: Siberian craton, lithospheric mantle, eclogite, fluid metasomatism, subduction.

Acknowledgements The study was funded by the Russian Science Foundation (Project No. 25-77-10027).

ANOXIC PHOTO-OXIDATION OF MN(II)-BEARING CARBONATES ON MARS AND EARLY EARTH

Jiye Guo, Yuke Zhu, Jihua Hao*

National Key Laboratory of Deep Space Exploration/State Key Laboratory of Lithospheric and Environmental Coevolution, School of Earth and Space Sciences, University of Science and Technology of China, China

Abstract Manganese oxides, thought to form almost exclusively through reactions between Mn^{2+} and O_2, catalyze oxidative transformations among redox-sensitive metals. Thus, the occurrence of Mn-oxides, either observed or inferred from sedimentary geochemical data, has formed the basis for multiple hypotheses concerning the evolution of the atmospheric redox state on the early Earth and Mars. Here, using theory and experiments, we report that the band gap of common Ca/Mg-carbonate minerals (including calcite, magnesite, and aragonite) is significantly lowered by trace incorporation (0.8 wt% or lower) of Mn(II) into their bulk structure or surface, conferring photochemical reactivity under UV conditions relevant to early Earth and Mars (200-400 nm). Moreover, we show that surface incorporation of Mn(II) reduces the fundamental band gap much more effectively (by >1 eV) than bulk incorporation. Our results suggest that photo-oxidation of Mn(II)-bearing carbonates could have occurred widely on planetary surfaces, resulting in the abiotic formation of manganese oxides without free molecular oxygen. Photochemically-driven redox cycling of manganese could help sustain redox disequilibria for microbial metabolisms, but compromises the use of manganese oxides as oxygen barometers.

Key words: Carbonate minerals, manganese photochemistry, oxygenic photosynthesis, early Earth, Mars

AQUEOUS ALTERATION EXPERIMENTS USING SYNTHETIC GEMS ANALOG MATERIALS: IMPLICATION FOR AQUEOUS ALTERATION AND PRECURSOR MATERIALS OF THE RYUGU PARENT BODY.

Akira Tsuchiyama[1,2], Haiyang Xian[1], Mingqi Sun[1], Xing Ding[1], Satomi Enju[3], Yuan Xu[1], Yao Xiao[1], Shengdong Chen[1], Jiarui Lin[1], Miaomiao Zhang[1], Chenyi Zhao[1], Kirika Otono[4], Megumi Matsumoto[5], Junya Matsuno[6], Shogo Tachibana[4].

1. State Key Laboratory of Deep Earth Processes and Resources/ Center for Advanced Planetary Science (CAPS), Guangzhou Institute of Geochemistry, Chinese Academy Sciences, China
2. Research Organization of Science and Technology, Ritsumeikan University, Japan
3. Faculty of Science, Ehime University, Japan
4. Department of Earth and Planetary Science, The University of Tokyo, Japan
5. Graduate School of Science, Tohoku University, Japan
6. Advanced Research Infrastructure for Materials and Nanotechnology in Japan, Kyoto University, Japan

Abstract Analyses of samples returned from asteroids Ryugu and Bennu by the Hayabusa2 and OSIRIS-REx missions have shown that these materials are similar to Ivuna-type (CI) carbonaceous chondrites. Most of the samples experienced extensive aqueous alteration and consist mainly of a phyllosilicate-rich matrix (serpentine and saponite) containing magnetite, pyrrhotite, and carbonates (calcite, dolomite, and magnesite). It has been suggested that primitive materials similar to cometary dust—mixtures of fine-grained amorphous silicates known as glass with embedded metal and sulfides (GEMS), together with organic matter and ice—accreted to form asteroid parent bodies, where aqueous alteration occurred through reactions between these materials and liquid water generated by the melting of ice.

To constrain such aqueous alteration processes, we conducted aqueous alteration experiments using GEMS analog materials. The GEMS analogs were synthesized by condensation in an induction thermal plasma (ITP) furnace with CI or average GEMS compositions. The products consist of spherical amorphous silicate particles (~several hundred nm) containing FeS and (Fe,Ni) nanoparticles, closely resembling the composition, texture, and size of natural GEMS. Approximately 20–30 mg of the GEMS analog material was reacted with pure water (water/rock ratio = 5 in mass) in sealed gold capsules or Teflon vessels at 200 °C for about two months. In some experiments, simulated molecular cloud organics or hexamethylenetetramine (HMT: $C_6H_{12}N_4$) were added as organic components, and/or ammonium bicarbonate was added as a carbon source. The run products were characterized using XRD, SEM/EDS, and TEM/EDS.

The experiments produced poorly crystalline phyllosilicates from the amorphous silicate starting

materials. In experiments conducted in Teflon vessels, hematite and anhydrite formed. This result indicates that H_2 gas generated by reactions between Fe and water escaped from the vessel, allowing oxidation reactions of Fe and S to proceed to completion. Such oxidized mineral assemblages are not observed in Ryugu samples, suggesting that H_2 gas was retained during aqueous alteration in the parent body. In contrast, experiments conducted in sealed gold capsules, where H_2 could not escape, produced minerals observed in Ryugu samples, such as magnetite, Fe(-Ni) sulfides including pyrrhotite, and carbonates (calcite, dolomite, and magnesite), together with phyllosilicates. These results suggest that the precursor materials were similar to cometary dust, including GEMS or GEMS-like materials. With increasing CO_2 abundance, carbonates became progressively enriched in Mg relative to Ca (calcite → dolomite → magnesite), and the abundance of saponite increased relative to serpentine. Because saponite has a lower Mg/Si ratio than serpentine, the formation of carbonates appears to influence the type of phyllosilicates produced. In terms of textures, the run products include two types of matrix similar to those observed in Ryugu samples. These textures reflect those of the starting materials, suggesting that the matrices in Ryugu samples may preserve the original accretionary textures of the parent body. However, the diverse crystal morphologies of magnetite observed in Ryugu samples were not reproduced in the present experiments.

Key words: CI chondrite, cometary dust, phyllosilicate, carbonate, H_2 gas escape

Acknowledgements A. Tsuchiyama was supported by Chinese Academy of Sciences President's International Fellowship Initiative, Grant No. 2025PVA0065_Y1. H. Xian was supported by National Natural Science Foundation of China (Grant No. 42522801). A. Tsuchiyama, M. Matsumoto and J. Matsuno were also supported by JSPS KAKENHI Grant Number 20H00205.

AQUEOUS MINERALS WITHIN THE EVOLUTIONARY SYSTEM OF MINERALOGY AND THE PARAGENETIC MODES OF MINERALS

Marko Bermanec

NAWI Graz Geocenter, Department of Earth Sciences, University of Graz, Graz, 8010, Austria

Abstract The evolutionary system of mineralogy classifies minerals according to their formation history rather than solely by chemistry and crystal structure. It links mineral diversity to planetary and biological processes—particularly on Earth—grouping minerals into stages of cosmic, geologic, and biological evolution that progressively increased mineral diversity over time. This contextual framework complements the mineral list of the International Mineralogical Association (IMA) by explicitly addressing mineral modes of formation and their paragenetic relationships.

Within this framework, the concept of paragenetic modes was introduced to assign all possible formation pathways to each IMA-approved mineral species. Previous efforts identified 57 distinct "paragenetic modes," defined as natural processes by which atoms in solid and/or fluid states are reorganized into one or more new solid phases. Each mode represented a specific combination of a physicochemical mineral-forming process, pressure–temperature–composition (PTX) conditions of the mineral-forming environment, and the geologic time context.

As mineral assemblages became increasingly complex through geologic time, limitations of the original paragenetic mode scheme became more apparent. In particular, work on Part IX of the evolutionary system—addressing aqueous mineralization prior to the Great Oxidation Event—highlighted conceptual and practical challenges that prompted a reassessment of how mineral-forming processes are defined and classified.

We propose a revised hierarchical framework for describing the paragenetic modes of minerals. Firstly, we define five principal mineral-forming processes based on fundamental physical mechanisms: (A) condensation from a vapor or plasma; (B) primary crystallization from a melt; (C) primary precipitation from aqueous or other solutions; (D) secondary alteration through fluid–mineral interactions; and (E) metamorphism and other solid-state reactions. Biomineralization, mediated by cellular activity, is treated as a distinct attribute and subdivided into 10 biological categories spanning processes A–E. Collectively, we recognize 5 primary and 9 secondary sub-processes, plus 10 biological categories, and assign each of the 6,188 IMA-approved mineral species to one or more of these sub-processes.

Since variables such as pressure, temperature, and composition all exist along a continuum, it was always possible to think of intermediate cases between any two of the previous paragenetic modes. By focusing on the states of matter that are participating in the mineral forming process, there is a

thermodynamic “anchoring” that is unambiguous, because it can be tied to state variables of the system. As a result, the new categories of mineral-forming processes encompass a more thermodynamically robust classification that can be used more universally to describe the formation processes of any solid, on any planet or moon. Furthermore, the same processes can operate within a variety of environments, leading to the formation of completely different mineral assemblages. And the operations of these processes within a certain environment is the driver of differentiation and chemical and mineral evolution of that environment, eventually creating a completely new environment which can enable other paragenetic processes to operate.

Together, this hierarchical approach provides a comprehensive, internally consistent, and broadly applicable framework for understanding mineral diversity in stellar, nebular, and planetary systems. Such separation of fundamental mineral-forming processes from the pressure–temperature–composition environments in which they operate is especially critical for better understanding of aqueous mineral evolution, where evolving fluid compositions, redox states, and water–rock interactions fundamentally reshaped Earth’s mineral diversity.

Key words: Mineral Evolution, Paragenetic modes, paragenetic processes, Aqueous minerals

A SPECTROSCOPIC PROBE OF EXPANDABLE CLAY MINERAL SURFACES: THE APPLICATION OF THE OD METHOD IN CHARACTERIZATION OF THE CRITICAL ZONE

Artur Kuligiewicz

Institute of Geological Sciences, Polish Academy of Sciences, Poland

Abstract Interactions between light and the mineral surfaces can be employed in many ways to extract information about the surface. One of the examples of such an application is the OD method, which uses the Attenuated Total Reflectance Infrared Spectroscopy (ATR-IR) of D_2O-saturated expandable clay minerals to probe the amount of the layer charge (LC) present in the expandable interlayers. Saturation of the clay sample with D_2O leads to the shift in the ATR-IR signature of adsorbed water, which effectively removes the overlap between the stretching modes of adsorbed H_2O and structural OH groups. This allows for the separate investigation of OH stretching modes of phyllosilicates and the broad envelope of O-D stretching modes coming from the adsorbed water molecules. Investigation of the latter resulted in the discovery of a linear relationship between the position of a sharp, high-frequency O-D stretching mode (νO-D) and the magnitude of LC present at the clay mineral's surface. The νO-D mode originates from a population of D_2O molecules situated in the direct vicinity of the siloxane surface and is involved in a weak hydrogen bonding with it. The OD method was primarily developed for dioctahedral smectites; however, the subsequent work demonstrated its applicability to all expandable clay minerals, including trioctahedral smectites, vermiculites, and mixed-layer minerals. The OD method can provide useful information about the magnitude of LC present on the surfaces available for interactions with the environment, including surfaces at which the formation of coatings can take place. The important feature of the OD method is that it provides information only on the average LC present on the wettable surfaces of the expandable portion of the clay mineral structure. It cannot measure the magnitude of LC present in collapsed interlayes, such as the illitic part of illite-smectite mixed-layer minerals. Additionally, if a part of the smectitic of vermicullitic structure is not accessible for the D_2O molecules, i.e., as a result of the formation of the inner sphere complexes, hydryxoy-interlayereing or coating, the OD method would return the average LC of the remaining part of the structure.

The aim of this presentation is to provide a brief overview of the application of the OD method to samples coming from the Critical Zone, including materials containing Fe-rich coatings. Examples coming from soils and weathering profiles, including bauxites, will be provided. The results of the OD method measurements will be compared with additional data such as X-ray diffraction patterns,

cation exchange capacity measurements, and chemical analysis in order to demonstrate how this spectroscopic tool can be used in the complex characterization of mineral samples.

Key words: FTIR, OD method, smectite, vermiculite, Critical Zone

ASSEMBLING A UNIFIED MINERALOGICAL MAP OF THE MOON THROUGH REMOTE SENSING, SAMPLE ANALYSIS, AND THE EXAMINATION OF PARAGENETIC MODES

Lindsay M. Podjasek[1], Shaunna M. Morrison[1], Jolyon Ralph[2], Barbara Lafuente[3]

1. Department of Earth and Planetary Science, Rutgers University, USA
2. Mindat.org, UK
3. SETI Institute, USA

Abstract Minerals preserve a record of the formational conditions, surface processes, and weathering mechanisms that have shaped planetary bodies over billions of years. The Moon is ideal for researching the mineral record due to the proximity, extensive collection of lunar materials, and rapidly growing collection of remote sensing data. This work consolidates the Moon's extensive mineralogical data into a single, tabulated dataset linked with an intuitive visualization through mapping. The comprehensive dataset and unified map of lunar mineralogy is categorized by three levels of uncertainty; 1) confirmed compositions based on Apollo samples and meteorites, 2) identified compositions from remote sensing data, and 3) hypothesized minerals derived from a study of paragenetic modes. The ongoing classification of Earth's minerals into well-defined paragenetic modes provides a foundational framework to analyze paragenetic modes and mineral assortment on the Moon. This work complements the USGS Unified Geologic Map of the Moon, which emphasizes large scale geologic units and stratigraphy rather than mineral distribution and abundance. The resulting map will be a valuable resource for future lunar exploration, influencing landing sites for robotic and human missions, conducting experiments that cannot be done on Earth, and identifying materials for In Situ Resource Utilization.

Key words: Moon, planetary, mineralogy, meteorites, map

ATOMIC RESOLUTION OBF-STEM IMAGING OF ANTIGORITE IN CLEAVABLE OLIVINE

Gen Koinuma[1], Kohei Sato[1], Ichiro Ohnishi[1], Naotaka Tomioka[2,3], Jun-ichi Ando[2,4]

1. JEOL Ltd. (Japan)
2. Hiroshima Univ. (Japan)
3. JAMSTEC (Japan)
4. Hiroshima Univ., HiPeR (Japan)

Abstract "Cleavable olivine" occurring in serpentinized ultramafic rocks exhibits cleavage mainly parallel to the (100) plane of antigorite, a serpentine-group mineral, preferentially forms. To better understand the serpentinization process of such cleavable olivine, detailed characterization of the interfacial structure between olivine and antigorite is essential. In this context, atomic-scale structural observation using aberration-corrected scanning transmission electron microscopy (STEM), which has rapidly advanced in recent years, provides a powerful analytical approach. STEM generally poses little difficulty when applied to minerals that are relatively resistant to electron-beam irradiation, such as common silicates. In contrast, hydrous minerals such as antigorite are highly susceptible to beam-induced structural damage, which significantly limits high-resolution imaging under conventional conditions. To address this challenge, we employed the recently developed Optimum Bright-Field (OBF) STEM technique to directly observe the atomic-scale structure at and near the olivine–antigorite interface.

The OBF-STEM technique enhances the signal-to-noise (S/N) ratio of STEM images by applying optimal filtering to each segmental image acquired from a segmented detector and then summing them. This approach enables the acquisition of high-contrast imaging even under low dose conditions, where conventional methods typically yield noisy and indistinct images. Indeed, atomic-resolution imaging has been achieved even for electron-beam-sensitive materials such as zeolites and metal–organic frameworks (MOFs).

The sample investigated in this study is cleavable olivine occurring in a dunite collected from Raijin Seamount in the northern Mariana forearc. After identifying cleavage domains using polarized light microscopy, TEM foils were prepared from these domains using a focused ion beam (FIB; JEOL JIB-PS500i). OBF-STEM observations were conducted using an aberration-corrected STEM (JEOL JEM-ARM300F2) operated at an accelerating voltage of 300 kV, with a convergence semi-angle of 14 mrad and a probe current below 0.4 pA.

As a result, the Mg, Si, and O atomic columns constituting antigorite were successfully visualized along the [010] zone axis. Furthermore, the periodicity of antigorite along the [100] direction was found to become progressively disrupted toward the olivine-antigolite interface. Previous studies based on selected-area electron diffraction (SAED) have reported that the [100] periodicity of

antigorite varies depending on temperature and pressure conditions. In contrast, the present study directly visualized local structural variations at the unit-cell scale. This observation highlights the utility of aberration-corrected STEM for direct structural observation. These findings demonstrate that OBF-STEM is a highly effective technique for the microstructural analysis of serpentine minerals.

In the presentation, we will discuss the formation process of antigorite based on OBF-STEM observations, together with complementary EDS analytical results.

Key words: OBF-STEM, Scanning Transmission Electron Microscopy, Low-Dose imaging, antigorite, cleavable olivine

BACTERIAL MINERALIZATION OF BARITE AND IMPLICATION FOR MARINE BARITE GENESIS

Kai-Rui Jiao[1], Xin Li[1], Qiu-Yu Qiao[1], Qi-Zhi Yao[2], Gen-Tao Zhou[1*]

1. State Key Laboratory of Lithospheric and Environmental Coevolution, University of Science and Technology of China, Hefei 230026, China
2. School of Chemistry and Materials Science, University of Science and Technology of China, Hefei 230026, China

Abstract Biogenic particulate barium (Ba_{bio}) serves as a geochemical proxy for the remineralization of particulate organic carbon in marine waters. As the primary carrier of Ba_{bio}, marine barite ($BaSO_4$) is widely distributed throughout the oceans and is commonly used to reconstruct past ocean export productivity. However, modern seawater is largely undersaturated with respect to barite formation. Consequently, the precise mechanism driving barite precipitation in Ba-undersaturated seawater remains unclear. Numerous natural observations indicated that marine barite formation is closely related to organic detritus (such as polysaccharides). Furthermore, the maximum distribution of barite particles in marine water column tends to occur in regions where bacterial carbon respiration is intense. Therefore, it is generally believed that barite precipitates in the microenvironments associated with the bacterial degradation of Ba-bearing organic matter. Moreover, results from laboratory simulation experiments further support the hypothesis that bacterial metabolic activities facilitate barite precipitation. However, these experimental protocols often conflict with conditions in the modern marine environment, where sulfate concentration (~28 mM) is high and barium exists primarily in an organically combined state. Polysaccharides are important components of marine primary producers and constitute a large fraction of marine dissolved and particulate organic matter. In addition, polysaccharides can form organic-metal complexes with metal ions. Therefore, this study induces barite mineralization by employing marine bacteria to degrade marine polysaccharide-Ba complexes under simulated seawater sulfate concentrations. The results showed that the degradation of polysaccharides by marine bacteria promoted barite precipitation, whereas no precipitation formed in the uninoculated control group. High-resolution transmission electron microscopy observations revealed that a Ba-containing, P-rich amorphous phase first formed on the bacterial surface, which subsequently transformed into P-poor barite crystals. Fourier-transform infrared spectroscopy analysis indicated that phosphoryl groups on the bacterial surface facilitated Ba^{2+} accumulation and induced the formation of the P-containing precursor phase. Solid-state ^{31}P magic-angle spinning nuclear magnetic resonance analysis further demonstrated that inorganic P species in the mineralization solution also participated in the formation of the P-containing precursor. As mineralization proceeded, the precursor phase detached from bacterial cells and further evolved into X-shaped, arrow-shaped, and pseudo-hexagonal prismatic crystals, which are commonly found in marine water columns and

sediments. These experimental findings deepen our understanding of the bacterial mineralization mechanism of marine barite.

Key words: Marine barite, Barium, Marine polysaccharides, Bacterial mineralization

Acknowledgements This work was supported by the National Natural Science Foundation of China (No. 42472059).

BIOREMEDIATION: LEARNING FROM BIO-GEO PROCESSES IN EXTREME ENVIRONMENTS

Onnis, P.[1]*, Falagan, C.[2], Ramos, V.[3], Medas., D.[1], De Giudici G.[1]

1. * Department of Chemical and Geological Sciences, University of Cagliari, Monserrato, Italy. patrizia.onnis@unica.it
2. School of Biological Sciences, King Henry Building, King Henry 1st St., University of Portsmouth, Portsmouth, United Kingdom.
3. Environment and Sustainability Institute and Camborne School of Mines, University of Exeter, Penryn Campus, United Kingdom.

Abstract Worldwide, legacy mine wastes pose a significant environmental challenge, creating extreme conditions that promote complex biogeochemical interactions. In such settings, biomineralisation processes play a key role in controlling elemental cycles, recording environmental change, and influencing ecosystem resilience. This contribution investigates biomineral formation and microbe–mineral interactions in an extreme coastal environment affected by coal-mining waste at Seaham Beach (UK).

Beach sediments, composed mostly of pyrite, jarosite, and traces of alumina-silicates and dolomite, showed ecotoxic metal(loid) concentrations above environmental guideline values (As 220 mg/kg, Pb 150 mg/kg, Zn 260 mg/kg, and V 350 mg/kg). Acidic water pools (pH ~ 3) covered the beach in contact with a dolostone outcrop and hosted average concentrations of the metal(loid)s at <0.2 mg/L, except for V, which reached 1 mg/L. Ongoing investigations suggest the presence of oxidative bacteria and fungal hyphae. Scanning electron microscopy of minerals and biofilms highlighted interactions between roots and dolomite microscale crystals, and between potential bacterial cells and jarosite-like phases.

These observations suggest that microbial communities actively influence pyrite oxidation, secondary mineral formation, and local pH buffering through biomineralisation processes. Such mechanisms highlight the role of microorganisms in driving mineral growth kinetics and stabilising contaminants under extreme conditions. Understanding these processes provides insights into the resilience of impacted environments and supports the development of nature-based technologies for remediation, environmental monitoring, and sustainable resource management.

Key words: Acid mine drainage, metal(loid)s, biominerals, secondary minerals

CHARACTERIZATION OF THE BLACK DUST FROM THE 2026 MARCH-APRIL DUSTFALL EVENTS IN THE TATRA MOUNTAINS (POLAND)

Artur Kuligiewicz[1], Agnieszka Rajwa-Kuligiewicz[2], Anna Bojarczuk[2], Łukasz Jelonkiewicz[2], Andrzej Adamski[3], Beata Kultys[3], Paweł Miśkowiec[3], Bartłomiej Zubek[4]

1. Institute of Geological Sciences, Polish Academy of Sciences, Poland
2. Faculty of Geography and Geology, Jagiellonian University, Poland
3. Faculty of Chemistry, Jagiellonian University, Poland
4. Tatra National Park, Poland

Abstract Long-range transport of mineral dust is a key atmospheric process linking arid source regions with distant receptor environments, with important implications for air quality, climate, and ecosystem functioning. In recent years, Central Europe has experienced an increasing frequency of dust intrusions; however, the complexity of transport pathways and post-emission transformations remains insufficiently constrained. This study investigates a sequence of dust episodes in March–April 2026 affecting Central Europe, with a particular focus on deposition recorded in the Tatra Mountains (Western Carpathians). The analysis integrates satellite observations with detailed laboratory characterization of deposited material.

A synoptic-scale circulation pattern in late March–early April 2026 facilitated the transport of air masses from southern to southeastern sectors toward Central Europe. This is evidenced by ERA5 reanalysis fields and elevated Sentinel-5P Aerosol Absorbing Index (AAI) values over the Mediterranean and southeastern Europe. A combined analysis of MERRA-2 dust column mass density, Sentinel-5P aerosol products, ERA5 wind fields, and precipitation data indicates that the Tatra snowpack records a composite depositional signal rather than a distinct single-source signature. The observations point to long-range transport of mineral dust followed by atmospheric mixing and precipitation-driven scavenging prior to deposition.

To characterize the deposited material, a multi-analytical laboratory approach was applied to snowpack samples collected during the early phase of the event. Mineralogical analyses, including X-ray diffraction (XRD), Thermogravimetric Analysis coupled with Mass Spectrometry (TG-MS), Fourier Transform Infrared (FTIR), and Raman spectroscopies, revealed a composition dominated by quartz, dioctahedral mica, kaolinite, feldspars, and chlorite, consistent with desert-derived mineral dust. FTIR spectra point to the presence of aliphatic organic compounds and amides. TG-MS analysis revealed the presence of black carbon in the investigated sample. Granulometric analysis of meltwater using a LISST-200X instrument shows that snowmelt-derived suspensions of aeolian material are strongly silt-dominated (84–90%), with minor clay (~1%) and a notable fraction of aggregates (10–15%). The particle size distribution has a median diameter (D50) of

15.5–19.4 µm, with a stable fine mode at ~3 µm (D10) and coarse fractions up to ~80 µm (D90), indicating aggregation during snowmelt.

Chemical analysis of the melted snow indicates a dominance of Ca^{2+} and HCO_3^-. At the same time, elevated concentrations of NH_4^+ and NO_3^-, together with measurable total organic carbon (TOC ≈ 2.15 mg L^{-1}), point to the presence of secondary inorganic aerosols and organic matter. These chemical characteristics deviate from those of pristine desert dust and indicate significant atmospheric processing, including mixing with polluted air masses and incorporation of secondary species.

The combined mineralogical, granulometric, and chemical evidence indicates that the observed plume represents a chemically and physically transformed dust aerosol rather than a simple single-source signal. While the mineral composition is consistent with desert dust typically attributed to North African sources, the presence of anthropogenic tracers and organic components suggests substantial modification along transport pathways, potentially involving regions influenced by industrial activity and petroleum-related emissions across the eastern Mediterranean and parts of Western Asia.

Overall, this study demonstrates that dust deposition in Central Europe during multi-episode transport events can reflect a hybrid natural–anthropogenic aerosol, shaped by both source characteristics and in-transit transformations. These findings highlight the importance of integrating remote sensing with laboratory analyses to better constrain the evolution of long-range transported dust and its environmental implications in mid-latitude regions.

Key words: mineral dust, long-range transport, snowpack deposition, Tatra Mountains

COUPLING OF MANGANESE OXIDATIVE CRYSTALLIZATION AND THALLIUM IMMOBILIZATION UNDER LIGHT IRRADIATION

Jielong Cao[1, 2, 3], Qingze Chen[1, 2, 3]*, Runliang Zhu[1, 2, 3]

1. State Key Laboratory of Advanced Environmental Technology & Guangdong Provincial Key Laboratory of Mineral Physics and Materials, Guangzhou Institute of Geochemistry, Chinese Academy of Sciences, China
2. Guangdong Research Center for Strategic Metals and Green Utilization, China
3. University of Chinese Academy of Sciences, China

Abstract Manganese (oxyhydr)oxides (MnO_x) are ubiquitously distributed across various geological settings, including marine, soil, and sediment. Due to their relatively high specific surface area and high redox and adsorption reactivity, MnO_x exert strong control over the geochemical processes on the Earth's surface, such as the redox cycling, as well as the migration and transformation of environmental substances. The formation and transformation of MnO_x play crucial roles in the biogeochemical cycling of thallium (Tl) due to the high geochemical affinity and strong correlation between MnO_x and Tl. Recent studies have revealed that light is a key abiotic driver of the Mn redox cycle. However, the coupled cycling of Mn and Tl under light irradiation in the Earth's surface environments remains poorly elucidated. Herein, we systematically investigated the interplay between Mn(II) oxidative crystallization and Tl immobilization in nitrate solution under light irradiation. Our findings revealed a ubiquitous yet previously overlooked light-driven Mn redox cycle, which specifically involves: (1) the oxidation of Mn(II) to vernadite (δ-MnO_2) by superoxide radicals generated from nitrate photolysis; (2) the reductive transformation of δ-MnO_2 to feitknechtite (β-MnOOH) and hausmannite (Mn_3O_4) by surface-adsorbed Mn(II); and (3) the reoxidation of Mn(II) derived from the photoreductive dissolution of MnO_x. The formed MnO_x effectively removed Tl(I) through adsorption and coprecipitation, with Mn(II) inhibiting the oxidation of Tl(I) to more toxic Tl(III). In turn, Tl(I) suppressed the reductive transformation of δ-MnO_2, which favored its own immobilization. These findings enhance the comprehension of the coupled environmental geochemical processes involving Mn and Tl in natural systems and offer new insights for treating industrial wastewater containing Mn and other metal contaminants.

Key words: manganese (oxyhydr)oxides, thallium, light, coupling effect

COUPLING OF TRACE METALS AND METALLOIDS TO MICROBIAL FE(III) REDUCTION; IMPACTS ON CE AND SB MOBILITY AND THE PRODUCTION OF NOVEL NANOMATERIALS TO SUPPORT THE ENERGY TRANSITION

Jinxin Xie, Victoria S. Coker, Brian O'Driscoll, Jonathan R. Lloyd

Department of Earth and Environmental Sciences, University of Manchester, Manchester M13 9PL, United Kingdom

Abstract Biogeochemical processes are widely recognised as key factors on metal fate in natural and engineered systems and can be exploited for the biotechnological synthesis of high value metallic nanoparticles. In this study, the fate of Ce and Sb was studied during the biotransformation of Fe(III) oxyhydroxides mediated via the dissimilatory metal-reducing bacterium *Geobacter sulfurreducens*. Cerium is among the most abundant rare earth elements (REEs) in the environment and is extensively used in industrial applications. In contrast, Sb is an emerging contaminant of concern due to its potential toxicity in aquifers.

Ce-bearing ferrihydrite was prepared by the co-precipitation of ferric chloride ($FeCl_3$) and cerium chloride ($CeCl_3$). Sb(V) was adsorbed to pre-made ferrihydrite before bioreduction. Across both systems, increased loadings of Ce and Sb impacted on the rate and extent of Fe(III) reduction, indicating that these elements can modulate Fe mineral biotransformation. Despite this inhibition, neither Ce nor Sb was measurably mobilised, suggesting a strong affinity between the Fe(III) mineral and Ce/Sb.

After bioreduction, magnetite was the dominant Fe(II)-bearing phase detected by XRD in the low Sb(V) or Ce-bearing samples (0.5% and 1%) with minor goethite detected. At higher Sb or Ce loadings, bioreduction of Fe(III) was inhibited, and goethite was the dominant end-point product detected. In both examples, Sb and Ce were retained within the iron mineral assemblage, suggesting that tight coupling to the iron redox cycle will not result in groundwater contamination, but could instead be used to control pollution in the environment. Beyond environmental immobilisation, this reductive bioprocessing route also generates functional nanomaterials. Here the biomagnetite prepared with 0.5% Ce was tested as an additive to Pt/C fuel cell electrodes, and improved their performance at lower loadings of Pt, suggesting that microbially produced Ce-magnetite (potentially from wastes) can provide a sustainable way to improve the performance of fuel cell catalysts. Ongoing work is focusing on the engineering of a wider range of doped biomagnetite nanoparticles for catalytic applications that support the clean energy transition.

Key words: Fe mineral biotransformation, Bioreduction, Geobacter sulfurreducens, Cerium (Ce) and Antimony (Sb)

CRYSTAL CHEMISTRY STUDIES OF SECONDARY MINERALS AND TECHNOGENIC MINERAL PHASES OF URANIUM TO ENSURE THE NUCLEAR FUEL CYCLE ENVIRONMENTAL SAFETY

Vladislav V. Gurzhiy[1], Evgeny V. Nazarchuk[1], Boris E. Burakov[1,2], Ilya V. Kornyakov[1], Sergey V. Krivovichev[1,3]

1. Department of Crystallography, Institute of Earth Sciences, St. Petersburg State University, University Emb. 7/9, 199034 Saint-Petersburg, Russian Federation; vladgeo17@mail.ru, vladislav.gurzhiy@spbu.ru
2. Ioffe Institute, 26, Politekhnicheskaya, 194021 St. Petersburg, Russian Federation
3. Nanomaterials Research Center, Kola Science Center, Russian Academy of Sciences, Fersmana str. 14, 184209 Apatity, Russian Federation

Abstract It is very difficult to overestimate the importance of uranium for modern civilization, and if consider the entire nuclear fuel cycle, then its initial and final stages (i.e. exploration of uranium deposits, mining and processing of uranium ores, storage and processing of radioactive wastes) are inextricably linked with mineralogical research: which rocks and their constituent minerals are best used for uranium mining, what happens to uranium compounds in contact with the environment, how do secondary uranium minerals differ in their physical and chemical properties? In this regard, it is very important to conduct crystal chemical studies involving both natural and synthetic objects. Stable and sparingly soluble uranium compounds can prevent the migration of radionuclides from the zones of uranium ores oxidation or from the repository of radioactive wastes, so, the study of the features of water-soluble uranium compounds is necessary to understand the processes of transfer of radionuclides in geological conditions.

Nowadays, there are more than 310 U-bearing minerals known that contain uranium in various forms. And this amount exceeds 5% of the total number of known minerals! The discovery of a large number of new U^{6+} minerals in recent years demonstrates the unique evolution of the natural material within the uranium deposits. At the same time, the processes of direct alteration of mineral species remain largely unexplored and not fully understood.

With this regard investigation of synthetic analogs of minerals and structurally related compounds shed the light on the formation mechanisms of such phases in nature, which in turn should help to implement a more balanced policy in the field of environmental safety.

Key words: Uranyl, mineral, crystal structure, topology, Chernobyl “lava”

Acknowledgements This work was supported by the Russian Science Foundation (grant No. 23-17-00080-P). The laboratory research was carried out using equipment of the Research Centre for X-ray Diffraction Studies of Saint-Petersburg State University.

DECIPHERING AND EMISSION ASSESSMENT OF KEY TOXIC COMPONENTS IN FINE PARTICLES FROM TYPICAL INDUSTRIAL SECTORS IN CHINA

Zuoshun Niu[1,2], Yi Yang[1*]

1. Key Laboratory of Geographic Information Science of the Ministry of Education, School of Geographic Sciences, East China Normal University, China
2. State Key Laboratory of Environmental Chemistry and Toxicology, Research Center for Eco-Environmental Sciences, Chinese Academy of Sciences, China.

Abstract Airborne particulate matter (PM) pollution has long been a major threat to human health worldwide, often ignored, but now coming into focus. Specifically in China, two atmosphere-polluting industrial sectors, coal-fired power plants (CFPPs) and iron-steel plants (ISPs), were taken as examples to decipher and estimate the emission of key toxic components of fine particles (FPs; < 1 μm). In vitro tests revealed ISP-emitted FPs induced 12.4 times higher oxidative stress and 4.4 times higher cytotoxicity on human bronchial epithelial cells than CFPP-emitted FPs. Single-particle ICP time-of-flight MS (spICP-TOF-MS) analysis showed that 60 ± 4% of the CFPP-emitted metal(loid)-containing FPs were multi-metal(loid)s FPs (mmFPs), mostly Si-rich mmFPs (~80%). In contrast, Fe-rich mmFPs dominated the ISP-emitted mmFPs, with their number concentrations 8.5 - 35.6 times higher than those from CFPPs. Random forest model and SHapley Additive exPlanation analysis identified Fe-rich mmFPs (especially Fe-sole fingerprinted FPs) as the top regulator of intracellular oxidative stress, while toxic metal(loid)s associated with Fe-rich mmFPs controlled cytotoxicity. Fe-rich FPs, including Fe-rich mmFPs and Fe-single-metal(loid) FPs, contributed over 30% of the total toxic potency induced by FPs, exceeding any other chemical component. Based on the latest available emission data of PMs in 2019, Fe-rich FPs emitted from CFPPs and ISPs in China were estimated to be about 1.7×10^{23} particles (ca. 5217 tons), annually. Among these emissions, ISPs contributed over 97%, with sintering and ironmaking being the major contributors. Magnetic components within FPs were further separated using a cyclic magnet extraction (CME) system. Results showed that magnetite accounted for up to 57% of the Fe-rich FPs. In addition, magnetite FPs exhibited single-particle multi-elements fingerprints similar to those of Fe-rich FPs, indicating that magnetite constitutes a key component of Fe-rich particles. Notably, despite accounting for only 10% of the total FP mass, magnetite FPs contributed up to 80% of the overall toxicity. Based on these findings, installing a magnetic field downstream of the dust removal system to eliminate magnetic compoments could effectively reduce the toxic potency of FPs.

Key words: Fe-rich FPs, Magnetite, spICP-TOF-MS, Toxic potency, Industrial sectors

DECODING QUARTZ TEXTURES: EXPERIMENTAL INSIGHTS INTO THE LINK BETWEEN FLUID STATES AND PRECIPITATION

Atsushi Okamoto

Graduate School of Environmental Studies, Tokoku University, Japan

Abstract Quartz veins are ubiquitous in hydrothermal systems and record dynamic crustal processes, including the formation of ore deposits and seismic activity. However, silica scaling along pipelines also poses a significant challenge to the sustainable development of geothermal energy. In the high-temperature crust, hydrothermal fluids transit between liquid, vapor, and supercritical states. Because silica solubility depends heavily on temperature and fluid density, these transitions induce silica precipitation at varying levels of supersaturation. While distinct cathodoluminescence (CL) zoning in natural quartz suggests fluid injection or pressure oscillations, the interpretation of these textures remains ambiguous. This study employs hydrothermal flow-through experiments to investigate silica precipitation under sub- to supercritical conditions to clarify how fluid state changes influence precipitation mechanisms and textures.

In the first set of experiments, we applied a temperature gradient (~300 °C to ~430 °C) under constant pressures of 10, 20, and 25 MPa. We used a granite-derived aqueous solution (~350 °C) containing 200–300 mg/kg Si and 5–10 mg/kg Al, Na, and K. At 25 MPa, the fluid transitioned from liquid to supercritical, while at 20 and 10 MPa, it transitioned from liquid to vapor, triggering high supersaturation. At 25 MPa, precipitates transitioned systematically from amorphous silica to nucleated quartz grains and quartz overgrowths. At 20 MPa, results were similar but included large voids within the amorphous silica. At 10 MPa, fine-grained quartz and amorphous silica formed complex, turbulent-like structures. Numerical simulations of coupled thermal-hydrological processes suggest that while precipitation occurred across a wide liquid-vapor bianry region at 10–20 MPa, the structural differences reflect variations in the Reynolds number of the flowing fluids. Furthermore, downstream quartz overgrowth at 20 MPa indicates that a liquid phase remained on the wall surfaces, facilitating growth. These results suggest that silica textures are strongly controlled by vapor-liquid and liquid-solid interfaces.

In the second set of experiments, we induced fluid pressure oscillations between 20 and 25 MPa at intervals of 4 or 8 hours. In the quartz growth regions, we observed distinct periodic CL zoning: CL-bright zones grew at 25 MPa (enriched in Al, K, and Li), while CL-dark zones grew at 20 MPa. The CL-dark bands were generally broader than the CL-bright bands, and square-wave oscillations produced sharper zoning than sine-wave oscillations. Additionally, primary fluid inclusions formed immediately following the CL-bright bands. These results suggest that the differences in growth

rate in response to the fluid pressure change produces the CL-zoning and the formation of fliud-inclusions at the specific growth duration.

In summary, quartz vein textures do more than record silica solubility; they serve as high-resolution recorders of pressure fluctuations, phase separation, and fluid flow dynamics. These findings suggest that CL and trace-element zoning in natural quartz can be directly linked to fluid-induced seismicity and pressure oscillations in the crust.

Key words: Hydrothermal experiments, quartz vein texture, superciritcal fluids, boiling, CL zoning

Acknowledgements This work was partly supported by the New Energy and Industrial Technology Development Organization (NEDO) under project number JPNP21001.

DIFFERENTIAL PRESERVATION OF ORGANIC BIOSIGNATURE IN MARS-ANALOG CLAYS AND EVAPORITES

Tongtong Huang [1], Wei Lin [1,2]

1. Key Laboratory of Planetary Science and Frontier Technology, Institute of Geology and Geophysics, Chinese Academy of Sciences, Beijing 100029, China.
2. College of Earth and Planetary Sciences, University of Chinese Academy of Sciences, Beijing 100049, China.

Abstract Clays and evaporites are considered potential hosts for organic biosignature preservation on Mars, yet the molecular-level constraints on their differential preservation potential remain poorly understood. Here, we investigate the composition of organic matter associated with clay and evaporite minerals from Mars-analog evaporitic sediments in the northwestern Qaidam Basin, China, by integrating bulk ultrahigh-resolution mass spectrometry analysis of dissolved organic matter (DOM) with in situ high-resolution NanoSIMS analysis. Our results demonstrate that clays (e.g., muscovite and chlorite) contain relatively higher organic carbon content, and evaporites (gypsum and halite) preserve a greater DOM diversity and exhibit lower degradation indices. In general, clays preferentially sequester nitrogen-containing organic compounds, whereas evaporites enrich sulfur-bearing organics. With increasing evaporation intensity, lipid abundance declines while unsaturated hydrocarbons and aromatic structures increase, suggesting that evaporation drives distinct molecular transformations. These results reveal a mineral-specific fractionation pattern governing organic matter preservation under arid conditions, providing important implications for organic geochemical cycling and biosignature detection on Mars.

Key words: Martian biosignatures, Clay minerals, Evaporitic minerals, the Qaidam Basin

DISSOLVED SILICA FROM HYDROTHERMAL EVENTS PROMOTED IRON CARBONATE FORMATION IN THE ARCHEAN EON

Mingjie Wang, Zhaoyi Dai*

State Key Laboratory of Geomicrobiology and Environmental Changes (GMEC), School of Earth Sciences, China University of Geosciences, Wuhan 430078, China

Abstract Iron formations (IFs) play a key role in the biogeochemical cycles of iron, carbon and silicon in the Archean Eon. Iron carbonate is one of the major mineral facies of various IFs and has been widely used to reconstruct the volcanism activities, evolution of the biosphere, and changes of seawater compositions. However, after decades of research, whether iron carbonate can precipitate directly from seawater remains debated. Previous studies suggested that iron carbonate formation is kinetically hindered, even though it is thermodynamically favorable. Here, we proposed that, hydrothermal events in the Archean Eon can supply dissolved silica (DSi) in the ocean and promote the direct precipitation of iron carbonate. By measuring the induction time of siderite crystallization, DSi was shown to accelerate the crystallization kinetics of siderite at different temperature, saturation state and *p*H conditions. Based on these experiments, a semi-mechanistic model was developed to quantify such promotion effects of DSi and was used to reconstruct the crystallization kinetics of siderite in the Archean Eon. The good match between the faster crystallization kinetics and more occurrence records of iron carbonate from 2.8 to 2.5 Ga confirms the critical role of DSi in iron carbonate formation. More importantly, the $\delta^{13}C$ values of iron carbonate became more negative and showed more contribution from the mid-ocean ridge hydrothermal venting events ($\delta^{13}C$ = ~-6.5‰) as stronger hydrothermal activity was recorded by the europium anomaly (Eu/Eu^*), indicating the correlation between hydrothermal events and the formation of iron carbonate. Such correlation is further confirmed by the coincidence between occasional inputs of wildfire ash and more siderite precipitation from the modern Canyon Lake sedimental records. This study provides new experimental constraints and a kinetic framework for understanding Archean iron carbonate formation, offering fresh insights into the cycling of iron, carbon and silicon.

Key words: BIF, GIF, silicates, Paleoarchean, MOR

EXPLORATIONS OF MINERAL SURFACE AREA QUANTIFICATION USING WATER-BASED BET: INSIGHTS FROM A SYSTEMATIC STUDY OF CLAY MINERALS

Xinru Hui[1], Nir Norbar Galili[2], Toshihiro Yoshimura[3], Michael Plötze[4], Thomas Michael Blattmann[1]

1. Asian School of the Environment, Nanyang Technological University, Singapore
2. Department of Earth and Planetary Sciences, Weizmann Institute, Israel
3. Biogeochemistry Research Center, Japan Agency for Marine-Earth Science and Technology (JAMSTEC), Japan
4. Institute for Geotechnical Engineering, ETH Zurich, Switzerland

Abstract Mineral surface area (MSA) is a fundamental parameter governing geochemical reactivity and organic matter preservation in soils and sediments. Nitrogen-based BET (N_2-BET) has established itself as the most widely used approach, yet as a non-polar adsorbate, nitrogen has limited access the interlayer spaces of expanding clay minerals such as smectite, systematically underestimating their total MSA. Water, as a polar and environmentally ubiquitous adsorbate, hydrates these interlayer spaces and thereby retrieve a measure of total hydratable mineral surface area (THMSA). However, the potential of water-based BET (H_2O-BET) remains underexplored due to a lack of systematic study. To evaluate this potential, we prepared a range of phyllosilicate reference materials — including smectites, illite, kaolinites, vermiculite, and chlorite — alongside environmental mineral matrices, following organic matter removal and homoionization with calcium and sodium. MSA was determined using multi-point H_2O-BET and N_2-BET, while X-ray diffraction (XRD), CEC and exchangeable cation assessments were used for additional control. We discuss the challenges of homoionization validation and outline a path towards a standardised, reproducible THMSA measurement framework, with broader implications for quantifying mineral reactivity in geological and environmental systems, especially where mineral-water interactions are involved.

Key words: Clay, Brunauer-Emmet-Teller, Soil, Sediment, Smectite

EXTRACELLULAR METABOLISM AND MEMBRANE INTERFACE ELECTRON TRANSFER REPROGRAMMING ENHANCE BIO-OXIDATION OF RHODOCHROSITE BY BIFA-DELETED PSEUDOMONAS PUTIDA MNB1

Lei GAO[1], Dongmei ZHANG[4], Huan LIU[2,3], Juan LI[2], Xiancai LU[2*]

1. School of Marine Science and Engineering, Nanjing Normal University, China
2. State Key Lab for Mineral Deposits Research, School of Earth Sciences and Engineering, China
3. Key Laboratory of Surficial Geochemistry, Ministry of Education, School of Earth Science and Engineering, Nanjing University, China
4. School of Life Sciences, Nanjing University, China

Abstract Microbially mediated Mn(II) oxidation is widespread in natural environments and represents a key driving process in the biogeochemical cycling of manganese. This process is jointly regulated by multiple mechanisms, including enzymatic oxidation, reactive oxygen species (ROS)-mediated reactions, extracellular polymeric substances (EPS), and cell surface mineralization interfaces. However, how biofilm-regulating signaling genes systematically influence Mn(II) oxidation efficiency through metabolic regulation remains poorly understood.

In this study, the Mn-oxidizing bacterium Pseudomonas putida MnB1 was employed as a model organism. A biofilm-enhanced Δ*bifA* mutant was constructed, and its Mn oxidation phenotype, proteomic profile, and extracellular metabolic composition were systematically compared with those of the wild-type strain. The results demonstrated that deletion of bifA significantly enhanced Mn(II) oxidation efficiency. This enhancement was not simply attributed to increased biofilm formation or EPS production, but rather to a coordinated strengthening of transmembrane transport capacity, energy metabolism supply, and the extracellular redox microenvironment. These changes stabilized low-and intermediate-valent manganese in precipitates, thereby systematically improving Mn(II) oxidation efficiency. Proteomic analysis revealed that bifA deletion led to significant downregulation of outer membrane modification and transport-related proteins (e.g., ArnT and PotA), while certain ABC transporters (e.g., BraF) were significantly upregulated. Additionally, characteristic catabolic pathways, including malonate decarboxylation (the mdc operon) and phenylacetate degradation (the paa gene cluster), were markedly enriched. These metabolic shifts increased the proportion of aromatic and quinone-like components at the cell membrane interface, while reducing alkyl and O-alkyl reductive fractions, thereby creating a more redox-active extracellular microenvironment. High-resolution Mn2p XPS peak deconvolution showed that precipitates from both the wild-type and ΔbifA strains were dominated by mixed-valence manganese species, including Mn(II), Mn(III), and Mn(IV). In the ΔbifA group, the relative proportion of Mn(II) increased from 23.6% to 27.0%, while Mn^{3+} and Mn^{4+} remained largely

unchanged. This indicates that bifA deletion did not significantly promote the complete oxidation of Mn^{2+} to high-valent MnO_2, but instead enhanced Mn(II) oxidation efficiency by stabilizing low- and intermediate-valent manganese species within the precipitates. This study reveals a molecular mechanism by which biofilm-regulating genes modulate microbial Mn(II) oxidation through metabolic reprogramming, providing new insights into the microbially driven manganese biogeochemical cycle at the molecular level.

Key words: Pseudomonas putida MnB1, gene bifA, microbial Mn(II) oxidation mechanisms, c-di-GMP

FIRE-INDUCED REDISTRIBUTION AND ISOTOPIC FRACTIONATION OF SOIL ORGANIC CARBON AMONG DENSITY FRACTIONS

Jinsuo Li [1,2], Luping Tian [1,2], Zhaofeng Chang [1,2*], Genghao Zhang [1,2], He Xu [1,2],Yunjiang Yu [3], Bo Pan [1,2*]

1. Yunnan Provincial Key Lab of Soil Carbon Sequestration and Pollution Control, Faculty of Environmental Science & Engineering, Kunming University of Science & Technology, Kunming 650500, Yunnan, China
2. Yunnan International Joint Laboratory for Emission Reduction and Carbon Sequestration in Agricultural Soils, Kunming 650500, Yunnan, China
3. School of Environmental Science and Engineering, Shanghai Jiao Tong University, Shanghai 200240, China

Abstract Fire-induced soil organic carbon (SOC) transformation and isotopic fractionation are typically ignored when investigating SOC turnover in post-fire vegetation recovery. To specifically focus on the fire-induced processes, laboratory-controlled pyrolysis of forest soils was studied in a temperature gradient (simulating fire intensities) by combining density fractionation, molecular biomarker, and $\delta^{13}C$ analysis. Results showed that increasing fire intensity reduced SOC content, enhanced carbon aromatization, and generated substantial pyrogenic carbon (PyC). The free light fraction (fLF) exhibited higher SOC loss and lower PyC yield compared to the heavy fraction. Preferential loss of light isotopes (^{12}C) enriched ^{13}C in residual pools, elevating $\delta^{13}C$ in bulk soil from -26.0‰ to -21.8‰. The most pronounced ^{13}C enrichment occurred in fLF due to extensive SOC loss, and this enriched carbon was readily solubilized into dissolved organic matter (DOM). Notably, the isotopic fractionation during fire significantly exceeded typical microbial-induced fractionation <3‰. DOM extracted from soils heated to 400 °C featured aromatic and phenolic-C structures, indicating PyC origins. But DOM extracted from soils heated to 550-700 °C contained mostly carboxyl and carbonyl-C, derived from highly oxidized SOC. These ^{13}C-enriched components intensified fractionation between DOM and residual organic carbon. This study clarifies mechanisms of fire-driven SOC redistribution and isotopic fractionation, highlighting the critical role of wildfire in soil carbon cycling.

Key words: Heating, Soil density fractionation, Molecular markers, 13C isotope fractionation, Dissolved organic matter

FORMATION PROCESS OF CALCIUM CARBONATE IN ANIONIC CHEMICAL HYDROGEL WITH COUNTER-DIFFUSION METHOD

Yanli Wang[1], Shinji Matsumoto[1], Jun Kawano[2], Takaya Nagai[2], Ayako Shinozaki[2], Takayuki Kurokawa[3]

1. Graduate School of Science, Hokkaido University, Japan
2. Faculty of Science, Hokkaido University, Japan
3. Faculty of Advanced Life Science, Hokkaido University, Japan

Abstract Calcium carbonate ($CaCO_3$) exhibits multiple formation mechanisms under different conditions and is widely used as a model system for studying crystal growth. In the last decades, the synthesis of calcium carbonate in gel matrix has been focused on as a method to mimic biomineralization. The porous structure and the specialty to suppress convective transport made the gel an ideal medium to resemble natural porous systems. However, the interaction between reacting ions and gel mesh remains unclear. To address this issue, chemical gel was introduced in this study in addition to the widely used physical gel (Agar gel, Agarose etc.). Chemical gels can be fully controlled with their pore size, charge and functional group to make the synthesis environment designable. Additionally, our group successfully visualized pH shift during synthesis in gel system by using a fluorescent probe whose fluorescence intensity varies with pH. In this study, we applied this visualization technique for the $CaCO_3$ formation process in a chemical gel in order to explore the interaction between gel and reacting ions.

For the experiment, agar gel (physical gel) and PNaAMPS gel (chemical gel) were used for the synthesis medium. They both are anionic hydrogels. The pore size of PNaAMPS gel can be estimated to be about 50 times smaller than that of agar gel. The crystal growth was conducted in a counter diffusion system where reacting solutions ($NaHCO_3$ and $CaCl_2$) slowly diffused from both sides. The crystallization process was captured by time-lapse recording with a certain time interval under optical microscopy. Characterization of resulting precipitates was mainly undertaken by Micro-Raman spectroscopy and their morphologies were observed by scanning electron microscopy (SEM). 8-hydroxypyrene-1,3,6-trisul-fonic acid (HPTS) was used as a pH indicator, and added into gels and reaction solutions at 40 mM. This synthesis was conducted under fluorescence microscopy, irradiating the sample with ultraviolet light to visualize the pH shift in real-time.

Optical microscopy revealed that in both physical and chemical gels, crystals directly nucleated close to the HCO_3^- side without the presence of an amorphous calcium carbonate (ACC) band observed in some previous researches. The resulting $CaCO_3$ crystals showed different polymorphs in different gel. In agar gel, rhombohedral calcite formed first, then aragonite formed gradually

much closer to the HCO_3^- reservoir side. In the PNaAMPS gel, only calcite formed in a relatively wider area. In this case, fewer but bigger crystals formed than those in physical gels.

Fluorescence microscopy showed significant differences in pH shift during the formation process in gels. After the experiment began, pH increased from the HCO_3^- reservoir side in both gels. In physical gels, nucleation of calcite occurs soon after reactants meet each other, with a sharp decrease of pH in the nucleation area. On the other hand, in chemical gels, even after pH increased from the HCO_3^- side all the way to the Ca^{2+} side, the nucleation did not occur. Nucleation was postponed for several hours, and no sharp decrease in the pH was observed. This may be due to the results that nanoscale chemical gel mesh limits ion diffusion and the nucleation of $CaCO_3$. These results suggest that the synthesis of $CaCO_3$ in the chemical gel with pH visualization has great potential for $CaCO_3$ formation research. We are considering further observation of $CaCO_3$ formation in chemical gels with different charges and pore sizes. It may confirm gel-crystal interactions and provide new insights of formation mechanisms.

Key words: Calcium carbonate, Chemical hydrogel, pH visualization

FROM DYNAMIC MARGINS TO THE GREAT OXIDATION EVENT: NANOSCALE IRON-ORGANIC CARBON COUPLING AND ITS BIOGEOCHEMICAL IMPLICATIONS

Heng Xiao, Zhe Zhou*

State Key Laboratory of Marine Geology, School of Ocean and Earth Science, Tongji University, China

Abstract Nanoscale iron (oxyhydr)oxides play a pivotal role in the global carbon cycle by preserving organic matter in modern marine sediments and potentially catalyzing the synthesis of complex organic macromolecules in early Earth environments. However, the mechanistic linkages between nanoscale mineral formation and the molecular alteration of organic carbon across varying spatiotemporal scales remain poorly constrained, particularly under non-steady-state redox conditions. This study investigates the dynamic coupling of iron (Fe) and dissolved organic matter (DOM) at the mineral-water interface, bridging modern estuarine processes with simulated Precambrian ferruginous ocean conditions.

First, focusing on modern dynamic margins, we conducted controlled incubations simulating rapid Fe(II) reoxidation in the Changjiang Estuary. Using Fourier-transform ion cyclotron resonance mass spectrometry (FT-ICR MS), we reveal that Fe(II) reoxidation acts as a highly selective "molecular filter." During the rapid nucleation of nanoscale Fe(III) (oxyhydr)oxides, terrestrial aromatic DOM is preferentially removed via association with these precipitating phases. Concurrently, the generation of reactive oxygen species (ROS) induces the degradation of specific organic components, while abiotic sulfurization and nitrogen incorporation into DOM are also evidenced. Ultimately, the presence of precipitating nanoscale iron minerals promotes the formation of new, complex polymeric structures, shifting the DOM pool towards a more aromatic and refractory composition.

Building upon these modern mechanistic insights, we extrapolate the Fe-carbon interactions to the Archean-Paleoproterozoic transition. During the Great Oxidation Event (GOE), episodic "whiffs of oxygen" into ferruginous and silicic oceans would have triggered massive precipitation of nanoscale iron and silica-iron phases. We present a highly controlled, strictly abiotic experimental framework simulating these GOE pulses using artificial Archean seawater. By introducing simple prebiotic precursors (e.g., ribose and glycine) and utilizing a multi-modal analytical approach (integrating ultra-high-resolution mass spectrometry and synchrotron X-ray spectroscopy), we explore how the specific mineralogy of nanoscale Fe-Si precipitates dictates the abiotic polymerization pathways of early organic matter. We hypothesize that the unique surface reactivity of these nanoscale minerals, coupled with silica-mediated ROS suppression, might have functioned as protective and catalytic

templates, facilitating the assembly of complex macromolecules and the covalent doping of essential elements like sulfur and phosphorus.

By bridging instantaneous interfacial reactions in modern estuaries with long-term geological processes, this research provides a comprehensive perspective on nanoscale mineral-organic interactions. Our findings highlight the dual role of nanoscale iron minerals in shaping the modern marine carbon reservoir and potentially orchestrating prebiotic chemical evolution during major Earth oxygenation events.

Key words: Iron-carbon coupling, Nanoscale minerals, FT-ICR MS, Great Oxidation Event, Organic matter preservation

IMPACT OF SELECTED BIOMOLECULES ON CACO3 CRYSTALLIZATION KINETICS

Mingjie Wang[#], Baohua Zhuo[#], Zhaoyi Dai[*]

State Key Laboratory of Geomicrobiology and Environmental Changes (GMEC), School of Earth and Planetary Sciences, China University of Geosciences, Wuhan 430078, China

Abstract Calcium carbonate ($CaCO_3$) is one of the most common carbonate minerals occurring in both geological processes and industrial operations. Understanding the impacts of typical biomolecules on $CaCO_3$ crystallization is critical for deciphering the biomineralization process of $CaCO_3$ and the development of biomimic scale inhibitors for industrial uses. However, to the best of our knowledge, systematic study of the quantitative effects of biomolecules on $CaCO_3$ crystallization kinetics remains scarce. In this study, the induction time (t_{ind}) of $CaCO_3$ with or without nine biomolecules, including four amino acids (L-aspartic acid (L-Asp), L-glutamic acid (L-Glu), L-histidine (L-His), and L-arginine (L-Arg)), three polysaccharides (pullulan (PL), xanthan gum (XG) and carboxymethyl cellulose (CMC)), and two phospholipids (phosphatidyl ethanolamine (PE) and phosphatidyl serine (PS)) were measured using a laser apparatus at condition of a calcite saturation index ($SI_{calcite}$) from 1.00 to 1.90, *pH* from 7.78 to 8.05, temperature (T) from 25 to 90 °C and biomolecule concentrations from 0 to 500 mg/kg H_2O. The results showed that negatively charged amino acids (L-Asp, L-Glu) and polysaccharides (CMC) show inhibitive effects, while the positively charged amino acid (L-Arg) shows promotion effects and the neutral biomolecules (L-His, PL and XG) show negligible effects. However, the positively charged PE also shows inhibitive effects while the negatively charged PS shows negligible effects. As a result, it is proposed that the interactions between aqueous ions, crystals (or nuclei), and the biomolecules are not only based on electrostatic interaction, but also competition and surface adsorption, governing $CaCO_3$ crystallization kinetics. The morphology changes measured by Scanning Electron Microscope showed that the biomolecules that inhibit the $CaCO_3$ crystallization (L-Asp, L-Glu, CMC, and PE) tend to precipitate near-spherical $CaCO_3$ solid with smooth surfaces and edges, whilst the biomolecules promoting the $CaCO_3$ crystallization (L-Arg) are inclined to precipitate $CaCO_3$ with better structured rhombohedral crystals, and biomolecules showing no impact (L-His, PL and XG) on the crystallization have no effects on morphology.

Key words: green inhibitor, scale inhibition, amino acid, polysaccharide, phospholipid

IRON MINERAL-ORGANIC MATTER INTERACTIONS DRIVE THE BIOGEOCHEMICAL CYCLES OF HEAVY METALS AND CARBON IN SOILS

Xinde Cao*, Xiaoyun Xu, Wenfeng Huang, Zibo Xu, Ling Zhao, Bo Chen
School of Environmental Science and Engineering, Shanghai Jiao Tong University, China

Abstract Minerals such as iron oxides and organic matter are fundamental soil constituents, whose interactions and interfacial behaviors govern element cycling and pollutant transformation. This study systematically investigated the reciprocal interactions between minerals and organic matter and their implications for heavy metal mobility, redox state, and carbon sequestration. Key findings include: (1) Ferrihydrite (Fh) catalyzed the polymerization of small organic molecules (e.g., glucose and glycine), yielding predominantly recalcitrant lignin-like compounds. The catalytic mechanisms involved electron acceptance from reducing sugars and cation bridging via dissolved metal ions. Notably, 52.2–84.8% of Maillard-like molecules were detected in natural soil dissolved organic matter, suggesting that mineral-catalyzed Maillard reactions represent a significant yet overlooked pathway in soil organic matter formation. (2) During organic matter humification, increasingly mature organic matter strongly inhibited Fe(II)-mediated Fh crystallization, reducing its transformation to lepidocrocite/goethite. This inhibition was closely associated with the accumulation of highly unsaturated and phenolic compounds (HUPs), which disrupted interfacial electron transfer and mineral nucleation. Consequently, the impeded crystallization promoted selective adsorption of HUPs and their conversion to condensed aromatics, thereby enhancing preservation of advanced humification-stage organic carbon. (3) Organic matter humification also redistributed As associated with Fh in paddy soil. Substantial As was released during the degradation stage but was re-immobilized in the maturation stage. Throughout this process, low-crystalline As/Fe species evolved into more stable forms. Release was driven by HUP accumulation and enriched *Enterobacter* and *Sphingomonas*, which promoted Fh and As(V) reduction. Re-immobilization was facilitated by carboxylic-rich alicyclic molecules, while C–O–Fe bonds in organo-mineral complexes contributed to solid-phase As/Fe stabilization. (4) The iron-bearing minerals enhanced Cr(VI) reduction by organic carbon across soils, with iron-rich red soil showing the highest reduction capacity. Iron minerals facilitated both direct reduction (by neutralizing organic carbon's negative charge) and indirect reduction (by mediating electron transfer from organic carbon to Cr(VI)). Mineral crystallinity further influenced the electron transfer pathway: low-crystallinity ferric oxyhydroxides favored indirect reduction via inner-sphere Cr(VI) complexation and C–O–Fe electron shuttling, whereas higher crystallinity promoted direct electron transfer between organic carbon and Cr(VI). Collectively, this work advances the mechanistic understanding of iron mineral–organic carbon interactions and their critical role in governing the

biogeochemical cycles of heavy metals and carbon in soils.

Key words: Soil chemistry, Iron mineral-organic matter interactions, Electron transfer, Pollutant transformation, Carbon sequestration

LI-FE INTERACTIONS: A TALE OF THE ROLE OF INTERFACES IN THE UPTAKE OF LI BY FE-OXIDES

Helen E. King[1], Xu Yvon Zhang[2], Oliver Plümper[1]

1. MARUM, University of Bremen, Bremen, Germany
2. Department of Earth Sciences, Utrecht University, Utrecht, The Netherlands

Abstract Chemical weathering processes play a key role in regulating the global climate over geological time scales. Lithium (Li) isotope compositions have proven to be a robust proxy for tracing weathering processes that produce secondary minerals, such as clays and oxides. These materials do not contain Li as a dominant ion and thus, the interaction of Li with these phases occurs as a trace element during mineral growth or through interactions across the interface between the precipitated minerals and a fluid reservoir. In particular, the interaction between Li and Fe-oxides has long been inferred based on field observations, but experimental constraints on this process are lacking. Here, I will present a paper recently published from my group led by Dr. Zhang investigating the geochemical behavior of Li its interaction with different forms of Fe-oxides: goethite, hematite, wüstite, and magnetite. We observed that solution pH plays an important role in the uptake of Li with poorly crystallized goethite nanoparticles take up ~20% of dissolved Li over a pH range from ~4 to ~10. This rises to ~90% at pH ~12. In contrast, the sorption of dissolved Li is insignificant for well-crystallized Fe-oxides (hematite, wüstite, magnetite, and goethite). This implies that simply adsorption to goethite surfaces is not the dominant mechanisms of Li uptake, as minimal uptake occurs with the highly crystalline forms. Instead, a dynamic process of dissolution and reprecipitation at the mineral surfaces could explain the higher uptake in less crystalline goethite. This process is cryptic as direct evidence for newly formed materals cannot be easily distinguished in the less crystalline goethite material. Incorporation of Li into newly formed goethite that is promoted by the recrystallisation preferentially takes up light ^{6}Li isotopes, resulting in an isotope fractionation of $\Delta^{7}Li_{oxide\text{-}fluid} \sim -16.7$ to -20.1‰. Overall, the study provides valuable data to better understand the processes occurring in highly weathered soil and sediment profiles that are rich in Fe-oxides, such as laterites. This research also emphasizes the importance of chemical conditions at mineral surfaces during mineral–water interactions and illuminates the mechanisms of large-scale Li extraction for future applications.

Key words: Lithium, isotope fractionation, iron oxides, recrystallisation

Acknowledgements This research was funded by the Dutch Research Council (OCENW.M20.156) and was supported by technical assistance with Dr. Hamers at Utrecht

University for electron microscopy imaging as well as Dr. Wilson at Univeristy College London for Li isotope analysis. The project was completed in close association with Prof. Pogge von Strandmann, now at Johannes Gutenberg University Mainz. All of these collaborators are also co-authors on the original work.

LIGHT-INDUCED COUPLING PROCESS OF FE REDOX CYCLING AND NATURAL DISSOLVED ORGANIC MATTERS OXIDATIVE DECOMPOSITION AT GOETHITE SURFACE

Shanshan Yang[1], Anhuai Lu[2]

1. China University of Geosciences (Beijing), Beijing, China
2. Peking University, Beijing, China

Abstract The interactions between widespread iron (oxyhydr)oxides (Fe oxides) and natural soil dissolved organic matters (DOM) are the dominant drivers in the geochemical behavior of Fe and the cycle of carbon in soil. Under visible light irradiation, their interactions become more complex due to the unique semiconducting structure of Fe oxides and complex components in DOM, which have not been deeply studied. In this study, the complex reactions occurred at the DOM-goethite interface under irradiation were investigated in detail. $Fe^{2+}_{(aq)}$ from goethitereductive dissolution was accumulated at the DOM-goethite interface, along with the generation of reactive oxidative species (ROS). The reasons could be ascribed to the enhanced generation of photoelectron from the conduct band of goethite, ligand-to-metal charge transfer and photolysis of Fe(III)-carboxylate complexes. Moreover, the generated ROS were the main driving forces in the coupling process of Fe redox cycle and oxidative decomposition of DOM at goethite surface, inducing the formation of secondary Fe minerals and chemical composition change of DOM. This work provided new insights into the light-induced coupling process of Fe semiconducting minerals reductive dissolution and dissolved organic matters oxidation in top soil.

Key words: Goethite, Soil dissolved organic matters, Reductive dissolution, Oxidative decomposition

LIGHT TO LIFE: ROLES OF MINERAL PHOTOCHEMISTRY IN PLANETARY HABITABILITY

Jihua Hao

School of Earth and Space Sciences, University of Science and Technology of China, China

Abstract The surfaces of early Earth and Mars were likely exposed to intense ultraviolet radiation because of the absence or weakness of protective ozone layers, allowing high-energy photons to drive widespread photochemical reactions involving surface materials. Minerals, as ubiquitous components of planetary surfaces, are not merely passive substrates but can directly participate in or catalyze photochemical processes relevant to planetary habitability. In this talk, I will synthesize previous studies and our recent findings on the photochemical reactivity of common surface minerals and the key factors that regulate these reactivities. I will further discuss how mineral-driven photochemistry may have contributed to the origin of life and early metabolic evolution by promoting the synthesis of prebiotic molecules, regulating the cycling of bioessential elements, generating redox gradients, and translating high-energy photons to bioavailable electrons. Finally, by integrating laboratory experiments with geological observations, I will explore how mineral photochemistry may have influenced the redox evolution of planetary surfaces and the preservation of potential biosignatures in the geological record.

Key words: photochemistry, early Earth, Mars, habitability, biosginatures

MANGANESE OXIDE FACILITATES PREBIOTIC EVOLUTION ON EARLY EARTH AND MARS

Zening Yang[1,2,3], Yamei Li[*1,3], Ryuhei Nakamura[*1,2,3]

1. Earth-Life Science Institute, Institute of Future Science, Institute of Science Tokyo, Meguro-ku, Tokyo 152-8550, Japan.
2. Department of Chemical Science and Engineering, School of Materials and Chemical Technology, Institute of Science Tokyo, Ookayama, Meguro-ku, Tokyo 152-8552, Japan.
3. Biofunctional Catalyst Research Team, RIKEN Center for Sustainable Resource Science, Wako, Saitama 351-0198, Japan. Present address for Yamei Li: School of Earth and Space Sciences, University of Science and Technology of China, Hefei 230026, China. (yamei.li@ustc.edu.cn)

Abstract Hydrogen cyanide (HCN) is widely recognized as one of the most important feedstock molecules for prebiotic chemistry because it participates in the synthesis of amino acids, nucleobases, lipids, sugars, and protometabolic intermediates. However, most traditional models for HCN production rely on highly reducing methane-rich atmospheres, which are increasingly considered unlikely for the Hadean Earth and ancient Mars. Therefore, identifying alternative geochemical pathways capable of sustaining cyanide production under nonreducing conditions is essential for understanding the emergence of life.

Here we report a mineral-facilitated pathway for aqueous HCN synthesis from prebiotically abundant amino acids under ambient conditions. Systematic screening of 38 naturally occurring minerals revealed that manganese dioxide (MnO2) efficiently promotes the conversion of glycine into cyanide in anaerobic aqueous environments. The reaction proceeds across a broad range of geochemically plausible conditions, including pH 2–12.6, temperatures from 6–60 °C, and substrate concentrations from 1 μM to 100 mM. Cyanide generation reached millimolar levels with a maximum selectivity of 57%.

Isotopic labeling experiments demonstrated that cyanide originates from the α-carbon of amino acids, indicating that MnO2 activates the α-C–H bond through an oxidative dehydrogenation pathway distinct from conventional amino acid decarboxylation chemistry. In addition to cyanide, the reactions simultaneously generated ammonium and multiple α-keto acids, including intermediates related to the reverse tricarboxylic acid (rTCA) cycle and glyoxylate chemistry. Cyanide formation was further confirmed for a broad range of proteinogenic amino acids and short glycine peptides, demonstrating that amino acids could function not only as stable end products of prebiotic synthesis but also as dynamic reservoirs for reactive carbon and nitrogen species.

These findings suggest that manganese oxides may have played a central role in coupling amino acid chemistry, cyanide production, and protometabolic network development on the early Earth. Because amino acids can be synthesized through methane-independent pathways using CO2, CO,

nitrate, and nitrite, the amino acid-to-HCN conversion pathway alleviates the dependence of prebiotic cyanide synthesis on reducing atmospheres. Furthermore, manganese minerals are geochemically plausible on both early Earth and Mars. Photochemical oxidation of dissolved Mn(II), oxyhalogen-mediated oxidation, and transient oxidative processes could have continuously regenerated Mn(IV) oxides in shallow aqueous environments, sustaining long-term HCN production.

The mechanistic similarity between this mineral-mediated chemistry and modern biological cyanide biosynthesis pathways also suggests a possible evolutionary continuity from geochemistry to biochemistry. Our results therefore support a broader view in which manganese oxides acted as multifunctional geochemical catalysts that promoted the coevolution of metabolism and information-bearing molecules on habitable rocky planets.

Key words: Hydrogen cyanide, Origin of life, Prebiotic chemistry, Early Earth and Mars

METABOLOMICS-BASED ANALYSIS OF THE INTERACTION EFFECTS AND STRESS RESPONSE MECHANISMS IN THE CO-CULTURE SYSTEM OF FUNGI AND MICROALGAE UNDER CADMIUM STRESS

Junjun Wang[1], Qinghua Tian[2], Jue Kang[2], Hao Zhou[2], Xinyi Yu[2], Guanzhou Qiu[2], Li Shen[b*]

1. School of Environment and Resource，Southwest University of Science and Technology，Mianyang, Sichuan, 621010
2. School of Metallurgy and Environment, Central South University, Changsha, Hunan, 410083,

Abstract Research on the co-culture of fungi and microalgae to harvest microalgae and enhance the adsorption capacity for heavy metals to reduce contamination is well demonstrated, but the study of the correlation mechanism among critical metabolites, system stability, and stress response in the system under cadmium stress based on metabolomics analyses has not been reported in detail. In this study, the co-culture system of *Aspergillus allahabadii* and *Synechocystis* sp. PCC6803 was taken as the object of investigation, and isotope labelling (^{13}C-Na_2CO_3 and ^{15}N-$(NH_4)_2SO_4$) and nanoscale secondary ion mass spectrometry were used to confirm the existence of carbon and nitrogen nutrient exchange. The adsorption behavior of the system after Cd treatment was investigated by Fourier Transform Infrared Spectroscopy, X-ray Photoelectron Spectroscopy, and Scanning Electron Microscope/ Transmission Electron Microscope. The content of extracellular polysaccharides in the system was increased from 40.8 mg/g to 80.12 mg/g, and the content of extracellular proteins was increased from 22.3 mg/g to 55.68 mg/g after 96 h of Cd treatment. Metabolomics results revealed 235 differential metabolites co-expressed after Cd treatment, with 95, 15, and 77 unique differential metabolites. In particular, the synthesis of extracellular polymeric substances was a factor affecting the stability of the symbiotic system, the up-regulation of the expression of the transporter system was one of the reasons for the improvement of the system's tolerance and resistance to heavy metals; and the nutrient metabolism between the fungus and the microalgae was the main defense mechanism to reduce the extent of the impairment of the system's carbon sequestration capacity by Cd. This provides a theoretical basis for the green and economically friendly application of the symbiotic system in microalgae harvesting, efficient carbon dioxide fixation and reduction of heavy metal pollution.

Key words: fungi-microalgae symbiotic system, cadmium, extracellular polymeric substances, metabolomics, nanoscale secondary ion mass spectrometry

METASTABLE MINERALS AS KEY CONTROLS ON WATER CHEMISTRY EVOLUTION AND CARBONATE PRECIPITATION IN ALKALINE LAKES

Daehyeon An[1], Shuukhaaz Ganbat[1], Baasansuren Gankhurel[2,3], Noriko Hasebe[3], Shinya Ochiai[3], Davaadorj Davaasuren[2], Keisuke Fukushi[3]

1. Graduate School of Natural Science & Technology, Kanazawa University, Japan
2. Department of Geography, National University of Mongolia, Mongolia
3. Institute of Nature and Environmental Technology, Kanazawa University, Japan

Abstract Alkaline lakes are high-pH, high-alkalinity closed-basin systems that host productive ecosystems and offer useful settings for investigating water-rock-carbonate interactions (Heins et al., 2023; Fukushi and Matsumiya, 2018). Their water chemistry evolves through inflow, evaporation, gas exchange, and mineral precipitation, yet conventional evaporative concentration models that assume stable carbonate and silicate phases do not adequately explain the dissolved Ca and Mg behavior observed in natural lakes (Garrels and Mackenzie, 1967). Recent mineralogical and experimental studies instead suggest that metastable phases can govern lake-water chemistry during active evaporation (Fukushi et al., 2020; Fukushi and Matsumiya, 2018; Zeyen et al., 2021). This mismatch is important because it affects not only interpretation of dissolved chemistry, but also discussion of carbonate precipitation during lake-water evolution. In this study, we constructed an evaporative concentration model for Boon Tsagaan Lake in southern Mongolia to examine whether metastable minerals better explain alkaline-lake evolution than conventional stable-phase models. Boon Tsagaan Lake is a terminal lake with no surface outflow and receives inflow mainly from the Baidrag River. The model was developed using field observations of lake water and inflow water, hydrological constraints, and mineralogical observations showing monohydrocalcite in lake suspended solids but not in river samples, consistent with previous evidence for authigenic MHC formation in Boon Tsagaan Lake (Fukushi et al., 2020). It initializes the lake with inflow-like water chemistry under open-system conditions with respect to atmospheric CO^2 and simulates evaporation balanced by river inflow. The model explicitly considers precipitation of phases regarded as important for alkaline-lake chemistry, including monohydrocalcite, amorphous Mg carbonate, and Mg-silicate hydrate. The metastable-mineral model reproduces the present water chemistry of Boon Tsagaan Lake more consistently than the conventional equilibrium model of Garrels and Mackenzie (1967), particularly for reactive dissolved ions such as Ca, Mg, HCO^3, and Si. This improved reproduction of lake-water chemistry provides a stronger basis for discussing carbonate precipitation during evaporative evolution. The results indicate that metastable phases are not minor by-products, but key controls on aqueous speciation, Ca and Mg behavior, and carbonate mineral formation in this alkaline-lake system. This case study also suggests that, in Boon Tsagaan Lake,

stable minerals preserved in sediments may reflect later transformation rather than the phases that directly regulated the water column during active evaporation. The geochemical model developed here provides a basis for realistic reconstruction of water-chemistry evolution in alkaline lakes. For Boon Tsagaan Lake, improved constraint on the present geochemical stage along the modeled evaporation trajectory enables quantitative evaluation of carbonate precipitation at the present stage of the lake. More broadly, such quantitative prediction of carbonate precipitation provides a framework for assessing the magnitude of alkaline-lake contributions to the terrestrial carbon cycle. The same framework may also be applied to quantitative evaluation of the effectiveness of enhanced rock weathering in alkaline-lake systems through its influence on carbonate precipitation.

Key words: Alkaline Lake, Geochemical Modeling, Metastable Phases, Carbonate Precipitation, Evaporative Concentration

MICROBIAL CONTROLS ON HYDROZINCITE FORMATION IN MINE DRAINAGE

Salvatore Guerrieri [1] *, Mario Borrelli[1], Giovanni Battista De Giudici [2], Jonathan Lloyd [3], Daniela Medas [2], Edoardo Perri[1]

1. Dipartimento di Ingegneria dell'Ambiente, Università della Calabria, Rende, Cosenza, Italy
2. Department of Chemical and Geological Sciences, University of Cagliari, Cagliari, Italy
3. Department of Earth and Environmental Sciences, The University of Manchester, Manchester, UK

* Corresponding author: salvatore.guerrieri@unical.it

Abstract Environmental pollution from mine drainage represents a critical global challenge, due to the mobility of potentially toxic elements, released from mine wastes and contaminated waters. In Neutral Mine Drainage (NMD) systems, inhabitant microbial communities that can mediate the precipitation of metal and metalloid rich secondary (bio)minerals, represent a natural attenuation mechanism for pollutant dispersion. Along the Rio Roia Cani, one of the mine drainages within the Montevecchio mining district (Sardinia, Italy), microbial-mediated hydrozincite, a secondary zinc carbonate hydroxide [$Zn_5(CO_3)_2(OH)_6$] precipitates forming biosedimentary deposits, which shape the streambed as a "pools and barrages" morpho-structure. Such natural processes have positive impacts on the local environment, strongly reducing the dispersion of zinc, furnishing a potential new source of zinc, and sequestring free CO_2. The stream water exhibits circumneutral pH and a dominant SO_4-Zn-Ca composition, while the hydrozincite deposit, covering the streambed, is composed of two main depositional facies. The first are granular facies, consisting of a slightly hardened silt to fine sand grains filling the pool floors and coating river plants and pebbles of low-gradient barrages. Laminated (stromatolite-like) hard crusts also form with alternated porous and denser laminae, forming pseudo-planar and mamelonar bodies developing transversal to the water flow, forming in barrages and waterfalls. Regardless of the different degree of lithification, typical microbial microfabrics such as peloidal or globular and filamentous, characterize both the facies. Moreover, the basic mineral structure is unique between the facies, and given by 25-40 µm diameter hydrozincite globules, deriving from the isooriented to chaotic accumulation of platelet-like crystallites; 10-200 nm the shortest side, and 1-2 µm the longest. Microbial cells and extracellular polymeric substances (EPS) are strictly associated with the mineral units throughout the deposit, which partially to fully replace the organic mass. Mineral crystallites below 10 nm nucleates inside EPS surrounding the cells, suggesting that EPS serves as the main substrate for hydrozincite nucleation and growth. Data from 16S and 18S rRNA gene sequencing reveals a complex biota, related to the hydrozincite-forming biofilm: prokaryotes are dominated by Alphaproteobacteria (18.75%), Planctomycetes (13.26%), Chloroflexia (11.03%), Deinococci (10.84%) and Cyanobacteriia (10.08%) with *Phormidium* spp. as the most abundant genus. Eukaryotes are dominated by Dactylopodida (61,38%), and Centramoebida (38.62%), with *Angulamoeba* spp. and

Balamuthia sp. as the main genera. Among these, the cyanobacterium *Phormidium* spp. is thought to play a crucial role in the mediation of hydrozincite.

Key words: Biomineralization, hydrozincite, mine drainage, zinc

MICROBIAL-INDUCED PRECIPITATION OF APATITE-LIKE PRECIPITATES AND STABLE AMORPHOUS CALCIUM PHOSPHATE BY SALINITY-ACCLIMATIZED MARINE CYANOBACTERIA

Maria Dittrich[1, 2], M., David Aceituno-Caicedo[1,2]

1. Department of Physical and Environmental Sciences, University of Toronto, 1065 Military Trail, Toronto, ON, M1C1A4, Canada
2. Earth Sciences Department, University of Toronto, University of Toronto, 22 Ursula Franklin Street, M5S 3B1, Toronto, Canada

Abstract Microbial biomineralization governs key processes in aquatic geochemistry, yet the role of stress-induced cell lysis in the formation of precipitates remains underexplored. We investigated how salinity acclimation in marine cyanobacterium Synechococcus sp. PCC8806 influences precipitate formation following exposure to hypoosmotic shock. Using a combination of Scanning Electron Microscopy with Energy Dispersive X-ray Spectroscopy, Attenuated Total Reflection Fourier Transform Infrared Spectroscopy, and X-ray Diffraction, we tracked precipitates over 40 days for lineages pre-acclimated to freshwater-, marine-, or hypersaline conditions. Lineage-specific differences in OD_{650} and microscopy observations were consistent with varying degrees of membrane destabilization and release of intracellular material. Across treatments, we observed nanogranular, spherical aggregates, and colloidal morphologies tentatively classified as amorphous calcium carbonate (ACC) and amorphous calcium-magnesium phosphate (AMCP) that transformed over time into tentatively assigned amorphous calcium-phosphate (ACP), and apatite-like precipitates. FTIR bands associated with phosphate and carbonate varied among lineages, and EDS revealed treatment-specific Ca:P:Mg trends. Together, these observations demonstrate that salinity acclimation is associated with differences in intracellular release under osmotic-stress, which likely shapes precipitate composition and persistence. The results demonstrate that salt-induced stress can initiate biomineralization pathways independent of metabolic activity. The findings offer new insights into phosphorus cycling, amorphous precipitate stabilization, and lysis-driven mineralization mechanisms relevant to microbial mat systems, stromatolite formation, and sustainable biomineralization technologies such as bioremediation and bioconcrete. Confirmation of crystalline ordering and mechanistic steps will require additional targeted analyses.

Key words: Cyanobacteria, Synechococcus, Salinity, Amouphous CaCO3, Calcium-phosphate

MINERAL COMPOSITION OF MODERN BOTTOM SEDIMENTS SALT LAKES OF THE NORTH AND WEST OF THE CRIMEAN PENINSULA

Anna Mikhailovna Bessonova, Marina Valentinovna Charykova, Elena Pavlovna Kayukova
St. Petersburg State University, Institute of Earth Sciences, St. Petersburg, Russia

Abstract On the Crimean Peninsula, four groups of salt lakes are distinguished: Yevpatoria, Tarkhankut, Perekop, and Kerch. This study focuses on the Yevpatoria and Perekop groups. The Yevpatoria lakes are located along the coast of the Kalamitsky Bay (Black Sea), are of marine origin. They are historically associated with the development of the chemical industry and balneology. The Perekop lakes are situated on the Perekop Isthmus and include large continental lakes that have been actively exploited for chemical production since the mid-20th century.

The aim of this study is to determine the mineral and chemical composition of bottom sediments, taking into account both macro- and microcomponent composition of brines.

Fieldwork was conducted in June 2025. Samples of brines and surface bottom sediments were collected from eight lakes of the Yevpatoria group (Sasyk-Sivash, Saki, Adzhi-Baichi, Airchi, Konradskoye, Moinaki, Kyzyl-Yar, Bogaily) and five lakes of the Perekop group (Staroye, Krasnoye, Kiyatskoye, Kirleutskoye, Aigulskoye). Due to high moisture content, sediments could not be air-dried, therefore, brines were removed by drying samples between filter paper layers to prevent salt crystallization.

Mineral composition was determined using powder X-ray diffraction and scanning electron microscopy, while elemental composition was analyzed by X-ray fluorescence. Major ions in brines were determined by titrimetric and gravimetric methods, and trace elements by ICP-MS. Saturation indices were calculated using Geochemist's Workbench 9 software, applying Pitzer equations to estimate activity coefficients.

The calculations indicate that most brines are supersaturated with respect to calcium and magnesium carbonates. Halite saturation has not been reached, although in some lakes (Sasyk-Sivash and Staroye) brines approach equilibrium. Gypsum is saturated or supersaturated in most lakes.

Comparison of saturation indices with mineral composition shows that precipitation of halite, gypsum, and calcium carbonates is controlled by ion ratios and the degree of saturation. Compared to the Yevpatoria lakes, Perekop brines are enriched in Mg^{2+} and Cl^{-}, and their sediments contain dolomite along with calcite and gypsum. In contrast, Yevpatoria sediments consist mainly of calcite, aragonite, magnesian calcite, and gypsum.

The distribution of trace elements is important for both industrial and balneological applications. Concentrations of major ions, as well as Li, B, Sr, and Ba, in most brines exceed average seawater values due to evaporative concentration. The highest enrichment factors are observed for Fe, Mn, and Zn, possibly reflecting anthropogenic influence.

In bottom sediments, most trace element concentrations are close to average crustal values. In general, trace element content in minerals shows weak correlation with brine composition, except for Sr, which may precipitate as sulfate.

Spatial differentiation of authigenic minerals has been identified: framboidal pyrite is typical of the Yevpatoria lakes, whereas strontium and barium sulfates occur in the Perekop lakes. These differences reflect variations in redox conditions and sulfate deposition.

The Perekop lakes, which are actively exploited, are of particular environmental concern. Elevated concentrations of Mg, K, B, Li, Fe, and Mn were recorded in Lake Staroye, while Lake Krasnoye is characterized by high pH and enrichment in Ca, Ba, and Sr.

Comparison with data from the early and mid-20th century reveals significant changes in brine composition in several lakes (Staroye, Krasnoye, Kiyatskoye), including shifts in hydrochemical type, pH, and salinity, likely related to industrial activity.

Overall, the formation of bottom sediments is controlled by the combined influence of brine composition, lithogenic input, redox conditions, authigenic mineral formation, and anthropogenic factors. Saturation calculations agree well with the observed mineral composition for halite, gypsum, and calcium carbonates. However, the formation of magnesian carbonates appears to be influenced not only by supersaturation but also by additional processes, possibly including biogenic ones.

Key words: salt lakes, bottom sediments, halite, gypsum, carbonate minerals

Acknowledgements The research was carried out with the support of the Russian Science Foundation (grant No. 25-27-00167 «Salt lakes of Crimea: geochemical state, features of mineral formation and modeling in the brine-bottom sediment system»). When performing the work, the equipment of the Science Park of St. Petersburg State University was used (Resource centers «X-ray diffraction research methods» and «Methods for analyzing the composition of matter»).

MINERAL CONTROL ON ARSENIC MOBILITY: ANOXIC ARSENOPYRITE DISSOLUTION AND SCORODITE CRYSTALLIZATION

H. Henry Teng, Pei Chang, Minghao Tang, Yuebo Wang, Xiangyu Zhu

School of Earth System Science, Tianjin University

Abstract The environmental fate of arsenic depends on its release from primary sulfides and sequestration in secondary arsenate minerals. This study examines two under-characterized steps in this cycle: anoxic arsenopyrite leaching and the crystallization of amorphous iron-arsenate precursors into scorodite. Arsenopyrite dissolution is well studied under oxidizing conditions but poorly constrained in the anoxic settings typical of groundwaters and paddy soils. Using batch and flow-through experiments, we characterized arsenopyrite dissolution kinetics and speciation as a function of pH under anoxic conditions. Dissolution was near-stoichiometric for As and S but Fe-deficient, with alkaline pH mildly promoting As release. Unexpectedly, oxidized species (H_2O_2, SO_4^{2-}, $S_2O_3^{2-}$) and mixed-valence surface species were detected under nominally anoxic conditions, implicating intrinsic interfacial electron transfer rather than simple surface reactions—suggesting existing models are inadequate for oxygen-limited settings. Measured dissolution rates were fast enough to exceed the WHO 10 μg/L arsenic guideline within a single day. On the sequestration side, amorphous iron arsenate precipitates are important As sinks and common precursors to scorodite ($FeAsO_4 \cdot 2H_2O$). The ferric end-member (AFA) has been extensively characterized, but its ferrous counterpart (AFEA) has received comparatively little attention. We synthesized both phases and compared their composition, local structure, and crystallization behavior. AFEA (~53% Fe(III) by Fe K-edge XAS) carries a longer Fe–O bond (2.02 Å) than AFA or scorodite (1.99 Å), and this structural difference translates into measurably higher stability: AFEA crystallizes to scorodite more slowly under both atmospheric and aqueous conditions, apparently because it limits the availability of aqueous Fe^{3+} needed for the phase transition.

Taken together, these results clarify distinct geochemical controls on arsenic cycling—anoxic release governed by surface redox dynamics on sulfides, and downstream sequestration modulated by the Fe oxidation state and local structure of amorphous precursors—with direct relevance to groundwater risk assessment and industrial arsenic immobilization.

MINERAL-ENHANCED SEMI-ARTIFICIAL PHOTOSYNTHESIS IN PLANTS

Anhuai LU

School of Earth and Space Sciences, Peking University, China

Abstract The latest research in the international biological field reveals that the substance in plant chloroplasts responsible for absorbing sunlight to split water and produce oxygen and hydrogen is actually the inorganic mineral manganese cluster. What's even more interesting is that not only do plant chloroplasts contain manganese clusters on the Earth's surface, but similar manganese clusters also develop on rock surfaces after being exposed to solar radiation. They are all called birnessite, a high-performance semiconductor mineral. The similarity in structure and function between birnessite from mineral membrane and manganese clusters in biological chloroplasts suggests that the minerals have the foundation for converting solar energy. Inorganic world photocatalysis of minerals and organic world photocatalysis of organisms are jointly, mutually affected by solar radiation.

We have found that there are layered or membranous black materials widely distributed on the rock and soil surfaces. The mineral membrane from the Earth's surface is distributed so widely, and plays so important role in converting solar energy like artificial solar film covering the surface of the earth. It should be divided into a new Earth's sphere: mineral membrane. A variety of redox processes can occur on the Earth's surface, which is comparable to the photosynthesis status of the Earth's surface organisms. It is worth pointing out that the iron and manganese mineral membrane we found on the Earth may also exist on Mars. The black matter on Mars surface is estimated to be manganese oxide. Some people describe Mars surface as coated with a layer of sunscreen.

It should be emphasized that the mineral membrane we have found on the Earth's surface are also distributed in nano particles, which is very similar to the manganese clusters in plant chloroplasts. A new understanding has been proposed that birnessite and chloroplast manganese cluster have similarities in local structure and oxygen production function. It is believed that organic chloroplasts and inorganic mineral membrane have similarities. The formation of manganese clusters in chloroplasts is promoted by the presence of birnessite in the surface of mineral membrane.

However, the natural photosynthesis of plants utilizes no more than 2% of solar energy, significantly limiting the global production of agricultural food and vegetables. It should be pointed out that the efficiency of photosynthesis depends on the degree of photocatalytic water splitting. How to improve the photocatalytic activity of manganese clusters in chloroplasts towards water. In fact, the vibration frequency of far-infrared light is very close to the frequency of water molecule motion. We have found that certain semiconductor minerals can release far-infrared light under the

action of solar radiation, which directly affects the motion state of water molecules, at least weakening the hydrogen bonding strength of water molecules and reducing the free energy of water molecule photocatalytic cracking. By developing mineral infrared emission spectroscopy characteristics outside chloroplasts, water function can be improved, and the degree of functional water being cleaved by plant manganese clusters by sunlight can be enhanced, opening up a new way: semi-artificial photosynthesis to improve plant photosynthetic efficiency. Based on this, we have invented a method for preparing functional water. The results of the field experiment have achieved incredible increases in yield and quality, all due to the improved efficiency of plant photosynthesis. Not only does the plant grow well, but the root system of the plant is particularly developed, which can enhance the crop's strong resistance to lodging and insect pests. We have obtained disruptive new technologies for mineral enhanced semi-artificial biological photosynthesis, being extended to global agricultural production and provide certain guarantees for the food crisis faced by humanity.

Key words: mineral membrane, birnessite, manganese cluster, water function, semi-artificial photosynthesis

MINERAL EVOLUTION AS A CASE STUDY OF A NEW NATURAL LAW

Hazen, Robert M. and Wong, Michael L.

Earth and Planets Laboratory, Carnegie Institution for Science, Washington DC, USA; rhazen@ciw.edu

Abstract A pervasive wonder of the natural world is the evolution of varied systems, including stars, planets, minerals, and life—all of which have increased in diversity and patterning over deep time. However, no law of nature describes and explains, much less quantifies and predicts, the behaviour of complex evolving systems. Accordingly, we propose a new law of nature, the "law of increasing functional information," that applies to the evolution of both abiotic systems (notably minerals) and life [*1,2*]. This postulated increase in functional information represents a second arrow of time—one that is consistent with the increase in entropy (the first arrow of time) but is not derivable from the laws of thermodynamics [*3*].

This concept is now being applied and tested by other groups in fields as wide-ranging as the evolution of languages, the behaviour of AI systems, prebiotic chemical evolution, the seasonal variations of soil microbiomes, and the search for new cancer therapies [*4-7*]. Mineral evolution, which explores the diversification of Earth's mineral kingdom on more than 4.5 billion years, is an especially revealing test case of this proposed law of nature [*8*].

Key words: Mineral Evolution, Laws of Nature, Functional Information, Complex Systems

MINERAL-MICROBE COEVOLUTION THROUGH GEOLOGICAL TIME

Hailiang Dong

Department of Earth Sciences and Resources, China University of Geosciences-Beijing, China

Abstract Mineral-microbe interactions play important roles in environmental change, biogeochemical cycling of elements, and formation of ore deposits. Minerals provide both beneficial and detrimental effects to microbes, resulting in mineral-specific microbial colonization. Microbes impact dissolution, transformation, and precipitation of minerals through their activity, resulting in either genetically-controlled or metabolism-induced biomineralization. Through these interactions, minerals and microbes coevolve through Earth history. The mineral-microbe interactions typically occur at microscopic scale but the effect is often manifested at global scale.

One example is on N_2 fixation. The largest reservoir of nitrogen on Earth is nitrogen gas (N_2). To make it bioavailable, N_2 gas is fixed into ammonia by N_2-fixing microbes. N_2-fixation requires nitrogenases, within which Fe, Mo, or V serve as metal cofactors. Mo-based nitrogenase (Nif) is the most common and efficient. However, on early Earth Mo was bound in solids and presumably not bioavailable, yet nitrogen isotopes of sedimentary rocks and phylogenetic analysis suggest that Mo-based nitrogenase was the predominant class of enzymes in Archaean oceans. Therefore, the emergence of the Mo-based nitrogenase before the Great Oxidation Event, raises an apparent paradox. By incubating N_2-fixing microorganisms of different ages with Mo-bearing minerals and rocks, our results demonstrated that microorganisms can extract Mo from molybdenite and other minerals/rocks by secreting molybdophores and by expressing Mo transport proteins. Significant changes in surface chemistry of Mo-bearing minerals/rocks occurred after their interaction with microbes. These findings provide novel explanations for the prevalence of Mo-nitrogenase on early Earth, with significant implications for nitrogen fixation in modern Mo-deficient environments.

The second example is focused on how Ni bioavailability affects the growth and function of methanogens by incubating crushed igneous rocks with a model methanogen *Methanosarcina acetivorans*. These rocks significantly promoted the growth and methanogenesis. The released trace metals from peridotite and basalt, especially Fe, Ni, and Co, accounted for the promotion effect. Proteomic analysis revealed that rock amendment significantly enhanced the expression of core metalloenzymes in the methylotrophic methanogenesis pathway. These results have important implications for evolution of methane flux over geological time and also for using enhanced rock weathering as an approach to sequester atmospheric CO_2.

The third example is aerobic microbial methane oxidation, which plays an important role in methane cycle. This process is catalyzed by enzyme methane monooxygenase (MMO). Particulate MMO

requires Cu as a cofactor. However, studies have shown aerobic methanotrophic activity in environments with low aqueous Cu. We hypothesize that minerals can serve as a source of Cu. Laboratory experiments show that the presence of chalcopyrite significantly promote cell growth and methane oxidation, with similar rates and extents to those of aqueous Cu^{2+}. Aerobic methane oxidizers extract Cu from chalcopyrite by secreting a chalkophore through expressions of specific genes and proteins. These results provide insights into Cu bioavailability and have important implications for methane cycling on early Earth and in modern environments.

Key words: coevolution, methane cycle, microbe, mineral, nitrogen fixation

MINERALOGICAL CHARACTERIZATION OF FINE-GRAINED MATRICES IN RYUGU AND CARBONACEOUS CHONDRITES USING MG K-EDGE XANES SPECTROSCOPY

Reon Okumura[1], Haruki Oya[1], Kosuke Inoue[1], Takuma Fujiya[1], Keisuke Fukushi[2], Yoshio Takahashi[3], Ryoichi Nakada[4], Mizuho Koike[5], Takahiro Kawai[3,6], Tomohiro Ono[3], Shohei Yamashita[7], and Yoko Kebukawa[8]

1. Division of Geosciences and civil Engineering, Kanazawa University, Japan
2. Institute of Nature and Environmental Technology, Kanazawa University, Japan
3. Department of Earth and Planetary Science, The University of Tokyo, Japan
4. Kochi Institute for Core Sample Research, Japan Agency for Marine-Earth Science and Technology (JAMSTEC), Japan
5. Earth and Planetary Systems Science Program, Hiroshima University, Japan
6. NanoTerasu, National Institute for Quantum Science and Technology (QST), Japan
7. Institute of Materials Structure Science Photon Factory, High Energy Accelerator Research Organization (KEK), Japan
8. Department of Earth and Planetary Sciences, Institute of Science Tokyo, Japan

Abstract Carbonaceous chondrites, particularly CI chondrites, are among the most primitive meteorites in the Solar System and contain abundant water and organic matter. Their fine-grained matrices are dominated by Mg-rich hydrous silicates that record the physicochemical conditions of aqueous alteration on their parent bodies, providing important constraints on the environments in which organic matter formed and evolved. However, the dominant Mg-bearing phase in these matrices remains poorly constrained because conventional techniques such as XRD, EPMA, and TEM have limited ability to characterize poorly crystalline and compositionally heterogeneous materials.

Mg K-edge X-ray absorption near-edge structure (XANES) spectroscopy is highly sensitive to local coordination rather than long-range crystallinity, making it a powerful method for identifying poorly crystalline Mg-bearing phases. In addition to comparison with reference spectra, linear combination fitting of XANES spectra enables quantitative evaluation of the contributions of different Mg coordination environments. In particular, for Mg-rich layered hydrous silicates considered to be major constituents of CI chondrites, differences in spectral shape can be used to distinguish among mineral species.

The aim of this study is to directly constrain the average local coordination environment of Mg in the matrices of CI chondrites (Ivuna and Orgueil), Ryugu returned samples, and the ungrouped carbonaceous chondrite Tarda using Mg K-edge XANES spectroscopy.

All samples show broadly similar spectral features, indicating generally similar Mg coordination

environments among these primitive materials. However, the observed spectra are not fully reproduced by the previously proposed crystalline two-component model of saponite (or Fe-saponite) plus serpentine. Instead, the fits are consistently improved when a poorly crystalline Mg-silicate hydrate (pc-MgSH)-like component is included, suggesting that a substantial fraction of Mg resides in a local coordination environment distinct from fully crystalline phyllosilicates.

These results suggest that a pc-MgSH-like local Mg coordination environment makes a significant contribution to the matrices of C-type asteroid materials. The persistence of metastable pc-MgSH implies that aqueous alteration on the parent bodies proceeded under lower-temperature, metastable, and more disequilibrium conditions than previously assumed, rather than under more equilibrated conditions involving extensive nucleation and crystal growth of serpentine or saponite. Such conditions may also have favored the synthesis and preservation of organic matter by suppressing excessive degradation while promoting adsorption, concentration, and reaction on the metastable mineral with highly reactive surfaces.

Key words: Mg K-edge XANES, C-type asteroid materials, Mg-rich hydrous silicates

MODELLING IN-SITU MINERAL DUST CHARACTERIZATION FOR TRACE ELEMENT LOAD MEASUREMENTS AND PROVENANCE ANALYSIS

Bruno A. A. Monteiro[1], Kim Berlo[1], Vincent van Hinsberg[1], Eleanor J. Berryman[2]

1. Earth and Planetary Sciences/Faculty of Science, McGill University, Canada
2. CanmetMINING, Natural Resources Canada, Canada

Abstract Airborne mineral particles affect the environment and human health, whether produced by human activity or natural processes. Commonly called “dust”, it generically consists of particles smaller than 75 µm in diameter, suspended in the atmosphere and settling under their own weight. These particles come from multiple sources, including desert storms, volcanic eruptions, traffic, and mining or industry-related processes. The heterogeneous make-up and mixing of sources during transport challenge dust provenance studies. Moreover, dust composition does not always directly reflect its source, as different minerals and particle sizes settle at different rates, and morphological features are altered during transport.

Mineral associations and geochemical characterization have often been employed to delineate dust fingerprints traceable to their sources. Trace element data is often used because it provides a strong geochemical fingerprint for provenance analysis. Bulk sample measurements are common in geochemical analysis, but they reflect the whole sample's geochemistry. Whereas, in-situ analysis of individual particles can provide precise mineral information. By characterizing individual particles, it is possible to have isolated content of trace elements and elements of concern, providing information on provenance, bioaccessibility and potential hazards. Nevertheless, dust samples can exhibit significant compositional contrasts, as many elements can be preferentially hosted in accessory phases, posing a major challenge to determining element deportment across mineral phases.

For particle characterization, in-situ characterization by SEM-EDX is sufficient for most major elements when rastering a sample at 1 µm resolution. However, provenance identification can be improved by combining mineral associations with trace-element content. Trace elements in a mineral typically reflect the geological processes it has undergone, and trace elements such as rare earth elements are resistant to secondary processes. The acquisition of in-situ analysis of such elements provides more reliable fingerprints, thereby identifying their sources with higher precision.

Laser Ablation (LA)-ICP-MS is commonly used to obtain in-situ composition for trace elements and can be used to obtain individual dust particle analysis. It is, however, limited in practice by the number of analysis spots and samples, and by the fact that a laser spot can encompass multiple fine-dust particles, thereby generating mixed signals. Therefore, a major challenge lies in selecting

representative sampling positions.

We used Monte Carlo simulations to demonstrate that random allocation of in-situ analysis spots fails to yield representative dust subsamples. The dust-simulated design represents small, heterogeneous phases with high compositional contrast. These simulations illustrated how varying the number of spots, changing spot size and aiming for more isolated particles affect in-situ subsampling. They show that random subsampling, typically used for powder-like samples, undersamples accessory phases, even when hundreds of spots are acquired. They also show that increasing the spot size makes it possible to retrieve the bulk composition. However, bigger spot sizes won't allow for individual particle characterization. In contrast, targeting phases, especially more isolated particles, allows for characterizing them individually and can provide a better understanding of element deportment. This provides a better definition of mineral endmembers and the unmixing of mixed geochemical data.

The proposed workflow to optimize sample characterization integrates SEM-EDX mapping with targeted in-situ trace-element analysis via LA-ICP-MS. Mineral segmentation is achieved by acquiring SEM-EDX maps for the whole sample. The phase maps can be used to locate particles of each mineral in the sample and to select more isolated particles. This enables the characterization of particles individually, the identification of mineral endmembers, and the understanding of their element deportment. The composition of minerals and their relative abundance can provide a deeper understanding of the distribution of elements in dust, which can be used for provenance, bioavailability, and hazard assessment studies, supporting more informed decision-making and mitigation strategies.

Key words: Airborne particulates characterization, In-situ analysis of particles, Dust provenance, Dust sampling, Monte Carlo simulations

MOLECULAR DYNAMICS FREE ENERGY CALCULATIONS OF HYDRATION AND SWELLING IN MONOVALENT CATION INTERCALATED BIRNESSITES

Gerica Joie P. Castro, Kideok D. Kwon
Department of Geology, Kangwon National University, Republic of Korea

Abstract Birnessite is one of the most reactive minerals in terrestrial and marine environments, playing a critical role in the sequestration of alkali and alkaline earth metals. The structural stability and swelling behavior of these minerals are fundamentally governed by the hydration properties of interlayer cations. However, the relative thermodynamic stability of discrete hydration states across varying environmental conditions remains poorly characterized. In this study, we utilize molecular dynamics (MD) simulations and thermodynamic integration (TI) to calculate the Gibbs free energy of water intercalation (ΔG_{int}) for a full series of alkali-saturated triclinic birnessites (Li^+, Na^+, K^+, Rb^+, and Cs^+). Our results show that Li- and Na-birnessite exhibit spontaneous, barrier-less hydration promoting continuous swelling to more hydrated phases. In contrast, the larger cations (K^+, Rb^+, Cs^+) impose thermodynamic penalties at low water contents, indicating the resistance of larger cation systems to transition to expanded phases. This thermodynamic hierarchy is consistent with trends in ionic hydration energies, suggesting that interlayer cation identity is a primary determinant of hydration state stability. Larger monovalent cations impose thermodynamic penalties inhibiting swelling, whereas smaller more hydrated monovalent cations promote interlayer expansion, offering molecular-scale insights into the role of monovalent cations in the hydration and swelling behavior of layered manganese oxides. These findings provide a quantitative framework for predicting birnessite stability, transformation into the two layer water phase (buserite) and ion exchange selectivity, with broader implications for trace metal mobility and contaminant cycling in natural environments.

Key words: birnessite, thermodynamic integration, swelling and hydration, alkali metals, molecular dynamics

NANOSCALE CONTROL OF DISORDERED DOLOMITE FORMATION: THE ROLE OF MICROBIAL BIOMASS AND POLYSACCHARIDES IN STABILIZING AMORPHOUS PRECURSORS

Ting Chen, Deng Liu*

State Key Laboratory of Geomicrobiology and Environmental Changes, China University of Geosciences, China

Abstract The "dolomite problem" remains a central enigma in geobiology because precipitating dolomite under ambient conditions is notoriously difficult. While microbial extracellular polymeric substances are known to facilitate this process, the specific nanoscale interactions between organic matrices and mineral precursors have remained elusive. Here, we integrate experimental results from microbial and organic systems to elucidate how nanoscale mineral-organic interactions govern Ca-Mg carbonate crystallization under ambient conditions. In microbial systems, we show that a halophilic bacterium (*Halomonas* sp. JBHLT-1) induces the formation of disordered dolomite via a non-classical pathway involving an amorphous calcium-magnesium carbonate (ACMC) precursor. Microbial cells promote Mg incorporation into ACMC through surface functional groups, facilitating the formation of a dolomite-like amorphous phase. During subsequent crystallization, microbial biomass suppresses dissolution-reprecipitation processes and favors a solid-state transformation pathway, thereby preserving Mg content and enabling the formation of disordered dolomite with nanoscale, spherulitic textures. In parallel, abiotic experiments with polysaccharides of contrasting charge properties (negatively charged xanthan gum vs. neutral guar gum) demonstrate that polymer charge density alone does not control Mg incorporation. Instead, polysaccharides act by reducing local water activity, stabilizing ACMC, and inhibiting Mg loss during phase transformation. Solution chemistry remains the primary control on carbonate composition, while polysaccharides provide a critical secondary modulation of crystallization pathways. Together, these results reveal that both microbial cells and organic polymers can independently promote dolomite formation through a shared non-classical pathway mediated by ACMC, but via distinct mechanisms: cation binding and templating in microbial systems versus water-activity modulation in polymer-rich environments. These results expand the range of potential organic-rich environments where low-temperature dolomite might form and underscore the importance of nanoscale mineral-organic interactions in shaping carbonate mineralogy throughout Earth's history.

Key words: Dolomite problem, Amorphous calcium magnesium carbonate (ACMC), Non-

classical crystallization, Polysaccharides, Microbial EPS

NON-NUTRITIVE MINERALS AS REGULATORS OF MICROBIAL GENE EXPRESSION AND ANTIBIOTIC RESISTANCE

H. Henry Teng, Luhan Li, Beibei Wang, Jianchao Zhang

School of Earth System Science, Tianjin University

Abstract Minerals and the evolution of life have been intimately intertwined since the origin of life, yet their influence on microorganisms beyond serving as nutrient sources—particularly as physical signals or evolutionary drivers—remains underappreciated. Whether biochemically inert minerals also shape microbial physiology has received far less attention. Here, we address this at both single-species and community levels by integrating high-resolution transcriptomic analysis with long-term evolution experiments.

In pure culture, exposure of *E. faecalis* to Al_2O_3 and SiO_2 phases triggered extensive transcriptional reprogramming. Both minerals induced an "iron paradox," with strong upregulation of iron acquisition and oxidative stress genes. The bacterium compensated by rerouting metabolism through a Lactate–Pyruvate–Thiol axis, suppressing serine catabolism while enhancing cysteine and glutathione synthesis. Additionally, an OmpR–SigV regulatory axis was identified as a discriminator of particle size, with nano-scale minerals eliciting the strongest stress responses. At the community level, serial passage experiments demonstrated that minerals act as potent selective pressures regardless of nutritional value. Both inert kaolinite and nutrient-rich olivine drove significant divergence in community structure, selecting for specific taxa (Acinetobacter, Clostridium) and enhancing pathways for complex organic matter degradation.

A critical convergence across both cellular and community scales was the stimulation of the resistome in drug-free environments. Mineral stress upregulated virulence factors (biofilm formation) and expanded antibiotic resistance genes (ARGs), specifically for multidrug and macrolide resistance. Notably, kaolinite enriched pathways for streptomycin biosynthesis. These results demonstrate that minerals function as physical cues and evolutionary filters, driving metabolic adaptation and the propagation of antimicrobial resistance independent of their potential as nutrients.

Key words:

OXALATE MINERALS FORMATION UNDER THE ACTION OF BROWN ROT FUNGI

Alina R. Izatulina[1], Marina S. Zelenskaya[2], Dmitry Yu. Vlasov[2], Olga V. Frank-Kamenetskaya[1]

1. Crystallography Department, Institute of Earth Sciences, St. Petersburg State University, 7/9, University Emb., 199034 St. Petersburg, Russia
2. Department of Biology, St. Petersburg State University, University Emb. 7/9, 199034 St. Petersburg, Russia

Abstract In the present work, we clarified the contribution of brown rot fungi to oxalate formation in nature. We first found oxalates formed under the action of brown rot fungi on stone in natural conditions (Rogoselga adit, Karelia, Russia), proposed a model for their formation, and thus confirmed the hypothesis that frequent occurrence of metal oxalates in subsurface space (mines, adits, and so on) may be associated with the activity of these fungi. Brown rot fungi belong to the wood-rotting fungi, which produce oxalic acid and actively decompose wood. We synthesized under the action of four species of brown-rot fungi (Serpula himantioides, Serpula lacrymans, Coniophora puteana, Antrodia xantha) on different mineral substrates analogs of all known biofilm oxalate minerals and oxalates of such toxic heavy metals as Pb, Cu, Mn. In addition, we compared the features of oxalate formation under the action of brown rot fungi and soil fungus Aspergillus niger, an active oxalic acid producer, widely used in model experiments and recommended for application in biotechnologies. It is shown that in contrast to A.niger, the contribution of the metabolic activity of brown rot fungi to oxalate crystallization exceeds the contribution of the underlying minerals. The prospects for the use of brown rot fungi such as Serpula himantioides, Coniophora puteana, and Antrodia xantha in modern environmentally friendly biotechnologies are justified.

Key words: microbial biomineralization, brown rot fungi, oxalates

Acknowledgements This research was funded by the Russian Science Foundation (grant 25-27-00487). The laboratory research was carried out in the Research Park of Saint Petersburg State University

OXIDATION OF AS(III) BY FE(II)-RICH CLAY MINERALS: PERFORMANCE, MECHNISM AND ENVIRONMENTAL GEOCHEMICAL IMPLICATIONS

Hongling Bu, Hanjie Chen, Peng Yuan

School of Environmental Science and Engineering, Guangdong University of Technology, Guangzhou 510006, China

Abstract Arsenic (As) poses a severe threat to ecosystems and human health due to its high toxicity and carcinogenicity. As(III) is more toxic and mobile than As(V), so oxidizing As(III) to As(V) is critical for arsenic pollution control. Iron-bearing clay minerals, widely distributed in high-arsenic groundwater areas, are key carriers regulating As biogeochemical cycling via Fenton-like reactions of structural Fe(II) with O_2 to generate reactive oxygen species (ROS). Unlike unstable secondary iron oxides, primary iron-bearing clay minerals with unique 2:1/1:1 crystal structures and long-term stability can reconstruct authentic arsenic cycling processes, making them core objects for exploring high-arsenic groundwater evolution. This study compared Fe(II)-rich clays, reduced natural Fe(III)-bearing nontronite, and Ca-montmorillonite to reveal their regulatory mechanisms on As(III) in heterogeneous systems.

As(III) oxidation-adsorption under different pH conditions was measured, and a Mössbauer spectroscopy-based quantitative characterization system for iron species transformation and ROS generation pathways was established, focusing on structural Fe(II) electron transfer and induced oxidants. Results showed Fe(II)-rich clays had excellent As(III) treatment performance (60% oxidation, 99% removal) under neutral-weakly acidic conditions, far superior to other minerals, attributed to abundant active structural Fe(II) sites. Structural Fe(II) drove electron transfer to generate •OH, O_2•$^-$ and Fe(IV) for synergistic As(III) oxidation, while natural Fe(III)-bearing minerals had limited redox activity. Fe(II)-rich clays maintained high reactivity and anti-passivation stability via sustainable Fe(II) supply and renewable surface sites. These findings deepen the understanding of interfacial redox processes of iron-bearing clays in environmental geochemistry, clarify their role in As biogeochemical cycling, and provide scientific basis for improving As cycle prediction models and designing efficient iron-based clay remediation materials.

Key words: Fe (II)-rich clay minerals, Arsenite (As (III)), Oxidation mechanism, Reactive oxygen species (ROS), Environmental geochemistry

Acknowledgements The research was supported by the National Natural Science Foundation of China (No. 42472060).

PERFORMANCE OF FE-MODIFIED BIOCHARS AND CARBO-IRON IN REMEDIATING ARSENIC IN GROUNDWATER

Mingyu Feng, Laura A. Richards, David A. Polya, and Jonathan R. Lloyd
Department of Earth and Environmental Sciences, The University of Manchester, Manchester, UK

Abstract Geogenic arsenic (As) mobilisation in aquifers, sometimes influenced by anthropogenic activities, can give rise to a widespread and serious hazard, leading to human health and ecological risks that can require mitigation. Here, we investigate the efficiency of Fe-modified biochars and Carbo-Iron in remediating As in groundwaters, focusing on their adsorption capacities and long-term performance under varying biogeochemical conditions.

24-hour adsorption (initial As 100 µg/L) in a deionized water system demonstrated that Fe-modified biochars and Carbo-Iron significantly enhanced As (both As(V) and As(III)) removal compared to pristine biochar, likely through surface complexation/co-precipitation and electrostatic interactions. Among the tested materials, Carbo-Iron exhibited stable and high removal capacity across a pH range of 3.5 – 7.4, whereas magnetite-containing biochar (M+BC) and ferrihydrite-containing biochar (FH+BC) showed stronger pH dependence and reduced performance under alkaline conditions. Extended 6-month performance under circumneutral conditions indicated that both M+BC and Carbo-Iron effectively sustained As retention, maintaining aqueous As below 1.4 µg/L.

Anaerobic microcosm incubations containing high-As aquifer sediments showed that microbial interactions influenced As fate in groundwater environments. The presence of lactate and acetate stimulated microbially mediated Fe(III)/As(V) reduction, which was associated with incresed As release (up to 105 µg/L). The addition of remediation materials nevertheless effectively inhibited As mobilization. Notably, Carbo-Iron maintained aqueous As concentrations below 3.8 µg/L throughout the incubation, demonstrating its potential for long-term groundwater remediation.

Key words: Fe-modified biochar, Carbo-Iron, Arsenic, groundwater remediation

Acknowledgements We acknowledge support from a China Scholarship Council-The University of Manchester joint scholarship (CSC-UoM, 202208440009) to M.F., the Natural Environment Research Council (NERC; NE/X010813/1 to L.A.R. and D.A.P.) and a UKRI Future Leaders Fellowship (MR/Y016327/1 to L.A.R et al; see www.aquaroad.org).

PROBING CLOSED REDOX SYSTEMS ON EARTH AND MOON SURFACES AT THE NANOSCALE

Qian Fang[1], Zhong-Qiang Chen[1], Anhuai Lu[2]

1. State Key Laboratory of Geomicrobiology and Environmental Changes, China University of Gesciences, Wuhan, China
2. School of Earth and Space Sciences, Peking University

Abstract The "mineral coatings" on Earth's surface, referred to as Earth's fourth sphere, play important roles in material cycling and energy transformation from multiple perspectives. Similar "mineral coatings" exist on the surfaces of the Moon and Mars, though their formation mechanisms and mineral compositions differ. Therefore, studying analogous materials on Earth holds significant implications for understanding surface processes on the Moon and Mars. In this talk, we present our recent research advances on the nanoscale characteristics of "mineral coatings" on Earth and the Moon. Within relatively sealed fractures beneath Earth's "mineral coatings" we discovered nanoscale Mn- and Ca-rich oxide clusters. Laboratory simulation experiments demonstrated the oxygen-producing capacity of these clusters. We calculated that appreciable concentrations of free oxygen can be generated within these sealed fractures, and this oxygen may have promoted the evolution of the earliest oxygenic photosynthesis. On the outermost surfaces of lunar regolith grains, at the micron to nanometer scale, vesicular reactors within impact melts or semi-permeable membrane reactors covered by micro- to nanoscale glass are commonly observed. Inside these reactors, we observed a variety of distinctive reaction products, including metallic iron, hematite, and phyllosilicate minerals. These sealed reactors in the outermost lunar surface share notable parallels with certain features found on Earth. We propose that these microscale reactors on planetary surfaces may represent previously unrecognized mechanisms for redox reactions and aqueous alteration.

QUANTITATIVE CONSTRAINTS ON THE MINERALOGY OF EARTH'S EARLY PALEOZOIC CLAY MINERAL FACTORY FROM THERMODYNAMIC-KINETIC PATHWAY MODELLING

Meitong Song[1,2,3], Yuyan Zhao[1,2], Xiaodan Tang[1,2,*], Simon A. T. Redfern[3,4,5,*]

1. College of Geo-exploration Science and Technology, Jilin University, Changchun 130026, China
2. Jilin Provincial Key Laboratory of Soil Exploration and Analysis, Jilin University, Changchun 130026, China
3. Asian School of the Environment, Nanyang Technological University, 50 Nanyang Avenue, Singapore 639798
4. Earth Observatory of Singapore, Nanyang Technological University, 50 Nanyang Avenue, Singapore 639798
5. School of Materials Science and Engineering, Nanyang Technological University, 50 Nanyang Avenue, Singapore 639748.

Abstract The earliest Paleozoic expansion of continental clay mineral production fundamentally altered ocean chemistry and has previously been linked to metazoan diversification, yet the thermodynamic and kinetic controls determining which clay phases this weathering factory produced remain unresolved. Here, thermodynamic and kinetic modelling are combined to reconstruct mineral transformation pathways in temperate soil systems. Temperate black-soil systems serve as modern analogues of the moderate-intensity continental weathering conditions that characterized early Paleozoic land surfaces. Forty-three mineral reactions involving feldspars, mafic silicates, micas and clay minerals were evaluated using thermodynamic stability analysis and kinetic rate calculations.

Three dominant transformation pathways are identified: (1) muscovite → illite → montmorillonite, (2) phlogopite → vermiculite → montmorillonite, and (3) mafic silicates → serpentine → montmorillonite. Montmorillonite emerges as the dominant product of all three pathways, governed by its thermodynamic stability under moderate-temperature, near-neutral, Si- and Al-sufficient conditions and by the sluggish precipitation kinetics of kaolinite. Feldspars persist as inherited primary phases owing to the high activation energy barriers of Si–O and Al–O bond hydrolysis.

These results provide a quantitative mechanistic basis for understanding the smectite-dominated clay mineral assemblages inferred from earliest Paleozoic sedimentary records and geochemical proxies. Apportioned against published early Paleozoic silicate weathering budgets, the dominant pathways collectively yield approximately 5 Tmol yr^{-1} of Mg^{2+} and 0.8 Gt yr^{-1} of montmorillonite, consistent with independent geochemical estimates for the Cambrian weathering flux. These element releases, delivered to early Paleozoic oceans via riverine transport, would have contributed

to the biogeochemical conditions conducive to metazoan diversification. The abiotic thermodynamic framework presented here establishes the mineralogical baseline against which the biological amplification of continental weathering during the Cambrian Explosion can be evaluated.

Key words: Mineral evolution, Pathway modelling, element fluxes, Earth's early Paleozoic, Clay mineral factory

Acknowledgements This study was supported by National Key Research and Development Program of China (2021YFA0715104), the China Scholarship Council (No. 202506170078), Singapore Ministry of Education (MOE) AcRF Tier 2 grant MOE-T2EP50222-0019, and MOE AcRF Tier 3 Climate Transformation Programme MOE-T32022-0006.

RAMAN SPECTROSCOPY OF CALCIUM OXALATE DIHYDRATE (COD) AND TRIHYDRATE (COT)

Nicole Horáková [1, 2], Jan Cempírek [2]

1. Department of biochemistry, molecular biology and biotechnology, Wrocław University of Science and Technology, Poland
2. Department of Geological Sciences, Masaryk University, Czech Republic

Abstract Calcium oxalate hydrates ($CaC_2O_4 \cdot nH_2O$) are common biominerals found in lichens, fungi, plants, and also in sedimentary rocks or on monument surfaces; they are common due to their strong affinity for divalent cations and interaction with weak organic acids (Izatulina et al. 2018). In nature, Ca-oxalates are represented by three hydrated forms: whewellite ($CaC_2O_4 \cdot H_2O$; COM), weddellite ($CaC_2O_4 \cdot 2H_2O$; COD), and caoxite ($CaC_2O_4 \cdot 3H_2O$; COT). The most common biomineral is COM, while COD and COT are considered to be metastable phases; however, COT is expected to be precursor of COD crystal formation (Conti et al. 2015) and may play an important role in calcium oxalate nucleation dynamics.

Since COD and COT have very similar Raman spectra, their identification requires careful calibration and measurement, and high-quality reference spectra. In order to obtain monocrystals of COD and COT for oriented Raman spectra measurements, we used syntheses according to Ouyang et al. (2006), Horáková (2022) and Echigo et al. (2005). Crystals of COD and COT were examined using single-crystal X-ray diffraction and their oriented Raman spectra were subsequently collected using the Horiba LabRamHR microspectrometer with Si-based Peltier-cooled CCD detector.

Our results show orientation-dependent variations in band intensities and positions in both COD and COT. They improve the high potential of Raman spectroscopy in studies of calcium oxalate nucleation and growth in organisms.

Key words: Caoxite, Weddellite, Raman spectroscopy

REGULATION OF FE(II) SUPPLY RATES AND EXTRACELLULAR POLYMERIC SUBSTANCES ON FERRIHYDRITE BIOTRANSFORMATION

Sheng, Anxu[1,2], Ding, Yuefei[2], Deng, Yurong[2], Li, Xiaoxu[2, 3], Rosso, Kevin M.[3], Liu, Juan[2].

1. Hubei Key Laboratory of Multi-media Pollution Cooperative Control in Yangtze Basin, School of Environmental Science and Engineering, Huazhong University of Science and Technology, Wuhan 430074, China
2. The Key Laboratory of Water and Sediment Sciences, College of Environmental Sciences and Engineering, Peking University, Beijing 100871, China
3. Pacific Northwest National Laboratory, Richland, Washington 99354, United States

Abstract Biotransformation of ferrihydrite (Fh) nanoparticles by dissimilatory iron-reducing bacteria (DIRB) into diverse secondary minerals assemblages is widespread in anaerobic environments. Our previous studies have shown that aqueous Fe(II) accelerates Fh transformation by promoting Fh dissolution and, consequently, enhancing the formation of a reactive intermediate, labile Fe(III) ($Fe(III)_{labile}$), through interfacial electron transfer (IET) from sorbed Fe(II) to structural Fe(III) within Fh. Once $Fe(III)_{labile}$ reaches a critical concentration, it repolymerizes and condenses into more stable mineral phases. To elucidate how DIRB respiration rates regulate Fh biotransformation, we conducted transformation experiments using 1 mM biogenic Fe(II) (BioFe(II)), supplies at different rates to mimic Fe(II) release rates driven by DIRB respiration. For comparison, parallel experiments with $FeSO_4$ alone and $FeSO_4$ plus citrate (CitFe(II)) were performed at the same supply rates to disentangle the respective effects of Fe(II) supply rate and extracellular polymeric substances (EPS) associated with BioFe(II). Lower $FeSO_4$ supply rates favored the transformation of Fh to lepidocrocite (Lp) rather than Gt, as well as the subsequent transformation of Lp to magnetite (Mt), shifting the overall transformation pathway from Fh→Lp/Gt→Gt to Fh→Lp/Gt→Mt/Gt. These results highlight the critical role of aqueous Fe(II) supply rate in governing the competition between olation and oxolation of $Fe(III)_{labile}$ intermediates into different secondary minerals. In BioFe(II) and CitFe(II) systems, EPS or citrate slightly increased Fe(II) adsorption and $Fe(III)_{labile}$ generation, while this effect was minor compared with the variation in aqueous Fe(II) concentration induced by different supply rates. At the same Fe(II) supply rates, EPS or citrate notably inhibited the transformation of Fh to Gt and the further conversion of Lp, shifting the pathway from Fh→Mt/Gt/Lp to predominantly Fh→Lp. This inhibitory effects became more pronounced with the decrease of BioFe(II) and CitFe(II) supply rates. Our findings provide new insights into how DIRB respiration rates control kinetics, pathways, and mineral products of Fh transformation, which is crucial for elucidating the relevant biogeochemical cycling of nutrients and (im)mobilization of contaminants.

Key words: Dissimilatory iron reduction, Fe(II)-catalyzed ferrihydrite transformation, Biogenic Fe(II) supply rates, Extracellular polymeric substances, Transformation kinetics and pathway

Acknowledgements This work was financially supported by the National Natural Science Foundation of China (42192502, 42377228, 42102026, and 41820104003) and the National Key R&D Program of China (2023YFC3706503). This research used resources from the Advanced Photon Source, a U.S. Department of Energy (DOE) Office of Science User Facility operated for the DOE Office of Science by Argonne National Laboratory under Contract No. DE-AC02-06CH11357. We also acknowledge the support from beamlines 1W1B and 4B9A at Beijing Synchrotron Radiation Facility (BSRF).

ROLE OF RHODOCOCCUS STRAINS IN MICROBIAL CARBONATE BIOMINERALIZATION UNDER STANDARD AND METAL-STRESSED CONDITIONS

Francesca Benedetti [1] 2, Nora Ivani [2] , Patrizia Paganin [2] , Agnese De Carlo [1] 3, Giovanni Birarda [3], Chiaramaria Stani [3], Lisa Vaccari [3], Cristian Ambu [1], Flavia Tasso [2], Chiara Alisi [2], Giovanni De Giudici [1]

1. Department of Chemical and Geological Sciences, University of Cagliari, Cagliari, Italy
2. Department of Sustainability (SSPT), ENEA, Rome, Italy
3. Elettra Sincrotrone Trieste, Area Science Park, Basovizza, Trieste, Italy

Abstract The present work aims to elucidate the molecular mechanisms underlying microbial carbonatogenesis by drawing inspiration from natural biomineralization processes. Understanding how microorganisms mediate carbonate precipitation is essential for both fundamental science and the development of sustainable technologies. In particular, bacterial carbonate biomineralization represents a promising strategy for applications such as soil stabilization, sediment consolidation, and the conservation of weathered limestone and cement-based materials. This study clarifies the interplay between microbial activity, environmental conditions, and mineral formation.

As a preliminary step, eleven strains from the EMCC (ENEA Microbial Culture Collection), belonging to different species, were tested for their ability to induce carbonatogenesis in a culture medium without urea, in order to identify efficient calcium carbonate producers independent of ureolysis. In parallel, different culture media, with and without urea, were used to determine suitable experimental conditions for carbonate precipitation. Urease activity was subsequently assessed using Christensen Urea Agar, where the intensity and extent of the color change indicate the rate of urea hydrolysis and enzyme production.

Based on these results, OSS19b *Rhodococcus qingshengii* and TSNRS12 *Rhodococcus erythropolis* were selected for their high enzymatic activity, rapid reaction rates, and strong carbonate production. These strains showed the highest bioprecipitation efficiency under both conditions, with and without urea, demonstrating their ability to promote carbonate formation through multiple biomineralization pathways. Carbonate precipitation in the absence of urea suggests biologically influenced mineralization, where organic matrices such as cell surfaces or extracellular polymeric substances act as nucleation sites. In contrast, strong urease activity highlights the role of ureolysis in biologically induced mineralization, where metabolic activity increases pH and carbonate availability, accelerating precipitation. This dual capability makes the selected strains suitable for investigating the coexistence of different pathways under varying environmental conditions.

A central aspect of this work was the evaluation of the effect of heavy metal stress, specifically

zinc, on the precipitation processes. The resistance of the eleven bacterial strains was assessed by testing growth in a general culture medium supplemented with $ZnCl_2$ at 4 and 6 mM. Notably, OSS19b *Rhodococcus qingshengii* and TSNRS12 *Rhodococcus erythropolis* showed enhanced resistance, growing even at concentrations up to 8 mM. Their tolerance makes them suitable models for studying biomineralization under stressed conditions.

The biochemical response of these bacteria to zinc exposure and its impact on carbonate precipitation were analyzed. Heavy metals may interact with microbial metabolism and become incorporated into mineral phases, potentially altering their structure and properties. The selected strains were cultured under controlled conditions to monitor in situ carbonatogenesis over time. Mineral formation was investigated at different stages to evaluate nucleation, growth, and morphological changes. Crystalline and amorphous phases were characterized by infrared spectroscopy, powder X-ray diffraction (XRD), and environmental scanning electron microscopy (ESEM).

Comparisons between standard and zinc-stressed conditions revealed differences in microbial activity, mineralization kinetics, and physicochemical properties of the resulting carbonates, including variations in crystal morphology, size distribution, and composition. These results improve the understanding of microbial carbonatogenesis under both normal and stressed conditions and support the development of scalable, bio-based strategies for carbon sequestration and sustainable material production in contaminated environments.

Key words: Microbial carbonatogenesis, Biomineralization, Rhodococcus, Ureolysis, Zinc stress

Acknowledgements This research is part of the PRIN 2022 project “MeChanisms Of carbonate biomineraLizatiOn driVen by selected unicEllular oRganisms under Stress conditions. CO_2 Lovers”, involving the University of Cagliari, Elettra Sincrotrone Trieste (SISSI-Bio offline facility), and the Italian National Agency for New Technologies, Energy and Sustainable Economic Development (ENEA).

ROLES OF NATURAL CATALYSTS IN PROMOTING PRECIPITATION OF SEDIMENTARY DOLOMITE: FROM MOLECULES TO MOUNTAIN BUILDING

Huifang Xu

Department of Geoscience, University of Wisconsin–Madison, Madison Wisconsin 53706, USA

Abstract Sedimentary dolomite is abundant in earth history, but rare in Cenozoic and modern carbonate sediments. Although modern seawater contains high concentrations of Mg and Ca in molar ratio of ~50 mM / 10 mM, modern carbonate sediments are dominated by aragonite. The main factor inhibiting dolomite growth is strong solvation of Mg^{2+} in aqueous solution at low temperature. Natural catalysts that can lower the solvation energy of Mg^{2+} will promote incorporation of Mg^{2+} into Ca-Mg-carbonate and precipitation of dolomite. Identification of a catalysis process which would permit easy low temperature laboratory synthesis of dolomite would achieve the "holy grail of dolomitization" (Land, 1998). We have identified that natural catalysts of dissolved H_2S, CH_4, ethanol, polysaccharides (in microbial EPS), and $Si(OH)_4$ with low dipole moments (or low dielectric constants) can lower the solvation energy and promote dolomite precipitation through surface-induced nucleation and growth processes. Density functional theory calculation shows that dissolved H_2S can weaken the bond between surface Mg^{2+}-water and enhance removal water in surface Mg^{2+}-water complex and promote dolomite growth. Molecular dynamics modeling results show that adsorbed trisaccharide (to mimic polysaccharides) can lower activation energy of water removal in surface Mg^{2+}-water complex by ~1 kcal/mole. Molecular dynamics modeling shows that adsorbed $Si(OH)_4$ can promote surface water removal and carbonate anion binding to surface Mg cations, which is an important step for dolomite growth.

Our laboratory syntheses and molecular dynamics modeling results demonstrate that the dissolved silica (with concentrations of ~ 1 mM to 2 mM) can catalyze dolomite precipitation. Primary dolomite in the Great Salt Lake in Utah and Deep Springs Lake in California correlate with concentrations of dissolved silica in the lake waters. The dramatic drop in dolomite abundance in late Cretaceous was a result of global radiation of diatom that lowered the concentration of dissolved silica in seawater globally. Geochemical modeling of the Marinoan cap dolomite formation (~635 million years ago) after the deglaciation of the snowball earth shows that cap dolomite and silica (chert) bands precipitation were no isolated events, but rather the silicate weathering was the determining factor for the appearance of cap dolomite. Understanding the dolomite problem and carbon cycles in earth history can help us to solve the challenge CO_2 problem we are facing today.

Key words: dolomite, catalysis, surface-induced nucleation & growth, polysaccharides, dissolved silica

SIMULTANEOUS PH AND ION CONCENTRATION IMAGING OF NON-STOICHIOMETRIC REACTION ON THE MINERAL-SOLUTION INTERFACE

Jun Kawano[1], Kohsei Miki[2], Shinichi Hasegawa[2], Takaaki Nanri[2], Takashi Toyofuku[3], Yuki Sugiura[4], Takaya Nagai[1]

1. Department of Earth and Planetary Sciences, Faculty of Science, Hokkaido University, Japan
2. Department of Natural History Sciences, Graduate School of Science, Hokkaido University, Japan
3. Japan Agency for Marine-Earth Science and Technology (JAMSTEC), Japan
4. National Institute of Advanced Industrial Science and Technology (AIST), Japan

Abstract To elucidate weathering mechanisms in the Earth's surface and their environmental impacts, it is essential to understand mineral reactions in aqueous solutions by analyzing the local behavior of ions at the mineral-solution interface. We have successfully visualized changes in the pH and ion concentration distribution around crystals dissolving or growing in aqueous solutions by using fluorescent probes, whose fluorescence intensity changes depending on the pH and ion concentration. This method allows us to understand the formation and dissolution processes by directly observing the behavior of specific ions at the mineral-solution interface. In the present study, HPTS (8-hydroxypyrene-1,3,6-trisulfonic acid) and Rhod-FF (or Rhod-5N) were applied as the pH and cation concentration (Ca^{2+} or Mg^{2+}) indicators, respectively, for simultaneous imaging of these parameters. By using this method, we analyzed the ionic behavior during the dissolution of carbonate minerals and the solvent-mediated transformation of calcium phosphate.

The results of pH and Ca^{2+} imaging during the dissolution of calcite ($CaCO_3$) showed that both pH and Ca ion concentration increased concentrically soon after a crystal was exposed to the solution. However, the increase in pH was not as significant as would be estimated from the conventional reaction with the measured Ca^{2+} concentration, indicating excess HCO_3^- ions were released during the rapid dissolution of calcite. This is consistent with the previous study by using the state-of-the-art AFM, which reported that $Ca(OH)_2$ exists on the dissolving calcite surface. In the case of magnesite ($MgCO_3$) dissolution in water, the pH should also increase, considering the equilibrium calculation. However, the present results of the pH visualization showed that it decreased just above the surface when the pH of the initial solution was higher than 7.5, while it increased at the initial pH of ~ 6. This tendency, which differs from what would be expected based on bulk reactions, could be reflected in the variation of surface structures depending on pH.

In the $CaPO_4$-H_2O system, when stable hydroxyapatite (HAP) and metastable octacalcium phosphate (OCP) are placed a short distance apart in aqueous solutions, the solvent-mediated phase transformation should occur, where the metastable phase dissolves while the stable phase grows. The results of visualizing this process showed that there were conditions where the profiles of Ca^{2+}

concentration and pH between these two phases had opposite slopes, and that the flow of ions was not simply from the metastable to the stable phases.

These results indicate that the present visualization method introduced here can provide new insights into the local surface reactions of multicomponent substances that are different from bulk chemical reactions

Key words: imaging, pH, dissolution, solvent-mediated transformation

STRUCTURE AND REACTIVITY OF INTERMEDIATE FE(III) SPECIES IN FE(II)-CATALYZED FERRIHYDRITE TRANSFORMATION

Yuefei Ding, Juan Liu*

College of Environmental Sciences and Engineering, Peking University, China

Abstract In anaerobic environments, dissolved Fe(II) can accelerate the transformation of metastable ferrihydrite into more thermodynamically stable mineral phases (e.g., goethite and magnetite), which process significantly impacts the bioavailability of ferrihydrite, the redox state of aqueous systems, and the ferrihydrite-mediated transport of contaminants and cycling of nutrients. Fe(II) transfers electrons to ferrihydrite via interfacial electron transfer, leading to the reductive dissolution of ferrihydrite while simultaneously being oxidized to form reactive Fe(III). This reactive Fe(III) continuously accumulates as a precursor for the formation of secondary minerals and subsequently crystallizes into secondary mineral phases. Although the intermediate Fe(III) species plays a crucial role in the phase transformation of ferrihydrite, our understanding of its structure and reactivity remains limited.

Utilizing aqueous chemical extraction, synchrotron radiation characterization combined with theoretical spectral calculations and fitting, alongside mass spectrometry, we preliminarily revealed that the intermediate Fe(III) predominantly exists as monomers during the initial stages of Fe(II) oxidation. As reactive Fe(III) accumulates, the proportion of trimeric Fe(III) species increases, becoming the primary precursor form for the nucleation and growth of secondary minerals. Furthermore, by employing carboxylic organic molecules with a strong complexing affinity for Fe(III), we explored how coexisting substances affect the condensation reaction of reactive Fe(III). The results indicate that the complexation between carboxylic ligands and intermediate Fe(III) reduces its reactivity, leading to a decreased concentration of “effective reactive Fe(III)” in the system. This reduction subsequently alters the effective supersaturation of the solution and dictates the types of secondary minerals formed. Overall, these findings elucidate the structural evolution of intermediate Fe(III) during the phase transformation of ferrihydrite and the factors influencing its reactivity at the microscopic scale, thereby offering a novel perspective for understanding the environmental behavior of metastable iron minerals.

Key words: ferrihydrite phase transformation, intermediate Fe(III), structure evolution, reactivity, microscopic scale

SUNLIGHT-DRIVEN MARTIAN-ANALOG METABOLISM: ENERGY COUPLING AND ELECTRON TRANSFER BETWEEN BIRNESSITE AND R. RADIOTOLERANS

Feifei Liu, Hongrui Ding Anhuai Lu

School of Earth and Space Sciences, Peking University

Abstract Solar radiation-mineral interfacial interactions constitute a fundamental driver of chemical evolution and energy transduction in near-surface environments of terrestrial planets. On Mars, Mn-rich rock varnishes are common and increasingly recognized not only as potential repositories of biosignatures, but also as plausible energy-harvesting platforms in extreme environments. Here, we establish a coupled “light-mineral-microbe” system using semiconducting birnessite and the radiation-tolerant extremophile *Rubrobacter radiotolerans* as a model to investigate energy coupling and electron transfer mechanisms at the mineral-microbe interface.

Our results demonstrate that the conduction band edge of birnessite is energetically well aligned with extracellular electron acceptors of R. *radiotolerans*, forming an efficient interfacial energy-coupling pathway. Under simulated solar irradiation, the ~38 $\mu A \cdot cm^{-2}$ photogenerated current produced by birnessite can cross the cell-mineral interface and inject electrons into the microbial respiratory chain. This process significantly enhances metabolic activity, resulting in a 1.6-fold increase in biomass relative to dark controls, and induces extracellular secretion of protein-like substances and stress-related metabolites. Bioelectrochemical analysis reveals that the "light-birnessite-R. *radiotolerans*" interaction system achieves a photocurrent density of 287 $\mu A \cdot cm^{-2}$, representing increases of 165% and 248% compared to mineral-only and abiotic controls under dark conditions, respectively. These observations provide compelling evidence for a synergistically enhanced extracellular electron transfer (EET) process driven by photogenerated electrons.

This study reveals a "non-photosynthetic" light-harvesting pathway in which R. *radiotolerans* can utilize photoelectrons generated by the natural semiconductor birnessite. In hyperoligotrophic, radiation-intensive near-surface environments, such a “light-mineral-biological” energy coupling mechanism may constitute a critical energy compensation strategy for maintaining metabolic activity over geological timescales. This mechanism refines our understanding of Martian habitability and Mn-related spectral anomalies and provides a conceptual framework for identifying non-canonical biosignatures based on semiconductor-mediated metabolic processes.

Key words: Birnessite, Rubrobacter radiotolerans, Energy coupling, Extracellular electron transfer, Martian-analogous metabolism

SURFACE CHEMICAL AND STRUCTURAL PROPERTIES INFLUENCE BIOFILM FORMATION ON CALCITE

Yarong Qi[1,2,3,*], Christopher Zamora[2], Zhao Hao[2], Benjamin Gilbert[2,3,*]

1. Department of Environmental Science, Policy, and Management, University of California, Berkeley, CA, 94720, United States
2. Earth and Environmental Sciences Area, Lawrence Berkeley National Laboratory (LBNL), Berkeley, CA, 94720, United States
3. Department of Earth and Planetary Science, University of California, Berkeley, CA, 94720, United States

Abstract Natural hydrogen is widely distributed in diverse environments including sediments, groundwater, hydrothermal vents, springs, and fairy circles. Hydrogen is a highly reducing electron donor for microbial metabolic processes in those environments, including methanogenesis, acetogenesis, and sulfate reduction. Although the electron acceptors for these metabolisms include dissolved species including bicarbonate and sulfate ions, it is increasingly understood that carbonate and sulfate minerals are bioavailable sources of these metabolic substrates. We previously demonstrated that calcite, can act as electron acceptor and carbon source for methanogenic and acetogenic microorganisms and as substrate for biofilm formation. However, the governing factors for colonization, growth and biofilm formation on such mineral phases are not fully understood yet.

In this work, the growth of biofilms by hydrogenotrophic microorganisms was stimulated by incubating marsh sediment-derived microbial community in a high-salinity inorganic medium with hydrogen gas and calcite crystals of different surface roughness and surface charge properties. The headspace hydrogen concentration during the three-week incubation was monitored by Gas Chromatography, with decreased hydrogen concentration indicating the consumption of hydrogen during the biofilm formation. The development of biofilm on calcite surfaces was investigated using Scanning Electron Microscope (SEM), Atomic Force Microscope (AFM), and an Optical Microscope. Higher biofilm coverage and greater hydrogen metabolism were observed for calcite surfaces with higher surface roughness and negative surface charge, suggesting the surface structural and chemical properties influenced biofilm formation on calcite. The biochemistry of biofilm on calcite surfaces was provided by Optical Photothermal Infrared (O-PTIR) with the presence of signature peaks of nucleic acids, proteins, and polysaccharides, confirming the existence of cells and metabolites in the biofilm. The morphology of biofilm was further characterized by Atomic Force Microscope (AFM) suggesting the biofilm development stage influenced biofilm structure and growth. The growing boundary of the biofilm was more porous but contained more abundant cells and secreted metabolites. In contrast, the fully developed biofilm was dominated by a homogeneous, rigid polysaccharides with lower metabolite diversity. These

findings suggest that mineral surface properties including surface roughness and surface charge could play a vital role in microbial metabolism of mineral phase nutrients sources. This work has implications in advancing our understanding of mineral-microbe interactions in various geologic environments.

SYNTHESIS AND PURIFICATION OF PHASE-PURE GREIGITE FOR NON-ENZYMATIC CATALYSIS

Feiyang Liu[1], Yu Su[1], Huiwen Lin[2], Jingbo Nan[3]

1. China Pharmaceutical University, Nanjing, China
2. Southeast University, Nanjing, China
3. State Key Laboratory of Palaeobiology and Stratigraphy, Nanjing Institute of Geology and Palaeontology, Chinese Academy of Sciences, Nanjing, China

Abstract Iron sulfides play central catalytic roles in metabolism-first hypotheses for the origin of life, in which the mineral surface may have promoted non-enzymatic reactions before metabolism evolved. While previous studies commonly associate iron sulfides with deep-sea hydrothermal systems, these minerals may also have functioned in terrestrial hot-spring environments, where sunlight and geothermal heat could have jointly driven photothermal catalytic processes. As such, laboratory simulation experiments allow to test such non-enzymatic reaction networks directly, but mechanistic studies require mineral catalysts with well-defined phase purity and minimal organic contamination. However, synthesizing greigite (Fe_3S_4) that is both inorganic and organic phase-pure is challenging. Here, we develop an improved hydrothermal method to synthesize inorganic phase-pure greigite using L-cysteine as the sulfur source. We further optimize post-synthetic treatments to remove residual L-cysteine and obtain organically clean greigite in photothermal simulators. Our method provides a practical and reproducible mineral platform for future investigating greigite-driven photothermal catalysis and for evaluating its potential role in prebiotic chemistry in early Earth surface environments.

Key words: iron sulfides, non-enzymatic catalysis, photothermal, origin of life, contamination control

THE DISSOCIATION EFFECT OF INDIGENOUS MICROORGANISMS ON COBALT-BEARING MINERALS IN THE NANJIAN MINING AREA, CHINA

Meng-Yue Zhang[1]*, Hao Zhang[3], Yu-Xiang An[2], Yang-Ai Lei[4], Yi-Fan Bai[1], Wen-Yuan Gao[2], Yi-Xuan Zhang[1], Fei Huang[2]*

1. School of Life Science and Biopharmaceutics, Shenyang Pharmaceutical University, People's Republic of China
2. School of Resources and Civil Engineering, Northeastern University, People's Republic of China
3. College of Mining, Liaoning Technical University, People's Republic of China
4. Team 310 of Yunan Nonferrous Metals Geological Bureau, People's Republic of China

Abstract Weathering-type (laterite) cobalt-nickel deposits are an important occurrence type of global cobalt and nickel resources. In such deposits, cobalt and nickel are mostly dispersed in the lattice of iron-manganese oxides in the form of isomorphism, and their natural dissociation and element migration are profoundly influenced by supergene weathering. This study took in-situ soil samples from different depths in the Nanjian cobalt-nickel mining area, China, and used microbial pure culture techniques to complete the isolation, purification, and taxonomic identification of culturable microbial strains. Through screening experiments, dominant strains for element mobilization were identified. Based on these, a 40-day long-term dissociation experiment was conducted on raw ore samples, dynamically monitoring the evolution of metal ions, pH, ORP, and iron valence cycling in the system. Combined with microscopic characterization techniques such as SEM-EDS, the dissociation process of cobalt-bearing minerals by microorganisms was investigated.

The results showed that 85 culturable microbial strains were isolated and purified from the mining area soil samples, and three dominant strains capable of driving mineral weathering and dissociation were screened. Under optimal conditions, the dissociation rates of cobalt and nickel from raw ore samples by fungus B1-1F3 reached 40.5% and 58.7%, respectively. Combining macro- and micro-scale characterizations, three leaching mechanisms by which this dominant strain drives the supergene weathering of laterite cobalt-nickel ore were discussed: (1) A chemical acid dissolution mechanism that creates a highly acidic microenvironment through high-intensity metabolic acid production, where free protons (H^+) directly attack and destroy the lattice of iron-manganese oxides; (2) A redox mechanism where heterotrophic metabolites mediate local reductive dissolution of minerals, combined with a macroscopic aerobic system to establish a dynamic Fe^{3+}/Fe^{2+} cycle, raising the redox potential to accelerate element mobilization; (3) A complexation mechanism that secretes low-molecular-weight organic acids as ligands to specifically coordinate with target metals, thereby breaking the dissolution equilibrium, coupled with the biophysical weathering effect where fungal hyphae physically penetrate the secondary jarosite passivation layer and overcome

interfacial mass transfer resistance. These findings indicate that a multi-synergistic supergene bioleaching mechanism exists in the Nanjian cobalt-nickel mining area, Yunnan.

From the interdisciplinary perspective of geomicrobiology and supergene geochemistry, this study reveals the ecological characteristics and element mobilization mechanisms of indigenous microorganisms in weathering-type cobalt-nickel mining areas, enriching the supergene geochemical theory of laterite cobalt-nickel deposits.

Key words: Weathering-type cobalt-nickel deposit, Geomicroorganisms, Supergene weathering, Bio-mineral interface

Acknowledgements This project was supported by the New Round Prospecting Action and Provincial Geological Exploration Fund Project for 2025 (SJ[2025]KC007).

THE EFFECT OF CO2 ON HYDROGEN GENERATION DURING PERIDOTITE SERPENTINIZATION:

Ruifang Huang[1], Weidong Sun[2], Wenwen Li[1], Xiuqi Shang[2]

1. Key Labortary of Tropical Oceanography, Chinese Academy of Sciences, Guangzhou 510301, China.
2. Center of Deep Sea Research, Institute of Oceanology, Chinese Academy of Sciences, Qingdao 266071, China.

Abstract Hydrogen (H_2) is an important clean energy source, and its geological production is closely linked to serpentinization. Serpentinization is a low-temperature (≤500 °C) hydrothermal alteration of ultramafic rocks (typically komatiites and peridotite), where olivine and pyroxene of ultramafic rocks are transformed into serpentine, (±) talc, and (±) brucite. Serpentinization occurs in diverse geological settings, including the ocean floor, mid-ocean ridges, and subduction zones. Critically, the process generates hydrogen, which sustains microbial communities in hydrothermal ecosystems. The H_2 originates from the reduction of water-derived H^+, driven by the oxidation of ferrous iron (Fe^{2+}) in olivine and pyroxene to ferric iron (Fe^{3+}).

In spite of its significance, the effect of CO_2 on hydrogen generation has remain controversial. Some studies reported that CO_2-bearing solutions enhance H_2 generation, whereas other studies documented that CO_2-bearing solutions impedes H_2 generation. Most previous experiments were performed using olivine and CO_2-bearing solutions, with CO_2 concentrations largely scattered from 0.08 to 1.0 mol/kg. A few experiments have been conducted using peridotite and CO_2-bearing solutions, and effect of CO_2 on H_2 generation during peridotite serpentinization remains poorly constrained.

This study involved serpentinization experiments on peridotite at 300 °C and 300 MPa with the addition of CO_2-bearing saline solutions. We found that low concentrations of carbon dioxide slowed down serpentinization and reduced hydrogen yield. In contrast, higher concentrations accelerated peridotite serpentinization, especially altering its pyroxene minerals, releasing more silica, and cutting hydrogen levels nearly 10 times. Our results show carbon dioxide has different effects on olivine and peridotite and can either speed up or slow down serpentinization depending on its concentrations, revealing its complex role in deep Earth geochemical processes.

Key words: Serpentinization, Hydrogen, Carbon dioxide

THE FORMATION AND EVOLUTION OF HYDROUS MINERALS ON THE SURFACE OF MARS

Jiacheng Liu NWU-HKU Joint

Centre of Earth and Planetary Sciences, Department of Earth and Planetary Sciences, the University of Hong Kong, China (jcliu01@hku.hk)

Abstract Understanding the evolution of habitable aqueous environments on the martian surface is a central goal of planetary science. Because hydrous minerals are direct products of water–rock interaction, their occurrence and evolution preserve a valuable record of past surface water environments on Mars. Their evolution on Mars—from clay minerals on early Mars, to sulfates during the middle period, and finally to widespread Fe(oxyhydr)oxides in more recent times—is well documented. However, the mechanisms underlying their formation remain controversial, and the drivers of this evolution are still unclear, limiting our understanding of Mars's habitable aqueous environments. Drawing primarily on Mars rover observations, we propose a preliminary framework in which climate temperature and the coupling style of water–rock interaction jointly controlled hydrous mineral evolution. As the martian climate progressively cooled from the early stage ($T > 0$ °C), through the middle stage ($T \leq 0$ °C), to the late stage ($T \ll 0$ °C), changes in the availability and physical state of liquid water drove a shift in the dominant water–rock interaction regime—from in situ chemical leaching, to freeze–thaw cycling, and ultimately to ground-ice–magma interaction—thereby leading sequentially to the formation of clay minerals, sulfates, and Fe(oxyhydr)oxides. This framework suggests that habitable aqueous environments on Mars gradually shifted from surface settings to the near subsurface and, ultimately, to localized subsurface activity as the planet became progressively colder and drier with time.

Key words: Mars, hydrous minerals, water-rock interaction, climate evolution, habitable aqueous environment

Acknowledgements This study was financially supported by the Research Grant Council General Research Fund (Grant No. 17306623, No. 17308625), the Key Program of National Natural Science Foundation of China (Grant No. 42441803), Young Scientists Fund of National Natural Science Foundation of China (Grant No. 42302264), Young Scientists Project of the National Key R&D Program of China (Grant No.SQ2024YFF0800028).

THE INSIGHT INTO BEHAVIOR AND MECHANISM OF PHOSPHOGYPSUM DERIVED HYDROXYAPATITE EMBEDDED CHITOSAN GEL SPHERES FOR EFFICIENT SOLIDIFICATION OF URANIUM IN WASTEWATER

Faqin Dong[1,3], Qiulin Deng[2], Siyi Liao[2], Yao Fu[2]

1. School of Environment and Resource, Southwest University of Science and Technology, Mianyang 621010, PR. China.
2. School of Materials and Chemistry, Southwest University of Science and Technology, Mianyang 621010, PR. China.
3. Key Laboratory of Solid Waste Treatment and the Resource Recycle, Ministry of Education,P. R. China

Abstract Hydroxyapatite (HAP) is a low-cost, readily available phosphate mineral with high stability in oxidizing or reducing environments. large specific surface area, and strong affinity for uranium, making it a promising adsorbent for U(VI) removal. However, pristine HAP has drawbacks such as easy decomposition in acidic water, reduced adsorption capacity and selectivity in harsh environments with coexisting ions, easy aggregation, and difficulty in recycling. Thus, combining HAP with natural biopolymer Chitosan (CS) is an effective way to overcome these limitations.

Phosphogypsum (PG) mostly comprises calcium sulphate dihydrate ($CaSO4 \cdot 2\ H2O$) and contains con-taminants including phosphorus compounds, fluorides, heavy metals, and trace radioactive substances, as an industrial by-product rich in calcium resources, shows potential application value in the field of uranium-containing wastewater remediation. The oriented synthesis of hydroxyapatite (HAP) has attracted much attention, and such materials can not only inherit the advantages of calcium source of PG, but also significantly enhance the selective capture ability of uranium and environmental friendliness. Based on this, In view of this, this works prepared HAP using PG as a calcium source to achieve the resourceful utilization of PG. Meanwhile, to address the drawbacks of pristine HAP, we created biocompatible composite gel spheres using CS-embedded HAP to immobilize uranium in waste water. The purpose of this study was to investigate uranium immobili zation behavior, migration, and transformation using batch adsorption studies with HAP-CS. With the assistance of XRD and XPS analyses, the immobilization mechanism and phase transformation will be under stood through phase change and morphological transformation to solve the problem of uranium purification and waste reuse, reflecting the concept of “treating waste with waste”. The HAP-CS developed in this work is a highly efficient uranium removal material with an environ mentally friendly and simple solid–liquid separation.

The optimum pH for U(VI) removal was determined to be 4, the optimum dosage was 0.2 g/L, and qmax = 350.88 mg/g through batch experiments. When C0 = 10 mg/L, it was found that the removal rate of U(VI) by HAP-CS could be up to 99.92 %, and the residual uranium concentration was 0.008 mg/L. The removal rate of uranium can reach 95.92 % by applying it to high concentration uranium ore wastewater. Meanwhile, we found that Ca, –OH, and P-O play a dominant role in the uranium removal process, and the main mechanism of uranium removal by Hydroxyapatite-Chitosan gel spheres (HAP-CS) is surface complexation, ion exchange, and dissolution–precipitation binding. The HAP-CS has high uranium removal efficiency, simple solid–liquid separation, and good biocompatibility, and can be used to treat actual uranium-containing wastewater.

Key words: Uranium-containing wastewater, phosphogypsum, hydroxyapatite, adsorption

Acknowledgements This work was supported by the National Natural Science Foundation of China, China (41831285 and 51974261), Sichuan Science and Technology Program, China (2023YFS0359).

THE POTENTIAL ROLE OF NACL IN SHAPING PREBIOTIC CHEMICAL EVOLUTION

RuiqinYi

Guangzhou Institute of Geochemistry, Chinese Academy of Sciences，China

Abstract The origin of life remains a central unresolved question. Evidence indicates that life existed on Earth at least 3.5 billion years ago, implying that its molecular building blocks emerged even earlier. The formation of these essential biomolecular precursors remains a key challenge in origin-of-life research. Minerals are widely recognized as catalytic and regulatory agents in prebiotic chemical evolution, and even simple salts such as NaCl may significantly influence reaction pathways and molecular transformations. Here, we investigate the potential role of NaCl under radiation-driven conditions, examining its effects on nucleotide formation, nucleotide activation leading to RNA polymerization, and amino acid condensation into peptides. Our results highlight the importance of simple inorganic components in shaping prebiotic reaction networks and provide new insights into the physicochemical processes that may have facilitated the emergence of early biomolecular complexity.

Key words: Origins of Life, Chemical Evolution, RNA World, Chemical Activation

TIME EVOLUTION OF BACTERIAL CALCIUM CARBONATE BIOMINERALIZATION INVESTIGATED BY ADVANCED INFRARED SPECTROSCOPIC ANALYSIS

Agnese De Carlo [1] 2, Francesca Benedetti [1] 3, Patrizia Paganin [3], Chiaramaria Stani [2], Lisa Vaccari [2], Nora Ivani [3], Cristian Ambu [1], Flavia Tasso [3], Chiara Alisi [3], Giovanni De Giudici [1], Giovanni Birarda [2]

1. Department of Chemical and Geological Sciences, University of Cagliari, Cagliari, Italy
2. Elettra Sincrotrone Trieste, Area Science Park, Basovizza, Trieste, Italy
3. Department of Sustainability (SSPT), ENEA, Rome, Italy

Abstract Calcium carbonate ($CaCO_3$) is one of the most abundant compounds in the Earth's crust, approximately 5% of its mass. It occurs in sedimentary and metamorphic rocks and represents the main component of marine organism skeletons and shells. In industry, calcium carbonate is widely used in pharmaceuticals, plastics, and paper production, as well as in the construction sector as both a building material and an additive in cement. Moreover, calcium carbonate plays a crucial role in the global carbon cycle, making it a key system for studying minerals formation in natural environments, i.e., biomineralization processes.

This research aims to elucidate the molecular mechanisms of carbonate biomineralization (carbonatogenesis) by studying natural systems, with a focus on microbial mediation of carbonate precipitation. To this end, two bacterial strains, OSS19b *Rhodococcus qingshengii* and TSNRS12 *Rhodococcus erythropolis*, were selected from the EMCC (ENEA Microbial Culture Collection). Their biomineralization efficiency was evaluated in terms of rate and extent under standard conditions using two different culture media. Furthermore, the same bacterial strains were investigated under chemical stress conditions, particularly zinc exposure during the precipitation process, to assess the biochemical response of the bacteria to heavy metal pollution and its impact on the biomineralization processes.

Investigating bioprecipitation mechanisms in the selected microbial systems requires an advanced analytical approach. Here, a combination of fluorescence and Optical Photothermal Infrared microscopies (O-PTIR) is employed. O-PTIR is a cutting-edge technique enabling simultaneous submicron-resolution IR and Raman spectroscopy with submicrometric lateral resolution. Bacterial biomineralization process is investigated following the evolution of carbonatogenesis. Specifically, calcium carbonate formation and growth are monitored by O-PTIR analysis at time intervals of 24 and 48 hours post-inoculation of both bacterial strains, as well as after 5, 7, 15, 20, and 30 days, both for standard and stressed conditions.

To monitor mineral evolution over time, for each culture medium inoculated with the two bacterial

strains, samples were collected and deposited onto calcium fluoride (CaF_2) windows for O-PTIR analysis. Fluorescence imaging was performed using three emission filters: BFP (λ_{em} = 470 nm), GFP (λ_{em} = 525 nm), and mCherry (λ_{em} = 630 nm). The strong epifluorescence response of biologically precipitated calcium carbonate crystals was exploited to guide and complement data acquisition. IR and Raman spectra were then collected at the same position, together with hyperspectral maps over selected areas with 0.5 µm spatial resolution. IR data analysis focused on three key wavenumber regions associated with both bacterial structures and calcium carbonate-related signals: 1700-1480 cm^{-1} for proteins, 1580-1350 cm^{-1} and 875 cm^{-1} for the $CaCO_3$, and 3000-2800 cm^{-1} for lipids. After 48 hours, bioprecipitaes already exhibited differences depending of the bacterial strain and culture medium, suggesting distinct biomineralization dynamics, highlighting the presence of biostabilized amorphous calcium carbonate (ACC) phases or the presence of partially hydrated species. From 5 days onwards, $CaCO_3$-associated signals progressively increased relative to lipid and protein signals, reflecting the time-progression of biomineralization. On the other hand, Raman data analysis was used to assess calcium carbonate crystal growth, distinguishing calcite from the other polymorphic phases by following the characteristic $CaCO_3$ bands of the symmetric stretching mode ν_1 at ~1086 cm^{-1} and the lattice mode at ~284 cm^{-1}.

This research provides insights into biomolecular processes supporting the development of bio-based carbonatogenesis methods driven by bacteria. Indeed, the importance of bacterial carbonate biomineralization studies are the applications in soil and sediment stabilization and the restoration of weathered limestone and cement monuments, while also providing potential for CO_2 reduction from atmospheric and industrial emissions. By investigating the capability of different bacterial strains under standard and chemically stressed conditions, the results highlight their potential for future sustainable, bioinspired technologies.

Key words: Biomineralization, Carbonatogenesis, Calcium Carbonate, O-PTIR, Rhodococcus bacteria

Acknowledgements This research is part of the PRIN 2022 project “MeChanisms Of carbonate biomineraLizatiOn driVen by selected unicEllular oRganisms under Stress conditions. CO_2 Lovers”, involving the University of Cagliari, Elettra Sincrotrone Trieste (SISSI-Bio offline facility), and the Italian National Agency for New Technologies, Energy and Sustainable Economic Development (ENEA).

TOOTH ENAMEL NANOSTRUCTURE AS A PROXY TO RECONSTRUCT DIET CHANGES DURING HUMAN EVOLUTION: THE INTRODUCTION OF MEAT, AGRICULTURE, AND INDUSTRY

Pupa U. P. A. Gilbert[1,2] and Mackie C. O'Hara[3]

1. Department of Physics, University of Wisconsin, Madison, WI, USA.
2. Chemical Sciences Division, Lawrence Berkeley National Laboratory, Berkeley CA, USA.
3. School of Anthropology and Conservation, University of Kent, Canterbury, Kent, UK.

Abstract Tooth enamel is macroscopically similar across all vertebrate animals, but at the nanoscale it varied dramatically. Using PhotoEmission Electron Microscopy (PEEM) and Polarization-Enabled Large Input of Crystal Angles at the Nanoscale (PELICAN), we first revealed that enamel nanocrystal misorientation confers fracture toughness to the enamel material. Then, we compared tooth enamel before and after 3 major dietary shifts: the introduction of meat 2 million years before present (BP), of agriculture 12,000 BP, and the Industrial Revolution 200 years ago. Key findings are about to be published in *Nature*, and they include:

Comparing apes and monkeys with known soft-to-hard diets a clear trend emerges with misorientation of adjacent nanocrystals increasing with the hardness of food. The increase is huge, by a factor of 6.

After the introduction of meat, the misorientation of adjacent nanocrystals increased significantly, by a factor of 1.5.

After the introduction of agriculture, the misorientation increased even more, by a factor of 1.8.

After the Industrial Revolution, the misorientation did not change.

In our genus *Homo* there is a clear trend of increasing misorientation over the last 1.6 million BP.

These findings were obtained comparing the misorientation of millions of pixels, and they are all statistically highly significant. They provide crucial, quantitative evidence of enamel adaptations to dietary changes throughout the evolution of the human lineage. They reveal another hierarchical level of biomineral adaptations not previously observed, that could be harnessed as a proxy for prehistoric *Homo* populations whose teeth were found but their diets remain unknown.

Key words: human, enamel, teeth, diet, evolution

Acknowledgements European Union's Horizon 2020 programme, Marie Sklodowska-Curie

grant 101026776 to MCOH. Turkana Basin Institute-Simons Foundation grant to MCOH; DOE grant DE-FG02-07ER15899 and NSF grant DMR-2220274 to PUPAG. Experiments done at Advanced Light Source, a U.S. DOE Office of Science User Facility under Contract no. DE-AC02-05CH11231.

USING COMPUTATIONAL SIMULATIONS TO IDENTIFY THE ORIGIN OF VIBRATIONAL SIGNALS FROM BIOAPATITE

Helen E. King

MARUM, University of Bremen, Bremen, Germany

Abstract We all have at least one thing in common, we are full of nanosized mineral crystals that form parts of our bone and teeth. The minerals found within our bones not only play an important role in our mobility but also act as a reservoir for ions that are critical for cellular function. Investigating these materials and how they change as we age is imperative if we are to create targeted treatments for mineralization disorders and identify the implications of these disorders on the larger body system. Recent innovations in vibrational spectroscopy have meant that we are now able to use these techniques to look at the mineral phase within our mineralized tissues in vivo. However, the original of the vibrational signals related to the mineral phases are a matter of contention within the scientific community. Here I will examine how we can use computational simulations to evaluate the origin of different vibrational spectral features expected in bone minerals. This focuses on two recent studies from my group that have used density functional theory computational simulations of carbonated apatite to evaluate the effect of orientation on the vibrational signatures as well as the termination of the crystal structure at surfaces.

Bone is a hierarchical material with foundational building blocks at the nanometer scale that are a mix of organic-inorganic materials. The organization of these building blocks at longer length scales produces different types of bone materials, wherein the bone minerals are aligned so that their c-axis lies in the direction of the highest stress. This means that vibrational signatures taken from bone samples may be affected by orientation differences within different tissues. The simulations demonstrate that hydroxyl group signatures are highly sensitive to orientation and are only visible when the crystal is illuminated along the crystallographic c-axis, which aligns with the channels in which these ions sit within the apatite structure. This may be a reason that many researchers have highlighted the apparent lack of OH in bone tissues based on vibrational spectra. Similarly, carbonate content within bone minerals related to mineralization disorders and crystal maturation are estimated from vibrational spectroscopy data using the carbonate band intensity normalized to specific phosphate bands. However, the phosphate and carbonate band intensities are also found to be dependent on illumination orientation, but do not show the same sensitivity. The computational simulations thus demonstrate that estimates of carbonate are only robust when the samples are orientated to account for these descrepancies.

There is also an extensive discussion in the literature about the origin of anomalous vibrational bands reported in bone tissues. These bands have been used to suggest multiple different scenarios: from the presence of precursor inorganic phases to a layer of material distinctly different to apatite

that is present at the nanometer crystal surfaces. By forming slabs of carbonated apatite in silico, a second study from my group has demonstrated that simple termination of carbonated apatite to form a surface can also produce the same bands, bringing into question previous interpretations. As the surface of bone apatite is expected to be an important source of Mg for homeostasis, being able to probe the reactivity of this environment is imperative to predict how changes in mineralized tissues with ageing have knock-on effects in how bone it utilized within the larger body system. The two studies demonstrate the usability of current computational techniques for evaluating the origin of vibrational signatures, but also highlight their limitations in terms of chemical complexity and ability to replicate all features of apatitic materials.

Key words: carbonated apatites, density functional theory, vibrational spectroscopy, bone

Acknowledgements This presentation will build on two papers from my group that utilized work from Dr. Zivkovic and Dr. Gemeri conducted as part of a HPC-EUROPA3 grant for the use of key computational infrastructure (INFRAIA-2016-1-730897).

WARMING ENHANCES IRON-MEDIATED PROTECTION OF SOIL ORGANIC CARBON IN BOREAL SPHAGNUM PEATLANDS

Yunpeng Zhao[1,2], Xiaojuan Feng[1], Mari Pihlatie[3], Mika Aurela[4], Xuefei Li[2]

1. Institute of Botany, Chinese Academy of Sciences, Beijing, China
2. Institute for Atmospheric and Earth System Research (INAR)/Physics, Faculty of Science, University of Helsinki, Helsinki, Finland
3. Environmental Soil Science, Department of Agricultural Sciences, University of Helsinki, Helsinki, Finland
4. Climate System Research, Finnish Meteorological Institute, Helsinki, Finland

Abstract Boreal *Sphagnum* peatlands distributed at high latitudes (>45°N) are globally important carbon reservoirs and store nearly 30% of the world's soil carbon. Recent studies have shown that *Sphagnum* acts as an efficient "rust engineer" by promoting the formation of reactive (i.e. poorly crystalline or amorphous) iron (Fe) (hydr)oxides. These reactive Fe minerals can stabilize up to 40% of soil organic carbon (SOC) in wetlands as Fe-bound organic carbon (bound OC), representing an important stable carbon pool that underpins long-term carbon sequestration. However, boreal regions are warming faster than the global average, and boreal *Sphagnum* peatlands are highly sensitive to climate warming. Understanding how warming alters Fe-organic carbon interactions is therefore critical for predicting long-term SOC stabilization in boreal *Sphagnum* peatlands.

Here we leverage two field warming experiments in the typical boreal peatlands of Finland that last for 6 and 16 yr, respectively. Importantly, both warming experiments encompass a regime dominated by *Sphagnum* and a regime dominated by graminoids along the water-table gradients, enabling a comparative assessment of warming effects on wet ecosystems dominated by different plant groups. We find that warming increases the contents of reactive Fe (hydr)oxides and bound OC in *Sphagnum* peatlands. This enhancement appears to arise from two main mechanisms. First, warming promotes the growth of the "rust engineer" *Sphagnum*, which likely increases the release of acidic and phenolic metabolites that facilitate the accumulation of reactive Fe (hydr)oxides and strengthen iron-mediated SOC protection. Second, metagenomic analyses suggest that warming suppresses microbially mediated Fe reduction while enhancing microbial Fe oxidation potential, thereby favoring the accumulation of reactive Fe (hydr)oxides. Together, these results indicate that warming may enhance SOC accumulation in boreal *Sphagnum* wetlands by strengthening Fe-organic carbon interactions.

Key words: Global warming, Northern peatlands, Iron-organic carbon interactions, Fe oxidation and reduction, carbon cycle

WHY DO MOST HYPERURICEMIC PATIENTS NEVER GET GOUT? REVEALING HIDDEN CONTROLS ON URIC ACID AND GUANINE CRYSTALLIZATION

Zak Jibrin[1], Nathan Yee[2], Vikas Nanda[3], Shaunna Morrison[1]

1. Earth and Planetary Sciences, Rutgers University, New Brunswick, Piscataway, NJ, USA
2. Environmental Sciences, Rutgers University, New Brunswick, Piscataway, NJ, USA
3. Biochemistry and Molecular Biology, Rutgers University, New Brunswick, Piscataway, NJ, USA

Abstract Why do most hyperuricemic patients never get gout? Hyperuricemia, defined as blood urate at or above the supersaturation threshold, is widely considered a prerequisite for urate crystallization. Yet most hyperuricemic individuals never develop gout, while acute gout flares can also occur in individuals with otherwise normal blood urate concentrations. Supersaturation alone therefore cannot explain why crystallization occurs in some cases but not others. This paradox exposes a major gap in our understanding of oxopurine crystallization and points to decisive controls acting at the precursor stage, where particle size, stability, and attachment behavior shape downstream crystal morphology, ripening trajectory, and final phase outcome. Here we show that these hidden controls arise from ion hydration-shell effects that govern supramolecular self-assembly, attachment kinetics, scaffold architecture, and ultimately polymorph selection through crystallization by particle attachment.

Insight into these hidden controls comes from guanine, a similarly low-solubility oxopurine metabolite that provides a useful analogue system for uric acid because their crystallization pathways share many of the same underlying controls. Across a broad range of biologically controlled and influenced settings, guanine reveals how organisms can modulate precipitation, crystal morphology, phase selection, and crystallization trajectory. Across the tree of life, guanine crystals are exploited as functional materials, serving as reflectors in fish and spiders and as tunable photonic architectures enabling color change in chameleons. In a striking parallel, uric acid itself was recently shown to crystallize under biological control in medaka fish, where it produces white coloration. Guanine can also appear in non-functional settings, including metabolically induced spherulites in bacteria. Together, these examples show that oxopurine crystallization is not merely a waste-disposal accident, but a broader materials process whose outcome depends on how precursor populations assemble, attach, organize, and ripen. From this perspective, unusual morphologies and metastable polymorphs may arise not only from supersaturation or biomineralizing macromolecules, but also from ion-mediated control over the crystallization pathway itself.

To test these controls directly, parallel experiments with guanine and uric acid solutions were titrated with NaOH, KOH, CsOH, and NH4OH to probe cation- and pH-dependent effects on

aggregation and crystallization. Dynamic light scattering was used to monitor assembly kinetics and aggregate-size evolution, while X-ray diffraction, ATR-FTIR, and scanning electron microscopy characterized phase, structure, and morphology. Initial results reveal strong cation-specific effects on guanine assembly, with K+ promoting the fastest aggregation, followed by Na+, whereas Cs+ slows assembly and NH4+ produces the slowest aggregation. Ongoing experiments with kosmotropic and chaotropic solutes are testing whether hydration-shell stabilization or disruption further modulates precursor stability, stacking behavior, aggregate morphology, and pathway selection. Taken together, these findings support a molecular-to-mineral framework in which ion-dependent hydration environments regulate precursor stability and attachment kinetics, which in turn dictate scaffold architecture, ripening trajectory, morphology, and final polymorph outcome. This framework clarifies how biological systems may regulate guanine platelet formation, identifies upstream therapeutic targets for inhibiting uric acid assembly in gout, and informs the design of guanine-based photonic and bioelectronic materials, including electro-switchable windows, low-power reflective displays, and other technologies based on electrically tunable, wavelength-selective reflection from guanine nanocrystals.

Key words: Biomineralization, Crystallization, Guanine, Uric acid, Self-assembly

XANES AS A TOOL FOR RESOLVING PHOSPHORUS SPECIATION IN ENVIRONMENTAL BIOMINERALIZATION SYSTEMS

Cristian Ambu[1], Giovanni De Giudici[1], Carlo Meneghini[2], Patrizia Onnis[1], Daniela Medas[1], Giovanni Birarda[3], Carla Buosi[1], Lulu Al Luhaibi[4], Alexey Maximenko[4]

1. Department of Chemical and Geological Sciences, University of Cagliari, Italy
2. Department of Science, Roma Tre University, Italy
3. SISSI - Chemical and Life Science branch, Elettra-Sincrotrone Trieste S.C.p.A, Italy
4. SOLARIS National Synchrotron Radiation Centre, Jagiellonian University, Poland

Abstract Biominerals arise from the interplay between living organisms and their surrounding environment and often exhibit distinctive characteristics, including specific morphologies and variations in internal atomic order that reflect the influence of biological processes during mineral formation. When organisms exert direct control over biomineral precipitation, this process is typically mediated by the secretion of specific biomolecules, such as phosphoproteins and phospholipids, and by the development of organic matrices. However, conventional analytical methods, such as scanning electron microscopy (SEM) and X-ray diffraction (XRD), often fail to provide definitive information, as biological contributions are typically expressed at sub-micrometric and molecular scales. Robust identification of biomineralization processes therefore requires the integrated use of advanced analytical techniques capable of resolving both structural and chemical features at appropriate spatial scales. This limitation is particularly critical for phosphorus, a key component of many biological molecules and a potential proxy for biomineralization, whose mode of occurrence in biominerals remains difficult to resolve. In this context, X-ray Absorption Near Edge Spectroscopy (XANES) represents a suitable approach for investigating phosphorus speciation and local coordination environments in complex natural systems. The technique is element-selective and, due to its sensitivity to the local atomic structure, can be applied to a wide range of samples, regardless of crystallinity and physical state, including powders and intact materials.

The present study evaluates the suitability of P K-edge XANES for investigating phosphorus speciation and local atomic environments across different biomineralization systems, with the broader aim of elucidating the role of phosphorus in these processes. Most samples originate from metal-contaminated environments in the SW Sardinia mine district (Italy). The dataset includes several mineral and biomineral systems: three species of foraminifera (*Miliolids*, *Elphidium*, and *Ammonia*); plant-derived *Juncus acutus* materials (stem, root, and rhizosphere); and two samples from surface waters contaminated with Pb, Zn, Cd, As, and Fe. The latter include a mineralization system in which carbonate green rust phases are likely precipitated and stabilized through

Pseudomonas-mediated activity, and a dark, fine-grained mud collected from a tailings-impacted river pond. Measurements were carried out at the ASTRA beamline at Solaris (Poland), with data collected in fluorescence mode. Data processing and analysis were carried out using Larix, with interpretation based on comparison with an open-access database of reference spectra collected at multiple synchrotron facilities or from the literature.

Our results indicate that: (1) in dead foraminiferal shells and partially oxidised green rust samples, phosphorus exhibits local coordination environments consistent with calcium phosphate minerals, such as octacalcium phosphate (OCP) or hydroxyapatite (HAP); (2) in Juncus acutus materials, phosphorus is mainly associated with poorly ordered phases, including phosphorus in organic form, and the quantitative XANES analysis reveals the presence of a crystalline phase consistent with HAP and/or OCP; (3) In fine-grained mud, phosphorus occurs mainly in poorly ordered phases, but also in other forms that may include associations with metals and/or organic phosphorus compounds.

Overall, P K-edge XANES spectra provide sufficient structural sensitivity to distinguish between organic and inorganic phosphorus, as well as between crystalline and poorly ordered phases, enabling robust assessment of phosphorus speciation and local coordination environments in natural biomineral systems. These findings support the use of XANES as an effective tool for disentangling key steps in biomineralization processes.

Key words: Synchrotron techniques, P K-edge XANES, organic phosphorus, local atomic structure, heavy metal-polluted environmental samples

Acknowledgements This study was carried out within the national project CO2LOVERS, which involves a multidisciplinary research team of environmental microbiologists and biomineralogists from ELETTRA Sincrotrone Trieste (SISSI beamline), the University of Cagliari, and the National Agency for New Technologies, Energy and Sustainable Economic Development (ENEA). The XANES experiments were supported by the CERIC-ERIC program (exp. #20252145). The support of ASTRA (Solaris) beamline staff is gratefully acknowledged.

COMPARATION OF THE GEOTHERMOBAROMETERS APPLIED TO SPECIAL NATURAL ECLOGITE AND BLUESCHIST

Hui C.G. Zhang [1], Zhen M.G. Li [1,2], Chun-Ming Wu [1]

1. National Key Laboratory of Earth System Numerical Modeling and Application, College of Earth and Planetary Sciences, University of Chinese Academy of Sciences, Beijing 101408, China
2. Department of Earth and Space Sciences, Southern University of Science and Technology, Shenzhen 518055, China

Abstract The validity of commonly used geothermobarometers for eclogite and blueschist containing garnet + omphacite + phengite was evaluated. Our logic is based on the fact that for different rocks within a very limited outcrop without any faults, the pressure (*P*) conditions should be identical; or alternatively, the pressure–temperature (*P–T*) conditions should also be identical for interlayered diverse rocks. We collected interbedded different eclogite samples in the ~-long transverse without any faults in the Bixiling area, the Dabie Orogen, east-central China, and collated closely interlayered eclogite and blueschist in three different outcrops, southwestern Tianshan Orogen, northwestern China. Application of different combinations of the geothermobarometers to these rocks show that: (a) Most of the different combinations of the geothermobarometers correctly identified the coesite- or quartz-bearing eclogite or blueschist; (b) Metamorphic *P–T* conditions determined by different combinations of the geothermobarometers could not converge to small *P–T* clusters, within ideally small errors (e.g., ±50 ºC / ±2 kbar), suggesting that precision of the present garnet-omphacite-phengite geobarometers is possibly not within ±3 kbar; (c) Precisely determining Fe^{3+} contents of omphacite is essential in accurately estimating the pressure and temperature conditions; and (d) The garnet-clinopyroxene geobarometer involving the Ca-tschermakite molecular of omphacite cannot be applied to crustal eclogite and/or blueschist, mostly due to negligible contents of tetrahedral Al^{3+} cations of omphacite, and other geobarometers (Ti-in-phengite, Si-in-phengite, Cr-in-omphacite barometers) cannot be applied to eclogite due to limitations of mineral assemblages or compositional limitations. Furthermore, it is quite necessary to calibrate new, precise and accurate garnet-omphacite geothermometer as well as garnet-omphacite-phengite, garnet-omphacite-kyanite-SiO_2 and garnet-phengite-kyanite-SiO_2 barometers applicable to eclogite and blueschist.

Key words: application, blueschist, comparative study, eclogite, geothermobarometry

DISCOVERY OF UHT METAPELITIC GRANULITE IN THE GROVE MOUNTAINS, INLAND EAST ANTARCTICA, AND ITS GEOLOGICAL SIGNIFICANCE

Laixi Tong[1], Haobo Wu[2], Zhao Liu[1], Xiaohan Liu[3] State Key

1. Lab of Continental and Early Life, Deparment of Geology, Northwest University, Xi'an 710069, China (Email: tonglx@nwu.edu.cn);
2. The Second Geological and Mineral Exploration Institute, Gansu Provincial Bureau of Geology and Mineral Exploration and Development, Lanzhou 730020, China;
3. Institute of Tibetan Plateau, Chinese Academy of Sciences, Beijing 100085, China

Abstract The Grove Mountains area in inland East Antarctica is considered to represent a single Pan-African (550-500 Ma) high grade metamorphic terrane and an inland extension of the early Paleozoic Prydz tectonic belt resulting from the assembly of East Gondawa supercontinent (Liu et al, 2002, 2006). The Grove Mountains consist mainly of high grade metamorphic complex, including felsic orthogneisses, garnet-absent mafic granulites, charnockite sheets, granite dykes, and minor Mesoproterozoic metasedimentary rocks and calcsilicates (Liu et al, 2003). The region is considered to have experienced three phases of deformation, D1 is indicated by the relict foliations in the gneiss or granulite lenses, D2 is related to the development of regional tight isoclinal folds and low-angle foliations, whereas D3 is associated with the development of local strongly overprinting ductile shear zones (Liu et al, 2002). The protoliths of the felsic orthogneisses and mafic granulites are considered to form in the early Neoproterozoic (920-910 Ma), while the charnockites and granites are shown to form in the early Paleozoic (550-500 Ma) (Liu et al, 2006, 2007). The mafic granulites record Pan-African peak metamorphic P-T conditions of 850 ºC and 6.1-6.7 kbar (Liu et al, 2003). In addition, some Pan-African high pressure garnet-bearing mafic granulites and kyanite-bearing metapelitic granulites are also recognized to occur as boulders in the glacial moraines in the region, with peak metamorphic P-T conditions of ~14 kbar and ~830 ºC (Liu et al, 2009; Chen et al, 2018). However, up to recently, no UHT granulite has been reported from the region, and the metasedimentary rocks are rarely studied.

Here we firstly identified typical spinel-quartz UHT metapelitic granulite from a small Nunatak outcrop in the Wilson Ridge in the region, showing gneissic structures and widespread development of garnet-bearing leucosomes, with an assemblage of garnet, spinel, sillimanite, cordierite, biotite, perthite, plagioclase and quartz. Petrographical observations and mineral compositions suggest three metamorphic stages for the granulite: (1) Pre-peak M1 stage consists of a biotite-sillimanite-spinel-cordierite-bearing inclusion assemblage in garnet porphyroblast, with low Cr_2O_3 contents (0.5-1.2 wt%) for spinel; (2) Peak M2 UHT stage is composed of garnet, spinel, cordierite, perthite, plagioclase and quartz assemblage, with a coexisting spinel-quartz assemblage and high Cr_2O_3

contents (6.2-9.5 wt%) for spinel; (3) Post-peak M3 retrograde stage consists of plagioclase, cordierite and biotite reaction rim assemblage. Phase equilibria modelling shows that M1 metamorphic conditions are 844-852 ºC and 7.3-7.6 kbar, peak M2 P-T conditions are 974-1005 ºC and 6.6-7.0 kbar, consistent with P-T estimates of 984-1030 ºC at 7.0 kbar from ternary feldspar thermometry, while post-peak M3 retrograde metamorphic conditions are 718-787 ºC and 4.6-5.3 kbar. Thus, the above three-stage P-T conditions define a clockwise P-T path of post-peak decompression and cooling. Zircon U-Pb age dating and Ti-in-zircon thermometry results indicate that 850-810 Ma ages record UHT conditions (960-900 ºC) compatible with the M2 metamorphism, and 520-500 Ma ages record metamorphic condition (775 ºC and 750 ºC) consistent with the M3 retrograde metamorphism. Therefore, the above results suggest that M1 stage may occur in Grenvillian (990-900 Ma) likely related to the assembly of Rodinia supercontinent, peak M2 UHT metamorphic stage may occur in the mid-Neoproterozoic (850-810 Ma) possibly associated with the breakup of Rodinia supercontinent, whilst post-peak M3 retrograde stage may occur in the early Paleozoic (520-500 Ma) likely reflecting the overprinting of the Pan-African event.

Key words: East Antarctica, Grove Mountains, UHT metapelitic granulite, P-T path, Geological significance

Acknowledgements This study has been supported by the NSFC project (No. 42472068, 41372070), and the fieldwork was supported by the 32rd Chinese Antarctic Research Expedition.

EPIDOTE GROUP MINERALS PARTICIPATE IN THE DEEP-EARTH WATER AND RARE EARTH ELEMENT CYCLES

He Chao[1,2], Li Lin[1,3]

1. State Key Laboratory of Geological Processes and Mineral Resources, China University of Geosciences, China
2. School of Earth Science and Resources, China University of Geosciences, China
3. Institute of Earth Sciences, China University of Geosciences, China

Abstract Epidote group minerals are ubiquitous hydrous silicates within subducting oceanic crusts, serving as critical carriers for transporting water and rare earth elements (REEs) into the Earth's interior. Through the substitution of $Ca^{2+} \rightarrow REE^{3+}$, these minerals significantly influence the deep-Earth REE cycle. In this study, we simulated the high-pressure and high-temperature (HP/HT) conditions of subduction zones using diamond anvil cells (DACs). Combined with synchrotron radiation, single-crystal and powder X-ray diffraction (XRD), as well as infrared (IR) and Raman spectroscopy, we systematically investigated the five evolutionary stages of epidote-group minerals: synthesis, stability, activation, dehydration, and decomposition.

Our results demonstrate that secondary epidote group minerals can be synthesized from oceanic sediments under subduction zone HP/HT conditions and migrate to greater depths. Water within epidote and zoisite is activated at 573 K, initiating exchange with surrounding hydrous phases. Zoisite exhibits a distinct two-stage dehydration process during its migration to a depth of 360 km: a slow dehydration stage occurs before 120 km, followed by a rapid stage between 120 and 250 km. The dehydration rate in the second stage is 4.5 times higher than that of the first. Zoisite loses 78% of its water content at a depth of 250 km, but its structural framework remains stable up to 360 km. Upon reaching 1173 K, zoisite decomposes into anorthite, pyroxene, and quartz, while epidote contains hematite due to its high iron content.

Allanite plays a crucial role in the crust-mantle REE cycle, exhibiting an enrichment sequence of Ce > (La or Nd) > (Pr or Sm). During cold subduction, although allanite undergoes continuous dehydration (losing 41% of its water at 360 km), the REEs remain sequestered within its stable structure. Subsequently, allanite facilitates the transport of REEs from the deep mantle back to the surface through solid-state diapirism, contributing to REE mineralization.

In conclusion, this study clarifies the complete kinetic path of epidote group minerals and highlights their dual function as volatile reservoirs and REE carriers, providing essential experimental evidence for the coupling mechanisms of deep-Earth water and REE cycles.

Key words: HP/HT, Epidote group minerals, Water cycle, REE cycle, Elemental substitution

Acknowledgements This study was financially supported by the National Natural Science Foundation of China (grant numbers 91962101 and 41603063).

ERROR ANALYSIS OF THE GARNET-CLINOPYROXENE-COESITE/QUARTZ OXYBAROMETERS

Chun-Ming Wu[1], Hui C.G. Zhang[2]

College of Earth and Planetary Sciences, University of Chinese Academy of Sciences, China

Abstract Oxygen fugacity directly reflects the redox state of geological surroundings. But unfortunately, it is possibly the most poorly constrained parameter in geology and in fact, errors of the oxybarometers are on the order of several magnitudes. The garnet-clinopyroxene-coesite oxybarometer was theoretically constructed based on the thermodynamically internally consistent dataset and was certified by high-pressure-temperature petrological experiments (Stagno *et al*., 2015; Purwin *et al*., 2013), and it can be applied to coesite-bearing eclogite or jadeitite. Based on the transformation of coesite ↔ quartz at thermodynamic equilibria, this oxybarometer was extended to the garnet-clinopyroxene-quartz oxybarometer. However, the systematic and random errors of these oxybarometers have seldom been systematically estimated and in turn, limiting people's understanding of their accuracy and usage. In this work, we studied their errors based on the related high-pressure-temperature petrological experiments (Stagno *et al*., 2015; Purwin *et al*., 2013). The numerical simulation on errors of the oxybarometers suggests that: (1) Precision (systematic error) of the oxybarometers is ±0.83 log unit; (2) Analytical errors of $Fe^{3+}/\Sigma Fe$ of garnet (±0.01), analytical errors of EPMA (±1.5 wt.%), errors of input temperature (±50 ºC) or pressure (±0.4 GPa) conditions, may translate to errors of computed oxygen fugacities of ±0.10~0.70 (mean ±0.27), ±0.002~0.005 (±0.004), ±0.48~1.22 (mean ±0.71) and ±0.07~0.21 (mean ±0.11) log units, respectively. Therefore, the largest error sources are errors of Fe3+/ΣFe of garnet and input temperature conditions; (3) The total random and total errors of the oxybarometers are ±1.10~2.66 (mean ±1.68) and ±1.27~3.81 (mean ±1.92) log units, respectively. In applying the oxybarometers, people must apply direct experimental measurements (Mössbauer spectroscopy, flank method, EELS, XANES or XPS) rather than charge balance method, to determine the $Fe^{3+}/\Sigma Fe$ ratios of garnet. Furthermore, the present oxybarometers should be further calibrated by direct reversed phase equilibrium experiments at broad pressure and temperature conditions which cover the stability field of both coesite and quartz.

Key words: eclogite, jadeitite, oxybarometry, random error, systematic error

EVOLUTION OF GARNET PERIDOTITES FROM MICA HILL (POLAR URALS): FROM RIFTING TO SUBDUCTION AND EXHUMATION OF THE CONTINENTAL MARGIN OF THE BALTICA CRATON

Vladimir R. Shmelev[1], Nikolai V. Gubanov[1], Fancong Meng[2], Vasiliy S. Chervyakovskiy[1]

1. Zavaritsky Institute of Geology and Geochemistry, UB RAS, Yekaterinburg, Russia
2. Institute of Geology, CAGS, Beijing, China

Abstract Garnet peridotites and eclogites from Mica Hill occur within the Precambrian Marun-Keu gneiss-amphibolite complex of the Polar Urals, which belongs to the continental margin of the Baltica craton. During the Late Cambrian to Early Ordovician (500–470 Ma), the destruction of the Baltica continental margin was accompanied by the intrusion of basaltoid melts into the lower crust. Their crystallization resulted in the formation of a layered complex (Mica Hill), comprising a peridotite–gabbro sequence and a comagmatic basaltoid dike/sill series. The protolith of the garnet peridotites consisted of ultramafic, plagioclase-bearing cumulates that preserve relict poikilitic textures after metamorphism. Their cumulate origin is supported by a decrease in silicate magnesium content from orthopyroxene-bearing to two-pyroxene peridotite varieties, as well as by REE patterns similar to those of eclogites derived from gabbros, including a positive Eu anomaly. During the magmatic stage, oxides (proto-spinel, ulvöspinel) underwent Al-chromite–Cr-magnetite and Al-chromite–ilmenite solvus exsolution; primary pyroxenes and amphiboles experienced ilmenite–Al-chromite/Cr-magnetite exsolution. The parental melt for the ultramafic cumulates corresponds to high-Ti (TiO_2 ≥1.5 wt%) basaltoids of rift-type affinity. The presence of primary amphibole indicates that the cumulates crystallized from fluid-saturated melts near the water-saturated solidus at temperatures of 1000–1100°C and relatively low pressures (5–7 kbar).

In the Late Devonian (360–370 Ma), subduction of the Baltica continental margin led to metasomatism and UHP–HP metamorphism of the ultramafic cumulates. K–Na–Ca–CO_2/H_2O metasomatism of the peridotites resulted in the formation of phlogopite-bearing veins and carbonate segregations. The peridotites likely also experienced metasomatism producing Ti-clinohumite-bearing assemblages. During prograde UHP metamorphism, plagioclase peridotites, gabbros of the layered series, and basaltoids were transformed into garnet peridotites and metagabbroic/metabasaltic eclogites. This process is recorded by prograde zoning in garnet, reflected by increasing pyrope component and HREE contents toward grain rims. Carbonate segregations within the peridotites underwent solid-state dolomite exsolution, forming symplectitic aggregates of aragonite and magnesite (ferromagnesite) under UHP conditions (≥5 GPa, corresponding to depths >150 km) and moderate temperatures (up to 800°C).

Subsequent exhumation of the Baltica continental margin rocks was accompanied by retrograde metamorphism under decreasing pressure and temperature. At an early stage, still within the ultrahigh-pressure field (~3 GPa), ilmenite–olivine intergrowths formed via decomposition of the Ti-clinohumine phase. During further exhumation under high-pressure conditions (up to 12–15 kbar) and influx of aqueous fluid, pargasite-bearing garnet peridotites and eclogites developed; phase transformation of aragonite to calcite was completed in the carbonate inclusions. At the late stage, exhumation of the garnet peridotites and eclogites to shallow crustal levels was accompanied by low-temperature metamorphism and serpentinization of the peridotites, as well as hydration of magnesite intergrowths within segregations, with their replacement by brucite and pyroaurite. Low-temperature alterations in the peridotites are marked by the formation of serpentine veinlets and ophicalcite segregations.

Thus, the garnet peridotites and eclogites of the Polar Urals record a complex evolutionary history – from magmatic layered rift-related formations of the Late Cambrian within the continental margin of the Baltica craton to eclogite-facies metamorphic rocks, whose formation was associated with ultra-deep (>150 km) subduction and subsequent exhumation to crustal levels in the Late Devonian.

Key words: Garnet peridotites, Polar Urals, Subduction, HP–UHP metamorphism

Acknowledgements This work was funded by the state assignments of the Zavaritsky Institute of Geology and Geochemistry UB RAS (projects no. 123011800009-9 and 124020400013-1) and the National Natural Science Foundation of China (grant no. 41672031).

EXOGENOUS ORIGIN OF METALLIC NANOPARTICLES ON CARBONACEOUS ASTEROIDS: EVIDENCE FROM HYPERVELOCITY IMPACT EXPERIMENTS

Qi Sun[1], Wenbi Yu[2], Xin Nie[3], Zonghua Qin[3], Quan Wan[3]

1. College of Resource and Environmental Engineering, Guizhou University, China
2. College of Earth Sciences, Guilin University of Technology, China
3. State Key Laboratory of Critical Mineral Research and Exploration, Institute of Geochemistry, Chinese Academy of Sciences, China

Abstract Space weathering, predominantly driven by meteoroid impacts and solar wind irradiation, significantly alters the surface properties of airless bodies through the production of submicroscopic metallic iron (SMFe). In the lunar regolith, SMFe consists largely of pure metallic iron, which can be formed via the reduction of endogenous Fe in native anhydrous silicates (for example, olivine and pyroxene) during shock events. However, recent analyses have revealed that the impact glasses of Ryugu samples are dominated by Fe-Ni alloy and Fe-Ni sulfide nanoparticles, with endogenous pure iron being notably scarce. This compositional dichotomy points to distinct, yet poorly understood, mechanisms regarding SMFe generation on carbonaceous asteroids during hypervelocity impacts.

Considering the prevalence of phyllosilicates in carbonaceous asteroids, we designed a series of hypervelocity impact experiments to systematically investigate the formation mechanisms of metallic nanoparticles within hydrous phyllosilicate matrices. Chlorite was selected as the target mineral due to its presence in the returned Ryugu samples and its unique Mg-Fe solid solution series. To investigate the role of Fe source (i.e., endogenous iron in the target mineral versus exogenous iron from the metallic projectile) on the generation of metallic nanoparticles, different target-projectile configurations were employed. To evaluate endogenous iron, an Fe-rich chlorite target (FeChl, Fe: 10.32 wt.%) was impacted by a spherical fused silica projectile ($SiO_2 \geq 99.99\%$) at an impact velocity of 5.0 $km \cdot s^{-1}$. Conversely, to evaluate exogenous iron, targets composed of Mg-rich chlorite (MgChl, Fe: 0.50 wt.%) were impacted by stainless steel projectiles (Fe: 69.1 wt.%, Cr: 19.4 wt.%, and Ni: 7.4 wt.%) at impact velocities of 1.5, 2.8 and 7.0 $km \cdot s^{-1}$, respectively.

Our results demonstrate that endogenous metallic nanoparticles are not efficiently produced within the FeChl impact glass under the current experimental conditions. The release of structural water via shock-induced dehydroxylation of chlorite effectively inhibits the reduction of Fe^{2+} to metallic Fe^0. In contrast, abundant exogenous metallic nanoparticles with varying sizes and species were observed in the MgChl impact glasses generated by stainless steel projectiles at impact velocities above 1.5 $km \cdot s^{-1}$. Microstructural analysis reveals that these exogenous particles originate from micro-jetting at the projectile-target interface. These micro-jetted metallic

nanodroplets were captured by the shock-generated silicate melt, forming spherical particles composed of body-centered cubic (BCC) Fe-Ni-Cr alloys upon rapid quenching. Notably, we observed the shock-induced exsolution of chromium, which migrated to the particle surfaces and was subsequently oxidized by water released via the dehydroxylation of the target. This redox interaction led to the precipitation of chromite nanoparticles from the immiscible metal-silicate melt. With increasing impact velocities, the average size of small nanoparticles (diameter < 40 nm) generally grew due to Ostwald ripening and kinetically controlled crystal growth, while larger nanoparticles (diameter > 40 nm) slightly decreased in size owing to secondary fragmentation under high pressure. These results demonstrate that micro-jetting can be a key mechanism to generate exogenous metallic nanoparticles during impacts on carbonaceous asteroids.

Key words: carbonaceous asteroids, hypervelocity impact, submicroscopic metallic iron, exogenous origin, phyllosilicates

Acknowledgements This work was supported by the B-type Strategic Priority Research Program of the Chinese Academy of Sciences (XDB 41000000).

EXPERIMENTAL SIMULATION OF SHOCK METAMORPHISM

Falko Langenhorst[1,2]

1. Institute of Geoscience, Friedrich-Schiller University Jena, Lessingstr. 14, D-07749 Jena, Germany
2. Hawai'i Institute of Geophysics and Planetology, School of Ocean and Earth Science and Technology, University of Hawai'i at Manoa, Honolulu, HI, 96822, USA

Abstract About 80 years ago, the first experimental shock techniques were developed, along with the basic laws governing the propagation of shock waves. From an early stage, these experiments were capable of compressing minerals to half their original volume. In other words, the pressures prevailing in the Earth's core could be reproduced in laboratory shock experiments long before static compression techniques, such as the diamond anvil cell, could achieve this. The strength of shock experiments lies particularly in the fact that they can achieve a combination of high pressures and temperatures, whereas the attainment of very high temperatures remains problematic in diamond anvil cell experiments.

In the field of Earth and planetary sciences, there are numerous fundamental interests in employing shock techniques:

(1) shock experiments are concerned with measuring the shock wave equation of state of minerals and rocks under extreme conditions. It is possible to reproduce virtually the entire range of pressures and temperatures that prevail in the Earth's and planetary interiors in a laboratory setting. Significant applications of shock wave experiments include the correlation of the pressure–density function with the internal structure of planets and the assessment of the melting temperatures at which planetary magma oceans can be produced.

(2) Experimental simulation of hypervelocity collisions can also be used to understand impact crater mechanics. In such experiments, spherical projectiles are employed to produce and excavate a crater in an infinite half space medium via a spherically expanding shock wave. Therefore, these experiments are not capable to recover ejected, highly shocked material.

(3) Shock experiments aiming at the simulation of shock metamorphism employ however flat-plate projectiles that drive a planar shock wave through a similarly planar target. The target is usually a metallic container, encapsulating the sample in a fashion to allow its partial or complete recovery. The experiments may differ widely in the type of accelerating system: powder and light-gas guns, high-explosive charges, electric discharge guns, and laser irradiation techniques have been used and tested to successfully reproduce shock effects in minerals.

The latter shock experiments are indispensable for understanding the nature of shock-metamorphic

effects in minerals, because recovered samples are rapidly quenched directly after shock compression, avoiding the post-shock annealing, which commonly occurs in nature. However, the formation mechanism of shock-effects remained often elusive because a time-resolved study of minerals during shock compression was for a long time impossible due to the short pulse duration in experiments, being commonly less than 1 μs. This has recently dramatically changed with the new time-resolved experimental capabilities at modern synchrotron and free-electron laser facilities. These permit scientists to study ultrafast transformations in slow motion, including the recent identification of transient metastable high-pressure polymorphs such as a rosiaite-structured phase in the silica system. The new experimental capabilities promise even more groundbreaking new fundamental insights for the future.

Key words: Experimental shock techniques, shock transformation and deformation of minerals

EXPERIMENTAL SIMULATIONS OF SERPENTINIZATION AND METAMORPHISM UNDER SUBDUCTION-ZONE DEFORMATION

Jin LIU

Center for High Pressure Science, Yanshan University , China

Abstract Subduction zones are critical tectonic settings where intense deformation, fluid-rock interactions, and metamorphic processes converge, governing crust-mantle material cycling and plate dynamics. Serpentinization, a key hydration metamorphic process of ultramafic rocks, plays a pivotal role in modulating rock rheology, plate interface coupling, and seismicity in subduction zones. This study conducts systematic high-pressure and high-temperature (HPHT) experimental simulations to investigate the co-evolution of serpentinization and metamorphism under deformation conditions analogous to natural subduction zones. Ultramafic rock samples (e.g., peridotites) were subjected to controlled pressure, temperature, and strain regimes, mimicking the shallow to intermediate depths of subducting slabs. Microstructural observations, mineralogical analyses, and mechanical measurements were employed to quantify the extent of serpentinization, metamorphic mineral assemblage evolution, and their impacts on rock strength and deformation behavior. The experimental results demonstrate that serpentinization is accerated synchronously with metamorphic reactions under subduction deformation, significantly weakening rock strength and promoting ductile deformation by reducing friction at grain boundaries. Additionally, fluid release during metamorphic dehydration and serpentinization regulates the brittle-ductile transition of rocks, providing critical insights into the mechanisms of slow slip events and intermediate-depth seismicity in subduction zones. These findings not only clarify the coupling relationship between deformation, serpentinization, and metamorphism but also provide quantitative constraints for geodynamic models, enhancing our understanding of material cycling and tectonic dynamics in subduction systems.

Key words: High Pressure and High Temperature, Thermal Alteration, Deep Carbon, Deep Water, Subduction zones

EXTREME METAMORPHISM AND METAMORPHIC FACIES SERIES AT CONVERGENT PLATE MARGINS: IMPLICATIONS FOR SUPERCONTINENT DYNAMICS

Yong-Fei Zheng*

School of Earth and Space Sciences, University of Science and Technology of China, Hefei 230026, China

Abstract Crustal rocks may undergo different grades of regional metamorphism along converging and converged plate margins. The nature of metamorphism is affected by such three key variables as temperature (T), pressure (P) and time (t). For this reason, metamorphic P-T-t paths are widely used to interpret metamorphic processes. However, problems were encountered in interpreting not only clockwise P-T paths that exhibit decompressional heating but also anticlockwise P-T paths that are characterized by compressional cooling common. For this reason, metamorphic T/P ratios are developed to qualify prograde, peak and retrograde metamorphic processes, respectively. In doing so, it is recognized that metamorphism may take place under extreme P-T conditions, giving rise to characteristic mineral assemblages of either ultrahigh-pressure (UHP) or ultrahigh-temperature (UHT) metamorphism. The formation and evolution of these assemblages have important implications not only for the generation and differentiation of continental crust through the operation of plate tectonics but also for mountain building along both convergent plate margins.

In principle, the products of extreme metamorphism can be linked to their lower grade counterparts at the same metamorphic facies series. They range from UHP through high-pressure (HP) eclogite facies to blueschist facies at low geothermal gradients and from UHT through high-temperature (HT) granulite facies to medium-temperature (MT) amphibolite facies at high geothermal gradients. The former is produced by low T/P Alpine type metamorphism during compressional heating in active subduction zones, whereas the latter is generated by high T/P Buchan type metamorphism during extensional heating in rifting zones. In between is moderate T/P Barrovian type medium-pressure (MP) amphibolite to HP granulite facies series, which were brought about by compressional thickening of the continental crust during syn-collisional orogeny. The geothermal gradient of crustal metamorphism at convergent plate margins changes in both time and space, with lower T/P ratios in the compressional regime during cold to warm subduction but higher T/P ratios in the extensional regime during hot to ultrahot rifting. In particular, bimodal metamorphism, one colder and the other hotter, would develop one after the other at convergent plate margins. The first is caused by lithospheric subduction at lower geothermal gradients and thus proceeds in the compressional stage of converging plate margins; the second is induced by lithospheric rifting at higher geothermal gradients and thus proceeds in the extensional stage of converged plate margins. As a consequence, bimodal metamorphism is primarily dictated by changes in both thermal state

and dynamic regime along plate margins. Furthermore, the extreme metamorphism has great bearings not only on reworking of accretionary and collisional orogens for mountain building in continental interiors but also on supercontinent dynamics in the Wilson cycle.

In general, supercontinent assembly is associated with compressional metamorphism during continental collision, whereas supercontinent breakup is associated with extensional metamorphism during continental rifting. While successful rifting results in continental breakup and even seafloor spreading, aborted rifting leads to extrusion of metamorphic core complexes at converged plate margins. In either case, partial melting of the continental crust was induced by upwelling of the asthenosphere in response to foundering of the previously thickened lithosphere along fossil suture zones. During this process, zircon grows abundantly through felsic magmatism along converged plate margins, but its U-Pb ages noy only postdate the continental assembly but also predate the continental breakup. These ages are intermediate in the cycle of supercontinents and hence responsible for reworking rather than growth of the continental crust. As such, it is problematic to utilize the zircon U-Pb ages as a temporal proxy for the assembly of continental blocks in the geological history.

Key words: UHP metamorphism, UHT metamorphism, bimodal metamorphism, continental rifting, supercontinental cycle

FIRST FINDING OF CALCIUM POTASSIUM PYROPHOSPHATE $CAK_2P_2O_7$ IN LUNAR RETURN SAMPLE

Runlian Pang[1], Tianhao Niu[2], Kairui Tai[1], Yuyan Sara Zhao[1], Junliang Sun[2*], Wei Du[3*],

1. Research Center for Planetary Science, College of Earth and Planetary Sciences, Chengdu University of Technology, China.
2. College of Chemistry and Molecular Engineering, Peking University, China
3. State Key Laboratory of Critical Mineral Research and Exploration, Institute of Geochemistry, Chinese Academy of Sciences, China

Abstract Impact glass is a major component of lunar regolith and serves as an ideal carrier for studying lunar impact processes. During our investigation of the Chang'e-5 lunar impact glass beads, we identified a compositionally unique glass bead (GL-109), approximately 100 μm in size. This bead exhibits a pronounced enrichment of moderately volatile and volatile elements from its center to its margin. For example, Na_2O content increases from 0.73 wt% at the center to 2.93 wt% at the edge, K_2O increases from 0.53 wt% to 5.79 wt%, P_2O_5 increases from 0.53 wt% to 0.72 wt%, and SO_3 increases from 0.07 wt% to 1.01 wt%. The contents of moderately volatile elements at the center of this glass bead are far higher than those in glass beads from Chang'e-5 or other lunar samples (for instance, P_2O_5 in Chang'e-5 lunar impact glass beads is typically below 0.10 wt%, and Na_2O and K_2O rarely exceed 0.3 wt%), indicating a unique source region for this bead, probably one that is rich in KREEP components.

The enrichment of moderately volatile elements such as alkalis and phosphorus at the margins of impact glass beads is not uncommon and is generally interpreted as the result of condensation of alkali metals (mainly Na and K) during high-speed lunar impacts. However, enrichment levels comparable to those in GL-109 have never been reported. Furthermore, some adherent materials are present on the surface of GL-109. Using FIB-TEM techniques, we analyzed the composition of these adherent materials and found them to be K-, P-, and Ca-rich glasses and their compounds. TEM-EDS and SAED analyses indicate that one of the K-Ca phosphate minerals matches $CaK_2P_2O_7$. Meanwhile, we collected three-dimensional electron diffraction (3D-ED) data on the FIB foil using continuous precession electron diffraction tomography (cPEDT) to determine the crystal structure parameters of this mineral. $CaK_2P_2O_7$, here referred to as pyrophosphite (not yet approved by the IMA), was first discovered in ash resulting from the combustion of bat guano in a cave in South Africa. It has also been found as a combustion product of calcium hypophosphite (e.g., $Ca(H_2PO_2)_2$) using potassium nitrates or nitrites as oxidizers. No other natural occurrence of $CaK_2P_2O_7$ has been reported to date. Combining the petrographic and geochemical (trace element) characteristics of GL-109, we propose that the formation of this glass bead reflects the impact melting, evaporation, and condensation processes of KREEP-rich rocks. This finding deepens our understanding of the

cycles of phosphorus and alkali elements on the Moon.

Key words: Chang'e-5 sample, calcium potassium pyrophosphate, shock vaporization and condensation, phosphorus and alkali element cycles

Acknowledgements This work was supported by the Natural Science Foundation of Sichuan Province (Youth Science Fund Project, 2025ZNSFSC1180).

FORMATION OF SHOCK MELT VEIN THROUGH MULTIPLE SHEARING: RECORDS IN LUNAR METEORITE NORTHWEST AFRICA 14526

Tian-Ran Du[1], Ai-Cheng Zhang[1], Qiang Zheng[2], Chi Ma[3], Jia-Ni Chen[1], Yuan-Yun Wen[4], and Falko Langenhorst[5]

1. State Key Laboratory of Critical Earth Material Cycling and Mineral Deposits, School of Earth Sciences and Engineering, Nanjing University, Nanjing 210023, China.
2. CAS Center for Excellence in Nanoscience, National Center for Nanoscience and Technology, Beijing 100190, China.
3. Division of Geological and Planetary Sciences, California Institute of Technology, Pasadena 91125, USA.
4. Institute of Geochemistry, Chinese Academy of Sciences, Guiyang 550081, China.
5. Institute of Geoscience, Friedrich Schiller University Jena, Jena 07743, Germany.

Abstract Shock melt veins in meteorites formed through interaction between shock wave and rocks. Previous studies show that the duration of high-pressure conditions may exceed the solidification time of melt veins by orders of magnitude, allowing multiple shearing in one impact event. This multiple shearing will lead to remelting and solidification of the pre-existing solid material within melt veins. Here, we report the mineralogical behaviors of minerals within and surrounding a garnet-bearing shock melt vein in the lunar basaltic meteorite Northwest Africa (NWA) 14526 and discuss the key role of multiple shearing.

The melt vein (~40 μm wide) contains super-silicic garnet (Si ~3.34 apfu) in the center and olivine (Mg#=40–47) and Fe,Mg-rich tissintite along the edge, which are cemented by glassy matrix. The garnet grains exihibit fracturing and skeletal shapes and show local overgrowths by Al-richer garnet. Host olivine adjacent to the melt vein and relict olivine fragments (Mg#~30) have partially transformed into fine-grained assemblage of Fe^{3+}-bearing clinoenstatite + magnesiowüstite + metallic iron. Further away from shock melt veins, the olivine exhibits a zone (a few micrometers in width) with segmented texture. Metal particles are also present in the segmented regions. These shock metamorphic features cannot be explained with single melt-vein formation. Instead, their formation can be best explained with multiple shearing based on the following considerations.

1) Morphology and overgrowth of garnet. The morphology of garnet in NWA 14526 requires post-crystallization shearing and fracturing. And the overgrowth of Al-rich garnet indicates a second crystallization of garnet, probably before the solidification of the melt surrounding the skeletal garnet.

2) Reverse pressure zonation in mineral assemblage within the melt vein. The Si and Al contents of garnet in NWA 14526 indicate a crystallization pressure of ~15 GPa, while olivine and tissintite

at the edge indicate lower crystallization pressures. This zonation is contrary to typical zoned shock melt veins, considering that the melt-vein solidification typically occurs during decompression stage with the vein edge cooling earlier than the vein center. The mineral assemblage along the edge requires relatively low-pressure melting and recrystallization.

3) Complex phase transformation behaviors of olivine. The clinoenstatite + magnesianwustite assemblage is consistent with dissociation of olivine. The presence of Fe^{3+} in clinoenstatite indicates that it probably transformed from bridgmanite. The segmented texture of olivine and the presence of metal particles therein require the back-transformation of certain high-pressure polymorph of olivine (probably ringwoodite) and the migration of metal praticles along the boundaries between segmented olivine grains during a second deformation.

Key words: Super-silicic garnet, Phase transformation, Lunar meteorite, multiple shearing, Shock metamorphism

FROM EVIDENCE OF DEEP SUBDUCTION TO DECODING COLLISIONAL DYNAMICS: NEW PERSPECTIVES ON UHP METAMORPHISM

Tatsuki Tsujimori[1], Nami Takeda[1], Tan Furukawa[1], Tetsumaru Itaya[2]

1. Department of Earth Science, Graduate School of Sciece, Tohoku University, Japan
2. Japan Geochronology Network (jGnet), Japan

Abstract More than 40 years after the landmark discovery of coesite in regional metamorphic rocks by C. Chopin and D.C. Smith, and more than two decades after the influential reviews by J.G. Liou and co-workers, research on ultrahigh-pressure (UHP) metamorphism has clearly moved beyond the stage of merely demonstrating that continental crust can be subducted to mantle depths. UHP rocks are now regarded not only as evidence of deep subduction, but also as key archives of the thermal, mechanical, and temporal evolution of collisional belts. Recent work has increasingly focused on how UHP units are distributed and preserved within orogenic belts, how long continental materials reside at mantle depths, how rapidly they are exhumed, and how these processes are linked to deformation, fluid–rock interaction, and lithosphere-scale geodynamics. In this sense, the role of UHP metamorphic rocks has shifted from documenting deep subduction itself to decoding the dynamics of continental collision and crustal recycling.

In this broader context, tracking peak pressure and its evolution under UHP conditions has become increasingly important, because robust geodynamic interpretations depend on how reliably pressure records can be linked to burial depth, exhumation history, and tectonic processes. However, no breakthrough method has yet been established for resolving pressure changes within the coesite stability field, and a major challenge remains how to extract the most geologically meaningful pressure from UHP rocks. This talk highlights that problem and explores one promising approach based on coesite inclusions hosted by kyanite. Kyanite, a low-symmetry (triclinic) mineral, is strongly elastically anisotropic, which makes pressure interpretation challenging; however, once this anisotropy is properly resolved, it has the potential to serve as one of the best recorders of entrapment conditions in UHP rocks. As a major high-pressure phase in UHP eclogite and related rocks, including whiteschists, kyanite can preserve coesite inclusions that may retain a direct record of pressure within the coesite stability field. Using coesite-in-kyanite from UHP whiteschist of the Dora-Maira Massif as an example, this talk examines the validity of this approach and places it within the broader framework of emerging perspectives on UHP metamorphism and collisional geodynamics.

Key words: UHP metamorphism, coesite, kyanite, collisional dynamics, Dora-Maira Massif

F-TYPE OLIVINE FABRIC: RECORDING UHP DEFORMATION IN CONTINENTAL SUBDUCTION ZONES

Yong-Feng Wang[1,2], Jun-Feng Zhang[1,3], Wen-Long Liu[1], Da-Peng Wen[1], Yi Cao[1], Hai-Jun Xu

1. School of Earth and Planetary Sciences, China University of Geosciences, Wuhan 430074, China
2. State Key Laboratory of Deep Geothermal Resources, School of Sustainable Energy, China University of Geosciences, Wuhan, China
3. State Key Laboratory of Geological Processes and Mineral Resources, China University of Geosciences, Wuhan 430074, China

Abstract Olivine crystallographic preferred orientation (CPO, i.e., fabric) is widely regarded as the primary cause of seismic anisotropy in the upper mantle. Given that different olivine fabric types correspond to distinct seismic properties, elucidating their formation conditions and mechanisms is of great importance. Extensive natural observations and deformation experiments have demonstrated that olivine fabric types are jointly controlled by deformation conditions (e.g., temperature, pressure, water content, presence of melt), deformation regimes/mechanisms, and/or recrystallization processes (dynamic vs. static). To date, six main types of olivine fabrics have been identified in both nature and experimental studies, namely A-type, B-type, C-type, D-type, E-type, and AG-type.

Notably, Skemer et al. (2006) reported an unusual fabric in the Cima di Gagnone peridotite massif: one sample exhibited [100] axes nearly perpendicular to foliation and [010] axes subparallel to lineation, while three others displayed typical C-type fabrics. However, that study neither named this fabric type nor explored its genesis. Here, we present olivine fabric data from four garnet peridotite samples collected at Yangkou in the Sulu ultrahigh-pressure metamorphic belt. Except for one C-type sample, the other three display characteristics fully consistent with the anomalous fabric reported by Skemer et al. (2006). This finding suggests that such a fabric is not an isolated phenomenon but may be more common in nature than previously recognized. To draw attention and stimulate further research, we designate this fabric as F-type.

If dominated by dislocation creep, this fabric would require activation of the (100)[010] slip system. However, the long Burgers vector along [010] renders this system energetically unfavorable. This inference is highly consistent with our microstructural observations: olivine lacks intracrystalline deformation features (e.g., undulatory extinction or subgrain boundaries) but instead exhibits euhedral to subeuhedral tabular crystal shapes and straight grain boundaries. These characteristics imply that the dominant deformation mechanism is not dislocation creep. Therefore, we propose that the formation of F-type fabric may be closely related to the crystal habit of olivine.

Recent work by Dilissen et al. (2021) on the Almirez ultramafic massif in southern Spain provides key insights. They documented that in the peridotite formed by dehydration of antigorite

serpentinite, tabular olivine grains surrounding olivine porphyroblasts display a peculiar crystal habit: the flattening plane is (100), with relative axial lengths following c > b >> a. This contrasts markedly with the tabular olivine commonly found in igneous rocks, where the flattening plane is (010) and axial lengths are characterized by a > c >> b or a ≈ c >> b. Given that this crystal habit is characterized by the [100] axis being the shortest, while the [001] and [010] axes have similar lengths, it can be anticipated that when olivine exhibiting such a habit undergoes oriented growth during non-dislocation creep processes, the (100) plane will preferentially align parallel to the foliation. On this basis, depending on the direction of preferential grain elongation, this may further result in either the [001] axis aligning parallel to the lineation (i.e., C-type fabric) or the [010] axis aligning parallel to the lineation (i.e., F-type fabric). This model provides a reasonable explanation for the coexistence of C-type and F-type fabrics observed in both Skemer et al. (2006) and the present study. Given that samples from both study areas have experienced ultrahigh-pressure metamorphism, we further infer that F-type fabric (and the associated C-type fabric) may record processes of metamorphic growth or recrystallization of olivine under UHP conditions.

Key words: Olivine fabric, growth fabric, garnet peridotite, UHP metamorphism, Sulu terrane

Acknowledgements This research was financially supported by the National Natural Science Foundation of China (NSFC) under Grants 41872230.

GEOCHRONOLOGY OF ULTRAHIGH-PRESSURE METAMORPHISM IN THE WESTERN HIMALAYA AND IMPLICATIONS FOR THE INDIA-ASIA COLLISION

MingCheng Duan, Lifei Zhang

SKLab-DeepMinE, MOE Key Laboratory of Orogenic Belts and Crustal Evolution, School of Earth and Space Sciences, Peking University, Beijing, China

Abstract As the most significant collisional orogenic event on Earth during the Cenozoic, the India-Asia collision shaped the Tibetan Plateau and the Himalayas—the most magnificent geomorphic units in the world today—and profoundly triggered global-scale climate reorganization and environmental evolution. The initial collision between the Indian and Asian continents marks the onset of the Himalayan orogeny, which is of vital importance for understanding the continental collision process, the geodynamic mechanisms of the Tibetan Plateau uplift, and intracontinental deformation. The Tso Morari terrane, one of the two ultrahigh-pressure (UHP) terranes in the northwestern Himalaya, formed during the initial collision of the Indian continent. Over the past three decades, geochronological studies of the Tso Morari terrane have yielded a wide range of UHP peak metamorphic ages, varying from 55 Ma to 43 Ma. These discrepancies in age interpretations have led to contrasting estimates of exhumation rates for the Tso Morari terrane and differing understandings of the subduction dynamics of the Indian continental UHP terrane. Therefore, a comprehensive and precise geochronological reappraisal of the Tso Morari terrane is urgently needed.

We conducted detailed metamorphic petrology and phase equilibrium modeling on eclogites and their host gneisses in the Tso Morari terrane. The eclogites record prograde metamorphic conditions of 22-23 kbar/520-540°C and peak conditions of 27-29 kbar/590-610°C. The host gneisses record lower-grade prograde conditions of 13 kbar/500°C; however, the discovery of coesite inclusions in zircon constrains the peak metamorphic conditions of the host gneisses to be consistent with those of the eclogites. Combining U-Pb geochronology of zircon, monazite, titanite, and allanite, we performed a novel petrochronological analysis of the mafic eclogites and host gneisses. The zircon age from the mafic eclogite is 49.2 ± 1.2 Ma; its rare earth element (REE) profile indicates growth under eclogite-facies conditions, which we interpret as the peak metamorphic age. Due to the narrow metamorphic rims on zircons in the host gneiss, we employed both conventional LA-ICP-MS spot sizes and small-spot (10 μm) LA-MC-ICP-MS for dating. The small-spot dating yielded an age of 49.87 ± 0.34 Ma, while the conventional spot dating yielded two ages: 44.59 ± 0.59 Ma and 50.3 ± 1.1 Ma. Based on analytical spot locations, the presence of coesite inclusions in zircon, and REE distributions, we consider 50.3 ± 1.1 Ma to represent the peak metamorphic age and 44.59 ± 0.59 Ma to represent the early exhumation age. Additionally, the Puga gneiss contains F-rich,

high-Al titanite (often identified as UHP titanite). Despite its high common Pb content, dating of this titanite yielded an age of 48.2 ± 3.2 Ma, which overlaps with the peak ages obtained from zircons in both the mafic eclogite and the gneiss. We also conducted high-precision in-situ U-Pb dating on widely distributed allanite in the gneiss, yielding prograde metamorphic ages of 57-55 Ma, and found that some grains can record the continuous process from peak metamorphism through early exhumation and retrograde metamorphism. In-situ Rb-Sr dating of phengite in the weakly deformed host gneiss yielded an age of 59.5 ± 1.2 Ma. Because the closure temperature of muscovite (around 550-600°C) is slightly lower than the peak temperature, we interpret that the phengite records the timing of prograde metamorphism.

Synthesizing the geochronological and metamorphic petrological studies above, we conclude that the Tso Morari terrane experienced prograde metamorphism between 59 and 55 Ma, reached UHP peak metamorphism at ~50 Ma, and underwent early exhumation at 45 Ma. Based on these new geochronological data, we calculate the exhumation rate of the Tso Morari terrane to be 6–8 mm/yr, rather than the previously thought 30 mm/yr. In-situ allanite U-Pb and muscovite Rb-Sr dating constrain the timing of the India-Asia collision to be prior to 59 Ma. Based on the prograde and peak age data alongside the P-T conditions, the subduction rate of the Indian continent is constrained to 1.1 cm/yr, which is significantly slower than rates derived from plate reconstructions (5-10 cm/yr).

Key words: Tso Morari, UHP metamorphism, Allanite, Geochronology, India-Asia collision

HIGH-PRESSURE OLIVINE POLYMORPHS IN HIGHLY SHOCKED ORDINARY CHONDRITES AND THEIR ELEMENT DIFFUSION KINETICS

Xiaorui Wang[1.2.3], Zhipeng Xia[1.2.3], Bingkui Miao[1.2.3]

1. Institution of Meteorites and Planetary Materials Research (College of Earth Sciences,Guilin University of Technology,China)
2. Key Laboratory of Planetary Geological Evolution of Guangxi Provincial Universities (College of Earth Sciences, Guilin University of Technology, China)
3. Guangxi Key Laboratory of Hidden Metallic Ore Deposits Exploration (College of Earth Sciences, Guilin University of Technology, China)

Abstract Shock metamorphism is a pivotal process governing the evolution of early solar system materials, and highly shocked ordinary chondrites (S5–S6 impact grade) serve as an exceptional natural laboratory to explore high-pressure (HP) mineral transformations and the temporal constraints of extreme geological events. Olivine, the dominant phase in ordinary chondrites (accounting for 50–60 vol%), undergoes sequential solid-state phase transitions (olivine → wadsleyite → ringwoodite → bridgmanite) under shock pressures of 13–50 GPa. However, critical gaps remain in understanding the fine-grained mineralogical characteristics of HP olivine polymorphs and their element diffusion kinetics relative to shock parameters (pressure, temperature, duration).

In this study, we selected a suite of well-characterized highly shocked ordinary chondrite samples to address these uncertainties. Our integrated analytical approach includes: (1) Electron Probe Microanalysis (EPMA) and Raman spectroscopy for HP polymorph identification and major-trace element quantification; (2) Transmission Electron Microscopy (TEM) to resolve microstructural features (e.g., coherent phase boundaries, dislocation networks) of HP phases; (3) EPMA and Laser Ablation Inductively Coupled Plasma Mass Spectrometry (LA-ICP-MS) to map element concentration gradients across olivine-HP phase interfaces, with diffusion coefficients modeled via Fick's laws and thermodynamic equilibrium calculations.

Key preliminary results include: (1) Diverse occurrences of wadsleyite and ringwoodite, including nanoscale inclusions within host olivine grains (solid-state transformation) and fine-grained aggregates associated with shock melt veins (crystallization from supercooled melts); (2) Mg# (Mg/(Mg+Fe)) values of HP polymorphs ranging from 0.85 to 0.92, showing a positive correlation with host olivine composition, indicative of equilibrium phase transformation; (3) Fe-Mg diffusion coefficients of 10^{-14}–10^{-12} m²/s at inferred shock temperatures of 1200–1500 K, corresponding to shock durations of 10–100 seconds.

This work provides tight constraints on the thermodynamic conditions and temporal scales of shock metamorphism in ordinary chondrites. The diffusion kinetics of HP olivine polymorphs also establish a comparative framework for interpreting element transport in Earth's mantle transition zone, where wadsleyite and ringwoodite are dominant phases [8]. Our findings advance understanding of early solar system shock processes and high-pressure mineral physics.

Key words: Ordinary chondrites, Olivine-HP phase, Shock metamorphism, Element Diffusion

HIGH-PRESSURE PHASES OF SILICA IN CHANG'E LUNAR SOIL SAMPLES

Wei Du[1], Qiong Li[1,2], Jing Yang[3], Yonggang Wang[4], and Zhaoxiu Jiang[4]

1. State Key Laboratory of Critical Mineral Research and Exploration, Institute of Geochemistry, Chinese Academy of Sciences, Guiyang 550081, China
2. College of Earth and Planetary Sciences, University of Chinese Academy of Sciences, Beijing 100049, China
3. Center for Lunar and Planetary Sciences, Institute of Geochemistry, Chinese Academy of Sciences, Guiyang 550081, China
4. Key Laboratory of Impact and Safety Engineering (MOE), Ningbo University, Ningbo 315211, China

Abstract housands of craters across the lunar surface provide a unique opportunity to investigate impact processes in the inner Solar System. However, high-pressure minerals have been rarely documented in sample returns from the Apollo and Luna missions. To date, stishovite represents the only reported high-pressure mineral within the Apollo 15299 regolith breccia. Specifically, the Moon's mid-to-late impact history remains poorly constrained, owing to the scarcity of lunar samples preserving prominent shock metamorphic effects from this evolutionary stage. Most available lunar samples consist of mare basalts, with limited documentation of their impact-induced alterations.

Here, we identified multiple high-pressure silica phases, including seifertite, stishovite, and coesite, in Chang'e-5 and Chang'e-6 lunar regolith samples. These newly discovered high-pressure minerals, together with additional shock metamorphic features preserved in basalt clasts, record complex impact events on both the lunar nearside and farside during the Moon's mid-to-late evolutionary period. The co-occurrence of seifertite and stishovite in the investigated samples indicates that the host rock experienced peak shock pressures of approximately 11–40 GPa, with 30–40 GPa as the optimal pressure range for their formation. Shock experiments on individual silica grains yield results consistent with our sample analyses. Notably, the peak impact pressures recorded by these high-pressure minerals are substantially lower than values predicted by hydrostatic experimental measurements and theoretical calculations. These new findings demonstrate that equilibrium-based mineral phase diagrams are not universally applicable to high-pressure mineral assemblages formed via planetary surface impacts. Accordingly, dynamic processes and kinetic effects must be incorporated when constraining impact histories through high-pressure mineral phase inversion.

Key words: Chang'e samples, Silica, Seifertite, Stishovite, Shock experiments

HYPERVELOCITY MICROMETEOROID PROCESSING OF PLANETARY SURFACES WITH THE IMPACT DUST ACCELERATOR

Zach Ulibarri[1,2], Matt Izawa[3], Fengke Cao[4]

1. Sibley School of Mechanical and Aerospace Engineering, Cornell University, Ithaca, NY USA
2. Laboratory for Atmospheric and Space Physics, University of Colorado, Boulder, CO USA
3. Institute for Planetary Materials, Okoyama University, Misasa, Tottori, Japan
4. Research Center for Planetary Science, College of Earth and Planetary Sciences, Chengdu University of Technology, Chengdu, Sichuan, China.

Abstract Atmosphere-less planetary surfaces are subjected to a constant flux of interplanetary dust particle (IDP) impact, often at velocities of several km/s up to tens of km/s. These impacts have important implications for the long-term gardening and processing of the surfaces, as they can deposit material from external sources, alter and mix existing surface chemistry, and form new chemical species. Ejecta material may be launched on ballistic trajectories, eventually falling to land elsewhere on the planetary surface, or it may achieve escape velocity.

The IMPACT Dust Accelerator at the University of Colorado provides a unique capability to study such hypervelocity impacts in highly realistic conditions. Dust grains of hundreds of nanometers to a few microns in diameter can be accelerated at velocities of up to 100 km/s and impacted onto sample target surfaces in-vacuo. Mineral surfaces, be they natural or synthetic, can be used as target material at temperatures of 80 K to well above room temperature. Typical impactors are aluminum or iron dust grains, but other impactor species such as olivine, latex, or amino-acid bearing aluminum can be used as well.

Here we present ongoing studies of laboratory micrometeoroid bombardment of planetary surface analog material. Surfaces of various composition are exposed to hypervelocity impact, and the resultant ejecta plasma plumes are sampled with impact ionization time-of-flight mass spectrometry to provide instantaneous compositional information. The target surfaces may be studied after bombardment to further assess impact shock properties, chemical alteration, and surface morphology changes. These results have important implications for planetary science, for impact shock-induced chemistry, for gardening of planetary surfaces, especially with respect to organic species, and for impact ionization mass spectrometers onboard past, current, or future spacecraft, e.g., the Cassini Cosmic Dust Analyzer (CDA), or the Europa Clipper's Surface Dust Analyzer (SUDA).

Key words: Hypervelocity impact, micrometeoroid impact, surface processing

Acknowledgements This work was funded in part by the Heising Simons Foundation 51 Pegasi B Fellowship grant number (2024-5175).

IDENTIFICATION OF NEOARCHEAN UHT METAMORPHISM FROM INTERMEDIATE AND GREYWACKIC GRANULITES IN THE YINSHAN BLOCK, NORTH CHINA CRATON

Chunjing Wei, Zizhen Yang, and Hexiang Chang
School of Earth and Space Sciences, Peking University, Beijing 100871, China

Abstract Identifying UHT metamorphism in intermediate and greywackic granulites is challenging due to the lack of diagnostic mineral assemblages. The Yinshan Block from the North China Craton (NCC) experienced granulite-facies metamorphism during the Neoarchean, but the *P–T* paths and tectonic regimes remain debated. We conduct a comprehensive study of petrography, mineral chemistry, phase equilibrium modelling, and zircon dating for intermediate and greywackic granulites from the Xiwulanbulang and Helamendu areas, and for the first time, report UHT metamorphism from the Yinshan Block. The intermediate granulites from Xiwulanbulang are migmatitic including mesosomes and leucosomes. The mesosomes contain two-pyroxene granulite-facies assemblages (Opx + Cpx + Pl + Amp + Qz) and can further be subdivided into amphibole-bearing residues and small former melt pockets. They record UHT peak conditions of 1000–1050 ºC/8–9 kbar, with possible anticlockwise *P–T* paths dominated by the post-peak near-isobaric cooling. Phase equilibria modelling also suggests that the isopleths of the Al^{T}(Cpx), X_{An}(Pl), and Ti (Amp) in *P–T* pseudosections are potentially useful for defining the peak temperatures of two-pyroxene granulites. The greywackic granulites at Hadamendu are dominated by the assemblages of Grt + Opx + Bt + Pl + Qz + Ilm in Al-poor rocks, and of Grt + Crn + Bt + Pl + Ilm in Al-rich rocks. They record counterclockwise *P–T* paths involving pre-peak up-*P* and post-peak cooling processes. The UHT peak conditions are constrained to be 950–1020 °C, 10–12 kbar using the isopleths of Ti(Bt), X_{Prp} (Grt), X_{Grs}(Grt) and X_{An}(Pl) in *P–T* pseudosections and combined with the Ti-in-zircon thermometry. Moreover, T–X_{Melt} pseudosections indicate that the amphibole-bearing residues and melt pockets preserve distinct aspects of the metamorphic evolution. The residues tend to record UHT solidi >900 ºC, where amphibole or biotite can be stable above 1000°C, making Ti(Amp) and Ti(Bt) reliable indicators for constraining the lower limit of the peak temperature. Whereas the melt or felsic pockets record HT solidi likely at ~ 850 ºC, with amphibole or amphibole stable just above the solidi. Zircon dating constrains the timing of UHT metamorphism to ca. 2.50 Ga, with post-peak cooling to solidi lasting approximately 30 Myr, approximately coeval with the regional TTG magmatism. Combining other geologic data from the Yinshan Block, we prefer a sagduction model of vertical tectonics to account for the UHT metamorphism.

IMPACT-INDUCED PRESSURE AND TEMPERATURE EFFECTS ON THE REMANENT MAGNETIZATION OF MARTIAN METEORITES

Ting Cao[1], Shaochen Hu[1], Fengke Cao[2], Yicheng Wang[3]

1. Paleomagnetism and Planetary Magnetism Laboratory, School of Geophysics and Geomatics, China University of Geosciences, China.
2. Research Center for Planetary Science, College of Earth and Planetary Sciences, Chengdu University of Technology, China
3. School of Atmospheric Sciences, Sun Yat-sen University, China

Abstract Martian meteorites preserve valuable extraterrestrial magnetic signals despite experiencing high-velocity impact events. However, the mechanisms controlling the survival of primary remanent magnetization under shock conditions remain poorly understood. Here, we used the iSALE hydrocode to track the microscale evolution of pressure and temperature across multiphase mineral assemblages during impact events. Simulations are conducted using identical projectile parameters but varying mineral assemblages, consisting of a dominant silicate phase (pyroxene or plagioclase) and a magnetic mineral phase (titanomagnetite, pyrrhotite, or iron). The influence of magnetic grain size is also evaluated.

Our results show that the peak shock pressures are relatively homogeneous across mineral phases, while post-shock temperatures exhibit significant spatial heterogeneity. Due to similar densities, peak pressures in pyroxene and magnetic minerals are comparable, whereas magnetic minerals exhibit slightly higher peak pressures than plagioclase, reflecting their significant density difference. In addition, the peak pressure of magnetic minerals also increases with magnetic grain size, likely reflecting prolonged shock-wave loading within larger particles.

In contrast, post-shock temperatures vary substantially between plagioclase and magnetic minerals, with differences of up to ~600 K. At an impact velocity of 3 km/s, plagioclase reaches a mean peak pressure of 32 ± 2 GPa and a mean post-shock temperature of 1145 ± 65 K, whereas titanomagnetite records 39 ± 3 GPa and 582 ± 44 K. The elevated temperature in plagioclase is attributed to its lower density and elastic modulus, which promote higher particle velocity and consequently greater specific internal energy. Based on typical shock pressures in Martian shergottites, estimated post-shock temperatures for iron, titanomagnetite, and pyrrhotite are 531 ± 41 K, 582 ± 44 K, and 720 ± 57 K, respectively. Comparison with Curie temperatures indicates that iron and titanomagnetite may undergo partial thermal demagnetization, whereas pyrrhotite experiences complete demagnetization due to shock heating exceeding its Curie temperature (598 K). Notably, strongly magnetic Martian meteorites predominantly contain magnetite or titanomagnetite, suggesting that shock-induced heating does not significantly compromise remanent magnetization in such systems.

Micromagnetic simulations further evaluate stress-induced effects on remanent magnetization. We studied the remanent magnetization of single-domain (SD) and vortex particles under increasing stress field. Results indicate that SD particles remain unaffected under applied stresses of 1−30 GPa in the absence of an external magnetic field. In contrast, vortex-state particles exhibit irreversible reductions in magnetization of up to ~30% between 1 and 8 GPa, with no further decrease at higher pressures. Given that shock pressures in Martian shergottites typically reach ~30−55 GPa, these results suggest that pressure-induced demagnetization is limited and does not significantly affect high-coercivity magnetic particles. Taken together, both shock pressure and post-shock heating exert only minor effects on the high-coercivity, high-temperature components of Martian meteorites, which are widely used to constrain paleofield intensity. These findings highlight the resilience of the stable remanence component to both shock pressure and post-shock heating, reinforcing the use of Martian meteorites as robust and quantitative recorders of ancient Martian dynamo activity.

Key words: Mesoscale iSALE simulation, Evolution of pressure−temperature during shock, Micromagnetic simulation, Shock demagnetization, Martian meteorites

Acknowledgements This work is supported by the Open Project for Innovative Platform of Meteoritical Research, Shanghai Science and Technology Museum (to T. Cao).

INITIATION OF PARTIAL MELTING IN NOMINALLY-ANHYDROUS ECLOGITE FACIES MAFIC ROCKS DURING EXHUMATION

Zhuocheng Wang[1,2], Lu Wang[1*], Michael Brown[1,3], Simon Schorn[4], Tim E. Johnson[1,5]

1. State Key Laboratory of Geological Processes and Mineral Resources, and Centre for Global Tectonics, School of Earth and Planetary Sciences, China University of Geosciences Wuhan, 430074, China
2. Chengdu Center, China Geological Survey (Geosciences Innovation Center of Southwest China), Chengdu, 610218, China
3. Laboratory for Crustal Petrology, Department of Geological, Environmental, and Planetary Sciences, University of Maryland, College Park, MD, 20742-4211, USA
4. Institute of Geosciences, Johannes Gutenberg University, J. Becher Weg 21, Mainz, Germany
5. Curtin Frontier Institute for Geoscience Solutions (CFIGS), School of Earth and Planetary Sciences, Curtin University, GPO Box U1987, Perth, WA 6102, Australia

Abstract Partial melting of eclogite-facies mafic rocks may significantly influence their rheology, thus plays an important role in their exhumation from mantle depths. However, whether nominally-anhydrous garnet + omphacite/sodian augite ± rutile ± coesite/quartz rocks can melt during exhumation is largely unexplored. Here, we document evidence for the initiation of in situ partial melting of nominally-anhydrous eclogite-facies garnet pyroxenite from the northern Sulu belt, China. The garnet pyroxenite forms the cores of amphibolitized boudins hosted in strongly-foliated migmatitic felsic gneisses. The rock is strongly foliated and comprises interlayered garnet-rich and clinopyroxene-rich layers, the latter containing abundant pockets of plagioclase with either euhedral clinopyroxene (Pl + Cpx leucosome) or amphibole (Pl + Amp leucosome), locally accompanied by grain-boundary films of K-feldspar (K-bearing leucosome). These leucosome pockets are preferentially located at triple junctions between clinopyroxene grains and have microstructural features, including plagioclase seams extending along clinopyroxene grain boundaries in the host, that suggest crystallization from a locally-derived melt. The calculated bulk composition of the leucosome pockets is consistent with melting through a process combining breakdown of clinopyroxene garnet with a contribution of mobile components (including H_2O and K) from the host gneiss. Thermodynamic modelling suggests that decompression from eclogite facies PT conditions generated gradients in H_2O and K_2O (where μ is the chemical potential), driving diffusive transfer of material from the gneiss to the garnet pyroxenite. This interpretation is consistent with the elevated contents of large ion lithophile and light rare earth elements in most of the leucosome pockets. Thirteen leucosomes are nepheline normative and five are hypersthene normative, suggesting that partial melting of nominally-anhydrous eclogite-facies garnet pyroxenite produces alkaline to subalkaline basaltic melts. Our findings indicate that clinopyroxene-

breakdown melting is an intrinsic consequence of suprasolidus decompression in eclogite-facies rocks, implying pervasive, albeit volumetrically minor, melt generation and a fundamental control on lithospheric rheology during continental exhumation.

Key words: eclogite facies, garnet pyroxenite, partial melting, phase equilibrium modelling, Sulu belt

Acknowledgements We thank Chunjing Wei and E. Moulas for insightful discussion. This study was supported by National Natural Science Foundation of China (42572245, 42072228, 91755213, 41961144020), the Chinese Ministry of Education (BP0719022), and the MostSpecial Fund (MSFGPMR2025-7). The China Scholarship Council funded a 12-month PhD joint supervision for ZW at Curtin University, WA (CSC No. 202106410063). ZW acknowledges financial support from the Regional Geological Survey of the Western Margin of the Upper Yangtze Metallogenic Belt (DD202402083). SS acknowledges financial support from the Austrian Science Fund (grant P-3302-N) and the Alexander von Humboldt Foundation.

IN SITU QUANTIFICATION AND CALIBRATION OF SHOCK-RELATED STRAIN IN MINERALS BY MICRO X-RAY DIFFRACTION

Roberta L. Flemming

Department of Earth Sciences, The University of Western Ontario, Canada

Abstract XRD is primarily used to identify minerals by their crystal structure, where the set of diffraction peaks is related to the lattice *d*-spacings by Bragg's Law ($n = 2d \sin\theta$). For micro XRD, a two-dimensional area detector (2D XRD) facilitates measurement of additional textural (grain size and strain) diffraction information. Single crystals produce spots on the 2D XRD image, whereas fine-grained polycrystalline materials produce complete Debye rings. Single crystal mineral grains that have been non-uniformly strained (e.g. bent or curved) produce a mosaic spread of crystal subdomain orientations, termed strain-related mosaicity (SRM). This causes streaking of diffracted X-rays along the Debye ring or chi () dimension of 2D XRD image, which is quantified as the full-width-at-half-maximum of peak intensity (FWHM). If subdomains are large, and they have individually resolved their strain, streaking is replaced by asterism, a short row of orientationally-related diffraction spots, in the 2D XRD image. Undulatory or mosaic extinction, seen in polished thin section under cross polarized light, is observed as SRM in 2D XRD, and can be quantified by measuring the diffraction streak FWHM. Penetrative stress at the atomic level can produce lattice strain, which contributes to XRD line broadening in the 2θ dimension. Lattice strain (ε) is visible as broadening of the diffraction peaks with increasing $\tan\theta$, as measured using Williamson-Hall plots. Deformed minerals may exhibit both SRM and lattice strain. Both can be quantified in the same 2D XRD image.

Deformation of rock-forming minerals is pervasive on rocky bodies across the solar system, as recorded by olivine, enstatite, clinopyroxene and plagioclase. Different minerals in a sample have different responses to shock, and together they can encapsulate a fuller record of the shock history. Ordinary chondrites contain ubiquitous olivine as well as enstatite and clinopyroxene. Ureilites contain olivine and pigeonite/clinopyroxene. Diogenites and Eucrites from asteroid 4 Vesta contain orthopyroxene and plagioclase. Martian nakhlites contain clinopyroxene; olivine-phyric examples also contain olivine. Martian shergottites and regolith breccia samples (NWA 7034 and pairings) contain considerable plagioclase. Plagioclase is ubiquitous in Lunar samples and terrestrial target rocks as well. Plagioclase amorphizes at relatively low shock pressures compared to other rock forming minerals, such that crystal X-ray diffraction peaks are replaced by broad amorphous 'humps' on the XRD pattern.

Current work involves calibration of SRM and lattice strain using experimentally shocked samples.

Micro XRD analysis of these samples has enabled calibration of peak shock pressures for olivine, clinopyroxene and plagioclase, thus underpinning the quantification of peak shock pressures experienced during impacts. Quantification of the shock deformation history of planetary materials using multiple minerals is important, as impact is a major process on all rocky bodies.

Key words: Strain-related mosaicity, asterism, lattice strain, olivine, pyroxene

Acknowledgements Funding is acknowledged from the Canadian Foundation for Innovation (CFI 2002; 2023), NSERC Research Tools and Instrumentation (RTI 2010, 2016), Canadian Space Agency (2018-2020; 2021-2023), and NSERC Discovery Grants (ongoing). Finally, this work would not have been possible without my students and my collaborators. I especially thank the members of my Mineralogy Research Group!

MELT-FLUID-DEFORMATION EVOLUTION OF THE SULU UHP ECLOGITES AND IMPLICATIONS FOR EXHUMATION DYNAMICS

Lu Wang

State Key Laboratory of Geological Processes and Mineral Resources, and Center for Global Tectonics, China University of Geosciences, 430074 Wuhan, China

Abstract Our interdisciplinary research on eclogites of the Sulu belt, one of the most deeply subducted UHP localities known globally (P_{peak} > 5.5 GPa), has led to a new understanding of the relationship between fluid and/or melt and deformation mechanisms, with implications for exhumation dynamics in continental collisional belts.

1) The UHP eclogites at Yangkou Bay are the only known example with pristine intergranular coesite, preserved in rootless intrafolial isoclinal F1 fold noses, indicating a fluid-undersaturated environment throughout the exhumation process. Comparison of the H_2O content of nominally anhydrous minerals between eclogite types, plus microstructural, petrological and structural features, demonstrates that the fold noses have the lowest inherited H_2O content (Wang L. et al., 2018). The drier environment limited fluid connectivity along grain boundaries in the fold noses, which themselves acted as rigid low strain sites and remained immune to grain-scale fluid infiltration, allowing coesite to survive. Strain localization in exhuming UHP eclogites facilitated progressive fluid infiltration, retrogression and evolution of deformation mechanisms from brittle, plastic to dynamic recrystallization(Chen Z. et al., 2025).

2) Migmatized eclogites were first reported from General's Hill (Wang L. et al., 2014), central Sulu. Whether or not they contain hydrous minerals (e.g., phengite, zoisite), can develop a solute-rich supercritical fluid or melt along grain boundaries by dehydroxylation of NAMs during the early stages of exhumation (Wang S.J. et al., 2020), whereas partial melting by breakdown of phengite and/or omphacite occurs during the later stages of exhumation (Feng P. et al., 2021). Estimation of the leucosome volume at both microstructural and outcrop scale ranges between ~10 vol% and ~24 vol% for partially melted UHP eclogite, which exceeds the threshold for melt connectivity (7 vol.%) and reduces the peak eclogite density by 5-19% (Yan C. et al., 2026). At Taohang, the dominant deformation mechanism in eclogite changes from dislocation creep around peak metamorphic conditions to diffusion creep with increasing fluid–melt mobility. This is consistent with the hypothesis that fluid exsolution and partial melting were important in reducing the strength of UHP rocks, facilitating their fast exhumation from mantle depths, as suggested by numerical modelling and experimental studies.

Key words: UHP eclogites, Sulu belt, partial melting, continental geodynamics, deformation mechanism

METAMORPHIC EVOLUTION OF ULTRA-HIGH PRESSURE GARNET CLINOPYROXENITE IN THE SANWEISHAN AREA, DUNHUANG OROGENIC BELT

Xue-Li Jia[1], Yan-Lin Zhao[1], Hui C.G. Zhang[1], Yichao Chen[2], Zhen M.G. Li[3], Chang-Ming Lu[1] and Chun-Ming Wu[1*]

1. College of Earth and Planetary Sciences, University of Chinese Academy of Sciences, Beijing 100049, China;
2. State Key Laboratory of Ecological Safety and Sustainable Development in Arid Lands, Xinjiang Institute of Ecology and Geography, Chinese Academy of Sciences, Urumqi 830011, China;
3. Department of Earth and Space Sciences, Southern University of Science and Technology, Shenzhen 518055, China.

Abstract Garnet clinopyroxenite xenoliths entrained by granitic bodies in the Daquan area, the Sanweishan arc, northern Paleozoic Dunhuang Orogenic Belt, preserve three different metamorphic mineral assemblages. The prograde assemblage (M1) consists of amphibole, plagioclase and clinopyroxene as inclusions in the garnet porphyroblast. The metamorphic peak assemblage (M2) is consisted of garnet, clinopyroxene and rutile, and the retrograde assemblage (M3) is represented by symplectic minerals (amphibole + plagioclase + quartz) rimming the garnet. Phase equilibrium modeling and geothermobarometric calculation suggest that these garnet clinopyroxenite xenoliths record clockwise *P-T* trajectories passing from 5.2–6.3 kbar / 610–660 °C (M1) through ~16–35 kbar / 750–930 °C (M2) and finally to 5.6–5.9 kbar / 650–670 °C (M3), defining hairpin-like *P-T* paths and possibly recording orogenic metamorphism. The presence of minor secondary amphibole surrounding garnet and clinopyroxene, together with the lack of pronounced diffusion rims on garnet, suggest rapid ascent to shallow depths prior to invasion of the granite, with only a short residence time at shallow levels. Zircon U–Pb dating of a representative sample possibly yields a peak metamorphic age of 446±1.4 Ma, coincident with garnet growth, while previously reported titanite U–Pb ages (~389–370 Ma) likely record recrystallization or resetting during post-peak cooling and retrogression. Based on regional geological data, we infer that the garnet clinopyroxenite in the Daquan area formed at around 446 Ma in response to the northward subduction of the Hongliuxia Ocean, and subsequently began exhumation prior to 370 Ma.

Key words: Paleozoic Dunhuang Orogenic Belt, garnet clinopyroxenite, Metamorphic evolution

Acknowledgements Prof. Yong-Hong Shi and Dr. Juan Wang helped us with electronic microbe analyses. Prof. Shan Li and Dr. Longxiang Quek guided us in laser ablation

inductively coupled plasma mass spectrometry (LA−ICP−MS) U-Pb dating of zircon. This work was supported by the National Natural Science Foundation of China (42330303, 42372258).

MICROSTRUCTURAL INVESTIGATIONS ON THE PRESERVATION MECHANISMS OF INTERGRANULAR COESITE IN UHP ECLOGITE FROM YANGKOU BAY, SULU REGION

Jinyu Zheng[1], Tao Chen[1,2]*, Junfeng Zhang[1]*, Lu Wang[1], Wenlong Liu[1], Feng Shi[1], Xiaohu Xuan[1], Mingxing Gong[3], and Zhe Gong[3]

1. State Key Laboratory of Geological Process and Mineral Resource, School of Earth Sciences, China University of Geosciences, China
2. Gemmological Institute, China University of Geosciences, China
3. Faculty of Materials Science and Chemistry, China University of Geosciences, China

Abstract Intergranular coesite found in ultra-high pressure (UHP) eclogites provides critical insights into deep subduction and exhumation processes. However, its plastic deformation behavior remains not well understood. We report here the detailed deformation micro-ultramicrostructure of both intragranular and intergranular coesite, along with its surrounding minerals in UHP eclogites from the Yangkou Bay, Sulu UHP terrane. A combination analysis of electron backscatter diffraction (EBSD), focused ion beam (FIB), and transmission electron microscopy (TEM) was performed in this study. EBSD reverals that Retrograde quartz replacing both types of coesite displays palisade textures, whereas the quartz replacing intergranular coesite further develops bulging mosaic textures. TEM analysis shows coesite is nearly dislocation-free, while retrograde quartz exhibits abundant dislocations. The defect structures in retrograde quartz include free dislocations, dislocation tangles, and subgrain boundaries. The dislocation density, quantified from total dislocations, indicates that the retrograde quartz experienced plastic deformation under differential stress. Intragranular palisade quartz records 628–999 MPa differential stress, exceeding intergranular palisade values (517 MPa; 154–165 MPa with Brazil twins) and mosaic quartz (345–657 MPa). Lower differential stress in the intergranular coesite indicates grain boundary facilitated pressure release. Notably, the intergranular coesite is free of water-related defects; however, they were detected in the surrounding retrograde quartz. Based on these results, we proposed a "stress-controlled pressure vessel" model to explain the preservation mechanism of intergranular coesite, which can only survive among 2-3 omphacite grains during exhumation. In addition to a dry preservation environment, differential stress is a more important key factor governing the preservation of intergranular coesite. Our findings provide critical micro- to ultra-microstructural insights into the preservation mechanisms of this coesite type.

Key words: coesite, preservation mechanism, pressure vessel, defect structure, Yangkou Bay

MINERALOGY CONTROL ON GEOCHEMISTRY OF (U)HP/(U)HT ANATEXIS: KNOWNS AND UNKNOWNS

Aleksandr Stepanov

State Key Laboratory of Geological Processes and Mineral Resources, School of Earth Resources, China University of Geosciences, Wuhan, China

Abstract Anatectic terranes are the major sources of granitic magmas, crust formation, fractionation and generation of metal-laden magmas. A systematic survey of the geochemistry of restites from the major (U)HP/(U)HT terranes (including but not limited to HT Mount Stafford, U-HT Ivrea-Verbano zone, and UHP-UHT Kokchetav massif) demonstrates the significant differences in the behaviour of elements caused related to melting conditions. While the major elements suggest that loss of granitic melt is the only major agent of mass transfer in (U)HP/(U)HT rocks, the amount of melt extracted in anatexis is well constrained only in exceptional cases. The haviour of lithophile trace elements during the anatexis is controlled by the assemblage of rock-forming and accessory minerals, which are strongly affected by the PT conditions. Cordierite, garnet, micas, monazite/allanite, Ti oxides (rutile and ilmenite) all assert significant effect on specific (group of) elements. The presence of abundant hosts for trace elements at mild conditions of anatexis can result in inert behaviour of many. The chalcophile elements behaviour during anatexis was likely affected mostly by the sulfides, yet the intricacies remain not well constrained. The geochemistry of restitic rocks holds troves of information regarding mineralogy, magmas metal potential and crust fractionation, which yet remain untapped in the vast restitic terranes of the world.

Key words: (U)HP, (U)HT, anatexis, restite

NANOMINERALOGY OF SHOCKED METEORITES AND IMPACTITES: DISCOVERY OF NEW HIGH-PRESSURE MINERALS

Chi Ma (马驰)

Division of Geological and Planetary Sciences, California Institute of Technology, Pasadena, USA

Abstract Nanomineralogy is the study of Earth and planetary materials at nanoscales, focused on characterizing nanofeatures (such as inclusions, exsolution, zonation, coatings, pores) in minerals and rocks, and revealing nanominerals and nanoparticles. With advanced high-resolution analytical scanning electron microscope (FE-SEM with EDS and EBSD), we are now capable to characterize solid materials easier and faster down to nanoscales. Nanofeatures are being identified in many common minerals, providing insights into their origins and physical properties. New minerals of geological significance are being discovered at micro- to nanoscales.

Since 2009, our ongoing nanomineralogy investigations of shocked meteorites and impactites have led to the discovery of 12 new high-pressure minerals and 5 new high-pressure phases, including bridgmanite ($MgSiO_3$-perovskite, the most abundant mineral in Earth), ahrensite (Fe_2SiO_4-spinel), tissintite (clinopyroxene with feldspar composition), liebermannite ($KAlSi_3O_8$-hollandite), zagamiite ($CaAl_2Si_{3.5}O_{11}$), chenmingite ($FeCr_2O_4$-CF), stöfflerite ($CaAl_2Si_2O_8$-hollandite), tschaunerite (Fe_2TiO_4-CT), feiite (Fe_3TiO_5), and liuite ($FeTiO_3$-perovskite). The findings not only provide new insights into shock conditions and impact processes on small bodies in the early solar system or on Mars, but also help investigate phase transformation mechanisms in the deep Earth. Presented here are our discovery stories, demonstrating how nanomineralogy works and the unique role it plays in Earth and planetary sciences research.

Key words: Nanomineralogy, shocked meteorites, impactites, new high-pressure minerals

NANOSCALE STUDY OF NATURALLY SHOCK-INDUCED HIGH-PRESSURE POLYMORPHS OF OXIDE MINERALS IN TWO METEORITES

Xiande Xie[1], Xiangping Gu[2], Yiping Yang[1], Ming Chen[1]

1. Guangzhou Institute of Geochemistry, Chinese Academy of Sciences, Guangzhou, 510640, China
2. School of Gemology and Mineral Resources, Jiangxi Institute of Applied Science and Technology, Nanchang, 330100, China.

Abstract High-pressure minerals serve as a key window for understanding mineral assemblages in the deep Earth and planetary impacts. Using micro-area and micro-beam techniques, we have identified various high-pressure oxide polymorphs in two meteorites. Specifically, five high-pressure polymorphs of oxide minerals were detected in the Suizhou L6 chondrite, including xieite and chenmingite (the two postspinel high-pressure (HP) polymorphs of chromite), wangdaodeite (the HP polymorph of ilmenite), riesite (the HP polymorph of rutile), and magnesiowüstite. Nanoscale investigations of these polymorphs were conducted via FIB-STEM, yielding the following results: (1) Oxide minerals in the Suizhou meteorite can transform into their HP polymorphs under natural shock compression, with xieite, chenmingite, wangdaodeite, riesite, and magnesiowüstite forming either through crystallization from dense melts or solid-state transformation of their host minerals under high-pressure conditions. (2) All HP polymorph grains of these five oxide minerals are polycrystalline aggregates composed of numerous nanometer-sized polygonal or irregular microcrystals/particles, rather than monocrystalline phases. (3) The HP polymorphs of the first four oxide minerals exhibit the same chemical compositions as their host minerals, with compression mechanisms dominated by bond angle bending or polyhedral tilting. In contrast, magnesiowüstite, a newly crystallized phase from dense silicate melts, possesses a simple cubic structure with edge-sharing polyhedra, and its unit-cell parameters can vary continuously with pressure. (4) In addition to the scattered narrow chenmingite lamellae within chromite in the Suizhou chondrite, single lamellar-structured chenmingite grains were first observed within polycrystalline xieite grains in the Suizhou melt vein, indicating the coeval formation of xieite and chenmingite under high-pressure conditions. (5) A new HP phase of chromite was observed within chenmingite lamellae in a chromite grain, which would be the third postspinel phase of chromite following xieite and chenmingite. (6) The occurrence of nanometer-sized, polycrystalline HP oxide phases in the shocked Suizhou meteorite is primarily attributed to extremely short-duration compression and rapid cooling. Furthermore, we discovered Xiexiandeite, the highest-pressure polymorph of SiO_2 and a new mineral candidate for the Earth's lower mantle, in the Muonionalusta iron meteorite. This mineral occurs as nanocrystalline aggregates in a silica vein within a kamacite-troilite matrix, closely associated with stishovite. It is suggested that this new mineral is potentially

stable at pressures exceeding 130 GPa and temperatures up to 2500 K.

Key words: Meteorites, Shock-induced, High-pressure polymorphs, Oxide minerals

PETROGRAPHY AND MINERALOGY OF THE MARTIAN NAKHLITE METEORITE HASSI MESSAOUD 001

Xinyi Tian[1], Fengke Cao[1]*, Yuyan Sara Zhao[1], Matthew R. M. Izawa[1,2,3], Yuangao Qu[4], Ning Ma[1]

1. Research Center for Planetary Science, College of Earth and Planetary Sciences, Chengdu University of Technology, Chengdu, China.
2. Institute for Planetary Materials, Okayama University, Misasa, Japan.
3. Department of Earth Sciences, Western University, London, Canada.
4. Institute of Deep-sea Science and Engineering, Chinese Academy of Sciences, Sanya, China.

Abstract Hassi Messaoud 001 is a newly classified nakhlite meteorite. Nakhlites are Martian hypabyssal igneous rocks, interpreted to have crystallized from lava flows or sills. Many Nakhlites preserve records of post-magmatic water-rock interactions on Mars, providing a unique window into the interplay between crustal fluids and near-surface igneous rocks on Mars. To date, only 34 nakhlites have been registered in the Meteoritical Bulletin Database. In this study, we integrate volumetric and petrographic approaches to characterize the petrographic and mineralogical features of a 3.67 g block of Hassi Messaoud 001, with the aim of constraining its petrogenesis and alteration history.

X-ray computed tomography (XCT) with a voxel size of 9.95 μm provides quantitative modal abundances and enables visualization of internal fractures and void networks. The sample consists of pyroxene (59.8 vol.%), olivine (23.0 vol.%), Fe-oxides (1.4 vol.%), mesostasis (13.8 vol.%), and fractures/veins (2.0 vol.%). Two-dimensional petrography and the TESCAN Integrated Mineral Analyzer (TIMA) analyses of polished slabs reveal that the meteorite is dominated by euhedral to subhedral augite (~53.4 vol.%), subhedral to anhedral olivine (~23.0 vol.%), and low-Ca pyroxene (~7.5 vol.%). These phases are embedded within mesostasis composed of coarse-grained plagioclase (8.6 vol.%) with minor K-feldspar rims(<0.1 vol.%), Fe-oxides (1.4 vol.%), apatite (0.5 vol.%), sulfides (<0.1 vol.%), and a fine-grained, K-feldspar–dominated mesostasis (2.9 vol.%) Discrepancies between XCT and TIMA modal abundances reflect heterogeneous phase distributions that are not fully captured in 2D analysis, highlighting the advantage of XCT for bulk volumetric characterization.

Electron probe microanalysis (EPMA) reveals that augite exhibits clear compositional zoning, with Ca-rich cores ($En_{34.2}Wo_{39.0}Fs_{26.8}$; n=31) transitioning to Fe-rich rims ($En_{29.1}Wo_{37.9}Fs_{32.9}$; n=22). Olivine is compositionally homogeneous and fayalitic ($Fa_{72.0\pm1.4}$; n=65). Low-Ca pyroxene is dominated by Fe-rich orthopyroxene ($En_{39.2}Wo_{3.5}Fs_{57.4}$; n=30). Plagioclase compositions ($An_{30.3\pm8.1}Or_{4.5\pm1.7}Ab_{65.2\pm8.7}$; n=15) range from andesine to oligoclase, and K-feldspar (sanidine; $An_{1.3}Or_{68.7}Ab_{30.0}$; n=3) occurs as rims on selected plagioclase grains.

Alteration features are pervasive and record both Martian and terrestrial processes. Based on

petrographic features (e.g., cross-cutting relationships), we distinguish Martian alteration from possible terrestrial weathering and exclude the later when interpreting Martian processes. Alteration veins (up to 50 μm wide) commonly occur within olivine grains and along grain boundaries. Raman spectroscopy indicates that these veins are dominated by amorphous phases. They are spatially associated with plagioclase and pyroxene inclusions and commonly across-cut host minerals. Some veins within olivine display compositional zoning. In addition, the fine-grained mesostasis shows partial alteration, developing gel-like to rosette textures. Raman spectra reveal that these altered domains are dominated by potentially amorphous materials with and hematite.

Overall, this study provides new constraints on the petrography, mineral chemistry, and alteration history of Hassi Messaoud 001, contributing to our understanding of aqueous processes and crustal evolution on Mars.

Key words: Martian meteorite, nakhlite, petrography, alteration

QUANTIFYING SHOCK-INDUCED AMORPHIZATION IN PLAGIOCLASE-RICH ROCKS USING MICRO-XRD

Fengke Cao[1,2], Roberta Flemming[2], Matthew Izawa[1,2,3], Steven Jaret[4], Jeffrey Johnson[5], Phil McCausland[2]

1. Research Center for Planetary Science, College of Earth and Planetary Sciences, Chengdu University of Technology, China
2. Department of Earth Sciences, Western University, Canada
3. Institute for Planetary Materials, Okayama University, Japan
4. Department of Earth and Planetary Sciences, American Museum of Natural History, USA
5. Johns Hopkins University Applied Physics Laboratory, USA

Abstract Plagioclase feldspar is ubiquitous in planetary materials and widely used to evaluate shock pressures in meteorites and impactites. However, shock loading occurs over millisecond timescales and generates extreme pressure–temperature gradients, resulting in strong spatial heterogeneity. As a consequence, different grains—and even domains within a single grain—record variable shock conditions, leading to incomplete and heterogeneous amorphization (diaplectic glass). Conventional shock stage classifications (S1–S6) treat the occurrence of diaplectic glass as a binary criterion, limiting their ability to provide continuous and quantitative constraints on peak shock pressures.

Building on previous calibration between shock pressure (0–56 GPa) and Debye ring broadening (FWHMχ) in experimentally shocked plagioclase, this study further develops a micro–X-ray diffraction (micro-XRD) approach to quantify shock-induced amorphization in the 2θ domain. The amorphous fraction is determined by integrating diffraction intensities over 2θ = 20°–60°, and calculated as: amorphous ratio (%) = amorphous area / (crystalline area + amorphous area) × 100.

Application to experimentally shocked andesine and bytownite samples reveals a strong correlation between amorphous content and peak shock pressure. For andesine, the amorphous fraction increases from 16.1% to 56.5% between 28.4 and 29.6 GPa, indicating the onset of significant amorphization. With increasing pressure to ~50 GPa, the amorphous content reaches ~89%. Similarly, bytownite exhibits a rapid increase from 10.3% to 58.0% between 25.5 and 27 GPa, followed by continued growth to ~90% at ~50 GPa. Both compositions show a rapid transformation over a narrow pressure interval (~25–40 GPa), suggesting the presence of an amorphization (or energy) threshold near ~25 GPa.

These results demonstrate that shock-induced amorphization in plagioclase is highly pressure-sensitive and occurs over a continuous range, rather than as a binary transition. The micro-XRD–based method establishes a quantitative relationship between amorphous fraction and peak shock pressure, providing a new continuous shock barometer that complements traditional petrographic

classifications. This approach enables more robust quantification of heterogeneous shock histories in meteorites and terrestrial impactites, and is directly applicable to the analysis of limited but complex extraterrestrial samples, including future returned planetary samples.

Key words: Plagioclase, Shock metamorphism, Micro-XRD, Amorphization, Meteorites

QUANTIFYING SHOCK METAMORPHISM IN LUNAR METEORITES USING WARREN–AVERBACH ANALYSIS AND PAIR DISTRIBUTION FUNCTIONS

Matthew R. M. Izawa[1.3,4,6]*, Andrew P. Jephcoat[1], Laura E. Jenkins[2], Edward A. Cloutis[3], Daniel M. Applin[3], Kristi M. Peters[3], Roberta L. Flemming[4], Phillip J. A. McCausland[4], Brendon J. Hall[5], Fengke Cao[6]♯

1. Institute for Planetary Materials, Okayama University, Japan
2. Diamond Light Source Ltd., Harwell Science and Innovation Campus, United Kingdom
3. Department of Geography, University of Winnipeg, Canada
4. Department of Earth Sciences, University of Western Ontario, Canada
5. SFL Scientific, USA
6. Research Center for Planetary Science, Chengdu University of Technology, China *corresponding authors: *matthew.izawa@gmail.com; ♯caofengke@gmail.com

Abstract Shock metamorphism progressively modifies the crystal structures of rock-forming minerals, ultimately producing diaplectic glasses such as maskelynite from plagioclase feldspar. These structural modifications are encoded in powder X-ray diffraction (XRD) peak profiles, yet extracting quantitative shock intensity metrics from routine laboratory XRD data remains challenging, particularly for multi-phase and partially amorphous planetary materials. Here, we present a powder XRD peak-profile analysis of seven lunar meteorites spanning shock stages S2 to S6. Samples include Gadamis 004 and NWA 11182 (a and b) (S2), NWA 11788 and NWA 13788 (S3– S4), NWA 12593 (S4, with recrystallized impact melt), and NWA 10401 (S5–S6, with extensive X-ray amorphous material). Powder XRD data were collected using a Bruker D8 Advance (Co Kα, 5–80° 2θ; University of Winnipeg) and a Rigaku SmartLab (Cu Kα, 10–60° 2θ; Okayama University), and all analyses are presented in d-spacing to enable wavelength-independent comparison. The mineral assemblages are dominated by anorthitic plagioclase with subordinate forsterite, clinopyroxene (pigeonite and/or augite), and accessory phases. Reference-guided peak detection based on computed anorthite peak positions identifies 22 to 39 diffraction maxima per sample, with a 3-sigma noise cutoff and automated zero-point offset correction.

Conventional Williamson–Hall (W–H) analysis of these peaks yields poor linear corrections ($R^2 < 0.1$) for most samples, reflecting the inherent limitations of this method for systems with multiple plagioclase populations (e.g., primary crystals and recrystallized impact melt), and partially amorphous phases. We therefore focus on two approaches that are better suited to these materials. Warren–Averbach (W–A) analysis exploits harmonic (e.g., (001), (002), (003)) peak families within a single phase to separate size and strain broadening via Fourier decomposition of individual peak profiles. This method is applied only to peaks confirmed to belong to a single crystallographic

phase.

The W–A results reveal anisotropic crystallite size reduction along specific crystallographic directions: the heavily shocked NWA 10401 shows W–A crystallite sizes ranging from approximately 120 Å along (10-2) to 520 Å along (121), whereas the weakly shocked NWA 11182b yields sizes of 400 to 700 Å with less directional variation. Pair distribution function (PDF) analysis, derived from via sine Fourier transform of the reduced structure function, provides a complementary, model-independent measure of structural order that is applicable to both crystalline and amorphous components. Highly shocked NWA 10401 exhibits broader, lower-amplitude, and shifted PDF peaks relative to the other samples, with reduced pair correlations beyond approximately 8 Å, consistent with loss of long-range structural coherence. The PDF differences between shocked and unshocked samples are reproduced by both instruments, confirming the robustness of the approach.

The limited Q-range ($Q = 4\pi \sin\theta/\lambda$) of laboratory diffractometers ($Q_{max} \approx 4.0–4.5$ Å^{-1}) constrains the real-space resolution of the PDF to ~0.7–0.8 Å. Synchrotron XRD data extending to Q_{max} of 15 Å^{-1} or greater, would enable quantitative PDF peak-width measurements with sub-angstrom resolution, opening the possibility of characterizing the short-range order in maskelynite and other shock-produced glasses through the crystalline to amorphous transition with increasing shock .

Key words: Shock metamorphism, Warren–Averbach analysis, pair distribution function, lunar meteorites, maskelynite

Acknowledgements This work was supported by JSPS, NSERC, and the Canadian Space Agency. XRD measurements were conducted at the University of Winnipeg HOSERLab and the Institute for Planetary Materials, Okayama University. This work is also supported by the Open Project for Innovative Platform of Meteoritical Research, Shanghai Science and Technology Museum.

QUANTITATIVE SHOCK BAROMETRY OF PLAGIOCLASE FROM LONAR IMPACT CRATER USING MICRO-XRD AND MULTI-SCALE MICROSTRUCTURAL ANALYSIS

Satheesh T. Saji[1], Fengke Cao[1*], Matthew R. M. Izawa[1,2,3], Yuyan Sara Zhao[1], Roberta L. Flemming[3], Phil J. A. McCausland[3], Suraj P. Rajappan[4]

1. Research Center for Planetary Science, College of Earth and Planetary Sciences, Chengdu University of Technology, China.
2. Institute for Planetary Materials, Okayama University, Japan.
3. Department of Earth Sciences, Western University, Canada.
4. Department of Geology, Government College Kasaragod, Kannur University, India.

Abstract Hypervelocity impact events generate diagnostic shock deformation features in minerals that record impact pressure-temperature conditions and cooling/decompression rates. Lonar Crater, India, is a ~1.88 km simple impact structure formed in Deccan Trap basalts, which hosts well-preserved shock metamorphic features, including shock-deformed plagioclase and pyroxene, vesicular SiO_2, diaplectic glass, and glass quenched from superheated impact melts, making it an ideal terrestrial analog for impact-cratered basaltic planetary crusts. This study aims to quantify peak shock pressures recorded in plagioclase from Lonar Crater, with reference to experimentally calibrated plagioclase shock pressures. Shock deformation is quantified using micro-X-ray diffraction (micro-XRD) by measuring the angle of full width at half maximum (FWHMχ) of diffraction maxima distributed along Debye rings, compared with similar observations on established experimentally shocked plagioclase (andesine and bytownite) data (0–56.5 GPa).

Microstructural characterization combines micro-XRD, electron backscatter diffraction (EBSD), and transmission electron microscopy (TEM) to resolve shock effects across multiple spatial scales. Optical observations of thin sections document features such as mosaic extinction and the preservation of primary igneous concentric zoning within optically isotropic plagioclase (i.e., diaplectic glass *sensu stricto*, formed via solid-state transformation). EBSD (spatial resolution of ~0.1–1.0 μm) constrains crystallographic misorientations and subgrain development, while TEM (nanometer scale, <100 nm) reveals lattice defects related to shock deformation. These observations are systematically compared with micro-XRD measurements (50–100 μm scale) to directly link microstructural impact-induced deformation across various scales.

The integration of micro-XRD–based quantitative barometry with multi-scale microstructural analysis enables cross-validation of shock indicators and establishes robust criteria for shock deformation quantification using plagioclase in naturally shocked rocks. The methodology provides a calibrated terrestrial reference for interpreting shock metamorphism in shocked meteorites and other impact-modified planetary materials, enabling more quantitative reconstruction of impact

histories.

Key words: Lonar Crater, Shock metamorphism, Micro-XRD, EBSD, TEM

Acknowledgements This work was supported by the Open Project for Innovative Platform of Meteoritical Research, Shanghai Science and Technology Museum.

SHOCK EFFECTS ON IRON-RICH OLIVINE AND PYROXENE

Kairui Tai[1], Yu-Yan Sara Zhao[1, 2*], Youjun Zhang[1,3], Wenhao Song[3], Yazhou Yang[4], Runlian Pang[1], Chao Qi[5], Wei Du[6]

1. Research Center for Planetary Science, College of Earth and Planetary Sciences, Chengdu University of Technology, PR China
2. Chinese Academy of Sciences Center for Excellence in Comparative Planetology, PR China
3. Institute of Atomic and Molecular Physics, Sichuan University, PR China
4. State Key Laboratory of Space Weather, National Space Science Center, Chinese Academy of Sciences, PR China
5. Center for High Pressure Science and Technology Advanced Research, PR China
6. State Key Laboratory of Ore Deposit Geochemistry, Institute of Geochemistry, Chinese Academy of Sciences, PR China

Abstract Iron plays a crucial role in planetary crustal evolution. Global remote sensing and in situ investigations indicate that Martian crust is enriched in iron, with olivine averaging an iron number (Fa#; Fe mola fraction of the Mg-Fe solid solution) of approximately 50, and reaching up to 70. Silicates detected on Martian moons and some asteroids are thought to originate from Martian impact ejecta, implying that the primordial materials of Phobos and Deimos may also contain iron-rich olivine, consistent with its abundance in the Martian crust. However, due to the scarcity of terrestrial analogs with similar compositions, the shock behavior and preservation potential of Fe-rich olivine remain poorly understood, limiting our ability to assess how impacts modify its mineralogy and spectral properties on Mars and Phobos.

Shock recovery experiments were conducted on synthetic Fa_{50} olivine using light gas gun at shock pressures of 18, 31, 41, and 47 GPa, corresponding to impact velocities between 0.89 and 1.95 km/s. Additionally, synthetic Fa_{70} olivine and NWA 14682 were subjected to shock recovery experiments at 49 GPa. NWA 14682 is a low-grade metamorphosed eucrite composed mainly of anorthite, ferrosilite ($Wo_{4.8}Fs_{66.5}En_{28.7}$) and augite ($Wo_{26.5}Fs_{47.3}En_{26.2}$). Microstructural and compositional features were characterized on post-shock samples using scanning electron microscopy (SEM), focused ion beam (FIB) sectioning, and transmission electron microscopy (TEM).

The shocked olivine samples exhibited systematic microstructural changes that varied with increasing shock pressure. Shocked Fa_{50} olivine demonstrated shock-induced Fe migration and zoning at pressures ≥31 GPa, with the development of a three-layer Fe distribution pattern (core-intermediate-rim) accompanied by nanoscale α-phase (~120 nm) and γ-phase (20-50 nm) metallic iron particles. At shock pressures ≥41 GPa (corresponding to estimated transient temperatures ≥1188 K), minor magnetite particles (20-50 nm) were observed at olivine grain boundaries. Nanoscale vesicles, often associated with dislocations and grain boundaries, were also observed, indicating localized gas release. These phenomena indicate that magnetite can form not only

through the direct decomposition of olivine but also via the oxidation of nanoscale metallic iron particles by oxygen vesicles generated during the impact process. Despite these extensive shock effects, no high-pressure olivine phases were detected, likely due to the short duration of the shock events.

For Fa_{70} olivine shocked at 49 GPa, SEM revealed dense degassing voids. The sample displayed Fe migration and zoning similar to Fa_{50} olivine. Instead of nanoscale iron particles, the iron-rich zones contained 5 nm olivine grains and exhibited intense fracturing with flow-like textures. In shocked NWA 14682 meteorite, SEM showed grain fragmentation and occasional degassing voids. Post-shock augite and ferrosilite shifted compositions toward hedenbergite and pigeonite series, respectively, with decreased Fe and increased Ca. TEM revealed that exsolved hedenbergite lamellae in ferrosilite host, vesicles near pyroxenes, and edenbergite grain (~50 nm) with satellite spots in diffraction patterns.

Given that TEM analyses of unshocked Fa_{70} olivine and NWA 14682 are still pending, shock origin of these features requires confirmation. Nevertheless, the higher iron content (Fa_{70}) did not produce more abundant nanoscale iron particles than Fa_{50} under similar shock conditions, highlighting the unique shock behavior of Fa_{50} olivine. In addition, pyroxenes appear more resistant to shock-induced alteration than olivine.

This study suggests that impacts on Fe-rich silicates provide an alternative mechanism, independent of water-rock interactions, to influence the redox evolution of the Martian surface and the composition of its early atmosphere. Notably, longer cooling durations, more extensive Fe migration, and the formation of larger particles are more likely under natural conditions than in laboratory settings, underscoring the need for further experimental and observational studies on Mars and its moons.

Key words: Iron-rich olivine, pyroxene, light gas gun, nanoscale metallic iron particle, Fe migration and zoning

Acknowledgements This research was supported by the National Natural Science Foundation of China (Grant Nos. 42441803, 42525801, 42373042, 42422201, and 42003054). Youjun Zhang is supported by the Sichuan Science and Technology Program (Grant No. 2023NSFSC1910).

SHOCK METAMORPHISM IN JONNAGIRI MICROMETEORITE, INDIA

SUNDER RAJU VENKATA PERUMALA

CSIR-National Geophysical Research Institute, Hyderabad,Telanagan ,India

Abstract In Jonnagiri uncovered a compelling 5 cm meteorite specimen with classic features: regmaglypts, magnetism, vitreous luster, Widmanstätten patterns (interlocking kamacite-taenite), and chondrules (1 mm to <10 μm). Analyses confirm it's an iron chondrite—PXRD shows Mg-rich olivine (fayalite); EDXRF reveals high Fe_2O_3 (~46%), Cr (~70 ppm), V (~100 ppm), Pb (~120 ppm); microscopy identifies Fe-Ni-S phases, titanite, NiS, cobalt, and possible Pt/Au. Raman highlights ringwoodite ($(Mg,Fe)_2SiO_4$) doublets (790, 814/816 cm^{-1}) alongside olivine (820, 843 cm^{-1}), indicating high-pressure shock metamorphism (16.5–18.7 GPa, ~500–560 km depth). A 3200 cm^{-1} hump suggests mantle water.

Key words: Olivine, Jonnagiri, Raman, Ringwoodite, Chondrules

SHOCK METAMORPHISM IN PYROXENE FROM LUNAR SOILS: INSIGHTS INTO EVOLUTION OF LUNAR CRUSTAL MATERIALS.

Jiawei Zhao, Long Xiao, and Qi He

State Key Laboratory of Geological Processes and Mineral Resources, Hubei Key Laboratory of Planetary Geology and Deep-Space Exploration, School of Earth Sciences, China University of Geosciences, Wuhan, 430074, China. (Jiawei_zhao@cug.edu.cn).

Abstract Pyroxene is a major constituent of lunar mafic materials and an important recorder of both magmatic evolution and impact modification. Although pyroxene has been widely used to trace lunar magmatic processes, the effects of shock metamorphism- on its structure and composition in lunar regolith remain poorly constrained. Here we integrate results from Chang'e-5 (CE-5) and Chang'e-6 (CE-6) lunar soils to investigate shock-related modification of pyroxene and its implications for lunar crustal evolution.In CE-5 basaltic regolith, a shocked pyroxene grain within a basaltic clast was analyzed using Raman spectroscopy, analytical scanning electron microscopy, electron probe microanalysis, and scanning transmission electron microscopy. The pyroxene records abundant dislocations dominated by the glide system , deformation-induced pigeonite formation, and localized frictional melting along grain boundaries and within the crystal. Together with shock twins in adjacent ilmenite, these features indicate low- to moderate-shock conditions of about 9-17 GPa. Some shocked domains in a single shocked pyroxene also show additional anomalous Raman peaks, suggesting tetrahedral Si-Al substitution that may serve as a spectral indicator of shock modification. These observations show that even relatively weak shock can significantly alter pyroxene structure and chemistry. In CE-6 anorthositic breccias, shock-altered augite clasts preserve lamellar twinning, recrystallization into granular augite with inherited crystallographic orientations, and localized dissociation products including Fe metal and fayalite. The recrystallized augite contains elevated Al_2O_3 contents (>8 wt%), indicating intergranular diffusion between augite and plagioclase during post-shock thermal metamorphism. These features record a transition from transient high-pressure deformation to prolonged high-temperature re-equilibration, likely associated with slow cooling in a large impact melt body.Together, the CE-5 and CE-6 results demonstrate that pyroxene in lunar soils is highly sensitive to both shock deformation and post-impact thermal overprinting. Such processes can obscure primary magmatic signatures, but also provide new constraints on the mechanical and thermal evolution of the lunar crust composition.

Key words: pyroxene, shock metamorphism, Chang'e-5, Chang'e-6, lunar regolith

THE FATE OF C-O-H FLUIDS IN OCEANIC SUBDUCTION ZONE

Lijuan Zhang[1], Lifei Zhang[2]

1. Key Laboratory of Deep Petroleum Intelligent Exploratton and Development, Instttute of Geology and Geophysics, Chinese Academy of Sciences, Beijing, China
2. Key Laboratory of Orogenic Belts and Crustal Evolutton, MOE, School of Earth and Space Sciences, Peking University, Beijing, China

Abstract Metamorphic fluids in oceanic subduction zones play a critical role in arc volcanism, seismicity, and deep carbon cycling. However, the speciation and evolution of carbon during subduction and exhumation remain poorly constrained. This study investigates fluid inclusions in eclogites from the Western Tianshan high- to ultrahigh-pressure (HP-UHP) metamorphic belt, China. Abundant CH_4-bearing fluid inclusions are identified in HP-UHP eclogites and associated veins. Petrological features and C-H isotopic data confirm an abiotic origin for this methane. Reconstruction of P-T-fO_2-fluid trajectories, combined with Deep Earth Water modeling, demonstrates that prograde metamorphism at 50-120 km depth promotes large-scale CH_4 synthesis via redox reactions during slab dehydration. In contrast, retrograde exhumation leads to the generation of CO_2-bearing fluid. The global flux of abiotic CH_4 in modern subduction zones is estimated to reach 10.8 Mt/year, making it the largest known source of abiotic CH_4. Furthermore, two distinct types of fluid inclusions are identified both in eclogites and their veins: Type-I (water-rich, with CH_4 vapor) and Type-II (CH_4-rich, with little or no H_2O). Their coexistence indicates fluid immiscibility under high-pressure conditions. Quantitative 3D Raman spectroscopy analysis of CH_4:H_2O ratios underscores an evolutionary transition in C-O-H fluids during decompression and exhumation, driven by progressive immiscibility between CH_4 and H_2O. This phase separation enhances carbon transfer from the subducting slab to the mantle wedge, improves decarbonation efficiency, and may contribute to the formation of abiogenic natural gas accumulations.

Key words: Eclogite, Abiotic CH4, Fluid inclusions, Oceanic subduction zonecarbon cycling

THE LARGEST COLD ANCIENT SUBDUCTION OROGENIC BELT IN THE WORLD

Huining Wang, Fulai Liu

Institute of Geology, Chinese Academy of Geological Sciences, Beijing

Abstract The formation and evolution of the Paleo-Tethyan tectonic regime have become the academic frontier and focus in the international geoscience field. The Paleo-Tethyan tectonic regime is characterized by the occurrences of many suture zones that are separated by microblocks. Previous studies mostly focus on the formation and evolution of one single subduction zone, whereas little atterntion was paid to the interaction of different subduction zones and its kinematic mechanism, which is significant for depicting in detail the deep cyclic and evolution processes of the whole Paleo-Tethyan tectonic regime. Eclogites as produced by the slab deep subduction are ideal in describing in detail subduction-orogeny evolution history and unraveling evolution process of the orogeny. The Paleo-Tethyan subduction zones are mainly represented by the Changning-Menglian suture zone (CMSZ) and Song Ma-Ailaoshan-Jinshajiang suture zone (SAJSZ) in the southeastern Plateau Tibetan. These suture zones are separated by the Lanping-Simao-Indochina Block, and are ideal for exploring the interaction of subduction zones and related kinematic mechanism. Our previous studies have revealed that abundant lawsonite-bearing blueschists and eclogites are present in the CMSZ, which connects with the Longmu Co-Shuanghu suture zone (LCSSZ). The CMSZ and LCSSZ build a nearly 2000 km oceanic cold-subduction high-pressure (HP)-ultrahigh pressure (UHP) metamorphic belt. However, critical problems remain concerning the petrogenesis and metamorphic evolution of eclogites in the CMSZ and the Song Ma suture zone (SMSZ). Accordingly, in the present study, the HP rocks in the CMSZ and SMSZ are selected for an integrated study concerning their mineralogy, petrology, geochemistry and geochronology.

Our study reveals that the not only the ocean-type eclogites but also continent-type HP rocks occur in the CMSZ and SMSZ. Abundant relics of igneous minerals are newly discovered within the eclogitized metagabbro in the CMSZ. The eclogitized metagabbros and the SMSZ eclogites show typical MORB-type element patterns and εNd(t) isotopic values (the former = +1.0~+8.0; the later = -1.69~+5.15). Their protoliths formed in the depleted or metasomatic mid-oceanic ridge setting. The protoliths of the SMSZ eclogites with emplacement timing of 425.4 Ma represent so far the oldest Paleo-Tethyan oceanic crust, demonstrating that the Song Ma Ocean was a long-term (~160 Myr) ancient Paleo-Tethyan Ocean rather than a narrow seafloor or back arc basin as expected. The detrital zircon U-Pb age histograms of the rocks hosting the SMSZ eclogites demonstrate that, the protoliths of metasedimentary rocks originated from the massive margin (Nam Co complex) of the South China Block. The continent-type eclogites in the CMSZ exhibit element patterns (e.g., depletion of high-field strength elements and enrichments of Th and U) and εNd(t) isotopic values

(-18.1~-15.5) that resemble continental mafic rocks. The inherited detrital zircons within the continent-type eclogites record U-Pb age distributions that are similar to those of the hosted rocks (the Lancang Group) and the sediments within the Baoshan-Tengchong Block. It is revealed that the continent-type eclogites are derived from the mafic dykes, which would have captured detrital zircons from sedimentary rocks during the magmatic emplacement process.

The eclogitized metagabbros are characterized by the preservation of igneous minerals (diopside + bytowinte + ilmenite). Eclogitized metagabbros and continent-type eclogites document the peak-stage mineral assemblages (the former: Grt + Omp + Ky + Tlc + Rt + Ph; the later: Grt + Omp +Gln + Rt), peak metamorphic conditions (the former: 25.6-27.1 kbar/595-637 ℃; the later: 28.5-29.6 kbar/580-594 ℃), the P-T trajectory patterns and metamorphic ages (peak stage: 234-233 Ma; retrograde stage: 223.7 Ma) that are comparable to the cold subduction-derived eclogites in the CMSZ. Accordingly, we proposed that the continental crusts followed by the sinking of the Paleo-Tethyan Ocean in the CMSZ underwent steep and rapid cold subduction. It is the rapid cold oceanic subduction that was responsible for the insufficient fluid diffusion. The weak deformation as well as the dense nature of the coarse-grained gabbroic precursors might have hindered pervasive and intensive fluid infiltration, and contributed to the locally metastable persistence of gabbroic rocks under eclogite-forming conditions. The SMSZ eclogites are interpreted to be formed by warm subduction in terms of their peak-stage mineral assemblages (Grt + Omp + Ph + Ep/Cz + Wnc ± Ky + Rt), peak metamorphic conditions (20.1-24.0 kbar/606-705 ℃) and related geothermal gradient (8-10 ℃/km). Moreover, the SMSZ eclogites and their hosted rocks record similar P-T conditions, HP ages (239.2-233.4 Ma) and retrograde ages (231.0-229.4 Ma). Combined with previous results, we proposed that the rapid exhumation (6.4 km/Myr) and associated cooling process (-14.0~-21.6 ℃/Myr) of the SMSZ eclogites were facilitated by the hosted metasedimentary rocks due to their buoyancy in the transition of the oceanic final closure to the initial continental subduction-collision. From the continental initial collision to the mature collision stage, the breaking off of subducted oceanic slab results to asthenosphere upwelling, which would slow down the subduction angle, warm the subduction thermal structure and bring about high-temperature granulite facies metamorphism in the medium-pressure facies field. In this regard, the SMSZ documents the transition of warm to hot subduction during oceanic subduction and continental collision, respectively, which is in contrast with the cold subduction signature in the CMSZ. Based on the similarity of metamorphic evolution of high-pressure rocks in the SMSZ and the Ailaoshan-Jinshajiang suture zone, we build a NNW-extended HP metamorphic belt along the SAJSZ.

Key words: Eclogite, cold subduction, Changning-Menglian suture zone, Paleo-Tethys …

UHT METAMORPHISM IN THE JINING COMPLEX, NORTH CHINA CRATON

Bin Wang

School of Earth Sciences, Lanzhou University, China

Abstract There have been great difficulties on recovering the peak temperature of ultrahigh-temperature (UHT) metamorphism, which was dependent on a few thermometries such as Al-in-orthopyroxene and feldspar thermometers, and the tectonic settings of UHT metamorphism were strongly controversial. The Jining complex in Khondalite belt, North China Craton contains widely distributed UHT metamorphic rocks and anatectic granites. Peak temperature and timing of the regional metamorphism in the Jining complex were widely controversial. Two types of granulites from the Xuwujia and Tianpishan areas both recorded metamorphic evolutions of peak stage, post-peak near-isobaric cooling to the fluid-absent solidus at 0.8–0.9 GPa, and then sub-solidus decompression. The peak temperatures reach up to 1120–1140 °C, exceeding the rocks' dry solidi. Peak temperature of the spinel-bearing granulite from Xuwujia were mainly constrained by the survival ferrous-pseudobrookite in the multi-phase Ti–Fe oxides and the inferred feldspar-absent peak assemblage of spinel ± garnet, where the compositions of some spinel cores with magnetite exsolution recorded near-peak (~1100 °C) temperatures. The sapphirine-bearing granulite from Tianpishan displays marked heterogeneity. Peak temperature of sillimanite-rich domains was constrained by the coexistence of sillimanite-I + sapphirine + spinel + quartz, where sillimanite-I contains hematite exsolution and shows reintegrated Fe_2O_3 contents up to 2.1–2.3 wt.%; that of orthopyroxene-rich domains was constrained by the inferred peak assemblage of sapphirine + orthopyroxene, where the core of orthopyroxene has Al^{IV} of 0.22 (Al_2O_3 = ~9.5 wt.%). In-situ U–Pb dating of metamorphic zircon and Monte Carlo simulation on the collected regional geochronologic data both indicate a cooling duration during 1.94–1.90 Ga. This reveals a slow cooling process (i.e., the timescale) as long as ~40 Myr in the Jining complex for the first time, and confirms that the UHT peak stage occurred before ~1.94 Ga. From the perspective of mineral, in UHT metamorphic rocks, the composition of perthite (or CaO contents in K-feldspar), Fe_2O_3 contents in sillimanite, Al_2O_3 contents in orthopyroxene, the Al/(Al + Fe^{3+}) value of spinel and some specific Ti–Fe oxides such as ferrous-pseudobrookite can indicate and record peak temperatures. Sillimanite with hemetite exsolution and spinel with magnetite exsolution both can indicate UHT metamorphism in pelitic granulites. These would also enlighten the researches on UHT metamorphism in other regions.

Key words: UHT metamorphism, Jining complex, Peak temperature, Slow cooling, Mineral

ULTRAHIGH-TEMPERATURE METAMORPHISM OF GRANULIZED ECLOGITES IN THE EAST-CENTRAL HIMALAYAN OROGENIC BELT, CHINA

Lifei Zhang[1*], Guibin Zhang[1], Chenguang Wu[1], Yang Wang[2], and A. Alexander G. Webb[3]

**Corresponding author ()*

1. Key Laboratory of Orogenic Belts and Crustal Evolution, School of Earth and Space Sciences, Peking University, Beijing 100871, China
2. Key Laboratory of Computational Geodynamics, College of Earth and Planetary Sciences, University of Chinese Academy of Sciences, Beijing, China
3. Department of Earth Sciences and Laboratory for Space Research, University of HongKong, China

Abstract Ultrahigh temperature (UHT) metamorphism is the most thermally extreme form of regional crustal metamorphism, with temperatures exceeding 900 ℃. The duration and heat source of UHT metamorphism are critical constraints on the tectonic evolution of orogenic systems. The Himalayan Orogen resulted from the continental collision between India and Asia, which has been ongoing since the early Cenozoic. It is a large and hot orogenic belt in the world. Based on the petrological studies, we have identified a more than 200 km long HP metamorphic eclogite belt which was formed by the continental subduction after collision of India plate beneath Europe continent. They had undergone UHT metamorphism overprinting during their uplift in the east-central Himalayan orogenic belt. At the Yadong area in East-central Himalaya, we have find UHT overprintized eclogite facies rocks: sapphirine-bearing granulites and granulitized eclogites. The petrological and geochronological studies show that the peak eclogite facies metamorphic stage happened at near 17 Ma with the P-T conditions of >1.9 GPa and >700 °C, the UHT metamorphic stage occur at about 15 Ma with 0.8–0.9 GPa/>900 °C. The reconstructed pressure-temperature-time path indicates the temperature increased by almost 200 °C within ~2 Myr. Numerical simulations show that this rapid heating may have resulted from juxtaposition of the deep crustal accretionary system with the upwelling asthenospheric mantle through newly-developed apertures generated by slab break-off and/or associated vertical tearing of down-going Indian lithosphere. Spatial-temporal consistencies amongst the UHT metamorphic phases, post-collisional magmatism, geophysical constraints, and crustal deformation indicate that slab break-off or tearing controls broad swaths of Himalayan tectonics. The consequent upwelling asthenosphere may have been a significant heat source for the Miocene Himalaya, and for similar ancient collisional orogenic systems.

WADSLEYITE RIMS AROUND RINGWOODITE CORES IN SHOCK MELT VEINS OF L5 CHONDRITE NORTHWEST AFRICA 7458

Feng Yin

Center for High Pressure Science and Technology Advanced Research, Shanghai, China

Abstract Strongly shocked meteorites often contain melt veins, which host a variety of high-pressure minerals, indicating that these meteorites experienced extreme pressure and temperature conditions during impact events. The high-pressure polymorph of olivine, ringwoodite and wadsleyite, have been observed in many chondrites as well as in lunar and martian meteorites. Common occurrences of ringwoodite include polycrystalline ringwoodite assemblages, sets of ringwoodite lamellae within host olivine, and ringwoodite rims of olivine clasts. In contrast, wadsleyite occurs as ringwoodite–wadsleyite assemblages in shock veins of a few chondrites (e.g., Peace River, ALH78003, Y-74445, Alfianello), suggesting fractional crystallization from a melt with olivine composition. Here, I present a preliminary study of unique wadsleyite and ringwoodite assemblages in a heavily shocked L5 ordinary chondrites Northwest Africa (NWA) 7458.

NWA 7458 contains pervasive shock melt veins up to 5 mm thick that host abundant high-pressure phases, including ringwoodite, wadsleyite, majorite, jadeite, tuite, and xieite. Ringwoodite is the most common high-pressure mineral in NWA 7458 and occurs in three forms: (1) ringwoodite lamellae intergrown with host olivine adjacent to shock melt veins; (2) polycrystalline assemblages of ringwoodite within shock melt veins; and (3) polycrystalline assemblages of coexisting wadsleyite and ringwoodite within shock melt veins. The wadsleyite and ringwoodite polycrystalline assemblages consistently show wadsleyite rims surrounding ringwoodite cores, with the wadsleyite rims being <5 μm in width. Individual wadsleyite crystallites are up to 2 μm in size. The chemical compostion of ringwoodite core (Fa≈28) is enriched in FeO relative to the wadsleyite rim (Fa≈11) and the host olivine (Fa≈25).

Wadsleyite occurs as the rim of polycrystalline assemblages in direct contact with the melt, experiencing higher tempertature than the ringwoodite in the core. This occurrence is consistent with the P–T phase diagram of olivine, which shows that higher temperatures promote the formation of wadsleyite+ringwoodite rather than the foemation of ringwoodite alone under the same shock pressure. The Fe-Mg partitioning between wadsleyite and ringwoodite implies that the transformation mechanism is a diffusion-controlled solid-state transformation. The presence and distribution of these olivine polymorphs hightlight the importance of temperature heterogeneity during shock in the formation of high pressure phases.

Key words: ringwoodite, wadsleyite, formation mechanism, shock vein

ZIRCON DIFFUSION CHRONOMETRY REVEALS BRIEF ULTRAHIGH-TEMPERATURE METAMORPHISM IN A PROLONGED PALEOPROTEROZOIC OROGEN

Yi Zou

State Key Laboratory of Lithospheric and Environmental Coevolution, Institute of Geology and Geophysics, Chinese Academy of

Abstract Ultrahigh-temperature (UHT) metamorphism (≥900°C) represents the most extreme thermal record of continental crust evolution. Whether such extreme conditions occurred as short-lived thermal pulses (~1 Myr) in Precambrian orogens—akin to those observed in Phanerozoic settings—remains a fundamental question in understanding early Earth geodynamics. In this study, we integrate phase equilibria modeling, conventional thermobarometry, and high-resolution NanoSIMS trace-element mapping (Ti, Dy, Yb) with diffusion modeling in zircon to resolve the timescales of UHT metamorphism in the Paleoproterozoic Jiao-Liao-Ji orogen, North China Craton.

Petrological analysis of pelitic granulites reveals a three-stage pressure-temperature path: an initial peak presssure assemblage at ~1.30 Ga and 850 °C, followed by decompression heating to ~0.65 Ga and ≥940 °C and subsequent cooling to ~600 °C. Zircon grains from these granulites preserve Archean detrital cores (2500–2750 Ma) with primary oscillatory zoning in Ti and rare earth elements (Dy, Yb), overgrown by metamorphic rims dated at ca. 1.85 Ga. These sharp compositional gradients in the detrital cores provide a unique opportunity to quantify the duration of the UHT event via diffusion chronometry. Using a plane-sheet diffusion model with step-function initial conditions and fixed boundary compositions, we simulated the relaxation of Dy, Yb, and Ti profiles across oscillatory-zoned lamellae. Uranium profiles, which are resistant to diffusion under these conditions, were used to define the initial interface geometry and account for analytical convolution effects. Our modeling results yield consistently brief timescales: best-fit durations range from 0.02 to 0.62 m.y. for the entire heating event, with UHT residence times of only 0.05 to 1.3 m.y. These results provide the first robust evidence for ultrafast (~0.1 m.y.) UHT pulses in the Paleoproterozoic, demonstrating that extreme thermal regimes in Precambrian orogens could be as transient as those documented in modern collisional settings.

Furthermore, the Ti zoning profiles allow us to empirically constrain Ti diffusivity in natural zircon under crustal metamorphic conditions. The derived diffusion coefficients are three to five orders of magnitude faster than those predicted by experimental calibrations, highlighting the importance of natural constraints for accurate timescale retrieval.

The UHT event is spatially and temporally linked to ca. 1.85 Ga mafic intrusions, suggesting that transient mantle upwelling—possibly triggered by slab break-off, tearing, or ridge subduction—

provided the heat source. These findings indicate that vigorous crust-mantle interactions under early plate tectonic regimes were capable of generating short-lived, high-grade thermal perturbations comparable to those in the Phanerozoic. Our study underscores the power of NanoSIMS-guided zircon diffusion chronometry in resolving the tempo of Precambrian thermal-tectonic processes and offers new insights into the dynamics of continental crust differentiation and stabilization.

Key words: Ultrahigh-temperature metamorphism, zircon, diffusion chronometry, Paleoproterozoic, North China Craton

ABIOTIC ORGANIC CHEMISTRY COMPLEXIFICATION UNDER SHOCK: THE CASE OF GLYCINE

Razvan Caracas

Institut de Physique du Globe de Paris, Université Paris Cité, CNRS

1 rue Jussieu, Paris 75005 France

caracas@ipgp.fr

Abstract Glycine, the simplest amino acid, is a model system for studying organic molecules due to its structural simplicity and presence in meteorites and interstellar clouds. Amorphous glycine, lacking a well-defined structure, is more adaptable and reflects extreme conditions found in space. Here, we perform multiple ab initio molecular dynamics simulations to explore the compressibility and physical properties of amorphous glycine, providing insights into its behavior under static and shock compression.

The static compressibility of amorphous glycine is challenging to measure experimentally due to its lack of crystallinity. Our theoretical results yield a density at 0 pressure that represents a 10% reduction in density compared to the crystalline phase.

We compute the Hugoniot shock equation of state and monitor the structural transformations under shock. We show that above 1000K the dissociation of the glycine molecule is associated to racemization reactions. The resulting organic molecules show large-scale polymerizations that are associated with the densification.

Our simulations show a different path towards organic chemistry evolution that is purely abiotic, being mediated by shocks. The arrival of meteorites rich in organics that dominated the Precambrian times and could have served as fuel for the heterotrophic fauna of the early Earth.

Key words: prebiotic chemistry, shock physics, polymerization

AI-BASED EXTRACTION OF DETRITAL INDICATOR MINERAL INFORMATION AND ITS APPLICATION FOR MINERAL EXPLORATION

Haiming Liu*[1], Yang Song[1], Hanyu Wang[2], Yang Wang[2], Yan Nie[1]

1. Ministry of Natural Resources (MNR), Key Laboratory of Metallogeny and Mineral Assessment, Institute of Mineral Resources, Chinese Academy of Geological Sciences, Beijing, 100037, China
2. School of Earth Sciences and Resources, China University of Geosciences, Beijing, 100083, China

Abstract Placer gold is a significant indicator mineral for gold-bearing deposits. The chemical composition of placer gold in diverse geological settings is a function of the composition of its parental hydrothermal fluids in diverse geological settings. Thus, trace elements contained in placer gold could present a particular geochemical signature that can be used to discriminate placer gold grains from different mineralization types and to trace the source of placer gold. As placer gold particles are transported across Earth's surface in stream sediments, their morphologies evolve, and microscopic surface textures develop as well as the trace element compositions change. Since transport mechanisms differ among depositional processes, the shape and characteristic micro-textures on gold surfaces integrating with geochemical signatures can offer valuable insights into their transport histories and depositional processes. In this study, we applied a deep neural network model to extract grain morphological information and used various machine learning tools to investigate geochemical compositions of placer gold from proximal to detrital locations to predict unknown gold deposits in the Duolong porphyry-epithermal ore district, western Xizang, China. Specifically, the deep learning framework utilized the ResNet-50 convolutional neural network (CNN) architecture. By leveraging transfer learning paradigms pre-trained on the ImageNet dataset, this approach enables the robust extraction of complex high-dimensional morphological features—specifically local edge curvatures and textural roughness—despite the inherent constraint of limited geological training samples. This study characterizes the composition of placer gold grains from stream sediments and yields geochemical discrimination models for application to mineral exploration for gold deposits. The micro-textures of placer gold grains were investigated by scanning electron microscopes (SEM). Furthermore, gradient-based Class Activation Mapping (CAM) applied to these SEM images enhances model interpretability. It reveals that the algorithm specifically activates in regions exhibiting high-frequency textural variations, such as edge angularity and impact pits. These micro-structures serve as direct physical proxies for quantifying sediment transport distance and cumulative abrasion intensity. Trace element contents of placer gold grains were measured in-situ by laser ablation ICP-MS (LA-ICP-MS) to identify systematic

changes in gold compositions associated with different transportation environments, and, where possible, to identify the distinctive geochemical signature of Au in different transportation distances. Our results demonstrate the robustness and versatility of the model in rapidly and automatically constraining the transport histories recorded in individual grains of placer gold through their morphological and geochemical features.

Key words: Placer gold, Machine learning, ResNet50, Mineral exploration, Porphyry deposit

AN ALTERNATIVE PHOSPHORUS SINK IN ORGANIC-RICH SEDIMENTS: INSIGHTS FROM THE PREDOMINANCE OF AUTHIGENIC GORCEIXITE IN THE EDIACARAN–CAMBRIAN TRANSITIONAL SUCCESSION

Tongxuan Du[1,2], Xiqiang Zhou[1,2,*], Run Li[1,2], Dongjie Tang[3], Kangjun Huang[4], Xiangli Wang[1,2], Zhuyin Chu[1]

1. State Key Laboratory of Lithospheric and Environmental Coevolution, Institute of Geology and Geophysics, Chinese Academy of Sciences, Beijing 100029, China
2. College of Earth and Planetary Sciences, University of Chinese Academy of Sciences, Beijing 100049, China
3. State Key Laboratory of Biogeology and Environmental Geology, China University of Geosciences (Beijing), Beijing 100083, China
4. State Key Laboratory of Continental Dynamics, Department of Geology, Northwest University, Xi'an 710069, China

Abstract Phosphorus is a key bioessential element that regulates marine primary productivity and exerts fundamental feedbacks on Earth's redox evolution. Authigenic carbonate fluorapatite (CFA) has traditionally been regarded as the dominant long-term phosphorus sink in marine sediments; however, increasing evidence suggests that non-apatite phosphorus-bearing minerals may constitute an underestimated reservoir. Therefore, the occurrence, controlling factors, and geological implications of such unconventional phosphorus sinks in deep-time burial merit systematic investigation. Here, we examine the siliceous rock-black shale succession of the Liuchapo Formation, South China, to constrain phosphorus sink characteristics and governing mechanisms in anoxic, organic-rich depositional environments. Integrated mineralogical and geochemical analyses demonstrate that gorceixite, rather than CFA, represents the dominant authigenic phosphorus phase within this interval. The extensive formation of gorceixite during early diagenesis is attributed to porewater conditions beneath the sulfate-methane transition zone (SMTZ), characterized by elevated P and Ba but depleted Ca and Fe. These conditions, coupled with low sedimentation rates and reduced carbonate particulates flux, suppress apatite and vivianite precipitation, thereby favoring gorceixite as the principal phosphorus sink. Furthermore, gorceixite-enriched samples exhibiting relatively low C_{org}/P_{tot} ratios indicate enhanced retention of reactive phosphorus and limitimation of phosphorus remobilization and recycling. Moreover, the occurrence of anomalously high P/Ca ratios in some fine-grained siliciclastic rocks in geological records implies that gorceixite (and/or vivianite) may have been widely developed in analogous marine environments and may have partially replaced apatite as major phosphorus sinks. Overall, this study identifies gorceixite as a previously underappreciated yet efficient phosphorus sink, defining an

alternative pathway for deep-time phosphorus sequestration and providing robust mineralogical constraints on marine phosphorus cycling and its feedbacks on Earth's surface environments and biological evolution.

Key words: Phosphorus sink, Gorceixite, Apatite, Authigenesis, Ediacaran–Cambrian transition

AN EVOLUTIONARY SYSTEM OF MINERALOGY, PARTS X TO XII: ON THE CO-EVOLUTION OF THE GEOSPHERE AND BIOSPHERE

Robert M. Hazen

Earth and Planets Laboratory, Carnegie Institution for Science, Washington DC, USA

Abstract The "Evolutionary System of Mineralogy" complements the official system of the International Mineralogical Society by classifying all minerals according to the processes of their formation (i.e., their paragenetic modes), coupled with their distinctive *P-T-X* formation environments and the geological time intervals in which they emerged. In this classification system, some IMA-approved mineral species are split into as many as 21 different historical natural kinds, whereas some closely-related IMA species—those that form solid solutions in the same environments and time intervals—are lumped into a single natural kind. In addition, the evolutionary system embraces a variety of amorphous solids, including volcanic glass, impact glass, and low-temperature gel-derived solids, which play important roles in the crustal evolution of Earth and other worlds. The result of this lumping and splitting is that the ~6200 IMA-approved mineral species are distributed among ~11,000 mineral natural kinds.

The Evolutionary System of Mineralogy is being released in 12 parts, of which Parts I to VIII are published [2] and Parts IX to XII are in preparation. The final three parts are of special interest because they focus on minerals that have arisen on Earth as a consequence of the biosphere. Remarkably, approximately half of all IMA-approved mineral species are known to form via microbial or other biological processes, with more than one-third of all species formed exclusively because of direct or indirect biological mediation. This presentation will review mineral-forming processes based on microbial metabolism (Part X); the Great Oxidation Event (Part XI); and Phanerozoic biomineralization, including shells, teeth, and bones (Part XII).

Key words: Mineral Evolution, Biomineralization, Great Oxidation Event, Systems of Mineralogy, Classification

APATITE CONSTRAINTS ON VOLATILE EVOLUTION IN OROGENIC NI–CU SYSTEMS

Ya-Jing Mao[1*], Xu-Yang Zheng[1], Jun Duan[2], Jinxiang Li[3]

1. State Key Laboratory of Lithospheric and Environmental Coevolution, Institute of Geology and Geophysics, Chinese Academy of Sciences, Beijing 100029, China
2. College of Earth Sciences and Resources, Chang'an University, Xi'an 710054, China
3. State Key Laboratory of Tibetan Plateau Earth System, Environment and Resources (TPESER), Institute of Tibetan Plateau Research, Chinese Academy of Sciences, Beijing 100101, China

Abstract Oregenic belt Ni-Cu deposits have become an important nickel source in recent decades. Volatiles may play an important role in the formation of magmatic Ni–Cu deposits, particularly those emplaced in orogenic belts. Apatite is widely used as an indicator mineral for tracing the composition and evolution of magmatic volatiles. In this study, we present in situ textural characteristics, trace-element compositions, and hydrogen isotopic data for apatite from the Xiarihamu Ni–Cu deposit hosted by websterite and lherzolite in the East Kunlun Orogenic Belt. These in-situ observations and apatite, together with the apatite composition from numerous Ni-Cu deposits in NW China (southern Central Asian Orogenic Belt), are used to reveal the crystallization sequence of apatite and to elucidate magma and volatile evolution of Ni-Cu systems in oregonic belts. Texturally, apatite is classified into seven groups based on host minerals and inclusion relationships: apatite enclosed in clinopyroxene, amphibole, plagioclase, biotite–phlogopite, sulfide, quartz, and interstitial domains. Geochemically, apatite hosted by silicate minerals is dominantly OH-rich, whereas some interstitial apatite is Cl-rich. All apatite grains are enriched in light rare earth elements (REE) and depleted in heavy REE, with Cl-rich apatite showing more pronounced heavy REE depletion. In contrast, apatite enclosed in pyrrhotite within massive sulfide breccia is F-rich and displays relatively flat REE patterns accompanied by a strong negative Eu anomaly. These features suggest that OH-rich, Cl-rich, and F-rich apatite record crystallization from silicate melt, vapor-saturated interstitial melt, and degassed silicate melt, respectively. Similarly, apatite from Ni-Cu deposits in NW China shows a wide variation in volatile components. Thus, apatite from the Ni-Cu system preserves a detailed record of magmatic evolution, including fractional crystallization, magma degassing, and late-stage fluid exsolution. These apatite data indicate that orogenic Ni–Cu systems have achieved vapor saturation during the very late stages of differentiation. We hightlight that the expanding compositional dataset of apatite can be used to indicate mineralization processes of mafic-ultramafic systems, although detailed structural studies are essential.

Key words: Apatite, mafic-ultramafic intrusions, Ni-Cu sulfide deposit, exploration

Acknowledgements Financial support for this research was provided by the National Natural Science Foundation of China (NSFC, Grant No. 42072105) and the Deep Earth Probe and Mineral Resources Exploration National Science and Technology Major Project (2024ZD1002306). We thank Shitou Wu, Lihui Jia, Xu Tang, and Jialong Hao for their assistance in LA-ICP-MS, electron microprobe, and XRF laboratory work. The comments and suggestions from Jun Duan on the first draft improved the manuscript.

APATITE VOLATILE CONTENTS OF PORPHYRY CU DEPOSITS CONTROLLED BY DEPTH-RELATED FLUID EXSOLUTION PROCESSES

Ming-Liang Huang[1], Jing-Jing Zhu[1], Massimo Chiaradia[2], Rui-Zhong Hu[1, 3], Lei-Luo Xu[1], Xian-Wu Bi[1,†]

1. State Key Laboratory of Ore Deposit Geochemistry, Institute of Geochemistry, Chinese Academy of Sciences, Guiyang 550081, PR China
2. Department of Earth Sciences, University of Geneva, rue des Maraîchers 13, Geneva 1205, Switzerland
3. College of Earth and Planetary Sciences, University of Chinese Academy of Sciences, Beijing 100049, PR China

Abstract Porphyry Cu deposits are formed by Cu- and volatile (e.g., Cl, S)-rich fluids exsolved from underlying magma reservoirs. Intuitively, higher magmatic Cl and S contents likely correspond to higher magma fertility. However, the Cl contents of syn-ore magmatic apatite, one of the major Cl-bearing mineral phases in magmas, are highly variable among deposits (from <0.1 to >2 wt %). These variations may be controlled by different timing of apatite crystallization relative to fluid saturation among deposits, but the causes of these different relative timings remain obscure. Here we compile existing chemical data of magmatic apatite and amphibole phenocrysts from 25 porphyry Cu deposits worldwide and use these data to calculate magmatic physical-chemical conditions, such as water contents and magma reservoir depths. We find that the porphyry Cu deposits associated with deeper magma reservoirs are characterized by systematically higher magmatic H_2O contents and apatite Cl, but lower apatite F contents and F/Cl ratios compared to shallower deposits. These correlations are best explained by early fluid exsolution and Cl loss that predate apatite crystallization in shallower porphyry Cu systems, which leads to elevated apatite F/Cl ratios. This is supported by the common occurrence of primary fluid inclusions in apatite from shallower systems. Postsubduction porphyry Cu deposits are normally associated with lower apatite Cl contents and shallower magma reservoirs, which is attributed to their formation under relatively extensional tectonic regimes. Our results demonstrate that the magma reservoir depth exerts an important control on the timing of fluid exsolution and accompanying Cl loss. In contrast, relatively high and constant apatite S content among deposits is minimally affected by fluid exsolution, possibly due to buffering of early-saturated sulfate in oxidized and S-rich magmas, and therefore might be used as a better potential fertility indicator than Cl.

Key words: Apatite, volatile contents, porphyry Cu deposits, fluid exsolution

ATOMIC-SCALE INSIGHTS INTO PYROXENE EXSOLUTION: AN HRTEM STUDY OF GARNET PERIDOTITE FROM THE POLAR URALS

Yazhou Fan [1,2], Fancong Meng [2], Vladimir R. Shmelev [3]

1. College of Geosciences and Engineering, North China University of Water Resources and Electric Power, Zhengzhou 450046, China
2. Institute of Geology, Chinese Academy of Geological Sciences, Beijing 100037, China
3. Institute of Geology and Geochemistry, Ural Branch, Russian Academy of Science, Ekaterinburg, 620016, Russia

Abstract The exsolution of minerals contains abundant information about temperature, pressure, and material migration under UHP conditions. The highly typical exsolution of pyroxenes in the UHP garnet peridotites from Mica Hill in the Polar Urals was investigated using various techniques (EPMA, LA-ICP-MS, SEM, FIB, and HRTEM). The aim was to explore the exsolution mechanism and the phase-state information of minerals in the ultradeep Earth. The following are the main findings:

(1) The exsolved pyroxenes are hosted in the garnet peridotites, whose protoliths are cumulate troctolite and troctolite-gabbro. (2) The exsolved pyroxene is bronzite, and the associated olivine and chromite are chrysolite (Fo value 80-87), Cr-rich hercynite and Al-rich chromite, respectively. (3) The system of exsolution is closed but fairly complex, and the exsolution minerals (approximately 2%-5%) include clinopyroxene, chromite, ilmenite, and their combinations. (4) The lattice interface between the pyroxenes and exsolution minerals is continuously matched, with a lattice adjustment domain exhibiting co-lattice phase boundary characteristics. (5) The crystallographic relationship is established: $(401)_{cpx}//(121)_{opx}$, $(006)_{Ilm}//(122)_{opx}$, $(132)_{Ilm}//(511)_{opx}$, $(211)_{Chr}//(121)_{opx}$, $(220)_{Chr}//(511)_{opx}$. (6) The clinopyroxene exsolution has the same lattice type and orientation as the host bronzite, and the interplanar spacing $(401)_{cpx}$ is 3.45 Å, suggesting a minimum exsolution pressure of 9.5-12.5 GPa. (7) The primary mineral of these pyroxene exsolutions is speculated to be UHP clinopyroxene or majorite, indicating a pressure of >10 GPa.

Key words: Pyroxene Exsolution, Crystallographic Orientation, HRTEM, UHP, Polar Urals

BANDED IRON FORMATION: TEXTURE STUDY AND IMPLICATION FOR REDOX EVOLUTION DURING GOE

Yuanfeng Cai, Qilin Huang, Siyi Huang, He Zhang, Yuguan Pan, Yuli Yuan
State Key Laboratory of Critical Earth Material Cycling and Mineral Deposits, Nanjing University, Nanjing 210023, China

Abstract The first major oxidation event, termed the Great Oxidation Event (GOE), occurred during the early Paleoproterozoic and late Archean (ca. 2.22–2.45 Ga) and profoundly restructured global surficial environments. This dramatic transition is recorded in the widespread, large-scale deposition of banded iron formations (BIFs) and siliceous successions worldwide. A suite of geochemical proxies has been developed to trace these changes, including redox-sensitive elements, biological productivity, carbonate-associated phosphate and minerals (Davín et al., 2025; Dodd et al., 2025).

However, the emergence of microbes in the Archean by at least 3.6 Ga also gradually modified the surficial system (Dong et al., 2023). The earliest documented iron formations date to approximately 3.3 Ga. Redox conditions are preserved in these iron formations, expressed by iron minerals with variable valence states. Between 4.0 and 3.0 Ga, iron minerals were dominated by Fe(II) phases, but evolved toward mixed-valence assemblages including siderite, magnetite, greigite ($Fe_2^+Fe_3^+{}_2S_4$), and franklinite.

During 3.0–2.22 Ga, massive iron formations accumulated globally. Hematite or its precursors subsequently became the dominant iron minerals, coinciding with a sharp rise in atmospheric oxygen to roughly 0.01% of the present atmospheric level (PAL). By the end of the GOE interval, elevated atmospheric oxygen supported a more habitable surface environment and likely facilitated the emergence of eukaryotes. Widespread ferric iron minerals thereafter became abundant in sediments and stratigraphic successions.

Nevertheless, the linkage between redox evolution and microbial development remains poorly constrained and highly debated. In this study, we conduct microscale observations and in-situ analyses to characterize reaction textures among different iron minerals. Our aims are to identify redox-sensitive iron phases, establish a mineral redox sequence, and integrate these with geochemical proxies to reconstruct the co-evolution of oceanic and atmospheric redox conditions.

Key words: Texture, Redox Mineral, Banded Iron Formation, Precambrian Era

Acknowledgements This work is supported by the National Natural Science Foundation of

China (Nos. 42192504).

CALCITE AS A STAGE-SPANNING ARCHIVE OF CRITICAL METAL ENRICHMENT IN CARBONATITE-ASSOCIATED DEPOSITS: INSIGHTS FROM MINERAL CHEMISTRY AND IN SITU ISOTOPE COMPOSITIONS

Wei Chen

State Key Laboratory of Geological Processes and Mineral Resrouces, China University of Geosciences, Wuhan, China

Abstract Carbonatite-associated deposits are important sources of rare earth elements, Nb, and other critical metals, but their enrichment commonly reflects a combination of magmatic crystallization, wall-rock interaction, and later hydrothermal modification. Calcite is one of the most abundant minerals in these systems and may form or be modified during different stages of carbonatite evolution. Its trace element and isotopic compositions therefore provide a useful record of changing melt-fluid-rock conditions.

This contribution examines the role of calcite as a mineral-scale tracer of ore-forming processes in carbonatite-associated REE-Nb deposits, mainly using examples from the Miaoya carbonatite complex in the South Qinling orogen and the Wu carbonatite dyke at Bayan Obo. At Miaoya, texturally distinct calcite records variable Sr and REE contents, REE patterns, and C-Sr isotopic compositions, reflecting modification of earlier carbonatite signatures by later hydrothermal activity. Dissolution–reprecipitation of calcite and associated apatite may have contributed to the redistribution of REEs and the formation of secondary REE minerals. In contrast, calcite from the Bayan Obo Wu dyke and associated sodic fenites records interaction between evolved alkali-carbonatite melts and quartz-rich wall rocks. Elevated Sr isotopic ratios and lower carbon isotope values in fenite calcite are consistent with wall-rock interaction and decarbonation during fenitization, which may have influenced melt alkalinity, ligand availability, and REE fractionation. These examples illustrate that calcite chemistry and in situ isotope compositions can help distinguish magmatic, hydrothermal, and wall-rock interaction processes in carbonatite-associated deposits. Integrated mineral-scale analysis of calcite provides a framework for evaluating how carbonatite systems evolve from primary carbonatitic magmatism to later fluid-mediated modification, and how these processes contribute to the redistribution and enrichment of critical metals.

Key words: Carbonatite, Calcite, REE–Nb mineralization, In situ C–Sr isotopes, Hydrothermal reworking

CARRIER MINERALS, ENRICHMENT MECHANISMS, AND PROSPECTING SIGNIFICANCE OF SCANDIUM IN THE ZHUJIABAOBAO ORE BLOCK, PANZHIHUA LAYERED INTRUSION, SW CHINA

Wenyuan Gao, Jianmin Yang, Fei Huang

Department of Geology, School of Resources and Civil Engineering, Northeastern University, China

Abstract Scandium is a critical metal for high-performance aluminum alloys, solid oxide fuel cells, and advanced functional materials. However, Sc is generally highly dispersed in nature and rarely forms independent ore deposits. In mafic-ultramafic layered intrusions, Fe-Ti oxide deposits may represent significant potential sources of by-product Sc, yet the carrier minerals, modes of occurrence, and enrichment mechanisms of Sc in these systems remain incompletely constrained. Here, we focus on the Zhujiabaobao ore block of the Panzhihua layered intrusion, situated along the western margin of the Emeishan Large Igneous Province, SW China. To investigate how Sc is hosted and enriched during the differentiation of high-Ti basaltic magma, we integrate petrographic observations, in situ LA-ICP-MS trace-element analyses of minerals, and AlphaMELTS modeling. Systematic sampling covered the Middle, Lower, and Marginal Zones, including gabbro, amphibole-bearing gabbro, Fe-Ti oxide-rich ore, and marginal microgabbro.

In situ LA-ICP-MS analyses show that Sc is mainly hosted by ilmenite and clinopyroxene. Amphibole can be a locally important Sc-rich mineral, whereas titanomagnetite, olivine, and plagioclase make only minor contributions to the bulk Sc budget. Sc concentrations are 68–91 ppm in clinopyroxene, 70–114 ppm in amphibole, and approximately 45.7 ppm on average in ilmenite. In contrast, titanomagnetite contains approximately 8.9 ppm Sc on average, and olivine approximately 5.3 ppm. Ilmenite and clinopyroxene are therefore the main Sc-carrier minerals because of their relatively high modal abundances and Sc concentrations. Although amphibole has high Sc contents, its low modal abundance suggests that it mainly records local redistribution of Sc during late-stage hydrous melt or fluid activity. Titanomagnetite, despite being abundant in the ores, has low Sc contents and thus makes only a minor direct contribution to the Sc budget. The generally smooth LA-ICP-MS time-resolved signals indicate that Sc is mainly incorporated into mineral crystal lattices by lattice substitution.

AlphaMELTS modeling suggests that fractional crystallization in a deep magma chamber could have led to preliminary enrichment of Sc in the residual melt. Subsequent crystallization in the shallow magma chamber occurred under conditions of approximately 0.5 wt.% H_2O and fO_2 close to the FMQ buffer, with plagioclase, olivine, clinopyroxene, and Fe-Ti oxides crystallizing at about 1156, 1150, 1132, and 1025 °C, respectively. The crystallization sequence, modal proportions of

clinopyroxene and Fe-Ti oxides, and residual melt mass jointly determined the amount of Sc captured by carrier minerals. Extensive Fe-Ti oxide crystallization further modified the residual melt mass, Fe-Ti composition, and Sc budget, thereby controlling the final Sc incorporation into ilmenite, clinopyroxene, and amphibole.

In summary, Sc enrichment in the Zhujiabaobao ore block can be interpreted as a multistage process involving high-Ti basaltic parental magma, preliminary Sc enrichment during fractional crystallization, coupled enrichment in ilmenite and clinopyroxene, and local redistribution during late-stage amphibole formation. The ilmenite-clinopyroxene assemblage may serve as an important mineralogical indicator for evaluating by-product Sc resources in Panzhihua-type Fe-Ti oxide deposits.

Key words: Scandium, Ilmenite, Clinopyroxene, Layered intrusion, Panzhihua

CHARACTERISTICS OF TRACE ELEMENTS OF PYRITES AND AU-AG-TELLURIDES IN THE SANHETUN GOLD DEPOSIT, HEILONGJIANG PROVINCE: IMPLICATIONS FOR THE METALLOGENESIS

Huajuan Gu [1], Huilin Shi [1], Chenglu Li [1,2*], Bowen Li [1], Yuanjiang Yang [1], Lili Liu [1]

1. Natural Resources Survey Institute of Heilongjiang Province, Harbin, China
2. Northeast Geological Science and Technology Innovation Center, Shenyang Liaoning, China

Abstract The Sanhetun gold deposit is a recently discovered, medium-sized gold deposit within the Nenjiang-Heihe tectonic metallogenic belt in Heilongjiang Province, China. It is the third telluride-rich gold deposit to have been recognized in this region, after the Sandaowanzi and Yongxin deposits. Orebodies are mainly hosted in the contact zone between a ductile shear zone and a volcanic–stratigraphic succession. The mineralization process of the deposit is characterized by being doublly influenced by the ductile deformation and the magmatic–hydrothermal fluid. In order to determine the metallogenic environment and controlling mechanism of the Sanhetun gold deposit, we have systematically analyzed gold-bearing pyrites and Au-Ag-bearing tellurides of different paragenetic stages in the deposit by usng the in-situ analytical techniques. Based on the characteristics of in-situ trace elements of Au-bearing minerals, the genetic characteristics of goldbearing minerals can be determined and the formation process of the deposit can be constrained. The research results show that main Au-bearing minerals of the Sanhetun gold deposit are pyrite and tellurides. Gold occurred dominantly as natural gold and telluride inclusions within pyrite and along microfractures of pyrite. A small amount of gold occurred between quartz and pyrite particles. On the basis of characteristics of pyrite petrography, ore textures and cross-cutting relationships,four types of pyrites (Py1, Py2a, Py2b, Py3) are classified. (1) The Py1 is a Ni-rich pyrite formed during the first mineralising stage. (2) The Py2a is a kind of pyrite with enriched Au, Ag, Pb, Bi and Te. (3) The Py2b is a kind of pyrite with enriched Cu, Zn, Se and As. Both of the Py2a and Py2b were formed during the second stage. (4) The Py3 is a kind of Sb-Co-enriched pyrite formed in the third stage. Gold and tellurium are present mainly as visible gold particles and telluride minerals. Minor Au and Te occurred in nano-scale particle or as isomorphous substitution within the lattice of pyrite. Results of trace elements of pyrites show that there are strong positive correlations between Au+Ag and Pb+Bi, between Au +Ag and Cu+Pb+Zn, and between Au and individual elements of Pb, Ag and Cu. These correlations indicate that there is the accompanied enrichment of Ag, Bi, Pb, Cu and Zn in the Au mineralization process. This is consistent with the characteristics that Au grade of the ore in chalcopyrite-rich zone is obviously increased and that Au-Ag minerals are closely intergrown with altaite and tetradymite. Co/Ni ratios of pyrites suggest that the pyrite is mainly of the metamorphichydrothermal type, with obviously superimposed

volcanic and magmatic- hydrothermal signatures. Combined with the metallogenetic geological setting and characteristics of the deposit, it is infered that the Santuntun gold deposit was formed by the superimposition of two mineralising events including the early-stage ductile-deformation-related one and the latestage hydrothermal one.

Key words: pyrite, Au-Ag-telluride, trace element, Sanhetun gold deposit, Heilongjiang Province

Acknowledgements This work was financially supported by the Heilongjiang Provincial Natural Science Foundation of China (No. LH2023D028) and the National Science and Technology Major Project of China (No. 2025ZD1008706).

COBALT OCCURRENCE AND ENRICHMENT MECHANISM IN SKARN IRON DEPOSITS OF THE NORTH CHINA CRATON

Xian Liang[1,2,3], Ju-Quan Zhang[1,2,3*], Fangyue Wang[4*], Jun-Wu Zhang[5] * Corresponding author: E-mail: juquan1983@163.com

1. School of Earth Sciences, Hebei GEO University, Hebei, Shijiazhuang, 052161, China
2. Key Laboratory of Strategic and Critical Mineral Resources of Hebei Province, Hebei GEO University, Hebei, Shijiazhuang, 052161, China
3. Collaborative Innovation Center for Strategic and Critical Mineral Resources of Hebei Province, Hebei, Shijiazhuang, 052161, China
4. Ore Deposit and Exploration Centre (ODEC), School of Resources and Environmental Engineering, Hefei University of Technology, Anhui, Hefei 230009, China
5. Institute of Earth Sciences, China University of Geosciences, Beijing 100083, China

Abstract The central-eastern North China Craton is characterized by numerous skarn iron deposits that also represent significant cobalt resources. However, the occurrence state and enrichment mechanisms of cobalt within these deposits remain incompletely understood. This study investigates the Handan-Xingtai and Laiwu districts, employing them as representative examples to elucidate cobalt behavior. Results indicate that cobalt primarily occurs as an isomorphous substituent within magnetite and pyrite, with a minor contribution from discrete cobalt-bearing minerals. Notably, pyrite exhibits a significantly higher cobalt concentration compared to magnetite.

Laser Ablation Inductively Coupled Plasma Mass Spectrometry (LA-ICP-MS) trace element mapping of pyrite from the Baijian deposit reveals a heterogeneous Co distribution, characterized by Co-rich growth zones, potentially indicative of multiple hydrothermal fluid pulses. At the Zhangjiawa deposit, magnetite can be categorized into two compositional groups: (1) a high-Mg group (Mg > 10,000 ppm), exhibiting an average Co content of 191 ppm, with a maximum of 822.3 ppm; and (2) a low-Mg group (Mg < 10,000 ppm), with an average Co content of 37.8 ppm. These observations suggest that Co-rich magnetite may represent a significant contribution to the overall Co endowment and should be considered during resource assessments.

Magmatic hydrothermal fluids represent the primary source of Co within these skarn systems. For example, pyrite within diorite at the Baijian deposit displays an average Co content of 9,264 ppm, substantially exceeding the average Co content of 921 ppm observed in pyrite from the ore zone. The major factors governing Co precipitation within the ore zones, however, appear to vary among individual skarn deposits. Within the Baijian ore zones, close to the hydrothermal mineralization center, magnetite exhibits higher concentrations of Co, Ti, V, Al, and Mn, while pyrite is enriched in Co. This implies that early hydrothermal fluids were rich in Co, and that Co concentrations in both minerals decline with decreasing temperature. At the Zhangjiawa deposit, Co, Mg, and Mn

concentrations in magnetite and pyrite decrease with increasing distance from the mineralization center, while V in magnetite and Ni, As, and Se in pyrite display an opposing trend. These observations indicate that early-stage fluids were enriched in Mg and Co, and that Co concentrations in magnetite and pyrite decrease with decreasing temperature and oxygen fugacity.

A comparison among the Baijian, Xishimen, and Beiminghe deposits in the Handan - Xingtai area and the Zhangjiawa deposit in the Laiwu area reveals that high Co contents in magnetite are associated with higher sulfur isotope compositions of the deposits. This indicates that the addition of evaporites to the ore-forming hydrothermal fluids increased the salinity and oxygen fugacity of the fluids, thereby promoting cobalt enrichment.

Key words: Cobalt, Occurrence state, Enrichment mechanism, Skarn iron deposits, North China Craton

CONSTRAINTS FROM SULFIDE TRACE ELEMENTS AND S–ZN ISOTOPES ON THE GENESIS OF THE KANGJIAWAN PB–ZN POLYMETALLIC DEPOSIT, NANLING METALLOGENIC BELT, SOUTH CHINA

Yi Zhang, Xin-Shui Wang

School of Earth Sciences, China University of Geosciences, Wuhan 430074, China

Abstract The Kangjiawan Pb-Zn polymetallic deposit, located on the northwestern margin of the Cathaysia Block, is an important component of the Nanling metallogenic belt, South China. No obvious igneous rocks are exposed in the mining district, and the orebodies are mainly hosted within silicified fracture zones controlled by both stratigraphic and structural factors. Consequently, the genetic type, source of ore-forming materials, and ore-forming processes of the deposit remain poorly constrained. To constrain the material source and genesis of the Kangjiawan Pb-Zn polymetallic deposit, this study systematically investigated trace elements and S-Zn isotopes of sulfides (pyrite and sphalerite). Based on crosscutting relationships and mineral assemblages, the mineralization process can be divided into three stages: (I) quartz-pyrite stage; (II) quartz-pyrite-galena-sphalerite stage; and (III) calcite-pyrite-sphalerite stage. Sphalerite can be further classified into four types (Sp1–Sp4), characterized by enrichment in Cd, Fe, Mn, and In, but depletion in Ga and Ge. Trace-element thermometry of sphalerite yields formation temperatures ranging from 230 to 392 °C, indicating a medium- to high-temperature hydrothermal system. Principal component analysis (PCA) of sphalerite trace elements reveals that the Kangjiawan deposit is distinctly different from MVT-, SEDEX-, and VMS-type Pb-Zn deposits, whereas its trace-element signatures and formation temperatures show strong affinity with skarn-related mineralization. The $\delta^{34}S$ values of sphalerite range from -3.1‰ to 2.0‰, while those of pyrite vary from -2.9‰ to 3.4‰. The sulfides display a tower-shaped $\delta^{34}S$ distribution centered around 0‰, falling within the typical range of granitic magmatic sulfur (-5‰ to 5‰), suggesting that the sulfur was mainly derived from deep magmatic-hydrothermal fluids. In addition, the Kangjiawan sphalerite samples exhibit relatively homogeneous $\delta^{66}Zn$ values (0.12‰-0.24‰), comparable to those of granitic rocks, further supporting a magmatic origin of the ore-forming fluids. Although no igneous rocks are exposed at the surface, skarn alteration, and intense silicification were identified in deep drill cores, indicating concealed magmatic-hydrothermal activity at depth. Collectively, these results suggest that the Kangjiawan Pb-Zn polymetallic deposit is a medium- to high-temperature magmatic-hydrothermal vein-type deposit related to deep magmatic activity, and that significant potential exists for further exploration of concealed magmatic-related mineralization at depth.

Key words: Sulfide, S-Zn isotopes, Nanling Metallogenic Belt, Trace element geochemistry Kangjiawan Pb–Zn Deposit

CONSTRAINTS ON THE SERPENTINITE NATURE IN QINGSHUIQUAN AREA OF THE EAST KUNLUN OROGENIC BELT

Fancong Meng[1] Songyong Chen[1] Hua Xiang [1] Xuepeng Duan[2]

1. - Institute of Geology, Chinese Academy of Geological Sciences, Beijing 100037, China

2. -Development Research Center of China Geological Survey, Beijing, 100037, China

Abstract The main types of peridotite in orogenic belts are as follows: (1) mantle peridotite in ophiolite not only indicates plate suture zones, but also may form chromitite in peridotite, such as in the Himalayan orogenic belt and the Urals orogenic belt. (2) mantle wedge peridotite in continental subduction zones. It often associated with eclogites and has undergone high-pressure - ultra-high-pressure metamorphism (garnet phase) or metasomatism by melts/fluids in subduction zone (spinel phase). Such as the Sulu-Dabie high-pressure - ultra-high-pressure metamorphic belt. (3) mafic-ultramafic complex formed in island arcs or continental margin rift environments. Sometimes magmatic copper-nickel sulfide deposits or platinum deposits are produced. Such as Jinchuan and Xiarihamu in China, as well as the Urals platinum belt and SE Alaska. Although peridotites are rare exposed, but their identification is significance for understanding the tectonic evolution of orogenic belts. Due to the usully serpentinization of peridotite, it is difficult to recognize its genesis.

The serpentinite in Qingshuiquan area of East Kunlun studied have always been considered as ophiolite units(e.g. Yang et al., 1996).The major elements of serpentinite indicates that the protolith may have been harzburgite, and the disseminated and banded chromian spinel components suggest that it was formed in a subduction zone environment(Feng et al., 2015a,b). Base on detailed mapping, we found graphite-bearing garnet amphibolite lenses in the serpentinite. Genetic mineralogy of garnet, amphibole, graphite and zircon were studied. Geochemistry and Sm-Nd isotope analysis of bulk-rocks were also carried out. The results show that the garnet is mainly composed of almandite and pyrope component, and the amphibole is mainly composed of pargasite and a small amount of edenite. The mica is mainly phlogopite, a small amount of biotite. Pyroxene is residue and trace. Graphite is mainly associated with phlogopite and pargasite.The carbon isotope $\delta^{13}C_{VPDB}$ values of graphite range from -17‰ to -5‰, and most of them are between -13‰ ~ -5‰, which is inorganic carbon. Geochronology of zircon results show that the garnet amphibolite was formed at 500Ma, and the P-T conditions are approximately 1.0GPa and 680-750°C (middle and lower crust depth), peak metamorphism may reach high temperature granulite facies. The garnet amphibolite has low in SiO_2 (minimum 38wt.%), rich in MgO (12-19wt.%), and showing mantle affinity. The differentiation between light and heavy rare earth elements is not strong, and the Eu is obviously negative anomaly ($\delta Eu = 0.23 \sim 0.29$); $\varepsilon Nd(t)$ values of whole rock vary from -14 to -

13. It has a strong continental crust signal. By comparison, we exclude it as a tectonic block of mafic granulite in the surrounding rock and metamorphic sole of ophiolite. It is proposed that crust-derived metamorphic fluids react with mantle wedge-peridotite to form garnet amphibolite. This study reveals the process of crust-mantle material exchange in the shallow subduction zone and the formation of enriched components in the mantle wedge peridotite.

Key words: garnet amphibolite, graphite, serpentinite, mantle wedge, subduction zone

Acknowledgements This work was supported by the National Natural Science Foundation of China (42072049) and the China Geological Survey project (DD20230340, DD20221649 and DD20190006).

CONTROLS ON CU ± AU, MO CONCENTRATIONS IN PORPHYRY SYSTEMS REVEALED BY MACHINE LEARNING

Bin Wang[1], Renguang Zuo[1],*, Oliver P. Kreuzer[2],[3]

1. State Key Laboratory of Geological Processes and Mineral Resources, China University of Geosciences, Wuhan 430074, China
2. Corporate Geoscience Group (CGSG), P.O. Box 5128, Rockingham Beach, WA 6969, Australia
3. Economic Geology Research Centre (EGRU), College of Science and Engineering, James Cook University, Townsville, QLD 4811, Australia

Abstract Porphyry deposits are the primary global sources of copper (Cu) and molybdenum (Mo) and a major source of gold (Au). Yet, the fundamental controls on the relative abundance of Cu, Mo and Au in porphyry deposits remain poorly understood. Here, we leverage global geological databases and a machine learning (ML) algorithm to investigate first-order geological controls on Cu/Mo/Au ratios in porphyry systems. First, association rule data mining of mineral assemblages identifies subtype-specific mineralogical fingerprints across hundreds of porphyry deposits. Second, supervised machine learning (ML) models trained on zircon trace element data classify deposits by Cu/Au, Cu/Mo, and Au/Mo ratio thresholds, and SHapley Additive exPlanations (SHAP) analysis, a technique used to explain ML predictions, defines the dominant predictors. The zircon models achieve high classification performance and consistently highlight Yb/Dy, U, Th, Hf, and redox proxies (ΔFMQ-related metrics) as key features, indicating that pre-mineralization magma evolution exerts a strong influence on the relative availability and partitioning behavior of Cu, Au, and Mo. We interpret these results as evidence that magmatic preconditioning provides an important, globally detectable signal in porphyry deposit metal ratios, while acknowledging that hydrothermal focusing and precipitation efficiency can further modulate final endowments. As a whole, the combined mineralogical and zircon-based framework offers not only a quantitative basis for refining porphyry subtype classification but also for improving Cu-Au-Mo exploration targeting.

Key words: Porphyry deposits, Machine learning, Mineral assemblage, Zircon trace-element geochemistry

CORE-MANTLE-SHELL SPHEROIDAL MICROFOSSILS FROM THE PALEOPROTEROZOIC YUANJIACUN BANDED IRON FORMATION: DIRECT EVIDENCE FOR MICROBIAL IRON OXIDATION

Qilin Huang[1], He Zhang[1], Siyi Huang[1], Yuanfeng Cai[1,*]

State Key Laboratory of Critical Earth Material Cycling and Mineral Deposits, Nanjing University, Nanjing 210023, China

Abstract A long-standing gap in understanding of the origin of banded iron formations (BIFs) is the lack of direct microfossil evidence for microbial iron oxidation. Here, we report spheroidal microfossils (5–35 μm) from the hematite subfacies of the Paleoproterozoic Yuanjiacun Formation BIF (ca. 2.23–2.20 Ga, North China Craton). These microfossils exhibit a previously unrecognized core-mantle-shell tripartite architecture. Using correlative nanoscale imaging (SEM, TEM), Raman spectroscopy, nanoSIMS, and synchrotron XANES, we establish a multi-proxy biogenicity chain. The core consists of radially arranged hematite nanocrystals; the mantle is an organic–mineral nanocomposite of hematite and amorphous carbon; and the shell is a continuous carbonaceous film. NanoSIMS reveals coupled C–N–S enrichments in the mantle and shell, with highly negative $\delta^{13}C$ values (from −22.4‰ to −39.1‰; average −31.5‰). XANES spectra show aromatic carbon and carboxyl groups, aromatic nitrogen, and an Fe(III) signature consistent with Fe(III)-carboxyl complexes in the extracellular polymeric substances (EPS) of iron-oxidizing bacteria. We propose a two-stage formation model: (I) planktonic Fe(II)-oxidizing bacteria drove water-column Fe^{2+} oxidation, precipitating a hematite-dominated core; (II) after settling, these cores were overgrown within benthic microbial mats, where microbially templated mineralization via EPS produced the organic-rich mantle and shell. This discovery provides direct microfossil evidence for microbe-driven iron oxidation and organic carbon burial during the Great Oxidation Event, thus filling a critical gap in BIF genesis.

Key words: Microbial iron oxidation, Banded iron formations, Microfossils, XANES, Great Oxidation Event

CRUSTAL FAULTING DRIVES BIOLOGICAL REDOX CYCLING AND SUSTAINS THE DEEP BIOSPHERE

Xiao Wu[1,2,3], Jianxi Zhu[1,2,3*], Xiaoliang Liang[1,2,3], Mang Lin[1,2,3*], Barbara Sherwood Lollar[4,5], Kurt O. Konhauser[6*], Hongping He[1,2,3]

1. State Key laboratory of deep earth Processes and Resources, Guangzhou institute of Geochemistry, Chinese Academy of Sciences, Guangzhou, P.R. China.
2. Guangdong Provincial Key laboratory of Mineral Physics and Materials, Guangzhou institute of Geochemistry, Chinese Academy of Sciences, Guangzhou, P.R. China.
3. Guangdong Research center for Strategic Metals and Green Utilization, Guangzhou, P.R. China.
4. Department of earth Sciences, University of toronto, 22 Ursula Franklin Street, Toronto M5S 3B1, Canada.
5. Institut de Physique du Globe de Paris (IPGP), Université Paris Cité, 1 rue Jussieu, Paris, France.
6. Department of Earth and Atmospheric Sciences, University of Alberta, Edmontont6G 2e3, Canada

Abstract Crustal faulting is a key geodynamic process that generates mineral radicals on fresh rock surfaces via homolytic cleavage of Si–O bonds, which further induce water splitting to produce reactive redox pairs (e.g., •H, H_2, •OH, H_2O_2) in the deep subsurface. Recently, two basic fault-induced rock fracturing modes (extension and shear fractures) with quartz as the model mineral were conducted to investigate redox gradient formation and subsequent Fe redox transformations (Wu et al., 2025). Our results show that extension fractures generate more robust redox gradients with substantial •H production (far exceeding oxidant yields), while shear fractures produce redox pairs continuously but lack H_2O_2 accumulation. In the presence of Fe, low concentrations of oxidants (•OH, H_2O_2) only marginally oxidize Fe^{2+} to Fe^{3+}, whereas reactive hydrogen atoms (•H) efficiently reduce Fe^{3+} (including dissolved Fe ions and Fe-bearing minerals (ferrihydrite, goethite, hematite)) back to Fe^{2+}. Calculations based on experimental data reveal that earthquake-induced faulting produces redox pairs at extremely high local fluxes (e.g., H_2: 33.1 mol m^{-2} $year^{-1}$; •H: 737.2 mol m^{-2} $year^{-1}$), which are several orders of magnitude higher than the levels required to sustain lithoautotrophic microbial ecosystems, and far exceed H_2 fluxes from radiolysis and serpentinization on a unit fault surface area. Faulting-derived redox pairs establish a broad redox potential range (–0.41 to +0.82 V) in fracture systems, driving the biogeochemical cycling of Fe, C, N, and S and forming multiple redox pairs that support high metabolic diversity in the deep biosphere.

DECIPHERING ORE-FORMING FLUID EVOLUTION PROCESSES OF THE QINGLONGGOU GOLD DEPOSIT, NORTHERN MARGIN OF QAIDAM BASIN, QINGHAI PROVINCE, CHINA

Abstract The Qinglonggou gold deposit is a large-scale deposit located within the Tanjianshan gold orefield on the northern margin of the Qaidam Basin. Recent exploration has achieved significant breakthroughs at depth and along its periphery. However, the occurrence of gold in deep ores and the evolution of the ore-forming fluids remain debated. This study, grounded in detailed fieldwork, involved systematic drill-core logging and deep sampling, followed by in-situ micro-analysis of native gold, pyrite, and arsenopyrite. Visible gold occurs mainly as micron-sized native gold (Au^0), with mineralization divided into three main stages (III–V). Stage III pyrite (Py3) occurs as veins within carbonaceous mylonite and phyllite, primarily along quartz-calcite fractures. It is characterized by high Co content and Co/Ni ratios, with $\delta^{34}S$ values ranging from +5‰ to +20‰, suggesting contributions from both magmatic and seawater sulfur sources. Native gold occurs as inclusions within Py3. Stage-IV mineralization comprises Py4, arsenopyrite (Apy), minor native gold, and chalcopyrite (Ccp) in quartz-calcite veins. Py4 shows extremely high Co/Ni and Co content, whereas Apy has variable Co and Ni with lower Co/Ni. Py4 $\delta^{34}S$ values (+20‰ to +25‰) lie within the seawater sulfur field. Ccp values (+5‰ to +10‰) in Stage-IV indicate a magmatic source, and Apy values (+10‰ to +15‰) reflect mixing. Native gold occurs adjacent to arsenopyrite, with nano-gold hosted in arsenopyrite, arsenian pyrite, and tellurobismuthite. Stage-V pyrite (Py5) occurs as thin veins in calcite with tetrahedrite. Py5 has a moderate Co/Ni ratio, and yields $\delta^{34}S$ values (+10‰ to +15‰) indicative of a mixed sulfur source. Minor native gold is found in calcite fractures. Py3 and Py4 show intermediate Pd/Pt ratios with low Pd and Pt contents, whereas Py5 has a lower Pd/Pt ratio but higher Pt. Three fluids contributed to the main mineralization: magmatic, metamorphic, and seawater. Magmatic and metamorphic fluids were active over a prolonged period. Sulfur was derived from mixed sources, and ore-forming materials were mainly sourced from magmatic rocks with a minor mantle component (enriched in the Wandonggou Group).

DECODING RARE-METAL PEGMATITE PETROGENESIS: INSIGHTS FROM MINERAL GEOCHEMISTRY

Xin Chen， Nan Chao

State Key Laboratory of Geological Processes and Mineral Resources and School of Earth Resources, China University of Geosciences, Wuhan 430074, China

Abstract The relative contributions of source composition, magmatic differentiation, and fluid-driven processes to rare-metal enrichment in pegmatite systems remain debated. Zircon, through its trace-element chemistry and Zr stable isotopes (δ94/90ZrIPGP), has the potential to record this entire evolutionary pathway, yet the behaviour of Zr isotopes during the magmatic–hydrothermal transition remains incompletely constrained. Here we present an integrated study of zircon U–Pb geochronology, Hf isotopes, trace elements, and Zr isotopic compositions from a cogenetic sequence of tourmaline granite, barren pegmatite, and spodumene pegmatite in the Himalayan orogen (Qiongjiagang and Zhaguopu deposits), spanning conditions from magma-dominated to fluid-influenced regimes. Four zircon populations are identified, defining a progressive sequence of increasing modification. Type I (inherited cores) and Type II (magmatic rims) in tourmaline granite preserve primary magmatic signatures with low δ94/90ZrIPGP, low LREE contents, and negligible common Pb. Type III zircons in barren pegmatite show intermediate compositions with partially preserved oscillatory zoning and moderate rare-metal enrichment, whereas Type IV zircons in spodumene pegmatite display pervasive spongy and patchy textures, the highest δ94/90ZrIPGP values (up to 2.32‰), pronounced LREE enrichment, and substantial common Pb incorporation. All populations are Cenozoic and yield overlapping U–Pb ages (ca. 24–22 Ma) and coherent εHf(t) values, supporting a shared magma source and indicating that the observed chemical and isotopic variations are primarily process-driven rather than source-controlled. The zircon record delineates three stages of rare-metal enrichment. Anatexis, recorded by melt-driven dissolution–reprecipitation of inherited zircon, established the initial metal budget with preferential Li and Be extraction and limited Zr isotope fractionation under near-equilibrium conditions. Fractional crystallisation during the granite-to-barren pegmatite transition produced further pre-enrichment, particularly of Nb and Ta, with δ94/90ZrIPGP fractionation consistent with diffusion-limited crystallisation. However, calculated melt Li concentrations remained well below the spodumene saturation threshold, indicating that differentiation alone was likely insufficient for economic mineralisation. The transition to spodumene pegmatite records a shift toward fluid-dominated conditions, marked by the largest δ94/90ZrIPGP increase (~0.5–0.8‰), strong within-population variability, and coupled enrichment in LREE and common Pb. These features are best interpreted as reflecting kinetic Zr isotope fractionation associated with fluid exsolution and advective transport, significantly exceeding equilibrium zircon–melt fractionation. Comparison between the two

deposits shows that the more intensely mineralised Zhaguopu system records higher δ94/90ZrIPGP values and lower Zr/Hf ratios than Qiongjiagang, pointing to a genetic link with the extent of the magmatic-hydrothermal transition. This suggests that the separation and advection of magmatic fluids (fluid exsolution) play a critical role in governing the final metal endowment. These results highlight the complementary and sequential roles of anatexis, fractional crystallisation, and fluid exsolution in rare-metal pegmatite formation, and indicate that zircon δ94/90ZrIPGP, combined with Zr/Hf ratios and common Pb contents, may provide a useful empirical framework for assessing the metallogenic potential of pegmatite systems.

Key words: Zircon, Zr isotopes, Magmatic-hydrothermal transition, Dissolution-reprecipitation, Li mineralization

DETRITAL MAGNETITE AS A SAMPLING MEDIUM IN FUTURE MARS SAMPLE RETURN MISSIONS: AN ANALOG STUDY IN THE WESTERN QAIDAM BASIN

Qi-Tao Hu[1,2], Wen-Ping Liu[3], Yi-Liang Li[4], Qi-Zhi Yao[5], Gen-Tao Zhou[1,2,*]

1. Deep Space Exploration Laboratory/School of Earth and Space Sciences, University of Science and Technology of China, Hefei 230026, China
2. State Key Laboratory of Lithospheric and Environmental Coevolution, University of Science and Technology of China, Hefei 230026, China
3. Hunan Automotive Engineering Vocational College, Zhuzhou, Hunan, China
4. Department of Earth and Planetary Sciences, the University of Hong Kong, Hong Kong Special Administrative Region of China
5. School of Chemistry and Materials Science, University of Science and Technology of China, Hefei 230026, China

Abstract Detrital magnetite has been identified in Martian sediments and regolith, and it is expected to be a component of sedimentary samples from Mars slated for return to Earth. Magnetite can preserve detailed records of formation conditions through its trace element composition and microstructures, giving it a high information density. In addition, its widespread occurrences, resistance to weathering, and ease of collection further make it a promising sampling medium for reconstructing Martian geological history. However, a robust framework for interpreting the genetic environments of detrital magnetite remains lacking. To address this gap, we conducted an integrated mineralogical and geochemical study on detrital magnetite from the western Qaidam Basin, a well-established terrestrial analog for Mars. Magnetic grains were extracted using a hand magnet from diverse settings, including sedimentary rocks, regolith, and a hydrothermal spring. They were characterized by X-ray diffraction, electron microscopy, and laser ablation inductively coupled plasma mass spectrometry. Magnetite, the only ferromagnetic mineral identified, dominates all samples. Backscattered electron imaging shows that magnetic grains occur either as mineral fragments (predominantly magnetite) or lithic fragments (composite grains of magnetite with silicates, occasionally with calcite). In both occurrences, magnetite is either monomineralic or exhibits microstructures such as inclusions, exsolution features, and martitization. Compositional analyses show that the iron content of detrital magnetite is slightly below the stoichiometric value, while trace element concentrations are highly variable. Given the likelihood that sediments at a site or within a region represent mixtures from multiple sources, an exploratory analysis was conducted to assess whether the magnetic grains originated from distinct sources using dimensionality reduction and clustering techniques. Principal component analysis (PCA) showed a continuous distribution with no apparent clusters, whereas t-distributed stochastic neighbor embedding (t-SNE) revealed a largely continuous distribution with a segregated group. Hierarchical density-based

spatial clustering of applications with noise (HDBSCAN) further confirmed the existence of two clusters, one of which corresponds to the group identified by t-SNE. However, projections of the compositional data onto three commonly used discrimination diagrams for distinguishing between hydrothermal and igneous magnetite yielded conflicting and unreliable results. To better discriminate between igneous, hydrothermal, and sedimentary origins, a new Random Forest classifier based on the eleven key elements (Mg, Al, Ti, V, Cr, Mn, Co, Ni, Zn, Ga, and Sn) was developed. The model indicates multiple sources for the detrital magnetite crystals, with a dominant igneous source from surrounding granitic terrains, accompanied by subordinate hydrothermal and sedimentary contributions. We further demonstrated that application of the single-mineral $T_{Mg\text{-}mag}$ geothermometer to Mg-poor magnetite from felsic systems requires caution, as the low Mg content primarily reflects bulk rock composition rather than crystallization temperature. Overall, this study highlights that integrating multiple analytical methods is essential for extracting complementary information preserved within detrital magnetite. As such, our analog study provides a reference for maximizing the scientific return from detrital magnetite in future Martian samples.

Key words: Magnetite, Mars, Qaidam Basin, Random Forest

Acknowledgements This work was supported by the National Natural Science Foundation of China (No. 42430201 and 42488101), the Seed Fund for Collaborative Research from the University of Hong Kong (No. 2307102420), and the Key Technology Research Project of TW-3 (TW3004).

DIAGENETIC AND METALLOGENIC AGES OF THE JIAZISHAN MO DEPOSIT, INNER MONGOLIA, CHINA: CONSTRAINTS FROM ZIRCON U-PB AND MOLYBDENITE RE-OS DATING

Zhenliang Wang[1,2], Yong Li[1,2], Jianweng Gao[1,2], Jianzhou Yang[1,2], Keqiang Zhao[1,2], Yangang Fu[1,2], Youmao Deng[1,2]

1. Institute of Geophysical and Geochemical Exploration, Chinese Academy of Geological Sciences, Tianjin 300309, China;
2. National Center for Geological Exploration Technology, Tianjin 300309, China

Abstract The Jiazishan Mo deposit in Inner Mongolia is located in the Cu-Pb-Zn-Mo polymetallic metallogenic belt in the middle section of the Great Xing'An Range, which is an important polymetallic metallogenic belt in China. In this study, LA-ICP-MS zircon U-Pb dating and molybdenite Re-Os dating were adopted to carry out the diagenetic and metallogenic chronology research of the deposit. The zircon U-Pb age of the granite is 149.19±0.47Ma, and the molybdenite Re-Os isochron age is 147.4±1.4Ma, which clearly confirms that the deposit was formed in the Late Jurassic and is a product of the large-scale molybdenum metallogenic event during the Yanshan period in eastern China. The $^{176}Hf/^{177}Hf$ values of the granite in the mining area range from 0.28290 to 0.28296, the $\varepsilon_{Hf}(t)$ values are 7.82 to 9.86, and the two-stage model age (t_{DM2}) are 744 to 929Ma. These results indicate that the granitic magma was formed by re-melting after the Neoproterozoic lower crust, which was formed by partial melting of depleted mantle material. The Re content of molybdenite ranges from 37.62×10^{-6} to 401.34×10^{-6}, with an average of 121.28×10^{-6}, revealing that the metallogenic materials of the deposit have a significant crust-mantle mixed source characteristics. Comprehensive analysis shows that the formation of the deposit is closely related to the transformation of the tectonic environment from compression to post-collisional extension after the closure of the Mongol-Okhotsk Ocean, and may be superimposed by the back-arc extension caused by the subduction of the Paleo-Pacific Plate. This study clarifies the diagenetic and metallogenic ages and material sources of the Jiazishan Mo deposit, and provides an important geological basis for the research on metallogenic regularity, metallogenic prediction and prospecting exploration of the polymetallic metallogenic belt in the middle section of the Great Xing'An Range.

Key words: Inner Mongolia, Jiazishan Mo deposit, U–Pb age, Trace elements, Hf isotope

Acknowledgements This research was jointly supported by National Nonprofit Institute

Research Grant of Institute of Geophysical and Geochemical Exploration, Chinese Academy of Geological Sciences (No. AS2024J13 and No. AS2017J04) and the China Geological Survey Program (No. DD20230309).

DISCOVERY OF MAGNESIO-FERRI-HORNBLENDE: A NOVEL INDICATOR MINERAL FOR PORPHYRY–SKARN CU POLYMETALLIC SYSTEMS

Yongmei Zhang[1], Xuexiang Gu[1], Tao Wang[1], Guang Fan[2], Ting Li[2]

1. State Key Laboratory of Geological Processes and Mineral Resources, School of Earth Sciences and Resources, China University of Geosciences (Beijing), Beijing 100083, China
2. Beijing Research Institute of Uranium Geology, Beijing 100029, China

Abstract Magnesio-ferri-hornblende, $\square Ca_2(Mg4Fe^{3+})[(Si_7Al)O_{22}](OH)_2$, is a newly discovered mineral of the amphibole supergroup (IMA2021-100). It predominantly crystallizes in intermediate–acidic magmatic systems under relatively low temperature and pressure (P–T), coupled with high oxygen fugacity (fO_2). This mineral is not only abundant but also commonly serves as a major rock-forming phase in fertile intrusions, whereas it remains exceedingly rare in barren intrusions. Statistical analysis of amphibole types and compositions from felsic magmas worldwide underscores the diagnostic value of magnesio-ferri-hornblende in distinguishing fertile from infertile intrusions in porphyry-skarn Cu polymetallic systems. In barren intrusive rocks, amphiboles are predominantly magnesio-hastingsite and hastingsite, together accounting for over 60 % of the total amphibole population. These minerals crystallize under high P–T and low fO_2 conditions. In contrast, fertile felsic magmas, which form under low P-T and high fO_2 environments, are characterized by a dominance of magnesio-ferri-hornblende (>70%) together with subordinate magnesio-hornblende. Notably, in intrusions where magma mixing is evidenced by the presence of mafic microgranular enclaves (MMEs), the proportion of magnesio-ferri-hornblende reaches exceptionally high levels (exceeding 80%), highlighting its pivotal role in porphyry-system mineralization. The occurrence of MMEs directly attests to the injection of mantle-derived mafic magmas into felsic magma chambers. This mantle input is also reflected in the elevated magnesium index (Mg#) of coexisting amphiboles. High Mg# values thus serve as a robust indicator of such mantle contribution, which introduces chalcophile elements (Cu, Au) and volatiles into the magmatic system. These mantle-derived components not only supply essential metals but also enhance the fertility of the system for porphyry–skarn mineralization. Because magnesio-ferri-hornblende is the dominant amphibole phase precisely in these mantle-influenced, high-fO_2, high-Mg# magmas, its widespread occurrence directly signals the presence of oxidized magmatic systems with enhanced ore-forming potential.

Building on these findings, we propose that the ore-forming potential of intermediate–felsic magmas can be quantitatively assessed by integrating three key parameters: (1) the modal abundance of magnesio-ferri-hornblende (≥2/3), (2) the Mg# value of amphiboles (≥0.5), and (3) the fO_2 estimated from amphibole compositions ($\Delta NNO \geq +1$). This integrated approach enables a

robust evaluation of magma redox state and mantle contribution—two critical factors controlling porphyry–skarn mineralization. Intrusive bodies that simultaneously satisfy all three criteria are thereby identified as highly fertile systems with exceptional mineralization potential. This tripartite threshold constitutes a validated, quantitative indicator for porphyry-skarn systems. Importantly, all three parameters can be readily calculated from routine electron microprobe analysis of amphiboles in standard thin sections, offering a cost-effective and efficient alternative to more labor-intensive geochemical methods. Amphiboles are readily accessible in felsic intrusions and amenable to routine mineralogical and geochemical analysis. This contrasts favorably with conventional whole-rock or single-mineral proxies, which often suffer from low elemental concentrations, difficult mineral separation, and high analytical costs. As a direct crystallization product that faithfully records magmatic conditions and metallogenic affinity, magnesio-ferri-hornblende provides a novel, mineralogically grounded exploration indicator for porphyry-skarn Cu polymetallic deposits.

Key words: Magnesio-ferri-hornblende, Porphyry-skarn deposit, Oxygen fugacity, Magnesium index, Mineral exploration indicator

Acknowledgements The research was jointly funded by the National Natural Science Foundation of China (42130804 and 42573067), the National Science and Technology Major Project on Deep Earth (2024ZD1001800), and the Key Research and Development Program of Xinjiang Uygur Autonomous Region(2023B03016).

DISCRETE MINERALIZATION OF REES AND NB IN CARBONATITE-ALKALINE COMPLEX TRIGGERED BY MAGMATIC EVOLUTION AND METASOMATISM

Ronglin Ma[1,2], Haiyang Xian[2,3], Zhihui Zha[4], Xiaoliang Liang[2,3], Yiping Yang[2,3], Jianxi Zhu[2,3], Wei Terry Chen[4], Hongping He[2,3], Wubin Yang[2,3*] Corresponding Author: E-mail: yangwubin@gig.ac.cn

1. School of Geological Engineering, Qinghai University, Xining 810016, Qinghai, China;
2. State Key Laboratory of Deep Earth Processes and Resources, Guangzhou Institute of Geochemistry, Chinese Academy of Sciences, Guangzhou 510640, Guangdong, China;
3. Guangdong Research Center for Strategic Metals and Green Utilization/Guangdong Provincial Key Laboratory of Mineral Physics and Materials, Guangzhou 510640, Guangdong, China;
4. State Key Laboratory of Critical Mineral Research and Exploration, Institute of Geochemistry, Chinese Academy of Sciences, Guiyang 550081, Guizhou, China;

Abstract Carbonatite-alkaline complexes are primary sources of rare earth elements (REEs) and niobium (Nb). However, the factors governing the spatio-temporal partitioning and enrichment of these metals within a single alkaline complex remain poorly constrained. The Shaxiongdong complex in South Qinling, Central China, which consists of pyroxenites, syenites, and carbonatites and hosts significant REEs and Nb mineralization, offers a well-preserved lithofacies framework to investigate these controlling factors. Zircon and primary titanite from the pyroxenites both yield U-Pb ages of ~430 Ma. The three lithofacies share homogeneous C-O-Sr-Nd isotopic compositions, and pyroxenite-hosted diopside exhibits consistently low Al_2O_3 contents (< 5 wt.%). Together, these lines of evidence establish a magmatic, rather than metasomatic, origin for the pyroxenites. Whole-rock geochemical trends further delineate a coherent evolutionary sequence involving fractionation, immiscibility, and metasomatism. Pyroxenites are depleted in both REEs and Nb, whereas carbonatites are strongly enriched in REEs yet contain less Nb than the syenites. This discreting is reinforced by contrasting mineralization styles: Nb mineralization in syenite occurs exclusively as disseminated Ti-rich phases, while REEs in carbonatites form both disseminations and veinlets. Syenites record elevated mafic indices and alkali/alkaline-earth cation ratios, high magmatic H_2O contents (0.05-0.21 wt.%) in titanite, and high crystallization pressure (~220 MPa) estimated from biotite, indicating that advanced differentiation proceeded under hydrous, alkaline, high-pressure conditions. Such conditions efficiently partitioned REEs into the conjugate carbonatitic melt, while the high alkali activity in the residual carbonated syenitic melt promoted the crystallization of Nb-rich Ti-phases (e.g., titanite, ilmenite, and rutile), accounting for the relatively high Nb content in the syenites. Following melt separation, carbonatitic melts metasomatism, texturally recorded by biotite aggregates and minor titanite within the carbonatites, scavenged Nb into pyrochlore and REEs into apatite. Continued hydrothermal activity, dated by secondary titanite at ~ 400 Ma, led to

the formation of REE-mineralized veinlets. We therefore propose a two-stage metallogenic model in which H_2O-alkali-modulated magmatic differentiation at high pressure governed the primary segregation of Nb and REEs into distinct lithological hosts, while late-stage, element-specific hydrothermal mobilization amplified the REE enrichment. Consequently, exploration for economic Nb should target early melt-metasomatic domains, whereas high-grade REE ores are predicted in zones of intense hydrothermal activity.

Key words: titanite, REEs and Nb mineralization, discrete distribution, carbonatite-alkaline complex

EFFICIENT GOLD SCAVENGING BY MINERAL REPLACEMENT REACTIONS: AN EXPERIMENTAL STUDY OF HEMATITE SULFIDATION IN IOCG SYSTEMS

Ruping Gan, Jingbo Xu, He Zhang, Yuanfeng Cai*

State Key Laboratory of Critical Earth Material Cycling and Mineral Deposits, School of Earth Sciences and Engineering, Nanjing University, PR China

Abstract Trace metal enrichment in hydrothermal deposits is often linked to fluid evolution, but the role of mineral interface reactions in scavenging and redistributing trace elements remains unclear—especially in iron oxide copper-gold (IOCG) systems, where the processes controlling gold sequestration are still not well understood. Here, we report hydrothermal experiments (240–300°C) that examine gold behavior during hematite sulfidation under acidic (pH=4) and alkaline (pH=10) conditions. Our results show that pH-dependent sulfide replacement reactions are the key factor controlling gold distribution, with mineral interfaces serving as critical sites for gold reactivation and remobilization. Under acidic conditions, chalcopyrite forms as the only sulfide product. Gold is initially hosted in chalcopyrite as invisible lattice-bound species, but these are gradually remobilized as the reaction proceeds, due to the limited number of structural sites available for gold in chalcopyrite. In contrast, alkaline conditions trigger the sequential formation of chalcopyrite and bornite. Interface-coupled dissolution-reprecipitation (ICDR) reactions create high-energy chalcopyrite–bornite interfaces that trap mobilized gold. As a result, gold becomes re-enriched as visible micron-scale grains at phase boundaries, while invisible gold in chalcopyrite falls below detection limits. These findings demonstrate that ICDR reactions—not bulk fluid chemistry alone—are the primary drivers of gold upgrading in IOCG deposits. The flexible, vacancy-rich structure of bornite, together with reactive sulfide-sulfide boundaries, allows for efficient trapping and coarsening of gold. This provides a unifying explanation for the spatial association of iron oxides, sulfides, and high-grade gold in natural systems. Our work establishes a new framework for understanding trace metal enrichment in hydrothermal systems, highlighting mineral interface reactions as key controls on the formation of economic mineralization.

Key words: Gold mineralization, Mineral-fluid interaction, IOCG deposits

Acknowledgements This research was supported by grants from the Natural Science Foundation of China (Grant No. 42372052, 42202036).

EPISODIC MAGMATISM CONTRIBUTES TO SUB-SEAFLOOR COPPER MINERALIZATION: INSIGHTS FROM TEXTURES AND GEOCHEMISTRY OF ZONED PYRITE IN THE ASHELE VMS DEPOSIT

Bing Xiao, Huayong Chen

Key Laboratory of Mineralogy and Metallogeny, Guangzhou Institute of Geochemistry, Chinese Academy of Sciences, China

Abstract Prolonged and episodic magmatic-hydrothermal processes have been proposed to be important in forming large-tonnage Cu volcanogenic massive sulfide (VMS) deposits but are difficult to document and remain poorly understood in ancient VMS systems. In this study, we combine textural evidence, in situ analysis of sulfur isotopic composition with trace elements of pyrite from the well-preserved, large-tonnage Ashele VMS deposit (Central Asian Orogenic Belt, NW China) to elucidate the origin of the ore-forming materials and controlling factors of VMS deposits. The distribution of hydrothermal alteration and mineralization allows the Ashele deposit to be divided into five zones: massive sulfide, quartz-pyrite, chlorite-chalcopyrite-quartz-pyrite, quartz-chlorite-sericite-pyrite, and quartz-sericite-pyrite zones. Cu mineralization is mainly hosed in the massive sulfide and chlorite-chalcopyrite-quartz-pyrite zones. Three texturally and compositionally distinct types of pyrite from the Cu mineralization zones have been recognized. The first type of growth zones with high Cu, As, and volatile elements (e.g., Hg and Tl) concentrations and negative $\delta^{34}S$ values (-7.83‰–-0.35‰) observed in pyrite grains from the massive sulfide zone most likely formed from the input of magmatic volatiles from degassing of the underlying magmatic systems. The second type of Cu-As-rich growth zones in pyrite grains from the chlorite-chalcopyrite-pyrite zone is not enriched in volatile elements and has positive $\delta^{34}S$ values (2.59‰–6.56‰), which is interpreted to have precipitated during fluid boiling. The third type of growth zones, without Cu-As enrichment but having positive $\delta^{34}S$ values in pyrite grains from both mineralization zones, was probably formed without boiling or magmatic volatile input. Our results suggest that multi-stage magmatic degassing or fluid boiling accompanied by Cu precipitation recorded in individual pyrite grains can reveal episodic magmatic-hydrothermal activities, which are essential factors in forming large-tonnage VMS deposits.

Key words: pyrite chemistry, in situ analysis, episodic magmatic activity, VMS deposit

EQUILIBRIUM PRESSURE – TEMPERATURE CONDITIONS, WATER CONTENT AND IMPLICATIONS OF OLIVINE INCLUSIONS IN ALLUVIAL DIAMONDS FROM THE YUANSHUI RIVER BASIN

Yuqian Zhan, Weizhang Liang, Zhili Qiu*

School of Earth Sciences and Engineering, Sun Yat-sen University, China

Abstract The formation, evolution and long-term preservation mechanisms of cratonic lithospheric mantle associated with diamonds are key scientific issues in deep Earth research. Diamonds from the Yuanshui River Basin of the Yangtze Craton are well known for their high quality and have been discovered and used for more than 100 years. Although previous studies have investigated their composition, structural characteristics and formation conditions, and have achieved substantial progress, the origin and nature of their source region remain poorly constrained.

In this study, based on crystal morphology analysis of newly collected Yuanshui diamonds, 17 samples containing mineral inclusions were sectioned, and the mineral inclusions in this batch of diamonds were identified using micro-Raman spectroscopy. Among them, three olivine inclusions suitable for detailed analysis were further investigated using micro-Fourier transform infrared spectroscopy and compositional analysis. The equilibrium temperatures and pressures of the olivine inclusions were estimated using the Al-in-olivine thermometer modified by Bussweiler et al. (2017) and the pressure calibration of Izraeli et al. (1999), their water contents were calculated using the Beer–Lambert law, following Bell et al. (2003) and Withers et al. (2012). The main results are as follows: (1) The equilibrium crystallisation temperatures of the diamonds indicated by syngenetic olivine inclusions range from 1022 to 1335 °C, corresponding to pressures of 3.81–4.21 GPa. These results are consistent with previously reported pressure–temperature estimates for Yuanshui diamonds (Qiu et al., 2014); (2)The average water content of olivine inclusions in the tested diamonds is approximately 40 ppm, with all measured values below 50 ppm. This low water content suggests that the lithospheric mantle source had high viscosity and rigidity, implying relatively high tectonic stability (Novella et al., 2015; Taylor et al., 2016).

These new results from olivine inclusions further indicate that some diamonds from the Yuanshui River Basin may have formed in an ancient and stable lithospheric mantle environment and subsequently experienced a relatively slow cooling and preservation history.

Key words: Diamond, Inclusion, Olivine, Water Content, Yangtze Craton

EXPERIMENTAL CONSTRAINTS ON CHROMIAN SPINEL EVOLUTION UNDER HYDROUS AND ANHYDROUS CONDITIONS: IMPLICATIONS FOR MANTLE GEOCHEMISTRY

Weibin Gui[1], Jin Liu[2], Fahui Xiong[1*]

1. Key Laboratory of Continental Dynamics of Ministry of Natural Resources, State Key Laboratory of Deep Earth and Mineral Exploration, Institute of Geology, Chinese Academy of Geological Sciences, China
2. Center for High Pressure Science, State Key Laboratory of Metastable Materials Science and Technology, Yanshan University, China

Abstract Chromian spinel is one of the most important indicator minerals in mantle rocks. Its Cr–Al–Mg–Fe major-element systematics are highly sensitive to partial melting, melt–rock interaction, redox conditions, and changes in mineral phase equilibria, and have therefore been widely used to trace mantle evolution and related petrogenetic processes (Arai, 1994; González-Jiménez et al., 2014; Arai et al., 2016; Zhang et al., 2024). Traditionally, high-Al and high-Cr podiform chromitites, as defined by the compositions of chromian spinel, have been interpreted as indicators of different tectonic environments. However, recent studies have shown that these two types of chromitite can coexist within the same ophiolitic massif, suggesting that their compositional differences cannot be fully explained by tectonic setting or a single parental magma composition alone (Rollinson, 2008; Uysal et al., 2009; Zaccarini et al., 2011; Miura et al., 2012; Xiong et al., 2013, 2017). This observation implies that, in addition to primary geological information, natural chromian spinel compositions may also be modified by subsequent evolutionary processes. However, systematic experimental constraints on these processes remain limited. In this study, we conducted high-pressure and high-temperature experiments using a multi-anvil apparatus to systematically investigate the interaction between chromian spinel and silicate minerals under anhydrous and hydrous conditions, and to evaluate the compositional evolution of chromian spinel and associated element redistribution under these contrasting conditions.

The experimental results show that: (1) Under anhydrous conditions, chromian spinel evolution exhibits a clear pressure–temperature dependence. At relatively low temperatures of 600–750 °C, local low-temperature immiscibility occurs in the system, producing an Al-rich end-member component. With increasing temperature, the spinel solid-solution field expands, and the previously differentiated Al-rich compositions progressively converge toward more homogeneous chromian spinel compositions. At higher pressures, spinel compositions further evolve toward Cr-rich compositions. Meanwhile, the appearance of Al- and Cr-bearing coexisting phases, including garnet, pyroxene, and melt, indicates that Al and Cr in the system are controlled not only by intracrystalline

substitution within spinel, but also by multiphase equilibria and interphase element partitioning. (2) Under hydrous conditions, fluid-induced modification is progressively enhanced during heating from 600 to 900 °C at 2 GPa. This modification is mainly reflected by a marked increase in Mg# in chromian spinel, accompanied by a limited increase in Cr# and relatively elevated Fe^{3+}#. However, when the temperature reaches 1200 °C and the system enters partial melting, Mg# continues to increase, whereas Cr# and Fe^{3+}# decrease, indicating a transition from fluid-dominated modification to melt–mineral equilibrium. Compared with the temperature effect, the pressure effect is more pronounced: at 1200 °C, increasing pressure from 2 to 3–5 GPa produces significantly higher Cr# and Mg# in chromian spinel, indicating that high-pressure hydrous environments are more favorable for the formation of Cr- and Mg-rich chromian spinel.

Overall, this study demonstrates that chromian spinel geochemistry is controlled not only by primary melt-related processes, but is also highly sensitive to subsequent pressure–temperature re-equilibration and hydrous fluid/melt interaction. The experimental results provide process-based constraints and a comparative framework for interpreting compositional variations of chromian spinel in natural mantle rocks and chromitites, and offer new experimental petrological insights into the geochemical significance of high-Cr# and high-Mg# chromian spinel in subduction-related mantle systems.

Key words: Chromian spinel, Podiform chromitite, Experimental petrology, Spinel geochemistry, Mantle processes

FACTORS CONTROLLING RARE EARTH MINERALIZATION IN REGOLITH AND EFFECTIVE INDICATORS FOR EXPLORATION

Wei Tan[1,2*], Lianying Luo[1,2,3]

1. State Key Laboratory of Deep Earth Processes and Resources, Guangzhou Institute of Geochemistry/Guangdong Provincial Key Laboratory of Mineral Physics and Materials, Guangzhou Institute of Geochemistry, Chinese Academy of Sciences, Guangzhou 510640, China
2. Guangdong research center for strategic metals and green utilization, Guangzhou 510640, China
3. University of Chinese Academy of Sciences, Beijing 100049, China

Abstract Ion-adsorption type rare earth element (REE) deposits originate from intensive chemical weathering of REE-rich granitoid and volcanic rocks under warm and humid climates and low hilly terrains. This study examines the hydrodynamic zonation, topographic characteristics, geochemical and mineral composition of regolith in the Menghai area, to reveal variables influencing the migration, enrichment, and differentiation of rare earth elements in tropical deposits. The tropical climate has concurrent rainy and hot season, which induce intense chemical weathering in the Menghai area. Primary minerals undergo extensive weathering, resulting in the development of thick regolith with elevated CIA values. The REE minerals serve as the primary source of exchangeable REE in the orebody. Thereby, dissolution of REE minerals is promoted, especially for the weather-resistant minerals, thereby facilitating the release of REE ions from REE minerals. The migration, enrichment, and differentiation of REE ions are regulated by the hydrological zonation of regolith. REEs were vertical leached in the rapidly percolating vadose zone and subsequently accumulated in the capillary fringe where seepage velocity diminishes. As REE-bearing fluids permeate the capillary fringe, LREEs and HREEs undergo fractionation, resulting in the accumulation of LREEs in the upper level and HREEs in the lower level.

The hydrodynamic zonation also influences the evolution of clay minerals and iron oxides. The alternating wet and dry conditions dissolve kaolinite and significantly transform it into halloysite, leading to a sharp reduction in kaolinite abundance and structural order. Meanwhile, when the capillary fringe shifts from wet to dry condition, goethite progressively dehydroxylates to form hematite, hence increasing hematite abundance. Changes in the resistivity of the regolith, as well as the abundance and structure of clay minerals and iron oxides, can be distinguished by high-density electrical resistivity tomography (ETR) and near-infrared spectroscopy (NIRS), respectively. Therefore, combining ETR and NIRS effectively identify the hydrodynamical control on REE leaching and accumulation processes in the ion-adsorption type REE deposits, thereby expediting field exploration and ore body delineation of such deposits.

Key words: rare earth mineralization, evolution of clay minerals and iron oxides

FAST ALKALI DIFFUSION IN THE NAL PHASE AS A SOURCE FOR HIGH CONDUCTIVITY IN THE DEEP LOWER MANTLE

Shun-Feng Yan[1,2], Lin Li[1,2,*]

1. Institute of Earth Sciences, China University of Geosciences, 29 Xueyuan Road, Beijing 100083, China
2. State Key Laboratory of Geological Processes and Mineral Resources, China University of Geosciences, 29 Xueyuan Road, Beijing 100083, China

Abstract The high spatial consistency between the stagnation of subducted slabs in the lower mantle and geophysically observed electrical conductivity anomalies (0.1–10 S/m) suggests an intrinsic genetic link between them. Although hydrous minerals are often considered the primary cause of high conductivity anomalies, the high-temperature environment during slab penetration of the 660-km discontinuity likely leads to dehydration, making the mechanism of water retention in the deep mantle highly questionable. In contrast, the NAL phase, as a stable aluminous mineral phase in subducted MORB under lower mantle pressure conditions, is capable of hosting high concentrations of alkali metal ions (Na^+ and K^+) and is a key candidate mineral for explaining lower mantle conductivity heterogeneity.

Ion diffusion is a rare event on long timescales, and AIMD is limited by the simulated atomic scale and time scale, making it difficult to accurately capture slow diffusion processes. This study combined the r2SCAN meta-GGA functional with the DP-GEN active learning strategy to train a high-precision MLP. Compared with the PBE functional, r^2SCAN can more accurately describe atomic interactions and lattice volume. Using this potential, we performed large-scale molecular dynamics simulations up to 1 ns under a wide range of temperature and pressure conditions (25–125 GPa, 2000–4000 K).

Trajectory analysis and MSD calculations show that Na^+ and K^+ exhibit significant one-dimensional superionic conductor characteristics within the hexagonal channel structure of the NAL phase. The hopping energy barrier for alkali metal ions along the c-axis is extremely low, resulting in extremely fast axial diffusion rates, while in the x-y plane perpendicular to the channel, their migration is strictly restricted by the rigid framework, exhibiting strong diffusion anisotropy. Calculations based on the Nernst-Einstein equation indicate that relying solely on intrinsic alkali metal ion migration, the electrical conductivity of the NAL phase at the depth of the top of the lower mantle can reach 2.67 S·m−1, a value sufficient to explain the magnitude of the observed high conductivity anomalies. Furthermore, Bader charge analysis further reveals that as pressure increases, the Bader charge values of alkali metal ions gradually decrease, indicating that the covalency of alkali-oxygen bonds is enhanced under high-pressure environments. This study confirms that the NAL phase in anhydrous systems can serve as an effective source of lower mantle high conductivity anomalies,

providing new mineral physics constraints for understanding deep Earth material cycling.

Key words: NAL phase, Alkali diffusion, Electrical conductivity, MLP

FORMATION OF REACTION RINDS BY EPISODIC HYDRATION–METASOMATISM OF AN OCEANIC ECLOGITE BLOCK AND IMPLICATIONS FOR SUBDUCTION INTERFACE PROCESSES

Dadi Cao*, Liqing Xu, Xiangxin Zhang

Hebei Key Laboratory of Strategic Critical Mineral Resources, Hebei GEO University, Shijiazhuang, China

Abstract The rarity of natural rocks that specifically record the physicochemical conditions of subduction interface strongly hampers pertinent studies on metamorphic trajectories of high-pressure (HP) rocks and related fluid–rock interaction. This study examines an oceanic eclogite block from the Huwan shear zone in Hong'an orogen. Eclogites from different domains exhibit considerable differences in texture, mineral assemblage and major-element zoning patterns. Garnet porphyrobglasts show distinct major-element zoning patterns, including homogenous zoning, step-changed-type zoning, and uniform-changed type zoning. Pseudosection modelling and geothermobarometry on representative eclogites yield distinct pressure–temperature (*P*–*T*) paths with divergent evolutionary vectors. Coupled Lu–Hf and Sm–Nd dating on an eclogite with three garnet generations yields a reverse age relationship, with the Lu–Hf date (273.7 ± 0.6 Ma) approximately constraining the growth age of garnet rim given its higher weight fraction of Lu. Multiple age clusters of metamorphic zircons (~353–237 Ma) are interpreted as reflecting the time of disparate HP metamorphic events. Combined with previous dates, a long-term yo-yo-like path is delineated in response to multiple subduction–exhumation cycles within the subduction interface. We attribute the discrepant *P*–*T* estimates and isotopic dates of eclogites to formation of reaction rinds through episodic hydration–metasomatism, facilitated by the external-derived aqueous fluid, carbon-bearing fluid, and sulfur-bearing fluid. The subduction interface thermal structure, hotter than that of the subducted crust, can be perturbed by punctuated heating pulses in localized high-strain zones, presumably owing to shear heating and/or exothermic hydration. Within the interface, reduced sulfur species (e.g., HS^-) in up-dip migrating fluids can be effectively filtered by reprecipitating as pyrite through redox reactions with detached HP rocks, sometimes accompanied by carbonate dissolution and silica metasomatism.

Key words: Subduction interface, Eclogite, Garnet, P–T–t path, Fluid–rock interaction

FOSSIL RECORD OF PRECAMBRIAN OXYGENIC PHOTOAUTOTROPHS

Qing Ouyang, Chuanming Zhou

State Key Laboratory of Palaeobiology and Stratigraphy, Nanjing Institute of Geology and Palaeontology, Chinese Academy of Sciences, Nanjing 210008, China

Abstract Fossil records of oxygenic autotrophs, primarily cyanobacteria but also eukaryotic algae, are abundant and diverse in Precambrian strata. The oldest widely accepted fossil record of cyanobacteria is found in cherts of the ~2.0 Ga Belcher Group, and this taxon and its co-occurring silicified microfossils that are generally compared to cyanobacteria proliferated throughout most of the Proterozoic Era, exhibiting notably high taxonomic diversity. These microfossils emerged alongside the global rise of stromatolitic ecosystems in shallow-water carbonate platform environments and the opening of a taphonomic window that plays a crucial role in preservation of cellular structures of microbial life. Microfossils from Meso- and Neoproterozoic strata also record several critical evolutionary innovations of cyanobacteria, such as the divergence of thylakoid-bearing cyanobacteria and the appearance of endolithic cyanobacteria.

Fossil cyanobacteria have also yielded crucial geological records of behavioral and ecological adaptations to the changing Precambrian environment. During the mid-Proterozoic (~ 1.8—0.8 Ga), silicified microfossils preserved in stromatolites provide fossil evidence of various adaptive strategies developed by benthic microbial communities. Based on observed differences in substrate colonization preferences between coccoidal and filamentous microfossils from Meso- to Neoproterozoic silicified assemblages, previous studies have proposed a co-evolutionary pattern between benthic microbial communities and marine geochemistry. This pattern interprets the secular change in dominant mat-builders—from coccoidal microbes in the Palaeoproterozoic to filamentous microbes in the late Meso- to Neoproterozoic—as an ecological response to the transition from cemented seafloor substrates to micritic substrates in peritidal environments. Our new data provide fossil evidence supporting this pattern, together with records of planktonic cyanobacterial communities, thus contributing to the broader picture of Proterozoic cyanobacterial evolution.

Key words: microfossils, oxygenic photoautotrophs, cyanobacteria, co-evolution, Precambrian

FROM CRUSTAL THICKENING TO POST-COLLISIONAL EXTENSION: REASSESSING ZIRCON AGE PEAKS USING TRACE ELEMENTS AND TEXTURAL DOMAINS

Di Pang , Xiaowei Li

School of earth science and resources, China University of Geosciences (Beijing), China

Abstract Zircon U–Pb age spectra are widely used to identify magmatic pulses and reconstruct the tempo of orogenic evolution. However, individual zircon age peaks may not carry equivalent tectonic or crustal-thickness significance, particularly in orogenic belts that evolved from subduction-related crustal thickening to post-collisional extension. Here, we integrate zircon U–Pb depth-profile dating and trace-element analyses of four granitoid samples from the Wulanwuzhuer area, Qimantagh region, western East Kunlun Orogen, to test how different zircon age populations record changing magmatic and tectonic processes.

We examined 663 zircon analyses between 350 and 550 Ma and evaluated their suitability for crustal-thickness proxy interpretation using three commonly applied screening criteria: Th/U > 0.1, La < 1 ppm, and Ce/U > 0.01. The compiled age spectrum defines three main populations at ca. 455 Ma, ca. 423 Ma, and ca. 383 Ma. These populations show distinct trace-element signatures, textural-domain distributions, and markedly different proportions of proxy-valid analyses. The ca. 455 Ma population contains the highest proportion of analyses that pass the screening criteria, reaching 60.0%. It is further characterized by relatively low La contents, high Ce/U ratios, and a large contribution from zircon cores or single-age domains. We therefore interpret this population as the most reliable record of crustal-thickness evolution, reflecting subduction-related arc magmatism and associated crustal thickening.

By contrast, the ca. 423 Ma population has a much lower proportion of proxy-valid analyses, at 27.5%, and is characterized by higher La contents, lower Ce/U ratios, elevated Hf contents, and a greater contribution from zircon rim domains. These features argue against interpreting the ca. 423 Ma peak as a simple second crustal-thickening event. Instead, this age population more likely records a transitional magmatic stage during the shift from subduction- or collision-related magmatism to post-collisional extension. The youngest population at ca. 383 Ma is dominated by zircon rim domains and has the lowest proxy-valid proportion, at only 15.6%. Although this peak is a real feature of the unfiltered age spectrum, it does not correspond to a robust crustal-thickness maximum. Its trace-element characteristics instead point to enhanced involvement of evolved melts, crustal anatexis, melt–fluid interaction, or zircon rim recrystallization and re-equilibration during late post-collisional extension.

Our results demonstrate that zircon age peaks may change their geological meaning through time

within a single orogenic system. In the Wulanwuzhuer granitoids, the ca. 455 Ma population records crustal thickening, the ca. 423 Ma population marks a tectono-magmatic transition, and the ca. 383 Ma population reflects post-collisional reheating, anatexis, and/or zircon modification. More broadly, this study shows that zircon age peaks should not be interpreted automatically as equivalent magmatic or crustal-thickness signals. Robust tectonic interpretation requires the joint evaluation of age spectra, trace-element filters, and zircon textural domains.

Key words: Zircon, trace elements, crustal thickness, post-collisional extension, East Kunlun Orogen…

FROM MANGANESE MINERAL EVOLUTION HISTORY TO ATMOSPHERIC OXYGEN RECONSTRUCTION

Yan Li[1,2]*, Rongzhang Yin[1,2], Ziyi Zhuang[2], Anhuai Lu[2], Robert M. Hazen[3]

1. SKLab-DeepMinE, MOEKLab-OBCE, School of Earth and Space Sciences, Peking University, Beijing 100871, China
2. Beijing Key Laboratory of Mineral Environmental Function, School of Earth and Space Sciences, Peking University, Beijing 100871, China
3. Earth and Planets Laboratory, Carnegie Institution for Science, Washington, DC 20015, USA

Abstract Understanding the evolution of Earth's atmospheric oxygenation over the past 4.0 billion years, and utilizing the existing Earth records to infer changes in O_2 concentration, are fundamental challenges for revealing the co-evolution of both Earth's interior and near-surface environments. Manganese (Mn), as Earth's second most abundant transition metal with three valence states in crustal environments, exhibits exceptional sensitivity to environmental redox states. The compositional and structural diversity of Mn minerals reflects a broad range of O_2 fugacity, emerging them as an ideal candidate for pO_2 reconstruction. In this study, by building a global Mn mineral dataset (144,200 entries across 25 feature dimensions), we developed a URD (Unequal-size feature matrix, Re-coupling relationship, Disaccord labels) deep-learning model to reconstruct continuous atmospheric oxygen level (pO_2) changes over 4.0 billion years. By identifying age-specific Mn mineral assemblages most strongly linked to pO_2, we provide global-scale mineralogical evidence that the timing and tempo of Earth's oxygenation were tightly coupled to plate tectonics and biosphere evolution. Our findings establish mineral informatics as a novel approach for paleoenvironmental quantification, demonstrating how deep-learning-driven analysis of mineralogical big data can reveal co-evolutionary dynamics among Earth's tectonic, mineralogical, and atmospheric systems. Moreover, the presented methodology is readily transferable to other paleoenvironmental parameters and provides a generalizable framework for investigating the deep-time co-evolution of the lithosphere, hydrosphere, and biosphere.

Key words: mineral informatics, Mn mineral dataset, atmospheric oxygenation history, Mn crystal chemistry, deep-learning

FROM MINERALIZATION MECHANISMS TO GEOLOGICAL RECORDS: ESTABLISHING COMPREHENSIVE IRON MINERAL BIOSIGNATURES

Jiahao Chen[1],[2] , Yuefei Ding[1], Juan Liu[1]*

The Key Laboratory of Water and Sediment Sciences, College of Environmental Sciences and Engineering, Peking University, Beijing, China

Abstract Iron mineral deposits, such as Banded Iron Formations (BIFs) and Cretaceous Oceanic Red Beds (CORBs), are crucial geological archives for reconstructing paleoenvironments and the evolution of early life. However, whether the deposition of these minerals was driven solely by abiotic redox fluctuations or deeply coupled with microbial metabolic activities remains highly debated. While organic and isotopic biosignatures are widely utilized, robust mineralogical biosignatures are still critically lacking. Here, under simulated paleo-oceanic conditions, we systematically investigate the abiotic transformation of metastable ferrihydrite, alongside its modulation by biogenic Fe(II) and extracellular polymeric substances (EPS), to establish comprehensive iron mineral biosignatures.

Our results reveal that EPS components (e.g., polysaccharides) reduce nucleation barriers and inhibit crystal coarsening, forming ultrafine hematite nanoparticles (~5 nm) consistent with geological records. Simultaneously, specific organics like tryptophan dictate morphology, promoting star-shaped goethite growth via oriented attachment. Furthermore, the dynamic supply rate of biogenic Fe(II) coupled with EPS concentrations regulates secondary mineral phase partitioning, successfully simulating the hematite-magnetite alternating interlayers frequently observed in BIFs. Conventionally, distinct features like hexagonal plate-like morphology or specific low-temperature magnetic properties (e.g., shifts in the Verwey transition) are utilized to differentiate biogenic magnetite from abiotic sources. However, our abiotic heating experiments and comparative analyses reveal that strictly non-biological processes can yield remarkably similar morphological and magnetic characteristics. This exposes the inherent limitations of relying on any single proxy, as single-parameter identification is intrinsically ambiguous. Overall, this study highlights that a multiproxy approach—integrating particle size, morphology, mineral association, and magnetic properties—is essential for establishing reliable iron mineral biosignatures, providing a more rigorous framework for tracing ancient microbial activities.

Key words: ferrihydrite phase transformation, magnetite, banded iron formations, mineral biosignatures

FROM ORBICULES TO VEINLETS: TOURMALINE RECORDS B-RICH FLUID EVOLUTION DURING THE MAGMATIC–HYDROTHERMAL TRANSITION IN AN INTERMEDIATE–FELSIC INTRUSIVE SYSTEM

Wenlu Wang , Xiaowei Li

School of earth science and resources, China University of Geosciences (Beijing), China

Abstract Tourmaline is a sensitive recorder of magmatic–hydrothermal processes and provides valuable constraints on the origin, evolution, and physicochemical conditions of B-rich fluids in intrusive systems. Here, we present in situ major- and trace-element compositions, together with B-isotope data, for tourmaline from intermediate–felsic intrusive rocks in the Changmu area, Western Qinling, with the aim of constraining the late-stage magmatic–hydrothermal evolution of the Lancai pluton.

Four textural types of tourmaline were identified on the basis of their occurrence and BSE contrast: (1) dark tourmaline in tourmaline–quartz orbicules from the Lancai diorite porphyry (Tur-OD); (2) light tourmaline in the same orbicules (Tur-OL); (3) dark tourmaline in tourmaline veinlets from the Lancai granodiorite (Tur-DD); and (4) light tourmaline in these veinlets (Tur-DL). All analyzed tourmalines belong to the alkali group and plot within the schorl–dravite solid-solution series, but they display systematic compositional and textural variations that are closely linked to their host-rock type, occurrence, and BSE brightness.

Tourmaline–quartz orbicules in the diorite porphyry commonly show radial textures. Although the relative crystallization sequence of the dark and light tourmaline domains is difficult to resolve, their orbicular textures indicate rapid crystallization from a B-rich magmatic–hydrothermal medium under strongly supersaturated conditions in a hypabyssal setting. In contrast, tourmaline from the granodiorite occurs mainly as relatively euhedral crystals in veinlets and commonly exhibits well-developed oscillatory zoning, reflecting sustained input of B-rich magmatic–hydrothermal fluids and episodic crystal growth under comparatively deeper, plutonic conditions.

On the basis of tourmaline textures, compositions, and geological occurrence, the magmatic–hydrothermal evolution of the Lancai pluton can be divided into five stages: (1) emplacement of an early calc-alkaline dioritic magma; (2) separation of B-rich fluids from the evolving dioritic melt, followed by rapid crystallization and preservation of tourmaline–quartz orbicules within a viscous hypabyssal magma; (3) emplacement of a later granitic magma; (4) extensive exsolution of B-rich magmatic fluids from the granitic magma, followed by their migration along fractures and the formation of tourmaline-bearing veinlets; and (5) continued fluid replenishment and cyclic fluid–rock interaction after the formation of primary tourmaline cores, producing oscillatory zoning in

the veinlet-hosted tourmaline.

Key words: Tourmaline, Orbicules, Veinlets, magmatic–hydrothermal, Western Qinling…

GARNET COLOR AND GARNET–CLINOPYROXENE CHEMISTRY AS EXPLORATION VECTORS FOR SKARN CU AND CU–ZN–PB MINERALIZATION IN THE JIAMA PORPHYRY–SKARN SYSTEM, TIBET, CHINA

Junfeng Zhao[1,2], Huayong Chen[1,2]

1. State Key Laboratory of Deep Earth Processes and Resources, Guangzhou Institute of Geochemistry, Chinese Academy of Sciences, Guangzhou 510640, China
2. University of Chinese Academy of Sciences, Beijing 100049, China

Abstract The Jiama porphyry–skarn Cu polymetallic system, in the Gangdese belt, Tibet, is one of the largest Cu deposits in China. Miocene intermediate–felsic intrusions emplaced into Upper Jurassic carbonate rocks and Lower Cretaceous siliciclastic rocks formed the Main-zone Cu–Mo–Au porphyry–skarn center and the Tongshan Cu–Zn–Pb skarn center. This study assesses garnet color and garnet–clinopyroxene major-element chemistry as exploration vectors in this unusually oxidized skarn system.

Prograde skarn in both centers is dominated by garnet and wollastonite, with sparse clinopyroxene and no well-developed clinopyroxene-rich outer zone. Garnet color provides a first-order field vector: dark red-brown to brown garnet is common in endoskarn and intrusion-proximal skarn, whereas pale yellow-green garnet becomes increasingly abundant outward, providing a visual guide to skarn zonation and fluid evolution.

Garnet and clinopyroxene define a composite Fe trend distinct from that of classical calcic skarns developed against reduced wall rocks. From proximal to intermediate positions, both minerals become less Fe rich away from causative intrusions, with garnet shifting toward grossular-rich compositions and clinopyroxene toward diopsidic compositions. This coupled trend is interpreted to reflect declining Fe availability in the evolving skarn-forming fluid. At the far-distal margin, the two minerals diverge: garnet continues toward grossular-rich compositions, whereas clinopyroxene returns toward more hedenbergitic compositions, indicating stronger control by fluid–wall-rock redox contrast.

These relationships define a practical exploration tool. At Jiama, Cu and Cu–Zn–Pb skarn mineralization is concentrated mainly in the inner domain where garnet and clinopyroxene Fe contents vary together, whereas distal redox-controlled divergence corresponds to a largely barren outer fringe. Garnet color and garnet–clinopyroxene chemistry can therefore help distinguish mineralized to weakly mineralized inner skarn from barren distal skarn and indicate the direction of fluid evolution in oxidized magma–oxidized wall-rock skarn systems.

Key words: Jiama, skarn, garnet, clinopyroxene, exploration vector

GENESIS OF COPPER-DEFICIENT SKARN IRON DEPOSITS IN THE NORTH CHINA CRATON: INSIGHTS FROM APATITE AND WHOLE-ROCK GEOCHEMISTRY

Junwu Zhang[1], Lin Li[1*], Juquan Zhang[2], Fangyue Wang[3], Xian Liang[2]

1. National Key Laboratory of Geological Processes and Mineral Resources and Institute of Earth Sciences, China University of Geosciences, Beijing, China
2. Hebei Key Laboratory of Strategic Critical Mineral Resources and College of Earth Sciences, Hebei GEO University, Shijiazhuang, China
3. Ore Deposit and Exploration Center, School of Resources, Environmental Engineering, and Anhui Province Engineering Research Center for Mineral Resources and Mine Environments, Hefei University of Technology, Hefei, China

Abstract The North China Craton (NCC) hosts several skarn iron ore clusters characterized by significant Cu depletion relative to those in the Middle–Lower Yangtze River Metallogenic Belt, but their genesis remains unclear. We collected apatite major element data and whole-rock major and trace element data from intermediate-felsic intrusions with different fertility levels (barren, Fe-fertile, and Cu-bearing) across both regions. A comparison of the whole-rock and apatite geochemistry of plutons with different fertility levels reveals that mineralized plutons result from multiple coupled factors.

We employed a Random Forest model to classify pluton fertility based on apatite-equilibrium melt parameters (melt F, Cl, SO_3, and ΔFMQ). SHAP analysis reveals that: Barren intrusions are defined by significantly lower melt-volatile (F, Cl, SO_3) contents. Fe-fertile plutons exhibit the highest Cl_{melt} concentrations and elevated fO_2 (oxygen fugacity). Cu-bearing plutons show high $SO_{3(melt)}$ but lower Cl_{melt} and ΔFMQ relative to Fe-fertile intrusions.

Based on integrated geochemical proxies, the following diagnostic thresholds for metallogenic fertility were established: Barren plutons are distinguished by lower median values of La/Yb ratio (17), AST (apatite saturation temperatures; 845 °C), melt F (1180 ppm) and SO_3 (32 ppm) contents in apatite. Cu-bearing plutons are defined by higher median values of La/Yb ratio (35), $\varepsilon_{Nd}(t)$ (–6.93), AST (944 °C), melt F (1819 ppm) and SO_3 (64 ppm) contents, and moderate fO_2 (ΔFMQ −1.8 – +2.9). Fe-fertile plutons are characterized by lower median values of La/Yb ratio (16), $\varepsilon_{Nd}(t)$ (–13.31), and AST (865 °C), coupled with higher median values of melt F (1637 ppm), Cl (2366 ppm), and SO_3 (66 ppm) contents, and higher fO_2 (ΔFMQ −0.8 – +4.3). These indicators provide a practical tool for identifying Cu-fertile plutons within the North China Craton.

Based on these findings, comparative analysis suggests that the copper deficiency in intrusions of NCC's skarn iron ore clusters results from lower La/Yb, $\varepsilon_{Nd}(t)$, and AST values, and higher fO_2. This implies two probable reasons: first, derivation from a magma source inherently depleted in

copper, which is unfavorable for copper mineralization; second, the high fO_2 likely dispersed copper within the iron-dominated ore system, preventing the effective concentration and formation of discrete copper orebodies.

Key words: Apatite, Whole-rock, Skarn, intermediate-acid plutons, Iron-copper fertility

Acknowledgements This study is financially supported by the Deep Earth Probe and Mineral Resources Exploration - National Science and Technology Major Project (2025ZD1004902, 2025ZD1008700, 2025ZD1009202), the National Natural Science Foundation of China (Nos. U2444208, 42273065), the Scientific Innovation Program (202303AA08000601), and the Youth Top-notch Talent Program (BJ2026188).

GEOCHEMICAL SIGNATURES OF KEY MINERALS IN THE LONGTOUSHAN GOLD DEPOSIT, GUANGXI：IMPLICATIONS FOR HYDROTHERMAL ALTERATION PATTERNS, AND ORE-FORMING MECHANISMS

Yu-Qing Yin[1,2,3], Bo Xu[1.2,3*],Mao-Wen Yuan[1,2]

1. National Mineral, Rock and Fossil Resource Center, and Deep Space Exploration Laboratory, China University of Geosciences, Beijing 100083, China
2. State Key Laboratory of Geological Processes and Mineral Resources, School of Gemology, China University of Geosciences, Beijing 100083, China
3. School of Gemmology, China University of Geosciences, Beijing 100083, China

Abstract The Longtoushan gold deposit is located in the southwestern plunging end of the Longshan brachyanticline in the Dayaoshan uplift area, Guangxi province. It is a typical subvolcanic-cryptoexplosion breccia type gold deposit. This paper systematically reviews the mineralogical research progress of the deposit. The main minerals in the mining area include quartz, K-feldspar, plagioclase, pyrite, sericite, tourmaline, native gold, and electrum. The widespread development of tourmaline is a distinctive feature that distinguishes this deposit from other continental volcanic-hosted gold deposits. Gold minerals are dominated by silver-bearing native gold (accounting for >80%), occurring mainly as intergranular gold and fracture gold. Pyrite, as the main carrier mineral of gold, can be divided into five generations. Its crystal forms are mainly cube and pentagonal dodecahedron. Electron microprobe analysis shows that the Au content ranges from 0.12×10^{-6} to 3.85×10^{-6}, accounting for about 60% of the total native gold. The sulfur isotope $\delta^{34}S_{CDT}$ values range from $+1.29\times10^{-3}$ to $+2.01\times10^{-3}$, and the Pb isotope μ values range from 9.63 to 9.84 with Th/U ratios from 3.87 to 4.00, indicating that the ore-forming materials originated from a deep magma source. Hydrothermal alteration is dominated by silicification, pyritization, and sericitization, among which tourmalinization, silicification and pyritization are most closely related to gold mineralization. The alteration zones are clearly zoned, and the mineral formation sequence is: K-feldspathization → silicification + pyritization → sericitization → carbonatization. H and O isotopes ($\delta^{18}O_{H_2O}$ = 10.8‰–10.2‰, δD = -76‰ to -48‰) reveal that the fluid was mainly derived from deep magmatic hydrothermal fluid mixed with a small amount of meteoric water. Collectively, the Longtoushan gold deposit is considered to be a medium-low temperature epithermal gold deposit. The ore-forming materials and fluids originated from deep magmatic rocks formed by re-melting of the basement crust, and the mineralization was jointly controlled by Late Yanshanian magmatism and regional tectonic movements. These results provide important mineralogical evidence for the study of epithermal gold deposit metallogeny in South China and for regional

exploration and deep prospecting.

Key words: Longtoushan gold deposit, mineralogy, pyrite, hydrothermal alteration, ore-forming fluid

GEORGELIUITE, CA2MN3+3O2(ASO4)3(H2O)2·H2O, A NEW MINERAL FROM THE JOTE MINE, ATACAMA REGION, CHILE.

Xiangping Gu[1], Hexiong Yang*2, Robert A. Jenkins[2], Ronald B. Gibbs[2], Robert T. Downs[2]

1. Guanghua School of Gems and Art Design, Jiangxi Institute of Applied Science and Technology, Nanchang, Jiangxi 330100, China.
2. Department of Geosciences, University of Arizona, 1040 E. 4th Street, Tucson, AZ 85721-0077, USA *E-mail: hyang@arizona.edu

Abstract Georgeliuite (IMA2025-093) is discovered from the Jote mine, the Atacama Region of Chile. The Atacama Region hosts more than 428 valid minerals and is the type localities of 22 new minerals and georgeliuite is the 23rd new mineral from this region. It occurs as a secondary mineral in fractures and vugs in the oxidized upper portion of the hydrothermal veins hosted by volcanoclastic rocks, associated with conichalcite, joteite, mansfieldite, manganlotharmeyerite, rruffite, and scorodite. Georgeliuite occurs as aggregates up to 0.5 mm in size. Individual platy crystals are black brown in specimen and dark-red in micropcope, and less than 0.05 mm in grain size (Fig. 1). The Raman spectra are composed of strong peaks at 950, 917, 866, 547, 195 cm^{-1} (Fig. 2). The empirical formula, $(Ca_{2.10}Na_{0.21})_{\Sigma 2.31}(Mn^{3+}_{2.70}Cu^{2+}_{0.19})_{\Sigma 2.89}O_2(As_{1.01}O_4)_3(H_2O)_2\cdot H_2O$, is obtained from 5 microprobe analyses. Georgeliuite is monoclinic, space group: *Cm*, a = 11.3129(7) Å, b = 20.1338(14), Å, c = 8.9690(6) Å, β = 100.567(4)°, V = 2008.2(2) $Å^3$, Z = 6. The crystal structure is isomorphous with sailaufite and built up from the $[Mn^{3+}_9O_6(AsO_4)_9]^{12-}$ sheets parallel to (001), which are interconnected by double layers of 7- or 8-coordinated Ca-polyhedra and hydrogen bonds provided by H_2O molecules (Fig. 3a). In the $[Mn^{3+}_9O_6(AsO_4)_9]^{12-}$ sheet, $Mn^{3+}O_6$ octahedra share edges to form nine-membered pseudo-trigonal rings (the Kagomé net), and $As^{5+}O_4$ tetrahedra are corner-connected to $Mn^{3+}O_6$ octahedra either at the centers of the rings or on both sides of the sheet (Fig. 3b). Georgeliuite (symbol: Gliu) is named in honor of Dr. Guanghua George Liu (b. 1954), an emminent geologist and mineral collector, and founder of Institute of Gemmology and Mineral Resources, Jiangxi Institute of Applied Science and technology.

GUIXIANGITE, NIBIS, A NEW MINERAL FROM THE LONGHUA NI-CO HYDROTHERMAL VEIN DEPOSIT, DAYAOSHAN AREA, SOUTH CHINA

Xiao Nie [1], Yuan Xue [2]

1. Chinese Academy of Geological Sciences, China
2. China University of Geosciences (Beijing), China

Abstract Guixiangite (IMA2025-019), ideally NiBiS, is a new member of the cobaltite group discovered in the Longhua Ni–Co hydrothermal vein deposit (N24°04.190′, E110°06.825′) in the Dayaoshan area, South China. The mineral occurs mainly in quartz–arsenide–sulfide veins and is commonly associated with ullmannite, parkerite, cobaltite, and galena. Guixiangite forms anhedral grains ranging from several micrometers to approximately 15 μm. It is steel-grey with a grayish-black streak and metallic luster, is brittle with uneven fracture, and has a calculated density of 8.29 g/cm3. Electron microprobe analyses (wt.%) yield: Bi 52.90, S 11.86, Co 0.85, Sb 11.77, As 0.42, Ni 21.89, and Fe 0.51. The empirical formula, calculated on a basis of three atoms, is $A(Ni_{1.00}Co_{0.04}Fe_{0.02})_{S1.06}M(Bi_{0.68}Sb_{0.26}As_{0.01})_{S0.95}X_{S0.99}$, which simplifies to the ideal formula NiBiS. In guixiangite, substitution of Bi for Sb is limited, with Bi/(Bi+Sb) ranging from 0.457 to 0.629. Co and Fe, together with minor Ni, are divalent and contribute to charge balance. Guixiangite is cubic, space group $P2_13$ (#198), with a = 5.9875(5) Å, V = 214.65(5) Å3, and Z = 4. Its crystal structure was solved by three-dimensional electron diffraction, yielding a final R1 = 0.118 for 145 unique reflections with $I > 2\sigma I$, enabling an ab initio structure solution and dynamical refinement from a few-μm-sized grain prepared in a FIB lamella. Guixiangite commonly occurs as a replacement texture around the rims of ullmannite, indicating an increase in Bi content during late-stage fluid activity and suggesting enhanced involvement of moderately acidic magmatic–hydrothermal fluids. Previous studies divided the formation of the Longhua Ni–Co hydrothermal vein system into an arsenide stage and a sulfoarsenide–sulfide stage. The discovery of guixiangite further refines this scheme by subdividing the latter into medium–high-temperature and medium–low-temperature substages. This insight provides new constraints on multi-element coupling and mineralization processes in arsenide–sulfide vein-type deposits.

Key words: New mineral, 3-dimensional electron diffraction, guixiangite, Longhua Ni-Co deposit, multi-stage vein mineralization

IN-SITU IRON ISOTOPE ANALYSIS OF MAGNETITE: IMPLICATIONS FOR THE GENESIS OF IRON-OXIDE APATITE DEPOSITS

Wang Liao, Xin-Fu Zhao*

State Key Laboratory of Geological Processes and Mineral Resources, and School of Earth Resources, China University of Geosciences, Wuhan, Hubei 430074, China

Abstract Magnetite is a common mineral in various types of ore deposits, and its trace element and iron isotope compositions can be used to trace ore-forming processes. Nevertheless, magnetite in magmatic-hydrothermal systems (including porphyry copper deposits, skarn iron deposits, iron oxide-copper-gold deposits) is susceptible to modification by late-stage fluids, resulting in significant variations in its trace element compositions. However, the iron isotope behavior of magnetite during fluid modification remains poorly constrained. Meanwhile, notable overlaps exist in iron isotope signatures between magmatic magnetite and high-temperature hydrothermal magnetite, hindering the effective application of magnetite iron isotopes in magmatic-hydrothermal systems.

The genesis of iron oxide-apatite deposits remains highly controversial. Proposed ore-forming models include iron magma emplacement, suspension of magmatic magnetite microcrystals, and hydrothermal metasomatism, among others. The composition and formation mechanism of magnetite are the key to interpreting the genesis of such deposits. Nevertheless, published trace element and iron isotope data of magnetite from different deposits show substantial discrepancies, leading to divergent interpretations of ore-forming processes and genetic mechanisms. Our previous studies indicate that magnetite in this type of deposit generally exhibits complex textural features, implying pronounced overprinting and fluid metasomatism, which may bias the genetic interpretation of the deposits.

To address the above issues, systematic in-situ trace element and iron isotope analyses were carried out on magnetite hosted in volcanic wall rocks and ores from the Luohe iron deposit in the Middle-Lower Yangtze River Metallogenic Belt, China. Primary magnetite (Mag1) in this deposit develops ilmenite exsolution textures. Although its iron isotope composition partially overlaps with that of magmatic magnetite (MagM) in volcanic rocks, it overall possesses distinctly different trace element and iron isotope signatures. Moreover, Mag1 shows similar trace element and iron isotope characteristics to magnetite from high-temperature magmatic-hydrothermal deposits (porphyry copper deposits, skarn iron deposits, iron oxide-copper-gold deposits), indicating a high-temperature hydrothermal origin. This demonstrates that the combined in-situ analysis of iron isotopes and trace elements can effectively distinguish magmatic from high-temperature

hydrothermal processes.

In addition, primary magnetite (Mag1) underwent recrystallization as well as dissolution-reprecipitation via hydrothermal metasomatism by late-stage fluids, forming secondary magnetite (Mag2 and Mag3). Significant variations in trace element and iron isotope compositions of magnetite occur during such hydrothermal-magnetite re-equilibration processes. This accounts for the compositional heterogeneity of magnetite in some iron oxide-apatite deposits, particularly the formation of magnetite with low-temperature hydrothermal affinities in these deposits.

Key words: Magnetite, In situ Fe isotope, IOA deposits, Mineralization Processes

IN SITU SULFIDE GEOCHEMISTRY REVEALS TE-BI-AU MINERALIZATION IN THE DASHUIGOU DEPOSIT, SW CHINA

Qingqing Zhao[1], Degao Zhai[1]*, Manuel Keith[2], Panagiotis Voudouris[3], Stylianos Tombros[4], Jiajun Liu[1]*

1. School of Earth Sciences and Resources, and State Key Laboratory of Geological Processes and Mineral Resources, China University of Geosciences Beijing, China
2. GeoZentrum Nordbayern, Friedrich-Alexander-Universität (FAU) Erlangen-Nürnberg, Erlangen, Germany
3. Faculty of Geology & Geoenvironment, National and Kapodistrian University of Athens, 15784 Athens, Greece
4. Department of Geology, University of Patras, Rion, Greece

Abstract The Dashuigou deposit in Sichuan, China, is the only known independent Te-Bi-Au deposit globally, with substantial reserves of Te (508 t) and Bi (768 t). Despite its significance, the sources of metals and the enrichment mechanisms remain poorly understood. Two distinct pyrite types were identified: stage I euhedral pyrite, characterized by high Co and low Ni, Te, Bi, and Au; and stage II colloform pyrite, exhibiting enriched rims of Ag, Te, Au, and Bi, suggesting complex mineralization processes that might involve multiple stages of fluid evolution. The analysis of both types of pyrite sample yielded similar $\delta^{34}S$ values (-0.5 to 5.1‰), and the narrow $\delta^{34}S$ variations observed within several pyrite crystals suggested a homogeneous magmatic origin. It is proposed that fluid supersaturation resulting from rapid cooling is the primary mechanism responsible for the formation of colloform pyrite, and the increases in fTe_2 and fO_2 play an important role in the Te-Bi-Au mineralization. These findings provide new insights into the metallogenic processes of Te-Bi-Au deposits and contribute to our understanding of magmatic-hydrothermal ore-forming systems.

Key words: Sulfur isotopes, Trace elements, Te-Bi deposits, Dashuigou, SW China

Acknowledgements This work was supported by the National Natural Science Foundation of China (92462306 and 92062219).

INTRACELLULAR NANOPARTICLE ACCUMULATION PROMOTES METABOLIC ADAPTATION OF METHANOGENS TO METAL SULFIDE UTILIZATION

Yidi Zhang [1,2], Donglei Zhang [1,2], Yizhi Sheng [1,3], Hongyu Chen [1,4], Gaoyuan Li [1], Hailiang Dong [1,2,3*]

1. Center for Geomicrobiology and Biogeochemistry Research, State Key Laboratory of Biogeology and Environmental Geology, China University of Geosciences, Beijing 100083, China.
2. School of Water Resources and Environment, China University of Geosciences, Beijing 100083, China.
3. Frontiers Science Center for Deep-time Digital Earth, China University of Geosciences, Beijing 100083, China.
4. School of Earth Sciences and Resources, China University of Geosciences, Beijing 100083, China.

Abstract Methanogens are thought to have originated in the ferruginous oceans of the Hadean or early Archean (>3.8 Ga). Following the Great Oxidation Event (~2.4 Ga), methanogens were largely restricted to anoxic environments enriched in HS^-, consistent with the high-HS^- composition of modern cultivation media used for methanogens. Since sulfide has a strong affinity for divalent metal ions, their interaction initially forms metastable aqueous metal-sulfide clusters that progressively precipitate into metal-sulfide minerals. Therefore, methanogens may utilize sulfide minerals rather than free metal ions or HS^-. In one of our studies, methanogens *Methanococcus maripaludis* S2 were cultivated in a system containing FeS_{Mack}, with additional Fe^{2+} or HS^- supplied to simulate ferruginous and Sulfidic environments, respectively. Compared to cells grown under high-HS^- conditions, cells grown under high-Fe^{2+} conditions accumulated substantial intracellular FeS nanoparticles while maintaining stable methanogenic activity and growth. The intracellular FeS nanoparticles perturbed metal homeostasis, leading to increased expression of genes and proteins involved in sulfur recycling and metal homeostasis regulation. Meanwhile, key enzymes participating in carbon metabolism exhibited enhanced metabolic stability and improved energy utilization efficiency. In another study using amorphous nickel sulfide and crystalline nickel sulfide as the sole nickel source for methanogens, it was found that exposure of methanogens to crystalline nickel sulfide caused cell deformation, along with the presence of intracellular iron-bearing mineral particles. When mineral-attached cells were transferred to fresh medium, they resumed normal growth and returned to a healthy state, with the disappearance of intracellular particles and the secretion of abundant extracellular substances that isolated the cells from the minerals. These findings suggest that during evolution, methanogens gradually adapted to fluctuations in ferrous iron and sulfide availability, underscoring their critical role in shaping the co-evolution of life and Earth's surface systems.

Key words: Methanogenesis, Metal Sulfide, TEM-EDS, Transcriptomics, Proteomics

ISOTOPIC APPLICATION IN HIGH SALINE CONDITIONS

Minghui Li[1], Xiaomin Fang[1], Jiao Li[2], Maodu Yan[1], Shurui Sun[1]

1. Institute of Tibetan Plateau Research, CAS, Beijing 100085, China
2. School of Geography Science, Shanxi Normal University, TaiYuan 030031,China

Abstract Evaporite minerals record the hydrogeochemical conditions in which they precipitated. And therefore they can be used to reconstruct the paleoclimate and paleoenvironments. Evaporite minerals are also major sources of industrial minerals including gypsum, halite, borates, lithium concentrates, and others. Because of their scientific significance and economic importance, evaporite minerals and their isotopic hydrochemical processes linked to their formation have been the focus of many geologists and paleoclimatologists. This study will discuss the application of isotopes of hydrogen, oxygen, sulfur, strontium, and boron in saline conditions. This will include the following: the $\delta^{18}O$ and δD of hydrated water of gypsum and their paleoclimate since 2.2 Ma in the Qaidam Basin, NE Tibetan Plateau; the $\delta^{18}O$ and δD of the interlayer water of clay minerals in salar lacustrine sediments; and the $^{87}Sr/^{86}Sr$, $\delta^{34}S$, and $\delta^{11}B$ of halite from evaporite deposits in Khorat Plateau, Laos, and Yunnan and their application in the origins of brine.

Key words: Oxygen and hydrogen, Sr isotope, sulfur isotope, boron isotope, salt minerals

LA^{3+} SPECIATION IN F-RICH ALKALINE HYDROTHERMAL FLUIDS AND ITS ROLE IN RARE-EARTH MINERAL FORMATION

Qi Cao, Jiaxin Wang*

MLR Key Laboratory of Metallogeny and Mineral Assessment, Institute of Mineral Resources, Chinese Academy of Geological Sciences, Beijing 100037, China

Abstract In fluorine-bearing hydrothermal systems, fluorine is one of the important ligands controlling the migration, complexation, and precipitation processes of rare earth elements (REE). The pH conditions of the fluid significantly affect the speciation and coordination activity of fluorine. Under acidic conditions, fluorine mainly exists in the form of HF, and the activity of free F^- is relatively low. Under alkaline conditions, however, fluorine mainly exists as free F^- ions, which have stronger coordination ability and are therefore more favorable for rare earth elements to form fluoride complexes and enhance their mobility in hydrothermal fluids. Previous experimental studies have shown that the stability of REE–F complexes has an important influence on the migration of rare earth elements in fluorine-bearing fluids. At the same time, alkaline fluids may promote the formation of rare earth fluorocarbonate minerals by transporting REE, F, and related ore-forming components. However, theoretical calculations and atomic-scale understandings of the influence of F^- on the complexation structures of rare earth ions and the mineral precipitation transformation process under alkaline conditions remain relatively insufficient.

In this study, molecular dynamics simulations were used to systematically investigate the complexation characteristics of La in fluorine-bearing alkaline fluids at the atomic scale. The focus was placed on the influence of F^- on the local complexation of La and the coordination structures among La^{3+}, F^-, OH^-, and H_2O. The simulation results show that La^{3+} does not exist only as a simple hydrated ion in fluorine-bearing alkaline fluids, but tends to form mixed coordination structures with F^-, OH^-, and H_2O, showing local structures with certain mineralogical significance. Among them, F^- has an obvious promoting effect on the complexation of La^{3+}, which is consistent with the understanding proposed by Migdisov et al. (2009) that REE–F complexes are stable and that fluorine enhances the hydrothermal mobility of REE. Furthermore, with the participation of OH^- in the first coordination shell of La^{3+}, the local complexation environment of La shows a tendency to transform from fluoride-complexation-related migration toward hydroxyl-participating precipitation structures, indicating that a local structural evolution process related to mineral precipitation precursors may exist in fluorine-bearing alkaline hydrothermal systems. This result suggests that the joint regulation of the coordination environment of La^{3+} by F^- and OH^- may be an important microscopic mechanism controlling the transformation of rare earth elements from

hydrothermal migration to mineralized precipitation.

Overall, this study indicates that in fluorine-bearing alkaline hydrothermal fluids, La^{3+} mainly exists in complexed forms with mixed coordination of F^-, OH^-, and H_2O, rather than in the form of a simple hydrated ion. This understanding not only provides atomic-scale evidence for understanding the promoting effect of F^- on the complexation and migration of rare earth elements under alkaline conditions, but also provides new mineralogical insight into revealing the formation and precipitation mechanisms of rare earth minerals in fluorine-bearing alkaline hydrothermal systems.

Key words: fluorine-bearing alkaline hydrothermal fluid, rare earth element migration, La^{3+} complexation, mixed coordination structure, molecular dynamics simulation

Acknowledgements This project is supported by special fund of Deep Earth Probe and Mineral Resources Exploration-National Science and Technology Major Project, (No. 2024ZD1003402) .

LATE PALEOZOIC MANGANESE DEPOSITS IN NORTHWEST CHINA: INSIGHTS FROM GENETIC MINERALOGY AND IMPLICATIONS FOR EXPLORATION

NIU Sida[1,4], ZHAO Liqun[1,4], MO Lingchao[1,4], CHAO Wendi[2], ZHANG Zhenfu[3], CHEN Heqi[5]

1. Institute of Mineral Resources Research, China Metallurgical Geology Bureau, Beijing 101300, China
2. Northwest Geological Exploration Institute of China Metallurgical Geology Bureau, Xi'an, Shaanxi 710119, China
3. Northwest Bureau of China Metallurgical Geology Bureau, Xi'an, Shaanxi 710119, China
4. Mineral Comprehensive Utilization Research and Development Center, China Metallurgical Geology Bureau, Beijing 101300, China
5. China Metallurgical Geology Bureau, Beijing 100025, China

Abstract Manganese is a critical strategic metal, and Late Paleozoic manganese deposits account for approximately one-third of the total manganese resources in Northwest China, which are mainly hosted in the West Tianshan and West Kunlun orogenic belts. However, the genetic mechanisms of the distinct differences in oxidation depth and mineral assemblages between these two key metallogenic belts remain controversial, which severely restricts the theoretical understanding and exploration practice of regional manganese deposits. In this study, we systematically characterized the geological, mineralogical, and geochemical features of the Late Paleozoic manganese deposits in Northwest China via integrated optical microscopy, scanning electron microscopy (SEM), electron probe microanalysis (EPMA), X-ray diffraction (XRD), and whole-rock geochemical analysis. We identified the typomorphic mineral assemblages of manganese deposits from different regions and metallogenic epochs, and classified the manganese silicate minerals into three groups based on MnO contents, providing robust genetic mineralogy constraints on the metallogenic environment. We further established a four-stage metallogenic framework for the regional manganese deposits, including initial manganese accumulation, manganese precipitation, post-depositional overprinting and reworking, and supergene oxidation and leaching. The contrasting mineralization and oxidation features between the West Tianshan and West Kunlun manganese deposits are ultimately controlled by the coupling of tectonic evolution, paleogeographic and paleoclimatic conditions. This study bridges the genetic mechanism of manganese mineralization with regional exploration practice, and establishes a robust conceptual metallogenic model to guide future exploration for Late Paleozoic manganese deposits in Northwest China.

Key words: Manganese deposits, Genetic mineralogy, Late Paleozoic, Northwest China, Prospecting implications

MAGMA SOURCE AND EVOLUTION CONTROL PORPHYRY METAL ENDOWMENT: EVIDENCE FROM UST QUARTZ

Jingxin Hong[1], Degao Zhai[1]*, Manuel Keith[2], Anthony E. Williams-Jones[3], Zhiming Yang[4], Qingqing Zhao[1], Reiner Klemd[2], Jiajun Liu[1], Zengqian Hou[4]*

1. School of Earth Sciences and Resources, China University of Geosciences, Beijing, China
2. GeoZentrum Nordbayern, Friedrich-Alexander-Universität (FAU) Erlangen-Nürnberg, Erlangen, Germany
3. Department of Earth and Planetary Sciences, McGill University, Quebec, Canada
4. Key Laboratory of Deep-Earth Dynamics, Institute of Geology, Chinese Academy of Geological Sciences, Beijing, China

Abstract Despite robust genetic models for porphyry Au, Cu, and Mo deposits, the key factors controlling metal metallogeny remain elusive. Unidirectional solidification textured (UST) quartz, which crystallizes at the magmatic-hydrothermal transition stage, offers a unique window into these processes. Here we present trace element and in-situ SIMS oxygen isotope data for UST quartz from three typical porphyry deposits: Bilihe (Au), Qulong (Cu), and Chalukou (Mo). Oxygen isotopes reveal distinct magma sources. The Au-related magma is mantle-derived with contamination from subducted oceanic crust, the Cu-related magma originated from partial melting of slab-metasomatized lithospheric mantle and juvenile lower crust, and the Mo-related magma was generated from ancient metasomatized sub-continental lithospheric mantle. Consistent with source differences, the Au deposit exhibits limited magma fractionation (low Ge/Ti, Al/Ti, Li/Ti, and (Sb+Ge)/Ti ratios), high temperature, rapid crystallization, and shallow emplacement depth (high Li content). In contrast, the Mo deposit shows extensive fractional crystallization, lower temperature, prolonged magmatic-hydrothermal pulses, and deep emplacement. The Cu deposit displays intermediate characteristics in temperature, timescale, and fractionation degree. We conclude that the source and composition of the parental magma exert a first-order control on porphyry Au, Cu, and Mo fertility. Furthermore, statistical analysis of a global compilation of UST quartz compositions identifies this mineral as a promising tool for predicting porphyry metal endowment.

Key words: UST quartz, in-situ SIMS oxygen isotope, trace element, time scale, porphyry Metallogeny

MAGMATIC CONTROLS ON AG MINERALIZATION IN THE SHUANGJIANZISHAN DEPOSIT, NE CHINA: INSIGHTS FROM ZIRCON AND APATITE

Hang-Jin Jiang, Jian-Wei Li*, Jin-Hao Liu

School of Earth Resources, China University of Geosciences, Wuhan 430074, China

Abstract The Shuangjianzishan, located in the southern Great Xing'an Range of NE China, is the largest Ag polymetallic ore deposit in Asia, with proven reserves of > 18,000 t Ag (@128.5 g/t). This ore district has witnessed multiple magmatic events, including coarse- to fine-grained granitic intrusions and diorite porphyry. Previous studies suggested that this granitic suite represents a continuous magma differentiation process from coarse- to fine-grained phases, and the late-stage fine-grained units are genetically related to ore mineralization. However, whether early-stage granitic magmatic evolution has contributed to the formation of this deposit remains poorly constrained and the relationship between magma properties, such as water content, oxidation state, and fractionation, and ore formation is still unclear. To address this issue, we integrated textures, trace elements, and U-Pb isotopes of zircon, along with major element analyses of apatite, from the granitic suite and diorite porphyry to constrain magmatic evolution and its genetic relationship to Ag mineralization.

Zircon U-Pb dating indicates that the coarse-, medium-, and fine-grained granites were all emplaced during the Early Cretaceous of ~135 Ma, consistent with the timing of Ag mineralization and clearly postdating the Triassic diorite porphyry (~246 Ma). In addition, these granitic rocks show a closely spatial association with ore bodies at different levels and they are hydrothermally altered in most cases. These combined results allow us to propose that the granitic suite can be better considered as causative intrusions at the Shuangjianzishan. Zircon grains extracted from three granitic units yield undistinguishable ΔFMQ (Fayalite-Magnetite-Quartz) values of −0.96 to 0.83, suggesting that they crystallized at the similar redox state. Additionally, similar Dy/Yb ratios (0.22–0.40) and Ti contents (1.31–7.69 ppm) in these zircons indicate relatively hydrous magmas with slightly oxidized conditions, which promoted Ag solubility in the exsolved ore fluids. Triassic diorite porphyry formed under a relatively reduced, anhydrous condition as evi-denced by lower ΔFMQ values (−2.39 to −0.60), higher Dy/Yb ratios (0.33–0.41) and higher Ti contents (8.49–14.33 ppm). This may explain the absence or scarcity of Ag mineralization in these rocks, consistent with previous proposals that Ag fertility is associated with highly evolved, felsic to rhyolitic magmas. These characteristics are consistent with its low fluid exsolution and limited contribution to Ag mineralization, supporting previous proposals that Ag fertility is linked to highly evolved, felsic to rhyolitic magmas. Apatite compositions from the three granitic intrusive phases exhibit highly variable halogen ratios (XF/XCl = 33.10–6,212.51; XCl/XOH = 0–3.07), reflecting extensive fluid

exsolution throughout the granitic suite. The very low to below-detection-limit Cl contents in these apatites further support this interpretation, as the partitioning of Cl between silicate melts and fluids favors its preferential incorporation into exsolved magmatic fluids. These results indicate that the protracted evolution of the granitic magmas contributed throughout their entire history to ore formation, facilitating the development of this world-class Ag deposit. In contrast, zircons from the Triassic diorite porphyry show minimal fluid exsolution, as indicated by narrow ranges of apatite halogen ratios (XF/XCl = 8.25–14.86; XCl/XOH = 0.08–0.19), further reinforcing their low fertility. Collectively, the formation of the giant Shuangjianzishan Ag polymetallic deposit is genetically controlled by the protracted evolution of hydrous, fractionated granitic magmas and continuous fluid exsolution under moderately reduced to weakly oxidized conditions.

This study also highlights that the critical role of zircon and apatite can be used as probes to trace magmatic evolution and fluid exsolution related to mineralization.

Key words: Zircon, Apatite, Magmatic evolution, Fluid exsolution, The Shuangjianzishan Ag polymetallic deposit

MAGMATIC-HYDROTHERMAL EVOLUTION AND NIOBIUM ENRICHMENT MECHANISMS TRACED BY MULTI-STAGE PYROCHLORE GROUP MINERALS

Zhi-Hao Jiang[1], Chang-Zhi Wu[1,3*], Can Rao[2], Xiang-Ping Gu[4], Hong-Dian Yuan[1], Ru-Xiong Lei[1], and Matthew J. Brzozowski[1]

1. Key Laboratory of Western China's Mineral Resources and Geological Engineering, Ministry of Education, School of Earth Science and Resources, Chang'an University, Xi'an 710054, China
2. Key Laboratory of Geoscience Big Data and Deep Resource of Zhejiang Province, School of Earth Sciences, Zhejiang University, Hangzhou 310027, China
3. Xinjiang Natural Resources and Ecological Environment Research Center, Urumqi, 830000, China
4. School of Gemmology and Mineral Resources, Jiangxi Institute of Applied Science and Technology, Nanchang 330100, China

Abstract Niobium (Nb) is a critical high-field-strength element (HFSE) of strategic importance, yet the mechanisms governing its enrichment—ranging from fractional crystallization and liquid immiscibility to hydrothermal mobilization—remain a subject of intense debate. This study investigates a paragenetic suite of Nb-bearing minerals, including Fluornatropyrochlore, Oxyplumbopyrochlore, Hydroxyplumbopyrochlore, Pb-poor pyrochlore, and columbite, to reconstruct the magmatic-hydrothermal evolution of the Boziguoer deposit system. Our results indicate that Nb underwent a multi-stage enrichment history synchronized with host-rock evolution. In the syenite stage, Nb initially attained primary enrichment through the crystallization of fluornatropyrochlore. As the system evolved into biotite/amazonite granites, progressive fractional crystallization led to the accumulation of Pb, a highly incompatible element. This facilitated the metasomatic replacement of early fluornatropyrochlore by oxyplumbopyrochlore, a process marked by a transient decline in Nb concentration alongside a substantial influx of Pb. During the culminating amazonite-pegmatite stage, intensified hydrothermal activity triggered a pervasive coupled dissolution-reprecipitation (CDR) process. In this late stage, the heightened mobility of hydrothermal fluids promoted the mobilization and removal of Pb, which in turn facilitated the localized secondary re-enrichment of Nb. The mineralogical evolution concluded with the crystallization of secondary columbite, signifying the final concentration of Nb into high-grade ore.

Otherwise, we found a potential new mineral species, a "Pb-poor pyrochlore", which occurs as yellow-brown crystals ranging from 30 to 200 μm in size and is in association with Oxyplumbopyrochlore and Hydroxyplumbopyrochlore. Single-crystal X-ray diffraction and structure refinement confirm its cubic symmetry with an empirical formula of $(Pb_{0.97}Na_{0.12}U_{0.16}Ce_{0.08}\square_{0.67})_2(Nb_{1.67}Ta_{0.12}Ti_{0.12}Si_{0.02}Sn_{0.04})_{1.97}O_{6.63}$. The discovery of this vacancy-bearing, Pb-dominant pyrochlore phase provides a unique window into the extreme chemical

fluctuations at the magmatic-hydrothermal transition and offers a robust indicator for tracing the mobilization and redistribution of Nb in alkaline-related mineral systems.

Key words: Niobium mineralization, Pyrochlore group, Metasomatism, Coupled dissolution-reprecipitation, Pb-poor pyrochlore

Acknowledgements Financial assistance for this research came from the Xinjiang Key R&D Program (2024B03004), the "Tianchi Talent" Plan to C.Z. Wu, together with the Central Universities' Fundamental Research Funds, CHD (300102274303). We express our sincere gratitude to the Aksu Geology Party (Xinjiang Geology Bureau) for their invaluable assistance during field sampling. We are also deeply grateful to Professor Can Rao from Zhejiang University and Xiang-Ping Gu from Jiangxi Institute of Applied Science and Technologyfor his meticulous guidance and assistance during the research process.

MAGNETITE GEOCHEMISTRY OF THE LARGE ERDAOKAN AG DEPOSIT IN HEILONGJIANG, NE CHINA: CONSTRAINTS ON THE ORE-FORMING PROCESS

Anzong Fu [1,2], Chenglu Li [1*], Wenpeng Yang [1,2], Masroor Alam [3], Changzhou Deng [4], Yuanjiang Yang [1], Bo Zheng [1], Ruijun Zhao [1], Maowen Yuan [2]

1. Natural Resources Survey Institute of Heilongjiang Province, Harbin, China
2. School of Earth Science and Resources, China University of Geosciences, Beijing, China
3. Department of Earth Sciences, Karakoram International University, Gilgit, Pakistan
4. State Key Laboratory of Ore Deposit Geochemistry, Institute of Geochemistry, Chinese Academy of Sciences, Guiyang, China

Abstract The Erdaokan Ag deposit in Heilongjiang is a large hydrothermal Ag-polymetallic deposit discovered in the past decade, and magnetite, as a key persistent mineral, has geochemical characteristics that impose important constraints on the ore-forming process. Magnetite at Erdaokan is classified into seven types: disseminated magnetite (Mag1), coarse-grained magnetite (Mag2a), radial magnetite (Mag2b), fragmented fine-grained magnetite (Mag2c), vermicular gel magnetite (Mag3a1 and Mag3a2), colloidal magnetite (Mag3b) and dark gray magnetite (Mag4). In this study, EPMA, LA-ICP-MS, and *in situ* Fe isotope analysis were employed to determine the major and trace element compositions as well as Fe isotopic compositions of magnetite from the ores. Our results show that all of the magnetite types are generally low in Ni (<800 ppm) and Ti (<400 ppm), while being enriched in light Fe isotopes ($\delta^{56}Fe < 0$), indicating a hydrothermal origin. However, they exhibit different geochemical signatures. EPMA data show Mag1 has a higher MnO content when compared to other magnetite types, ranging from 6.651 to 17.939 wt%. Mag2a-c have a lower SiO_2 content (< 1 wt%) while Mag3a-b, Mag4 have a higher SiO_2 content (> 1 wt%), and Mag4 has a higher MnO content (> 0.2 wt%). LA-ICP-MS data show that the Si, Ba, Sr, Y, P, Pb, Zn, Li, B, Na and Cs contents of Mag3b and Mag4 are higher than those of Mag2a. Mag4 shows higher levels of Ca (1232.5–4576.5 ppm), Mn (9586–17614 ppm), Mg (148.69–931.08 ppm), Ga (0.67–2.51 ppm), B (120.55–321.20 ppm) and Na (123.28–203.54 ppm), which are significantly different from those of Mag2a and Mag3b. On the other hand, Mag3b exhibits high Sn (7.40–12.62 ppm) and Sb (6019.76–8366.16 ppm) contents. Based on mineralogy, elemental geochemistry, Fe isotopes, temperature trends, $T_{Mg\text{-}mag}$ and (Ti + V) vs. (Al + Mn) diagrams, we propose that the Erdaokan Ag deposit underwent multi-stage mineralization, which can be broken down into four stages and nine sub-stages. Mag1, Mag2a-c, Mag3a-b and Mag4 were formed during the first sub-stage of each of the four stages, respectively. In stage I_1, Mag1 is disseminated and coexists with jakobsite and pyrite, occurring within Fe-Mn carbonates. The crystallization temperature of Mag1 ranges from 540 to 728°C, corresponding to the initial temperature of the hydrothermal fluid. In stage II_1, low-silicon

magnetite (Mag2a-c) was replaced by hematite, reflecting the high oxygen fugacity conditions during this stage. The crystallization temperatures of Mag2a-c range between 265 and 477°C, higher than those of sub-stage I_2. The high oxygen fugacity and elevated fluid temperatures may have been caused by the superposition of the hydrothermal fluids in stages II and I. In stage III_1, the high-silicon magnetite types (Mag3a-b) exhibit distinctive structures that might result from dissolution-reprecipitation processes. Mag3a-b have similar crystallization temperature ranges to Mag2a-c, although Mag3b shows a heavier Fe isotope composition compared with Mag2a. This could be due to the superposition of hydrothermal fluids, which increased both the temperature and δ^{56}Fe. In stage IV_1, Mag4 primarily appears as thin veins along the edges of Mag2a-c and Mag3b. The crystallization temperatures of Mag4 range from 314 to 561°C, which are significantly higher than those of Mag3a-b. This increase may be attributable to the superposition of hydrothermal fluids. Mag4 has a narrow δ^{56}Fe ‰ range from −0.87 to −0.36, indicating a relatively short crystallization process, which is consistent with the small amount of Mag4 found in the silver ore. Additionally, fluid mixing, cooling and depressurization boiling were identified as the main mechanisms for mineral precipitation. The enrichment of Ag was significantly enhanced by the superposition of multi-stage ore-forming hydrothermal fluids in the Erdaokan Ag deposit.

Key words: multi-stage mineralization, magnetite geochemistry, in situ Fe isotope, Erdaokan Ag deposit

Acknowledgements This work was financially supported by the Heilongjiang Provincial Key R&D Program Project (No. GA21A204), the National Science and Technology Major Project of China (No. 2025ZD1008706), Heilongjiang Provincial Natural Science Foundation of China (No. LH2022D031) and the Research Project of Heilongjiang Province Bureau of Geology and Mineral Resources (No. HKY202302).

MANGANESE (HYDR)OXIDES RECORD THE DYNAMIC EVOLUTION OF A MILLION-YEAR HESPERIAN OCEAN IN UTOPIA PLANITIA, MARS

Bingxu Hou[1,2,#], Heng Sun[3], Xiangzhi Bai[4], Yan Li[1,2,*]

1. SKLab-DeepMinE, MOEKLab-OBCE, School of Earth and Space Sciences, Peking University, Beijing 100871, China.
2. Beijing Key Laboratory of Mineral Environmental Function, School of Earth and Space Sciences, Peking University, Beijing 100871, China.
3. College of Computer Science, Beijing University of Technology, Beijing 100124, China.
4. School of Astronautics, Beihang University, Beijing 102206, China.

Abstract The evolutionary and duration history of ancient surface water on Mars remains one of the most significant challenges in unraveling the planet's past habitability. Utopia Planitia, a vast basin in Mars' northern lowlands, serves as a critical region for deciphering the past aqueous activity. Here, we present the quantitative evidence of dynamic aqueous evolution and the persistence history of the Hesperian Ocean in Utopia Planitia. By developing a novel deep learning Spectral Contrastive-Aware Network (SCANet), we conduct quantitative analyses of Mn (hydr)oxides in the short-wave infrared (SWIR) spectra from the Zhurong rover, OMEGA and CRISM spectrometer. Our findings reveal a distinctive altitude-dependent "bathtub ring" pattern of Mn (hydr)oxides, strongly supporting the presence of a large ancient water body. By mapping the spatiotemporal distribution of Mn (hydr)oxides, we reconstruct the evolution of the ancient Hesperian Ocean, detailing its origin, flourishing, regression, and eventual extinction. Quantitative modelling of Mn (hydr)oxides deposition rates further constrains the ocean's duration, providing refined temporal estimates for the persistence of Martian water bodies. These results enhance our understanding of Mars' aqueous evolution, with implications for its past and future habitability.

Key words: Manganese (hydr)oxides, deep learning, infrared spectra, ancient ocean, Mars

METAL UTILIZATION STRATEGIES IN METHANOGENS WITH DIVERGENT EVOLUTIONARY ORIGINS UNDER MINERAL-CONTROLLED LOW-METAL CONDITIONS

Qiang Zeng, Wenhui Zhang, Hailiang Dong

Center for Geomicrobiology and Biogeochemistry Research, State Key Laboratory of Geomicrobiology and Environmental Changes, China University of Geosciences, Beijing 100083, China.

Abstract This study examined the physiological responses and metal utilization traits of methanogens with distinct evolutionary origins within a mineral-controlled, low-metal supply regime. Significant strain-specific differences in metal dependency were observed. The earlier-originating *Methanococcus maripaludis* S2 sustained stable growth and methanogenesis despite metal limitation, whereas the later-originating *Methanolacinia paynteri* exhibited heightened metal dependency, accumulating greater intracellular metal loads without corresponding metabolic enhancement. Transcriptomic analysis revealed that under low-metal conditions, *M. maripaludis* S2 maintained core metabolic integrity through transcriptional regulation of genes associated with metal transport, metal binding, and electron transfer. These findings suggest that methanogens have evolved divergent metal acquisition and utilization strategies, patterns that align with long-term geological trends in metal bioavailability and supply mechanisms across Earth's history.

Key words: Methanogens, Metal Utilization, Mineral, Evolutionary Origins

METAMORPHIC OR IGNEOUS ZIRCON? CLASSIFICATION THROUGH RARE EARTH ELEMENTS, MACHINE LEARNING, AND LOGISTIC REGRESSION

Jarrod M. Burges[1], Chris Yakymchuk[2], Michael P. DiMaio[1], Timothy C.C. Lui[3], and Shaunna M. Morrison[1]

1. Department of Earth and Planetary Sciences, Rutgers University, Piscataway, New Jersey, USA
2. Department of Earth and Environmental Sciences, University of Waterloo, Waterloo, Ontario, Canada
3. Department of Earth and Planetary Sciences, Stanford University, Stanford, California, USA

Abstract Zircon is a common, highly refractory accessory mineral found in sedimentary, igneous, and metamorphic rocks that forms through various processes (e.g., magmatic, hydrothermal, metamorphic growth, recrystallization). Trace element compositions of detrital zircon have been widely applied to understanding tectonic processes and continental reconstruction. Previous studies have shown that no single compositional parameter (i.e., REE pattern, Th/U) can distinguish zircon petrogenesis. Here, we employ novel machine learning methods to differentiate between metamorphic and igneous zircon, independent of researcher-labeled lithologies. With advancements and the adoption of machine learning algorithms by the geochemical community, we holistically analyze n-dimensional geochemical data (14 dimensions for the full REE suite) to ascertain or confirm complex geological processes. We utilize a dataset of previously identified zircon with varying proposed origins (i.e., metamorphic, igneous, S-type granites, early Earth detrital) and unsupervised machine learning algorithms (i.e., UMAP, Mclust), which reveal two distinct clusters that we interpret as the dominant magmatic and metamorphic REE signatures. The two REE signature clusters are used to define a comprehensive REE equation that matches an unknown zircon into the most similar interpreted cluster (igneous or metamorphic) through probabilistic bimodal logistic regression. The logistic regression equation was derived exclusively from REE signatures independent of previous classification. Model validation was achieved using confusion matrices and yielded a mean accuracy of 0.7986 (balanced accuracy = 0.7604), with average precision = 0.7447, recall = 0.6651, F1 = 0.6510, and AUC = 0.7938, indicating moderate discriminative performance with higher precision than recall. Unsupervised machine learning demonstrates that two distinct REE signatures emerge, which vary in their HREE enrichment and LREE depletion. We demonstrate that machine learning can decipher complex multi-elemental relationships in zircon REE data and can be used to classify zircon.

Key words: zircon, machine learning, rare earth elements, petrogenesis

MICROBE-MEDIATED IRON PRECIPITATION IN THE PALEOPROTEROZOIC ASTINGBULAKE BIF, XINJIANG: INSIGHTS FROM REE CHARACTERS

Jingyi Yuan, Qilin Huang, He Zhang, Yuanfeng Cai

School of Earth Science and Engineering, Nanjing University, China

Abstract Mineral-microbe co-evolution is a key process in the evolution of Earth's surface system during the Precambrian Era. Direct evidence of microbial activity in banded iron formations (BIFs) remains scarce, though the microbes were thought to affect the evolution of surface system. This study presents a petrographic and rare earth element (REE) geochemical study of the Paleoproterozoic Astingbulake BIF in the northeastern Tarim Craton, Xinjiang.

Petrographic analysis reveals that magnetite is the main ore mineral, interbedded with silicious material to form typical banded structures. Magnetite grains in iron bands are euhedral, whereas those in siliceous ironstones are anhedral and spindle-shaped. The present of spindle magnetite may indicate deformation resulted from regional stress. Further analysis of trace elements using PAAS-normalized REE patterns displays two diagnostic features: (1) pronounced positive Eu anomalies (Eu/Eu* = 0.97- 4.5, average 1.56), indicating high-temperature hydrothermal fluid input; and (2) distinctly negative Ce anomalies (Ce/Ce* = 0.54- 0.96, average 0.86), verified as true negative anomalies by Pr/Pr* cross-plots. Previous simulation experiment suggested that the oxidation of Ce^{3+} to insoluble Ce^{4+} was thought to be mediated primarily by manganese-oxidizing bacteria in modern sea floor. The preservation of negative Ce anomalies in magnetite bands thus may suggest microbially mediated Ce oxidation in Paleo-proterozoic Ocean. Furthermore, Y/Ho versus Eu/Sm discrimination diagrams indicate a dominantly crustal source for the ore-forming materials.

Combined with the prominent positive Eu anomalies, we propose a two-stage model for the Astingbulake BIF: hydrothermal leaching of crustal materials - seawater transport- microbe-mediated precipitation. Specifically, microbial oxidation of Fe^{2+} and Ce^{3+} in oxygenated surface waters was followed by dissimilatory iron reduction in anoxic deep waters, driving the precipitation of magnetite. This study also differs from previous ones in that a new recognition of Ce anomalies may be present in banded iron formations.

Key words: Banded Iron Formation, Astingbulake, Rare Earth Elements, Ce Anomaly, Mineral-Microbe Coevolution

Acknowledgements This work was performed with the approval of the State Key Program

of the National Natural Science Foundation of China (No. 42192504).

MINERAL CONTROL OF BIOLOGICAL NITROGEN FIXATION ON EARLY EARTH

Yizhi Sheng[1], Xinyi Zhou[1], Dongyi Guo[2], Shuaidi Wang[1], Xiaowen Zhang[1], and Hailiang Dong[1]

1. Center for Geomicrobiology and Biogeochemistry Research, State Key Laboratory of Geomicrobiology and Environmental Changes, China University of Geosciences, Beijing 100083
2. Department of Geology and Environmental Earth Science, Miami University, Oxford, OH 45056, United States

Abstract Nitrogen is an essential nutrient for life on Earth, and biological nitrogen fixation is the primary pathway by which atmospheric dinitrogen (N_2) is converted into bioavailable ammonia (NH_3). This process is catalyzed by nitrogenase enzymes, which predominantly employ molybdenum (Mo) as a metal cofactor, although iron (Fe)- and vanadium (V)-based nitrogenases can function as alternative systems. Although the evolutionary origin of nitrogenase has long been debated, accumulating evidence indicates that Mo-dependent nitrogenase emerged during the Archean, despite the extremely low dissolved Mo concentrations in early oceans. In contrast, the less efficient Fe- and V-nitrogenases are thought to have evolved approximately one billion years later, potentially in response to environments where Mo bioavailability was constrained relative to Fe and V, thereby favoring the activation of alternative enzymatic pathways. While hydrothermal systems may have supplied trace metals locally, the bioavailability of mineral-bound Mo was likely critical for sustaining nitrogen fixation in shallow marine and coastal environments, where early diazotrophs were most abundant.

Emerging evidence suggests that metal bioavailability is governed not only by bulk concentration but also by mineralogical association and chemical speciation. Our previous work demonstrated that diazotrophs can mobilize metal ions directly from Mo, V, and Fe minerals to sustain nitrogenase expression and nitrogen fixation through diverse strategies. More recently, we observed that even in euxinic environments characterized by Fe–S-mediated Mo sequestration and elevated dissolved V concentrations, conditions traditionally assumed to favor alternative nitrogenases, anoxygenic phototrophs can still mobilize Mo via metallophore production and maintain Mo-nitrogenase activity. In contrast, within the overlying water column where Mo is removed, isotopic signatures and functional gene analyses

indicate activation of V-nitrogenase. We further found that, in the presence of organic ligands such as metallophores, the methanogen Methanosarcina acetivorans was unable to directly utilize metal-metallophore complexes to fix N , leading to reduced metal bioavailability and a likely shift toward expression of alternative nitrogenases. Metallophore addition also reshaped transcriptional profiles associated with metal transport systems and cellular energy metabolism in these anaerobic

diazotrophs. Notably, when mineral phases such as molybdenite and basalt were introduced, nitrogen fixation activity was restored despite the presence of metallophores, indicating that mineral can buffer ligand-induced metal limitation and sustain diazotrophic function. Together, these findings highlight the central role of metal speciation in regulating nitrogenase utilization and biological nitrogen fixation in ancient redox-stratified environments.

Key words: Biological nitrogen fixation, Molybdenum paradox, Molybdenite, Pyrite, Great Oxidation event

MINERAL INFORMATICS WITH INTERPRETABLE MACHINE LEARNING FOR APATITE BIOSIGNATURE DETECTION

Yanzhang Li[1], Anirudh Prabhu[1], Bingxu Hou[2], Michael L. Wong[1], Jieqi Xing[2], Don Ngo[1], Bo Xu[3], Robert M. Hazen[1]

1. Earth and Planets Laboratory, Carnegie Institution for Science, USA
2. School of Earth and Space Sciences, Peking University, China
3. State Key Laboratory of Geological Processes and Mineral Resources, China University of Geosciences (Beijing), China

Abstract Reliable identification of mineral biosignatures remains a central challenge in astrobiology and deep-time geochemistry. Apatite, a ubiquitous phosphate mineral in terrestrial and extraterrestrial settings, preserves complex structural and chemical signals that may record biogenic influence, yet quantitative and interpretable diagnostic frameworks remain limited. Here we develop a mineral informatics approach that integrates Raman spectroscopy with interpretable machine learning to discriminate biotic from abiotic apatite. We compiled a curated dataset of 331 apatite Raman spectra from literature sources, public databases, and laboratory measurements. After baseline correction, normalization, and full-spectrum peak fitting, 21 band-resolved quantitative features were extracted. Principal component analysis reveals systematic separation between abiotic and biotic endmembers. A random forest classifier achieves 96.8% accuracy on an independent test set, and robustness is confirmed through multiple validation schemes, including leave-one-source-out cross-validation across 60 independent data sources, demonstrating generalization beyond instrument- and source-specific effects.

Feature attribution identifies two dominant controls: (1) phosphate-band broadening as a structural proxy for lattice disorder and (2) carbonate-band intensity as a chemical indicator of substitution. Density-functional calculations reproduce the observed spectral trends and show that carbonate incorporation approximately doubles phosphate tetrahedral distortion and increases formation energies on the order of 10^2 kcal/mol, providing a mechanistic basis for reduced crystallinity and Raman band broadening. Building on these insights, we construct a transparent two-parameter decision map that jointly captures structural disorder and carbonate incorporation, enabling rapid probabilistic screening of unknown apatite samples. This work demonstrates how mineral informatics can transform Raman datasets into physically interpretable biosignature metrics and provides a mission-relevant framework for deep-time archives and future planetary exploration.

Key words: biosignatures, astrobiology, Raman spectroscopy, machine learning, apatite

MINERALOGICAL AND IN-SITU CARBON ISOTOPIC EVIDENCE FOR MICROBIAL INVOLVEMENT IN THE OOID MINERALIZATION PROCESS OF XUANLONG-TYPE IRON ORES

TANG Ganyu, LAI Yong*

The Key Laboratory of Orogenic Belts and Crustal Evolution, Peking University, Beijing 100871, China

Abstract Xuanlong-type iron ore is one of the most significant sedimentary iron deposits in North China, playing a crucial role in China's mining and industrial development. This study collected samples from the Chuanlinggou Formation in the North China Craton and systematically analyzed the mineralogical characteristics and carbon isotopic compositions of hematite ooids and siderite ooids using optical microscopy, Environmental Scanning Electron Microscopy (ESEM), Energy Dispersive X-ray Spectroscopy (EDS), and Laser Ablation-Gas Stable Isotope Ratio Mass Spectrometry (LA-IRMS).

The study found that the $\delta^{13}C$ values of oolitic hematite (whole-rock average $\delta^{13}C_{Avg}$=-11.41‰) and oolitic siderite (whole-rock $\delta^{13}C_{Avg}$=-8.68‰) both exhibit significant negative anomalies. Compared with the general characteristics of inorganic carbonate minerals ($\delta^{13}C$ > -5‰) and organic carbon-derived carbonate minerals ($\delta^{13}C\approx$-25‰), this confirms microbial involvement in the mineralization process of Xuanlong-type iron ores.

In-situ laser ablation sampling results show that the $\delta^{13}C$ of hematite ooids exhibit a trend of first decreasing and then increasing from the core ($\delta^{13}C_{Avg}$=-8.72‰), mantle (average -12.05‰), shell ($\delta^{13}C_{Avg}$=-14.64‰) to the matrix ($\delta^{13}C_{Avg}$=-10.86‰). In contrast, the $\delta^{13}C$ of siderite ooids display an entirely opposite trend of first increasing and then decreasing from the core ($\delta^{13}C_{Avg}$=-8.02‰), shell ($\delta^{13}C_{Avg}$=-3.57‰) to the matrix ($\delta^{13}C_{Avg}$=-13.37‰).

Combined with the mineralogical characteristics of the samples, the following ooid mineralization model can be established. Microorganisms participated in and promoted the formation of oolitic hematite by altering environmental properties, leaving evidence within the carbon-bearing materials encapsulated between ooid layers. Prior to the formation of siderite ooids, microbial activity led to the development of euhedral carbonate crystals, which, after fragmentation under high-energy hydrodynamic conditions, were re-cemented to form the ooid cores. During the intermediate stage, hydrodynamic forces dominated ooid formation, with minimal microbial involvement. In the later depositional cementation stage, microorganisms once again played an extensive role in mineralization.

This study is the first to reveal, through in-situ carbon isotopic evidence and other data, the

mechanisms by which inorganic environmental conditions and microbial interactions manifest at different stages of Xuanlong-type iron ore ooid formation. It illustrates the energy flow processes among the environment, minerals, and microorganisms, offering a new perspective for understanding microbe-mineral co-evolution and providing important insights for research on the genesis of sedimentary iron deposits.

Key words: Xuanlong-type Iron Ores, Oolitic Hematite, Oolitic Siderite, Co-evolution, In-situ Carbon Isotope

MINERALOGICAL CHARACTERISTICS AND GENESIS STUDY OF BANDED IRON FORMATIONS IN THE HAMERSLEY BASIN, WESTERN AUSTRALIA

Siyi Huang, He Zhang, Qilin Huang, Yuanfeng Cai, Jingyi Yuan, Yuli Yuan, Jingbo Xu
State Key Laboratory for Mineral Deposit Research, Nanjing University, China Affiliation

Abstract As the world's most significant source of iron ore, banded iron formations (BIFs) serve as a crucial rock archive for understanding the evolution of Precambrian Earth surface systems and early life. However, due to their great antiquity and widespread post-depositional alteration, major controversies remain regarding the BIFs genesis mechanisms. Here, we systematically investigated BIFs from the Hamersley Basin through mineralogical and geochemical studies. The mineral composition is largely consistent between the iron-rich and silica-rich bands, dominated by quartz and iron minerals. Based on the XRD quantitative analysis results, the iron minerals can be ranked as follows: iron (hydro)oxides (hematite, magnetite, goethite) > iron silicates (chamosite, stilpnomelane, cummingtonite) > iron carbonates (ankerite, siderite). Carbonate and silicate minerals are extremely rare, indicating that most BIFs in the Hamersley Group have experienced only low-grade metamorphism. Hematite "dust" and euhedral magnetite grains likely derive from initial $Fe(OH)_3$ precursors in the primary sediment and may preserve primary geochemical signatures. The formation of magnetite likely involved microbial dissimilatory iron reduction. Within magnetite-hematite intergrowths, hematite is produced by partial oxidation of magnetite, while in goethite-hematite assemblages, hematite results from partial dehydration of goethite. Crystallographic orientation relationship preserved between iron minerals reflect coherent phase transformations, whereas goethite occurring along grain fractures or rims lacks such features, indicating later weathering products. Al_2O_3, TiO_2, and HFSE concentrations are generally low in the BIFs. Weak correlations among elements in both iron-rich and silica-rich bands suggest limited influence from terrigenous clastic input during BIFs deposition. The BIFs exhibit a consistent rare earth element (REE) distribution pattern: HREE is relatively enriched compared to LREE, with positive anomalies for La, Y, and Eu. In Zr-Y/Ho plots, samples cluster between the average continental crust and/or high-temperature hydrothermal fluids and modern seawater. The Ge/Si ratios in iron-rich bands are close to those of hydrothermal fluids, while those in silica-rich bands approximate values typical of continental runoff. The relatively heavy $\delta^{56}Fe$ values are associated with the partial oxidation of Fe(II) from hydrothermal fluids. Integrated geochemical evidence indicates that the sources of iron and silica were decoupled in the Hamersley Group BIFs, with hydrothermal fluids and seawater mixing providing the dominant iron source and silica having a continental weathering origin.

Key words: banded iron formations, mineral genesis, iron minerals

MOBILIZATION AND EXTREME ENRICHMENT OF TI IN HYDROTHERMAL SYSTEMS DURING CONTINENTAL COLLISION

Qiuping Qiang [1], [2], Xin Chen [1]

1. State Key Laboratory of Geological Processes and Mineral Resources and School of Earth Resources, China University of Geosciences, Wuhan 430074, China
2. Geological Team of East China Metallurgical Geological Exploration Bureau.

Abstract Activation, migration, and extreme enrichment of high field strength elements (HFSEs) in hydrothermal fluids represent a frontier topic in modern geochemistry. Titanium, a typical HFSE, has traditionally been considered immobile in aqueous fluids; however, the mechanisms enabling its mobilization, transport, and concentration to form economic deposits remain poorly understood. Recently, several rutile-barite-quartz veins with TiO_2 grades reaching up to 77 wt% have been discovered in the Archean metamorphic basement of the Fengyang area, on the southeastern margin of the North China Block. These veins record exceptional Ti enrichment in a continental collisional setting and provide an ideal natural laboratory to investigate the above scientific questions.

The TiO_2 grade in these veins ranges from 2.5% to 77.2%, with $BaSO_4$ contents between 26.9% and 53.5%, accompanied by associated metals such as Pb, Mo, Nb, and Ta, and localized Au mineralization. Rutile occurs in massive, radial, and disseminated forms within quartz and barite. Hand specimen and microscopic observations reveal two rutile generations—dark brown and red—exhibiting well-developed compositional zoning. The first generation is enriched in Nb and depleted in Ti compared to the second generation. U-Pb dating of the two rutile types yields ages of 229 ± 2 Ma and 210 ± 3 Ma, respectively. These ages are close to or slightly later than the peak metamorphic age (231–225 Ma) of the Dabie-Sulu ultrahigh-pressure metamorphic rocks, but are consistent with the early exhumation stage (225–214 Ma), indicating the activity of Ti-rich fluids in continental collisional orogenic belts.

Future work will focus on micro-scale geochronology, multi-isotopic tracing techniques (Ti-Ba-S-Hf-O), and in-situ analyses of minerals and fluid inclusions. The objectives are to constrain the source and timing of Ti-rich fluids, reconstruct the evolution of P-T-X conditions (including fO_2 and volatile components) during fluid activity, and evaluate the role of volatiles in controlling Ti partitioning, mobilization, and enrichment in hydrothermal systems. The findings will advance the theoretical understanding of Ti behavior and enrichment mechanisms during fluid processes in continental collisional orogens.

Key words: Rutile, Titanium enrichment, High field strength elements (HFSEs),

Hydrothermal fluid, Continental collisional orogen

MULTI-STAGE REE MINERALIZATION IN THE BAYAN OBO FE-REE-NB DEPOSIT: CONSTRAINTS FROM GEOCHRONOLOGY AND MINERAL GEOCHEMISTRY

Pei Liang[1, 2], Yuling Xie[1]

1. School of Resources and Safety Engineering, University of Science and Technology Beijing, Beijing 100083, China
2. Key Laboratory of Metallogenic Prediction of Nonferrous Metals and Geological Environment Monitoring (Central South University), Ministry of Education, Changsha 410083, China

Abstract The Bayan Obo deposit, situated on the northern margin of the North China Craton, stands as the largest rare earth elements (REE) deposit in the world. Despite extensive research, the controversies remain regarding the ore-forming ages, genesis and metallogenic models of REE within the carbonatite and the role of subsequent hydrothermal fluids. The new discovery of a silicate-calcite complex pluton in the Bayan Obo Formation, North China Craton, characterized by zoned petrographic units: biotite-, calcite-biotite-, calcite-, and carbonatite units from the outer to inner zones, provides a unique window into the magmatic-hydrothermal evolution of REE mineralization. Given their high sensitivity to the chemical and physical factors associated with magmatic crystallization fractionation and fluid activities, biotite and apatite from the Bayan Obo deposit were subjected to detailed petrographic, geochronological, and geochemical analyses. Two groups of biotite and apatite were identified: (1) primary magma-related minerals with an age of 1231 Ma (Mesoproterozoic), characterized by relatively high K/Rb ratios and formation temperatures ranging from 564°C to 643°C; and (2) altered hydrothermal minerals with ages ranging from 280 to 240 Ma (Paleozoic, Hercynian), characterized by relatively high X_{Mg} (Mg/(Mg+Fe)), Al, F, and REE contents, high oxygen fugacity, and low formation temperatures. The distinctly different geochemical characteristics between the two groups of biotite and apatite indicate contrasting REE mineralization processes during magmatic and hydrothermal stages. During the magmatic stage, the fractional crystallization of REE-poor silicate minerals (such as biotite) within the evolving silicate-carbonatite complex played a crucial role in concentrating REE and differentiating light REE (LREE) from heavy REE (HREE) in the residual carbonatitic magma. Subsequently, during the hydrothermal stage, a separate REE- and F-rich late-stage hydrothermal fluids, likely sourced from Hercynian magmatic activities, percolated through the system. The high F content in these late fluids is considered a critical factor facilitating the transport and eventual precipitation of REE minerals.

Key words: Bayan Obo, REE, Geochronology, In situ geochemistry, Ore-forming process

Acknowledgements This study was financially supported by the National Natural Science Foundation of China (Nos. 42002076, 41930427), the Open Research Fund Program of Key Laboratory of Metallogenic Prediction of Nonferrous Metals and Geological Environment Monitoring (Central South University), Ministry of Education (No. 2025YSJS01), and the Young Elite Scientists Sponsorship Program of the Beijing High Innovation Plan (No. 20250959).

NANOSCALE MINERALOGY AND FORMATION MECHANISMS OF TYPE II TCIS IN THE CM2 CARBONACEOUS CHONDRITE GRV 13051

Jiayu Wang[1,2], Lin Li[1,3,*], Xiaochao Che[4], Xiaowei Li[1,2,] Corresponding author: clark.li@cugb.edu.cn

1. State Key Laboratory of Geological Processes and Mineral Resources, China University of Geosciences (Beijing), China
2. School of Earth Sciences and Resources, China University of Geosciences (Beijing), China
3. Institute of Earth Sciences, China University of Geosciences (Beijing), China
4. Beijing Sensitive High Resolution Ion Micro Probe Center, Institute of Geology, Chinese Academy of Geological Sciences, Beijing, China.

Abstract Tochilinite–cronstedtite intergrowths (TCIs) are key secondary phases in CM carbonaceous chondrites and record aqueous alteration on primitive parent bodies. Among them, the formation mechanism of fibrous Type II TCIs remains poorly constrained at the nanoscale. Here we report a TEM-based study of well-developed Type II TCIs in the CM2 carbonaceous chondrite GRV 13051 using FIB sections, HRTEM, FFT, and STEM-EDS mapping.

The studied TCIs occur in the matrix and show a consistent core–mantle–matrix architecture, comprising an Fe–Ni–S-rich vein-like core, a fibrous tochilinite mantle, and an outer cronstedtite-rich matrix. Two distinct core assemblages were identified: one dominated by monoclinic 4c pyrrhotite, and another containing a Ni-rich linear domain with pentlandite and nanoscale magnetite. Elemental distributions indicate strong nanoscale partitioning, with Ni preferentially retained in the core, whereas Fe and S are concentrated in the vein-centered alteration domain and Si is enriched in the surrounding matrix. The tochilinite mantle shows coherent layered domains with progressive orientation gradients, while the cronstedtite-rich matrix records intense lattice bending and distorted stacking.

These observations suggest that fibrous Type II TCIs formed through localized replacement in a confined microporous environment rather than by simple open-space precipitation. The recurrent core–mantle–matrix organization reflects spatially coupled mass transfer and strong local chemical gradients during aqueous alteration. This study provides new nanoscale mineralogical constraints on the formation of Type II TCIs and on the microenvironmental evolution of aqueous processes in CM chondrite parent bodies.

Key words: CM chondrite, TCI, aqueous alteration, parent-body processes

Acknowledgements The sample was provided by the Polar Research Institute of China. *

NEW RARE-METAL MINERALS FROM THE XIANGHUALING SKARN (SOUTH CHINA)

Can Rao[1*], Xiangping Gu[2], Rucheng Wang[3], Frédéric Hatert[4]

1. School of Earth Sciences, Zhejiang University, Hangzhou 310027, China
2. School of Earth Sciences and Info-physics, Central South University, Changsha, 410083, China
3. State Key Laboratory for Mineral Deposits Research, School of Earth Sciences and Engineering, Nanjing University, Nanjing, 210046, China
4. Laboratoire de Minéralogie, B18, Université de Liège, B-4000 Liège, Belgium

Abstract The Xianghualing skarn is a typical tin-polymetallic (Sn-W-Be-Li) deposit in Linwu County, Hunan Province, in southern China. It occurs in the exocontact zone between the Laiziling granitic pluton and the Middle-Upper Devonian carbonate rocks of the Qiziqiao Formation. The U-Pb dating of the zircon of the protolithionite granite from the Laiziling granitic pluton indicated the age of 155 Ma. Owing to its relatively high concentrations of Li, Be, Sn, W, Rb, Nb, and Ta, the Laiziling granite is generally regarded as the main Sn source of the Xianghualing orebodies, with average Sn concentrations in the Laiziling granite of 65 ppm. The predominant accessory minerals in the Xianghualing skarn include Sn minerals (cassiterite, hulsite, and nigerite group minerals), W minerals (wolframite and scheelite), Be minerals (hsianghualite, liberite, chrysoberyl, hambergite, bertrandite, and taaffeite group minerals), and Li minerals (hsianghualite and liberite). New species of hsianghualite $Ca_3Li_2Be_3(SiO_4)_3F_2$, liberite $Li_2Be(SiO_4)$, and ferrotaaffeite-2*N*'2*S* $BeFe_3Al_8O_{16}$ have been found in this skarn. Focus on rare-metal minerals in the Xianghualing skarn, we discovery four new rare-metal minerals: mengxianminite, chukochenite, zinconigerite-2*N*1*S* and zinconigerite-6*N*6*S*.

(1) Mengxianminite, ideally $Ca_2Sn_2Mg_3Al_8[(BO_3)(BeO_4)O_6]_2$, is closely associated with fluorite, phlogopite, hsianghualite, magnetite, dravite, magnesiotaaffeite-2*N*'2*S* and calcite. The mean chemical composition of mengxianminite (Be and B were measured by secondary ion mass spectrometry, average of 6 electron microprobe analyses and in wt%) is Al_2O_3 40.00, SnO_2 25.96, MgO 6.57, CaO 8.56, FeO 4.83, B_2O_3 6.53, BeO 4.37, ZnO 1.81, MnO 1.23, Na_2O 1.13, TiO_2 0.10, SiO_2 0.04, sum 101.12. The strongest 8 lines of the powder XRD pattern [d in Å (I)(hkl)] are: 3.000(35)(16 2 0); 2.931(100)(17 1 1); 2.475(29)(022); 2.430(30)(13 3 1); 2.375(100)(14 0 2/640); 2.028(52) (21 3 1); 1.807(35)(913); 1.530(98)(14 6 0/15 3 3). Mengxianminite is orthorhombic, space group *Fdd*2; unit-cell parameters refined from single-crystal X-ray diffraction data are: a = 60.689 (3), b = 9.907 (1), c = 5.740 (1) Å, V = 3451.0 (3) Å^3, Z = 8. The structure of mengxianminite is characterized by the alternating O-T1-O-T2-O'-T2 layers stacked along the a axis.

(2) Chukochenite, $LiAl_5O_8$, occurs as subhedral to euhedral crystals up to 200 μm across in the green rock of Xianghualing skarn, closely associated with fluorite, phlogopite, chrysoberyl,

matgarite, chlorite, ferronigerite-2*N*1*S*, and zinconigerite-2*N*1*S*. Electron microprobe analysis (Li by LA-ICP-MS) yielded in wt.% Al_2O_3 80.70, Fe_2O_3 8.16, Li_2O 3.68, ZnO 3.25, MnO 2.49, MgO 1.70, Na_2O 0.11, CaO 0.08, TiO_2 0.02, K_2O 0.01, Cr_2O_3 0.01, total 100.24 wt.%. Chukochenite is orthorhombic, *Imma*, a = 5.659 (1), b = 16.898 (1), c = 7.994 (1) Å, V = 764.46 (8) Å^3, and Z = 6. The stronger nine lines of the powder XRD pattern [d in Å (I) (hkl)] are: 2.405 (53) (231); 1.996 (29) (260); 1.535 (77) (303); 1.413 (100) (264); 1.260 (52) (2 12 0); 1.068 (36) (1 13 4); 1.039 (61) (503); 0.999 (59) (008); and 0.942 (35) (3 13 4). Chukochenite has a framework structure of spinel with low symmetry (orthorhombic *Imma*) due to Li cations ordering in octahedral sites, which is not previously reported for the synthetic analogue $LiAl_5O_8$.

(3) Zinconigerite-2*N*1*S* $ZnSn_2Al_{12}O_{22}(OH)_2$ and Zinconigerite-6*N*6*S* $Zn_3Sn_2Al_{16}O_{30}(OH)_2$, are two new minerals with different numbers and ratios of nolanite (*N*) and spinel (*S*) modules. Both phases have trigonal symmetry; the unit cell parameters of zn-2*N*1*S* (*Pm*1) and zn-6*N*6*S* (*Rm*), refined from single-crystal X-ray diffraction data, are, a = 5.7191 (2) and 5.7241 (2) Å, c = 13.8380 (6) and 55.5393 (16) Å, V = 391.98 (3) and 1575.96 (12) Å^3, and Z = 1 and 3, respectively.

Key words: New minerals, chemical composition, crystal structure, polysomatic series

NEW USES FOR ANCIENT PROCESSES; ENGINEERING MICROBIAL ELECTRON TRANSFER FOR CLEAN INDUSTRIAL GROWTH

Jonathan R Lloyd

Dept of Earth and Envornmental Sciences, University fo Manchester, UK

Abstract The ability to respire high valence metals is distributed widely throughout the prokaryotic world, and can result in the formation of nanoparticles with a range of potential applications. Subsurface Fe(III)-reducing bacteria are a particularly useful resource, capable of converting waste iron oxides to catalytically active magnetic nanoparticles. They also have the potential to target non ferrous metals in waste streams, forming mono and bimetallic nanoparticles with tunable properties, with the ability to drive catalytic reactions that could simplify the production of pharmaceuticals and fine chemicals. Building on these natural, and likely ancient systems, the careful application of Engineering Biology approaches has the potential to deliver the next generation of nature-based solutions to recover waste metals, converting them to valuable functional nanomaterials that can underpin clean industrial growth.

Starting with the conversion of waste Fe(III) oxides, downstream applications including the bioremediation of land and water contaminated with toxic organics, metals and radionuclides will be described, in addition to new work encompassing the energy and agricultural sectors. Other Fe-based bionanoparticle applications that will be discussed will include optimisation of the reactivity and magnetic properties of nano-scale biomagnetite, including the incorporation of transition metal dopants.

Finally the bioreduction of a range of non-ferrous metals to form catalytically active bionanoparticles will also be discussed, aiming to produce industrial catalysts from a range of waste-streams. Single and multi-step catalysis will be reviewed; including the production of high value chiral compounds by combining biosynthesised metallic bionanoparticles and recombinant enzymes, in a single genetically engineered bacterium. A wider discussion of this “biometallic” approach will be given, including the bioproduction of other highly active catalytic nanoparticles for processes including “click chemistry” reactions. The likely impact of Engineering Biology approaches to underpin the optimisation of these potentially disruptive biotechnologies at scale will also be discussed.

Key words: Bioreduction, electron transfer, nanoparticles, bioremediation, catalysis

OCCURRENCE AND ENRICHMENT MECHANISM OF INVISIBLE AU IN CARLIN-TYPE AU DEPOSITS

Zhuojun Xie

State Key Laboratory of Critical Mineral Research and Exploration, Institute of Geochemistry, Chinese Academy of Sciences, China

Abstract A defining characteristic of Carlin-type gold deposits is that invisible gold is primarily hosted in arsenian pyrite, setting them apart from other gold deposit types. In this study, we employed focused ion beam–scanning electron microscopy (FIB-SEM), spherical aberration-corrected transmission electron microscopy (AC-TEM), and atom probe tomography (APT) to investigate the nature of invisible gold and its evolution during subsequent geological events. TEM analyses show that high-grade arsenian pyrite contains extensive gold-enriched domains. These domains display trace element signatures asso-ciated with gold (Sb, Tl, Hg, Cu) in energy-dispersive X-ray spectroscopy (EDS), but no detectable me-tallic nanoparticles. APT data reveal that invisible gold is distributed in complex, oscillatory-zoned mi-cro- to nanoscale bands, with gold occurring homogeneously at the atomic scale rather than as discrete nanoclusters. Importantly, AC-TEM confirms that gold is structurally incorporated by substituting for iron in the lattice and occupying vacancy sites. The widespread presence of stacking faults and na-noscale fluid inclusions in gold-bearing arsenian pyrite points to rapid crystallization conditions. Curved dislocations pinned by solid inclusions record subsequent annealing processes.

By integrating nanoscale textural observations with geologic context, we propose that invisible gold was initially incorporated into the arsenian pyrite crystal structure during rapid precipitation. Later post-ore thermal events induced annealing of the ionic gold-bearing arsenian pyrite, leading to trace element redistribution and the formation of gold-bearing nanoparticles. The dominant occurrence of ionically bound gold in arsenian pyrite suggests that the ore-forming fluids were undersaturated with respect to gold during pyrite crystallization. This process of gold deposition from gold-undersaturated, arsenic-rich ore fluids ultimately produced the giant Carlin-type gold deposits..

Key words: Carlin-type gold deposits, occurrence of invisible gold, enrichment mechanism of invisible gold

ON THE CONCEPTUAL FOUNDATIONS, CONTEMPORARY RESEARCH PARADIGMS, AND EVOLVING KNOWLEDGE ARCHITECTURE OF GENETIC MINERALOGY

Sheng-Rong Li[1,2*], Lin Li[1,3], Mao-Wen Yuan[1,2] , Masroor Alam[4] * Corresponding author: E-mail: lisr@cugb.edu.cn

1. National Key Laboratory of Geological Processes and Mineral Resources, China University of Geosciences, Beijing, 100083
2. School of Earth Science and Resources, China University of Geosciences, Beijing, 100083
3. Institute of Geoscience, China University of Geosciences, Beijing, 100083
4. Department of Geology and Mountain Hazards, Karakoram International University, Gilgit 15100 Pakistan

Abstract Genetic mineralogy is a foundational branch of modern mineralogy that investigates the thermodynamic conditions and kinetic processes governing the formation, stability fields, and compositional variations of minerals and mineral assemblages, along with their diagnostic typomorphic features. The term "genetic mineralogy" was first coined by Soviet mineralogist D.S. Fedorovski in the 1920s. In the 1980s, Chinese mineralogist Chen Guangyuan and his colleagues established a disciplinary framework, and proposed six diagnostic characteristics of mineral typomorphism, and four fundamental operational principles for mineralogical mapping. After decades of development, the current theoretical system of genetic mineralogy has been gradually improved and covers eight core components, including: (1) Mineral ontogeny and phylogeny (mineral or mineral group / assemblage formation, spatiotemporal distribution and evolution, deep-Earth and planetary mineralogy); (2) Mineral typomorphism (mineral index or fingerprint; typomorphic mineral assemblage / species / characteristics; indicator Minerals); (3) Mineral thermobarometry (high / low temperature - high / low pressure simulaton experimental / computational mineralogy); (4) Mineral paragenesis (paragenetic assemblages / models / sequences and paragenetic analysis); (5) Mineral genetic classification (system, genetic / prospecting groups); (6) Application of mineralogenetic information (geodynamic events, geo-processes, resources, environment, life / medicion); (7) Discipline historiography for genetic mineralogy (development history, systemics, major achievements and lessons, represent intellectual pioneers and future research frontiers); (8) Genetic mineralogical research methodology (epistemology and workfow, mineralogical mapping, artificial intelligence (AI), big-data). Among the 8 aspects, mineral typomorphism serves as the disciplinary cornerstone. Since the 21st century, methodologies for genetic mineralogical study have undergone substantial refinement, revealing highly-resolved mineral growth patterns through advanced analytical techniques. Contemporary research has robustly elucidated the geodynamic significance, tectonic implications, and evolutionary signatures

of mineral typomorphism. Genetic mineralogy has progressively integrated with environmental and biological processes, crystallizing into the subdiscipline of environmental and bio- and vita-mineralogy, thereby expanding the conceptual frontiers of genetic mineralogy. We suggest that future research in genetic mineralogy should priorities the systematic integration of scientific findings; experimental investigations of mineral ontogeny combined with AI-assisted mineral identification; the convergence of mineral big-data analytics with studies on phylogenetic evolution and genetic classification. Furthermore, enhanced global knowledge exchange is essential to transform genetic mineralogical advancements into collective intellectual heritage.

Key words: Theoretical fundamentals, Research domains, Disciplinary architecture, Evolutionary trajectories, Philosophy of mineralogy

ORIGIN OF MO-RICH SCHEELITE IN THE RUANJIAWAN OXIDIZED SKARN TUNGSTEN SYSTEM

Shitao Zhang [1], Jian-Feng Gao [1,2*], Yihui Lyu [1,3], He Zhang [4], Yuzhou Feng [5], Qiang Zhang [1], Bing Xiao [6], Hao Xu [1,2], Di Ding [1] *Corresponding Author: e-mail, gaojianfeng@mail.gyig.ac.cn (Jianfeng Gao)

1. State Key Laboratory of Critical Mineral Research and Exploration, Institute of Geochemistry, Chinese Academy of Sciences, Guiyang 550081, China
2. University of Chinese Academy of Science, Beijing 100049, China
3. Daye Nonferrous Metals Co., Ltd., Huangshi 435005, China
4. State Key Laboratory of Critical Earth Material Cycling and Mineral Deposits, School of Earth Sciences and Engineering, Nanjing University, Nanjing 210023, China
5. Department of Geological Sciences, University of Saskatchewan, Saskatoon, Saskatchewan S7N 5E2, Canada
6. State Key Laboratory of Deep Earth Processes and Resources, Guangzhou Institute of Geochemistry, Chinese Academy of Sciences, Guangzhou 510640, China

Abstract Skarn-type tungsten deposits constitute one of the primary sources of global tungsten resources, hosting more than 70% of the world's total tungsten reserves. Scheelite, the dominant tungsten-bearing mineral in skarn systems, acts as an essential geochemical tracer for recording the physicochemical evolution of ore-forming processes throughout multiple hydrothermal stages. Scheelite from oxidized skarn deposits generally contains higher Mo contents than that from reduced skarn counterparts. However, the controls on Mo enrichment in scheelite remain insufficiently understood and widely debated. Current models mainly attribute Mo enrichment either to intrinsically Mo-rich and oxidized ore-forming fluids or to oxidation induced by meteoric-water influx.

The Middle–Lower Yangtze River Metallogenic Belt (MLYRB) is an important skarn–porphyry Cu–Au-W metallogenic belt in eastern China. Mineralization within this belt is genetically linked to Late Mesozoic high-K calc-alkaline granitoids, which were traditionally considered to possess limited tungsten metallogenic potential. However, several concealed medium-to-large W(–Cu–Mo) deposits have been recently discovered along the periphery of these granitoid systems. The Ruanjiawan tungsten deposit represents a typical skarn tungsten deposit in the MLYRB and provides an ideal case for investigating the formation of Mo-rich scheelite. Petrographic observations and paragenetic analysis reveals four distinct generations of scheelite corresponding to different hydrothermal stages. The earliest generation (Sch1) in the prograde skarn stage occurs as anhedral grains with weak zoning. Sch2, formed during the retrograde alteration stage (S2), consists of anhedral grains characterized by bright cores and dark jagged rims. Sch3, precipitated during the quartz–scheelite stage (S3), displays well-developed concentric oscillatory zoning with

enhanced luminescence along crystal margins or on one side of the grains. The latest generation, Sch4, formed during the quartz–scheelite–sulfide stage (S4), exhibits complex replacement textures distinguished by contrasting CL responses. Sch4a is characterized by a dark core surrounded by a bright mantle and oscillatory-zoned rim, whereas Sch4b displays metasomatic texture in which residual dark domains (Sch4b-core) are overprinted by irregular bright replacement fronts (Sch4b-rim). EPMA and LA–ICP–MS analyses indicate that most scheelite generations have comparable major element compositions. In contrast, the Sch4b-core is characterized by exceptionally high MoO_3 contents (6.21–9.14 wt%), elevated CaO and SO_3. This generation also exhibits lower Nb and higher total REE contents than other scheelite generations, deviating from the normal evolutionary trend of Nb and REE differentiation in hydrothermal system. Both the core and rim of Sch4b display weak Eu anomalies and distinctive REE partitioning patterns compared with earlier scheelite generations. TEM observations further reveal that Mo enters the crystal lattice primarily through substituting for W, and that extensive Mo incorporation induces crystal dislocations without forming independent Mo-bearing mineral phases.

From Sch1 through Sch2, Sch3 and Sch4a, scheelite records progressively increasing Mo contents accompanied by decreasing δEu and δCe values, reflecting an overall evolution toward increasingly oxidized hydrothermal conditions. Combined with regional geology and previous studies, the extreme Mo enrichment observed in Sch4b-core is interpreted to result from the combined influence of local evaporite strata and episodic influxes of Mo-rich hydrothermal fluids. These processes promoted localized formation of high-Mo scheelite during the quartz–scheelite–sulfide stage of the Ruanjiawan tungsten deposit. This study demonstrates that highly Mo-rich scheelite can develop locally under transient oxidizing conditions during the late quartz–sulfide stage of skarn tungsten systems, a stage that is typically characterized by reducing hydrothermal environments.

Key words: Scheelite, LA–ICP–MS, Redox condition, Tungsten skarn deposit, Eastern China

Acknowledgements This research was financially supported by the National Key R&D Program of China (2023YFC2906802), and the Key Research and Exploration Fund for Critical Minerals of the State Key Laboratory (202403).

OXYGEN ISOTOPE STUDY OF UV-INDUCED PHOSPHITE OXIDATION

Dongjun Kim[1,2], Sae Jung Chang[2], Ruth E. Blake[3] Kideok D. Kwon[1]

1. Department of Geology, Kangwon National University, Republic of Korea
2. Metropolitan Seoul Center, Korea Basic Science institute, Republic of Korea
3. The Department of Earth and Planetary Sciences, Yale University, USA

Abstract It is generally accepted that phosphate (PO_4^{3-}, P(V)) is the dominant phosphorus species at Earth's surface and does not undergo redox reactions under ambient conditions. However, recent geological evidence suggests that reduced phosphorus species, particularly phosphite (PO_3^{2-}, P(III)), may have predominated in early anoxic oceans, where intense UV radiation could have subsequently oxidized phosphite to phosphate (P(III) to P(V)). The oxygen isotopic composition ($^{18}O/^{16}O$, $\delta^{18}O$) of phosphate has been proposed as a biomarker for early microbial life. It is crucial to determine the isotopic signatures of abiotic reactions/oxidation of reduced phosphorus, in order to establish an abiotic baseline value for $\delta^{18}O$ as well as to clearly distinguish biotic from abiotic $\delta^{18}O$ signatures. In this study, we determined the $\delta^{18}O$ values of dissolved phosphate produced by UV-induced oxidation of phosphite. This reaction was conducted using ^{18}O-labeled phosphite and water at pH 7 under both ambient air and Ar-purged conditions. After 12 hours of UV exposure (1,200 W), more than 93% of the aqueous phosphite was oxidized to phosphate. The $\delta^{18}O$ values of the product phosphate covaried with those of the ambient water, with linear regression slopes of approximately 0.2. This indicates that only ~20% of the oxygen atoms in the product phosphate were derived from the ambient water, while the majority of oxygen were inherited from the phosphite precursor. No significant difference in $\delta^{18}O$ values was observed between ambient air and Ar-purged conditions, suggesting that atmospheric oxygen species (e.g., O_2, CO_2) were not incorporated into the product phosphate. Consequently, the $\delta^{18}O$ values of UV-oxidized phosphate remain distinct from known biotic signatures. These findings have important implications for interpreting phosphate $\delta^{18}O$ biosignatures preserved in ancient terrestrial and extraterrestrial samples.

Key words: Phosphate, Phosphite, Oxygen isotopes, Biomarker, Ultraviolet radiation

P-FE-MN CO-EVOLUTION REVEALED BY MINERAL NETWORKS AND ITS CONTROLS ON GLOBAL ANCIENT OXYGENATION

Ziyi Zhuang[1,2], Yan Li[1,2,†], Rongzhang Yin[1,2], Ganyu Tang[2], Junqi Wu[1,2], Chunjiang Li[1,2], Yong Lai[2]

1. SKLab-DeepMinE, MOEKLab-OBCE, School of Earth and Space Sciences, Peking University, Beijing 100871, China
2. Beijing Key Laboratory of Mineral Environmental Function, School of Earth and Space Sciences, Peking University, Beijing 100871, China †Corresponding author. Email: liyan-pku@pku.edu.cn

Abstract Phosphorus (P) dominates primary productivity, organic carbon burial and oxygenic photosynthesis, whereas the linkage between its elemental couplings and atmospheric oxygen evolution remains poorly constrained. This study integrates mineral network, phylogenetic and correlation analyses, combined with spectroscopic and microscopic techniques, to explore the co-evolution of P, Fe and Mn throughout Earth's history. Before the Great Oxidation Event (GOE), P-bearing minerals originated mainly from magmatic and sedimentary processes, and shifted to mixed intrusive and weathering origins after the Mesoproterozoic. The material supply for photosynthetic Mn clusters gradually transformed from deep-Earth-dominated to coupled deep-surface processes during the GOE–Neoproterozoic Oxygenation Event (NOE). Low-valent Fe and Mn prevailed in the Archean, whereas mixed redox states in the Mesoproterozoic indicate dynamic elemental cycling. Multiple geological and biological processes jointly regulated bioavailable P, amplifying oxygen production during two major oxygenation events. Future integrated approaches will clarify how P-mineral evolution controlled the tempo and heterogeneity of ocean–atmosphere oxygenation.

PORPHYRY FERTILITY EVALUATION AND HYDROTHERMAL CENTER VECTORING IN THE PERIPHERY OF THE SANDAOWANZI EPITHERMAL AU DEPOSIT, NE CHINA

Zong-Yong Yang [1], Jing-Jing Zhu [1]*, Xing-Chun Zhang [1], Dongyan Shi [2], Kun Zhang [2], Shitao Zhang [1] Corresponding author, e-mail: zhujingjing-vip.gyig.ac.cn

1. State Key Laboratory of Critical Mineral Research and Exploration, Institute of Geochemistry, Chinese Academy of Sciences, Guiyang 550081, China
2. Heilongjiang Mining Group Co. Ltd., Harbin 150036, China

Abstract At present, the exploration of shallow porphyry deposits is challenged by increasing exploration expenditure accompanied by decline discovery efficiency. So, mineral exploration increasingly focused on searching under cover, e.g., greenfield (without any previous exploration basis) and brownfield areas (with limited existing exploration works). The prophylitic alteration characterized by the occurrence of chlorite and epidote, is typically the most ubiquitous and laterally extensive alteration in porphyry ore systems. The eastern Great Hinggan Range, NE China, is well known for epithermal Au deposits and porphyry Mo deposits. Large-scale chloritization alteration is developed within the volcanic rocks in the periphery of the Sandaowanzi epithermal Au deposit, however, its porphyry Cu-Au endowment and potential mineralization center remain unclear.

Systematic mineral analyses of zircon, apatite, chlorite and epidote were carried out on altered rocks in the Sandaowanzi mining area, with aims to evaluate the metallogenic potential and identify the potential hydrothermal/mineralization center. Chemical composition of zircon and apatite suggest these Early Cretaceous magmas were characterized by high magma oxygen fugacity, high H_2O and S contents, conditions favorable for the formation of porphyry deposit. Epidote from these altered rocks is enriched in distal pathfinder elements such as As, Sb, Pb and Zn. Combined with the high Zn and Mn concentrations in chlorite, indicating favorable conditions for porphyry mineralization. The high Ti/Sr and V/Ni ratios of chlorite indicates the region defined by holes of ZK801, ZK805 and ZK802 represents a potential hydrothermal center. This conclusion is consistent with the observation of intensive silification, occurrence of dickite–alunite–pyrophyllite assemblage, and the spectral character of muscovite group minerals with high maturity (IC value) from the same region, providing supportive evidence for future mineral exploration and prospecting in the region.

PREDICTING COMPLEX MINERAL COMPOSITIONS IN GALE CRATER, MARS BASED ON CHEMIN INSTRUMENT X-RAY DIFFRACTION AND MACHINE LEARNING

Shaunna M. Morrison[1], Anirudh Prabhu[2], Jarrod Burges[1], Zak Jibrin[1], Ahmed Eleish[3]

1. Department of Earth and Planetary Science, Rutgers University, USA
2. Earth and Planets Laboratory, Carnegie Institution for Science, USA
3. Tetherless World Constellation, Rensselaer Polytechnic Institute (RPI), USA

Abstract The CheMin X-ray diffractometer onboard the NASA Mars Science Laboratory (MSL) Rover, Curiosity, performs X-ray diffraction (XRD) experiments on martian rock and sediment collected in Gale crater. To gain a greater understanding of the formational conditions and geologic history of Gale crater and the minerals found therein, the CheMin team developed a crystal-chemical method to predict limited chemical compositions of the minerals observed in the CheMin samples (e.g., Fe-Mg olivine, Na-Ca plagioclase, K-Na alkali feldspar, Mg-Fe-Ca pyroxene, alunite-jarosite). Previous methods were chemically constrained due to the complexity of the crystal chemical relationships beyond three chemical components. However, in this study we adapt a machine learning technique, Label Distribution Learning (LDL), to predict multicomponent chemical compositions of Gale crater mineral phases, thereby allowing for more detailed petrologic interpretation of the geologic history of the martian surface.

LDL is a novel framework for classification problems with small datasets and has been widely applied to facial recognition problems such as age estimation. In this study, we adapt the LDL algorithm such that it can predict chemical elements (labels) and their abundances (degrees) for each martian mineral sample, based on crystallographic parameters. We evaluate performance using distance and similarity between label distributions as well as mean square error and also compare the results to traditional machine learning methods.

This work is expanding our understanding of Gale crater, Mars, and the processes that formed the terrestrial bodies in our solar system.

Key words: Mars, Machine Learning, Planetary Mineralogy, Crystal Chemistry, Gale crater

PYRITE AS A MULTI-PROXY RECORDER OF HYDROTHERMAL EVOLUTION: INSIGHTS INTO CU–AU DECOUPLING IN PORPHYRY–EPITHERMAL SYSTEM, MANGLA DEPOSIT, TIBET

Yan Nie, Yang Song*, Haiming Liu, Nan Wang

Institute of Mineral Resources, Chinese Academy of Geological Sciences, Beijing

Abstract The Gangdese metallogenic belt in southern Tibet represents one of the most significant Cu-producing provinces in China, hosting a wide spectrum of mineralization styles, including porphyry Cu–Au, Cu–Mo, Mo (±Cu), skarn, and epithermal systems. Representative deposits such as Qulong, Jiama, and Zhunuo are Miocene collision-related porphyry Cu polymetallic systems. Despite the belt's substantial endowment (>43 Mt Cu), intense uplift and erosion associated with the India–Eurasia collision have largely removed shallow epithermal systems. In contrast, the western Gangdese segment preserves well-developed Miocene volcanic sequences due to relatively limited exhumation, providing favorable conditions for the preservation of porphyry–epithermal systems. The Mangla deposit, discovered in 2024, is the first recognized Miocene porphyry–epithermal Cu–Au system in this region. This discovery extends the western limit of the Gangdese Cu belt by nearly 1,000 km and highlights the strong exploration potential of Miocene continental volcanic terranes, offering new constraints on regional metallogenic models.

Pyrite, a ubiquitous sulfide in hydrothermal systems, exhibits semiconducting behavior and measurable thermoelectric properties arising from charge carrier diffusion under a temperature gradient. Depending on composition and defect chemistry, pyrite may exhibit both N-type (electron-dominated) and P-type (hole-dominated) conductivity. The spatial distribution of these conductivity types has been shown to record hydrothermal processes and constrain orebody architecture. This property has been successfully applied in exploration across diverse deposit types, including hydrothermal Au, Pb–Zn–Ag, skarn Mo, porphyry, and Co–Ni systems, demonstrating its broad applicability.

In this study, we integrate LA–ICP–MS trace element geochemistry, thermoelectric measurements, electrical resistivity, and machine learning classification to reconstruct the evolution of the Mangla Cu–Au magmatic–hydrothermal system. Pyrite textures and compositions define three generations (Py1–Py3), recording progressive overprinting from early high-temperature Co–Ni-rich fluids, through intermediate Au–Ag–As–Sb-rich epithermal fluids, to late Cu–Pb–Bi-rich hydrothermal events. Machine learning results consistently indicate a dominant epithermal affinity.

Trace element systematics reveal strong Au–As coupling and Au–Ag co-precipitation, consistent with bisulfide complex transport and coupled substitution mechanisms. In contrast, Cu shows

decoupled behavior, occurring both as lattice-bound Cu and inclusion-hosted sulfides, reflecting distinct physicochemical controls. Thermoelectric measurements document a systematic transition from P-type pyrite at shallow levels to N-type at depth, recording vertical gradients in redox conditions and temperature. Estimated formation temperatures (~78–379 °C) are consistent with independent geothermometric constraints.

Collectively, these results demonstrate that the Mangla deposit represents a vertically zoned porphyry–epithermal transitional system in which Cu and Au mineralization formed during temporally discrete hydrothermal pulses rather than from a single evolving fluid. This decoupling reflects variations in metal transport mechanisms, ligand stability, and structurally focused fluid flow. Our study highlights pyrite as a robust multi-proxy recorder of hydrothermal evolution and a powerful tool for constraining orebody architecture, providing a new framework for exploration in continental volcanic terranes.

Key words: Pyrite, Thermoelectricity, Gangdise metallogenic belt, Tibet

Acknowledgements This study was supported by the National Key R&D Program of China (Deep Earth Project; Grant No. 2025ZD1006200), the National Natural Science Foundation of China (Grant No. 42172100), and the China Geological Survey Program (Grant No. DD202302034).

PYRITE-HOSTED PRIMARY AND SECONDARY GOLD-TELLURIDE MINERALIZATION AT XIAOYINGPAN: DISCRIMINATING THE ROLES OF COUPLED DISSOLUTION-REPRECIPITATION AND TE-AU-AG MELTS

Dazhao Wang[1,2], Dahong Xiao[1,2]

1. National Key Laboratory of Uranium Resources Exploration-Mining and Nuclear Remote Sensing, East China University of Technology, Nanchang, China
2. School of Earth and Planetary Sciences, East China University of Technology, Nanchang, China

Abstract The Xiaoyingpan Au-Te deposit (55 t Au, 50 t Te) in the Zhangjiakou district, North China Craton, is characterized by complex pyrite textures and an abundance of gold and telluride minerals, recording multistage mineralization and deformation. Three pyrite generations (Py1, Py2, Py3) are identified, with Py2 being the main gold-bearing generation. This study integrates petrography, electron back-scattered diffraction (EBSD), electron probe microanalysis (EPMA), LA-ICP-MS trace element, and in-situ sulfur isotopes to distinguish primary and remobilized gold and tellurides, and to unravel the mechanisms of Au-Te hyper-enrichment.

Py1 occurs as euhedral, undeformed crystals with primary inclusions of tellurides and native gold. Py2 is the product of deformation-assisted coupled dissolution-reprecipitation (CDR) of Py1, and can be subdivided into Py2a (porous, with relict primary textures) and Py2b (highly porous, inclusion-rich, and lattice-distorted). Py3 forms through dynamic recrystallization of Py1 and contains minor gold. Primary and secondary native gold and tellurides are identified in the deposit. Primary native gold consists of Au2a (coarse, euhedral grains hosted within Py2a) and Au2b (irregular grains filling fractures in Py2a or oxidized ores); both precipitated directly from the early ore-forming fluid. Secondary native gold comprises Au2c and Au2d. Au2c occurs as fine grains intimately intergrown with remobilized tellurides in Py2b, precipitating synchronously with the consolidation of a Te-Au-Ag melt. Au2d forms unique bamboo-shoot-like aggregates growing perpendicular to telluride surfaces; these are interpreted to result from the oriented attachment of gold nanoparticles that nucleated on tellurides during CDR-driven dissolution of primary gold-telluride inclusions. Primary tellurides, including petzite, hessite, altaite, stützite, sylvanite, and melonite, are found as large composite inclusions in Py2a or galena. They formed either by direct precipitation from the magmatic-hydrothermal fluid or by crystallization of a primary Te-Au-Ag melt. Secondary tellurides occur exclusively within Py2b as irregular, small (<10 μm) grains with low interfacial angles, indicative of melt crystallization. These formed when primary telluride assemblages were remelted due to elevated temperatures (260–350 °C) coupled with the low-melting-point depression caused by Pb, Bi, and other elements. The resulting Te-Au-Ag melt, with viscosity comparable to water, migrated along micro-fractures and pores, scavenging reduced Au,

Ag, and Te atoms that were released by CDR or reduced on pyrite surfaces. This melt acted as an efficient collector and transport medium for precious metals, carrying them to Py2b domains where it subsequently solidified, forming calaverite, petzite, hessite, and electrum.

The CDR process itself liberated inclusion-hosted elements (Au, Ag, Te, Cu, Pb) from Py1, while lattice-bound Co and Ni remained immobile. Mass-balance estimates suggest significant gold and silver were lost to the fluid phase before being captured by the melt. Homogeneous sulfur isotope values (δ^34^S = –11.7 to –8.7‰) across all pyrite generations confirm that sulfur and metals were internally recycled without significant external input, consistent with a magmatic source linked to the Devonian Shuiquangou alkaline complex.

We propose that the exceptional Au-Te endowment of Xiaoyingpan resulted from a two-stage process: initial deposition of primary gold and tellurides from a magmatic fluid, followed by deformation-assisted CDR and generation of low-melting-point Te-Au-Ag melts that efficiently remobilized and concentrated precious metals within Py2b. This model underscores the importance of micro-scale dissolution-reprecipitation and melt-mediated transport in forming high-grade telluride-gold deposits and provides a framework for interpreting complex ore textures in polydeformed terranes.

Key words: Pyrite, Tellurides, Native gold, Coupled dissolution-reprecipitation, Te-Au-Ag melt

Acknowledgements This study was funded by the China National Natural Science Foundation (92462306 and 42373072) and the Jiangxi Provincial Natural Science Foundation (grant 20252BAC220018).

PYRITE THERMOELECTRICITY AND IN-SITU TRACE ELEMENTS: IMPLICATIONS FOR DEEP PROSPECTING AT THE QINGLONGGOU GOLD DEPOSIT, NORTHERN MARGIN OF QAIDAM BASIN

Yiming Xie[1]，Min Chen[1,*]，Jian Li[2,3]，Genhou Wang[1,4]，Wentao Zhao[1]，Hailin Xie[2,3]，Jinhua Ma[1]

1. Shool of Geological Engineering, Qinghai University, China;
2. The No.1 Geological Survey Institute of Qinghai Province, China;
3. Qinghai Qaidam Large-Superlarge Gold Deposit Deep Exploration Technology Innovation Engineering Research Center, China;
4. School of Earth Sciences and Resources, China University of Geosciences, China

Abstract The Qinglonggou gold deposit is located in the Tanjian Mountain giant gold field along the northern margin of the Qaidam Basin, the sole super-large gold field in this region. In recent years, significant breakthroughs have been made in deep and peripheral exploration, yet understanding of its genesis and metallogenic environment remains limited. Orebodies are hosted in Mesoproterozoic Wandonggou Group phyllite and marble and are distinctly controlled by structures. Pyrite is the principal gold-bearing mineral, and its thermoelectric properties(N-type indicating high temperature, P-type indicating medium-low temperature) combined with in situ trace element compositions provide important constraints on ore-forming fluids and deposit genesis. Ore-stage pyrite samples from different depths of drill cores along exploration line 51 in the No. II ore belt were analyzed for thermoelectric characteristics and trace elements, to infer the mineralization stages and model of the Qinglonggou gold deposit, summarize deep prospecting indicators, and provide a scientific basis for future exploration. The test results show that, pyrite from different depths is predominantly of mixed P-N type, with thermoelectric coefficients mainly ranging from -250 μV/℃ to 0. Formation temperatures cluster at 50–150 ℃ and 350–525 ℃. Mineralizing fluids are enriched in As, Au, Cu, and Sb. Most pyrite samples show Co/Ni ratios of 0.1–1, whereas a minor proportion ＞1. Deep-level pyrite contains mantle platinum-group elements (Pd, Pt). It indicates that the Qinglonggou Gold Deposit exhibits characteristics of both low-temperature and medium- to high-temperature mineralization, with elemental features analogous to those reported in previous studies on Carlin-type gold deposits. Mineralization was influenced by both hydrothermal and sedimentary processes, with possible incorporation of mantle materials into the ore-forming fluids. Overall, the Qinglonggou deposit is interpreted as a Carlin-orogenic composite-type gold deposit. Shallow mineralization is dominated by medium- to low-temperature hydrothermal processes influenced by sedimentary metamorphism, whereas deep mineralization reflects the combined effects of sedimentary metamorphism and high-temperature hydrothermal

activity, recording multi-stage mineralization with mantle material input. Exploration should focus on structurally altered zones characterized by As-Au-Cu-Sb assemblages and P-N-type pyrite thermoelectric signatures.

Key words: Qinglonggou Deposit, pyrite, thermoelectricity, LA-ICP-MS, prospecting implications

Acknowledgements We thank Zhengzhi Zhang and Tongpeng Xie from the First Institute Geology and Mineral Exploration of Qinghai Province for helps during our field work; and Yafang Liu for her technical supports in running the LA-ICP-MS analyses. We are grateful to two anonymous reviewers and editors for their constructive suggestions and efficient handling. This work was funded by the Bureau of Geological Exploration and Development of Qinghai Province, Xining, China(2024-79-19).

QUANTITATIVE MINERAL-GEOCHEMICAL CONSTRAINTS ON OROGENIC GOLD FORMATION: QUARTZ–PYRITE INSIGHTS FROM THE NIANZHA DEPOSIT, YARLUNG–TSANGPO SUTURE ZONE

Xiangfa Song[1], Degao Zhai[1*], Jinchao Wu[1], Zijun Qiu[1], Qingqing Zhao[1], Jian-Feng Gao[2]

1. School of Earth Sciences and Resources, and State Key Laboratory of Geological Processes and Mineral Resources, China University of Geosciences Beijing, China
2. State Key Laboratory for Critical Mineral Research and Exploration, Institute of Geochemistry, Chinese Academy of Sciences, China

Abstract Orogenic gold deposits represent a class of mineral systems characterized by coherent tectono-thermal histories and deposit-scale features, yet the sources of their fluids and metals remain debated. Here, we investigate the Nianzha gold deposit in the Yarlung–Tsangpo suture zone (YTSZ) using a trace-element-based XGBoost classification framework applied to quartz and pyrite, aimed at quantifying fluid and metal sources. Trace-element datasets of quartz and pyrite from global orogenic (metamorphic-fluid) and porphyry–skarn (magmatic hydrothermal fluid) gold systems were used to train XGBoost classifiers, distinguishing magmatic from metamorphic fluid systems. The model demonstrates that the combined effect of multiple trace elements enables robust discrimination, whereas single-element proxies alone are often insufficient. Applied to the Nianzha deposit, quartz consistently records metamorphic-fluid signatures, whereas pyrite exhibits mixed affinities, reflecting selective incorporation of magmatic-derived solutes. Monte Carlo integration of mineral-specific XGBoost probabilities confirms a predominantly orogenic character at the deposit scale. These observations, supported by fluid-inclusion and stable-isotope evidence, are consistent with a model in which low-salinity metamorphic fluids generated during prograde metamorphism remobilized pre-enriched S–Au reservoirs in the lower crust or lithospheric mantle, transporting metals along structural pathways and precipitating gold. We term this the "subduction–devolatilization reservoir preconditioning–metamorphic remobilization" model. Our results demonstrate that integrating high-resolution mineral geochemistry with multivariate machine learning and probabilistic modeling provides a robust framework for resolving fluid and metal sources in complex orogenic gold systems.

Key words: Orogenic gold deposits, Trace elements, XGBoost, Yarlung–Tsangpo suture zone

Acknowledgements This work was supported by the National Key R&D Program of China

(2023YFC2906805).

QUARTZ TEXTURES AND TRACE ELEMENT GEOCHEMISTRY AS TRACERS OF FLUID EVOLUTION IN OROGENIC GOLD SYSTEMS

Parfait M. Mupenge, Degao Zhai*, Xiangfa Song, Gaoxin Zhang, Qingqing Zhao, Gang Zhao
School of Earth Sciences and Resources, and State Key Laboratory of Geological Processes and Mineral Resources, China University of Geosciences Beijing, China

Abstract Quartz, a ubiquitous gangue mineral in veins and veinlets of orogenic gold deposits, precipitates throughout the evolution of hydrothermal systems, and its resistance to later alteration makes its trace-element composition a reliable tracer of crystallization conditions and ore-forming processes. Quartz samples from different hydrothermal stages in the Wangu and Huangjindong Au-W deposits of the Jiangnan Orogenic Belt, South China, were investigated using petrography, SEM cathodoluminescence (CL), and in situ LA-ICP-MS trace-element analyses to constrain the evolution and physicochemical conditions of ore-forming fluids. Distinct paragenetic quartz stages identified in both deposits record successive hydrothermal events through characteristic CL textures and trace-element signatures. Quartz trace-element systematics indicate crystallization temperatures below 350 °C, while zoning patterns reflect short-lived fluctuations in fluid temperature and chemistry. Variations in Al, Li, K, Sb, and As suggest lattice-controlled substitutions, with Al-Li defect centers dominating quartz luminescence. Quartz chemistry records fluid evolution from early near-neutral, CO_2-rich W-bearing fluids, to acidic Au-As-bearing ore fluids during main-stage mineralization, followed by late low-temperature Ca-rich fluids associated with quartz-calcite veining. Collectively, quartz textures and geochemical signatures from the Huangjindong and Wangu deposits indicate that different quartz generations formed during discrete hydrothermal fluid pulses under progressively evolving physicochemical conditions. Comparison with published global and regional quartz trace-element datasets shows that the Wangu and Huangjindong quartz compositions overlap closely with those of orogenic gold systems and rule out SEDEX, porphyry, and epithermal systems. Overall, the results of this study demonstrate that integrated quartz petrography, CL imaging, and trace-element geochemistry provide an effective framework for reconstructing fluid evolution and metal deposition in orogenic gold systems.

Key words: *Quartz textures, *Trace element geochemistry, *Hydrothermal fluid, *Orogenic Au-deposits

Acknowledgements This work was supported by the National Key R&D Program of China (2023YFC2906800).

QUARTZ TRACE ELEMENTS AS INDICATORS OF FLUID EVOLUTION AND MINERALIZATION IN LOW- TO MEDIUM-TEMPERATURE HYDROTHERMAL SYSTEMS

Shen Gao[1,2*]

1. State Key Laboratory of Geological Processes and Mineral Resources, China University of Geosciences, Beijing 100083, China
2. School of Earth Sciences and Resources, China University of Geosciences (Beijing), Beijing 100083, China

Abstract Quartz is the most common gangue mineral in hydrothermal ore deposits. However, its trace element geochemistry remains underutilized as a tool for deciphering fluid evolution and discriminating mineralization types. We integrate detailed quartz textural and compositional analyses from three distinct hydrothermal systems: adularia-sericite epithermal Ag-base metal deposits, low- to medium-temperature Sb-Au deposits, and granite-related U deposits. Using scanning electron microscope cathodoluminescence (SEM-CL), laser ablation-inductively coupled plasma-mass spectrometry (LA-ICP-MS), and electron spin resonance (ESR), we identify systematic relationships between quartz trace-element signatures, CL spectral features, and ore-forming processes. In epithermal Ag-base metal systems, magmatic quartz exhibits homogeneous CL with peaks at 360 and 415 nm and low Sb (median 0.1 ppm). Hydrothermal type I quartz (cooling origin, zonal textures, base metal sulfides) has low Sb (median 4.5 ppm) and positive Sb-Al and Li-Al correlations, whereas type II quartz (boiling origin, high-intensity 580 nm CL peak, associated with Ag minerals) shows the highest Sb (median 71 ppm) and elevated E'1 centers indicating rapid crystallization. In Sb-Au systems, Ti/Al ratios discriminate host-rock affinities (>0.005 for igneous-hosted, <0.005 for sedimentary-hosted), and Sb-As plots link Sb mineralization with metamorphic-hosted systems and Au mineralization with igneous-hosted systems. Li-Al trends further distinguish fluid evolution in vein-type Sb, intrusion-related Au, and Carlin-type Au deposits. In granite-hosted U systems, ore-stage quartz is CL-dark (650 nm peak), U-rich, with elevated Mn, Al, and Sb, and formed via late-stage fluid events following early barren hydrothermal quartz. Altered magmatic quartz records low-temperature fluid-rock reactions, and rimmed textures mark the U-mineralizing event. Collectively, these results demonstrate that quartz texture, CL spectra, trace elements (particularly Sb, Al, Li, Ti, Ge, and As), and ESR centers can effectively discriminate cooling from boiling, magmatic from hydrothermal origins, and identify key mineralization stages. Such quartz-based fingerprints provide robust exploration guides for Ag-base metal, Sb-Au, and granite-related U deposits in low- to medium-temperature hydrothermal systems.

Key words: Quartz, Cathodoluminescence, Trace elements, Fluid evolution, Hydrothermal

systems

RECYCLED VOLATILES AND POST-SUBDUCTION PORPHYRY ORE SYSTEMS

Author name (Bo, Xu)[1,2], Author name (Zeng-Qian, Hou)[3], Author name (Massimo, Chiaradia)[4], Author name (Zhuang, Miao)[1, 2], Author name (Zi-Hao, Wen)[1, 2]

1. Affiliation (National Mineral, Rock and Fossil Resource Center, and Deep Space Exploration Laboratory, China University of Geosciences (Beijing), China)
2. Affiliation (State Key Laboratory of Geological Process and Mineral Resources, Frontiers Science Center for Deep-time Digital Earth, China University of Geosciences (Beijing), China)
3. Affiliation (SinoProb Lab, Institute of Geology, Chinese Academy of Geological Sciences, China)
4. Affiliation (Department of Earth Science, University of Geneva, Switzerland)

Abstract The role of volatiles in post-subduction porphyry ore systems within continental collision zones remains poorly constrained. Using the eastern Tethyan domain as an example, we combine mineralogical analyses of apatite and phlogopite with isotope tracing to investigate how Cl, S, and Hg control collisional orogenic mineralization.

Our results show that economically viable ore-bearing porphyries in the collision zone are significantly enriched in Cl and S within key volatile-rich minerals, with enrichment levels far exceeding those in contemporaneous barren intrusions. This confirms that a volatile-rich melt environment is the primary control on the mobilization and transport of copper and gold. Further analysis reveals that widespread zoning in phlogopite from syn-mineralization lamprophyres, together with isotopic compositions of key minerals, records the continuous injection of mantle-derived melts into the lower crust. This process not only delivered mantle-derived volatiles but also triggered water-rich melting of the lower crust, jointly driving the formation of the ore-bearing porphyry magma system.

Research on Hg isotopes provides direct constraints on the source of deep-seated volatiles. Ore-bearing porphyries and associated mantle-derived melts exhibit high δ^{198}Hg signatures that are distinct from barren intrusions and consistent with marine sediments in subduction zones. This strongly demonstrates that the volatiles required for collision-related mineralization did not originate from simple lower crustal melting, but were derived from an enriched lithospheric mantle source metasomatized by prior subduction of oceanic sediments. These fluid components and their complexed ore metals were ultimately remobilized and released by partial melting events induced by deep mantle upwelling during the post-collisional stage of the India–Eurasia collision.

Integrating the mineralogical evidence, we propose a new model for porphyry mineralization in collisional settings. The mantle volatile reservoir established during the early subduction stage serves as the foundation for metal transport, while lithospheric mantle remelting triggered by collision orogeny provides the driving force for the ascent of ore-forming magmas. Sustained

injection of mantle-derived melts into the crustal system maintains high magma oxygen fugacity and significantly prolongs the lifespan of the hydrothermal system, thereby enabling efficient metal enrichment in the residual melt. This continuous deep volatile supply accounts for the marked difference between large-scale Cu mineralization in the eastern Gangdese belt and the barren intrusions in the western segment. Accordingly, relative enrichment of Cl and S in apatite and phlogopite can serve as an effective indicator of ore potential. This study mineralogically establishes deep volatile recycling as the decisive factor in collision-type porphyry mineralization, offering a new theoretical basis for giant metal accumulation in collisional orogenic belts.

Key words: Post-subduction porphyry ore systems, Continental Collisonal orogen, Volatile components, Apatite and phlogite, Hg isotopes

REVEALING THE GENETIC RELATIONSHIP BETWEEN GOLD MINERALIZATION AND MAGMATISM IN JIAODONG PENINSULA THROUGH ZIRCON, APATITE AND HORNBLENDE CHEMISTRY

Lichuan Pan[1], Haodong He[1,2], Haidong Zhang[3], Zhuojun Xie[1], Qian Liu[1,2], Jingdan Xiao[1], Chusi Li[4], Ruizhong Hu[1,2]*

1. State Key Laboratory of Ore Deposit Geochemistry, Institute of Geochemistry, Chinese Academy of Sciences, Guiyang 550081, China
2. College of Earth and Planetary Sciences, University of Chinese Academy of Sciences, Beijing 100049, China
3. School of Earth Science and Resources, Chang'an University, Xi'an 710000, China
4. Department of Geological Sciences, Indiana University, Bloomington, IN 47405, USA

Abstract The Jiaodong Peninsula, Eastern China, is renowned for its extensive Mesozoic gold (Au) mineralization, yet the genetic link between this mineralization and coeval felsic–mafic magmatism remains elusive. This study investigates the temporal variations in magma redox conditions, Cl, S, and H_2O contents, as well as the emplacement depth of Mesozoic granites and associated mafic dikes in the region, using the chemical compositions of zircon, apatite, and hornblende. Zircons and apatites were also analyzed to determine U–Pb ages and Sr–Nd isotope compositions, respectively. Our results indicate that the granites formed in three distinct episodes: (1) 165.5–154.7 Ma (Linglong granitic suite), (2) 136.2–126.3 Ma (Guojialing granitic suite), and (3) 119–116.7 Ma (Weideshan granitic suite). The mafic dikes, divided into low and high Ti varieties, are relatively contemporaneous (126.1–110 Ma) with the youngest granites (episode 3) and lode Au deposits. Data show that fO_2 (ΔFMQ) and contents of H_2O, Cl, and S in felsic magmas increase with decreasing formation age. This trend likely results from the gradual increase in oxidized and volatile-rich mafic melts added to felsic magmas with time. This interpretation is supported by the variation in apatite $\varepsilon_{Nd}(t)$ and $(^{87}Sr/^{86}Sr)_i$ values from older to younger granites. The estimated depths of magma emplacement decrease from generally >10 km for older granites (episodes 1 and 2) to generally <7 km for younger granites (episode 3), indicating rapid Early Cretaceous crustal uplift that enhanced structural permeability. These findings reveal a progressively increasing affinity for Au ore in regional granites over time, with the youngest granites (episode 3), formed concurrently with the ore deposits, exhibiting the highest magma fertility in Au. The observed correlation between magma fertility of granites and Au mineralization intensity suggests a potential genetic relationship between regional felsic magmatism and lode Au deposits, although direct Au-mineralized granites have not yet been identified. The implications of this study highlight the role of subduction-related magmatism in Au mineralization, suggesting that

the Au deposits in the Jiaodong Peninsula may represent a unique type closely associated with subduction and craton destruction.

Key words: Jiaodong gold deposits, Magma fertility, North China Craton destruction, Mineral chemistry

REVISITING METAL SOURCES IN THE SOUTHERN TIBET ANTIMONY METALLOGENIC BELT

Jinchao Wu[1], Degao Zhai[1]*, Anthony E. Williams-Jones[2], Manuel Keith[3]

1. School of Earth Sciences and Resources, and State Key Laboratory of Geological Processes and Mineral Resources, China University of Geosciences Beijing, China
2. Department of Earth and Planetary Sciences, McGill University, Canada
3. GeoZentrum Nordbayern, Friedrich-Alexander-Universität (FAU) Erlangen-Nürnberg, Germany

Abstract The metal sources of globally distributed low-temperature Sb mineralization remain poorly constrained and have long been debated. The Cenozoic Sb metallogenic belt in southern Tibet, formed in response to Himalayan post-collisional extension and manifested as well-preserved stibnite-quartz veins hosted in Mesozoic sedimentary rocks, provides a natural case for resolving this question. Earlier studies have primarily focused on individual deposits within the belt, while marked isotopic heterogeneity among deposits has obscured the regional source signatures of ore-forming metals. As the principal Sb-bearing mineral in these deposits, stibnite preserves key information for constraining the metal sources of Sb mineralization. This study integrates new *in-situ* S-Pb isotope analyses of stibnite from six representative Sb deposits across the Southern Tibet Metallogenic Belt (STMB) with regional isotopic data for potential source reservoirs, and applies quantitative mixing models to evaluate the relative contributions of different metal sources. At the deposit scale, stibnite $\delta^{34}S$ compositions are broadly consistent with those of the corresponding local Mesozoic sedimentary rocks, suggesting a dominant sulfur contribution from the local Mesozoic host strata. In addition, stibnite Pb isotope compositions vary markedly across the metallogenic belt, but show limited variation within individual deposits. Together with crust-mantle Pb isotope mixing models, these suggest that the ore-forming metals were derived from mixed crustal sources, mainly the Mesozoic sedimentary rocks and the Precambrian gneissic basement. End-member mixing calculations further quantitatively suggest that the Mesozoic ore-hosting sedimentary rocks supplied the dominant proportion of the Sb budget in these deposits. These findings highlight the critical role of the host rocks in Sb mineralization systems, which served both as major metal reservoirs and as favorable sites for Sb deposition, thereby providing new insights into the formation of similar Sb-bearing ore systems elsewhere.

Key words: Metal source, S-Pb isotope, Sb mineralization, Ore genesis, Southern Tibet

Acknowledgements This work was supported by the National Key R&D Program of China (2023YFC2906805).

ROBUST MULTIMODAL MINERAL IDENTIFICATION BASED ON A PARAMETER-EFFICIENT METHOD

Hongxiang Liao, Xiaohui Ji,*

School of Artificial Intelligence, China University of Geosciences, Beijing, China

Abstract Automatic mineral image identification plays a crucial role in geological exploration and related applications. Although multimodal data, such as physical attributes and spectral information, can enhance recognition accuracy, field environments often suffer from missing or corrupted modalities, leading to reduced system robustness. A parameter-efficient method is proposed to solve the above problems, requiring only about a 13.8% increase in parameters compared to the baseline while enabling adaptive recognition across various modality combinations. The method is evaluated on a dataset containing 36 mineral classes and more than 110,000 images and achieves 93.7% accuracy under complete-modality conditions, which is 1.7% higher than the baseline, and maintains 71.4% accuracy under extreme scenarios with 100% modality corruption, surpassing the baseline by 28.3%. These results demonstrate that the method exhibits strong robustness and practicality in complex field environments and provides a promising solution for real-world multimodal mineral recognition.

Key words: Mineral identification, multimodal, missing modalities, robust identification

SCALABLE DATA SCIENCE AND AI FOR MINERALOGY: OUR RECENT WORK WITH MINDAT

Xiaogang Ma[1], Jolyon Ralph[2], Jiyin Zhang[1]

1. Department of Computer Science, University of Idaho, Moscow, ID 83844, USA
2. Hudson Institute of Mineralogy, Keswick, Virginia 22947, USA

Abstract Mindat is one of the world's largest databases of mineral species and their global occurrences. Since its launch in the early 2000s, Mindat has evolved into an open resource for mineralogy and related geoscience disciplines. To meet the increasing demand from researchers, Mindat has established an open data service that provides programmatic access to curated records, along with supporting Python and R packages. Building on this infrastructure, researchers have advanced data-driven approaches that move mineralogy toward predictive science. Using statistical, network-based, and machine learning methods, researchers can predict mineral species occurrences and summarize paragenetic modes within mineral deposits. The Mindat database team have scaled up those studies to tens of thousands of localities and allow users to quickly browse those records and interpretate mineral associations and deposit evolution for any areas of interest. Most recently, the Mindat open data service has been extended through the integration of large language models (LLMs). An LLM-assisted interface has been established to translate natural language questions into executable data queries and analytical workflows. Through this interface, visual outputs such as mineral–element networks and locality density maps can be automatically generated. In parallel, a modular, multi-agent system has been developed to extract structured datasets from legacy geological documents. Together, these developments demonstrate how the coupling of open mineral databases with scalable data science and AI can enhance data accessibility and accelerate scientific discovery, and we welcome broader usage of the Mindat open data from the geoscience community.

Key words: Mindat, Open Data, Scalable Data Science, Large Languange Models

SCHEELITE TRACE ELEMENTS FRINGPRINTING OF THE EVOLUTION FROM HIGH-TEMPERATURE W TO LOW-TEMPERATURE SB-AU-W MINERALIZATION IN SOUTH CHINA

Hongwei Peng, Shanling Fu

State Key Laboratory of Critical Mineral Research and Exploration, Institute of Geochemistry, Chinese Academy of Sciences, Guiyang 550081, China

Abstract which produced high-temperature W–Sn mineralization in the eastern Cathaysia Block and low-temperature Au–Sb mineralization in the western Yangtze Block. The Xiangzhong Metallogenic Province (XZMP), located in central South China, hosts both granite-related high-temperature W deposits and low-temperature sediment-hosted Sb–Au–W deposits. These two deposit types formed coevally, implying a potential genetic linkage between them, which, however, remains poorly constrained to date. Scheelite is a widespread W-bearing mineral in both deposit types and retains key geochemical fingerprints of ore-forming fluids and processes, making its trace element systematics a robust tool for deciphering fluid evolution and metallogenic affinity. In this study, we present in situ LA-ICP-MS trace element data of scheelite from four representative high-temperature W deposits (Shaxi, Zhongcun, Zhaixishan, Niujiaojie) and two typical low-temperature Sb–Au–W deposits (Zengjiaxi, Zimuchong) in the XZMP. These data are used to investigate the physicochemical properties of the ore-forming fluids and the possible genetic linkage between the two deposit types.

Scheelite from the high-temperature W deposits shows elevated concentrations of rare earth elements (REE), Mo, Nb, Mn, Na, and Y, with relatively low Sr contents and Sr/Mo ratios, and variable Eu anomalies. In contrast, scheelite from the low-temperature Sb–Au–W deposits is characterized by low REE, Mo, Nb, Mn, Na, and Y contents, but significantly higher Sr contents and high Sr/Mo ratios, along with consistently positive Eu anomalies. These chemical features indicate that the ore-forming fluids of the high-temperature and low-temperature deposits were dominated by high-temperature magmatic-hydrothermal fluids and by low-temperature meteoric water that interacted with the regional Precambrian metamorphic basement, respectively. Notably, systematic compositional variations in scheelite are observed from the coeval high-temperature W mineralization to the low-temperature Sb–Au–W mineralization in the XZMP: decreasing REE, Mo, Nb, Mn, and Na, coupled with increasing Eu anomalies, Sr contents, and Sr/Mo ratios. Such chemical evolution points to a linked hydrothermal system, involving magmatic fluids for the high-temperature W deposits and circulating meteoric water for the low-temperature deposits.

The potential genetic linkage allows us to propose a comprehensive model for the high-temperature

W and low-temperature Sb–Au–W mineralization in the XZMP. Following the emplacement of granitic magma and fluid exsolution, high-temperature W mineralization occurred in proximal locations relative to the granite, as a result of magmatic fluid exsolution. Meanwhile, the thermal gradient from the granitic intrusions induced circulation of meteoric water, which leached W, Sb, and Au from Neoproterozoic metasedimentary rocks. This process, combined with minor contributions from long-distance transported magmatic-hydrothermal fluids and tungsten, formed ore bodies in locations distal to the granites. Based on the decreasing mineralization temperatures—from high-temperature W (>350 °C) to Au (250–350 °C) and Sb mineralization (<250 °C)—a mineralization zoning pattern can be broadly inferred, ranging from W, through Au ± W and Sb–Au–W, to Sb, extending from the granites outward into the metasedimentary rocks. This genetic model highlights the potential for high-temperature W mineralization in deeper regions associated with the known low-temperature Sb–Au–W deposits in the XZMP.

Key words: Scheelite trace elements, Low-temperature Sb-Au-W deposits, High-temperature W deposits, Genetic linkage, South China

SHORT-WAVE INFRARED SPECTRAL AND GEOCHEMICAL CHARACTERISTICS OF CHLORITE AS EXPLORATION INDICATORS FOR MAGMATIC CU-NI SULFIDE DEPOSIT

Shuang Li [1, 2], Huayong Chen [1, 2 *]

1. State Key Laboratory of Deep Earth Processes and Resources, Guangzhou Institute of Geochemistry, Chinese Academy of Sciences, Guangzhou 510640, China
2. University of Chinese Academy of Sciences, Beijing 100049, China

Abstract Magmatic Cu-Ni sulfide deposits are commonly accompanied by hydrothermal alteration. The potential utility of alteration minerals in prospecting remains inadequately explored. This study investigated the Kalatongke Cu-Ni deposit, characterized by pervasively developed hydrothermal alteration, to assess the exploration potential of alteration minerals.

Short-wave infrared (SWIR) spectral identification reveal that chlorite is the most pervasive alteration mineral in the Kalatongke Cu-Ni deposit, exhibiting a distinct spatial trend: from tuff to mineralized gabbro, the composition evolves from Fe-chlorite to Fe-Mg-chlorite/Mg-chlorite. The characteristic absorption peaks at 2250 nm and 2350 nm (Pos2250 and Pos2350) exhibit a systematic shift to shorter wavelengths, which can serve as a spectral ore indicator.

Six chlorite types were identified based on petrography: Chl1–Chl4 (alteration of pyroxene, feldspar, amphibole, and biotite) dominate the proximal mineralized gabbro; Chl5 (amphibole-derived) occurs in distal barren gabbro; and vein-type Chl6 is found in the distal tuff. Chl1–Chl6 are trioctahedral, dominated by Fe^{2+} = Mg^{2+} substitution. Geochemically, Chl1–Chl4 are characterized by high SiO_2, MgO, Co, Ni, Sr, Cs, and Pb; Chl5 by higher SiO_2, MgO, Co, Ni, and Cs than Chl6; and Chl6 by higher Al_2O_3, FeO_T, Ti, Mn, Li, V, Sc, Zn, and Ga than Chl1–Chl5. These geochemical variations are primarily controlled by temperature, protolith, precursor minerals and fluid compositions.

Hydrothermal-derived Chl6 shows metamorphic-like Al_2O_3, FeO_T, MgO, Li, and Zn contents. Combined with higher formation temperatures for Chl5–Chl6 versus Chl1–Chl4, this indicates a tectono-metamorphic hydrothermal overprint at Kalatongke. From distal tuff to mineralized gabbro, temperature-driven decreases in Si/Sr, Al/Pb, and Ga/Pb ratios, coupled with increases in Mg/Si and Mg/Al, provide geochemical vectors for exploring concealed orebodies in the Kalatongke Cu-Ni deposit.

Key words: Short-wave infrared spectroscopy, Chlorite geochemistry, Magmatic Cu-Ni sulfide deposit, Hydrothermal alteration, Central Asian Orogenic Belt

SOMBRERETEITE, NACA3(AL7SI9)O32, A NEW MINERAL FROM THE SOMBRERETE IRON METEORITE IN THE CERRO DEL SOMBRERETILLO, ZACATECAS, MEXICO

Xiangping Gu[1, 4], Zuokai Ke[1], Hexiong Yang[2*], Kai Qu[3], Guanghua Liu[1], Yixuan Liu[1], Yizhou Chen[1], Ran Gao[1], Qun Ai[1], Shuting Huang[1], Baihui Ma[1], Yang Liu[1]

1. School of Gemology and Mineral Resources, Jiangxi Institute of Applied Science and Technology, Nanchang, 330100, China.
2. Department of Geosciences, University of Arizona, 1040 E. 4th Street, Tucson, AZ 85721-0077, USA.
3. Tianjin Center, China Geological Survey, Hedong, 300170 Tianjin, China.
4. School of Geosciences and Infophysics, Central South University, Changsha, Hunan 410083, China. *Corresponding author: hyang@arizona.edu

Abstract Sombrereteite (IMA2025-095a) is discovered from the Sombrerete iron meteorite in the Cerro del Sombreretillo, Zacatecas, Mexico, which is known for its rich silicate inclusions (~8% in volume), and is considered as IIE type or an ungrouped iron meteorite. Sombrereteite occurs as euhedral to subhedral platy crystals, 10-100 μm in length, and accounts for about 6 vol.% of the silicate inclusions, in association with kumdykolite+albite (~50%), orthopyroxene (~13%), chlorapatite (~19%), chromite (~3%), and yagiite (~1.2%) of the silicate inclusions, plus trace merrillite, sanidine, ilmenite, and rutile (Fig. 1). It is colorless with vitreous luster and estimated Mohs hardness 6.5. The Raman spectrum is characterized by strong peaks at 485 cm^{-1} and 422 cm^{-1}, apparently distinguished from albite, sanidine and kumdykolite (Fig. 2). The empirical formula from 7 microprobe analyses is $Na_{1.06}K_{0.03}Ca_{2.77}(Al_{6.60}Si_{9.39})_{\Sigma 15.99}O_{32}$. Sombrereteite is monoclinic, space group: *C*2/*c*, *a* = 10.23584(13) Å, *b* =17.8056(3) Å, *c* = 14.9349(3) Å, β = 90.4200(14)°, *V* = 2721.88(8) $Å^3$, *Z* = 4. It is structurally related to wodegongjieite and the cymrite group, but chemically similar to plagioclase (layered type feldspar). The crystal structure is composed of double-layer sheets of TO_4 tetrahedra with three *A* sites sandwiched between the sheets. Each single tetrahedral layer in a sheet consists of 6-membered rings of corner-shared TO_4. The *A*1 and *A*2 sites are 8-coordinated and dominated by Ca, whereas *A*3 is 6-coordinated and dominated by Na, leading to an ideal formula $^{A3}Na^{[A1,A2]}Ca_3(Al_7Si_9)O_{32}$. The mineral name, sombrereteite (symbol: Som), is derived from the Sombrerete iron meteorite.

SOURCE OF THE DAHONGSHAN CU-FE DEPOSIT, YUNNAN, CHINA: EVIDENCE FROM IN-SITU TRACE ELEMENTS AND SULFUR ISOTOPES OF SULFIDES

Kangping Shi, Jiaxi Zhou* Corresponding author, Email: zhoujiaxi@ynu.edu.cn
Key Laboratory of Critical Minerals Metallogeny in Universities of Yunnan Province, School of Earth Sciences, Yunnan University, Kunming 650500, Yunnan, China

Abstract The Dahongshan copper deposit in Yunnan Province is the largest and most representative Cu-Fe polymetallic deposit in the Kangdian Cu-Fe metallogenic province of China, but its ore-forming material sources and metallogenic model have long been subjects of debate. In this study, in situ analytical techniques were employed to determine the trace element and sulfur isotopic compositions of sulfides from two stages of the main ore body. Combined with the geological characteristics of the Dahongshan copper deposit and deep information revealed by newly drilled deep boreholes (~1500 m), the sources of ore-forming materials are discussed, and a more comprehensive metallogenic model is tentatively established. The sulfides in the Dahongshan deposit mainly comprise those formed during the diagenetic–mineralization stage (chalcopyrite–pyrite–magnetite) and those formed during the later-stage reworking stage (quartz–calcite–chalcopyrite–bornite). Both trace element and sulfur isotope data indicate that the fluid properties of the two stages are distinct. The earlier stage is characterized by magmatic affinities, with low $\delta^{34}S$ values (1.1‰~-2.3‰), high Se (up to 908×10^{-6}), Zn (up to 619×10^{-6}), and Co (up to $10{,}288\times10^{-6}$) contents, and high Co/Ni ratios (10~230). In contrast, the later stage exhibits higher $\delta^{34}S$ values (8.3‰~8.6‰) and relatively lower Se, Zn, and Co contents as well as lower Co/Ni ratios, indicative of a non-magmatic fluid source. Combined with previous data and the discovery of copper mineralization in the Laochanghe Formation from deep drilling (implying strata-transgressive mineralization), it is inferred that the later reworking fluids may be related to regional metamorphism or tectonic thermal events. Comparative analysis shows that, relative to VMS deposits, the Dahongshan deposit is characterized by abundant magnetite + chalcopyrite ± bornite assemblages and only minor quartz–sulfide veins, which are more consistent with the diagnostic features of IOCG deposits. On this basis, a more comprehensive metallogenic model is proposed.

Key words: In-situ trace elements, In-situ sulfur isotopes, Sources of ore-forming materials, Metallogenic model, IOCG deposits

Acknowledgements This study is supported by the National Natural Science Foundation of China (U2444206), the Fundamental Research Major Project of Yunnan Province

(202501BC070002), the Major Science and Technology Special Plan Project of Yunnan Province (202402AB080006), the Scientific and Technological Innovation Team (2025-01) and Master's Supervisor Team (2023-15) Projects of Critical Metal Metallogeny and Prospecting Prediction of Yunnan Provincial Education Department to J.-X. Zhou. *

SPECIAL RESEARCH METHODS FOR ORE-FORMING ALTERATION MINERALS

Jian-Ling Xue [1,2*], Sheng-Rong Li[3], Zhen-Shan Pang[1,2], Zhi-Zhong Cheng[1,2], Hui Chen [1,2], Xiao-Fei Zhang [1,2], Ru-Ya Jia [1], Bang-Lu Zhang[1], Bing Yu [1,2], Ni-Ni Mou [1,2] * Corresponding author: E-mail: xuejianling369@126.com

1. Development and Research Center, China Geological Survey, Beijing 100037, China
2. Mineral Exploration Technical Guidance Center, Ministry of Natural Resources, Beijing 100037, China
3. China University of Geosciences (Beijing), Beijing 100083

Abstract Exploration for concealed and deep-seated ore deposits represents a major challenge in contemporary mineral exploration, where conventional prospecting approaches often yield limited efficacy in targeting deep orebodies. Hydrothermal alteration minerals are genetically associated with mineralization and act as robust indicators for tracking ore-forming fluid evolution, changes in physicochemical conditions, and orebody localization. This paper systematically addresses the linkage between hydrothermal alteration and metal precipitation, the evolution of mineralization stages, and the theory of ore-forming geochemical barriers, emphasizing the critical value of extensive early-stage alteration in predicting concealed orebodies. We outline core research components of alteration mineral studies, including mineral characteristics, spatio-temporal alteration zoning, ore-forming geochemical barriers, and localization of ore-forming centers. Working methodologies are comprehensively reviewed, encompassing alteration-specific mapping, microscopy, spectral analysis, and fluid inclusion analyses. The typomorphic implications of over ten key alteration minerals (e.g., quartz, sulfates, iron oxides, biotite, hornfels, skarn) are categorized, and criteria are established to differentiate ore-related alteration from barren alteration. Results demonstrate that recognizing alteration assemblages, zoning patterns, and physicochemical transition markers enables precise delineation of geochemical barriers and spatial prediction of concealed orebodies, providing a systematic methodological framework for deep-seated mineral exploration.

Key words: Alteration minerals, Hydrothermal alteration, Ore-forming geochemical barrier, Concealed orebody, Mineral exploration

SPHALERITE TRACE ELEMENTS AS PROXIES FOR ORE-FORMING FLUID EVOLUTION IN THE WUXU SB–PB–ZN ORE DISTRICT, SOUTH CHINA

Hao Xu[1,2], Jian-Feng Gao[1,2*], Shi-Tao Zhang[1], Jiang-Bo Lan[1], Xue-Biao Li[3], Zhen-Zhou Xiao[4], Xin-Yu Li[1,2], Kang Min[1], Wei Lou[1,2], Wan-Ting Ge[1]

1. State Key Laboratory of Critical Mineral Research and Exploration, Institute of Geochemistry, Chinese Academy of Sciences, Guiyang 550081, China
2. University of Chinese Academy of Sciences, Beijing 100049, China
3. China Nouferrous Metal (Guilin) Geology and Mining Co., Ltd, Guilin 541004, China
4. Guangxi No.215 Geological Team Co., Ltd., Liuzhou 545006, China

Abstract The Wuxu ore district, located in the southeastern segment of the Danchi metallogenic belt in South China, hosts medium- to low-temperature Sb–Pb–Zn polymetallic mineralization and exhibits pronounced ore-district-scale metal zonation. This contrasts sharply with the adjacent Dachang ore district within the same metallogenic belt, which is dominated by medium- to high-temperature Sn mineralization. To better constrain the genetic relationship between these contrasting mineralization systems and clarify the mechanisms controlling metal zonation, this study investigates sphalerite as a stage-spanning mineral capable of recording the physicochemical evolution of ore-forming systems throughout multiple hydrothermal stages. Petrographic observations and LA-ICP-MS trace-element analyses were conducted on sphalerite from four representative deposits in the Wuxu ore district, including the Bawang Sn–Zn, Jianzhupo Sb–Pb–Zn, Furongchang Sb–Pb–Zn, and Shuiluo Sb–Pb–Zn deposits. The resulting data were further compared with sphalerite compositions from the Dachang ore district and from a broad range of mineralization systems worldwide, including MVT, SEDEX, skarn, porphyry, and VMS deposits. Sphalerite from the Wuxu ore district is generally enriched in Sn, Ga, Sb, and Ag, whereas sphalerite from the Dachang ore district is characterized by enrichment in Fe, In, and Mn. Partial least squares discriminant analysis (PLS-DA) indicates that sphalerite from Wuxu preserves mixed geochemical signatures of magmatic-hydrothermal and sediment-derived fluids, whereas sphalerite from Dachang records a typical magmatic-hydrothermal affinity. Among the studied deposits in Wuxu, sphalerite from the Bawang deposit is characterized by homogeneous dark-black textures, enrichment in Fe, Ga, In, and Sn, and relatively stable high-temperature and high-sulfur-fugacity conditions (281–300 °C; log fS_2 = −11.5 to −10.8), indicating a strong magmatic-hydrothermal affinity. Sphalerite from the Jianzhupo deposit commonly exhibits dark-brown coloration with locally developed reddish-brown heterogeneous textures and weak oscillatory zoning, accompanied by enrichment in Cu and Sn and moderate Sb contents. Its strongly fluctuating temperature and sulfur fugacity conditions (271–352 °C; log fS_2 = −11.2 to −8.3) suggest a dominantly magmatic-

hydrothermal system mixed with sediment-derived components. In contrast, sphalerite from the Shuiluo deposit displays dense light-yellow to reddish-brown oscillatory zoning and enrichment in Cd, Ge, As, Sb, and Pb, together with relatively low and highly variable temperature–sulfur-fugacity conditions (112–308 °C; log fS_2 = −20.4 to −10.0), indicating dominant sediment-derived contributions and possible involvement of meteoric water. Sphalerite from the Furongchang deposit is characterized by homogeneous greenish-brown textures and relatively stable lower-temperature and lower-sulfur-fugacity conditions (226–242 °C; log fS_2 = −12.8 to −12.0), with selective enrichment in Sb, suggesting limited magmatic input but substantial sediment-derived contributions. Collectively, sphalerite from the Wuxu ore district records lower and more variable temperature and sulfur fugacity conditions (112–352 °C; log fS_2 = −20.4 to −8.3), reflecting the evolution of a comparatively open hydrothermal system. In contrast, the Dachang ore district formed within a relatively stable magmatic-hydrothermal environment characterized by high temperatures (324–401 °C) and elevated sulfur fugacity (log fS_2 = −9.5 to −7.0). Integrated trace-element compositions, temperature–sulfur-fugacity conditions, and fluid-source characteristics indicate that, in contrast to the proximal, high-temperature, and relatively closed magmatic-hydrothermal system of the Dachang ore district, the Wuxu ore district represents a more distal and open metallogenic system formed through the interaction of magmatic-hydrothermal and sediment-derived fluids. Ore-district-scale metal zonation was jointly controlled by fluid mixing, progressive physicochemical evolution, and structurally controlled fluid migration pathways. Variations in metallogenic position, hydrothermal system openness, and fluid-material sources are therefore considered the principal factors controlling the spatial separation and contrasting metal associations between medium- to low-temperature Sb–Pb–Zn mineralization and high-temperature Sn mineralization within the Danchi metallogenic belt.

Key words: Sphalerite, LA-ICP-MS trace element, Wuxu ore Field, Metal zonation, Metallogenic System

Acknowledgements This study was supported by the National Key Research and Development Program of China (2023YFC2906802), the Guangxi Key Research and Development Program of China (GuiKe AB24010058) and the Key Research and Exploration Fund for Critical Minerals of the State Key Laboratory (202403).

STIBNITE GEOCHEMISTRY AS A TRACER FOR FINGERPRINTING FLUID FLOW AND ORE EXPLORATION

Degao Zhai[1], Jinchao Wu[1], Xiangfa Song[1], Anthony E. Williams-Jones[2], Zijun Qiu[1], Qingqing Zhao[1], Jian-Feng Gao[3]

1. School of Earth Sciences and Resources, and State Key Laboratory of Geological Processes and Mineral Resources, China University of Geosciences Beijing, China
2. Department of Earth and Planetary Sciences, McGill University, Canada
3. State Key Laboratory for Critical Mineral Research and Exploration, Institute of Geochemistry, Chinese Academy of Sciences, China

Abstract Stibnite samples collected from a variety of depths in the world-class Xikuangshan Sb deposit in south China were used to determine their trace element and Sb isotope signatures and identify features of these signatures that could be used in the exploration for similar deposits elsewhere. An important finding of the analyses is that the As, Zn and Tl contents of the stibnite vary systematically with depth in the deposit. Therefore, we propose that these trace elements and their ratios can serve to reconstruct the pathways of ore fluid migration and target the exploration for orebodies. We have compiled published data on the trace element compositions of stibnite for Sb, Sb-W, Au-Sb-W, and Au ore systems worldwide, and discovered that trace elements involving Cu, Pb, Se, As, and Ag+Sn+In can be used to distinguish distinct metal associations in natural hydrothermal ore systems. In addition, a gradual increase of Sb isotope ratios from the proximal to the distal parts was observed in stibnite ores, showing that distal stibnites possess higher Sb isotopic values. In this way, we consider that separation of stibnite from a Sb-bearing fluid related to reaction kinetics as a cause for Sb isotope fractionation. The modeled data constrain a Sb isotope fractionation factor ($\alpha_{\text{fluid-stibnite}}$) between hydrothermal fluid and stibnite at approximately 0.9994. Overall, this study implies that trace element and Sb isotope analyses for stibnite have critical implications for fingerprinting fluid flow paths and could shed new light on guiding ore exploration.

Key words: Antimony isotopes, Trace element, Hydrothermal system, Stibnite

Acknowledgements This work was supported by the National Key R&D Program of China (2023YFC2906805).

STUDY ON FE-CU DECOUPLING IN ZHUCHONG SKARN FE-(CU) DEPOSIT -INSIGHTS FROM CHALCOPYRITE IN-SITU SULFUR AND COPPER ISOTOPE ANALYSIS

FangYue Wang[1,2], Ting Liu[1,3], Yonghong Guo[1,2]

1. Ore Deposit and Exploration Center, School of Resources and Environmental Engineering, Hefei University of Technology, Hefei 230009, China
2. Anhui Province Engineering Research Center for Mineral Resources and Mine Environments, Hefei 230009,China
3. Anhui Technical College of Industry and Economy, Hefei 230051, China

Abstract Iron (Fe) and copper (Cu) mineralization often coexist in skarn deposits but can also occur independently. The Zhuchong skarn iron deposit is a typical case of Fe-Cu decoupling in a single magmatic-hydrothermal system, featuring a deep Fe-dominant skarn ore body (Fe/Cu ~197) and widespread overlying vein-type Cu mineralization (marble-type, diorite-type, and breccia-type). Tthis study conducted integrated analyses of chalcopyrite from different orebodies, including petrography, LA-ICP-MS trace element analysis, and LA-MC-ICP-MS in-situ S and Cu isotope analysis.

The results show a temperature transition from high-temperature conditions in the deep skarn stage (chalcopyrite Zn > 600 ppm) to medium-low temperatures in the shallow vein-type ores (Zn: 17.63–51.72 ppm). Significant spatial variation in $\delta^{34}S$ values (+0.5‰ to +3.2‰ in breccia-type, +2.8‰ to +9.4‰ in diorite-type, +13.2‰ to +15.9‰ in marble-type ores) indicates fluid evolution from primitive magmatic fluid to one heavily contaminated by stratigraphic sulfur (mainly gypsum layers). The decoupling between $\delta^{65}Cu$ values (-0.07‰ to +0.76‰) and $\delta^{34}S$ confirms a persistent deep magmatic source for copper, with gypsum layers only contributing sulfur. Copper isotope fractionation is controlled by temperature and fluid immiscibility. High temperatures at depth suppressed fractionation and favored light Cu isotopes ($\delta^{65}Cu \approx$ -0.07‰), while shallow residual fluids enriched heavy Cu isotopes ($\delta^{65}Cu \approx$ +0.76‰). Additionally, fluid boiling and phase separation under low pressure dominate the large $\delta^{65}Cu$ dispersion (-0.26‰ to +2.59‰) in diorite-type chalcopyrite. This study provides new insights into Fe-Cu decoupling mechanisms in magmatic-hydrothermal systems.

Key words: Zhuchong skarn iron deposit, Fe-Cu decoupling, magmatic-hydrothermal system, in-situ S-Cu analysis, fluid boiling

SYNTHETIC ANALYSIS OF PREBIOTIC CHEMISTRY ON METAL SULFIDES IN HYDROTHERMAL SYSTEMS

Chunjiang Li[1,2], Jincheng Guo[1,2], Siyu An[3,4,5], Xiangzhi Bai[3,4,5], Yan Li[1,2]* * Corresponding author: Yan Li

1. SKLab-DeepMinE, MOEKLab-OBCE, School of Earth and Space Sciences, Peking University, Beijing 100871, China
2. Beijing Key Laboratory of Mineral Environmental Function, School of Earth and Space Sciences, Peking University, Beijing 100871, China
3. Image Processing Center, School of Astronautics, Beihang University, Beijing 102206, China
4. State Key Laboratory of Virtual Reality Technology and Systems, Beihang University, Beijing 100191, China
5. Key Laboratory of Spacecraft Design Optimization and Dynamic Simulation Technology, Ministry of Education, Beihang University, Beijing 102206, China

Abstract The transition from abiotic geochemistry to proto-biochemistry requires overcoming severe thermodynamic and kinetic barriers that limit dilute, solution-phase reactions. Deep-sea hydrothermal systems, abundant in catalytic transition metal sulfides (e.g., FeS, NiS, FeS_2), offer a compelling environment where minerals provide the reducing power and adsorption sites necessary to drive early carbon and nitrogen fixation. Experimental simulations have validated numerous isolated mineral-catalyzed reactions such as iterative carbon chain elongation and analogues of the reverse tricarboxylic acid (rTCA) cycle. However, understanding their synergistic integration within a complex geochemical mixture remains a fundamental system-level challenge. To address this, we developed a comprehensive Chemical Reaction Network (CRN) incorporating a curated library of hydrothermal mineral-promoted reaction rules. Our network simulations reveal that mineral catalysis profoundly alters the topology of prebiotic chemical space. Compared to purely solution-phase baselines, mineral-inclusive networks dramatically accelerate the generation of key metabolic precursors and unlock constructive autocatalytic cycles. However, integrating mineral catalysis into CRNs inherently generates a combinatorial explosion of output molecules. To identify species with genuine prebiotic significance, we introduce a machine learning-based framework. Our pipeline filters the massive network outputs through various complementary criteria. By synergistically combining mineral-inclusive CRNs with molecular screening, this work provides a quantitative evaluation of how hydrothermal sulfide minerals sculpted the early chemical landscape. We demonstrate that the emergence of foundational metabolic pathways is intricately linked to mineral catalysis, offering a novel computational paradigm for exploring the origins of biochemical complexity.

Key words: Chemical reaction network, mineral-catalyzed reactions, deep-sea hydrothermal

sulfides, prebiotic geochemistry

TANTALAESCHYNITE-(CE), A NEW TA-DOMINANT MEMBER OF AESCHYNITE-GROUP FROM TA-ENRICHED PEGMATITE AT HUANGSHAN, SOUTH CHINA

Zeying Zhu[1]*, Hong Yu[1], Zhenyu Chen[1], Bin Wu[2], Rucheng Wang[3, 4], Jiankang Li[1], Denghong Wang[1]

1. MNR Key Laboratory of Metallogeny and Mineral Assessment, Institute of Mineral Resource CAGS, Beijing 100037, China
2. National Key Laboratory of Uranium Resources Exploration-Mining and Nuclear Remote Sensing，East China University of Technology, 330013, Nanchang
3. State Key Laboratory for Mineral Deposits Research, School of Earth Sciences and Engineering, Nanjing University, Xianlin University Town, Nanjing 210023, China
4. Frontiers Science Center for Critical Earth Material Cycling, Nanjing University, Nanjing 210023, China

Abstract Tantaleaschynite-(Ce), ideally $Ce(TiTa)O_6$, is newly discovered and approved by the IMA-CNMNC (IMA 2023-058), as Ta-dominant member of aeschynite-group mineral in Huangshan pegmatite, South China. Tantaleaschynite-(Ce) was discovered at the border of pegmatite dyke, and occurs as subhedral or anhedral granular, tabular crystals and radiating clusters, 10 to 50 μm in size, and paragenetically associated with Ta-rich titanite, and fluorcalciomicrolite. Tantaleaschynite-(Ce) is translucent to opaque and yellowish-orange color in thin section scale, conchoidal fracture and resinous lustre. The density is calculated 6.88 $g \cdot cm^{-3}$ on the basis of empirical formula of $Ce(TiTa)O_6$. The Raman spectrum of tantalaeschynite–(Ce) shows the bending of O−Ta−O, O−Ti−O and the stretching Ti−O vibrations in the range of 200−450 cm^{-1}, the bands of Ta−O stretching vibrations at 659 and 856 cm^{-1}. The aeschynite–group minerals have the general formula AB_2O_6, and electron microprobe analyses yield an empirical formula for tantaleaschynite-(Ce) of $(Ce_{0.38}Ca_{0.38}Nd_{0.12}La_{0.07}Pr_{0.04}Sm_{0.01}Eu_{0.01}Fe_{0.01})_{1.02}(Ti_{0.94}Ta_{0.74}Nb_{0.21}Si_{0.08}W_{0.02}Al_{0.01})_{2.00}(O_{5.69}OH_{0.22}F_{0.09})_{6.00}$, calculated on the basis of two *B*-site cations per formula unit. The ideal formula is $Ce(TiTa)O_6$. The crystal structure, determined by transmission electron microscopy (TEM) and aberration-corrected transmission electron microscopy (AC-SEM), is consistent with that of synthetic $Ce(TiTa)O_6$. Structural refinement confirms that tantaleaschynite-(Ce) adopts the aeschynite-type orthorhombic structure, space group *Pnma* (#62), with unit-cell parameters a = 10.969(4) Å, b = 7.551(9) Å, c = 5.421(7) Å, V = 449.1(3) $Å^3$. This structure consists of chains of $[CeO_8]$ polyhedron and edge-sharing $[Ti(Ta)O_6]$ octahedron. Tantaleaschynite-(Ce) co-occurs with other Ta-rich minerals, including fluorcalciomicrolite and Ta-rich titanite, in a narrow zone adjacent to the blocky K-feldspar unit within the Huangshan Ta-rich pegmatite. The constitutional zone refining model provides the most robust explanation for the sharp, localized Ta

enrichment observed in this boundary layer, consistent with its classification as a highly evolved pegmatite. The presence of tantalaeschynite-(Ce), together with widespread Ta-metasomatic minerals, underscores the critical role of this boundary layer in the petrogenesis of highly evolved pegmatites at Huangshan.

Key words: Tantalaeschynite-(Ce), boundary layer, highly evolved pegmatite, Huangshan pegmatite

TEMPORAL EVOLUTION OF CONTROLLING FACTORS IN SEDIMENTARY MANGANESE MINERALIZATION REVEALED BY MACHINE LEARNING

Fengping Chen, Xiaolin Zhang

School of Earth and Space Sciences, University of Science and Technology of China, Hefei, China

Abstract Sedimentary manganese (Mn) deposits are both economically important ore resources and sensitive archives of marine redox chemistry. However, the factors controlling their spatial and temporal distribution, as well as the relative importance of different mineralization processes through Earth history, remain poorly constrained. In this study, we present a global compilation of 5,184 screened whole-rock geochemical records from sedimentary Mn deposits and Mn-rich strata, spanning the Archean to the Cenozoic. Using a combination of Random Forest regression, SHAP attribution, Spearman correlation, and partial dependence analysis, we investigate how the importance of various controlling factors and the dominant mineralization mechanisms changed over geological time. Our results reveal that ocean oxygenation, linked to the rise of atmospheric oxygen levels, was the most important controlling factor for sedimentary Mn mineralization during the intervals of the Great Oxidation Event and the Neoproterozoic Oxygenation Event. In contrast, productivity emerged as the dominant controlling factor during the Boring Billion and the Phanerozoic. These findings indicate that the redox evolution of the global ocean fundamentally modulated the spatial distribution pattern of sedimentary Mn deposits across different intervals of Earth history.

Key words: Sedimentary manganese deposits, Redox evolution, Machine learning, Major and trace elements

THE MINERALIZATION AGE OF XIANGTANZI GOLD DEPOSIT IN THE WESTERN QINLING AREA, CHINA: EVIDENCE FROM SERICITE RB-SR DATING, GARNET AND ZIRCON U-PB DATING

Lin Chenggui [1,2,3*], Cheng Zhizhong [2*], Du Zezhong [2], Pang Zhenshan [2], Xue Jianling [2], Mao Jingwen [1,3]

1. MNR Key Laboratory for Exploration Theory and Technology of Critical Mineral Resources, China University of Geosciences, Beijing 100083, P.R.China
2. Development and Research Center, China Geological Survey, Beijing 100037, P.R. China
3. MNR Key Laboratory of Metallogeny and Mineral Assessment, Institute of Mineral Resources, Chinese Academy of Geological Sciences, Beijing 100037, P.R. China

Abstract The western Qinling area is the western extension of the Qinling orogenic belt. It is an important gold polymetallic metallogenic belt in China. Due to its unique tectonic environment, complex geological evolutionary history, and strong magmatic activity, it has developed abundant gold polymetallic resources, which have received extensive attention from geologists. Regarding the metallogenic age of gold deposits in the West Qinling region, there is significant controversy among previous research results. However, due to the often unclear metallogenic age of gold deposits in this area, there is a significant controversy on the genetic types of the gold deposits. The Xiangtanzi gold deposit is a large-scale gold system located in the eastern part of the West Qinling orogenic belt. Gold orebodies are predominantly hosted within Neoproterozoic mica quartz schists of the Muqitan Formation and are structurally controlled by high-angle fault zones. Significant debate concerning the age and genesis of gold deposits in this region has hindered the development of a comprehensive genetic model and effective exploration strategies.

To resolve this, new high-precision geochronological data from the intrusive rocks, skarn, and ores of the Xiangtanzi deposit are presented. A mineralized monzonitic granite yielded a zircon U-Pb age of 227.4±3.4 Ma, interpreted as the magmatic emplacement age, which provides a maximum age constraint for mineralization. U-Pb dating of garnet from associated skarn yielded a concordant age of 228.6±5.3 Ma, directly linking alteration to this magmatic event. Hydrothermal sericite from a pyrite-sericite gold ore sample yielded a Rb-Sr isochron age of 221.3±9.6 Ma, which directly dates the gold-related hydrothermal alteration. Together, these data constrain the timing of gold mineralization at Xiangtanzi to the Late Triassic, between ca. 227 and 221 Ma. This timing is coeval with a major metallogenic event throughout the western Qinling belt, which occurred during a period of post-collisional extension following the amalgamation of the North and South China Blocks. Integrating the new geochronology with existing geological, structural, and S-Pb-H-O isotope data, the Xiangtanzi gold deposit can be classified as an intrusion-related, magmatic-

hydrothermal gold system genetically linked to Late Triassic magmatism.

Key words: Rb-Sr dating of sericite, U-Pb dating of garnet, U-Pb dating of zircon, Late Triassic, Xiangtanzi gold deposit

THE ROLE OF MINERALS IN PREBIOTIC EVOLUTION: A KEY TO HABITABLE WORLDS DETECTION

Houze Lu[1], Yan Li[1], Dehai Liang[2]

1. School of Earth and Space Sciences, Peking University, Beijing 100871, China
2. College of Chemistry and Molecular Engineering, Peking University, Beijing 100871, China

Abstract Understanding the origin of life requires unraveling the chemical and geological processes that enabled abiotic molecules to evolve into the first living systems. Minerals are increasingly recognized as critical agents in this trajectory, acting as adsorbents, catalysts and protective and structural scaffolds. In this review, we integrate current research insights into the roles of minerals across successive stages of prebiotic evolution—from the synthesis of simple precursors, through the formation of biomolecular monomers and polymers, to compartmentalization and protocell assembly. We emphasize that these processes were unlikely confined to a single environment due to the energy constraints. Instead, diverse geological settings such as hydrothermal vents, terrestrial hot springs, and even extraterrestrial bodies contributed complementary reactions, coupled through spatial and temporal transport. By categorizing mineral functions and mapping them to distinct prebiotic stages, we propose mineralogical signatures as potential indicators of prebiotic reactivity. Such signatures, detectable through remote sensing and spectroscopy, may serve as robust proxies for habitability assessments on rocky exoplanets. This mineral-centered perspective complements conventional biosignature approaches and highlights new avenues for integrating geoscience into the search for life beyond Earth.

Key words: minerals, origin of life, prebiotic evolution, habitability, mineralogical indicators

THE TWO-STAGE MANTLE ENRICHMENT PROCESSES IN SOUTHERN TIBET: IMPLICATIONS FROMM IN-SITU COMPOSITIONS AND RB-SR ISOTOPES OF PHLOGOPITE

Yumin Ai [1,2], Junfeng Zhao [1,2] Pete Hollings [3] Huayong Chen [1,2,4*]

1. State Key Laboratory of Deep Earth Processes and Resource, Guangzhou Institute of Geochemistry, Chinese Academy of Sciences, Guangzhou 510640, China
2. University of Chinese Academy of Sciences, Beijing 100049, China
3. Department of Geology, Lakehead University, 955 Oliver Road, Thunder Bay, Ontario P7B 5E1, Canada
4. Guangdong Provincial Key Laboratory of Mineral Physics and Materials, Guangzhou 510640, China

Abstract Potassium-rich volcanism in the southern Tibetan Plateau provides vital indicators for understanding geodynamic mechanisms and associated mineralization processes in post-collisional environments. However, the specific mechanisms underlying the enrichement of the mantle source for potassic rocks and their relationship with post-collisional porphyry copper deposits are not fully understood. This study investigates the geochronology, mineral and whole-rock geochemistry of potassic and ultrapotassic lamprophyres from the Zhunuo-Beimulang porphyry copper deposit. Phlogopite phenocryst in potassic lamprophyres (Phl-A) show high Al- Fe-Ti content and low Mg#, and the in-situ Rb-Sr isotope results fall on an isochron age. Primary phlogopite phenocrysts (Phl-B) in ultrapotassic lamprophyres are characterized by enriched Mg-Cr-Ni signatures and elevated Mg#. Phl-B exhibits hybrid in-situ Rb-Sr isotopic signals with significant radiogenic Sr enrichment compared to Phl-A. Zircon U-Pb dating of the ultrapotassic lamprophyres yields an later age than potassic lamprophyres. This, combined with the presence of Phl-A xenocrysts within some phlogopite grains (Phl-C), and significant increase of initial $^{87}Sr/^{86}Sr$ ratios from potassic lamprophyre to ultrapotassic lamprophyre, demonstrate that the enriched signatures of ultrapotassic lamprophyre likely resulted from subsequent incorporation of upper continental crustal materials into the mantle source following the formation of potassic lamprophyre. We propose that these observations reflect a two-stage enrichment process in the southern Tibetan lithospheric mantle following the India-Asia collision: (1) initial mantle enrichment through slab-derived fluids/melts during early subduction, and (2) subsequent metasomatism by Indian continental crustal materials during Miocene asthenospheric upwelling triggered by slab break-off. Subsequent extension then induced partial melting of lithospheric mantle, generating strongly enriched ultrapotassic magmatism.

Key words: post-collision, potassium-rich rocks, phlogopite, in-situ composition, porphyry

copper deposit

TRACING VOLATILE SOURCE AND EVOLUTION IN COLLISIONAL PORPHYRY DEPOSITS USING APATITE S AND CL ISOTOPES

Qiushi Zhou[1], Rui Wang[1], Heejin Jeon[2]

1. State Key Laboratory of Geological Processes and Mineral Resources, Institute of Earth Sciences, Frontiers Science Center for Deep-time Digital Earth, China University of Geosciences, Beijing 100083, China
2. Swedish Museum of Natural History, Stockholm SE-10405, Sweden

Abstract The source and evolution of volatiles in collisional porphyry deposits have long been a popular research topic. Apatite, due to its wide solidus temperature, is widely applied in porphyry mineralization research to trace the evolution of volatiles. In recent years, advances in first-principles calculations and experimental petrology focusing on S- and Cl-bearing minerals have enabled numerical modeling of S and Cl isotope partitioning between apatite and melt, allowing for new insights into porphyry mineralization processes. Our study focuses on two giant porphyry deposits on the Tibetan Plateau: Qulong and Jiama, both with prospected Cu reserve above 5 Mt. In situ S and Cl isotope analyses of apatite were conducted at the NordSIMS laboratory, Swedish Museum of Natural History, using Durango apatite as the primary reference material. The external reproducibility (1 SD) for S and Cl isotopes of the analyzed apatite samples is 0.21 ‰ and 0.19 ‰, respectively. The results show that apatite S isotopes are more effective in tracing magmatic S evolution: $\delta^{34}S$ values of apatite from the Jiama deposit initially remain constant with increasing S content, then decrease with decreasing S content. Combined with numerical modeling of magmatic evolution, this trend can be explained either by anhydrite fractionation under high oxygen fugacity ($\Delta FMQ > +1$) or by sulfide fractionation under low oxygen fugacity ($\Delta FMQ < +1$). Given that low oxygen fugacity is inconsistent with mineralization conditions, anhydrite fractionation under high oxygen fugacity is considered a more plausible explanation. In contrast, apatite in porphyry systems is predominantly fluorapatite with low Cl content, making it difficult to record Cl evolution. Therefore, Cl isotopes in apatite are more suitable for tracing material sources. After correcting for apatite-melt fractionation, the $\delta^{37}Cl$ values of apatite from the Qulong deposit can be reasonably explained by a mixture of ~60% mantle-derived juvenile magma and ~40% ultrapotassic magma, indicating that the Cl required for mineralization was mainly derived from the mantle. This conclusion is consistent with the average $\delta^{34}S$ values of apatite from Qulong.

Key words: apatite, porphyry deposit, sulfur isotope, chlorine isotope

TRANSFORMATION OF MAGNETITE TO HEMATITE DRIVEN BY EVAPORITE-DERIVED SULFATE REDUCTION: EVIDENCE FROM EBSD AND TOURMALINE GEOCHEMISTRY IN THE LONGQIAO IRON SKARN DEPOSIT, EASTERN CHINA

Yi-Zhe Fan, Li-Ping Zeng, Xian-Kang Wang, Shi-Xun Chen, Xin-Fu Zhao

State Key Laboratory of Geological Processes and Mineral Resources, and School of Earth Resources, China University of Geosciences, Wuhan 430074, China

Abstract Magnetite replaced by hematite is widely observed in the Earth's crust, particularly in magmatic-hydrothermal iron oxide deposits. The transformation of magnetite to hematite has been commonly attributed to oxidization at elevated oxygen fugacity and relatively high temperatures (>200 °C), yet the characteristics and source of the oxidizing agents responsible for this process in deep crustal environments remain poorly constrained. Here, we present electron backscatter diffraction (EBSD) analyses of magnetite-hematite pairs and in situ elemental and isotopic analyses of associated tourmaline, sulfides to constrain the mechanism of magnetite oxidation in the Longqiao iron skarn deposit, Eastern China.

Longqiao developed typical skarn minerals (e.g. garnet, diopside) and exhibits three stages of hydrothermal alteration that contain tourmaline: pre-ore prograde skarn alteration (Tur I), syn-ore Na-(K)-Fe-Ca alteration and iron skarn mineralization (Tur II), and post-ore sulfide-carbonate alteration stage (Tur III). Tourmaline from stage I and II belongs to the calcic group and plot in dravite and uvite field along the "oxy-dravite"- povondraite (O-P) join, which is indicative of precipitation from hydrosaline liquids. Post-ore tourmaline of stage III belongs to alkali group and plot in schorl field with high proportions of X-site vacancy ($X_{□}$ 0~0.59 apfu), suggesting that low salinity fluids condition. The range of B-isotopic compositions in Tur I ($\delta^{11}B$ values ranging from -6.1‰ to -4.5‰) is consistent with a magmatic source and this is supported further by Sr-isotopic compositions in Tur I (0.70623 to 0.70790), which are identical to the host intrusions. Higher $\delta^{11}B$ values (-7.6‰ to -0.1‰) obtained from Tur II are mainly ascribed to Rayleigh fractionation in the magmatic-hydrothermal system as tourmaline precipitated. Post-ore Tur III has s wide range of mostly higher B-isotopic compositions (-4.3‰ to +7.6‰) that record heavy boron component input, which is likely the infiltration of meteoric ground water from adjacent evaporites of sedimentary country rocks. Tourmaline chemistry and B-Sr isotope data indicate that the ore-forming fluids evolved from relatively reduced magmatic-hydrothermal fluids of pre- and syn-ore stages to more oxidized, sulfate-rich fluids through mixing with evaporite-dissolution fluids during the post-ore stage with hematitization. This is consistent with EBSD results that hematite preserves a

crystallographic relationship with precursor magnetite, with hematite (0001) and planes parallel to magnetite (111) and magnetite (110), respectively, indicating oxidation-driven transformation of magnetite. Pyrite intimately associated with hematite shows heavy sulfur isotopic compositions (+10.0‰ to +18.0‰), suggesting incorporation of sulfur produced by thermodynamic reduction of evaporite-derived sulfates. These observations suggest that sulfate-rich fluids generated by evaporite dissolution acted as an effective oxidizing agent, driving magnetite oxidation to hematite through coupled sulfate reduction. Our finding highlights that magnetite oxidation in hydrothermal systems can be mediated by sulfate reduction involving evaporitic components, providing a key mechanism for formation of iron oxide ore systems in evaporite-bearing areas.

Key words: Magnetite-hematite transformation, Oxidizing reaction, Tourmaline geochemistry, iron oxide deposits, evaporite-sourced sulfate reduction

ULTRAFAST ELECTRON TRANSFER KINETICS AT MINERAL-MICROBE INTERFACE: KEY TO EFFICIENT EXTRACELLULAR PHOTOELECTRON UTILIZATION

Yimei Du[1, 2], Yan Li[1, 2], Yanzhang Li[1, 2]

1. SKLab-DeepMinE, MOEKLab-OBCE, School of Earth and Space Sciences, Peking University, Beijing 100871, China.
2. Beijing Key Laboratory of Mineral Environmental Function, School of Earth and Space Sciences, Peking University, Beijing 100871, China.

Abstract The coupling of excited-state photoelectrons generated by surface semiconducting minerals under light with non-photosynthetic microbes provides a novel light-driven metabolic pathway that does not rely on photosynthetic pigments. However, the underlying mechanisms of this energy utilization, particularly why microbes continue to harness photoelectrons, remain unclear. This study investigates the impact of ultrafast electron transfer kinetics at $Cd_xZn_{1-x}S$/*Shewanella oneidensis* MR-1 interfaces on the overall efficiency of hybrid systems. The reduction efficiency of direct blue 71 dye by $Cd_xZn_{1-x}S$/MR-1 is significantly enhanced under light, leveraging the synergy of extracellular photoelectron transfer in various $Cd_xZn_{1-x}S$ nanoparticles and associated redox pathways in MR-1. Notably, CdS/MR-1 achieved a 98% reduction compared to 31% for ZnS/MR-1 after one hour, despite ZnS exhibiting a more favorable conduction band potential of −1.37 V *vs*. NHE. Time-resolved spectra and density functional theory calculations reveal that the efficiency advantages of CdS/MR-1 is attributed to its longer photoelectron lifetime (1.14 0.12 ps *vs*. 0.18 0.03 ps for ZnS/MR-1) and higher electron mobility (119.71 cm2/V·s for CdS/MR-1 *vs*. 62.47 cm2/V·s for ZnS/MR-1), providing MR-1 with superior kinetic advantages in utilizing photoelectron energy. Additionally, experiments with exogenous cytochrome c demonstrate its crucial role in modulating extracellular and intracellular electron transfer kinetics at the $Cd_xZn_{1-x}S$/MR-1 interface. Transcriptomic analysis reveals similar photoelectron transfer pathways in CdS/MR-1 and ZnS/MR-1, supporting that CdS/MR-1's superior efficiency stems from kinetic advantages at the interface, leading to greater bioavailable photoelectron accumulation. This study proposes that the key to chemotrophic microbes activating extracellular photoelectron energy transfer pathways lies in the picosecond-scale ultrafast photoelectron transfer kinetic advantage at the sulfide mineral–microbe interface. This kinetic advantage substantially improves microbial energy utilization efficiency, thereby offering a competitive edge that may have shaped the co-evolution of minerals and microbes in diverse surface environments.

Key words: Non-photosynthetic microbes, Semiconducting minerals, Ultrafast electron transfer, Interfacial kinetics, Extracellular photoelectron utilization

UNRAVELING THE CRUCIAL ROLE OF PULSED METEORIC WATER INFLUX IN OROGENIC GOLD FORMATION: CONSTRAINTS FROM IN-SITU QUARTZ GEOCHEMISTRY

Shuling Song[1], Yu Zhang[1], Huayong Chen[2]

1. School of Geosciences and Info-Physics, Central South University, China
2. State Key Laboratory of Deep Earth Processes and Resources, Guangzhou Institute of Geochemistry, Chinese Academy of Sciences, China

Abstract Orogenic gold mineralization is traditionally modeled as a steady-state process governed by deep-seated auriferous fluids. However, the Chaxi deposit (Jiangnan Orogenic Belt, South China) serves as a premier natural laboratory for decoding more complex, multi-stage mineralization processes. By integrating high-resolution cathodoluminescence (CL) imaging, fluid inclusion microthermometry, and in situ SIMS oxygen-isotope analysis, this study tracks the chemical evolution of nine distinct quartz generations across five paragenetic stages. A recurring internal signature across Stages I-IV is identified: early, CL-bright, high-temperature quartz is consistently overprinted by CL-dark generations characterized by lower temperature and salinity. This textural transition coincides with sharp negative $\delta^{18}O_{fluid}$ excursions and synchronized depletions of trace elements (Al, Sb, Ge) in the late generations of each stage, indicating episodic infiltration of meteoric water into the primary metamorphic regime. These meteoric pulses acted as a primary engine for gold precipitation by triggering rapid cooling, oxidation, and neutralization, a mechanism further supported by the mineralogical shift from Bi-rich to Te-rich assemblages and extensive gold-sulfide intergrowths within the late quartz generations. At the deposit scale, features such as wall-rock sulfidation, hydrothermal brecciation, and crack-seal veins reveal that fault-valve phase separation and subsidiary fluid-rock interactions functioned as auxiliary mechanisms dynamically coupled with meteoric water infiltration. These results show that periodic faulting transforms crustal-scale shear zones from simple conduits into dynamic interfaces, facilitating early-stage suction of meteoric water and multi-process coupling. By linking micro-scale quartz geochemistry to tectono-fluid pulses, this research provides a new framework for fluid mixing dynamics in global orogenic gold systems.

Key words: Orogenic gold deposit, Jiangnan Orogenic Belt, oxygen isotope, fluid evolution, meteoric water incursion

Acknowledgements This research was financially supported by the National Natural Science Foundation of China (42172077). The authors would like to thank Hunan Jintong Mining Co.,

Ltd for their assistance in sampling.

USING THE APRIORI ALGORITHM TO PREDICT MINERALS ON MARS USING MINERAL ASSOCIATION ANALYSIS

Kate Hendrickson [1], Forest Yee[2], Anirudh Prabhu[3], Rachel Sheppard[4,5], Elizabeth B. Rampe[6], Zakaria Jibrin[1], Michael T. Thorpe[7,8], Shaunna M. Morrison[1]

1. Rutgers University, Department of Earth and Planetary Sciences, United States of America
2. Trinity School, United States of America
3. Carnegie Institution for Science, Earth and Planets Laboratory, United States of America
4. Planetary Science Institute, United States of America
5. Institut d'Astrophysique Spatiale, Université Paris-Saclay, CNRS, France
6. NASA Johnson Space Center, United States of America
7. NASA Goddard Space Flight Center, United States of America
8. University of Maryland, Department of Astronomy, United States of America

Abstract Minerals on Mars yield insights into the planet's geologic history, environmental change, and aqueous activity. Recently, Mineral Association Analysis (MAA) was used to predict previously unknown localities of several economic mineral species in the United States of America by analyzing patterns in the Mineral Evolution Database (MED), part of the RRUFF Project. Many of these mineral predictions were later ground-truthed through citizen science and approval on Mindat.org. Mineral Association Analysis utilizes the apriori algorithm to mine association rules based on large scale trends of mineral co-occurrences across the United States. Our reference dataset included 93,419 localities across the United States of America, which spanned 2,622 different mineral species and generated 8,139,004 association rules.

This method was previously applied at Mars analogue sites like Tecopa Basin, California, in preparation for planetary applications. The shared physical and chemical fundamentals of mineral formation throughout the solar system support the model's viability on Mars and allow for nuanced interpretation related to the distinctions in geologic history between the planetary bodies. One excellent dataset to apply this model to is the set of minerals identified by the NASA Mars Science Laboratory (MSL) CheMin (Chemistry and Mineralogy) X-ray diffraction (XRD) instrument. This XRD on the Curiosity rover is the most robust mineralogical instrument we have sent to another planetary body. By assessing crystallographic information from CheMin, we have high confidence in the mineral interpretations coming from Gale Crater.

In this study, we apply the MED MAA model to these minerals identified in Gale crater to predict previously unknown mineral occurrences of known martian minerals and hypothesize the presence of species not yet found on the red planet. The model generated mineral predictions beneath instrument detection limits,in the general locality but not sampled by the drill, amorphous phases, or minerals with substantial peak overlap at CheMin's resolution. Notably, the MAA analysis

yielded repeated high-confidence predictions of opal; phyllosilicates including clay species; sulfates including gypsum, baryte, alunite; carbonates including calcite, dolomite, siderite; and sulfides including pyrite, galena, sphalerite, chalcopyrite.

In our modern age of large-scale data availability, this research illustrates one instance of advancement and possibility in mineral informatics. This research shows that mineral association rules generate statistically sound and geologically insightful predictions. The breadth of predicted minerals also indicates that mineral diversity at Gale Crater localities is likely greater than currently recognized.

Key words: Minerals, Mars, Apriori Algorithm, Gale Crater, Informatics

Acknowledgements To the Geological Society of America and Rutgers Univeristy for funding this work.

VERTICAL AND TEMPORAL EVOLUTION OF LONG-PERIOD BIOTITE POLYTYPES IN THE LONG VALLEY MAGMATIC SYSTEM: A NON-EQUILIBRIUM CRYSTALLIZATION MODEL

Jiaxin Xi[1], Yiping Yang[1*], Huifang Xu[2], Hongping He[1]

1. State Key Laboratory of Deep Earth Processes and Resources (Guangzhou Institute of Geochemistry, Chinese Academy of Sciences, China)
2. Department of Geoscience (University of Wisconsin-Madison, USA)

Abstract Minerals with compositional zoning in volcanic products are widely used to decipher the history of magmatic evolution. However, structural information, which reflects physical conditions and crystallization equilibrium, has often been overlooked. This study presents the first report on the structural zoning of deep-derived biotite phenocrysts through investigations of metaluminous rhyolite from Long Valley, CA, providing key insights into their vertical and temporal evolution. Biotite is enriched in Si, Mg, and K and depleted in Fe^{3+}, Ti, and Al^{IV} in core zones compared with rims. In situ structural analyses, including micro X-ray diffraction, Raman spectroscopy, and transmission electron microscopy, were conducted to identify cores with perfect $2M_1$ polytype and disordered rims of biotite. The results demonstrate the effectiveness of these methods in revealing various (micro-)polytypes of a single species, which occur at different crystallization temperatures, pressures, supersaturation levels, and oxygen fugacities. The concept of structural zoning is introduced here to describe the different structural features distributed systematically in various parts of minerals, which record both vertical (deep-to-shallow) and temporal (early-to-late) changes. By combining structural and chemical zoning, we illustrate a two-step growth for samples: equilibrium crystallization of the highly ordered cores in a deep magma reservoir with high temperature and pressure, followed by rapid growth of disordered rims during magma mixing in a crystal mush. This two-step model captures a vertical transition from deep to shallow levels and a temporal progression from early equilibrium to late non-equilibrium conditions. We further discuss the implications of these findings for reflecting the plumbing system structure and eruption history of rhyolitic magma over extended periods. Our study underscores the remarkable sensitivity of structural zoning in delineating the crystallization conditions of minerals and documenting the environmental changes within magma, particularly the vertical stratification and temporal evolution of the magmatic system.

Key words: Igneous crystals, biotite structural zoning, temporal and vertical evolution, TEM, non-equilibrium crystallization

VERY COLD SUBDUCTED SLAB INDICATED BY 3.65 Å PHASE IN UHP SERPENTINITE

Tingting Shen[1], Lifei Zhang[2]*, Richard Wirth[3], Jing Chen[2], Max Wilke[3],[5], Bernd Wunder[3], Marine Cotte[4]

1. Institute of Geology, Chinese Academy of Geological Sciences, Beijing, 100037, China.
2. MOE Key Laboratory of Orogenic Belts and Crustal Evolution, School of Earth and Space Sciences, Peking University, China (* corresponding author: Lfzhang@pku.edu.cn).
3. Deutsches GeoForschungsZentrum, Potsdam, Germany.
4. European Synchrotron Radiation Facility, Grenoble, France.
5. Institut fuer Erd- und Umweltwissenschften, Universitaet Potsdam, Potsdam, Germany.

Abstract Water can be transported into the deep mantle through cold subduction zone. The studies of experimental petrology have shown that the dense hydrous magnesium silicates (DHMS) phases should be the main potential carriers of water in a very cold subduction zone. However, no DHMS phase has been found in nature rocks except the 10 Å phase. Here, we report Raman spectroscopy data, TEM data and synchrotron X-ray diffraction measurements of nanometre-sized inclusions found in ultrahigh pressure serpentinites from SW Tianshan, China. All these data together strongly suggest that these relict lamellar inclusions in UHP serpentinites are the 3.65 Å phase. The high pressure/low temperature stability of the 3.65 Å phase indicates that the host rock unit was part of a very cold subducted slab, which is a pre-requisite to preserve such an extreme phase. Such a very cold subducted slab would be existed as a possible transport medium for cycling water from the Earth's surface into the deep upper mantle.

Key words: 3.65 Å phase, TEM, serpentinite, water, subduction zone

VESUVIANITE SUPERGROUP NOMENCLATURE

Taras L. Panikorovskii

Laboratory of Nature-Inspired Technologies and Environmental Safety of the Arctic, Nanomaterial Research Center of the Kola Science Centre, Russian Academy of Sciences, Russia

Abstract Vesuvianite-group mineral nomenclature is based on the general chemical formula $(^{8}X1)_2(^{7}X2)_8(^{9}X3)_8(^{8}X4)_1(^{5}Y1)_1(^{6}Y2)_4(^{6}Y3)_8(^{4}T1)_{0\text{-}4}(^{3}T2)_{0\text{-}1}(^{4}ZO_4)_{10}(^{4}Z_2O_7)_4(W1)_2(W2)_8(W3)_{0\text{-}2}$, where the most common elements or vacancies in the group of sites are *X* = Ca, Na, *REE*, Sr, K, Pb, Sb, Bi, U and Th; *Y* = Al, Mg, Fe, Ti, Mn, Cu, Cr and Zn; *Z* = Si, H_4O_4; *T* = vacancy, B, Al and Fe; *W* = OH, O, F, Cl and vacancy. The different vesuvianite polytypes (*P*4/*nnc*, *P*4/*n* and *P*4*nc*) are considered jointly as structural polytypes without using any additional suffixes. The subdivision of groups (vesuvianite, wiluite, potential manaevite and five potential new groups) is based on the different populations of *X*, *Y*, Z and *T* groups of cationic sites. The different occupancies of anionic *W*-group sites are considered for the species definition within groups. Vesuvianite supergroup species are defined according to the dominant-valency rule where the dominant ion of the dominant valence state at each site is used as basis for the nomenclature. We propose a scheme of classification and ways of normalization and formula calculation procedures. We recommend a procedure for allocating cations from complete chemical data that is based on normalization to 19 X cations, and normalization to 50 cations when only EDS or WDS chemical data are available There are 12 possible mineral species described in the literature, which require further investigations.

Key words: vesuvianite, nomenclature, supergroup, formula, mineral

Acknowledgements This work were carried out in accordance with the state task, registration number FMEZ-2025-0046

YULINITE, SRNB2O6, A NEW MINERAL FROM THE BAYAN OBO DEPOSIT, INNER MONGOLIA, CHINA

Guanghua Liu[1], Zhixiang Liu[1], Jianchao Song[1], Jingyi Wu[1], Wenyi Wang[1], Haiyang Wang[1], Siyun Li[1], Zhuqing Ding[1], Xiangping Gu[1*,2] *Corresponding author: guxp2004@163.com

1. School of Gemology and Mineral Resources, Jiangxi Institute of Applied Science and Technology, Nanchang, 330100, China
2. School of Geosciences and Infophysics, Central South University, Changsha 410083, China

Abstract Yulinite (IMA2025-093) is discovered from the West Mine of the Bayan Obo deposit, Inner Mongolia, China, which is the type locality of 28 new minerals and hosts more than 200 minerals. Yulinite is the 29th new mineral from this mine. It occurs as a platy crystal, about 10 μm in size, in the matrix of magnetite of banded Fe-REE-Nb ores (Fig. 1). Associated minerals include magnetite, columbite-(Fe), nioboaeschynite-(Ce), clinofergusonite-(Ce), ilmenite-pyrophanite series, pyrite, sphalerite, fluorite, fluorapatite, fluorophlogopite, dolomite, baryte etc. It is translucent in microscopre, grey in color with a reflectance of 15.6-15.9%. The Raman spectrum is composed 18 well-resolved peaks obviously distinguished from pyrochlore and fersmite (Fig. 2). The empirical formula from 6 microprobe analyses is $Sr_{1.08}(Nb_{1.86}Fe_{0.10}Ti_{0.06})_{\Sigma 2.02}O_6$. Yulinite is monoclinic, space group: $P2_1/c$, a = 7.7184(3) Å, b = 5.5954(2) Å, c = 10.9905(4) Å, β = 89.772(3)°, V = 474.64(3) Å^3, Z = 4. Yulinite is a member of the aeschynite-(Ce) group. The crystal structure is composed of edge-shared dimers of NbO_6 octahedra, which are corner-connected to form double chains along the a-axis (Fig. 3a). The planes of the double chains are zigzag-aligned, respectively parallel to (0 -5 -1) and (0 5 -1), and are further corner-connected to form a network with open channels along the a-axis occupied by Sr coordinated with 8 O atoms (Fig. 3b). Yulinite (symbol: Yul) is named in honor of Mr. Yulin Huang (b. 1961), a promoter for privately-funded higher education, and the sponsor and founder of Institute of Gemmology and Mineral Resources, Jiangxi Institute of Applied Science and Technology.

ZIRCON AND APATITE COMPOSITIONS: INSIGHTS INTO MAGMATIC FERTILITY OF THE QIMANTAGE BELT, EAST KUNLUN OROGEN

Jing-Jing Zhu, Ju-Ting Deng, Lichuan Pan, Xianwu Bi, Ruizhong Hu

State Key Laboratory of Critical Mineral Research and Exploration, Institute of Geochemistry, Chinese Academy of Sciences

Abstract Magma oxygen fugacity and volatile contents are critical parameters governing the formation of porphyry Cu deposits. Zircon and apatite inclusions hosted in zircon are common accessory phases in intermediate–felsic intrusive rocks, and their compositional characteristics can preserve information on early magmatic conditions. Accordingly, mineral-geochemical proxies based on these phases provide an economical and efficient approach for evaluating porphyry Cu potential at the regional scale.

The Qimantage metallogenic belt in the East Kunlun Orogen, located along the northeastern margin of the Tibetan Plateau, hosts numerous porphyry Cu occurrences and medium-sized skarn Cu polymetallic deposits; however, large porphyry Cu deposits are relatively rare. In this study, ore-related intrusions from skarn-type Cu polymetallic deposits in the study area, including the Kaerqueka and Lalingzaohuo deposits, were investigated. The results indicate that these magmas were characterized by moderate oxygen fugacity, with zircon ΔFMQ values of 0.36 ± 0.36; low water contents, as reflected by zircon EuN/EuN* values of 0.31 ± 0.10; sulfur-poor conditions, with apatite S contents below the detection limit; and Cl enrichment, with apatite Cl contents of 0.65 ± 0.29 wt.%. These features are less favorable than those of globally typical porphyry Cu-forming magmatic systems, probably suggesting limited porphyry Cu potential. Zircon copper fertility index (ZCFI) which jointly proxies magmatic water content and oxygen fugacity, yields values of 3.8 ± 1.1, lower than those typical of porphyry Cu-fertile magmas, further explaining why the porphyry Cu deposits are much less than typical arc belts.

While these intrusions host rare porphyry Cu deposits, they are closely linked to skarn Cu mineralization. Their occurrence indicates that Cl-rich magmas exert a more critical control on skarn Cu mineralization than oxygen fugacity and H_2O-S contents. Notably, apatite inclusions in amphibole from the same samples have lower Cl (0.47 ± 0.24 wt.%) and higher F (2.84 ± 0.34 wt.%) than those in zircon. This suggests amphibole-hosted apatite compositions have been modified, so exceptional caution is needed when using them alone to reconstruct magmatic volatile budgets.

Key words: Porphyry-skarn Cu deposits, Magma fertility, Zircon, Apatite

ZIRCON FINGERPRINTS THE CRITICAL MAGMATIC-HYDROTHERMAL TRANSITION FOR CRITICAL ENRICHMENT IN THE BAERZHE PERALKALINE GRANITE

Hui-Min Su, Shao-Yong Jiang, Tao Jin

School of Earth Resources, China University of Geosciences, Wuhan 430074, PR China

Abstract Rare metals and rare earth elements (REE) are globally critical resources and reach exceptional enrichment in peralkaline granite systems, yet the mechanisms linking magmatic evolution to hydrothermal concentration remain debated (Vasyukova and Williams-Jones, 2020). Here we present new textural, geochemical, and geochronological constraints from multi-generation zircon of the spherulite granite in the giant Baerzhe Zr-REE-Nb deposit, Northeastern China.

Three process-defined zircon types record a continuous magmatic–hydrothermal evolution. Type-I zircon crystallized from highly evolved melts enriched in REE, Y, Th, U, Nb, and Hf. Type-II zircon irregularly overprints Type-I and formed during fluid-mediated recrystallization at the magmatic–hydrothermal transition. Extremely high Y (5.1–6.0 wt%) and Nb (up to 9,020 ppm) indicate formation in alkaline, F-rich fluids capable of efficiently mobilizing HFSE. Type-III zircon, characterized by spongy textures, depleted Y-Th-U and enrichment in Al-Fe, formed via dissolution–reprecipitation driven by late hydrothermal fluids. In situ LA-ICP-MS U-Pb dating demonstrates indistinguishable ages of ~126 Ma for all types, indicating that melt crystallization, fluid exsolution, and hydrothermal modification occurred within a short-lived and continuous metallogenic pulse rather than multiple discrete events. The data reveal that the magmatic–hydrothermal transition represents the critical window for Y and Nb enrichment, whereas subsequent fluid influx promotes LREE redistribution through monazite and bastnäsite precipitation.

This process-based interpretation refines earlier views of Baerzhe mineralization (e.g., Yang et al., 2014) and is consistent with recent studies emphasizing the importance of fluid-driven zircon modification in highly evolved granitic systems. The results indicate that zircon textures and compositions provide a direct record of how metals were redistributed between melt and fluid, and they help identify the stages most closely associated with economically significant enrichment.

Key words: Zr-REE-Nb mineralization, zircon chemistry, peralkaline granite, Baerzhe deposit

ZIRCONS REVEAL THE HISTORY OF FLUCTUATIONS IN OXIDATION STATE OF CRUSTAL MAGMATISM AND SUPERCONTINENT CYCLE

Rui Wang[1, 2]*, Shao-chen Wu[1], Roberto F. Weinberg[3], William J. Collins[4], Peter A. Cawood[3]

1. State Key Laboratory of Geological Processes and Mineral Resources, Institute of Earth Sciences, China University of Geosciences, Beijing 100083, China
2. Frontiers Science Center for Deep-time Digital Earth, China University of Geosciences (Beijing), Beijing 100083, China
3. School of Earth, Atmosphere and Environment, Monash University, Clayton, VIC 3800, Australia
4. The Institute for Geoscience Research, Curtin University, Perth, WA 6102, Australia

Abstract We apply a zircon redox index to a global compilation of detrital zircons to track the variation of oxidation state, expressed as ΔFMQ, through Earth's history. Those from I-type rocks, which comprise mantle and crustal igneous protoliths, including Tonalite–trondhjemite–granodiorites (TTGs), generally have a high oxidation state (ΔFMQ > 0). In contrast, zircons from igneous rocks derived from supracrustal source rocks (S-type) are commonly reduced (ΔFMQ < 0). With the probability density function derived from the Gaussian-Kernel-Density-Estimation, we use the maximum likelihood estimation (MLE) to distinguish S-type from I-type zircons through Earth's history using zircon redox. Voluminous S-type magma production shows a ca. 600 Ma cyclicity that is closely related to the supercontinent cycle. We link a cyclic drop in redox values after 2.6 Ga to periodic S-type magma generation associated with burial and melting of metasedimentary rocks during supercontinent assembly and amalgamation. The ΔFMQ of the detrital zircons rise at ~3.5 Ga followed by a consistent average ΔFMQ > 0 over the last 3 Ga. Given that the redox state of magmas is independent of crustal thickness and silica variation, and elevated values are likely more closely related to tectonic setting, we suggest that the consistent average ΔFMQ > 0 from ca. 3.5 Ga onwards relates to recycling of oceanic lithosphere back into the mantle in what eventually became established as subduction zones. The more reduced magmas associated with sedimentary sources, became established at 2.6 Ga, presumably in response to continental rocks rising above sea-level, and follow peaks of productivity associated with the supercontinent cycle.

Key words: oxidation state, supercontinent, weathering, subduction, zircon

A GENERAL MACHINE LEARNING MODEL FOR THE VISCOSITY OF ALUMINOSILICATE MELTS

Charles Le Losq[1,2], Clément Ferraina[1,3], Paolo Sossi[4], Charles-Édouard Boukaré[5]

1. Université Paris Cité, Institut de physique du globe de Paris, CNRS, Paris, France

2. Institut Universitaire de France, Paris, France

3. Université de Lorraine, CNRS, CRPG, F-54000 Nancy, France

4. Institute of Geochemistry and Petrology, ETH Zürich, Zürich, Switzerland

5. York University, York, Canada

Abstract In planetary interiors, magmas transport heat and matter between the mantle, crust, and surface. Their chemical composition governs atomic structure, which in turn controls physical properties. Among these, viscosity is critical, as it regulates magma mobility, crystallization, outgassing, and fragmentation. Viscosity spans many orders of magnitude as a function of temperature, pressure, and composition, including volatile content. Existing models, however, remain limited: they are often restricted to specific compositional domains and generally lack robust uncertainty quantification.

In recent years, machine learning (ML) has emerged as a promising approach to predict the viscosity of geological and industrial melts. Among the tested methods, artificial neural networks (ANN) are widely used, either as purely data-driven models or in combination with physically motivated formulations. However, the relative performance and robustness of these approaches remain unclear. In addition, most ML models provide limited insight into the uncertainties associated with their predictions.

Here, we present a new model for predicting molten magma viscosity, applicable in diverse scenarios, including magma oceans on lava planets. Using a database of 28,898 viscosity laboratory measurements on phospho-aluminosilicate melts, spanning superliquidus to undercooled temperatures and pressures up to 30 GPa, we trained a greybox artificial neural network, refined by a Gaussian process. This model achieves high predictive accuracy (RMSE ≈ 0.4 $\log_{10}$ Pa·s) and can handle compositions from SiO_2 to multicomponent magmatic and industrial glasses, accounting for pressure effects up to 30 GPa for compositions such as peridotite.

Key words Magma, Viscosity, Pressure, Machine Learning, Magma Ocean

ABSENCE OF WATER CONTENT CONTRAST AT LAB BENEATH CHINA: STUDY ON XENOLITHS IN NUSHAN MAAR, ANHUI

PROVINCE

Yuto Sato[1,2], Eiichi Takahashi[2], Kenji Shimizu[1], Takayuki Ushikubo[1]

1. Kochi core sample research, JAMSTEC, Japan

2. State Key Laboratory of Deep Earth Processes and Resources, Guangzhou Institute of Geochemistry, Chinese Academy of Sciences, China

Abstract Fluids in mantle rocks play a vital role in mantle metasomatism and in the generation of various types of magma. Water in mantle minerals, particularly in olivine, is considered to exert a strong control on mantle rheology. It has been proposed that the origin of the lithosphere–asthenosphere boundary (LAB) is related to a contrast in water content in olivine (Karato, 2012). We previously investigated the water contents of olivine and pyroxenes in spinel peridotite xenoliths from Ichinomegata maar and found no significant contrast in olivine water content between the lithosphere and asthenosphere in a subduction setting (Sato et al., 2023, EPSL).

Mantle xenoliths from Nushan maar are among the most extensively studied in China. Because the host magma is inferred to have been relatively cool, and because the xenoliths were emplaced in a cold maar deposit without significant dehydration, volatiles in mantle minerals, including olivine, are likely better preserved than in xenoliths from lava flows (Hao et al., 2016; Xia et al., 2019). In this study, we analyzed 30 spinel peridotite xenoliths from Nushan and estimated their depths of origin using geothermobarometry as described in our previous work. The geotherm derived from these spinel peridotites agrees well with that estimated from garnet pyroxenite and garnet peridotite xenoliths from Nushan (Huang et al., 2004). A sharp textural transition occurs at ~55 km depth. Xenoliths from shallower levels are coarse-grained with granoblastic textures, whereas those derived from depths greater than ~55 km are finer-grained and porphyroclastic. Hornblende commonly occurs in xenoliths from <55 km but is absent in those from greater depths.

OH species in olivine (OL), orthopyroxene (OPX), and clinopyroxene (CPX) were analyzed by FTIR spectroscopy. In olivine, OH associated with Ti-clinohumite–type defects and Mg-site vacancies predominates. The OH absorption peaks in olivine show highly variable peak-height ratios within individual samples, suggesting partial dehydration during xenolith transportation. In contrast, pyroxenes generally exhibit homogeneous OH peak patterns, indicating better preservation, with only minor exceptions. Estimated water contents determined by FTIR are 0.8–8.0 ppm for OL, 53–143 ppm for OPX, and 92–423 ppm for CPX.

Volatile contents (H_2O, CO_2, and F) in OPX and CPX were measured by SIMS, using the FTIR-derived water contents as H_2O standards. For CO_2 and F, calibration curves of basaltic glass standards (Shimizu et al., 2017, Geochem. J.) were employed because appropriate mineral standards are unavailable. At mineral cores, H_2O contents are 51–441 ppm in CPX and 58–142 ppm in OPX; CO_2 contents are 1.6–5.9 ppm and 0.6–2.4 ppm; and F contents are 11–54 ppm and

3–23 ppm, respectively. The distribution coefficients of H_2O and F correlate systematically with temperatures estimated by geothermobarometry. In both pyroxenes, CO_2 and F contents increase with depth, whereas the H_2O/F ratio decreases. Elevated H_2O/F ratios at shallower depths (35–55 km) can be explained by addition of H_2O-rich slab-derived fluids, consistent with the H_2O–F mantle trend (Shimizu et al., 2019). In contrast, lower H_2O/F ratios at greater depths (55–80 km) may reflect contributions from MORB-like mantle and recycled materials.

Comparison with results from Ichinomegata (Sato et al., 2023) indicates lower water concentrations in the mantle beneath Nushan, suggesting reduced slab-fluid input with increasing distance from the trench. This may result in a deeper and hotter LAB beneath Nushan than beneath Ichinomegata. Although accurate water contents in mantle olivine are obscured by dehydration during xenolith transport, the water contents of OPX and CPX suggest that any contrast in water content between shallow lithospheric peridotite (30–55 km) and deeper asthenospheric peridotite (55–80 km) is likely small.

Key words water, fluids, lithosphere, asthenosphere, mantle dynamics

ATMOSPHERE DISSOLUTION IN MAGMA OCEANS IN EXOPLANETS

Razvan Caracas

Institut de Physique du Globe de Paris, Université Paris Cité, CNRS, 1 rue Jussieu, Paris 75005 France

Abstract The question of hydrogen dissolution in a silicate planet is longstanding within the Earth and planetary science community. Its presence and amount can drastically change the functioning of the planet from the redox state to the characteristics of its atmosphere. This question becomes of utmost importance when studying exoplanets sub-Neptunes and super-Earths. Here, we employ ab initio molecular dynamics to compute the solubility of hydrogen in a magma ocean with bulk silicate Earth composition. We find that magma oceans can dissolve almost 2 wt% hydrogen at typical conditions relevant to their interface with hot and dense atmospheres. The hydrogen influx changes the redox state of the magma ocean (which becomes reduced), and generates a massive outflux of oxygen, which combines with atmospheric hydrogen to form large amounts of water vapor. Numerous other complex chemical species are released into the atmosphere. This changes profoundly the thermal and chemical evolution of the primitive atmosphere for early Earth-like conditions. For sub-Neptune exoplanets, this offers an amazing diagnostic tool, as their atmospheres would bear spectral signatures observable from space telescopes. These atmospheric composition changes are a testable signature of hidden magma oceans on exoplanets. Moreover, the uptake of volatiles by the magma implies that sub-Neptunes are more volatile-rich than once thought.

Key words extreme conditions, molecular dynamics, chemical speciation

COMPOSITION AND NATURE OF HYDROTHERMAL FLUIDS RELATED TO GOLD MINERALIZATION IN THE MENGE GOLD DEPOSIT, WESTERN ETHIOPIA

Mesfin Tadesse Wolde[1], Yonggang Feng[1*,2]

1. School of Earth Science and Resources, Chang'an University, China

2. Key Laboratory of Western Mineral Resources and Geological Engineering, Ministry of Education, China

Abstract Understanding the nature, origin, and evolution of hydrothermal fluids is critical for constraining the mechanisms of gold mineralization in orogenic systems. The Menge gold deposit, located in Western Ethiopia within the Neoproterozoic Arabian–Nubian Shield, provides an excellent natural laboratory for investigating fluid–rock interaction processes associated with auriferous mineralization. This study integrates field observations, hand specimen characterization, and petrographic analysis of representative lithologies, quartz vein textures, and fluid inclusion assemblages to constrain the physicochemical properties of ore-forming fluids and their role in gold deposition. Macroscopic observations reveal that gold mineralization is predominantly hosted in quartz veins and silicified zones developed within mafic to intermediate metavolcanic rocks and metasedimentary units (graphite-rich schist). Petrographic observation shows that quartz veins exhibit multiple generations of quartz subject to recrystallization, micro-fracturing, and fluid-assisted deformation. Textural relationships, including crack-seal structures, healed microfractures, and disseminated opaque minerals (likely sulfides), indicate episodic fluid flow and pressure fluctuations during vein formation. The presence of abundant primary and secondary fluid inclusions indicates a complex fluid evolution history. Both primary and secondary fluid inclusions are predominantly carbonic LLV inclusions. with subordinate vapor-rich ones. A great number of primary inclusions contain multiple solids including. Raman spectroscopy suggests that the vapor phase is dominated by CO_2 with minor N_2 and that nahcolite, quartz, lithium metaborate, brookite, and higher hydrocarbons are present as solid phases. The presence of higher hydrocarbons is likely due to the involvement of graphite in host schist. Fluid immiscibility and phase separation appear to have played a significant role in gold precipitation, as evidenced by inclusion assemblages and vein textures. The integration of petrographic and textural evidence suggests that gold deposition at Menge was controlled by structural conduits, fluid pressure cycling, and evolving fluid composition. These findings support a model in which deep-sourced metamorphic fluids migrated along shear zones, underwent decompression and phase separation, and precipitated gold in structurally favorable sites. This study provides new insights into the hydrothermal system of the Menge gold deposit. It contributes to a broader understanding of orogenic gold systems in the Arabian–Nubian Shield.

Key words gold mineralization, ore-forming process, metamorphic fluid, Arabian–Nubian Shield, Alteration, Western Ethiopia

COMPOSITION OF ZONED OLIVINES FROM MEIMECHITES OF THE KONTOZERO COMPLEX (KOLA PENINSULA): EVIDENCE FOR EXTREMELY MAGNESIAN MANTLE MELTS

Anna M. Dymshits[1,2], Julia A. Mikhailova[1], Pavel Yu. Plechov[3]

1. Geological Institute, Kola Science Center, RAS, Russia

2. Institute of the Earth's crust, SB RAS, Russia

3. Fersman Mineralogical Museum, Russia

Abstract In the northeastern part of the Kola Peninsula, Archean gneisses of the Kola Series are intruded by rocks of the Kontozero Complex, which is interpreted as a paleovolcano. Its stratigraphic section is tripartite and includes (from bottom to top): a terrigenous-volcanic sequence (ultramafic rocks and their tuffs), a volcanic sequence (composed mainly of melilitites and nephelinites), and a carbonatite sequence. In the lowermost part of the terrigenous-volcanic sequence, relatively thin interlayers of ultramafic lavas, interpreted as meimechites, were discovered. Meimechites are rare high-Mg, high-Ti ultramafic volcanic rocks that represent primary mantle melts, offering critical insights into the composition of the lithospheric mantle and associated melting processes. In this study, the major and trace element compositions of olivines from the meimechites of the Kontozero massif were investigated using EPMA and LA-ICP-MS techniques.

According to EPMA data, olivine Fo values [100×Mg/(Mg+Fe) in mol%] range from 81 to 92. Typical impurities include Ca, Ni, and Mn. Calcium content reaches up to 1.42 wt.% CaO (minimum 0.12 wt.% CaO), NiO concentrations vary from 0.17 to 0.47 wt.%, and MnO content ranges from 0.11 to 0.47 wt.%. All olivine grains are zoned. A notable compositional gap exists, with olivine compositions between Fo_{88} and Fo_{90} being absent. Two distinct populations of high-Mg olivine (Fo $\geqslant$ 90) were identified: rare mantle xenocrysts (characterized by deformation textures and low CaO < 0.1 wt.%) and dominant magmatic phenocrysts (weakly zoned, with higher CaO). Low-Mg olivines (Fo $\leqslant$ 88) are enriched in Ca and plot below the equilibrium envelope, suggesting crystallization from a melt modified by volatile loss. Distinctly zoned grains are rare and includes phenocrysts with a high-Mg core (Fo_{90-92}) and Fe-rich rim (Fo_{84-87}). Phenocrysts with reverse zoning exhibit narrow embayments infilled by groundmass and contain low-Ca, low-Mg cores. Compositional heterogeneity is also expressed as "spots" in some phenocrysts are presented by local areas of Fe- and Ca-rich olivine. Trace elements in olivine show wide concentration ranges: Cr from 50 to 1099 ppm, Ca from 542 to 10547 ppm, V from 2 to 13 ppm, and Mn from 408 to 2626 ppm. Nickel content varies from 1892 to 3060 ppm, Co from 84 to 220 ppm, Ti from 74 to 302 ppm, and Sc from 3.8 to 15 ppm. High-Mg olivine grains are characterized by high Ni and low Ca contents. However, from the core to the rim of these grains, the Ni concentration can either decrease or increase. Similarly, for Cr, high-Mg olivine

grains are enriched in Cr, and its content can either increase or decrease from the core to the rim. Low-Mg olivines are always relatively enriched in Ca and Mn, but the concentrations of these elements vary quite irregularly from the cores to the rims of the grains. Both low- and high-Mg olivine grains contain comparable amounts of aluminum. Numerical modelling, thermobarometry and oxibaromenty calcaltions indicate that the primary magma was generated in a relatively oxidazed source at the base of the lithosphere (~ 180 km, 60 kbar and 1400–1450°C). Physical separation from the mantle substrate occurred at ~23.3 kbar (olivine–clinopyroxene cotectic). Rapid magma ascent (~2.6 km/day) inhibited the formation of clinopyroxene phenocrysts, preserved olivine zoning, and facilitated the survival of mantle xenocrysts.

Key words meimechites, olivine, xenocrysts, phenocryst, mantle melts

Acknowledgements Sampling and microprobe analysis were funded by the Ministry of Science and Higher Education of the Russian Federation, project no. FMEZ-2024-0008. Analytical studies (LA-ICP-MS) were supported by the Russian Science Foundation grant No. 25-77-30006, https://rscf.ru/project/25-77-30006/.

CONSTRAINING MANTLE REDOX CONDITIONS USING FERRIC IRON IN CLINOPYROXENE XENOLITHS: A MACHINE LEARNING APPROACH

Chen-Yang Ye, Chun-Tao Liu, J. ZhangZhou

Research Center for Earth and Planetary Material Sciences, School of Earth Sciences, Zhejiang University, Hangzhou 310058, China

Abstract The oxygen fugacity (f_{O_2}) of the mantle governs the behaviors of multivalent elements (e.g., Fe, V) and the speciation of C–O–H fluids, influencing mantle melting, magmatic evolution and volatile distribution across tectonic settings. However, the estimation of mantle f_{O_2} is limited by challenges in measuring Fe^{3+} in minerals like clinopyroxene (Cpx) due to analytical constraints and inconsistencies between oxybarometer methods. Here, we applied machine learning (ML) to predict Cpx Fe3+ content and equilibrium pressure-temperature and f_{O_2} conditions. We employed a nested cross-validation approach to minimize coincidental perfomance biases. Our models outperformed previous ferric iron and thermobarometer models on both metrics and generalization. The ML-based oxybarometer shows adequate generalization with R2 peaking at 0.74. We compiled a application dataset comprising of 9,832 global mantle xenolith samples. For the subset with Fe^{3+} measurements (n≈600), ML-predicted f_{O_2} closely matches thermodynamic estimates, supporting the robustness and global applicability of our approach. Applying the model to the rest samples lacking Fe^{3+} analyses expands geographic coverage to data-sparse provinces (e.g., South America, India, and Eastern Europe), and reveals coherent global redox gradients. Xenoliths from cratonic mantle domains show no temporal f_{O_2} trends since Mesoproterozoic. Comparative analysis across cratonic mantle xenoliths, abyssal peridotites, and oceanic intraplate xenoliths indicates that mantle residues are initially oxidized by short-term metasomatism, but eventually equilibrate to stable redox conditions through interactions with neutral or reducing agents.

Key words oxygen fugacity, machine learning, mantle xenolith, peridotite

CONSTRAINTS ON MELT AND FLUID IN THE CONTINENTAL CRUST FROM ELECTRICAL CONDUCTIVITY ANISOTROPY

Song Luo[1,3], Haiying Hu[2], Lidong Dai[2] and Yu He[1,3]

1. Key Laboratory of High-Temperature and High-Pressure Study of the Earth's Interior, Institute of Geochemistry, Chinese Academy of Sciences, Guiyang, 550081, China
2. School of Physics and Electronic Science, Guizhou Normal University, Guiyang, 550025, China
3. University of Chinese Academy of Sciences, Beijing, 100049, China

Abstract Electrical anisotropy, widely observed by magnetotelluric surveys at crustal depths of ~15–50 km, is generally attributed to rock microfabric, lithologic layering, or oriented fluids and melts. However, these mechanisms have not been effectively verified in the continental crust due to the lack of experimental and computational evidence. Laboratory measurements on the electrical anisotropy of crustal rocks are extremely challenging when considering microfabrics and oriented microcracks filled with fluids or melts. In contrast, numerical modeling, being an effi-cient approach, can be used to compute the anisotropic physical properties of complex rock system. Here, we calculated electrical anisotropy using the available data on mineral conductivity and rock fabrics by circuit simu-lation technique to evaluate these mechanisms. Our results show that oriented fluids or melts within rocks generate much higher electrical anisotropy than mineral alignment and lithologic layering, and thus can explain the geo-physically observed electrical anisotropy anomalies. Correspondingly, ~0.5 vol.% fluid with 3.5 wt.% salinity in the middle crust and ~3.0 vol.% fluid with 5.0 wt.% salinity in the lower crust are necessarily present for inter-preting the electrical anisotropy observed in the middle and lower crust, respectively. For the finger-shaped melt intrusions beneath the Kunlun Fault in Tibet Plateau, 7–19 vol.% granitic melts with 6–8 wt.% water contents is required to match the observed electrical anisotropy. Our results provide not only fundamental data for forward and inverse modeling of MT sounding, but also independent constrains on the crustal fluids and melts.

Key words Electrical anisotropy, Rock fabrics, Fluid, Melt, Continental crust

Acknowledgements This study was financially supported by the Guizhou Normal University Academic New Talent Fund (Grants No. GZNUD[2025] 10 and GZNUD[2025] 12) and National Natural Science Foundation of China (Grant Nos. 42274137).

DEVELOPMENT AND APPLICATIONS OF HYDROTHERMAL DIAMOND-ANVIL CELL

I-Ming Chou

Institute of Deep-sea Science and Engineering, Chinese Academy of Sciences, China

Abstract The hydrothermal diamond anvil cell (HDAC) was developed by the late Professor William A. Bassett (1931–2026) of Cornell University around 1990, specifically for conducting hydrothermal experiments at temperatures up to 1000 °C and pressures up to 3.5 GPa. The HDAC was first introduced to the European Earth science community at an international conference in France in 1992, and subsequently to researchers in other countries, including the United States, Canada, Japan, and China.

To enhance its operational flexibility and broaden its applicability, several modifications have been made to the HDAC design: (1) A recess approximately 300 μm in diameter and 50 μm deep was created at the center of the lower diamond anvil face, on which a groove was milled from the edge of the diamond toward the center of the recess, leaving about 160 μm of diamond thickness before reaching the recess. This configuration allows X-ray absorption fine structure (XAFS) signals—generated when synchrotron X-rays interact with the sample solution confined in the recess—to be collected effectively while minimizing X-ray absorption by the diamond along the groove path. (2) The metal gasket, typically used to form a sample chamber in its central hole and to seal the fluid sample through deformation under compression by the two opposing diamond anvils, was eliminated to avoid contamination of the sample solution in the recess by the gasket. (3) The protecting gas (Ar + ~2% H_2) chamber, originally designed to prevent oxidation of the diamonds and molybdenum heating wires at elevated temperatures, was reduced in size so that the two guide posts—used to compress the diamond anvils against a metal gasket—remained outside the heating zone of the gas chamber. This modification simplified disassembly of the HDAC after each heating experiment, facilitating the setup of subsequent runs.

The HDAC has been employed in a wide range of studies on Earth materials, including: (1) determining the stability and solubility of minerals in aqueous fluids, melts, and supercritical fluids under elevated pressure and temperature conditions; (2) formulating equations of state for aqueous solutions (e.g., isochores of NaCl–H_2O systems); (3) identifying and characterizing dissolved complexes in aqueous solutions, primarily through Raman and XAFS spectroscopies; and (4) applying external pressures to fluid inclusions within the HDAC to minimize deformation or decrepitation during heating, thereby enabling the determination of liquid-vapor homogenization and total homogenization temperatures of the fluid inclusions.

Future HDAC research will focus on improving the sensitivity of in-situ spectroscopic analysis and developing in-situ redox control and measurement techniques for hydrothermal experiments involving multivalent elements.

Key words Hydrothermal diamond-anvil cell (HDAC), mineral–fluid interaction, Raman and X-ray absorption fine structure (XAFS) spectroscopies, complexes in fluids, in-situ redox control and measurement in HDAC

Acknowledgements I wish to honor Bjorn Mysen, a dedicated user of the HDAC, in recognition of his exceptional contributions to the study of fluids and melts in planetary interiors. I am deeply grateful to the late Professor William A. Bassett for his thoughtful scientific mentorship and for more than 35 years of close collaboration, which resulted in a total of 31 co-authored papers. I also extend my thanks to many former and current colleagues, visiting scientists, and students at the U.S. Geological Survey and the Institute of Deep-sea Science and Engineering, Chinese Academy of Sciences, for their assistance and support. This study was supported by the National Natural Science Foundation of China (Grant No. 42130109).

EXPERIMENTAL STUDY OF APATITE AS A PROXY OF VOLATILE AND METAL BUDGETS IN CARBONATITE MELTS

Haihao Guo[1,2], Johann Tuduri[2], Zineb Nabyl[3], Saskia Erdmann[2], Xiaochun Li[4], Fabrice Gaillard[2]

1. State Key Laboratory of Geological Processes and Mineral Resources, School of Earth Sciences, China University of Geosciences, Wuhan 430074, China

2. Univ. Orléans, CNRS, BRGM, ISTO, UMR 7327, F-45071, Orléans, France

3. CEA, DES, ISEC, DE2D, Univ Montpellier, Marcoule, France

4. Key Laboratory of Mineral Resources, Institute of Geology and Geophysics, Chinese Academy of Sciences, Beijing 100029, China

Abstract Carbonatites are silica-poor, volatile-rich magmatic rocks that host significant deposits of rare earth elements (REE) and high field strength elements (HFSE). However, reconstructing primary carbonatite melt compositions is challenging due to their intrusive nature and common metasomatic overprints. Here we employ apatite as a geochemical proxy to retrieve the volatile and metal concentrations of carbonatite melts. We experimentally determined apatite–melt partition coefficients for alkali-rich carbonatite melts with variable volatile contents (H, F, S, Cl) using internally heated pressure vessels (200 MPa, 800°C) and piston-cylinder apparatus (400–800 MPa, 725–1050°C). The results show partition coefficients (D) of 1–6 for Sr, Y and REE, <0.5 for HFSE, and for volatiles: DF = 0.97, DCl = 0.14, and DS = 0.031. Temperature, pressure and oxygen fugacity have only minor effects on the partitioning of volatiles, REE and HFSE. Using these experimentally calibrated partition coefficients, we analysed over 700 natural apatite compositions from carbonatites in diverse geodynamic settings. Reconstructed carbonatite melts show more than two orders of magnitude variation in REE contents, while Cl and F concentrations range from 0.88 to 6.01 wt% and 0.04 to 1.34 wt%, respectively. No correlations are observed between REE, HFSE, Cl and F in the melts, suggesting that some carbonatite melts are inherently enriched or depleted in these elements, likely reflecting silicate–carbonate immiscibility processes. This study demonstrates that apatite is a robust archive for deciphering the volatile and metal signatures of carbonatite systems, with direct implications for understanding their ore-forming potential.

Key words Apatite, Volatiles, Carbonatite, REE

EXTREMELY SLOW HORIZONTAL MIGRATION RATE OF SILICATE MELT IN THE ASTHENOSPHERE

Zhaowen Li, Baohua Zhang*, Hongzhan Fei*, Dongliang Jiang, Changze He, Shan Zhou, Fang Xu, Suyu Fu, Qunke Xia

Research Center for Earth and Planetary Material Sciences, School of Earth Sciences, Zhejiang University, Hangzhou 310058, China

Abstract The migration of silicate melts in the Earth's mantle plays a critical role in governing mantle dynamics, heterogeneity, and the transport of volatiles and incompatible elements. However, the rates at which melts migrate through upper mantle rocks remain poorly constrained. Here we experimentally determine the horizontal migration rate of basaltic melt along grain boundaries in polycrystalline olivine aggregates at 3 GPa and 1673 K using a Kawai-type multi-anvil press with a horizontally oriented capsule to minimize gravitational and thermal effects. By measuring Mg# (Mg/[Mg+Fe]) compositional profiles across the melt–olivine interface, we quantify melt infiltration distances as a function of time. The migration follows a diffusion-controlled process, yielding an average melt migration rate of $D = 2.4 \times 10^{-11}$ m^2/s. Extrapolation to geological timescales indicates that horizontal melt migration is limited to only ~55 m over 1 Myr and ~1.7 km over 1 Gyr. These results demonstrate that horizontal melt migration is extremely inefficient in homogenizing the mantle over large scales. By applying these findings to two major melt reservoirs, the lithosphere-asthenosphere boundary (LAB) and the dehydration melting layer above the 410-km discontinuity, we infer that partial melt layers are unlikely to be globally extensive features. Instead, observed seismic anomalies such as shear-wave velocity reductions at the LAB likely result from localized melt accumulation, possibly organized into horizontal melt-rich bands or lenses by plate motion. For the 410-km discontinuity, the limited horizontal migration distances imply that any dehydration melting layer must be sustained by nearly global upwelling fluxes from the mantle transition zone, rather than by lateral melt redistribution. Our study provides quantitative constraints on melt mobility in the upper mantle and offers new insights into the origin and preservation of mantle heterogeneities.

Key words melt migration, olivine, mantle heterogeneity, lithosphere-asthenosphere boundary, 410-km discontinuity

Acknowledgements This study was financially supported by the National Natural Science Foundation of China (Grant No. 42325203, 92579204) and Deep Earth Probe and Mineral Resources Exploration-National Science and Technology Major Project (Grant No. 2025ZD1005200) to B.H. Zhang, and the National Key Research and Development Program of China (2024YFF0809700), the New Cornerstone Science Foundation through the Xplorer Prize to H. Fei.

FLUID–MINERAL EQUILIBRIA AND THERMODYNAMIC MIXING PROPERTIES OF FLUID SYSTEMS

Leonid Aranovich
IGEM RAS, Russia

Abstract I present a review of an experimental method to quantitatively constrain thermodynamic mixing properties of fluid systems at high temperature T and pressure P. The method is based on bracketing equilibrium parameters of simple fluid–mineral reactions. Experimental data obtained with this technique for the H_2O–CO_2, H_2O–N_2, and H_2O–H_2 binary systems were utilized to calculate mixing parameters (WVL) corresponding to the simplified van Laar model. The WVL values for the three mixtures correspond to 202, 219, and 331 kJ cm^3/mol. The empirical correlation $WVLH_2O$–X (kJ cm^3/mol) = 887.012 QX – 16.674, where Q = Pc (critical pressure, bar)/Tc (critical temperature, K) for gas X (where X = CH_4, CO, H_2S, O_2, Ar, and NH_3) is used to evaluate the van Laar parameters for a number of petrologically important water–gas mixtures. The H_2O–H_2 system is characterized by the greatest positive deviation from the ideal mixing and can decompose into two immiscible fluid phases under the P–T parameters typical of deep lithospheric zones. The exsolution in the H_2O–CO_2 and H_2O–N_2 binary systems may occur only under high pressure and low temperature, that is, may be expected only in the environment of cold subduction. Salts (highly soluble simple salts and/or silicates) should significantly expand the exsolution regions in petrologically important fluids.

Key words Petrologic fluids, thermodynamic mixing properties

Acknowledgements: Support of the RSF grants 25-47-00073(RSF, Russia) and W2412052 (China) is appreciated.

FORMATION AND ISOTOPIC EVOLUTION OF EARTH'S EARLIEST OCEANS

Yu Zhang[1], Wenzhong Wang[1], Zhongqing Wu[1], Zhengbin Deng[2], Chao He[2], Lu Pan[1], Fang Huang[2], Bowen Chen[1]

1. Laboratory of Seismology and Physics of the Earth's Interior, School of Earth and Space Sciences, University of Science and Technology of China, China

2. State Key Laboratory of Lithospheric and Environmental Coevolution, School of Earth and Space Sciences, University of Science and Technology of China, China

Abstract How Earth's earliest oceans formed, and whether their hydrogen and oxygen isotope composition has remained constant since the Hadean, are two long-standing and fundamental questions in Earth and planetary sciences. Although numerous studies have debated the secular evolution of seawater isotopes (Knauth and Lowe, 2003; Robert and Chaussidon, 2006), progress has been limited by the absence of quantitative constraints on the isotopic composition of Earth's earliest oceans—the baseline from which all subsequent evolution proceeds. Here we employ machine learning–accelerated path-integral molecular dynamics to quantify equilibrium hydrogen and oxygen isotope fractionation between silicate melt and coexisting vapor at pressures and temperatures relevant to magma ocean degassing. By integrating these fractionation factors into thermal evolution models, we derive the first quantitative estimates of the hydrogen and oxygen isotope composition of Earth's earliest oceans. Our results show that Earth's earliest oceans formed through magma ocean degassing followed by atmospheric condensation during planetary cooling. These oceans likely exhibited elevated δ18O values and δD values comparable to or more negative than those of Archean (Pope et al., 2012; Johnson and Wing, 2020) and modern seawater (~0‰). We further demonstrate that ocean isotope compositions have evolved since ~4.5 Ga rather than remaining static, providing a dynamic framework that reconciles previously conflicting hydrogen and oxygen isotope records from the Archean to the present (Pope et al., 2012; Galili et al., 2019; Johnson and Wing, 2020; Isson and Rauzi, 2024). In addition, we identify a major transition in surface processes, from early serpentinization-dominated alteration of an ultramafic crust to a weathering-dominated surface regime. This shift links the evolution of ocean isotopes to fundamental changes in geodynamics, crustal composition, and surface environment.

Key words Ocean formation and evolution, Isotope fractionation, Machine learning potential

HIGH-PRESSURE DENSITY MEASUREMENTS ON SODIUM ALUMINOSILICATE MELTS ALONG THE NEPHELINE-ALBITE JOIN AND RECALIBRATION OF A MODIFIED HARD-SPHERE EQUATION OF STATE FOR SILICATE MELTS

Man Xu[1,2,3], Zhicheng Jing[4], James A. Van Orman[5], Qingyang Hu[1], Qi Chen[3], Tony Yu[3], Yanbin Wang[3]

1. Center for High Pressure Science and Technology Advanced Research, Shanghai, China
2. Shanghai Advanced Research in Physical Sciences, Shanghai, China
3. Center for Advanced Radiation Sources, The University of Chicago, Chicago, IL, USA
4. Department of Earth and Space Sciences, Southern University of Science and Technology, Shenzhen, China
5. Department of Earth, Environmental, and Planetary Sciences, Case Western Reserve University, Cleveland, OH, USA

Abstract Silicate melts play a crucial role in planetary differentiation. The density contrast between silicate melts and the surrounding solid residue exerts a primary control on many magmatic processes. However, direct measurements of the density of silicate melts at high pressure (P) and temperature (T) conditions remain challenging, particularly for the highly viscous and reactive silica- and alkali-rich melts. Here we determined the high P-T densities of three sodium aluminosilicate melts with nepheline ($NaAlSiO_4$), jadeite ($NaAlSi_2O_6$), and albite ($NaAlSi_3O_8$) compositions, using the high-P X-ray microtomography technique up to 4.1 GPa and 2020 K. Our results suggest that the substitution of $(NaAl)^{4+}$ for Si^{4+} along the $NaAlSiO^{4-}$ $NaAlSi_3O_8$ join leads to higher melt density and lower melt compressibility. In addition, our new data, combined with a wide range of literature data, were employed to re-calibrate a modified hard-sphere equation of state (HS-EOS) for silicate melts, which provides a unified framework for calculating the density and other compressional properties of multi-component silicate melts in the CaO-MgO-Al_2O_3-SiO_2-FeO-Na_2O-K_2O (CMASFNK) system up to ~25 GPa. The calibration also reveals that SiO2, alkalis, and CaO are the major components contributing to the compositional dependence of melt elastic properties. The HS-EOS was then applied to alkali basaltic melts at cratonic mantle conditions and silica- and alkali-rich melts at early planetesimal melting conditions, with implications for the gravitational stability and extraction of melts in Earth's mantle and planetesimal settings.

Key words silicate melts, density, equation of state, melt extraction, X-ray microtomography

Acknowledgements Funding support from the National Key R&D Program of China (2024YFF0807401), Shanghai Pujiang Program (24PJA095), NSFC (92479108), and US NSF (EAR - 2246803) are acknowledged.

HYDROUS SILICATE MAGMA AND SILICATE-SATURATED AQUEOUS FLUIDS AT HIGH TEMPERATURES AND PRESSURES: SIMILARITIES AND DIFFERENCES

Bjorn O. Mysen

Carnegie Institution of Washington, USA

Abstract Water plays central roles in igneous and metamorphic processes. As a component of silicate magma, H_2O affects chemical properties including phase relations and element partitioning between magma, minerals and fluids thus affecting chemical evolution. Physical properties of magma such as density, compressibility, and viscosity are affected by dissolved H_2O, which impacts on magmatic transport. Those properties reflect changes of silicate speciation.

The major rock-forming component of igneous and metamorphic rocks are SiO_2, Al_2O_3, iron oxides and alkali and alkaline earth oxide ($M^{n+}O_{n/2}$). Characterization of the role of H_2O in magmatic and metamorphic processes can, therefore, be carried out by study of the structural interaction between H_2O and silicate and aluminosilicate components in the SiO_2-H_2O, $M^{n+}O_{n/2}$-SiO_2-H_2O, and $M^{n+}O_{n/2}$-Al_2O_2-SiO_2-H_2O systems. In these systems, their structure, whether in hydrous magma or silicate-rich aqueous fluid can be described in terms of Q^n species. The Q denotes Si^{4+} and/or Al^{3+} and the superscript, n, defines the number of bridging oxygen in silicate structures. Its value is an integer between 0 and 4. The types, proportions and equilibria among the Q^n species in fluids and melts resemble one another. However, at temperatures and pressures below the critical point, solvation spheres surrounding the Q=species in fluids lead to immiscibility between fluid and melt.

As SiO_2 is the dominant oxide in most rocks, the characterization of fluid and melt structure in the SiO_2-H_2O system is fundament for our understanding of how H_2O interacts with silicate components. Water dissolves in hydrous SiO_2 melt by replacing bridging oxygens with OH-groups via equilibria of the type $2Q^4+nH_2O=2Q^3(OH)_n$, where n increases with increasing H_2O content. When n exceeds 3, all bridging oxygens in Q^3-species have been replaced by OH-groups thus forming isolated tetrahedra of the type, $Q^0(OH)_4$. This latter situation also is that which governs interaction between H_2O solvent and SiO_2 solute in aqueous solutions, $Q^4+H_2O=Q^0(OH)_4$.

Addition of metal oxide to SiO_2-H_2O, to form the $M^{n+}O_{n/2}$-SiO_2-H_2O results in competition between protons, H^+ and metal cations, M^{n+}, for nonbridging oxygens in hydrous melts and aqueous fluids. Moreover, the electronegativity of the M^{n+}-cation or cations affects this competition. This feature also governs the how H_2O solubility in $M^{n+}O_{n/2}$-SiO_2-H_2O melts affects the H_2O solubility and the extent to which these silicate components are dissolved in aqueous fluids. The H_2O solubility in $M^{n+}O_{n/2}$-SiO_2-H_2O melts increases the more electropositive the M-cation. The solubility mechanisms of H_2O are of the types, $Q^4+2Q^3(ONa)+2H_2O=2Q^2(ONa)+Q^0(OH)_4$ for an electropositive cation such as Na^+. For more electronegative cations such as Ca^{2+} or Mg^{2+}, there is less cation fractionation and the solution mechanism is of the type, $Q^4+2Q^2(OCa)+2H_2O=2Q^0(OCa)+Q^0(OH)_4$.

The solubility of $M^{n+}O_{n/2}$-SiO_2 components in aqueous fluids also increases the more electropositive the M^{n+}-cation(s). This is governed by how the cations and H^+ are distributed among the nonbridging oxygen in the silicate solute. This structural behavior is somewhat similar to that of silicate speciation in hydrous $M^{n+}O_{n/2}$-SiO_2-H_2O melts, and depends on the electronic properties of the cation much like that indicated by the equations above.

The solubility behavior of H_2O in aluminosilicate melts and aluminosilicate solubility in aqueous fluids are more complex because of the extent to which Al^{3+} is charge-balanced ion 4-fold coordination and by how Al^{3+} may between Q^n-species of different degrees of polymerization. In general, H_2O solubility in aluminosilicate melts in positively correlated with proportion of charged-balanced Al^{3+} and the electronic properties of the charge-balancing cation. Equivalent relations govern aluminosilicate solubility in aqueous fluids.

The relations summarized above explain how and the extent to which H_2O affect rock-forming processes. For example, these H_2O interaction with alkali aluminosilicate rocks results in greater effects on alkali than alkaline earth aluminosilicate rocks. Melt viscosity and compressibility is greater, as are solidus temperature depression, for example. Alkali aluminosilicate-bearing fluids also are more efficient mass transport agents than alkaline earth aluminosilicate-bearing fluids.

NEW PERSPECTIVES ON NATURAL DIAMOND-FORMING FLUIDS

Fabrizio Nestola[1], Maxwell C. Day[1], Martha G. Pamato[1], Davide Novella[1], Suzette Timmerman[2], Nils Gies[2], Fernando Cámara[3], D. Graham Pearson[4]

1. Dipartimento di Geoscienze, Università degli Studi di Padova, Italy.
2. Institute of Geological Sciences, University of Bern, Switzerland.
3. Dipartimento di Scienze della Terra, Università degli Studi di Milano, Italy.
4. Department of Earth and Atmospheric Sciences, University of Alberta, Canada.

Abstract Natural gem-quality diamonds do not usually contain fluid inclusions and therefore the nature of the fluids or melts from which diamonds form has remained poorly understood. In contrast, "fluid-rich" diamonds (more generally referred to as "fibrous diamonds") contain millions of submicrometric fluid inclusions (commonly described as "high-density fluids" - HDFs). Although the fluid inclusions in fibrous diamonds represent the deepest natural fluids that can be directly investigated, they remain understudied compared to normal gem-quality diamonds. It is still unclear whether the fluids observed in fibrous diamonds are universally the same as those from which gem-quality diamonds form. Previous work identified, by micro-Raman spectroscopy, a possible fluid in gem-quality diamonds occurring as thin films (~1–5 μm) surrounding a wide variety of mineral inclusions. This fluid film is currently the only form of fluid recognized in gem-quality diamonds and although its composition remains largely unknown, it appears to be a Si–O–H-bearing fluid. Subsequently, researchers attempted to measure the composition of this fluid film using slow LA-ICP-MS depth profiling. These authors were able to distinguish the respective contributions of the diamond, fluid film, and mineral inclusions, and detected elements such as Ba, Sr, Ce, Nb, La, Nd, and Th within the fluid film. These elements are typically found in HDF inclusions in fibrous diamonds, suggesting a possible genetic link between the two types of diamond-forming fluids. In order to provide new insights into the composition and possible sources of both gem-quality and fibrous diamond-forming fluids, we investigated a unique diamond from the Democratic Republic of Congo (DRC) which consists of a gem-quality core overgrown by a fibrous rim (i.e., a "coated" diamond). Within the gem core we observed clusters of isolated circular droplets of a fluid with similar composition to that found in films around mineral inclusions, but in this case not associated with solid inclusions. Such fluids have been described previously as isolated inclusions along twinning planes in only one gem-quality diamond. In addition, we observed, for the first time, the same fluid in the fibrous region of the studied diamond close to the boundary between the gem core and fibrous rim. Several coesite inclusions, surrounded by a fluid film, were also observed at the core-rim boundary. Nitrogen-aggregation (FTIR) thermochronometry suggests the gem core resided within the mantle at ~1100 °C. Elastic geobarometry applied to coesite inclusions

show the fibrous rim formed at a pressure of ~5.5 GPa. The presence of unaggregated nitrogen (i.e., C-centers) in the fibrous region suggest the rim formed during or shortly before kimberlite eruption at temperatures similar to that for the gem core.

Key words Diamond, mantle, inclusions, minerals, fluids

Acknowledgements Funding: ERC Advanced Grant MADAM (grant agreement n. 101199315), ERC Starting Grant INHERIT (grant agreement n. 101041620).

ORIGIN OF WATER IN THE DEEP EARTH INTERIOR: CONSTRAINS FROM HYDROGEN ISOTOPE OF LARGE IGNEOUS PROVINCES

Jia Liu, Qunke Xia，Jingjun Zhou

Research Center for Earth and Planetary Material Sciences, School of Earth Sciences, Zhejiang University, China

Abstract Large Igneous Provinces (LIPs) are commonly considered to originate from partial melting of mantle plume heads. In recent years, numerous studies have shown that many LIPs distributed on both continental and oceanic plates worldwide exhibit characteristics of water-rich mantle sources. However, the origin of this water in their mantle sources remains poorly constrained. The hydrogen isotopic composition of water (D/H) is an important tracer for identifying the source of water in the mantle. Here we report new measurements of water contents and hydrogen isotopic compositions from several continental and oceanic LIPs, including West Greenland, Emeishan, Agulhas, and Manihiki. The analyzed materials include melt inclusions hosted in olivine and submarine volcanic glasses. All measurements were conducted using secondary ion mass spectrometry (SIMS). The results show that samples from different LIPs display distinct characteristics. Submarine glasses from the Manihiki Plateau exhibit relatively low water contents (~0.2 wt.%), high H_2O/Ce ratios, and δD values of −40 to −50‰. In contrast, glass samples from Hole U1582 of the Agulhas Plateau contain ~0.45 wt.% H_2O and show the highest H_2O/Ce ratios among all studied oceanic plateau samples (~650), while their δD values range from −78 to −80‰, which fall within the typical range of mid-ocean ridge basalts (MORB). For the Emeishan Large Igneous Province (ELIP), melt inclusions in olivine from picrites generally contain less than 0.8 wt.% H_2O, significantly lower than the melt water contents calculated from coexisting clinopyroxene phenocrysts in the same samples. The δD values vary widely, from −100 to −60‰. Together with their high Nb/La ratios, low K/La ratios, and $\mu^{182}W$ values close to that of the bulk silicate Earth (BSE), these observations rule out the possibility that the water originated from arc-related subduction fluids, early Earth primordial reservoirs, or the core. Considering the enrichment in incompatible elements and other geochemical signatures, we suggest that the water in the mantle source of the ELIP was mainly derived from deeply subducted oceanic lithosphere. In Paleocene picrites from West Greenland, melt inclusions in olivine show a negative correlation between δD and H_2O content. Based on elemental correlations and diffusion-kinetic modeling, this trend is interpreted to result from hydrogen diffusing inward through the host olivine during the late stages of magmatic evolution. Melt inclusions with the highest Fo values (>92) and the highest δD values (−72 ± 18‰) most likely preserve the hydrogen isotopic composition of the primary magma. Overall, our results demonstrate significant heterogeneity in both water contents and δD values among the mantle sources of different LIPs. Nevertheless, none of the studied samples show extremely low δD values that would indicate a solar nebula origin of water, as previously proposed. Instead, the data are more consistent with a

water source related to subducted oceanic lithosphere.

Key words water, hydrogen isotope, mantle, large igneous provinces

SERPENTINITE-DERIVED FLUID METASOMATISM IN CONTINENTAL SUBDUCTION ZONES

Yi-Xiang Chen[1], Hans-Peter Schertl[2]

1. School of Earth and Space Sciences, University of Science and Technology of China, Hefei 230026, China

2. Institute of Geosciences, Ruhr-University Bochum, 44780 Bochum, Germany

Abstract Serpentinites play an important role in fluid mobility, crust-mantle interaction and arc magma formation in subduction zones. However, it is usually difficult to trace the serpentinite signature in deeply subducted crustal rocks, especially in continental subduction zones. Therefore, we need to develop effective geochemical tracers to address this issue. Boron and Mg isotope compositions have been increasingly used to track the effect of serpentinite derived fluids in subduction zones. This is because serpentinite derived fluids have been documented to show high Mg-B contents and heavy Mg-B isotope compositions even at subarc depths, which are distinct from fluids released from altered oceanic crust (AOC) and sediments. In addition, B and Mg are trace and major elements in most rocks, respectively. Therefore, combined B and Mg isotope compositions can give unique constraints on the contribution of serpentinites in fluid mobility and fluid-rock interaction even in continental subduction zones. In this talk, I will introduce our work on Mg-Fe-B isotope studies of fluid-metasomatized rocks mainly from the western and eastern Alps. We show that the greatly elevated Mg and B isotope compositions in the fluid-metasomatized rocks formed at forearc to subarc depths of Alps can be unambiguously ascribed to the infiltration of fluids derived from serpentinites. The great Fe isotope composition variation suggested the serpentinite derived fluids are reduced with Fe mobility in the form of Fe^{2+}-(HS) or Fe^{2+}-Cl complexes. The inference of serpentinite derived fluids is consistent with geophysical detections that showed the occurrence of a serpentinite channel between the subducted continental slab and mantle wedge interface beneath the western Alps. Therefore, the western Alps represents an excellent example whose geological structure and subduction process can be cross-checked by geochemical and geophysical methods.

Key words Fluid mobility, fluid-rock interaction, subduction zones, stable isotopes, serpentinites

SPATIAL CLUSTERING OF DEEP EARTHQUAKES CONTROLLED BY WATER CARRIERS

Wen-Yuan Zhao[1], Feng Wang[1, 2, 3*]

1. College of Earth Sciences, Jilin University, China

2. Key Laboratory of Mineral Resources Evaluation in Northeast Asia, Ministry of Natural Resources, China

3. International Center of Future Science, Jilin University, China

Abstract Deep earthquakes within subducting slab into the mantle transition zone (MTZ) exhibit along-strike variations, but the controlling mechanisms remain poorly understood. Here, we investigate spatial co-variations between boron isotopes of basalts and deep earthquakes in Northeast Asia. Arc basalts from the northern segment of the NE Japan arc show heavy and variable δ11B values (−14.55‰ to +6.47‰), whereas basalts from the corresponding intraplate basalts have light δ11B values (−10.44‰ to −5.15‰). In contrast, southern arc basalts display homogeneous and light δ11B values (−4.7‰ to −3.1‰), against variable intraplate ranges (−8.42‰ to +7.71‰). These contrasts reflect distinct carriers transporting water into the MTZ. In the north, dehydration of hydrous minerals leaves minimal water carried by nominally anhydrous minerals, corresponding to the absence of earthquakes in the MTZ. In the south, dense hydrous magnesium silicates transport large amounts of water, consistent with clustered deep-focus earthquakes. We conclude that water carriers control along-strike earthquake clustering.

Key words Water cycling, boron isotope, deep earthquakes

STABILITY OF THE TRISULFUR RADICAL ION $S_3^{\bullet-}$ IN SUBDUCTION ZONE FLUIDS

Renbiao Tao[1], Jianjiang Zhu[2], Jintao Zhu[1,3], Zengli Guo[1,3], Lifei Zhang[3]

1. Center for High Pressure Science and Technology Advanced Research, Haidian District, Beijing 100193, China

2. Institute of Geology, Chinese Academy of Geological Science, Beijing 100037, China

3. SKLab–DeepMinE, MOEKLab–OBCE, School of Earth and Space Sciences, Peking University, Beijing 100871, China

Abstract The sulfur cycle in subduction zones plays a fundamental role in regulating the redox evolution of the mantle wedge. The trisulfur radical ion ($S_3^{\bullet-}$) has been proposed as a key carrier of ore-forming elements in subduction-zone fluids; however, its formation mechanisms and stability under relevant conditions remain poorly constrained. In this study, we employ a diamond anvil cell (DAC) coupled with in situ Raman spectroscopy to investigate the generation of $S_3^{\bullet-}$ via redox reactions between pyrite and water at high pressure–temperature (P–T) conditions. We systematically quantify the effects of pressure, temperature, and oxygen fugacity (fO_2) on $S_3^{\bullet-}$ stability in subduction-zone fluids. Our results demonstrate that $S_3^{\bullet-}$ represents a relatively oxidized sulfur species that can persist along a range of subduction geotherms. By integrating large-volume press (LVP) experiments with thermodynamic modeling of altered oceanic crust (AOC) systems containing C–H–O–S volatiles, we propose that $S_3^{\bullet-}$ acts as a major carrier of oxidized sulfur from subducting slabs to the mantle wedge. During arc magma ascent, $S_3^{\bullet-}$ decomposes into S^{2-} and SO_4^{2-} at temperatures below ~200 °C. The reduced sulfur (S^{2-}) is sequestered by FeO-rich mantle minerals through sulfidation reactions, whereas sulfate (SO_4^{2-}) remains mobile and contributes to the oxidation of arc magmas and the formation of porphyry ore systems. These findings highlight a previously underappreciated role of $S_3^{\bullet-}$ in linking slab-derived fluids, mantle wedge redox state, and arc-related metallogenesis.

Key words subduction zone fluids, sulfur cycle, high pressure and high temperature, experimental geochemistry

SUPERHEATED CORE–DRIVEN DYNAMO DELAYS: A CONSTRAINT ON MOON-FORMING MODELS?

You Zhou[1], Yun Liu[1, 2*]

1. Earth and planet science college, Chengdu university of technology,China

2. Institute of Geochemistry, Chinese Academy of Sciences, China

Abstract Recent studies have underscored the significance of impact-induced heating in planetary evolution. For example, Carter et al. (2020) and Lock et al. (2020) demonstrated that giant impacts can deliver substantial energy to planetary cores, affecting their thermal histories and internal energy balance. Nakajima et al. (2021) further developed mantle melting scalings to quantify heat redistribution and pressure contrasts between global and local melt reservoirs. Marchi et al. (2023) proposed that late accretion shocks may haveheated Venus's core, influencing its thermal and volcanic evolution. Building on these efforts, Zhou et al. (2024) employed SPH simulations to show that a canonical Moon-forming impact could raise the core– mantle boundary temperature to ~11,000 K, potentially delaying the onset of the geodynamo by ~250 million years. Here, we explore the outcomes of impact heating and the melting of the mantle by superheated cores through extensive SPH simulations. Our results indicate that dynamo delays caused by impact-generated core heating are likely a common phenomenon among rocky planets and could postpone the onset of magnetic fields by several hundred million to over a billion years. This suggests a possible causal link between the formation and cooling of superheated cores and the timing of dynamo initiation, which may, in turn, provide a new constraint on giant impact models—for instance, in distinguishing whether the Moon-forming event involved a high- or low-energy collision. Tackley (2025) argued that core superheating has only short-term effects on planetary evolution, a view consistent with earlier interpretations by Ke and Solomatov (2009). However, Boukaré et al. (2025) demonstrated that a basal magma ocean (BMO) can inevitably form through the gravitational segregation of iron-rich melts, regardless of where the mantle geotherm intersects the melting curve, which will inhibit the loss of core superheating. These results imply that a portion of the thermal energy from a superheated core may be retained over long timescales.

Key words Superheated core, Dynamo onset, Moon-forming giant impact, Basal magma ocean

SUPER-HYDROUS ARC MAGMAS DELAY MAGNETITE SATURATION AND SULFIDE PRECIPITATION

Lanqin Li [1,2], Xingcheng Liu [1,2], Jintuan Wang[1], Zhongxing Sun[1,3], Xiaolin Xiong[1,2,3]

1. State Key Laboratory of Deep Earth Processes and Resources, Guangzhou Institute of Geochemistry, Chinese Academy of Sciences, China

2. University of Chinese Academy of Sciences, China

3. College of Earth Sciences, Jilin University , China

Abstract Magnetite crystallization strongly influences iron (Fe) behavior, sulfide saturation, and redox evolution in arc magmas. However, the combined effects of H2O and oxygen fugacity (fO2) on magnetite solubility in hydrous silicate melts remain unclear. We conducted piston-cylinder experiments on hydrous dacitic melts at 1–2 GPa, 850–1000 °C, and fO2 from FMQ−1.5 to FMQ+5.0 (FMQ = Fayalite-Magnetite-Quartz buffer). Magnetite solubility (melt FeOtot at magnetite saturation) increases with temperature and melt H2O content but decreases with rising fO2. Increasing melt H2O from 5 to 15 wt% at ~FMQ+2 doubles melt FeOtot (3 to 7 wt%), whereas increasing fO2 from FMQ+1 to FMQ+3 at fixed H2O (5 wt%) decreases FeOtot (4 to 1 wt%). Highest FeOtot occurs at intermediate fO2 (FMQ+2) when melt H2O exceeds 10 wt%. Additionally, increasing FeOtot content in the melt enhances the sulfur solubility. Thereby, elevated H2O delays magnetite and sulfide saturation, significantly affecting Fe and chalcophile element evolution in hydrous arc magmas.

Key words Hydrous magmas, oxygen fugacity, magnetite solubility, sulfide solubility

THE FORMATION MECHANISM OF THE LOW-VELOCITY LAYER ABOVE THE 410-KM DISCONTINUITY

Longjian Xie

Center for High Pressure Science & Technology Advanced Research, Shanghai, 201203, China

Abstract Seismic observations have identified a low-velocity layer atop the 410-km discontinuity, characterized by lateral discontinuity, variable thickness, and a locally stratified double-layer structure. Although this layer is generally attributed to low-degree melting resulting from dehydration of nominally anhydrous minerals (the "410-melt layer"), its specific formation mechanism remains enigmatic. To address this, we conducted high-pressure experiments at ~13 GPa to determine the composition and viscosity of the 410-melt. Our results reveal an exceptionally high water content (~43 mol%) and an ultra-low viscosity (~0.01 Pa·s) for this melt. Such a high water content necessitates significant iron enrichment to achieve a density comparable to the surrounding mantle, a prerequisite for its stable retention. Consequently, stable melt layers can only form in iron-enriched domains, such as those hybridized by recycled oceanic crust. In contrast, melts generated in normal mantle are buoyant and migrate upward, precluding layer formation. Furthermore, using a one-dimensional finite element model of continuous dehydration melting during mantle upwelling, we show that melt preferentially accumulates at two dynamically stable depths: the 410-km and a shallower neutral buoyancy depth. Under conditions of a low mantle upwelling rate or a significant density difference, the melt between the two dynamically stable depths is rapidly drained, forming a distinct "gap zone" and resulting in a vertically double-layered structure. Conversely, under opposite conditions, the melt layers may merge into a single continuous layer. These combined experimental and numerical results provide a coherent framework to explain the complex structure of the low-velocity layer above the 410-km discontinuity.

Key words low-velocity layer, composition, viscosity, 410-km discontinuity, high pressure

ULTRA-LOW DEUTERIUM ISOTOPES REVEAL LONG-LIVED PRIMORDIAL HYDROGEN IN THE MANTLE TRANSITION ZONE BENEATH EAST ASIA

Xiang Wu, Fabin Pan, Junfeng Zhang

State Key Laboratory of Geological Processes and Mineral Resources, School of Earth and Planetary Science, China University of Geosciences, Wuhan 430074, P.R. China

Abstract Water plays a dominant role in the development of Earth and formation of habitable world, but its origin and agglomerate timing are still in debated. Thermodynamic models proposed that the proto-Earth accreted in the early solar system with hydrogen-rich nebular gas which was gathered during the Magma Ocean era. Original water was also brought to Earth by water-rich chondrites and comets. The primordial water dissolved in the Magma Ocean and affected the early Earth's differentiation and partially stored in the Earth's interior. Impact-driven accretion of the proto-Earth, however, synchronously resulted in significant loss of moderately and highly volatile elements relative to the Sun and carbonaceous chondrites. Thus, it remains unclear that the amount of primordial water store in the Earth's interior after the Moon-forming giant impact, which represents the final dominant growth of the proto-Earth.

Hydrogen is believed to exist in the mantle transition zone (MTZ) primarily as hydroxyl (OH^-), ice-VII (H_2O), and molecular hydrogen (H_2). Recently, we observed centimeter-sized garnet peridotite fragments derived from the MTZ, offering a valuable opportunity to investigate hydrogen's provenance. Within olivine formed by retrograde transformation of wadsleyite/ringwoodite, we identified both hydroxyls and molecular hydrogen. Total hydrogen concentrations decrease from 1786 ppm to 118 ppm H_2O weight, recording its evolution during transport from the MTZ to the lithosphere-asthenosphere boundary. Extremely light deuterium isotopes (δD = -280‰ to -375‰) in olivine indicate that hydrogen in the MTZ dominantly comprises primordial hydrogen with minor (nearly 2-9%) subducted surficial water. These findings provide compelling evidence for the occurrence, abundance, origin, and evolution of hydrogen in the deep mantle, shedding new light on Earth's internal water cycle.

ULTRAMAFIC MELT VISCOSITY

Russell, K.[1], Hess, K-U.[2] and Dingwell, D.B.[2]

1. Volcanology and Petrology Laboratory, Department of Earth and Ocean Sciences, University of British Columbia, Vancouver, British Columbia, V6T 1Z4, Canada
2. Department für Geo- und Umwelwisseschaften, Ludwig-Maximilians-Universtät München, Munich, 80333, Germany

Abstract A model for the non-Arrhenian, Newtonian viscosity (η) of ultramafic melts based on experimental literature data is presented. The model predicts the viscosity of ultramafic melts as a function of temperature (T), pressure (P) and for a restricted range of melt compositions (70 < Mg# < 100), including H2O content. Viscosity measurements span 14 orders of magnitude of η (10-2 to 1011.8 Pa s), over a T range of 880 to 2700K, pressures of 7 to 25 GPa, and include measurements on hydrous melts containing 0.2 to 4.4 wt% H2O. The viscosity model is continuous across T-P-composition space and can predict ancillary transport properties including glass transition temperatures (Tg) and melt fragility (m). The predictive capacity of this model for ultramafic melt viscosity makes it pertinent to model the lifetime of magma oceans of terrestrial planets and the evolution of planetary atmospheres.

Key words silicate melts, viscosity, model

VARIATION IN PETROLOGICAL AND MICROSTRUCTURAL CHARACTERISTICS OF THE HOROMAN PERIDOTITE COMPLEX

Kazuki Matsuyama[1,2], Yumiko Harigane[3,4], Itsuki Natsume[5], Romain Tilhac[2], Benoit Ildefonse[2], Katsuyoshi Michibayashi[1,6]

1. Department of Earth and Planetary Sciences, Graduate School of Environmental Studies, Nagoya University, Japan

2. Géosciences Montpellier, University of Montpellier, CNRS, France

3. Research Institute of Geology and Geoinformation, Geological Survey of Japan, AIST, Japan

4. Department of Marine Resources and Energy, Tokyo University of Marine Science and Technology, Japan

5. Kanagawa Prefectural Museum of Natural History, Japan

6. Volcanoes and Earth's Interior Research Center, JAMSTEC, Japan

Abstract The Horoman peridotite complex in southern Hokkaido, Japan, represents one of the most extensively studied exposures of the uppermost mantle. This complex exhibits considerable variations in microstructures, crystal preferred orientations (CPOs), and petrological characteristics. In this study, we investigated the major-element compositions of olivine, orthopyroxene, clinopyroxene, and spinel obtained by electron probe microanalysis (EPMA) for peridotite samples whose microstructures and crystal-fabrics were previously characterized using electron backscatter diffraction (EBSD).

The mineral compositions show clear contrasts between the Basal Shear Zone in the southern part of the complex and the Equigranular Zone in the northern part. Olivine Mg# values are relatively restricted in the Basal Shear Zone but display a wider range in the Equigranular Zone. Clinopyroxene TiO_2 contents are generally low in the Basal Shear Zone, whereas significantly higher values occur in the Equigranular Zone. Systematic differences are also observed in spinel compositions. In particular, spinel Mg#–Cr# relationships indicate that samples from the Basal Shear Zone fall within the compositional range typically observed for abyssal peridotites, whereas those from the Equigranular Zone tend to show lower Mg# values relative to this reference field. In addition, spinel TiO_2 contents are markedly higher in the Equigranular Zone than in the Basal Shear Zone.

Thermodynamic modeling of mantle partial melting suggests that the observed mineral compositional trends are broadly consistent with progressive melt extraction. In particular, relationships among olivine MgO–FeO, clinopyroxene Mg#–TiO_2, and olivine Mg#–spinel Cr# closely follow predicted melting trajectories. These results indicate that the degree of melting increases from plagioclase-bearing lherzolite through spinel lherzolite to harzburgite. Furthermore, the spatial distribution of melting degrees suggests a systematic increase toward the structurally lower part of the complex.

These observations suggest that the lithological and microstructural variations in the Horoman

peridotite complex reflect a combination of partial melting and subsequent melt–rock interaction processes within the uppermost mantle. Integrating mineral chemistry, thermodynamic modeling, and previously documented deformation fabrics provides new constraints on the relationships among mantle melting, melt migration, and deformation in this well-exposed mantle section.

Key words mantle peridotite, partial melting, melt–rock interaction, crystal preferred orientation, Horoman peridotite complex

Acknowledgements Electron probe microanalysis was performed using a JXA-iHP200F at the GSJ-Lab, AIST, Japan. We appreciate the logistical assistance provided by Samani-cho and Mt. Apoi Geopark Visitor Center.

VISCOSITY OF EXTREMELY DEPOLYMERIZED SILICATE MELTS

Bissbort, T.[1], Hess, K-U.[2] and Dingwell, D.B.[2]

1. Experimental Petrology and Geochemistry, Institute of Geosciences, Ruhr-University Bochum, Germany

2. Department für Geo- und Umwelwisseschaften, Ludwig-Maximilians-Universtät München, Munich, 80333, Germany

Abstract Properties of extremely depolymerized melts and glasses have always been elusive due to their inaccessibility in experiments. Information on viscosity, for example, was previously restricted to very high temperatures. Yet, theory and experimental details about peridotites suggest that highly depolymerized melts exhibit exceptional properties, such as extremely non-Arrhenian viscosity-temperature relationships. Studies at low temperatures, i.e., just above the glass transition temperature, required for investigating such phenomena have been impossible for many compositions due to their rapid crystallization and thus extremely poor glass-forming ability. Here, we have developed a novel method combining synthesis by pulsed laser deposition with characterization by fast differential scanning calorimetry (FDSC) to deposit glassy thin films, from a plasma directly onto FDSC sensors, combined with calorimetric analysis at very high heating-cooling rates (3500–9500 °C s−1). In this way we have been able to explore the glass transition of the glasses (at or near olivine stoichiometry): Mg1.30SiO3.3, Fe0.34Mg1.67SiO4.0, Fe0.49Mg1.53SiO4.0, Fe1.21Mg0.91SiO4.1, and Fe2.26SiO4.3. The peak glass transition temperature at 5000 °C s−1 increases from 550 °C for Fe2.26SiO4.3 with decreasing (Fe + Mg)/Si and with increasing Mg/(Fe + Mg) to 736 °C for Mg1.30SiO3.3. Viscosities derived through the shift factor approach range from 105.61 to 106.04 Pa·s in that temperature range. These results thus extend the experimentally available viscosity range by ca. seven log units and were employed here, together with high-temperature superliquidus viscosity data to fit the Vogel-Fulcher-Tammann (VFT) equations for these melts. The viscosity-temperature relationships are all strongly non-Arrhenian (m = 82–123 ± 15). We provide a comparison with other experimental studies of ultrabasic melts and with predictions from viscosity models. The inability of the latter to predict the observed viscosities highlights the necessity of direct experimental studies such as that presented here

Key words silicate melts, viscosity

WATER PARTITIONING BETWEEN NAM AND DHMS AND ITS IMPLICATIONS FOR SUBDUCTING SLAB DYNAMICS

Eiji Ohtani[1], Takayuki Ishii[2]

1. Department of Earth Science, Graduate School of Science, Tohoku University, Japan

2. Institute for Planetary Materials, Okayama University, Japan

Abstract Water is transported into the mantle by nominally anhydrous minerals (NAMs) and hydrous minerals such as dense hydrous magnesium silicates (DHMS) in subducting slabs, and it plays important roles in chemical evolution and dynamics of the mantle. For example, water in olivine enhances deformation due to hydrolytic weakening and transformation kinetics. Such effects can control dynamic processes of slab deformation and deep seismicity during slab subduction. Therefore, it is important to clarify the storage of water and the roles of NAMs and DHMS phases in the water bearing slabs.

We studied the water partitioning between wadsleyite and hydrous phase A, ringwoodite and superhydrous phase B, and bridgmanite and hydrous phase D/hydrous phase δ-AlOOH at high pressures and temperatures. We also studied the water partitioning between silica phases (stishovite and $CaCl_2$-silica phase) and hydrous δ-AlOOH, which are the important constituent in the crustal layer of the descending slabs. We revealed that water strongly partitions to hydrous minerals such as phase A, superhydrous phase B, hydrous phase D, and hydrous phase δ resulting in water depletion in wadsleyite, ringwoodite, and bridgmanite even in the wet slabs. DHMS phases are important water carriers in the slabs which can transport water into the mantle transition zone and lower mantle. We also revealed depletion of alumina and water in the silica phases by absorption of these components by hydrous phase δ.

These partitioning behaviors provide important consequences for subducting slab dynamics, i.e., dry rheology and dry phase transition kinetics of the major minerals of olivine and its high-pressure polymorph work even under the wet slab containing DHMS phases. The metastable mantle wedge in some slabs observed at the mantle transition zone depths is not a signature of the dry slabs, but it occurs even in water bearing slabs. Deep earthquakes occurring in slabs descending into the mantle transition zone can be triggered by the dry phase transformation kinetics even in the wet slabs. It has been suggested that the grain size reduction of olivine due to dry phase transformation kinetics has been proposed to explain a large deformation of the slabs such as formation of stagnant slabs. This mechanism also works in the water bearing slabs due to existence of dry olivine. Ultradeep earthquakes occurs at the depths exceeding 650 km in some subductions such as the Izu-Bonin subduction may be originated from dehydration of hydrous minerals such as super hydrous phase B in the wet slabs.

Key words Water, partitioning, NAMs, DHMS, subducting slabs

Acknowledgements This work was supported by JSPS KAKENHI Grants, Number

20H00187 and 24K00722 to EO, and 23K19067 and 24K00735 to TI.

WATER-INDUCED MANTLE OVERTURNS AND GREAT OXIDATION EVENT

Zhongqing Wu [1,2*] , Xin Deng [1], Jian Song [1]

1. School of Earth and Space Sciences, University of Science and Technology of China, Hefei 230026, China

2. State Key Laboratory of Precision Geodesy, University of Science and Technology of China ,Hefei, 230026, China

Abstract As a consequence of the evolution of the water-bearing basal magma ocean (MO), water-induced mantle overturn can well account for many puzzling observations in the early Earth, such as the formation of the Archean continents, the Archean–Proterozoic boundary, and high Archean paleomagnetic field (Wu et al., 2023; Wang and Wu 2026). The early Earth may have experienced a deep-water cycle totally different from the current. High pressure studies suggest that the whole-mantle MO evolved into an outer MO and a basal MO. With the solidification, water in the basal MO moved toward the core-mantle boundary and the basal MO eventually became gravitationally unstable because of the enrichment of water. The instability triggered the massive mantle overturns and resulted in the major pulses of the thick SCLM and continental crust generations in the Neoarchean. The mantle overturns eventually got rid of the whole basal MO and the mechanism which generated the Archean-type SCLM and continents likely no more worked after the overturns. Thus, water-induced mantle overturns can account for why Archean-type SCLM and continents basically occurred in the Archean (Wu et al., 2023). The mantle overturn can substantially accelerate the cooling of the core and strengthen the geomagnetic field, which explains well the high paleointensity records from ~3.5–2.5 Ga (Wang and Wu 2026).

Besides the enrichment of water, the basal MO was enriched with ferric iron because its ferrous iron undergoes disproportionation reactions. This study shows that the ascent of ferric-rich basal MO and its mixing with the upper mantle could account for the observed shift in the redox state of the upper mantle during the Archean. Both the redox state shift and the generation of Archean continents result from these mantle overturns. Therefore, it is expected that the shift in mantle fO_2 aligns with the timing of continental generation, which is supported by the observations. The mantle overturns are rare with age > ~ 3.6 Ga, but their frequency increases with age < ~3.6 Ga and reaches the maximum in the Neoarchean. The combined effects of the ascent of the deep oxidized material, the emergence of continents, and oxygenic photosynthesis generated the broader First Redox Revolution of the Earth system, ultimately initiating the GOE shortly after the end of the Archean.

Key words volatile, deep water cycle, high temperature and high pressure, early Earth

ELECTRICAL CONDUCTIVITY MEASUREMENTS OF AQUEOUS FLUIDS UNDER CRUSTAL CONDITIONS IN MULTI-ANVIL APPARATUS

Jinyan Wu[1,3], Haiying Hu[2], Lidong Dai[2], Ziming Hu[1,3], and Song Luo[1,3]

1. Key Laboratory of High-Temperature and High-Pressure Study of the Earth's Interior, Institute of Geochemistry, Chinese Academy of Sciences, Guiyang, 550081, China

2. School of Physics and Electronic Science, Guizhou Normal University, Guiyang, 550025, China

3. University of Chinese Academy of Sciences, Beijing, 100049, China

Abstract Aqueous fluids are pivotal carriers of material transport in the Earth's interior, and their electrical conductivity is a key parameter for interpreting magnetotelluric geophysical anomalies of planetary interiors. Electrical conductivity measurements of aqueous fluids at high temperature and high pres-sure have been realized via cold-sealed pressure vessels, hydrothermal diamond anvil cells and pis-ton-cylinder devices, yet such research based on multi-anvil apparatus (MAA) remains unreported. Conventional sample capsules for these measurements mainly include single-crystal quartz and pre-cious metal sleeves, which suffer from fluid leakage due to microcracking under high pres-sure-temperature conditions and high manufacturing cost with poor processability, respectively. To address these limitations, we adopted polytetrafluoroethylene (PTFE)–a low-cost and easily ma-chinable material–to fabricate novel sample capsules, and for the first time achieved electrical con-ductivity measurements of NaCl aqueous solutions in a multi-anvil apparatus under crustal condi-tions of 323−598 K and 0.5 GPa[1]. The experimental results show excellent consistency with those obtained from diamond anvil cells and piston-cylinder devices, verifying the reliability of the PTFE capsule-based MAA measurement method. This innovative approach not only provides a cost-effective pathway for determining aqueous fluid electrical conductivity, but also can be further extended to a wider pressure-temperature range by replacing PTFE with metal components, provid-ing a new technical means for the study of physical properties of fluids and melts as well as flu-id-rock interaction in planetary interiors under high pressure-temperature conditions.

Key words Aqueous fluids, Electrical conductivity, Multi-anvil apparatus, High temperature and high pressure

Acknowledgements This study was financially supported by the Guizhou Normal University Academic New Talent Fund (Grants No. GZNUD[2025] 10 and GZNUD[2025] 12) and National Natural Science Foundation of China (Grant Nos. 42274137).

GLOBAL RESURFACING ON VENUS BY VOLATILE-INDUCED MANTLE OVERTURN

Yajie Zhao, Zhongqing Wu*, Jian Song

Deep Space Exploration Laboratory/ School of Earth and Space Sciences, University of Science and Technology of China, Hefei, China.

Abstract Understanding why Venus and Earth, two planets of similar size and bulk composition, evolved starkly different surfaces remains a central question in planetary science. Here, we demonstrate that crystallization of the basal magma ocean (BMO) and subsequent volatile-induced mantle overturn provide a coherent framework to explain these divergent surface histories. On Earth, mantle overturn likely drove the formation of Archean cratons, whereas on Venus, it may cause the global resurfacing at ~1.0 Ga. The timing of mantle overturn, primarily controlled by the initial volatile content and lifetime of the BMO, reflects that Venus's BMO had fewer volatiles and persisted longer than Earth's. The relative areas of Earth's cratons and Venusian tesserae, which are interpreted as analogues of cratons, further suggest that Venus's BMO last roughly twice as long as Earth's and hosted a significantly smaller volatile inventory, about 1/5 to 1/2 that of Earth. Our results show that the Earth's craton formation and Venus' global resurfacing with the formation of Tessera terrains could be better understood within a comparative planetology framework. We infer that Venusian global resurfacing lasted for ~1.6 Ga and represented an intermediate style between equilibrium and catastrophic resurfacing.

Key words Venus, global resurfacing, volatile-induced mantle overturn, comparative planetology

MACHINE LEARNING PREDICTION OF PYROXENITE PARTIAL MELTING BEHAVIOR

Le Huangfu, Jia Liu, Zhikang Luan, Tianting Lei, Denggang Lu

School of Earth Sciences, Zhejiang University, Hangzhou 310027, China

Abstract Pyroxenite is recognized as a important mantle source component for basalts alongside peridotite, comprising approximately 2-15% of the upper mantle. However, previous high-temperature and high-pressure partial melting experiments indicate that pyroxenite possesses a lower solidus temperature and a narrower melting interval. This characteristic enables pyroxenites to contribute 15-40% to mantle-derived melts, significantly enhancing the geochemical diversity of basalts. However, quantitatively predicting pyroxenite melting behavior remains elusive owing to its broad compositional variability and the highly non-linear mixing behaviors that often challenge traditional thermodynamic models.

To accurately predict the partial melting behavior of pyroxenite—specifically, the melt fraction and resulting melt composition for diverse initial chemical compositions under varying temperature and pressure conditions—we developed a two-stage machine learning approach utilizing the XGBoost algorithm. The model was trained on a compiled dataset of 431 high-temperature and high-pressure experimental records compiled from previous literature , covering conditions from 1000 to 2200 °C and pressures up to 20 GPa. Stage 1 applies binary classification to predict if a given pyroxenite composition will melt under specific P-T conditions, while Stage 2 applies regression analysis to predict the melt fraction and the resulting major oxide geochemical composition. To alidate the efficacy of the developed machine learning model, we additionally conducted new high-temperature and high-pressure piston-cylinder experiments at 1.0 to 2.0 GPa and 1200to 1400°C , utilizing garnet websterite xenoliths and a mixed KLB/MORB composition as starting materials.

Our results demonstrate that the XGBoost framework effectively captures the compositional trends associated with pressure changes and melt fraction variations. Applied to the test dataset, the model achieves R^2 values exceeding 0.8 for key major oxides and predicts the degree of partial melting with a mean squared error of 0.08. Serving as a robust, data-driven complement to traditional thermodynamic simulations, this machine learning approach refines our ability to constrain the geochemical signatures of pyroxenite melts under diverse mantle P-T conditions, ultimately providing quantitative new insights into the generation and transport of heterogeneous mantle melts.

Key words Pyroxenite, Partial melting, Machine learning, Mantle heterogeneity, Basalt genesis

Acknowledgements We would like to express our sincere gratitude to Dr. Hongzhan Fei and Dr. Jiejun Jing for their invaluable guidance and technical support on the high-temperature and

high-pressure experiments.

MELTING AND CRYSTALLIZATION EXPERIMENTS CONSTRAINTS OF WATER AND FLUORINE ON HIGHLY FRACTIONATED GRANITIC MAGMA EVOLUTION

Yao Lu, Haihao Guo*

State Key Laboratory of Geological Processes and Mineral Resources, School of Earth and Planetary Sciences, China University of Geosciences, Wuhan 430074, China

Abstract Highly fractionated granites have attracted significant attention because of their extreme enrichment in rare metals, including W, Sn, Nb, Ta, Zr, Hf, Li, Be, and REE. Volatiles, especially fluorine and water, play key roles in generating granites, by reducing solidus temperature, governing liquid-crystal equilibria, and decreasing magma viscosity. Due to its melt affinity, fluorine can remain in magma until saturation and exsolves in highly fractionated granites, which contain elevated volatiles. However, the petrogenesis and fractionation mechanisms, as well as the roles of fluorine and water in the physical-chemical properties and evolutionary process of such magma, remain poorly understood.

A series of melting and crystallization experiments were performed to investigate the effects of H_2O and F on the evolution of highly fractionated granitic magma. Melting experiments on a representative lower crust composition with addition of 0-4 wt% H_2O and 0-3 wt% F were performed at 200 MPa, 800-1000 °C under an fO_2 of ~NNO+0.5 in cold seal pressure vessels (CSPV) or internally heated pressure vessels (IHPV). The results show that H_2O and F significantly increase the melt fraction, and produce silica-rich (74.2 wt%) melt at 800°C, 4 wt% H_2O and 1 wt% F. Experimental melt compositions indicate that F depolymerizes the melt, increasing NBO/T from 0.02 (800 °C, 4 wt% H_2O, 1 wt% F) to 0.06 (800 °C, 4 wt% H_2O, 3 wt% F). We have also addressed the phase equilibria in highly evolved magma system through crystallization experiments using F-bearing (0.79 wt% F) highly fractionated granites of South China (Qitianling phase-3 granites) as the starting material, with 0-8 wt% water at 200 MPa, 650-900 °C. The results show that the minimum solidus occurs at 650-700 °C with the mineral assemblage of 35% quartz, 35% alkali feldspar, 20% plagioclase, 5% biotite, plus accessory mineral phases of fluorite, zircon, ilmenite, and apatite (<5%). This assemblage is consistent with that observed in Qitianling phase-3 granites. Phase diagrams have been constructed at 200 MPa, 650-900°C, with the initial water conditions being 0-8 wt%, and H_2O and F effects on the evolution of highly fractionated granites of South China have been discussed.

Key words Highly fractionated granites, Melting experiments, Crystallization experiments, Water, Fluorine

SPECIATION OF W AND MO IN HYDROTHERMAL AND DEEP SUBDUCTION ZONE FLUIDS

Naoko Takahashi[1,2*], Michihiko Nakamura[1], Shigeru Yamashita[3], Hiroyuki Kagi[2]

1. Department of Earth Science, Graduate School of Science, Tohoku University, Japan

2. Geochemical Research Center, Graduate School of Science, The University of Tokyo, Japan

3. Institute for Planetary Materials, Okayama University, Japan

Abstract Tungsten (W) and molybdenum (Mo) are highly mobile in aqueous fluids in both magmatic-hydrothermal ore-forming and deep subduction zone systems, yet their dominant dissolved species at elevated pressure and temperature remain unresolved. This uncertainty limits the prediction of metal mobility and the mechanistic understanding of W and Mo stable isotope fractionation in high-temperature geological environments. Here, we combine in situ Raman spectroscopy in an externally heated hydrothermal diamond anvil cell with density functional theory calculations to investigate the aqueous speciation of W(VI) and Mo(VI) under crustal conditions. Above 400 °C, new Raman bands appear at higher frequencies than those of the tetrahedral oxyanions MoO_4^{2-} and WO_4^{2-}, suggesting the metal speciation changes. We show that these bands are best explained by protonated monomeric tungstate and molybdate species rather than by the polynuclear species previously proposed. For tungsten, the combined experimental and theoretical results identify tetrahedral HWO_4^- and higher-coordinated H_2WO_4 as the most plausible assignments. Addition of NaCl or NaF further enhances WO_3 solubility, with anionic monomers or their Na-bearing ion pairs dominating dissolved W transport. Our results resolve previous ambiguities in Raman band assignments, including the distinction between HWO_4^- and paratungstate A ($W_7O_{24}^{6-}$), and indicate that polynuclear tungstate species are negligible in high-temperature ore-forming fluids. Protonated monomeric species, particularly HWO_4^- in saline metamorphic fluids, therefore play key carriers of W and are likely controls on isotope fractionation during deep fluid-rock interaction.

Key words tungsten, molybdenum, aqueous speciation, hydrothermal fluids, subduction zone

TRACE ELEMENT VARIATIONS IN THE SETOUCHI HIGH-MG ANDESITES: IMPLICATIONS FOR SLAB-DERIVED MELT CONTRIBUTIONS AND ALONG-ARC HETEROGENEITY

Hironao Shinjoe[1], Yuji Orihashi[2], Takahito Osawa[3]

1. Center for General Education, Tokyo Keizai University, Japan

2. Graduate School of Earth and Environmental Sciences, Hirosaki Universty, Japan

3. Materials Sciences Research Center, Japan Atomic Energy Agency (JAEA), Japan

Abstract The Setouchi Volcanic Rocks (SVR), which were active in the near-trench region of Southwest Japan during the Middle Miocene, are characterized by the occurrence of high-Mg andesites (HMAs), suggesting equilibration with mantle peridotite. These rocks were mainly active between 14 Ma and 15 Ma and are considered to have formed during igneous activity associated with subduction of the Philippine Sea Plate immediately after the opening of the Japan Sea. In this study, we sampled HMAs and coexisting basalts over a distance of approximately 700 km along the arc and examined variations in trace element compositions, including boron concentrations measured by prompt gamma-ray analysis (PGA). PGA was conducted using instruments installed at the JRR-3M research reactor of the Japan Atomic Energy Agency. Previous studies have discussed the origin of HMA magmas on the basis of whole-rock chemical compositions, including Sr-Nd-Pb-Hf isotopic compositions, for samples from representative regions. Most researchers have suggested that these magmas were generated by reaction between slab melts and mantle wedge peridotite. The slab melts were inferred to have been derived from subducted sediments composed mainly of terrigenous clastic materials with minor altered oceanic basalt. This genetic model involves forced subduction of the young Shikoku Basin (ca. 0-20 Ma) of the Philippine Sea Plate beneath these regions as a result of the clockwise rotation of Southwest Japan during the Miocene. We modeled the trace element compositions of fluids derived from sediments and altered oceanic crust, as well as those of their partial melts, and used the resulting fluid-mobile/immobile element ratios (e.g., B/Nb and Ba/Nb) to evaluate the contribution of slab-derived components to the source of HMA magmas. For many element ratios, HMAs plot between the mixing lines defined by depleted mantle and melts derived from sediments and altered oceanic crust. Furthermore, addition of a fluid phase cannot account for these element ratios, because even a very small amount of fluid would cause a marked increase in B/Nb. These results therefore support the previously proposed model that melt, rather than fluid, was added to the mantle source. The boron concentrations of HMAs vary widely, ranging from approximately 1 to 70 μg/g, whereas B/Nb ratios range from approximately 0.1 to 13. Samples with high boron concentrations and high B/Nb ratios are concentrated in several regions. In contrast, HMAs from Kyushu, in the western part of the distribution area, generally show extremely low boron concentrations and B/Nb ratios. The presence of such regional compositional variations suggests that these changes may be related to the heterogeneity of the subducting Shikoku Basin.

Key words Arc volcanism, Philippine Sea plate, slab melting, boron, Prompt gamma-ray analysis

CHARACTERISTICS AND PROPERTIES OF GERAISITE, A NEW TEKTITE STREWN FIELD UNVEILED IN BRAZIL

Alvaro P. Crósta

Geosciences Institute, Universidade Estadual de Campinas, Brazil

Abstract Tektites are natural glasses formed during hypervelocity meteorite impacts under extreme temperature and pressure conditions and are typically distributed in strewn fields located hundreds to thousands of kilometers from their source crater. Because only a few such strewn fields are known on Earth, each new occurrence provides important constraints on the terrestrial impact record and on the processes governing large-scale impact ejecta transport. A new tektite occurrence, named geraisite, was recently identified in northern Minas Gerais State, Brazil, representing distal impact ejecta from a still unidentified impact event. This discovery adds a previously unrecognized strewn field to the limited global inventory, which currently includes the Australasian, Central European, Ivory Coast, North American, and Belize fields, and provides new insights into Neogene impact processes involving continental crustal targets.

Although visually similar to volcanic glass (obsidian), tektites display distinctive characteristics, most notably their extremely low water contents (typically <0.03 wt.% compared to >0.07 wt.% in obsidian). This reflects the extreme conditions during formation (temperatures up to several thousand °C and pressures approaching ~100 GPa), which result in rapid melting and partial vaporization of target rocks and soils. Geraisite specimens range in mass from ~1 to 85 g, and approximately 600 specimens have been documented to date. They display typical tektite features, including diverse morphologies (spherical, ellipsoidal, teardrop, discoid, and dumbbell), pitted surfaces, lechatelierite inclusions, and olive-green to brown colors.

Here we report the chemical, magnetic, and isotopic properties of geraisite, including Sr, Nd, and Hf isotopic compositions, Nd and Hf model ages, and new $^{40}Ar/^{39}Ar$ ages. Measured H_2O contents range from 70 to 110 ppm (0.007–0.011 wt.%). Major element compositions are relatively homogeneous and plot within the dacite–rhyolite fields of the total alkali versus silica diagram, while some trace elements show variability, including Cr (10–48 ppm) and Ni (9–63 ppm).

Mass-normalized magnetic susceptibility (MS) measured in 61 specimens ranges from 19 to 300×10^{-9} m³/kg for samples weighing 0.88–19.96 g, consistent with values reported for other tektites. MS exhibits a logarithmic dependence on specimen mass that stabilizes above ~10 g. Many specimens show frequency-dependent susceptibility >10%, indicating the presence of superparamagnetic ultrafine-grained particles. Paramagnetic phases dominate the magnetic response, as indicated by hysteresis curves similar to those observed in other tektites. A ferromagnetic component is also present, with remanent magnetization between 10^{-5} and 10^{-8} A·m² and remanent coercivities of 0.02–0.03 T, likely reflecting the presence of magnetite.

$^{40}Ar/^{39}Ar$ dating constrains the impact event to 6.33 ± 0.02 Ma. Average isotopic compositions

(four samples) yield εNd = −39.5, εSr = 608.1, and εHf = −61.2, with $^{176}Lu/^{177}Hf$ = 0.0052 and $^{147}Sm/^{144}Nd$ = 0.094. The calculated Sm-Nd model age (TDM) of 3.2 Ga indicates a continental crustal source, most likely Mesoarchean felsic rocks. Considering the regional geological context, granitic rocks of the São Francisco Craton represent the most plausible source. The felsic character of the target is further supported by the K_2O/Na_2O (1.6) and SiO_2/Al_2O_3 (4.9) ratios and the high SiO_2 content (71.9 wt.%). These results support the interpretation of geraisite as distal impact ejecta derived from felsic crust and define a new tektite strewn field in South America.

Key words tektite, impact glass, strewn field, impact melt

Acknowledgements The results presented here arise from a collaborative effort involving: G.G. Silva (Institute of Chemistry, University of São Paulo, Brazil); L. Ferrière (Natural History Museum of Abu Dhabi, United Arab Emirates); M.A. Nunes and R.I.F. Trindade (Institute of Astronomy, Geophysics, and Atmospheric Sciences, University of São Paulo, Brazil); P. Nonnotte (Geo-Ocean, University of Brest, France); E. Libowitzky (University of Vienna, Austria); and F. Jourdan (Curtin University, Australia).

EVOLUTION OF CHEMICAL DURABILITY AND MECHANICAL PROPERTIES OF SILICATE GLASSES AFTER AQUEOUS SOLUTION CORROSION

Qiuju Zheng

School of Materials Science and Engineering, Qilu University of Technology, China

Abstract Borosilicate glasses have wide applications in many fields. Chemical durability and mechanical properties are two important properties for borosilicate glasses. We have conducted a series of static corrosion tests on different types of borosilicate glasses. We revealed the underlying mechanism of the influence of water content on the mechanical properties of glass. After corrosion, the glass surface underwent nearly complete leaching of network-modifying ions, leading to structural alterations and increased water content within the layer. Importantly, we found that both the water content and the hydrogen bonding strength of hydrous species in the alteration layer affect the mechanical properties of glass. Strong hydrogen bonds enhanced the nano adhesion force of the glass surface, while reducing the nano-hardness, elastic modulus, and Vickers hardness of glass. These findings offer new insights into the glass-water interaction and its influence on the mechanical properties of glass materials.

Key words Borosilicate glasses, Chemical durability, Mechanical properties

MECHANICAL BEHAVIOUR OF OBSIDIAN RESOURCES OF PRE-HISPANIC CIVILIZATIONS OF CENTRAL MESOAMERICA

Luiz Pereira[1,2*], Geovana L. Santana[3], Qiuju Zheng[4], Ricardo F. Lancelotti[3], Augusta Isaac[5], Alejandro Pastrana[6], Hugo Delgado-Granados[7], Edgar D. Zanotto[3], Donald B. Dingwell[1,2].

1. GEOLAB, Hangzhou International Innovation Institute Beihang University, China.
2. Dep of Earth and Environmental Sciences, Ludwig-Maximilians-Universität München, Germany.
3. Dep of Materials Engineering, Federal University of São Carlos, Brazil.
4. School of Materials Science and Engineering, Qilu University of Technology, China.
5. Metallurgical and Materials Engineering Department, Federal University of Minas Gerais, Brazil.
6. Dirección de Estudios Arqueológicos, Instituto Nacional de Antropología e Historia, Mexico.
7. Instituto de Geofísica, Universidad Nacional Autónoma de México, Mexico.

Abstract Obsidian – natural volcanic glass – was an essential material for pre-Hispanic societies of central Mesoamerica. Large quantities were used for domestic cutting tools, weapons, and a wide range of ornamental and ritual objects. The choice of obsidian types from specific deposits was closely linked to their appearance and mechanical performance; however, the latter remains poorly understood. In this investigation, we investigate some mechanical properties of obsidians from the Sierra de Las Navajas deposit – the most important obsidian source in Mexico – using ball-on-three-ball (B3B) fracture-strength measurements and, for the first time, nanoindentation to quantify hardness. We complemented these analyses with X-ray tomography to characterise the internal three-dimensional microstructures. Mechanical behaviour varies widely across the different obsidian families and collected locations, and it is governed by textural characteristics, notably the size, amount, and shape of inclusions. These textures reflect distinct volcanic formation processes, which in turn shaped the performance of the material in its daily use. This work brings a clear message: pre-Hispanic civilisations were able, using locally available knowledge and the technologies of their time, to identify and select the most appropriate obsidian types for specific purposes.

Key words glass, Aztecs, volcanology, mechanical properties, archaeology

RELATIONSHIP BETWEEN TITANIUM COORDINATION AND IONIC CONDUCTIVITY IN SODIUM SILICATE GLASSES

Oscar Bonnet[1], Sohei Sukenage[2], Neo Takakusagi[1], Yoshiyuki Gambe[2], Arunkumar Dorai[2], Hiroyuki Shibata[2]

1. Graduate School of Engineering, Tohoku University, JAPAN

2. Institute of Multidisciplinary Research for Advanced Materials, Tohoku University, JAPAN

Abstract Ionic conductivity in glasses is strongly ruled by the local structural environment surrounding charge carriers, which directly depends of the type of network-forming species. Titanium oxide, for instance, plays an decisive role in the short- and medium – range order of the glassy network depending of its coordination state. This effect significantly impacts cation mobility, either enhancing or hindering conductive pathways. Nonetheless, substantial uncertainty remains regarding Ti coordination in silicate glasses, and no consensus has yet been established.

The present study focuses on the Ti coordination state – ionic transport relationship in Na_2O–SiO_2–TiO_2 glasses. By introducing TiO_2 from 5 up to 20 mol%, ionic conductivity was determined by impedance spectroscopy over a wide range of temperature (from room temperature up to glass transition temperature). The amount of Na_2O was kept constant to ensure the same number charge carriers for each samples. In parallel, structural analysis spectroscopies such as Raman and ^{29}Si NMR were used to probe the network connectivity and Titanium coordination state.

The results show a non-monotonic effect: While low content of TiO_2 increases ionic conductivity, further addition leads to an noticeable decrease, with a conductivity dropping by 15% compared to the undoped sodium silicate glass. The reason for this behavior is mainly due to the structural reorganization within the silicate network induced by Titanium oxide. These findings suggest that the predominantly five-coordinated Titanium species promote conductive pathways for sodium ions at low TiO_2 content, whereas higher concentrations favor the formation of TiO_4 tetrahedra, increasing network polymerization and inhibiting cation mobility.

These results provide new insight into the relationship between titanium coordination and ionic transport in silicate glasses. They highlight the role of local structural variations in controlling ion mobility and contribute to improving predictive models for glass compositions.

Key words Titanium coordination, Ionic conductivity, Silicate glass

VISCOSITY AND STRUCTURE OF IRON ALUMINOSILICATE MELT

Sohei Sukenaga[1], Juson Kokubo[2], Masanori Tashiro[1], Jiang Liu[3], Gen Kamimura[1], and Hiroyuki Shibata[1]

1. Institute of Multidisciplinary Research for Advanced Materials, Tohoku University, Japan
2. Department of Metallurgy, Graduate School of Engineering, Tohoku University, Japan
3. Sumitomo Metal Mining Co., Ltd., Japan

Abstract Viscosity of aluminosilicate melts strongly depends on the local structure near aluminum cations, which is sensitive to the types of non-framework cations (e.g., Ca^{2+}) that exist in the silicate melts. Previous studies have demonstrated that the average coordination number of aluminum cations tends to increase with an increase in the field strength (Z/r^2, Z: cationic valence, r: cationic radius) of the non-framework cations. Then, calcium aluminosilicate melts generally have higher viscosity than magnesium aluminosilicate melts at comparable alumina content because the Z/r^2 of magnesium is higher than that of calcium cation. Although the iron aluminosilicate melt is an important system that forms as slag in metallurgical processes, little is known about the local structure near aluminum cations in these iron-containing systems owing to the difficulty of using a gold-standard method, nuclear magnetic resonance. The present study aims to investigate the correlation between the viscosity and structure of the iron aluminosilicate system. We measured the viscosity of the melts at temperatures above the liquidus. The structure of the quenched glasses were characterlized to understand the local structure near aluminum cations. The effect of $61FeO–39SiO_2$ (mol%) was chosen as the composition, labeled as "FS." To investigate the effect of alumina content on the viscosity of the FS melt, FS with varying alumina contents (0, 3, 6, 9, or 12 mol%) were synthesized by the melt-quench method using an iron crucible. The viscosity of these melts was measured using a rotating crucible method under an argon atmosphere in a molybdenum crucible. The viscosity of the FS melt increased with increasing alumina molar content. Mössbauer spectra of the quenched glassy slags after the viscosity measurement indicated that the iron cations in the slag are mainly present in a divalent state (Fe^{2+}). The increase in viscosity with an increase in alumina content can be attributed to the structural role of alumina, which acts as a network former. This conclusion is consistent with the structural information obtained by the synchrotron X-ray total scattering and X-ray absorption spectroscopy for the quenched glasses.

Key words Iron aluminosilicate melt, glasses, viscosity, structural characterization

Acknowledgements We would like to thank Sumitomo Metal Mining Co., Ltd. for financial support.

ABNORMAL PHASE RELATIONS IN FE-LIGHT ELEMENT TERNARY MELTS AND IMPLICATIONS FOR PLANETARY MAGNETIC FIELDS

Feng Zhu, Yuanjing Li, Wei Wang, Liangliang Zhang, Shengchun Chen

State Key Laboratory of Geological Processes and Mineral Resources, School of Earth Sciences, China University of Geosciences, Wuhan, Hubei, China.

Abstract The liquid cores of terrestrial planets may contain multiple light elements (LEs). Recent studies have shown that the phase relations in Fe-LE ternary systems can be more complex than that in simple ternary eutectic system. Abnormal phase behaviors such as liquid immiscibility and simultaneous dissolution with shared solubility can provide new dynamic mechanism to power the core dynamo and produce magnetic fields. In this study, we performed high-pressure and hight-temperature multi-anvil apparatus experiments combined with first-principles and machine-learning force-field molecular dynamics calculations, to investigate the phase relations in Fe-LE ternary melts. The results indicate that light element exsolution during core cooling process in the simultaneous dissolution system such as Fe-Si-C and Fe-O-H may account for the long-term magnetic fields of Mercury, Earth, and Ganymede, particularly prior to core crystallization. The miscible-immiscible transition in immiscible system such as Fe-C-O, on the other hand, may drive short-term dynamo that can explain the early magnetic fields of Moon and Mars. The different Fe-LE core compositions and their diverse phase relations may thus provide distinct mechanisms to interpret the varied magnetic field behaviors among the terrestrial planets in the Solar System.

Key words Light element, Fe melt, Liquid Cores of Terrestrial Planets, Phase relation, Magnetic Field

CONSTRAINTS ON LITHOLOGY AND FLUORINE-CHLORINE VOLATILIZATION CHARACTERISTICS OF MANTLE SOURCE IN LAIWU , SHANDONG PROVINCE IN EASTERN CHINA

Qi Yu , Gang Zeng

School of Earth Sciences and Engineering, Nanjing University, Nanjing

Abstract Cycling of volatiles plays a critical role in deep melting, ore formation, and the development of Earth's habitability. As important volatiles in the Earth's interior, fluorine (F) and chlorine (Cl) significantly influence mantle-derived magmatic processes. Basalt, the direct product of mantle melting, is a key target for constraining deep F and Cl compositions; however, the F and Cl compositions of basalt are significantly modified by degassing during magma ascent. Melt inclusions trapped in early-formed minerals (e.g., olivine) preserve primitive magma compositions, providing a robust record of mantle volatiles. Here we present in-situ major and trace element analyses of olivine phenocrysts, coupled with precise determinations of F, Cl, and Pb isotopes of melt inclusions from Laiwu basalts in eastern China. The olivine phenocrysts in Laiwu basalts show high Ni and Mn contents, moderate Ni/(Mg/Fe) and low Mn/Fe ratios, indicating an eclogitic source. Their high Ca contents imply the source has been carbonated. The melt inclusions trapped within these olivine phenocrysts are generally characterized by high silica and alkali enrichment. Primitive magma calculations indicate that the samples fall within the silica-rich pyroxenite field, further supporting the influence of recycled materials. Pb isotopes of these melt inclusions show a good correlation, with the low-206Pb/204Pb endmember similar to the lower continental crust. The high F/Cl ratios of low-206Pb/204Pb endmember also suggest the important influence of lower continental crust during the formation of Laiwu basalts.

Key words Eastern China, Cenozoic basalts, Olivine phenocryst, Melt inclusion, F-Cl Volatile

DISORDER-DRIVEN SYNTHESIS OF C_{2+} ABIOTIC HYDROCARBONS VIA DIRECT CARBON-HDROGEN REACTIONS UNDER UPPER MANTLE CONDITIONS

Shaojie Wang[1,2,3], Mingtao Li[3], Zhongyan Wu[2*], Saichao Cao[4], Penghui Li[2], Xiang Zhang[2], Zhiwei Shen[1,2], Hongkai Li[1,2], Ke Yang[4], Li Zhang[3*], Guoying Gao[2*], Lin Wang[1,2*], Yongjun Tian[2]

1. Key Laboratory for Microstructural Material Physics of Hebei Province, School of Science, Yanshan University, Qinhuangdao 066004, P. R. China

2. Center for High Pressure Science, State Key Laboratory of Metastable Materials Science and Technology, Yanshan University, Qinhuangdao, 066004, China

3. Center for High Pressure Science and Technology Advanced Research, Shanghai 201203, China

4. Shanghai Synchrotron Radiation Facility, Shanghai Advanced Research Institute, Chinese Academy of Sciences, Shanghai 201210, China

Abstract Recent advances in geoscience have underscored the critical role of abiogenic processes in petroleum formation, especially the formation and polymerization of methane. However, whether a direct carbon–H_2 reaction can produce C_{2+} hydrocarbons (e.g., ethane and propane) beyond methane remains an open question. Here, we demonstrate the direct synthesis of ethane and propane via reactions between amorphous carbon and H_2 under upper mantle conditions (2–10 GPa and 1000–1200 K). A systematic investigation reveals that increasing structural disorder in carbon precursors, from graphite to glassy carbon-II and carbon black, enhances the production of C2–C3 hydrocarbons. Through integrated X-ray diffraction and reverse Monte Carlo simulations, we establish that the continuous random atomic network structures in amorphous carbon enable one-step synthesis of heavy hydrocarbons with H_2. These models establish a direct link between atomic-scale carbon structures and the one-step synthesis of C_{2+} hydrocarbons under H_2-rich, high-pressure, and high-temperature conditions—potentially revealing an efficient mechanism for the abiotic production of C_{2+} hydrocarbons in the upper mantle.

Key words C_{2+} abiotic hydrocarbons, deep-Earth carbon cycling, upper mantle conditions

EXOTIC CHEMISTRY IN VOLATILE-BEARING SILICATE MELTS ALONG THE SHOCK AND AT EXTREME PLANETARY CONDITIONS

Razvan Caracas, Adrien Saurety

Institut de Physique du Globe de Paris, Université Paris Cité, CNRS, 1 rue Jussieu, Paris 75005 France

Abstract Giant and large-scale impacts dominate the end of the accretion stage in early solar systems. As the accretion advances, the size of the leftover planetesimals increases and, therefore, the impacts between them become increasingly energetic. Here we use atomistic simulations based on *ab initio* molecular dynamics and machine learning to study the behavior under shock of a series of silicates, representative of various rocky worlds, like the bulk silicate Earth (BSE) and several chondritic compositions.

The atomic structure of the silicate fluid and thus its properties vary enormously as a function of shock conditions and during shock release. Fluffy short-lived chemical species dominate the hot low-density regime, while long-lasting dense polymers abound in the higher-pressure regions. During release, liquids and gases separate according to the liquid-vapor stability dome.

These variations challenge us to define the chemical speciation in a melt/fluid. For fluids, one of the most common way to define bonding is geometrical: we compute statistically the pair distribution functions (PDF) between all pairs of atoms in that system. Then, by convention, the first local minimum of the PDF marks the radius of the first coordination sphere. Atoms within that distance are considered "bonded", while atoms outside of that distance are considered not bonded. With this definition, we may determine the chemical speciation in a melt, identify coordination polyhedra, track polymerization, calculate volatile speciation, etc. We can even pursue our analysis and monitor the formation of bubbles in natural melts, at low densities/pressures. But are these geometrical method always right? Or shall we use more sophisticated method, like the electron localization function (ELF)?

Here we use and compare these two different methods to analyze the behavior of various volatile-bearing complex silicate melts along shocks expected to occur during large and giant planetary impacts. We show how the balance between temperature and pressure affects the chemical speciation along the Hugoniot. We identify the formation of bonds between Fe and C; Si and C, Si and H, and we analyze their transient character We discuss the formation of molecular CO_2 and the induced varying oxidizing condition along the shock trajectory. Finally, we discuss in detail the formation of gas bubbles in silicate melts during the release trajectory.

Key words extreme conditions, molecular dynamics, chemical speciation

EXPANDING THE GEOCHRONOLOGICAL TOOLBOX OF THE EPIDOTE SUPERGROUP

Marko Bermanec[1], Jesse B. Walters[1,2,3], Christoph Hauzenberger[1], Axel Gerdes[2,3], Andreas Karlsson[4], Horst R. Marschall[2,3]

1. NAWI Graz Geocenter, Department of Earth Sciences, University of Graz, Graz, 8010, Austria
2. Department of Geosciences, Goethe University Frankfurt, 60438 Frankfurt am Main, Germany
3. Frankfurt Isotope and Element Research Center (FIERCE), Goethe University Frankfurt, 60438 Frankfurt am Main, Germany
4. Department of Geosciences, Swedish Museum of Natural History, P.O. Box 50007, 10405 Stockholm, Sweden

Abstract Epidote-supergroup minerals are common rock-forming phases that crystallise in a wide range of magmatic, metamorphic, and hydrothermal environments. To date, U-Th-Pb petrochronology within the epidote supergroup has focused almost exclusively on the allanite endmembers, with limited attempts to date the epidote-clinozoisite solid solution. Consequently, it remains unclear whether other epidote-supergroup minerals can be dated and which crystal-chemical or geochemical factors control their suitability for U–Th–Pb petrochronology. Because epidote-supergroup minerals commonly participate directly in major mineral-forming reactions and fluid–rock interaction processes, expanding geochronology to additional endmembers could provide new opportunities to directly date metamorphic, metasomatic and particularly fluid-mediated alteration reactions in systems which cannot be dated by other conventional chronometers such as zircon or monazite-(Ce). The key question is therefore whether epidote-supergroup minerals beyond allanite and epidote contain sufficient U and Th and sufficiently low common Pb to allow meaningful age determinations.

We address under what analytical and geological conditions meaningful U–Th–Pb dates can be obtained. To achieve this, we have assembled a globally sourced collection of approximately 100 samples representing at least 15 epidote-supergroup endmembers spanning diverse tectonic settings and metamorphic conditions, providing an unprecedented framework for systematic evaluation. This dataset provides an initial framework for assessing how mineral chemistry, REE substitution mechanisms, and bulk-rock composition influence actinide incorporation and Pb systematics in the epidote supergroup. Major- and trace-element compositions were characterized by electron microprobe and LA–ICP–MS in order to evaluate the intra-grain distribution of U, Th, and Pb.

Preliminary LA–ICP–MS analyses demonstrate that epidote-supergroup minerals beyond allanite can yield robust U–Th–Pb ages. In particular, we present the first U–Th–Pb dates obtained from dissakisite-(Ce) and dollaseite-(Ce). Dissakisite-(Ce) from the Trimouns talc quarry in France contains up to 5 µg/g U, but very low Th (~0.01 µg/g) and Pb (~0.02 µg/g). Although the actinide concentrations are modest compared to typical allanite samples, the very low Pb

concentrations suggest minimal common Pb incorporation, creating favourable conditions for U–Pb geochronology. The analyses yield a concordia intercept age of 99.9 ± 4.8 Ga (2σ), consistent with the latest stages of hydrothermal crystallization of zircon from the same locality which records ages from 112 to 97 Ma.

Analyses of dollaseite-(Ce) from Norberg, Sweden yield a concordia intercept age of 1.7 ± 0.12 Ga (2σ), which is within statistical uncertainty with the 1.88 ± 0.11 Ga Sm–Nd isochron age obtained for REE-rich minerals from the same skarn system, often recording extremely protracted crystallisation periods. Uranium, Th, and Pb concentrations in the dollaseite-(Ce) reach up to 2.5, 1.5, and 1.4 µg/g, respectively.

These results indicate that the ability to date epidote-supergroup minerals is not controlled solely by high U and Th concentrations but is also heavily dependent on the relative abundance of common Pb. Minerals such as dissakisite-(Ce) and dollaseite-(Ce), despite containing relatively low actinide concentrations, may still yield meaningful ages when common Pb is sufficiently low. Preliminary observations from our broader dataset suggest that other epidote-supergroup minerals commonly contain measurable U at the µg/g level, while Pb concentrations vary significantly between mineral compositions and geological environments.

We demonstrate that the petrochronological potential of the epidote supergroup extends beyond the traditionally studied allanite and epidote endmembers. Expanding U–Th–Pb dating to additional epidote-supergroup minerals opens new opportunities to directly date mineral growth, metamorphic reactions, and fluid–rock interaction processes in geological environments where conventional accessory mineral chronometers are absent or rare.

Key words Epidote, U-Th-Pb petrochronology, LA-ICPMS

FIRST-PRINCIPLES CONSTRAINTS ON FRACTIONATION OF RARE EARTH ELEMENTS IN METAMORPHIC GARNET

Meng Chen[1,2,*], Yancheng Lou[1,2]

1. State Key Laboratory of Deep Earth Processes and Resources, Guangzhou Institute of Geochemistry, Chinese Academy of Sciences, Guangzhou, 510640, China.

2. Guangdong research center for strategic metals and green utilization, Guangzhou, 510640, China.

Abstract Garnet is ubiquitous in the upper mantle and crust and records valuable information about metamorphic and metasomatic reactions associated with geodynamic and geochemical evolution. In metamorphic rocks, garnet commonly occurs as porphyroblasts with compositional zoning. Due to the slow elemental diffusion in the crystal, these zoning patterns can preserve records of local chemical equilibrium between growth stages of garnet and the surrounding fluid. Consequently, compositional zoning profiles in garnet can be used to infer fluid flow, chemical mass transfer, seismic cycles, and tectonic histories in subduction zones. However, multiple interpretations have been proposed for the origin of elemental zoning, which complicates the reconstruction of geodynamic and geochemical processes from these profiles.

Given these uncertainties, it is necessary to use first-principles simulations to understand the partitioning mechanisms of Y and rare earth elements (Y+REEs) between garnet and fluids over a wide range of pressure–temperature–fluid composition (*p*–*T*–*X*) conditions. Such an approach can help verify elemental distribution records and provide constraints on the underlying geodynamic and geochemical processes. In addition, elucidating the partitioning behavior of REEs during garnet growth is fundamental for geochronological studies based on REE isotopes, which can provide time-resolved constraints on geodynamic and geochemical evolution.

In this study, we model two major end-member components of the garnet solid solution: pyrope and grossular. Using thermodynamic integration to combine thermodynamic data—including the free energies and stability constants of stepwise complexation reactions of La(III), Gd(III), and Y(III) in Cl-rich aqueous fluids, as well as the free energies of ion-exchange reactions in pyrope and grossular systems—we quantify the fractionation behavior of La(III), Gd(III), and Y(III) in garnet that is in local equilibrium with aqueous fluids over a wide range of p–T–X conditions. These fractionation data help interpret the geochemical records preserved in garnet porphyroblasts and thereby provide insights into past geodynamic events and geochemical processes.

Key words Rare earth element complexes, Aqueous fluid, Garnet, Elements partitioning, First-principles molecular dynamics

GENESIS OF THE NOUGOUA GOLD DEPOSIT IN THE ABOISSO, CÔTE D'IVOIRE: CONSTRAINTS FROM GEOCHRONOLOGY, FLUID INCLUSION, AND H-O-S ISOTOPES

Peng Hu[1, 2], Xin Chen[1*], Youye Zheng[1]

1. School of Earth Resources, China University of Geosciences, China

2. Wuhan Center, China Geological Survey (Geosciences Innovation Center of Central South China), China

Abstract The Nougoua gold deposit is located in the Kumasi Basin of the Paleoproterozoic Birimian terrane, which hosts one of the world's most significant gold provinces in West Africa. However, the ore-forming fluid source, metal precipitation mechanisms, and precise mineralization age of the deposit remain poorly constrained. This study integrates fluid inclusion microthermometry, H-O-S isotopes, in-situ trace elements and U-Pb dating of zircon and rutile, as well as in-situ Ti isotope analyses of rutile to decipher the genesis of the Nougoua deposit. Fluid inclusion analyses in quartz from auriferous quartz-sulfide veins reveal aqueous-carbonic fluids with homogenization temperatures of 200–350 °C and low salinities (2–10 wt% NaCl equiv.), typical of orogenic gold systems. Hydrogen and oxygen isotopic compositions (δD = –68‰ to –34‰; $\delta^{18}O$= 3.85‰ to 8.34‰) indicate a dominantly metamorphic fluid source, with minor late-stage meteoric water incursion. In-situ sulfur isotopes of pyrite ($\delta^{34}S$ = –2.36‰ to –5.81‰) suggest a magmatic or metamorphic sulfur reservoir, possibly derived from leaching of Birimian volcanic-sedimentary rocks. U-Pb dating of rutile yields a lower intercept age of 2146± 34 Ma (n=39, MSWD = 3.4) and zircon yields age of 2146± 6 Ma (n=25, MSWD =1.3), interpreted as the timing of gold mineralization, coeval with the late Eburnean orogenic event. Importantly, in-situ Ti isotope analyses of the same rutile grains show $\delta^{49}Ti$ values ranging from –0.17‰ to +0.40‰ (mean = 0.10‰, n = 50), with 80% of data positive and a unimodal distribution peaking at 0.00–0.20‰. The slightly positive $\delta^{49}Ti$ signature, relative to mantle rutile (≈0 ± 0.1‰), relatively high-pH hydrothermal fluid, where heavy Ti isotopes preferentially partition into rutile. The narrow range and near-normal distribution indicate a stable fluid chemistry and homogeneous precipitation environment. Together, these results support an orogenic gold model for the Nougoua deposit, where metamorphic fluids released during the Eburnean orogeny migrated along shear zones, leaching Au and S from Birimian greenstones, and precipitated gold in response to fluid-rock interaction and cooling. Rutile Ti isotopes serve as a novel tracer for fluid evolution and gold-coupling processes, offering a new tool for exploration in Paleoproterozoic terranes.

Key words Nougoua gold deposit, Rutile Ti isotopes, Orogenic gold, Eburnean orogeny, Kumasi Basin, West Africa

GLOBAL SUB-ARC MANTLE OXIDATION IN THE MID-PROTEROZOIC

J. ZhangZhou, Chun-Tao Liu, Chen-Yang Ye, Qun-Ke Xia

Research Center for Earth and Planetary Material Sciences, School of Earth Sciences, Zhejiang University, Hangzhou 310058, China

Abstract The redox state of Earth's mantle fundamentally impacts mantle melting processes, volcanic degassing, and crustal composition, but its long-term evolution remains uncertain. Here we use a machine-learning classifier to identify primitive arc basalts with high accuracy and reconstruct global sub-arc mantle oxygen fugacity (fO_2) from ~3.2 to 0.8 billion years ago (Ga). Our results show that the sub-arc mantle fO_2 remained stable during ~3.2–1.6 Ga, increased gradually between ~1.6 and 1.2 Ga, attaining near-modern conditions by ~1.2 Ga. This Mesoproterozoic oxidation was asynchronous with the Great Oxidation Event and Neoproterozoic Oxygenation Event, suggesting that deep-Earth processes, such as the establishment of modern-style subduction and enhanced fluxes of serpentinite-derived fluids drove the oxidation of the mantle wedge. The establishment of an oxidized sub-arc mantle may have diminished volcanic oxygen sinks, contributing to long-term accumulation of atmospheric oxygen in the Mesoproterozoic and a habitable environment for early eukaryotic life.

Key words Machine learning, Arc, Redox

MANTLE CATIONS DEFINE THE FATE OF OXIDIZED SULFUR IN DEEP FLUIDS

Xi Zhu, Razvan Caracas

Université Paris Cité, Institut de Physique du Globe de Paris, CNRS, Paris 75005, France

Abstract Macroscopic models of subduction-zone volatile cycling typically assume major divalent cations act as charge balancers. Here, we use machine-learning molecular dynamics to evaluate the physical structure and chemical speciation of aqueous $MgSO_4$, $CaSO_4$, and $FeSO_4$ under deep-Earth conditions (1–7 GPa, 1000–1500 K).

We find that all three systems share a consistent structural response to compression, systematically shifting toward solvent-dissociated states. However, pronounced chemical divergence occurs within these similar structures. At 1500 K, the Mg- and Ca-bearing systems remain dominated by SO_4^{2-}. By contrast, the Fe-bearing fluid uniquely enters a protonated sulfate regime in which HSO_4^- becomes more abundant than SO_4^{2-}, at a low-pressure window of 1–3 GPa. This structural-chemical decoupling demonstrates that chemical fate in deep aqueous systems cannot be inferred from physical association alone. Ultimately, oxidized sulfur transferred into the mantle wedge is not a monolithic fluid. Cation identity can split deep fluids into fundamentally distinct chemical endmembers.

Key words oxidized sulfur, aqueous, deep fluids, machine learning potential.

METASTABLE CO_2-CO FLUIDS IN THE DEEP OCEANIC LITHOSPHERE CHALLENGE MODELS OF CARBON TRANSPORT AND FIXATION AT MANTLE DEPTH

Maria Luce Frezzotti, Andrea Maffeis

Dipartimento di Scienze dell'Ambiente e della Terra, Università degli Studi di Milano-Bicocca, Milan, Italy

Abstract Equilibrium thermodynamics predicts that carbon introduced into the reduced lithospheric mantle by oxidised fluids or melts should be immobilised as graphite via redox reactions with Fe^{2+}-bearing silicates. This prediction underpins current models of deep carbon storage, in which the CCO and EMOD/EMOG buffers delineate the boundaries between oxidised and reduced carbon phases. Yet graphite is virtually absent from the mantle xenolith record outside Archean cratons, suggesting that carbon may not be predominantly stored in solid form under these conditions. In this context, alternative reduced carbon species must be considered, with CO in particular receiving almost no attention.

We present fluid inclusion data from spinel peridotite xenoliths from Sal Island (Cape Verde), sampling the oceanic lithospheric mantle to depths exceeding 100 km. The xenoliths are ultradepleted spinel harzburgites and fertile spinel lherzolites, recording *P-T* conditions of 2.1-3.5 GPa and ~1000-1200 °C within a thick, depleted lithospheric root. The deep lithosphere was metasomatised by silicate-carbonate melts, whose carbonatitic component reacted with orthopyroxene to produce clinopyroxene, olivine, spinel, and a C-O fluid via a wehrlitisation-type reaction at pressure conditions above the carbonate ledge. The reaction is incomplete in harzburgites, where relic orthopyroxene is preserved within thick metasomatic coronae. Two inclusion populations record distinct stages of the process: Type I inclusions in olivine preserve oxidised CO_2 degassed from the carbonate-rich melt, whereas Type II inclusions in reacting orthopyroxene within metasomatic coronae contain CO_2-CO mixtures with CO up to 22 mol%, but no graphite. Within individual inclusion trails, CO content and, when present, disordered carbonaceous material show a systematic inverse relationship, indicating post-entrapment CO disproportionation ($2CO \rightarrow C + CO_2$) and demonstrating the metastability of the trapped fluids.

Fluid fO_2 and aC were calculated independently from fluid compositions using the thermodynamic relations for the anhydrous C-O system, in which a graphite-free fluid at fixed *P* and *T* is univariant. In harzburgites, aC exceeds unity in all CO-bearing inclusions free of solid carbon, confirming that the CO_2-CO mixtures are metastable within the graphite stability field. Supersaturation increases with host-rock depth. Rock fO_2, determined by spinel-olivine-orthopyroxene oxybarometry, shows that the fluid and rock are not in redox equilibrium. In sample SAL1G (3.38 GPa), fluid fO_2 reaches ΔFMQ -3.4, whereas the metasomatic coronae record ΔFMQ +0.1 to +0.5, nearly 4 Δlog units apart, produced by the same incomplete redox reaction.

In the C-O system, carbon saturation ($aC = 1$) and fluid-rock redox equilibrium (fO_2 fluid = fO_2 rock) cannot be satisfied simultaneously. Without graphite to impose invariance and buffer fO_2 at the CCO, the oxidising potential of the infiltrating carbonate melt is transferred directly to Fe^{2+} in silicates and spinel, driving rock fO_2 above the CCO buffer, a condition that equilibrium models cannot reproduce. Open-system modelling confirms that only models suppressing graphite reproduce the observations; equilibrium models sequester all carbon as graphite at the EDDOG buffer, leaving no free fluid phase. In lherzolites, the more fertile assemblage provides greater redox capacity. Unmetasomatised rock fO_2 is already near the CCO buffer, and the fluid equilibrates as pure CO_2 without supersaturation when the metasomatic reaction reaches completion.

Carbon supersaturation and fluid metastability arise when the redox capacity of the peridotites is insufficient to equilibrate the fluid-rock system during metasomatism. Therefore, in the deep, depleted lithospheric mantle, carbon may not be fixed as graphite and remains mobile in metastable CO_2-CO fluids, potentially rising through the lithosphere. This challenges the role assigned to the oceanic lithospheric mantle as a carbon sink in current models of the deep carbon cycle.

Key words fluid inclusions, carbon supersaturation, C-O system, mantle metasomatism, deep carbon cycle

MOLECULAR SIMULATION OF THE STRUCTURES AND TRANSPORT PROPERTIES OF SUPERCRITICAL GEOFLUIDS

Yicheng Sun[1*], Yifan Lu[1], Xiandong Liu[2], Xiancai Lu[2]

1. College of Oceanography, Hohai University, China.

2. School of Earth Sciences and Engineering, Nanjing University, China.

Abstract Supercritical geofluids are formed by the complete miscibility of silicate melts and aqueous fluids under the high-temperature and high-pressure conditions of the Earth's deep interior. They serve as crucial carriers for mass transport and chemical evolution in subduction zones. We have conducted systematic research on several typical supercritical fluid systems using various theoretical calculation methods. The study reveals that with increasing water content, the sharp decline in viscosity for felsic silicate-water systems is driven by the reduction of Q4 species and the increase of protonated silicate units, whereas the key factor driving the drastic viscosity drop in ultramafic silicate-water systems is primarily the increase of protonated silicate units.The typical structural feature of supercritical fluid is that it contains a large amount of easy-to-flow partially polymerized or depolymerized protonated silicate units, which leads to a low viscosity while being enriched in silicate. This unique structural characteristic endows supercritical fluids with exceptional element migration capabilities, with mobilities several orders of magnitude higher than those of basaltic melts. Notably, supercritical fluids of different compositions exhibit similar viscosity values under identical temperature and pressure conditions; therefore, we propose a modified Arrhenius equation for the viscosity of supercritical fluid systems as a function of P-T-H_2O. This model demonstrates an excellent fit to the simulation data and effectively captures the response mechanisms of viscosity to temperature, pressure, and water content. Based on this equation, we explored the element migration capacities of supercritical fluids with varying compositions. Additionally, we found that the reaction between ultramafic melts and water produces a significant amount of OH^-, which may represent an important source of OH^- in deep subduction zones.

Key words Supercritical geofluid, Transport properties, Structures, First Principles, Machine learning

PERVASIVE HYDROUS CARBONATITIC LIQUIDS MEDIATE TRANSFER OF CARBON FROM THE SLAB TO THE SUBARC MANTLE

Wei Chen

School of Marine Sciences, Sun Yat-Sen University, China

Abstract Carbonatitic liquids, as a medium for transferring carbon from the slab to the mantle at subarc depths, are thought to be restricted either to the hottest conditions or to be the hydrous melting of calcium-rich lithologies (i.e., carbonated gabbro and limestone rocks) in subduction zones. In this study, high-pressure experiments on carbonated hydrous pelites demonstrate that while silicate melts are produced at 2.5–4 GPa, hydrous carbonatitic liquids clearly dominate at 5–6 GPa. The stability of Ca-rich carbonate is strongly depressed by water at pressures exceeding ~4 GPa, promoting the formation of hydrous carbonatitic liquids at temperatures as low as ~850–900 °C; these temperatures correspond to intermediate thermal regimes at depths of 150–180 km. Hence, the transfer of carbon from the slab to the subarc mantle was pervasively mediated by hydrous carbonatitic liquids. Silica-undersaturated rocks in subduction zones have higher Nb/Ta ratios than MORB, confirming the production of carbonatitic liquids by melting/dissolution of subducted carbonated rocks.

Key words Deep carbon cycle, Subduction zone, High-pressure experiment, Carbonatitic liquids

RAMAN SPECTROSCOPIC INVESTIGATION OF SULFUR SPECIATION IN AQUEOUS FLUIDS WITH MULTIPLE SOLUTES

Kang Liu[1], Huaiwei Ni[1, 2]

1. State Key Laboratory of Lithospheric and Environmental Coevolution, School of Earth and Space Sciences, University of Science and Technology of China, China

2. Deep Space Exploration Laboratory, China

Abstract Understanding sulfur speciation in aqueous fluids is essential for elucidating sulfur partitioning, recycling, and isotope fractionation in fluid-mediated geological processes. However, the effects of redox state, fluid acidity, and different solutes on sulfur speciation in aqueous fluids under high-pressure (*P*)-temperature (*T*) conditions are not totally clear. In this study, in situ Raman spectroscopy was used to determine sulfur speciation in S-H_2O ± HCl/$Na_3AlSi_5O_{13}$ and $Na_2S_2O_3$-H_2O ± $Na_3AlSi_5O_{13}$ systems in a hydrothermal diamond anvil cell at up to 800°C and 2 GPa. Experimental results show that in the S-H_2O system, the predominantly detected sulfur species were S_3^-, H_2S, and SO_2, and the proportion of S_3^- decreased with increasing temperature. Elevated acidity in the presence of HCl boosted the concentration of SO_2 and polymeric S_8 molecules at the expense of S_3^-. In contrast, in the $Na_2S_2O_3$-H_2O ± $Na_3AlSi_5O_{13}$ system, the predominantly detected sulfur species were S_3^-, HS^-, and SO_4^{2-}, and the proportion of S_3^- increased with increasing temperature. Furthermore, the presence of dissolved silicate boosted S_3^- in the S-H_2O system but depressed S_3^- in the $Na_2S_2O_3$-H_2O system. These results are generally consistent with the predictions of sulfur speciation in aqueous fluids by the Deep Earth Water (DEW) model, with the thermodynamic properties of S_3^- adopted from Pokrovski and Dubessy (2015). We inferred that slab-derived fluid at forearc depths can contain a substantial sulfur fraction in the form of S_3^- (up to 20 %) under typical redox and acidity conditions (ΔFMQ=0–2, ΔpH=1–2).

Key words Sulfur speciation, S_3^- ion, Aqueous fluids, Raman spectroscopy, DEW model, Subduction zone

REVISITING SILICATE MELT STRUCTURE VIA DYNAMIC BONDING ANALYSIS: DISTINGUISHING STABLE SPECIES FROM TRANSITION STATES

Junhai Xu[1], Yonghui Huang[1], Yunguo Li[1,2], Huaiwei Ni[1,2]

1. State Key Laboratory of Lithospheric and Environmental Coevolution, School of Earth and Space Sciences, USTC, Hefei 230026, China

2. Deep Space Exploration Laboratory, Hefei 230088, China

Abstract Understanding the behavior of melts and fluids requires detailed and accurate knowledge of their atomic structures. However, rapid liquid dynamics and the constant interconversion of chemical species pose significant challenges for both experimental and theoretical studies. In traditional analyses, stable and transition-state species often cannot be clearly distinguished. To address this, we utilized a recently developed dynamic bonding analysis strategy to unambiguously identify stable and transition-state species in silicate melts. Moving beyond purely spatial constraints, this method introduces a time-domain kinematic stability criterion. By precisely tracking the relative distance of "center-ligand" atomic pairs along ab initio molecular dynamics trajectories, our algorithm evaluates time-resolved bonding to determine the true coordination environment.

We applied this algorithm to a hydrous potassium feldspar melt, revealing a chemically rigorous and physically sound distribution of coordination numbers (CN):

Network-Forming Cations (Si and Al): The analysis reveals that dominant configurations are strictly concentrated in tetrahedral (CN=4) environments—exceeding 75% for Si and 50% for Al. This effectively eliminates the artificially inflated populations of 5-coordinated species typically observed in static analysis.

Network-Modifying Cations (K): While static analysis yields a broad, high-coordination artifact peaking at CN=11, our dynamic method uncovers a fundamentally different, tighter coordination environment peaking sharply at CN=8. This more accurately reflects the effective binding of Potassium within the melt framework.

This study provides high-fidelity structural data for understanding the topological evolution of complex silicate melts. Furthermore, it offers a powerful new analytical tool for deciphering microscopic ion hopping and macroscopic transport properties in magmatic systems.

STRUCTURES AND TRANSPORT PROPERTIES OF SUPERCRITICAL PERIDOTITE-H_2O SYSTEM

Yifan Lu[1], Yicheng Sun[1*], Kai Wang[2*], Xiancai Lu[2]

1. College of Oceanography, Hohai University, China.

2. School of Earth Sciences and Engineering, Nanjing University, China.

Abstract Supercritical fluids, owing to their exceptional capacity to efficiently mobilize elements that are typically insoluble under conventional conditions, have emerged as critical agents in the study of material transport in subduction zones and even global elemental cycling. The unique transport capabilities and behavioral patterns are fundamentally governed by the microscopic structural characteristics and macroscopic transport properties of the fluid. Therefore, a deep understanding of the structure and properties of supercritical fluids is the basis for comprehending their complex behavior in geological processes and for accurately assessing their geodynamic implications. Currently, although numerous theoretical computational studies have explored the properties of various supercritical mineral-water fluid systems, a systematic understanding of supercritical rock-water systems remains very limited, and no relevant theoretical computational research has been conducted to date. This study employs machine learning potential model trained on a first-principles dataset to systematically investigate the microscopic structures and transport properties of the supercritical peridotite-H_2O system under various temperature and pressure conditions. Based on the simulation results, we have elucidated the evolution of the structure of this system and quantitatively evaluated the transport efficiency of the supercritical fluid under varying water contents, temperatures, and pressures. As peridotite is the primary representative rock of the upper mantle, this theoretical calculation of the microstructure and transport properties of the supercritical peridotite-H2O fluid reveals its structural response and behavioral patterns during transport processes at the scale of subduction zones and the upper mantle, which provides a new theoretical foundation for understanding the role of supercritical fluids in the deep Earth.

Key words Machine learning, Supercritical fluids, Peridotite, Transport properties, Species

THE ROLE OF HALOGENS (F-CL-BR-I) IN RARE-METAL MINERALIZATION: INSIGHTS FROM THE RIRIWAI A-TYPE GRANITES, NORTH-CENTRAL NIGERIA

Yu-Xiang Zhu[1], Lian-Xun Wang[1, 2], Zhen-Bing She[1, 2], Chao Zhang[3], Dan-Zhen Ma[1]

1. School of Earth and Planetary Sciences, China University of Geosciences, China

2. Hubei Key Laboratory of Planetary Geology and Deep-Space Exploration, China University of Geosciences, China

3. State Key Laboratory of Continental Dynamics, Department of Geology, Northwest University, China

Abstract Spatially associated peralkaline and aluminous A-type granites from the Ririwai region (Nigeria) were investigated for their halogen (F, Cl, Br, I) budgets to elucidate the role of halogens in rare metal mineralization. Mineralogical mass balance reveals that the primary F carriers transition from fluorite, arfvedsonite, and biotite in the less evolved rocks to predominantly cryolite in the highly evolved albite granite. During peralkaline magma evolution, whole-rock F contents increase progressively (from 544–820 to 13,000–25,000 μg/g), exemplifying the role of fractionation in driving the magmatic enrichment of HFSEs, HREEs, and other trace elements (e.g., Rb, Pb, Sn, Zn) in the residual melt. In contrast, the aluminous biotite-bearing granites are relatively F-poor (1480–5580 μg/g) and lack significant Nb-Zr-REE mineralization. The presence of Ca- and Na-rich fluoride melt inclusions, enriched in LREEs, MREEs, and Y, within arfvedsonite confirms the onset of early-stage fluoride-silicate melt immiscibility, which likely dictated the two distinct evolutionary trends of the Ririwai granites. While F was continuously retained in the residual melt, Cl and Br contents initially increase from the fayalite-bearing (mean Cl: 41 μg/g; Br: 390 ng/g) to the arfvedsonite-bearing granites (72 μg/g; 512 ng/g), followed by systematic depletion in the cryolite-bearing (37 μg/g; 303 ng/g) and biotite-bearing granites (53 μg/g; 363 ng/g). This decoupling, marked by strongly rising F/Cl ratios and relatively low Cl/Br ratios in the cryolite-bearing granites, reflects the preferential retention of F in the melt versus efficient extraction of Cl and Br into an exsolving aqueous fluid, with Br partitioning more strongly into the fluid than Cl. Iodine contents vary widely (13–2,397 ng/g) but show no systematic variation across the granitic suite. We suggest that extreme F enrichment plays a crucial role in rare-metal mineralization, while Cl-Br systematics serve as effective tracers for the magmatic-hydrothermal transition.

Key words Halogens (F, Cl, Br, I), Fluoride-silicate immiscibility, Peralkaline granite, Rare metal mineralization, Ririwai complex

UNDERWORLD MODELING OF GRANITIC CRYSTAL MUSH SYSTEMS

Xinhang Lin, Haibin Yang, Can Rao

School of Earth Sciences, Zhejiang University, China

Abstract Granite plutons commonly exhibit lithofacies zonation, vertical compositional and textural variations, and composite pluton, recording complex elements redistribution and structural reorganization during the evolution of granitic magmatic systems. However, the relative contributions of magmatic differentiation, crystal settling, melt segregation and migration, and repeated magma recharge and mush rejuvenation remain poorly constrained. The crystal mush model suggests that granitic magma reservoirs were not maintained as long-lived, completely molten bodies, but instead existed as heterogeneous systems composed of a crystal framework, interstitial melt, and locally extractable melt. This model provide a useful framework for interpreting internal heterogeneity within granitoid plutons. In this study, we use the Underworld numerical platform to construct a two-dimensional simplified thermo-mechanical model of a granitic crystal mush system, in which crystals are represented as high-viscosity, high-density phases and melt as a low-viscosity continuous medium. By varying crystal abundance, spatial distribution, and contrasts in physical properties, we simulate the settling, accumulation, reorganization, and progressive stratification of the mush under gravitational forcing. The simulations show that crystal populations may progressively evolve toward vertically differentiated configurations characterized by relative crystal enrichment in the lower part of the system and relatively melt-rich domains in the upper part, producing marked vertical heterogeneity. As crystal abundance increases and particle interactions become stronger, the degree of internal stratification becomes more pronounced, and local crystal accumulation becomes more evident. These results suggest that crystal-melt property contrasts coupled with gravitational settling may promote vertical differentiation within granitic crystal mush systems. It may provide a plausible explanation for crystal-rich lower zones, relatively melt-rich upper residual domains, and vertical lithofacies transitions observed in some granite plutons. Furthermore, combined with repeated magma recharge, mush rejuvenation, and localized melt extraction, such an evolutionary framework may help explain the multi-stage emplacement, lithological superposition, and internal structural complexity characteristic of composite plutons.

Key words granitic crystal mush, Underworld, vertical zonation, composite pluton, numerical modeling

UNIQUE PROPERTIES OF SUPERCRITICAL GEOFLUIDS

Huaiwei Ni

State Key Laboratory of Lithospheric and Environmental Coevolution, School of Earth and Space Sciences, University of Science and Technology of China, Hefei 230026, China

Abstract Multiphase fluid inclusions found in subduction zone rocks and pegmatites are possible relics of supercritical geofluids, which form due to enhanced miscibility between H_2O and silicate melts driven by the addition of specific components or increases in pressure and temperature. The coexistence of H_2O and depolymerized structural units (such as monomers and dimers) endows supercritical geofluids with unique physical properties, including low density, low elastic moduli, low viscosity, high diffusivity, and high electrical conductivity. These fluids can efficiently mobilize a wide range of elements, and their chemical signatures can be inherited by metasomatized mantle and mantle-derived melts. Supercritical geofluids are shown to maintain a high $Fe^{3+}/\Sigma Fe$ ratio even under moderate oxygen fugacity, thereby acting as oxidizing agents. They can induce electrical anomalies and low seismic velocities near the top of subducted slabs and may be linked to intermediate-depth earthquakes. Furthermore, supercritical geofluids can account for the oxidation characteristics observed in arc magmas.

Key words Supercritical geofluids, density, electrical conductivity, redox, metasomatism

UPPER MANTLE LOW-VELOCITY LAYER TIED TO VOLATILE-CHARGED CARBONATE MELTS

Yongsheng Huang[1,2*], Guoji Wu[1,2,3], Xuran Liang[4], Kaiwei Tao[1,2,3], Yu Wang[1,2], Michihiko Nakamura[5], Yuan Li[6]

1. State Key Laboratory of Deep Earth Processes and Resources, Guangzhou Institute of Geochemistry, Chinese Academy of Sciences, Guangzhou 510640, China
2. CAS Center for Excellence in Deep Earth Science, Guangzhou 510640, China
3. College of Earth and Planetary Sciences, University of the Chinese Academy of Sciences, Beijing 100049, China
4. Southern Marine Science and Engineering Guangdong Laboratory (Guangzhou), Guangzhou 511458, China
5. Department of Earth Science, Graduate School of Science, Tohoku University, Sendai, 980-8578, Japan
6. Bayerisches Geoinstitut, University of Bayreuth, Bayreuth 95440, Germany

Abstract: Recent geophysical observations indicate the presence of small-volume, carbonate-rich melts in Earth's deep interior. However, the mechanisms by which such minute melt fractions migrate through largely solid rocks and generate large-scale geophysical anomalies have remained unclear. Here, our high-pressure experiments demonstrate that in the presence of H_2O and NaCl, carbonate-rich melts act as super-spreaders, completely wetting and coating the surfaces of surrounding mantle minerals. This perfect wetting enables even trace amounts of melt (0.02–0.08 vol%) to form fully interconnected networks. Such connectivity facilitates efficient melt migration and chemical exchange, driving global material recycling between the surface and planetary interior.

Key words upper mantle, low velocity layer, volatile-charged carbonate melt, dihedral angle, complete wetting

SOURCE VERSUS PROCESS CONTROLS HIGH SR/Y SIGNATURES? A CASE STUDY OF EARLY PALEOZOIC GRANITES FROM THE WUYI–YUNKAI OROGEN, SOUTH CHINA

Yuanlan Tang[1], Anthony I. S. Kemp [2], Junhong Zhao*[1,3]

1. School of Earth Sciences, China University of Geosciences, Wuhan 430074, China

2. ARC Centre for Critical Resources for the Future, School of Earth and Oceans, University of Western Australia, Crawley 6009, Australia

3. State Key Laboratory of Ore Deposit Geochemistry, Institute of Geochemistry, Chinese Academy of Sciences, Guiyang 550081, China

Abstract High-Sr/Y granitic rocks are widely used to infer deep crustal melting, garnet-stable residues and palaeo-crustal thickness, and therefore provide an important geochemical tool for reconstructing crustal evolution and tectonic setting. However, increasing recognition of long-lived, crystal-rich magmatic reservoirs has shown that whole-rock Sr/Y ratios may also be modified by crystal accumulation, melt extraction and crystal–melt segregation during magma storage. This creates a fundamental ambiguity: do high Sr/Y signatures mainly record source conditions and melting pressure, or can they be generated and amplified during intracrustal differentiation? Resolving this ambiguity is critical because these alternatives imply fundamentally different petrogenetic interpretations of crustal evolution and geodynamic history.

Here we investigate the Early Paleozoic Duntou pluton in the Wuyi–Yunkai Orogen, South China, where high- and low-Sr/Y granitic rocks occur within a single composite intrusion. The pluton comprises biotite granodiorite (BGD), two-mica granodiorite (TGD) and K-feldspar-rich monzogranite (KMG), with Sr/Y ratios ranging from high values in BGD and TGD to markedly lower values in KMG. We integrate petrography, whole-rock geochemistry, zircon U–Pb geochronology, zircon O–Hf isotopes and trace elements, apatite geochemistry and Nd isotopes, phase-equilibrium modelling and REE batch-melting modelling to distinguish source-related from differentiation-related controls. Zircon U–Pb data indicate emplacement at ca. 410 Ma, and zircon Hf–O together with apatite Nd isotopes show that the BGD, TGD and KMG form a broadly cogenetic suite derived mainly from a juvenile-dominated lower-crustal source with minor ancient crustal input. The KMG further records assimilation of evolved upper-crustal material during emplacement. Phase-equilibrium and REE modelling indicate that the parental magma was generated under hot, moderately hydrous conditions (~900 °C, ~3 wt.% H_2O) over a mid- to low-pressure range of 4–12 kbar, leaving amphibole-dominated residues. The weak pressure sensitivity of the modelled melts, together with the lack of systematic coupling between Sr/Y, Y and Dy/Yb, indicates that variable melting depth, melt fraction or garnet-stable residual assemblages cannot explain the large Sr/Y range. Instead, the Sr/Y variation is mainly associated with Sr and Eu anomalies, pointing to feldspar-controlled mass redistribution. Plagioclase-rich cumulate textures, feldspar glomerocrysts, antecrystic zircon populations, apatite–whole-rock Sr–Eu decoupling and Rb–Sr–Ba modelling collectively support multi-stage crystal–melt

segregation. In this framework, the high-Sr/Y BGD and TGD represent crystal-rich residual mush products formed during different stages of reservoir evolution, whereas the low-Sr/Y KMG represents an extracted and evolved melt.

The Duntou pluton therefore demonstrates that high Sr/Y signatures can be process-amplified rather than directly source-diagnostic. Although high Sr/Y granitic rocks are commonly used as proxies for deep crustal melting, crustal thickening and tectonic setting, this case shows that similar signatures may be produced by reservoir-scale differentiation in hot, long-lived orogenic magmatic systems. These results caution against a straightforward use of Sr/Y as a palaeo-crustal thickness proxy without first evaluating crystal–melt processes using integrated petrographic, mineral-scale and whole-rock evidence. More broadly, the Duntou case highlights the role of trans-crustal mush evolution, episodic melt extraction and crystal–liquid segregation in generating compositional diversity and promoting continental crustal differentiation.

Key words high Sr/Y granites, crystal–melt segregation, zircon and apatite geochemistry, Wuyi–Yunkai Orogen, South China

WATER-ROCK INTERACTION IN THE HIGH-TEMPERATURE GEOTHERMAL SYSTEM OF THE NORTHEASTERN DATONG BASIN, NORTH CHINA: EVIDENCE FROM FLUID INCLUSIONS IN HYDROTHERMAL ALTERATION VEINS OF DRILL CORES

Dongdong Yuan[1],Qiang Liu[1, 2]

1.School of Earth and Planetary Sciences, State Key Laboratory of Deep Geothermal Resources, China University of Geosciences, Wuhan, China

2.School of Sustainable Energy, China University of Geosciences, Wuhan, China

Abstract High-temperature (HT) geothermal energy is a critical renewable resource for addressing global energy demands and mitigating environmental concerns. Characterizing geothermal fluids and their interactions with reservoir rocks is essential for evaluating the formation and evolution of HT geothermal systems. Located in the northeastern Datong Basin, the Yangtian geothermal field is the hottest (~160°C) and highest-discharge system associated with Cenozoic extension in northern China. In this study, we present the petrographic observations, Raman and microthermometric data of **fluid inclusions (FIs)** in quartz veins from a geothermal drill core to constrain water-rock interaction in the HT reservoir. The HT geothermal reservoir, hosted primarily in Archean gneiss, exhibits various hydrothermal alterations, including silicification, chloritization, and carbonatization. The hydrothermal alteration veins (e.g., quartz, calcite, and fluorite) thus represent products of interaction between HT fluids and the reservoir rocks. As typical alteration features, quartz veins commonly crosscut the foliation and host abundant primary FIs.

Raman analyses reveal that these FIs consist primarily of H_2O and CO_2, with minor CH_4. Microthermometry indicates homogenization temperatures (Th) ranging from ~120 to 180 °C, displaying a systematic increase with depth. Final ice melting temperatures vary between −2.5 and −18.5 °C, corresponding to salinities of about 5.7 to 22.7 wt.% NaCl equiv. These data indicate moderate-to-high salinities for the investigated HT geothermal fluids. Peak Th values rise rapidly from ~140 to 155 °C between 465 and 848 m, then increase gradually from ~155 to ~170 °C from 1104 to 2416 m. This trend is consistent with drilling data, suggesting that Th values of FIs from the drill core serve as a reliable proxy for deep reservoir temperatures where direct measurements are lacking. FIs in samples at 465–1104 m show uniform salinities (~10 wt.% NaCl equiv.), increasing gradually to ~17 wt.% at 2306 m. At the well bottom (2416 m), two distinct salinity populations (~7 and ~18 wt.% NaCl equiv.) suggest fluid mixing or multiple fluid sources in the deep geothermal system. These results improve understanding of mineralogical records tracing fluid circulation in HT reservoirs of Cenozoic rift basins. These findings have implications for geothermal exploration in continental cratons.

Key words High-temperature geothermal system, Water-rock interaction, Fluid inclusions, Datong Basin

ATOMISTIC BEHAVIOUR OF HYDROGEN IN DIAMONDS

Martha G. Pamato[1], Maxwell C. Day[1], Mattia La Fortezza[1], Francesca Innocenzi[1], Davide Novella[1], Fabrizio Nestola[1], Razvan Caracas[2,3]

1. Department of Geosciences, University of Padova, Italy

2. Institut de Physique du Globe de Paris, Université de Paris Cité, CNRS, France

3. The Research Institute of the university of Bucharest, University of Bucharest, Romania

Abstract Hydrogen (H), is the most important impurity (after nitogen, N) in diamonds and understanding the types defects it forms provides key insights into the type of diamond-forming fluids and deep Earth volatile cycles. Moreover, determining the H isotopic composition of diamonds may provide constraints about the origin of Earth's water, as these isotopic signatures may reflect primordial H_2O reservoirs. However, interpreting these geochemical signatures requires understanding of the extent to which H re-equilibrates during mantle residence. To this end, it is essential to investigate the formation and evolution of H-related defects during the initial stages of diamond formation and subsequent high temperature mantle residence. Furthermore, it is fundamental to understand H diffusivity in diamonds at realistic mantle P-T conditions.

In this study, we analysed FTIR spectra from rare H-bearing *Type Ib* diamonds that reflect N/H-defect aggregation states shortly after diamond formation. Two new H-related defects were identified and their structures were determined using ab initio simulations and machine-learning molecular dynamics. Our results suggest that interstial hydrogen is trapped by substitutional N defects much earlier than previously thought, preventing diffusive loss of H during mantle residence. In addition, the diffusivity of H in diamond was computed using *ab initio* molecular dynamics (AIMD) as implemented in the Vienna Ab Initio Simulation Package (VASP). Simulations were performed over a wide range of pressures and temperatures conditions, compatible with those expected for diamond-stable regions in the Earth's mantle. Our results indicate that diamonds may act as closed systems throughout geological timescales, preserving the original H isotopic signatures and thus acting as tracers of primordial H_2O reservoirs.

Key words diamonds, hydrogen defecs, FTIR spectroscopy, diffusivity, Ab-initio simulations

Acknowledgements This work was funded by the European Union (ERC, INHERIT, Starting Grant No.101041620

CO-EVOLUTION OF CARBON AND SULFUR RECORDED BY FLUID INCLUSIONS IN SUBDUCTION ZONE: A CASE STUDY OF THE SOUTHWESTERN TIANSHAN

Jiayang Lyu, Jilei Li, Zhipei Ma, Zhongrui Wang

Institute of Geology and Geophysics, Chinese Academy of Sciences, Beijing

Abstract The vein is hosted within the blueschist, with eclogite-facies selvages developed on both sides of it. Subduction zones are important hubs for volatile cycle. Fluids are the main medium for the migration of elements. Fluid inclusions are the most direct record of deep Earth fluid information. Carbon and sulfur cycle have been researched on many topics, such as speciation, distribution and flux. And researchers find there are many similarities between the two elements in their properties. However, the research on co-evolution of carbon and sulfur has not been systematically developed from the perspective of fluid inclusions. (Jin et al., 2023) and (Fei et al., 2025) are the only two cases. Also, detailed studies on it are scarce, especially for oceanic subduction zones, and the mechanisms remain unclear, such as the distribution patterns of the two at different metamorphic stages; whether the disproportionation of sulfur affects the speciation of carbon; and whether it is a promoting or inhibitory effect. In response to these problems, this study focuses on the garnet-calcite vein system in the Southwestern Tianshan high-pressure to ultrahigh-pressure metamorphic belt, which is rich in carbon and sulfur species associations.

The vein is hosted within the blueschist, with eclogite-facies selvages developed on both sides of it. The analyses of petrology, geochemistry and mass-balance calculations have been conducted. The texture of barroisite transforming into omphacite in eclogite garnet indicates that the vein is the product of fluid-blueschist reaction during the peak metamorphism. Approximately 90% of the mineral compositions in the vein are calcite, with small amounts of garnet (5%), quartz (5%), epidote and pyrite. Based on the mass-balance calculations, the vein is Pb-rich and Sr-rich comparing to the host rock. And the fluid which finally precipitated as the vein is composed of both external and internal fluid in an open system. The $\delta^{34}S$ value of pyrite suggests that the fluid is mainly from metasediments and a small amount is from altered oceanic crust. By developing detailed analysis of fluid inclusions in the vein, we have identified two types of them in calcites, and three types in garnets. In calcites, "H_2S-CH_4-CO_2-N_2-H_2O" type and "H_2S-CH_4-N_2-ZnS-H_2O" type were found. And in garnets, there are a large number of "Cv-Gr-Dol" type fluid inclusions, with some amounts of "CH_4-H_2O" type and "Qz-Cal-H_2O" type inclusions. Additionally, ethylene (C_2H_4), muscovite, and topaz are the composition preserved in the fluid inclusion in garnet.

The existence of calcite and pyrite preliminarily suggests the coupling of carbon and sulfur, and also indicates that the fluid represented by the vein is Ca-rich, C-rich and S-containing.

Mineral compositions in the vein are almost calcite, and CO_2 has also been detected. Therefore, we think the fluid presented by the vein is mainly oxidizing. However, we still found the reducing fluid composition represented by H_2S and CH_4. This suggests that the fluid has experienced a low oxygen fugacity environment. Based on previous studies, the carbon released from subducting slabs is mainly CO_2, with the presence of CO_3^{2-} and HCO_3^-. At relatively low oxygen fugacity conditions, carbonate minerals also undergo disproportionation reactions to form methane and graphite. There is textural and thermodynamic evidence that the slab fluid is dominated by reductive sulfur species, with a pulse peak of sulfur (mainly H_2S and HS^-) at 90 km. In this study, the discovery of fluid inclusions indicates that the species pairs of carbon and sulfur may be complex, and this study can provide potentially critical information on the carbon and sulfur co-evolution in subduction zone fluids.

Key words High-pressure vein, Fluid inclusions, Subduction zone fluid, Carbon and sulfur co-evolution

EFFECTIVE RETENTION OF WATER IN FLUORINE-BEARING OLIVINE

Cheng Gao , Yan Yang *

Key Laboratory of Geoscience Big Data and Deep Resource of Zhejiang Province, School of Earth Sciences, Zhejiang University, Hangzhou 310027, China.

Abstract The Earth's mantle has long been recognized as an important reservoir of water, and the presence of water would significantly influence the geodynamic and geochemical evolution of the mantle. Although great progress has been made in understanding the distribution and cycling of water in the mantle, there still exist many inconsistencies and uncertainties. Coexisting volatiles may influence the behavior of water in the mantle. However, their roles have rarely been considered. It is worth noting that the mantle also serves as a major reservoir of fluorine. There is a lot of evidence showing that fluorine and water are coupled in the mantle, and the nominally anhydrous minerals are the main carriers of both fluorine and water. The composition of melt inclusions in the Archaean komatiites (2.7 billion-years-old) indicates the early deep mantle is rich in both fluorine and water. The kimberlite-hosted xenoliths from Kaapvaal craton show the samples metasomatised by fluorine-rich melts can contain a higher content of water. However, little is known about the impact of fluorine on water in the mantle. Considering the volume fraction of olivine, we investigate the water retention in the F-bearing olivine. We carried out annealing experiments on the F-bearing hydrous olivine at 900-1200 ℃ to study the effect of fluorine on the water stability in the mantle. The results show that (1) Fluorine would promote water incorporated in hydrogen defects associated to Si vacancy (labelled as [Si]). (2) The presence of fluorine would influence the diffusion mechanism of [Si], [Si] tend to diffuse through the slowest Si vacancy exchange mechanism in the F-bearing olivine. These results suggest that the [Si] in the F-bearing olivine are more stable, and have a good retention during magma ascent. The F-bearing olivine would preserve the more original water signature, and can be a better probe for the mantle water research.

Key words Fluorine, Water retention, Olivine, Si vacancy, Diffusion

FLUORINE INCORPORATION IN OLIVINE UNDER WATER-SATURATED CONDITIONS

Yuhao Chen, Yan Yang*

School of Earth Sciences, Zhejiang University, China

Abstract The Earth's mantle serves as a reservoir for both water and fluorine, but their abundances and distribution remain unclear. As the dominant mineral phase in the upper mantle, olivine plays a crucial role in controlling the mantle water and fluorine budget. Although fluorine storage capacity in olivine has been reported (Grützner et al., 2017), it is still unknown water effect. To evaluate the fluorine storage capacity in the shallow mantle, this study reveals fluorine incorporation in olivine at 2-4 GPa under water-saturated conditions through high-temperature and high-pressure experiments. The results show that: (1) Fluorine storage capacity in olivine greatly increases with temperature, which is consistent with the trend in the anhydrous system; and increases with pressure as well, which is in contrast to the trend in the anhydrous system. (2) Fluorine concentrations in olivine are significantly enhanced in hydrous system compared to those in anhydrous system extrapolated from Grützner et al. (2017). (3) The partition co-efficient of fluorine between olivine and enstatite is significantly higher than the results obtained by previous studies for the aluminum-bearing systems (e.g. Beyer et al., 2012; Dalou et al., 2014). These findings provide new insights for re-evaluating the occurrence of fluorine and water in olivine from the perspective of volatile interactions, and contribute to a deeper understanding of the storage and distribution of water and fluorine in the mantle.

Key words Olivine, Water, Fluorine

FORMATION OF GASEOUS MOLECULAR WATER IN COESITE: FROM OH^- TO H_2O CLUSTER

Wei Yan[1,2], Yan Yang[3], Li Zhang[4], Xiaohu Li[1,5], Weidong Sun[6], Xi Liu[2,*]

1. State Key Laboratory of Submarine Geosciences, Second Institute of Oceanography, Ministry of Natural Resources, Hangzhou 310012, China

2. School of Earth and Space Sciences, Peking University; Key Laboratory of Orogenic Belts and Crustal Evolution, Ministry of Education of China, Beijing 100871, China

3. Institute of Geology and Geophysics, School of Earth Sciences, Zhejiang University, Hangzhou 310027, China

4. Center for High Pressure Science and Technology Advanced Research (HPSTAR), Shanghai 201203, China

5. School of Oceanography, Shanghai Jiao Tong University, 200240 Shanghai, China

6. Center of Deep Sea Research, Institute of Oceanography, Chinese Academy of Sciences, Qingdao 266071, China

Abstract Water, either as hydroxyl water (OH^-) or as molecular water (H_2O), plays a key role in numerous geological processes. The mechanism for water to enter or leave the structures of silicates is yet uncertain. Here we show how OH^- water leaves coesite (Coe) by conducting a systematic in situ high-*T* Infrared (IR) spectroscopic study supplemented by transmission electron microscopy (TEM) analysis. The used Coe sample contained ~96(32) wt ppm water and showed IR peaks for OH^- water only. By heating up to ~1473 K at 1 atm, a new IR band developed at ~3659 cm^{-1}, and was likely caused by gaseous H_2O water nanoclusters. This attribution was supported by our TEM observation, which exhibited numerous nanobeads of H_2O water ubiquitously and evenly distributed in the Coe crystal. It is thus clear that as the water solubility of Coe decreases, extra OH^- water transforms into gaseous H_2O water and leaves the Coe structure. This implies that nanoclusters of H_2O water and even larger water-rich fluid inclusions in natural Coe and other silicates with unusual H and O isotopes can be intrinsic origin, not necessarily a result of micro-fractural infiltration of external fluids.

Key words Coesite, Water clusters, Hydroxyl water, High-*T* IR spectroscopy, TEM

FREEZE-THAW CYCLES AS A CHEMICAL WEATHERING DRIVER TO SINK VOLATILES ON MARS

Yuan Zou and Jiacheng Liu*

NWU-HKU Joint Centre of Earth and Planetary Sciences, Department of Earth and Planetary Sciences, the University of Hong Kong, China (yuanzou@connect.hku.hk)

Abstract While modern Mars is cold, arid, and oxidizing, early Mars is believed to be episodically warm and wet. From early Mars to the present day, how volatile elements (e.g., C, H, O, S) in the martian atmosphere were consumed over time remains an unsolved question. Previous models suggest that most surface water on Mars was sequestered into the crust through water-rock interactions. However, the accumulated warm climate on early Mars was estimated to be only tens of millions of years to allow chemical weathering to occur at T > 0°C. Such a short duration is insufficient to sequester abundant volatiles into the crust. Notably, temperature fluctuations resulting from orbital, seasonal, and diurnal changes make freeze-thaw cycles a common natural process on the martian surface. While often mentioned as a physical process, we propose that freeze-thaw cycles are potentially an efficient process to drive chemical weathering and sink volatiles into secondary minerals. Based on the study of remote sensing and Mars rover data, we have hypothesized that freeze-thaw cycles could have been responsible for the formation of sulfates observed on the surface of early Mars. This research intends to conduct systematic laboratory experiments to unveil these riddles by examining the mineralogical, elemental, dissolution rate, and isotopic behaviors of chemical weathering of the most susceptible materials driven by freeze-thaw cycles. We expect that freeze-thaw cycles may serve as a critical yet overlooked driver of chemical weathering on Mars, offering a key pathway to unravel the planet's volatile consumption and climate transition.

Key words Freeze-thaw cycles, Volatile on Mars, chemical weathering, Climate

Acknowledgements: This study was financially supported by the Research Grant Council General Research Fund (Grant No. 17306623, No. 17308625), the Key Program of National Natural Science Foundation of China (Grant No. 42441803), Young Scientists Fund of National Natural Science Foundation of China (Grant No. 42302264), Young Scientists Project of the National Key R&D Program of China (Grant No.SQ2024YFF0800028).

GLOBAL SYSTEMATICS OF NITROGEN IN DIAMOND

Michael Jollands, Henry Towbin

Gemological Institute of America, 50 W. 47th St, New York, USA

Abstract Most natural diamonds contain trace to minor amounts of nitrogen. The prevailing model involves N being incorporated into diamonds as single substitutional atoms ("C centres"), which then aggregate (combine) to form pairs ("A centres") then tetrads ("B centres"). The extent of aggregation is a function of temperature, time and total nitrogen content, and the relevant aggregation rates have been calibrated experimentally. The concentrations of these defects can be determined using infrared spectroscopy, as they all show mutually distinctive absorption features in the ~1000-1350 cm^{-1} wavenumber region.

Published compilations of diamond aggregation states from global datasets show no clear trends. But, these represent the relatively small number of diamonds (hundreds to thousands) available for study by academic researchers. In contrast, gemmological laboratories may routinely handle considerably larger numbers of diamonds (hundreds of thousands to tens of millions). Here, we study a database of infrared spectra recorded from >1 million diamonds which were submitted for analysis at the laboratories of the Gemological Institute of America (GIA). We assume that this database is large enough that it can be considered as representative of all diamonds mined for gem purposes.

After processing, these spectra show trends that have not been previously observed, specifically at least four, and likely more, distinct series which can be interpreted as narrow ranges of temperature/residence time conditions. While we do not have locality information for the majority of diamonds, it appears that these trends are not defined by their geographic origins. Rather, these trends are global. Together, they suggest that diamond formation is defined by global systematics, either related to discrete bands of residence time (secular) or common formation temperatures (thermal). Whilst there are caveats, the use of big datasets such as those available to commercial gemmological laboratories can show trends that would otherwise be inaccessible to academia.

Key words Diamond, Nitrogen, Aggregation

HYDRATION AT THE BASE OF THE MANTLE TRANSITION ZONE BY ANCIENT SUBDUCTIONS IN ASIA

Jiyu Liu [1], Zhongqing Wu [1,2], Wenzhong Wang [1,2], Wenjiao Xiao [3,4], Zhu Mao [1,2]

1. State Key Laboratory of Precision Geodesy, School of Earth and Space Sciences, University of Science and Technology of China, Hefei 230026, China
2. Mengcheng National Geophysical Observatory, University of Science and Technology of China, Mengcheng, 233500, China
3. National Key Laboratory of Ecological Safety and Sustainable Development in Arid Lands, Xinjiang Institute of Ecology and
4. Institute of Geology and Geophysics, Chinese Academy of Sciences, Beijing 100029. China

Abstract Whether and how subduction results in water enrichment at the base of the mantle transition zone (MTZ) remain elusive. The major orogenic belts of the Asian continent, including the Central Asian, Tethyan, and Alpine–Himalayan belts, which record extensive subduction processes, offer an ideal target to address the hydration of the MTZ and its relationship with subduction. Here, we map water content at the MTZ base by combining mineral physics constraints on hydrous pyrolite and global seismic observations of velocity structure and 660-km discontinuity topography. Our results indicate an average global water content of approximately 0.13 wt%, with pronounced hydration anomalies in parts of Asia. Linking these anomalies with reconstructions of past subduction events since 410 Ma reveals extensive water delivery to the MTZ, particularly beneath the Baikal region and across northwestern China, Kyrgyzstan, Uzbekistan, Kazakhstan, Afghanistan, Turkmenistan, Iran, and western Pakistan, where water content exceeds 0.5 wt%. These results connect ancient subduction history to present-day mantle hydration, offering new insights into Earth's deep water cycle and highlighting the MTZ as a key reservoir for water.

Key words mantle transition zone, water in mantle, subduction, deep water cycle, seismic structure

IN SITU EPMA ANALYSIS OF TRACE NITROGEN IN POTASSIUM FELDSPAR AND BASALTIC GLASS

Yue-Er Zhang, Shui-Yuan Yang, Shao-Yong Jiang, Hua-Jun Wang, Ke Shi

State Key Laboratory of Geological Process and Mineral Resources, China University of Geosciences, Wuhan 430074, P. R. China

Abstract Nitrogen is a critical volatile component in minerals and magmatic-hydrothermal systems. Its occurrence and distribution in mineral phases can provide key constraints on volatile cycling, fluid evolution, and element enrichment in the Earth. However, accurate in situ quantification of trace nitrogen in minerals by electron probe microanalysis (EPMA) remains highly challenging. These difficulties mainly arise from the intrinsic characteristics of the N Kα signal, including its low intensity, strong matrix absorption, and high sensitivity to peak position shifts, spectral interference, and background curvature. In this study, we developed and validated an EPMA method for the quantitative determination of trace nitrogen in potassium feldspar, with the aim of providing a reliable analytical approach for investigating nitrogen as a volatile component in geological materials.

To improve analytical precision and reduce the detection limit, both analyzing crystal selection and analytical conditions were carefully optimized. The LDE1L crystal has a larger diffraction area than the conventional LDE1 crystal, and delivers approximately 1.8 times higher count rates. We further optimized the instrumental parameters for N Kα detection. An accelerating voltage of 10 kV was confirmed to provide the optimal peak-to-background ratio, while a beam current of 500 nA improves counting statistics and further lowers the detection limit. TDI testing also verified that a 20 μm defocused beam can maintain a stable nitrogen signal even under high current conditions. Under identical test conditions, the LDE1L crystal achieved a detection limit of approximately 138 ppm (3σ), while the detection limit obtained with the conventional LDE1 crystal was only approximately 190 ppm, confirming the superior sensitivity of LDE1L for nitrogen detection.

To enhance the accuracy of the analysis, we investigated peak position correction, background subtraction, spectral overlap correction, and carbon coating absorption correction. To eliminate the error caused by the shift of the N Kα peak position in samples relative to the BN standard, we adopted a fine wavelength-scan method to determine the peak and background positions, and applied polynomial fitting to model the curved background shape. Additionally, we established the overlap correction coefficient to correct the influence of titanium spectral interference on the nitrogen Kα peak. Finally, we constructed a calibration curve between carbon film thickness and nitrogen X-ray intensity based on measurements of boron nitride standards with different carbon coating thicknesses, and corrected the systematic error caused by carbon coating absorption.

The method was validated using natural hyalophane and nitrogen-bearing synthetic basaltic glasses with independently confirmed nitrogen contents. Using the optimized LDE1L-based protocol, analyses of natural hyalophane yielded 1166 ± 240 ppm N (1σ, n = 12), which is

consistent with the reported reference value of ~1130 ppm. Measurements of synthetic basaltic glasses gave 540 ± 71 ppm for NS-9, 186 ± 33 ppm for NS-10, and 240 ± 34 ppm for NS-12, all of which agree well with published independent values. These results demonstrate that the developed EPMA protocol provides a robust and reliable in situ method for quantifying trace nitrogen in minerals and silicate materials, and offers an important analytical basis for studies of nitrogen as a volatile component in mineral-hosted geological systems.

Key words EPMA, Trace Nitrogen Electron, Quantitative Analysis

LOW WATER CONTENT OF THE LOWER CONTINENTAL CRUST INDUCED BY DECOMPRESSION MELTING: EVIDENCE FROM THE WEICHANG GRANULITE XENOLITHS IN THE NORTHERN NORTH CHINA CRATON

Yuanyuan Liu, Dongya Zou*, Xiaoyan Gu, Yantao Hao*, Hongfu Zhang, Shenghua Zhou

Research Center for Earth and Planetary Material Sciences, School of Earth Sciences, Zhejiang University, Hangzhou 310058, China

Abstract The water content of granulite xenoliths from the Cenozoic Weichang basalts in the northern North China Craton (NCC) is investigated to constrain the nature and evolution of the lower crust. The granulites are categorized into felsic and mafic groups, both characterized by widely developed glass-bearing sieve textures in their constituent minerals. Spinel-plagioclase-clinopyroxene symplectites after garnet are observed in one mafic granulite. Compared to the Archean crystalline basement, felsic granulites exhibit similar mineral compositions, whereas mafic granulites display higher Mg# and Al_2O_3 content in pyroxenes. Notably, the Al_2O_3 content of clinopyroxene in some felsic granulites decreases progressively from core to rim and extends into the sieve-textured zones. Minerals within these sieve-textured zones exhibit higher Mg# in pyroxenes and higher CaO in plagioclases relative to the clean zones. Water content in clinopyroxene varies at both inter- and intra-grain scales and shows a positive correlation with Al_2O_3. Overall, the water contents of clinopyroxene (89–286 wt. ppm) and orthopyroxene (38–192 wt. ppm) in the Weichang granulites are lower than those reported for Precambrian granulites representing the ancient lower crust of the NCC. These observations indicate that the present-day lower crust beneath Weichang is composed predominantly of reworked Precambrian felsic granulites and newly accreted Phanerozoic mafic granulites, which experienced decompression melting during the Cenozoic and consequently exhibit low water contents. The ubiquitous glass-bearing sieve textures and heterogeneous distribution of water verify that decompression melting served as an efficient mechanism for water loss. Considering the widespread decompression melting and granitic magmatism along the northern NCC during the Carboniferous-Cretaceous, we propose that the lower crust underwent a prolonged dehydration process. This resulted in a water-poor, high-strength lower crust that has persisted from the Cretaceous to the present, which critically governed the cessation of felsic magmatism and influenced the chemical properties of the Cenozoic basalts in the northern NCC.

Key words Water contents, Hydrogenzonation, Granulite, Continental lower crust

MAGMATIC WATER PROMOTES FE–TI OXIDE MINERALIZATION IN LARGE IGNEOUS PROVINCES

Huan Chen[1,2]*, Jia-Min Zhong[1], Yao Bi[3], Qun-Ke Xia[2]

1. College of Oceanography, Hohai University, Nanjing 210098, China

2. Research Center for Earth and Planetary Materials, School of Earth Sciences, Zhejiang University, Hangzhou, 310027 China Affiliation

3. Zhejiang Nuclear Industry 262 Brigade, Huzhou, 313000 China

Abstract Fe–Ti oxide deposits are major sources of Ti and V, yet the processes controlling their formation in mafic magmatic systems remain debated. Here we investigate the role of magmatic H_2O in Fe–Ti oxide mineralization using samples with variable oxide enrichment from the Tarim large igneous province. Analyses of early-crystallized clinopyroxene indicate magma H_2O contents of ~1.3–2.3 wt.%, significantly higher than typical intraplate basalts. Correlations between H_2O indicators (H_2O/Ce) and Ti enrichment proxies (Ti/Y) show that stronger Fe–Ti oxide mineralization is associated with higher magmatic water contents. These results provide natural evidence that magmatic H_2O promotes early Fe–Ti oxide saturation and enrichment. Elevated water contents likely enhance mineralization by suppressing silicate crystallization, increasing oxygen fugacity, and modifying melt density and viscosity. Our findings suggest that variations in mantle source hydration may influence the metallogenic potential of mantle plume-related mafic magmatic systems.

Key words water content, Fe–Ti oxide deposit, large igneous province

NITROGEN IMPACTS ON STRUCTURAL STABILITY OF FELDSPAR: CONSTRAINTS FROM HIGH TEMPERATURE AND HIGH PRESSURE SPECTROSCOPY AND MACHINE LEARNING

Weihua Huang, Yan Yang

Key Laboratory of Geoscience Big Data and Deep Resource of Zhejiang Province, School of Earth Sciences, Zhejiang University, Hangzhou 310027, China

Abstract Nitrogen recycling between the Earth's surface and deep interior is fundamental to the long-term evolution of the atmosphere, biosphere, and solid Earth. Silicate minerals are major nitrogen hosts in geological systems, and their stability exerts important control on the efficiency of nitrogen transport into the deep Earth. Although silicate stability has been widely investigated, the effects of nitrogen incorporation on structural stability remain poorly constrained. Feldspar is one of the most important nitrogen-bearing silicates, with nitrogen mainly incorporated as NH_4^+.

Here, we investigate the effect of ammonium on feldspar stability using in situ high-temperature and high-pressure spectroscopy combined with machine-learning analysis. Feldspar containing 0.12 wt% NH_4^+ has a thermal expansion coefficient of $14.9 \pm 0.5 \times 10^{-6}$ K^{-1}, lower than the machine-learning-predicted value for a compositionally similar nitrogen-free feldspar ($18.3 \pm 1.83 \times 10^{-6}$ K^{-1}). Under compression, the NH_4-bearing feldspar undergoes a structural transition at ~15.3 GPa, whereas nitrogen-free feldspars generally transform below 13 GPa. These results indicate that ammonium incorporation significantly modifies the thermal and compressional behavior of feldspar.

Comparison with previous studies suggests that ammonium has contrasting effects on different silicate groups. In tectosilicates, sufficiently high NH_4^+ contents may reduce thermal stability, whereas in phyllosilicates, ammonium appears to enhance thermal stability over a broad compositional range. This contrast implies that the influence of nitrogen on mineral stability is strongly structure-dependent.

These findings provide new constraints on the density and phase stability of nitrogen-bearing silicates at elevated pressure and temperature. Relative to nitrogen-free counterparts, NH_4-bearing feldspar is likely denser and may remain stable to greater depths. Nitrogen-bearing feldspar should therefore be considered important phases in deep nitrogen recycling and may also influence the physical properties of subducting slabs.

Key words Nitrogen cycling, NH_4-bearing feldspar, Structural stability, High-temperature and high-pressure spectroscopy, Machine learning

QUANTITATIVE NMR ANALYSIS OF VOLATILES IN LUNAR ANORTHITES INDICATES SIMILAR F AND P DEPLETION IN THE NEAR- AND FAR-SIDE MANTLE

Yunhua Fu[1,2], Renbiao Tao[1*], Thomas Meier[3,1], Shijie Li[4,1], Lifei Zhang[2]

1. Center for High Pressure Science and Technology Advanced Research (HPSTAR), Beijing, China.

2. SKLab-DeepMinE, MOEKLab-OBCE, School of Earth and Space Sciences, Peking University, Beijing, China.

3. Institute for Shanghai Advanced Research in Physical Sciences, Pudong, Shanghai, China

4. Institute of Geochemistry, Chinese Academy of Sciences, Guiyang, China.

Abstract Trace fluorine (F) and phosphorus (P) in silicate minerals are volatile elements that are essential for revealing the interior evolution of celestial bodies, such as the Moon. While the nearside lunar mantle is extensively characterized, the deep volatile budget of the farside remains fundamentally enigmatic. Reconstructing pristine mantle signatures is inherently challenging due to the highly fractionated nature of late-stage apatite and the vulnerability of melt inclusions to secondary modifications. Although early-crystallizing nominally anhydrous minerals (NAMs) offer a robust alternative to bypass these late-stage overprints, their ultra-trace volatile abundances have long eluded conventional analytical capabilities. Here, we breach this analytical barrier by deploying high-sensitivity micro-scale quantitative Nuclear Magnetic Resonance (μQ-NMR) spectroscopy to quantify F and P in anorthites from Chang'e-5 (nearside) and Chang'e-6 (farside) basalts. Coupling these measurements with comprehensive Monte Carlo simulations informed by compiled partition coefficients, we estimate the F and P abundances of the CE5 mantle source to be 0.12–0.92 and 99–780 μg·g-1, respectively. The CE6 farside source exhibits strikingly consistent and highly overlapping abundances (0.12–0.45 μg·g-1 for F; 196–759 μg·g-1 for P). These findings reveal an equivalent degree of volatile depletion beneath both hemispheres, conclusively indicating that the Moon's deep interior maintained a globally homogenized volatile inventory despite its profound crustal dichotomy.

Key words μQ-NMR Analysis (^{19}F,^{31}P), Chang'e-5 and Chang'e-6 lunar anorthites, Mantle Source Inversion

Acknowledgements This work is supported by the Original Exploratory Program from the National Natural Science Foundation of China (42150104 to R. Tao).

RECYCLED MARINE SEDIMENT AND FLUID IN THE SOURCE OF THE EARLY CRETACEOUS BASALTS IN LIAONING, EASTERN CHINA: EVIDENCE FROM OXYGEN ISOTOPES AND VOLATILE (CL, S, H_2O) CONTENTS

Qi-Hu Xu[1, 2*], Qun-Ke Xia[2], Jia Liu[2], Lu Wang[3]

1. Key Laboratory for the Evolution and Intelligent Regulation of Coastal Zone Resources and Environment in Jiangsu Province, College of Marine and Geographical Sciences, Yancheng Teachers University, Yancheng 224007, China

2. Key Laboratory of Geoscience Big Data and Deep Resource of Zhejiang Province, School of Earth Sciences, Zhejiang University, Hangzhou 310027, China

3. Key Laboratory of Silicate Cultural Relics Conservation, Shanghai University, Shanghai 200444, China

Abstract Understanding volatile recycling in subduction zones is crucial for constraining the nature of mantle, magma formation, and Earth's habitability. Recent research indicates that the lithosphere mantle during the peak time of North China craton (NCC) destruction was enriched in volatiles. Most scholars speculated that these volatiles may stem from the recycled Paleo-Pacific slabs. However, there is still controversy over the enriched components from subducted slabs, such as fluids, sediments, altered oceanic crust, and lithospheric mantle. This study investigates the volatile contents (H_2O, S, Cl) and oxygen isotope compositions of clinopyroxene (cpx) phenocrysts from the Early Cretaceous Yixian and Sihetun basalts in the Liaoning Province, eastern NCC. The cpx phenocrysts exhibit significantly elevated $\delta^{18}O$ values (7.18‰–9.17‰) compared to typical MORB mantle values (5.4‰–5.8‰), with a notable positive correlation between $\delta^{18}O$ and Mg#. FTIR analysis reveals distinct H_2O contents in the equilibrium melts, ranging from 0.23–0.74 wt.% for Yixian basalts to substantially higher values of 1.70–4.19 wt.% for Sihetun basalts, far exceeding typical MORB or OIB source levels. The integration of volatile ratios (H_2O/Ce, Cl/K, Cl/Nb) with whole-rock Sr-Nd-Pb isotopes and trace element patterns (elevated Li/Yb) reveals that shallow-level processes such as crustal contamination, degassing, or fractional crystallization cannot explain the observed geochemical anomalies. Instead, the elevated $\delta^{18}O$ values of the cpx phenocrysts and high H_2O/Ce and Cl/Nb ratios in the basalts indicate that the mantle source was metasomatized by recycled marine sediments and slab-derived fluids. These findings highlight the critical role of mineral-scale volatile and isotopic records in deciphering the interaction between the stagnant Pacific slab and the overlying lithospheric mantle, contributing new insights into volatile flux and mantle enrichment processes in continental subduction zones.

Key words Volatiles, Clinopyroxene, Oxygen Isotope, Basalts, NCC

SEQUESTRATION OF CARBON IN THE SUBDUCTING SEDIMENTS

Linzhe Du[1], Yongsheng Huang[2,*]

1. School of Earth Sciences, Zhejiang University, China

2. State Key Laboratory of Deep Earth Processes and Resources, Guangzhou Institute of Geochemistry, Chinese Academy of Sciences, China

Abstract The contribution of subducting sediments to the carbon fluxes within subduction zones with the presence of fluids remains poorly understood. Recent studies indicate that through carbonation induced by carbon-bearing fluids, subducted metasedimentary rocks can sequester 20%–50% of the carbon flux derived from ascending slab devolatilization fluids at a depth of ~80 km. To understand the effects of pressure and temperature variations during subduction on the capacity of subducting sediments to sequester fluid-derived carbon, we conducted high-temperature and high-pressure (HT-HP) experiments at 450–1000 °C and 1–3 GPa. The experimental results demonstrate that elevated pressure promotes the carbonation reaction, whereas elevated temperature inhibits it. At a lower pressure (2 GPa), the fluid-induced carbonation of subducting sediments primarily produces iron-bearing carbonates (siderite and ankerite), whereas at a higher pressure (3 GPa), more Ca-rich carbonates (dolomite and calcite) are formed. Furthermore, an increase in fluid carbon content leads to the formation of more ankerite, with its iron content increasing as a function of pressure. Based on these experimental results, we estimated the amount of fluid-derived carbon fixed via carbonation. The findings suggest that sediments in cold subduction slabs can effectively sequester a considerable portion (20%–30%) of carbon from carbon-bearing fluids at forearc depths; even in hot subduction slabs, sediments retain the potential to fix a minor fraction (~3%) of carbon. Ultimately, this study provides new insights into the specific carbonation reaction mechanisms within subducting sediments and the estimation of global carbon fluxes across subduction zones.

Key words Carbon, Subducting sediments

THE COMPOSITIONS AND PROPERTIES OF THE DEHYDRATION MELTING LAYER NEAR THE 410-KM DISCONTINUITY

Hongzhan Fei, Juan Chen

School of Earth Sciences, Zhejiang University, Hangzhou, China

Abstract Since wadsleyite and ringwoodite within the mantle transition zone are widely considered as water rich, dehydration melting could occur near the 410 km discontinuity when they are transferred to olivine into the upper mantle, which has a much lower water storage capacity. Nevertheless, the properties of this dehydration melting layer, which may play a key control on mantle dynamics, remain poorly constrained. In this study, we determined the water contents and compositions of hydrous melts under conditions corresponding to the 410 km discontinuity using high pressure and high temperature multi anvil experiments. Our experimental results show a melt water content of ~13 wt.% and a melt fraction of approximately 10 wt.%. Accordingly, hydrous melts generated near the 410 km discontinuity should be buoyant and are expected to migrate upward rapidly. These melts are also enriched in FeO, resulting in FeO depletion in coexisting minerals at the bottom of the upper mantle. While water rich conditions act to thicken the 410 km discontinuity, FeO depletion driven by melt migration tends to narrow it. Namely, a water saturated mantle is consistent with the seismically observed sharp 410 km discontinuity.

Key words dehydration melting, 410-km discontinuity, water, upper mantle

THE RETENTION OF VOLATILES (H, F, C) IN APATITE DURING HIGH TEMPERATURE PROCESSES

Junyu Wang, Yan Yang

Affiliation (Department/School, University, Country) Research Center for Earth and Planetary Material Sciences, School of Earth Sciences, Zhejiang University, Hangzhou 310027, China.

Abstract Apatite not only exists in igneous, sedimentary, and metamorphic rocks on Earth but is also commonly found in extraterrestrial rocks. The special hexagonal structure provides apatite space to contain various volatiles such as hydrogen, fluorine, chlorine and carbon, making it an excellent volatile carrier in geological thermal events. But experimental data concerning the mobilities of volatiles out of its lattice remains scarce. Despite several investigations elucidating the diffusivities of F, Cl, and OH, their interplay mechanism remains poorly understood. In addition, the behavior of carbon in apatite at high temperatures is poorly known either.

In this study, we carry out annealing experiments at 900, 1000, and 1100 ◦C on two apatite samples with distinct fluorine contents and analyze the mobilities of volatiles (H, F, C) with FTIR and EPMA. The results show that (1) diffusion coefficient of OH is 2-3 orders of magnitude higher than that of F for both the samples; (2) the OH and F diffusion coefficients and diffusion activation energies of the F-poor Imilchil apatite are both higher than those of the F-rich Durango apatites, indicating fluorine impacts on OH diffusion; (3) no C diffusion occurs in both of the samples at these temperatures.

These differences in diffusivity may suggest that hydrogen diffuses as OH^- along the a-axis and as H^+ along the c-axis, while fluorine diffusion relies on hydrogen diffusion along the c-axis. Based on these new data, the capacity of apatite to record volatiles can be evaluated. All volatiles, including hydrogen, is likely preserved within the core of apatite during thermal events from several days to years, such as rapid volcanic eruptions. However, for prolonged thermal events lasting hundreds of millions of years, apatite preserves volatiles for F, Cl and C, but not hydrogen.

Key words Volatiles, apatite

THE ROLE OF IRON- AND CHLORIDE-RICH HYDROSALINE LIQUIDS IN THE FORMATION OF KIRUNA-TYPE IRON OXIDE-APATITE DEPOSITS

Li-Ping Zeng and Xin-Fu Zhao

State Key Laboratory of Geological Processes and Mineral Resources, and School of Earth Resources, China University of Geosciences, Wuhan Hubei Province, China

Abstract Kiruna-type iron oxide-apatite (IOA) deposits, an important source of iron, show close associations with andesitic subvolcanic intrusions. However, the processes of ore formation and the mechanism controlling iron concentration remain uncertain. Several genetic models have been proposed, including iron oxide or sulfate (- carbonate) melts formed via magma immiscibility, flotation of igneous magnetite micro-aggregates, and replacement by magmatic hydrothermal fluids. Recent studies have focused on high-temperature melt/fluid inclusions, as these provide critical clues for understanding the nature and origin of the initial ore-forming fluids/liquids or iron-rich melts.

Here, we report the widespread presence of high-temperature, water-poor, multi-phase chloride-rich hydrosaline liquid inclusions in pre- and syn-ore minerals (including albitized zircon, garnet, diopside, and magnetite) from representative IOA deposits in eastern China. These inclusions commonly contain abundant transparent daughter minerals, including halite + sylvite (~20 to 60 vol.%), anhydrite (<~40 vol.%), Fe-chlorides, and possibly minor barite as well as fluorite, as identified by Raman spectroscopy and scanning electron microscope-energy dispersive X-ray spectroscopy (SEM-EDS) on exposed inclusions. The inclusions consistently homogenize to a liquid phase upon vapor disappearance during heating at temperatures ranging from 787 to 928 °C (average 865°C). These homogenization temperatures roughly represent the entrapment temperatures of the hydrosaline liquids, supported by other independent geothermometric data. Additionally, the hydrosaline liquids can be stable at temperatures and pressures of subvolcanic settings in the simplified H_2O-NaCl phase diagram. LA-ICP-MS analyses show these inclusions predominantly contain 3 to 10 wt.% Fe, highlighting their significant iron transport capacity. Furthermore, elemental ratios (e.g., K/Na and Ca/K) of the hydrosaline liquids and B-Sr-O isotopic data from associated minerals suggest that such hydrosaline liquids were likely immiscible from the dioritic magmas with high Cl/H_2O in subvolcanic settings, typically at depths ≤2.5 km.

Therefore, we propose a novel genetic model in which high-temperature alkaline alteration and magnetite ores were formed simultaneously through host-rock interaction with, and/or decompression and cooling of, the hydrosaline liquids. The proposed model of Fe- and Cl-rich hydrosaline liquids could have implications for other mineralization systems associated with shallow intrusions, such as iron skarn and iron oxide-copper-gold deposits, where extensive alkaline alteration and the presence of HLIs have been documented

Key words Hydrosaline liquids, Fluid inclusions, Iron oxide-apatite deposits, Magmatic-hydrothermal ore systems, Alkaline alteration

COUPLING OF WATER AND FLUORINE IN FORSTERITE AND ITS IMPLICATIONS FOR UPPER MANTLE VOLATILES

Zhicheng Zhu[1], Xiang Wu[2]

1. School of Earth and Planetary Sciences, China University of Geosciences, Wuhan, China
2. State Key Laboratory of Geological Processes and Mineral Resources, China University of Geosciences, Wuhan, China

Abstract Water is the most abundant and important volatile on Earth. In the Earth's interior, it predominantly occurs as structural OH^- incorporated into crystal structures, significantly influencing the physical and chemical properties of minerals such as defect chemistry, atomic diffusivity, rheology, and melting. Fluorine (F), the most abundant halogen in the mantle, may exert similar effects due to its comparable ionic radius and identical charge to OH^-, tending to permit substitution and potential coupling with hydrogen in mineral structures. Olivine, the dominant mineral in the upper mantle, can incorporate both H_2O and F via clumped F–OH defects that substitute for $[SiO_4]^{4-}$ tetrahedra. However, the interaction between F and H_2O in olivine remains poorly constrained. In this study, we conducted high-pressure and high-temperature experiments with $MgO–SiO_2 + MgF_2 + Mg(OH)_2$ systems at 1200–1400 °C and 3–6 GPa. The experimental products are primarily forsterite coexisting with humite-group minerals, and F and H concentrations were analyzed by electron microprobe and Fourier-transform infrared spectroscopy, respectively. Forsterite contains 565–2847 ppm F, but F solubility is reduced in the presence of H_2O compared with anhydrous systems, particularly at higher temperatures(1400 °C). In contrast, humite-group minerals host significantly higher F contents (2.01–8.65 wt.%), indicating these phases as the primary reservoir for F partitioning. The H_2O content in forsterite ranges from 131 to 558 ppm, increasing with pressure but showing little dependence on temperature, consistent with F-free systems and suggesting a limited influence of F on H_2O incorporation. Infrared spectra show sharp OH-stretching bands at 3400–3700 cm^{-1}, attributed to Si-site defects. These results indicate a decoupled behavior between F and H_2O in forsterite, with F incorporation largely controlled by coexisting hydrous phases. This provides new constraints on F–H_2O interactions and highlights the role of humite-group minerals in regulating halogen and water cycling in the upper mantle.

Key words Water, Fluorine, Forsterite

DEEP CARBON CYCLING AND CLIMATIC RESPONSE OF THE WESTERN PACIFIC SUBDUCTION SYSTEM RECORDED BY CENOZOIC INTRAPLATE BASALTS

Zhuocheng Cai, Yiwen Ju*, Peiyun Guan

State Key Laboratory of Earth System Numerical Modeling and Application, College of Earth and Planetary Sciences, Beijing

Abstract Since the Cenozoic, continuous subduction of the western Pacific plate beneath East Asia has transported carbonate- and clastic sediment-bearing oceanic crust into the Northeast Asian big mantle wedge. During subduction, the slab undergoes metamorphic dehydration, partial melting, and carbonate dissolution at various depths, releasing carbon-rich fluids and melts that metasomatize the overlying mantle wedge, induce intraplate magmatism, and regulate deep carbon cycling. However, the degree of carbonate enrichment in mantle sources, its along-strike spatial heterogeneity within the subduction system, and the associated volcanic carbon fluxes remain poorly quantified. This study investigates basalts from Changle in Shandong Province (~10 Ma) and Jeju Island in South Korea (~1.7 Ma), integrating petrographic observations, whole-rock major and trace elements, Sr–Nd–Mg isotopes, and CO_2/Nb and CO_2/Ba volatile proxies to systematically trace subducted carbonate metasomatism, volcanic carbon release, and its climatic response. The Changle and Jeju Island basalts both display typical OIB-like geochemical affinities, characterized by enrichment in LREEs and Nb–Ta, together with relative depletion in K and Pb. Their Sr–Nd isotopic compositions indicate derivation mainly from an asthenospheric mantle source. Covariations between major elements and MgO, compatible-element systematics, and K/U, Ce/Pb, and Ba/Th ratios collectively indicate that the magmas experienced only limited fractional crystallization of olivine and clinopyroxene. Positive εNd values and low initial $^{87}Sr/^{86}Sr$ ratios below 0.7045 preclude substantial crustal contamination. Both basalt suites show markedly light Mg isotopic compositions, with $\delta^{26}Mg$ values of –0.478‰ to –0.418‰ for Changle and –0.417‰ to –0.320‰ for Jeju Island, significantly lighter than the normal mantle value of -0.25 ± 0.07‰. Combined with low Fe/Mn, low Hf/Hf^* and Ti/Ti^*, and high CaO/Al_2O_3 characteristics, a carbonated eclogite origin can be excluded. The low $\delta^{26}Mg$ signatures are instead attributed to metasomatism of the mantle source by subducted recycled Mg-rich carbonates, probably dominated by magnesite-bearing components. Quantitative $\delta^{26}Mg$–$^{87}Sr/^{86}Sr$ mixing models indicate that recycled carbonates contributed approximately 15–22% to the Changle mantle source, corresponding to 2.1–3.1 wt% carbon input, and 6–16% to the Jeju Island mantle source, corresponding to 0.8–2.3 wt% carbon input. The east-to-west increase in carbonate input records lateral heterogeneity in slab decarbonation efficiency along the western Pacific

subduction system. Based on CO_2/Nb and CO_2/Ba proxies, the primitive magma CO_2 contents are estimated to be 1.83–4.53 wt% for the Changle basalts, with a mean volcanic CO_2 release of ~1,532 Mt, and 0.40–3.89 wt% for the Jeju Island basalts, with a mean volcanic CO_2 release of ~20,103 Mt. These results quantitatively reveal the metasomatic effect of western Pacific subduction-derived Mg-rich carbonates on the East Asian mantle wedge, document along-strike variations in carbon input, and constrain regional Cenozoic volcanic carbon fluxes and their climatic effects. Although CO_2 emissions from the Cenozoic basalts in eastern Shandong and adjacent offshore regions likely exerted only limited direct influence on global climate, their geochemical signatures provide critical constraints on the coupling among material recycling in the western Pacific subduction zone, regional basaltic magmatism, and the global carbon cycle.

Key words Cenozoic basalt, Mg isotope, recycled carbonate, magmatic CO_2, western Pacific plate subduction

Acknowledgements This study was jointly supported by the National Key Research and Development Program of China (No. 2023YFF0804304) and the National Natural Science Foundation of China (Nos. 42372153 and 41530315).

MACHINE LEARNING CONSTRAINTS ON CARBON AND CHLORINE DISTRIBUTION IN THE MANTLE

Tian-Ting Lei, Jia Liu, and Qun-Ke Xia

School of Earth Sciences, Zhejiang University, Hangzhou 310058, China

Abstract The mantle is a major reservoir of deep-Earth volatiles, and mid-ocean ridge basalts (MORB) and ocean island basalts (OIB) provide key constraints on the cycling of carbon (C) and chlorine (Cl). However, accurate reconstruction of primary volatile contents in mantle-derived magmas remains challenging due to degassing and contamination. Existing approaches largely rely on volatile/incompatible element ratios, but these are hindered by considerable variability, and limited sample representativeness, leading to substantial uncertainties at the global scale. Here we develop two machine learning models to predict primary C and Cl contents in MORB and OIB using major and trace element compositions, enabling a systematic reconstruction of mantle volatile distributions. The results show that MORB generally exhibit low volatile contents, but previously unrecognized C-Cl enrichments occur along specific ridge segments, reflecting the combined effects of plume-ridge interaction, recycled material input, and lithospheric metasomatism. In contrast, OIB display systematically higher C and Cl contents, indicating enriched deep mantle reservoirs, with spatial patterns linked to mantle plume upwelling and subduction recycling. Notably, the enrichment of C and Cl in the HIMU mantle endmember suggests contributions from deeply subducted, serpentinized lithosphere, implying that these volatiles could be transported through the upper mantle into deeper reservoirs. Flux estimates indicate comparable annual carbon and chlorine fluxes from ocean islands and mid-ocean ridges. Overall, this study provides new quantitative constraints on the abundance, spatial distribution, and fluxes of C and Cl in the mantle, highlighting the critical roles of mantle heterogeneity, plume dynamics, and subduction recycling in deep volatile cycling and offering new insights into Earth's long-term habitability.

Key words carbon content, chlorine content, mantle, machine learning

HP-METAMORPHIC ROCKS IN SERPENTINITE-HOSTED MÉLANGES OF THE DOMINICAN REPUBLIC AND THE ROLE OF JADE

Hans-Peter Schertl[1,2], Walter V. Maresch[1]

1. Institute of Geosciences, Ruhr-University Bochum, Bochum 44780, Germany

2. Frontiers Science Center for Deep Ocean Multispheres and Earth System, Key Lab of Submarine Geosciences and Prospecting Techniques, MOE and College of Marine Geosciences, Ocean University of China, Qingdao 266100, China

Abstract Jadeitite, jadeite quartzite, and jadeite-lawsonite quartzite from the Rio San Juan Complex (RSJC) of the northern Dominican Republic are found in serpentinite mélanges associated with a former intra-oceanic subduction zone. In addition, these mélanges contain blocks of various high-pressure (HP) metamorphic rocks, such as different types of blueschist and eclogite, orthogneiss, rare cymrite-bearing rocks, marble and metapelite. Detailed petrological studies on different types of eclogite and blueschist reveal a broad diversity of PTt-paths which are closely interrelated. In the early stages of the evolution of the subduction zone, PT-paths are both clockwise and anticlockwise, with low ("hot") P/T-gradients; maximum PT-conditions derived from eclogites are about 800°C/2.5 GPa (a Lu-Hf-age on eclogite is 103.9 Ma). Omphacite-bearing blueschists document a continuous cooling and steepening of the PT-gradient; their recorded peak metamorphic conditions are 500-550°C/1.6-1.8 GPa at 80.3 Ma (Rb-Sr on Phe-Amp-WR). Very steep ("cold") P/T-gradients are derived from jadeite blueschists; Rb-Sr-ages (Phe-Amp-WR) of 62.1 Ma and Ar-Ar ages of 71.9 Ma date the peak metamorphic conditions of 360-380°C at about 17 kbar.

Jadeitites are known from only about 20 localities worldwide and are interpreted to have either precipitated from a high-pressure aqueous fluid (“vein precipitation” or “P-type”) or to have formed through comprehensive metasomatic replacement of an igneous protolith (“R-type”). The principal types of jadeite-rich rocks observed in the RSJC can be categorized as (1) jadeitite *s.str*. (quartz-free, albite-bearing, >90 vol% jadeite), which have so far been found only as loose blocks/boulders in the mélange, and (2) jadeitite *s.str*. (quartz-bearing) and jadeite quartzite (JQ) which grade into jadeite-lawsonite quartzite (JLQ). A very unusual feature of the RSJC is that the latter type, although also found as loose blocks/boulders, can also occur as concordant layers and discordant veins in jadeite-lawsonite blueschist and omphacite-garnet blueschist country rocks. In addition, monomineralic omphacitite veins have been found in such blueschists. Thus, evidence is found for both direct crystallization from a HP aqueous fluid as well as formation by metasomatic replacement. Dated zircon of concordant jadeitite documents that old domains of 113 to 117 Ma are indistinguishable from igneous zircon of the oceanic crust; related REE patterns and Th/U ratios also suggest an igneous origin. On the other hand, younger domains of about 78 Ma ages are interpreted to be contemporaneous with the metasomatic replacement

process that formed the jadeitite.

First isotope studies document low $\delta^{26}Mg$ and relatively high $\delta^{56}Fe$ values; the jadeitite-forming fluids are best explained as mixtures derived from both altered oceanic crust and serpentinizing fluid components from forarc depths, which either directly precipitate P-type jadeitites or metasomatize igneous protoliths to form R-type jadeitites. Jadeitite and jadeite-rich rocks have a wide range of $\delta^{30}Si$ values; P-type samples exhibit slightly higher $\delta^{30}Si$ values than R-type samples. Whereas the highest $\delta^{30}Si$ values of P-type rocks can be achieved through direct precipitation from the metasomatic fluids, the observed mean $\delta^{30}Si$ values of R-type rocks can be achieved through an interaction between plagiogranite/trondhjemite and metasomatic fluid with low water/rock mass ratios.

Key words Jadeitite, P-type, R-type, HP-rocks, Rio San Juan Complex

INSIGHTS FROM FLUID INCLUSION STUDIES OF JADEITITE ON FLUID MIGRATION IN SUBDUCTION ZONES

Jiabao Wen, Guanghai Shi

State Key Laboratory of Geological Processes and Mineral Resources, China University of Geosciences, Beijing 100083, China

Abstract Subduction zone fluids are key to magmatism, metamorphism, element transfer, and seismicity. Based on depth, they are divided into deep (>80 km) and shallow (<80 km) fluids with distinct salinities, elements, and volatile contents. Deep Na-Al-rich fluids are inferred from metamorphic rocks like jadeitite, which often contain methane in fluid inclusions. Na originates from dehydration of altered oceanic crust/sediments or from Na-rich protoliths like plagiogranites. Methane is generated via abiogenic and thermogenic processes (carbonate reaction, Fischer-Tropsch, organic decomposition). However, the genetic link between Na-rich fluids and methane, especially at shallow depths (<80 km), remains unclear.

We report primary methane-water inclusions in jadeitite from Central Kazakhstan. Two-phase inclusions (3 – 20 μm) yield homogenization temperatures of 195 – 270 °C, salinities of 4.96 – 10.49 eq mass% NaCl, and estimated formation pressures of ~0.5 – 1.0 GPa (corresponding depths of ~16 – 33 km). $\delta^{13}C_{CH_4}$ (– 27.6‰ to – 31.0‰) and δD_{CH_4} (– 238‰ to – 205‰) of methane within the inclusions indicate a thermogenic origin, while δD_{H_2O} (– 134.8‰ to – 113.9‰) of water is the lowest reported in jadeitites. suggesting a mixture of dehydrated subduction fluids and meteoric water.

Globally, methane-bearing fluid inclusions in jadeitites have been documented under blueschist- to eclogite-facies conditions at depths of ~16 – 90 km (Myanmar, Guatemala, Japan, Dominican Republic, Polar Urals, Italy, Cuba). These fluids are consistently Na-rich, with salinities mostly above seawater (3 – 10 eq mass% NaCl). We found that the isotopic signatures vary with depths: shallow (<50 km) methane shows $\delta^{13}C$ of −50‰ to −30‰ and δD of −265‰ to −120‰, typical of thermogenic organic decomposition; with increasing depth (>50 km), $\delta^{13}C$ rises (> −30‰) and δD becomes more variable, reflecting carbonate dissolution or Fischer-Tropsch reactions. Importantly, CH_4-bearing fluids are not restricted to jadeitite. They occur widely in HP-UHP rocks down to ~120 km, including eclogite (West Tianshan), plagioclase-bearing mantle rocks (Germany), meta-peridotites, mafic cumulates, ophicarbonates, amphibolites, and marbles. In cold subduction zones, reducing conditions (below FMQ buffer, <400 °C) stabilize CH_4 over CO_2, making methane a major deep carbon carrier. The co-occurrence of Na-rich and CH_4-bearing fluids is particularly common at shallow to intermediate depths (<80 km), where dehydration of altered oceanic crust supplies Na, and

thermogenic or abiogenic reactions produce CH_4. Meteoric water infiltration, as recorded in Kazakhstan, could indicate that surficial fluids can penetrate shallow subduction interfaces and mix with slab-derived fluids. These findings have major implications for carbon transport and redox evolution along subduction zones. Gemologically, these findings provide implications on the quality assessment of jadeite jades: Coarse, loose textures of Kazakhstan jadeitite reflect its low P–T formation (coolest yet reported) and stress conditions, contrasting with high-quality jadeite jades from Myanmar/Guatemala formed under higher P–T conditions and strain.

Key words jadeitite, retrograde metamorphism, subduction zone, fluid-rock interaction, gemological quality

ISOCHEMICAL METAMORPHISM GENESIS OF THE NEWLY DISCOVERED BAQING JADEITOID AND BLUESCHIST, EASTERN-CENTRAL TIBET, CHINA

Xin Jin[1], Tatsuki Tsujimori[2], Donna L. Whitney[3], Yu-Xiu Zhang[4], Kai-Jun Zhang[4]

1. Research Institute for Intelligent Earth Systems, Marine Science and Technology College, Zhejiang Ocean University, Zhoushan 316022, China

2. Center for North East Asian Studies, Tohoku University, Sendai 980-8576, Japan

3. Department of Earth and Environmental Sciences, University of Minnesota, Minneapolis, Minnesota 55455, USA

4. College of Earth and Planetary Sciences, University of Chinese Academy of Sciences, 19A Yuquan Road, Beijing 100049, China

Abstract The formation of most jadeitites and jadeite-rich rocks is attributed to precipitation (P-type) and metasomatism (R-type) driven by infiltration of external Na-Al-Si-rich aqueous fluids, which compositionally resemble subduction-derived fluids. In contrast, the existence of isochemical metamorphic jadeite-rich rocks—formed by internally generated fluids within subducted slabs—remains debated. To address this, we propose the term "I-type" for isochemical metamorphic genesis, and introduce "jadeitoid" as a collective term for metamorphic rocks containing 50–100 vol% jadeite, to enhance clarity and avoid ambiguity. I-type jadeitoids exhibit a subducted-plate affinity and record prograde metamorphism similar to that of eclogite. This contrasts with P- and R-type jadeitoids, which are typically hosted in serpentinite from the mantle wedge: P-type lacks a prograde history, while R-type shows a prograde evolution that is often obscured by high-variance jadeite-dominated assemblages and fluid alteration.

The newly discovered Baqing jadeitoid and blueschist (eastern-central Tibet) are enclosed in quartzo-feldspathic schist. Their peak assemblages are garnet + jadeite/omphacite + phengite/paragonite + rutile + quartz (jadeitoid) and garnet + glaucophane + phengite/paragonite + rutile + quartz (blueschist). Using pseudosections, Zr-in-rutile thermometry, and conventional geothermobarometers, we constrain their metamorphic evolution. Both rocks record a clockwise P–T path, from early conditions of 5–7 kbar / 350–440 °C, to peak conditions of either 27–29 kbar / 730–760 °C or 20–23 kbar / 670–710 °C, and finally to retrograde conditions of 6–7 kbar / 530–600 °C. This path mirrors that of Baqing eclogite, indicating a shared subduction-to-exhumation history. Furthermore, the jadeitoid and blueschist showsimilar major-element (Na-Al-Si enrichment) and trace-element compositions to greywacke and plagiogranite. We therefore propose an I-type origin for the Baqing jadeitoid and its preformed rocks–blueschist.

Key words jadeitite, jadeitoid, blueschist, isochemical metamorphism, protolith

Acknowledgements This study was financially supported by the Deep Earth Probe and Mineral Resources Exploration-National Science and Technology Major Project (grants

2025ZD1005100), the National Natural Science Foundation of China (grants 41472209, 40802048, and 42002218), the Strategic Priority Research Program of the Chinese Academy of Sciences (grants XDA22050103 and XDB42020303), and the College of Science and Engineering (funding for work done at the University of Minnesota).

JADEITITES AS ARCHIVES OF SUBDUCTION-ZONE FLUIDS AND BEYOND: PROGRESS AND PERSPECTIVES SINCE IMA 2010

Tatsuki Tsujimori[1], Yi-Xiang Chen[2]

1. Department of Earth Science, Graduate School of Sciece, Tohoku University, Japan

2. State Key Laboratory of Lithospheric and Environmental Coevolution, University of Science and Technology of China, Hefei 230026, China

Abstract Jadeitite is a rare jadeite-rich rock that commonly occurs as veins and blocks in serpentinite-matrix mélanges, together with eclogite, blueschist, and other high-pressure metasomatic rocks. Because jadeitite forms through intense fluid–rock interaction under high-pressure conditions, it provides a sensitive archive of aqueous fluids, chemical mass transfer, and metasomatic processes in subduction zones.

At IMA 2010, the first dedicated session on jadeitites, convened by G.E. Harlow, S.S. Sorensen, and T. Tsujimori, highlighted the importance of jadeitites as records of subduction-channel fluids and brought together studies from a limited number of well-documented occurrences worldwide; the state of knowledge at that time was later synthesized in a special issue of the *European Journal of Mineralogy* edited by Harlow et al. (2012). Since then, progress in jadeitite research has been driven not only by additional field studies, but more importantly by advances in analytical methods and conceptual frameworks. Integrated petrography, mineral chemistry, high-precision trace-element and isotope geochemistry, fluid-inclusion studies, geochronology, and thermodynamic and numerical modeling have refined our understanding of the timing, mechanisms, and geodynamic significance of jadeitite formation.

This introductory talk revisits the scientific themes raised at IMA 2010 and summarizes major developments over the past decade and a half. Particular emphasis is placed on jadeitites as records of focused fluid flow, changing fluid compositions, slab-derived components, serpentinite-mélange dynamics, and slab–mantle-wedge interaction. I will also outline key questions for future work: What are the sources and pathways of jadeitite-forming fluids? How do jadeitites record temporal changes in fluid composition during subduction and exhumation? How are jadeitites linked to high-pressure vein systems, eclogite and blueschist evolution, serpentinite rheology, and arc magmatism? This talk introduces the session by framing jadeitites as key archives of subduction-zone fluids and as a basis for discussing fluid-mediated mass transfer at convergent margins.

Key words jadeitite, jadeite, jadeitite research, subduction-channel fluids, jadeitite-forming fluids

LARGE-SCALE METAMORPHIC FLUID FLOW IN A CONTINENTAL SUBDUCTION CHANNEL RECORDED BY COESITE-BEARING JADEITE QUARTIZITES

Gao Xiao-Ying

School of Earth and Space Sciences, University of Science and Technology of China, Hefei, China

Abstract Metamorphic fluids generated by dehydration of subducting crust play a crucial role in transporting mass and energy along the slab-mantle interface within subduction channels. While fluid flow is widely considered significant in oceanic subduction systems, it has commonly been regarded as negligible in continental subduction channels. This conventional view is now challenged by an integrated study of whole-rock geochemistry, Mg-O-Ba isotopes, zircon U-Pb geochronology, and trace-elements analyses of coesite-bearing jadeite quartzites from the Dabie orogen, China. Although the studied samples were collected from disparate outcrops across an area of ~50 km^2, zircon U-Pb dating consistently yields discordiant arrays defined by congruent upper-intercept ages of 1.9–2.0 Ga and lower-intercept ages of 224–235 Ma. This results indicate a shared Paleoproterozoic protolith and uniform Triassic metamorphism for all jadeite quartzites. Oxygen isotope analysis of mineral separates and whole-rocks reveal variable $\delta^{18}O$ values ranging from 6.3‰to 9.4‰, suggesting incorporation of supracrustal components. Most samples exhibit variable $\delta^{26}Mg$ values from −0.16‰ to +0.61‰, significantly elevated relative to typical mantle values. Whole-rock Mg isotopic compositions display strong positive correlations with both MgO contents and Rb/La, Rb/Gd and Rb/Nb ratios, but a negative correlation with Na_2O contents. These observations imply that: (1) the mid-Paleoproterozoic protolith of the jadeite quartzites experienced weathering and subsequent deposition as sedimentary rocks along a passive continental margin; and (2) these rocks later underwent substantial metasomatism by metamorphic fluids characterized by high $\delta^{26}Mg$ signatures during Triassic continental subduction. We infer that these metamorphic fluids were liberated primarily through the breakdown of biotite in the metasedimentary rocks during their subduction to subarc depths for ultrahigh-pressure metamorphism. They would have acquired their geochemical compositions not only from the biotite breakdown but also through leaching reaction with the TTG provenance. In view of the spatial occurrences of the target samples, the metamorphic fluids would have flowed inside the continental subduction channel on a large scale. This is the first report of the large-scale fluid flow in the continentalsubduction zone and therefore demonstrates that fluid flow can be significant in continental subduction channels.

Key words Jadeite quartzite, continental subduction, metamorphic fluid, metasomatism

SOURCES AND EVOLUTION OF SUBDUCTION-ZONE FLUIDS AT FOREARC DEPTH: MULTI- ISOTOPE CONSTRAINTS FROM DOMINICAN JADEITITES AND RELATED ROCKS

*Kun Chen[1,2], Yi-Xiang Chen[1], Tatsuki Tsujimori[2], Hans-Peter Schertl[3,4], Hui-Min Yu[1], Naoko Takahashi[2], Walter V. Maresch[3], Sergei Skuzovatov[5], Fang Huang[1]

1. State Key Laboratory of Lithospheric and Environmental Coevolution, University of Science and Technology of China, Hefei 230026, China

2. Department of Earth Science, Tohoku University, Sendai, Miyagi 980-8578, Japan

3. Institute of Geosciences, Ruhr-University Bochum, 44780 Bochum, Germany

4. College of Earth Science and Engineering, Shandong University of Science and Technology, Qing- dao, 266590, China

5. Vinogradov Institute of Geochemistry SB RAS, 1A Favorsky Str., Irkutsk, 664033, Russia

Abstract Subduction-zone fluids control mass transfer and crust-mantle evolution, yet their detailed sources and the effects of fluid-rock interaction remain debated. Jadeitites in forearc ser- pentinite mélanges, formed either by direct precipitation from Na–Al–Si-rich fluids (P-type) or by metasomatic replacement of magmatic protoliths (R-type), serve as a unique archive of subduction- zone fluids. We present high-precision radiogenic Sr–Nd and stable O–Si–Mg–Fe isotopic data for jadeitites and related jadeite-rich rocks from the Rio San Juan Complex (RSJC), Dominican Re- public. P-type jadeitites display low $(87Sr/86 Sr)_i$ values (0.70346–0.70505), high εNd(t) values (4.6– 6.8), and low $\delta^{18}O$ of the forming fluids (4.7‰–6.4‰), indicating a primary contribution from altered oceanic crust (AOC) rather than subducted sediments. Si isotope compositions show that both P-type and R-type jadeitites have relatively high $\delta^{30}Si$ values (−0.20‰ to 0.25‰), significantly above the igneous array. Combining Rayleigh distillation and binary mixing simulations, we pro- pose that fluids derived from altered oceanic crust progressively obtained high $\delta^{30}Si$ values after crystallization of minerals enriched in light Si isotopes (e.g., omphacite and epidote). RSJC jade- itites exhibit low $\delta^{26}Mg$ values (−0.92‰ to −0. 16‰) that lack correlations with carbonate indicators (CaO/Al_2O_3, CaO/TiO_2, and Sr/Nd), precluding a significant carbonate contribution. Instead, the coupling of light Mg isotopes with MgO–Ni–Cr enrichment indicates a substantial contribution from serpentinizing fluids. In contrast to the light Fe isotope signatures of Myanmar jadeitites, Dominican jadeitites display relatively high $\delta^{56}Fe$ values (−0.08‰ to 0.29‰). Systematic covaria- tions between $\delta^{56}Fe$ values, TFe_2O_3 contents and redox-sensitive proxies ($Fe^{3+}/\Sigma Fe$, V/Sc, U/Th, Ce anomalies, and Sb/As) indicate that Fe isotope heterogeneity is primarily controlled by the fluid redox state. By integrating petrological and geochemical constraints, we propose that forearc serpentinization acts as a critical redox filter governing the coupled Mg–Fe isotope heterogeneity of jadeitites. Olivine-dominated serpentinization generates reducing conditions that promote light Fe isotope fractionation, as recorded by Myanmar jadeitites, whereas orthopyroxene-involved

ser- pentinization buffers the system under relatively oxidizing conditions, preserving heavier Fe iso- topic signatures in RSJC jadeitites. Overall, the Dominican jadeitites demonstrate that the subduc- tion-zone fluids are primarily sourced from altered oceanic crust with an additional contribution from serpentinizing fluids, and that fractional crystallization coupled with serpentinization-related redox buffering jointly governs the evolution of Si, Mg, and Fe isotopes. These fluids either directly precipitate P-type jadeitites or metasomatize igneous protoliths to form R-type jadeitites. The sub- duction and melting of jadeitites may transfer light Mg and distinct Fe isotopic signatures to the mantle wedge and related arc magmas.

Key words Jadeitite, subduction-zone fluids, serpentinization, multi-isotope system, mantle heter- ogeneity

SUBDUCTION ZONE FLUID-ROCK INTERACTION REVEALED BY FE-O ISOTOPES IN UHP JADEITE QUARTZITE FROM THE DORA MAIRA MASSIF, WESTERN ALPS

Jia-Wei Xiong[1], Yi-Xiang Chen[2]

1. Department of Ocean System Sciences, Laoshan Laboratory, China

2. School of Earth and Space Sciences, University of Science and Technology of China, China

Abstract In addition to jadeitite *sensu stricto* associated with serpentinite in oceanic subduction channels, jadeite-bearing quartz-rich rocks of continental affinity have also been recognized as valuable recorders for activities of subduction zone fluid. A representative example is the coesite-bearing jadeite quartzite from the Dora-Maira Massif, Western Alps, where jadeite-rich quartzite bands occur within Mg-rich whiteschist blocks enclosed by metagranitoids. Previous studies have shown that the whiteschists were produced by fluid-metasomatism related to dehydration of serpentinite, which was most likely linked to fluids introduced during earlier stages of oceanic subduction.

In-situ zircon U–Pb ages and oxygen isotope compositions of relict magmatic domains demonstrate that the jadeite quartzite, whiteschist, and host metagranitoid all share a common Permian granitic protolith. Metamorphic zircon rims from these lithologies record synchronous ultrahigh-pressure metamorphism at ca. 35 Ma, indicating that they participated in the same Alpine UHP event. However, both whiteschist and jadeite quartzite show distinctly lower $\delta^{18}O$ values (~6–7‰) than the relatively unmetasomatized metagranitoid (~10‰), pointing to substantial fluid-mediated modification during subduction. An additional and independent line of evidence is provided by whole-rock Fe isotopes; $\delta^{56}Fe$ values of jadeite quartzite are significantly higher than those of the unmetasomatized metagranitoid (0.69–0.87‰ vs. 0.18–0.38‰) and overlap with the high-$\delta^{56}Fe$ whiteschist (0.32–1.03‰). Because prograde metamorphism alone would not be expected to produce such large Fe isotopic fractionation, as also indictaed by the normal $\delta^{56}Fe$ values of the metagranitoid, these data confirm that jadeite quartzite was not produced by simple closed-system UHP metamorphism of the granitic protolith, but instead records externally mediated mass transfer.

Importantly, jadeite quartzite is chemically distinct from the enclosing whiteschist. Whereas the whiteschist is characterized by extreme Mg enrichment coupled with strong depletion in Na and Ca, the jadeite quartzite is marked by strong depletion in K and other LILE, while Na and Ca are comparatively retained. This contrast indicates that the two metasomatized lithologies did not form through the same fluid-rock interaction process. In line with previous geochemical and fluid-inclusion studies, we propose a two-stage fluid history for these jadeite-bearing rocks in the continental subduction channel. In the first

stage, Mg-rich fluids infiltrated granitic protoliths along structural pathways and formed whiteschist. In the second stage, a later UHP fluid, likely generated during continued evolution of previous metasomatized rocks, infiltrated adjacent granitic precursor domains. These fluids were characterized by Si–Al-rich compositions with variable Mg, Fe, Na, and Ca, promoting phengite breakdown and the development of jadeite-rich assemblages.

The coupled Fe–O isotope signatures clearly demonstrate that coesite-bearing jadeite quartzite records fluid-mediated mass transfer in a continental subduction environment.Our results show that jadeite-rich rocks in continental UHP terranes, although distinct from classical jadeitites in serpentinite mélanges, can likewise provide robust geochemical constraints on subduction-channel fluid compositions and multistage fluid-rock interaction.

Key words Jadeite quartzite, Subduction zone, Fluid-rock interaction, Fe isotopes, Serpentinite

RETROGRADE METAMORPHISM RECORDED BY THE MINERAL ASSEMBLAGE OF GUATEMALAN JADEITITE

Guanghai Shi[1], Biqian Xing[1,2], Jiabao Wen[1], Jiayi Lun[1]

1. State Key Laboratory of Geological Processes and Mineral Resources, China University of Geosciences, Beijing 100083, China

2. China National Academy of Educational Sciences, Beijing 100088, China

Abstract Retrograde metamorphism is the process which high-temperature/pressure mineral assemblages would react or decomposite into low-temperature reactant minerals during cooling and exhumation. Research indicates that external fluid influx might be involved into the retrograde metamorphism, often accompanied by significant fluid-rock interaction. In subduction zone settings, retrograde metamorphism typically occurs and characterized by a decompression and cooling P-T path during the exhumation.

Jadeitites and related rocks hosted within serpentinite mélanges on both sides of the Motagua Fault Zone in Guatemala serve as ideal samples for studying the late-stage retrograde processes of subduction zones. The translucent to transparent jadeitite samples contain white to grayish-white lumpy and flocculent albite. This albite is randomly distributed with varied shapes, and some lumpy aggregates even look like “sea urchins”. Different jadeitite may have varying ratio of such albite, reflecting certain degree of retrograde metamorphism. Microscopically, some albites exhibit metasomatic replacement along the cleavage planes and margins of jadeite, showing that retrogression might have fluid influx.

In the jadeitites of the Motagua Fault Zone in Guatemala, alteration and recrystallization of the existed mineral assemblages occurred and a series of mineral assemblages appeared at relatively lower pressure–temperature conditions. The mineral assemblages may include analcime, albite, amphibole, (clino)zoisite, paragonite. Jadeitites could even undergo extensive albitization and evolve into albitite. The coexistence of albite + analcime and albite + nepheline indicates fluid participation and rock decomposition. These reactions involve significant chemical element migration, with fluids transporting elements such as Ca, Ba, Sr, and REE, forming characteristic minerals like apatite, titanite, muscovite and banalsite. The termination of retrogression is marked by the crystallization of late-stage veins and the stabilization of greenschist-facies mineral assemblages.

Retrograde metamorphism might significantly influence quality of jadeite jade (Feicui). Two major Feicui deposits from Myanmar and Guatemala formed in intra-oceanic subduction settings. The Sagaing strike-slip fault into the Himalayan Syntaxis resulted in a significantly rapid exhumation relative to that the Motagua fault between the North American and Caribbean plates in Guatemala. During rapid uplift, the high-pressure mineral remained in a thermodynamically metastable state for an extended period,

preventing complete phase transitions. However, during slower exhumation it might facilitate widespread retrograde metamorphism, extensively forming retrograde minerals such as albite with flocculent and patchy distributions. Consequently, its transparency and overall quality of jade from this locality would diminish. On the other hand, as newly phase with lower relative gravity grow, which might compress the host pyroxene mineral more tightly, the later might be more compact and tougher.

Key words jadeitite, retrograde metamorphism, subduction zone, Guatemala

COUPLED DISSOLUTION AND DEHYDRATION REACTIONS OF TALC IN SUBDUCTION-ZONE FLUIDS: IMPLICATIONS FOR SLAB-MANTLE WEDGE DECOUPLING DEPTH

Nanfei Cheng[1,*], I-Ming Chou[2], Zhenhao Duan[2], Zhou Gui[3], Haiyan Zhang[2], Hao Yan[2], Jianhui Sun[2]

1. State Key Laboratory of Deep-Sea Science and Intelligent Technology, Institute of Deep-sea Science and Engineering, Chinese Academy of Sciences, Sanya, Hainan 572000, China
2. Department of Experimental Study under Deep-sea Extreme Conditions, Institute of Deep-sea Science and Engineering, Chinese Academy of Sciences, Sanya, Hainan 572000, China
3. Key Laboratory of Ocean Observation and Forecasting, Institute of Oceanology, Chinese Academy of Sciences, Qingdao, Shandong 266000, China

Abstract Talc, a hydrous Mg-silicate and the softest mineral, plays a dual role in subduction zones: it transports water into Earth's interior and lubricates the slab-mantle wedge interface. Its stability influences subduction geodynamics and thermal structure as well as metasomatism and partial melting of the mantle wedge, which has received extensive experimental attention. However, most experimental studies have focused on water-poor, quartz-saturated (high-silica) conditions, despite evidence that external fluid infiltration and the coexistence of silica-poor phases (e.g., antigorite and olivine) can suppress silica activity. To address this gap, this study focused on the dehydration behavior of talc under water-rich and thus low-silica conditions (up to 800 ℃ and 33.8 kbar), supported by two comparative experiments under relatively high-silica conditions (up to 850 ℃ and 19.8 kbar) and a preliminary examination of enstatite dissolution, and the experimental results were interpreted in light of those from thermodynamic calculations. The combined usage of hydrothermal diamond anvil cell and Raman spectroscopy ensures real-time observations and analyses. Previous studies have shown that under the quartz-saturated conditions at 10–30 kbar, talc undergoes dehydration at approximately 800 °C via the reaction: talc → enstatite + quartz/coesite + H_2O. In contrast, our experimental results demonstrate that in a water-rich and low-silica environment at ~10 kbar, talc undergoes a coupled dissolution and dehydration reaction at significantly lower temperatures (~705 °C): talc → forsterite + silica-bearing aqueous fluid, with silicon preferentially dissolved into the fluid phase while magnesium is retained in forsterite. At ~30 kbar, the decomposition temperature drops to ~650 °C, approximately 170 °C lower than that under silica-saturated conditions. This indicates that low-silica conditions markedly reduce the dehydration temperatures of talc, an effect amplified by pressure through enhanced silicate solubility in aqueous fluids. Critically, this shift implies talc dehydration may occur at ~80 km depth in both cold (e.g., Mariana) and hot (e.g., Cascadia) subduction zones, coinciding with the maximum depth of decoupling (MDD) between slab and mantle wedge. These results demonstrate that fluid composition, not merely

pressure and temperature conditions, affect hydrous mineral stability, with direct implications for deep water cycling, fluid-mediated element transport, and the rheological and thermal evolution of subduction zones.

Key words subduction zone, talc dehydration, fluid-rock interaction, slab–mantle decoupling, hydrothermal diamond anvil cell

Acknowledgements We appreciate Prof. David Jenkins (SUNY Binghamton) for his comments on the work and Prof. Ikuko Wada (UMN) for providing thermal models of subduction zones. We also thank Dr. Yibing Li (ZJOU) for discussions on pyDEW and Haiyan Sun (IDSSE) for XRD analysis assistance. This research was funded by the Deep Earth Probe and Mineral Resources Exploration – National Science and Technology Major Project (2025ZD1005100), the National Natural Science Foundation of China (42130109, 42102056), and the Nanhai New Star Project (NHXXRCXM202337).

EXPERIMENTAL CONSTRAINS ON TRACE ELEMENT PARTITIONING BETWEEN MOBILE PHASES AND CARBONATED METASEDIMENTS DURING SLAB DEVOLATILIZATION

Marija Putak Juriček[1], Andreas Audétat[2], Hans Keppler[2], Jason Kirk[1], Ananya Mallik[1]

1. Geosciences Department, University of Arizona, USA

2. Bayerisches Geoinstitut (BGI), University of Bayreuth, Germany

Abstract Isotopic and elemental signatures in arc magmas bear similarities to the marine sediments from the forearc, which has been used to infer ubiquitous sediment melting along the slab-mantle wedge interface, whereas aqueous fluids were deemed too inefficient at mobilizing trace elements to account for arc magma compositions. While most primitive arc melts have elevated $^{206,207,208}Pb/^{204}Pb$ and lower $^{143}Nd/^{144}Nd$ compared to MORB, reflecting a sediment component in the melt source, this is in contrast to their low $^{87}Sr/^{86}Sr$ that almost always plot below the range of pelagic sediments. Such isotope decoupling is difficult to explain by models that assume sediment melts are the predominant mobile phase in subduction zones. However, most experimental studies on trace element partitioning between subducted sediments and mobile phases were performed in chlorine- and CO_2-free systems, even though it is expected that trace element solubility in aqueous fluids may be enhanced by the formation of chloride complexes, while the residual carbonates could preferentially retain Sr in the slab during mobile phase extraction. We performed several series of piston cylinder experiments at 2–4.5 GPa and 500–1200°C in the sediment-H_2O-NaCl, $CaCO_3$-H_2O-NaCl and sediment-H_2O-CO_2 systems to investigate trace element partitioning between residual and mobile phases (fluids and alkaline silicate melts) during sediment subduction. Trace element compositions of silicate melts and residual phases were obtained by LA-ICP-MS. Different strategies were employed to analyze aqueous fluids. The fluids from experiments in the sediment-H_2O-NaCl system were separated using the diamond trap metod and analyzed in frozen state. The captured fluids (along with quench precipitates) from the $CaCO_3$-H_2O-NaCl system were analyzed in solution. We combined our partitioning data with published literature to demonstrate that saline fluids and sediment melts have a comparable efficiency in extracting incompatible elements from subducted sediments, producing similar element fractionation during mobile phase expulsion.The Sr, Pb and Nd isotopic signatures of arc magma suggest that the mantle wedge is infiltrated by mobile phases derived from both the sediment and basalt sections of the subducted oceanic crust. Several percent of either sediment-derived saline fluid or melt can account for the isotopic and elemental compositions of most arc magma. Geochemical similarities between arc magma and forearc sediments are not necessarily evidence of slab melting.

Key words subduction, sediments, trace elements

EXPERIMENTAL CONSTRAINTS ON CARBON SEQUESTRATION IN THE MANTLE WEDGE

Guoji Wu[1,2,3], Yongsheng Huang[1,2*]

1. State Key Laboratory of Deep Earth Processes and Resources, Guangzhou Institute of Geochemistry, Chinese Academy of Sciences, Guangzhou 510640, China

2. CAS Center for Excellence in Deep Earth Science, Guangzhou 510640, China

3. College of Earth and Planetary Sciences, University of the Chinese Academy of Sciences, Beijing 100049, China

Abstract Subduction zones play a crucial role in regulating the global carbon (C) cycle. Recent geochemical and geophysical findings have revealed widespread carbonation of mantle rocks, including serpentinite and olivine, within mantle wedges, indicating the existence of a potentially vast C reservoir. Nevertheless, the quantitative assessment of C inventory resulting from the carbonation of mantle rocks in multicomponent subduction fluids remains poorly understood. In this study, we investigated serpentinite and olivinite carbonations in H_2O–CO_2–NaCl fluids under various pressure-temperature conditions mimicking those in the mantle wedge. Our results indicate that the carbonation reaction extent increases with rising pressure-temperature and CO_2 concentration in fluids, but decreases with increasing salinity, especially at low levels (< 10 wt%). This decrease is due to reduced fluid pH, decreased CO_2 and H_2O activities, and increased magnesite solubility in salt-bearing fluids. Based on previous and our data, we derived an empirical equation to describe the carbonation reaction extent in these fluids. In this study, we employed van Keken (2011) subduction dehydration model. Subsequently, we utilized Lan (2023) and Li (2022) carbonate solubility models respectively to calculate the decarbonation amounts at various depths for each subduction zone. Then, by integrating our fitted empirical formula for C precipitation, we computed the C precipitation capacity of every global subduction zone. Our calculation results indicate that the C precipitation in global mantle wedges ranges from 1.53 - 1.60 million tons of C per year (by Li) and 2.68 - 2.74 million tons of C per year (by Lan). The C precipitation efficiency in mantle wedges exhibits significant variations across different subduction zones, particularly between cold and warm subduction zones. In warm subduction zones, the C precipitation capacity is less than 30%, with the lowest values dropping below 10%. In contrast, cold subduction zones generally show a C precipitation capacity exceeding 40%, and in some cases, it can even approach 90%. Warm subduction zones experience earlier dehydration, but under relatively low temperature and pressure conditions, the carbonation reaction degree of olivine is not high, making it difficult to sequester a large amount of C. Consequently, mantle wedges in cold subduction zones emerge as ideal sites for C precipitation. Some of this stored C may remain in cold, stagnant regions of the wedge, potentially contributing to long-term C storage and seismic activity.

Additionally, processes like down-dragging and subduction erosion can transport C to partial melting regions, leading to volcanic emissions in arc regions. This study provides valuable insights into the C cycle and seismic responses within subduction zones.

Key words Carbonation, Subduction, C cycle.

FLUID-FLUXED MÉLANGE MELTING TO FORM ARC MAGMA CONSTRAINED BY MULTIPLE STABLE ISOTOPE SYSTEMATICS

Yi-Xiang Chen, Xin-Yue Qiao

School of Earth and Space Sciences, University of Science and Technology of China, Hefei 230026, China

Abstract Arc magma records key information of mass recycling and crust-mantle interaction in subduction zones. However, the detailed formation process and slab component contributed to arc magma source are highly debated. For the slab component, aqueous fluids, hydrous melts, or some form of solids (sediment vs. sepentinite) are proposed based on different aspects of geochemical compositions. For the transport mechanism, it is suggested that arc magmas are formed either by fluid-fluxed melting of mantle wedge or by mélange melting. Currently, the above debates need to be further constrained by integrated novel geochemical tracers like Mg-B-Ba isotopes. Mg, as a major element in mantle, whose isotopic composition is insensitive to fluid addition, but rather sensitive to addition of serpentinites. In contrast, B and Ba, as trace elements in mantle, whose isotopes are highly sensitive to addition of various kinds of fluids. Integrated such isotope systematics can give unique insights into the formation mechanism of arc magmas. In this talk, I will introduce our recent work on Mg-B-Ba isotope studies of some typical arc magmas, including those from the South Sandwich arc and Izu arc. We show that these arc magmas show elevated Mg and B isotope compositions, which require a component of heavy Mg-B isotopes with high Mg-B contents, the most likely candidate is serpentinite. In addition, Ba isotopes show the contribution of slab-derived aqueous fluids. Taken together, both slab-derived aqueous fluids and serpentinite-dominated mélange are essential to form some typical arc magmas. Consequently, a new model, i.e., fluid-fluxed mélange melting, is proposed for arc magma formation.

Key words Arc magma, mélange melting, crust-manlte interaction, mass recycling, fluid mobility

FLUID-ROCK INTERACTION AND DEEP CARBON CYCLING IN THE FOREARC MANTLE: INSIGHTS FROM NUMERICAL MODELS

Ryosuke Oyanagi

Graduate School of Environmental Studies, Tohoku University, Japan

Abstract The geological carbon cycle, in which subduction zones are a key component, regulates the habitability of Earth. The forearc mantle, primarily composed of peridotite, represents a significant potential reservoir for carbon sequestration as carbonate minerals through reactions with fluids released from subducting slabs. These slab-derived fluids transport aqueous carbon and interact with the overlying mantle wedge, potentially promoting carbonation reactions that stabilize carbon over geological timescales.However, the extent of carbonation and the role of the forearc mantle in the deep carbon cycle remain largely unclear. In this study, we utilize numerical modeling to predict fluid characteristics (chemical composition and flux) and mineral assemblages at the subduction interface across depths from ~20 km to ~80 km. We accounted for variations in subducting sediments and the thermal structures of a typical cold subduction zone (NE Japan) and a warm subduction zone (SW Japan).The calculations demonstrate that the amount and composition of fluids generated in these two subduction zones differ significantly, leading to distinct types and quantities of altered minerals in the forearc mantle at the subduction interface. In the forearc mantle of NE Japan, carbonate minerals do not form, and talc appears only at a depth of about 70 km. In contrast, in SW Japan, both talc and magnesite are produced over a wide depth range (35–70 km); the abundance of these minerals increases from 40 km, with thicker layers existing at greater depths. These modeling results suggest that carbonation of the forearc mantle reduces the carbon flux into the deep mantle. In this presentation, we provide additional constraints from numerical modeling and discuss the extent of carbonation and the role of the forearc mantle in the deep carbon cycle of modern subduction zones.

Key words Forearc mantle, Serpentinization, Carbonation, Deep carbon cycle

OSCILLATORY ZONING IN LOW-TEMPERATURE ECLOGITIC GARNET REVISITED: FINGERPRINTS OF OPEN- AND CLOSED-SYSTEM REACTIONS

Ryo Fukushima[1,2], Tatsuki Tsujimori[2], Jesse B. Walters[3,4,5], Dominik C. Hezel[4,5], Richard Albert[4,5], Axel Gerdes[4,5], Horst R. Marschall[4,5]

1. Kochi Institute for Core Sample Research, JAMSTEC, Japan
2. Graduate School of Science, Tohoku University, Japan
3. NAWI Graz Geocenter, University of Graz, Austria
4. Department of Geosciences, Goethe-University Frankfurt, Germany
5. Frankfurt Isotope and Element Research Center (FIERCE), Goethe-University Frankfurt, Germany

Abstract Low-temperature (*T*) eclogite (a.k.a. Group-C eclogite), which occurs in Phanerozoic high-pressure/ultrahigh-pressure (H*P*/UH*P*) metamorphic complexes, preserves records of fluid-rock interaction at forearc- to subarc-depth conditions. Prograde-zoned garnet rimmed by oscillatory-zoned garnet is common, but the mechanisms of these compositional oscillations are controversial. One possibility is that oscillatory-zoned garnet rims are produced by metasomatic (open-system) reactions due to fluid infiltration. Alternatively, metamorphic (closed-system) reactions driven by *P–T* fluctuation have also been proposed. Here we petrographically characterize Guatemalan eclogite samples (lawsonite-eclogite facies metabasalt) to unravel mechanisms of zoned garnet formation. Garnet porphyroblasts in the sample are characterized by metasomatic rims (~200 μm in width) with compositional oscillations in major elements (Mg, Ca, Mn, Fe). The Mn-oscillation profile——a sensitive measure of Mn budget around the growing/dissolving garnet rim——consists of: (1) an inner rim comprising two major annuli, and (2) an outer rim with a mostly flat profile followed by an enrichment at the grain edge. Some garnet porphyroblasts contain multiphase solid inclusions that indicate the titanite-to-rutile transition, a potential source of heavy rare earth elements (HREEs), but they are clearly enclosed in garnet mantles. HREE profiles in the representative garnet show positive correlations with Mn-concentrations at the inner rim, but are decoupled within the outer rim. In addition, Ga, Ba and Rb concentrations increase rimward within the outer rim (Ga: 3 to 15 μg/g; Ba: 0 to 50 μg/g; Rb: 0 to 3 μg/g). Taken together, we interpret that the inner rim was formed by repeated cycles of dissolution and regrowth of garnet in a semi closed-system, whereas the outer rim precipitated from a solute-bearing aqueous fluid. We show that open- or closed-system reactions can be distinguished using detailed in situ measurements of the major- and trace-element profiles.

Key words metasomatism, oscillatory zoning, garnet, low-temperature eclogite, Guatemala

PETROLOGY AND THERMODYNAMIC MODELLING REVEAL AN IMPORTANT SOURCE OF ABIOTIC H_2 AND CH_4 DRIVEN BY SLAB REHYDRATION

Zeng-Li Guo[1,2], Ren-Biao Tao[2†], Jesse B. Walters[3], Vincenzo Stagno[4], Ning Qi[5], Chao Wang[1], Li-Fei Zhang[1†]

1. School of Earth and Space Sciences, Peking University, China

2. Center for High Pressure Science and Technology Advanced Research (HPSTAR), China

3. NAWI Graz Geocenter, University of Graz, Austria

4. Department of Earth Sciences, Sapienza University of Rome, Italy

5. State Key Laboratory of Shale Oil and Gas Enrichment Mechanisms and Efficient Development, SINOPEC, China

Abstract The origin and flux of geologically sourced abiotic hydrogen (H_2) and methane (CH_4) in Earth's crusts are fundamental to understanding deep carbon and hydrogen cycles, the formation of deep energy resources, and the potential to sustain subsurface biospheres. While forearc serpentinization has long been considered the dominant abiotic hydrocarbon source in subduction zones, our study reveals a distinct and previously overlooked pathway: intraslab fluid–reactive transport at much greater depths. We investigated abundant CH_4–H_2-bearing fluid inclusions in carbonated eclogites from the Southwestern Tianshan paleo-subduction zone using high-resolution 3D Raman imaging. Thermodynamic and numerical modeling indicate that oxidized altered oceanic crust may be insufficiently reduced to generate CH_4–H_2-rich fluids. Alternatively, our modeling results reveal that enhanced hydration of subducting fresh oceanic crust can markedly lower oxygen fugacity, generating abundant abiotic CH_4 and even H_2 in metamorphic fluids. Prograde deserpentinization fluids thus migrate upward and react with relatively unaltered oceanic crust, providing a significant and persistent source of CH_4–H_2-bearing fluids, particularly in cold subduction zones. Given the substantial fluid fluxes from deserpentinization and associated carbon mobilization, we estimate that intraslab fluid transport has the potential to generate CH_4–H_2 fluxes comparable in magnitude to those produced by ridge-spreading hydrothermal alteration and deep serpentinization. This process may significantly modify the redox gradient in subduction zones, thereby contributing to the accumulation of abiotic crustal energy sources and influencing shallow biosphere ecosystems.

Key words Subduction zones, Fluid–rock interactions, Abiotic hydrocarbons

Acknowledgements This research was supported by the National Key Research and Development Program of China (2019YFA0708501) and the National Natural Science Foundation of China

(42150104, U25A202984).

AN OCCURRENCE OF THE YTTRIUM-VANADATE WAKEFIELDITE IN AN EPIDOTE AMPHIBOLITE OF THE HOROKANAI UNIT KAMUIKOTAN METAMORPHIC BELT, CENTRAL HOKKAIDO, JAPAN

Kosuke Naemura[1], Taro Kato[1] , and Toru Takeshita[2]

1. Faculty of Education, Iwate University, Japan (Department/School, University, Country)

2. Pacific Consultants, Japan (Department/School, University, Country)

Abstract At the Horokanai area in the central Hokkaido of northern Japan, lawsonite-bearing blueschist facies metabasite terrane distributed that formed during late Cretaceous subduction at 100 Ma. Metamorphic grade increase near the contact with overlying ophiolitic mantle rocks, and lawsonite disappear near the contact zone III, which attributed prograde dehydration reaction. At zone III, exotic epidote amphibolite rocks that formed in a warm subduction at early Cretaceous 130 Ma, occurs as lenses in blueschist. One of such amphibolite lense contains wakefieldite-(Y). The amphibolite experienced polymetamorphism with initial low P/T condition in epidote amphibolite facies, followed by recrystallization under pumpellyite blueschist facies (250 ºC and 5 kbar), and experienced ductile shear deformation at (300 ºC) that produced pumpellyite-chlorite-actinolite-epidote assemblage. All the wakefieldite grains occur in association with pumpellyite blueschist facies metamorphic minerals. In particular, several minute wakefieldite occur as intergranular crystals in the albite vein as well as submicron crystals in fluid cavities associated with carbonate enclosed in albite, thought to have been deposited from hydrocarbonate fluids. The wakefieldites contain the high level of MREE in particular Dy and are relatively depleted in LREE. In detail, wakefieldite grains at the pull apart fractures display negative Ce anomaly while those as constituents in albite veins show positive Ce anomaly. Since Ce could replace Y site of the wakefieldite-Y (YVO_4), wakefieldite prefer Ce^{3+} relative to Ce^{4+} because the same charge and similar ionic radius. Therefore, the wakefieldite in the pull-apart zone was formed in a highly oxidizing environment dominated by Ce^{4+}, whereas that in the albite vein may have formed in a slightly reducing environment. If the wakefieldite-forming fluids caused hydrofracturing during rock decompression, it can be inferred that the Albite vein formed in an early stage of hydrofracturing in a relatively reducing environment, while the wakefieldite in pull-apart fratures formed in a more oxidizing environment as the fractures widened and connected to the surface.

Key words wakefieldite, blueschist facies metamorphism, amphibolite, Kamuikotan metamorphism

A RAMAN STUDY OF MINERAL INCLUSIONS IN MEROVINGIAN GARNETS

Frédéric Hatert[1], Nelly Kieffer[1], Cédric Malherbe[2], Britt Claes[3], Femke Lippok[3], Line Van Wersch[4] and Grégoire Chêne[4]

1. Laboratory of Mineralogy, University of Liège B18, B-4000 Liège, Belgium
2. Mass Spectrometry Laboratory, Chemistry Department, University of Liège, B-4000 Liège, Belgium
3. Royal Museums of Art and History, Brussels, Belgium
4. European Center for Archaeometry, University of Liège B15, B-4000 Liège, Belgium

Abstract On the Merovingian jewellery, garnets are extremely popular. They offer the advantage of having chemical compositions characteristic of their provenance, as shown by the publications of Calligaro and co-workers. According to these authors, in the entire Merovingian world, garnets have the same origins: India and/or Rhajastan, Ceylan, and possibly Bohemia. For the current territory of Belgium, between 2002 and 2007, François Mathis and Olivier Vrielyncks analyzed more than 805 garnets decorating 116 objects originating from 10 sites. They came to preliminary conclusion that the garnets found in Belgium were merely from India, with a late emergence of Bohemian garnets before the disappearance of this jewelry style.

In the framework of the Merojewel project, more analyses were performed on material from the Harmignies necropolis. In 2025, 14 jewels coming from 9 graves were analyzed by PIXE-PIGE at ULiège Laboratory. One of them was and earring and the 13 others were brooches going by pairs in three cases. Most of these objects can be situated before the 7th century. 107 points were measured on garnets and almost all the stones seem homogeneous and coming from Asia.

A very interesting feature of the garnets decorating Merovingian jewels is the presence of numerous inclusions, that can be constituted either by solid inclusions of minerals, or by fluid inclusions. In geology, the characterization of such inclusions is of crucial importance, since they are able to give accurate data on the geochemistry of the deposit, on the physico-chemical parameters occurring during the crystallization of the garnets (pressure, temperature), as well as on the composition of the fluid phase. A deep characterization of the inclusions found in the garnets from Harmignies therefore appeared as necessary.

Inclusions were first observed under the binocular microscope, in order to estimate their abundance, and to define the most interesting samples. A total of 13 jewels were examined, decorated by 117 garnets,

6 glass beads, 2 amber beads, 2 resin beads, and 2 metallic insets. Most garnets (92 %) showed inclusions, among which a majority of colorless (25 %) or black (19 %) inclusions, as well as rutile (19 %) or zircon and monazite (10 %). Some garnets showed large fractures (5 %), as well as rare orange, brownish or yellowish inclusions (6 %). Finally, spherical bubbles were observed in 5 % of the garnets; these bubbles appear to be linked with recent restorations with Epoxy resin.

In order to confirm the visual observations, analyses of the inclusions were conducted with a micro-Raman spectrometer (Labram300, 785 nm laser, Chemistry Department ULiège). The colorless inclusions appear to be constituted by apatite, quartz, or by fluid inclusions. The Raman spectra of apatites were characterized by a strong luminescence, produced by the Rare-Earth Elements (REEs) occurring as traces in this mineral. A detailed characterization of these spectral lines will allow us to determine those REEs, and consequently to obtain accurate data on the geochemistry of the deposit in which apatites crystallized. The black inclusions were generally identified as hematite or ilmenite, but some spectra also correspond to possible amphibole-group minerals such as richterite or pargasite. Rare dark lamellae were identified as phlogopite, and brownish grains showing a strong pleochroism under the binocular microscope correspond to staurolite.

A comparison of these mineral inclusions with those found in the Asian garnet deposits will now be conducted, and hopefully will give us new insights on the complex questions concerning the origin of these beautiful stones.

Key words mineral inclusions, garnets, Merovingian jewels, Raman spectroscopy

APPLYING GEOCHEMICAL LEAD ISOTOPE ANALYSIS FOR RECONSTRUCTING THE RAW MATERIAL PROVENANCE OF ARCHAEOLOGICAL OBJECTS

Sabine Klein[1,2,3], Katrin J. Westner[1], Thomas Rose[4], Tim Greifelt[1], Yiu-Kang Hsu[1], Annette Hornschuch[5], Helge Wiethoff[6]

1. Forschungsbereich Archäometallurgie, Leibniz-Forschungsmuseum für Georessourcen/Deutsches Bergbau-Museum Bochum, Bochum, Germany
2. Institut für Archäologische Wissenschaften, Ruhr-Universität Bochum, Bochum, Germany
3. Frankfurt Isotope & Element Research Centre (FIERCE), Goethe-Universität Frankfurt a.M., Germany
4. Massachusetts Institute of Technology, Department of Materials Science and Engineering, Cambridge, MA, United States
5. Forschungsbereich Montanarchäologie, Leibniz-Forschungsmuseum für Georessourcen/Deutsches Bergbau-Museum Bochum, Bochum, Germany
6. Rechenzentrum, Technische Hochschule Georg Agricola, Bochum, Germany

Abstract Lead isotope data are used in geochemistry to determine the geological age of rocks, minerals and ore-forming events. Due to its information potential, the geochemical method has been rapidly recognised as a practical tool for reconstructing the provenance of raw materials in non-ferrous metals and other materials in the archaeological sciences. It is now an established standard method in the archaeometric and archaeometallurgical disciplines. A comprehensive database of lead isotope values for ores and minerals worldwide is required to achieve meaningful results. Due to the interdisciplinary character of the applied method, the data are widely distributed and reported heterogeneously, hence often lacking comparable information and impending comparison. Given the large volume of data, the common lack of metadata, the highly dispersed reference data, and the need to compare results from reference data and objects, digital approaches are crucial. For a digital management of analytical data, efficient research data infrastructures are pivotal, but data infrastructures optimised for the archaeological sciences are currently missing. TerraLID aims to fill this gap for the lead isotope method. Key features of TerraLID are the FAIRification of lead isotope data of ores and its community-driven development. Currently under development, TerraLID is developing a universal metadata profile. It provides workflows for publishing data according to this metadata profile, and services to access the database, interact with the data, and carry out the most common visualisations and statistical tests. An additional project branch, ASTR, develops an interactive toolbox, an R package to improve the computational interoperability and reproducibility of scientific data in the archaeological sciences. TerraLID further develops open education resources about the lead isotope method.

Key words TerraLID, GlobaLID, lead isotopes, archaeology, metadata profile

Acknowledgements GlobaLID and ASTR are funded by the Deutsche Forschungsgemeinschaft (DFG), the German Science Foundation, project numbers 524790825 and 57120551. Acknowledged are the Core Team, the Regional Editors, and the Material Editors of GlobaLID/TerraLID (https://terralid.org/team.html), who dedicate substantial time and effort to contributing to the success of TerraLID, and all contributors to ASTR.

BEYOND THE NEAREST SOURCE: MULTI-PROXY PROVENANCE OF TURQUOISE AT XUEWEI TOMB NO. 1 ALONG THE SILK ROAD CORRIDOR, NORTHEASTERN TIBETAN PLATEAU (RESHUI, QINGHAI, CHINA)

Bahareh Shirdam[1,2]*, Mingxing Yang[1,2], Jianhua Han[3], Yue Yang[1,2], Yuwei Zheng[1,2], Wenlong Bai[4]

1. Gemmological Institute, China University of Geosciences, Wuhan 430074, China

2. Hubei Jewelry Engineering Technology Research Center, Wuhan 430074, China

3. Institute of Archaeology, Chinese Academy of Social Sciences, Beijing 100101, China

4. Qinghai Provincial Institute of Cultural Relics and Archaeology, Xining 810007, China

Abstract Establishing where a gemstone came from is rarely straightforward, least of all for turquoise, whose chemistry reflects both lattice-bound substitutions and contributions from accessory microphases, while intra-deposit variability and incomplete reference datasets routinely complicate source attribution. This study presents a multi-scale, multi-proxy provenance investigation of 32 turquoise ornaments from Xuewei Tomb No. 1 (Reshui cemetery, Dulan County, Qinghai Province), an elite Tang-period burial (7th–9th century CE) situated along the Silk Road corridor on the northeastern Tibetan Plateau, a landscape where local mineral resources, regional exchange networks, and long-distance connectivity converge.

The assemblage was characterised through a tiered analytical protocol: FTIR and Raman spectroscopy for mineral authentication; SEM–EDS for microtextural documentation; and LA–ICP–MS for trace-element and REE geochemistry (53 spot analyses across 24 specimens). Provenance inference was structured as a stepwise narrowing across four spatial scales, deposit type, mining zone, ore belt, and locality, with each level evaluated independently before proceeding to the next. At every scale, an open-set "none-of-the-above" (NOA) classification scheme was applied to flag unresolved specimens rather than forcing them into the nearest reference group, providing explicit uncertainty control throughout the workflow.

Spectroscopy confirms a turquoise-dominated phosphate assemblage, with minor variscite and mixed turquoise–variscite domains. SEM imaging reveals porous cryptocrystalline fabrics with Fe-(oxyhydr)oxide and carbonaceous associations, consistent with formation in sedimentary host rocks. At zone scale, geochemical patterns place the assemblage confidently within the Qinghai–Gansu–Hami (QGH) mineralisation corridor, with the strongest affinity toward Gansu reference materials, and clearly distinguish the artefacts from Hubei–Henan–Shaanxi signatures. The overwhelming dominance of unworked rough fragments (30 of 32 specimens) points to raw material delivery and on-site craft working at Reshui, rather than the circulation of finished ornaments.

At locality scale, open-set screening reveals that a meaningful subset cannot be resolved within the current reference framework, specimens that lie, in the precise sense of the multi-scale model, beyond the nearest sampled source. When considered alongside independent evidence for Central Asian glass imports from the same tomb, this unresolved fraction raises a testable hypothesis: that some turquoise may have reached Reshui through exchange routes extending beyond the immediate QGH corridor, reflecting the cosmopolitan connectivity of this Tibetan Plateau elite.

These findings carry a broader methodological message: an unresolved provenance result is not a failure of analysis, it is an observation in its own right, and one that demands the same rigor as a confident attribution. Future work should prioritise denser reference sampling within the Northwest corridor and the development of deposit-resolved Central Asian comparative datasets to distinguish unsampled regional variability from genuine long-distance supply.

Key words turquoise, archaeometry, LA–ICP–MS, Silk Road, Tang dynasty

Acknowledgements The authors thank the Qinghai Provincial Institute of Cultural Relics and Archaeology for access to the Xuewei Tomb No. 1 assemblage.

CHARACTERISTICS AND PROVENANCE STUDY OF JADE ARTIFACTS UNEARTHED FROM THE GUOZISHAN TOMB M1 IN ZHANGSHU CITY, JIANGXI PROVINCE, CHINA

Ting Fang[1,2,3,6*], Beibei Zheng[4], Jifu Liu[1,2,3], Longcai Zhou[4], Yile Wang[5], Mingxing Yang[1,2,3*]

1. Gemmological Institute, China University of Geosciences, Wuhan 430074, China

2. Hubei Province Gem and Jewelry Engineering Technology Research Center, Wuhan 430074, China

3. Hubei Key Research Base of Humanities and Social Sciences-Center for Jewelry Heritage and Innovation, Wuhan 430074, China

4. Jiangxi Provincial Institute of Cultural Relics and Archaeology, Nanchang 330095, China

5. Zhangshu Museum, Yichun 331299, China

6. Institute for Geosciences, Johannes Gutenberg University of Mainz, Mainz 55128, Germany

Abstract This study presents a multi-analytical investigation of jade and related artifacts excavated from the Guozishan Tomb M1 (Zhangshu City, Jiangxi Province, China), a crucial site for exploring Yue–Chu cultural interactions during the Warring States period. The assemblage primarily comprises nephrite, along with quartzite, turquoise, and faience (including eye beads and old glass beads/tubes). Our mineralogical and geochemical characterization aims to trace raw material provenance and reconstruct ancient technological choices. By combining X-ray diffraction (XRD), Raman spectroscopy, and laser ablation inductively coupled plasma mass spectrometry (LA-ICP-MS), we directly correlate the artifacts with their geological sources. Results indicate that the faience beads were likely produced locally in China and incorporated indigenous aesthetic styles. Notably, trace element and isotopic signatures link nephrite artifacts to the West Kunlun–Altun–Beishan metallogenic belt, with specific origins identified in the Altun Mountains and Gansu Province. These findings provide new insights into Pre-Qin period resource economies, long-distance trade networks, and the transfer of mineralogical knowledge. The study demonstrates how applied mineralogy and geochemistry can effectively address archaeological questions concerning innovation, social structures, and cultural connections across ancient China.

Key words Nephrite provenance, Archaeometry, Warring States period, Ancient trade network

Acknowledgements We would like to thank Professor Yang Mingxing's Jade and Jade Culture Research Team of China University of Geosciences (Wuhan) for their assistance in sample testing. Special thanks are due to Ms. Liu Jia and Mr. Xu Xing from the Gem Testing Laboratory of China University of Geosciences (Wuhan) for their guidance on experimental testing techniques.

FORMATION AND STABILITY MECHANISMS OF MAYA BLUE: A MINERALOGICAL PERSPECTIVE ON NANOSCALE CONFINEMENT EFFECTS

Guanzheng Zhuang [1], Peng Yuan [1], Maguy Jaber [2]

1. School of Environmental Science and Engineering, Guangdong University of Technology, China

2. Laboratoire d'Archéologie Moléculaire et Structurale, UMR 8220, Sorbonne Université, Paris, France

Abstract Maya Blue is a greenish-blue hybrid pigment composed of indigo and fibrous clay minerals, typically palygorskite or sepiolite, and is renowned for its exceptional durability. However, its formation process and the origin of its remarkable stability remain incompletely understood. In this study, we investigate the optical properties, stability, and synthesis mechanism of Maya Blue, and further evaluate its implications for the design of modern mineral-based functional pigments.

Results show that the channels (0.64 × 0.37 nm) of the palygorskite matrix and the state of water confined within these channels are key factors controlling pigment formation and stability. Under mild thermal treatment (150–200°C), zeolitic water is removed, while indigo diffuse into the channels. This nanoscale confinement markedly enhances the photochemical, thermal, and chemical stability of indigo molecules. Comparative investigation of the sepiolite-based system further demonstrates that the match between channel size and guest molecules plays a decisive role in determining material performance. Although the larger channels of sepiolite favor stronger initial coloration and improved photostability, they are less effective in protecting guest molecules from external chemical attack. Molecular dynamics simulations indicate that indigo and related organic molecules can enter the channels of both palygorskite and sepiolite and diffuse along the channel direction. Although weak and dynamic hydrogen bonding may occur between organic molecules and coordinated water, such interactions are not the dominant origin of pigment durability. Instead, the tight encapsulation and confinement of organic molecules within mineral nanochannels are responsible for the outstanding stability of Maya Blue.

These findings provide new mineralogical insight into the long-standing question of why Maya Blue remains stable over centuries, and they highlight the potential of minerals as versatile platforms for the development of high-performance hybrid materials.

Key words Maya Blue, clay minerals, organic dyes, hybrid materials, confinement

SALINE EFFLORESCENCES AT ARCHAEOLOGICAL SITES IN THE SERRA DAS CONFUSÕES NATIONAL PARK, MUNICIPALITIES OF CARACOL AND GUARIBAS, PIAUÍ, BRAZIL

Daniel Atencio, Tatiane de Souza

Instituto de Geociências, Universidade de São Paulo, Brazil

Abstract Mineralogical studies of saline efflorescences in rock art shelters are underway in archaeological sites of the Serra das Confusões National Park, in the state of Piauí, Brazil, at Baixão do Milho, in the municipality of Caracol, and Bom Sucesso and Bom Jardim, in the municipality of Guaribas. The efflorescences form on sandstone walls of the Cabeças Formation, attributed to the Middle Devonian, in the Parnaíba Basin. The sandstones of the Cabeças Formation constitute important rock supports for archaeological sites with rock art, as their texture and fracturing favor the formation of rock shelters and surfaces suitable for the execution and preservation of graphic representations. Among the minerals already identified are the oxalates weddellite [$Ca(C_2O_4)(H_2O)_2$] and whewellite [$Ca(C_2O_4)(H_2O)$], the sulfates gypsum [$Ca(SO_4)(H_2O)_2$], alunite [$KAl_3(SO_4)_2(OH)_6$], and alunogen [$Al_2(SO_4)_3(H_2O)_{12}\cdot 5H_2O$], the phosphates gorceixite [$BaAl_3(PO_4)(PO_3OH)(OH)_6$] and goyazite [$SrAl_3(PO_4)(PO_3OH)(OH)_6$], and the nitrate sveite [$KAl_7(NO_3)_4(OH)_{16}Cl_2\cdot 8H_2O$]. A new chalcoalumite group mineral species is under study.

In previous studies conducted on similar occurrences in rock shelters with petroglyphs in sandstone from the Furnas Formation (Silurian/Devonian of the Paraná Basin), in the municipalities of Ponta Grossa, Piraí do Sul, and Tibagi, Paraná State, Brazil, the following minerals were identified: the phosphates tinsleyite [$KAl_2(PO_4)_2(OH)(H_2O)_2$] and taranakite [$K_3Al_5(PO_3OH)_6(PO_4)_2(H_2O)_{12}\cdot 6H_2O$]; the sulfates gypsum [$Ca(SO_4)(H_2O)_2$], baryte [$Ba(SO_4)$], and alunite [$KAl_3(SO_4)_2(OH)_6$]; the minerals that are both phosphates and sulfates, sasaite [$(Al,Fe^{3+})_{14}(PO_4)_{11}(SO_4)(OH)_7\cdot 83H_2O$] (and an unnamed dehydration product) and rossiantonite [$Al_3(PO_4)(SO_4)_2(OH)_2(H_2O)_{10}\cdot 4H_2O$]; the nitrates sveite [$KAl_7(NO_3)_4(OH)_{16}Cl_2\cdot 8H_2O$] (or an undescribed isostructural mineral) and a more hydrated unnamed phase, among others.

In rock shelters with petroglyphs, the formation of saline efflorescences is one of the most common and potentially destructive physicochemical deterioration processes. These efflorescences result from the migration of solutions rich in dissolved ions through the rock or adjacent sediments. When water evaporates on the surface of the rock support, soluble salts precipitate, often in the form of sulfates, nitrates, chlorides, or carbonates.

These salts can directly affect paintings through different mechanisms. One of the main ones is saline

crystallization, which occurs when salts precipitate in the pores and microfissures of the rock or between the pigment and the mineral support. The growth of crystals exerts mechanical pressure on the substrate, which can cause microfractures, flaking, and detachment of the pictorial layer. In repeated cycles of wetting and drying—common in rock shelter environments—the salts can dissolve and recrystallize several times, progressively amplifying the damage.

In addition to the mechanical effect, some salts can also produce chemical interactions with the pigments and minerals of the support. Depending on the composition of the pigment—for example, iron oxides, manganese oxides, or clay minerals—the presence of saline solutions can favor dissolution processes, ionic mobilization, or mineralogical alteration. This can lead to loss of chromatic intensity, alteration of tonality, or complete disintegration of the pictorial material.

Another relevant effect is the formation of superficial saline crusts, which can partially or totally cover the paintings. These crusts not only visually obscure the graphic elements, but can also trap particles, promote moisture retention, and create microenvironments that accelerate chemical reactions and biological processes, worsening deterioration.

In this way, saline efflorescences represent an important agent of alteration in rock art contexts, as they combine physical (crystallization pressure), chemical (reactions with pigments and minerals of the support), and environmental (humidity cycles) processes. The mineralogical identification of these salts and the understanding of their dynamics in the shelter environment are, therefore, fundamental steps for the conservation and interpretation of rock art heritage.

Key words Saline efflorescences, archaeological sites, Serra das Confusões, Piauí, Brazil

Acknowledgements DA acknowledges FAPESP (Fundação de Amparo à Pesquisa do Estado de São Paulo) for financial support (process 2024/02850-6) and CNPq (Conselho Nacional de Desenvolvimento Científico e Tecnológico) for a research productivity scholarship (process 305656/2023-6).

A CROSS-CULTURAL STUDY ON MALACHITE FROM TANG DYNASTY CHANGSHA KILN GLAZES AND ANCIENT EGYPTIAN FAIENCE

Shangjia Wen[1], Xinxin Gao[2],Yimiao Liu[3], Ren Lu[4]

1. Hunan City University

2. Institute of Deep-sea Science and Engineering, Chinese Academy of Sciences

3. Gemmological Institute, China University of Geosciences, Wuhan

4. Independent Consultant

Abstract The intersection of mineralogy and archaeology provides a fruitful approach to understanding the dynamic relationship between nature and culture in ancient craftsmanship. Existing research on mineral-based crafts, such as ceramics and enamel, has generated significant results in both scientific analysis and humanistic interpretation. However, a coherent, dynamic interpretive framework that bridges the natural properties of minerals with artisans' technical choices and cultural perceptions has yet to be established. To this end, this study takes malachite as its central subject. Through an interdisciplinary approach, it asks why the same mineral produces such different craft productions across cultures, and what those differences reveal about how each tradition understood and worked with its materials.

The study is grounded in experimental archaeology and integrates scientific analysis with documentary comparison. Focusing on the green glaze of the Tang Dynasty Changsha Kiln, a glaze system comprising kaolinite, calcite, feldspar, and quartz. Controlled firing experiments grounded in archaeological data were conducted to investigate the coloration and high-temperature behavior of malachite within this system. Experimental samples were characterized using thermogravimetric–differential scanning calorimetry (TG-DSC), Raman spectroscopy, and UV-Vis-NIR reflectance spectroscopy. In parallel, the study systematically reviews existing scholarship and data on the use of malachite in ancient Egyptian faience. Building on this foundation, it conducts a cross-cultural comparative analysis by integrating the experimental results from the Changsha Kiln with Egyptian faience documentary sources, as well as their mineral origins and archaeological contexts.

When fired in the Changsha Kiln glaze system, malachite yields an olive-green with gray undertones; in the quartz-soda glaze of ancient Egyptian faience, the same mineral produces a bright, saturated turquoise blue. The contrast goes beyond differences in formulation and temperature. It reflects how artisans in each tradition developed a distinct sense of what this mineral could and should look like, shaped by the materials available to them and the aesthetic values they worked within.

These findings show that malachite's thermal behavior and color response under different glaze conditions directly shaped what each tradition could produce, and, in turn, what each tradition came to value aesthetically. Tracing one mineral across two craft cultures proves more revealing than studying either the chemistry or the historical record in isolation.

Key words Malachite, Cross-cultural comparison, Material culture

A REVIEW ON THE EXPLOITATION AND UTILIZATION OF NEPHRITE (CALCIC AMPHIBOLITE) RESOURCES IN PREHISTORIC EUROPE

BAO Tongmei[1,3], YANG Jiong[1,2*,3]

1. College of Earth Sciences, Guilin University of Technology, Guilin 541004, China

2. School of Tourism //Taishan Jade and Stone Research Institute, Taishan University, Tai 'an 271000, China

3. Key Laboratory of Guangxi Concealed Metal Mineral Exploration, Guilin University of Technology / Key Laboratory of Electronic Functional Materials and Devices of Nonferrous Metal Oxides in Guangxi Universities, Guilin 541004, China

Abstract Nephrite, a significant green nephrite material used in prehistoric Europe from the Neolithic to the Chalcolithic period, has been discovered at many sites across the continent. Due to scattered occurrences, inconsistent nomenclature, and a lack of clear archaeological contexts, our understanding of its resource distribution, exploitation, circulation, and social functions remains fragmentary. This paper synthesizes previous research on nephrite in prehistoric Europe and presents the following key conclusions: (1) From the 7th to the 5th millennium BC, the Balkan Peninsula, centred on Bulgaria, pioneered the use of nephrite, forming Europe's earliest "Balkan nephrite culture". From the 5th to the 4th millennium BC, nephrite spread widely to Central, Western and Southeastern Europe, reaching its peak in distribution range and social prestige, with the furthest finds located over 800 km away. The Danube, the Rhine and other rivers served not only as transport routes but also as bridges for cultural exchange and trade. From the 3rd to the 2nd millennium BC, with the rise of bronze and gold artefacts, its core functions were replaced;nephrite was only used for simple regional tools, or even disappeared entirely. (2) In terms of function and distribution, European nephrite shows distinct regional differences. Nephrite in Central Europe served both utilitarian and ritual functions, while nephrite in Southeastern Europe was typified by small amulets and frog-shaped amulets. (3) As the highest-ranked ritual jade implements in prehistoric Central, Western and Southern Europe, nephrite axes share broadly comparable social functions with large jadeite axes and other green lithic materials. Together with jadeite,serpentinite and variscite, nephrite formed part of a shared symbolic system and identity markers centered on "green sacred stones", serving as a vital material carrier for early complex societies and long-distance interaction in prehistoric Europe. (4) Based on petrographic and geochemical provenance analyses, prehistoric

nephrite artefacts unearthed across Europe derive primarily from three sources: Lower Silesia (Jordanów) in Poland, the Swiss Alpine region (Valais), and the Pyrenees. Among these, Jordanów in Poland has been confirmed by numerous studies as the primary supply centre of nephrite for prehistoric Central Europe, while the Swiss Alpine region served as the main source for Western Europe. In the Balkans, nephrite originated from at least two distinct provenances; no local primary nephrite deposits exist, and the region relied entirely on external imports.

Key words nephrite(calcic amphibolite), prehistory, Resource exploitation and utilization, Jade culture

FROM MINERAL RESOURCES TO GEOTOURISM: DESIGNING A GEMSTONE ROUTE IN CHANTHABURI, THAILAND

Kannatee Fueangaksorn, Boonyapak Aksorn, Chanikarn Seangrit, Namrawee Susawee,
Pakakorn Nampadon, Rungarun Chankhonkaen
The Gem and Jewelry Institute of Thailand (Public organization), Thailand

Abstract This study examines how geotourism can be used to present geological heritage in Chanthaburi through tourism activities that also support public learning and local development. In this context, geological and mineral resources can be interpreted in ways that link earth science with local culture, community participation, and conservation-oriented tourism. Areas with notable mineral resources and clear geological features may offer strong potential for geotourism planning. Chanthaburi Province in eastern Thailand, widely known as the "Gem Capital of Thailand," has long been a major center of gemstone mining, processing, and trade ,making it an important case for this study. The province is known for ruby and sapphire, together with other gem-related minerals such as zircon, garnet, spinel, and tourmaline. Many of these gemstones are found in secondary alluvial and/or eluvial deposits derived from Cenozoic alkali basaltic sources, reflecting the region's complex geological evolution and making it an excellent case study for geotourism development.

Our study investigates how Chanthaburi's mineral resources can be organized into geotourism attractions through the design of gemstone tourism routes. Field investigations were conducted at selected sites, including the Ploi Waen Gem Learning Center, where ten representative specimens were collected within weathered reddish sediments, and later were characterized by using gemological microscopy alongside advanced instrument identification techniques, including UV-Vis-NIR spectroscopy, EDXRF, FTIR, and Raman analysis, as well as detailed geological field observations. Our field surveys further identified a range of significant geological and cultural sites, such as former mining areas, gemstone-bearing deposits, community learning centers, local markets, and notable natural attractions. Based on these findings, a two day guidebook was prepared for general tourists, families, students, and people interested in gemstones and jewelry. The route is designed as a weekend program so that visitors can experience Chanthaburi's gemstone heritage, local culture, and natural attractions within a short trip. The journey highlights ten key destinations, including Khao Ploi Waen temple, Ploi Waen Gem Learning Center, Bo Phloi Lek Phet Learning Center, Phlio Waterfall National Park, Chanthaburi City Pillar Shrine, Gem and Jewelry Promotion Center, Chanthaburi Riverside Community, Pak Nam Khaem Nu temple, Kung Krabaen Bay, and Proet Island. Together, these destinations offer a unique blend of geological emphasis, cultural heritage, and natural beauty, making Chanthaburi an exceptional destination for both

educational exploration and creative travel.

The SWOT analysis indicates that Chanthaburi possesses strong advantages, including its international reputation as a gemstone center and its diverse tourism resources. However, several challenges remain, such as limited interpretive activities, insufficient integration of scientific information into tourism experiences, and a shortage of specialized geotourism guides.

The findings suggest that mineral resources can support sustainable geotourism development when integrated with conservation and tourism planning. The proposed tourism routes offer a possible model for sustainable geotourism development in Chanthaburi and may also be adapted for other gemstone-producing areas with similar goals.

Key words geotourism, gemstone route, basaltic sources, Chanthaburi

ORIGIN OF GEM SAPPHIRES FROM THE ANAKIE GEMFIELDS, CENTRAL QUEENSLAND, AUSTRALIA.

Ian Terence Graham[1], Nicholas Raffan[1], Karen Privat[1,2] and Yi-Jen Lai[3]

1. Earth and Sustainability Science Research Centre, School of Biological, Earth and Environmental Sciences, UNSW Sydney, Australia

2. Electron Microscope Unit, Mark Wainwright Analytical Centre, UNSW Sydney, Australia

3. Macquarie Analytical and Fabrication Facility, Faculty of Science and Engineering, Macquarie University, Australia

Abstract The Anakie sapphire fields of central Queensland are world famous for producing gem-quality blue, yellow, orange and parti-coloured (especially blue-green and blue-yellow) sapphires of the highest quality. They have also produced some of the largest and finest star sapphires ever found, including the famous 4 USA presidents heads (largest is 1444 carats). Other famous sapphires include the Stonebridge green at 212 carats, Pride of Tomahawk Creek at 225 carats, Eifel Tower at 144 carats and Tomahawk Tiger at 82.4 carats. The main diggings include Policemans Creek, Retreat Creek, Tomahawk Creek, Glen Alva, the Willows, Scrub lead, Bedford Hill, Mount Newsome, Graves Hill and the Divide while the main towns are Anakie, Sapphire and Rubyvale. Inlcluded with the sapphires in the gemmiferous gravels are gem-quality zircons (mainly colourless to deep orange) and spinels.

The Anakie sapphire fields are within the Cenozic Hoy Basalt Province with basalts ranging in age from 34 to 18.1 Ma. The basement units comprise the Late Cambrian to Ordovician Anakie Metamorphics, Devonian granites and Carboniferous metasedimentary and volcanic rocks of the Drummon Basin to the west. The sapphire fields are bound between two major faults the Chinaman Fault to the west and south, and the Kettle Creek fault to the northeast. During the course of this investigation, a Carboniferous intrusive complex, the 'Billaboo Complex' was found wihin the Drummond Range sequence and this includes abundant Carboniferous lamprophyres and is capped by a newly-discovered Cenozoic basalt flow. However, no sapphires were found within either the lamprophyres or basalt flow.

The sapphires are found within both present-day alluvial sediments but most commercial production comes from palaeoalluvial deposits (though these may be lahar deposits) overlying the Devonian granites. The gem deposits are found from the surface to depths of 6 metres, with the gem-bearing gravels mostly ranging in thickness from 0.2 to 1 metre. Many of the sapphires occur within distinctive powdery white volcaniclastic beds. Although there are abundant basalt cobbles within the plaeoalluvial deposits (in places over 60%), none of the miners have ever found any sapphires in these. The only location where sapphires occur as megacrysts within the basalts is at Mount Leura and these have prominent reaction rims.

Sapphires show abundant evidence of magmatic corrosion and resorption, with little sign of any significant alluvial transport. Also, subhedral to euhedral grains are very rare. Mineral inclusions comprise rutile, ilmenite, fayalite, zircon, pyrrhotite, diopside and tantalite.

The sapphires vary widely in chemistry though all have extremely low Mg (bdl to only 0.02 ppm) and high Fe (range 6699 to 14926 ppm). They all consistently plot as magmatic in origin using various ratios with Fe/Mg from 323 to 11125 and Ga/Mg from 4 to 259. Ti ranges from 6 to 248 ppm, Cr from 1.8 to 144.8 ppm, and V from 1.1 to 58.9 ppm. Sapphire inclusions in basalt from Mount Leura plot within the same area as the gemfield sapphires. Based on their Fe/Mg index, 11 geochemical groups of sapphires occur, while based on their Ga/Mg index this is expanded to 16 groups. However, different geochemical types are found within the same field.

Evidence from the sapphires, associated zircons, volcaniclastics and basalts collectively suggests that the sapphires crystallised in a highly alkaline environment involving varying degrees of interaction between carbonatitic and alkaline basaltic magmas in the subcontinental lithospheric mantle. The sapphires were then brought to the surface during sporadic short duration explosive volcanic eruptions from the mid Cretaceous to the mid Eocene.

Key words sapphires, zircons, alkaline volcanics, lamprophyres, Anakie gemfields

GEMOLOGICAL CHARACTERIZATION OF PINK OPALS FROM BINTHALYA PROSPECT, AUSTRALIA

Bowen Zhao[1,2], Zhibin Li[3]

1. Gemmological Institute, China University of Geosciences, China

2. Shanghai Institute of Measurement and Testing Technology Co., Ltd., China

3. Shanghai Jewelry Testing and Appraisal Office, China

Abstract A new type of pink opal was discovered in 2011 at the Binthalya Prospect, Mooka Creek, Carnarvon Shire, Western Australia. Sharing the same geological origin with mookaite, this pink opal is part of the silicified radiolarite in the Carnarvon Basin. Its gemological characteristics were tested non-destructively with conventional and spectroscopic methods, revealing significant differences from those of Peruvian and Mexican pink opals, which are primarily composed of opal-CT and palygorskite, with their coloration attributed to Mn ion and biogenetic quinones. The Binthalya pink opal exhibits a unique porcelain-like appearance with parallel or swirling banding and brecciated patterns. White dots scattered throughout the pink opal are believed to be radiolarian skeletons, base on their cage-like microstructure and their diameters ranging from 60~92 μm, as observed and measured under 500× magnification. Despite the pink opal's sedimentary origin, its infrared spectra display typical opal-CT features without any presence of phyllosilicate, although some minor areas of the samples (e.g., white banding) show the absorption features of low-crystallinity chalcedony. The ultraviolet-visible-near infrared (UV-Vis-NIR) spectra are featured with absorption peaks at 460 nm, 493 nm, and 533 nm with gradually increasing intensity, along with shoulders at 400 nm, 429 nm, 564 nm, and 630 nm resolved by second derivative analysis. Under long-wave UV, the samples exhibit red and bright blue fluorescence in the zoning corresponding to the opal's parallel or swirling banding. On each specific sample, areas with intense coloration tend to fluoresce red, while paler areas tend to fluoresce blue. The 370 nm UV-excited fluorescence spectra show a superposition of red fluorescence composed of emission bands at 543 nm, 568 nm, 588 nm, and 643 nm, along with blue fluorescence composed of emission bands at 435 nm, 474 nm, 510 nm, and 550 nm. As the blue fluorescence was attributed to oxygen-related intrinsic defects of opal, the red fluorescence is probably induced by the pink chromophore. After baseline correction to suppress fluorescence bands centered at ~540 nm and ~580 nm, the Raman spectra reveal a group of peaks at 1619 cm^{-1}, 1572 cm^{-1}, 1401 cm^{-1}, 609 cm^{-1}, 531 cm^{-1}, 388 cm^{-1}, 353 cm^{-1}, 305 cm^{-1}, and 255 cm^{-1}, which are obviously not derived from inorganic minerals. Trace amounts of K, Ca, Ti, Cr, Mn, Fe, Ni, and Cu were detected by X-ray fluorescence analysis (XRF), however, no correlation was observed between the intensity of the pink coloration and the concentration of these potentially color-inducing elements. Based on the spectroscopic results above, the coloration of the Binthalya pink opal is likely due to some kind of

organic pigment that differs significantly from quinone and does not match common pink-red pigments found in marine organisms, such as phycoerythrobilin, phenazine, prodigiosin, bacterioruberin, astaxanthin, etc. Further tests and analyses are required to determine the specific category and structure of the pink pigment. However, micro-Raman tests on areas of colors other than pink indicate that the brownish red brecciated areas and the purple shades on the pink matrix are both colored by dispersed hematite microparticles.

Key words pink opal, radiolarite, opal-CT, color genesis

GEOCHEMICAL FINGERPRINTING OF RED SPINEL FROM MYANMAR VIETNAM AND TANZANIA

Montira Seneewong-Na-Ayutthaya[1], Bhuwadol Wanthanachaisaeng[1], Thanong Leelawatanasuk[1], Sirinapa Saengdech[1], Pimlapat Kamkeaw[1], Boonyapak Aksorn[1], Tasnara Sripoonjan[2], Muanfan Wantong[3]

1. The Gem and jewelry Institute of Thailand (Public Organization), Bangkok, Thailand

2. G-I D Laboratories, Bangkok, Thailand

3. Department of Earth science, Kasetsart University, Bangkok, Thailand

Abstract Red spinel is a highly valued red gemstone in the gem and jewelry industry. The origin determination of red spinel is a critical factor in enhancing the commercial value of gem in the trade, as variations in properties, rarity, and chemical composition reflect differences in formation conditions and geological settings. In addition, the global trend toward responsible sourcing has increased the demand for reliable information on gemstone provenance throughout the supply chain. This study aims to develop a method for determining the geographic origin of red spinel from importantly global sources, including Myanmar, Vietnam, and Tanzania. The approach focuses on origin determination through internal feature observation and trace-element analysis using Energy-Dispersive X-ray Fluorescence (EDXRF) and Laser Ablation Inductively Coupled Plasma Mass Spectrometry (LA-ICP-MS). A total of 278 samples were analyzed, comprising 122 from Myanmar (Mogok), 99 from Vietnam (Luc Yen), and 57 from Tanzania (Mahenge). The chemical composition analysis of red spinel from the three sources reveals clear differences, reflecting their distinct geological environments. Myanmar red spinel is associated with pure marble and exhibits low Fe content. In contrast, Vietnamese red spinel shows higher Fe content, linked to calcic to dolomitic marble and kyanite-sillimanite bearing micaschists, garnet amphibolites. Tanzanian red spinel is characterized by elevated Zn content, likely derived from high-grade metamorphic processes under high temperature and pressure conditions. Key elements used as indicators of origin include Mg, Ti, V, Fe, Ni, Zn, and Ga, which can be related to the geological environments of the respective regions. These elemental characteristics enable clear differentiation of spinel from the three geographic sources.

Key words Red spinel, Geographic origin, Geochemical fingerprinting

Acknowledgements The authors sincerely acknowledge the support provided by the Gem and Jewelry Institute of Thailand (GIT) and its staff throughout the course of this research.

INTERPRETABLE MACHINE LEARNING FOR GEMSTONE PROVENANCE DETERMINATION: A COMPARATIVE STUDY OF ALGORITHMS AND GEOLOGICAL ANALYSIS FOR PERIDOT AND JADEITE

Heng Luo, Shao Kui Pan, Ping Ma, Yuan Zhong, Zhi Qing Zhang, Andy Hsitien Shen*

Gemmological Institute China University of Geosciences (Wuhan), Wuhan 430074, China

Abstract This study systematically evaluates machine learning for gemstone provenance determination by comparing nine algorithms across two gem materials. The datasets comprise peridot, a single-crystal mantle gem (470 samples from five origins: Jilin and Hebei, China; South Hwanghae, North Korea; Khyber Pakhtunkhwa, Pakistan; and Arizona, USA), and jadeite, a polycrystalline metamorphic rock (122 samples from Myanmar, Guatemala, and Russia). The discrimination analyses rely on the chemical compositions of the materials: trace element data were acquired by LA-ICP-MS for both materials, while major element compositions were determined by EDS for peridot and by EPMA for jadeite. Algorithms include linear models (LDA, LR), support vector machine (SVC), back-propagation neural network (BPNN), and ensemble tree methods (RF, ET, LightGBM, XGBoost and CatBoost). The analytical framework employed stratified nested cross-validation with Bayesian hyperparameter optimization to ensure robust performance estimates. SHAP analysis quantified each variable's contribution and linked its directional influence to geological processes.

The results demonstrate that ensemble tree methods offer the most balanced and robust performance for gemstone provenance classification. For peridot, mean accuracy ranged from 89.79% (LDA) to 96.81% (Extra Trees). Extra Trees achieved the highest raw accuracy (96.81%) and macro F1-score (97.17%), while CatBoost proved most robust to class imbalance (balanced accuracy 97.66%). LightGBM and XGBoost both attained mean accuracies of 96.17%, with LightGBM showing a balanced accuracy of 96.53%. BPNN reached 96.38% accuracy but exhibited weaker minority-class generalization than the top ensemble models, and SVM achieved 95.74%. Logistic Regression (94.47%) outperformed LDA, whose low accuracy (89.79%) stems from violation of the equal covariance assumption across peridot origins. For jadeite, ensemble performance was even stronger: CatBoost reached 98.37% overall accuracy, 98.33% balanced accuracy, and 98.37% macro F1-score. LightGBM followed with 97.57% accuracy, while XGBoost and Extra Trees exceeded 96.7%. Logistic Regression achieved 96.70%, reflecting strong linear separability among the three origins; LDA again performed poorly (85.23%) due to heterogeneous covariance structures. SHAP analysis identified specific trace elements as consistent discriminators and aligned their directional contributions with geological processes. In peridot, Ge, B, Al, Zn, and Co

exhibited large SHAP values. Low Ge was associated with depleted mantle sources (USA, Hebei), whereas elevated B in Pakistani samples indicated fluid-related metasomatism. High Al and Zn in USA samples were consistent with higher equilibration temperatures and limited melt extraction. In jadeite, key discriminators included Sr, Zr, Fe, Mn, and total REE. High Sr in Myanmar and Guatemalan jadeite reflected subduction-related fluid sources, while low Sr and high Ba in Russian jadeite suggested sediment-derived fluids. Elevated Fe and Mn in Guatemalan and Russian samples indicated more mafic protoliths and distinct redox conditions relative to Myanmar jadeite.

In conclusion, this study provides a validated and reproducible framework for applying machine learning to gemstone provenance determination. Careful algorithm selection—particularly ensemble tree methods such as Extra Trees and CatBoost—yields high classification accuracy while maintaining robustness to common data challenges, including class imbalance and high dimensionality. Importantly, the integration of SHAP analysis ensures that models are not merely "black boxes" but offer meaningful insights into the geological processes governing trace-element distributions. This approach bridges data-driven classification and geochemical understanding, thereby supporting more transparent and scientifically grounded gemological practices.

Key words Ensemble learning, Nonlinear classification, SHAP (SHapley Additive exPlanations), Geochemical characteristics, LA-ICP-MS

RAINDROP MICROTEXTURES AND PROVENANCE SIGNATURE OF SUPERGENE TURQUOISE FROM DELINGHA MOUNTAIN, QINGHAI, CHINA

Bahareh Shirdam[1,2]*, Mingxing Yang[1,2], Jinhan Dun[1,2], Yue Yang[1,2]

1. Gemmological Institute, China University of Geosciences, Wuhan, 430074, China

2. Hubei Jewelry Engineering Technology Research Center, China

Abstract The Delingha turquoise deposit also known as Duancengshan turquoise deposit, situated in Wulan County near Delingha City at the eastern edge of the Qaidam Basin, Qinghai Province, China, is characterized by a distinctive microtextural–geochemical signature, Fe–Mg–Ca-enriched 'raindrop' micro-disks (present in 28% of examined specimens) and a consistent, deposit-specific trace-element fingerprint, that differentiates it from turquoise reported at other localities worldwide. The turquoise notably occurs within Precambrian basement rocks, primarily migmatized gneisses and schists of the Sinian System (800–541 Ma), overlain by Cambrian sediments. Detailed analyses were performed using petrography, scanning electron microscopy, Raman spectroscopy, X-ray diffraction, and trace-element geochemistry. The turquoise is found within carbonaceous slate and black shale and is characterized by features such as vein-like structures, raindrop-shaped aggregates, and microfold textures. Geochemically, it is distinguished by elevated levels of iron, calcium, magnesium, lithium, chromium, and strontium, alongside notably low barium content. Significantly, this research records, to our knowledge, this is the first time in turquoise, the occurrence of Mg phosphate solid solutions such as segelerite as part of turquoise paragenesis. The associated mineral assemblages, including quartz, goethite, hematite, jarosite, muscovite, illite, anatase, and phosphosiderite, reflect complex formation processes driven by episodic low-temperature meteoric leaching (supergene alteration). We also compare Delingha Mountain raindrop-textured turquoise with the well-known "raindrop turquoise" from Zhushan, Hubei Province, differentiating the two based on their compositional and mineralogical signatures. These results provide critical geochemical markers for turquoise provenance studies, thereby enhancing authentication and contributing to our understanding of historical trade along ancient Silk Road routes.

Key words Turquoise, phosphate associated mineral, Provenance signature

THE EFFECT OF CR CONTENT ON THE ACTIVATION ENERGY OF ORDER-DISORDER TRANSITION IN MG-AL SPINEL

Chengsi Wang[1], Andy H. Shen[2], Jiling Zhou[3], Xin-Yi Chen[4], Jingcheng Pei[3]

1. College of Earth and Planetary Sciences, Chengdu University of Technology, China

2. Gemmological Institute, China University of Geosciences, China

3. State Key Laboratory of Geological Processes and Mineral Resources, China University of Geosciences, China

4. School of Earth and Space Sciences, University of Science and Technology of China, China

Abstract Mg-Al spinel ($MgAl_2O_4$, MAS) is a common rock-forming mineral widely distributed in the upper mantle, crust, and extraterrestrial bodies. The order-disorder transition (ODT) in spinel is a critical physical characteristic that significantly affects its properties and applications as a geothermometer for probing the thermal history of Earth and extraterrestrial bodies. Although activation energy—a key thermodynamic parameter of ODT—is reported to be influenced by Cr content, the relationship between these two factors remains unclear.

Six natural gem Mg-Al spinel samples with varying Cr contents (419 – 6918 ppma) were heated to seven different temperatures (550–850 ˚C), and their photoluminescence (PL) spectra were subsequently collected at liquid nitrogen temperature. The PL spectrum emitted by Cr in the samples consists of zero-phonon lines (ZPL) and phonon sidebands, with a spectral range between 13800 and 14640 cm^{-1}. The ZPL, located between 14500 and 14640 cm^{-1}, comprises R peaks (R_1 and R_2) and N peaks (n_5, N_2, n_3, and N_1). R_1 and R_2 are emitted by the Cr^{3+} ions around which the cation arrangement is ordered, while the N peaks are emitted by the disordered arrangement. The intensity of the N peaks in the zero-phonon line range and the N_4 peak increased with increasing Cr content. By integrating parameters extracted from these spectra into a thermodynamic model which we established in previous work based on the Arrhenius relationship, we calculated the ODT activation energies which decreased from 335 to 163 kJ/mol with the Cr content increasing. A quantitative relationship between activation energy and Cr content was established: $Ea = -0.03[Cr] + 356.28$. As a result, we clarify the negative correlation between ODT activation energy and Cr content in Mg-Al spinel, which may be attributed to local structural distortion caused by the presence of Cr-pairs.

This study provides a method to correct the influence of Cr content on ODT thermodynamic models, thereby enhancing the viability of spinel as geothermometers and deepening the scientific understanding of how elemental composition affects the thermal stability of spinel.

Key words Mg-Al spinel, Order-disorder transition, Activation energy, Chromium content

VOLCANIC OPAL WITHIN A TRADITIONAL SEDIMENTARY OPAL FIELD: THE LIGHTNING RIDGE OPAL FIELD, NORTHERN NSW, AUSTRALIA.

Ian Terence Graham[1], Tully Ritter[1], Rory Carter[1], David French[1], Alan Greig[2] and Elizabeth Smith[3]

1. Earth and Sustainability Science Research Centre, School of Biological, Earth and Environmnetal Sciences, UNSW Sydney, Australia

2. School of Geography, Earth and Atmospheric Sciences, University of Melbourne, Australia

3. Lightning Ridge, NSW, Australia

Abstract Gem opals are generally classified as being of either 'sedimentary' or 'volcanic' in origin based on their hostrock, opal type (i.e. opal-CT, opal-A) and geochemistry (i.e. Ba < 110 ppm). The 'classic' sedimentary opal fields are those of Andamooka and Coober Pedy in South Australia, White Cliffs and Lightning Ridge in northern NSW, and the boulder opal fields of south-western Queensland. The 'classic' volcanic opal fields include those of Slovakia, Hungary, Nevada (USA), and Mexico.

In the Lightning Ridge field, gem opal mainly occurs within claystone lenses (Finch clay facies) within the sandstones (Wallungulla Sandstone Member) of the Late Cretaceous Griman Creek Formation. The opal occurs lining fractures (seam opal), as space-fill (nobbies), or as replacments of a wide range of Cretaceous fossils (molluscs, plesiosaurs, early mammals).

For this study, we obtained a large sample of fresh and unaltered flow-banded rhyolite containing obvious seam opal from the Lightning Ridge field, along with seam opal hosted within reworked ash fall tuffs from south of Lightning Ridge.

The seam opal in the rhyolite is a distinctive yellow to creme-coloured glassy opal, and is sometimes termed 'caramel potch'. The seams are up to 8 mm wide and continuous for 155 mm. The contact with the surrounding rhyolite is sharp, with the opal clearly occurring as a fracture-fill phase. In thin-section, the flow-banded rhyolite contains partially reworked phenocrysts of albitic plagioclase, sanidine and volcanic quartz in a fine-grained spherulite-rich felsic groundmass.

Opal within the reworked tuff occurs as a white to pale grey fracture-fill phase. In thin-section, this opal has a finely concentric banded structure suggesting progressive deposition from a fluid phase without any deposition of any other phases. In thin-section, the tuff comprises small grains of altered plagioclase, angular K-feldspar, muscovite and quartz shards, along with aggregates of vermicular kaolinite and illite overprinting kaolinite, and hematite flooding.

We have also investigated a cabochon of what is termed 'magpie potch', also from Lightning Ridge. This material comprises clasts of host sandstone within a complex vari-coloured matrix of caramel potch, black potch, whte potch and crystal opal.

In terms of trace elements, there are a wide range of differences between the rhyolite-hosted and tuff-hosted opals. However, their Ba content is 39 and 80 ppm respectively, clearly within the volcanic opal field of < 110 ppm. In addition, their Ca contents are 566 and 2064 ppm respectively, above the average content for sedimentary opal. However, their Zr/Hf of 31.6 and 34.2 fall at the higher value for published sedimentary-origin Lightning Ridge opals of 29.2-31.7. Compared to classic 'sedimentary opal' from Lightning Ridge, they are much lower in Ti, Cr, V, Rb, Zr, and Hf, but have comparable Sn and Gd. On chondrite-normalised diagrams, they have relatively flat curves but with significant negative Ce and Eu anomalies which again suggests that they are volcanic in origin. The tuff-hosted opal also has significantly high Li (124 ppm), and is also more enriched in Be, Sc, Ti, V, Cr, Co, Ni, Cu, Ga, Rb, Sr, Y, Zr, Nb, In, Sn, Sb, Ta, W, Tl, Pb, Bi and Th compared to the rhyolite-hosted opal which is more enriched in P, Zn, As, Cd, Cs and U. However, overall they are similar and have sub-parallel CN curves.

These results suggest that there is at least a minor component of volcanic origin opal within the dominantly sedimentary origin Lightning Ridge field. A number of authors have described distinctive former glass shards in thin-sections from the Griman Creek Formation, Suggesting that it is at least partially volcanic in origin, perhaps a partially reworked tuff. The field also contains abundant petrified wood.

Key words opal, volcanic, sedimentary, trace elements, Lightning Ridge

LOCAL PROCUREMENT OR LONG-DISTANCE EXCHANGE? A NEW TECTONIC-GEOCHEMICAL PROVENANCE FRAMEWORK FOR PREHISTORIC JADE ARTIFACTS BASED ON LI–BE–δCE

Yuefeng Zhang[1], Jiong Yang[1, 6], Zhili Qiu[1*], Mo Wu[1, 4], Xianzi Gu[1, 8], Han Luo[1, 9], Lifeng Zhong[2], Fengchun Li[7], Hui Wang[3, 5], Guoke Chen[3], Zhichao Liu[1] and Kangyou Huang[1]

1. School of Earth Sciences and Engineering, Sun Yat-sen University, Zhuhai 519082, China.

2. Southern Marine Science and Engineering Guangdong Laboratory (Zhuhai), Zhuhai 519082, China

3. Gansu Provincial Institute of Cultural Relics and Archaeology, Lanzhou 730000, China

4. Guangdong Museum, Guangzhou 510623, China

5. Institute of Archaeological Science, Fudan University, Shanghai 200433, China

6. School of Tourism, Taishan Research Institute, Taishan University, Tai'an 271000, China

7. Testing Center of Shandong Bureau of China Metallurgical Geology Administration, Jinan 250014, China

8. Shanghai Museum, Shanghai 200003, China

9. The Palace Museum, Beijing 100009, China

Abstract The question of "local procurement" versus "long-distance exchange" is a central and pressing issue in Chinese jade archaeology. However, traditional provenance methods either rely heavily on subjective experience or are highly destructive. Meanwhile, recently proposed machine learning discrimination methods are highly dependent on database completeness and lack grounding in geological principles, falling into the dilemma of "black-box" models. This study aims to reveal the intrinsic relationship between the chemical composition of jade materials and their ore-forming tectonic settings, providing a new research framework to address these issues. We employed near-non-destructive laser ablation inductively coupled plasma mass spectrometry (LA-ICP-MS) technology to systematically analyze 352 carbonate-related nephrite (C-nephrite) samples from 15 key deposits across East Asia. The study reveals that fine-grained tremolite (Tr-II), the major mineral in C-nephrite from different tectonic units, exhibits significant systematic differences in lithium (Li) and beryllium (Be) contents and cerium (Ce) anomaly characteristics. These variations in Li-Be-δCe signatures are primarily controlled by the source of ore-forming hydrothermal fluids, the depositional age and environmental conditions of the carbonate host rocks, making them reliable "tectonic-geochemical fingerprints" that reflect their mineralization tectonic units. Accordingly, we classify East Asian C-nephrite into three types: North China Craton type (NCC-type): characterized by low Li (< 1.5 μg/g), high Be (> 6 μg/g), and no Ce anomaly (e.g., Xiuyan, Liaoning); Yangtze Craton type (YC-type): characterized by high Li (> 6 μg/g),

low Be (< 1.5 μg/g), and strong negative Ce anomaly (e.g., Liyang, Jiangsu; Luodian, Guizhou); Phanerozoic Orogenic Belt type (POB-type): showing intermediate Li-Be contents (satisfying 1.5×Li-7.5 < Be < 6×Li+6) and generally no Ce anomaly (e.g., Hetian, Xinjiang; Mazongshan, Gansu). This classification system provides a scientific discrimination framework for archaeological provenance. By comparing the "tectonic-geochemical fingerprint" of an excavated jade artifact obtained through LA-ICP-MS analysis with the "tectonic domain" of its excavation site, it becomes possible to scientifically determine whether it was locally sourced or transported over a long distance. The method is near-nondestructive, interpretable, and reliable, offering substantial potential for decoding prehistoric jade circulation paths and reconstructing early "Jade Roads", and it may open a new research paradigm for East Asian jade archaeology. Moreover, this methodological approach can provide valuable insights for provenance studies of serpentinite-related nephrite (S-nephrite) and other precious gemstone artifacts.

Key words Carbonate-related nephrite, Tectonic-geochemical fingerprint, Li-Be-δCe, Provenance, Local sourcing, Long-distance transport

NON-DESTRUCTIVE TESTING AND TRACEABILITY OF PEARLS BASED ON MICROWAVE RESONANCE AND X-RAY MICRO-COMPUTED TOMOGRAPHY

Yuan Sun[1], Hongcai Chen[2], Zhonghua Song[3], Jianxia Ye[4] , Zelong Chen[1]

1. Key laboratory of non-ferrous metal oxide electronic functional materials and devices (Guilin University of Technology), Education Department of Guangxi Zhuang Autonomous Region, MOE Key Laboratory of New Processing Technology for Nonferrous Metals and Materials,Guilin University of Technology, Guilin 541006, China

2. Beihai Product Quality Testing Institute, Beihai 536000, China

3. National Gems & Jewelry Testing Co. Ltd. , Beijing 100013, China

4. Beihai Intellectual Property and Quality Service Center, Beihai 536000, China

Abstract As a precious organic gemstone, the genetic identification, quality evaluation, and geographic origin traceability of pearls have long been critical topics in the field of gemology, which directly determine the commercial value of pearls and the standardized development of the industry. With the continuous innovation of modern pearl culture technology, a large number of non-bead freshwater cultured pearls and new types of bead-cultured pearls have emerged in the market. Conventional X-ray radiography, limited by structural overlap in two-dimensional (2D) imaging, has greatly increased difficulty in identifying the subtle internal structural features of pearls, making it difficult to meet the demand for high-precision identification. Meanwhile, characteristic saltwater pearls represented by Chinese Nanhai pearls (Nanzhu) are facing industry pain points such as an imperfect anti-counterfeiting traceability system and difficulty in verifying geographic origin. Therefore, there is an urgent need to establish an integrated, high-precision non-destructive testing technology system. To address the above issues, this study proposes an integrated method for pearl non-destructive testing and traceability combining microwave resonance detection and X-ray micro-computed tomography (μ-CT), aiming to achieve the dual objectives of high-precision imaging of pearl internal structures and extraction of identity characteristic parameters.

In this study, natural saltwater pearls, natural freshwater pearls, saltwater cultured pearls, non-bead/bead-cultured freshwater pearls, and Nanzhu from the Beibu Gulf were taken as the research objects. For microstructural characterization, X-ray micro-computed tomography (μ-CT) was applied. Based on the differential X-ray absorption by materials, this technology realized micron-level visualization of the internal structure of pearls (with a spatial resolution up to 4 μm) through multi-angle scanning and 3D reconstruction algorithms. Compared with conventional X-ray radiography that can only provide 2D compressed images, μ-CT can clearly reveal key identification features, including the unique onion-like

nacreous layer structure and tiny organic core of natural pearls, the typical "beard-like" twisted cavities of non-bead freshwater cultured pearls, and the demarcation line between the bead nucleus and nacreous layer of bead-cultured pearls, effectively solving the problem of feature blurring caused by structural overlap in 2D images.

For microwave resonance-based traceability, Nanzhu was taken as the main research object. Based on the "quark" dynamic model and string wave equation, this study utilized the resonance effect generated by the coupling between microwave electromagnetic force and different material components in Nanzhu (aragonite, calcite, organic matrix, etc.). A fluctuation model describing the unique characteristic parameters of Nanzhu identity was established through the variation law of amplitude and power spectral density, and a millimeter-wave-based non-invasive pearl traceability detection system was developed. Under the synergistic effect of light waves of specific wavelengths and microwaves, the unique characteristic parameters of each Nanzhu were extracted and an identity code (Pearl ID) was generated, realizing the accurate traceability of "one code per pearl". It has been verified that the accuracy of identity authentication for per 10,000 pearls reaches over 98%.

The synergistic application of the two technologies can break through the limitations of single-dimensional traditional detection technologies, effectively distinguish natural pearls from bead/non-bead cultured pearls, and realize accurate traceability of pearls from specific producing areas such as Nanzhu. This study provides technical support for pearl quality inspection, anti-counterfeiting traceability, and industrial standardization. Future research will further expand the pearl sample database covering different producing areas and categories, optimize the feature discrimination criteria and traceability algorithms, and promote the large-scale application of this technology in gemstone testing institutions and the industrial end.

Key words Pearl, Microwave Resonance, X-ray Micro-computed Tomography, Non-destructive Testing, Traceability

Acknowledgements This work is supported by the Guangxi Science and Technology Program (Guike XT2600870042) and Open Fund Project (24KFGMY-03).

THE KIMBERLEY PROCESS AND THE GLOBAL GOVERNANCE OF NATURAL ROUGH DIAMOND TRADE: INSTITUTIONAL POWER, MARKET ACCESS, AND THE INTEREST STRUCTURE OF NON-RESOURCE NODE STATES

Liang Weizhang, Qiu Zhili*

School of Earth Science and Engineering, Sun Yat-Sen University, Zhuhai 519082, China

Abstract The Kimberley Process Certification Scheme (KPCS) is more accurately understood as a certification-based arrangement for the governance of mineral trade than as a narrowly defined compliance mechanism directed only at "conflict diamonds." Existing scholarship has examined the internationalization of the conflict diamonds issue, the formation of the Kimberley Process, and the normative and implementation limits of the KPCS, yet the scheme is still often treated primarily as an instrument of conflict management. Such a reading is too limited to capture its wider institutional role in organizing the legal circulation of natural rough diamonds in the international market. Through the institutional combination of participation status, certificate accompaniment, and inter-member trade restrictions, legality is converted into a condition of market access, and state interests become embedded in a rule-based international trading order.

Qualitative institutional analysis, process tracing, and policy text analysis make it possible to identify how this governance arrangement operates and how it distributes interests. The relevant materials include United Nations resolutions, KPCS core documents, World Trade Organization waivers, the European Union implementing regulation, Chinese customs regulations, official Kimberley Process statistics, participant materials, and academic and policy literature. The central concern is not the net trade effect of the KPCS as such, but the way in which a certification-based trade-governance mechanism generates distributive consequences by organizing legality, access qualifications, and institutional participation. Four dimensions of institutional power emerge from this structure: rule-definition power, market-access power, interpretive power, and reform influence.

Several findings follow from this framework. First, the KPCS does not merely identify and exclude conflict-related goods. More fundamentally, it institutionalizes the legal trading status of natural rough diamonds and reconstructs the conditions under which rough diamonds can circulate internationally. Its significance therefore lies not only in conflict prevention, but also in the governance of legal market access for a high-value mineral commodity. Second, competition within the KPCS is not best understood as competition over resource possession alone. More important are struggles over who defines the boundary of "conflict diamonds," who remains inside the legal trading network, who interprets implementation standards, and who influences the future direction of institutional reform. The politics of

the KPCS are therefore more usefully understood as struggles over institutional power within a trade-governance framework than as simple disagreements over compliance.

The position of China helps clarify how such a system generates interests for participants that lack major upstream resource advantages but occupy important places within global trade networks. Dependence on external compliant supply, the mainland–Hong Kong composite trade-node structure, and sustained participation in Kimberley Process institutions together produce clear interests in market access, chain security, and rule participation. In this setting, the significance of the KPCS is not exhausted by formal compliance. Equally important are continued access to legal supply channels, maintenance of key trade and processing nodes, and participation in processes of institutional interpretation and adjustment. Interests in the governance of natural rough diamonds thus derive not only from resource possession, but also from access to compliant markets, nodal positioning, and institutional embeddedness.

The implications of diamond governance extend beyond the certification of natural rough diamond origins. The rise of synthetic diamonds points toward a broader governance space involving substitute materials, production capabilities, end-use boundaries, and fragmented compliance regimes. The KPCS accordingly belongs within a wider analytical framework concerned with the international governance of mineral resources, the ordering of global trade, and the distribution of institutional power.

Key words Kimberley Process, natural rough diamonds, certification-based trade governance, institutional power, non-resource node states

COLLECTION AND CURATION OF TYPE SPECIMENS OF NEWLY DISCOVERED MINERAL SPECIES IN A GEOLOGICAL MUSEUM: A CASE STUDY

Xiao-Nan Yang, Ze Shen, Ying Ye, Zhu-Nan Geng, Qing-Pei Ye, Jing Li, Liang-Feng Yang*

The Geogogical Museum of China, Beijing 100034, P. R. China

Abstract Type specimens of newly discovered mineral species serve as permanent reference samples for the definition of mineral species, and a standardized collection and management process in a geological museum is essential for subsequent research and material sharing. The Geological Museum of China, which undertakes the responsibilities of acquisition, registration, preservation, and curation of geoscience specimens, has systematically accessioned type specimens of over 120 mineral species originally discovered in China. To further enhance the management and utilization of these mineral type specimens, the museum has implemented four key measures based on recent study and practice: (1) establishing a new numbering system and an information-based retrieval workflow for newly discovered mineral species; (2) formulating management protocols for collaborative research including sampling and analysis of accessioned specimens; (3) introducing streamlined approval procedures for further studies of accessioned mineral specimens; and (4) organizing thematic exhibitions on new mineral studies to strengthen public science education with representative newly discovered mineral species. These measures have effectively resolved issues such as ambiguous specimen numbering, cumbersome procedures for accessioned specimen sampling and research, difficulty in obtaining type mineral specimens for necessary studies, and public unawareness of new discoveries of mineral species. As a result, they ensure the safety of museum collections while promoting the unlocking of the scientific value of significant specimens. Practice demonstrates that this collection and curation management model, jointly driven by institutionalization and informatization, provides a replicable paradigm for the management of mineral type specimens in specialized museums.

Key words Mineral type specimens, Mineral collection, Collection management, Promoting Research, Mineral curation

INVESTIGATION OF SILICEOUS MATERIALS IN HISTORICAL PIETRA DURA: A COMPARATIVE STUDY OF PORTABLE AND LABORATORY ANALYTICAL APPROACHES

ŠTĚPÁN JAROMĚŘSKÝ[1], RICHARD PŘIKRYL[1], ADAM CULKA[1], FILIP KOŠEK[1] & MARTIN RACEK[2],

1. Institute of Geochemistry, Mineralogy and Mineral Resources, Faculty of Science, Charles Univesity, Albertov 6, 128 43, Prague 2, Czech Republic

2. Institute of Petrology and Structural Geology, Faculty of Science, Charles University in Prague, Albertov 6, 128 43 Prague 2, Czech Republic

Abstract Artworks created using the Pietra Dura mosaic technique represent a unique intersection of artistic craftsmanship and natural materials in the form of coloured minerals and rocks. These materials were carefully selected in order to achieve the specific aesthetic effects that are characteristic of this technique. Among the studied materials are jaspers, valued for their wide range of colours and textures as well as their high hardness. Despite their relatively frequent occurrence in historical objects, the mineralogical characterisation of these materials remains limited, particularly with regard to their provenance and the identification of potential source localities. A better understanding of the mineralogical composition of jaspers used in historical artefacts may therefore contribute both to studies of material provenance and to the development of appropriate conservation and restoration process.

This study focuses on the characterisation of jasper materials from selected European localities that may have served as sources of raw material for the production of Pietra Dura objects in Central Europe, particularly during the late sixteenth and early seventeenth centuries, when a prominent workshop led by the Castrucci family operated in Prague. The primary objective of this research is to link non-destructive analyses carried out directly on historical artefacts with detailed laboratory investigations of reference samples from potential source regions. This integrated approach enables a better understanding of the mineralogical composition, colouring impurities and genetic characteristics of jasper materials, while also identifying diagnostic features that may help relate historical objects to specific geological sources.

The analysis of historical artefacts is based primarily on non-destructive methods. Portable Raman spectroscopy, handheld X-ray fluorescence, and spectrophotometric colour measurements were employed to characterise the mineralogical composition and colour variability of SiO_2 materials directly on the investigated objects. The data obtained from these measurements were subsequently compared with analytical results from reference samples originating from historically important jasper localities in Central and Southern Europe, particularly in the Czech Republic, Germany and Italy.

Reference materials were subjected to more detailed laboratory analyses. Polished thin sections were

prepared from selected samples and examined using optical microscopy in both transmitted and reflected light, providing fundamental information on rock texture, grain size and arrangement, as well as the presence of pigmenting mineral phases. The mineralogical composition was further investigated using powder X-ray diffraction performed on powders prepared from differently coloured portions of the jasper samples. Detailed information on microstructure and chemical composition was obtained using scanning electron microscopy combined with elemental mapping. The identification of individual mineral phases was subsequently verified using Raman spectroscopy, which enables the discrimination of SiO_2 polymorphs and associated minerals based on their characteristic vibrational spectra.

The combination of these analytical approaches provides a comprehensive insight into the mineralogical composition, texture and genesis of the studied materials. At the same time, it allows the interpretative potential of portable analytical methods to be compared with detailed laboratory results and their applicability in cultural heritage research to be evaluated.

This research revealed a complex mineralogical composition of the investigated jasper materials, dominated by microcrystalline SiO_2 with variable contributions of iron-bearing phases responsible for the characteristic red, brown and green colouration. Comparative analysis of reference materials indicates that certain mineralogical features may serve as potential indicators of specific mineralogical deposits. These preliminary results demonstrate the potential of integrating non-destructive and laboratory-based analytical approaches for a deeper interpretation of microcrystalline SiO_2 materials used in historical Pietra Dura objects.

Key words jasper, Pietra Dura, silica, cultural heritage

Acknowledgements This research is part of Štěpán Jaroměřský's doctoral study under the supervision of Prof. Richard Přikryl. The study was financially supported by the Charles University Grant Agency under project no. 456725. The authors would like to express their sincere gratitude to the Lobkowicz family and to the management of the Lobkowicz Collections for granting access to the artefact and for enabling the research to be conducted. The authors also extend their sincere gratitude to the Museum of Decorative Arts in Prague for granting access to the artefact and facilitating this research.

WORKING IN A SYSTEMATIC MINERAL COLLECTION – A NEVER ENDING STORY!

Jörgen Langhof

Department of Geosciences, Swedish Museum of Natural History, Box 50007, 104 05 Stockholm, Sweden

Abstract How to build up, maintain and expand a systematic mineral collection from a museum point of view is of course not an easy question to answer. History, laws and regulations, traditions, national geology, collecting tradition, mining, education etc are key words to describe what affects the possibility to perform the work in a systematic mineral collection, wherever you are situated around the globe. Of course there are no strict rules or easy roads to build up and expand a systematic collection. Questions like; acquisition by field collecting, trade, exchange, gifts etc., de-acquisition by sorting out, reduction of specimens, exchange etc. are always following staff involved in this work. Some main issues will be touched upon in this talk, reflecting the authors personal experience from working in a systematic mineral collection for more than twenty-five years.

Key words minerals, collection, aquisition

NON-DESTRUCTIVE TESTING OF JADE ARTIFACTS FROM THE DAWENKOU-LONGSHAN CULTURE IN THE COLLECTION OF SHANDONG MUSEUM AND A DISCUSSION ON THEIR PROVENANCE

Yang Jiong[1, 3], Zhou Ena[2], Qiu Zhili[3], Zhang Yuefeng[3], Bai Dongzhou[3], Sun Qirui[4]

1. School of Tourism// Taishan Jade and Stone Research Institute, Taishan University, Tai'an 271000, China

2. Shandong Museum, Ji'nan 250014,China

3. School of Earth Science and Engineering, Sun Yat sun University//Southern Marine Science and Engineering Guangdong Laboratory (Zhuhai) , Zhuhai 519082, China

4. Shandong Provincial Institute of Cultural Relics and Archaeology, Ji'nan 250000, China

Abstract The typological study of archaeological artifacts suggests that the prehistoric Hai Dai archaeological cultural area was an important transit station for the northward transmission of jade and the westward transmission of jade during Longshan culture period. However, the research on the sources of jade materials and the specific time and path of jade cultural exchanges during the Dawenkou - Longshan culture period is relatively weak. This paper conducts non-destructive tests on 102 pieces of ancient jade artifacts unearthed during the Dawenkou - Longshan culture period in Shandong Museum, using portable infrared spectroscopy (FTIR) and handheld energy dispersive X-ray fluorescence spectrometer (P-XRF). The results show that jade artifacts during the Dawenkou - Longshan culture period were mainly composed of various materials such as amphibole jade, serpentine jade, etc; among them, the proportion of tremolite - actinolite jade of Dawenkou culture was 61.8%, and serpentine jade accounted for 31.5%; the proportion of tremolite and actinolite jade of the Longshan culture was 61.5%, and serpentine jade accounted for 38.5%; the origin of jade materials of amphibole jade was of contact - alteration type of marble. The amphibolite jade deposits were formed by contact metasomatism of marble, and Serpentine jade artifacts can be divided into two distinct genetic types: magnesium - rich marble contact metasomatic metamorphism (M - type) and ultrabasic rock hydrothermal alteration (U - type); the Fe, Cr, Ni contents of the serpentine jade were relatively high, and there were more magnetite inclusions, with strong magnetism, and the Cr/Ni ratio was generally less than 1 (most less than 0.7), etc., which are consistent with the characteristics of Taishan serpentine jade. So, it is speculated that the jade materials of this type were sourced from the Taishan jade mine on-site. The composition of the marble-type (M - type) serpentine jade cannot currently be determined with accuracy of its exact source, but it has very fine structural characteristics and strong whitening features, and its characteristics are consistent with Hongshan culture jade artifacts. The above test results further indicate that the jade mine resources in Taishan began to be used as late as the middle and late stages of the Dawenkou culture; considering that

no nephrite jade mines (including ancient nephrite jade sites) have been discovered in the Hai Dai area, and the geographical relationship between the Liaodong Peninsula and the Shandong Peninsula, and Liaoning Xiuyan jade has both nephrite jade and serpentine jade belong to M - type, it was deduced that some jade materials in the Hai Dai area might be related to the Liaodong Peninsula, which is nearly one thousand kilometers away. Apart from Taishan jade, Junan jade, Laiyang jade, and Laoshan jade also belongs to serpentine jade materials, indicating that in addition to local and nearby sourcing, there are also distant sources of jade materials, but further testing data of jade materials is needed for confirmation. The research results provide mineralogical evidence for the understanding that the Hai Dai region might have been an important area for jade artifact exchanges during the middle and late Neolithic period.

Key words Unearthed jades, Dawenkou - Longshan culture, non-destructive testing, provenance of jade materials, Shandong Museum

2D AND 3D ZEOLITES CONTAINING TETRAHEDRAL LAYERS WITH THE APOPHYLLITE-TYPE TOPOLOGY: POLYMORPHISM, POLYTYPISM, AND SYSTEMATICS

Sergey M. Aksenov

FRC Kola Science Centre RAS, Russia

Abstract Materials related to apophyllite are of significant industrial and technological interest because they are analogs of natural single-layer silicates. The varying orientation of tetrahedra relative to the tetrahedral layer plane, which determines the formation of structural isomers, creates prerequisites for their combination into multilayer tetrahedral polyanions (up to zeolite-type tetrahedral frameworks). Among compounds containing such multilayer polyanions, the most representative are those based on layers with the apophyllite-type topology. These layers combine either directly through layer-by-layer (topotactic) stacking or *via* additional tetrahedra linking adjacent layers. Furthermore, several compounds feature tetrahedral frameworks in which layers with the apophyllite-type topology can also be distinguished. The discovery of the first three-layer silicate, gunterblassite, made it possible to establish a fundamental crystal-chemical relationship between microporous silicate minerals and synthetic materials containing silicate layers with apophyllite-like topology.

The most representative family consists of silicates containing tetrahedral layers $[Si_4O_9(OH)]^{3-}$ and $[Si_4O_{10}]^{4-}$, found in the crystal structures of the mineral shlykovite and cryptophyllite. Such layers were first discovered as part of double layers in the structures of minerals of the rhodesite group and their synthetic analogs. The discovery of shlykovite and cryptophyllite confirmed the general topological and stereoisomeric features of these layers, as well as the possibility of their condensation to form multilayer silicate polyanions. The formation of double-layer polyanions can be represented as the polycondensation of shlykovite-type layers through free apical vertices ($Ø^{ap}$) of tetrahedra oriented in opposite directions, leading to the formation of rhodesite-type double layers.

Further direct condensation of shlykovite-type layers is unlikely (or extremely rare), therefore polycondensation mechanisms were not considered for a long time. Possible transformation pathways, using the synthetic K,Sr-analog of rhodesite (AES-19) as a model, involved the extraction of alkaline earth elements from the original structure followed by topotactic condensation of rhodesite-type double layers. Based on the assumptions described above, a model of a hypothetical framework structure was proposed; however, to date, it has not been realized in either natural or synthetic compounds.

The determination of the crystal structure of the mineral gunterblassite revealed for the first time a three-layer polyanion retaining the apophyllite-type topology. This structure is formed by inserting an additional TO_4 tetrahedron between the single $[T_4O^{br}_6Ø^{ap}_4]$ layers of the shlykovite/cryptophyllite type

and the double [$T_8O^{br}_{13}Ø^{ap}_6$] layers of the rhodesite type, leading to the formation of a triple layer [$T^{add}T_{12}O^{br}_{23}Ø^{ap}_6$] of the gunterblassite type. The günterblassite condensation mechanism (insertion of additional tetrahedra) suggests a pathway toward silicates with extended tetrahedral blocks (with more than three shlykovite-type layers) and, ultimately, zeolite-like frameworks (**EDI**, **THO** or **NAT** types).

The prepared review by Aksenov et al. (2025) details the significant potential of apophyllite-type layers as versatile building blocks for creating both two-dimensional and three-dimensional zeolitic materials. The unique reactivity of these natural single-layer silicates, expressed in their ability to form hybrid organosilicate polymers with tunable hydrophobic-hydrophilic properties, underscores their industrial importance. Moreover, the discovery of multilayer analogs, such as gunterblassite, was key, as it revealed a fundamental crystal-chemical relationship unifying different families of microporous minerals and synthetic zeolites.

Based on the identified patterns, a classification scheme is presented, founded on the topological and symmetry differences of apophyllite-type layers. This system provides a much-needed method for categorizing and classification known materials and serves as a predictive tool for the targeted synthesis of new zeolites. The modular nature of these layers, demonstrated in various synthesis strategies, opens up a vast design space for hierarchical porous materials with predefined diffusion pathways and active site distributions.

Key words apophyllite, rhodesite, günterblassite, topology, modularity

Acknowledgements This research was funded by the Ministry of Science and Higher Education of Russia (grant agreement No. 075-15-2025-585).

A NEW FORMULA FOR TERLINGUACREEKITE

Marcus J. Origlieri[1], Shiyun Jin[2], Milan Gembick´y[3], and Michael L. Shannon[4]

1. Mineral Zone, 1370 N. Silverbell Road, Suite 140, Tucson, Arizona 85745 U.S.A.

2. Gemological Institute of America, 5345 Armada Drive, Carlsbad, Califor nia 92008 U.S.A.

3. Department of Chemistry, University of California at San Diego, La Jolla, California 92093 U.S.A.

4. Shannon Family Minerals, 1013 N. Palm Street, Gilbert, Arizona 85234 U.S.A.

Abstract Terlinguacreekite is an exotic mercury mineral found in the Mariposa mine, Terlingua, Texas, U.S.A. (Roberts et al. 2005), its type locality, and also in the McDermitt mine, Nevada, U.S.A. (Dunning et al. 2019). This multi-method in vestigation of co-type terlinguacreekite proposes a new formula for the species. While originally assigned the ideal formula $Hg_3^{2+}O_2Cl_2$, terlinguacreekite con tains essential nitrogen, undetected by electron microprobe. Raman spectra of terlinguacreekite show modes consistent with N–Hg stretching but not those typical of Hg–O stretching (Cooper et al. 2013). An X-ray diffraction study of a tediously selected 25 × 25 × 45 μm single crystal found a *C*-centered monoclinic unit cell: a = 26.1356(12) Å, b = 6.6797(3) Å, c = 11.0849(5) Å, β =102.265(2)°, V = 1891.01(15) Å^3. The crystal yielded an intensity dataset spanning indices $\overline{37} \le h \le 37$, $\overline{9} \le k \le 9$, $\overline{15} \le l \le 15$, with maximal res olution 0.70 Å. Terlinguacreekite exhibits pronounced orthorhombic pseudo symmetry associated with pervasive twinning by reflection on (100). The crys tal structure solved with *C*2/*m* symmetry, which after implementing a twin model, refined to R_{all} = 0.0598 for 3137 unique reflections. Fundamental build ing blocks of the crystal structure consist of anion-centered NHg4 tetrahedra with r(N–Hg) = 2.04–2.14 ˚ A and edge lengths r(Hg–Hg) = 3.31–3.44 ˚ A. Four nonequivalent NHg_4 tetrahedra polymerize into microporous double sheets of $[N_4Hg_9]_n^{6+}$ stoichiometry stacked ∥ **a***. Two independent Cl^- terminate non bridging Hg atoms and one further disordered Cl^- in the interlayer together af ford weak interactions between sheets. Commodious $N_{12}Hg_{15}$ cages enclose split Hg atoms and their first coordination spheres, $HgCl_5$ trigonal bipyramids, which assemble into infinite chains of $[HgCl_4]_n^{2-}$ stoichiometry ∥ c. Fittingly the b di mension of terlinguacreekite matches the *c* dimension of comancheite (6.6976 Å, Cooper et al. 2013) and also that of gaildunningite (6.6840 Å, Cooper et al. 2019), which correspond to *dreier* periodicities along extended chains of NHg_4 tetrahedra. Although first described as a mercury oxychloride, terlinguacreekite is instead a mercury nitride chloride with unit cell content $4[N_4Hg_9][HgCl_4]Cl_4$ or ideally $Hg_5^{2+}N_2^{3-}Cl_4$ with Z = 8.

ATOMIC-RESOLUTION OBF-STEM IMAGING OF LAYERED AND MULTIPLE-CHAIN SILICATES IN CROCIDOLITE ASBESTOS

Ichiro Ohnishi

JEOL Ltd., 3-1-2 Musashino, Akishima, Tokyo, 1996-8558

Abstract Crocidolite asbestos is known for its extremely fine and highly elongated asbestiform morphology, which contributes to its persistence in the human body and its higher toxicity compared with other asbestos types. Previous studies have suggested that the presence of multiple-chain silicates and sheet silicates within crocidolite plays an important role in promoting fibrillation, because these silicate species can act as structural defects that weaken the amphibole framework. However, detailed structural observation of these phases has long been hindered by their strong susceptibility to electron-beam damage.

The recent development of optimum bright-field scanning transmission electron microscopy (OBF-STEM) has enabled low-dose atomic-resolution imaging of beam-sensitive materials such as zeolites. In this study, OBF-STEM was applied to cross-section specimens (~10–20 nm thick) of crocidolite asbestos prepared by ion milling. Observations were conducted using an aberration-corrected 300 kV STEM (JEM-ARM300F2) equipped with an eight-segment detector, with a probe current of ~4 pA to minimize beam-induced damage. This approach allowed us to obtain damage-free atomic-resolution images of the amphibole fibrils and the associated defect phases.

The crocidolite sample consists of numerous small amphibole fibrils, and abundant sheet silicates were found within the inter-fibril spaces. Atomic-resolution OBF-STEM images clearly resolved all atomic columns, including oxygen. The sheet silicate exhibits a basal spacing of 0.9 nm and shows no evidence of interlayer cations, which is consistent with a talc-like structure. Compositional analysis using energy-dispersive X-ray spectroscopy at low magnification shows that this phase is enriched in Mg and depleted in Fe and Na, further supporting its identification as talc. In addition, the (010) interface between amphibole and the sheet silicate is atomically sharp, and the two structures share oxygen and sodium columns across the boundary, suggesting a crystallographically coherent interface.

OBF-STEM imaging also revealed the presence of multiple-chain silicates—triple-chain and higher order—within the crocidolite amphibole structure. These chain variants coexist with the double-chain amphibole structure and form a variety of defect configurations, indicating that crocidolite contains a more complex network of silicate units than previously recognized. The abundance of these defects suggests that they may locally weaken the amphibole structure and facilitate fragmentation into extremely thin fibrils.

The results of this study demonstrate that OBF-STEM is highly effective for characterizing the

atomic-scale structure of beam-sensitive asbestos samples, enabling direct observation of defect-forming silicate species previously inaccessible by conventional TEM. The findings support a mechanism in which layered silicates and multiple-chain silicates contribute to the mechanical weakening and fibrillation of crocidolite, thereby helping to explain its characteristic high aspect ratio and associated health risk. The presentation will further discuss the diversity of defect structures identified by OBF-STEM in crocidolite and their implications for the formation processes of asbestiform amphiboles.

Key words Asbestos, Crocidolite, Amphibole, Talc, OBF-STEM

CRYSTAL CHEMISTRY OF AXINITE-(MN)–TINZENITE SERIES MINERALS FROM THE VAL GRAVEGLIA MANGANESE DISTRICT (ITALY), AND RELATIONS WITH AXINITE-GROUP MINERALS

Giovanni B. Andreozzi[1,2], Ferdinando Bosi[1,2], Ulf Hålenius[3], Alessandra Altieri[1], Marco E. Ciriotti[4,5]

1. Department of Earth Sciences, Sapienza University of Rome, Rome, Italy

2. CNR-IGAG c/o Department of Earth Sciences, Sapienza University of Rome, Italy

3. Department of Geosciences, Swedish Museum of Natural History, Stockholm, Sweden

4. AMI - Associazione Micromineralogica Italiana, Devesi-Ciriè, Torino, Italy

5. Department of Earth Sciences, Università degli Studi di Torino, Torino, Italy

Abstract Fifteen Mn-rich axinite samples from the Val Graveglia Manganese District (Liguria, Italy) were investigated by electron microprobe and single-crystal X-ray diffraction to define the crystal chemistry of the axinite-(Mn)–tinzenite solid solution. The samples span the full compositional range between the two endmembers (5–83 mol% tinzenite) and are described by the general crystal-chemical formula: $^{X1}Ca_2{}^{X2}(Ca_{2-x}Mn^{2+}{}_x)^{Y}(Mn^{2+}{}_{2-w}Mn^{3+}{}_w)^{Z1}(Al_{2-y}Mn^{3+}{}_y)^{Z2}Al_2{}^{T5}B_2{}^{(T1-4)}Si_8O_{30}(OH_{2-w}O_w)$, where $0 \le x \le 2$ apfu, $0 \le w \le 0.1$, and $0 \le y \le 0.2$.

Unit-cell parameters *a*, *b*, *c*, and *V* increase linearly from axinite-(Mg) to axinite-(Fe) to axinite-(Mn) due to occupancy of the *Y* site by the larger divalent cations Fe^{2+} and Mn^{2+} (up to 2 apfu), whereas they decrease sharply from axinite-(Mn) to tinzenite, that is for $Mn_{tot} > 2$ apfu, due to incorporation of the additional Mn^{2+} at *X*2 site replacing Ca. The unit-cell contraction, particularly along the **b** axis, reflects the coupled cation substitutions involving $^{X2}Mn^{2+}$ and $^{Z1}Mn^{3+}$.

Structural analysis reveals that the cation distribution correlates with the relative size and distortion of the coordination polyhedra, with cations with larger ionic radii preferentially occupying the larger and more distorted octahedra. The structural site *X*1 is fully occupied by Ca, whereas *X*2 hosts variable amounts of Ca and Mn^{2+}, which control the evolution from axinite-(Mn) to tinzenite. The *Y* site is dominated by Mn^{2+}, and both *Z*1 and *Z*2 sites are dominated by Al. Minor contents of Mn^{3+} are present, mainly ordered at the *Z*1 site, with Mn^{3+} partially substituting Al and showing the same substitution mechanism and ordering arrangement previously observed for Fe^{3+} in (Fe,Mn)-axinite samples. For all samples, the Mn^{3+}/Mn_{tot} ratio averages ~8%, a value that is consistent with sub-oxidizing metamorphic conditions. Homogeneous compositions are only observed near the endmembers, whereas most intermediate samples display strong chemical zoning, with axinite-(Mn)-rich cores and tinzenite-rich rims. The observed zoning recorded a progressive Mn enrichment and Ca depletion during late-stage re-equilibration under decreasing temperature conditions.

The mineral assemblage observed in the Val Graveglia Manganese District [braunite + axinite-(Mn) or tinzenite + quartz ± rhodonite ± piemontite ± carbonates] formed under sub-oxidizing conditions,

within the prehnite–pumpellyite to lower greenschist facies. Results obtained indicate that axinite-group minerals can record subtle variations in redox state and Ca activity during low-grade metamorphism, providing potential structural proxies for Mn oxidation and fluid–rock interaction in metamorphosed Mn deposits.

Key words axinite-group minerals, tinzenite, crystal chemistry, Mn ore deposits, Val Graveglia

HYDROCALUMITE PUZZLE

Elena S. Zhitova

Institute of Volcanology and Seismology, Russian Academy of Sciences, Bulvar Piypa 9, Petropavlovsk-Kamchatsky 683004, Russia (laboratory of mineralogy)

Abstract Hydrocalumite is a hydrotalcite-supergroup mineral with the 90-year history. The currently accepted chemical formula of the mineral is $Ca_4Al_2(OH)_{12}(Cl,CO_3,OH)_2 \cdot 4H_2O$ and as it has been suggested in the hydrotalcite-supergroup nomenclature, that it may correspond to several mineral species: Cl-, CO_3- and OH-end-members. The recent investigation of hydrocalumite from Boisséjour (Puy-de-Dôme, France) undertaken by our group has shown the ordering CO_3 and Cl anion and their stoichiometric ratio as $Cl : CO_3 = 2 : 1$. This means that both anions play species-defining role in contrast to the previous suggestions on mono-anionic end-members and expands the number of potential mineral species that are currently named `hydrocalumite` to six. The crystal chemical study of hydrocalumite from Bellerberg volcano (Vordereifel, Germany) shows its structural difference from the Boisséjour sample by the unit-cell parameters, and, thus, polytype (that is previously unknown). Preliminary data indicate disordering of CO_3 and Cl anions. All this points to the need for a systematic crystal chemical study of hydrocalumite by joint efforts of different mineralogical scientific societies in deciphering the scientific puzzle. A special collaboration is required to find and study any specimen from the type locality Scawt Hill (Larne, County Antrim, Northern Ireland, UK) that are not currently mentioned in the Museum`s collections.

Key words hydrocalumite, layered double hydroxide, hydrotalcite, crystal structure polytype

OCTAHEDRAL CATION SUBSTITUTION MECHANISMS OF MONTMORILLONITE

Bao Cheng Guo[1,2], Jie Yang[1,2] Chun Hui Zhou[1,2]*

1. Research Group for Advanced Materials & Sustainable Catalysis (AMSC), State Key Laboratory of Green Chemical Synthesis and Conversion, College of Chemical Engineering, Zhejiang University of Technology, Hangzhou 310032, China

2. Anhui International Exchange and Cooperation Base, Qingyang Institute for Industrial Minerals, Youhua, Qingyang 242804, China

Abstract The hierarchy of octahedral cation substitution and the associated structural perturbations during low-temperature montmorillonite formation remain poorly constrained, despite the established influence of isomorphic substitution on layer charge and swelling behavior. Notably, our recent advances in quantifying the layer charge of synthetic smectites demonstrate that the measured charge is exquisitely sensitive to the specific substitution pathway, highlighting a fundamental gap: the mechanisms of cation competition and site occupancy during dioctahedral sheet crystallization are unresolved. To address this gap, a systematic hydrothermal synthesis of montmorillonite was conducted under rigorously controlled conditions of pH (9–12), temperature (90–200 °C), and precursor gel aging states (raw, dried, and calcined gels). A comprehensive suite of Mg-, Fe-, and Ni-doped specimens was prepared and characterized to probe local octahedral architecture, layer charge distribution, and interlayer expandability. Characterization techniques included X-ray diffraction, Fourier-transform infrared spectroscopy, ^{27}Al magic-angle spinning nuclear magnetic resonance, nitrogen physisorption, and transmission electron microscopy. This work provide critical constraints on the paragenetic conditions and cation incorporation pathways governing the formation of montmorillonite, thereby advancing the mechanistic understanding of dioctahedral smectite genesis in low-temperature geochemical environments.

Key words montmorillonite, isomorphic substitution, octahedral sheet, cation doping

Acknowledgements The authors wish to acknowledge the financial support from the National Natural Science Foundation of China (42572045; W2433034; 22072136). This work was also supported by the Central Government Guided Local Science and Technology Development Fund Project (No. 2025ZY01113), and by the projects from Qing Yang Institute for Industrial Minerals (KYY-HX-20220336; KYY-HX-20170557).

PROBING SITE OCCUPANCY IN MINERAL STRUCTURES VIA 3DED

Haiyang Xian[1,2,3*], Wenlin Yang[4], Yiping Yang[1,2,3], Jianxi Zhu[1,2,3]

1. State Key Laboratory of Deep Earth Processes and Resources, Guangzhou Institute of Geochemistry, Chinese Academy of Sciences, Guangzhou 510640, China

2. Guangdong Research Center for Strategic Metals and Green Utilization, Guangzhou 510640, China

3. Guangdong Provincial Key Laboratory of Mineral Physics and Materials, Guangzhou Institute of Geochemistry, Chinese Academy of Sciences, Guangzhou 510640, China

4. College of Materials and Chemistry and Chemical Engineering, Chengdu University of Technology, Chengdu 610059, China

Abstract Three-dimensional electron diffraction (3DED) is a crystallographic technique analogous to single-crystal X-ray diffraction (SCXRD). Compared with traditional SCXRD, this technique offers unique advantages in handling nanoscale and weakly diffracting samples. However, due to the significant dynamical effects inherent in electron diffraction, the intensities of diffraction spots obtained via this method are often inaccurate. Consequently, doubts remain regarding its ability to accurately identify common isomorphous substitution atoms in minerals. To evaluate the reliability of 3DED in addressing such scientific questions, we applied this technique to analyze the crystal structures of two mineral samples: rare-earth-bearing apatite and arsenic-bearing pyrite. In the apatite sample, the distribution and content of rare-earth elements across two Ca sites were determined. The results align with numerous reported experimental findings, confirming that light rare-earth elements (represented by Ce) exclusively occupy the Ca2 site. For the arsenic-bearing pyrite analysis, two types of pyrite were prepared—one with As substituting for S sites and the other with As substituting for Fe sites—followed by 3DED characterization of As occupancy and content. Although 3DED failed to accurately quantify As content in this experiment, it successfully identified the substitution of As for S and Fe atoms, with results consistent with XPS analysis. These findings demonstrate that 3DED holds unique value in mineral structural research, particularly excelling in identifying the occupancy of isomorphous substitution atoms. With future advancements in dynamical effect correction methods, 3DED is poised to become a vital tool for nanoscale mineralogical studies, providing critical structural insights into the mechanisms of isomorphous substitution.

Key words 3DED, site occupancy, apatite, arsenian pyrite, crystal structure

PROPOSAL FOR THE ESTABLISHMENT AND CLASSIFICATION OF THE WUMUITE SUPERGROUP

Xue Yuan, Sun Ningyue, Li Guowu

Science Research Institute, China University of Geosciences (Beijing), China

Abstract This proposal seeks the establishment of the Wumuite Supergroup, which currently comprises two mineral groups: the Wumuite Group and the Xianhuaite Group. Minerals assigned to the Wumuite Supergroup are defined by the following key characteristics: a general stoichiometric formula of A_xBX_3 (where $0 < x < 1$) and a typical tungsten bronze (TB) crystal structure. In this structure, *A*-site cations occupy structural channels, while *B*-site cations coordinate with *X* anions to form three-dimensional frameworks composed of corner-sharing BX_6 octahedra. While the Wumuite and Xianhuaite groups both adopt the tungsten bronze (TB) structure, they differ in their specific framework topologies. Minerals of the Wumuite Group exhibit the characteristic hexagonal tungsten bronze (HTB) structure, distinguished by the presence of hexagonal and triangular channels. This group includes wumuite and morningstarite. In contrast, minerals of the Xianhuaite Group possess the typical tetragonal tungsten bronze (TTB) structure, which is characterized by pentagonal, quadrilateral, and triangular channels; its members include xianhuaite-(Ce), xianhuaite-(La), and zuolinite. Although only five minerals are currently recognized as members of the Wumuite Supergroup, its structural framework composed of corner-sharing octahedra is analogous to that of the Pyrochlore and Perovskite Supergroups, both of which are highly diverse in composition. The six-coordinated octahedra in these three structure types are linked exclusively and completely by corner-sharing, thereby constructing three-dimensional framework structures that can accommodate highly coordinated cations within their channels or holes. This structural similarity suggests that the Wumuite Supergroup has comparable potential for compositional variation. The formal establishment of the Wumuite Supergroup will provide a critical framework to guide and predict the discovery of additional new minerals within this supergroup.

Key words Wumuite supergroup, wumuite group, xianhuaite group, tungsten bronze structure, hierarchial classification

RARE EARTH MINERALS: CHEMICAL AND COORDINATION DIVERSITY,

COMPLEXITY, NEW RESULTS

Sergey V. Krivovichev[1,2]

1. Department of Crystallography, St. Petersburg State University, Russia

2. Nanomaterials Research Centre, Kola Science Centre, Russia

Abstract Rare earth elements (lanthanides, Y and Sc) are important constituents of materials needed for the fabrication of modern high-technological devices and therefore are of great industrial and geopolitical importance. Their prominent role in today's world determines the high demand of their natural sources, i.e., REE minerals. Among more than 400 REE minerals known and approved by the International Mineralogical Association (IMA), all are either oxygen-based compounds (in order of importance: silicates, carbonates, complex oxides, phosphates, etc.) or fuorides, which is the result of a strongly lithophile character of rare earth metal ions. Eight out of seventeen REEs play the role of essential mineral-forming constituents: Y, Sc and six lanthanides, Ce (most common), La, Nd, Sm, Gd, Yb. Geometrical analysis of 473 REE coordination polyhedra occurring in crystal structures of minerals indicates that there are 23 topological types with coordination numbers 6, 7, 8, 9, 10, and 12. The eightfold coordination is prevalent with bicapped trigonal antiprism and square antiprism being the most common topological types. The high coordination numbers make the task of structure description of REE oxysalts uneasy, since REE polyhedra may share corners, edges and faces, and even in the same structure these three possibilities may be realized. The application of the topological procedure that abstracts itself from the number of shared ligands between the adjacent REE polyhedra results in interesting insights that allow to establish remarkable topological similarities between structure architecture of REE oxysalts and topologies of 2D and 3D networks in metal-organic and organic compounds. The efficiency of this approach will be illustrated using recently studied REE minerals from Kola peninsula (Russian Arctic), including kuliokite-(Y), caysichite-(Y), seidite-(Ce), kainosite-(Y), and the mineral closely related to ashcroftine-(Y). The latter mineral possesses an extraordinary structural complexity, which is the result of the presence in its structure of porous silicate nanotubules that can be considered as topological derivaties of the LTA zeolite framework.

Key words Rare earths, coordination, diversity, complexity

Acknowledgements This work was supported by Russian Science Foundation, grant 24-17-00083.

SCHREIBERSITE FROM THE WEDEL IAB COMPLEX IRON METEORITE

Natalia Dubrovinskaia[1,2], Leonid Dubrovinsky[1],

1. The Bavarian Research Institute for Experimental Geochemistry and Geophysics, University of Bayreuth, Germany

2. Material Physics and Technology at Extreme Conditions, University of Bayreuth, Germany

Abstract Schreibersite, an Fe–Ni phosphide, $(Fe,Ni)_3P$, is a characteristic accessory phase in many iron and stony-iron meteorites, where it is typically associated with metallic Fe–Ni assemblages including kamacite and taenite. Because it concentrates phosphorus within meteoritic metal, this mineral provides important constraints on the behavior of phosphorus during metal segregation, core formation, and the crystallization history of differentiated planetary bodies. Beyond its cosmochemical significance, schreibersite has also received attention in origin-of-life studies, since alteration of meteoritic phosphides may generate reduced and soluble phosphorus compounds that could have contributed to prebiotic phosphorylation pathways on early Earth.

Schreibersite investigated in this study originates from the Wedel iron meteorite, which was discovered in 2024 in the federal state of Schleswig-Holstein, northern Germany. Following classification work, Wedel was approved by the Meteoritical Society on 18 October 2025 and officially listed in Meteoritical Bulletin 114 (2025) as an iron meteorite belonging to the IAB complex.

Schreibersite in the Wedel meteorite occurs between coarse kamacite grains as thin layers approximately 20–30 μm thick and up to ~500 μm in length, locally thickening to ~40–50 μm to form irregularly shaped pockets. In addition, needle-like schreibersite inclusions were observed within individual kamacite grains. Owing to their small size and irregular geometry, mechanical extraction of schreibersite from the meteorite proved impractical. To overcome this limitation, we employed focused ion beam (FIB) techniques to isolate two plates from schreibersite-bearing regions, each with approximate dimensions of 20 × 10 × 2 μm^3. These fragments were mounted on a diamond anvil in a BX90-type diamond anvil cell (DAC) and studied at the Extreme Brilliant Source of the European Synchrotron Radiation Facility (EBS-ESRF).

Both schreibersite samples extracted from the meteorite were found to be monodomain single crystals. The high quality of the diffraction data (Rint $\approx$ 2%, resolution 0.57 Å, completeness $\approx$ 65%, redundancy $\approx$ 3, ~450 independent reflections, and more than nine reflections per refined parameter) enabled an accurate crystal structure solution and refinement. The mineral crystallizes in the non-centrosymmetric space group $I\bar{4}$ and contains phosphorus in a single crystallographic site, while metal

atoms are distributed over three distinct sites (M1, M2, and M3). All structural sites have equal multiplicity, corresponding to eight formula units per unit cell.

Published data remain inconsistent regarding whether iron and nickel are distributed among all metal sites or preferentially occupy specific crystallographic positions, and whether natural terrestrial, synthetic, and meteoritic schreibersite differ in their metal-site occupancies. We found that the Ni distribution in the studied schreibersite samples is ordered: within the precision of the refinement, Ni is absent from the M1 site, present at the M2 site, and dominant at the M3 site. Details of these investigations will be discussed in the presentation.

Key words schreibersite, iron meteorite, single crystal XRD

STRANDITE, $PB_3MN^{3+}{}_4MN^{4+}{}_3O_{15}$, A NEW HEXAGONAL MINERAL FROM LÅNGBAN, SWEDEN

Andreas Karlsson[1], Dan Holtstam[1], Luca Bindi[2] and Daniel Buczko[3]

1. Department of Geosciences, Swedish Museum of Natural History, Stockholm, Sweden

2. Dipartimento di Scienze della Terra, Università degli Studi di Firenze, Firenze, Italy

3. Department of Earth Sciences, Uppsala University, Uppsala, Sweden

Abstract Hexagonal lead-manganese oxides have attracted some interest due to their unusual magnetic and electric properties, particulary for their magnetoresistance. Hitherto only one natural occurring mineral of this type is known, zenzénite, $Pb_3Fe^{3+}{}_4Mn^{4+}{}_3O_{15}$, that is endemic to the Långban Fe-Mn-(Ba-As-Pb-Sb-W-Be-B) deposit in Värmland. We have now found and named a second one, the nominally Fe-free member strandite, ideally $Pb_3Mn^{3+}{}_4Mn^{4+}{}_3O_{15}$, which is also known as an synthetic compound. It occurs as an accessory phase within the manganese ore at the deposit, primarily composed of braunite and hausmannite, and is found in close association with an unnamed triclinic Pb-Mn-oxide, barytocalcite, calcite, and kinoshitalite. Strandite and the triclinic Pb-Mn-oxide are frequently alterated to a fine-grained intergrowth of quenselite and manganite. Strandite is interpreted to have formed at approximately 1.8 Ga during peak metamorphic conditions (~600°C, ~3.5 kb), and possibly represents the equivalent of oxidized Mn-Pb rich ore precursors.

The new mineral occurs as black, anhedral platy grains reaching up to 250 µm in size, and with a metallic lustre and a black to dark brown streak. The Mohs hardness is approximately 5; a distinct cleavage parallel to {0001} is noted, furthermore strandite is brittle with an uneven fracture. The calculated density is 6.927 g/cm3. In reflected light, the mineral is white with moderate bireflectance, strong anisotropy, and dark red internal reflections. Electron microprobe analyses yielded a mean composition (in wt.%) of PbO 54.79, Mn_2O_3 22.96, MnO_2 21.67, Al_2O_3 0.52, Fe_2O_3 0.66, and MgO 0.15, totalling 100.76. The empirical formula, calculated on the basis of 10 cations, is $Pb_{3.04}(Mn^{3+}{}_{3.60}Al_{0.13}Fe^{3+}{}_{0.103}+Mn^{4+}{}_{0.09}Mg_{0.05})_{\sum=3.96}Mn^{4+}{}_{3.00}O_{15}$. Raman spectroscopy confirmed the absence of volatile components and showed Mn−O vibration modes consistent with mixed-valence (Mn^{3+} and Mn^{4+}) manganese. Strandite is hexagonal, space group $P6_3/mcm$, with unit-cell parameters a = 10.0255(11) Å, c = 13.640(2) Å, V = 1187.3(3) Å^3, and Z = 4. Crystal structure refinement from scXRD data ($R1$ = 1.92%) show that is is isotypic with zenzénite. It consists of layers of edge-sharing MnO_6 octahedra forming an incomplete kagome net perpendicular to the c-axis, bridged by inter-layer doublets of face-sharing octahedra. Lead atoms occupy positions between these layers, showing displacement due to stereo-active $6s^2$ lone-pairs. Bond-valence sums indicate that Mn^{3+} is preferentially ordered at larger, more distorted site labelled $M2$. Overall, the structure can be interpreted as a six-layer hexagonal close-packed (HCP) arrangement of large atoms within the

unit cell, (・*hhhhhh*・). In every third layer, half the oxygen atoms are substituted by lead atoms.

Strandite is the 81st type mineral described from Långban, highlighting Långban's mineral diversity and function as a "natural laboratory" for unexpected chemical compositions that could serve as an inspiration for research about novel and useful material for high-tech applications.

Key words New mineral, lead manganese oxide, systematic mineralogy, skarn, Långban

SUPERGENE NEW MINERALS AND MINERAL ASSEMBLAGES IN THE OXIDATION ZONE OF THE DONGCHUAN CU–PB–ZN POLYMETALLIC DEPOSIT, YUNNAN, CHINA, AND THEIR ENVIRONMENTAL IMPLICATIONS

Ningyue Sun[1,2], Yuan Xue[1], Guowu Li[1,3]*, Fabrizio Nestola[2], Jinhua Hao[1], Hongtao Shen[3], Chang Li [4]

1. Science Research Institute, China University of Geosciences, 100083 Beijing, China

2. Department of Geosciences, University of Padua, , 35131 Padua, Italy

3. State Key Laboratory of Geological Processes and Mineral Resources, China University of Geosciences, 430074 Wuhan & 100083 Beijing, China

4. Independent researcher, 364000 Longyan, China

Abstract The Xueling deposit in the Dongchuan ore district, Yunnan, China, hosts an Cu–Pb–Zn polymetallic sulfide assemblage dominated by galena, sphalerite, and tennantite-(Zn), together with a strongly developed supergene oxidation zone. Buffering by carbonate host rocks of the Dengying Formation, combined with a regionally P-enriched geological background, promoted the formation of a complex supergene mineral assemblage dominated by phosphates and arsenates. This system provides an excellent natural laboratory for studying the crystal chemistry of supergene arsenate–phosphate minerals and the crystalline immobilization of environmentally hazardous elements.

Based on field investigation and multiscale mineralogical characterization, including electron microanalysis, Raman spectroscopy, powder and single-crystal X-ray diffraction, X-ray photoelectron spectroscopy, and complementary theoretical and microbiological approaches, we investigated the mineral assemblages, crystal structures, and element redistribution processes in the Dongchuan oxidation zone.

A total of 26 supergene minerals were identified, including 17 arsenates, phosphates, phosphate–arsenates, and phosphate–sulfates. Six new phosphate–arsenate minerals were discovered and approved by the IMA-CNMNC, including four members of the newly established dongchuanite group, together with arsenoveszelyite and qiumingite. These results substantially expand the mineralogical diversity known from the Dongchuan supergene system.

The study further establishes a coupled weathering–element migration–mineral fixation model for an iron-poor polysulfide assemblage and reveals crystal-chemical controls on multielement immobilization. In particular, the dongchuanite group shows ordered As/P distribution, whereas Cu/Zn ordering is controlled by the Jahn–Teller effect of Cu^{2+}. Carbonates act as relatively labile short-term sinks, whereas phosphate–arsenate minerals provide more stable long-term immobilization for hazardous elements such as Pb, Cu, Zn, As, Sb, and Cd. These results provide new insight into supergene mineral evolution and

offer a structural basis for mine-pollution control and mineral-inspired crystalline immobilization materials.

Key words Dongchuan, supergene oxidation zone, new minerals, crystal chemistry

THALLIUM MINERALS AT THE NANOSCALE: SPECIATION, PARTITIONING AND STABILIZATION IN SECONDARY ARSENATES AND OXIDES

Tamara Đorđević[1,2], Miguel Angel Gomez-Gonzalez[3] and Andreas Voegelin[4]

1. E057-02 USTEM, Vienna University of Technology (TU Wien), Austria

2. Department of Mineralogy and Crystallography, University of Vienna, Vienna, Austria

Diamond Light Source Ltd, Didcot, United Kingdom

3. Eawag - Swiss Federal Institute of Aquatic Science and Technology, Dübendorf, Switzerland

Abstract Thallium (Tl) is a highly toxic trace metal that can reach very high concentrations in hydrothermal ore systems. However, its mineralogical hosts and retention mechanisms at the nanoscale that govern the release of Tl during the weathering of such deposits are not well understood. This study investigates the partitioning and speciation of Tl in secondary phases from the northern part of the Allchar Sb–As–Tl–Au deposit in North Macedonia.

Previous microanalytical work involving SEM-EDX, EMPA, Raman spectroscopy and TEM revealed the formation of poorly crystalline Tl arsenates during weathering. These occur as micaceous, subparallel aggregates in pore spaces and represent at least one previously unknown mineral species. These phases form two distinct compositional groups with different Tl:As ratios (approximately 2 and 3.4–4.4) and varying amounts of calcium. Further TEM investigations identified nanoscale intergrowths of needle-like Tl_2O crystals, suggesting complex Tl redistribution and re-precipitation pathways during supergene alteration.

In this study, we build upon this work by employing synchrotron-based nano-focused X-ray fluorescence (nano-XRF) and X-ray absorption spectroscopy (nano-XANES) techniques to determine the spatial distribution and oxidation state of Tl at a sub-micrometre scale in mining wastes from the Crven Dol locality, as well as in technosols near orpiment-rich tailings near the former Adit 25 mine, where Tl concentrations in the bulk material can reach up to 17,000 mg/kg. The measurements targeted Tl-arsenates, Tl–Me–arsenates (where Me = Mn, Ca, Fe or Mg) and As-bearing Tl oxides.

Our results demonstrate that, irrespective of variations in mineral chemistry or Tl concentration, Tl is predominantly present as Tl(III) in secondary arsenates and oxides. This indicates a strong preference for the incorporation of trivalent Tl and highlights its remarkable stability in secondary mineral hosts under highly variable geochemical conditions. The nanoscale distribution patterns also show that Tl is efficiently retained within poorly crystalline and structurally complex phases, including amorphous phases that lack any long-range order.

These findings provide new insights into the crystal chemistry, redox behavior and mineral systematics

of Tl, emphasizing the role of nanoscale processes and metastable phases in controlling Tl release from mineral deposits. More broadly, this study shows how advanced synchrotron techniques combined with micro- and nano-mineralogical approaches can improve our understanding of how toxic and critical elements are distributed, how minerals are structured and how they evolve in extreme geochemical environments.

Financial support of the Austrian Science Fund (FWF) [P 36828-N] to T. Đorđević is gratefully acknowledged. Diamond Light Source Ltd (Didcot, UK) is acknowledged for the allocation of beamtime at beamline I14 [MG38328].

Key words Thallium, nano mineralogy, Tl-secondary minerals, nano-XRF, nano-XANES

THE PYROXENE NOMENCLATURE AND CLASSIFICATION: A REVIEW.

Fernando Cámara[1], Luca Bindi[2], Chi Ma[3], Aaron J. Lussier[4], Mariko Nagashima[5], Sabrina Nazzareni[6], Silvio Mollo[7], Günther Redhammer[8], Mark Welch[9]

1. Earth Sciences Department, University of Milan, Italy
2. Earth Sciences Department, University of Florence, Italy
3. Division of Geological and Planetary Sciences, California Institute of Technology, Pasadena, USA
4. Canadian Museum of Nature, Mineral Scences Section, Ottawa, Canada
5. Graduate School of Sciences and Technology for Innovation, Yamaguchi University, Japan
6. Department of Chemistry, Life Sciences and Environmental Sustainability, University of Parma, Italy
7. Department of Earth Sciences, Sapienza – University of Rome, Roma, Italy
8. Institute of Mineralogy, University of Salzburg, Hellbrunstr. 34, A-5020 Salzburg, Austria
9. Natural History Museum, London, United Kingdom

Abstract The pyroxene classification approved by the IMA Commission on New Minerals and Mineral Names (CNMMN) in 1987 has been widely used, but numerous new nomenclature rules and guidelines have since been introduced. These updates address issues such as mineral naming conventions, end-member definitions, chemical modifiers, dominant-constituent and dominant-valency rules, and the preservation of historical names. Many new pyroxene root names have been added over the past 38 years and, as a result, a revision of the classification is needed to align with current standards and properly classify newly defined end-members. For this purpose, the officers of the IMA Commission on New Minerals, Nomenclature and Classification (CNMNC) have established a new Subcommittee on Pyroxene Nomenclature and Classification. Our aim is to create a comprehensive and consistent nomenclature and classification for pyroxenes that accommodates future species, respects crystal-chemical compositional limits, and minimizes changes to historical names without compromising scientific accuracy. Ambiguity should be avoided and any reclassification clearly explained, helping future generations to adopt the updated nomenclature easily. We believe that the Amphibole Nomenclature & Classification report (Hawthorne et al. 2012) serves as a model for pyroxenes, ensuring a consistent approach for two closely related mineral groups. Work is in progress and the current state of the art will be presented.

Key words Nomenclature, pyroxene group.

THE ROLE OF TRANSITION METALS IN HEAT-INDUCED COLOR CHANGE IN CU-BEARING TOURMALINES FROM MAVUCO, MOZAMBIQUE

Riccardo Luppi[1], Federico Pezzotta[2], Henrik Skogby [3], Ulf Hålenius[3], and Ferdinando Bosi[1]

1. Department of Earth Sciences, Sapienza University of Rome, Rome, Italy
2. MUM – Mineralogical Museum Luigi Celleri, San Piero in Campo, Elba Island, Italy
3. Department of Geosciences, Swedish Museum of Natural History, Stockholm, Sweden

Abstract Crystal chemistry and spectroscopy play a fundamental role in understanding the mineral properties, particularly color, which is an important factor in the commercial value of gemstones. Laboratory treatments aimed at modifying color to enhance gem value are therefore widely used. Tourmalines, chemically complex borosilicates, represent an excellent example of mineral color variability, displaying hues across the entire visible spectrum. The most prized tourmaline variety is Paraíba, renowned for its vivid turquoise to neon-blue color caused by the presence of Cu (hundreds of ppm), typically associated with Fe contents below 1 wt%. This rare Cu-bearing tourmaline, sourced from Brazil, Nigeria, and Mozambique, can reach prices of up to USD 50,000 per carat. Transition metals like Ti, V, Cr, Mn, Fe, and Cu occupy octahedrally coordinated sites in the tourmaline structure and act as chromophores, strongly influencing hue and color saturation. Understanding both natural and treatment-induced color mechanisms is essential for distinguishing treated from natural gems, and it also represents an open challenge in tourmaline crystal chemistry.

In this contribution, more than 40 Cu-bearing tourmalines of different colors from Mavuco (Mozambique), the world's largest residual eluvial deposit of cuprian tourmalines, were heated under both oxidizing and reducing conditions at different temperatures. Colors were classified using the Munsell system in transmitted and incident light along and perpendicular to the **c**-axis, before and after heating. Samples displaying enhanced neon-blue tones, together with representatives of other color categories, were characterized using electron microprobe analysis, optical absorption spectroscopy, and Fourier-transform infrared spectroscopy. The results show elbaitic compositions, with color controlled by the combination, concentration and oxidation states of Cu, Mn, Fe, and Ti. Purple and bicolored (purple and grayish blue) samples changed most effectively toward neon-blue hues after heating. The three main purple subcategories exhibited different behaviors depending on Cu content and the Cu/Mn ratio. As both parameters increase, the color after heating progressively shifts toward the characteristic Paraíba hue. Particular attention was given to Mn during heating. Under reducing conditions at around 500 °C, Mn^{3+} is reduced to Mn^{2+} and, in samples with low Ti and Fe contents, Cu^{2+} absorptions become dominant, producing the neon-blue Paraíba color. Conversely, when these samples are heated in air at higher

temperatures (~750 °C), they develop a reddish coloration due to the oxidation of Mn^{2+} to Mn^{3+}. In Cu-bearing tourmalines with higher Fe and Ti contents, green tones become dominant. Green samples heated up to 600 °C generally show no significant color change; under reducing conditions they may exhibit slight shifts toward yellowish-green tones due to Mn^{2+}-Ti^{4+} intervalence charge transfer (IVCT), whereas under oxidizing conditions and temperatures above ~700 °C they develop reddish shades associated with Mn^{3+}. Dark green colors are instead attributed to Fe^{2+}-Fe^{3+} electronic exchange pairs together with Fe^{2+}-Ti^{4+} IVCT. Observations during heating also revealed that treatment conditions critically affect the final color. More reducing environments promote faster and more intense shifts toward Paraíba-like hues. Heat treatment also tends to homogenize the color of multicolored tourmalines and reduces or even eliminates pleochroism. These findings may provide preliminary indications useful for distinguishing natural from treated stones. However, further analyses, including single-crystal X-ray diffraction and electron paramagnetic resonance spectroscopy, will be necessary to refine the crystal-chemical model of color origin in natural and heated Cu-bearing tourmalines. Such work will help link color evolution to chemical composition and treatment conditions, ultimately aiding the distinction between treated and natural gems and contributing to greater transparency in the gem market.

Key words Tourmaline, thermally treated, spectroscopy analyses

THE YTTROTUNGSTITE GROUP REVISITED

Frédéric Hatert[1] and Simon Philippo[2]

1. Laboratory of Mineralogy, University of Liège B18, B-4000 Liège, Belgium

2. Musée national d'histoire naturelle de Luxembourg, 25 Rue Münster, 2160 Luxembourg, Luxembourg

Abstract The crucial importance of tungsten in our modern technologies explains why this element is included in the list of critical raw materials published by the European Union. In most geological contexts, only two mineral substances are carrying this rare element: scheelite, $CaWO_4$, and "wolframite", that designate members of a solid solution between the two species hubnerite, $MnWO_4$, and ferberite, $FeWO_4$.

In the Central African tungsten province, that extends from southwestern Uganda to central Rwanda and eastern Congo, most tungsten-bearing minerals of economic value are constituted by varieties of ferberite. This species generally occurs as black platy crystals, showing a characteristic perfect cleavage plane, and crystallizing as a primary phase in mineralized quartz veins. A remarkable variety of ferberite, called "reinite", forms large pseudo-octahedral crystals without any cleavage plane, and shows a dull black colour and an earthy lustre. This unusual variety mainly occurs in the "tungsten belt" of central Rwanda, and is produced by a pseudomorphic replacement of scheelite by ferberite.

In such "reinite" pseudomorphs occur numerous late alteration phases, among which the new mineral species yttrotungstite-(Nd) that was found in the famous Nyakabingo tungsten mine, close to Kigali.

The mineral, with an ideal formula $NdW_2O_7(OH)(H_2O)$, is the Nd-equivalent of yttrotungstite-(Ce) and yttrotungstite-(Y), has been named in agreement with the nomenclature of the yttrotungstite group. It has been approved by the Commission on New Minerals, Nomenclature, and Classification of the International Mineralogical Association (IMA-CNMNC) under number IMA 2023-064, and forms transparent crystals reaching a length of maximum of 100 µm, and frequently forming radiated groups. The dominant form is {010}, and a twinning has been observed parallel to (001). The streak of yttrotungstite-(Nd) is white, the lustre vitreous, and the mineral is non-fluorescent. The Mohs hardness is 1, the tenacity is brittle, and observed cleavage planes are (010) perfect, (100) and (001) excellent. The calculated density is 6.25 $g \cdot cm^{-3}$, and refraction indices are $\alpha = 1.90(2)$, β and $\gamma > 2.00$. The mineral is optically biaxial, its optical plane is parallel to (010), and the optical orientation is $X \wedge c = 6°$, $Z \wedge a = 9°$. Pleochroism is from light yellow (X) to yellow (Z). The empirical formula of yttrotungstite-(Nd), calculated on the basis of 15 positive charges assuming 1 (OH) group and 1 H_2O molecule per formula unit, corresponds to: $(Nd_{0.36}Sm_{0.13}Ce_{0.12}Pr_{0.08}La_{0.06}Gd_{0.06}Y_{0.05}Dy_{0.03}Yb_{0.02}Ca_{0.01})_{\Sigma 0.92}(W_{2.02}P_{0.02})_{\Sigma 2.04}O_7(OH)(H_2O)$.

The crystal structure of yttrotungstite-(Nd) was refined in space group $P2_1/m$, to the final R1 value

0.0362, and the measured unit-cell parameters are a = 5.8534(3), b = 8.6881(3), c = 7.0488(4) Å, β = 105.336(5)°, V = 345.70(3) Å^3. The structure is characterized by edge-sharing WO_6 octahedra, forming kinked chains parallel to the b axis. The NdO_8 complex polyhedra connect three chains together, by sharing edges or corners with adjacent WO_6 octahedra. A view perpendicular to the b axis shows that the NdO_8 and WO_6 polyhedra occur in two different types of planes, stacked parallel to the [-101] direction. Neodymium occurs in a very large 8-coordinated site, which can be described as two tetragonal pyramids sharing one common basal edge, and sharing the opposite basal edge with a square.

According to the structural data, the end-member formula of yttrotungstite-(Nd) is written as $NdW_2O_7(OH)(H_2O)$, since it appears that the mineral contains 1 OH group and 1 water molecule per formula unit. In order to uniformize the nomenclature of minerals belonging to the yttrotungstite group, the formulae of yttrotungstite-(Ce) and yttrotungstite-(Y) were also modified to $CeW_2O_7(OH)(H_2O)$ and $YW_2O_7(OH)(H_2O)$, respectively.

Key words yttrotungstite-(Nd), tungsten belt, Rwanda, new mineral, nomenclature revision

THERMAL AND VACUUM-INDUCED EVOLUTION OF HYDRATED IRON SULFATE MINERALS

Oleg I. Siidra[1], Artem S. Borsiov[2], Veronika R. Abdulina[1], Astrid Holzheid[2], Mikhail P. Sobolev[1]

1. Department of Crystallography, Institute of Geosciences, Saint-Petersburg State University, Russia

2. Institute of Geosciences, University of Kiel, Germany

Abstract Hydrated iron sulfates are common minerals occurring in various oxidation zones, volcanic fumaroles, and other terrestrial geological environments. A diversity of such phases has been identified spectroscopically on Mars. Understanding the transformation pathways of these minerals under variable physicochemical conditions is critical for interpreting the mineralogical and chemical composition of the Martian surface. Furthermore, the study of iron sulfates and their formation mechanisms on Mars provides constraints on the composition of the ancient atmosphere and aqueous reservoirs. In light of the planned Mars Sample Return mission, iron sulfates have garnered substantial attention. A key concern during sample transport to Earth is the potential for partial or complete dehydration induced by temperature fluctuations and vacuum exposure. Such dehydration may be either reversible or irreversible.

In this work, we investigated the thermal and vacuum-induced evolution of several hydrated iron sulfate minerals using *in situ* low- and high-temperature single-crystal and powder X-ray diffraction, Raman spectroscopy, and thermal analysis. The examined phases include: quenstedtite, $Fe_2(SO_4)_3(H_2O)_{11}$; botryogen, $MgFe^{3+}(SO_4)_2(OH)(H_2O)_7$; aluminocopiapite, $(Al_{0.54}Fe^{3+}_{0.12})_{\Sigma=0.66}Fe^{3+}_4(SO_4)_6(OH)_2(H_2O)_{20}$; parabutlerite, $Fe^{3+}(SO_4)(OH)(H_2O)_2$; coquimbite, $AlFe^{3+}_3(SO_4)_6(H_2O)_{18}$; and römerite, $Fe^{2+}Fe^{3+}_2(SO_4)_4(H_2O)_{14}$. Experimental conditions were designed to simulate those expected on the Martian surface. A diverse array of phase transitions and transformations was observed as a function of increasing temperature and/or exposure to vacuum.

Notably, several rare single-crystal-to-single-crystal (SC-SC) transformations were identified. In botryogen, heating induces partial dehydration and the formation of a post-phase with the composition $MgFe^{3+}(SO_4)_2(OH)(H_2O)_3$. This phase is structurally based on metal-sulfate blocks characterized by a structural topology previously unknown in metal sulfates. Upon heating or vacuum application, aluminocopiapite transforms into a post-copiapite phase with the composition $(Al_{0.64}Fe^{3+}_{0.02})_{\Sigma=0.66}Fe^{3+}_4(SO_4)_6(OH)_2(H_2O)_{12.44}$. Concurrently, a thin film of schwertmannite ($Fe_8O_8(OH)_{8-2x}(SO_4)_x \cdot nH_2O$) forms on the crystal surface. This topotactic transition is reversible: when the post-copiapite crystal is stored under ambient conditions for one week, it reverts to its original composition and copiapite-type structure, and the schwertmannite film disappears. In parabutlerite, a lock-in phase transition from an incommensurately modulated to a commensurately modulated structure was observed with increasing temperature.

Among the studied minerals, coquimbite and römerite exhibited are the most stable. Quenstedtite loses one water molecule upon gradual heating. However, almost all of the studied phases—including quenstedtite, botryogen, and the post-botryogen phase—remain stable under low vacuum in the absence of thermal stress. In contrast, copiapite-group minerals are highly unstable and are unlikely to persist on the Martian surface. Instead, the post-copiapite phase (as yet undescribed as a mineral species) is expected to be widespread. Finally, the identification of the lock-in transition in parabutlerite and the determination of its modulation vector may serve as a marker for thermal exposure experienced by the mineral. Consequently, caution is required in multiple contexts, including the interpretation of remote sensing data, the modeling of the Martian near-surface environment, and the analysis of samples returned from Mars. Particular attention must be paid to the sulfur and oxygen isotopic compositions of sulfates that have undergone repeated dehydration and hydration cycles, as demonstrated by terrestrial analogs, where the dehydration of hydrated sulfates induces significant isotopic fractionation.

Key words Iron sulfates, phase transitions, SC-SC transformations, thermal and vacuum dehydration

Acknowledgements This work was financially supported by the Russian Science Foundation through the grant 25-17-00157.

TÖRNEBOHMITE-(CE): CRYSTAL STRUCTURE REFINEMENT, PHASE TRANSITION, AND THERMAL EXPANSION

M.S. Avdontceva[1], S.V. Krivovichev[1,2], A.A. Agakhanov[3], V.N. Bocharov[4], I.V. Pekov[5]

1. Department of Crystallography, Institute of Earth Sciences, St. Petersburg State University, St. Petersburg, Russia

2. Nanomaterials Research Centre, Kola Science Center, Russian Academy of Sciences, Apatity, Russia

3. Fersman Mineralogical Museum of the Russian Academy of Sciences, Moscow, Russia

4. Centre for Geo-Environmental Research and Modelling, St. Petersburg State University, St.Petersburg, Russia

5. Faculty of Geology, Moscow State University, Moscow, Russia

Abstract Törnebohmite-(Ce), $Ce_2Al(SiO_4)_2(OH)$, a hydroxyl-containing silicate of light rare earth elements (REE) and aluminum from Bastnäs mine was investigated using *in situ* high-temperature (300-1200 K) single crystal X-ray diffraction analysis, and chemical microprobe analysis. The empirical formula of törnebohmite-(Ce) can be presented as $(Ce_{0.96}Nd_{0.20}La_{0.78}Pr_{0.06}Sm_{0.02}Eu_{0.01}Gd_{0.01})_{\sum 2.04}(Al_{0.94}Fe_{0.06})_{\sum 1.00}(SiO_4)_2(OH)$ and is in a good agreement with the ideal formula of mineral. The most intense bands of Raman spectrum of törnebohmite-(Ce) correspond to the region 800-1000 cm^{-1} and belong to symmetric and assymetric stretching vibrations modes of silicate tetrahedra. The crystal structure of törnebohmite-(Ce) ($P2_1/c$, a = 7.6422(2), b = 5.6033(1), c = 16.7948(4) Å, β = 112.292(2)°, V = 665.43(3)Å^3, R_1 = 0.025) is based on octahedral-tetrahedral backbone consisting of $[AlO_4(OH)_2]$ octahedra linked through common edges and formed chains alongated along [010], isolated SiO_4 tetrahedra connect chains to a framework. The REE^{3+}(Ce) cations are located in the cavities of the framework. Recently, Krivovichev (2025) suggested that, with increasing temperature, a phase transition should be observed for the mineral with a twofold decrease in the volume of the unit cell without an increase in symmetry. Single crystal X-ray diffraction analysis has shown that increasing the temperature to 1200 K leads to an irreversible phase transition. The HT modification of törnebohmite-(Ce) is also monoclinic ($P2_1/m$, a = 7.9162(7), b = 5.5662(4), c = 8.6367(7) Å, β = 114.530(9)°, V = 346.21(5) Å^3, R_1 = 0.044) and has practically the same structural architecture as LT-modification. Calculation of the thermal expansion coefficients presented that the structures of both modifications expand sharply anisotropically, and the maximum thermal expansion is observed along α_{33}. This type of thermal expansion can be explained by shear deformations, often observed in monoclinic structures. The structural complexity analysis showed that both modifications of törnebohmite-(Ce) are intermediate in complexity ($I_{G,total}$ = 213.12 bits/cell for LT and $I_{G,total}$ = 105.207 bits/cell for HT polymorphs). These values of complexity are correlated well with the general observations of the

increasing symmetry and descreasing complexity of minerals and inorganic compounds under heating.

Key words törnebohmite-(Ce), thermal evolution, phase transition, X-ray diffraction, complexity

Acknowledgements This research was funded by the Russian Science Foundation, grant No 24-17-00083, https://rscf.ru/project/24-17-00083/. The X-Ray diffraction studies were carried out at the Center for X-ray diffraction research and Raman spectra were performed at the centre for Geo-Environmental Research and Modelling of the Research Park of St.Petersburg State University.

CHANGESITE-(CE): A NEW REE MINERAL FROM LUNAR

Yanjuan Wang[1*,2], Fabrizio Nestola[2,1], Kai Qu[3], Arianna E. Lanza[4], Jiayang Cong[5], Xiaochao Che[6], Zhenyu Chen[7], Guang Fan[8], Xiangping Gu[9], Ze Liu[7], Cheng Yue[6], Tao Long[6], Shuping Yin[6], Anna Barbaro[2], Simone Molinari[2], Ziyao Wang[10], Zhehao Huang[5], Zengqian Hou[1*]

1. State Key Laboratory of Deep Earth and Mineral Exploration, Chinese Academy of Geological Sciences, China

2. Department of Geosciences, University of Padova, Italy

3. Tianjin Center, China Geological Survey, China

4. Department of Chemistry, University of Copenhagen, Denmark

5. Electron Microscopy Center, School of Emergent Soft Matter, South China University of Technology, China

6. Institute of Geology, Chinese Academy of Geological Sciences, China

7. Institute of Mineral Resources, Chinese Academy of Geological Sciences, China

8. Beijing Research Institute of Uranium Geology, China

9. School of Gemmology and Mineral Resources, Jiangxi Institute of Applied Science and Technology, China

10. North Campus, Hebei GEO University, China

Abstract Changesite-(Ce) (IMA2025-098) is a new Ce-dominant member of the merrillite group discovered in samples returned by the Chang'e-5 (CE-5) mission from northern Oceanus Procellarum on the Moon. The mineral crystallized during the late-stage evolution of mare basaltic magmas and typically occurs as 3–15 μm subhedral to euhedral granular or columnar crystals along the margins of anorthite, pigeonite, and ilmenite. In some cases, it forms composite inclusions [changesite-(Ce) + pigeonite + troilite] within ilmenite, indicating co-precipitation from residual Fe-rich melts. The empirical formula, based on five electron microprobe analyses and calculated on the basis of Si + P + S + Al = 7 apfu, can be expressed as: $^{A}(Ca_{8.16}Ce_{0.25}Y_{0.22}Nd_{0.16}La_{0.08}Gd_{0.05}Pr_{0.03}Dy_{0.03}Sm_{0.02})_{\Sigma 9.00}{}^{X}(\square_{0.80}Ca_{0.15}Fe_{0.05})_{\Sigma 1.00}{}^{M}(Fe_{0.99}Mg_{0.01})_{\Sigma 1.00}{}^{T}(P_{6.88}Si_{0.11}S_{0.01})_{\Sigma 7.00}O_{28.05}$. The ideal endmember formula is $(Ca_8Ce)\square Fe^{2+}(PO_4)_7$. A platy fragment of Changesite-(Ce) (3 × 2 × 0.1 μm) extracted from CE-5 material was used for three-dimensional electron diffraction (3D ED) data collection. The results demonstrate that Changesite-(Ce) is isostructural with merrillite and crystallizes in the trigonal system, space group *R*3*c* (#161). Refined unit-cell parameters are a = 10.3513(2), c = 37.0806(5) Å, V = 3440.83(14) Å^3, and Z = 6. The refinement converged to R_1 = 0.1547 for 5035 unique reflections with $I > 2\sigma(I)$, and R_{all} = 0.1709 for all 6417 unique reflections. The Raman spectrum of changesite-(Ce) is generally consistent with previously reported merrillite group minerals. Unlike other planetary merrillite-type minerals, in which Na or Ca occupies the X site and the v_1 region typically exhibits a well-resolved doublet at 953-960 and 970-976 cm^{-1},

changesite-(Ce) as well as previously reported lunar REE-merrillite and synthetic REE-rich merrillite, displays either an asymmetric single peak at ~968 cm^{-1} or a poorly resolved doublet at 952~953 cm^{-1} and 968~972 cm^{-1}. The difference between lunar REE merrillite and other planetary Na-, Ca-merrillite suggests that coupled substitution of REE^{3+} for Ca^{2+} at the A sites, accompanied by vacancy at the X site, results in a more uniform bonding environment for phosphate groups. If more data can be obtained to verify the above phenomenon, as a result, the difference in Raman spectra could also serve as a potential spectroscopic fingerprint to distinguish vacancy-merrillite from other merrillite group minerals under ambient conditions. The discovery of changesite-(Ce) also provides new mineralogical constraints on late-stage lunar magmatism, REE behavior, and the thermal evolution of young mare basalts.

Key words Changesite-(Ce), REE minerals, Lunar, Merrillite, Phosphate

CRYSTAL CHEMISTRY OF KYRGYZSTANITE, $ZNAL_4(OH)_{12}(SO_4)\cdot 3H_2O$

E.S. Zhitova[1], R.M. Sheveleva[1,2], A.A. Zolotarev[1,2], A.N. Kupchinenko[1], V.N. Bocharov[2], V. Yu. Karpenko[3], I.V. Pekov[4]

1. Institute of Volcanology and Seismology FEB RAS, Petropavlovsk-Kamchatsky, Russia
2. St. Petersburg State University, St. Petersburg, Russia
3. Fersman Mineralogical Museum RAS, Moscow, Russia
4. Lomonosov Moscow State University, Moscow, Russia

Abstract The crystal structure of kyrgyzstanite, ideally $ZnAl_4(OH)_{12}(SO_4)\cdot 3H_2O$, a layered double hydroxide (LDH) was determined for the first time. The sample originates from the type locality, Kara-Tangi U-V deposit, Kyrgyzstan. The single-crystal X-ray diffraction (XRD) data were processed in the space group $P2_1/n$, a = 10.2718(4), b = 8.8955(3), c =17.1119(7) Å, β = 95.562(3) °, V = 1556.20(10) Å^3, and Z = 4. The structure has been solved by the Intrinsic Phasing method and refined to R_1 = 0.0402 for 3593 unique reflections with $F_o > 4\sigma(F_o)$. The crystal structure consists of alternating dioctahedral [or $Al(OH)_3$-derived] layers with half of octahedral cavities occupied by Zn, i.e. $\{ZnAl_4(OH)_{12}\}^{2+}$ and interlayer of composition $\{(SO_4)(H_2O)_{2.4}\}^{2-}$. Each of metal-hydroxide layers contains one Zn site, four Al sites and 12 O [of $(OH)^-$ groups] sites with <Zn–O(H)> 2.085 Å, <Al–O(H)> 1.898–1.902 Å. The metal-hydroxide layers are shifted along stacking for ½t in b direction, resulting in a two-layer unit-cell. The interlayer SO_4 tetrahedra and 3 symmetrically independent (H_2O) molecules are connected by complex hydrogen-bonding system. The H atoms of both $(OH)^-$ and $(H_2O)^0$ groups have been localized. The refined unit-cell parameters of kyrgyzstanite from powder XRD data are a = 10.2792(8), b = 8.8995(5), c = 17.1425(8) Å, β = 95.652(7) °, and V = 1560.58(17) Å^3. The Raman spectra of kyrgyzstanite contains bands corresponding to O–H stretching vibrations at 3666–3455 cm^{-1} and 3283 cm^{-1}; asymmetric, symmetric and bending vibration of SO_4 groups in the 1137–467 cm^{-1} region and lattice vibrations at 439–75 cm^{-1}. Kyrgyzstanite is a Zn-analogue of chalcoalumite and nickelalumite and ancestor of rather novel type of synthetic layered double hydroxide of MAl$_4$ stoichiometry with perspectives in industrial application. Kyrgyzstanite and other members of the chalcoalumite group should be considered as hydrotalcite-supergroup members.

This research was funded by the Russian Science Foundation project no. 22-77-10036-P for ESZ, RMS, AAZ and ANK. Technical support of the St. Petersburg State University Resource Centres “X-ray diffraction research methods” and “Geomodel” is carried out within the framework of SPbSU, grants No. 125021702335-5 and 124032000029-9, for both Resource Centres, respectively.

Key words kyrgyzstanite, layedred double hydroxide, chalcoalumite, crystal structure, LDH

INSIGHT INTO THE CRYSTAL CHEMISTRY OF PUMPELLYITE-GROUP MINERALS: JULGOLDITE FROM KOURAGAHANA AND PUMPELLYITE FROM SUGASHIMA

Mariko Nagashima[1], Daisuke Nishio-Hamane[2]

1. Division of Earth Science, Graduate School of Science and Technology for Innovation, Yamaguchi University, Japan

2. The Institute for Solid State Physics, the University of Tokyo, Japan

Abstract Pumpellyite-group minerals, $^{VII}W_2{}^{VI}X^{VI}Y_2{}^{IV}Si_3O_{14-n}(OH)_n$ with $4 \geq n \geq 3$ ($Z = 4$, space group A2/m), are formed under low-grade metamorphic conditions and at low-temperature hydrothermal activity. Due to the compositional and structural complexity of this mineral group, its crystal chemistry is still not well understood. Since both octahedral divalent and trivalent cations occupy the X site, they are balanced by the number of hydroxyl groups, resulting in at least two hydrogen bond systems observed. Despite earlier studies on pumpellyite-group minerals, a method for estimating the cation distribution at the X site remains undeveloped. Therefore, examining these minerals with various compositions precisely from a crystal-chemical perspective is essential. To gain insights into the comprehensive crystal chemistry of the pumpellyite-group minerals, we studied the relationship between cation distribution and structural variation, as well as the hydrogen-bond system of these minerals from two localities: (1) Kouragahana, Shimane, Japan, and (2) Sugashima, Mie, Japan.

Single-crystal X-ray crystal-structure refinements and electron-microprobe analyses of Kouragahana and Sugashima specimens determined the compositions of $^{W}Ca_{2.00}{}^{X}(Fe_{0.69}Mg_{0.20}Al_{0.11})_{\Sigma 1.00}{}^{Y}(Fe^{3+}{}_{1.46}Al_{0.54})_{\Sigma 2.00}Si_{3.00}O_{14-n}(OH)_n$ and $^{W}Ca_{2.00}{}^{X}(Al_{0.56}Mg_{0.35}Fe_{0.09})_{\Sigma 1.00}{}^{Y}Al_{2.00}Si_{3.00}O_{14-n}(OH)_n$ ($4 \geq n \geq 3$), respectively. The latter was classified as pumpellyite-(Al), while the former can only be concluded to be either julgoldite-(Fe^{3+}) or julgoldite-(Fe^{2+}). The OH groups determined by structure refinement are consistent with those known for pumpellyite. The length of the *b*-axis most accurately reflects the average ionic radius at the Y site, based on structural and chemical data for pumpellyite-group minerals. In contrast, the lengths of the *a*- and *c*-axes demonstrate a favorable correlation with the mean ionic radius of the Y site; however, they exhibit greater dispersion compared to the *b*-axis. This is attributed to lateral expansion or shrinkage of the (010) plane due to variations in the size of the X site. Therefore, the pumpellyite group minerals with longer *a*- and *c*-axes may be rich in divalent cations at the X site. Since a weak correlation was observed between the mean ionic radius of the X site and the volume of the X site from pumpellyite-julgoldite series samples, where the oxidation state was determined directly, clarifying this correlation and enhancing the regression line with additional high-quality structural studies may enable the determination of cation distribution at the X site of the pumpellyite group.

Key words pumpellyite, julgoldite, crystal chemistry

Acknowledgements This study is supported by the MEXT Project, JPMXS0440400024, and JSPS, no. 23K0355.

LOW-DOSE ATOMIC-RESOLUTION IMAGING OF VATERITE USING OBF-STEM

Taiga Okumura[1], Hayato Miura[2], Toshihiro Kogure[1,3]

1. Department of Earth Sciences, Waseda University, Japan

2. JEOL, Ltd., Japan

3. Department of Earth and Planetary Science, The University of Tokyo, Japan

Abstract Anhydrous calcium carbonate ($CaCO_3$) crystallizes into three distinct polymorphs: calcite, aragonite, and vaterite. Vaterite, a metastable phase, is rarely found in Earth's surface environments. However, it is formed in specific biominerals such as fish otoliths. The precise crystal structure of vaterite has been a subject of debate for over a century; however, structural determination using single-crystal X-ray diffraction (XRD) has been challenging due to the presence of dense stacking faults.

In a previous study, we directly observed calcium atoms and carbonate groups (CO_3^{2-}) in vaterite constituting the asteriscus otoliths of goldfish (*Carassius auratus*) using annular bright-field (ABF) scanning transmission electron microscopy (STEM) (Okumura et al., 2024). The ABF images revealed that vaterite consists of alternating layers of calcium planes forming a hexagonal sublattice, with carbonate sheets sandwiched between them. We confirmed that adjacent carbonate sheets are rotated by +60°, −60°, or 180°, and that these three rotations are subject to certain constraints. Although powder XRD simulations based on this model generally reproduced experimental measurements, discrepancies remained in some peak intensities. These inconsistencies may be attributed to slight deviations between the actual atomic positions and the proposed model, which necessitates a more precise determination of all atomic coordinates. While carbon atoms within the carbonate groups could be observed in the ABF images, some oxygen atoms remained difficult to resolve, limiting our understanding of the exact positions of the carbonate groups. Furthermore, electron beam damage hindered the acquisition and statistical analysis of a sufficient number of high-resolution images using conventional STEM.

To overcome these limitations, the present study employed optimum bright-field (OBF) STEM using a segmented detector, which enables observations with a high signal-to-noise (S/N) ratio even under extremely low electron doses. As in the previous study, goldfish asteriscus otoliths were used as samples. Ultrathin sections were prepared using a focused ion beam and underwent final polishing with a precision ion polishing system. The S/N ratio was further enhanced by applying non-rigid registration to the acquired images. In the resulting OBF images, the oxygen positions that were obscured in conventional ABF images were successfully resolved. These images revealed that the triangular planes of the carbonate groups are slightly tilted with respect to the stacking direction. Furthermore, the spacing between the adjacent calcium atoms was uneven, indicating a deviation from the vertices of an ideal hexagonal lattice.

These minute atomic displacements may provide direct observational evidence for the structural model estimated by precession electron diffraction in a previous study (Mugnaioli et al., 2012). In the future, we intend to further refine the atomic coordinates to completely elucidate the crystal structure of vaterite.

Key words vaterite, OBF-STEM, crystal structure, low-dose imaging, biomineral

LÅNGBANITE REVISITED

Fernando Cámara[1], Dan Holtstam[2]

1. Dipartimento di Scienze della Terra 'A. Desio', Università degli Studi di Milano, Milan, Italy

2. Department of Geosciences, Swedish Museum of Natural History, Stockholm, Sweden

Abstract The crystal structure of långbanite, ideally $Mn^{2+}_4Mn^{3+}_9Sb^{5+}O_{16}(SiO_4)_2$, a nesosilicate and a rare skarn mineral from Sb-anomalous Mn deposits, was determined independently by Moore et al. (1991) and Giuseppetti et al. (1991). Although both studies arrived at a similar general topology for the atomic arrangement, they differed in their symmetry descriptions (hexagonal *vs*. monoclinic) and in reported metal–oxygen bond distances.

To resolve these discrepancies, type material originally used by Flink (1889) for the description of the mineral – named after its discovery locality, the Långban mine, Värmland, Sweden – was reinvestigated. In addition, a specimen of "ferrostibian" from the Sjögruvan mine, Örebro, Sweden (Igelström, 1889), representing the most Fe-rich variety found to date, was examined.

Both the Långban type specimen (11.5 wt.% Fe_2O_3) and the Sjögruvan specimen (20.3 wt.% Fe_2O_3) are shown to be monoclinic, space group *C*2/*m*. Structure refinements ($R1 = 0.042$) yielded the following unit-cell parameters for the type specimen: $a = 11.5680(3)$, $b = 20.0467(5)$, $c = 11.0754(5)$ Å, $\beta = 90.071(3)°$, $V = 2568.39(15)$ Å^3 for $Z = 6$ – values very close to those previously reported by Giuseppetti et al. (1991). The Sjögruvan specimen gives similar parameters ($R1 = 0.034$), with only a slightly larger unit-cell volume [$V = 2577.54(16)$ Å^3], confirming the identity of "ferrostibian" with långbanite.

Raman spectra collected for långbanite differ radically from those reported in previous work by Bahfenne & Frost (2010), raising questions about the validity of the published data. New ^{57}Fe transmission Mössbauer spectroscopy results show that Fe is present only in the trivalent state and distributed over octahedrally coordinated sites, in agreement with an earlier study by Nysten & Ericsson (1994).

Key words långbanite, crystal structure, Raman spectroscopy, Mössbauer spectroscopy, Långban mine

RECENT ADVANCES IN TRANSITION METAL-CONTAINING BORATES WITH TUNABLE PROPERTIES

Yaroslav P. Biryukov[1], Almaz L. Zinnatullin[2], Andrey P. Shablinskii[1], Margarita S. Avdontceva[3], Yulia S. Gokhfeld[4], Maria G. Krzhizhanovskaya[3], Natalia V. Kazak[4], Rimma S. Bubnova[1], Farit G. Vagizov[5], Stanislav K. Filatov[3]

1. Institute of Silicate Chemistry, Russian Federation
2. Federal Research Center Kazan Scientific Center of RAS, Russian Federation
3. Institute of Earth Science, St. Petersburg State University, Russian Federation
4. Kirensky Institute of Physics, Federal Research Center KSC SB RAS, Russian Federation
5. Institute of Physics, Kazan Federal University, Russian Federation

Abstract Transition metal-containing (*TM*) borates have attracted significant interest over the past decade due to their rich crystal chemistry and diverse functional properties including multiferroic, ferroelectric, electrochemical, magnetic, resonance and optical. Of particular interest are exotic phenomena recently discovered in *TM* borates such as cascades of magnetic transitions within independent magnetic subsystems, spin liquid, spin glass and spin ice states, geometric frustration and high magnetic ordering temperatures. Owing to this unique combination of properties, these compounds are utilized in the design of key commercial single-crystal materials for Mössbauer spectroscopy sources, electrodes for metal-ion batteries and promising components for MRAM in spintronic applications.

This study presents a comprehensive investigation of *TM* borates characterized by X-ray diffraction alongside known magnetic and thermal properties. Thermal data were obtained through the development of original methodological approaches employing complementary *in situ* techniques – primarily variable-temperature X-ray diffraction and Mössbauer spectroscopy – enabling a simultaneous analysis of local structural and bulk phenomena in magnetic materials. This work summarizes our findings alongside existing literature on the temperature-dependent crystal chemistry of synthetic and natural *TM* borates. We demonstrate that, in addition to chemical composition, the anisotropy of magnetic and thermal properties is largely governed by specific features of the crystal structure. These comprehensive insights significantly advance the fundamentals of crystal-chemical prediction and the rational design of promising magnetic materials.

Key words Borates, X-ray diffraction, Thermal expansion, Magnetics, Mineral-like materials

Acknowledgemengts The work was funded by the Russian Science Foundation Grant No. 25-73-00080, https://rscf.ru/project/25-73-00080.

RETENTION-ACTIVE OXIDE MATRICES AS DYNAMIC SINKS FOR ARSENIC AND ANTIMONY IN LEGACY MINE TAILINGS

Katharina Vacek[1] and Tamara Đorđević, T.[1,2]

1. Department of Mineralogy and Crystallography, University of Vienna, Vienna, Austria

2. E057-02 USTEM, Vienna University of Technology (TU Wien), Austria

Abstract Legacy flotation tailings from historical mining represent both a secondary resource and a long-term environmental concern due to the mobility of toxic metalloids. The realgar-rich tailings at Lojane, originating from an abandoned Sb-As-Cr mine in North Macedonia, provide an opportunity to investigate the retention of arsenic (As) and antimony (Sb) within metastable, cement-like secondary phases formed during weathering of primary sulphides.

Using vertically resolved sampling combined with scanning electron microscopy (SEM), this study characterises the role of secondary oxide matrices as dominant hosts for As and Sb. These phases occur as pore-filling and grain-coating materials and exhibit strongly heterogeneous compositions, forming three principal types: Fe-rich, Fe-poor (Sb-rich), and S-rich matrices. The Fe-rich phases (5–15 at% Fe; 15–25 at% As) are consistent with Sb-bearing Fe–As oxyhydroxides (e.g., scorodite-like or poorly crystalline Fe–As gels), while Fe-poor phases (<10 at% Fe; up to 30 at% Sb) correspond to mixed Sb–As oxides. S-rich matrices (up to 20 at% S) represent partially oxidised sulphide relics that act as a continuing source of metalloids.

These metastable oxide phases act as the primary retention sites for As and Sb through a combination of adsorption, co-precipitation, and incorporation into poorly crystalline matrices formed during oxidative weathering. The Fe-rich oxyhydroxides preferentially retain As, whereas Sb is more effectively sequestered in Fe-poor, Sb-rich oxide phases, indicating phase-dependent partitioning of metalloids. The S-rich phases sustain this system by releasing As and Sb, thereby promoting ongoing formation of secondary retention phases.

Despite their transient nature, these cement-like matrices exert a strong control on metalloid mobility by temporarily immobilising As and Sb. However, their metastability implies that changes in environmental conditions (e.g., redox or pH) may destabilise these phases, potentially leading to remobilisation.

Overall, this study highlights the critical role of metastable oxide phases as dynamic but effective sinks controlling the retention and release of metalloids in mine tailings systems.

Financial support of the Austrian Science Fund (FWF) [P 36828-N] to T. Đorđević is gratefully acknowledged.

Key words antimony, arsenic, secondary oxides, electron microscopy

SHOJIITE: A NEW AMPHIBOLE SUPERGROUP MINERAL FROM HOKKAIDO, JAPAN.

Maki Hamada[1], Mariko Nagashima[2], Terumi Ejima[3], Tomoyuki Mizukami[1], Noriko Hasebe[4], Koichi Momma[5], Akihiro Tamura[1], Akihiro Ishii[6], Kiwamu Okamoto[7], and Tomoaki Morishita[1.8]

1. College of Science and Engineerig, KanazawaUniversity, Japan
2. Division of Earth Science, Graduate school of Sciences and Technology for Innovation, Yamaguchi University, Japan
3. Faculty of Science, Shinshu University, Japan
4. Institute of Nature and Environmental Technology, Kanazawa University, Japan
5. National Museum of Nature and Science, Japan
6. Shibetsu City Museum, Japan
7. Department of marine Biology and Sceices, Biological Sciences, Tokai University, Japan
8. Volcanoes and Earth's Interior Research Center, Japan Agency for Marine-Earth Science and Technology, Japan

Abstract The amphibole supergroup represents one of the most chemically complex and geologically significant mineral groups in the Earth's crust and upper mantle. We report the discovery of a new mineral species, shojiite (IMA 2024-023a), a sodium-(magnesium-iron-manganese) amphibole found in the Horokanai ophiolite, Hokkaido, Japan. The mineral is named in honor of Professor Shoji Arai, a world-renowned expert on peridotites and their metasomatism. Shojiite, $Na(NaMg)_2Mg_5Si_8O_{22}(OH)_2$, is the Mg-analogue of richterite and hjalmarite, specifically characterized by the dominance of Mg over other divalent cations at the *B* site. Shojiite was discovered in boulders found in the Mamushinosawa Creek in the Horokanai ophiolite. It occurs as aggregates of prismatic crystals that form an almost monomineralic rock, associated with minor amounts of serpentine and chlorite. The mineral is transparent and green in color with pale green streaks and has a vitreous luster. It exhibits perfect {110} cleavage and has a Mohs hardness of 5 1/2. Its density is approximately 3.04 g/cm³. Shojiite is optically biaxial(-), with $\alpha = 1.612$, $\beta = 1.626$ and $\gamma = 1.633$, and is pleochroic, with pale green to pale yellowish green to pale reddish brown. Under the microscope, shojiite shows positive elongation. It is non-magnetic and does not adhere to a neodymium magnet. Chemical analysis using electron probe microanalysis and wet chemical methods (for Fe^{2+}/Fe^{3+} determination) confirms that shojiite is chemically homogeneous. The empirical formula calculated on the basis of (O, OH, F, Cl) = 24 is $^{A}(K_{0.01}Na_{0.80}\square_{0.19})_{\Sigma 1.00}{}^{M4}(Na_{0.900}Mg_{0.512}Ca_{0.332}Fe^{2+}{}_{0.256})_{\Sigma 2.000}{}^{M1}Mg_{2.000}{}^{M2}(Mg_{1.799}Cr_{0.166}Fe^{3+}{}_{0.128})_{\Sigma 4.997}{}^{M3}Mg_{1.000}{}_{0}{}^{T}(Si_{7.89}Al_{0.11})_{\Sigma 8.00}O_{22}(OH)_2$. The critical feature of shojiite is the occupancy of the *B* site, where Mg (0.44

apfu) is greater than Ca (0.33 apfu). This dominance of Mg at the 8-coordinated *B* site requires a new root name within the amphibole classification system. By crystal structural analysis, the structural refinement converged to R_1 = 3.51%. Shojiite is monoclinic with the space group $P2_1/m$. Its unit cell parameters are a = 9.7912(5) Å, b = 17.9438(9) Å, c = 5.2721(3) Å, β = 103.548(5)° and V = 900.49(8) Å^3. While many sodic amphiboles belong to the space group, reflections violating *C*-lattice extinction rules were observed in shojiite, confirming the primitive lattice. Fourier-transform infrared spectroscopy shows absorption bands at 3671 and 3720 cm^{-1}, which are assigned to MgMgMg-OH-^{A}□ bond facing a vacant *A* site and MgMgMg-OH-^{A}Na bond facing an occupied *A* site, respectively.

Key words **s**hojiite, amphibole supergroup, new mineral

STILLWELLITE-(LA): A NEW MINERAL FROM THE GEJIU INTRUSION, YUNNAN, CHINA

Kai Qu[1,2*], Guochen Dong[3], Guang Fan[4], Xiangping Gu[5], Junping Ren[1], Alei Gu[1], Hang Zhang[1], Yanjuan Wang[6,7]

1. Tianjin Center, China Geological Survey, Hedong, Tianjin, China

2. School of Earth Sciences and Engineering, Nanjing University, Xixia, Nanjing, China

3. School of Earth Sciences and Resources, China University of Geosciences (Beijing), Haidian, Beijing, China

4. Beijing Research Institute of Uranium Geology, Chaoyang, Beijing, China

5. Jiangxi University of Applied Science, Xinjian, Nanchang, China

6. State Key Laboratory of Deep Earth and Mineral Exploration, Chinese Academy of Geological Sciences, Beijing, China

7. Department of Geosciences, University of Padova, Padova, Italy

Abstract Stillwellite-(La), ideally $LaBSiO_5$, is a new rare lanthanide borosilicate discovered in feldspathoid syenite of the Gejiu intrusion, Honghe Hani and Yi Autonomous Prefecture, Yunnan Province, China. It is associated with stillwellite-(Ce), fluorbritholite-(La), moxuanxueite, låvenite, baddeleyite, phlogopite, aegirine, jadeite, magnetite, orthoclase and albite. Stillwellite-(La) forms subhedral granular crystals, commonly 2–100 μm in size, and is pale brown to pale yellow in color. Electron microprobe analyses, complemented by boron confirmation using Time-of-Flight Secondary Ion Mass Spectrometry, yielded the empirical formula (based on 5 anions, O + F): $(La_{0.45}Ce_{0.40}Pr_{0.10}Ca_{0.07}Nd_{0.03}Na_{0.02}Th_{0.01})_{\Sigma 1.08}BSi_{0.94}(O_{4.92}F_{0.08})_{\Sigma 5.00}$, corresponding to the simplified formula (La,Ce,Ca,Pr,Na,Th)(B,Pr,Nd)BSi(O,F)$_5$. Raman spectra are generally consistent with those of synthetic $LnBSiO_5$ (Ln = REE) phases and stillwellite-(Ce), with the strongest band at 903 cm^{-1} assigned to stretching vibrations of SiO_4 and BO_4 groups. A platy fragment of stillwellite-(La) (15 × 10 × 7 μm) was selected for single crystal X-ray diffraction using a Rigaku XtaLAB Synergy diffractometer with Cu$K\alpha$ radiation. The results demonstrate that stillwellite-(La) crystallizes in the trigonal system, space group $P3_221$ (#154). Refined unit-cell parameters are a = 6.9061(5), c = 6.7549(5) Å, V = 279.01(5) Å^3, and Z = 3. The refinement converged to R_1 = 0.0383 for 388 independent reflections with $I > 2\sigma(I)$. Stillwellite-(La) is the La-dominant analogue of stillwellite-(Ce), previous synthetic studies of stillwellite-type materials generally report $P3_1$ symmetry at low temperature and $P3_221$ at high temperature. The new mineral and its name were approved by the IMA-CNMNC (IMA2024-074). The type material is deposited at the Geological Museum of China, No. 16, Yangrou Hutong, Xisi, Beijing 100031, People's Republic of China, under catalogue number GMCTM2024010.

Key words Stillwellite-(La), borosilicate, REE mineral, new mineral, Gejiu intrusion

STRUCTURAL ORIGIN OF THERMAL EXPANSION IN $RBSO_4$ AND $RB_2CA_3(SO_4)_3$

Sofya Vladimirovna Demina[1,2], Andrey Pavlovich Shablinskii[1,2], Rimma Sergeevna Bubnova[1], Maria Georgievna Krzhizhanovskaya[2], Stanislav Konstantinovich Filatov[2]

1. Laboratory of structural chemistry of oxides, Institute of Silicate Chemistry, Russian Federation

2. Institute of Earth Science, St. Petersburg State University, Russian Federation

Abstract In this work, the nature of the anisotropy of thermal expansion is explained in terms of crystal structure data, and the positive and negative thermal expansion behavior of langbeinite-, arcanite-, and metathenardite-type compounds is considered. Thermal expansion of Rb_2SO_4 and langbeinite-type $Rb_2Ca_2(SO_4)_3$ was investigated by high-temperature powder X-ray diffraction in the temperature ranges 25–900 °C and 25–1000 °C, respectively. A temperature-induced structural phase transition *Pmcn* ↔ $P6_3/mmc$ (or β- ↔ α-Rb_2SO_4) is observed at 663 ± 12 °C. Thermal expansion of Rb_2SO_4 is highly anisotropic: for β-Rb_2SO_4 (at 300 °C) $\alpha_a = 35.9(1)$, $\alpha_b = 28.9(2)$, $\alpha_c = 70(1)$, $\alpha_V = 127(2) \times 10^{-6}$ °C^{-1}; for α-Rb_2SO_4 (at 800 °C) $\alpha_a = 55(5)$, $\alpha_c = 115(9)$, $\alpha_V = 224(12) \times 10^{-6}$ °C^{-1}. Thermal expansion coefficients for $Rb_2Ca_2(SO_4)_3$ are: $\alpha_a = 10.4(2)$, $\alpha_V = 31.1(6) \times 10^{-6}$ °C^{-1} (at 25 °C). The crystal structure of the high-temperature α-Rb_2SO_4 was refined at 700 and 1000 °C. The anisotropy of the expansion of both Rb_2SO_4 modifications is explained by the rotation of SO_4 tetrahedra. The crystal structure of the langbeinite-type $Rb_2Ca_2(SO_4)_3$ is described in terms of $M(TO_4)_6$ microblocks. The interpretation of the expansion of $Rb_2Ca_2(SO_4)_3$ is based on a mechanism of rocking polyhedra and hinge deformation of the $M(TO_4)_6$ microblocks. The crystal-chemical reasons for changes in hinge angles at the level of the microblocks are considered..

Key words Sulfates, Thermal expansion, Crystal structure

Acknowledgements This work was supported by the RSF (No. №23-77-10066-P) and utilized equipment from the "RDMI".

THERMAL EXPANSION OF THE NOVEL BORATE-PHOSPHATE $Y_7O_6(BO_3)(PO_4)_2$

Sofya Vladimirovna Demina[1], Andrey Pavlovich Shablinskii[1], Rimma Sergeevna Bubnova[1], Maria Georgievna Krzhizhanovskaya[2], Stanislav Konstantinovich Filatov[2]

1. Laboratory of structural chemistry of oxides, Institute of Silicate Chemistry, Russian Federation

2. Institute of Earth Science, St. Petersburg State University, Russian Federation

Abstract This work reports the synthesis of a novel borate-phosphate, $Y_7O_6(BO_3)(PO_4)_2$, which belongs to the $Ln_7O_6(BO_3)(PO_4)_2$ family. The compound was synthesized via a high-temperature solid-state reaction at 1350 °C for 24 hours. The resulting sample consists predominantly of the target phase, with minor YPO_4 and Y_2O_3 impurities. The borate-phosphate crystallizes in the monoclinic system, space group $P2_1/n$. The unit cell parameters, refined from powder X-ray diffraction data, are: a = 6.6128(3), b = 17.2658(8), c = 12.5441(6) Å, β = 96.38(3) , V = 1423.35(3) Å^3. The crystal structure features seven independent crystallographic sites for rare-earth cations, two for phosphorus, and one for boron. The rare-earth polyhedra form layers parallel to the *ab* plane, with the rare-earth cations coordinated by seven or eight oxygen atoms. The structure contains three types of anions: additional O^{2-} anions, along with isolated $[BO_3]^{3-}$ and $[PO_4]^{3-}$ complex anions. The isolated BO_3 and PO_4 groups are oriented parallel to the (100) plane.

High-temperature powder X-ray diffraction was performed to investigate the thermal expansion of $Y_7O_6(BO_3)(PO_4)_2$. The compound remains stable up to 870 °C; upon further heating, a polymorphic transition occurs, as evidenced by the temperature dependence of the unit cell parameters. The thermal expansion coefficients are as follows: at 30 °C, α_a = 9.37(3), α_b = 6.31(2), α_c = 5.33(2), α_β = -1.55(4), α_V = 21.01(7) × 10^{-6} °C^{-1} (at 30 °C), α_a = 10.61(2), α_b = 14.47(3), α_c = 12.52(2), α_β = -0.24(5), α_V = 37.62(7) × 10^{-6} °C^{-1} (at 800 °C). Thermal expansion is maximal along the *b*-axis, which is perpendicular to the preferred orientation of the BO_3 triangles located in the *ac* plane. Future research will focus on growing single crystals of $Y_7O_6(BO_3)(PO_4)_2$ and solving its crystal structure using single-crystal X-ray diffraction data at both room temperature and 850 °C to fully characterize the high-temperature polymorph.

Key words Borate-phosphate, Thermal expansion, Crystal structure

Acknowledgements This work was supported by the RSF (No. №26-73-00196) and utilized equipment from the "RDMI".

AMBIENT-CONDITION TRANSFORMATION FROM LAYERED TO TUNNELED MANGANESE OXIDES DRIVEN BY MONOLAYER ASSEMBLY

Chunjiang Li[1,2], Huan Ye[1,2], Ziyi Zhuang[1,2], Zhaoyang Hu[1,2], Anhuai Lu[1,2], Yan Li[1,2,*]

1. SKLab-DeepMinE, MOEKLab-OBCE, School of Earth and Space Sciences, Peking University, China

2. Beijing Key Laboratory of Mineral Environmental Function, School of Earth and Space Sciences, Peking University, China

Abstract In Earth's surface settings, layered manganese (Mn) oxides tend to spontaneously convert into tunneled structures, which is a thermodynamically favored and widespread phenomenon. Previous work has intensively studied this conversion and its controlling variables (e.g., pH, interlayer cations) using high-energy hydrothermal systems or repeated redox cycling. However, how this transformation proceeds under low-energy supergene conditions is still not well understood, especially whether the intrinsic stacking tendency of birnessite layers can by itself drive the process.

To address this gap, we used monolayer Mn oxide—inspired by the few-layer habit of natural birnessite—as a simplified starting model. We examined how these monolayers assemble at room temperature under different pH and K^+ levels. Negatively charged sheets adsorb H^+ and K^+, which induces layer stacking. Strikingly, we discovered that mere stacking can trigger phase transformation even under mild conditions. After 20 days, synchrotron X-ray diffraction and X-ray absorption fine structure analyses revealed that acidic media produce tunneled cryptomelane (2×2) and groutite (1×2), while neutral or alkaline conditions yield only multilayered birnessite. In acidic solutions, higher K^+ concentrations speed up the conversion and promote cryptomelane. Electron microscopy shows that individual monolayers appear as flexible, silky sheets, whereas rapidly stacked aggregates exhibit lattice distortion and strain. These deformations allow Mn^{3+} to migrate from intra- to interlayer positions, relieving Jahn-Teller strain and enabling tunnel wall construction. Density Functional Theory calculations confirm that the monolayer's high formation energy substantially lowers the energy barrier for phase transformation, making the reaction feasible at ambient conditions.

Combining these observations, we built a phase diagram illustrating the thermodynamic stability of monolayer birnessite, multilayered birnessite, and the two tunneled oxides as functions of pH and K^+ concentration. Our work thus outlines a comprehensive kinetic-thermodynamic framework for the oxidation of aqueous Mn^{2+} into monolayer oxides and their subsequent evolution into few-layer or tunneled phases in supergene environments. We attribute the phase conversion to a kinetic mismatch between layer formation and layer assembly, with pH and metal cations exerting thermodynamic control over the final assemblage. These insights offer a new perspective on Mn oxide distribution and

transformation in soils, sediments, and other low-energy aquatic systems.

Key words Manganese oxides, Birnessite, Monolayer assembly, Ambient condition mineral transformation, Phase diagram

Acknowledgements This work was supported by the National Natural Science Foundation of China (42372049, 42192502, and 92351302), the Chinese Academy of Geological Sciences Basal Research Fund (JKYDM2025110), the National Science and Technology Major Project (2025ZD1010301), and the Regional Special Program (KCX2024003). The authors acknowledge beamline BL13SSW at Shanghai Synchrotron Radiation Facility for the SXRD experiments supports. The DFT calculations were computed on the High-Performance Computing Platform of Peking University. The authors acknowledge Electron Microscopy Laboratory of Peking University, China for the use of FEI Tecnai F20 transmission electron microscopy.

ATOMIC MECHANISM OF AU–AS COUPLING IN PYRITE

Xin Liu[1*], Xiancai Lu[2], Hao Liu[3], Huan Liu[2], Kunfeng Qiu[4]

1. Engineering Research Center of Ministry of Education for Geological Carbon Storage and Low Carbon Utilization of Resources, Beijing Key Laboratory of Materials Utilization of Nonmetallic Minerals and Solid Wastes, National Laboratory of Mineral Materials, Hebei Key Laboratory of Resource Low-carbon Utilization and New Materials, School of Materials Science and Technology, China University of Geosciences, Beijing, 100083, China
2. State Key Laboratory of Critical Earth Material Cycling and Mineral Deposits, School of Earth Sciences and Engineering, Nanjing University, Nanjing 210023, China
3. School of Science, China University of Geosciences, Beijing, 100083, China
4. State key Laboratory of Geological Processes and Mineral Resources, Frontiers Science Center for Deep-time Digital Earth, School of Earth Sciences and Resources, China University of Geosciences, Beijing 100083, China

Abstract Strong coupling between Au and As in pyrite has been observed in many types of gold deposits. However, the valence states and solubility of Au and As remain controversial, and the microscopic coupling mechanism between Au and As is still poorly understood. In this study, pyrite solid solutions with varying As contents were simulated with density functional theory (DFT). Detailed investigation of the microscopic crystal structure of As-bearing pyrite reveals that As tends to aggregate in a specific triangle within the FeS_6 octahedron, and this may be key for Au incorporation into the pyrite lattice. When two or three As atoms occupy this specific triangle, Au is most readily stabilized in the pyrite structure. Analysis of the energy differences for Au substituting at Fe sites versus interstitial sites under varying As contents shows that the most energetically favorable configuration is Au located at the center of the same Fe–S octahedron where three S atoms are replaced by As, while the original Fe atom at that site is displaced to an interstitial position, forming an Fe–S tetrahedron. Nevertheless, this does not preclude the possibility of other substitution mechanisms. When two As atoms substitute for S in the same Fe–S octahedron, the central Fe site is also readily occupied by Au, but the statistical thermodynamic probability of this configuration is significantly lower than that of the aforementioned one. Based on these results, statistical thermodynamic calculations were performed to define the upper limit of Au content in pyrite as a function of specific As content. These calculated results are in good agreement with a lot of previously published experimental data. This study elucidates the atomic-scale mechanism of Au–As coupling, discusses the enrichment mechanism of Au in pyrite from a theoretical computation perspective, and provides a new research approach for studying coupled element behavior in minerals.

Key words Pyrite**,** Au–As coupling, DFT simulation, Statistical thermodynamic calculation

Acknowledgements This work was supported by the National Natural Science Foundation of China (41802036, 42572041). We are grateful to the High Performance Computing Platform of China University of Geosciences Beijing and the High Performance Computing Center of Nanjing University for using the FLEX Blade cluster system.

COMPETING CRYSTALLIZATION PATHWAYS IN CALCIUM ARSENATES

Xiangyu Zhu[1], Minghao Tang[1], Xiancai Lu[2], Rucheng Wang[2], Hui Henry Teng[1]

1. Institute of Surface-Earth System Science, School of Earth System Science, Tianjin University, Tianjin 300072, China

2. State Key Laboratory of Critical Earth Material Cycling and Mineral Deposits, School of Earth Sciences and Engineering, Nanjing University, Nanjing 20046, China

Abstract Crystallization in natural geochemical environments rarely follows a single deterministic pathway; instead, multiple mineralization routes often operate concurrently and compete for solutes, generating complex polymorphic outcomes. Yet the dynamic interplay among these pathways and its control by physicochemical conditions remain poorly resolved. Here, using calcium arsenate systems forming pharmacolite (Pmc), haidingerite (Hdi), and guérinite (Gué) as a model, we uncover how competing crystallization pathways reorganize under varying pH and temperature. At mildly acidic conditions (pH ≈ 6.0), two classical pathways coexist, yielding Pmc or Hdi depending on kinetic–thermodynamic preferences: Pmc dominates at low temperature, whereas Hdi prevails at elevated temperature. Near critical boundary conditions (e.g., pH 6.0, 25°C), where nucleation barriers converge, stochastic fluctuations amplified by autocatalytic growth dictate the final polymorph, producing exclusively Pmc or Hdi under nearly identical conditions. Increasing pH (~6.45) or temperature (40–60 °C) activates a non-classical route via amorphous calcium hydrogen arsenate (ACHA), producing metastable core–shell guérinite-rimmed spherical compounds (GRSCs). During subsequent crystallization of Pmc and Hdi, GRSCs undergo Kirkendall-effect-driven dissolution into hollow structures when the growth rate of Gué exceeds that of its counterparts. These results establish a hierarchical framework for polymorph selection governed by accessibility and competition among crystallization pathways and provide a predictive basis for polymorphic evolution in both synthetic and natural systems.

Key words Competitive crystallization, Polymorph selection, Non-classical pathways, Kirkendall effect, Calcium arsenates

DECOMPOSITION PATHWAYS OF S_6 AND FORMATION OF POLYSULFIDE CHROMOPHORES IN SODALITE-GROUP MINERALS

Maria Fedyaeva,[1,2,*] Sergey Lepeshkin,[1, 2, 3], Nikita V. Chukanov[4] and Artem R. Oganov[2]

1. Vernadsky Institute of Geochemistry and Analytical Chemistry, Russian Academy of Sciences, Kosygina, 19, Moscow, 119991, Russia

2. Skolkovo Institute of Science and Technology, Bolshoy Boulevard 30, bld. 1, Moscow 121205, Russia

3. Lebedev Physical Institute, Russian Academy of Sciences, 53 Leninskii prosp., 119991 Moscow, Russia

4. Federal Research Center of Problems of Chemical Physics and Medicinal Chemistry, Russian Academy of Sciences, Chernogolovka 142432, Russia

Abstract This study examines the thermal transformations of polysulfide chromophore species in sodalite-group minerals such as haüyne, lazurite, and slyudyankaite, where sulfur-bearing extra-framework species play a key role in determining mineral color. Using density functional theory calculations, the authors focus on the decomposition of the cyclic S_6 molecule in order to identify the most probable reaction pathways and final products formed during heating. Several possible mechanisms were analyzed, including decomposition of neutral S_6, one-electron capture followed by ring opening and fragmentation, and sequential capture of two electrons. The calculations show that direct decomposition of neutral S_6 is unfavorable because it requires relatively high energy barriers, whereas the most favorable pathway begins with spontaneous capture of one electron, which leads to opening of the S_6 ring and formation of a chain radical anion. This intermediate then decomposes with a low limiting barrier of about 0.4 eV, mainly producing the radical-anion pairs $S_3^{\bullet-} + S_3^{\bullet-}$ and $S_2^{\bullet-} + S_4^{\bullet-}$. In contrast, capture of a second electron is associated with a much higher barrier of about 2 eV, making this route much less likely. The study also shows that radical anions $S_n^{\bullet-}$ are generally the most stable sulfur species for a given number of atoms. Overall, the results provide a theoretical explanation for experimentally observed sulfur transformations in sodalite-group minerals and help clarify the origin of their color by linking specific chromophore species with energetically preferred reaction pathways.

Key words polysulfides, sodalite-group minerals, chromophores, DFT calculation

INTEGRATED APPLICATION OF FIB-SEM IN 3D RECONSTRUCTION, MICROSTRUCTURE ANALYSIS AND MULTI-TECHNIQUE COMBINED CHARACTERIZATION OF MINERALIZED FOSSILS AND MINERAL SOLID SOLUTIONS

Qian Chen

State Key Laboratory of Palaeobiology and Stratigraphy, Nanjing Institute of Geology and Palaeontology, Chinese Academy of Sciences, Nanjing 210008, China

Abstract Focused ion beam scanning electron microscopy (FIB-SEM) technology, with its precision micro- and nano-fabrication capabilities and three-dimensional characterization capabilities, has become a key tool for analyzing the structure of mineral solid solutions, characterizing their composition, and conducting phase analysis. Broadly speaking, mineralized fossil materials also fall under the category of solid solutions. This report systematically reviews three core applications of FIB-SEM in paleontological fossil research, with the hope that these techniques will be widely applied to the study of mineral solid solutions in the future. (1) Sequential sectioning and scanning by FIB-SEM enable three-dimensional reconstruction of the structure and composition of mineralized fossils, thereby identifying the 3D spatial distribution of different minerals and their assemblages. Furthermore, combined with the large field-of-view and non-destructive scanning advantages of micro-CT, we have established a workflow for rapidly locating regions of interest inside mineralized fossil specimens, enabling multi-modal, cross-scale analysis of specific minerals and mineral assemblages. (2) By preparing sections with thicknesses less than 100 nm at specific locations, the FIB-SEM instrument allows subsequent scanning transmission electron microscopy observation to be performed directly on the same device, enabling rapid characterization of sub-nanometer morphological and structural features. Meanwhile, transmission electron backscatter diffraction analysis can also be completed in situ with this integrated system, efficiently acquiring phase and orientation distribution information of mineral grains in a convenient and cost-effective manner. Nevertheless, the above convenient workflow is inapplicable to ultrafine mineral particles, making conventional TEM methods such as selected area electron diffraction essential for further characterization. To enable analysis by nano-secondary ion mass spectrometry and nano-infrared spectroscopy, especially for samples with uneven surfaces or difficult-to-polish textures, slices thinner than 2 μm can be prepared and mounted flat on silicon wafers, through which in-situ molecular structure and chemical bonding information can be effectively obtained. (3) Prepare three-dimensional atomic probe samples to achieve atomic-level three-dimensional reconstruction of mineral solid solutions. This report presents multi-technique combinations bridged by FIB-SEM, which integrate information on morphology, crystal structure, elements and chemical bonds. It provides a new approach for multi-

dimensional, multi-scale, and multi-modal in-situ characterization of the formation mechanisms of mineral solid solutions and the study of diagenetic and mineralization processes. This approach not only holds broad application prospects in the field of paleontology but also shows great potential in numerous geological disciplines, including petrology, mineralogy, sedimentology, as well as in hydrocarbon exploration.

Key words FIB-SEM, Mineralized Fossils, Mineral Solid Solutions, Multi-Technique

MICRO- TO NANO-SCALE GEOCHEMICAL CHARACTERISTICS OF PYRITE AND ARSENOPYRITE: IMPLICATIONS FOR GOLD MINERALIZATION AT THE JIAGANTAN GOLD DEPOSIT, WEST QINLING OROGEN

Yu-Hui Wang , Ya-Fei Wu*

State Key Laboratory of Geological Processes and Mineral Resources and School of Earth Resources, China University of Geosciences, Wuhan, Hubei Province 430074, China

Abstract The West Qinling Orogen is one of the most important orogenic gold provinces in China, where gold is mainly hosted in pyrite and arsenopyrite. However, the occurrence and enrichment mechanisms of gold in these sulfides remain unclear. This study investigates the micro- to nano-scale geochemical characteristics of auriferous pyrite and arsenopyrite from the world-class Jiagantan gold deposit (>150 t Au, average grade 2~3 g/t), aiming to elucidate their implications for gold mineralization. Detailed mineralogical observations reveal that four generations of pyrite (Py1–Py3) and three generations of arsenopyrite (Apy1–Apy2) occur at Jiagantan: fine-grained disseminated pyrite (Py1) and arsenopyrite (Apy1); euhedral pyrite (Py2a) intergrown with radial arsenopyrite (Apy2a); subhedral to anhedral pyrite (Py2b) intergrown with radial arsenopyrite (Apy2b); and coarse-grained euhedral pyrite (Py3) with a core-rim texture. LA-ICP-MS analyses demonstrate that all sulfide generations are enriched in Au and As. Among the pyrite generations, Py1 contains the highest Au concentration (mean = 606 ppm) and is enriched in As (mean = 68,260 ppm). Arsenopyrite generally contains higher Au contents than pyrite, with Apy2b showing the highest mean Au content (mean = 706 ppm). These features indicate that the sulfides precipitated from a long-lived, Au–As-rich hydrothermal fluid system. TEM observations reveal that gold predominantly occurs as a solid solution within the crystal lattice of pyrite and arsenopyrite rather than as nanoparticles. These results indicate that Au is most likely incorporated into the sulfide lattice via Au–As coupled substitution mechanisms.

Key words Aurifeorus sulfides, Invisible gold, Jiagantan gold deposit, West Qinling Orogen

SPECIATION OF NICKEL AND COBALT DURING FE(II)-MEDIATED BIRNESSITE TRANSFORMATION

Jing Hu[1], Maximilian Mann[1], Jessica Hamilton[2], Andrew Frierdich[*, 1]

1. School of Earth, Atmosphere and Environment, Monash University, Australia

2. Australian Synchrotron, Australian Nuclear Science and Technology Organisation (ANSTO)

Abstract The accumulation of anthropogenic CO_2 intensifies global warming, driving the search for carbon-negative strategies to recover critical metals. Cobalt (Co) and nickel (Ni), indispensable for batteries and renewable infrastructure, are mainly hosted in laterite deposits within iron and manganese (oxyhydr)oxides. To address this challenge, we applied Fe(II)-catalysed recrystallisation and reductive dissolution as an environmentally friendly extraction route. Unlike high-pressure acid leaching, this method efficiently releases Co/Ni from goethite and hematite at ambient temperature (25 °C) and circumneutral pH (~7.5). Yet, the role of Fe(II) in mobilising Ni and Co from birnessite (δ-MnO2), another key Ni/Co-bearing host in laterites, remains poorly understood. In this study, synthetic Co/Ni-incorporated birnessite was subjected to controlled Fe(II) reductive dissolution, which substantially accelerated the concomitant release of Ni and Co. Post-reaction X-ray diffraction (XRD) and X-ray absorption spectroscopy (XAS) revealed mineralogical transformations, confirming birnessite reductive dissolution and secondary Fe(oxyhydr)oxide formation. These findings elucidate trace-metal cycling in Fe(II)-rich, redox-active systems and inform carbon-negative strategies for critical metal recovery from laterites. By clarifying reaction pathways and guiding process optimisation, this work supports the development of environmentally friendly technologies to secure critical metals essential for the global energy transition.

Key words Birnessite, Critical metals, Fe(oxyhydr)oxide, X-ray absorption spectroscopy

SPONTANEOUS POLARIZATION OF TOURMALINE SUBSPECIES AND ITS ENHANCEMENT ON PHOTOCATALYTIC CO_2 REDUCTION

Jiaqi Liu, Qingxin Liu, Xin Liu*, Yingmo Hu, Guocheng Lv, Libing Liao

Engineering Research Center of Ministry of Education for Geological Carbon Storage and Low Carbon Utilization of Resources, Beijing Key Laboratory of Materials Utilization of Nonmetallic Minerals and Solid Wastes, National Laboratory of Mineral Materials, Hebei Key Laboratory of Resource Low-carbon Utilization and New Materials, School of Materials Science and Technology, China University of Geosciences Beijing, 100083, China

Abstract: Tourmaline exhibits spontaneous polarization arising from its noncentrosymmetric structure with space group *R*3*m*, positioning it as a potential built-in electric field source for photothermal synergistic catalytic CO_2 reduction. In this study, three typical subspecies—schorl from USA, dravite from Xinjiang, China, and elbaite from Brazil were selected for systematic analysis of their chemical composition, crystal structure, and spontaneous polarization properties. XRD, LA-ICP-MS, and FT-IR confirm the high purity of all samples, and isomorphous substitution of Y-site cations ($Fe^{2+}\rightarrow Mg^{2+}\rightarrow Li^{+}$) induces regular variations in lattice parameters. Rietveld refinement reveals intrinsic dipole moments in the order: elbaite > schorl > dravite. The superior polarization of elbaite stems from severe [XO_9] polyhedron distortion within a Li, Al, and F-rich environment, whereas polarization in schorl and dravite is primarily governed by [SiO_4] tetrahedron distortion. Furthermore, both polarization intensity and pyroelectric coefficient increase first linearly and then exponentially with rising temperature. At room temperature, elbaite shows the strongest spontaneous polarization; at elevated temperatures, schorl becomes dominant. Compositing elbaite with various semiconductors such as ZnO, g-C_3N_4, MgAl-LDH, $CuInS_2$, and CuO, the photocatalytic CO_2 reduction performance improved significantly, with CO yield increasing by 1.76 to 4.6 times. Among these, the ZnO/Elbaite composite shows the most pronounced improvement, with a 4.6-fold increase. This study elucidates the composition–structure–polarization relationship in tourmaline, offering a theoretical foundation for its targeted application in synergistic catalytic CO_2 reduction.

Key words Tourmaline, Crystal structure, Spontaneous polarization, Intrinsic dipole moment, Photocatalytic CO_2 reduction

VISIBLE-LIGHT-DRIVEN REDOX PROCESSES AND STRUCTURAL EVOLUTION OF LAYERED MANGANESE OXIDES TOWARD TUNNEL-STRUCTURED PHASES

Zhaoyang Hu[1,2], Huan Ye[1,2], Yan Li[1,2]

1. State Key Laboratory of Deep Earth and Mineral Exploration, School of Earth and Space Sciences, Peking University, Beijing 100871, China

2. Beijing Key Laboratory of Mineral Environmental Function, School of Earth and Space Sciences, Peking University, Beijing 100871, China

Abstract Layered manganese oxides (most commonly as birnessite) are widely distributed in Earth's surface environments and play critical roles in elemental cycling and redox reactions. Their transformation into tunnel-structured manganese oxides, such as todorokite and cryptomelane, is commonly considered to require hydrothermal conditions or prolonged diagenesis, and the mechanisms governing such transitions under ambient conditions remain poorly constrained. Here, we investigated the coupled effects of light and organic matter on the reduction and structural evolution of birnessite. Batch experiments demonstrated that light significantly enhances the reduction of birnessite by low-molecular-weight organic compounds, with formate exhibiting the strongest light-promoted reactivity compared to formaldehyde and methanol. Transient absorption spectroscopy confirmed the higher electron-donating capacities of formate and formaldehyde than methanol and water. Structural characterization using X-ray absorption spectroscopy indicated systematic changes in MnO_6 octahedra connectivity from edge-sharing to conner-sharing during reaction, implying the initiation of tunnel structure formation. This structural rearrangement was more pronounced under light conditions, which was in accordance with density functional theory calculations. Field samples of Mn-rich rock varnish and soil cutan further exhibited systematic variations in Mn oxidation state and mineral structure with depth, with more significant differences between surface and subsurface in organic-rich soil environments than desert varnish. The different patterns reflect synergistic effect of light and organic matter, which contributes to the active redox cycling of manganese oxides and its resultant structural transformation. These results suggest that light-driven redox processes can destabilize layered Mn oxides and promote their structural evolution, providing a potential pathway for layer-to-tunnel transformation in surface environments. Since Mn-rich rock varnish is also detected on Mars, the detailed investigation of composition and structure for manganese minerals in Martian rock and soil may help to evaluate the potential existence of organic matter as its importance in the transformation of manganese mineral phases.

Key words Manganese oxides, Birnessite, Light, Organic matter, Structural transformation

FORMATION MECHANISM OF MICRON-SCALE CHALCOPYRITE AND PYRRHOTITE BLEBS IN SPHALERITE FROM THE XIANGLUSHAN TUNGSTEN DEPOSIT, JIANGXI PROVINCE

Jing Zhou [1], Feng Zhu [1], Chang Xu [1], Jun gang Pang [2]

1. School of Earth and Planetary Sciences, China University of Geosciences, Wuhan, China.

2. School of Earth Sciences and Engineering, Xi'an Shiyou University, China.

Abstract The chemical and crystallographic associations between sulfide inclusions and their sphalerite host preserve key information on the thermal and fluid conditions of hydrothermal ore formation. Micron-scale chalcopyrite and pyrrhotite blebs in sphalerite host were found from Xianglushan tungsten deposit in Jiangxi Province, China. To characterize the chemical characteristics and crystallographic orientation relationships (COR) between sulfide inclusions and their sphalerite host, as well as reconstructing their formation mechanism, electron backscatter diffraction (EBSD), energy dispersive spectrum (EDS) and electron microprobe analysis (EPMA) measurements were carried out for the sphalerite samples. EPMA and EDS results reveal negligible compositional variations across different testing points within the sphalerite domain, indicating a relatively homogeneous composition. However, when approaching the sphalerite-chalcopyrite boundary, the Fe content increases gradually, the Cu content decreases progressively, and the Zn content exhibits a W-shaped oscillatory variation trend. Meanwhile, when approaching the pyrrhotite within the sphalerite-pyrrhotite intergrowth regions, the Fe content increases gradually, the Cu exhibits a W-shaped variation pattern, and the Zn content decreases progressively. EBSD measurements identified specific CORs $(100)_{Sph}$ // $\{100\}_{Ccp}$, $(100)_{Sph}$ // $\{001\}_{Ccp}$, $(110)_{Sph}$ // $\{110\}_{Ccp}$, and $(111)_{Sph}$ // $\{112\}_{Ccp}$ between the sphalerite host and chalcopyrite inclusions, and $(100)_{Sph}$ // $(10\bar{1}0)_{Po}$ and $(111)_{Sph}$ // $\{0001\}_{Po}$ between the sphalerite host and pyrrhotite inclusions. These CORs are mainly controlled by the crystal structure similarity, lattices coherency, and sulfur packing configurations. Overall, the chalcopyrite and pyrrhotite blebs hosted in sphalerite are interpreted to be formed via a combination of exsolution and metasomatism.

Key words Chalcopyrite, Sphalerite, Exsolution texture, EPMA, EBSD

AL_2O_3 IN ANORTHOSITIC SLABS: A NEW PERSPECTIVE ON LLSVPS AND SEISMIC VELOCITY VARIATIONS

Ishita Das[1], Gaurav Shukla[1,2]

1. Department of Earth Sciences, Indian Institute of Science Education and Research, Kolkata, India

2. National Center for High Pressure Studies, Indian Institute of Science Education and Research, Kolkata, India

Abstract Al_2O_3 is among the very first condensations during the cooling of the early solar nebula, and bears significance throughout the universe due to its highly refractory nature. It undergoes a series of high-pressure phase transitions beyond the temperature-pressure regime of the Earth, possibly owing to its presence in other planetary interiors.

These Al_2O_3 polymorphs owe their significance in evolution of the earth's mantle through their presence in the ancient crust which known to have subducted into the mantle. We study these polymorphs pertaining to pressure temperature regime of the earth, namely corunudum and Rh_2O_3(II)-type Al_2O_3 through first principles study. Our study shows significant contribution of Rh_2O_3(II)-type Al_2O_3 in the lower mantle Large Low Shear Velocity provinces and of corundum in the cold high velocity regions. Furthermore our multiphase model of anorthositic crust containing these polymorphs show its penetration into the lower mantle and stagnation near the D" layer. Thus, this study adds to the idea that ancient crust can survive deep mantle cycling and contribute to compositional and seismic anomalies in the lowermost mantle.

Key words Al_2O_3 polymorphs , Large Low Shear Velocity provinces, anorthositic crust, Lowermost Mantle

ATOMIC-SCALE INSIGHTS INTO THE FRICTIONAL BEHAVIOR OF CLAY MINERALS FROM MOLECULAR DYNAMICS SIMULATIONS

Juhyeok Kim, Kideok D. Kwon

Department of Geology, Kangwon National University, Chuncheon 24341, Republic of Korea

Abstract Clay minerals are recognized as key agents in the reactivation of many faults, and tribological studies have focused on their mechanical behavior. According to Byerlee's law, most rocks have a friction coefficients (μ) of about 0.6, and this value is widely used to explain fault behavior within the brittle crust. However, some faults slips at much lower shear stresses (i.e., $\mu << 0.6$), which is attributed to the presence of abundant clay minerals, whose layered structures inherently show low frictional strength. To systematically examine the frictional properties of clay minerals, we have employed molecular dynamics (MD) simulations. Saponite (trioctahedral smectite) exhibited slightly higher shear stress than montmorillonite (dioctahedral smectite) due to the differences in local charge density. We calulcated μ values as a function of water content. The shear stress followed a distinct rise-and-fall pattern with increasing water content. This is driven by structural changes in the interlayer water, specifically the occupation of ditrigonal cavities by water molecules during intermediate states, which effectively strengthens the frictional coupling. Among anhydrous minerals, specifically kaolinite, lizardite, pyrophyllite, and talc, trioctahedral structures exhibited significantly higher μ values than their dioctahedral counterparts. In 1:1 minerals, while only 60% of the surface hydroxyl groups in kaolinite form interlayer hydrogen bonds, the full participation of OH groups in lizardite leads to a higher μ value. For 2:1 minerals, the trioctahedral structure promotes enhanced interlayer geometric interlocking, thereby increasing the effective contact area and frictional resistance. We discuss the implications of clay minerals for fault strength and reactivation, based on these MD-derived atomic-scale mechanisms.

Key words Clay mineral, friction coefficient, molecular dynamics simulation, fault behavior

COMPOSITIONAL SIGNATURES OF (FE,AL)OOH AND THEIR IMPLICATIONS FOR THE LOWERMOST MANTLE

Sparsh Sharma[1], Gaurav Shukla[1,2]

1. Department of Earth Sciences, IISER Kolkata, India

2. National Center for High Pressure Studies, IISER Kolkata, India

Abstract Recent studies have proposed a crucial role of hydrous oxyhydroxides like FeOOH and AlOOH in being potential hydrogen carriers into the Earth's deep mantle. In addition, individual studies have suggested the presence of high-pressure FeOOH and AlOOH phases at the depths of the lowermost mantle. However, their relevance to realistic mantle compositions remains poorly constrained. In particular, FeOOH and AlOOH form extensive solid solutions, and the role of Al incorporation in governing the phase stability and thermoelastic properties of Fe-bearing high-pressure oxyhydroxides is yet to be systematically explored. In our study, we investigate the thermoelastic properties and phase stability of (Fe,Al)OOH solid solutions across ε/δ-type and pyrite-type (Py) structures at lower-mantle pressures and temperatures, with a focus on cold-slab geotherms. Our results demonstrate that Al incorporation substantially modifies the ε-(Fe,Al)OOH to Py-(Fe,Al)OOH phase boundary, shifting transition depths and stabilizing solid oxyhydroxide phases over an expanded pressure–temperature range compared to pure FeOOH. Along cold slab geotherms, (Fe,Al)OOH solid solutions exhibit pronounced contrasts in density and seismic velocities relative to surrounding mantle assemblages. These findings indicate that Al can act as a key compositional control on the depth distribution and physical properties of hydrous Fe-bearing phases in the lower mantle. We propose that such compositional filtering may contribute to the spatially heterogeneous occurrence of seismic velocity anomalies in the deep mantle, particularly in regions influenced by long-lived, cold subducted slabs. Our study highlights the importance of considering realistic solid solutions when assessing the role of hydrous phases in deep Earth structure and dynamics.

Key words **(**Fe,Al)OOH, Lower mantle, Mantle heterogeneities, Hydrous minerals

ELECTRICAL AND THERMAL CONDUCTIVITIES OF (FE,MG)SIO3 MELTS AT CORE-MANTLE BOUNDARY: INSIGHTS FROM MACHINE LEARNING POTENTIAL AND FIRST-PRINCIPLES CALCULATIONS

Yonghui Huang[1], Yunguo Li[1,2], Huaiwei Ni[1,2]

1. State Key Laboratory of Lithospheric and Environmental Coevolution, School of Earth and Space Sciences, University of Science and Technology of China, Hefei 230026, China

2. Deep Space Exploration Laboratory, Hefei 230026, China

Abstract The existence of a basal magma ocean (BMO) in the early Earth has profound implications for the thermal and magnetic evolution of the planet. It has been proposed that an early magnetic field could have been generated by a silicate dynamo operating within a highly electrically conductive BMO. However, the feasibility of this hypothesis strongly depends on the transport properties of iron-bearing silicate melts at core-mantle boundary conditions. In this study, we investigate the electrical and thermal conductivities of (Fe,Mg)SiO_3 melts across the full compositional range (X_{Fe}=Fe/(Fe+Mg) from 0 to 1) at 135 GPa and 4500 K.

To accurately capture the distinct transport mechanisms, we employed a comprehensive ab initio molecular dynamics (AIMD) framework. The electronic conductivities were evaluated using the Kubo-Greenwood formulation based on atomic snapshots extracted from the AIMD trajectories. The ionic electrical conductivity was also computed from the AIMD simulations facilitated with a machine learning potential via the Green-Kubo method. Our results reveal a strong compositional dependence for both electrical and thermal properties. For the pure magnesium end-member ($MgSiO_3$), the total electrical conductivity is relatively low (~3,300 S/m). However, as the iron content increases, the total electrical conductivity rises dramatically, reaching over 60,000 S/m for the iron end-member ($FeSiO_3$). This significant enhancement is fundamentally driven by the electronic contribution. In contrast, the ionic electrical conductivity remains a minor component (~1,500–3,000 S/m) and is largely overshadowed by the electronic part in iron-enriched melts. Similarly, the total thermal conductivity increases from approximately 5 W/m/K at X_{Fe}=0 to roughly 15 W/m/K at X_{Fe}=1. While the ionic thermal conductivity remains relatively low and stable across the compositional range, the electronic thermal conductivity exhibits a sharp increase, emerging as the dominant heat transport mechanism at high iron concentrations.

The pronounced increase in electrical conductivity with iron enrichment provides robust support for the silicate dynamo hypothesis. Assuming the BMO is denser and enriched in iron compared to the bulk mantle (e.g., $X_{Fe} \geqslant 0.25$), the calculated electrical conductivity reaches values ($\geqslant$8,000 S/m) closely approaching or exceeding the critical threshold required to sustain a geodynamo. Furthermore, the elevated thermal conductivity of these iron-rich melts implies a more efficient heat transfer mechanism at

the core-mantle boundary, which would significantly influence the cooling rate and the ultimate lifespan of the early Earth's basal magma ocean.

Key words Basal magma ocean, (Fe,Mg)SiO_3 melts, Electrical and thermal conductivities, First-principles molecular dynamics, Silicate dynamo

ELEMENT COVARIATION REVEALS DIVERSE CORE DIFFERENTIATION HISTORIES AMONG MAGMATIC IRON METEORITES

Tong Zhou[1,2], Kun-Feng Qiu[1], Razvan Caracas[2]

1. State Key Laboratory of Geological Processes and Mineral Resources, Frontiers Science Center for Deep-time Digital Earth, School of Earth Sciences and Resources, China University of Geosciences, Beijing, China.

2. Université Paris Cité, Institut de Physique du Globe de Paris, CNRS, Paris, France

Abstract Iron meteorites preserve key records of early planetary differentiation and core formation processes. However, the combined effects of metal–silicate separation, core crystallization, and subsequent impact modification have produced complex and variable geochemical signatures, complicating efforts to reconstruct their parent-body origins and evolutionary histories. To address this challenge, we compiled a comprehensive geochemical dataset of iron meteorites and developed an integrated statistical framework to characterize their internal chemical architectures across different meteorite groups and to distinguish source-sensitive signatures from those modified by later differentiation processes. The results reveal distinct and internally consistent geochemical structures among major magmatic iron meteorite groups. IIAB and IIIAB irons show strong positive correlations among HSEs and systematic anticorrelations with Ni, consistent with well-developed metal crystallization trends and relatively continuous core differentiation histories. In contrast, IVA and IVB irons exhibit weaker coupling between HSEs and other elements, together with subdued or decoupled Ga–Ge behavior, suggesting more complex or non-equilibrium differentiation pathways. The IID group displays intermediate and less coherent correlation structures, indicating greater heterogeneity in internal processes or parent-body conditions. This process-oriented framework provides a quantitative basis for comparing the internal geochemical architectures of iron meteorite groups and offers new perspectives on the diversity of differentiation histories recorded by metallic planetary cores.

Key words Iron meteorite, core differentiation, elemental correlation, planetary cores

EXPLORING PLANETARY CORE FORMATION WITH MACHINE LEARNING MOLECULAR DYNAMICS SIMULATIONS

Haiyang Luo[1,2]

1. School of Earth Sciences and Engineering, Nanjing University, China

2. Department of Geosciences, Princeton University, USA

Abstract Planetary core formation is often described as the gravitational segregation of metallic iron from silicate magma oceans. However, gravitational segregation can operate efficiently only after a distinct Fe-rich metallic liquid first separates from the silicate melt. In this study, I will present machine-learning molecular dynamics simulations that examine the conditions under which this first step of core formation may be inhibited. Two mechanisms will be discussed. First, at sufficiently high pressures and temperatures, metallic and silicate liquids may become increasingly miscible, preventing complete separation of an Fe-rich liquid phase in hot super-Earths and sub-Neptunes. Second, in water-rich magma oceans, water can oxidize metallic iron and redistribute Fe, Si, O, Mg, and H between metal and silicate liquids, thereby reducing the amount of metal available for core formation and modifying the final core and mantle compositions. Together, these results suggest that planetary core formation is controlled not only by gravitational separation, but also by the thermodynamic and chemical conditions that determine whether a metallic liquid phase can form in the first place. Machine-learning molecular dynamics provides a direct way to connect atomistic reactions and phase behavior to planetary-scale differentiation.

Key words Magma ocean, Core formation, Miscibility, Element partition, Machine learning

FINDING AND FIXING ERRONEOUS MINERAL SOLUBILITIES IN SOFTWARE: PHREEQC, SUPCRT92, HCH, AND REAKTORO

Zhenhao Duan and Haoran Sun

Department of Experimental Study under Deep-sea Extreme Conditions, Institute of Deep-Sea Sciences and Engineering, Chinese Academy of Sciences, Sanya, Hainan, 572000, China

Abstract Computer software packages—including PHREEQC, SUPCRT92, HCH, and Reaktoro—are widely used to calculate thermodynamic properties of aqueous species and mineral solubilities. Geochemists commonly rely on these tools as dependable "black boxes" in practical applications. However, they can produce substantial errors (e.g., in calcite and barite solubility calculations) under certain natural conditions, particularly in deep-sea environments characterized by low temperatures and high pressures.

In this study, we comprehensively review available mineral solubility data and systematically compare experimental observations with computational results from the aforementioned software packages, which are generally not user-friendly and can pose challenges for many researchers. To address these computational inaccuracies, we developed a novel thermodynamic correction model grounded in the Helgeson–Kirkham–Flowers (HKF) equation of state for aqueous species, the Pitzer activity coefficient model, and a rigorously integrated treatment of aqueous speciation.

The improvements embodied in our model are threefold:

Using updated and expanded experimental datasets, we refitted key thermodynamic parameters, including mineral heat capacities and standard partial molar Gibbs free energies of aqueous ions.

1. incorporating a more complete representation of equilibrium reactions and speciation during mineral dissolution, with special attention to interactions among ions released by mineral dissolution.

2. The Pitzer model is comprehensively employed to compute the activities of diverse aqueous species.

Comparisons between existing models and our new model for barite and calcite solubility demonstrates that the new model significantly improves the accuracy of mineral solubility calculations, substantially reducing discrepancies between computational predictions and experimental data. Calculations for an expanded range of minerals will be integrated into our web-based software package, available at https://efs.idsse.ac.cn.

NOVEL SUPERIONIC STATES IN DEFECTIVE SILICATE MINERALS AND THEIR ROLES IN DEEP EARTH AND PLANETARY INTERIORS

Zifan Wang[1,4], Yu He[1,2], Ho-kwang Mao[1,3] and Duck Young Kim[1*]

1. Center for High Pressure Science & Technology Advanced Research (HPSTAR), Shanghai, P.R. China.
2. State Key Laboratory of Critical Mineral Research and Exploration, Institute of Geochemistry, Chinese Academy of Sciences, Guiyang, Guizhou, P.R. China.
3. Shanghai Key Laboratory of Material Frontiers Research in Extreme Environments (MFree), Institute for Shanghai Advanced Research in Physical Sciences (SHARPS), Shanghai, P.R. China.
4. Department of Chemistry, Pohang University of Science and Technology, Pohang, Republic of Korea.

Abstract Superionic behavior has been increasingly recognized as a key phenomenon in deep-Earth minerals, with profound implications for the planet's volatile cycling, electrical conductivity, and magnetic field generation. In this presentation, I will introduce our recent computational studies uncovering novel superionic phenomena in silicate minerals through two distinct defect mechanisms: oxygen vacancy and hydrogen substitution. First, machine learning molecular dynamics (MLMD) simulations on oxygen-deficient davemaoite ($CaSiO_x$) reveal that oxygen ions undergo superionic diffusion under extreme conditions, enhancing electrical conductivity and potentially serving as a major source of mobile oxygen in the deep mantle, with implications for early mantle oxidation and the deep-Earth oxygen cycle. Second, structure predictions identify stable hydrous magnesium silicates under mantle transition zone conditions, revealing a pressure-induced hydrogen substitution transfer from Mg to Si sites that reduces electrical conductivity and implies higher water storage than previously estimated. Notably, an unexpected double superionic state with simultaneous diffusion of H^+ and Mg^{2+} was discovered in hydrous wadsleyite and ringwoodite above 2000 K, with potential implications for magnetic field generation in super-Earths. These findings provide new perspectives on the dynamics, evolution, and volatile cycling in deep Earth and planetary interiors.

Key words Superionicity, Hydrous minerals, Davemaoite, Mantle transition zone, Machine learning molecular dynamics

QUANTIFYING IRON DISPROPORTIONATION IN SILICATE MELTS USING MACHINE LEARNING POTENTIALS

Xin Deng[1,2], Michael Walter[1], Zhongqing Wu[2], R.E. Cohen[1]

1. Earth and Planets Laboratory, Carnegie Institution for Science, USA

2. School of Earth and Space Sciences, University of Science and Technology of China, China

Abstract The oxidation state of Earth's mantle influences its chemical differentiation, mantle dynamics, and volatile evolution, yet how it was initially established after core formation and magma ocean crystallization remains poorly constrained. The disproportionation of iron (i.e., $3FeO = Fe + Fe_2O_3$) in a silicate magma-ocean played a crucial role in setting the solid mantle's initial redox state. For example, an initially reducing mantle can become progressively more oxidized if disproportionated Fe metal segregates to the core as the magma ocean solidifies. To calculate the potential for mantle oxidation by disproportionation, it is required to understand how pressure and temperature affect the disproportionation reaction. Here we combine *ab initio* calculations, machine-learning potentials, and thermodynamic integration to quantify iron disproportionation in silicate analogs to a deep magma ocean at 20-140 GPa and 3000-6000 K, conditions relevant to Earth's deep magma ocean stage. The results reconcile discrepancies among previous experiments, and identifies secular cooling as a potential primary driver of the oxidation of Earth and terrestrial planetary mantles, and by extension, their earliest atmospheres.

Key words magma ocean, iron disproportionation, oxygen fugacity, machine learning potentials, thermodynamic integration

VISUALIZATION OF CRYSTAL STRUCTRUES HAVING SYMMETRIES BEYOND 3D

Koichi Momma

National Museum of Nature and Science, Japan

Abstract In the study of crystal structures, it is important to visually examine how each atom is derived from atoms within the asymmetric unit through symmetry operations. In recent years, VESTA, a program for visualizing crystal structures, has been extended to visualize magnetic structures and quasicrystals while preserving symmetry information. In magnetic space groups (MSGs), both atomic position and magnetic spin of each atom are derived by applying the same symmetry operations. For magnetic spins, an additional symmetry element—'time reversal', which flips the spin—is also considered. Thus, by incorporating 'time reversal' to the 230 crystal space groups results in total of 1651 magnetic space groups. A more comprehensive group, known as the spin space group (SSG), is gaining growing attention because it provides a foundation for fully classifying and understanding the topological phases of magnetic materials. SSGs treat spin rotations independently from spatial lattice operations, giving greater degrees of freedom than MSGs. VESTA can read and visualize magnetic structures based on MSGs and SSGs from crystallographic information files (CIF). At special positions that overlap symmetric elements, the result of the symmetry operation to a spin must match the original spin component; therefore, constraints are placed on the possible component values. VESTA automatically checks such constraints, and if a vector component does not satisfy the constraints, the conditions required to satisfy the symmetry are displayed in a text area.

Quasicrystals lack translational symmetry and therefore have no unit cell as a repeating unit, yet they exhibit a high degree of order in their atomic arrangement. They possess symmetries—such as 5-, 8-, 10-, and 12-fold symmetry—that are forbidden in periodic crystals, and unlike amorphous materials, they produce discrete diffraction patterns. In nature, two quasicrystal minerals are known in meteorites. VESTA represents quasicrystal structures as a three-dimensional cross-section of a periodic structure in five- or six-dimensional space. In structural representations using high-dimensional space, atoms are no-longer 0 dimensional points, but treated as two- or three-dimensional objects (occupation domains) that extend in dimensions parallel to complementary space, which is orthogonal to physical space. Atoms appear in physical space where the occupation domains intersect with physical space. The shape of the occupation domain is highly complex in actual quasicrystals, and its shape and position are specified in separate files. Visualization of quasicrystal structures is not necessarily centered at the origin; instead, the center can be specified at any point in physical space or in the complement space, at any distance from the origin. By applying a distortion (phaseon strain) parallel to the complement space of a quasicrystal

structural model such that lattice points periodically intersect with physical space, we can derive a three-dimensionally periodic structure called approximant crystal. Vector components such as magnetic moments and electric dipoles are also supported in high-dimensional spaces of up to six dimensions.

Key words Visualization, crystal structure, quasicrystal, magnetic space group, spin space group

WATER-INDUCED MANTLE OVERTURN EXPLAINS HIGH ARCHEAN PALEOINTENSITIES

Dong Wang, Zhongqing Wu*

School of Earth and Space Sciences, University of Science and Technology of China, Hefei

Abstract As a consequence of the evolution of the water-bearing basal magma ocean, water-induced mantle overturn can suitably explain many puzzling observations in the Archean, including the formation of continents and the Archean–Proterozoic boundary. The upwelling of the hot basal magma ocean during mantle overturn drastically affects the thermal state of the core–mantle boundary and geomagnetic field. We model the thermal evolution of the core–mantle boundary to investigate the effects of mantle overturn on the geomagnetic field. Our results demonstrate that mantle overturn substantially accelerates core cooling and increases the heat flow across the core–mantle boundary. Such enhanced heat flow would have strengthened the geomagnetic field, which explains well the high paleointensity records from approximately 3.5 to 2.5 Ga. The strong geodynamo and formation of Archean continents generate a concordant picture on the evolution of water-induced mantle overturn.

Key words magma ocean, mantle overturn, paleomagnetic field, early earth

ACTIVE-LEARNING DEEP POTENTIAL MOLECULAR DYNAMICS OF PHOSPHORUS OXYANION REACTIONS UNDER HIGH-TEMPERATURE AND HIGH-PRESSURE CONDITIONS

Chenyang Zhao[1], Zhongqing Wu[1,2,*], Bowen Chen[1], Wenzhong Wang[1]

1. State Key Laboratory of Precision Geodesy, School of Earth and Space Sciences, University of Science and Technology of China, Hefei 230026, China

2. Mengcheng National Geophysical Observatory, University of Science and Technology of China, Bozhou 233500, China

Abstract The availability and transformation of phosphorus on the early Earth remain important issues in prebiotic geochemistry. Although surface phosphorus is commonly associated with relatively insoluble phosphate minerals, reduced phosphorus species may represent more reactive reservoirs in some reducing environments. The structural evolution and molecular-scale reactivity of phosphorus oxyanions in hot, compressed aqueous fluids, however, remain difficult to resolve because conventional ab initio molecular dynamics is limited in accessible time scale and unbiased machine-learning-potential simulations may undersample rare reactive configurations. Here we develop an active-learning Deep Potential molecular dynamics framework for the P-O-H system at 500-1500 K and 1-9 GPa. VASP first-principles calculations provide energy, force, and stress labels for iterative Deep Potential training, while ensemble-based model deviation guides the selection of configurations requiring additional labeling. LAMMPS enables longer-timescale molecular dynamics exploration, and PLUMED-enhanced sampling increases access to underrepresented regions associated with P-O-P bridge formation and local phosphorus coordination environments. Candidate configurations are reduced by PCA/FPS-based representative selection before VASP labeling, followed by a quality-assurance step that removes configurations with extreme forces, nonphysical short contacts, or numerical anomalies before incorporation into the training set. The current model achieves an energy RMSE of approximately 6 meV/atom, a force RMSE of 0.209 eV/A, and a stress RMSE of 0.207 GPa on a validation set. These results indicate that the workflow provides a useful basis for preliminary longer-timescale exploration of reactive P-O-H configurational space and may help investigate phosphorus speciation and reactivity in reducing aqueous environments relevant to early Earth geochemistry.

Key words phosphorus geochemistry, early Earth, Deep Potential, enhanced sampling, high-pressure aqueous fluids

FIRST-PRINCIPLES PATH INTEGRAL MOLECULAR DYNAMICS (PIMD) CALCULATIONS OF THE ELASTICITY OF D_2O ICE VII UNDER PRESSURE

Takuya Iwata, Jun Tsuchiya

Department of Earth and Space Science, Graduate school of Science, The university of Osaka, JAPAN

Abstract H_2O is one of the most fundamental constituents of planetary bodies, and understanding its physicochemical properties under planetary interior conditions is of great importance. In particular, ice VII is stable over a wide pressure range of approximately 2 to 100 GPa, and accurate characterization of its structure and physical properties is essential as a basis for such studies.

Nuclear quantum effects (NQEs), arising from the light mass of hydrogen, can significantly influence the structure and elasticity of hydrogen-bonded systems. A previous study (Tsuchiya et al., 2024) compared the elastic constants of ice VII calculated using conventional first-principles molecular dynamics (AIMD), which neglects NQEs, and first-principles path-integral molecular dynamics (PIMD), which incorporates them. That study demonstrated that NQEs significantly increase the elastic constants in the dynamically disordered phase by approximately 20% at ~300 K and 77 GPa, due to transient hydrogen-bond symmetrization.

These effects are expected to be strongly mass-dependent, and thus isotope substitution (H → D) provides a powerful means of probing their impact. Here, we performed AIMD and PIMD simulations to determine the equation of state and elastic constants of D_2O ice VII at 300 K under pressure. The results were compared with those for H_2O ice VII to evaluate isotope effects.

Our results show that, in D_2O ice VII, nuclear quantum effects increase the elastic constants of the dynamically disordered phase by approximately 10% near 300 K and 77 GPa, which is significantly smaller than the effect observed for H_2O. These results indicate that isotope-dependent nuclear quantum effects, mediated by transient hydrogen-bond symmetrization, play a key role in controlling the elastic properties of high-pressure ice.

Key words Nuclear quantum effects, isotope effects, high pressure ice VII

A DUAL-ENDMEMBER NUMERICAL FRAMEWORK CONSTRAINED BY MINERAL PHASE TRANSFORMATION: REPRODUCING MINERAL-FLUID INTERACTIONS AND ELEMENT TRANSPORT IN A HYDROTHERMAL EXPERIMENTAL SYSTEM

Jingbo Xu[1], Ruping Gan[1], He Zhang[1], Linhong Wei[2], Yuanfeng Cai[1*]

1. State Key Laboratory of Critical Earth Material Cycling and Mineral Deposits, School of Earth Sciences and Engineering, Nanjing University, PR China

2. School of Frontier Science, Nanjing University Suzhou Campus, PR China

Abstract To investigate how coupled phase transformation and element redistribution develop during hematite replacement in hydrothermal systems; we numerically reproduce an experiment in which hematite grains react with an acidic Cu-Au-bearing fluid enriched in As and S. To capture both interface-scale reactions and internal replacement, we develop a dual-endmember numerical framework that combines titration modeling with diffusion-infiltration modeling.

Experimental observations indicate that the primary reaction can be summarized as the transformation of hematite into an alteration assemblage dominated by pyrite. At the external mineral-fluid interface, chalcopyrite and Fe-As-S mixed phases form preferentially, whereas during continued fluid infiltration, secondary pyrrhotite, pyrite, and magnetite form locally along the internal reaction front. These phases are spatially differentiated rather than uniformly distributed. Cu-bearing secondary phases mainly grow along the outer rim of the grain and show overgrowth textures at the mineral-fluid interface, where a significant amount of detectable gold is hosted. In contrast, pyrite, pyrrhotite, and magnetite mainly occur as intergrown phases that advance with the internal reaction front and display displacement textures within hematite. This pattern suggests that the observed phase transformation reflects the combined action of local interfacial equilibrium reactions at the mineral-fluid interface and diffusion-infiltration-driven replacement within the grain.

Within this framework, titration modeling is used to constrain the local reaction pathway associated with hematite dissolution and fluid interaction, including phase-stability changes, preferential nucleation, and replacement relationships leading to Fe-As-S mixed phases and Cu-bearing secondary phases. Diffusion-infiltration modeling is used to track the redistribution of S-, As-, Fe-, Cu-, and Au-bearing species within the mineral, together with reaction-front propagation and the development of secondary mineral zonation.

The simulations show that when Cu is present in solution, early dissolution favors formation of a Cu-bearing mineral band at the mineral-fluid interface. As diffusion-infiltration-driven replacement proceeds, a pyrite-dominated alteration band becomes the principal product, whereas Cu-bearing secondary phases

shrink to the outermost interface or may disappear entirely. Additional tracking of Au behavior shows that both modeling approaches predict extensive native gold precipitation along the chalcopyrite-pyrite interface. In every case of native gold precipitation, the activity of As-S compounds decreases, whereas the activity of arsenate increases. These coupled features cannot be fully resolved by either modeling approach alone.

Therefore, for numerical studies of mineral-fluid interaction, neither titration modeling nor diffusion-infiltration modeling is sufficient by itself to explain the coupled evolution of phase transformation and element redistribution observed in the experiment. The former resolves interface-scale phase-transformation pathways during mineral dissolution but cannot represent internal diffusion-infiltration-driven replacement. The latter captures internal mass transfer and zonation development but cannot independently constrain the evolution of newly formed secondary phases in solution. Only their combination can more fully reproduce the experimentally observed replacement sequence and associated element redistribution.

Key words Mineral-fluid interaction, Reactive transport modeling, Element redistribution

Acknowledgements This research was supported by grants from the Natural Science Foundation of China (Grant No. 42372052, 42202036).

APPLICATION OF STABLE ISOTOPES AS "STRUCTURE-SENSITIVE PROBES" FOR MINERAL-FLUID INTERFACIAL REACTIONS

Wei Li

School of Earth Science & Engineering, Nanjing University, China

Abstract The application of metal stable isotopes as "structure-sensitive probes" for mineral-water interfacial reactions requires a rigorous theoretical foundation linking isotopic fractionation to atomic coordination environments. This paper presents a systematic exposition of the physical chemical chain connecting equilibrium isotope fractionation to crystal structural parameters. We trace the theoretical lineage from the quantum statistical mechanics origins of isotope effects through the semi-empirical force constant-bond length relationships to the quantitative increment method for mineral systems. We demonstrate how modern Density Functional Theory (DFT) calculations validate these classical relationships in metal isotope systems (e.g., Zn, Cu, Mo), confirming that heavy isotopes preferentially partition into sites with shorter bond lengths and lower coordination numbers. This theoretical framework establishes the scientific legitimacy of using metal isotope fractionation to discriminate among interfacial reaction mechanisms (outer-sphere vs. inner-sphere complexation, surface precipitation, lattice incorporation), offering a methodological solution for systems where synchrotron-based spectroscopy faces inherent limitations (low-Z elements, low concentrations, mixed-phase assemblages). For example, we studied the sorption behavior of Zn on calcite across a wide range of reaction times, pH values, and Zn concentrations. The underlying sorption mechanisms were examined through a combination of Zn stable isotope measurements and X-ray absorption fine structure (XAFS) spectroscopy. At pH 6.5 and a low Zn concentration of 5 μM, the surface coverage reached 0.9 μmol/m^2, accompanied by a pronounced $\Delta^{66}Zns_{orbed\text{-}aqueous}$ of + 0.40 ‰, which is indicative of a tetrahedral inner-sphere surface complexation mechanism. Conversely, at pH ≥ 7.5 and a higher Zn concentration (100 μM), the surface coverage surpassed 57.6 μmol/m2, resulting in diminished Zn isotope fractionation (+0.20 ‰), suggesting the formation of hydrozincite precipitates. These results revealed a continuous transition from inner-sphere tetrahedral surface complexes to hydrozincite precipitates as the pH and/or Zn concentration increased. Notably, the sensitivity of Zn isotope fractionation to distinct Zn sorption mechanisms was supported by an inverse linear relationship between Zn isotope fractionation and the Zn-O bond distance. The synergistic application of Zn stable isotopes and XAFS spectroscopy provides a robust framework for probing metal-mineral interactions under environmentally relevant conditions.

Key words Stable metal isotope, mineral surface, XAFS, isotope fractionation

FLUID-ROCK INTERACTION MECHANISMS CONTROL THE DYNAMICS OF THE LITHOSPHERE.

Andrew Putnis[1,2] and Christine V. Putnis[1]

1. Institut für Mineralogie, University of Münster, Germany
2. School of Earth Sciences, Curtin University, Perth, Australia

Abstract The strength of rocks and the reactions between their constituent minerals as a function of temperature and pressure is the basis of our traditional understanding of rock deformation and metamorphic petrology. The lithosphere is, by definition, mechanically strong yet it is also dynamic and constantly evolving. Recent papers have questioned the paradigm that this apparent paradox can be reconciled by temperature-dependent rheology and slow metamorphic reactions, controlled by lithostatic pressure and temperature, while maintaining equilibrium.

Geological processes of rock transformation throughout the Earth's crust are dependent on the presence of aqueous solutions and here we will briefly review the hypothesis that the aqueous fluid at mineral interfaces controls the coupling between mineral reactions, volume changes, stress generation, mass transport and deformation mechanisms on a wide range of spatial and time scales. The feedback between fluid-induced reactions, porosity generation and maturation, rock weakening and deformation mechanisms provide the context for the dynamics that has shaped the lithosphere.

In the first instance, understanding interface-coupled dissolution-precipitation as the key mechanism of mineral reactions in experiments and in nature explains how permeability can be introduced and eventually eliminated during reactions and how close coupling results in pseudomorphic replacement. Examples of such processes will demonstrate the universality of the mechanism. Volume changes during metamorphic reactions can be accommodated by mass transport, and this is most dramatically demonstrated during rock weathering. Introducing non-hydrostatic stress uncouples the dissolution and precipitation steps of the mechanism (as in pressure solution) and results in dissolution-precipitation creep as the primary mechanism of rock deformation during metamorphic reactions. As pointed out by Holger Stünitz in a landmark paper (J.Struct. Geol. 2020), experiments on mineral deformation where the only available mechanism is by dislocation creep are not adequate to explain rock deformation when coupled with mineral reactions. More recently the grain-scale feedback between deformation mechanisms and deformation mechanisms has been described in lower crustal rocks by Mérit et al. (EPSL 2025).

IN SITU EXPERIMENTAL CONSTRAINTS ON THE DIFFERENTIAL HYDROTHERMAL BEHAVIOR OF YTTRIUM AND SCANDIUM IN HYPER-ALKALINE CARBONATE FLUIDS

Ze Yuan, Tianzi Guo, Xiang Wu

State Key Laboratory of Geological Processes and Mineral Resources, China University of Geosciences, Wuhan 430074, China

Abstract The geochemical fractionation of yttrium (Y) and scandium (Sc) in magmatic and hydrothermal systems is a key factor in understanding the formation of carbonatite-hosted rare earth element (REE) deposits. Yet, the processes governing their spatial decoupling remain poorly constrained. In deposits such as Bayan Obo, Sc precipitates early in proximal zones, while Y migrates to distal domains. Most experimental studies on REE transport rely on low-temperature halogen and sulfate systems. However, ore-forming carbonatitic fluids feature extreme alkalinity with high Na^+ and CO_3^{2-} concentrations under supercritical conditions. In such environments, reliance on quenched samples may alter actual phase equilibria. Direct *in situ* observations of metal behavior at relevant pressure and temperature conditions minimize these post-experiment changes, although direct data on Y and Sc in hyper-alkaline carbonate fluids remain scarce.

Here, we address this issue by using a hydrothermal diamond anvil cell (HDAC) coupled with *in situ* Raman spectroscopy. This approach allows us to directly observe Y and Sc in highly concentrated sodium carbonate fluids (40 to 50 wt% Na_2CO_3) under conditions up to ~750 °C and ~2 GPa. Characterization of the experimental products was performed using SEM-EDS and single-crystal X-ray diffraction (XRD). These experiments reveal contrasting thermal behaviors of Y and Sc under extreme alkalinity. For the Y system, high sodium carbonate concentrations significantly enhance its hydrothermal solubility. Upon heating, Y undergoes dynamic phase transitions, sequentially precipitating intermediate phases before completely dissolving into the supercritical fluid by ~750°C. During cooling, the high-temperature intermediate phase re-precipitates and remains stable down to room temperature. In contrast, Sc exhibits a strong tendency to crystallize. While it forms a low-temperature intermediate phase, the Sc-carbonate complexes destabilize as the temperature reaches 486 °C. This leads to the precipitation of a new, stable, and insoluble Sc-bearing high-temperature phase. *In situ* Raman spectroscopy confirms that this precipitation is irreversible upon further heating to 750 °C, and the precipitated phase remains stable during subsequent cooling.

Crystal chemical analysis indicates that Sc^{3+}, having a smaller ionic radius and higher charge density than Y^{3+}, exhibits stronger polarizing power. As a result, Sc strongly binds carbonate ligands to form highly charged anionic clusters, requiring a higher ratio of alkali metals for charge balance. This makes

Sc precipitation highly dependent on Na^+ activity. Furthermore, the strong fluorophile nature of Sc restricts its mobility in carbonatite fluids. These findings provide support for understanding the spatial decoupling in REE deposit, where Sc precipitates early near the hydrothermal core, while Y migrates outward for late-stage distal enrichment.

Key words Hydrothermal diamond anvil cell (HDAC), Yttrium, Scandium, Carbonatite, Mineral solubility

INTERCONNECTED CU–FE SULFIDE NETWORKS IN CHIMNEYS AND THERMOELECTRIC CONVERSION AT DEEP-SEAFLOOR HYDROTHERMAL VENTS

Kentaro Toda[1], Atsushi Okamoto[1], Dandar Otgonbayar[1], Misaki Takahashi, Yoshinori Sato[1], Tomonori Ihara[2], Tatsuo Nozaki[3,4]

1. Graduate School of Environmental Studies, Tohoku University, Japan
2. Faculty of Marine Technology, Tokyo University of Marine Science and Technology, Japan
3. Faculty of Science and Engineering, Waseda University, Japan
4. School of Engineering, The University of Tokyo, Japan

Abstract Hydrothermal vents occur at mid-ocean ridge, island arcs, back-arc basins, and rift zones, where rapid mixing of hydrothermal fluid and seawater forms chimney-like structures composed of sulfide and sulfate minerals. Previous studies have suggested that electrons may be supplied to the deep seafloor driven by redox potential difference of hydrothermal fluid-seawater and the conductivity of sulfide minerals (Yamamoto et al., 2018). However, the electron transport mechanism remains poorly understood because few studies have focused on electrical conductivity of chimney textures. In addition, sulfide minerals are known as semiconductors that exhibit the Thermoelectric Effect, converting temperature gradients into electromotive force. Therefore, part of the approximately 11 TW of thermal energy transported by global hydrothermal circulation may be directly converted into electrical potential, although the thermoelectric performance of chimneys has rarely been evaluated (Okamoto 2026). In this study, we measured electrical conductivity and Seebeck coefficient of chimney samples collected from hydrothermal vents in the Izu-Bonin Arc and the Okinawa Trough. We also conducted hydrothermal experiments using chimney sample reacted with simulated hydrothermal fluid (T = 200–300 °C). In addition, X-ray CT analyses to evaluate the three-dimensional mineral distribution were carried out, and the relationship between chimney textures and electricity generation was examined.

Samples from the Izu-Bonin Arc and Okinawa Trough can be classified into three types: (i) porous barite ($BaSO_4$) and sphalerite (ZnS) rich samples; (ii) sphalerite with spherical pyrite (FeS_2); and (iii) sphalerite-pyrite assemblages partly replaced by galena (PbS) or chalcopyrite ($CuFeS_2$) around hydrothermal conduits. These correspond to the birth, growth, and mature stages of chimney concentric zoning, with increasing hydrothermal fluid temperature. Surface electrical conductivity σ [S cm^{-1}] is on the order of 10^{-12} in sphalerite, whereas galena and chalcopyrite reach ~10^{-2}. We further calculated the Seebeck coefficient S [mV K^{-1}] and the power factor $S^2\sigma$ [mV^2 K^{-1} S cm^{-1}], which represent thermoelectromotive force (TEMF) per unit temperature gradient and power generation performance based on TEMF, respectively. Chalcopyrite and galena exhibit a power factor approximately six orders of

magnitude higher than sphalerite, suggesting that mineralogical evolution accompanyied with the growth of zoned structure may initiate electricity generation.

X-ray CT analyses of natural samples revealed that, in early-stage samples, most pores are mutually interconnected. In late-stage samples, chalcopyrite precipitates on the pore surfaces and forms connected, mesh-like mineral textures within the chimney wall. When electrodes were placed in contact with the chimney wall approximately 1 cm apart, long-distance conduction was confirmed only in the late-stage samples, suggesting the connectivity of conductive minerals inside the chimney wall can govern the bulk electrical conductivity.

Hydrothermal experiments were conducted under closed-system conditions using highly-porous chimney samples composed of sphalerite and spherical pyrite, and a simulated hydrothermal fluid (T = 200–300 °C, P = saturation vapor pressure, pH = 3.0). The solution contained high concentrations of $CuCl_2$ and $FeCl_2 \cdot 4H_2O$ (0.3 M) and was adjusted to reducing conditions using $Na_2S_2O_3$. $Cu_{2-x}S$ formed on the surface of the sphalerite, while $CuFeS_2$ formed on the exterior of the Cu_{2-x} S layer. Notably, the products of the experiment were distributed along the chimney wall, forming a network-like structure similar to that of natural samples. Electrical conduction over a distance and thermoelectric power generation were also confirmed.

Overall, early-stage porous chimneys composed mainly of poorly conductive sphalerite evolve into structures containing dense, highly conductive minerals. Consequently, high-power-factor ($S^2\sigma$) networks form within the chimney wall, functioning as bridges for electron transport. The thermoelectric effect can then convert the internal temperature gradient into thermoelectromotive force comparable to the redox potential difference. It suggests that the structural evolution of chimney interiors can give rise to thermoelectric conversion in seafloor hydrothermal environments.

Key words Seafloor Hydrothermal Vents, Thermoelectric Conversion, Sulfide Mineral Replacement, Micro X-ray Computed Tomography, Water-Rock Interaction

INTERFACE-CONTROLLED GOLD ENRICHMENT DURING HEMATITE SULFIDATION: IMPLICATIONS FOR AU DISTRIBUTION IN IOCG SYSTEMS

Ruping Gan, Jingbo Xu, He Zhang, Yuanfeng Cai*

State Key Laboratory of Critical Earth Material Cycling and Mineral Deposits, School of Earth Sciences and Engineering, Nanjing University, PR China

Abstract Iron oxide copper-gold (IOCG) deposits host economically significant gold, and understanding how gold is distributed is critical for both resource evaluation and ore genesis. However, the relationships between gold occurrence and sulfide minerals remain unclear, and the processes controlling Au sequestration in these hydrothermal systems are still poorly understood.

Here, we present an experimental study investigating the distribution of Au during the sulfidation of hematite to chalcopyrite and bornite under hydrothermal conditions (240-300 °C) similar to those in IOCG deposits. The experimental results show that Au-bearing sulfides form at temperatures above 240 °C, and that pH plays a key role in controlling how gold is distributed among the reaction products. Under acidic conditions (pH=4), chalcopyrite dominates throughout the reaction, and gold is mainly incorporated as invisible, lattice-bound gold in chalcopyrite, with the highest concentrations observed at the early stages of the reaction. Under alkaline conditions (pH=10), chalcopyrite and bornite are the main products, and gold occurs as nanoparticles distributed within the sulfides and becomes enriched in larger particles along chalcopyrite-bornite interfaces. LA-ICP-MS analyses further show that the concentration of invisible gold in chalcopyrite decreases rapidly with increasing reaction time under alkaline conditions.

Textural and compositional evidence indicates that hematite sulfidation proceeds primarily via pseudomorphic dissolution-reprecipitation. During this process, gold is partially remobilized and can subsequently form micron-scale grains. The replacement of hematite by chalcopyrite is accompanied by a decrease in sulfur fugacity at the reaction interface, which destabilizes Au-S complexes and promotes the initial incorporation of gold into chalcopyrite. However, because chalcopyrite provides only limited structural sites for gold, some of this gold is remobilized as the reaction continues, likely driven by thermal effects and evolving fluid chemistry. Under alkaline conditions, the subsequent replacement of chalcopyrite by bornite creates new mineral interfaces that serve as favorable sites for gold deposition, promoting the nucleation, growth, and enrichment of remobilized gold.

Overall, these results show that gold mineralization in IOCG systems is fundamentally controlled by dynamic fluid–rock interaction and interface-coupled redox processes, rather than by bulk fluid evolution alone. This provides a process-based explanation for the mineral assemblages and paragenetic relationships commonly observed in IOCG deposits, demonstrating that pre-existing iron oxide veins act

as chemical traps for ore-forming fluids and promote the precipitation of gold as well as sulfides during Cu–Au mineralization. Our findings further constrain the physicochemical evolution of Cu-rich, Au-bearing fluids and the associated replacement processes. This interface-controlled model provides a unified explanation for the spatial association of iron oxides, sulfides, and gold, and offers a mechanistic framework linking fluid evolution, mineral replacement, and gold deposition in hydrothermal systems, with broad implications for gold mineralization in iron oxide-rich environments.

Key words Gold mineralization, Mineral-fluid interaction, IOCG deposits

Acknowledgements This research was supported by grants from the Natural Science Foundation of China (Grant No. 42372052, 42202036).

LINK BETWEEN GOLD MINERALIZATION AND FLUID EVOLUTION IN EPITHERMAL SYSTEMS: A CASE STUDY OF THE DONGYANG GOLD DEPOSIT, CHINA

He Zhang[1], Gujie Qian[2], Wei Tan[3], Joël Brugger[4], Allan Pring[5] and Yuanfeng Cai[1]

1. State Key Laboratory of Critical Earth Material Cycling and Mineral Deposits, Nanjing University, Nanjing, Jiangsu Province 210023, China

2. College of Science and Engineering, Flinders University, Adelaide, SA 5042, Australia

3. CAS Key Laboratory of Mineralogy and Metallogeny/Guangdong Provincial Key Laboratory of Mineral Physics and Materials, Guangzhou Institute of Geochemistry, Chinese Academy of Sciences (CAS), Guangzhou 510640, China

4. School of Earth, Atmosphere and Environment, Monash University, Clayton, Victoria 3800, Australia

5. Australian Critical Minerals Research Centre, University of Adelaide, Adelaide, South Australia 5005, Australia

Abstract Epithermal deposits are commonly regarded as products of processes related to fluid evolution within and/or around volcanoes. They form at convergent plate margins, as well as in intra-arc, back-arc, and post-collisional rift settings. These deposits occur at shallow crustal levels, where their mineralization is intimately coupled with the physicochemical evolution of fluids during complex fluid–rock and fluid–fluid interactions. However, the factors controlling the partitioning of gold and arsenic into sulfide minerals within the evolutionary framework are still poorly understood.

Here, we interpret the spatial zoning of mineral assemblages, trace elements, and sulfur isotopic fractionation at the Dongyang epithermal gold deposit in southeastern China. The vertical zonation is defined by a distinct transition from an upper (surface to ~100 m) sulfide assemblage with negative-$\delta^{34}S$ values to a lower zone (below ~100 m) where sulfides with near-zero $\delta^{34}S$ coexist with ferric iron oxides and sulfosalts, indicative of an increase in the oxygen fugacity of the hydrothermal fluids with depth. The distribution of arsenian sulfides (e.g., pyrite and arsenopyrite) exhibits an opposite trend relative to the variation in oxygen fugacity, indicating that low oxygen fugacity favors arsenic partitioning into sulfides, which is consistent with reduction of As(III) aqueous complexes to As^{-} in the structures of pyrite and arsenopyrite. Meanwhile, the increased arsenic partitioning into sulfides also enhances mineralization of "invisible" gold in the upper part of the deposit. HRTEM imaging reveals that the substitution of arsenic for sulfur triggers an atomic-scale transformation in the pyrite structure, which in turn lowers the energy barrier for gold to substitute for iron. This observation highlights a dynamic feedback between pyrite composition and nanostructure, linking arsenic incorporation to gold enrichment. Consequently, the vertical zonation, mineralogical, textural and sulfur isotopic signatures at the Dongyang deposit are consistent with a model involving boiling at depth, and rapid upwards migration of reducing (H_2), H_2S-

rich vapors. The integration of paragenetic, mineral compositions, and S-isotopic information provides critical insights into the formation of epithermal gold deposits.

Key words "invisible" gold, arsenic, structural transformation, fluid evolution, epithermal gold deposit

Acknowledgements This research was financially supported by the National Natural Science Foundation of China, grants 42202036, 42192504, and 42372052. We thank Liang Li, Li Zhang, Youwei Chen, and Bohao Yin for assistance with LA-ICP-MS, EBSD, and NanoSIMS analyses, respectively. Parts of this research were also undertaken on the XFM beamline at the Australian Synchrotron, part of the Australian Nuclear Science and Technology Organisation (ANSTO).

MICROBIAL MINERAL INTERACTIONS DURING HYDROXYAPATITE AND CALCIUM CARBONATE PRECIPITATION: MINERALOGICAL PERSPECTIVE FROM NANO TO MOLECULAR SCALES

Pelina Toprak[1], Anant Aishwarya Dubey[1], Abhijit Mukherjee[1], Carlos Rodriguez-Navarro[2], Allan Pring[3], Navdeep K Dhami[1,4*]

1. School of Civil and Mechanical Engineering, Curtin University, WA , Australia

2. Department of Mineralogy and Petrology, University of Granada, Spain

3. Department of Earth Sciences, University of Adelaide, Australia

4. School of Molecular and Life Sciences, Curtin University, WA, Australia

Abstract Microbial processes are increasingly recognised as powerful drivers of mineral nucleation, growth and transformation. Amongst these processes, microbially induced calcium carbonate precipitation (MICP) and phosphate precipitation (MIPP) have attracted considerable interest because of their widespread occurrence in natural systems, including beach rocks, coral reefs, molluscs, phosphorites, bones, and teeth. Their synthesis via microbial routes under lab conditions has been widely demonstrated, offering several advantages over conventional approaches including mild reaction conditions, operational simplicity, lower cost and low carbon footprint. But despite extensive research and progress, however, the mechanisms controlling precipitation pathways and the resulting mineral properties remain incompletely understood because of the complexity of bio-mineral interactions.

We are have investigated the role of microbial surfaces, metabolic route, extrapolymeric substances (EPS) on carbonate and hydroxyapatite formation from nano to molecular scales. Two different bacterial cultures *Sporosarcina pasteurii (SP)* and *Pseudomonas fluorescens (PF)* and ^{44}Ca isotope tracing were used for the study. Mineral formation and cell surface interactions were characterised using Zeta potential, Scanning electron microscopy (SEM), Confocal laser scanning microscopy (CLSM), Energy dispersive spectroscopy (EDS), Raman spectroscopy, Fourier transform infrared spectroscopy (FTIR) and Time-of-Flight Secondary Ion Mass Spectrometry (ToF-SIMS).

Our results provide new mechanistic insight into microbe-mineral interactions by demonstrating that cell interfaces, EPS and metabolic pathways exert fundamental control over polymorph selection in calcium carbonate and crystallographic architecture of hydroxyapatite. We show for the first time that isotopic doping represents a robust tool for tracing the formation and transformation of biogenic calcite, enabling direct linkage between microbial activity and mineral products. These findings advance fundamental understanding of biomineralization processes in natural systems, particularly the role of microbial mediation in mineral phase, structure and isotopic signatures. The outcome has broader implications for interpreting biogenic signatures in the geological record and for predicting mineral evolution in microbially active environments.

Key words MICP, MIPP, EPS, Biomineral architecture, Biocementation

MYRMEKITE AND ANTIPERTHITE FORMATION IN DEFORMED GRANITE: CHEMICAL AND CRYSTALLOGRAPHIC CONSTRAINTS ON FORMATION MECHANISMS

Yueting Song[1, 2, 3], Thomas A. Griffiths[2], Shanrong Zhao[1] and Rainer Abart[2]

1. School of Earth Sciences, China University of Geosciences (Wuhan), China

2. Department of Lithospheric Research, University of Vienna, Austria

3. State Key Laboratory of Palaeobiology and Stratigraphy, Nanjing Institute of Geology and Palaeontology, Chinese Academy of Sciences, China

Abstract The chemical and crystallographic characteristics of myrmekite and antiperthite in deformed Tiantang Zhai granite of the Central China Orogen are studied to reveal their origin. We infer two paths of silica transfer during formation of myrmekites: (1) silica released by magmatic quartz during formation of early coarse-grained myrmekites, and (2) silica released from the myrmekitic vermicular quartz during formation of a second generation of fine-grained myrmekites. Formation of myrmekites occurred during syn-kinematic deformation of the granite. The silica transfer was promoted by the high density of crystallographic defects in the proto-quartz and by the low interfacial energy, as indicated by crystallographic orientation relationship(s) (CORs) of defect-free myrmekitic quartz.

Systematic lattice correlation of {110}feldspar // {11-21}quartz is observed in nearly all myrmekites, attributed to the close lattice spacing match between feldspar and quartz within these lattice planes. The myrmekites formed under high silica supersaturation developed multiple subdomains with different orientations of quartz. Subdomain lacking CORs between quartz and plagioclase tapered out, indicating that the interfacial energy differences control the orientation evolution in each subdomain. The variations in CORs among different subdomains reveal the processes of quartz nucleation, propagation, and possible dissolution in myrmekite. The study introduces an approach for investigating the growth features and evolution of intergrowth through the occurrence of CORs within intergrowths, wherein the constituent minerals do not share comparable crystallographic structures.

Antiperthite comprising faceted inclusions of alkali feldspar developed in the vicinity of myrmekite. Precipitation of alkali feldspar in plagioclase was mediated by fluid present along cracks in the plagioclase host. Compositional evidence indicates that myrmekite and antiperthite may have formed simultaneously, serving as mutual sources and sinks for Na, K, and Ca exchanged between their respective domains during formation. This study reveals ubiquitous mass transfer among intergrowths formed during the late magmatic hydrothermal stage, accompanied by ongoing adjustments in the crystallographic orientations of their constituent minerals, aimed at reducing strain energy and achieving minimal interfacial energy.

Key words Myrmekite, antiperthite, metasomatism, crystallographic orientation relationships, EBSD

Acknowledgements We thank Callum Hetherington and an anonymous reviewer for their thoughtful comments, which improved and clarified this reseach. We acknowledge financial support from the Visiting Ph.D. program of China Scholarships Council and from the National Natural Science Foundation of China (Grant No. 41372058). We are grateful to Chang Xu for his generous help and support during the two field trips to the Dabie Orogen. We thank Yuelian Lu for all the support and Jie Tan for providing assistance with optical microscopy imaging.

REACTION-INDUCED POROSITY DURING FLUID-MINERAL INTERACTION: COMBINING 4D SYNCHROTRON IMAGING WITH AI-BASED PERMEABILITY RECONSTRUCTION

Oliver Plümper[1], Hamed Amiri[2], and Florian Fusseis[3]

1. Faculty of Geosciences and MARUM, University of Bremen, Germany

2. Department of Earth Sciences, Utrecht University, the Netherlands

3. Applied Structural Geology, RWTH Aachen, Germany

Abstract Fluid-rock interactions underpin fundamental lithospheric processes as well as applied challenges such as geological CO_2 sequestration and geothermal energy production. In deep crystalline basement where intrinsic permeability is negligible and deformation is absent, fluid migration relies on transient pathways generated by chemical reactions between minerals and fluids out of equilibrium. The resulting reaction-driven pore networks modulate rock permeability dynamically, yet their transient character renders direct observation difficult.

Here, we present an integrated approach that couples time-resolved synchrotron X-ray microtomography (4DSµCT) with generative artificial intelligence to track and quantify the evolution of reaction-induced porosity. Using 4DSµCT, we monitored the spatio-temporal development of pore networks during KBr–KCl replacement, a well-characterised analogue system for interface-coupled dissolution–precipitation. Statistical microstructural descriptors and Minkowski functionals expose the tight interplay between dissolution–precipitation mechanisms, solute transport regimes, and the evolving connectivity that governs transient permeability.

To move beyond the constraints of direct experimentation, especially for high-temperature environments (>500 °C) where in-situ imaging is not yet feasible, we developed Pore-Edit GAN (Generative Adversarial Network), a StyleGAN2-ADA (Adaptive Discriminator Augmentation) architecture trained on approximately 29,000 tomographic slices. The model produces statistically faithful synthetic microstructures while permitting targeted semantic manipulation of porosity and connectivity. We applied this workflow to hydrothermally altered monzonite from the Oslo Rift, in which feldspar replacement reactions at roughly 10 km depth generated pore networks that are now texturally isolated. By traversing the GAN latent space along identified connectivity vectors, we reconstructed plausible transient pore geometries, effectively reversing the isolation that accompanied reaction cessation.

Voxel-based finite element simulations of incompressible Stokes flow through these AI-generated networks yield permeabilities up to 4.5×10^{-15} m², an enhancement of approximately two orders of magnitude upon pore reconnection, in good agreement with published transient crustal permeability–depth relationships. The integration of synchrotron imaging, deep generative modelling, and computational fluid dynamics provides a quantitative framework for estimating transport properties in reactive geological

systems that remain inaccessible to direct measurement.

Key words Fluid-Rock Interaction, 4D Synchrotron X-ray Tomography, AI, Permeability

TO RUST OR NOT TO RUST: MINERAL-DRIVEN IRON REDOX DYNAMICS AND CRUSTAL REDOX HETEROGENEITY

Joël Brugger[1], Bin Hu[1], Barbara Etschmann[1], Denis Testemale[2], Huan Chen[3], Chris R. Voisey[1], Richen Zhong[3], Weihua Liu[4], Yanlu Xing[1,4], Xinfu Zhao[5], Andrew G. Tomkins[1]

1. School of Earth Atmosphere and Environment, Monash University, Australia

2. CNRS, Université Grenoble Alpes, Institut Néel, France

3. School of Civil and Resource Engineering, University of Science and Technology Beijing, China

4. CSIRO Mineral Resources, Australia

5. School of Earth Resources, China University of Geosciences, China

Abstract Mass transfer of essential metals and volatiles through the Earth's crust is governed primarily by redox conditions, largely mediated by iron, sulfur and carbon. Ferric iron [Fe(III)] is conventionally considered unstable in crustal hydrothermal fluids, conflicting with the ubiquitous presence of ferric minerals in crustal ore systems. Under the anoxic conditions of the deep earth, the most likely oxidant in geofluids is sulfur (as sulfate), but many Fe-rich ore systems (e.g. IOCG, IOA) as well as most rocks are sulfur-deficient relative to the amount of Fe. Under such condition, the widespread distribution of Fe(III)-bearing mineral in hydrothermal systems is difficult to explain.

Using *in-situ* spectroscopy in quartz capillaries, we demonstrate that Fe(III) remains stable up to 600 ˚C as tetrahedral $FeCl_4^-$ complexes in Fe(III)-only brines (no mineral and contact with hematite). In contrast, in magnetite-bearing samples, Fe(II) and Fe(III) are released into solution, with the Fe(III) fraction declining rapidly with temperature, concomitant with magnetite replacement by hematite.

These results highlight the importance of fluid-rock interaction for maintaining a high ferric content in geofluids. Hydrothermal fluids migrate through porous media and through fluid-focussing structures, dissolving and precipitating minerals as local physicochemical conditions change. We hypothesize that elevated Fe(III)/Fe(II) ratio occur mainly along altered, high-flux pathways (Fe-poor with limited fluid:rock interaction), while fluids interacting with 'fresh' magnetite-bearing rocks quickly lose dissolved Fe(III). These results identify a mechanism independent of external oxidants whereby coupled thermodynamic and kinetic controls via fluid-mineral interactions generate crustal redox heterogeneity, shaping mass transfer of essential metals and volatiles.

Key words Iron, Hydrothermal Fluids, Redox, Magnetite, Hematite.

VACANCIES IN SULFIDES FACILITATE FLUID-INDUCED SOLID-STATE DIFFUSION

Zheng-Jie Qiu[1] Yanlu Xing[2] Joël Brugger[3] Denis Fourgerous[4] Jing Xu[5] Hong-Rui Fan[1]

1. Institute of Geology and Geophysics, Chinese Academy of Sciences, Beijing, China

2. CSIRO, Mineral Resources, Melbourne, Australia

3. School of Earth, Atmosphere and Environment, Monash University, Melbourne, Australia

4. School of Earth and Planetary Sciences, Curtin University, Perth, WA, Australia

5. Zijin School of Geology and Mining, Fuzhou University, Fuzhou, China

Abstract Understanding element uptake and release during mineral-fluid interaction is crucial for clarifiying the accumulation of critical metals, yet the mechanisms and kinetics of element mobilization at the atomic scale remain poorly constrained. Fluid-induced coupled dissolution-reprecipitation (FI-CDR) is widely recognized as an efficient mechanism for trace element transport in mineral-fluid systems. By contrast, solid-state diffusion (SSD) is rarely invoked as effective mechanism of element mobility as it is often a much slower process than FI-CDR. However, recent hydrothermal experiments have challenged this view by showing that fluid-induced solid-state diffusion (FI-SSD) can occur at surprisingly high rates in sulfide minerals when coupled with element release into fluids.

To test this idea in a natural system, we investigated cobalt-rich pyrite from metamorphosed black shales in the Zhongtiao Mountains, China. Atomic-resolution aberration-corrected scanning transmission electron microscopy (AC-STEM) observations and image simulations confirm that Fe vacancies are widespread in the pyrite lattice. First-principles calculations indicate that these vacancies significantly lower the diffusion energy barrier for Co migration, and vacancy clustering creates fast diffusion pathways that greatly enhance Co transport. High-resolution compositional mapping further shows that Co zoning in pyrite is better described by steady-state diffusion (constant flux) rather than transient-state diffusion with time-evolving concentrations. Diffusion modelling suggests that vacancy-assisted steady-state diffusion is 2–3 orders of magnitude more efficient than traditional vacancy-mediated lattice diffusion over geological timescales.

We propose that Co release from pyrite is governed by a coupled FI-SSD and FI-CDR mechanism, in which vacancy-assisted steady-state diffusion first promotes preferential Co transfer into interfacial fluids, followed by vacancy accumulation that triggers dissolution-reprecipitation and sustains further Co release.

Key words fluid-induced solid-state diffusion, vacancy-assisted diffusion, Atomic-scale

characterization, cobalt mobilization, pyrite

Acknowledgements This research was supported by the National Science Foundation of China (42330804 and 42372094).

CONTRASTING LITHIUM SITING MECHANISMS IN CLAY MINERALS: EVIDENCE FROM CENTRAL YUNNAN, CENTRAL GUIZHOU, AND NORTHERN GUIZHOU

Song Yan[1,2], He Zhang[3], Jingbo Xu[3], Yuli Yuan[3], Siyi Huang[3], Ruping Gan[3], Tao Sun[3], Jinhai Yu[3], Jianxi Zhu[1,2]*, Yuanfeng Cai[3]*

1. State Key Laboratory of Deep Earth Processes and Resources, Guangzhou Institute of Geochemistry, Chinese Academy of Sciences, Guangzhou 510640, PR China

2. University of Chinese Academy of Sciences, Beijing 100049, PR China

3. State Key Laboratory of Critical Earth Material Cycling and Mineral Deposits, School of Earth Science and Engineering, Nanjing University, Nanjing, China

Abstract Lithium (Li) is a critical metal for the global energy transition and controlled nuclear fusion. By 2030, conventional sources (brine and hard rock) are projected to meet only about half of global demand, making clay-hosted Li resources a key supplementary supply. Although recent ex-ploration in China has identified widespread Li enrichment in clays, the underlying genetic mechanisms remain poorly constrained. This study advances the understanding of Li occur-rence to the atomic scale using molecular-level approaches. Results indicate that, in systems with multiple clay minerals, Li enrichment is often dominated by specific mineral hosts. In central Yunnan, central Guizhou, and northern Guizhou, the principal Li-bearing clays are cookeite, kaolinite, and chamosite/kaolinite assemblages, respectively. Although clays provide multiple potential Li sites, including surface sites, pseudo-hexagonal cavities, and octahedral vacancies, Li enrichment is controlled by preferential site occupation. Li is mainly hosted in lattice sites, pseudo-hexagonal cavities, and surface sites (central Yunnan), pseudo-hexagonal cavity sites (central Guizhou), and octahedral vacancy sites (northern Guizhou). These differences lead to distinct binding strengths and structural responses: surface Li is weakly bound and readily exchangeable; cavity Li is more strongly bound via H–Li exchange and F-induced stabilization, allowing acid leaching without structural collapse; octahedral Li is strongly bound, requiring structural disruption and promoting dioctahedral-to-trioctahedral transformation. Overall, Li metallogenesis in clays is governed by both mineral type and site-specific incorporation, providing a basis for understanding Li enrichment and guiding extraction strategies.

Key words Lithium resources, Clay minerals, Molecular-scale, Lithium siting, Structural evolution

SILVER: THE MAGIC "BULLET" FOR CHALCOPYRITE DISSOLUTION

Barbara Etschmann, Luis Verdugo, Maryam Olamide Abdus-Salam and Joël Brugger
School of Earth, Atmosphere and Environment, Monash University, Clayton, VIC, Australia

Abstract For the last 50 years it has been recognised that a 'Goldilocks' concentration of silver can catalyze copper extraction from chalcopyrite in a ferric-sulfate leaching solution; too little silver yields no effect, whereas excess silver promotes silver sulfide precipitation that inhibits further leaching. The dissolution of chalcopyrite, without added silver, is a well described multistep process. We propose a new integrated model for Ag-catalysed dissolution that incorporates recent advances in sulfide mineral reactivity arising from the field of geochemistry.

Dissolution initiates via an incongruent step in which Fe diffuses from the chalcopyrite lattice to the surface and into solution, producing a Fe-deficient layer ('*Fluid-Induced Solid State Diffusion Mechanism*'). This is followed by dissolution of this layer and its replacement by a porous, Fe-bearing copper sulfide via *interface-coupled dissolution–reprecipitation*, releasing additional Fe. The final stage involves dissolution of this (Fe-bearing) copper sulfide, accompanied by the formation of porous elemental sulfur and jarosite, locally developed at the reacting surface.

The presence of ~1 mg per kg silver in the ferric-sulfate leaching solution accelerates the dissolution of chalcopyrite, but chalcopyrite dissolution essentially follows the same process as in the Ag-free case. Based on the FIB-SEM evidence and the evidence from 50 years of research, we propose the following role for Ag. In solution, Ag^+ (from $AgNO_3$) exists as $Ag(H_2O)_{4\text{-}6}^+$, which either rapidly transforms to $Ag(HS)_2^-$ or $Ag(HS)(H_2O)(aq)$ in the presence of aqueous sulfur near the surface of dissolving chalcopyrite. These complexes sorb to onto the surface of the chalcopyrite. Ag^+ and Cu^+ ions can readily exchange: the resulting substituted Ag^+ distorts the structure, making it structurally and energetically unstable and more susceptible to dissolution. This releases Ag^+ back into near-surface solution as $Ag(HS)_2^-$ or $Ag(HS)(H_2O)(aq)$ complexes, which can again sorb to the surface of the chalcopyrite, and so repeating the reaction. In this way, Ag^+ remains as Ag^+ throughout the reaction, it does not change oxidation state. In the meantime, Cu^+-sulfur species rapidly precipitate as a copper-sulfide phase, with widely varying stoichiometries (nearly metallic Cu, Cu_2S, CuS) controlled by local conditions at the reacting surface and in micro-cracks('local microreactor'). The catalytic effect of Ag^+ hence reflects a complex reaction pathway that depends on the unique coordination chemistry of monovalent cations of Column 11 in the Periodic Table.

Experiments synthesizing chalcocpyrite with and without silver demonstrate that low concentrations of silver incorporated into chalcopyrite can aid in dissolution by supplying Ag to this catalytic cycle,

whereas high concentrations of silver released into solution slow leaching kinetics, by precipitating silver sulfide and blocking access to the chalcopyrite. These results reconcile longstanding observations of both catalytic and inhibitory roles of silver, and emphasise that its effect is governed by concentration-dependent feedbacks between solution chemistry, mineral structure, and interfacial reaction pathways.

Key words chalcopyrite, silver, dissolution mechanism

BATTLE BETWEEN THE BANDS: COMPETITIVE PRECIPITATIONS OF FERRIHYDRITE AND SILICA GEL LEAD TO THE BANDS IN BANDED IRON FORMATIONS

Huifang Xu

Department of Geoscience, University of Wisconsin–Madison, Madison Wisconsin 53706, USA

Abstract Banded iron formations (BIFs) are massive chemical deposits composed of alternating layers of chert and iron-rich minerals (such as hematite, magnetite and siderite), with three scales of bandings: microbands, mesobands (1 mm - 10 cm) and macrobands. Their abundance in the Archaean/early Proterozoic era and their absence thereafter suggest that chemical conditions and iron transport pathways on the early Earth surface were different from those after 1.7 billion years ago. Thermodynamic calculations show that Fe-silicate metal complex can be generated by hydrothermal leaching of low-Al oceanic crustal rocks such as komatiites, which suggest that the presence of low-Al ultramafic rocks (for example, komatiitic rocks) in the early oceanic crust were the reason for both the formation of BIFs and their abundance in the Archaean/early Proterozoic era (Wang et al., 2009: doi:10.1038/ngeo652). This is consistent with the findings that the ages of komatiites are correlated strongly, at the 99% confidence level, with the ages of BIFs (Isley and Abbott, 1999: doi.org/10.1029/1999JB900066).

We used the PHREEQC geochemical modeling package was used to test the chemical reactions that may have led to the banding pattern in the BIFs based on competitive precipitation of ferrihydrite (precursor of hematite and magnetite) and silica gel (precursor of chert) (Zhou et al., 2024: doi.org/10.1016/j.chemgeo.2024.122091). After aqueous ferrous silicate metal complex decomposition in O_2-sufficient condition ($pO_2 \geq 10^{-4}$), the faster Fe^{2+} oxidation and precipitation rate led to Fe-rich layer preceding Si-rich layer with ferrihydrite and amorphous silica as the precursor to the hematite and quartz, respectively. Episodic $Fe(H_3SiO_4)_2$ input resulted in successive cycles of layering. O_2-deficient environments ($pO_2 < 10^{-4}$) results in jaspilite (no bands). The kinetic model also works well for the formation of siderite bands under O_2-deficient environments when pCO_2 is high. Greenalite precipitated as granular iron formation (GIF) when the concentration (flux) of Fe-silicate metal complex was high and atmospheric oxygen level was low (Wang et al., 2009: doi:10.1038/ngeo652; Xu et al., 2025: DOI: 10.2138/gselements.21.3.170). In summary, the precipitation process model proposed in this study offers an alternative abiotic explanation for the formation of distinct bands within the BIFs.

Key words banded iron formation, Fe-silicate metal complex, komatiite, Precambrian atmospheric oxygen level, precipitation kinetics

ENHANCED IMMOBILIZATION OF CD AND CR DURING CARBONATE-ACCELERATED TRANSFORMATION OF FERRIHYDRITE-METAL COPRECIPITATES

Ying Li and Yuxiao Zhang

National Observation and Research Station of Coastal Ecological Environments in Macao, Macau

University of Science and Technology, Macao SAR 999078, China

Abstract An elevated activity of (bi)carbonate in soils and sediments (pCO_2, ~3%) above current atmospheric CO_2 (~0.04%) could influence the metal cycling at mineral-water interface. Although it is known that the ferrihydrite (Fh) transformation is promoted by carbonate, it is unclear how increasing carbonate activities exert the transformation of Fh-metal coprecipitates and the fate of heavy metals. Herein, cadmium (Cd) and chromium (Cr) as models of cationic and anionic metals were selected to evaluate these processes at near-neutral pH using experimental geochemistry coupled with several state-of-the-art techniques. Resuts show that carbonate promoted the transformation of Fh-Cd and Fh-Cd coprecipitates to hematite through enhancing the olation reaction by weak inner-sphere complex. Moreover, carbonat modified the morphology of hematite from regular rhombic to disk-shaped. Chemical analysis indicate the different fate of Cd and Cr. For Cd, with increasing carbonate concentration, the release of Cd to solution kept relative constatant, accompanied by a decrease in the fraction of 0.4 M HCl extractable Cd and a increase in the fraction of structural substitution into the newly formed crystalline iron (oxyhydr)oxides. For Cr as oxyanion, the content of aqueous Cr increased and the fration of 1.0 M Na_2HPO_4 extractable Cr was lower than that of 0.4 M HCl extractable Cd due to the competitive desorption of carbonate and the decrease in the specific surface area during the phase transformation. Besides the aqueous Cr and surface adsorption, a portion of Cr may be incorporated into the lattice strucures of and/or physical encapsulation by crystallized products, which was facilitated by carbonate. These findings not only suggest that carbonate is an important geochemical parameter controlling the occurrence of hematite, but also are useful in predicting the fate of heavy metals during mineral transformation and developing strategies for simultaneously immobilizing heavy metals and carbon in the critical zone.

Key words Ferrihydrite-metal coprecipitate, Transformation, Carbonate, Cadmium, Chromium

EVOLUTION CHARACTERISTICS OF IRON (HYDR)OXIDES IN REGOLITH AS EFFECTIVE INDICATOR FOR REE MINERALIZATION

Lianying Luo[1,2,3], Wei Tan[1,2*]

1. State Key Laboratory of Deep Earth Processes and Resources, Guangzhou Institute of Geochemistry/Guangdong Provincial Key Laboratory of Mineral Physics and Materials, Guangzhou Institute of Geochemistry, Chinese Academy of Sciences, Guangzhou 510640, China

2. Guangdong research center for strategic metals and green utilization, Guangzhou 510640, China

3. University of Chinese Academy of Sciences, Beijing 100049, China

Abstract Regolith-hosted rare earth element (REE) deposits hosted by the granitic regolith in South China provide over 90% of the world's heavy REEs. Iron (hydr)oxides are one of the carriers of REE in regolith, and their formation and transformation processes are closely genetically linked to the activation, migration, and mineralization of REEs. The formation and evolution of iron (hydr)oxides in regolith respond to supergene environmental conditions such as hydrology and climate. However, the distribution characteristics of iron (hydr)oxides in regolith have not yet been systematically elucidated. Meanwhile, the coupling mechanisms between iron (hydr)oxides and REEs remain poorly understood, particularly regarding the evolutionary patterns of iron (hydr)oxides within the vertical zoning of regolith and their potential as indicators for REE mineralization. In this study, we systematically investigate typical regolith-hosted REE deposits in South China using mineralogical and geochemical methods, aiming to elucidate the evolutionary characteristics of iron (hydr)oxides and their genetic links to REE enrichment. The results demonstrate that the evolution of iron (hydr)oxides in the regolith is synergistically controlled by chemical weathering intensity and hydrodynamic conditions. With increasing chemical weathering intensity, iron-bearing primary minerals (e.g., biotite and amphibole) first release ferric ions to form ferrihydrite, which subsequently transforms into goethite or hematite within different hydrological zones of the regolith. In the saturated zone and capillary fringe, the wet environment facilitates the preservation of goethite, whereas in the vadose zone, the relatively dry and strongly oxidizing environment promotes the formation of hematite. Notably, the relatively high seepage velocity and alternating wetting-drying conditions in the vadose zone facilitate the formation and preservation of Al-rich hematite. Furthermore, the enrichment of REEs exhibits a significant spatial coupling with the distribution of iron (hydr)oxides. In the capillary fringe, characterized by gradually increasing water saturation and low permeability, REEs are readily adsorbed by secondary minerals within the regolith, leading to the formation of REE enrichment. Therefore, the evolution of iron (hydr)oxides in the regolith is governed by the synergistic interplay between chemical weathering intensity and hydrodynamic conditions, and their evolutionary characteristics serve as effective indicators for REE mineralization.

Key words Iron (hydr)oxides, regolith-hosted rare earth element deposit

FACET-DEPENDENT HETEROGENEOUS FENTON REACTION MECHANISMS ON HEMATITE NANOPARTICLES FOR (PHOTO)CATALYTIC DEGRADATION OF ORGANIC DYES

Ping Chen[1,2,3], Tianhu Chen[2], Kevin M. Rosso[1], Xin Zhang[1]

1. Physical & Computational Science Directorate, Pacific Northwest National Laboratory, USA

2. School of Resources and Environmental Engineering, Hefei University of Technology, China

3. Zijin School of Geology and Mining, Fuzhou University, China

Abstract Hematite (α-Fe_2O_3) nanoparticles are naturally occurring semiconducting minerals that play important roles in environmental redox processes, particularly in the photo-Fenton degradation of organic pollutants. However, the roles of charge transfer and reactive oxygen species (ROS) generation in the reaction mechanism remain debated, largely because previous studies have overlooked the influence of facet-dependent differences in surface atomic structure. This study systematically investigates the facet-dependent heterogeneous (photo)-Fenton reactivity of hematite nanoparticles with dominant (001), (104), and (116) facets, using methylene blue (MB) as a model dye. Three types of facet-engineered hematite nanoparticles were synthesized via simple hydrothermal methods, achieving high facet purity (>88% for each sample).

Adsorption isotherms show that MB adsorption capacity (total amount per mass) follows (001) > (104) > (116). In contrast, photocatalytic kinetic experiments reveal that the overall photodegradation capacity follows (104) > (116) > (001). When normalized by surface area, the intrinsic adsorption/photodegradation activity follows (116) > (104) > (001). Electron paramagnetic resonance (EPR) spectroscopy reveals two main pathways of radical generation. Path One involves photogenerated electrons from hematite reacting directly with H_2O_2. Path Two involves photoexcited MB donating electrons to hematite, generating surface Fe^{2+}, which then reacts with H_2O_2. Furthermore, EPR results show that at pH 5.5, the dominant reactive oxygen species is •OOH, whereas at pH 9.0, •OH is predominantly generated. The (116) facet supports both pathways, while (104) is limited to Path One and (001) shows low activity in both. For reasons, under visible light irradiation, the (116) facet exhibits superior photodegradation activity due to its smaller optical bandgap (1.8–2.2 eV in the order (116) < (104) < (001)), faster charge transfer (approximately one order of magnitude higher than the other facets as measured by IMPS showing (116) > (104) > (001)), and lower energy barrier for H_2O_2 decomposition (0.018 eV for (116) vs. 0.390 eV for (104) from DFT calculations). In contrast, the (104) facet achieves the highest overall photodegradation capacity because of its high density of surface active sites ((001) > (104) > (116)). Time-of-flight secondary ion mass spectrometry (ToF-SIMS) identifies intermediates (e.g., m/z 130, 167) at low pH, indicating a less efficient degradation route compared to the direct pathway at

high pH. Additionally, at high pH (9.0), a dark Fenton reaction occurs. In this path, hematite oxidizes H_2O_2 to form Fe^{2+} and •OOH in a first step; the resulting lattice Fe^{2+} then reduces another hydrogen peroxide molecule, producing •OH. Under these conditions, the (001) facet degrades over 95% of MB without illumination and maintains 92.1% degradation after three cycles, attributed to its high H_2O_2 adsorption capacity.

These findings demonstrate that facet engineering of hematite nanoparticles can optimize either intrinsic activity (via high-energy facets like (116)) or overall capacity (via high-site-density facets like (001) or (104)), depending on the reaction conditions. This work advances the fundamental understanding of facet-dependent photo-redox chemistry at mineral-water interfaces and provides design principles for sustainable wastewater treatment catalysts, highlighting the need to balance electronic properties, surface site density, and operational parameters in catalyst development.

Key words (photo)catalytic degradation, facet-dependent reactivity, hematite, photofenton reactions, redox chemistry

Acknowledgements This material is based upon work supported by the U.S. Department of Energy, Office of Science, Office of Basic Energy Sciences, Chemical Sciences, Geosciences, and Biosciences Division through its Geosciences program at Pacific Northwest National Laboratory (FWP 56674). PC and THC acknowledge support from the National Science Foundation of China (41572029).

FERRIHYDRITE PHASE TRANSFORMATION ACROSS EARTH-SURFACE THERMAL REGIMES

Juan Liu, Jiahao Chen, Yuefei Ding

College of Environmental Sciences and Engineering, Peking University, Beijing 100871, China

Abstract Ferrihydrite is a ubiquitous, metastable Fe(III) oxyhydroxide in Earth-surface environments, and its transformation strongly influences iron mineral assemblages, nutrient and trace-element cycling, and microbial respiration. Although temperature is a key control on ferrihydrite transformation, its effects across environmentally relevant thermal regimes remain poorly understood. Fe(II)-catalyzed ferrihydrite transformation has primarily been studied at room temperature, despite the fact that many Earth-surface environments, such as glaciers and tropical soils, experience markedly different thermal conditions. As a result, how temperature variability shapes ferrihydrite transformation pathways and products remains unclear, limiting our ability to predict ferrihydrite-mediated biogeochemical processes.

Here, we investigate how contrasting Earth-surface thermal regimes regulate ferrihydrite transformation pathways. We focus on two end-member scenarios: (i) ancient warm seawater conditions spanning 25–65 °C, relevant to Precambrian ferruginous surface environments, and (ii) repeated freeze–thaw cycling characteristic of modern and past cold-region settings. Our results show that temperature variations across this Earth-surface range can fundamentally alter the pathway, rate, and products of ferrihydrite transformation. By linking warm and cold Earth-surface regimes within a common mineralogical framework, this study identifies temperature variability as a first-order control on ferrihydrite transformation beyond conventional high-temperature or diagenetic perspectives. These findings provide a mineralogical basis for understanding how ferrihydrite responds to thermal forcing across diverse geological settings, from Precambrian iron formations to glacially influenced critical zones. More broadly, they demonstrate that environmentally relevant temperature fluctuations can reshape phase transformation pathways, mineral reactivity, and the biogeochemical functions of Fe oxyhydroxides in both ancient and modern Earth-surface systems.

Key words Ferrihydrite, Phase transformation, Temparture, Ancient seawater warming, Glacial Freeze–Thaw

Acknowledgements This work was financially supported by the National Natural Science Foundation of China (42192502).

FROM MOLECULAR COORDINATION TO LANDSCAPE EVOLUTION: ZINC ISOTOPE FRACTIONATION MEDIATED BY FE-(OXYHYDR)OXIDES DURING SILICATE WEATHERING

Ting Gao[1,2], Yuhui Liu[1], Meng Qi[1], Zihan Xia[1], Chengshuai Liu[1,2]

1. Institute of Geochemistry Chinese Academy of Sciences, Guiyang, Guizhou 550081, P.R. China

2. South China Agricultural University, Guangzhou, Guangdong 510642, P.R. China

Abstract Iron (oxyhydr)oxides are fundamental regulators of the biogeochemical cycling of zinc (Zn) in terrestrial environments. This study integrates molecular-level mechanisms with field-scale geochemical tracing to elucidate how Fe-(oxyhydr)oxides shape the Zn isotopic signatures of Earth's surface during silicate weathering. By combining laboratory synthesis, synchrotron-based EXAFS spectroscopy, and multi-scale weathering profile analyses, we bridge the gap between microscopic coordination and macroscopic landscape evolution.

Molecular investigations demonstrate that the mode of Zn uptake by Fe-(oxyhydr)oxides dictates the direction of isotopic fractionation. During adsorption on ferrihydrite, Zn is dominated by tetrahedral coordination (R_{Zn-O} ~ 2.00 Å), leading to the enrichment of heavy isotopes in the solid phase ($\delta^{66}Zn_{ads-aq}$ ~ 0.42-0.53‰). Conversely, structural incorporation via coprecipitation triggers a transition to octahedral coordination (R_{Zn-O} ~ 2.06-2.07 Å), which results in a distinct isotopic shift, characterized by slightly negative or limited fractionation $\delta^{66}Zn_{stru-aq}$ ~ -0.08‰) compared to surface adsorption.

Field evidence from granitic and basaltic weathering profiles across diverse climatic zones validates these molecular controls. In granitic regoliths, advanced weathering promotes the formation of crystalline Fe oxides (goethite and hematite) that preferentially incorporate light Zn isotopes ($\delta^{66}Zn_{goethite-aq}$ down to -0.54‰; $\delta^{66}Zn_{hematite-aq}$ down to -1.94‰), causing the bulk regolith to become isotopically lighter than the parent bedrock. Similarly, in extremely weathered basalt profiles, while incipient weathering is dominated by the dissolution of Mg-bearing primary minerals (releasing light Zn and leaving heavy residues), the subsequent formation of secondary Fe oxides acts as a major sink for light Zn isotopes ($\delta^{66}Zn_{Fe\ oxide-bulk}$ ~ -0.31‰). This sequestration within Fe oxide lattices significantly reduces Zn mobility and bioavailability, providing a mechanistic explanation for the paradox of Zn deficiency in plants grown in Zn-rich tropical soils.

Our findings demonstrate that Zn isotopes are powerful proxies for tracing Fe-oxide-mediated processes across scales. This integrated understanding, from molecular coordination to soil profile evolution, provides a robust framework for evaluating nutrient cycling and chemical weathering signals in terrestrial ecosystems.

Key words Fe-(oxyhydr)oxides, Zn isotopes, Coprecipitation, Silicate weathering, Molecular geochemistry

GLACIER RETREAT UNVEILS A HIDDEN ABIOTIC SOURCE OF NITROUS OXIDE ON THE TIBETAN PLATEA

Lei Zhong

Tianjin University, Tianjin 300072, China

Abstract Glacier retreat on the Tibetan Plateau, driven by rapid warming, is exposing vast areas of iron-rich parent material, yet the impact of this process on nitrous oxide (N_2O) emissions remains unknown. Here we show that chemo-denitrification, the abiotic reduction of nitrite by ferrous iron (Fe(II)), dominates N_2O production in Tibetan glacier forelands. In proglacial wetlands and meadows, chemo-denitrification contributed 50–69% of total N_2O production from denitrification, and in three additional glacier retreat zones (Jiali County, Mount Everest, Cho Oyu) its contribution exceeded 60%. Unlike tropical peatlands where chemo-denitrification outcompetes an active microbial community, here denitrification functional genes and microbial activity was extremely low. Consequently, N_2O is produced abiotically through Fe (II) driven nitrite reduction without subsequent microbial consumption a “naturally dominant” mode distinct from the “competitively dominant” mode observed elsewhere. With glaciers on the plateau shrinking by 0.5% per year, the expanding Fe (II)-rich forelands are becoming an overlooked source of abiotic N_2O. Our findings challenge the paradigm that denitrification is primarily a biological process and call for inclusion of iron-driven chemo-denitrification in Earth system models to accurately project high-alpine greenhouse gas emissions under continued warming.

HEAVY METAL ISOTOPE FRACTIONATION DURING ADSORPTION AND INCORPORATION ONTO IRON (HYDR)OXIDES

Hui Yin[1,*], Chuanwei Zhu[2], Wei Li[3], Xionghan Feng[1], Wenfeng Tan[1]

1. Key Laboratory of Arable Land Conservation (Middle and Lower Reaches of Yangtse River), Ministry of Agriculture and Rural affairs, College of Resources and Environment, Huazhong Agricultural University, Wuhan 430070, China.

2. State Key Laboratory of Ore Deposit Geochemistry, Institute of Geochemistry, Chinese Academy of Sciences, Guiyang 550002, China

3. Key Laboratory of Surficial Geochemistry, Ministry of Education, School of Earth Sciences and Engineering, Nanjing University, Nanjing 210023, China

Abstract In terrestrial and marine environments, iron (hydr)oxides widely exist and have high reactivity towards heavy metals through adsorption and incorporation processes. This will cause isotopic fractionation, and hinder the application of metal stable isotope in the environment. But the underlying mechanisms are not clear yet. In this study, the isotope fractionation behaviors and mechanisms of zinc (Zn) during interactions with iron (hydr)oxides were elucidated. It shows that, heavy Zn isotopes are preferentially enriched onto solids, with almost similar isotopic offsets ($\Delta^{66/64}$Znsolid-solution = 0.25−0.36‰) for goethite, lepidocrocite, and feroxyhyte. This is consistent with the same average Zn−O bond lengths for adsorbed Zn on these solids as revealed by Zn K-edge X-ray absorption fine structure spectroscopy. In contrast, at an initial Zn/Fe molar ratio of 0.02, incorporation of Zn into goethite and lepidocrocite by substituting for lattice Fe preferentially sequesters light Zn isotopes with $\Delta^{66/64}Zn_{substituted\text{-}stock\ solution}$ of −1.52 ± 0.09‰ and −1.18 ± 0.15‰, while Zn-substituted feroxyhyte (0.06 ± 0.11‰) indicates almost no isotope fractionation.This is closely related to the different crystal nucleation and growth rates during the Zn-doped FeOOH formation processes. Further, Zn distributions and isotope compositions were coupled during lepidocrocite nucleation and crystallization in the presence of different initial Zn concentrations. Light Zn isotopes are preferentially incorporated into the mineral, and follow first dynamic and then equilibrium fractionations, probably related to the aqueous chemistry, kinetic isotope fractionation, and the mineral nucleation and growth mechanisms. Increasing the initial metal concentration greatly decreases the mineral nucleation and growth rates, and results in significant increases in the isotope fractionations between the solid and solution. However, further increase in the metal concentration may prolong the time required for fractionation equilibrium. These results not only deepen our understanding of Zn geochemical behaviors mediated by iron (hydr)oxides, but also enrich the non-traditional stable isotope fractionation theories in low temperature geochemistry.

Key words iron (hydr)oxides, metal isotope fractionation, interface reactions, isomorphous substitution, adsorption

LUOGUFENGITE (ε-Fe_2O_3): A NANO-MINERAL WITH GIANT COERCIVE FIELD AND ITS IMPLICATIONS FOR NATURAL REMANENT MAGNETIZATION

Seungyeol Lee[1] and Huifang Xu[2]

1. Department of Earth and Environmental Sciences, Chungbuk National University, Republic of Korea

2. Department of Geoscience, University of Wisconsin–Madison, USA

Abstract The mineral luogufengite (IMA 2016-005), a natural Fe_2O_3 polymorph analogous to synthetic ε-Fe_2O_3, was first discovered in late Pleistocene basaltic scoria from the Menan Volcanic Complex near Rexburg, Idaho, USA. This mineral forms as an oxidation product of Fe-bearing basaltic glass at elevated temperatures and is commonly associated with maghemite and hematite. It occurs as euhedral to subhedral nanocrystals ranging from approximately 20 to 120 nm in size. Recent studies have further confirmed the occurrence of luogufengite in young scoria, red obsidian, and paralava from various localities worldwide, establishing it as a far more widespread phase than initially recognized.

Luogufengite is a magnetically significant mineral capable of recording paleomagnetism in volcanic rocks owing to its exceptionally large magnetic coercivity. This unique magnetic property may account for the anomalously high remanent magnetization observed in certain igneous and metamorphic rocks, and potentially in Martian rocks that exhibit strong remanent magnetization. Furthermore, in lodestones and hemoilmenite-bearing rocks, intergrowths of magnetite with ilmenite exsolution lamellae, or hematite with magnetite lamellar precipitates, display luogufengite-like two-dimensional crystalline characteristics featuring doubled hexagonal close-packing at the interface between cubic and rhombohedral structures. These luogufengite-like nanodomains at magnetite–hematite interfaces may be responsible for the large coercive field of lodestones, which consist of partially oxidized magnetite containing hematite microprecipitates. Our findings suggest that both discrete luogufengite nanominerals and luogufengite-like nanodomains play a critical role in enhancing magnetic coercivity and remanent magnetization, thereby providing new insights into the diverse magnetic anomalies observed on Earth and other planetary bodies.

Key words Luogufengite, ε-Fe_2O_3, Magnetic coercivity, Natural remanent magnetization, Lodestone

MAGNETITE TEXTURE AND CHEMISTRY: PRESENT AND FUTURE

Xiaowen Huang

State Key Laboratory of Critical Mineral Research and Exploration, Institute of Geochemistry, Chinese Academy of Sciences, China

Abstract Magnetite (Fe_3O_4) is one of the most ubiquitous and information-rich minerals in geological systems, occurring in a wide range of environments from magmatic and hydrothermal deposits to metamorphic and sedimentary settings. Its robustness, capacity to incorporate a variety of trace elements, and sensitivity to physicochemical conditions make magnetite a powerful recorder of ore-forming processes. Over the past decades, advances in microanalytical techniques and mineral chemistry have significantly enhanced our understanding of magnetite textures and compositions, positioning this mineral as a key tool in genetic interpretation and mineral exploration. This contribution reviews the current state of research on magnetite texture and chemistry, and outlines future directions in this rapidly evolving field.

Magnetite textures provide fundamental insights into its growth history and the evolution of the host system. Primary magmatic magnetite commonly exhibits euhedral to subhedral grains with exsolution lamellae, reflecting crystallization from evolving melts. In contrast, hydrothermal magnetite often displays complex textures such as oscillatory zoning, dissolution–reprecipitation, and recrystallization. More recently, nanoscale analytical tools such as transmission electron microscopy have revealed submicron- to atomic-scale features, including nanoparticle inclusions and diffusion profiles. The integration of textural observations with paragenetic relationships has proven essential for distinguishing between different mineralization stages, especially in complex systems such as iron oxide–copper–gold and skarn deposits.

Magnetite can incorporate a wide range of trace elements. The partitioning behavior of these elements is strongly controlled by temperature, oxygen fugacity, fluid composition, and host rock chemistry. For instance, Ti and V contents are commonly used as indicators of magmatic versus hydrothermal origin, whereas elements such as Co and Ni may reflect fluid sources related to mafic magma. Recent studies have emphasized the diagnostic value of multivariate geochemical discrimination diagrams and machine learning approaches for classifying magnetite from different deposit types. These diagrams are useful for revealing ore genesis and assisting mineral exploration. In addition to elemental composition, *in situ* Fe isotopic studies of magnetite are emerging as a promising frontier. Coupled with trace element data, Fe isotope signatures offer a powerful means of reconstructing the physicochemical conditions of magnetite formation.

Several key directions are expected to shape future research on magnetite texture and chemistry. First,

the integration of multiscale observations, from field relationships to nanoscale features, will be essential for building comprehensive genetic models. Second, the application of big data analytics and artificial intelligence to large geochemical datasets holds great promise for improving classification accuracy and uncovering hidden patterns. Third, experimental studies under controlled conditions are needed to better constrain element partitioning and isotopic fractionation mechanisms. Finally, the development of reference materials and data-sharing platforms will facilitate interlaboratory comparisons and enhance reproducibility.

Key words Magnetite texture, Trace elements, Ore genesis, Nanomineralogy, Big data

MAGNETOFOSSIL ASSEMBLAGES AS RECORDERS OF PALEOENVIRONMENT CONDITIONS: EVIDENCE FROM THE EOCENE-OLIGOCENE EQUATORIAL PACIFIC

Yang Lu[1,2,3], Dunfan Wang[1],Xiaodong Jiang[1], Zhiyong Lin[2], Yiping Yang[4,5], Qingsong Liu[1,6,7]

1. Centre for Marine Magnetism (CM2), Department of Ocean Science and Engineering, Southern University of Science and Technology, China
2. Institute für Geologie, Centrum für Erdsystemforschung und Nachhaltigkeit, Universität Hamburg, Germany
3. State Key Laboratory of Tropical Oceanography, Laboratory of Ocean and Marginal Sea Geology, South China Sea Institute of Oceanology, Chinese Academy of Sciences, China
4. CAS Key Laboratory of Mineralogy and Metallogeny, Guangdong Provincial Key Laboratory of Mineral Physics and Materials, Guangzhou Institute of Geochemistry, Chinese Academy of Sciences, China
5. CAS Center for Excellence in Deep Earth Science, China
6. Laboratory for Marine Geology, Pilot National Laboratory for Marine Science and Technology (Qingdao), China
7. Southern Marine Science and Engineering Guangdong Laboratory (Guangzhou), China

Abstract Magnetofossils — fossil magnetite crystals produced by magnetotactic bacteria (MTB) — are typically single-domain magnetic particles with three dominant morphologies: cuboctahedral, elongated prismatic, and bullet-shaped. Because different MTB species thrive under distinct redox conditions, the relative abundance of each magnetofossil morphology in sediments is potentially a sensitive proxy for paleoenvironmental changes, particularly variations in sediment redox gradients.

The Eocene–Oligocene transition (EOT, ~34 Ma) represents a critical shift from greenhouse to icehouse climates, accompanied by Antarctic glaciation, reorganization of ocean circulation, and significant changes in aeolian dust supply and marine productivity. This interval therefore provides an ideal natural laboratory to test the environmental response of biogenic magnetite assemblages.

Here we present a combined environmental magnetism and transmission electron microscopy study of pelagic sediments from ODP Site 1218 and IODP Site 1333 in the eastern equatorial Pacific Ocean. Our results show that across the EOT: (1) the absolute abundance of all magnetic particles decreases, consistent with a reduced aeolian input after the EOT; (2) however, the relative proportion of magnetofossils within the magnetic assemblage increases, as indicated by higher ARM/χ and ARM/IRM ratios and confirmed by first-order reversal curve (FORC) diagrams and IRM component analyses; (3) among magnetofossils, the fraction of anisotropic forms – especially bullet-shaped magnetosomes – obviously increases after the EOT.

Concurrently, the mass accumulation rate of total organic carbon (TOC MAR) increases, implying enhanced preservation of organic matter in the sediment despite similar or slightly reduced surface productivity. We interpret this as a result of lower bottom-water temperatures after the EOT, which reduced basal metabolic consumption of organic carbon. The higher organic carbon flux intensified the redox gradient within the oxic–anoxic transition zone (OATZ), creating more favorable conditions for MTB that produce bullet-shaped magnetite.

Our study demonstrates that magnetofossil assemblage variations — in particular the relative increase of bullet-shaped biogenic magnetite — faithfully record changes in sedimentary redox conditions driven by organic carbon supply. These findings confirm that biogenic magnetite morphology is a robust mineralogical proxy for paleo-redox and paleoproductivity regimes, highlighting the tight coupling between iron oxide biomineralization and the evolving chemistry of ancient oceans.

Key words Biogenic magnetite, Magnetofossil morphology, Redox-controlled mineralization, Eocene-Oligocene transition, Equatorial Pacific Ocean

MECHANISMS OF HEXAVALENT CHROMIUM REDUCTION IN FE(II)-BEARING CLAY MINERAL AND FE (HYDR)OXIDE BINARY SYSTEMS: COMPETITIVE ADSORPTION VERSUS MEDIATED ELECTRON TRANSFER

Ao Qian[1, 2], Yunsong Zheng[1], Peng Zhang[1, 3,*], Yuxi Lu[1], Chenglong Yu[4], Wenjuan Liao[5], Songhu Yuan[1, 3]

1. State Key Laboratory of Geomicrobiology and Environmental Changes, China University of Geosciences, Wuhan, 430078, P. R. China
2. Hubei Key Laboratory of Environmental and Health Effects of Persistent Toxic Substances, School of Environment and Health, Jianghan University, Wuhan, 430056, P. R. China
3. Hubei Key Laboratory of Yangtze Catchment Environmental Aquatic Science, School of Environmental Studies, China University of Geosciences, Wuhan, 430078, P. R. China
4. State Key Laboratory of Geohazard Prevention and Geoenvironment Protection, Chengdu University of Technology, Chengdu, 610059, P. R. China
5. College of Resources and Environment, Hunan Agricultural University, Changsha, 410128, P. R. China

ABSTRACT Fe(II)-bearing clay minerals are widespread reductants of hexavalent chromium (Cr(VI)) in subsurface environments. However, the influences of coexisting Fe (hydr)oxides on Cr(VI) reduction by Fe(II)-bearing clay minerals remain elusive. Here, Cr(VI) reduction was investigated in pre-mixed systems of reduced nontronite NAu-2 (rNAu-2) and various Fe (hydr)oxides. Results showed that coexisting ferrihydrite significantly facilitated Cr(VI) reduction during the quick stage (0–2.5 min) across pH 5.5–9.0. During the subsequent slow stage (2.5–205 min), ferrihydrite inhibited Cr(VI) reduction at pH 5.5–7.0 but enhanced it at pH 9.0. In contrast, coexisting goethite had negligible effects. Without Fe (hydr)oxides, direct reduction by rNAu-2 dominated for Cr(VI) removal. In the presence of Fe (hydr)oxides, competitive adsorption was found to inhibit direct Cr(VI) reduction, yet Fe (hydr)oxide-mediated electron transfer effectively offset this inhibitory effect. Both competitive adsorption and mediated electron transfer were influenced by the type and dosage of Fe (hydr)oxides, as well as solution pH. Kinetic modeling revealed that ferrihydrite-mediated electron transfer contributed 2.6–67.2% of the total Cr(VI) reduction, with greater contributions observed at higher solution pH and ferrihydrite dosage. Our findings provide new insights into mineral-mineral electron transfer and its role in regulating Cr(VI) fate in subsurface environments.

Key words Hexavalent chromium, Fe(II)-bearing clay minerals, Fe (hydr)oxides, Electron transfer, Adsorption

MINERALOGICAL EVOLUTION OF FE (HYDR)OXIDES AND ITS CONTROL ON CERIUM SPECIATION AND ANOMALY FORMATION IN MATURE REGOLITH

Mei Lu[1, 2*], Wei Tan[3, 4, 5], Jing Liu[6], Xiaoliang Liang[3, 4, 5], Yiping Yang[3, 4, 5], Hongping He[3, 4, 5]

1. School of Resources and Materials, Northeastern University at Qinhuangdao, China
2. School of Resources and Civil Engineering, Northeastern University, China
3. State Key Laboratory of Deep Earth Processes and Resources, Guangzhou Institute of Geochemistry, Chinese Academy of Sciences, China
4. Guangdong Research Center for Strategic Metals and Green Utilization, China
5. Guangdong Provincial Key Laboratory of Mineral Physics and Materials, Guangzhou Institute of Geochemistry, Chinese Academy of Sciences, China
6. State Key Laboratory of Lunar and Planetary Sciences, Macau University of Science and Technology, China

Abstract Cerium (Ce) exhibits unique geochemical behavior among rare earth elements (REEs) due to its redox sensitivity. The Ce anomaly is a vital proxy for tracing weathering processes and redox conditions, yet detailed mineralogical characterization of this phenomenon in natural regolith profiles has been limited. This study examines the geochemical and mineralogical evolution of Ce through a 90-meter-long drill core from the Huangshe ion-adsorption type REE deposit in South China, specifically linking the alteration of Fe and Mn (hydr)oxides to Ce speciation. The evolution of Fe oxides plays a critical role throughout the chemical weathering process. In the initial weathering stage (C horizon), primary Fe-bearing minerals dissolve, leading to the formation of poorly crystalline goethite. As weathering proceeds through the completely weathered horizon (B horizon), the crystallinity of goethite increases, and hematite begins to appear as intergrowths. In the mature topsoil (A horizon), characterized by a Chemical Index of Alteration (CIA) > 90, hematite becomes the predominant Fe phase, forming faceted crystals, while goethite gradually disappears. The transformation of these Fe phases significantly constrains Ce speciation and the resulting anomaly. In the early stages, the interaction between poorly crystalline goethite and mobilized Ce ions immobilizes the latter, generating a slightly positive Ce anomaly. As the weathering intensity increases, Ce-Fe-Mn ternary-mixed (hydr)oxides form. Within these composites, Mn (hydr)oxides (e.g., hausmannite) facilitate the oxidation of Ce^{3+} to Ce^{4+}, resulting in the precipitation of nano-scale cerianite (CeO_2). The phase transformation from goethite to hematite further influences this process by reducing surface hydroxyl density and specific surface area, which decreases direct Ce uptake by Fe (hydr)oxides and favors the separation of cerianite as a discrete phase. In the final stage of mature regolith development, well-crystallized hematite and cerianite become ubiquitous in the topsoil, trapping

Ce while other REEs migrate downward to form enriched zones in the lower horizons. This decoupling results in a profound positive Ce anomaly (up to 57.7) in the surface zone. These findings provide a mineralogical basis for using the Ce anomaly as a complementary geochemical indicator for prospecting REE deposits in mature regolith systems.

Key words Cerium anomaly, chemical weathering, Fe-Mn (hydr)oxides, mineral evolution, ion-adsorption-type REE deposit

MOLECULAR MECHANISMS OF PHOSPHATE-INDUCED MIDDLE-REE ENRICHMENT DURING REE ADSORPTION ON GOETHITE

Xiaoju Lin, Xiaoliang Liang

State Key Laboratory of Deep Earth Processes and Resources, Guangzhou Institute of Geochemistry, Chinese Academy of Sciences

Abstract Rare earth elements (REEs) are widely used as geochemical tracers, but their mobility and fractionation in supergene environments are strongly influenced by adsorption onto Fe (hydr)oxides. Phosphate is a particularly important ligand because it has a high affinity for Fe oxide surfaces and can form stable complexes with REEs. However, how phosphate modifies REE adsorption and fractionation at mineral–water interfaces remains insufficiently constrained. Here, we investigate the co-adsorption of phosphate and REEs on goethite. Batch adsorption experiments show that phosphate shifts the REE adsorption edge toward lower pH and markedly enhances REE uptake, with stronger effects at higher phosphate concentrations. More importantly, the presence of adsorbed phosphate changes the REE fractionation pattern from HREE-enriched to MREE-enriched, especially under acidic conditions. Molecular-scale evidence from in situ ATR-FTIR spectroscopy combined with 2D-COS, DFT calculations, and SCM collectively indicates that this shift is driven by the formation of ternary inner-sphere complexes among goethite surface sites, adsorbed phosphate, and REEs. At lower pH, REEs are mainly incorporated into phosphate-bearing surface complexes through monodentate ternary configurations, whereas bidentate ternary complexes become more favorable under near-neutral conditions. DFT calculations further show that MREEs form more stable phosphate-bridged ternary complexes than both LREEs and HREEs, providing a molecular explanation for the observed MREE enrichment. These results demonstrate that phosphate is an active mediator of REE fractionation on Fe oxide surfaces. This mechanism provides a mineral-surface basis for interpreting MREE-enriched signatures in natrual terrestrial waters.

Key words Rare earth elements, Phosphate, Goethite, Fractionation, MREE enrichment

REMOVAL PERFORMANCE OF IRON-LOADED CLAY MINERAL COMPOSITES FOR HEAVY METAL IONS

WU Limei[1], TANG Ning[1], LV Guocheng[2*], LIAO Libing[2*],

1. School of Materials Science and Engineering, Shenyang Jianzhu University, Shenyang 110168, China

2. School of Materials Science and Technology, China University of Geosciences, Beijing 100083, China

Abstract Based on the layered structural characteristics and surface/interface properties of clay minerals, this study successfully prepared a series of iron-loaded clay mineral composites, including nZVI/montmorillonite(Mnt) composites, nZVI/halloysite(HNT) composites, nano-Fe_3O_4/saponite composites, and nano-Fe_3O_4/Mnt composites. The phase composition, interactions between components, and iron speciation of the iron-clay mineral composites were characterized using XRD, XPS, SEM, TEM, and EDS, among other techniques. For example, the characteristic diffraction peaks of nZVI@HNT appear at 2θ = 44.7° (110)， 65.0° (200), and 82.3° (211), which match well with the standard card of elemental iron (JCPDS:06-0696). Moreover, no other diffraction peaks are observed in the XRD pattern of nZVI@HNT, indicating the high purity of the synthesized nZVI. The elemental composition and chemical valence states on the surface of nZVI@HNTs were determined using XPS. To further analyze the valence state of Fe in nZVI@HNTs, peak fitting of the Fe2p spectrum was performed using Avantage software. In the XPS spectrum, four characteristic peaks at binding energies of 725.0, 711.5, 731.2, and 716.9 eV are observed, corresponding to $Fe^{2+}2p_{1/2}$, $Fe^{2+}2p_{3/2}$, $Fe^{3+}2p_{1/2}$, and $Fe^{3+}2p_{3/2}$, respectively. However, no typical characteristic peaks of Fe^0 are observed at 706.9 eV or 719.9 eV.

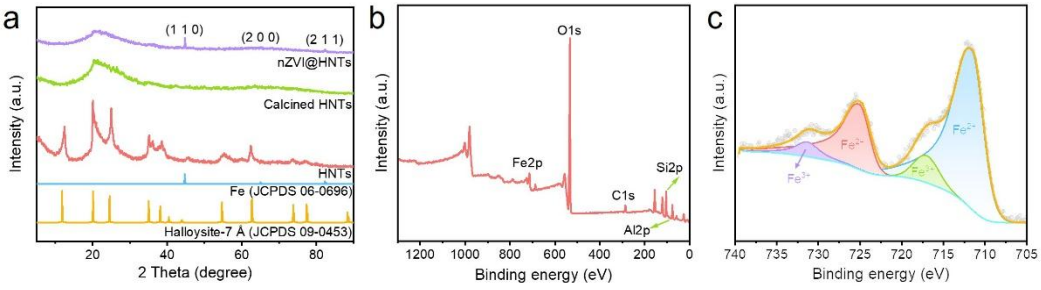


Fig.1 The XRD and XPS characterization of nZVI@HNTs.

This may be attributed to the fact that the Fe^{2+} and Fe^{3+} signals detected by XPS originate from the oxidation of a small amount of nZVI remaining on the external surface of HNTs, forming Fe_2O_3 or Fe_3O_4. Furthermore, the absence of an Fe^0 signal is because XPS cannot effectively capture information from the

nZVI protected within the inner lumen of HNTs. Characterization methods such as SEM, TEM, and EDS confirmed that almost no nZVI is loaded on the external surface of HNTs. nZVI is mainly distributed inside the tubular cavities of HNTs, with particle sizes equal to or smaller than the inner diameter of HNTs, and is aggregated from nZVI particles of approximately 2 nm in size.

Iron-loaded clay mineral composites exhibit excellent redox performance for heavy metal ions. Clay minerals possess a layered structure, a large specific surface area, and abundant surface active sites, demonstrating outstanding adsorption capability that can effectively enrich heavy metal ions in water, thereby providing a high-concentration local microenvironment for subsequent removal reactions. Meanwhile, nZVI and Fe_3O_4 have strong redox capacity and can convert the adsorbed heavy metal ions into lower valence, less toxic, or readily precipitable forms through electron transfer-mediated redox reactions, thus achieving efficient removal. These composites hold great application prospects in the field of environmental pollution remediation.

STEPWISE SUPERGENE OXIDATION OF PRIMARY AURIFEROUS PYRITE LEADS TO THE FORMATION OF BONANZA GOLD ORES

Fengxia Huang, Yage Wu, Yafei Wu*

State Key Laboratory of Geological Processes and Mineral Resources and School of Earth Resources, China University of Geosciences, Wuhan, Hubei Province 430074, China

Abstract Supergene weathering and oxidation of primary gold ores result in the formation of supergene gold ores with upgraded gold grades. During this process, oxidation of auriferous pyrite forms iron (oxyhydr)oxides, such as ferrihydrite, goethite, and hematite, and releases Au and other trace elements. However, the detailed processes of pyrite oxidation and gold remobilization remain poorly understood.

In this study, we integrated scanning electron microscopy (SEM), laser Raman spectroscopy, and laser ablation inductively coupled plasma mass spectrometry (LA-ICP-MS) to characterize the detailed textures and compositions of residual pyrite and iron (oxyhydr)oxides in high-grade supergene gold ores (206 g/t Au) from the Longtougou gold deposit, South Qinling orogen. SEM observations reveal that residual pyrite is successively overgrown by banded goethite (Gth1 and Gth2), followed by fine-grained (Gth3) and acicular (Gth4) goethite. Hematite (Hem) occurs at the interfaces between Gth1–Gth2 and Gth3–Gth4, where pyrite is absent. Microscopic gold grains are hosted in Gth4. LA-ICP-MS analyses reveal the lowest Au in residual pyrite (mean = 2.56 ppm), the highest Au in Gth1–Gth2 (mean = 239 ppm Au), and lower values in Hem (mean = 3.55 ppm) and Gth3–Gth4 (mean = 11.8 ppm).

Our results demonstrate stepwise supergene oxidation of primary auriferous pyrite, producing multiple generations of iron (oxyhydr)oxides under progressively evolving fluid physicochemical conditions. Pyrite dissolution released Fe^{2+}, which is oxidized to Fe^{3+} and hydrolyzed to thermodynamically unstable ferrihydrite that subsequently transforms into more stable Gth1. Gth1 is then converted to Gth2 via dissolution-reprecipitation. Progressive consumption of pyrite increases the local pH at the mineral-fluid interface, favoring the transformation of Gth2 to hematite. Gth3 precipitates rapidly from a Fe^{3+}-oversaturated fluid and recrystallizes into acicular Gth4. Concomitantly, Au and associated trace elements are remobilized from pyrite, forming microscopic gold within iron (oxyhydr)oxides. These findings provide new insights into the processes responsible for supergene gold upgrading.

Key words Supergene oxidation of pyrite, Gold-rich iron (oxyhydr)oxides, Gold remobilization, Longtougou, South Qinling Orogen

A 4 X 4 X 4 UNIT-CELL SUPERSTRUCTURE FOR URANIUM-BEARING HEMATITE WITH LONG-RANGE ORDERING OF METAL VACANCY

Jie Yao[1], Cristiana L. Ciobanu[1], Nigel J. Cook[1], Kathy Ehrig[1,2], Ashley D. Slattery[3], Eugene Ilton[4], Nobuyoshi Miyajima[5], Gerd Steinle-Neumann[5]

1. School of Chemical Engineering, Adelaide University, Adelaide, SA 5005, Australia
2. BHP Copper SA, 10 Franklin Street, Adelaide, SA 5000, Australia
3. Adelaide Microscopy, Adelaide University, Adelaide, SA 5005, Australia
4. Pacific Northwest National Laboratory, 902 Battelle Boulevard, Richland, WA 99354, USA
5. Bayerisches Geoinstitut, University of Bayreuth, 95440 Bayreuth, Germany

Abstract There is much interest in finding long-term barriers that can hinder environmental migration of radionuclides. Iron oxides, hematite (α-Fe_2O_3) and magnetite (Fe_3O_4) are recognized candidates due to their thermodynamic stability and abundance in surface environments. Uranium-bearing hematite from the Olympic Dam deposit (South Australia) is reported to contain as much as 2.5 wt% UO_3, as measured by energy dispersive X-ray spectrometry in a scanning transmission electron microscope (STEM). This natural hematite shows 12-fold long-range modulation along the $<\bar{1}100>^*$ directions on high-angle annular dark field STEM images. This feature was reproduced using an empirical 4 x 4 x 1 hematite superstructure model ($Fe_{1.467}O_3$) with 12 layers of variable Fe occupancy. To fit the analytical data on the $[2\bar{2}01]$ zone axis, the model was further expanded into a 4 x 4 x 4 unit-cell superstructure. Due to its structural complexity and relatively large size, the superstructure model cannot be directly constrained by ab initio calculations. Instead, it was approximated by using the simplified long-range iron and oxygen vacancy ordering model ($Fe^{3+}_{1.969}U^{5+}_{0.010}O^{2-}_{2.979}$) within the 4 x 4 x 4 unit cell, also utilizing the previous fitted double-corner or edge- and face-sharing local Fe vacancy configurations. Electron diffraction patterns of both DFT relaxed structures exhibit a good match with experimental data. Bader charge and magnetic moment calculation confirm incorporation of pentavalent uranium within the supercell. To completely constrain the original superstructure, it requires averaging hundreds of 4 x 4 x 4 supercells with unique positions of long-range ordering in local Fe vacancy configurations. This could potentially be achieved by training machine learning potential for Fe, O and U atoms using DFT datasets.

Key words Uranium-bearing hematite, long-range ordering, superstructure, ab initio calculation, scanning transmission electron microscopy

Acknowledgements N.J.C and K.E. acknowledge funding from Australian Research Council grant LP200100156. E.S.I. acknowledges support from the US DOE BES Geosciences program at PNNL (FWP: 56674).

MINERALOGICAL AND GEOCHEMICAL CHARACTERISTICS OF IRON METEORITE: BASELIN DATA FOR METAL-RICH ASTEROID EXPLORATION

Heejeong Jeon, Seungyeol Lee*

Department of Earth and EnvironmentalScience, Chungbuk National University, Republic of Korea

Abstract With the anticipated arrival of NASA's Psyche mission at the metal-rich asteroid (16) Psyche in 2029, along with the progress of other international small-body exploration programs such as China's Tianwen-2 and the UAE's MBR Explorer, scientific interest in metal-rich asteroids has grown significantly. Iron meteorites are widely regarded as fragments of metallic cores formed during the differentiation of early Solar System planetesimals, and therefore serve as direct analogs for understanding the composition and structure of metal-rich asteroids. Characterizing the mineralogical and chemical textures of iron meteorites through laboratory analyses thus provides a means to indirectly investigate metallic asteroid interiors and core formation processes during planetary differentiation. Accordingly, this study employed portable X-ray fluorescence spectrometry (XRF), scanning electron microscopy with backscattered electron imaging (SEM-BSE), and powder X-ray diffraction (XRD) to systematically characterize three representative iron meteorite samples: Campo del Cielo (IAB-MG octahedrite), Gibeon (IVA octahedrite), and Muonionalusta (IVA octahedrite), with the aim of establishing fundamental reference data for interpreting future Psyche mission results. . Powder XRD analysis identified major peaks at approximately 2.03 Å, 1.43 Å, and 1.17 Å in all three samples, corresponding to the bcc α-Fe (kamacite) phase and confirming that kamacite is the dominant constituent mineral. Furthermore, subtle peak shifts observed relative to literature values may reflect minor variations in Ni content within the α-Fe (kamacite) solid solution. SEM-BSE imaging of Gibeon and Muonionalusta revealed the typical Widmanstätten pattern, characterized by the intergrowth of kamacite and taenite, providing constraints on the formation environment and cooling history within their respective parent bodies. The XRF analysis revealed that Campo del Cielo has a relatively low Ni concentration, whereas Gibeon and Muonionalusta exhibit comparatively higher Ni concentrations. These mineralogical and geochemical characteristics offer valuable insights into parent-body differentiation and core formation processes in the early Solar System, and the results of this study can serve as a comparative baseline for interpreting future Psyche mission data and for advancing our understanding of metallic asteroids and their planetary interiors.

Key words Psyche mission, iron meteorites, cooling processes, kamacite, Metal-rich asteroid

AG-RICH MINERALS AND GOLD FROM THE NORTHWEST AND AEGEAN ZONES OF THE INTERMEDIATE SULFIDATION EPITHERMAL BOWDENS AG-(PB-ZN-AU) PROSPECT, LUE, NSW, AUSTRALIA

Rory Carter[1], Ian Graham[1], David French[1], Karen Privat[1,2], Huixin Wang[3], David Biggs[4], Tom Klein[4]

1. Earth and Sustainability Science Research Centre, School of Biological, Earth and Environmental Sciences, University of New South Wales, Australia

2. Electron Microscopy Unit, Mark Wainwright Analytical Centre, University of New South Wales, Sydney, Australia

3. Solid State Analysis Unit, Mark Wainwright Analytical Centre, University of New South Wales, Sydney, Australia

4. Bowdens Silver Pty Ltd, Lue, NSW, Australia

Abstract Silver has a wide range of applications due to its favorable properties such as conductivity, reflectivity, and antimicrobial properties. As a result, silver finds use in electronics, medicine, photography, solar energy, and industrial applications. Epithermal systems are a common source of silver, frequently co-occurring with a polymetallic assemblage of copper, lead, zinc, and gold.

This study focused on two silver-rich zones (Northwest and Aegean) of the intermediate-sulfidation Bowdens Ag-Pb-Zn-Au epithermal deposit, near Lue, NSW, Australia. Mineralization at Bowdens is hosted in the Late Carboniferous Rylstone Volcanics (RV) and unconformable underlying deformed Late Ordovician metasedimentary rocks of the Coomber Formation (CF). The Northwest and Aegean zones are hosted in the highly welded, crystal, lithic rhyolite-andesite tuffs in the lower horizons of the RV.

The Northwest and Aegean zones have exceptionally enriched silver intersections (>5,000 ppm Ag), with assay results in the Northwest zone also showing significant gold. These zones were of particular interest because they are believed to sit at a transitionary level of the Bowdens system, between the characteristically intermediate mineralization in the underlying Coomber Formation, and overlying mineralization in the upper horizons of the Rylstone Volcanics that display some low-sulfidation characteristics. Four drill holes (two in each zone) were sampled for this study, with the aim of characterizing their overall mineralogy and developing a paragenesis of mineralization through the two zones.

Through petrography, electron microscopy, and complementary electron microprobe analysis (EPMA), this study identified at least seven different Ag-bearing sulfosalt minerals across the two zones. Argentopearceite ($(Ag_{15.03}Cu_{1.94})_{16.97}(As_{1.39}Sb_{0.35})_{1.74}S_{10.20}$), argentopolybasite

($(Ag_{16.17}Cu_{1.53})_{17.70}(As_{0.51}Sb_{1.26})_{1.77}S_{9.50}$), and Ag-rich tetrahedrite ($Cu_{6.00}[Cu_{1.05}Ag_{3.66}(Fe_{0.34}Zn_{1.51})](As_{0.41}Sb_{3.54})S_{12.50}$) were observed as common phases in both zones. Furthermore, pyrargyrite ($Ag_{3.19}Sb_{0.93}S_{2.82}$) was only noted in the Aegean zone, while pearceite ($(Ag_{11.80}Cu_{4.63})_{16.43}(As_{1.63}Sb_{0.15})_{1.78}S_{10.68}$), Ag-bearing tennantite ($Cu_{6.00}[Cu_{3.32}Ag_{0.58}(Fe_{0.53}Zn_{1.52})_{2.05}](As_{3.34}Sb_{0.53})_{3.87}S_{13.18}$) and tennantite ($Cu_{6.00}[Cu_{3.91}(Fe_{0.44}Zn_{1.60})_{2.04}](As_{3.79}\ Sb_{0.15})_{3.94}S_{13.11}$) were identified only in the Northwest zone. Of particular interest is the common occurrence of exceptionally Ag-rich species such as argentopearceite and argentopolybasite in both zones. In the Northwest zone only, Au occurs as grains with a high fineness (Au76) as a late phase of this second major ore stage mineralizing event. The presence of these minerals can help explain the exceptionally high grades observed (>5,000 ppm Ag).

In addition to the Ag mineralogy, this study particularly identified a close correlation between the intensity of adularia alteration and high-grade Ag mineralization in both zones. Adularia is suggested to be an important vector towards high-grade Ag mineralization at Bowdens. Furthermore, the co-occurring sulfide assemblages in combination with the vein and breccia types observed in each zone are markedly distinct. The Northwest zone hosts polyphasal, polymetallic, Ag-rich vein breccias in the rheologically competent welded vitric tuff, with common chalcopyrite, and an As-rich Ag-bearing sulfosalt assemblage. In comparison, the Aegean zone hosts Ag in thinner veins and veinlets with only minor wall-rock brecciation, displaying an Sb-rich Ag-bearing sulfosalt dominant assemblage with common galena and pyrite, but rare sphalerite and no chalcopyrite. These observations suggest that the Northwest zone represents a major upflow zone at Bowdens, with higher intensity of deformation and hotter temperatures. Conversely, the Aegean zone is part of a vein network envelope around this upflow conduit, formed in a more distal, cooler environment.

Finally, the use of micro-X-ray fluorescence mapping proved very effective at delineating key paragenetic relationships. In particular, mapping the variations in co-occurring carbonate chemistry through highly cryptic, multiply deformed samples was able to visualize the major ore-forming generations. Mn-rich carbonates were noted as indicative of the Ag-rich generation of mineralization. Critically two major polymetallic sulfide mineralization events were identified, with the entirety of Ag and Au mineralization within the later ore-stage mineralization, post-dating an earlier base metal sulfide-rich generation.

Key words Epithermal, Bowdens, intermediate-sulfidation, argentopearceite, argentopolybasite

CHARACTERISTICS OF CLAY SOILS FROM CENTRAL SEMIACHIK'S NORTH CRATER (KAMCHATKA)

Ruslan Alexeevich Kuznetsov[1], Andrey Borisovich Ermolinsky[2], Anton Alekxeevich Nuzhdaev[1]

1. Volcanochemistry, Institute of Volcanology snd Seismology FEB RAS, Russia

2. Faculty of Geology, Lomonosov Moscow State University, Russia

Abstract Clay minerals and the soil strata composed of them, formed as a result of hydrothermal transformations of volcanic rocks, are widely developed in the thermal fields of Kamchatka and have been described in considerable detail for some of them. These include the thermal fields of the Pauzhetka and Mutnovsky deposits, as well as the thermal fields associated with the Koshelevsky and Kambalny volcanic massifs. However, detailed studies of clay formations have not been conducted previously for the thermal fields associated with post-volcanic processes in the area of Central Semiachik.

Central Semiachik is a destroyed basaltic volcano with two craters: the Northern and the Southern. Its western part has been destroyed as a result of erosion, hydrothermal and fumarolic activity. On the northern slope of the volcano there is an extrusive dome of dacitic composition (Polukupol), and in the southern and eastern parts – a group of andesitic domes of Upper Pleistocene–Holocene age. Present-day active hydrothermal activity is observed in the central destroyed part of the volcano, as well as on its southeastern slope, in the upper reaches of the Kisly Stream.

The Northern crater of Central Semiachik has been substantially altered as a result of hydrothermal processes. Moreover, the area of rocks transformed to clays significantly exceeds the area of the present-day thermal field.

Samples were collected from various points in different areas of the thermal field within the Northern crater of Central Semiachik. These areas had undergone alteration due to hydrothermal processes, but by the time of sampling, most of them had cooled down.

The chemical composition of clayey soils on the surface of the Northern crater of Central Semiachik is dominated by SiO_2, the content of which varies from 32 % to 90%; Al_2O_3 content is 15–20%; S content reaches 9%; $FeO+Fe_2O_3$ accounts for 13%; and CaO for 8%. The loss on ignition of samples at 1050°C is quite high, ranging up to 35%.

The mineral composition is dominated by kaolinite and montmorillonite; calcite, pyrite, cristobalite, and opal may be present in smaller amounts.

During simultaneous thermal analysis, the studied samples lose up to 20% of their mass at the dehydration stage and up to a further 15% during dehydroxylation, indicating their high hygroscopicity.

In their natural state, the samples have a moisture content of 40% to 80%, a density of 1.3 to 2 g/cm³, and a plasticity index of 11% to 38%. Based on compression test results, all samples are classified as

highly compressible, which is quite typical for soils of such mineral composition and natural structure.

Key words hydrothermal alteration, clay minerals, Kamchtka, Semiachik, volcanoes

Acknowledgements The work was carried out within the framework of the state assignment of the Institute of Volcanology and Seismology FEB RAS “Geochemistry of products of modern volcanic and post-volcanic activity” (FWME-2024-0013 under the leadership of A.A. Nuzhdaev), aproved by the Ministry of Education and Science of Russia (topic no. 124080600037-9).

In addition, the authors would like to express their gratitude to the Centre for X-ray Diffraction Studies of Saint-Petersburg State University Research Park; Laboratory of Mineralogy (IVS FEB RAS); The Chair of Engineering and Ecological Geology of Lomonosov Moscow State University.

EXHALATION MINERALS FROM SOLFATARAS OF THE PYROCLASTIC FLOW IN 2023 OF THE SHIVELUCH VOLCANO (KAMCHATKA, RUSSIA)

1. A.N. Kupchinenko[1], E.S. Zhitova[1], R.M. Sheveleva[1,2], E.Yu. Plutakhina[1] and N.S. Vlasenko[2]

2. Institute of Volcanology and Seismology FEB RAS, Petropavlovsk-Kamchatsky, Russia

St. Petersburg State University, St. Petersburg, Russia

Abstract Exhalation minerals from solfataras of the pyroclastic flow in 2023 of the Shiveluch volcano (Kamchatka, Russia) have been characterized by the combination of analytical techniques: electron-probe microanalysis, powder X-ray diffraction. Among the most common minerals are alunite-group (alunite, natroalunite, jarosite, natroarosite), voltaite-group (ammoniomagnesovoltaite, magnesiovoltaite), halotrichite-group (pickeringite), alunogen, tamarugite, gypsum, bassanite, anhydrite, chlorides (salammoniac, halite, bischofite), fluorides (hydrokenoralstonite) have been found.

The Shiveluch volcanic complex is located in the northern part of the Central Kamchatka Depression, 50 km north of Klyuchi settlement. The minerals studied therein were formed on a degassing pyroclastic flow resulting from the paroxysmal explosive eruption of Shiveluch volcano that occurred on April 10–13, 2023. Pyroclastic deposits filled dry valleys of temporary streams with thicknesses up. After the eruption, so-called rootless (not connected to the magmatic source) fumaroles and solfataras formed on the flow. Gases in such fumaroles are released both during degassing of volcanic material and due to boiling of meteoric waters. The mineral samples were collected in September 2023, when the temperature of solfataras ranged from 220 to 405 °C.

The work was performed under Institute of Volcanology and Seismology FEB RAS state assignment within the research topic “Mineral formation in the Northern Pacific suprasubduction zone” No. FWME-2024-0004, registration number 124031900001-9. Mineral studies were conducted using equipment of Saint-Petersburg State University Scientific Park at Resource Centers “X-ray Diffraction Research Methods” and “Geomodel” under projects 125021702335-5 and 124032000029-9, respectively. We thank O.A. Girina, R.A. Kuznetsov, A.A. Nuzhdaev, and V.O. Davydova for providing samples and the field photographs.

Key words Shiveluch, pyroclastic flow, solfatara, Kamchatka, exhalation minerals.

FUMAROLE SUBLIMATES OF KRASHENINNIKOV VOLCANO (KAMCHATKA, RUSSIA)

Elena S. Zhitova

Institute of volcanology and seismology FEB RAS (Mineralogy, Russia)

Abstract The report is devoted to the mineralogical study of volcanic sublimates formed on the lava flow of the Krasheninnikov volcano (Kamchatka, Russia) during its first historical (in 500 years) eruption. Among the sublimates formed at a temperature of about 100 ºC, ammonium minerals were found: kremersite and salammoniac in association with wilcoxite, coesite, halite, ralstonite and krasheninnikovite. Sublimation thallium minerals were found in the higher temperature parts of the lava flow (300-500 ºC). Among them, kremersite is rare; most of its few discoveries are associated with coal fires. However, as the 2025 eruption of Krasheninnikov volcano demonstrated, this mineral can form abundant manifestations on lava flows. The presentation will examine its main crystal chemical characteristics and demonstrate the importance of this mineral as a potential phase-concentrator of biogenic nitrogen on other planets.

The study is carried out by the Institute of volcanology and seismology FEB RAS state assignment within the research topic "Mineral formation in the Northern Pacific suprasubduction zone" No. FWME-2024-0004, registration number 124031900001-9.

Key words Krasheninnikov volcano, kremersite, fumarole, ammonium, Kamchatka

GENESIS OF GEM SAPPHIRE FROM THE PLIOCENE ALKALI BASALTS OF THE WESTERN CARPATHIANS

Stefan Farsang

Institute of Geological Sciences, University of Bern, Switzerland

Abstract Most gem sapphire deposits worldwide are spatially associated with alkali basalts, although sapphire is not a stable mineral phase in such magmas. Basalts therefore act only as transport agents, entraining sapphire xenocrysts from their source and delivering them to the surface. Because sapphire occurs predominantly as isolated xenocrysts and only exceptionally within xenoliths representing its original host rock, its primary formation environment remains unresolved and highly debated. This study investigates sapphire occurrences in Pliocene alkali basalts from the Nógrád-Gömör/Novohrad-Gemer Volcanic Field in the Western Carpathians, where sapphire is found both as xenocrysts and within sapphire-bearing syenite xenoliths. A comprehensive analytical approach combining optical petrography, cathodoluminescence imaging, scanning electron microscopy, electron probe microanalysis, Raman spectroscopy, and laser ablation inductively coupled plasma mass spectrometry was applied to characterise (1) xenocrysts, including their reaction rims and solid and fluid inclusions, and (2) syenite xenoliths and their mineral assemblages. Sapphire hosts abundant primary solid inclusions composed of minerals identical to those in the syenite xenoliths, directly linking xenocrysts to this lithology. In addition, secondary fluid inclusions containing multiple daughter minerals are present in sapphire and indicate the former presence of a carbonatitic liquid. Besides the major minerals, the syenite xenoliths contain carbonates, accessory phases such as zircon and apatite, and minerals belonging to the monazite, pyrochlore, betafite, and columbite groups, reflecting an evolved system enriched in incompatible elements. Integrated petrographic, mineralogical, and geochemical data support a syenitic-carbonatitic genetic environment for sapphire formation.

Key words sapphire, syenite, carbonatite, gemstone

Acknowledgements Ladislav Oravec is acknowledged for the rediscovery of sapphires in the studied area. I thank Ladislav Oravec, Peter Chalachan, and Daniel Šoltés for donating samples for this research. Thomas Pettke, Kalin Kouzmanov, Agathe Martignier, Pavel Uher, Daniel Ozdín, László Előd Aradi, Zoltán Zajacz, and Csaba Szabó are acknowledged for analytical assistance and discussion of the results.

MODULAR STRUCTURES OF BUBNOVAITE $K_2Na_8CA(SO_4)_6$, DOBROVOLSKYITE $Na_4CA(SO_4)_3$ AND A_2SO_4 SERIES (A = NA, K, RB, CS): INHERITANCE OF MINERAL STRUCTURE FROM HIGH TEMPERATURE DISORDERED MODIFICATIONS

Andrey Pavlovich Shablinskii[1,2], Sofya Vladimirovna Demina[1], Olga Yurievna Shorets[1], Margarita Sergeevna Avdontceva[2], Yaroslav Pavlovich Biryukov[1], Rimma Sergeevna Bubnova[1], Stanislav Konstantinovich Filatov[2]

1. Grebenshikov Institute of Silicate Chemistry, St. Petersburg, Russia

2. St. Petersburg State University, St. Petersburg, Russia

Abstract Currently, the already classic concept of “From minerals to advanced materials” is being actively developed, which in some cases proves to be much more effective for predicting and obtaining new synthetic compounds than the traditionally used trial-and-error synthesis. The Tolbachik volcano (Kamchatka Peninsula, Russia) is one of the leading geological objects both in the number of new mineral species discovered there and in the number of new structure types, many of which serve as prototypes for the creation of mineral-like materials. Since volcanic minerals typically originate at high temperatures, temperature is a key factor in their formation.

The crystal structures of minerals of the Na_2SO_4–K_2SO_4 series, bubnovaite $K_2Na_8Ca(SO_4)_6$ and dobrovolskyite $Na_4Ca(SO_4)_6$, many of which were discovered on the Tolbachik volcano, were considered by us as modular. It is quite rare to succeed in applying the modular approach to substantiating the genesis of mineral species. The microblock, module [$M(TO_4)_6$], or structural unit consisting of an octahedron sharing six common vertices with six adjacent tetrahedra, was considered as an inherited fragment of crystal structures from a disordered high-temperature parent structure. The relations between the "parent" microblock and the microblocks formed upon cooling from high temperature is described. The driving force for the formation of a certain module upon cooling of the parent module is the tendency of the structure to become ordered upon cooling. If the parent block is cooled, due to the difference in charge and ionic radius of the cations, crystalline structures can be formed from different microblocks, which have different physical properties.

The results are confirmed by experimental data: polymorphic transformations of $K_2Na_8Ca(SO_4)_6$, $Na_4Ca(SO_4)_6$ and A_2SO_4 series (A = Na, K, Rb, Cs) were studied using high-temperature single-crystal and powder X-ray diffraction methods.

The formation of minerals with these described structural features facilitates great prospects for the synthesis of compounds with useful properties. Initial reagents consisting of similar microblocks can be selected for successful synthesis. Then, during the synthesis, compounds with these crystal structures are

formed from these microblocks and can potentially exhibit useful properties.

Experiments and its data evaluation were supported by the Russian Science Foundation (grant No. 22-13-00317]). The X-ray diffraction experiments were performed at The Center for X-ray Diffraction Studies (Saint Petersburg State University).

Key words Modular structures, Tolbachik volcano, phase transformations, high-temperature X-ray diffraction

NATURE OF OLIVINE MACROCRYSTS IN HAWAIIAN PICRITES

Eiichi Takahashi, Fangfang Huang and Li Li

State Key Laboratory of Deep Earth Processes and Resources, Guangzhou Institute of Geochemistry, Chinese Academy of Sciences, China

Abstract Picrites containing abundant olivine phenocrysts (macrocrysts), commonly up to 30 vol.%, have long been considered representative of primary magmas in large igneous provinces such as Hawaii. In this study, we investigated picrites collected from the submarine flanks of six Hawaiian shield volcanoes (Kilauea, Mauna Loa, Mauna Kea, Loihi, Haleakala, and Koolau) during the Japan–US joint Hawaii cruises conducted by JAMSTEC (see Hawaiian Volcanoes: Deep Underwater Perspectives, AGU Special Volume, 2002, eds. Takahashi, Garcia, Lipman, et al.).

The studied picrites were classified into three categories. Type-1 picrites contain only euhedral olivine phenocrysts showing normal zoning from magnesian cores (Fo90–88) to Fe-rich rims (Fo86–84). Type-2 picrites contain a mixture of Type-1 and Type-3 olivines. Type-3 picrites contain only xenocrystic olivine macrocrysts with a wide range of core compositions (Fo90–75), magnesian olivines with well-developed kink banding indicative of subsolidus deformation, most olivines showrounded shapes indicating resorption during magma ascent. Type-1 picrites are rare and are restricted to the Puna Ridge of Kilauea volcano, whereas Type-3 picrites were found only in the submarine part of Koolau volcano. Most Hawaiian picrites belong to Type-2, in which olivine macrocrysts represent mixtures of phenocrysts and xenocrysts.

The origin of the olivine xenocrysts in Koolau volcano can be explained by the following model. Koolau is an enigmatic outlier among Hawaiian volcanoes, characterized by high-SiO_2 tholeiitic magmas with enriched EM1-type isotopic signatures. These features suggest derivation from a mantle source containing a high proportion of recycled ancient oceanic crust. We investigated rock specimens collected from the northern flank of Koolau volcano at depths of approximately 2500–3000 m, in areas unaffected by the Nuuanu landslide. Picritic rocks dominate at deeper levels, whereas aphyric basaltic andesite occurs at shallower depths. Sr–Nd–Pb isotope data indicate that both rock types belong to the final Makapuu stage of Koolau volcanism.

The olivine macrocrysts in the Koolau picrites are highly heterogeneous (Fo90–75), showing complex zoning patterns and curved crystal surfaces suggestive of partial dissolution during magma ascent. Experimental studies demonstrate that olivine can crystallize from Koolau magmas (7–15 wt.% MgO) only at pressures below 0.5 GPa, whereas orthopyroxene and clinopyroxene crystallize at higher pressures. These results imply that the magma erupted under superheated conditions (~1300 °C), resulting in olivine

resorption during ascent followed by olivine crystallization at shallow crustal levels (possibly after eruption).

We conclude that all olivine macrocrysts in the Koolau picrites are xenocrystic and that the primary Koolau magma was a superheated basaltic andesite produced by partial melting of eclogite, rather than by crystallization from a picritic magma derived from partial melting of a mafic garnet pyroxenite source. The low CaO contents of Koolau olivines (<0.2 wt.%) further support a lithospheric origin. This model provides an alternative explanation for the NiO enrichment of Koolau olivines proposed by Sobolev et al. (2005), and suggests that the persistence of eclogite, rather than mafic pyroxenite, at the top of the Hawaiian plume during the final stage of Koolau volcanism either by a lower plume potential temperature than previously proposed by Herzberg et al.(2009) or by very depleted hurzburgitic host peridotite (Béguelin et al 2025).

Key words olivine, phenocryst, xenocryst, picrite, Hawaiian volcano

ROCK-FORMING MINERALS AS INDICATORS OF PROCESSES IN MAGMATIC SYSTEMS: THE CASE OF KRENITSYN PEAK VOLCANO (ONEKOTAN ISLAND, KURIL ISLANDS, RUSSIA)

Vesta O. Davydova[1,2], Anton A. Nuzhdaev[1], Ilya E. Bolshakov[1,2], Ruslan A. Kuznetsov[1], Andrey B. Ermolinskiy[2], Elena S. Zhitova[1], Vasiliy O. Yapaskurt[1]

1. Institute of Volcanology and Seismology FEB RAS, Russia

2. Geology Faculty, Lomonosov Moscow State University, Russia

Abstract Krenitsyn Peak is a post-caldera volcano that started forming after the caldera-forming eruption of Tao-Rusyr volcano (~7.5 ka) on Onekotan Island (Kuril Islands). The earliest eruptive products of Krenitsyn Peak are noticeably more felsic than the most SiO_2-rich rocks of Tao-Rusyr and belong to a different magmatic series: Tao-Rusyr lavas are tholeiitic, while the rocks of Krenitsyn Peak are calc-alkaline. Additionally, the volcanic products of Krenitsyn Peak show a progressive shift toward more mafic compositions over time. In this study, we analyze the composition, zoning patterns, and textural features of rock-forming minerals to reconstruct the evolution of the magmatic system feeding the volcano.

Plagioclase and pyroxenes show clear signs of disequilibrium crystallization and magma interaction processes. Plagioclase phenocrysts often contain relic high-Ca cores (up to An_{94}) surrounded by more sodic zones (up to An_{52}). The presence of spongy sieve textures (An_{80-85}), patchy zoning (An_{51-90}), and resorption surfaces indicates repeated changes in pressure-temperature conditions and magma composition. Rhythmic zoning at plagioclase rims and partial melting along growth-zone boundaries support the idea of repeated magma recharge and mingling episodes.

Pyroxenes also record complex crystallization histories. Large clinopyroxene phenocrysts may contain relic cores, while reverse zoning in pyroxenes suggests sudden changes in melt composition, temperature, or volatile content. The groundmass mineral assemblage includes orthopyroxene of the enstatite-ferrosilite series, augite, and pigeonite. The coexistence of these pyroxenes indicates high-temperature crystallization just before eruption. The presence of pigeonite, along with stable sulfides in the groundmass, points to relatively reduced conditions during late-stage crystallization.

The strong compositional difference between relic high-An plagioclase cores and the rhyolitic matrix glass indicates that the system experienced injections of significantly more mafic magma. The occurrence of pigeonite in the groundmass and relic high-An plagioclase support the interpretation that compositionally and thermally contrasting basaltic melts were periodically injected into a reservoir containing more evolved dacite–andesite magma.

Whole-rock trace element ratios (e.g., Rb/Sr, La/Nb, Zr/Hf, and Sr/Y) show limited variability, which

suggests that fractional crystallization was the main, but not the only, process controlling magma evolution. The relatively uniform distribution of incompatible elements indicates that magma mixing mainly occurred between related magmas at different stages of fractional crystallization, whereas assimilation of crustal material probably occurred earlier, during the formation of the large magma chamber before the Tao-Rusyr caldera-forming eruption.

Therefore, the compositions, zoning patterns, and mineral assemblages of rock-forming minerals provide important insights into the development of the magma plumbing system beneath Krenitsyn Peak, indicating a relatively felsic subsurface reservoir periodically recharged by basaltic magma injections.

Key words rock-forming minerals, mineral zoning, Krenitsyn Peak, Kuril Island arc, post-caldera volcanism

Acknowledgements The work was carried out within the framework of the state assignment of the IVIS of the Far Eastern Branch of the Russian Academy of Sciences within the framework of the research topic “Geo-chemistry of products of modern volcanic and post-volcanic activity” (FVME-2024-0013), ap-proved by the Ministry of Education of the Russian Federation and Science of the Russian Federa-tion (topic No. 124080600037-9). The authors would like to thank the MSU Development Program for its support. The authors would like to thank the Russian Geographical Society and the head of the expedition, A. P. Kalemberg, for their assistance in conducting fieldwork and primary pro-cessing of materials.

SILICATE-SULFIDE MELT IMMISCIBILITY AND NOBLE-METAL BEHAVIOR IN MANTLE-DERIVED MAGMAS: KEY DISCOVERIES FROM NATURAL OBSERVATIONS

Vadim S. Kamenetsky

Center of Deep Sea Research, Institute of Oceanology, Qingdao, China

Abstract Understanding how mantle-derived magmas concentrate chalcophile and highly siderophile elements remains central to igneous petrology and economic geology. Over the past decade, our research has focused on direct natural observations of silicate–sulfide melt immiscibility and the behavior of noble metals in primitive oceanic and arc magmas. By studying sulfide melt inclusions preserved in early-crystallizing minerals (olivine and Cr-spinel), we were able to capture the earliest stages of sulfide segregation and metal enrichment that are normally erased during magmatic evolution. These studies reveal several key discoveries about the formation of metal-rich sulfide melts and the distribution of platinum-group elements (PGE) in magmatic systems.

One of the central results of this work is the recognition of <100 micrometer globules of immiscible sulfide melt preserved in olivine phenocrysts and volcanic glasses from primitive mantle-derived magmas. These globules represent quenched droplets of sulfide liquid that segregated from silicate magma once sulfur concentrations exceeded the sulfur content at sulfide saturation (SCSS). Because these droplets are trapped early within growing olivine crystals, they preserve the compositions of primitive sulfide liquids that are otherwise rarely accessible in natural systems. The compositions of these incipient sulfide melts demonstrate their strong enrichment in chalcophile elements (Ni and Cu) relative to coexisting silicate melts.

Island-arc magmas are generally thought to remain sulfide-undersaturated because of their relatively oxidized conditions, where sulfur is present mainly as sulfate rather than sulfide. However, studies of basalts from Tolbachik volcano (Kamchatka) show that sulfide immiscibility can occur early in the evolution of primitive arc magmas despite their oxidized character. This finding challenges the long-standing paradigm that arc magmas rarely form sulfide liquids. Instead, it demonstrates that sulfur-rich primitive arc melts can reach sulfide saturation during early crystallization and generate metal-bearing sulfide droplets capable of scavenging large quantities of chalcophile elements and PGE.

The third key finding is that even extremely small volumes of sulfide melt can extract large amounts of noble metals from silicate magma. Sulfide globules from primitive arc basalts contain PGE and gold at concentrations several orders of magnitude higher than in their host silicate melts. This observation confirms theoretical predictions that sulfide melts strongly partition noble metals and explains why orthomagmatic Ni–Cu–PGE deposits do not require exceptionally large volumes of metal-rich magmas.

A striking feature of many sulfide globules is the presence of nano- to micrometer-scale particles of Pt-, Pd-, and Au-rich phases embedded in or attached to sulfide melts. These particles represent metallic alloys, sulfides, or intermetallic compounds that occur both within the sulfide matrix and on the surfaces of globules. Their presence indicates that noble metals may exist in magmas as discrete nanoparticles prior to or during sulfide segregation. Growing sulfide droplets can therefore concentrate noble metals not only through diffusive partitioning from silicate melt but also through physical capture of pre-existing metal-rich particles.

Our studies of sulfide inclusions from oceanic picrites and arc basalts reveal that primitive sulfide liquids undergo significant compositional evolution during cooling and crystallization. Immiscible sulfide melts commonly crystallize into assemblages of monosulfide and intermediate solid solutions, followed by crystallization/ exsolution of phases such as pentlandite, chalcopyrite, and pyrrhotite. These processes produce strong fractionation of Ni, Cu, and noble metals between coexisting sulfide phases and explain the complex metal distributions observed in natural magmatic sulfide systems.

Finally, the study of sulfide melt inclusions entrapped in primitive olivine phenocrysts provides a rare glimpse into the earliest stages of magmatic sulfide mineralization before later magmatic and hydrothermal processes overprint magmatic signatures. Our observations provide direct constraints on the composition of primitive sulfide melts and the mechanisms by which mantle-derived magmas concentrate economically critical metals.

Key words Sulfide, immiscibility, magma, fractionation, mineralization

STRUCTURAL AND CHEMICAL DIVERSITY OF THE AVERIEVITE FAMILY, (MX)$Cu_5O_2(TO_4)_2$ (M = K, RB, CS; X = CL, BR, I; T = P, AS, V)

Ilya V. Kornyakov, Sergey V. Krivovichev

Department of crystallography, St. Petersburg State University, Russia

Abstract One of the most interesting and diverse mineralogical objects of our time is the fumarolic fields of Tolbachik volcano, Kamchatka, Russia. Between 1976, the time of the Great Fissure Tolbachik Eruption, and 2020, investigations of fumarolic formations led to the discovery of more than 120 new mineral species. From all minerals known from this locality at 2020, more than half are Cu^{2+}-bearing, and 15 additional new minerals have been discovered since. One of the minerals first found in the Tolbachik fumaroles is averievite, $Cu_5O_2(VO_4)_2 \cdot n MCl_x$ (M = Cu, Cs, Rb, K). Its structure is based on pyrochlore-like $[O_2Cu_5]$ layers composed of anion-centered OCu_4 tetrahedra. Vanadate tetrahedra are attached to these tetrahedra in a 'face-to-face' manner, while the channels of the resulting $[Cu_5O_2(VO_4)_2]$ framework are occupied by halide anions (in the plane of the kagomé lattice of Cu^{2+} cations) and alkali cations (between the $[O_2Cu_5]$ layers). Owing to this unique structure, the physical properties of this mineral have attracted considerable interest. Since 2018, ten papers devoted to the crystal chemistry and magnetic properties of compounds belonging to the averievite family have been published, nine of which concern with phosphates and vanadates with different M cations and X anions. At present, six main polymorphs of averievite-type structures are known: (i) $P\bar{3}m1$ aristotype with $a_0 = b_0$, and c_0, (ii) $P321$ with $a_0 = b_0$, and c_0, (iii) $P\bar{3}$ with $a = b \approx 2a_0$, and $c = c_0$, (iv) $C2/c$ with $a \approx \sqrt{3}a_0$, $b = b_0$, $c \approx 2c_0$, and $\beta \approx 95°$, (v) $I2/a$ with $a \approx \sqrt{3}a_0$, $b = b_0$, $c \approx 2c_0$, and $\beta \approx 90.6°$, and (vi) $P2_1/c$ with $a = c_0$, $b = a_0$, $c \approx \sqrt{3}a_0$, and $\beta \approx 90°$. In addition, we have recently identified two other polymorphs: (vii) $P31m$ (or $P\bar{3}$) with $a = b \approx \sqrt{3}a_0$, and $c = c_0$, and (viii) an incommensurately modulated $X2/c(\alpha 0 \gamma)00$ phase with $a \approx \sqrt{3}a_0$, $b = b_0$, $c \approx 2c_0$, and $\beta \approx 92°$. Whereas some polymorphs have so far been observed only once (polymorphs iii, v, vi, and viii), others are more frequent. Polymorphs iii, vi, and vii are characteristic only for vanadates; polymorphs v and viii are found only in arsenates, whereas among phosphates only one unique polymorph, namely ii, is known. The aristotype structure occurs in all chemical classes and undergoes a structural transition upon cooling, while polymorph iv is common to phosphates and arsenates only. Such a diverse polymorphism is caused primarily by the chemical interplay among the M, X, and T sites. However, some questions still remain unresolved. For example, polymorph vi was proposed on the basis of powder X-ray diffraction data and has not yet been experimentally confirmed by single-crystal X-ray diffraction. In addition, some phase transitions remain unclear, although they have been observed by X-ray diffraction. It is also worth noting the possibility of substitution of Cu^{2+} by Zn^{2+}, which drastically changes the crystal chemistry and

physical properties of averievite-family compounds. Such crystal-chemical diversity, even if observed under laboratory conditions, raises the question of whether other averievite-family minerals may also exist in nature. Indeed, compounds containing KCl and $Cu^{+}Cl$ have already been studied for the phosphate members of the averievite family. At the same time, arsenates are among the most common compounds in the fumaroles of Tolbachik volcano, while the possibility of Cu-Zn substitution further expands the crystal-chemical diversity of these systems. Given the chemical diversity of minerals found in the fumaroles of Tolbachik volcano, it seems highly likely that the discovery of new averievite-family minerals is only a matter of time.

Key words crystal chemistry, crystal structure, phase transitions, divalent copper, averievite

Acknowledgements This work was supported by Russian Science Foundation, grant 24-17-00083.

SULFATE MINERALOGY OF THE TOLBACHIK VOLCANO FUMAROLES: BRIDGING GEOSCIENCES AND MATERIALS SCIENCE

Oleg I. Siidra

Department Crystallography, Institute of Geosciences, Saint-Petersburg State University, Russia

Abstract The fumaroles of the Tolbachik volcano in Kamchatka, Russia, constitute a globally unique high-temperature natural laboratory. To date, these fumaroles have yielded more than 150 new mineral species, with a predominance of exotic sulfates. This remarkable mineralogical diversity arises from the interaction between volcanic gases and basaltic host rocks, which produces an exceptionally complex and variable mineral environment. Notably, many of these minerals exhibit crystal structures that have no precedent among synthetic compounds, thereby bridging the fields of mineralogy and materials design. Moreover, knowledge of the sequential crystallization pathways of minerals in fumaroles, as well as of the mineral associations formed during their coeval growth, allows us to significantly reduce the number of synthesis attempts and to obtain pure single-phase products for property studies.

Due to the natural conditions of slow crystallization from gas and/or fluids within the fumaroles, the resulting anhydrous sulfate mineral crystals are often sufficiently large to allow detailed determination of their structural features. Systematic study has revealed that the stoichiometries of anhydrous sulfates of divalent transition metals and alkali metals fall into only three families: (i) the saranchinaite family, $A_2^+M^{2+}(SO_4)_2$; (ii) the itelmenite family, $A_2^+M_3^{2+}(SO_4)_4$; and (iii) the langbeinite family, $A_2^+M_2^{2+}(SO_4)_3$. The first two large sulfate families were completely unknown in inorganic chemistry prior to our discovery of saranchinaite and itelmenite a decade ago. These compositional and structural characteristics have served as the primary motivation for our extensive synthetic efforts directed toward producing analogs of such minerals. Beyond the aforementioned families, our synthetic investigations into sulfates have enabled the preparation of a large number of mineral-like oxosulfate phases (e.g., Na–Cs solid solutions of the puninite series).

In addition, detailed knowledge of fumarolic mineralogy has found several other applications in inorganic chemistry. One illustrative example is the elucidation of the highly complex sequence of transformations and thermal evolution of the well-known copper Tutton's salts—compounds that have been studied for more than a century. Furthermore, rare examples of crystal-to-crystal topotactic transitions have been investigated using both mineral and synthetic samples of anhydrous sulfates.

All of the examples described above, together with numerous other recent experimental findings on fumarolic sulfate mineralization and their applications across various scientific disciplines, will be presented herein.

Key words Mineralogy, fumaroles, sulfates, Tolbachik volcano, materials science

Acknowledgements This work was financially supported by the Russian Science Foundation through the grant 25-17-00157.

THE EVOLUTION OF AN ACTIVE VOLCANIC SYSTEM: INSIGHTS FROM TEXTURES OF BASALTIC SCORIA AND ISOTOPIC SIGNATURES OF FUMAROLIC MINERALS OF THE TOLBACHIK VOLCANO

Astrid Holzheid[1], Artem S. Borisov[1], Oleg I. Siidra[2], Kun Wang[3], Harald Strauss[4]

1. Institute of Geosciences, Kiel University, Germany

2. Department of Crystallography, St. Petersburg State University, Russia

3. Department of Earth, Environmental, Planetary Sciences, Washington University in St. Louis, USA

4. Institute of Geology and Paleontology, University of Muenster, Germany

Abstract The Great Tolbachik Fissure Eruption (GTFE) in Kamchatka, Russia, features fumaroles that serve as a distinctive natural laboratory for studying mineral evolution and unraveling the processes behind their formation. The mineral assemblages found in the Yadovitaya fumarole were examined using a variety of techniques to provide a comprehensive description of the fumarole. This study specifically highlights insights obtained from high-resolution X-ray computed tomography (CT) of the basaltic scoria and isotope measurements (^{34}S, ^{18}O, ^{65}Cu) of fumarolic minerals.

The textural features obtained by CT reveal clear similarities to the original hand specimens, particularly in the large amount of precipitate covering the scoria fragments' surfaces. The transition between the scoria fragments and the precipitate is especially evident along the edges of larger scoria fragments, suggesting sharp boundaries and limited alteration of the scoria. In contrast, smaller fragments exhibit more diffuse boundaries, possibly reflecting enhanced alteration. The spongy surface texture of the scoria fragments likely promotes the nucleation and crystallization of exhalation minerals. Regarding pore densities, larger scoria fragments often display zonation, with higher pore densities in their cores and lower densities toward the surfaces. Smaller scoria fragments, on the contrary, show little to no identifiable pores and appear as clasts embedded in a matrix of high-density phases (primarily different copper sulfates). The presence of micropores and visible channel systems suggests that these microstructures may have acted as microreactors, aiding the crystallization of diverse mineral species.

Unlike previous studies of Tolbachik fumaroles, the isotopic compositions of individual mineral phases from anhydrous sulfates, oxysulfates, and hydrated sulfates from the Yadovitaya fumarole were investigated. Two overlapping groups were examined: (i) Cu-free and Cu-containing species, and (ii) sulfates with and without an additional oxygen atom. For comparison, native sulfur from the Mutnovsky volcano (Kamchatka) and La Fossa crater (Vulcano Island, Sicily), as well as an arsenate from the Arsenatnaya fumarole (GTFE), were used as reference phases. The positive $\delta^{34}S_{VCDT}$ values in Cu-containing sulfates range from 1 to 4 ‰, suggesting that most sulfate sulfur originates from steam-heated environments (oxidation of H_2S) and, to a lesser degree, from magmatic-hydrothermal sources

(disproportionation of SO_2). The differences in oxygen isotopes between sulfates and oxysulfates, with higher $\delta^{18}O$ values in exhalative oxysulfate minerals, point to the significant influence of atmospheric oxygen in the formation of these minerals. An empirical correlation between increased $\delta^{65}Cu$ and Cu:O ratios in fumarolic copper oxysalts indicates a greater role for the ^{65}Cu isotope in oxidation processes. The lack of significant differences in $\delta^{65}Cu$ between sulfates and oxysulfates suggests that $\delta^{18}O$ fractionation plays a more substantial role than $\delta^{65}Cu$ fractionation in the formation of the oxysulfates.

Together, these findings, along with the observed mineral assemblages, the migration, and concentration of individual elements in fumarolic minerals, helped to outline the spatial evolution of the mineral assemblages in the Yadovitaya fumarole that vary in complexity, chemistry, and their interactions with the surrounding environment.

Key words Tolbachik volcano, Yadovitaya fumarole, Basaltic scoria, Isotopic signatures

A HISTORICAL CU-SULFATE FUMAROLIC ASSEMBLAGE FROM THE 1872 ERUPTION OF VESUVIUS COLLECTED BY ARCANGELO SCACCHI

Ningyue Sun[1,3], Manuela Rossi[2], Fabrizio Nestola[1*]

1. Department of Geosciences, University of Padua, 35131 Padua, Italy

2. Department of Earth Sciences, Environment and Resources, University of Naples Federico II, 80126 Naples, Italy

3. Research Institute, China University of Geosciences, 100083 Beijing, China

Abstract Vesuvius is one of the most important European localities for fumarolic minerals. During its active period from 1631 to 1944, abundant fumarolic products formed, and the 1872 eruption was among the most intense events. Since 1944, fumarolic activity has markedly declined, and many sublimates and related alteration assemblages formed during historical eruptions can no longer be sampled from modern outcrops. Historical museum specimens with well-documented provenance therefore represent important mineralogical archives for reconstructing past fumarolic processes.

Here we investigate a historical Vesuvian specimen collected after the 1872 eruption by Arcangelo Scacchi, then director of the Royal Mineralogical Museum of Naples, University Federico II. The sample was sealed in a glass tube immediately after collection, limiting prolonged interaction with the atmosphere. It consists of green and brown fine-grained crystals coating a basaltic rock fragment. The tube was recently opened, and the sample was studied by X-ray diffraction and scanning electron microscopy. The results reveal a sulfate-dominated fumarolic assemblage including the anhydrous phases euchlorine, $KNaCu_3(SO_4)_3O$, dolerophanite, $Cu_2(SO_4)O$, chalcocyanite, $CuSO_4$, anhydrite, $CaSO_4$, and anglesite, $PbSO_4$, together with the hydrated sulfates chalcanthite, $Cu(SO_4)(H_2O)_4 \cdot H_2O$, and cyanochroite, $K_2Cu(SO_4)_2 \cdot (H_2O)_6$. Hematite, Fe_2O_3, and corundum, Al_2O_3, were also identified.

These minerals record a complex formation and evolution history. During single-crystal X-ray refinement of euchlorine, we identified a previously unrecognized structural site with an electron density of ~ 7 e $Å^{-3}$. Its coordination resembles zeolite-type molecular-water positions, suggesting that the structure may have retained a minor volatile component even under fumarolic conditions. Corundum also shows an unusual nanocrystalline pseudomorphic texture, possibly indicating a volatile-rich precursor phase later transformed into corundum. Chalcanthite and cyanochroite are more likely related to hydration after exposure to air. This is especially clear for chalcanthite, which rapidly forms by alteration of chalcocyanite after the tube was opened. More broadly, this assemblage is comparable to sulfate-rich fumarolic associations described from Tolbachik, where mineral diversity reflects coupled effects of oxygen fugacity, gas-rock interaction, temperature gradients, and atmospheric water; comparable

assemblages may develop at about 150–200 ℃.

This study shows that a historically documented Vesuvian specimen can preserve mineralogical, volcanological, and historical significance simultaneously. It provides direct evidence for Cu-rich fumarolic assemblages at nineteenth-century Vesuvius and demonstrates that historical museum collections are scientific archives capable of yielding new insights through modern analytical study.

Key words Vesuvius, fumarolic minerals, historical specimen, Cu sulfates, Arcangelo Scacchi

THE YADOVITAYA FUMAROLE (TOLBACHIK VOLCANO): FROM MINERALOGY AND GEOCHEMISTRY TOWARD DRIVING FACTORS OF MINERAL DIVERSITY

Artem S. Borisov[1], Oleg I. Siidra[2], Natalia S. Vlasenko[2], Astrid Holzheid[1], Natalia V. Platonova[2]

1. Kiel University, Germany

2. St. Petersburg State University, Russia

Abstract Active volcanic fumaroles are among the most spectacular natural objects in terms of mineral diversity. The Great Tolbachik Fissure Eruption (GTFE, Kamchatka) fumaroles host an exceptional number of mineral species, with over 400 minerals reliably identified – approximately 6.5% of all known minerals to date. Among the GTFE fumaroles, special attention is drawn to the Yadovitaya fumarole, which exhibits rich exhalative and secondary sulfate mineralization. We performed a comprehensive study of the mineral assemblages of the Yadovitaya fumarole using a wide range of techniques including bulk chemistry, microprobe analysis and powder X-ray diffraction. Tomographic investigations of the basaltic scoria as a matrix for the crystallization and recrystallization of fumarolic minerals were carried out, as well as isotopic studies of $\delta^{34}S$, $\delta^{18}O$ and $\delta^{65}Cu$ in fumarolic minerals (these results are presented in a separate contribution). The comprehensive set of mineralogical and geochemical studies carried out allowed us to identify patterns of mineral formation, characterize element distribution trends, and generalize the key factors responsible for the unique mineral diversity.

This contribution presents part of the work devoted to the mineralogical and geochemical study of the mineral assemblages of the Yadovitaya fumarole. We present the first systematic description of this fumarole, which exhibits zonation in the succession of mineral assemblages in the following generalized sequence: (1) high-temperature anhydrous Cu-free sulfates → (2) anhydrous Cu sulfates → (3) Cu-sulfate hydrated offsprings → (4) Ca-sulfate- and fluoride-rich (sub)surface mineralization. For all zones of the fumarole, the chemical and morphological characteristics of primary exhalative and secondary hydrated mineralization of basaltic scoria fragments composing the fumarole were studied. Basaltic scoria pieces have a highly spongy surface that encourages the nucleation and crystallization of exhalation minerals. The zonation of mineralization of the Yadovitaya fumarole is associated with the gradual distribution of a number of key mineral-forming elements, primarily S, Cu, Pb, Zn, As, as well as trace elements, with the most pronounced patterns shown by Rb and Cs. Our results highlight several key factors on fumarolic mineral formation: high oxygen fugacity, interaction of minerals with atmospheric oxygen and seasonal precipitation (producing abundant hydrated phases), temperature gradients influencing spatial distribution of mineral-forming components, gas-rock interactions, and the morphology of basaltic

scoria providing ideal conditions for crystallization.

Key words Mineral diversity, Volcanic fumaroles, Tolbachik volcano, Sulfates, Mineral evolution

ADSORPTION AND ACTIVATION OF O_2 AT FE-BEARING MONTMORILLONITE SURFACES: A FIRST-PRINCIPLES MOLECULAR DYNAMICS STUDY

Ziheng Zhang, Chi Zhang*

College of Natural Resources, Northwest Agriculture & Forestry University, China

Abstract Understanding the activation of molecular oxygen (O_2) at clay mineral interfaces is critical for elucidating redox processes in natural environments. Here, we employ first-principles molecular dynamics (FPMD) simulations to investigate O_2 adsorption and activation at Fe-bearing montmorillonite – water interfaces, with a focus on the facet- and site-specific reactivity of different surface terminations. Multiple representative surfaces and cationic sites, including Al-, Mg-, and Fe^{2+}-dominated environments, are systematically examined to evaluate their respective affinities toward O_2. Our results demonstrate that O_2 exhibits negligible adsorption at Al and Mg sites, whereas Fe^{2+} sites serve as the exclusive active centers for effective O_2 binding. At these sites, O_2 forms a stable inner-sphere bidentate complex via coordination with surface Fe^{2+}, and the adsorption process is thermodynamically spontaneous. Importantly, O_2 adsorption is intrinsically coupled with interfacial electron transfer: upon binding to Fe^{2+}, O_2 undergoes one-electron reduction to generate superoxide. The resulting superoxide species can remain coordinated to Fe^{2+} and further participate in subsequent reduction steps, leading to the formation of peroxide species or hydrogen peroxide.These findings reveal a clear site-specific mechanism for O_2 activation at Fe-bearing clay mineral surfaces and highlight the pivotal role of Fe^{2+} in mediating coupled adsorption-reduction processes. This work provides molecular-level insights into oxygen activation pathways at mineral/water interfaces, with important implications for understanding reactive oxygen species formation and redox transformations in soil and geochemical systems.

Key words Molecular Oxygen Activation, Fe-bearing Montmorillonite, Reactive Oxygen Species, Dynamic Reaction Mechanism, FPMD

ADSORPTION OF MOLYBDENUM ON GOETHITE SURFACE: A FIRST-PRINCIPLES MOLECULAR DYNAMICS SIMULATION

Mengjia He[1], Xiancai Lu[2*]

1. School of Environmental and Biological Engineering, Nanjing University of Science and Technology, Nanjing 210094, P. R. China

2. State Key Laboratory of Critical Earth Material Cycling and Mineral Deposits, School of Earth Sciences and Engineering, Nanjing University, Nanjing, Jiangsu 210023, P. R. China

Abstract Understanding the interfacial behavior of molybdate on iron oxides is essential for constraining the geochemical behavior of Mo in natural environments and for elucidating its geochemical cycle in comparison to tungsten (W), which exhibits similar chemical properties. However, the molecular-scale structures and thermodynamic stabilities of Mo complexes on iron oxides remain poorly resolved. In this work, we investigate the adsorption mechanism of monomeric molybdate on the goethite (110) surface by using first principles molecular dynamics (FPMD) method. Considering molybdate (MoO_4^{2-}) and its possible protonation states ($HMoO_4^-$ and $H_2MoO_4^0$), as well as their different coordination environments, free FPMD results show that bidentate corner-sharing complexes remain stable for all species while protonated species spontaneously deprotonate during the simulations. These results indicate that deprotonated states are common under environmentally relevant pH conditions, while protonated species are thermodynamically unstable and undergo spontaneous deprotonation. The free-energy profiles show that 4-coordinated bidentate Mo complexes are thermodynamically favored over 5-coordinated bidentate, monodentate, and outer-sphere species. Comparison with our previous study of W adsorption on goethite shows that, although Mo and W display comparable desorption free energies, W more readily forms 5-coordinate structures whereas Mo prefers 4-coordinate binding, implying that W may more easily incorporate into iron oxide lattices. These findings provide molecular-level insight into Mo–iron oxide interactions and contribute to a mechanistic understanding of Mo and W mobility in natural environments.

Key words Molybdate, Goethite, Surface complexation, First-principles molecular dynamics, Potentials of mean force

AN ACCURATE AND EFFICIENT FRAMEWORK FOR MODELLING MULTI-METAL COMPETITIVE ADSORPTION ON CLAY MINERALS

Pengyuan Gao [1,2], Xiandong Liu [1,2], Xiancai Lu [1,2], Christophe Tournassat [3,4]

1. State Key Laboratory of Critical Earth Material Cycling and Mineral Deposits, School of Earth Sciences and Engineering, Nanjing University, P. R. China

2. Frontiers Science Center for Critical Earth Material Cycling, Nanjing University, P. R. China

3. Institut des Sciences de la Terre d'Orléans, Université d'Orléans, CNRS, BRGM, OSUC, France

4. Energy Geosciences Division, Lawrence Berkeley National Laboratory, USA

Abstract Multiple toxic metal elements usually coexist and thus their competitive adsorption always occur in natural and engineered clay-rich systems. Currently, however, the competitive adsorption mechanisms of multicomponent metal systems on clay mineral surfaces are still unclear, hindering the accurate prediction of toxic metal distribution in soil-water environments. In this study, we uncovered the microscopic mechanism of competitive adsorption of multi-metals on heterogeneous clay mineral surfaces using first principles calculation, which indicates that metal ion size largely dominates their complexation on clay mineral surfaces, and competitive adsorption of metals plays a key modulatory role in the adsorption process on clay minerals. By integrating theoretically and experimentally derived multi-scale information, a state-of-the-art surface complexation model (SCM) framework has been developed for modeling competitive adsorption. Extensive tests showed that the new SCM framework accurately and efficiently reproduces the toxic metal distribution, which enables the quantitative prediction and understanding in realistic environmental conditions. Our results have wide applications in future fundamental studies and the design of environmental materials for toxic metal removal from aquatic systems.

Key words competitive adsorption, multiscale modeling, metals, clay

CONSTRAINING THE PHYSICAL STATE OF THE TERRESTRIAL MAGMA OCEAN VIA MACHINE LEARNING FORCE FIELD

Yicheng Sun[1*], Kai Wang[2*], Xiancai Lu[2]

1. College of Oceanography, Hohai University, China.

2. School of Earth Sciences and Engineering, Nanjing University, China.

Abstract Geochemical evidence suggests that the early Earth underwent multiple global-scale melting events, which not only facilitated the formation of the nascent crust but also drove the chemical differentiation between the metallic core and the silicate mantle. During this evolutionary process, silicate melts served as the primary carriers for mass and energy transport, with their transport properties and thermodynamic parameters deeply governing the chemical and thermal evolution paths of the magma ocean. Specifically, melt viscosity directly influences the chemical equilibration between the descending metallic phases and the surrounding silicate melt following giant impacts, while significantly modulating the cooling rate of the magma ocean. Concurrently, the interplay between the melt's adiabatic temperature profile and the mantle liquidus dictates the crystallization sequence of the magma ocean. In this study, we employed first-principles-based machine learning force fields to calculate the thermodynamic properties and viscosities of multi-component silicate melts, subsequently constructing a comprehensive viscosity model for the terrestrial magma ocean. Based on our findings, we calculated the adiabatic temperature and viscosity profiles within the magma ocean, providing new insights into the physical state and evolutionary trajectory of the early Earth.

Key words Magma ocean, Thermodynamic properties, Viscosity, First principles, Machine learning

DEVELOPMENT OF A GENERAL-PURPOSE REAXFF REACTIVE FORCE FIELD FOR MINERAL SYSTEMS VIA MACHINE LEARNING ACCELERATION

Yingchun Zhang[1,2], Xiandong Liu[1], Adri van Duin[2], Xiancai Lu[1], and Evert Jan Meijer[3]

1. State Key Laboratory of Critical Earth Material Cycling and Mineral Deposits, School of Earth Sciences and Engineering, Nanjing University, Nanjing, Jiangsu 210023, P. R. China

2. Department of Mechanical Engineering, The Pennsylvania State University, University Park, PA, 16802, USA

3. Van't Hoff Institute for Molecular Sciences, University of Amsterdam, Amsterdam 1012 WX, The Netherlands

Abstract Over the past two decades, the ReaxFF reactive force field has established itself as a vital link between traditional non-reactive molecular dynamics and high-fidelity quantum mechanical calculations. However, its application to complex mineral systems, such as interfaces, multi-component phases, and extreme high-P-T conditions, remains constrained by a shortage of reliable parameters. In this study, we present the development and validation of a ReaxFF force field covering essential crustal elements, i.e., Si/Al/Mg/Fe/Na/K/Ca/C/O/H, parameterized through a novel machine-learning (ML) accelerated optimization framework. This approach enables efficient training against an extensive DFT-derived database, including charges, bond/angle distortion curves, equation of states, ion migration energy profiles, and condensation reaction energies. The resulting force field demonstrates high fidelity in reproducing the reference quantum mechanical data. Its predictive power was further demonstrated through applications to mineral-water interfaces, hydrous melts, supercritical geofluids, and bulk crystals, where it accurately captured structural, thermodynamic, and transport properties. The ML-optimized force field holds good promise to model complex geochemical processes, significantly expanding the utility of ReaxFF in the mineralogical sciences.

Key words ReaxFF, Machine learning optimization, Mineral systems, Reactive molecular dynamics

ELUCIDATING ZEOLITE NUCLEATION BY MOLECULAR SIMULATION

Johan Bergsma, Gadi Rothenberg, Evert-Jan Meijer

Van 't Hoff Institute for Molecular Sciences, University of Amsterdam, The Netherlands

Abstract Zeolites are an important class of crystalline aluminosilicate minerals bearing a nonoporous structure. They are commonly sythesized starting from an aqueous solution of ortho-silicate monomers in the presence of anionic structure directing agents (SDAs) A fundamental understanding of the full crystallization process is still lacking. Employing both atomistic and coarse grained models we address the early stages of zeolite crystallization by molecular simulation. Using all-atom first principle molecular dynamics simulation we elucidate the mechanism and energetics of various silicate oligomerization reaction pathways, also addressing the effect of SDAs. This reveals how formation of specific oligomers are kineticly and/or thermodynamically favored, and how this balance among the oligomer types is affected by the presence of SDAs. To assess the phase beyond the oligomerization stage, we designed a coarse grained model that is employed to model the early stage of crystal nucleation. Initial results appear to reveal how the size and shape of the SDAs can direct the formation of crystallites with specific pore structures, that are identified to be very similar to specific zeolite frameworks, including LTA and AST, and may well be the seeds for the crystallization pathways of these zeolite frameworks.

Key words Zeolites, Nucleation, Molecular Dynamics, DFT, Coarse Graining

FATE OF PRIMORDIAL NOBLE GASES DURING CORE-MANTLE DIFFERENTIATION FROM AB INITIO SIMULATIONS

Yajie Zhao[1], Tianhua Wang[2], Bowen Chen[1], Razvan Caracas[2], Wenzhong Wang[1], Zhongqing Wu[1]

1. School of Earth and Space Sciences, University of Science and Technology of China, Hefei, China

2. Université Paris Cité, Institut de Physique du Globe de Paris, CNRS, Paris, France

Abstract Early planetary accretion and giant impacts likely generated a global magma ocean on the proto-Earth, enabling extensive dissolution of primordial volatiles from the solar nebula into silicate melts. During subsequent core-mantle differentiation, the partitioning of noble gases between pyrolitic silicate melts and iron (Fe with light elements) melts would have controlled their redistribution and long-term preservation in Earth's deep interior. The contrasting noble gas signatures observed in mid-ocean ridge basalts and mantle plume sources, particularly in He/Ne ratios, motivated the existence of a deep primitive reservoir potentially linked to early core-mantle differentiation. Here, we use ab initio molecular dynamics simulations combined with thermodynamic integration to quantify the partition coefficients of He, Ne, Ar, Kr, and Xe between pyrolitic silicate melts and Fe-S melts. We further assess the effects of melt composition by comparing pyrolite with MgSiO3 melts and Fe-S with metallic iron melts. Our results reveal systematic variations in noble gas partitioning with atomic size and melt chemistry. Based on these partitioning coefficients, we estimate the potential noble gas inventories preserved in the mantle and core. These results provide new quantitative constraints on the fate of primordial noble gases and the origin of deep-mantle volatile reservoirs.

Key words Noble gas, pyrolite, iron, thermal integration, partition coefficient

FORMATION OF CALCIUM SILICATE PEROVSKITE ABOVE THE CORE-MANTLE BOUNDARY DURING SOLIDIFICATION OF EARTH'S MAGMA OCEAN

Tianhua Wang[1], James Badro[1], Razvan Caracas[1,2], Héloïse Gendre[1], Cécile Hébert[3]

1. Université Paris Cité, Institut de Physique du Globe de Paris, CNRS, Paris, France.

2. Center for Planetary Habitability, University of Oslo, Oslo, Norway.

3. LSME, École Polytechnique Fédérale de Lausanne, Lausanne, Switzerland.

Abstract Calcium silicate perovskite (CaPv) is the host for many large ion lithophile elements including the heat-producing elements in the lower mantle. Whether, when, and where it forms during the solidification of the magma ocean is fundamental to understanding the geochemical and geodynamical evolution of the early Earth and the trace element distribution in the lower mantle. In this study, we performed first-principles molecular dynamics simulations to investigate the partitioning behavior of Ca (alongside other alkali-earth elements, Sr and Ba) between bridgmanite and molten pyrolite. Our results show that the bridgmanite-melt partition coefficient of Ca remains smaller than 1 along the liquidus across the lower mantle, and decreases further between the magma ocean liquidus and solidus, indicating that Ca is incompatible in bridgmanite at all relevant crystallization conditions in the lower mantle. This results in a progressive enrichment of Ca in the magma ocean as it solidifies, leading unavoidably to the crystallization of CaPv during the final stages of solidification in the deep mantle. Laser-heated diamond anvil cell experiments performed to replicate the crystallization of pyrolitic melt in the same conditions as our simulations confirm the crystallization of CaPv in the last stages of solidification. From Ca to Sr to Ba, the bridgmanite-melt partition coefficients decrease by orders of magnitude, indicating a significant enrichment of these large ion lithophile trace elements in the residual melt. Combined with previous experimental studies at lower P-T conditions, our findings infer that both large ion lithophile elements and their host, CaPv, will be concentrated in the deep mantle at the end of magma ocean solidification.

Key words Element partitioning, magma ocean, bridgmanite, deep mantle, first-principles molecular dynamics (FPMD)

GROWTH RATE-DEPENDENT LITHIUM ISOTOPE FRACTIONATION DERIVED FROM MACHINE LEARNING-ENABLED MOLECULAR SIMULATION

Qin Li, Xiancai Lu, Kai Wang, Xiandong Liu, Rucheng Wang

State Key Laboratory of Critical Earth Material Cycling and Mineral Deposits, School of Earth Sciences and Engineering, Nanjing University, Nanjing Jiangsu 210023, China

Abstract Lithium (Li) isotopes have emerged as a promising tracer for various geological processes and clay minerals serve as key Li carriers in Earth surface systems, but the underlying mechanism driving Li isotope fractionation remains poorly understood. Based on a deep potential (DP) trained with density functional theory (DFT) data, path integral molecular dynamic (PIMD) simulations reveal the equilibrium and kinetic Li fractionation factors of -11.5‰ and -23.5‰ during clay precipitation, respectively. Further modeling indicates that high clay growth rate intensifies Li isotope fractionation, which can be well described by the surface kinetic model. The unified mechanistic framework involving equilibrium and kinetic fractionation not only elucidates the intrinsic Li isotopic fractionation factors and pH dependencies observed in both natural and experimental contexts, but also highlights the critical roles of reactive kinetic fractionation during rapid clay precipitation, such as estuarine and hydrothermal systems.

Key words Li isotope fractionation, clay mineral, molecular simulation, deep potential

LINKING KINETIC PARTITIONING AND COORDINATION CHEMISTRY OF SR^{2+} IN CALCITE

Kideok D. Kwon

Department of Geology, Kangwon National University, Chuncheon 24341, Republic of Korea

Abstract The partition coefficient of Sr^{2+} in calcite ($CaCO_3$) is a key input parameter of surface reaction kinetic models (SRKM), a widely used framework for growth rate-dependent trace element partitioning. The equilibrium partition coefficient (D_{eq}), which defines the reference state in SRKM, remains poorly constrained. Here, we constrained D_{eq} using density functional theory (DFT) with the SCAN functional, yielding 0.01 at 25°C, near the lower bound of reported values. Incorporating this DFT-predicted D_{eq} into the SRKM successfully captured the experimentally observed rate-dependent partitioning behavior. To understand the structural basis of this partitioning behavior, an ensemble DFT approach was applied, revealing that seven-fold coordinated Sr^{2+} in calcite is thermodynamically favorable over six-fold states at elevated Sr concentrations. This heterogeneous coordination chemistry is further validated by comparison of DFT-calculated Sr *K*-edge XANES spectra for $Ca_{1-x}Sr_xCO_3$ and experimental spectra. These results demonstrate that calcite precipitation rate governs Sr^{2+} coordination state, providing a direct mechanistic link between growth rate, coordination chemistry, and partitioning behavior. This work enables mechanism-based parameterization of Sr coprecipitation in large-scale geochemical models, with implications for paleoclimate reconstruction and radioactive waste management.

Key words Strontium, calcite, density functional theory, SRKM, XANES, equilibrium partition coefficients

MINING-ENVIRONMENT COUPLING KNOWLEDGE GRAPH AND MULTI-SCALE DIGITAL PLATFORM

Liang Bian

School of Environment and Resource, Southwest University of Science and Technology, Mianyang, Sichuan, 621010

Abstract In response to the digital transformation of mineralogy and the need for coordinated governance between the mining industry and the environment, this project aims to construct a mineral-environment coupled knowledge graph and a multi-scale digital platform to address the bottlenecks in China's foundational mineral databases, as well as the digital challenges related to mine environments, geological hazards, and resource utilization. Building on the trend of mineralogy evolving from the macro- to the micro-scale and advancing toward computational and big data stages, this project addresses the current situation where China's mineral databases and analytical technologies have long lagged behind and core data relies on foreign sources. By integrating multi-scale simulation, machine learning, and remote sensing IoT technologies, we will establish a database on mineral structural evolution that synergizes experimental and theoretical approaches, develop a new geospatial-aerial mineral spectroscopy system, and ensure the security of deep-space exploration data. The platform covers three core application scenarios: environmental pollution, geological exploration hazards, and mineral processing. In the environmental sector, it enables ecological IoT monitoring in Xinjiang, remote sensing assessment of tailings pollution, and inversion of uranium and heavy metal migration; In the geological exploration and disaster mitigation sector, we have developed deep learning-constrained geophysical detection, intelligent noise reduction for seismic acoustic emission, and real-time flood forecasting systems for mountainous regions; in the mineral processing sector, we have completed big data optimization for the leaching of tellurium-bismuth ores and the performance of basalt fibers, supporting digital mining in smart mines. The team has independently developed multiple software solutions and non-destructive testing equipment, including an atmospheric mineral particulate database and the Sichuan Province Tailings Resource Platform. It has obtained numerous patents and software copyrights, with its achievements applied in fields such as mine ecological restoration, strategic mineral development, and aerospace inspection. These innovations provide end-to-end digital technical support for green and low-carbon mining, geological safety assurance, and efficient resource utilization.

Key words Computational Mineralogy, Multiscale Simulation and Machine Learning

MOLECULAR DYNAMICS STUDY ON THE CURLING MECHANISM OF HALLOYSITE NANOTUBES

Xin Liu, Yueyu Yu, Jiaxin Hou, Guocheng Lv*, Libing Liao

Engineering Research Center of Ministry of Education for Geological Carbon Storage and Low Carbon Utilization of Resources, Beijing Key Laboratory of Materials Utilization of Nonmetallic Minerals and Solid Wastes, National Laboratory of Mineral Materials, Hebei Key Laboratory of Resource Low-carbon Utilization and New Materials, School of Materials Science and Technology, China University of Geosciences, Beijing, 100083, China

Abstract Halloysite nanotubes (HNTs) exhibit significant application value in multiple fields owing to their unique one-dimensional hollow tubular structure. It has been suggested that natural HNTs are formed by the curling of kaolinite layers. Moreover, HNT-like structures have been successfully prepared through intercalation-exfoliation treatment of kaolinite. Although theoretical models based on tetrahedral–octahedral dimensional mismatch and tetrahedral rotation and bending partially explain the curling mechanism of HNTs, they struggle to account for key issues such as the orientation of the curling axis, and conventional experimental methods also face clear limitations in this regard. In this study, by constructing near-real-scale kaolinite layer models (100 nm × 100 nm) and employing large-scale molecular dynamics simulations, the dynamic curling behavior of kaolinite layers was investigated. Through quantitative analyses of structural parameters including bond lengths, bond angles, polyhedral volumes, and distortions, the curling mechanism of HNTs was explored in depth. The results show that: (1) the average volume of SiO_4 tetrahedra and the average area of six-membered silicate rings increase, indicating expansion of the tetrahedral (siloxane) sheet; (2) the average volume of AlO_6 octahedra and the average area of six-membered aluminate rings decrease, indicating contraction of the octahedral sheet; (3) the tetrahedral sheet is stretched both parallel and perpendicular to the curling axis, whereas the octahedral sheet is stretched parallel to the curling axis but contracted perpendicular to it. These findings directly support the classical tetrahedral–octahedral dimensional mismatch theory and suggest that anisotropic contraction of the octahedral sheet may be a key factor driving the curling of kaolinite layers. This study reveals, at the atomic scale, the structural evolution mechanism of the curling of kaolinite layers into tubular forms, which not only deepens the theoretical understanding of HNT formation but also provides a reference for their functional applications and performance optimization.

Key words Halloysite nanotubes, Curling mechanism, Molecular dynamics simulation, Anisotropic contraction

Acknowledgements: This work was supported by the National Natural Science Foundation of China (42072053). We are grateful to the High Performance Computing Platform of China University of

Geosciences Beijing

MOLECULAR MECHANISMS OF ENHANCED PROTON CONDUCTIVITY: LONG-RANGE GROTTHUSS DYNAMICS AT IRO_2/H_2O INTERFACES

Fei-Teng Wang[1], Marcos F. Calegari Andrade[1,2]

1. Chemistry and Biochemistry Department, University of California Santa Cruz, Santa Cruz, California 95064, USA

2. Quantum Simulations Group, Materials Science Division, Lawrence Livermore National Laboratory, Livermore, California 94550, USA

Abstract: Proton transfer (PT) is central to energy conversion, catalysis, and biological processes. Proton conductivity (σ) serves as the key macroscopic descriptor that quantitatively bridges microscopic PT mechanisms with material performance. For instance, a phenomenological relationship has been established to describe the performance of water dissociation catalysts in bipolar membranes, wherein proton conductance plays a critical role. However, a significant gap persists between the underlying proton transfer mechanisms and the resulting proton conductivity/conductance. To bridge this gap, we developed a machine learning potential and performed extensive machine learning molecular dynamics simulations spanning tens of nanoseconds at first-principles accuracy. These simulations reveal the nature of proton flux at the IrO_2/water interfaces and demonstrate how hydrogen bond dynamics govern long-range proton transport and proton conductivity.

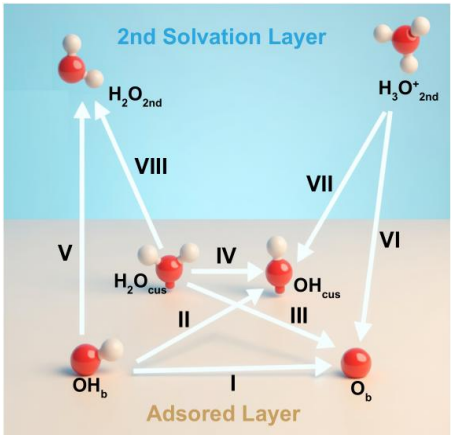


Figure1. Proton transfer steps at IrO_2/water interfaces.

Key words machine learning molecular dynamics, proton transfer, proton conductivity

MOLECULAR MECHANISMS OF H_2 GAS ADSORPTION IN CLAYS PROBED BY CLASSICAL ATOMISTIC SIMULATIONS IN THE CONTEXT OF RADIOACTIVE WASTE STORAGE

Andrey G. Kalinichev, Sylvia M. Mutisya, Pinar Citli

Laboratoire SUBATECH (IMT-Atlantique, Nantes Université, CNRS-IN2P3) Nantes, France

Abstract Clay minerals exhibit a unique combination of useful properties, (low hydraulic conductivity, high sorption and retention capacity for radionuclides, swelling/self sealing properties, etc.) which make them excellent host rock candidates for deep geological disposal of radioactive waste. Hydrogen gas (H_2) can be generated in the waste repository under storage conditions through radiolysis of water due to the residual radioactivity or through anoxic corrosion of steel waste containers ($3Fe+4H_2O=Fe_3O_4+4H_2(g)$). The accumulation of hydrogen gas can present a risk of overpressure and mechanical fracturing of the surrounding host rocks within the repository. Therefore, it is crucial to understand whether the gas can be either absorbed, diffused, or reacted with the constituent host rocks.

In order to develop a fundamental molecular-scale understanding of the physical and chemical processes governing the mineral-fluid interactions between H_2 and H_2O molecules in clay interlayers and interfaces under the thermodynamic conditions relevant to radioactive waste repository, we employ classical atomistic computer simulation techniques. Grand Canonical Monte Carlo (GCMC) simulations of H_2/H_2O mixtures in Na-, Cs-, and Ca-montmorillonite interlayers show that the adsorption of H_2 gas increases with increasing pressure and decreases with increasing temperature in accordance with the H_2 solubility in water. However, the amount of adsorbed H_2 in hydrated clay interlayers is significantly higher compared to its bulk water solubility. Site-specific structural and energetic characteristics of H_2 adsorption in the interlayer, basal, and edge surfaces of montmorillonite clay were quantitatively probed through the use of enhanced molecular dynamics (MD) techniques. In particular, the effects of local compositional and structural heterogeneity on the basal and edge surfaces of montmorillonite have been quantified, as well as the effects of different cations on the gas sorption mechanisms. We show that the energetics of H_2 adsorption on the edges and its intercalation into the interlayer pores is heavily controlled by the structuring of interfacial water.

Key words clay minerals, radioactive waste disposal, H_2 gas, adsorption, molecular simulations

Acknowledgements This work was supported by the industrial chair “Storage and Disposal of Radioactive Waste” at the Institut Mines-Télécom Atlantique, funded by ANDRA, Orano, and EDF.

NOBLE GASES IN THE DEEP SILICATE EARTH RESERVOIRS

Razvan Caracas[1,2], Ozge Ozgurel[2], Sarah Figowy[2], Anne H. Davis[2]

1. Institut de Physique du Globe de Paris, Université Paris Cité, CNRS
1 rue Jussieu, Paris 75005 France
2. Center for Planetary Habitability (PHAB), University of Oslo, Norway

Abstract We determine the chemical behavior of noble gases in the primordial magma ocean (MO) and selected silicate minerals by performing ab initio molecular dynamics simulations at temperatures and pressures along the mantle adiabat.

Our simulations show that at the bottom of the magma ocean, He partitions preferentially into the MO rather than the liquid core. The origin of the ocean island basalts reflects a large contribution and contamination from mantle sources and no necessary contribution from the top of the outer core, which is depleted in primordial He. We suggest searching for the He reservoirs at the base of the solid mantle.

At the top of the magma ocean, Helium degasses at low atmospheric pressures. The simultaneous presence of incompatible volatiles, such as CO2 and He, results in significant loss of He from the magma. Our findings indicate that the early Earth's atmosphere was carbon-rich, with a high concentration of He and other noble gases, and must have been thicker and hotter than previously believed.

Finally, during crystallization, He remains in the melt and continues to accumulate in the melt until the last droplets of the MO solidify. However, the heavier noble gases, such as Xe, which diffuse very slowly, may be partially trapped in the newly forming bridgmanite crystals, while Ne hovers on the brink of crystal entrapment. Consequently, Ar, Kr, and Xe, which are trapped in bridgmanite, would be more evenly distributed throughout the solid mantle, whereas He would concentrate in specific deep reservoirs.

We also find that once trapped in the mantle minerals, with the exception of He, all the other heavy noble gases are inert, not forming any chemical bonds. There escape rates from the bulk solids are close to zero, as the energy barriers for diffusion are extremely high. The only plausible escape mechanism is partial melting combined with diffusion along the grain boundaries during upwellings.

Key words diffusion, helium, xenon, silicate, magma ocean, core formation, atmosphere, Hadean

ORIGIN OF PREMELTING OF ICE IN CONTACT WITH CLAY MINERALS

Meng Chen[1,2,*], Yun Li [3,4]

1. State Key Laboratory of Deep Earth Processes and Resources, Guangzhou Institute of Geochemistry, Chinese Academy of Sciences, Guangzhou, 510640, China.

2. Guangdong research center for strategic metals and green utilization, Guangzhou, 510640, China.

3. College of Petroleum Engineering, Xi’an Shiyou University, Xi’an, Shaanxi, 710065, P.R. China

4. Shenzhen Key Laboratory of Natural Gas Hydrates & Institute of Major Scientific Facilities for New Materials, Southern University of Science and Technology, Shenzhen 518055, P.R. China

Abstract A quasi-liquid layer (QLL) composed of water molecules at the ice/clay mineral interface plays a critical role in ice melting, regelation, and water channeling. The associated mass transport and elemental cycling are of fundamental importance to Earth’s surface systems. Conventionally, QLL formation has been interpreted as a reorganization of the ice surface layers to minimize the system free energy. However, it remains unclear whether the entropy gain arising from water molecular reorganization alone can account for such free energy minimization.

In this work, we present a perspective from open system thermodynamics: the QLL at the ice/clay mineral interface is connected to supercooled liquid water, and is thus subjected to a differential pressure, defined as the difference between the pressure on the interface and that in the liquid. This framework is consistent with realistic environmental conditions. Using extensive molecular dynamics simulations, we reveal a cyclic variation in QLL thickness in response to excess water availability.

At temperatures near the melting point, global equilibrium under uniform pressure corresponds to a system with a thin QLL. In contrast, a nonzero differential pressure gives rise to a considerably thickened QLL. Systems with a thin QLL exhibit a highly ordered structure and can be superheated, whereas those with a thick QLL undergo spontaneous melting around the melting temperature. When the differential pressure exceeds the range of the disjoining pressure, a dynamic QLL drives continuous ice melting or growth, which may represent a key mechanism underlying regelation.

This study establishes a new paradigm for understanding the ice/solid interface within an open system framework.

Key words Clay minerals, ice, water, melting

PHOTOACTIVE ELEMENTAL SULFUR ALLOTROPES PROMOTE EXTENSIVE AMMONIA SYNTHESIS IN VENUS-LIKE ATMOSPHERE

Rongzhang Yin[1,2], Yanzhang Li[1,2], Yan Li[1,2*]

1. SKLab-DeepMinE, MOEKLab-OBCE, School of Earth and Space Sciences, Peking University, Beijing 100871, China

2. Beijing Key Laboratory of Mineral Environmental Function, School of Earth and Space Sciences, Peking University, Beijing 100871, China

Abstract Atmospheric chemistry in Venus remains elusive, especially the photochemical role of sulfur species and the unexplained presence of ammonia (NH_3). Here we show, through combined experiments and quantum chemical calculations, that elemental sulfur (S^0) can photoreduce nitrate (NO_3^-) to NH_3 under Venus-like acidic and UV-irradiated conditions. Up to 20% of NO_3^- can be converted to NH_3 within six hours, driven by surface-catalyzed photoreactions on S^0 allotropes with chain-like molecular configuration. Terminal sulfur atoms in S^0 chains act as reactive sites and become more active under higher proton concentrations and photon fluxes, enabling a thermodynamically favorable stepwise conversion of NO_3^- to NH_3 with a Gibbs free energy change ranging from −68.0 to −92.6 kcal·mol^{-1}. Based on vapor or aerosol models of S^0, the peak NH_3 production rate is estimated at ~10^{13} mol·yr^{-1}·km^{-1} within the 48–70 km sulfuric acid clouds. These findings identify an abiotic pathway sustaining NH_3 and coupling sulfur and nitrogen cycles in Venus-like atmosphere.

Key words native sulfur, ammonia synthesis, photochemistry, Venusian atmosphere

STRESS COUPLED VACANCY DIFFUSION IN CRYSTALS: A CAUCHY-NERNST-PLANCK CONTINUUM MODEL

Michiel Sprik

Yusuf Hamied Department of Chemistry, University of Cambridge, United Kingdom

Abstract Material scientists agree that the leading mechanism for diffusion in crystals is vacancy exchange. Atoms can only move to an unoccupied site nearby leaving a vacancy behind. This picture is the basis for the Larché-Cahn (LC) network theory of crystals[F. Larché and J.W. Cahn, *Acta Metallurgica* **21** (1973) 1051-1063]: i) Bulk lattice sites are conserved keeping their identity whether occupied or empty. ii) Elastic deformation (strain) is determined by the displacement of lattice sites, not by the unbounded displacement of migrating atoms. The rather disconcerting consequence is that elastic energies have become independent of the number of atoms complicating the definition of the chemical potential. This is solved in LC theory by adding a separate composition strain to the strain tensor. An alternative, applied here, is to have the site binding energy vary with the density of atoms in the deformed solid. This introduces a local "molecular" pressure similar to the hydrostatic pressure in liquids.

The thermodynamics of this model was worked out in a previous publication for uniform systems neglecting shear deformation[M. Sprik, *J. Chem. Phys.* **163** (2025) 114702]. This approach has now been extended to diffusive dynamics including shear elasticity. Neglecting inertial effects, the result is a Nernst-Planck expression for the vacancy flux with the gradient of the molecular pressure as drift force. The same molecular pressure gradient also acts as an effective one-body force density in the Cauchy equation for the elastic stress establishing a coupling between elastic and diffusive degress of freedom. In this talk we will try to elucidate the physics behind these equations omitting derivations. We closely follow the theory of diffusion in solids as found in our favourite textbook on continuum mechanics [M.E. Gurtin, E.Fried and L. Anand "*The Mechanics and Thermodynamics of Continua*". Cambridge University Press (2010)].

Key words Diffusion in solids, chemical potential of vacancies, coupling of diffusion to stress

THERMODYNAMIC AND TRANSPORT PROPERTIES OF $CACO_3$ MELT UNDER MANTLE CONDITIONS

Yifan Lu[1], Yicheng Sun[1*], Kai Wang[2*], Xiancai Lu[2]

1. College of Oceanography, Hohai University, China.

2. School of Earth Sciences and Engineering, Nanjing University, China.

Abstract Carbonate melts are key agents for the efficient migration and deep recycling of mantle materials. On the one hand, carbonate melts possess extremely low viscosity and exceptionally high migration rates, serving as the primary carriers of deep carbon transport and profoundly influencing the mantle carbon cycle. On the other hand, carbonate melts can lower the solidus temperature of mantle rocks, modify mantle rheology, and form carbonated mantle sources, participating in the petrogenesis of deep-seated magmas such as carbonatites and kimberlites. However, compared to silicate melts, understanding of the relevant properties of carbonate melts within the mantle remains limited. As the most representative carbonate melt, the $CaCO_3$ melt serves as the benchmark endmember and simplified model for understanding the physicochemical properties and reaction mechanisms of natural carbonate melts. In this study, we employ a machine learning potential model trained on first-principles datasets to systematically investigate the thermodynamic and transport properties of $CaCO_3$ melt across the entire mantle pressure-temperature range. Based on the equation of state (EOS) obtained from simulations, we derived the thermodynamic properties of the CaCO3 melt, providing physical property parameters for geophysical models. Using the calculated viscosity data of the $CaCO_3$ melt, we calculate the migration rate of carbonate melts within the mantle. The low viscosity and high mobility of the $CaCO_3$ melt indicate that carbonate melts are able to escape their source regions rapidly without fully equilibrating with the surrounding rocks, thus avoiding complete reaction and dissipation. This characteristic enables carbonate melts to efficiently transport deep carbon to shallow depths, which has significant implications for understanding the global deep carbon cycle and arc volcanic degassing fluxes.

Key words Machine learning, Mantle, $CaCO_3$, Thermodynamic properties,Transport properties

WATER INCORPORATION MECHANISMS AND EFFECTS IN MGSIO3-MAJORITE UNDER HIGH TEMPERATURE AND PRESSURE CONDITIONS

Yancheng Lou[1,2,3,*], Zhigang Zhang[3,4], Andrew M. Walker[5], Stephen Stackhouse[6], Meng Chen[1,2], and Hongping He[1,2,4]

1. State Key Laboratory of Deep Earth Processes and Resources, Guangzhou Institute of Geochemistry, Chinese Academy of Sciences, Guangzhou, 510640, China.
2. Guangdong Research Center for Strategic Metals and Green Utilization, Guangzhou, 510640, China.
3. Key Laboratory of Planetary Science and Frontier Technology, Institute of Geology and Geophysics, Chinese Academy of Sciences, Beijing 100029, China.
4. College of Earth and Planetary Sciences, University of Chinese Academy of Sciences, Beijing 100049, China.
5. Department of Earth Sciences, University of Oxford, South Park Road, Oxford OX1 3AN, United Kingdom.
6. School of Earth and Environment, University of Leeds, Leeds LS2 9JT, United Kingdom.

Abstract The incorporation of water in high-pressure minerals is essential for the water cycle within the interiors of terrestrial planets. Majoritic garnet, a major component in the mantles of Earth and Mars, plays a significant role in this context. In this study, we use first-principles simulations to explore water incorporation mechanisms in $MgSiO_3$-majorite, which is a key end-member of majoritic garnet, at conditions up to 2,000 K and 20 GPa. By dealing with the relationship between chemical potential and the Gibbs free energy changes for the reactions at equilibrium conditions, we determine the ratios of the seven potential hydrous defects. Our results reveal that the Si2 and Si3 defects, which are of the hydrogarnet-type, dominate water incorporation in $MgSiO_3$-majorite. In addition, we evaluate the effects of these hydrous defects on seismic wave velocities. The presence of Si2 and Si3 defects, with an expected water concentration of ~700 ppm, has a small effect on both P-wave and S-wave velocities. Nevertheless, the influence of water on lateral variations in the seismic wave velocities of $MgSiO_3$-majorite, which is opposite to that found for ringwoodite, offers a potential tool for investigating compositional heterogeneities in hydrated regions of planetary mantles.

Key words First-principles, majorite garnet, Water Incorporation Mechanisms, Hydrous Defect, Deep Earth

THE STRUCTURE AND TRANSPORT PROPERTIES OF DIOPSIDE SUPERCRITICAL FLUID FROM MACHINE LEARNING POTENTIAL

Dong Wang, Zhongqing Wu*

School of Earth and Space Sciences, University of Science and Technology of China, Hefei

Abstract In deep subduction zones with high temperatures and pressures, the miscibility gap between silicate melt and aqueous fluid diminishes, leading to the formation of a single phase with an intermediate composition, known as supercritical fluid. Supercritical fluids play a crucial role in mass transfer in the subduction zone due to their low viscosity and their ability to carry large amounts of elements. However, the structures and transport properties of supercritical fluids are poorly constrained. Conducting in-situ experiments at high temperatures is still challenging. First-principles calculations can only provide results at extremely high temperatures, since the computational cost required to make the results converge increases significantly as the temperature decreases. Machine learning potentials trained from first-principles data combine the computational efficiency of classical potentials with the accuracy of first-principles, providing a promising way to calculate the properties of supercritical fluid at relatively low temperatures.

Here, we obtained a representative train set of diopside supercritical fluid with 0 ~ 78 wt.% water ($CaMgSi_2O_6$-xH_2O) through a combination of concurrent learning, enhanced sampling, and principal component analysis. The train set was then used to train a machine learning potential for the diopside supercritical fluid. At high temperatures, the melt structure and transport properties calculated by the machine learning potential perfectly match the results from first-principles calculations. By using the efficient machine learning potential, we were able to obtain the structure and transport properties of diopside supercritical fluid down to 1000 K, building a bridge between experiments and theoretical calculations.

Key words Supercritical fluid, machine learning potential, first-principles calculations.